International Congress on Innovation Technologies & Engineering

September 02-04, 2022

Ege University, Izmir, Turkey

Proceedings Book

2022

EGE

INTERNATIONAL CONGRESS ON INNOVATION TECHNOLOGIES & ENGINEERING

September 02-04, 2022
Ege University, Izmir, Türkiye

PROCEEDINGS BOOK

Edited by

PROF. DR. BAHRI BAŞARAN
ASSIST. PROF. DR. AYSUN BALTACI

by
IKSAD GLOBAL PUBLISHING HOUSE
E-mail: info@iksad.com
iksad47@gmail.com www.egekongreleri.org

Issued: 03.10.2022

ISBN: 978-625-8213-60-7

CONGRESS ID

CONGRESS TITLE

EGE

INTERNATIONAL CONGRESS ON INNOVATION TECHNOLOGIES & ENGINEERING

DATE and PLACE

September 02-04, 2022
Ege University, Izmir, Türkiye

ORGANIZATION

Ege University, Türkiye
Graduate School of Natural and Applied Sciences, İzmir, Türkiye
ANAS, Azerbaijan
IKSAD Institute, Türkiye

HONORARY BOARD

Prof. Dr. Necdet BUDAK – Rector of Ege University
Prof. Dr. Cemil GÜRGÜN – Vice-Rector of Ege University
Prof. Dr. Mehmet ERSAN – Vice-Rector of Ege University
Prof. Dr. Hakan ATILGAN – Vice-Rector of Ege University

HEAD OF CONGRESS

Prof. Dr. Bahri BAŞARAN
Director of Ege University, Graduate School of Natural and Applied Science, Türkiye
Academic Arif HEŞİMOV
Director of ANAS, Institute of Physical Science, Azerbaijan
Prof. Dr. Nadim MACİT
Director of Ege University, Institute of Turkish World Studies, Türkiye

NUMBER of ACCEPTED PAPERS

120

NUMBER of REJECTED PAPERS

25

PARTICIPANT COUNTRIES (18)

Turkey, Nigeria, USA, India, Netherlands, Austria, Uganda, Pakistan, Morocco, Algeria, China, Iraq, Azerbaijan, Croatia, Brazil, Kazakhstan, Iran, Republic of Korea

TOTAL NUMBER of INTERNATIONAL PAPERS

Turkey (58), Other Countries (62)

EVALUATION PROCESS

All Applications Have Undergone A Double-Blind Peer Review Process

PRESENTATION

Oral and Poster Presentations

ORGANIZING BOARD

Prof. Dr. Bahri BAŞARAN
Ege University

Prof. Dr. M.Bahattin TANYOLAÇ
Ege University

Prof. Dr. Banu YÜCEL
Ege University

Prof. Dr. Uğur SUNLU
Ege University

Prof. Dr. Hasan YILDIZ
Ege University

Prof. Dr. Hüseyn İBRAHİMOV
ANAS Institute of Physics

Prof. Dr. Neriman REHMANOV
AMEA Institute of Physics

Prof. Dr. Kudret İSAKOV
AMEA Institute of Physics

Prof. Dr. Şebnem TAVMAN
Ege University

Prof. Dr. Ahmet ASLAN
Ege University

Assoc. Prof. Dr. Gülsüm ÖZTÜRK
Ege University

Assoc. Prof. Dr. Candaş ADIGÜZEL ZENGİN
Ege University

Assoc. Prof. Dr. Terane NURUBEYLİ
ANAS Institute of Physics

Assoc. Prof. Dr. Ali MEMMEDOV
ANAS Institute of Physics

Assoc. Prof. Dr. Kamil QURBANOV
ANAS Institute of Physics

Assist. Prof. Dr. Aysun BALTACI
Ege University

Dr. Tarık AYYILMAZ
Ege University

Res. Assist. Dr. Evrim KURTAY
Ege University

Res. Assist. Dr. Ö. ALPER ERDEM
Ege University

Res. Assist. Dr. Burcu TAYLAN
Ege University

Res. Assist. Enis KÖRPE
Ege University

Res. Assist. Devrim TÜMER
Ege University

Res. Assist. Hilal YILMAZKARASU
Ege University

Res. Assist. Zekeriya Anıl GÜVEN
Ege University

Res. Assist. Muhammet Serdar AVCI
Ege University

Res. Assist. Tunç DURDU
Ege University

Res. Assist. Özlem AKBAŞ
Ege University

Assist. Prof. Dr. Aysun BALTACI
Ege University

SCIENTIFIC COMMITTEE

Prof. Dr. M. Osman ÜNALIR - Ege University

Prof. Dr. Şebnem TAVMAN - Ege University

Prof. Dr. Erkan MEŞE - Ege University

Prof. Dr. Şemsi YAZICI - Ege University

Prof. Dr. Levent BALLİCE - Ege University

Prof. Dr. Yeliz PEKBEY - Ege University

Prof. Dr. Perrin KUMBASAR - Ege University

Prof. Dr. M.Bahattin TANYOLAÇ - Ege University

Prof. Dr. Ahmet ASLAN - Ege University

Prof. Dr. İbrahim DUMAN - Ege University

Prof. Dr. Mustafa GÜMÜŞ - Ege University

Prof. Dr. Harun UYSAL - Ege University

Prof. Dr. Erhan AKKUZU - Ege University

Prof. Dr. Hüseyn İBRAHİMOV - ANAS Institute of Physics

Prof. Dr. Neriman REHMANOV - AMEA Institute of Physics

Prof. Dr. Kudret İSAKOV - AMEA Institute of Physics

Prof. Dr. Abul Hashem - Khulna University of Engineering & Technology (KUET)

Prof. Dr. Mekonnen Heilemariam - ALLPI African Leather and Leather Product Institute

Prof. Dr. Hakan BAYRAKTAR - Ege University

Prof. Dr. Şule IŞIN - Ege University

Prof. Dr. Behçet KIR - Ege University

Prof. Dr. Engin NURLU - Ege University

Prof. Dr. Bülent ÇAKMAK - Ege University

PHOTO GALLERY

PHOTO GALLERY

PHOTO GALLERY

PHOTO GALLERY

PHOTO GALLERY

PHOTO GALLERY

PHOTO GALLERY

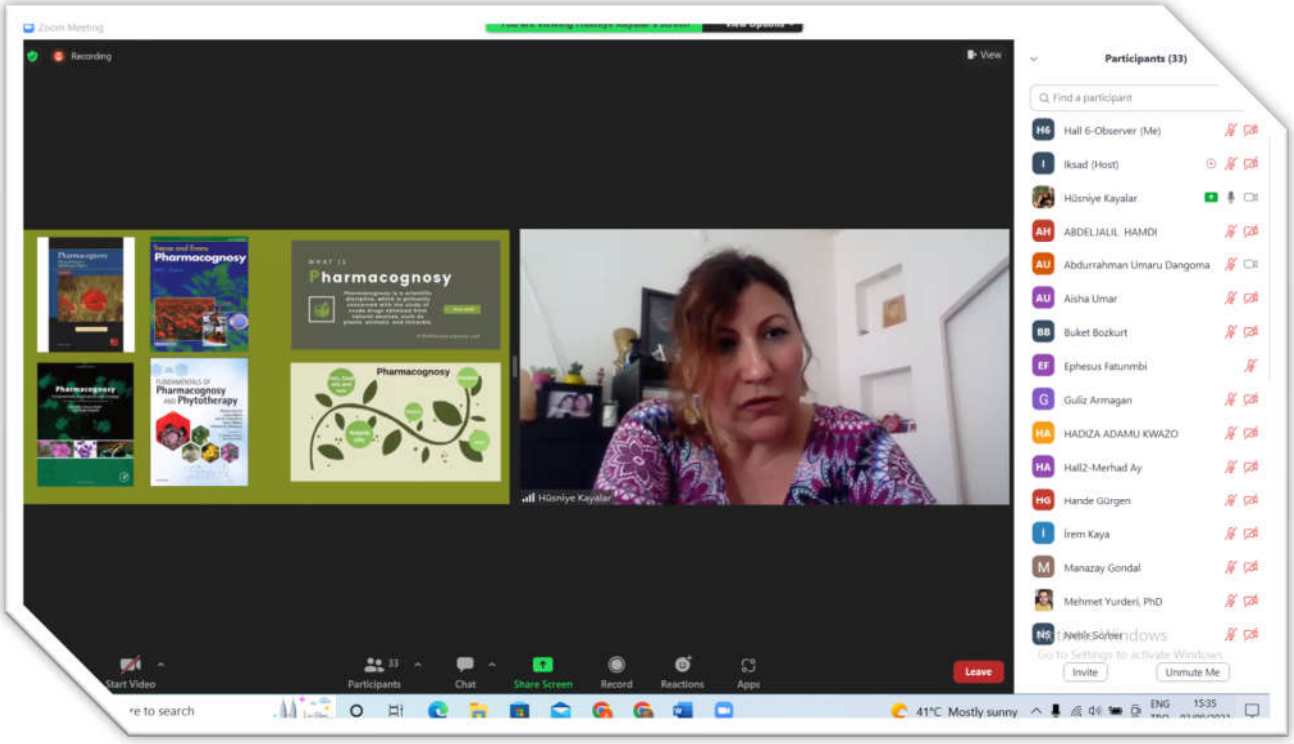

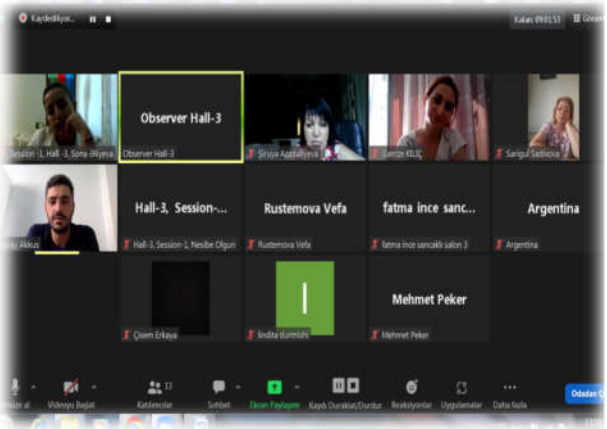

PHOTO GALLERY

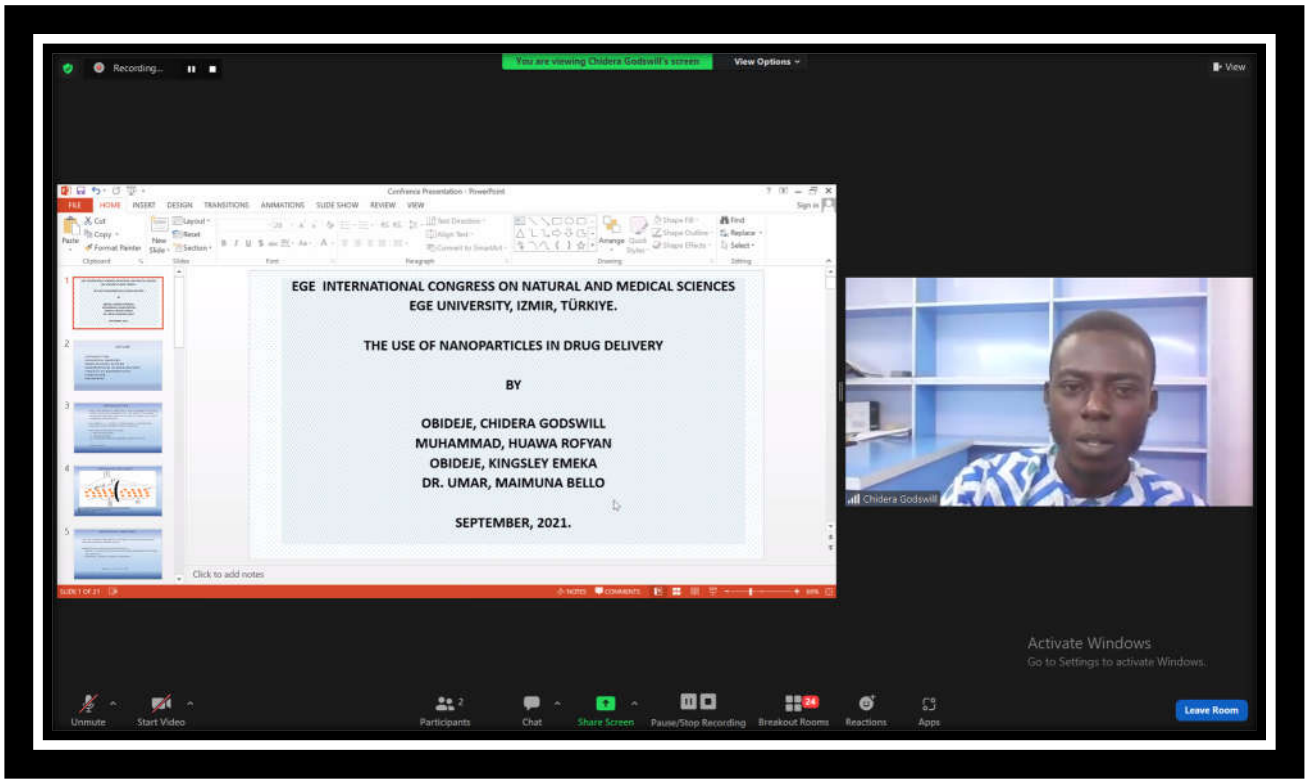

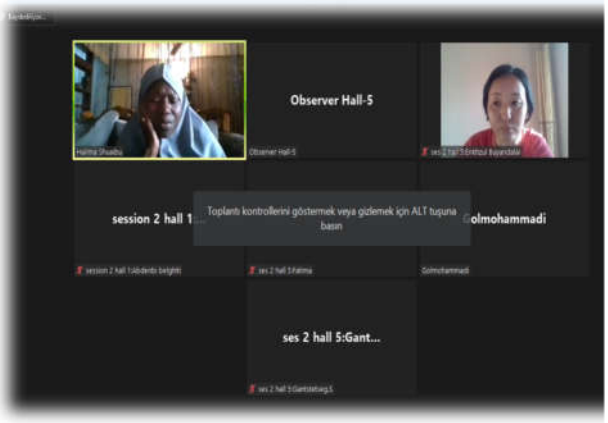

PHOTO GALLERY

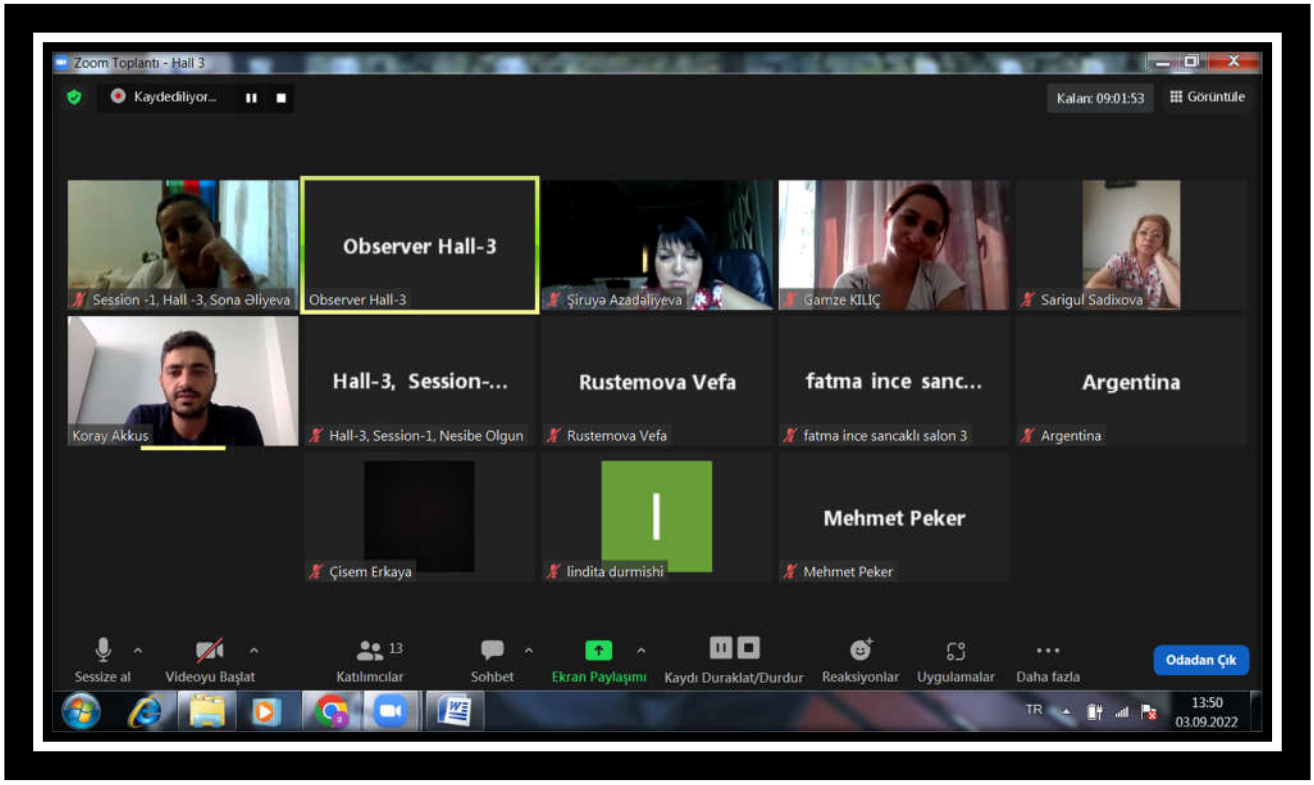

PHOTO GALLERY

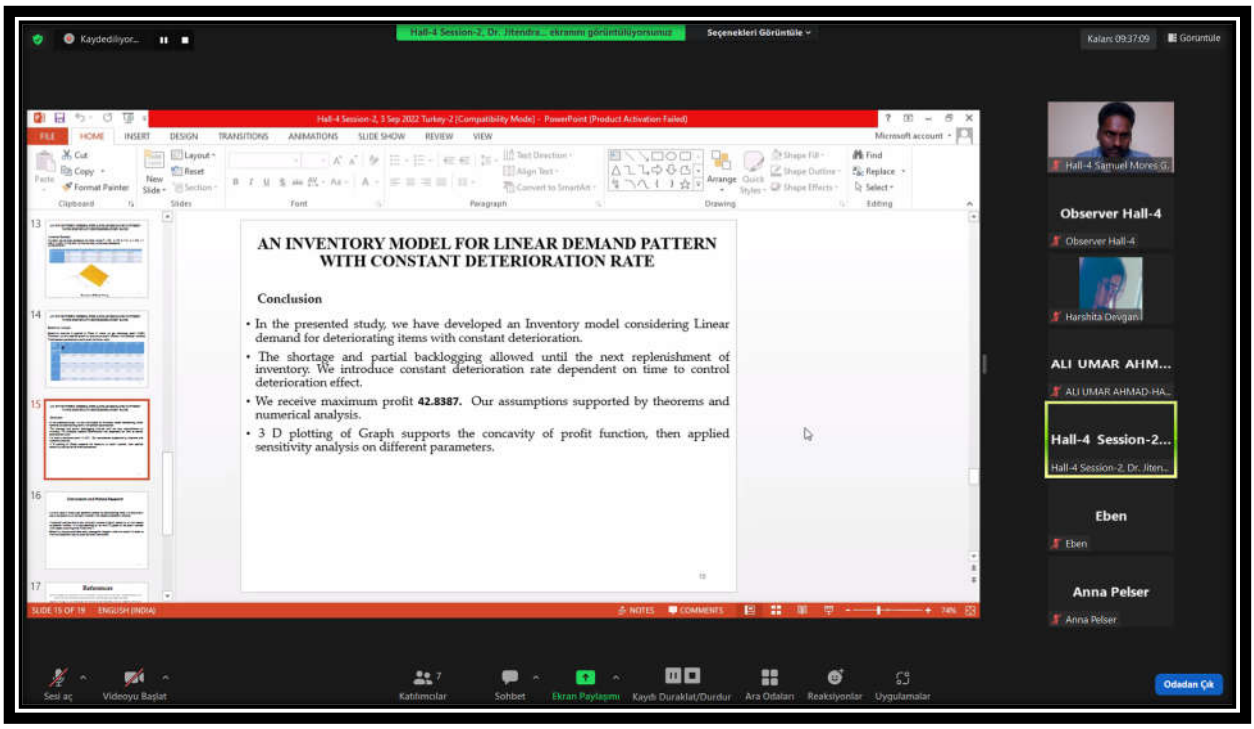

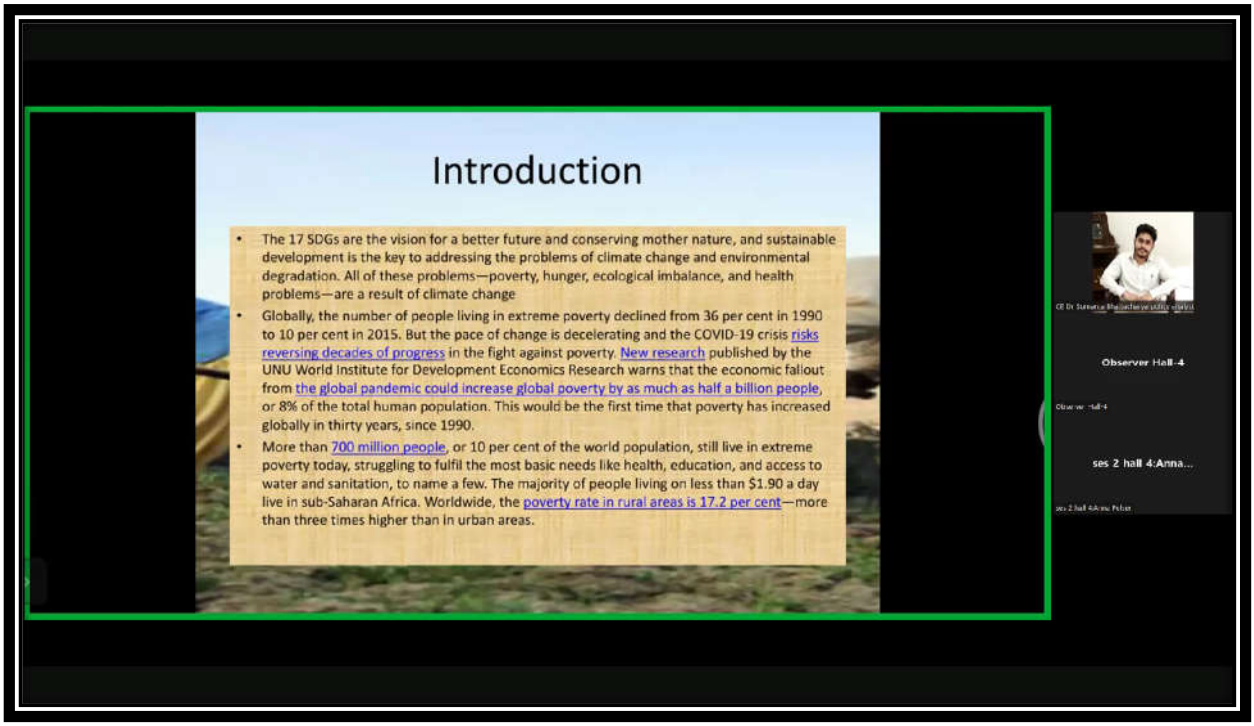

PHOTO GALLERY

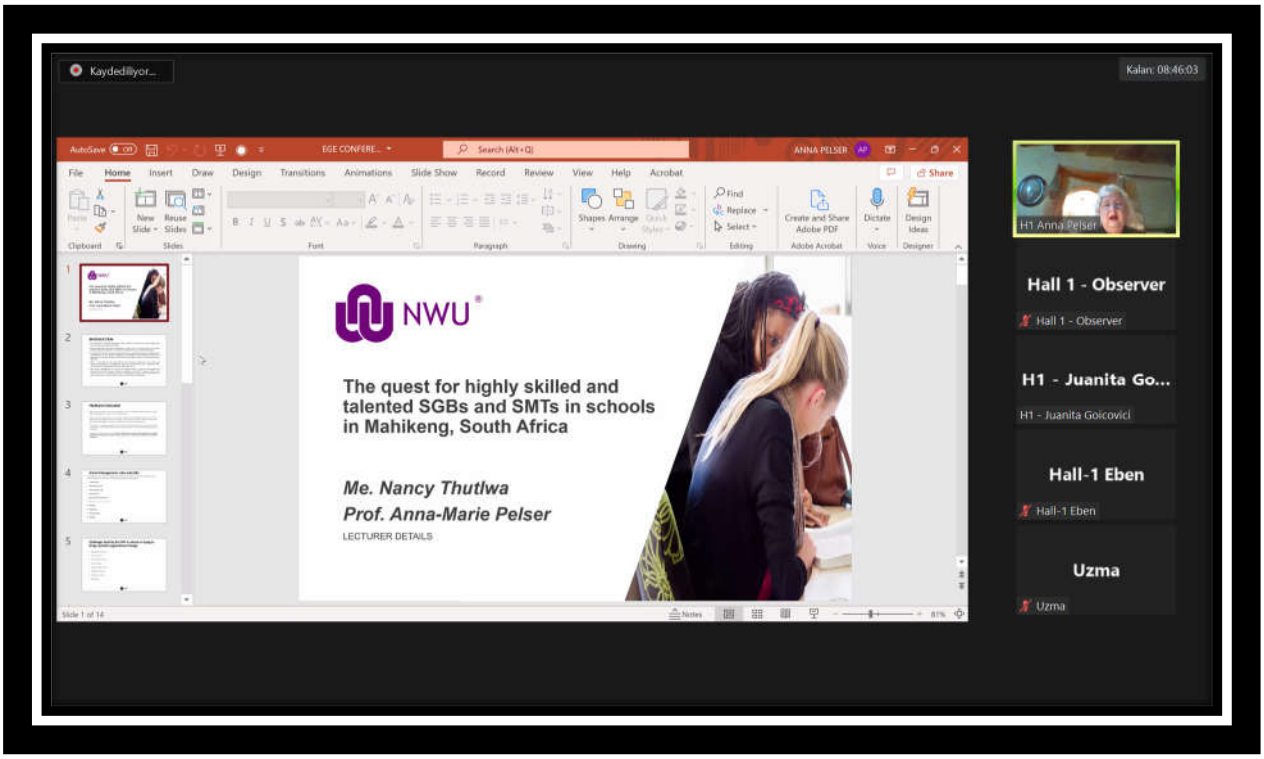

EGE

INTERNATIONAL CONGRESS ON INNOVATION TECHNOLOGIES & ENGINEERING

September 02-04, 2022
Ege University, Izmir, Türkiye

CONGRESS PROGRAM

Participant Countries: (18)

Turkey, Nigeria, USA, India, Netherlands, Austria, Uganda, Pakistan, Morocco, Algeria, China, Iraq, Azerbaijan, Croatia, Brazil, Kazakhstan, Iran, Republic of Korea

Önemli, Dikkatle Okuyunuz Lütfen

- Kongremizde Yazım Kurallarına uygun gönderilmiş ve bilim kurulundan geçen bildiriler için online (video konferans sistemi üzerinden) sunum imkanı sağlanmıştır.
- Online sunum yapabilmek için https://zoom.us/join sitesi üzerinden giriş yaparak "Meeting ID or Personal Link Name" yerine ID numarasını girerek oturuma katılabilirsiniz.
- Zoom uygulaması ücretsizdir ve hesap oluşturmaya gerek yoktur.
- Zoom uygulaması kaydolmadan kullanılabilir.
- Uygulama tablet, telefon ve PC'lerde çalışıyor.
- Her oturumdaki sunucular, sunum saatinden 5 dk öncesinde oturuma bağlanmış olmaları gerekmektedir.
- Tüm kongre katılımcıları canlı bağlanarak tüm oturumları dinleyebilir.
- Moderatör – oturumdaki sunum ve bilimsel tartışma (soru-cevap) kısmından sorumludur.

Dikkat Edilmesi Gerekenler - TEKNİK BİLGİLER

- Bilgisayarınızda mikrofon olduğuna ve çalıştığına emin olun.
- Zoom'da ekran paylaşma özelliğini kullanabilmelisiniz.
- Kabul edilen bildiri sahiplerinin mail adreslerine Zoom uygulamasında oluşturduğumuz oturuma ait ID numarası gönderilecektir.
- Katılım belgeleri kongre sonunda tarafınıza pdf olarak gönderilecektir.
- Kongre programında yer ve saat değişikliği gibi talepler dikkate alınmayacaktır.

Important, Please Read Carefully

- To be able to attend a meeting online, login via https://zoom.us/join site, enter ID "Meeting ID or Personal Link Name" and solidify the session.
- The Zoom application is free and no need to create an account.
- The Zoom application can be used without registration.
- The application works on tablets, phones and PCs.
- The participant must be connected to the session 5 minutes before the presentation time.
- All congress participants can connect live and listen to all sessions.
- Moderator is responsible for the presentation and scientific discussion (question-answer) section of the session.

Points to Take into Consideration - TECHNICAL INFORMATION

- Make sure your computer has a microphone and is working.
- You should be able to use screen sharing feature in Zoom.
- Attendance certificates will be sent to you as pdf at the end of the congress.
- Requests such as change of place and time will not be taken into consideration in the congress program.

***

Zoom'a giriş yapmadan önce lütfen örnekteki gibi salon numaranızı, adınızı ve soyadınızı belirtiniz
Before you login to Zoom please indicate your hall number, name and surname

exp. H-5, Dilshod ARTYKOV

OPENING CEREMONY

02.09.2022

Ankara Local Time: *10:30 – 12:00*

Place: *Mühendislik Fakültesi, Biyomühendislik Bölümü Konferans Salonu*

***

Prof. Dr. Fikret TÜRKMEN

Ege Üniversitesi, Türk Dünyası Araştırmaları Enstitüsü

5. ULUSLARARASI DEDE KORKUTTÜRK KÜLTÜRÜ, TARİHİ ve EDEBİYATI KONGRESİ

***

Prof. Dr. Metin EKİCİ

Ege Üniversitesi, Türk Dünyası Araştırmaları Enstitüsü

Türk Halk Bilimi Anabilim Dalı Başkanı

5. ULUSLARARASI DEDE KORKUTTÜRK KÜLTÜRÜ, TARİHİ ve EDEBİYATI KONGRESİ BAŞKANI

***

Prof. Dr. Ramazan GAFARLI

AMEA Folklor Enstitüsü

"Dede Korkut" şöbesinin müdürü, Dede Korkut dergisinin başkanı

5. ULUSLARARASI DEDE KORKUTTÜRK KÜLTÜRÜ, TARİHİ ve EDEBİYATI KONGRESİ BAŞKANI

***

Prof. Dr. Alimcan İNAYET

Ege Üniversitesi, Türk Dünyası Araştırmaları Enstitüsü Müdür Yardımcısı

***

Prof. Dr. Mustafa MUTLUER

Ege Üniversitesi, Sosyal Bilimler Enstitüsü Müdürü

ULUSLARARASI EGE SOSYAL VE BEŞERİ BİLİMLER KONGRESİ BAŞKANI

***

Prof. Dr. Bahri BAŞARAN

Ege Üniversitesi Fen Bilimleri Enstitüsü Müdürü

ULUSLARARASI SAĞLIK VE FEN BİLİMLERİ KONGRE BAŞKANI

ULUSLARARASI İNOVASYON VE MÜHENDİSLİK BİLİMLERİ KONGRE BAŞKANI

***

Dr. Mustafa Latif EMEK

İKSAD Enstitüsü Başkanı

***

Prof. Dr. Necdet BUDAK

Ege Üniversitesi Rektörü

EGE KONGRELERİ ONURSAL BAŞKANI

PANEL SESSION

02.09.2022

Ankara Local Time: *14:00 – 15:00*

Place: *Ege University, Faculty of Engineering, Department of Bioengineering*

Halil Ceylan, Ph.D., Dist.M.ASCE

Pitt-Des Moines, Inc. Endowed Professor in Civil, Construction and Environmental Engineering (CCEE)

ISU Site Director, PEGASAS - FAA Center of Excellence on General Aviation

Director, Program for Sustainable Pavement Engineering & Research (PROSPER)

Institute for Transportation, Iowa State Universit

- ELECTRICALLY CONDUCTIVE CONCRETE BASED HEATED INFRASTRUCTURE SYSTEMS FOR SUSTAINABLE AND RESILIENT WINTER MAINTENANCE

FACE TO FACE PRESENTATIONS

02.09.2022 / Session-1 / Hall-1

ANKARA LOCAL TIME		Ege University, Faculty of Engineering, Department of Bioengineering	
15 00 : 17 00			

HEAD OF SESSION: Halil Ceylan

AUTHORS	AFFILIATION	TOPIC TITLE
Mustafa ÇAKIR Emre AKIN Boran BERBEROĞLU	*Marmara University*	URETHANE ACRYLATE AND SILICON ACRYLATE CONTAINING NOVEL EPOXY ACRYLATE SYSTEMS FOR SLA 3D PRINTERS
Yavuz Bahadır Şahin Seydi Vakkas Şahin Sinan Zengin	*Ege University*	CALCULATING OPTIMUM TILT ANGLES OF PHOTOVOLTAIC MODULES FOR IZMIR PROVINCE
Bengi Kanat COŞKUN Onur SEVLİ	*Manisa Science and Art Center, MANİSA, TURKEY* *Burdur Mehmet Akif Ersoy University*	CLASSIFYING CARDIAC SPECT DATA USING MACHINE LEARNING METHODS AND FEATURE SELECTION
Ceren Bahar Yılmaz Oğuz Gövem Murat Osman Ünalır	*Litum Bilgi Teknolojileri Ar-ge Merkezi* *Litum Bilgi Teknolojileri Ar-ge Merkezi* *Ege University*	TRANSFORMING RTLS DATA ARCHITECTURE TO BIG DATA ARCHITECTURE: A CASE STUDY FOR POST-PROCESSING OF LOCATION DATA
Halil Ceylan, Ph.D., Dist.M.ASCE	*Pitt-Des Moines, Inc. Endowed Professor in Civil, Construction and Environmental Engineering (CCEE)* *ISU Site Director, PEGASAS - FAA Center of Excellence on General Aviation* *Director, Program for Sustainable Pavement Engineering & Research (PROSPER)* *Institute for Transportation, Iowa State Universit*	USE OF UNCREWED AIRCRAFT SYSTEMS/DRONES FOR HEALTH MONITORING AND MANAGEMENT OF INFRASTRUCTURE SYSTEMS
Prof. Dr. Banu YÜCEL	*Ege University*	NEW APPROACHES ON VALUE-ADDED BEE PRODUCTS; WHOLE BEE (PODMORE), BEE DRONE LARVAE (APILARNIL) AND BEE HIVE AIR APPLICATIONS
Lala R. Aliyeva Rahim M. Rzaev	*Institute of Mathematics and Mechanics of NAS, Baku, Azerbaijan* *Azerbaijan State Pedagogical University, Baku, Azerbaijan.*	SINGULAR INTEGRAL OPERATOR IN SPACES DEFINED BY GENERALIZED OSCILLATION
İrem PALABIYIK (POSTER SUNUM) Özgür BULUT	*FG Tekstil Konfeksiyon San. Tic. A.Ş. / R&D Center, İzmir, Turkey* *FG Tekstil Konfeksiyon San. Tic. A.Ş. / R&D Center, İzmir, Turkey*	DEVELOPMENT OF OZONE EFFECTING SYSTEM WITHOUT USING HARMFUL CHEMICALS

ONLINE PRESENTATIONS

03.09.2022 / Hall-1 / Session-1

Ankara Local Time		Meeting ID: 839 6259 8369	
10 ^{00} : 12 ^{30}		Passcode: 123456	

HEAD OF SESSION: Ömer ZOR

AUTHORS	AFFILIATION	TOPIC TITLE
Ahmet Ali Süzen Remzi Gürfidan	*Isparta University*	VULNERABILITY ASSESSMENT OF SERVER WITH SHODAN QUERY
Mustafa Feyzi TEMEL Raif BAYIR	*Karabük University* *Karabük University*	REALIZING LINEAR AXIS CONTROL FOR ROBOTIC APPLICATIONS WITH NEXT GENERATION SERVO DRIVES
Sabri BIÇAKÇI	*Balıkesir University*	FACTORS AFFECTING BULLET OUTPUT SPEED IN A COILGUN
Hakan ÇITAK	*Balıkesir University*	EFFICIENCY OF AMORF FERROMAGNETIC WIRES IN DETERMINING DISCONTINUITY
Ömer ZOR	*Bursa Technical University*	LORENTZ FORCE ACTING ON DYON AND DUALITY
Alperen SOYDAN	*TOBB Universtiy of Economy and Technology*	CREATING HOLISTIC THREAT HUNTING FRAMEWORK
Tutku Dilara AKKAYA Al MIZAN Bahri BAŞARAN	*Ege University* *Ege University, Khulna University of Engineering & Technology (KUET), BANGLADESH*	EXTRACTION OF COLLAGEN HYDROLYSATE FROM CHROME LEATHER SHAVINGS AND ITS PROPERTIES

ONLINE PRESENTATIONS

03.09.2022 / Hall-2 / Session-1

Ankara Local Time

10 00 : 12 30

Meeting ID: 839 6259 8369

Passcode: 123456

HEAD OF SESSION:

AUTHORS	AFFILIATION	TOPIC TITLE
S. Melike Bulut Tugce Tezel Volkan Kovan	*Akdeniz University*	FAILURE ANALYSIS OF A HELICAL HSS END MILL
S. Melike Bulut Tugce Tezel Volkan Kovan	*Akdeniz University*	POST-PRODUCTION COPPER COATING APPLICATIONS WITH ADDITIVE MANUFACTURING
Eray ERBAK Gökhan GÜRLEK Barış Oğuz GÜRSES Mert ŞENER	*Ege University*	FLOW ANALYSIS OF NON-NEWTONIAN FLUID INTO THE SYRINGE
Şeyma Özkan Gökhan Gürlek Barış Oğuz Gürses Yoldaş SEKİ Mehmet SARIKANAT Mert Şener Hicran Beşikci	*Dokuz Eylül University* *Ege University*	COPPER CHLORIDE AND SILVER SELENITE ADDITIVE PEDOT: PSS BASED THERMOELECTRIC THIN FILM MANUFACTURING
Gökhan ÖZDEMİR Mert ŞENER Barış Oğuz GÜRSES	*Ege University*	DETERMINING THE MECHANICAL PROPERTIES OF A HYPERELASTIC MATERIAL
Dr. Elif KOZAN Filiz KARADAĞ Dr. Agah KOZAN	*Ege University*	COMPARISON OF MACHINE LEARNING CLASSIFICATION TECHNIQUES IN R
Yuksel CELIK Dr. Murat TURE	*Multitek Elektronik Research and Development Centre, Istanbul, TURKIYE*	ETHERNET INTERFACE DESIGN AND REALIZATION FOR SMART HOME COMPONENTS
Ekrem YILMAZ Dr. Murat TURE	*Multitek Elektronik Research and Development Centre, Istanbul, TURKIYE*	SIP CHAT CONTROLLED CLOUD INTERCOM

ONLINE PRESENTATIONS

03.09.2022 / Hall-1 / Session-2

Ankara Local Time

13 00 : 15 30

Meeting ID: 839 6259 8369

Passcode: 123456

HEAD OF SESSION: John Chiwuzulum Odozi

AUTHORS	AFFILIATION	TOPIC TITLE
Isa Diadia Alhassan Lawal Adamu	*Department of Mathematics, Federal University of Technology, Minna, Nigeria*	APPLICATION OF GREY-MARKOV GMM (1, 1) MODEL FOR FORECASTING NIGERIA ANNUAL SOYBEAN PRODUCTION
Oyefeso, B.O. Udu, G.O.	*University of Ibadan, Ibadan, Nigeria*	EFFECT OF HEAT TREATMENTS ON PROXIMATE COMPOSITION OF SWEET POTATO TUBERS
Okonkwo, H.O Omokhua, G. E Chima U. D	*Swamp Forest Research station, Forestry Research Institute of Nigeria, Onne* *Dept of Forestry and Wildlife Management, Faculty of Agriculture, University of Port Harcourt*	SIZE AT REPRODUCTIVE MATURITY ONSET IN GARCINIA KOLA (HECKEL)
Micheal Taiwo AYANKOSO Azeez Olanrewaju YUSUF	*Adekunle Ajasin University. Federal University of Agriculture* *Federal University of Agriculture*	IMPACT OF UREA-SULPHUR MIXTURE ADDITIVE IN SWEET POTATO PEEL UTILIZATION ON PERFORMANCE, HAEMATOLOGY AND BLOOD CHEMISTRY OF WEST AFRICAN DWARF SHEEP
Mujahid ALI	*Water Management Research Farm, Renala Khurd, Okara, Pakistan*	GUAVA PRUNING PRACTICES-AN OVERVIEW
John Chiwuzulum Odozi	*Ajayi Crowther University, Oyo Town, Nigeria*	SOURCES OF AGRICULTURAL LABOUR PRODUCTIVITY GAP IN RURAL NIGERIA: A MICRO-LEVEL DECOMPOSITION
LAABAS S. Boukirat D. Chaker H. Berber F.	*University of Ahmed Ben Yahia el Wancharissi, Tissemsilt, Algeria*	EFFECT OF TREATING PEA SEEDS (PISUM SATIVUM) WITH FUNGICIDE ON THE ESTABLISHMENT OF SYMBIOSIS

ONLINE PRESENTATIONS

03.09.2022 / Hall-2 / Session-2

Ankara Local Time

13 00 : 15 30

Meeting ID: 839 6259 8369

Passcode: 123456

HEAD OF SESSION: Muhammad FAISAL

AUTHORS	AFFILIATION	TOPIC TITLE
Lasisi, A. R. Rajeev Nepal Prabesh Bajracharya Vinay Sharma	*Department of Physics, Federal College of Education, Kontagora, Nigeria* *Dixon Science Research Centre, Department of Physics, Morgan State University, Baltimore, MD, USA*	THERMOELECTRIC MEASUREMENT OF 2D Bi2Te3-Ni AND Bi2Te3-Cu THERMOELECTRIC JUNCTION DEVICES
Ephesus Olusoji Fatunmbi	*Department of Mathematics and Statistics, Federal Polytechnic, Ilaro, Nigeria*	FLOW AND HEAT TRANSFER PROPERTIES OF ELECTRICALLY CONDUCTING CARREAU HYBRID NANOFLUID OVER A 3-DIMENSIONAL ROTATING SHEET
Rafindadi Ibrahim Saad	*Department of Computer Science, Federal College of Education, Zaria Kaduna State Nigeria*	THE USE OF MOBILE APPLICATIONS IN TERTIARY INSTITUTION CLASS: A COMPARATIVE PILOT STUDY OF THE STUDENTS' PERCEPTIONS AND REAL USAGE (CASE STUDY: FEDERAL COLLEGE OF EDUCATION, ZARIA)
Muhammad FAISAL	*TOP-TECH Artificial Intelligence Institute, Karachi, Pakistan*	STRENGTH IN MEDICAL CARE FRAMEWORKS: CYBER SECURITY AND COMPUTERIZED CHANGE IN PAKISTAN
Abdessamad Belhaouzi Youssef Halimi Souad Zyade Mohamed Tahiri	*Hassan II Casablanca University*	NUMERICAL STUDY WITH EXPERIMENTAL COMPARISON OF THE THERMOPHYSICAL PROPERTIES OF POLYMER MATRIX POLYMER MATRIX COMPOSITES
Ibrahim Aliyu Jumare Aminu Bala Umar Dr. Mohammed Sani Jaafaru	*Federal University Birnin Kebbi, Kebbi State Nigeria* *Kaduna State University, Kaduna State Nigeria*	ASSESSMENT OF MAGNETIC FIELD FROM POWER LINES FOR ITS ENVIROMENTAL IMPACTS
Tannu Panchal	*Bhagat Phool Singh Mahila Vishwavidhalya*	ARTIFICIAL INTELLIGENCE
Dr. Mu'azu Jibrin Musa Assoc. Prof. Dr. Kabir Ahmad Abubilal Fatima Ashafa Yahaya Otuoze Salihu Man-Yahaya Sani	*Ahmadu Bello University Kaduna Polytechnic, Nigeria, Dept. of Computer Engineering* *Department of Electrical Engineering, Federal Polytechnic Bida, Niger, Nigeria*	DEVELOPMENT OF A SMART ARTIFICIAL INCUBATOR WITH A PETROLEUM LIQUID GAS ALTERNATIVE HEATING SOURCE CONTROL

ONLINE PRESENTATIONS

03.09.2022 / Hall-1 / Session-3

Ankara Local Time

16 00 : 18 30

Meeting ID: 839 6259 8369

Passcode: 123456

HEAD OF SESSION: Felix A. HIMMELSTOSS

AUTHORS	AFFILIATION	TOPIC TITLE
Felix A. HIMMELSTOSS Ferhat N. YAMAN	*University of Applied Sciences, Faculty of Electronic Engineering and Entrepreneurship, Power Electronics, Austria*	BUILDING BLOCK FOR A SPOT WELDER
Amadi Oko Amadi Lawrence Oborkahle Yabesh Toppo Ekikere Umoren Udo Lokesh Ganta	*"Department of Electrical Engineering and Computer Science, Texas A and M University, Kingsville"* *Department of Electrical/Electronic Engineering, Michael Okpara University of Agriculture Umudike* *Department of Chemical Engineering, Texas A and M University, Kingsville USA*	DETERMINATION OF HYDROCARBON PIPELINE TIME OF LEAK USING DISTRIBUTED ACOUSTIC SENSING MODEL
Mohammad Bakhtiary Masoud Shafiei Masoud Riazi Yousef Kazemzadeh	*School of Chemical and Petroleum Engineering Shiraz, University, Shiraz, Iran* *Enhanced Oil Recovery Research Center School of Chemical and Petroleum Engineering Shiraz, University, Shiraz, Iran* *"Department of Petroleum Engineering, Faculty of Petroleum, Gas, and Petrochemical Engineering, Persian Gulf University, Bushehr, Iran"*	HOW CAN ARTIFICIAL INTELLIGENCE INCREASE THE ACCURACY OF PRODUCTION FORECASTING?
Dalila Khalfa Hichem Bouras Oussama Meghlaoui Mounira Djemai	*Annaba University Algeria*	DYSFUNCTIONAL ANALYSIS OF A PRODUCTION SYSTEM BASED ON MOUNTED CARLO SIMULATION
Pushkar Pandey Renu Kundu	*Indian Institute of Technology, Department of Design, India*	UX STUDY ON HANDHELD AUGMENTED REALITY GAMES BY APPLYING SPRADLEY'S NINE DIMENSIONS DESIGN PRINCIPLE
Dr. Menaouer BRAHAMI Dr. Mohammed SABRI Chaya KEDİDİR Fatma DEHBI	*National Polytechnic School of Oran - MA, Systems Engineering Department, Algeria*	SENTIMENT ANALYSIS FOR PRODUCT RECOMMENDATION ON AMAZON'S MOBILE PHONE REVIEWS USING MACHINE LEARNING TECHNIQUES
Dr. Menaouer BRAHAMI Dr. Mohammed SABRI Oussama CHETA Ahlem KHIAR	*National Polytechnic School of Oran - MA, Systems Engineering Department, Algeria*	FEATURE ANALYSIS OF IOT BOTNET ATTACKS USING DEEP LEARNING

ONLINE PRESENTATIONS

03.09.2022 / Hall-2 / Session-3

Ankara Local Time

16 00 : 18 30

Meeting ID: 839 6259 8369

Passcode: 123456

HEAD OF SESSION: Gamze OKYAY

AUTHORS	AFFILIATION	TOPIC TITLE
Gamze OKYAY Münevver ERTEK AVCI Hilal BİLGİÇ	*Malatya Turgut Ozal University*	EFFECT OF PIGMENT COATING ON SOME PERFORMANCE PROPERTIES OF DENIM FABRICS
Dr. Mahamane Chapiou SOULEY GARBA Prof. Dr. Erol KAYA	*Dokuz Eylul University*	COMPARATIVE STUDY OF SLAKED LIME AND TSP ON HEAVY METAL IMMOBILIZATION FROM WASTEWATER
Ramazan Yasin AYYILDIZ Hatice Ahu KAHRAMAN	*Burdur Mehmet Akif Ersoy University*	EFFECT OF OHMIC HEATING ON THE INACTIVATION OF Listeria Monocytogenes IN PROTEIN-ADDED MILK
Merhad Ay Lale Ozbakir	*Erciyes University*	EFFECT OF DIFFERENT DISTANCE METRICS ON CLUSTERING OF GEOGRAPHIC POINTS
Merhad Ay	*Erciyes University*	INTEGRATION OF BIG & STREAMING DATA TECHNOLOGIES AND AN APPLICATION
Manazza Ayub Dr. Mustafa Fincan	*Erciyes University*	INDUCTION OF ENZYMATIC BROWNING IN BANANA PEELS BY PULSED ELECTRIC FIELD

ONLINE PRESENTATIONS

04.09.2022 / Hall-1 / Session-1

Ankara Local Time

10 00 : 12 30

Meeting ID: 839 6259 8369

Passcode: 123456

HEAD OF SESSION: Assoc. Prof. Dr. İbrahim İskender SOYASLAN

AUTHORS	AFFILIATION	TOPIC TITLE
Serhad YILDIZ Zühtü Onur PEHLİVANLI	*Kırıkkale University*	DEVELOPING A BARRIER MECHANISM FOR HAND GRENADE FUZES
Serhad YILDIZ Zühtü Onur PEHLİVANLI	*Kırıkkale University*	POSSIBLE ACCIDENTS RELATED TO MORTAR FUZES DEVELOPMENT OF NEW SAFETY SYSTEMS FOR PREVENTION
Fatih Nedim YORULMAZ Hüyla DURMUŞ	*Manisa Celal Bayar University*	INVESTIGATION OF CAVITATION EROSION RESISTANCE OF 308L COATINGS IN DIFFERENT PRODUCTION PARAMETERS
Necmi YARBAŞI Rıdvan KUL	*Atatürk University*	COMPRESSIVE STRENGTH OF CLAYEY SOILS REINFORCED WITH BAYBURT STONE (BAYBURT TUFFITE)
Assoc. Prof. Dr. İbrahim İskender SOYASLAN	*Burdur Mehmet Akif Ersoy University*	INVESTIGATION OF GEOLOGICAL AND HYDROGEOLOGICAL CHARACTERISTICS OF THE MARBLE QUARRY FIELD OF THE CAVDIR DISTRICT OF BURDUR PROVINCE
Ahmet APAYDIN	*Giresun University*	HOW TO OPERATE, MONITOR AND PROTECT UNDERGROUND DAMS: AN EVALUATION OF TECHNICAL, INSTITUTIONAL AND LEGAL ASPECTS
Ahmet APAYDIN	*Giresun University*	COMPARISON OF UNDERGROUND DAMS WITH SURFACE DAMS IN TERMS OF DAM BODY AND CAPACITY
Burcu Buram ÇOLAK İdil AYÇAM	*Gazi University*	ADAPTIVE ARCHITECTURE AND FUTURE POTENTIALS IN ACCORDANCE WITH CHANGING CLIMATE SCENARIOS
Fulya GÖKŞEN İdil AYÇAM	*Gazi University*	DEVELOPMENT OF SOLAR DECATHLON COMPETITIONS WITHIN THE SCOPE OF SUSTAINABILITY PRINCIPLES
Süleyman Nazif ORHAN Kemal SOLAK	*Erzurum Technical University*	2D FINITE ELEMENT SIMULATION OF ELLIPTIC HOLE AUXETICS

ONLINE PRESENTATIONS

04.09.2022 / Hall-2 / Session-1

Ankara Local Time

10 00 : 12 30

Meeting ID: 839 6259 8369

Passcode: 123456

HEAD OF SESSION: Mokhtar Noori Saddam

AUTHORS	AFFILIATION	TOPIC TITLE
Triumph Temitope AROWOSAFE	*Federal University Of Technology, Akure, Ondo State, Nigeria*	ASSESSMENT OF THE SAFETY AND SECURITY OF COMMERCIAL MOTORCYCLE OPERATION IN AKURE, ONDO STATE, NIGERIA
Opeoluwa Joseph Balogun Ayodeji Samuel Binuyo	*Department of Mechanical Engineering, Obafemi Awolowo University, Nigeria*	HEAT TRANSFER PERFORMANCE OF INTERRUPTED MICROCHANNEL HEAT SINK USING AL2O3-WATER NANOFLUID AND EULERIAN MULTIPHASE TECHNIQUE
Popoola Moshood Abiola	*Federal College of Animal Health and Production Technology, PMB Moor Plantation, Ibadan, Oyo state, Nigeria*	SAFETY ASSESSMENT OF MILKING PRACTICES AMONG SMALLHOLDER DAIRY CATTLE FARMERS IN OYO STATE, NIGERIA
Zakaria HABIBI S. OUKKASS S. MAJID Y. CHAOUQI M. HLAIBI K. TOUAJ	*Laboratoire Génie des Matériaux pour Environnement et Valorisation (GeMEV), Faculté des Sciences Aïn Chock, Université Hassan II, Casablanca, Maroc* *Laboratoire Génie des Matériaux pour Environnement et Valorisation (GeMEV), Faculté des Sciences Aïn Chock, Université Hassan II, Casablanca, Maroc. Laboratoire de Recherche sur les Matériaux Textiles (REMTEX),ESITH Casablanca, Maroc*	AFFINITY POLYMER MEMBRANE CONTAINING TOA AND TOPO AS CARRIERS FOR THE RECOVERY OF NI (II) AND CO(II) FROM WASTE LI-ION BATTERIES
Yosra Raji Meriem Saadouni Issam Mechnou Abdelfattah Elmahbouby Omar Cherkaoui Souad Zyade	*Hassan II University, Casablanca, Morocco* *Laboratory for Research on Textile Materials (REMTEX), Higher School of Textile and Clothing Industries (ESITH), Casablanca, Morocco*	PREPARATION AND CHARACTERIZATION OF A BIO-ADSORBENT FROM Moringa oleifera POD WASTE
Mokhtar Noori Saddam	*University of Thi-Qar, AL-Nasiriyah, Iraq*	STUDY OF DESIGN AND PERFORMANCE OF A HYBRID SOLAR-POWERED SYSTEM IN SUMMER CLIMATE
Rawan Adnan Mokhtar Noori Saddam	*University of Thi-Qar, AL-Nasiriyah, Iraq*	COMPARISON OF EVACUATED TUBE AND FLAT PLATE SOLAR COLLECTOR – A REVIEW
Dr. Mu'azu Jibrin Musa Yahaya Otuoze Salihu Abdullahi Ismail Beli Abubakar Abisetu Oreyemi	*Ahmadu Bello University, Nigeria* *Kaduna Polytechnic, Nigeria* *Kogi State Polytechnic Lokoja, Nigeria*	DEVELOPMENT OF AN IMPROVED SMS OPERATING EGG TRAY TURNING SYSTEM

ONLINE PRESENTATIONS

04.09.2022 / Hall-3 / Session-1

Ankara Local Time

10 00 : 12 30

Meeting ID: 839 6259 8369

Passcode: 123456

HEAD OF SESSION: Shamim Akhter

AUTHORS	AFFILIATION	TOPIC TITLE
Tolulope. O. James	*Department of Mathematics, Kebbi State University of Science and Techonogy, Aliero, Nigeria*	COMPARISON OF STATISTICAL NEURAL NETWORK AND LOGISTIC REGRESSION IN CLASSIFICATION OF CHILD HIV STATUS
I. O. Isah A. Ndanusa M. D. Shehu A. Yusuf	*Department of Mathematics, Federal University of Technology, Minna, Nigeria*	ON PARAMETRIC REACCELERATED OVERRELAXATION (PROR) METHOD FOR LINEAR SYSTEMS
Babayemi, A.W James, Tolulope O Isah, Z.F	*Department of Mathematics, Kebbi State University of Science and Technology, Aliero, Nigeria*	MARKOV CHAIN ANALYSIS OF THE ACADEMIC CAREER PROGRESSION
Mohammed Baba Abdullahi Amiru Sule	*"School of Mathematics and Computing, Department of Mathematics/Statistics Kampala International University, Kampala Uganda"* *Faculty of Science, Department of Mathematical Science, Federal University Gusau*	ANALYSIS AND NUMERICAL SOLUTION OF FRACTIONAL ORDER microRNA IN LUNG CANCER
Asha S. K Gayitri Mali	*Department of Mathematics, Karnatak University, Karnataka, India*	EFFECT OF DOUBLE-DIFFUSIVE STAGNATION POINT FLOW OF EYRING - POWELL NANOFLUID ON A SLENDER STRETCHING SHEET WITH NON-UNIFORM HEAT SOURCE SINK AND INCLINED MAGNETIC FIELD
Zaman V. Safarov	*Azerbaijan State Oil and Industry University, Baku, Azerbaijan*	TWO-WEIGHTED INEQUALITIES FOR GENERALIZED FRACTIONAL INTEGRAL OPERATOR IN GENERALIZED WEIGHTED MORREY SPACES
Shamim Akhter Muhammad Sajjad Ali Khan Wali Khan Mashwani	*Institute of Numerical Sciences, Kohat University of Science & Technology, Pakistan* *Department of Mathematics, Khushal Khan Khattak University, Karak, Pakistan*	FRANK OPERATOR WITH COMPLEX HESITANT FUZZY SETTINGS FOR DEALING WITH MULTIPLE-ATTRIBUTE DECISION-MAKING PROBLEMS

ONLINE PRESENTATIONS

04.09.2022 / Hall-1 / Session-2

Ankara Local Time

13 00 : 15 30

Meeting ID: 839 6259 8369

Passcode: 123456

HEAD OF SESSION: Dr. S. Bhuvaneswari

AUTHORS	AFFILIATION	TOPIC TITLE
Dr. S. Bhuvaneswari Ms. D. Divyasri Ms. Mayuri Dr. N.K. Udaya Prakash	*Department of Botany, Bharathi Women's College (A), Broadway, Chennai, India* *Research and Development, MARINA LABS, Nerkundram, Chennai, India* *Department of Biotechnology, Vels Institute of Science, Technology and Advanced Studies (VISTAS), Pallavaram, Chennai, India*	PHYLLOPLANE MYCOFLORA OF NERIUM OLEIFERA IN A NATIONAL HIGHWAY IN TAMIL NADU, INDIA
Mahendra Kumar Savita Vinay Dwivedi Prachi Srivastava	*Amity University, India* *Dr. APJ Abdul Kalam University* *Amity University, India*	POTENTIAL ANTIBACTERIAL ACTIVITY OF QUERCETIN AGAINST MULTIDRUG-RESISTANT STRAIN AEROMONAS HYDROPHILA
Rabiu Ahmad Abubakar	*The State Key Laboratory of Fluid Power Transmission and Control, Zhejiang University, Hangzhou, China*	NON-ISOTHERMAL MODELING OF 1D SMA SPRING INVOLVING ENTROPY CHANGE OF THE SYSTEM
Rabiu Ahmad Abubakar	*The State Key Laboratory of Fluid Power Transmission and Control, Zhejiang University, Hangzhou, China*	MODELING OF 1D SMA SPRING UNDER CONSTANT TEMPERATURE INVOLVING ENTROPY CHANGE OF THE SYSTEM
Rabiu Ahmad Abubakar	*The State Key Laboratory of Fluid Power Transmission and Control, Zhejiang University, Hangzhou, China*	NON-ISOTHERMAL MODELING OF 1D SMA SPRING USING CHEBYSHEV COLLOCATION METHOD
Ahmad Mohammad Abdullahi Abdu Zuru Chika Muhammad Musa Mu'azu Mohammad Adamu Garga	*Department of Mechanical Engineering, Faculty of Engineering and Environmental Design, Usmanu Danfodiyo University Sokoto, Nigeria* *National Biotechnology Development Agency, Abuja, Nigeria*	COMPARATIVE BIOGAS PRODUCTION MEASUREMENT FOR LABORATORY SCALE EXPERIMENT
Mohammad Imran Eun-Bi Kim Mohammad Shaheer Akhtar Dong-Heui Kwak Sadia Ameen	*Jeonbuk National University, Republic of Korea*	HEAVY METAL IONS DETECTION BY ELECTROCHEMICAL SENSING METHOD WITH LOW TEMPERATURE SYNTHESIZED OF NANOSTRUCTURED MGNIO2 BASED ELECTRODE
Loubna Rachidi Prof. Dr. Ghizlan Kaichouh Prof. Dr. Aicha Guessous	*University Mohammed V*	BIO-ELECTRO FENTON PROCESS FOR TREATMENT OF ANTIDEPRESSANT POLLUTANT: PERFORMANCE ENHANCEMENT

ONLINE PRESENTATIONS

04.09.2022 / Hall-2 / Session-2

Ankara Local Time

13 00 : 15 30

Meeting ID: 839 6259 8369

Passcode: 123456

HEAD OF SESSION: Hande Argunşah

AUTHORS	AFFILIATION	TOPIC TITLE
Sümeyra İBİŞ Erbil ÇETİN	*Ege University*	EXISTENCE OF THE SYMMETRIC SOLUTIONS FOR FOURTH ORDER BOUNDARY VALUE PROBLEMS ON TIME SCALE
Ozan Can Yıldız Burcu Palas Gülin Ersöz	*Ege University*	PHOTOCATALYTIC DEGRADATION OF SULFAMETHAZINE IN THE PRESENCE OF COPPER/PERYLENE DIIMIDE SUPRAMOLECULAR CATALYSTS
Saadet YILDIRIMCAN	*Mersin University*	METAL OXIDE BASED SOLAR CELLS: IMPROVEMENT IN CELL PERFORMANCE
Mert Şener Hicran Beşikci Şeyma Özkan Barış Oğuz Gürses Mutlu Boztepe Aysun Baltacı	*Ege University* *Dokuz Eylül University*	PRELIMINARY RESULTS ON THE ELECTROMAGNETIC ACTUATOR INTEGRATED MAGNETIC PARTICLE IMAGING SYSTEM
Saniye Elvan Öztürk	*Aksaray University*	ASPERGILLUS SPECIES: PATHOGENICITY ON DIFFERENT ORGANISMS, BIOTECHNOLOGICAL USE AND BIODEGRADATION CAPACITY
Hande Argunşah	*Acıbadem Mehmet Ali Aydınlar University*	CHANGES IN POSTURAL CONTROL AND KINEMATIC VARIABLES IN RESPONSE TO ANKLE JOINT TAPING IN PROFESSIONAL BASKETBALL PLAYERS

ONLINE PRESENTATIONS

04.09.2022 / Hall-3 / Session-2

Ankara Local Time

13 00 : 15 30

Meeting ID: 839 6259 8369

Passcode: 123456

HEAD OF SESSION: Assoc. Prof. Dr. Ömer Süha USLU

AUTHORS	AFFILIATION	TOPIC TITLE
Duygu Arıkan Ferruh Yıldız	*Konya Technical University*	INVESTIGATION OF URBAN HEAT ISLAND IN ISTANBUL USING LANDSAT 8 SATELLITE BETWEEN 2018–2021
Mert Çakır Bahar Sancar	*Süleyman Demirel University* *Kocaeli University*	THE ADVANTAGES OF ORNAMENTAL PLANTS FOR ENVIRONMENTAL AND HUMAN HEALTH
Bahar Sancar Mert Çakır	*Kocaeli University* *Süleyman Demirel University*	URBAN SCALE MICRO AGRICULTURE PRACTISES
Osman GEDİK Ömer Süha USLU Elif BOZDAĞ Ali ACAR	*Kahramanmaraş Sütçü İmam University*	DETERMINATION OF THE EFFECT OF DROUGHT STRESS ON GERMINATION AND SEEDLING DEVELOPMENT IN BLACK CUMIN
Osman GEDİK Ömer Süha USLU Orçun ÇINAR	*Kahramanmaraş Sütçü İmam University*	DETERMINATION OF ESSENTIAL OIL COMPONENTS AND PLANT NUTRIENT ELEMENT OF THYMBRA SPICATA SPECIES
Damla Kübra GÜRLENKAYA Levent GÜREL	*Pamukkale University*	THE POTENTIAL OF RAW TURKISH PUMPKIN SEED SHELLS ON DYESTUFF REMOVAL
Assoc. Prof. Dr. Ömer Süha USLU Asst. Prof. Dr. Osman GEDİK Assoc. Prof. Dr. Haroon KHAN	*Kahramanmaraş Sütçü İmam University* *The University of Agriculture, Pakistan*	THE EVALUATION OF THE CLIMATE CHANGE IN TERMS OF PLANT PROTECTION

ONLINE PRESENTATIONS

04.09.2022 / Hall-1 / Session-3

Ankara Local Time

16 00 : 18 30

Meeting ID: 839 6259 8369

Passcode: 123456

HEAD OF SESSION: Aysun BALTACI

AUTHORS	AFFILIATION	TOPIC TITLE
Dilan Deniz İlhan Veysel Bay	*Ege University*	THE ASSOCIATION BETWEEN RUMEN MICROBIOTA AND PRODUCTION PERFORMANCE IN DAIRY CATTLE
Veysel Bay Çağrı Kandemir Turgay Taşkın	*Ege University*	THE GENETICS OF CASEOUS LYMPHADENITIS IN SMALL RUMINANTS
Esra ACAR Ayça GÜLTEN	*Fırat University*	EXAMINATION OF ESKISEHIR ODUNPAZARI HOUSES WITH SPACE SYNTAX
Kenan YİĞİT	*Yildiz Technical University*	ALTERNATIVE TECHNOLOGIES FOR THE USE OF WIND ENERGY ON SHIPS: FLETTNER ROTOR
Begüm RAHMAN Prof. Dr. Aylin M. Deliormanlı Harika ATMACA	*Manisa Celal Bayar University*	INVESTIGATION OF IN VITRO BIOACTIVITY, CYTOTOXICITY AND 5-FLOROURACIL RELEASE BEHAVIOR OF Eu3+, Gd3+ AND Yb3+-DOPED SOL-GEL DERIVED BIOACTIVE GLASS POWDERS
Begüm RAHMAN Prof. Dr. Aylin M. Deliormanlı	*Manisa Celal Bayar University*	PREPARATION OF MESOPOROUS, GADOLINIUM (III) AND YTTERBIUM (III) CONTAINING 13-93 BIOACTIVE GLASS POWDERS BY EISA METHOD AND INVESTIGATION OF THEIR STRUCTURAL PROPERTIES AND IN VITRO BIOACTIVITY
Özge AKBÜLBÜL Aysun BALTACI Barış Oğuz GÜRSES	*Ege University*	A MATHEMATICAL MODEL OF THE EFFECT OF DRAG FORCE CREATED BY BODY FLUIDS ON THE POSITION OF THE MAGNETIC MICROROBOT

ONLINE PRESENTATIONS

04.09.2022 / Hall-2 / Session-3

Ankara Local Time

16 00 : 18 30

Meeting ID: 839 6259 8369

Passcode: 123456

HEAD OF SESSION: Asst. Prof. Samuel Mores G

AUTHORS	AFFILIATION	TOPIC TITLE
Adegbesan Ololade O Ayegbusi Olufunke O Omisande Larence A	*Department of Civil Engineering, The Federal Polytechnic, Ilaro Ogun State Nigeria*	INVESTIGATING THE ENGINEERING CHARACTERISTICS OF ANTHILL SOIL AND LATERITE SOIL
D.S.Pathania Pradeep Kumar	*GNDEC Ludhiana (Punjab) INDIA C T University Ludhiana (Punjab) INDIA*	MECHANICAL AND THERMAL MECHANICAL INTERACTIONS IN A FRACTIONAL ORDER MICROSTRETCH THERMOELASTIC HALF-SPACE
Sandra JURADIN Melina ČOTA Jelena LOVRIĆ VRANKOVIĆ Gabrijela GROZDANIĆ	*University of Split Faculty of Civil Engineering, Architecture and Geodesy, Split, Croatia*	USE OF E-WASTE CABLES AS PART OF AGGREGATE OR FIBERS IN CONCRETE
Asst. Prof. Samuel Mores G Kiran mai Yanamala	*Presidency University, Bangalore, India*	INDIA'S SMART CITIES MISSION AS A MEANS OF ACHIEVING UN NEW URBAN AGENDA 2016: INDIAN PERSPECTIVE POST COVID-19 ANALYSIS
Domingos Brasil da Silva Junior Sávio Torres Melo	*University Center of Piaui, Brazil*	ANALYTICAL AND NUMERICAL STUDY OF REINFORCEMENT IN CIRCULAR AND SQUARE PILLARS OF REINFORCED CONCRETE BRIDGES
João Leite Barbosa de Carvalho Filho Sávio Torres Melo	*University Center of Piaui, Brazil*	THE USE OF ELECTRIC VEHICLES IN THE CURRENT ENVIRONMENTAL SCENARIO
R. Sherwani W. Abdul Aqsa Qalb Syed H. Arshad Saima Gulzar	*National University of Science and Technology, Islamabad, Pakistan University of Management and Technology, C II, Johar Town, Lahore.*	IMPACTS OF URBAN FORM AND SOCIOECONOMIC ELEMENTS ON DOMESTIC ELECTRICITY CONSUMPTION WITH RESPECT TO ITS IMPACTS ON LAND SURFACE TEMPERATURE (LST) AND CLIMATE CHANGE IN PAKISTAN
Vəfa Vəliyeva	*Democratic Youth Public Union, Baku, Azerbaijan*	MODERN RECONSTRUCTION OF THE CITY OF SHUSHA AND INNOVATIVE PROPOSALS

ONLINE PRESENTATIONS

04.09.2022 / Hall-3 / Session-3

Ankara Local Time

16 00 : 18 30

Meeting ID: 839 6259 8369

Passcode: 123456

HEAD OF SESSION: Assoc. Prof. Dr. V. Thiyagarajan

AUTHORS	AFFILIATION	TOPIC TITLE
L.B. Umiraliyeva M.S. Amangeldin S.F. Kolosova A.T. Ibraikhan	*Kazakh Research Institute of Processing and Food Industry, Kazakhstan* *Sarsen Amanzholov East Kazakhstan University*	ANALYSIS OF PATENT INFORMATION SEARCH BASED ON ROYAL JELLY
Assoc. Prof. Dr. Haroon KHAN Assoc. Prof. Dr. Ömer Süha USLU Asst. Prof. Dr. Osman GEDİK	*The University of Agriculture, Pakistan* *Kahramanmaraş Sütçü İmam University, Turkey*	FOOD SECURITY AND BIODIVERSITY SUSTAINABILITY IN A CHANGING CLIMATIC SCENARIO IN PAKISTAN
Amitrajeet A. BATABYAL Karima KOURTIT Peter NIJKAMP	*Arthur J. Gosnell Professor of Economics, Rochester Institute of Technology, USA* *Open University, Heerlen, The Netherlands*	CLIMATE CHANGE AND RIVER WATER POLLUTION: AN APPLICATION TO THE GANGES IN KANPUR
Hassan Bouhsiss A. En-Naji A. Wahid Abdekarim Kartouni Mohamed El Ghorba	*Hassan II University of Casablanca, Sidi Othman, Casablanca, Morocco*	THE DAMAGE MECHANISMS OF ACRYLONITRILE BUTADIENE STYRENE
Seyedeh Golaleh Hosseini Prof. Kourosh Shahriar Dr. Mohammad Amin Karbala	*Amirkabir University, Iran*	CALCULATING THE AMOUNT OF WATER LEAKAGE INTO THE OPEN PIT MINE USING A DISCRETE FRACTURE NETWORK AND NUMERICAL SIMULATION AND WAYS TO CONTROL IT WITH A DRY PLAN FOR IT
Mokrane Salwa El azzouzi Rachid	*Sultan Moulay Slimane University, Morocco* *Agronomic and Veterinary Institute Hassan II – IAV, Morocco*	COMPARATIVE STUDY BETWEEN GNSS AND LASERGRAMMETRY
Assoc. Prof. Dr. V. Thiyagarajan	*Sri Sivasubramaniya Nadar College of Engineering, INDIA*	DESIGN AND ANALYSIS OF ADVANCED SPEED CONTROL METHODS FOR PLC AND HMI BASED INDUCTION MOTOR DRIVE

CONTENT

URETHANE ACRYLATE AND SILICON ACRYLATE CONTAINING NOVEL EPOXY ACRYLATE SYSTEMS FOR SLA 3D PRINTERS

Mustafa ÇAKIR

Doç. Dr., Marmara Üniversitesi, Teknoloji Fakültesi, Metalurji ve Malzeme Mühendisliği, Maltepe, İstanbul.

ORCID NO: 0000-0002-9409-2684

Emre AKIN

Arş. Gör. Dr., Marmara Üniversitesi, Teknoloji Fakültesi, Metalurji ve Malzeme Mühendisliği, Maltepe, İstanbul.

ORCID NO: 0000-0003-2067-1488

Boran BERBEROĞLU

ABSTRACT

As well known, epoxy acrylate resins have been widely used in 3D SLA printer applications. Epoxy acrylate systems have generally consisted of bisphenol-A glycerolate diacrylate (epoxy acrylate resin) and 1,6-Hexanediol diacrylate (HDDA, reactive diluent resin) in various weight percents. The purpose of this study is to develop novel epoxy acrylate systems without HDDA and investigate their properties. For this reason, two different reactive resins were used instead of HDDA in epoxy acrylate systems with various weight percents. One of these resins was urethane acrylate resin that was synthesized in our laboratory. Urethane acrylate resin was synthesized using monomeric aliphatic diisocyanate (commercial name; Desmodur H) and 2-Hydroxymethyl methacrylate (HEMA). The other reactive resin was mixture of silicone acrylate and photoinitiator (commercial name; TEGO RC 1002). These resins were added into epoxy acrylate resin in various weight percent such as 20%, 40%, 60% and 80%. Tensile, izod impact, shore-D hardness, taber abrasive, density and DSC tests were applied to these produced samples. Considering of the results, urethane acrylate containing epoxy acrylate system exhibited much more improved results compared to pure epoxy acrylate system and silicon acrylate containing epoxy acrylate systems. It also exhibited more enhanced properties than epoxy acrylate systems with HDDA. It exhibited substantial increases in terms of tensile strength, modulus and izod impact resistance. Moreover, they presented more enhanced abrasive resistance. Shore-D hardness values and densities showed almost no change. This synthesized urethane acrylate reactive resin can be used in applications that required higher mechanical and abrasive properties for epoxy acrylate systems of 3D SLA printers.

Keywords: SLA 3D Printer, epoxy acrylate systems, monomeric aliphatic diisocyanate (Desmodur H), 2-Hydroxyethyl methacrylate (HEMA), silicone acrylate (TEGO RC 1002)

INTRODUCTION

Currently, ultraviolet (UV)-curable products have received great interest due to both technological advances and the increasing environmental pressure to decrease the emission of volatile organic compounds (VOC) (Aerykssen and Khudyakov, 2011). In comparison with conventional solvent-based products, UV-curable products present the advantage of low VOC emission, rapid curing at ambient temperature, low energy consumption, high productivity and high degrees of cross-linking (cause to outstanding scratch, chemical resistance). Therefore, these products provide a wide range of economic and ecological benefits. UV-curable coatings usually contain four main components (Chemtob, Versace, Belon, Céline and Rigolet, 2008). the oligomer, the reactive diluent, the photoinitiator and various additives. Epoxy acrylate (EA) is a common

oligomer in UV-curable coatings, which is the most principal component for film formation (Çakir, Akin, Ulak, 2018). There have been two kinds of epoxy acrylate oligomers that have been widely used. These are bisphenol diglycidyl ether and epoxy novolac based epoxy acrylate oligomers. As reactive diluents, hexanediol diacrylate (HDDA) and tripropylene glycol diacrylate (TPGDA) have been generally used in epoxy acrylate systems. These reactive dilents dissolve and adjust the viscosity and crosslinking density of epoxy acrylate systems (Yildiz and Usta, 2018).

In this study, novel reactive diluents were used such as urethane acrylate and silicon acrylate instead of common aliphatic reactive diluents such as hexanediol diacrylate (HDDA) and tripropylene glycol diacrylate (TPGDA). Urethane acrylate was synthesized using aliphatic diisocyanate monomer (Desmodur-H) and 2-Hydroxymethyl methacrylate (HEMA). Therefore a novel aliphatic groups containing urethane acrylate reactive diluent was synthesized. The other used reactive diluent was silicon acrylate that has been exists as commerical product. Commerical name is Tego RC 1002 and this products contains photoinitiator (Tego A 18). Silicon acrylate has high thermal resistance due to the bonds of Si-O-Si. By using these novel reactive diluents novel epoxy acrylate systems were obtained. The properties of these novel systems were investigated. Tensile, izod impact, shore-D hardness, taber abrasive, density and DSC tests were applied to the produced samples. The novel epoxy acrylate system with urethane acrylate outshined in terms of tensile strength, modulus and izod impact resistance. Moreover, it presented more enhanced taber abrasive resistance.

EXPERIMENTAL

Materials

Bisphenol A glicerolate diacrylate (Bisphenol A based epoxy acrylate oligomer) was purchased from Sigma-Aldrich. Desmodur-H was used as aliphatic monomeric diisocyanate that purchased from Covestro, 2-Hydroxymethyl methacrylate (HEMA) was used to acrylate and terminate Desmodur H. Tego RC 1002 was used silicon acrylate that purchased from Evonik. Irgacure 819 was used as photoinitiator. Dibutyltin dilaurate (T12) was used as catalyst for urethane acrylate synthesis. Tetrahidrofuran (THF) was used to synthesis urethane acrylate as solvent.

Synthesis of urethane acrylate diluent resin

HEMA was added in a flask and THF was poured onto the diol. HEMA in THF were magnetically stirred. After that the diisocyanate (Desmodur-H) was added drop by drop into the flask. Then, the tin catalyst (T12) was added and stirred magnetically at 60 ºC in a nitrogen atmosphere for two hours. The diisocyanate was terminated with HEMA. The mole ratio was adjusted stochiometrically. Therefore urethane acrylate resin was obtained. The weight ratio of THF/solid in solution was ½. The flowchart of urethane acrylate synthesis was given in Figure 1.

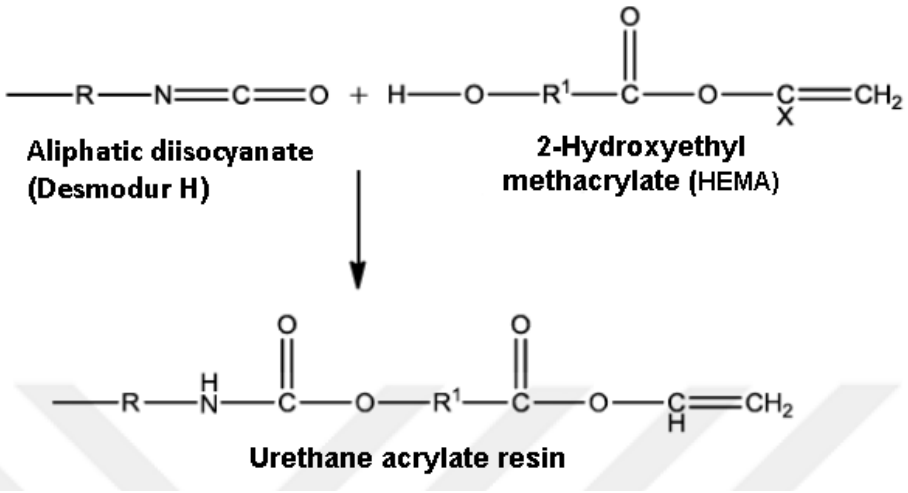

Figure 1. The flowchart of urethane acrylate synthesis

Measurements

Measurements were carried out for film and coating samples. Coating samples were used to characterize abrasion resistance. Film samples were used for the other tests. Fourier transform infrared spectroscopies (FT-IR) were conducted by Shimadzu 8303 FT-IR Spectrometer. Differential scanning calorimetry (DSC) is a thermoanalytical technique used to study thermal properties of the polymer temperature of a sample and reference is measured as a function of temperature. The samples were tested up to 150oC at a heating rate of 10oC/min. The samples were characterized mechanically by standard tensile test in order to determine in terms of tensile strength, failure strain and young modulus according to ASTM D638. Tensile test was carried out by using a crosshead speed of 5 mm/min. Izod impact resistance was measured using unnotched samples according to ASTM D 4812-99 (ASTM D 256) using Zwick B5113.30 with hammer of 5.4J at a striking rate of 3.96 m/s. For each sample, at least three for each sample, at least three measurements were taken, and the average value was used for the calculations. Hardness of the samples were measured according to Shore D. Coating samples were also produced besides film samples for abrasion test. Taber abrasion test were applied to the produced coating samples. Density was measured according to archimed principle for film samples.

RESULTS AND DISCUSSION

The FT-IR spectra of urethane acrylate is given in Figures 2. The absorption bands at 3000-3300, 1730 and 810 cm^{-1} relate to –NH stretching, C=O stretching and C=C twisting of acrylate, respectively. From the IR spectra, the disappearance of the characteristic absorption band at 2270 cm^{-1} related to isocyanate group (-NCO) indicates the completion of the reaction (Bayramoglu, Kahraman, Kayaman-Apohan and Güngör, 2006). These results confirmed the synthesizing of the urethane acrylate successfully.

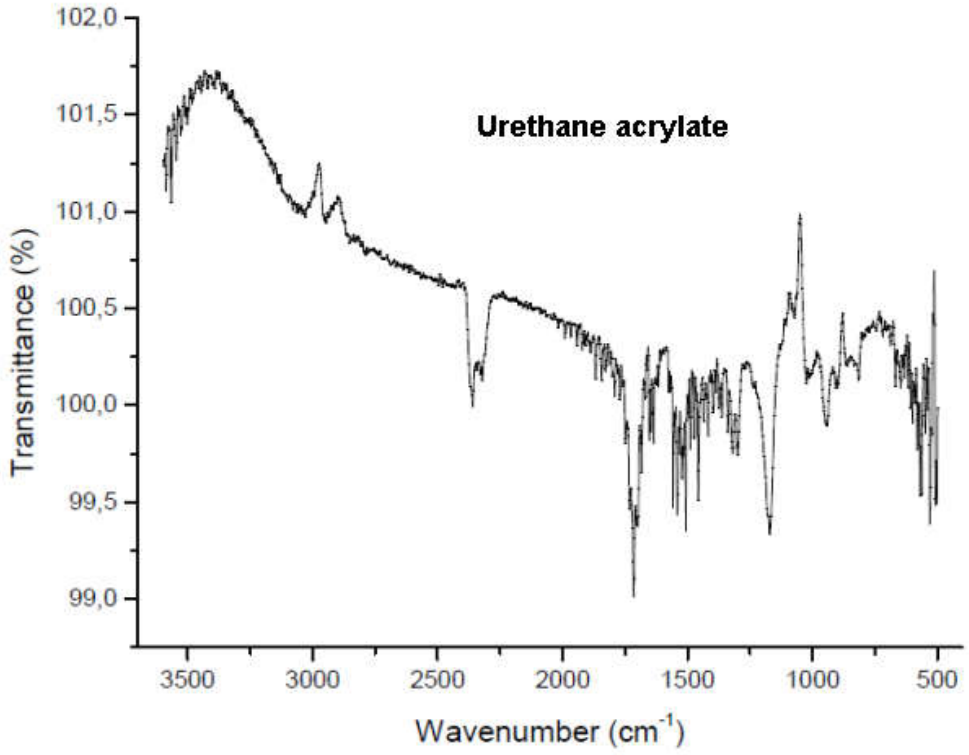

Figure 2. FT-IR spectrum of urethane acrylate

Main structure of epoxy acrylate system in this study was bisphenol A diglycidyl ether based epoxy acrylate as shown in Figure 3.

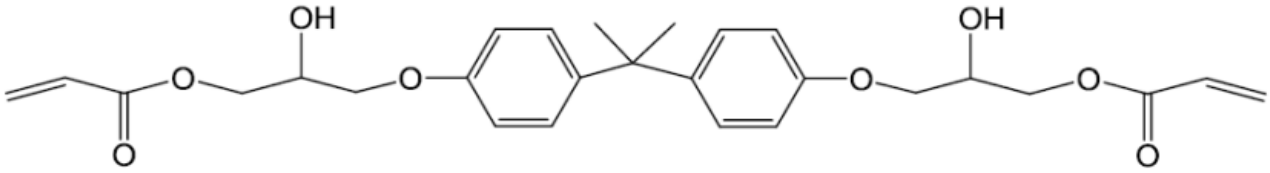

Figure 3. Bisphenol A glicerolate diacrylate

Two types reactive diluent crosslinking agents were used in this study such as silicon acrylate (commercial) and urethane acrylate (synthesized). Commercial silicon acrylate structure was shown in Figure 4.

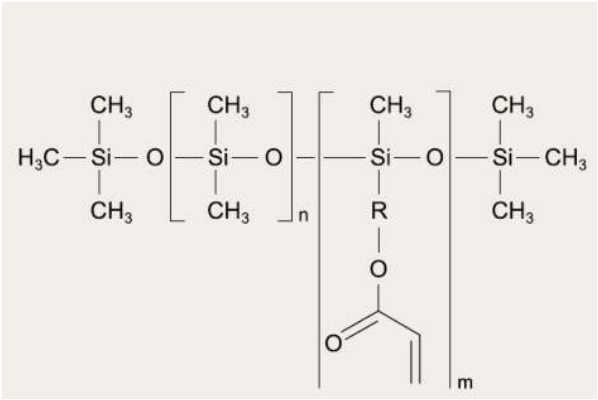

Figure 4. The structure of silicone acrylate

Mechanical tests were performed to determine the overall effect of urethane acrylate and silicon acrylate samples on the performance of epoxy acrylate. Mechanical properties of urethane acrylate samples showed that ultimate tensile strength increased up to 60% wt while impact resistance increased. Silicon acrylate samples exhibited continuous decrease up to 100% wt due to the incorporation of soft segment structure of silicon acrylate in epoxy acrylate system.

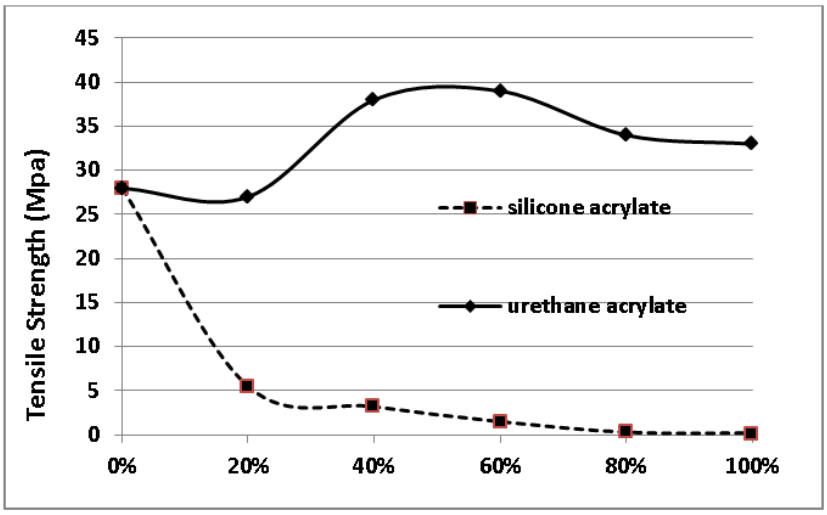

Figure 5. Tensile strength values of urethane acrylate and silicon acrylate samples

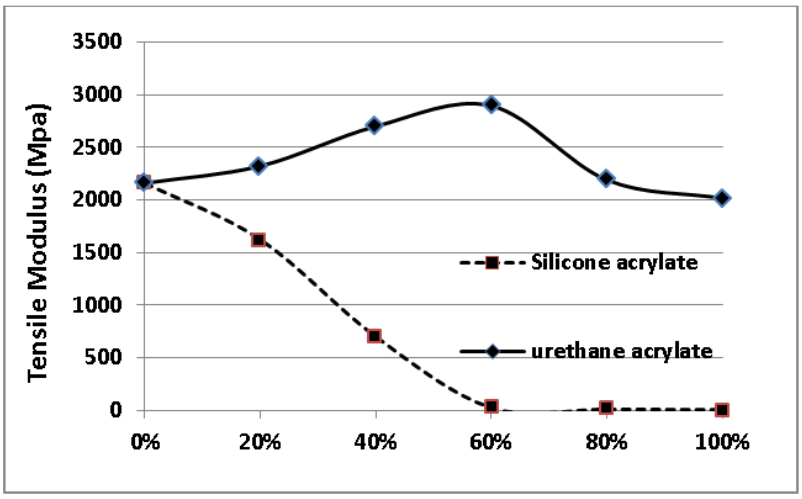

Figure 6. Tensile modulus values of urethane acrylate and silicon acrylate samples

Soft silicon acrylate groups and higher molecular weight of silicon acrylate groups decreased mechanical properties. However, these groups increase impact resistance of polymers.

Table 1. Mechanical properties of urethane acrylate samples

Uretane acrylate samples	Tensile Modulus (MPa)	Tensile Strength (MPa)	Izod Impact (kj/m^2)
%0	2160	28	6
%20	2323	27	21
%40	2700	38	22
%60	2895	39	20
%80	2190	34	18
%100	2016	33	17

In this study, silicon acrylate group was used as crosslinking agent. It decreased tensile modulus and strength so much and izod impact resistance test could not carry out for silicon acrylate samples. Figure 5 presents the relation of weight increase of silicon acrylate and urethane acrylate samples and tensile strength.

Table 2. Mechanical properties of silicon acrylate samples

Silicon acrylate samples	Tensile Modulus (MPa)	Tensile Strength (MPa)	Izod Impact (kj/m^2)
%0	2160	28	6
%20	1623	5.5	-
%40	699	3.2	-
%60	23	1.5	-
%80	9	0.3	-
%100	5	0.2	-

Similar trend was also observed for tensile modulus values in Figure 6. Table 1 and Table 2 give tensile strength, tensile modulus and izod impact resistance values.

Table 3. Density, taber abrasive resistance and hardness of urethane acrylate samples

Urethane acrylate samples	Density (g/cm^3)	Taber abrasive resistance	Shore D hardness
%0	1.2478	0.0016	67
%20	1.2507	0.0014	67.4
%40	1.2480	0.001	69
%60	1.24	0.0008	69
%80	1.2370	0.0009	68.6
%100	1.2360	0.0010	67

Neat epoxy acrylate presented a tensile strength of 28 MPa, which increased to 24.9 MPa (39% decrease, at 60 % wt.) by the addition of urethane acrylate within the range of 0 % wt. to 100 % wt. Tensile modulus of neat epoxy acrylate also exhibited a tensile modulus of 2160 MPa, which increased 2895 MPa (34% decrease, at 60 % wt.) by the addition of urethane acrylate. Izod impact resistance of urethane acrylate samples exhibited its highest value at 40 % wt but the value at 60 % wt. is substantially high.

Table 4. Density, taber abrasive resistance and hardness of silicone acrylate samples

Silicone acrylate samples	Density (g/cm^3)	Taber abrasive resistance	Shore A hardness
%0	1.2478	0,0016	-
%20	1.2460	0,0014	78
%40	1.24	0,0013	70
%60	1.2356	-	40
%80	1.2321	-	35
%100	1.2307	-	26

For this reason the urethane acrylate sample of 60 % wt became prominent among all samples. On the other hand, silicon acrylate samples exhibited opposite situation according to the trend of urethane acrylate samples. This situation could be derived from its higher molecular structure and the chemical structure of silicon oligomer. Urethane acrylate reactive group is at monomeric level and it can be crosslinked with epoxy acrylate at very higher amount. This situation can also affect on mechanical properties of epoxy acrylate systems.

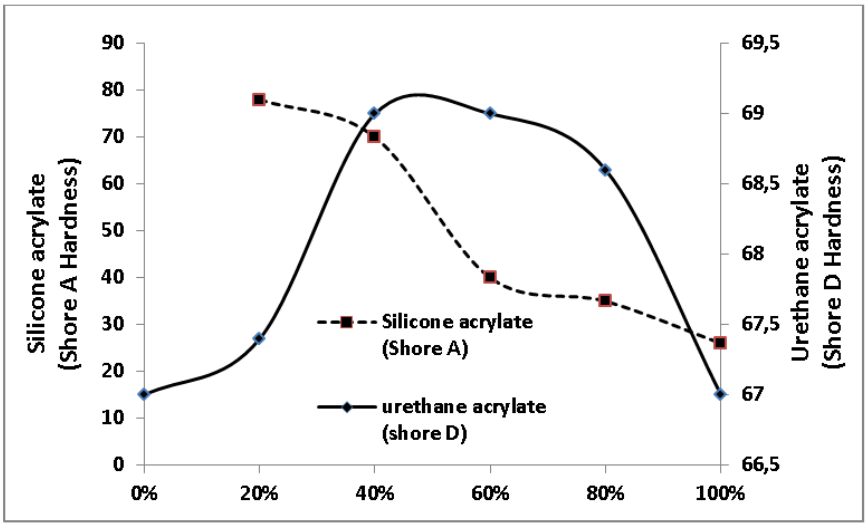

Figure 7. Hardness values of urethane acrylate and silicon acrylate samples

Densities of urethane acrylate and silicon acrylate samples presented very close values and similar trend. Taber abrasive resistance values exhibited similar trend up to 40 % wt.

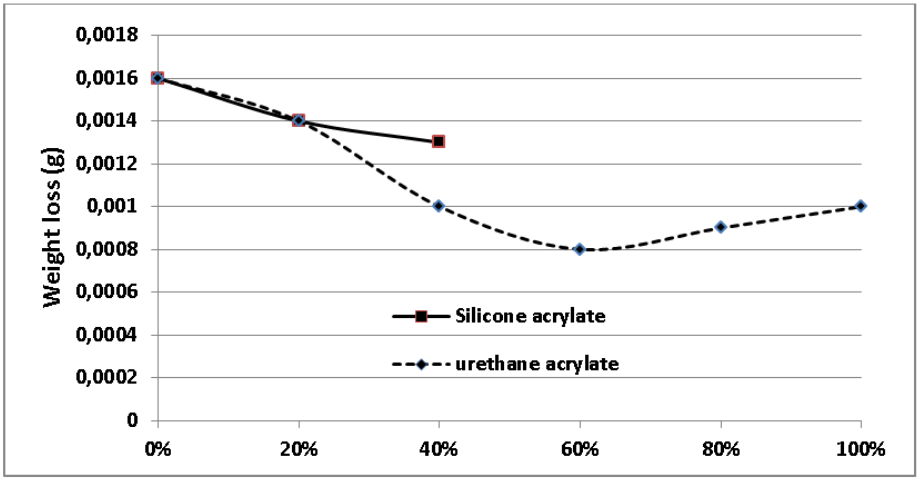

Figure 8. Taber abrasive values of urethane acrylate and silicon acrylate samples

However, silicon acrylate samples at higher than 40 % wt. could not be tested due to their very soft structure. Urethane acrylate sample of 40 % wt also has higher taber abrasive resistance than the silicon acrylate of 40 % wt. Moreover, hardness values of silicon acrylate samples were measured by Shore A method due to its very low hardness values. The hardness values of urethane acrylate samples were much more silicon acrylate samples.

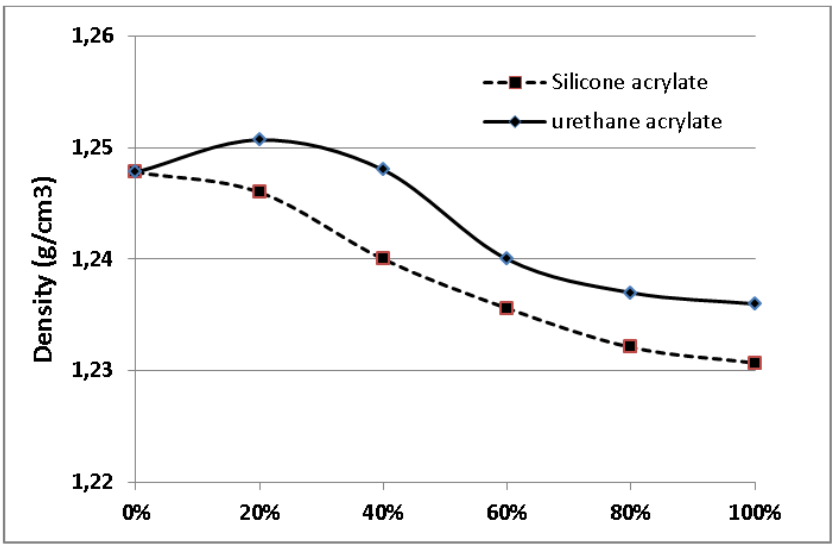

Figure 9. Density values of urethane acrylate and silicon acrylate samples

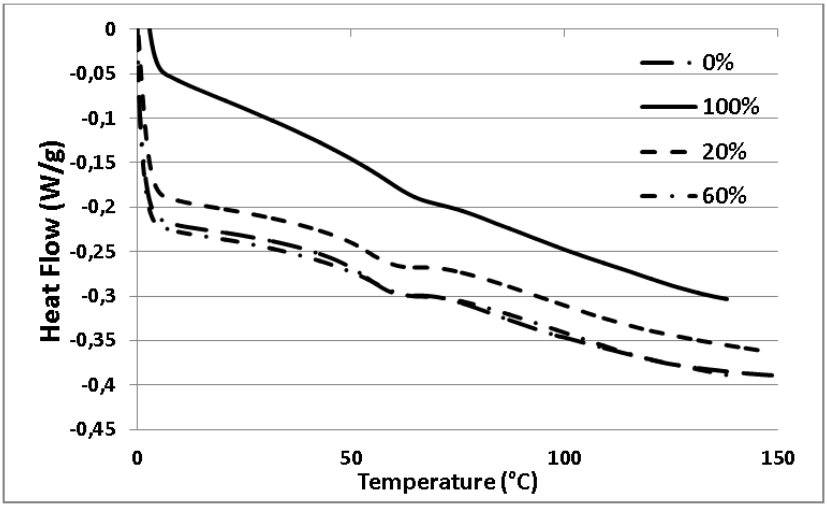

Figure 10. DSC curves of urethane acrylate samples

The thermal analyses of the samples were conducted by DSC. The amount of urethane acrylate in epoxy acrylate system increased glass transition temperature (Tg) little. However, the glass transition temperature of silicon acrylate samples decreased little.

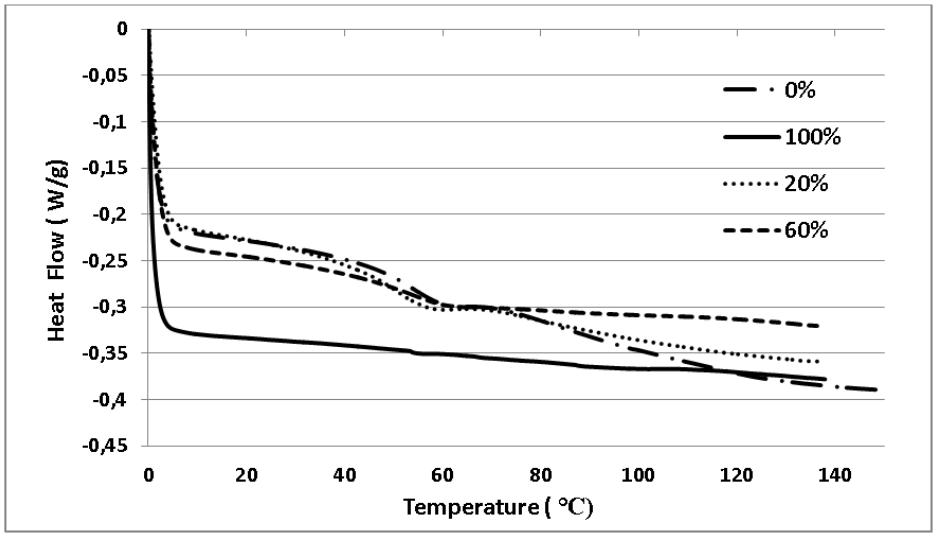

Figure 11. DSC curves of silicon acrylate samples

While urethane acrylate sample of 100% showed 65 °C Tg, pure epoxy acrylate showed 60 °C of Tg. Silicon acrylate sample of 100% also showed distinct curve. Figure 10 and Figure 11 showed glass transition temperatures of samples separately.

CONCLUSION

In this study, novel epoxy acrylate systems were developed without HDDA and investigate their properties. For this reason, two different reactive resins were used instead of HDDA in epoxy acrylate systems with various weight percents. One of these resins was urethane acrylate resin that was synthesized in our laboratory. Urethane acrylate resin was synthesized using monomeric aliphatic diisocyanate (commercial name; Desmodur H) and 2-Hydroxymethyl methacrylate (HEMA). The other reactive resin was mixture of

silicone acrylate and photoinitiator (commercial name; TEGO RC 1002). These resins were added into epoxy acrylate resin in various weight percent such as 20%, 40%, 60% and 80%. Tensile, izod impact, shore-D hardness, taber abrasive, density and DSC tests were applied to these produced samples. Considering of the results, urethane acrylate containing epoxy acrylate system exhibited much more improved results compared to pure epoxy acrylate system and silicon acrylate containing epoxy acrylate systems. It also exhibited more enhanced properties than epoxy acrylate systems with HDDA. It exhibited substantial increases in terms of tensile strength, modulus and izod impact resistance. Moreover, they presented more enhanced abrasive resistance. Shore-D hardness values and densities showed almost no change. This synthesized urethane acrylate reactive resin can be used in applications that required higher mechanical and abrasive properties for epoxy acrylate systems of 3D SLA printers.

REFERENCES

Aerykssen J.H. & Khudyakov IV. New acrylated oligomers with a sulfide group for radiation-curable coatings. Ind Eng Chem Res., 9, 50:1523, 2011.

Bayramoglu G., Kahraman M.V, Kayaman-Apohan N. & Güngör A. Synthesis and characterization of UV-curable dual hybrid oligomers based on epoxy acrylate containing pendant alkoxysilane groups, Progress in Organic Coatings, 2006.

Chemtob A., Versace D.L., Belon C., Céline C.B. & Rigolet S. Concomitant organic-inorganic UV-curing catalyzed by photoacids. Macromolecules, 41:7390, 8, 2008.

Çakir, M., Akin, E. & Ulak, P. Properties of UV-Curable bisphenol-A glycerolate diacrylate coatings containing 1H,1H,2H,2H-perfluorodecyl acrylate monomer. El-Cezerî Journal of Science and Engineering, 5, 3, 836-844, 2018.

Yıldiz Z. & Usta İ. Synthesis and characterization of dual-curable epoxyacrylates for polyester cord/rubber applications, Journal of Industrial Textiles, 46(2), 2018.

İZMİR İLİ İÇİN FOTOVOLTAİK MODÜLLERİN OPTİMUM EĞİM AÇILARI HESABI

CALCULATING OPTIMUM TILT ANGLES OF PHOTOVOLTAIC MODULES FOR IZMIR PROVINCE

Yavuz Bahadır Şahin[1], Seydi Vakkas Şahin[2], Sinan Zengin[3]*

[1-2-3]Ege Üniversitesi Elektrik Elektronik Mühendisliği Bölümü

[1-2-3]Ege University Electrical and Electronics Engineering Department

[3*]ORCID ID: 0000-0002-7357-4836

ÖZET

Elektrik enerjisi hayat standartlarını yükselten, ekonomik ve sosyal ilerlemeyi sağlayan en önemli enerji kaynaklarından birisidir. Elektrik enerjisinin kullanılmaya başladığı ilk zamanlarda genellikle fosil yakıtlardan enerji üretilmiştir. Fakat fosil yakıtların çevreye zararlı etkileri ve yakın gelecekte tükenecek olmalarından dolayı yenilenebilir enerji kaynaklarına talep son zamanlarda artmıştır. Yenilenebilir enerji kaynakları içerisinde güneş enerjisi sonsuz bir enerji kaynağı durumundadır ve diğer alternatif enerji kaynaklarının da temelini oluşturmaktadır. Ayrıca güneş enerjisi, dünyanın pek çok lokasyonunda kullanılabilmekte ve bakım maliyetleri de nispeten düşüktür. Bu nedenlerden dolayı güneş enerjisinin kullanımı diğer yenilenebilir enerji kaynaklarına göre avantajlı hale gelmektedir.

Güneş enerjisinden elektrik üretmek için fotovoltaik modüller kullanılmaktadır. Bu modüller, sabit eğim açılı mekanik sistemler ya da güneş takip sistemleri ile birlikte montaj edilir. Sabit sistemler, yataya göre belirlinen sabit bir eğim açısında konumlandırılır. Bu eğim açısının optimum değeri, güneş ışığından elde edilen enerji miktarını maksimize etmek için hesaplanmaktadır. Optimum açı değeri ise coğrafik konumuna göre değişmektedir. Sabit konumlandırılan bu sistemlerin kurulum maliyeti güneş takip sistemlerine göre çok daha düşüktür.

Bu çalışmada bir yıl boyunca yatay düzleme gelen saatlik güneş ışınım verileri kullanılarak; İzmir ili ve ilçeleri için gelen global ışınım büyüklüğünün bileşenlerine ayrılması, eğik düzleme gelen ışınım miktarı ve yanı sıra sabit açılı sehpalar için optimum açı bilgisi hesaplanıp, ara yüz programı vasıtası ile kullanıcının bilgisine sunulmuştur. Bu hesaplama yapılırken öncelikle İzmir iline ait atmosfer dışından gelen ışınım ve global ışınım verileri alınmıştır. Bu veriler sayesinde açıklık indeksi değerleri elde edilmiştir. Daha sonra İzmir'e gelen global ışınım değerleri direkt ışınım ve difüz ışınım olmak üzere bileşenlerine ayrılmıştır. Eğik düzleme gelen ışınım değerlerinin ayrıştırılmasında yatay düzlem için bulunan direkt ve difüz ışınım değerleri kullanılarak direkt ışınım, difüz ışınım ve bunların yanında yansıyan ışınım da hesaplanmıştır. Yansıyan ışınımın bulunmasında yüzey yansıtma katsayısı sonbahardaki orman yüzeyi katsayısı olan 0.26 olarak alınmıştır Son olarak bir yıl için alınan bu veriler yardımı ile eğim açısı 0˚ ve 90˚ arasında değiştirilmiştir. Buna göre İzmir ve çevresi için hasat edilen yıllık toplam enerjiyi maksimize eden optimum eğim açısı değeri yaklaşık 32˚ olarak hesaplanmıştır. Gelecek çalışmalarda yıllık veriler yerine mevsimsel veriler kullanılarak tüm Türkiye bölgesi için optimum mevsimsel eğim açılarının hesaplanması planlanmaktadır.

Anahtar Kelimeler: Güneş enerjisi, Fotovoltaik Modül, optimum eğim açısı.

ABSTRACT

The electrical energy is one of the most important source which increases the life standards, and progress of social and economic status. In the beginning of industrilization, electrical energy was generally produced from fossil fuels. However, due to the harmful effects of fossil fuels on the environment and the prediction of their depletion in the near future, the demand for renewable energy sources has increased recently. Among

the renewable energy sources, solar energy is an abundance source of energy and forms the basis of other renewable energy sources. In addition, solar energy can be used in many locations around the world and maintenance costs are relatively low. For these reasons, the use of solar energy becomes advantageous compared to other renewable energy sources.

Photovoltaic (PV) modules are used to generate electricity from solar energy. PV modules are mounted with fixed tilt angle mechanical systems or solar tracking systems. Fixed systems are positioned at a fixed angle of inclination relative to the horizontal. The optimum value of this tilt angle is calculated to maximize the amount of energy obtained from sun. The optimum angle value varies according to PV module's geographical location. On the other hand, the installation cost of fixed angle systems is much lower than solar tracking systems.

In this study, using hourly solar radiation data on the horizontal plane for a year; the division of the incoming global radiation magnitude into its components, the amount of radiation incident on the inclined plane, the optimum angle information for fixed angle systems are calculated and presented to the user through the interface program for the province and districts of Izmir. First of all, radiation coming from outside the atmosphere and global radiation data of Izmir province were taken. By using these data, clearness index values were obtained. Then, the global radiation values coming to Izmir are divided into its components as direct radiation and diffuse radiation. Direct radiation, diffuse radiation and reflected radiation were calculated by using the direct and diffuse radiation values found for the horizontal plane in the decomposition of the radiation values coming to the inclined plane. In finding the reflected radiation, the surface reflection coefficient was taken as 0.26, which is the forest surface coefficient in autumn. Finally, with the help of these data for one year, the angle of inclination was changed between 0˚ and 90˚. As a result, optimum tilt angle was calculated as 32˚ for Izmir province which maximize the annual total harvested energy value. In future studies, it is planned to calculate the optimum seasonal tilt angles for the whole of Turkey region by using seasonal data instead of the annual data.

Keywords: Solar energy, Photovoltaic modules, optimum tilt angle.

CLASSIFYING CARDIAC SPECT DATA USING MACHINE LEARNING METHODS AND FEATURE SELECTION

Bengi KANAT COŞKUN

Dr., Manisa Science and Art Center

Şehzadeler, Manisa.

ORCID NO: 0000-0002-7645-8136

Onur SEVLİ

Dr. Öğretim Üyesi, Burdur Mehmet Akif Ersoy University Faculty of Engineering and Architecture, Department of Computer Engineering, Burdur

ORCID NO: 0000-0002-8933-8395

ABSTRACT

Circulatory system has a vital importance in human life. Heart is the main organ of circulatory system and it pumps blood through the vessels to the organs and tissues. Blood, oxygen and other necessary materials are transported to different organs by heart or totaly circulatory system. Even one glitch in this sytem, will affect all human life. Cardiovascular or heart disease is one of that glitches, which includes coronary artery disease (CAD), coronary heart disease (CHD) and so on. The number of deaths due to cardiovascular diseases is 17.5 million and it is the 30% of all deaths every year. According to the study of Turkish Society of Cardiology, it is reported that the main reason of death, under the 70 year old people, is cardiovascular diseases with %37. Early detection is the main resort to prevent these cases. During the detection and treatment precess some imaging techniques like SPECT, EKG are used. SPECT (Single Photon Emission Computerized Tomography) is a widely used technique to evaluate the presence of many diseases and the degree of the deseasee progression. Thousands of SPECT images data is collected every day and scientists are studying on new methods to interpret these image data to ensure early detection systems by using machine learning methods. Some features of the data sets are rebundant and irrelevant and this affets the efficiency of the method that includes accuracy and speed. Hence, feature selection in other words variable elemination is needed to be used in some domains. Feature selection is one of the intelligent optimization methods and is used in data preprecessing to achieve efficient variable elimination. Pre-processing of the domains is used for the reduction of the size of the domain and for fitting the machine learning method to the domain. In this study, we present the results of some feature selection methods that applied to SPECT Heart Data Set. The dataset is a heart dataset consisting of inputs obtained by SPECT imaging. It consists of 267 SPECT images. Each image sample has 23 digitized features. We used Genetic Algorithm (GA), Binary Bat Algorithm (BBA), and Harmony Search (HS) Algorithm as feature selection methods with the combination of the classification method, Support Vector Machine (SVM). These hybrid methods provide %85, %83 and, %81 accuracies respectively.

Keywords: Cardiac Spect Data, Feature Selection, Machine Learning

1. INTRODUCTION

Today, while the world evolves in a positive direction with the development of industry and technology, it also goes in a negative direction due to reasons such as decrease in clean air, depletion of clean water resources and rapid urbanization. These negativities are most evident in human health. Especially heart is the most affected organ in this situation. According to the study of Turkish Society of Cardiology, it is reported that the main reason of death, under the 70 year old people, is cardiovascular diseases with %37 (Figure 1)

(Türkiye Kalp ve Damar Hastalıkları Önleme ve Kontrol Programı Raporu, 2022). Circulatory system is the most important system in a body. It includes blood, blood vessels and heart which is the vital organ in a body. Blood, oxygen and other necessary materials are transported to different organs by heart. There can be some hitches in circulatory system or cardiovascular system which cause cardiovasculaer diseaes (CVD) or heart diseases. Coronary artery disease (CAD), coronary heart disease (CHD) are the examples of these diseases. Like all other fatal diseases, early diagnosis is very important for cardiovascular diseases and besides genetic factors, it can be due to reasons such as tobacco and alcohol use, insufficient physical activity, unhealthy diet, obesity, as well as genetic factors.

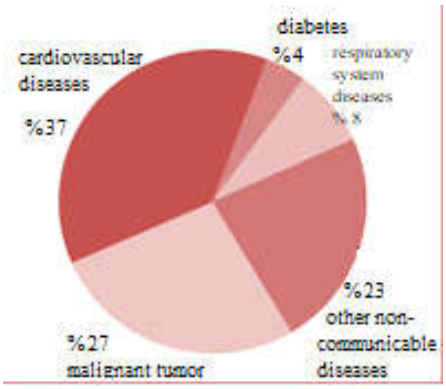

Figure 1. Global Distribution of deaths under 70 years of age by causes

With the developing technology, artificial intelligence techniques, which are used in economy, science and many other fields, are now frequently used in the field of health. Artificial Intelligence is a branch of computer science that develops intelligent machines that can act like humans, think like humans, and make decisions based on logic programs in memory (Hoşgör, 2022). It was tried to understand whether it could think like a human with the Turing test, which was firstly developed by Alan Turing, and after this appropriate methods were proposed. Artificial intelligence, which is frequently used in every field, has also been used at an advanced level in the field of health and the number of studies on it, is increasing day by day. In a study on the usage areas of artificial intelligence in health, the theses obtained from the National Thesis Center were researched and according to the data obtained, it was determined that the subjects of these theses were on 13 different health care (Hoşgör, 2022). Diagnosis of diseases, classification of diseases, detection of diseases, processing of medical images, prediction of diseases, development of medical support systems, identification of diseases, determination of the degree of risk of diseases, prognosis follow-up of diseases, monitoring of diseases, public health, healthcare services management, determination of physician opinions are the topics of these theses (Hoşgör, 2022) . Beside this, the majör areas fort he usage area of AI in health, are drug discovery, precision oncology, imaging and digital pathology, and patient data management (Hoşgör, 2022).

The advantages of the use of artificial intelligence and technological devices in the field of health are a phenomenon accepted by everyone. One of them is early diagnosis. The imaging techniques used offer the possibility of early diagnosis and are important factors in the early treatment of deadly diseases. It also provides great advantages for new drug discovery. The development of smart medicine systems which will replace traditional medicines, and the development of smart medicines which are suitable for people's DNA will be an important development in the treatment of diseases. Beside this, with the development of imaging techniques, high performance in the diagnosis, treatment and prognosis of common diseases such as cancer can be counted as another advantage. In the current pandemic period, it has been used in subjects such as early diagnosis of covid-19 disease, follow-up of contacted individuals, diagnosis, monitoring of treatments, and prevalence rate of the pandemic. It has an important place in reducing the workload of health workers all

over the world. Considering all these, the facilitating and healing role of the use of artificial intelligence in the field of health comes to the fore.

While new studies are being done every day for various artificial intelligence techniques that make more precise diagnoses, increasing data sizes pose a major problem . Speed is an important factor especially for health. High accuracy computation and speed are two important factors for measuring the efficiency of an algorithm. For this reason, size reduction methods are used to get faster and more effective results. Existing features in the data set enlarge the size of the data set and slow down the operations. Since the features used during the operation of some algorithms are found to be rebundant and irrelevant, size reduction methods are mostly based on reducing the number of features. For this, two methods; feature selection and feature extraction are used (Alpaydın, 2020). Some methods have been developed to use the smallest number of features that give the best results in feature selection which is based on the logic of preserving the important features and discarding the unimportant ones and these methods are used in the diagnosis of heart disease as an application. Tasci, M.E. and Şamlı, R. conducted a heart disease diagnosis study with 9 different algorithms applied to the heart data set (Taşçı, 2020). Görgün, M. made a study of diagnosing heart diseases by using different machine learning methods in his master's thesis (Görgün, 2020). Gündoğdu, S. used the classification method for heart disease in her study and found the random forest method to be the most accurate method (Gündoğdu, 2021). Boyraz et al. performed a heart disease detection study using artificial neural networks method (Boyraz, 2014). Ekrem, O. et al., after selecting the features in the heart dataset with particle swarm optimization, developed a diagnostic model with various classification methods (Ekrem, 2020). Göktaş, M.E., Yağanoğlu, M., determined that the C4.5 decision tree method was the method with the highest accuracy after applying various methods to the heart data set (Göktaş, 2020). Vatansever, B. et al. presented a similar study using feature selection and genetic algorithm (Vatansever, 2021). Atınç Yılmaz and Eda Sümer presented a hybrid model with Relief feature selection in their studies (Yılmaz, 2021).

Feature selection is one of the important steps of data preprocessing in data mining. In general, it can be defined as the process of searching for the smallest subset of features that improves the performance of the computational model. The feature selection process, which is increasingly important for knowledge discovery, can be used for many data types. Text mining, computational chemistry, bio-informatics or biomedical fields can be given as examples. It is more preferred especially in cases where the number of features is larger in size than the number of samples.

This preprocessing of data is deemed necessary for two reasons. First of all, reducing the size of the data provides more effective analysis (Jovic, 2022). The second reason is fitting the data set to the chosen analysis method (Jovic, 2022).

2. MATERIAL AND METHOD

2.1 Dataset

Many imaging techniques are used in the detection of the diseas and the treatment process. Radiography, mammography, fluoroscopy, CT, MRI, Ultrasound, SPECT, EKG are some of them. SPECT (Single Photon Emission Computerized Tomography) can be defined as the logical way of planar scintigraphy to obtain cross-sectional and 3D images of physiological activity (Atlan, 2021). In this study, we applied different feature selection methods to the Spect Heart Data Set obtained from UCI (University of California Irvine - Machine Learning Repository). The dataset is a heart dataset consisting of inputs obtained by SPECT imaging. Each patient is divided into two categories as normal and abnormal. It consists of 267 SPECT images. 44 continuous features are created for each patient. There are 267 samples defined by 23 binary feature patterns. Genetic Algorithm (GA), Binary Bat Algorithm (BBA) and Harmony Search (HS) methods are the methods used for feature selection. As the classification algorithm, SVM (Support Vector Machine) method is used. Feature selection algorithms were applied firstly and then classification was made for each method.

2.2 Feature Selection Methods

It has become an increasing need to get more effective data processing results from data sets of increasing size. The question of how to use such large sizes of data more is an important and necessary study, and therefore researchers have developed various size reduction methods. There are two ways to reduce size (Alpaydın, 2020). These are feature extraction and feature selection. In feature extraction, new features defined based on the features of the data set are used, while in feature selection, the ones that are suitable for the purpose are selected and the others are excluded. It is aimed to select the optimal smallest subset of the set of input features (Alpaydın, 2020). Feature selection can be considered as three types according to the status of labeled data in the data set. The first of these methods, which is also valid for machine learning methods, is Supervised methods, the second is Semi-supervised methods, and the last one is Unsupervised methods. The feature selection process according to the search methods can be examined in three categories. 1) Filter Methods 2) Wrapper Methods 3) Embedded Methods (Miao, 2018) (Akpınar, 2014). While the matrices formed in the datasets continue to grow in width and length, the transverse growth is called the curse of dimensionality (Akpınar, 2014). While increasing size reduces the efficiency of the methods used, it is often not understood without trying which features should be selected in order to increase efficiency, which ones serve the purpose better or which ones are noise for this purpose (Bins, 2001). The mathematical model of the feature selection problem can be defined as follows:

Given a set with the dimension M. There is a feature subset with the dimension n such that satisfies the following condition:

$$n \ll M$$

and increase the classification capability of the system (Bins, 2001). The following flow chart can be used for feature selection (Figure 2), which can be thought of as removing irrelevant and redundant data for the purpose of the study (Sevli, 2022a).

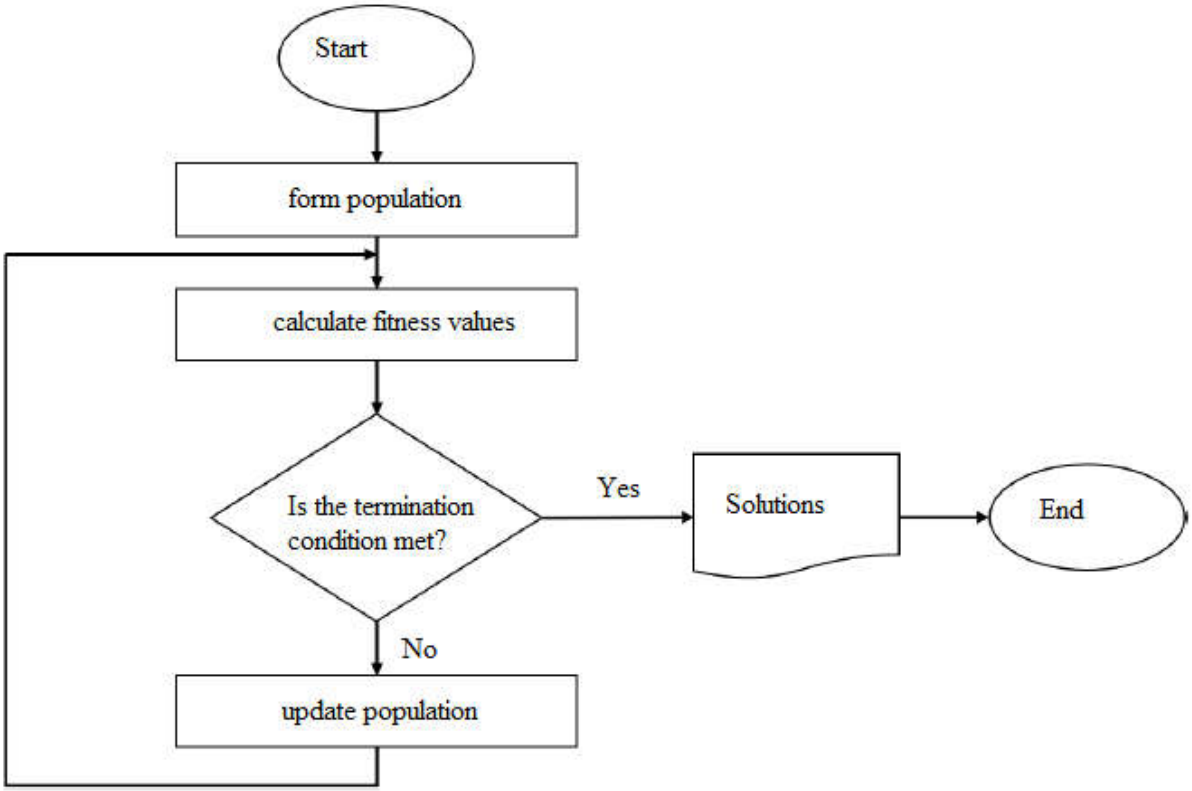

Figure2. Flowchart of the feature selection process

Feature selection algorithms used in this study are Genetic Algorithm (GA), Binary Bat Algorithm (BBA) and Harmony Search (HS) methods. The first of these is Genetic Algortihm. Genetic algorithms, named after Darwin's theory of evolution, are part of evolutionary computing (Nabiyev, 2018). First introduces in 1975 by J.H. Holland (Nabiyev, 2018). Genetic algorithms created using the principle of natural selection in nature and the modeling of the laws of conservation of the best are a search algorithm (Nabiyev, 2018). Vectors are called chromosomes and the well-being of each chromosome is measured with the help of objective function by forming a society (population) and generation. Genetic algorithms work with the help of operators such as repetition, crossover and mutation, and have an iterative structure.

Another method chosen is Binary Bat Algortihm. It is named like this because of some properties of bats. For example they behave like a sonar with their sensibile structure. They use echo and pulses of sound to understand the environmental conditions. In 2011 Yang developed bat algorithm which is an optimization technique (Yang, 2012). Bat Algorithm is as follows (Yang, 2012):

Objective function $f(x), X = (x^1, \dots, x^n)$
Initialize the bat population x_i and v_i, $i = 1,2, \dots, m$
Define pulse frequency f_i $at\ x_i$, $\forall i = 1,2, \dots, m$
Initialize pulse rates r_i and the loudness $A_i, i = 1,2, \dots, m$
1. While t<T
2. For each bat b_i, do
3. Generate new solutions through equation (1), (2) and (3)
4. if rand > r_i then
5. Select a solution among the best solutions.
6. Generate a local solution around the best solution
7. İf rand < A_i and $f(x_i) < f(\hat{x}), then$
8. Accept new solutions.
9. Increase r_i and $reduce$ A_i
10. Rank the bats and find the current best $\hat{x}$
Pseudo Code of Bat Algorithm

As the feature selection method, BBA in oher words Binary Bat Algorithm is used in this study. It is the binary version of the Bat Algorithm which includes bat's position as the binary values using a sigmoid function (Yang, 2012):

$$S(v_i^j) = \frac{1}{1+e^{-v_i^j}}$$

The other method is Harmony Search (HS). Its name comes from the music of an orchestra when aiming at composing the most harmonious melody as measured by aesthetic standarts (Manjarres, 2013). It is as follows:

1. Initialization of the Harmony Memory (HM)
2. İmprovisation of a new harmony
3. İnclusion of the newly generated harmony in the HM provided that its fitness improves the worst fitness value in the previous HM
4. Returning to step 2 until a termination criteria
Pseudo Code of Harmony Search

2.3 Classification Algorithm

Classification algorithm that applied to the SPECT Data Set is the Support Vector Machine (SVM) which is a widely used supervised learning algorithm because of high accuracy results that can be obtained from it. It is first developed by Vladimir Vapnik and the others in 1997 (Sevli, 2022b). A hyperplane boundary which is optimal is used to allocate data. It is a method based on statistical learning theory. In the plane where the data samples are located, a decision boundary is drawn at the furthest distance from the members of the two classes to separate the classes from each other (Sevli, 2022a).

3. FINDINGS AND DISCUSSION

The test results are measured by using accury test metric. The weight for the classification accuracy is chosen as 1. The percentage of data wanted for valdiation is 20. Three different number of agents are applied to each method and these are 10, 25 and 50. For every number of agent, each feature selection method is applied and after the selection process classification methos SVM has been run. In Table 1, the results of Support Vector Machine for 10 agents are given. Table 2 shows the accuracy results of SVM for 25 agents. In Table 3, the results of SVM accuracy for 50 agents are given.

Table 1. SVM Results for 10 agents

Number of agent 10	SVM-Results
	Accuracy
Binary Bat Algorithm (BBA)	0,8518
Genetic Algorithm (GA)	0,9074
Harmony Search (HS)	0,8148

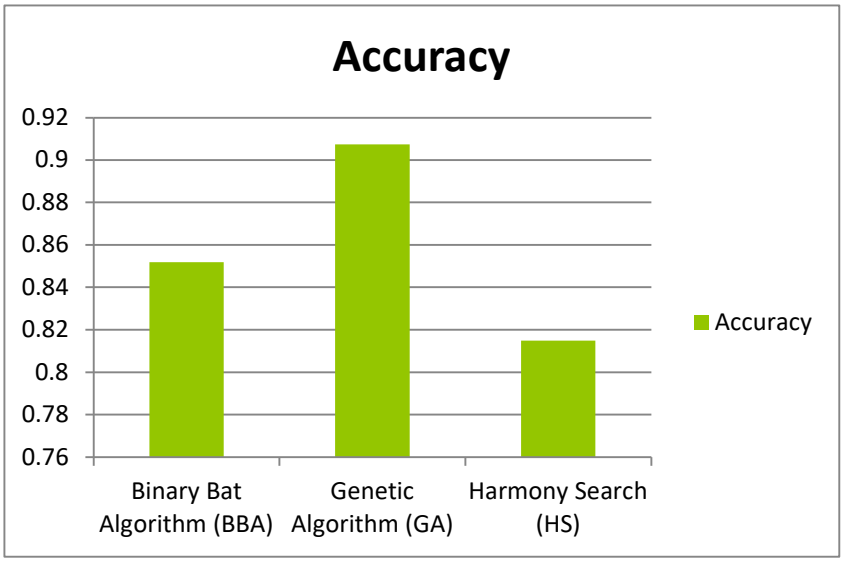

Figure 3. The results for Number of agent 10

Table 2. SVM Results for 25 agents

Number of agent 25	SVM-Results
	Accuracy
Binary Bat Algorithm (BBA)	0,8148
Genetic Algorithm (GA)	0,8888
Harmony Search (HS)	0,8888

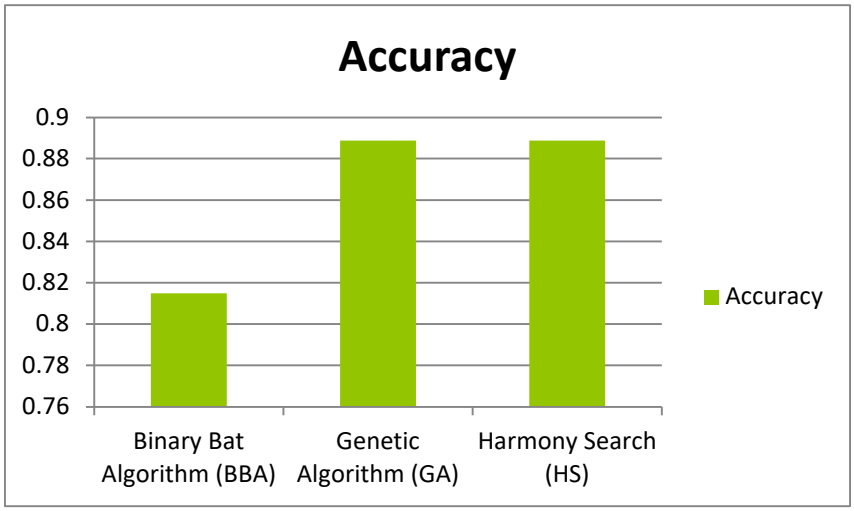

Figure 4. The results for Number of agent 25

Table 3. SVM Results for 50 agents

Number of agent 50	SVM-Results
	Accuracy
Binary Bat Algorithm (BBA)	0,8518
Genetic Algorithm (GA)	0,8148
Harmony Search (HS)	0,8148

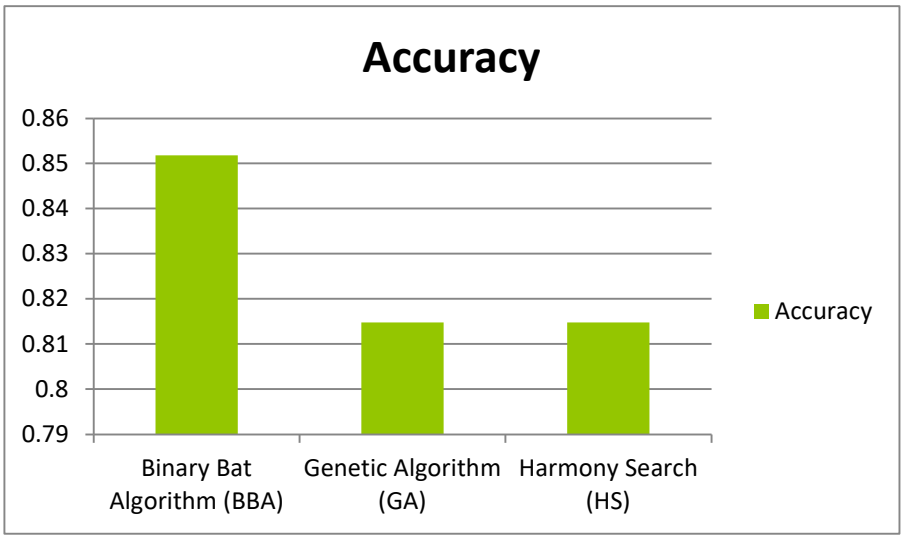

Figure 5. The results for Number of agent 50

Table 4. Accuracy Results of SVM for each number of agents

ACCURACY			
Number of Agent	BBA	GA	HS
10	0,8518	0,9074	0,8148
25	0,8148	0,8888	0,8888
50	0,8518	0,8148	0,8148

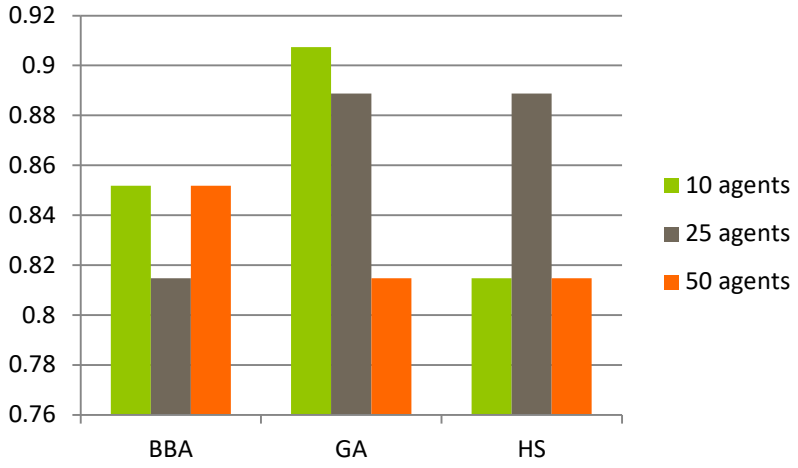

Figure 6. Comparative Graph of Feature Selection Methods

As it is shown in Figure 3, for 10 agents GA has the best accuracy result. For 25 agents, GA and HS has the same test scores and both of them work better than BBA (Figure 4). For 50 agents, BBA has better test scores than GA and HS (Figure 5). As the number of agent decreases, GA gives better results. In Figure 6, all results are given comparatively.

4. CONCLUSION

This preliminary study shows us the effectiveness of the feature selection methods. For the same data set, the other feature selection methods like Cuckoo Search Algorithm, Equilibrium Optimizer, Grey Wolf Optimizer, etc. can be applied and the results should be compared. For the next studies, it is planned to apply these and other feature selection methods to another health datasets and observe the accuracy of the methods. Thus, it can be contributed to the usage of artificial intelligence in the field of health.

5. REFERENCES

Akpınar, H., (2014), *Data Veri Madenciliği*, Papatya Yayıncılık

Alpaydın, E., (2020), *Yapay öğrenme Yeni Yapay Zeka*, Tellekt

Atlan,F., Pençe, İ., (2021), Yapay Zeka ve Tıbbi Görüntüleme Teknolojilerine Genel Bakış, *Acta Infologica*

Bins, Jose & Draper, Bruce. (2001). Feature selection from huge feature sets. In 8th IEEE International Conference on Computer Vision. 2. 159 - 165 vol.2. 10.1109/ICCV.2001.937619.

Boyraz, Ö.F., Seymen, V., Bozkurt, M.R., Çetin, Ö., (2014), Makine Öğrenmesi Algoritmaları Kullanılarak Kalp Hastalığı Tespiti, *International Conference on Education in Mathematics, Science and Technology*.

Ekrem, Ö., Salman, O.K.M., Aksoy, B., İnan, S.A., (2020), Yapay Zekâ Yöntemleri Kullanılarak Kalp Hastalığının Tespiti, *Mühendislik Bilimleri ve Tasarım Dergisi.*

Göktaş, M. E. & Yağanoğlu, M. (2020). Veri Bilimi Uygulamalarının Hastalık Teşhisinde Kullanılması: Kalp Krizi Örneği . Journal of Information Systems and Management Research, 2 (2), 26-32. Retrieved from https://dergipark.org.tr/tr/pub/jismar/issue/59183/844726

Görgün, M., (2020), *Makine Öğrenmesi Yöntemleri ile Kalp Hastalığının Teşhis Edilmes,*İstanbul Aydın Üniversitesi Yüksek Lisans Tezi.

Gündoğdu, S., (2021), Kalp Hastalık Risk Tahmini İçin Python Aracılığıyla Sınıflandırıcı Algoritmalarının Performans Değerlendirmesi, *Dokuz Eylül Üniversitesi Mühendislik Fakültesi Fen ve Mühendislik Dergisi.*

Hoşgör, H., Güngördü, H., (2022), Sağlıkta Yapay Zekanın Kullanım Alanların Üzerine Nitel Bir Araştırma, *Avrupa Bilim ve Teknoloji Dergisi.*

Jovic, A., Brkic, K., and Bogunovic, N., (March, 2022), Areview of feature selection methods with applications, Retrieved from: https://www.researchgate.net/profile/AlanJovic/publication/308871570_A_review_of_feature_selection_methods_with_applications/links/62792a8db1ad9f66c8ae5cf6/A-review-of-feature-selection-methods-with-applications.pdf

Khandelwal, R., (September, 2022), Genetic Algorithm Optimization Algotrithm, Retrieved from: https://pub.towardsai.net/genetic-algorithm-optimization-algorithm- f22234015113

Manjarres, Diana & Landa-Torres, Itziar & Gil-Lopez, Sergio & Del Ser, Javier & Bilbao, Nekane & Salcedo-Sanz, Sancho & Geem, Zong Woo., (2013), Survey A survey on applications of the harmony search algorithm, *Engineering Applications of Artificial Intelligence*. 26. 1818-1831. 10.1016/j.engappai. 2013.05.008.

Miao, J. and Niu, L., (2016), A Survey on Feature Selection, *Procedia Computer Science*

Nabiyev, V., (2018), *Yapay Zeka*, Seçkin Yayıncılık

Sevli, O., (2022a), Doğa İlhamlı Optimizasyon Kullanarak Özellik Seçimi, *Mühendislik Bilimleri ve Tasarım Dergisi.*

Sevli, O., (2022b), Farklı Sınıflandırıclar Ve Yeniden Örnekleme Teknikleri Kullanılarak Kalp Hastalığı Teşhisine Yönelik Karşılaştırmalı Bir Çalışma, *Zeki Sistemler Teori ve Uygulamaları Dergisi.*

Taşçı, M.E., Şamlı, R., (2020), Veri Madenciliği ile Kalp Hastalığı Teşhisi, *Avrupa Bilim ve Teknoloji Dergisi.*

Türkiye Kalp ve Damar Hastalıkları Önleme ve Kontrol Programı, (September,2022), Retirieved from: https://tkd.org.tr/TKDData/Uploads/files/Turkiye-kalp-ve-damar-hastaliklari-onleme-ve-kontrol-programi.pdf

Vatansever, B., Aydın, H., and Çetinkaya, A., (2021), Heart Disease Prediction With Machine Learning Algorithm Using Feature Selection By Genetic Algorithm, *Journal Of Scıentıfıc, Technology And Engıneerıng Research.*

Yang, (2012), "BBA: A Binary Bat Algorithm for Feature Selection", *2012 25th SIBGRAPI Conference on Graphics, Patterns and Images*, doi: 10.1109/SIBGRAPI.2012.47.

Yılmaz, A. and Sümer, E., (2021), Relief Özellik Seçim Yöntem Tabanlı Önerilen Hibrit Model ile Kalp Hastalığı Teşhisi, *Avrupa Bilim ve Teknoloji Dergisi.*

GZKTS VERİ MİMARİSİNİ BÜYÜK VERİ MİMARİSİNE DÖNÜŞTÜRMEK: KONUM VERİLERİNİN ART İŞLENMESİ İÇİN BİR DURUM ÇALIŞMASI

TRANSFORMING RTLS DATA ARCHITECTURE TO BIG DATA ARCHITECTURE:

A CASE STUDY FOR POST-PROCESSING OF LOCATION DATA

Ceren Bahar Yılmaz[1], Oğuz Gövem[1], Murat Osman Ünalır[2]

Litum Bilgi Teknolojileri Ar-ge Merkezi[1], Ege Üniversitesi Bilgisayar Mühendisliği Bölümü[2]

ORCID ID: 0000-0001-9808-4182, 0000-0001-6836-6197, 0000-0003-4531-0566

ÖZET

Gerçek Zamanlı Konum Takibi Sistemleri (GZKTS), bir radyo frekansı (RF) ağı tarafından kapsamı tanımlanmış bir bölge içindeki herhangi bir kişiyi veya varlığı bulur ve izler. Bu sistem, her bir varlığın takibi için, saniyede birkaç kezden birkaç dakikada bire kadar konum verisinin ne sıklıkta yenilenmesinin istendiğine bağlı olarak konum verisi üretir. Toplanması, saklanması, işlenmesi, analiz edilmesi ve raporlanması gereken veri hacmindeki artış, büyük veri teknolojilerinin gelişmesinin nedenlerinden biridir. Bu makale, GZKTS'nin hedeflenen kısa vadeli ve uzun vadeli analitik ihtiyaçlarına göre veri mimarisinin dönüşümünü açıklamayı ve geleneksel mimari ile büyük veri mimarisini okuma/yazma süreleri ve depolama maliyetleri açısından karşılaştırmayı amaçlamaktadır. Bunu sağlamak için ilişkisel veritabanı yönetim sistemi içerisinde günlük olarak tetiklenen bir mikroservis ile ilişkisel veritabanı sistemindeki veri, ham haliyle .csv dosyalarına çıkarılır. Veri, GZKTS'nin iki farklı raporlama gereksinimini karşılamak için Pandas ve Dask kütüphanelerinin kıyaslı olarak kullanılmasıyla Python dili ile işlenir. Her iki kullanım durumu için de analiz edilen veri, daha hızlı sorgulama amaçları için, sorgu parametreleri doğrultusunda farklı modellemeler yapılarak, sütun yönelimli bir NoSQL veritabanı olan Apache Cassandra'da depolanır. Konum verisinin ilişkisel veritabanı üzerinde arşivlenmemesi sayesinde GZKTS'nin operasyonel performans sağlığını etkilemeden bu veriden anlamlı sonuçlar üretilmekte ve sonuçlar uygulama üzerinde raporlanmaktadır. Günlük veri hacimleri bir kerede işlendiğinde, Dask kütüphanesi, Pandas kütüphanesine kıyasla umut verici bir performans sergilemiştir. CSV dosya işlemleri Apache Cassandra'ya yazma performansını kıyaslanamayacak şekilde hızlandırdığı için tercih edilen yöntem olan, işlenen veriyi .csv dosyalarına yazma performansında iki kütüphanenin hızlarında önemli bir fark görülmemektedir.

Anahtar Kelimeler: Gerçek Zamanlı Konum Takip Sistemleri, büyük veri mimarisi, konum verisi.

ABSTRACT

Real-time Location System (RTLS) locates and monitors any person or asset within a defined zone covered by a radio frequency (RF) network. This system produces location data for each entity to track from several times per second to every few minutes, depending on how often it is desired to refresh the location data. The increase in the volume of data that is required to be collected, stored, processed, analyzed, and reported, is one of the reasons for the development of big data technologies. This paper aims to explain the transformation of data architecture according to the target short-term and long-term analytical needs of RTLS and to compare traditional architecture and big data architecture on read/write times and storage costs. In order to achieve that, the data in the relational database system is extracted to .csv files in its raw form with a microservice triggered daily within the relational database management system. Data is processed in Python language using the Pandas and Dask libraries comparatively to meet the two different reporting requirements of RTLS. For both use cases, analyzed data is stored in a column-oriented NoSQL database Apache Cassandra by modeling differently in line with the query parameters for faster query purposes. Thanks to not archiving the location data on the relational database, without affecting the operational

performance health of RTLS, meaningful results are produced from this data and are reported on the application. When daily volumes of data are processed at once, Dask performed promisingly compared to Pandas. No significant difference is observed in the speeds of the two libraries in performance of writing the processed data to .csv files, which is the preferred method as .csv file operations accelerate the performance of writing to Apache Cassandra incomparably.

Keywords: Real Time Locating Systems, big data architecture, location data.

1. INTRODUCTION

The object of the project is to analyze the former architecture of Real-time Location System (RTLS) of Litum Inc., define the requirements of the system and transform it to big data architecture. The report will propose a better understanding of what is big data architecture, the components of location data, existing former RTLS architecture, additional big data architecture blocks.

Litum helps businesses transform their operations to accomplish their goals in increasing safety and efficiency. Through extensive research and development, Litum designs and manufactures its entire solution portfolio, with main divisions being Industrial IoT (Internet of Things), Healthcare RTLS, Passive RFID, and Software Applications. Litum produces a combination of hardware and software solutions used to determine and track the real-time location of mobile transmitting devices associated with objects and resources in application areas.

It is tried to enhance the Litum company's capability in reporting for the customers' business continuity with improved safety. A well-developed RTLS software program can also be tied into other systems throughout the customer's facility to further improve automation and safety. In order to achieve these goals, big data can be employed to uncover information such as hidden patterns, correlations, customer movements. Then it will be possible to provide data analytics, metrics, and conclusions within near time. Therefore, the customer company as an IoT adopter will ensure its staffs' and moving equipment's safety and peace, regulatory compliances, and less lost-time accidents.

The problem in providing data analytics reports is to process big data and to present report requirement results in near real-time. The data produced particularly by the RTLS of the Litum can be classified as big data due to its volume and velocity requirement. Since the solution of this problem cannot be provided with a relational database system, the data is collected from the relational database, stored, processed, and analyzed in big data architecture.

Abstraction among system components and domain requirements is an important skill for the new architecture. The abstracted needs should determine the abstracted services that will be offered without impacting the existing system. Former RTLS data architecture and big data architecture can work together coordinately through microservice architecture, and this is a deployment requirement of the new architecture.

A microservice triggered daily within the relational database management system extracts data in its raw form to .csv files from the relational database management system. Then, the data is processed in Python language using the Pandas and Dask libraries comparatively to meet the reporting requirements of RTLS. Queries searched for reports are listed. Analyzed data is stored in a column-oriented NoSQL database Apache Cassandra. The data model of NoSQL database is designed differently in line with the query parameters for faster query purposes. Meaningful results should be generated from this data and reported on the application, without affecting the operational performance health of existing RTLS. To obtain this, location data is processed on a big data architecture instead of accumulating on a relational database. In reading daily data volumes, Dask performed promisingly compared to Pandas. At the end of the process, .csv files containing the processed data were written to Apache Cassandra. It is reported in the RTLS web application by querying the NoSQL database through the web application.

Through the rest of the paper, background, and related work, former RTLS data architecture, requirements of RTLS in the big data era, case study and discussion regarding the study are going to be shortly explained.

2. MATERIALS AND METHODS

Background and Related Work

The amount of data produced and transferred grows linearly, so the need to store and process data efficiently increases. A simple big data architecture is designed to retrieve, process, and analyze data that is too large or complex for traditional database systems. Thus, the infrastructure for opportunities in the fields of data science, artificial intelligence, machine learning and deep learning has been prepared.

Elements incorporated into application systems that support an organization's ongoing operations and automate key business processes are sourced from transactional data (Getz, 2022). This type of data often includes numeric values and times and is recorded as transaction history. Transactional data is captured, recorded, and queried.

On the other hand, analytical data serves for different purposes on business performance instead of business events itself. Analytical data are the information used to provide data-driven decision making and support business intelligence. This type of data includes numerical measurements to be analyzed and does not necessarily need to be descriptive unlike transactional data.

Transactional data should be captured, streamed, and stored in big data analytics, which is essential to ensure transaction volumes, data rates for the velocity. Big data analytics systems in the big data architecture need to be integrated back into core systems to get prescriptive insights over analytical data.

NoSQL (not only SQL) databases are an alternative to traditional databases and environments that allow us to store diverse data types rather than relational databases. The data is stored without the need for a logical categorization and any schema in NoSQL databases. Multiple NoSQL database platforms are available. There are various NoSQL databases, some of which are Key-Value Store, Document Stores, Graph Database, Wide Column Stores, Time Series Database, Search Engines, etc. There are also databases like Geospatial Datastore, which are specialized for the purpose of use. Additionally, a few examples of multi-model or data lake technologies are:

- Hadoop: Software tools running on top of multiple databases
- MongoDB: Multiple data storage options in a single database software platform
- PostgreSQL: Row-oriented, column-oriented, key-value, and document-oriented data storage options

In analytics use cases, a columnar database may suit better. Below is the comparison of Relational Database vs Wide Column Store database types.

Database Type	Examples	Pros	Cons	Use cases
Relational Databases	Oracle, MySQL, SQL, DB2 etc.	ACID compliance (Atomicity, Consistency, Isolation, and Durability) Better support options	SQL databases cannot handle unstructured or semi-structured data Their tables do not necessarily map to objects They require complicated ETL (Extract, Transform, Load) and maintenance Have row locking, Pricing for some products (Oracle, SAP) can be expensive. *Note: While some RDBMS systems can now handle JSON, they are not purpose built to do so.* Scalability challenges and difficulties with sharding: RDBMSs have a more difficult time scaling up in response to massive growth compared to NoSQL databases. These databases also present challenges when it comes to sharding. Sharding is the process of dividing a large database into smaller parts for easier management.	Organize data into tables with columns, each with a specified name and data type. Rows are identified with a unique attribute, or grouping of attributes, called a primary key (typically a single column, called a field) Relationships between tables are defined through foreign keys which reference primary keys Strict schema (data model) enforcement Data accessed via Structured Query Language (SQL) Extra features like Triggers and Stored Procedures *ACID compliance, Data warehouse, OLAP, OLTP, structured data analysis.*
Wide Column Stores	Apache Cassandra, HBase, Azure Cosmos DB	Schema-agnostic databases that can handle querying of non-sequential data in real-time. Highly scalable: Well-suited for distribution across multiple data stores and computing nodes Sorting and some data manipulation: Directly from the database rather than relying solely on the application Indexing: Some databases index different levels of columns to help with data processing Increased granularity: Being able to update an individual column rather than having to replace all the data when something changes	Inefficient updates Inefficient joins / aggregations	Wide column stores have tables just like RDMBs, but these tables do not have a relationship with other tables The names of the columns and their types may be different for each row in the same table Complex data is grouped into a single table Tables have Column Families and Row Key Row Key can be interpreted as Primary Key in RDMBs Row Keys are also used to distribute records between servers It is a versioned sparse matrix with multi-dimensional mapping (row-value, column-value, timestamp). It is like a two-dimensional key-value store, with each cell value versioned with a timestamp. *Web analytics and analyzing data from sensors*

Table 2-1: Comparison of Relational and Columnar Databases

While functional requirements will be met over relational databases, non-functional requirements such as performance will be met over wide column stores, which is the most suitable database type.

The query first approach is a database modeling design which involves revision of the columns' usage frequencies and query paths for the design of tables to support these queries. If there is a need to implement another query model, there should be a new data model that supports that query model, which can be constructed easily and independently from the existing ones. This approach is preferred in NoSQL databases such as Apache Cassandra, a highly available and partition tolerant database that is often used in Big Data solutions.

Handling the data and processing it is one of the main procedures of IoT. It is required to have an analytical platform that extracts information from IoT data. IoT devices generate continuous streams of data at very high speeds, so the process of extracting valuable information is complicated. This platform also must have good mechanisms and protocols which guarantees the security and significance of the data. Big Data completes IoT in terms of these requirements (Gubbi, Buyya, Marusic & Palaniswami, 2022).

Former RTLS Data Architecture

RTLS can locate and track anything, anyone within a defined zone that is covered by radio frequency. RTLS system is a blend of hardware and software that work together to create a mesh network capable of overseeing the movement of RFID tags within a specific location. The main technology of Litum Ultra-Wideband RTLS, are specifically designed to provide accurate, real-time status updates of movement within a facility.

In practice, the system consists of transmitter (tag) and receiver (anchor) devices. As of system components, transmitters are mobile devices whose location will be tracked, and receivers are fixed devices that provide location calculation. There are various types for RFID tags and anchors. The location information is sent to the server by anchors. The location can be calculated by using multiple methods. This calculation is done by the location engine, which is a part of the RTLS software. In the case study, the location data which is the output of the location engine is the subject as transactional data.

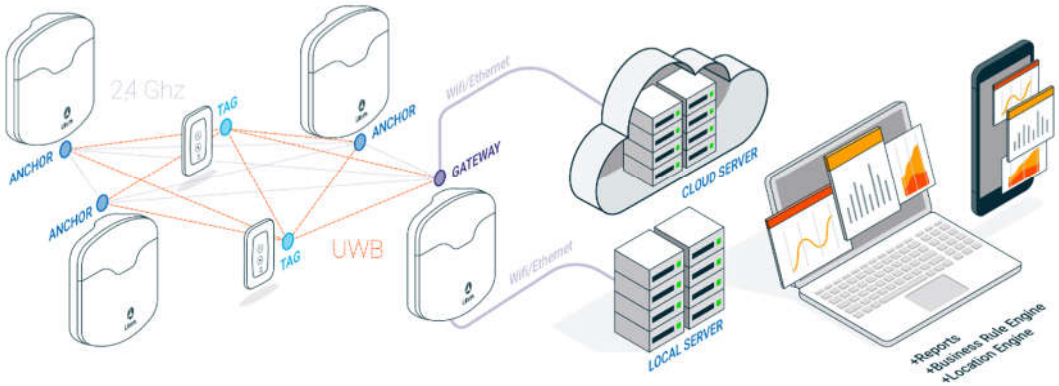

Figure 2-1: Litum's Mesh Network

Every RTLS system incorporates a combination of hardware and software to create an enclosed indoor positioning network. This meshed system uses several Radio-Frequency Identification (RFID) readers (anchors) placed throughout the area to receive the radio signals sent by active RFID tags that are attached to or worn by tag carriers.

There is a wide range of technologies developed for use in location tracking systems. Each of these systems offers a selection of unique benefits for businesses. Some technologies are better suited to passive monitoring of assets and personnel as they enter and exit a building. Other systems, such as Ultra-Wideband (UWB) RTLS, are specifically designed to provide accurate, real-time status updates of asset movement within a facility. Some of these technologies are the following.

- Radio Frequency Identification (RFID) solutions are a popular option for facilities and retailers that want to track the movement of merchandise or tools within a short-range, which is better for passive RFID that tracks tags as they are scanned by handheld scanners or when they pass through gateways.
- Global Positioning System (GPS) can be benefitted by open mining operations and other concerns that operate outdoors to track the movement of their vehicles and equipment by using satellites, which can only provide real-time tracking within a few meters and only outside of buildings.
- Wi-Fi which sends wireless signals in all directions to multiple access points, is a less expensive option for businesses and is useful for tracking arrival time, speed, and has a location accuracy to within 5-10 meters.
- Bluetooth low-energy beacons (BLE) are becoming more affordable, and they offer better location accuracy of within 3-4 m. for real-time tracking which is also a flexible technology that can be used for tracking objects as they pass gateways or active movement within a facility.

- Ultra-Wideband RTLS technology is one of the most popular options for facilities that require pinpoint accuracy. This low energy frequency provides location accuracy within a sub-meter range. It is ideal for monitoring the movement of fast vehicles and preventing collisions, tracking senior newborn babies, senior residents, patients, and improving their safety. UWB tags last for years with a single battery and require minimal maintenance.

Since most RTLS hardware is placed within industrial environments, it must offer longevity and complete durability against damage. The RFID tags are built to resist everyday damage from falls and impacts of any sort. A durable shell keeps the electronic components safe, along with very secure fittings and connections within. Some RFID tags are specifically for outdoor use or use in hazardous environments. These devices have nearly airtight and watertight cases that keep out dust, sand, general dirt, and water. Some can even be submerged in water for a short period without damage. This is the same for the RTLS anchors, also known as active RFID readers, that are posted throughout a work area. Anchors must also be weather-resistant for outdoor work areas that face wind, rain, and snow. RTLS systems can come with a range of features that improve personnel safety, prevent damage to equipment, and can provide important data for customer's employees ("What is RTLS - Real-Time Location System? | Litum", 2022).

RTLS Data Architecture has been created with the legend below of The Open Group Architecture Framework (TOGAF) Information Systems Architectures - Data Architecture ("Phase C: Information Systems Architectures - Data Architecture", 2022).

Symbol	Element
	Entity describing a Data Object
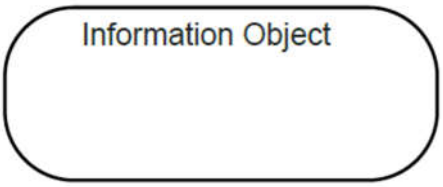	Information Object encompassing Entities
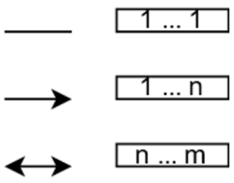	Relations between Entities and Information Objects

Table 2-2: Data Architecture

Entities (Data Objects) and Information Objects relate to each other as can be seen on the Figure 2-2: Entity Relationship Diagram. They can be nested hierarchically and have attributes.

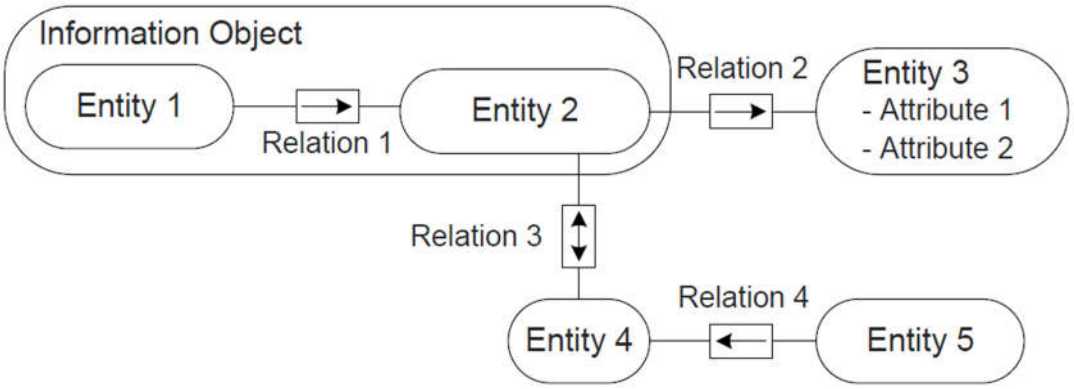

Figure 2-2: Entity Relationship Diagram

The data architecture is structured by means of a core model and extensions for specific business domains. The core model contains and describes the top-level business objects for the RTLS. Specific extensions add information objects to the core model for the sake of clarification and more detailed consideration. Figure 2-3: Overview of Core Data Model gives an overview of the core model entities.

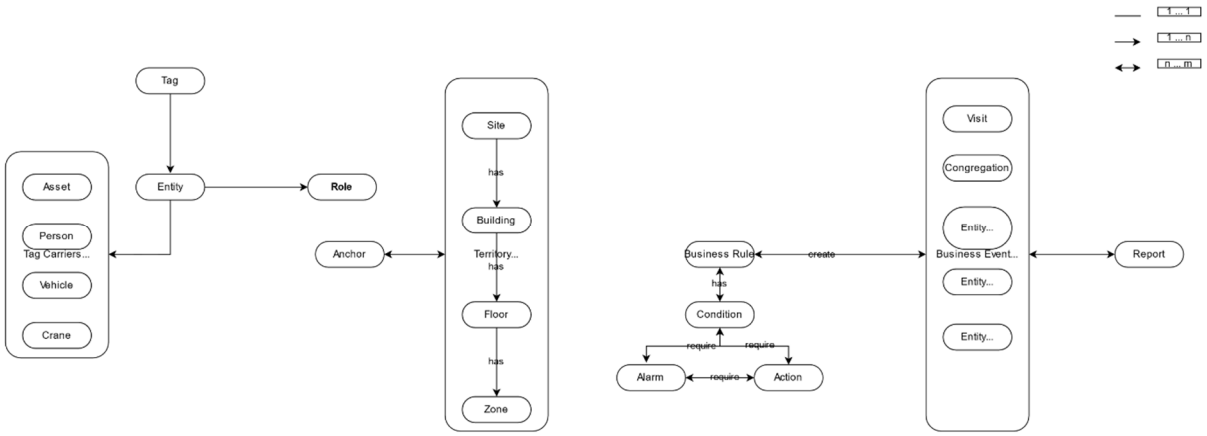

Figure 2-3: Overview of Core Data Model

In the core data model of Litum RTLS Data Architecture, you may see core data concepts relation with business concepts. This high-level architecture draws a connection between entities to be tracked and anchors as trackers on the territory to scan. Business rules, alarms, and actions can be defined on the location information. Then reports can be triggered regarding the business events.

Entity	Description

Tag	A tag is a mobile device that is carried for tracking purposes.
Entity	An abstraction for each tag carrier which can be vehicle, person, asset, object or thing.
Asset	An asset is the tag carrier which is expected to move less frequently as a resource with economic value.
Person	A person is the tag carrier which is expected to move within defined speed limits.
Vehicle	A vehicle is the tag carrier which is expected to move faster within defined speed limits and is used for transportation.
Anchor	Radio-Frequency Identification (RFID) readers placed throughout the area to receive the radio signals sent by RFID tags that are attached to equipment, merchandise, or worn by personnel. Anchors send out radio signals and receive radio signals. They can recognize the active RFID tags every time they come within the range of the anchor.
Site	The specific location where the wireless network is created by placing anchors. Site is the biggest abstraction for the territory to be tracked. Site has key points throughout and surrounding a facility.
Building	The specific location where the wireless network is created by placing anchors. Building is the structure with a roof and walls physically or virtually, such as a workplace, factory, or warehouse etc. in the territory to be tracked. Building has key points throughout and surrounding a facility.
Floor	The specific location where the wireless network is created by placing anchors. Floor is all the rooms or areas on the same level of a building. Floor has key points throughout and surrounding a facility.
Zone	The specific location where the wireless network is created by placing anchors. Zone is the smallest abstraction for the territory to be tracked such as room, corridor, highway, or specific business alarm territory etc. Zone has key points throughout and surrounding a facility.
Business Rule	A regulation that defines or restricts actions of operations of the organization.
Report	The document presented on a particular business event, thorough analysis.

Table 2-3: Relevant Data Architecture Entities

RTLS systems that utilize state-of-the-art UWB technology provide sub-meter location accuracy when tracking assets, equipment, and employees. UWB RTLS systems also form their own mesh networks and do not require network connectivity, which reduces the investment of network infrastructure and cabling. Some of the features of RTLS tags and anchors tracked through business events include:

- Monitoring environment temperature and humidity
- Gas level detection for CO, H2S, NO, O2, and CO2.
- Alert you when assets are overdue for maintenance, repair, or calibration.
- Monitoring the current temperature of motors and other equipment components.
- Alert you if an employee falls or stops moving for a specific length of time.
- Panic buttons for personnel to press if they need help.
- Track the speed and fuel usage of equipment or vehicles
- Keep track of inventory levels in a warehouse, facility, or store.

The communication of a tag and anchors produces position messages which is a time series data. The signal contains vital information about the location and status of each object or person inside the network, which is sent to the servers to be processed by RTLS software. When the anchors get a signal from an RFID tag, the location of the tag can be calculated by using triangulation, received signal strength (RSSI), time difference of arrival (TDOA), or similar methods. This calculation is done by the location engine, which is a part of the RTLS software and location data is produced. This data flow and relationships can be followed at Figure 2-4: Conceptual Data Diagram which improves intelligibility of the domain. In the diagram, the conceptual data model for time series features tags, entities, vehicles and anchors. Each tag has a unique ID and various specific types. Each entity has a unique ID and various specific characteristics. Each vehicle has a unique ID and various specific types. A vehicle is an entity, and an entity has a tag. Each anchor has a unique ID, ZoneID and FloorID specifying its location on the territory and various specific types. A position message has a MessageDate timestamp and Distance value, and some controlled features. Although a tag and anchors can generate many position messages, one location data is produced for the tag at each timestamp.

This conceptual data model is generic enough to demonstrate important concepts of time series data in the RTLS system.

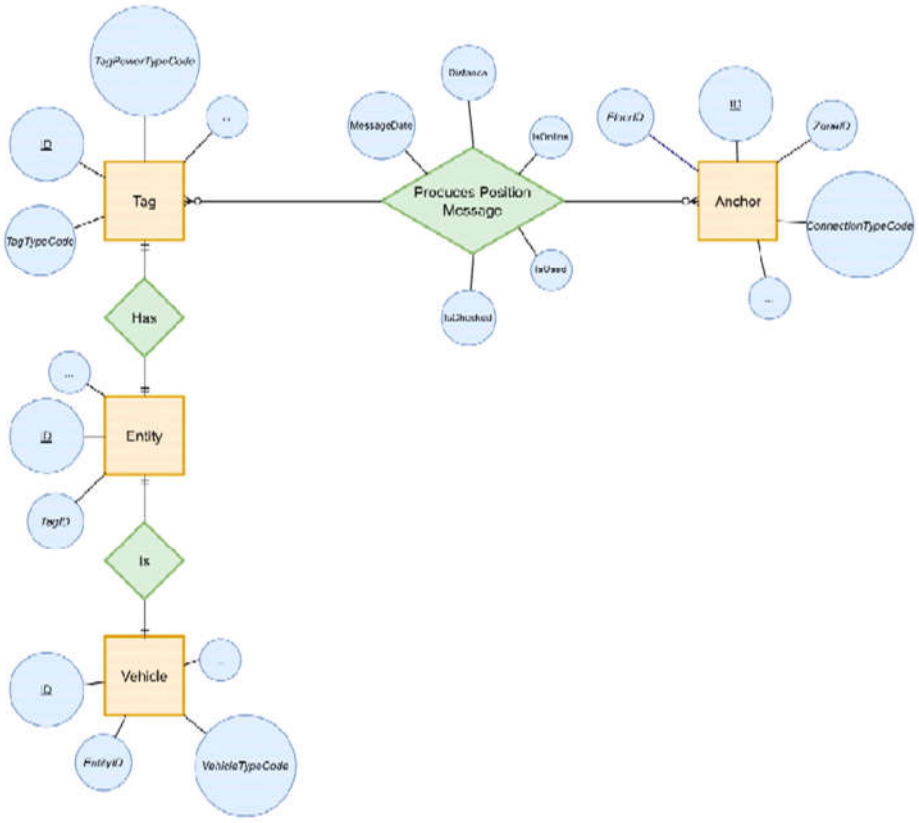

Figure 2-4: Conceptual Data Diagram

Tables in the RDBMS are classified according to the core data model. The metadata, types of data, table definitions, table properties, field properties, their default values, table types, model bases are documented.

Properties	**Values**
Table Type	Business table (APP_ENTITY) Parameter table (APP_PRM_ENTITY)
Table Content	Master (COM_USER) Detail of Master (COM_USER_GROUP_ASSIGN) Transaction (BRE_EntityZoneTransaction) Log (COM_NOTIFICATION_LOG) Summary
Sensitivity	Contains Personally Identifiable Information (PII) Retention Policy

Table 2-4: Table Properties

Properties	Values
Name	
Type	int datetime nvarchar
Length	
Nullable	Yes No
Encrypted	Yes No
Key Relation (Other … Main)	Primary Key (PK) Foreign Key (FK)
	Foreign key (PRM Table)
	1/n … 1/n/m
Default	
Sensitivity	Personally Identifiable Information (PII) Business information Classified information (Tier of sensitivity: Restricted, Confidential, Secret, or Top secret)
Details	Indicated values. Calculation rule for summary tables

Table 2-5: Field Properties

In relational modeling, every table in the database represents a real-world entity. These tables are tied using relationships. The primary keys, IDs, which uniquely represents a tag, an entity, a vehicle, etc. These real-world entities are represented by rows in the database. Joins are used in relational database queries. Joins are not very efficient because they require a lot of locks which means order requests occurring at the same time cannot be serviced. For a system where high throughput is required, this type will not reach or exceed the desired standard or performance.

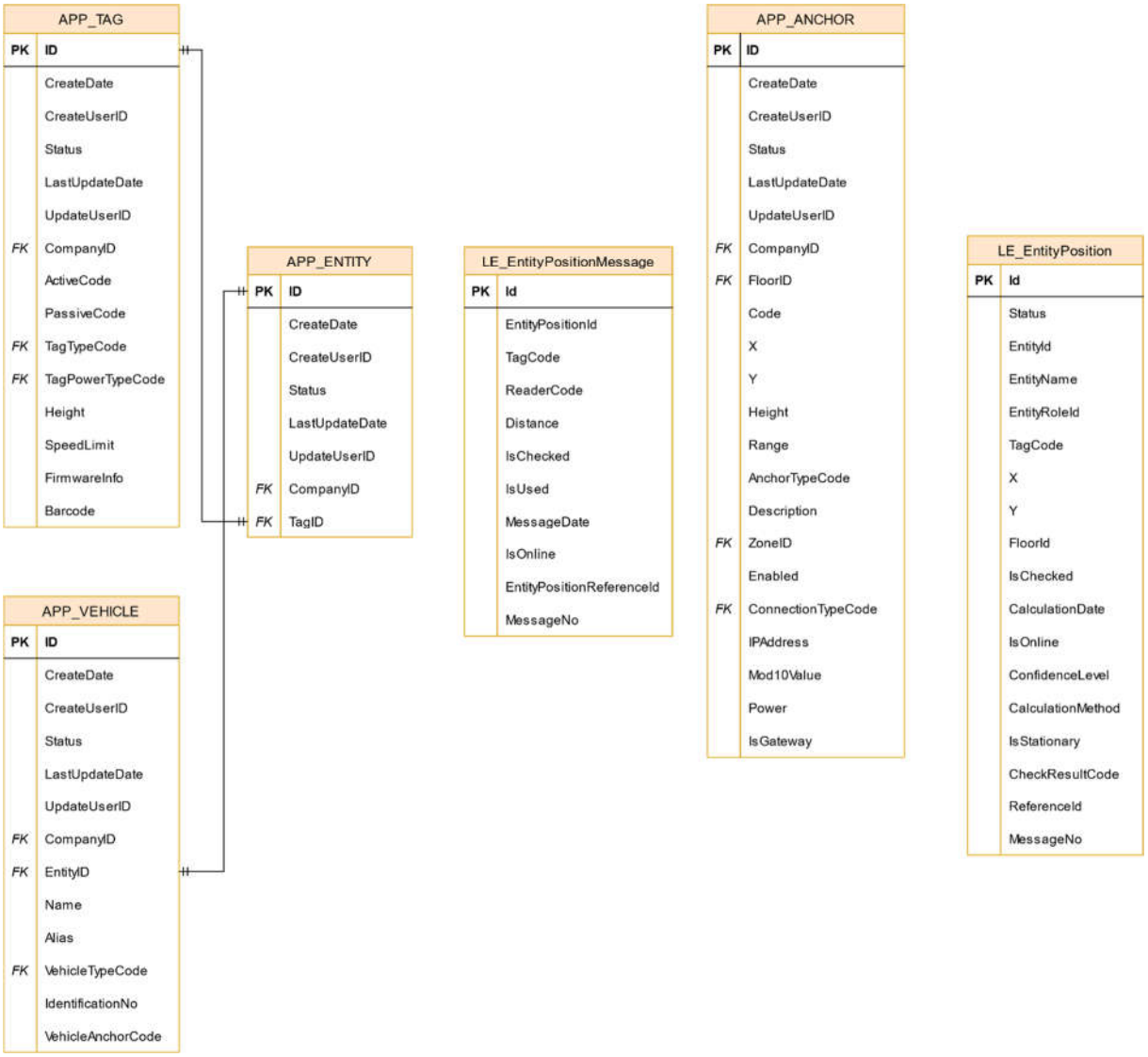

Figure 2-5: Entity Relationship Diagram (ERD)

Requirements of RTLS in The Big Data Era

Real-Time Location System gives companies the ability to track objects and people, while also gathering vital data about these assets and the surrounding environment. RTLS tracks locations and the movement of entities via continuous feedback. It can give the information about where an entity is at the present, where it has been, and provide an analysis of where it is going.

The RTLS software that Litum has developed serves multiple functions in reports, including:

- Displaying where assets are located on the map of the facility
- Showing the movement of assets
- Creating history reports for review
- Triggering alerts and automated actions

The RTLS software is a vital part of any RTLS system. It processes the information provided by the RFID anchors to calculate the location and displays it. RTLS software can show a map of the work area with a live display of personnel and equipment location. It can even alert designated personnel when an RFID tag leaves

the area or is tampered with, which could indicate a potential theft. Besides, RTLS software can provide you with a selection of organized reports using key data received by the anchors. These reports can:

- Show any employee tardiness or absences
- Show whether employees move around or remain at their workstation
- Track how many loads each piece of heavy mining equipment moved
- Display completed maintenance on vehicles and equipment
- Display how fast vehicles move and their routes

With the new era, the system should comply with the following requirements. Vehicles should not follow each other closer than 20 feet on a straight route. There is a report requirement to show these answers: How often do vehicles violate the 20 feet rule? What is the distance between vehicles when this violation is committed? How long do vehicles violate the 20 feet rule?

RTLS location data should be modeled by complying with the following levels

- Level 1: Requirements for querying and retention
- Level 2: Analytical requirements (These are domain-specific requirements from the customer.)
- Level 3: Data science focused requirements

Although Level 1 can be fulfilled on RDBMS with some time and space complexity restrictions, Level 2 and Level 3 forces the RTLS data architecture to evolve by developing these capabilities.

The total area monitored is around 584 meters x 213 meters, which is 124392 square meters. There are 1227 tags (985 of which are for people and 252 of which are for vehicles) monitored by 334 anchors. Cycle time is a requirement that each entity should produce location information shorter than or equal to cycle time, which is 1 second for the case. Therefore, 252 vehicles produce one location data per each vehicle at each second with each location data having a space of 0.11 KB approximately. With these requirements, the system ends up to 100 GB monthly data. The location data should be cleansed to improve its quality and processed to reveal the gist of knowledge; consequently, be organized, configured, and partitioned for analytical queries.

A typical row-based relational database is optimized for mass-storing rows of data, which stores each row in an individual file. Executing queries in this database causes every row to be entirely read even if only a few columns are needed. This is highly inefficient for big data, where huge volumes of data must be retrieved and processed. On the other hand, a columnar or column-oriented database separates the columns of data and stores them individually. This implementation allows queries to find and retrieve the data faster by only reading the required columns. A column-oriented database also takes advantage of storing the same type of data in a file, which allows it to apply the most efficient data compression on each individual column of data. Transferring these operations from RDBMS to a column-oriented database gives an advantage in IoT Big Data solutions, as this type of database can operate with huge amounts of data very efficiently.

During the transfer, query first approach must be taken into attention. A typical NoSQL database provides different types of keys to store and access the data efficiently. Some of these are primary keys, partition keys, and clustering keys.

- Primary keys uniquely identify each data in a database. A primary key consists of one or many partition keys and zero or many clustering keys. Data is partitioned into different groups by partition keys and sorted within a group by clustering keys, which directly affects the speed and cost of the queries.
- Partition keys must be selected by having the query model in mind, probably as filters of the query, which will help the database to find the correct partition faster.
- Clustering keys sort the data inside of a partition, implement multi-row partitions, and since they are also a part of the primary key, they provide uniqueness. They can be used as filters of a query model alongside with a partition key to retrieve specific data in a partition.
- Composite partition keys are formed by having multiple partition keys inside a primary key. This will divide data into more partitions and possibly decrease the amount of data stored in a single partition.

3. FINDINGS and DISCUSSION

Case Study

In the case study, big data architecture is utilized to eliminate this disadvantage of relational database systems.

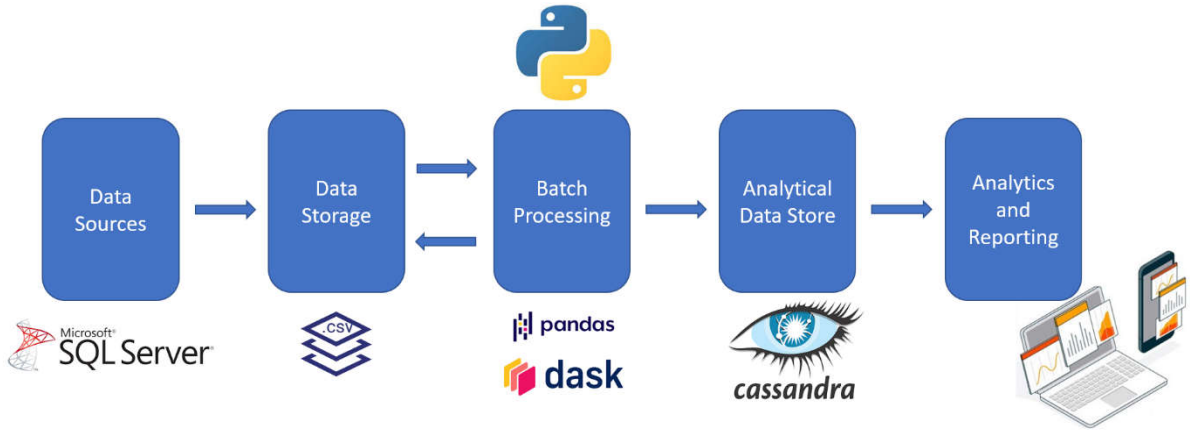

Figure 3-1: Transformed RTLS Data Architecture

In the traditional RTLS architecture, a SQL database is used which is Microsoft SQL Server. Then, a microservice for ETL (Extract, Transform, and Load) is triggered from the MSSQL Server and extracts raw data in .csv file format to a separate machine. The daily data is divided into hourly data and processed to obtain the required analytics. The process is in Python language using the Pandas and Dask libraries comparatively. For use cases, analyzed data is stored in a column-oriented NoSQL database Apache Cassandra by modeling differently in line with the query parameters for faster query purposes. Apache Cassandra gets a lot of its speed in database reads and writes from the fact that it never has to perform any joins on the database. It is impossible to perform joins on Apache Cassandra. Instead of taking the relational model approach, the query first approach is taken. Then, users can report them through the RTLS application by querying Apache Cassandra.

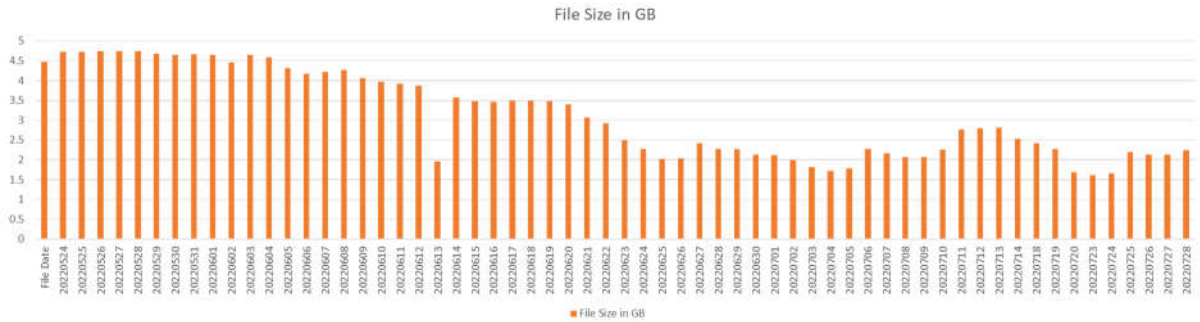

Figure 3-2: Sizes of Daily Data Files for Two Months

In the first step which is the raw data extraction for a two months' timeline, the sizes of files collected are depicted in Figure 3-2: Sizes of Daily Data Files for Two Months.

Descriptive Statistics	Results
Minimum	1.6 GB
Maximum	4.5 GB
Median	2.8 GB
Mean	3.1 GB
Standard deviation	1.0 GB

Table 3-1: Descriptive Statistics of Daily Data File Sizes for Two Months

At the beginning of processes, half-daily data files are read with both Pandas and Dask libraries to compare the read execution times. Daily data process duration average with Pandas is 122 seconds (2.03 minutes). The same metric for Dask is 110 seconds (1.83 minutes). On average, for daily data processing, Dask performed promisingly compared to Pandas by 12 seconds.

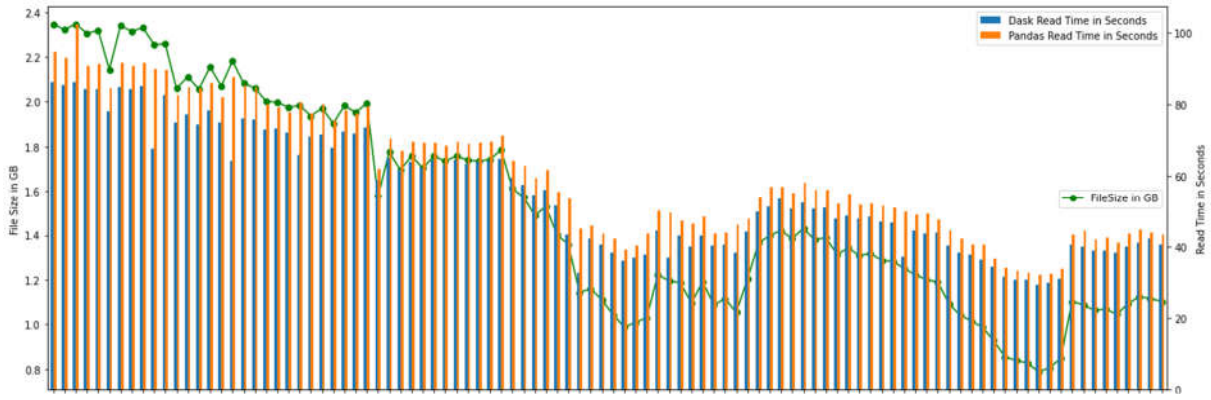

Figure 3-3: Half-Daily File Sizes and Execution Times

Figure 3-4: Process Times of Hourly Data in Minutes shows the mean of process times of hourly data in minutes around 10 minutes. Hourly data files have sizes around 0.1 to 0.2 GBs. No connection is made between file sizes and process times.

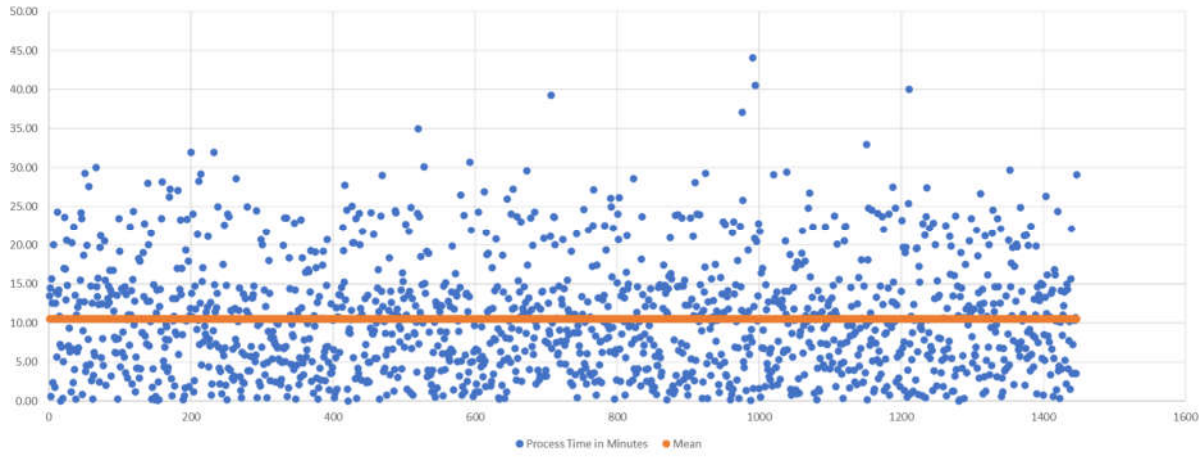

Figure 3-4: Process Times of Hourly Data in Minutes

The histogram of hourly data process times in Figure 3-5 shows that the process times are gathered around 0 to 13 minutes.

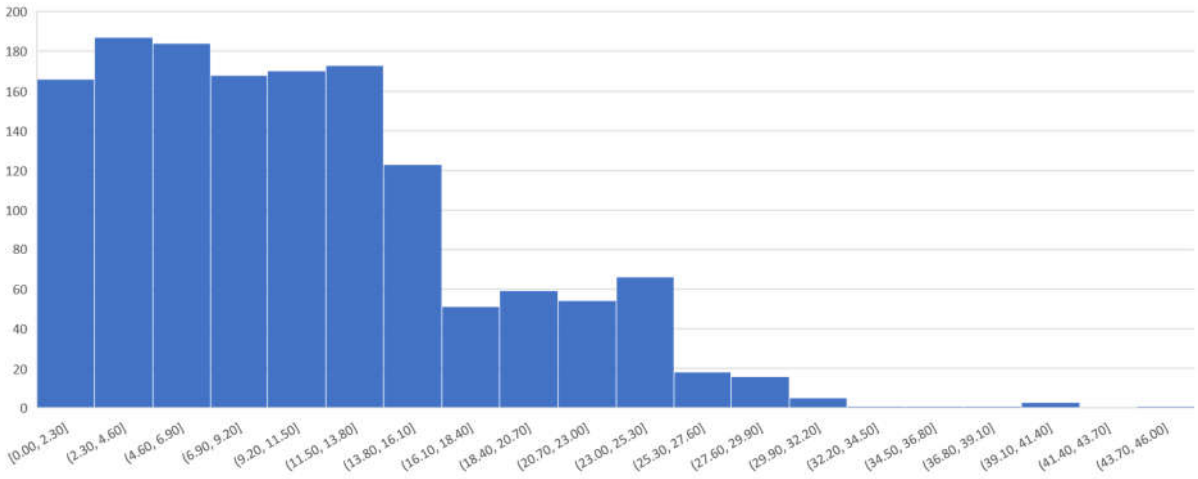

Figure 3-5: Histogram of Process Times of Hourly Data in Minutes

Tables are designed for a specific query rather than flexible tables such as tag, anchor, location data table. Every table in the columnar database must be catered for a specific query. If another data is required for reading, another query should be searching over another table. Likewise, in writing data, the data is written to the table or tables that is required to be written. There are consequences of writing the same data to multiple tables to satisfy different queries. However, it is ideal for Apache Cassandra's distributed architecture. Only one table will have to be queried. In a lot of databases that are under high load, denormalization is in the nature of best practices. The data model for location time series data is represented below. There are eight tables, each one supporting a unique data access pattern. Table vehicle_position_ts stores the distances closer than 20 feet between entities at a point in time.

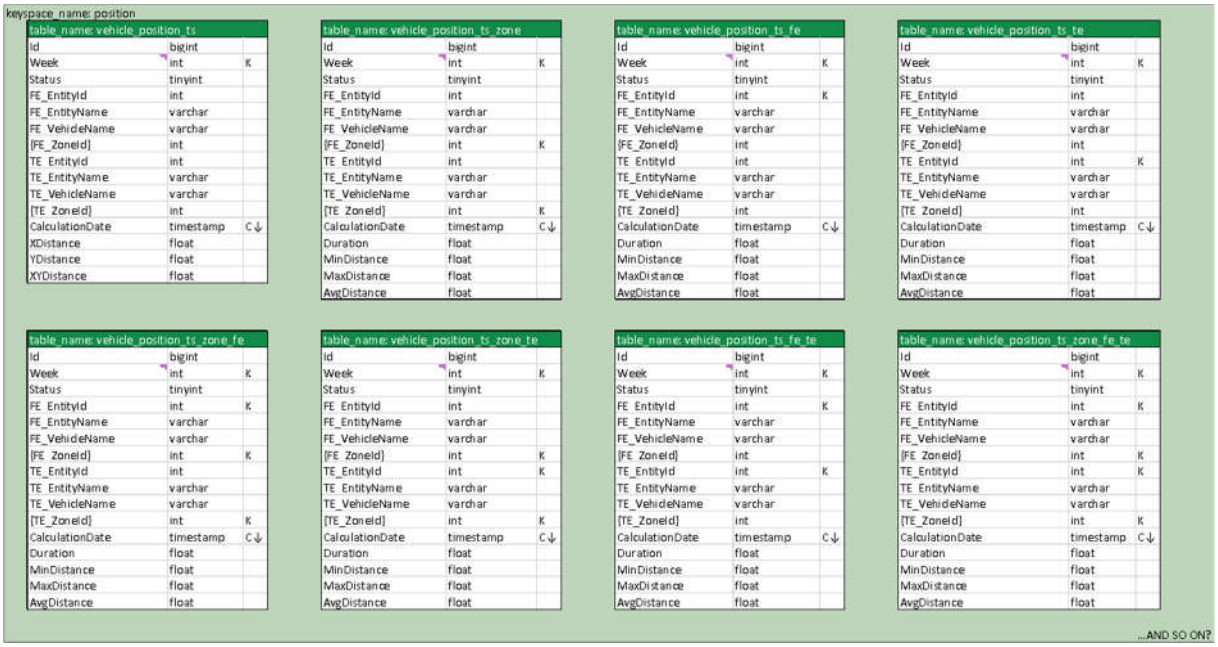

Figure 3-6: Cassandra Data Model

The remaining seven tables demonstrate the three common approaches to organizing time series data: modeling by entity; modeling by zone; and modeling by both entity and zone. While the table contents are

identical, they are intended for different report filters. They are designed to store aggregated data for a time series per partition. Aggregated data is also a time series with the resolution of duration. Then, potentially large partitions should be analyzed and optimized for performance. “Some common optimization techniques include splitting and merging partitions, data indexing, data aggregation and concurrent data access optimizations” ("Time Series Data Modeling | DataStax", 2022).

By adding column week as a partition key column, the design ensures manageable partition sizes and number of partitions.

Retrieve all violations

- from a defined vehicle
- to a defined vehicle
- with vehicle names) that are subject to the violation
- with the zones where the vehicles are
- with the minimum, maximum, average distance between vehicles
- in a defined time range
- order by the time violation happens (descending)

table_name: vehicle_position_ts_fe_te		
Id	bigint	
Week	int	K
Status	tinyint	
FE_EntityId	int	K
FE_EntityName	varchar	
FE_VehicleName	varchar	
{FE_ZoneId}	int	
TE_EntityId	int	K
TE_EntityName	varchar	
TE_VehicleName	varchar	
{TE_ZoneId}	int	
CalculationDate	timestamp	C↓
Duration	float	
MinDistance	float	
MaxDistance	float	
AvgDistance	float	

Figure 3-7: Table for Time and Entity Filters

Retrieve all violations

- with vehicles (ids, names) that are subject to the violation,
- with the zones where the vehicles are
- with the distance between vehicles
- in a defined time range
- order by the time violation happens (descending)

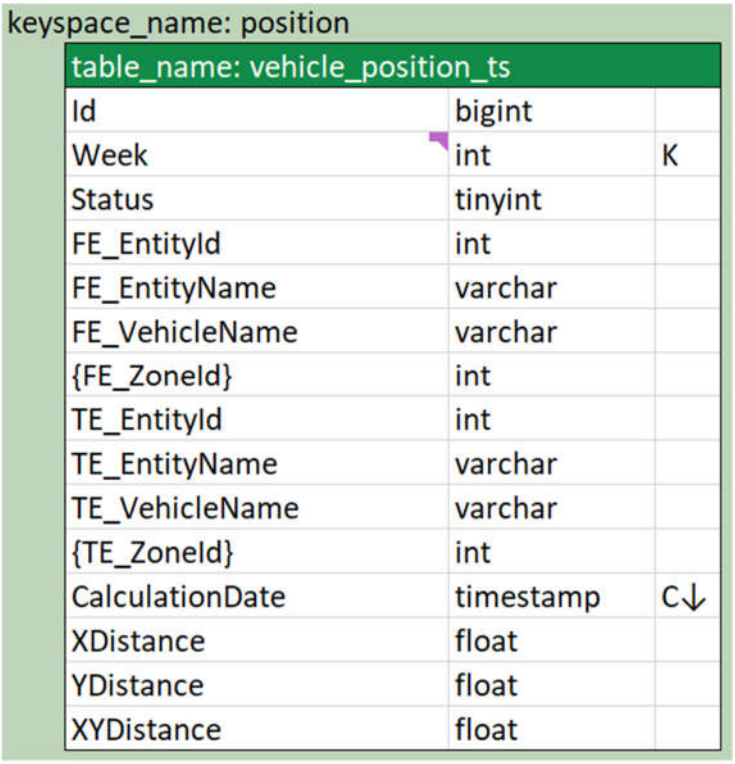

Figure 3-8: Table for Time Filter

```
SELECT *
FROM position.vehicle_position_ts
WHERE week = 26
  AND calculationdate >= '2022-07-01 00:55:00'
  AND calculationdate <= '2022-07-01 01:10:00';
```

Table 3-2: Sample CQL for Time Filter for 15 minutes

The output of batch processing, .csv files of processed hourly data, is written to a column-oriented NoSQL database Apache Cassandra. The processed hourly data file has 49175 rows and size of 0.13 GBs, on average. Apache Cassandra write time of a processed hourly data file is on average 4.38 seconds with the speed of 5026 rows/s. The magnitude of data storage is reduced to one-fifth when it is copied to Apache Cassandra without any content loss, which is also beneficial for storage areas.

The requirement for this use case is to get the vehicles' information, zone information and the distance within a defined timeframe. Moreover, the results should be in the historical order. Table 3-2: Sample CQL for Time Filter for 15 minutes can result in around 50K rows for different time frames. The execution takes 0.20 seconds on average.

By transforming to big data architecture, the volume and velocity problems that are faced within SQL databases are overcome. This is a technology agnostic solution whose components can be replaced with any alternative technology in the scope of SQL or NoSQL databases and data process tools. The case study implements the big data architecture solution for a specific query. Abundance of various queries that will be needed for new report requirements can be answered over the same architecture with new arrangements in data models of new columnar database tables.

4. CONCLUSION

The real-time location system is an answer to monitoring the status and movement of assets on the ground. Whether it is run in a production facility or needed to track down forklifts and equipment in a warehouse, the RTLS system can be advantageous. Companies looking for a better way to monitor their employees and equipment can have it with the utilization of a real-time location system.

In this research, it is studied on comparison of traditional RTLS architecture and big data RTLS architecture on read/write times and storage costs while considering overcoming the disadvantage of RDBMS in collecting data and responding to queries.

NoSQL data models are designed to query faster in line with different query parameters which store analyzed data in a column-oriented NoSQL database Apache Cassandra by using the real data of the Real-time Location System (RTLS) of Litum Inc. With the realization of big data transformation, which will also contribute to the realization of learning by data science techniques, the multi-year analytical data obtained from the raw data has been made quickly accessible via the NoSQL database.

Data is collected and transferred on a separate system, so that data abstracted from the former existing system. Therefore, more resources can be allocated for existing operational processes of RTLS software in the course of querying easily for new big data architecture. Ultimately, performance-related issues are solved.

Innovative RTLS technology is rapidly being implemented by many industries around the world. With the ability to track asset and worker movement in real-time using location monitoring equipment and software, companies are able to minimize production slowdowns, identify areas to improve and provide workers with added safety features. In these aspects, there are lots of potential future application directions of big data on the RTLS domain.

5. RECOMMENDATIONS

As part of future research directions, processing with Dask by testing different file types like Parquet and parallelism tools like Spark, implementing different use cases with the same big data architecture, implementing the requirements of other domains that the Litum serves with the same big data architecture are planned to be studied.

Therefore, it will be possible to see the validity of this big data architecture as a building block.

6. ACKNOWLEDGEMENT

Contribution provided by Ege Altıok during his Software Engineer Internship at Litum is greatly appreciated.

7. REFERENCES

Getz, A. (2022). Types of Enterprise Data (Transactional, Analytical, Master). Retrieved 10 September 2022, from https://bi-insider.com/posts/types-of-enterprise-data-transactional-analytical-master

Gubbi, J., Buyya, R., Marusic, S., & Palaniswami, M. (2022). Internet of Things (IoT): A vision, architectural elements, and future directions. Retrieved 10 September 2022, from

Phase C: Information Systems Architectures - Data Architecture. (2022). Retrieved 10 September 2022, from https://pubs.opengroup.org/architecture/togaf91-doc/arch/chap10.html

Time Series Data Modeling | DataStax. (2022). Retrieved 9 September 2022, from https://www.datastax.com/learn/data-modeling-by-example/time-series-model

What is RTLS - Real-Time Location System? | Litum. (2022). Retrieved 9 September 2022, from https://litum.com/blog/what-is-rtls-real-time-location-system-rfid/

NEW APPROACHES ON VALUE-ADDED BEE PRODUCTS; WHOLE BEE (PODMORE), BEE DRONE LARVAE (APILARNIL) AND BEEHIVE AIR APPLICATIONS

Prof. Dr. Banu YÜCEL

Ege University, Faculty of Agriculture, Department of Animal Science, Izmir/TURKIYE

ABSTRACT

Beekeeping is the ancient science of the honey bee (*Apis mellifera L.*), the most advanced social insect that has been cultivated for thousands of years and is a nature-dependent livestock activity. Even in countries where the most advanced beekeeping technique is applied, beekeeping largely depends on natural conditions such as climate and vegetation. Throughout history, the use of bee products, especially honey, for health and nutrition purposes and the scientific researches and the proof of these effects, their use has been increasing. In recent years, the production and processing of other value-added bee products other than honey has come to the fore among the important income generating activities for the beekeeper in terms of economic gain. Increasing the diversity of bee products and introducing innovative bee products to the market are not only economically attractive to beekeepers, but also raise awareness in terms of consumption of value-added bee products in importance of public health. In beekeeping, whole bee (podmore), drone larva (Apilarnil) and hive air applications have the potential to be evaluated as new approaches that can be applied within the scope of value-added bee products.

Keywords: Podmore, Apilarnil, bee hive air, honey bee, bee products.

Whole Bee (Podmore)

The whole bee (podmore) is a bee product obtained by extracting the biological contents of glands, internal organs and body parts. In its structure, chitin, heparin, heparinoid, glucosamine, melanin, acetic acid, honey, bee bread, propolis, pollen, royal jelly, apilarnil, bee venom, beeswax, melanin oil (Omega 3-6-9 and Q-10), proteins of worker and male bees. It contains carbohydrates, essential amino acids, polypeptides, flavonoids, proteins, enzymes, hormones, vitamins, fiber, sterine, polyunsaturated fatty acids, hemolymph, peptides (adolapin, melittin, MCD-peptide, apamin and protease inhibitors) (1,2). It is considered as an element of health protection and complementary therapy in apitherapy. It is important that the bees to be used for this purpose are obtained from healthy hives with organic beekeeping or good agricultural practices, especially in the spring, summer and autumn periods, and that they are fed with high quality honey and pollen in the said seasons. It is necessary to pay attention to the fact that the bees to be used in all bee production have died by physiological aging, hunger, cold, thirst, needle loss as a result of stings, and mechanical factors. All Bee production should be avoided if any synthetic drug is required to be used in the hive. Dead bees collected from the hives in summer and autumn are washed and dried in an oven at 45°C. It is important that the bees are completely free from moisture during the drying process in terms of preventing fungus production. After the whole Bee drying process, it is ground and prepared for extract production. It can be extracted in water, alcohol and oil. If it will not be extracted, it can be stored in a dry and cool place after grinding. After preparation, the whole bee must be kept in cold chain conditions and it must be determined that the people who will use it are not allergic to bee products (3).

The product has a unique smell, pH value of 6.5 and a rich biochemical structure. In properly dried bees, the organs and systems that make up the bee products are protected without being adversely affected by the heat. All Bee's; External application to the skin with conductors such as honey, oil and plant extracts allows the compounds in its content to penetrate the skin more effectively. It is recommended to be used together with propolis to strengthen the effect of the product (2,3).

The chitin in its structure prevents the formation of fat cells in the body, improves the skin, strengthens the hair structure and accelerates fat loss. Bee venom speeds up metabolism and improves the immune system. Amino acids strengthen muscles. In addition, it prevents the development of lamblia parasite (giarda lamblia) that can be found in the liver. Besides these; It balances high cholesterol and blood pressure, in wounds and burns, shows vascular opening (anticoagulant), cleans intestinal microflora, cleanses the body from toxins (antitoxic), stimulates the immune system, balances carbohydrate and lipid metabolism (hypolipidemic), reduces the risk of diabetes, radiation and severe It is used in removing metals from the body, preventing vascular lesions in the brain, preventing prostate gland inflammation (antiprostatitis), chronic lung, liver (hepatoprotective), gastrointestinal, muscle, joint and central nervous system diseases (3,4,5). It is recommended that the treatment with Whole Bee be applied by a specialist physician and in the form of a cure. It should not be used in children under the age of three, pregnant women, and people allergic to any of the bee products.

Bee Drone Larvae (Apilarnil)

Apilarnil is the 3-7 day larval stage of drone larvae before pupal stage. Apilarnil, which has very strong biological properties; It has a homogeneous, milky boza consistency, yellowish gray color and a bitter taste. It is easily adulterated and requires cold chain storage in raw form. After the larval eyes are closed, in the pupal stage, the nutrient composition of the larva changes, so it is appropriate to harvest it in the larval stage where the best quality food form is preserved. Ideally, the larvae should be at the same larval age (6,7).

Drone Larva is a bee product with a very high production potential in our country. The production and processing of this bee product will help reintegrate into the production cycle of a product that is seen as a waste material in the hive, thereby providing economic gain. The product should be harvested quickly, taking into account the temperature sensitivity, and care should be taken not to expose the larvae to direct sunlight. Before passing from the larval stage to the pupal stage, both the cleaning process is carried out and the larva harvest is carried out by giving water to the larva's eyes against the risk of defecation of the larva. If it needs to be stored until the processing stage, it should be frozen in series (-18 ºC) for this purpose. After lyophilization, which is the best processing method, the larva can be safely stored at -15ºC for 7 months. Production technique, hygiene, storage and marketing conditions significantly affect the quality of drone larvae (7,8).

In addition, the proteins, carbohydrates, fats, polyphenols, amino acids, vitamins and mineral substances in its structure determine the quality level, and the protein profile changes depending on the type of pollen consumed by the bees. The rich polyphenols in its structure enable it to have a high antioxidant capacity and show higher antioxidant properties than royal jelly (9,10).

It was determined that drone larvae showed a significant antibacterial effect on different bacteria, but was not effective on fungi. It has been found to have a very effective antibacterial effect especially on gram-positive bacteria (Bacillus aureus), but its effect on gram-negative bacteria (Escherichia coli and Pseudomonas aeruginosa) was found to be very low (11,12).

The drone larva, which triggers the release of androgenic hormones, but whose mechanism of action is not fully known, gives very successful results especially in male sexual performance (impotence), erection difficulty, premature ejaculation, sperm deficiency problems, and is sold as "natural viagra" in Far East countries (13). It is used in the treatment of insufficiency of reproductive functions and irregularities in the ovulation cycle (menstrual period) in women. As a natural anabolic stimulant in men, it increases the muscle weight in the body and promotes muscle contraction with natural methods in athletes engaged in body sports. Apilarnil, which is a powerful source that stimulates oxidative processes that cause energy production due to its strong catabolic effect in the body, prevents glycogen loss in the muscles (14,15).

Drone larva; in animal nutrition, healthy people, anorexia (due to its appetite-enhancing effect), hypoporoteinemia (protein deficiency), excessive physical and mental fatigue, development of premature children, development of intelligence and motor muscles of preschool children (due to its neurophysicochemical effect), depression, nervous system diseases (due to its neuromodulatory effect), in the treatment of Alzheimer's (due to its effect that prevents gray cell destruction in the brain), bone development problems and skeletal system diseases (bone resorption, bone tissue loss), endocrine (internal

secretion gland) disorders, insufficiency of the pituitary and adrenal glands, premenstrual pains. It is used in immune system diseases (as a biostimulant), geriatrics (due to its ability to increase the regeneration power in skin tissues), pure or lyophilized according to its chemical structure, in medicine, food and cosmetics (16,17,18,19,20).

It has been reported that the dose of use can be recommended by the physician according to the severity and type of the disease. Medical studies on its use in children are limited. In the treatment of chronic diseases, it is recommended that the patient first undergo an allergy test, then start the treatment at a low dose with the recommendation of the physician and follow a gradually increasing course. It is emphasized that it is necessary to take a break after the cure application and to avoid continuous use (21). Before the use of drone larvae, there is a great benefit in detoxing the body and increasing bioavailability in cleaning tissues and organs. Increasing blood circulation with activities such as light sports, walking, and massage will support the delivery of apilarnil's active substances to target tissues and cells (22,23).

It should not be used in case of an allergic reaction to any substance in the composition of drone larvae. If taken in high doses, digestive system complaints may occur, can cause toxicity, hyperandrogenism, hyperspermatogenesis and mild insomnia. If general discomfort, diarrhea, abdominal pain and vomiting occur after ingestion of drone larvae, its use should be avoided. It should be used under the supervision of a physician, as the wrong dose, application and interaction of methods may make the treatment negative (24).

Bee Hive Air

In bee air application, the system is the systematic and slow breathing of the air in the hive with a fan mechanism. The air in the hive is transmitted to the hose-mask by means of the fan assembly, which is prepared on the cover board and whose air flow rate can be adjusted with a regulator. Each patient breathes the air in the hive by inhalation with his own hose-mask apparatus and does not come into direct contact with the bees. The mask should be disinfected by keeping it in vinegar water once a week after each application. By breathing the warm air in the hive, very valuable components in the microclimate are taken directly into the body (25).

The presence of a healthy growing bee colony in the hive ensures the formation of a high quality microclimate. There are important volatile and aerosol-containing substances in the water vapor in the air breathed from the hive. The saturated water vapor, isoprenoids, carotenoids, terpenes and essential oils in the hive are refreshed by the bees by providing a continuous air flow. In addition, active substances in honey, pollen, beeswax, royal jelly, apilarnil and propolis in the microclimate, hormones, pheromones, phytohormones, volatile wax components, high-value alcohols, bees' mandibular gland secretions, aerosol, propolis-derived aerosol, trace elements, enzymes, choline (26).

The hives and shed where bee air will be applied should be made of natural wood material, and the hives should be placed inside the hut so that the entrance holes are open to the outside environment. The strength of the colonies, the fact that they contain individuals in different age periods, and the continuous flow of nectar and pollen to the colony are considered as factors that will help to obtain positive results from the application. In general, bee air application should be done in spring-summer seasons, in clean environmental conditions, in beehives where "good agricultural practices or organic beekeeping" is practiced. Care should be taken that the air temperature is not below eighteen degrees and that the application is not made in rainy weather. Care should be taken to limit the number of inhalations per hive per day to five patients. Before the bee air application, the patient should be informed by his doctor, a protocol should be prepared to comply with the practices during the treatment, and how the process works should be explained in detail. Supporting the application with other bee products such as honey, propolis, pollen and royal jelly during the application of bee air, adjusting the dose and duration of use by considering the physician's recommendation, provides more benefits from bee air (25,27). During the treatment application, the air in the hive should be taken rhythmically and slowly, rapid breathing should be avoided, and a fifteen-minute break should be taken between applications so that the air can be refreshed. Extremely rapid breathing can create a risk as it may cause both the blood pressure balance in the patient to deteriorate and the microclimate in which the bee colony is located to change rapidly. Patients can benefit from microclimatic changes by breathing the air in different hives in each session. In individuals who take bee air; relaxation, relaxation, uninterrupted and

quality sleep, expansion of lung capacity and accordingly comfortable breathing were detected. It has been determined that breathing half an hour of hive air twice a day for ten days in healthy individuals significantly strengthens the immune system (28).

In medicine, it is known that taking drugs by respiration (inhalation) is especially more effective. In this way, the active substances reach the target area directly. Inhaled molecules act quickly and directly. It is seen that bee air is extremely effective in diseases such as bronchitis, asthma, allergy, COPD (Chronic Obstructive Pulmonary Disease), Emphysema, Pseudocrup, immune system deficiency, migraine, depression. In various medical evaluations (attack observation, lung capacity measurement tests, blood tests, isotope measurements) made in these patients, a rapid and effective recovery course was determined (28).

Conclusion

With applications such as whole bee (podmore), drone larva (apilarnil) and bee hive air, which have just begun to be recognized in medical complementary and preventive treatment approaches in our country, but attracting attention with their promising results, it is possible for patients to regain their health with low-cost, side-effect and reliable treatment support. It is foreseen that it will be possible for people to lead a more fit and quality life. It is worth noting that these practices are "supportive" or "complementary" to modern medical treatment. These studies, which can give rational results with the partnership of multidisciplinary disciplines, need to be carried out with medical parameters that can be measured objectively on a larger number of patients and disease types, and there is a need for studies for their scientific use, especially by medical doctors. For the production of such innovative bee products that will be needed, it is necessary to organize trainings for beekeepers to make special production practices with the contracted production model, and to carry out studies for the determination and standardization of product quality by universities, ministries, research institutions and legal authorities.

Literature

1) **Kirilov, N.** 2007. Pçelnite produkti, hirana i leçebna sila. İzdatelstvo Enyoçe, 108-110.

2) **Anonim**, Erişim: http://great-beemaster.blogspot.com.tr/p/podmore.html Erişim Tarihi: 15.06.2017

3) **Anonim**, Erişim: http://symptomms.com/en/pages/1579307 Erişim Tarihi: 15.06.2022

4) **Anonim**, Erişim: http://menportals.com/en/pages/1471471 Erişim Tarihi: 15.06.2022

5) **Anonim**, Erişim: http://mymedinform.com/others/application-bee-podmore.html Erişim Tarihi: 15.06.2017

6) **Barnutiu, L.I.** 2013. Biological properties evaluation of the quality markers from royal jelly and apilarnil. University of Agricultural Sciences and Veterinary Medicine, Faculty of Animal Husbandry and Biotechnologies (PhD Thesis), Cluj-Napoca/Romania; 55.

7) **Bărnuţiu, L. I., Mărghitaş, L. A., Dezmirean, D., Bobiş, O., Mihai, C., Pavel, C.** 2013. Physicochemical composition of Apilarnil (bee drone larvae). Lucrări Ştiinţifice-Seria Zootehnie, 59: 199-202.

8) **Cornoiu, I.** 1995. Din produsele stupului Laptisorul de matca si Apilarnilul (Test de verificare a cunostintelor). Apicultura in Romania, 8: 30.

9) **Iliesiu, N.V.** 1975. A new biostimulating and energizing product on the basis of bee products, 25 th Apimondia Congress, Grenoble – France, 224-5.

10) **Iliesiu, N.V.** 1980. Apilarnil, The 8th biologically active bee product. Apicultura in Romania, 12: 4.

11) **Ioyrish, N., Derevici, A., Petrescu, A.** 1965. Virulicidal action in vitro of alcoholic extracts of drone larvae and propolis. Lucr. Stiint. ale Statiunii de Cercetari Apicole si Sericicole: 5 : 107-10.

12) **Kogalniceanu, S., Lancrajan, I., Ardelean, G.** 2010. Changes of the glucidic metabolism determined by the physical effort of the treatment with the Aslavital and Apilarnil. Arad Medical Journal, 3: 33-41.

13) **Drugeanu, C.** 1989. Rezultate obþinute în tratamentul cu “Apilarnil-potent” a tulburarilor de dinamicã sexualã. Apicultura in Romania, 10: 21.

14) **Iliesiu, N.V.** 1991. Apilarnil, Health, Strength and Longevity. Apimondia Publishing House.

15) **Iliesiu, N.V.** 1993. Preparation based on medicinal plants, bee products, apilarnil and pollen. Apicultura in Romania, 1: 8.

16) **Cosman, D., Iliesiu, N.V., Moldovan, O.** 1984. The efficacy of neurosis treatment with Apilarnil. Apicultura in Romania, 3: 21-4.

17) **Iliesiu, N.V.** 1993. Apilarnil lyophilised in honey. Apicultura in Romania, 3: 23.

18) **Iliesiu, N.V.** 1993. A bio-stimulative and dieto-therapeutic product” Apivitas-Forte". Apicultura in Romania, 4: 8.

19) **Iliesiu, N.V.** 1987. Contribution of Apilarnil and Apitotal N.V.I. to the strengthening of natural defensive factors of the body with special reference to the immune system. Apicultura in Romania, 10: 17-20.

20) **Speteanu, R., Cismaru, S., Iliesiu, N.V.** 1984. Apilarnil, an active compound in cosmetic products. Apicultura in Romania, 4: 23-4.

21) **Matsuka, M., Watabe, N., Taceuchi, K.** 1973. Analysis of the food of larval drone honeybees. Journal of Apicultural Research, 12: 3-7.

22) **Okada, I., Matsuka, M.** 1973. Artificial rearing of Harmonia axyridis on pulverized drone honey bee brood. Environ Entomol, 2: 301-2.

23) **Stangaciu, S.** 2002. Bee products and their medicinal uses. Honeybee Science, 23 (3): 97-104.

24) **Yücel, B., Kösoğlu, M. 2005.** Apiterapi’de Apilarnil. Arı Ürünleri ve Sağlık (Apiterapi). Sidas Yayınevi.

25) **Musch, H.** 2014. ApiAir – Die Bienenlufttherapie. Ochsenhausen, 15.

26) **Bengsch, E.** 2014. Studie über potenzial der biomedizinischen wirksamkeit von inhalierter bienenluft. Max Planck-Institute, 4.

27) **Uccusic, P.** 1985. Bienenprodukte: Ihre Heilkraft und Anwendung. Ariston Verlag.

28) **Yücel, B., Ceylan, H.** 2015. Arı (Kovan) Havası ve Sesi’nin Apiterapi’de Kullanımı. Arı Ürünleri ve Sağlık (Apiterapi). Sidas Yayınevi.

SINGULAR INTEGRAL OPERATOR IN SPACES DEFINED BY GENERALIZED OSCILLATION

1. Lala R. Aliyeva
Institute of Mathematics and Mechanics of NAS, Baku, Azerbaijan,
ORCID ID: https://orcid.org/0000-0002-5380-4841
2. Rahim M. Rzaev
Azerbaijan State Pedagogical University, Baku, Azerbaijan.

ABSTRACT

Let R^n be an n-dimensional Euclidean space of points $x=(x_1,x_2,\dots,x_n)$, $B(a,r):=\{x\in R^n:|x-a|\le r\}$ be closed ball in R^n of radius $r>0$ centered at the point $a\in R^n$, N be a set of all positive integers, $\nu=(\nu_1,\nu_2,\dots,\nu_n)$, $x^\nu=x_1^{\nu_1}\cdot x_2^{\nu_2}\cdots x_n^{\nu_n}$, $|\nu|=\nu_1+\nu_2+\dots+\nu_n$, where $\nu_1,\nu_2,\dots,\nu_n$ are non-negative integers. By $L_{loc}(R^n)$ we denote a totality of all locally summable functions in R^n. Let $f\in L_{loc}(R^n)$, $k\in N\cup\{0\}$. Consider the polynomial

$$P_{k,B(a.r)}f(x):=\sum_{|\nu|\le k}\left(\frac{1}{|B(a,r)|}\int_{B(a,r)}f(t)\phi_\nu\left(\frac{t-a}{r}\right)dt\right)\phi_\nu\left(\frac{x-a}{r}\right).$$

where $|B(a,r)|$ denotes the volume of the ball $B(a,r)$ and $\{\phi_\nu\}$, $|\nu|\le k$, is an orthonormal system obtained by applying orthogonalization process with respect to the scalar product $(f,g):=\frac{1}{|B(0,1)|}\int_{B(0,1)}f(t)g(t)dt$ to the system of power functions $\{x^\nu\}$, $|\nu|\le k$.

Denote by Ψ the class of all positive monotonically increasing functions $\phi(t)$ on $(0,+\infty)$ such that $\phi(+0)=0$. By definition, we will consider the function $\phi(t)\equiv 1$ also as an element of the class Ψ. By Ψ_k we denote the totality of all functions $\phi\in\Psi$ such that the function $\phi(t)\cdot t^{-k}$ is almost decreasing.

Let $\alpha>0, r>0,$ and let

$$\Phi^{(\alpha)}(x)=c_n^{(\alpha)}\cdot\frac{1}{1+|x|^{n+\alpha}},\quad \Phi_r^{(\alpha)}(x)=r^{-n}\Phi^{(\alpha)}\left(\frac{x}{r}\right),$$

where $c_n^{(\alpha)}$ is chosen in such a way that $\int_{R^n}\Phi^{(\alpha)}(x)dx=1$.

For the function $f\in L_{loc}(R^n)$ we denote

$$\Omega_{k,\alpha}\big(f,B(x;r)\big):=\int_{R^n}\Phi_r^{(\alpha)}(x-t)\big|f(t)-P_{k-1,B(x,r)}f(t)\big|dt\ \ (x\in R^n,\ r>0),$$

$$H_f^{k,\alpha}(\delta):=sup\big\{\Omega_{k,\alpha}\big(f,B(x,r)\big):\ 0<r\le\delta,\quad x\in R^n\big\},\quad \delta>0.$$

Let $f\in L_{loc}(R^n)$, $\alpha>0$, $k\in N$, $\phi\in\Psi_k$. We will also use the following notations:

$$A_{\phi,\theta}^{k,\alpha}(f):=\left(\int_0^\infty\left(\frac{H_f^{k,\alpha}(t)}{\phi(t)}\right)^\theta\frac{dt}{t}\right)^{1/\theta}\quad\text{for}\quad 1\le\theta<\infty,\ A_{\phi,\infty}^{k,\alpha}(f):=sup\left\{\frac{H_f^{k,\alpha}(t)}{\phi(t)}:\ t>0\right\}.$$

Let $\phi\in\Psi_k$, $k\in N$, $1\le\theta\le\infty$, $\alpha>0$, $k<\alpha+1$. By $HO_{\phi,\theta}^{k,\alpha}$ we denote the collection of all functions $f\in L_{loc}(R^n)$ such that $A_{\phi,\theta}^{k,\alpha}(f)<+\infty$. It is easy to see that $HO_{\phi,\theta}^{k,\alpha}$ is a linear pace.

In this class, we introduce the norm by the equality $\|f\|_{HO_{\varphi,\theta}^{k,\alpha}} := A_{\phi,\theta}^{k,\alpha}(f)$.

Let μ be a positive number. By Z_μ we denote the collection of all functions $\phi \in \Psi$ such that $\delta^\mu \int_\delta^\infty \frac{\phi(t)}{t^{\mu+1}} dt = O(\phi(\delta)), \quad \delta > 0$. In what follows, by $(\boldsymbol{\alpha})$ we denote the maximum integer smaller than $\boldsymbol{\alpha}$.

Consider a singular integral operator

$$A_k f(x) = \lim_{\varepsilon \to +0} \int_{R^n} \left\{ K_\varepsilon(x-y) - \left(\sum_{|\nu| \le k-1} \frac{x^\nu}{\nu!} D^\nu K(-y) \right) X_{\{|t|>1\}}(y) \right\} f(y) dy,$$

where $K(x) = \omega(x) \cdot |x|^{-n}$, $\int_{S^{n-1}} \omega(x) ds = 0$, $K_\varepsilon(x) = K(x) \cdot X_{\{|t|>\varepsilon\}}(x)$, $\omega(x)$ is a homogeneous function of power 0, $X_{\{|t|>\varepsilon\}}$ is the characteristic function of the set $\{t \in R^n: |t| > \varepsilon\}$, and S^{n-1} is a unit sphere in the Euclidean space R^n. Assume that, for $k = 1$, the function $K(x)$ is differentiable and has bounded partial derivatives of the first order and, for $k > 1$ the function $K(x)$ is k times differentiable on the sphere S^{n-1}; $v = (v_1, v_2, \dots v_n)$, $v_1, v_2, \dots, v_n$ are nonnegative integers, $|v| = v_1 + v_2 + \dots + v_n$, $v! = v_1! \, v_2! \dots v_n!$ $k \in N$, $D^v f := \frac{\partial^{|v|} f}{\partial x_1^{v_1} \partial x_2^{v_2} \dots \partial x_n^{v_n}}$.

Theorem. *Suppose that* $\alpha > 0$, $k \in N$, $k < \alpha + 1$, $1 \le \theta \le \infty$, $\mu = min\{\alpha, k\}$, $\phi \in Z_\mu$. *Then the operator* A_k *boundedly acts in the space* $HO_{\phi,\theta}^{k,\alpha}$.

Keywords: singular integral, integral operator, Euclidean space

DEVELOPMENT OF OZONE EFFECTING SYSTEM WITHOUT USING HARMFUL CHEMICALS

İrem PALABIYIK[1]

[1]FG Tekstil Konfeksiyon San. Tic. A.Ş. / R&D Center, İzmir, Turkey.

[1]https://orcid.org/0000-0003-4707-2362

Özgür BULUT [2]

[2] FG Tekstil Konfeksiyon San. Tic. A.Ş. / R&D Center, İzmir, Turkey.

[2]https://orcid.org/0000-0001-8160-4049

ABSTRACT

Denim fabric is a kind of woven fabric, which is mainly made of cotton fiber, and it is also produced from fibers such as polyester, elastane, linen, viscose. Formerly denim products were only desizing and sold with no washing process. Denim products had a stiff hand feeling. The effects and coloration on garment occurred by the wear of indigo dyestuffs, in which the warp yarn was dyed, over time during the use of the denim product. That is why denim products have acquired a special appearance after a long period of using and washing. Over time the demand for used appearance denim products has increased. Garment denim products began to undergo bleaching processes at washing plants. Denim washing processes are aimed at giving the products effects and color. The bleaching process is applied to achieve lighter color on garment denim product. This process is applied to achieve lighter color that cannot be achieved using pumice stones or enzymes. At this step, by various methods and chemicals, the indigo fabric acquires the requested color. In addition to the traditional methods, ozone bleaching, which is a sustainable method, is very important for denim garment products. Ozone as for that, is a compound consisting of three oxygen atoms and has a higher energy than atmospheric oxygen. Ozone is an oxidative substance and its redox potential is higher than that of hydrogen peroxide. Thanks to this oxidation property of ozone gas indigo molecules of denim fabric are degraded quickly. Achieved effects in traditional denim bleaching can be achieved with ozone gas and without any harmful chemicals. While there is excess water consumption for traditional denim washing, ozone bleaching system needs far fewer water and reuse of ozone bleaching wastewater is possible. With this study, it is aimed to save water and energy by ozone bleaching method compared to traditional bleaching method in denim products.

Keywords: Denim Bleaching, Ozone, Giving Effect

VULNERABILITY ASSESSMENT OF SERVER WITH SHODAN QUERY

Ahmet Ali Süzen[1*]

[1]Isparta University of Applied Sciences, Faculty of Technology, Computer Engineering, Isparta, Turkey.

[1*]ORCID ID: https://orcid.org/0000-0002-5871-1652

Remzi Gürfidan[2]

[2]Isparta University of Applied Sciences, Yalvaç Technical Sciences Vocational School, Isparta, Turkey.

[2]ORCID ID: https://orcid.org/0000-0002-4899-2219

ABSTRACT

The widespread use of IT assets also expands the attack surface that attackers exploit. Especially software-related vulnerabilities are the most preferred type of vulnerability by cyber attackers. The vulnerability of a system or application to cyber-attacks is called vulnerability. If a vulnerability is detected, it must be publicly announced and published by a specific authority. CVE (Common Vulnerabilities and Exposures) is known as the international vulnerability dictionary organized by MITER. A detected vulnerability receives a vulnerability number starting with CVE and is published on the web. There is also an NVD (National Vulnerability Database) vulnerability database that works simultaneously with the CVE. Shodan; It is an internet of objects search engine developed to make queries such as vulnerabilities, ports, locations on servers, applications and devices connected to the internet. Shodan's robots scan IP ranges periodically and index the results.

In this study, the risks and vulnerabilities of the servers were evaluated with the queries made using Shodan APIs. First, the server operating system (Windows Server, Ubuntu, Debian, Centos) query was performed on server IPs indexed by Shodan. In the second stage, vulnerable servers were detected by scanning for previously discovered vulnerabilities on the ports and services of the servers. In order to detect undiscovered vulnerabilities or potential configuration errors, risky servers with open remote desktop connection ports (Remote Desktop Connection, Secure Shell, etc.) and login page detected have been extracted. CVE and NVD database records were used to detect vulnerabilities. In line with the findings a risk assessment was made and solution, suggestions were presented for potential threats.

Keywords: Shodan, Server, Vulnerability.

INTRODUCTION

A vulnerability can be defined as a live system or software that can be made open to manipulation by unauthorized malicious attackers, malicious software, or cyber-attacks, or the service is interrupted [1]. All transactions performed by vulnerable systems are at risk. Data security and transaction security are at the forefront of these risks. These risks cause serious financial losses and legal liabilities.

One of the phrases describing vulnerabilities for cyber attackers to attack systems is the term zero-day. Zeroday is a term denoting that the victim has zero days to be safe from attack [2]. Targets in zero-day vulnerabilities include operating systems, web browsers, office applications, software, and IoT devices [3]. There are a few basic methods that can be followed to be protected from these attacks. These can be listed as keeping the software and operating systems up-to-date, keeping the firewall constantly active, and using up-to-date antivirus software.

CVE (Common Vulnerabilities and Exposures) is a dictionary structure for categorizing and informing about vulnerabilities that are accessible to everyone. The CVE dictionary is freely available to the public, and there are data stores about vulnerabilities in this structure. Among these data warehouses, there is a free-access data warehouse open to everyone and working simultaneously with the CVE dictionary named NVD (National Vulnerability Database) [4]. This database contains detailed information about vulnerabilities. Vulnerability scores calculated for vulnerabilities are also included in the NVD. A vulnerability score can be thought of as points awarded to a vulnerability over metrics. A high score indicates that the threat is a potential danger.

The most effective method used to eliminate vulnerabilities is penetration testing. After the completion of the in-house IT structuring, penetration tests are performed to identify possible risks and threats. According to the penetration test reports, the institution can go to IT again. However, penetration tests are performed once a year on average, which is too late for information technologies [5]. Therefore, IT personnel in the institution should perform daily, weekly, and monthly security checks. Especially the discovered vulnerabilities of the systems they use in server and web services is a process that needs to be taken daily action [6]. Servers are hardware structures that enable many users, such as web systems, to operate simultaneously and to use many services simultaneously. There are many systems and file types with different capabilities in the servers. Data such as databases, e-mail records, corporate documents, and accounting and finance documents, which are generally located on servers, are considered sensitive data for the institution.

Shodan (Sentient-Hyper-Optimized-Data-Access-Network) is known as the internet of things search engine [7]. Shodan indexes software and systems connected to the Internet. These systems include switches, routers, servers, cameras, operating systems, services, ports, etc. is located [8-9]. It can also scan for vulnerabilities of systems and software that occur at certain periods.

In order to instantly detect the possible risks of general information systems, in this study, the possible risks and threats of the servers were detected and examined via Shodan. Server operating systems on the servers were determined and port/service discovery of these operating systems was made. Afterward, the weaknesses in these results were evaluated. The main purpose of this study is to draw attention to existing server vulnerabilities and to contribute to the detection of vulnerabilities of instant information assets of institutions.

PREPARING SHODAN QUERIES

Shodan allows querying both from within its own web application and via the developer API and command-line interface (CLI). In this study, queries are performed via CLI. For this, shodan was installed with the command *"pip install -U --user shodan*". In order to query shodan queries via CLI, API KEY must be obtained in the web application and triggered with the "*shodan init YOUR_API_KEY*" command. In the next step, the scope of shodan queries must be created via the CLI. Since the scope of work includes server vulnerabilities, the operating systems running on the server were determined as given in Table 1, among the results that came with the country:TR query in order to extract frame queries.

Table 1. Server operating systems in Shodan

Operating System
Windows Server
Ubuntu
Debian
Unix
CentOS

In the second stage, each operating system determined in Table 1 was filtered with the country:TR + os:"OS_Name" query. Each server is separated as web, mail, application, and storage in terms of the service it offers and uses service/port accordingly. With Shodan queries, the open/closed ports on the servers and the

service version used are determined. At the same time, information can be obtained on whether the services have detected vulnerabilities or not. The generally preferred port of the service on the servers is between 0 and 65535. IT staff can sometimes change the services used on certain ports. For example, Secure Shell (SSH) protocol port 22 is used for remote control of servers. In some security configurations, this port address can be changed to 2222,2223,2323. Therefore, in some scenarios, the service name is preferred instead of the port address in queries. In Table 2, examples of service queries made separately for each operating system are given.

Table 2. Operating system specific queries

Shodan Query Samples	Output
country:tr os:"Ubuntu" product:"OpenSSH"	OpenSSH Detection
country:tr os:"Windows Server 2012 R2" port:3389	Remote Desktop Protocol Detection
country:tr os:"Debian" product:"OpenSSH"	OpenSSH Detection
country:tr has_vuln:true	Vulnerable Detection
country:tr os:"Debian" product:"OpenSSH" has_screenshot:true	OpenSSH Screenshot Detection
country:tr os:"Windows Server 2012 R2" port:3389 has_screenshot:true	Remote Desktop Protocol Screenshot Detection

ASSESSMENT OF SERVER VULNERABILITIES

In the first step, after the server evaluation scope of Turkey and the shodan queries were determined, the queries were run in the CLI and the results were evaluated in this section. A total of 220,137 systems appear to use a previously discovered vulnerability. Figure 1 gives a list of vulnerabilities that have previously received CVE numbers and are most commonly used in Turkey. As can be seen, the most vulnerable system usage belongs to the vulnerabilities detected in 2022. When the query results are examined, it has been determined that it was used in the vulnerabilities of 2006 and 2007, albeit in a small number (1,500).

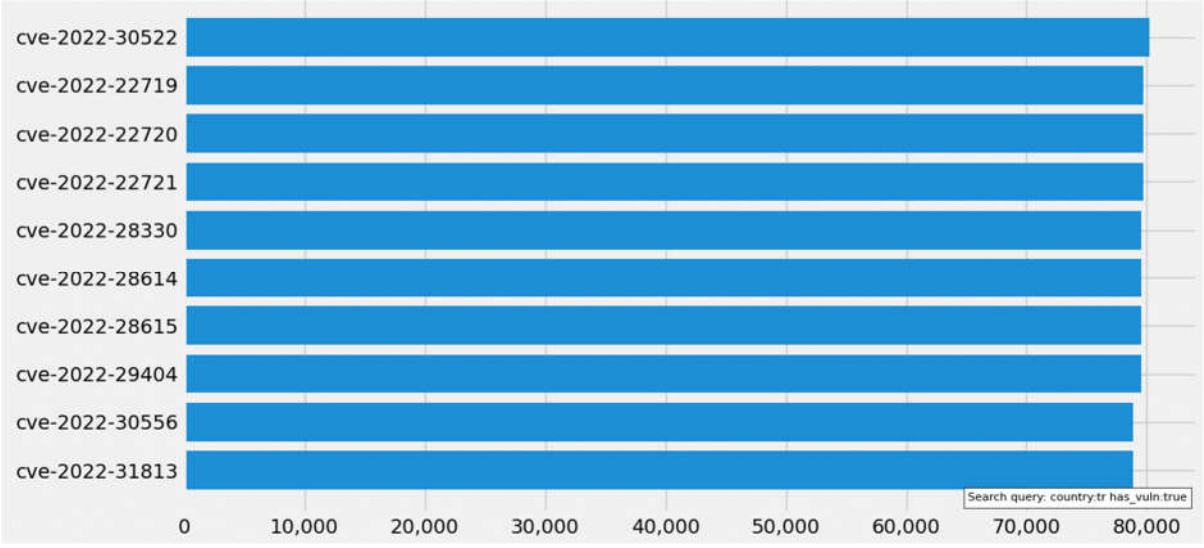

Figure 1. Top ten representations of the most used verified vulnerabilities

In Figure 2, the distribution of the discovered vulnerabilities according to the applications running on the server is given. Apache HTTP, which is open source code that runs on all server operating systems and is used as an HTTP server, has the most vulnerable use. Considering that many web pages are hosted on Apache servers, it is seen that web pages are at serious risk. OpenSSH, which is used to remotely control the server, comes second in the use of vulnerable systems, and Microsoft IIS, which is used as a web server in

Windows Server operating systems, comes in third place. As a result of the findings obtained as a result of the query, it is predicted that the vulnerabilities of the applications used on the servers are not monitored periodically and there are update delays.

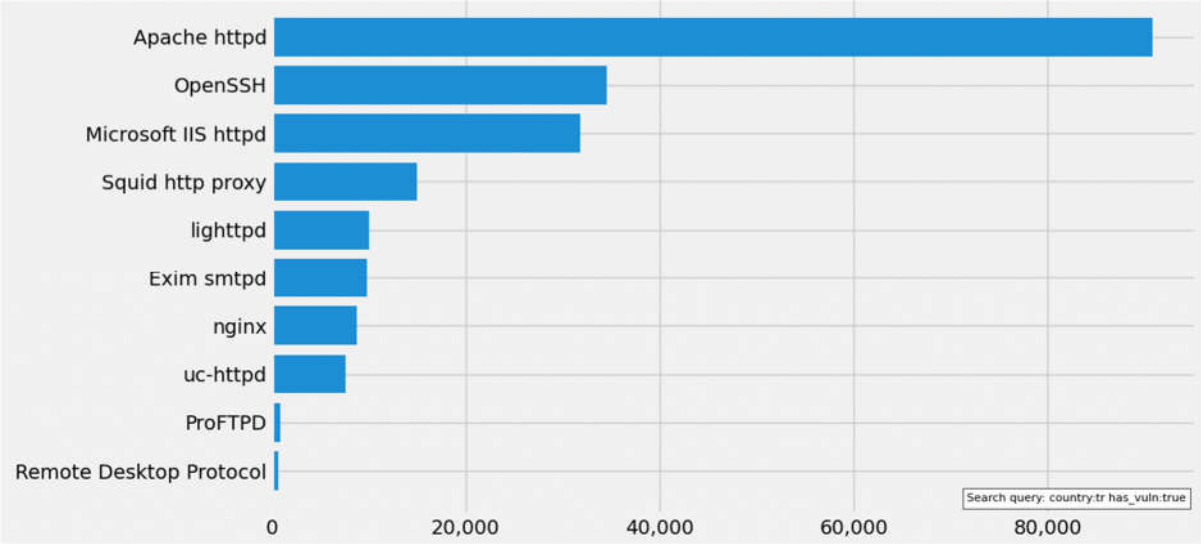

Figure 2. Application-based vulnerability usage used in servers

In Figure 3, the port type representation of vulnerable uses is given. Applications or protocols running on the server usually use fixed ports for their purpose. It is possible to change these ports as a security measure during the server configuration phase. Web servers using HTTP and HTTPS protocols use ports 80 and 443 in the standard. As it provides a secure connection between server-client in web server security configurations, HTTPS provides a connection from port 443. It is also directed to the HTTPS protocol on port 80 with HTTP connections. In this way, it is aimed to provide a secure connection. When Figure 3 is examined, it is seen that port 80 is the most vulnerable usage. The most important reason for this is that the secure port forwarding has not been configured. Although port 443 aims to provide a secure connection, it is seen that the vulnerabilities experienced in the applications given in Figure 2 pose a risk.

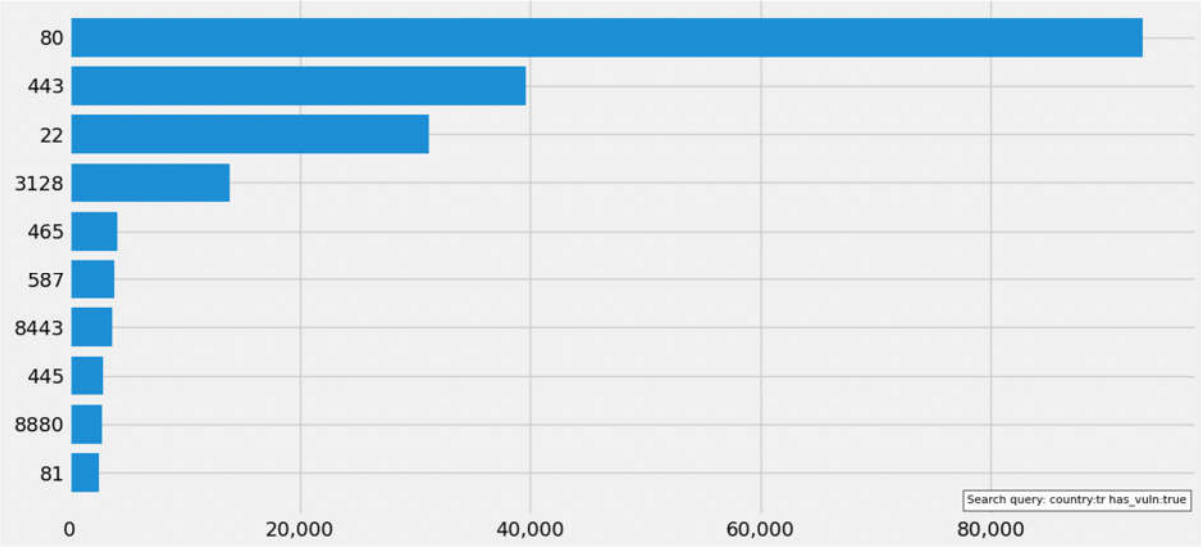

Figure 3. Port-based use of vulnerable systems

CONCLUSION

A potential attacker selects the system to attack, either on a targeted basis or randomly from search engines such as Shodan. The most important phase of the attack phase is the active and passive information gathering processes. Especially in terms of data and function, servers are the most vulnerable IT assets. In this study, the vulnerabilities of servers located in Turkey were evaluated through the Shodan search engine. As a result of the queries made on the CLI screen, it is seen that the updates of the discovered vulnerabilities are not made periodically and the necessary security measures are taken. In particular, versions of vulnerabilities experienced in applications on servers used as web servers are used extensively. Although the density in the vulnerability assessment belongs to 2022, the use of a vulnerability list that started in 2006 is seen. For web-based operations, it is not enough to have the operating system up-to-date in server use and the vulnerabilities of service/protocol applications serving on the server should be monitored periodically. In this context, it is an important precaution for IT personnel to check the indexing of server IP addresses or domain addresses in Shodan.

REFERENCES

[1]. Adger, W. N. (2006). Vulnerability. Global environmental change, 16(3), 268-281.
[2]. İlker, K. A. R. A. (2019). Kaba Kuvvet Saldırı Tespiti ve Teknik Analizi. *Sakarya University Journal of Computer and Information Sciences*, *2*(2), 61-69.
[3]. Ablon, L., & Bogart, A. (2017). *Zero days, thousands of nights: The life and times of zero-day* vulnerabilities *and their exploits*. Rand Corporation.
[4]. Yosifova, V., Tasheva, A., & Trifonov, R. (2021, May). Predicting vulnerability type in common vulnerabilities and exposures (CVE) database with machine learning classifiers. In *2021 12th National Conference with International Participation (ELECTRONICA)* (pp. 1-6). IEEE.
[5]. Bacudio, A. G., Yuan, X., Chu, B. T. B., & Jones, M. (2011). An overview of penetration testing. International Journal of Network Security & Its Applications, 3(6), 19.
[6]. Carley, S., Evans, T. P., Graff, M., & Konisky, D. M. (2018). A framework for evaluating geographic disparities in energy transition vulnerability. *Nature Energy*, *3*(8), 621-627.
[7]. Shodan (2022). Access Link: https://www.shodan.io/ Access Date: 15.08.2022.
[8]. Al-Alami, H., Hadi, A., & Al-Bahadili, H. (2017, December). Vulnerability scanning of IoT devices in Jordan using Shodan. In *2017 2nd International Conference on the Applications of Information Technology in Developing Renewable Energy Processes & Systems (IT-DREPS)* (pp. 1-6). IEEE.
[9]. Ercolani, V. J., Patton, M. W., & Chen, H. (2016, September). Shodan visualized. In *2016 IEEE conference on intelligence and security informatics (ISI)* (pp. 193-195). IEEE.

YENİ NESİL SERVO SÜRÜCÜLER İLE ROBOTİK UYGULAMALAR İÇİN DOĞRUSAL EKSEN KONTROLÜNÜN GERÇEKLEŞTİRİLMESİ

REALIZING LINEAR AXIS CONTROL FOR ROBOTIC APPLICATIONS WITH NEXT GENERATION SERVO DRIVES

Mustafa Feyzi TEMEL[1]

[1]Karabük Üniversitesi, Teknoloji Fakültesi, Mekatronik Mühendsiliği, Karabük, Türkiye.

[1]ORCID ID: https://orcid.org/0000-0001-5867-3951

Raif BAYIR [2]

[2] Karabük Üniversitesi, Teknoloji Fakültesi, Mekatronik Mühendsiliği, Karabük, Türkiye.

[2]ORCID ID: https://orcid.org/0000-0003-3155-8771

ÖZET

Endüstride ve robotik uygulamalarda fırçasız doğru akım motorları yüksek hassasiyet, dinamik yük değişikliği, verimleri, hız ve konum kontrolleri nedeniyle sıklıkla tercih edilmektedirler. Özellikle robot kollarda, medikal cihazlarda, hassas dozajlama makinelerinde ve elektrikli araçlar gibi sistemlerde kullanılmaktadırlar. Bu motorlarda en çok karşılaşılan zorluklardan biri motor sürücüsü ile bu motorların kapalı çevrim çalıştırılmasıdır. Bu çalışmada, fırçasız doğru akım motorun konuma bağlı hız kontrolü Siemens S7-1500 Programlanabilir Mantık Denetleyicisi (PMD) ile yapılmıştır. Motor sürücüsü olarak Siemens'in yeni nesil sürücülerinden Sinamics S120 servo motor sürücüsü tercih edilmiştir. Deneysel çalışmada fırçasız doğru akım motor hız, konum ve ivme kontrolü talep edilen referansa göre kontrol edilebilmektedir. Nümerik eksen kontrolünde ve robotik uygulamalarda bu sürücü ve motorların kullanılabilirliğini mümkün kılmaktadır. Robot kollarda doğrusal ve dönel eksenlerde bu sürücü ve denetleyicinin rahatlıkla kullanılabileceği görülmüştür. Sonuç olarak endüstride farklı kinematik konfigürasyonlarda robotik uygulamaları rahatlıkla gerçekleştirilebilir.

Anahtar Kelimeler: Servo Sürücü, PLC, Eksen Kontrolü, PID

ABSTRACT

The brushless direct current motors are frequently preferred in industry and robotic applications due to their high sensitivity, dynamic load change, efficiency, speed and position controls. Especially, they are used with robot arms, medical devices, precision dosing machines and electric vehicles etc. One of the most encountered difficulties in these motors is the closed-loop operation of these motors with the motor driver. In this study, position-dependent speed control of brushless direct current motor is made with Siemens S7-1500 Programmable Logic Controller (PLC). The motor driver of Siemens firm Sinamics S120 servo motor driver was preferred as a motor driver. In the experimental study, brushless direct current motor speed, position and acceleration control can be controlled according to the requested reference. This enables the usability of drives and motors in numerical axis control and robotic applications. It has been seen that this driver and controller can be used easily in linear and rotary axes in robot arms. As a result of this, robotic applications can be easily realized in different kinematic configurations in the industry.

Keywords: Servo Dirver, PLC, Axis Control, PID

BİR BOBİN SİLAHINDA MERMİ ÇIKIŞ HIZINI ETKİLEYEN FAKTÖRLER

FACTORS AFFECTING BULLET OUTPUT SPEED IN A COILGUN

Sabri BIÇAKÇI[1]

[1]Balıkesir Üniversitesi, Mühendislik Fakültesi, Elektrik -Elektronik Mühendisliği Bölümü, Balıkesir, Türkiye.

[1]ORCID ID: https://orcid.org/0000-0002-2334-8515

ÖZET

Klasik silahlarda merminin namludan çıkış hızının değiştirilmesi ancak üretim esnasında sağlanabilmektedir. Burada mermideki barut miktarı ve mühimatın depolama süreçleri en önemli unsurlardır. Bobin silahında ise mermi hızlandırma işlemi sıralı stator bobinleri üzerine uygulanan anlık değişken akımlarla sağlandığından mermi çıkış hızı üretim sürecinden bağımsızdır. Bir bobin silahının güç elektroniğinde kondansatör, tristörler önemli yer tutmaktadır. Hız ölçümü için genelde optik sensörler kullanılmaktadır. Optik sensörlerdeki durum değişikliği hem hız bilgisini hem de bir sonraki bobinin ateşleme zamanını belirlemektedir. Bu işlemler geliştiriecek bir yazılım ile bilgisayar ya da MyRIO gibi platformlarla sağlanmaktadır. Bir bobin silahında mermi çıkış hızı, anlık akımın genliği ile uygulanma süresine ve merminin hangi konumdayken uygulandığına bağlıdır. Akımın genliği ve uygulama süresi ise kondansatörün yük depolama kapasitesi ile bobinin geometrisi, indüktansı ve elektrik direnciyle ilişkilidir. Bununla birlikte optik sensörlerin ve tristörlerin tepki süreleri ile yazılımın işletim süresi de uygun ateşleme noktasını değiştirmektedir. Bu bildiri kapsamında bir bobin silahında mermi çıkış hızının etkileyen parametreler ayrıntılı bir şekilde incelenek ve mermi çıkış hızının iyileştirilmesi noktasında yapılması gerekenler ayrıntılı olarak tartışılacaktır.

Anahtar Kelimeler: Bobin Silahı, Mermi, Stator, Optik sensör, Hız

ABSTRACT

In conventional weapons, changing the muzzle velocity of the bullet can only be achieved during production. Here, the amount of gunpowder in the bullet and the storage processes of the ammunition are the most important factors. In the coil gun, on the other hand, the bullet exit velocity is independent of the production process, since the projectile acceleration process is provided by instantaneously variable currents applied on the sequential stator coils. Capacitors and thyristors have an important place in the power electronics of a coil gun. Optical sensors are generally used for velocity measurement. The state change in optical sensors determines both the speed information and the ignition time of the next coil. These processes are provided by a computer or platforms such as MyRIO with a software to be developed. In a coil gun, the projectile exit velocity depends on the amplitude of the instantaneous current, the time it is applied, and the position of the projectile. The amplitude of the current and the application time are related to the charge storage capacity of the capacitor and the geometry, inductance and electrical resistance of the coil. However, the response times of optical sensors and thyristors and the operating time of the software also change the appropriate firing point. In this paper, the parameters affecting the bullet exit velocity in a coil gun will be examined in detail and what needs to be done to improve the bullet exit speed will be discussed in detail.

Keywords: Coil Gun, Bullet, Stator, Optical sensor, Velocity.

AMORF FERROMANYETİK TELLERİN SÜREKSİZLİK BELİRLEMEDEKİ ETKİNLİĞİ

EFFICIENCY OF AMORF FERROMAGNETIC WIRES IN DETERMINING DISCONTINUITY

Hakan ÇITAK[1]

[1]Balıkesir Üniversitesi, Balıkesir Meslek Yüksekokulu, Elektrik ve Enerji Bölümü, Balıkesir, Türkiye.

[1]ORCID ID: https://orcid.org/0000-0002-5627-3601

ÖZET

Bir manyetik cihazın geliştirilirken istenilen özellikler verim, manyetik geçirgenlik ve kritik manyetik alandır. Bu özellikler, amorf ferromanyetik maddeleri bir adım öne çıkarmaktadır. Örneğin bu maddeler, elektrik çelikleriyle karşılaştırıldığında 3 kat daha verimlidir. Elektriksel direnci en az üç kat daha fazladır. Daha küçük kritik manyetik alana (H_c), daha büyük geçirgenliğe (μ) sahiptirler. Bu özellikleri sebebiyle amorf ferromanyetik tellerin manyetik alan algılayıcı olarak kullanımı yaygındır. Amorf tele AC akım uygulandığında, manyetik alan tel içinde dairesel mıknatıslanma oluşturmakta ve harici DC manyetik alanda asimetrik değişim göstermektedir. Bu sebeple telin empedans değişimi de asimetriktir ve küçük manyetik alanların belirlenmesinde oldukça faydalıdır. Literatürde manyetik algılayıcı yapımında daha çok manyetik alanda tavlanmış Co (Cobalt) esaslı amorf ferromanyetik tellerin tercih edildiği görülmektedir. Bu bildiri kapsamında literatür doğrultusunda Co esaslı AC-20 $(Co_{0.94}Fe_{0.06})_{72.5}Mo_{12.5}B_{15}$ kullanılarak soğuk haddelenmiş Grain-Oriented çeliklerde (CRGO) süreksizlik sebebiyle oluşan manyetik akı kaçaklarının tespit edilmesine çalışılmıştır. Telde oluşan empedans değişimi kullanılarak CRGO çelik üzerinde süreksizliğin konumu ve geometrik özelliklerinin belirlenmesindeki etkinliği araştırılmıştır. Sonuçlar bildiri kapsamında ayrıntılı olarak tartışılacaktır.

Anahtar Kelimeler: Amorf ferromanyetik madde, AC-20 Tel, Grain-Oriented çelik, Manyetik akı kaçağı

ABSTRACT

The desired properties when developing a magnetic device are efficiency, magnetic permeability, and critical magnetic field. These properties make amorphous ferromagnetic materials one step ahead. For example, these materials are 3 times more efficient compared to electrical steels. Its electrical resistance is at least three times higher. They have smaller critical magnetic field (Hc) and greater permeability (μ). Due to these properties, the use of amorphous ferromagnetic wires as magnetic field sensors is common. When AC current is applied to the amorphous wire, the magnetic field creates circular magnetization inside the wire and shows an asymmetrical change in the external DC magnetic field. For this reason, the impedance change of the wire is also asymmetrical and is very useful in detecting small magnetic fields. In the literature, it is seen that Co (Cobalt) based amorphous ferromagnetic wires annealed in magnetic field are mostly preferred in the construction of magnetic sensors. In this paper, it has been tried to determine the magnetic flux leakages due to discontinuity in cold rolled Grain-Oriented steels (CRGO) using Co-based AC-20 $(Co_{0.94}Fe_{0.06})_{72.5}Mo_{12.5}B_{15}$ in line with the literature. Using the impedance change in the wire, its effectiveness in determining the location and geometrical properties of the discontinuity on CRGO steel was investigated. The results will be discussed in detail within the scope of the paper.

Keywords: Amorphous ferromagnetic material, AC-20 Wire, Grain-Oriented steel, Magnetic flux leakage

LORENTZ FORCE ACTING ON DYON AND DUALITY

Ömer Zor[1]

[1] Bursa Technical University, Faculty of Engineering and Natural Sciences, Department of Electrical and Electronics Engineering, Bursa, Turkey.

[1]ORCID ID: https://orcid.org/0000-0001-6461-9812

ABSTRACT

The Lorentz force acting on point-like electric charges in microscopic domain is well defined. We wrote the Lorentz force equation for the dyon with electric and magnetic charges using Ampere's hypothesis in microscopic domain. We determined the duality expressions contained in this Lorentz force expression. Since the basic equations defining electrodynamics are in integrity, the symmetry that arises in one definition can be extended to the others. We obtained symmetric Maxwell equations in the medium with dyons using these duality expressions.

Keywords: Dyon, Lorentz force, duality, symmetric Maxwell equations.

INTRODUCTION

Although the existence of magnetic monopoles cannot be determined, the symmetry offered by nature causes scientists not to ignore the magnetic monopoles.

Poincaré (1896) studied a moving electric charge in the field of a standing magnetic charge. Thomson (1904) studied same problem and gave detailed explanation. Dirac (1931,1948) constructed quantization condition for the electric and magnetic charge. Schwinger (1969) and Zwanziger (1971) conceived quantization condition for the particle electric and magnetic charge on it (named dyon). Thus, accepting the existence of dual charges expands the theory of electrodynamics to dual forms.

FORMULATION

We can write Lorentz force acting on a single point electric charge moving with velocity $\vec{v}$ in an electric field $\vec{e}$,

$$\vec{f}_e = e\vec{e}_{eff}. \tag{1}$$

Here $\vec{e}_{eff}$ is effective electric field defined in co-moving frame. This field has additional field $\vec{e}_m$ beside the field before the motion. Thus we can write

$$\vec{e}_{eff} = \vec{e} + \vec{e}_m. \tag{2}$$

The electric field caused by the motion $\vec{e}_m$ can be written as

$$\vec{e}_m = \frac{\vec{v}}{c} \times \vec{b}(\vec{r}, t). \tag{3}$$

This field can be constructed from the wave equation (Schwinger, 1998). Thus we can write Lorentz force equation as

$$\vec{f}_e = e\left(\vec{e}(\vec{r}, t) + \frac{\vec{v}}{c} \times \vec{b}(\vec{r}, t)\right). \tag{4}$$

Similarly, we can write the force on moving magnetic charge in the field of magnetic field as

$$\vec{f}_m = g\vec{b}_{eff}, \tag{5}$$

here the effective field $\vec{b}_{eff}$ can be defined as

$$\vec{b}_{eff} = \vec{b} + \vec{b}_m. \tag{6}$$

where $\vec{b}_m$ is magnetic field caused by the motion of the electric charge which is based on the hypothesis of Ampere (Schwinger, 1998). This field can be written as

$$\vec{b}_m = -\frac{\vec{v}}{c} \times \vec{e}(\vec{r}, t). \tag{7}$$

Thus we can write the force on magnetic charge

$$\vec{f}_g = g\left(\vec{b}(\vec{r}, t) - \frac{\vec{v}}{c} \times \vec{e}(\vec{r}, t)\right). \tag{8}$$

If we expand the theory on dyon, we can write total force as the sum of (4) and (8). The reason why we write as the sum of two forces, dyon has electric and magnetic charge on the same particle.

$$\vec{F} = e\left(\vec{e}(\vec{r}, t) + \frac{\vec{v}(t)}{c} \times \vec{b}(\vec{r}, t)\right) + g\left(\vec{b}(\vec{r}, t) - \frac{\vec{v}(t)}{c} \times \vec{e}(\vec{r}, t)\right). \tag{9}$$

This force is only acting on a dyon. If there is some charges on a certain volume (q_e, q_g) and if the distance from charged volume is as far as we can consider this volumetric charges as pont-like charges, we can write Lorentz force equation as

$$\vec{F} = q_e\left(\vec{e}(\vec{r}, t) + \frac{\vec{v}(t)}{c} \times \vec{b}(\vec{r}, t)\right) + q_g\left(\vec{b}(\vec{r}, t) - \frac{\vec{v}(t)}{c} \times \vec{e}(\vec{r}, t)\right). \tag{10}$$

This Lorentz force is defined for some dyons in microscopic domain.

If we construct duality expressions from the definition of Lorentz force (10) acting on some dyons, we can write

$$\rho_e \to \rho_g, \vec{E} \to \vec{B}, \vec{j}_e \to \vec{j}_g,$$
$$\rho_g \to -\rho_e, \vec{B} \to -\vec{E}, \vec{j}_g \to -\vec{j}_e. \tag{11}$$

If we use duality expressions on the Maxwell equations in the medium with only electric charges

$$\frac{\partial}{\partial t}\begin{pmatrix}\vec{e}(\vec{r}, t)\\ \vec{b}(\vec{r}, t)\end{pmatrix} = -\begin{pmatrix}\vec{j}_e(\vec{r}, t)\\ 0\end{pmatrix} + c\vec{\nabla} \times \begin{pmatrix}\vec{b}(\vec{r}, t)\\ -\vec{e}(\vec{r}, t)\end{pmatrix}, \tag{12}$$

$$\nabla \cdot \begin{pmatrix}\vec{e}\\ \vec{b}\end{pmatrix} = \begin{pmatrix}\rho_e\\ 0\end{pmatrix}, \tag{13}$$

we get Maxwell equations in symmetric form in the medium with dyons.

$$\frac{\partial}{\partial t}\begin{pmatrix}\vec{e}(\vec{r}, t)\\ \vec{b}(\vec{r}, t)\end{pmatrix} = -\begin{pmatrix}\vec{j}_e(\vec{r}, t)\\ \vec{j}_g(\vec{r}, t)\end{pmatrix} + c\vec{\nabla} \times \begin{pmatrix}\vec{b}(\vec{r}, t)\\ -\vec{e}(\vec{r}, t)\end{pmatrix}. \tag{14}$$

$$\nabla \cdot \begin{pmatrix}\vec{e}\\ \vec{b}\end{pmatrix} = \begin{pmatrix}\rho_e\\ \rho_g\end{pmatrix} \tag{15}$$

Thus we expanded the symmetry from Lorentz force to Maxwell equations.

CONCLUSION

We extended the well-defined Lorentz force equation for dyons. We obtained the Lorentz force equation for dyons which are exposed to the electric and magnetic fields at the same time. Starting from this Lorentz force equation for dyons, we revealed the duality relations. Using the obtained duality relations, we constructed the symmetric Maxwell equations.

REFERENCES

Poincaré, H. (1896). Remarques sur une expérience de M. Birkeland. *Comptes Rendus,* 123, 530-533.
Thomson, J.J. (1904). *Electricity and Matter*. Scribners, New York.
Dirac, P. A. M. (1931). Quantised singularities in the electromagnetic field. *Proceedings of the Royal Society of London*, A133, 60-72.
Dirac, P. A. M. (1948). The theory of magnetic monopoles. *Physical Review*, 74, 817-830.
Schwinger, J. (1969). A magnetic model of matter. *Science*, 165, 757-761.
Zwanziger, D. (1971). Local-Lagrangian quantum field theory of electric and magnetic charges. *Physical Review D*, 3, 880-891.
Schwinger, J., DeRaad, L. L., Milton, K. A., Tsai, W. (1998). *Classical Electrodynamics.* Perseus Books.

BÜTÜNCÜL TEHDİT AVCILIĞI ÇERÇEVESİ OLUŞTURULMASI

CREATING HOLISTIC THREAT HUNTING FRAMEWORK

Alperen SOYDAN

YL Öğrencisi, TOBB Ekonomi ve Teknoloji Üniversitesi, Mühendislik Fakültesi, Siber Güvenlik

ORCID ID: 0000-0001-9794-6289

ÖZET

Bilgisayar sistemlerinin ve ağlarının ortaya çıkmasıyla birlikte, siber güvenlik kavramı da ortaya çıkmış ve o günden beri de giderek önem kazanmıştır. Siber güvenliğin ilk dönemlerinde saldırıların günümüzdeki kadar gelişmiş olmamasından dolayı güvenlik duvarı, saldırı tespit sistemleri gibi pasif siber savunma yaklaşımlar yeterli olmuştur. Teknolojinin gelişmesiyle birlikte siber saldırıların karmaşıklıkları ve saldırganların kabiliyetleri artmıştır. Genellikle devlet destekli olan gelişmiş kalıcı tehditlerin de ortaya çıkmasıyla birlikte geleneksel yöntemler yetersiz kalmaktadır. Siber Tehdit Avcılığı; önleme ve tespit mekanizmalarını atlatmış olan gelişmiş tehditlerin, sistem ve ağ içerisinde tespit ve izole edilmesini sağlayan proaktif ve tekrarlı bir süreç olarak ele alınmaktadır. Tehdit avcılığı süreçlerinin işletilmesi için hem siber güvenlik içerisinde farklı disiplinlerdeki çerçeveler hem de tehdit avcılığına özel tasarlanmış çerçeveler kullanılmaktadır. Siber Ölüm Zinciri, Elmas Modeli, Acı Piramidi, MITRE ATTCK, MITRE CAR, MITRE DEFEND, TaHiTI, Sqrll Çerçevesi, Practical Hunt Model gibi çerçeve ve modeller, ele alınarak değerlendirmeleri gerçekleştirilmiştir.

Bu çalışmanın amacı; belirtilen çerçeve ve modeller değerlendirilerek, kullanım yöntemlerinden dolayı karşılaşılan problemlerin ve eksikliklerin belirlenip ortadan kaldırılmasını sağlayacak bir çerçeve oluşturulmasıdır. Çalışma çerçevesinde gerçekleştirilmiş olan anket ile tehdit avcılığı alanında aktif rol alan kişilere sorulan sorularla; tehdit avcılığı süreçlerinde kullanılan çerçeveler, çerçevelerden kaynaklı problemler, karşılaşılan zorluk ve eksikliklerle ilgili bilgi toplanması sağlanmıştır. Ortak ve genel bir çerçevenin bulunmaması, sürecin adımlarının işleyişi ve bu adımlarla ilgili bilgilerin bulunmayışından ötürü katılımcılar problem yaşadıklarını belirtmişlerdir. Katılımcılar tarafından ifade edilen bütün problemler ele alındığında ve detaylı bir şekilde analiz edildiğinde; tehdit avcılığı süreçlerinde kullanılan çerçevelerin, bütüncül bir şekilde ele alınarak bütün bir süreci kapsayacak şekilde değerlendirilmediği görülmüştür. Gelişmiş kalıcı tehdit raporu ele alınarak senaryo bazlı olarak test edilen Bütüncül Tehdit Avcılığı Çerçevesi'nin; tehdit avcılığı süreçlerinin baştan sona kadar eksiksiz şekilde işletilmesi, işletilen süreç neticesinde elde edilen sonuçların aksiyona dönüştürülmesi ve bütün bir sürecin raporlanmasını sağladığı görülmüştür.

Anahtar Kelimeler: Aktif Siber Güvenlik, Gelişmiş Kalıcı Tehdit, Tehdit Avcılığı, MITRE

ABSTRACT

With the emergence of computer systems and networks, the concept of cyber security emerged and has become increasingly important since then. In the early stages of cyber security, passive cyber defense approaches such as firewalls and intrusion detection systems were sufficient because the attacks were not as advanced as they are today. With the development of technology, the complexity of cyber attacks and the capabilities of attackers have increased. With the emergence of advanced persistent threats, which are usually state-sponsored, traditional methods are insufficient. Cyber Threat Hunting, it is considered as a proactive and iterative process that ensures the detection and isolation of advanced threats, which have bypassed prevention and detection mechanisms, within the system and network. For the operation of threat hunting processes, both frameworks in different disciplines within cyber security and frameworks specially designed for threat hunting are used. Frames and models such as Cyber Chain of Death, Diamond Model,

Pyramid of Pain, MITRE ATTCK, MITRE CAR, MITRE DEFEND, TaHiTI, Sqrll Framework, Practical Hunt Model were discussed and evaluated.

The aim of this study is that by evaluating the specified frameworks and models, a framework is created to identify and eliminate the problems and deficiencies encountered due to usage methods. With the questions asked to the people who take an active role in the field of threat hunting with the survey conducted within the framework of the study, information about the frameworks used in the threat hunting processes, the problems arising from the frameworks, the difficulties and deficiencies encountered were collected. The participants stated that they had problems due to the lack of a common and general framework, the functioning of the steps of the process and the lack of information about these steps. When all the problems expressed by the participants are considered and analyzed in detail, it has been seen that the frameworks used in threat hunting processes are not evaluated in a holistic manner and cover the whole process. The Holistic Threat Hunting Framework, which was tested on a scenario-based basis by considering the advanced persistent threat report, it has been observed that the threat hunting processes are fully operated from start to finish, the results obtained as a result of the operated process are transformed into action and the whole process is reported.

Keywords: Active Cyber Security, Advanced Persistent Threat, Threat Hunting, MITRE

EXTRACTION OF COLLAGEN HYDROLYSATE FROM CHROME LEATHER SHAVINGS AND ITS PROPERTIES

Tutku Dilara AKKAYA[1], Al MIZAN[1,2], Bahri BAŞARAN[1*]

[1] Ege University, Department of Leather Engineering, İzmir, TURKEY

[2] Khulna University of Engineering & Technology (KUET), Department of Leather Engineering, Khulna, BANGLADESH

ORCID NO: 0000-0003-0390-2192

ABSTRACT

Leather industry uses and fixes raw hides/skins which is a by-product of the meat industry to produce final leather for manufacturing daily usable leather items. During the manufacturing process, 60-70% of waste is generated. Among them, high amounts of chrome shaving wastes are produced after the mandatory shaving operation of chrome-tanned leather and are being almost unutilized which could lead to environmental pollution. To tackle this unavoidable burden and minimize environmental pollution posed by metal Cr, a step has been taken to use shaving waste as the raw material of collagen hydrolysate. Chrome shavings were hydrolyzed at different temperatures and time duration under alkaline and enzymatic/alkaline conditions. A bunch of analyses has been carried out to determine the quality of the hydrolysate such as ash content, particle size, molecular weight, metal content, conductivity, solid matter, density, free amino acid content, etc. It was found that, the highest particle size (524.3 nm) and the lowest protein content (%5.1) were obtained in the alkali treatment applied at 60°C for two hours in the hydrolysate. In addition, hydrolysates with the highest protein content (%7.3) in small particle size (55.2 nm) were obtained in the alkali/enzymatic treatment applied for a total of four hours at 90°C. In light of these data, with the increase in temperature, time, and addition of enzyme increases the protein content in the hydrolysate, decreasing the particle size and lowering the chromium content in the hydrolysate. Therefore, it is a plausible way for waste utilization and a sustainable manufacturing process.

Keywords: Collagen hydrolysates, Chrome shavings, Leather wastes, Sustainability

FAILURE ANALYSIS OF A HELICAL HSS END MILL

S. Melike Bulut*[0000-0002-8024-3541], **Tugce Tezel**[0000-0003-0139-442X], and **Volkan Kovan**[0000-0002-0599-525X]

Akdeniz University, Engineering Faculty, Department of Mechanical Engineering, Antalya 07058, TURKEY

Abstract: A helical end mill is a cutting tool used for milling, expanding, and grooving cylindrical holes by removing chips from the processed material. It is produced by grinding, rolling, or milling from high-quality tool steels (HSS). It is used in different types and geometries depending on the material being processed and the requirement. On it, grooves give the end part a bent appearance and help cut the material by moving up and down during drilling. The number of these grooves varies depending on the end mill function.

This study studied the fracture failure of a short-end mill with a helical handle, a diameter of 13 mm, and high-speed steel material. Visual inspection, stereomicroscope examination, and shear force calculations were performed in this context. It was emphasized that the armor layer was damaged by sharpening many times. Considering that the helical end mill was subjected to excessive mechanical stress due to the first damage, it showed signs of fracture due to the torsional load effect and high cutting speed under static sudden forcing conditions.

Keywords: failure analysis, high-speed steel (HSS) end mill, drilling

1. Introduction

Helical end mills are one of the most important cutting tools because they are economical and drill holes quickly. They are used for drilling and expanding cylindrical holes. Helical end mills are subjected to heavy torsional loads and bending stresses during operation. Thanks to the slope and grooves provided by the helical angle, the cutting force is directed downward, resulting in lower vibration and a smoother cut with a reduced load on the cutting tool.

When producing high-speed tool steels, also known as air steels in Turkish, they have high hardness, heat, and wear resistance by undergoing specific alloying and heat treatment. These steels can operate at high cutting speeds (30-40 m/min) compared to other tool steels[1]. They have a high cutting capacity with forced chip removal in large proportions. Heat treatment considerably retains its hardness and cutting ability up to 400-600°C. They have a hardness of about 62-67 HRC. Their wear resistance is quite good at high temperatures. These mechanical properties are related to the number of carbides in the internal structure of the end mill and their distribution in the microstructure [1]. High-speed tool steels contain various amounts of Cr, Va, Mo, W, and Co alloying elements. Due to these, carbide-forming elements can maintain their mechanical properties, such as wear resistance, even at high temperatures. Because the rolled high-speed tool steel is formed at certain temperatures, its resistance to hardness, stress rupture, and deformation is high[2].

A literature review was conducted for this study, and sample studies were examined. As a result of the literature review, studies on parts with similar or close damage were considered. *Tjahjana et al. (2019)* conducted an experimental and numerical analysis of fracture damage of superhard end milling HSS-Co in their experimental work. They determined that the surface fracture is divided into two parts, thin and rough. Carbide points were formed due to alloying elements that are not evenly distributed over the entire microstructure. First, due to the maximum stress generated, carbide particles began to crack. Crack growth has occurred due to the applied torsional load. Then a split was observed in the matrix in the crack plane, and the fragment was broken. The study recommends improving the quality control of round blank material by increasing the number of checked samples[3]. *Yohanes Waloyo* et al. (2019) said that end-mills fractures

occur at high voltage and low hardness concentrations when the hardness test is applied [Vickers micro-hardness test]. The surface with varying grain size is seen as the beginning of failure. Damage is caused by defects in production processes that are not included in standard operating procedures. In the chemical composition test carried out by energy dispersive spectrometry (EDS), it was found that rough surfaces lose the leading elements tungsten (W) and cobalt (Co). Both of these elements have the function of forming carbide by increasing hardness and heat resistance[4]. *Vipindas and Mathew (2019) studied* the wear behavior and surface roughness analysis of Ti-6Al-4V's TiAlN coated WC specimens during micro-finger milling. To study the effect of the tool edge radius on tool wear, they conducted experiments at two feed rates. Since the machining mechanism is affected by the expansion of the tool edge radius, it has been found that this is one of the types of wear during micromachining. The processing mechanism has changed with the expansion of the cutting edge radius due to wear after a cutting length of 600 mm with a feed rate of 5 µm/tooth and a cutting edge radius of 600 mm. It has been observed that it passes from the cutting mechanism to the sliding mechanism and therefore wears out. It has been found that adhesive abrasion is the main wear mechanism that causes the tool material to crumble, granulate, delaminate and exfoliate from the side surface[5]. *M., Sokovic et al. (2004)* studied the wear of PVD-coated solid carbide end mills in high-speed dry cutting. The wear behavior on the cutting edges of the spherical end end end mills studied has been observed optically and metallographically. According to these observations, it has been suggested that two types of wear occur. Firstly, it was defined as the deformation of the upper point of the solid carbide end mill, i.e., side wear, which is mainly caused by the feed rate effect. Secondly, the central wear of the end mill was studied[6]. Q., Song et al. (2021) conducted a chemical composition and fractured analysis of the W6Mo5Cr4V2Al high-speed steel (HSS) end mill. OM, SEM, and EDS analyses were carried out to investigate the results of these studies. In the results, it was concluded that the grain boundary oxidation was caused by overheating of the end mill during the heat treatment process, a large number of network carbide structures were formed in the eutectic and matrix, and the high tensile stress formed on the drilling surface as a result of the cooling process caused the fracture. The stress caused the appearance of an intergranular crack in the material and finally caused the end mill to break dec to the action of external force[7]. *Viana R. et al. (2009)* analyzed the performance of TiN/TiCN, TiAlN, TiN/TiAlN, and TiN/TiAlN/WCC coatings on HSS M2 end mills used for drilling the aluminum-silicon alloy ISO 3522 ALSI8CU3FE and correlated the service life of the tools with the coating with adhesion characterization experiments. In the adhesion characterization experiments, it was found that there were no cracks or delamination in the coatings and that they performed better[8].

2. Material and Method

The damaged helical end mill examined in this study and its original form is shown in Figure 1. The tool is a short-end mill with a diameter of 13.0 mm, HSS (High-Speed Steel), right cutting direction, with a rolling cylindrical handle.

Figure 1. The original and broken state of the damaged end mill

This part used in the milling machine was broken during the drilling operation of the unalloyed steel car chassis. The fracture occurred on the middle sides of the cutting and handle parts, closer to the sharp edge. According to the information received during the preliminary research, no abnormal conditions would have caused the damage before the damage was revealed. Mugshot MD50B Stereomicroscope images were taken in this study, and examinations were performed.

Material	*Norm*	*Type*	*Point Angle*	*Cutting Direction*	*Dimensional tolerance*
HSS	DIN 338 TS ISO 235	N	118	Right	h8

Figure 2. Technical information[9]

The damaged part is used in the milling machine with belt speed adjustment. The cutting speed (v_c) is the path a point on the end mill diameter takes in one minute. The rotation speed (n) is the number of turns the drill takes around its axis in a minute. The advance (s_z) is the path the milling cutter takes on the workpiece linearly in mm per minute.

Cutting speed; $v_c = \frac{d \cdot \Pi \cdot n}{1000}$

Rotation speed; $n = v_c \cdot \frac{1000}{d.\pi}$

Feed; $s_z = \frac{s}{z} = \frac{s}{2}$

Rate of feed; $u = s_z \cdot z \cdot n$

The cross-section of sawdust corresponding to one mouth; $A_{sz} = \frac{s_z \cdot d}{2}$

Total chip cross-section; $A_s = 2 \cdot A_{sz}$

The shear force corresponding to a mouth is; $F_{sz} = A_{sz} \cdot k_s$

The total shear force; $F_s = z \cdot F_{sz}$

* The average value was taken as 0.10 and calculated ($0.05 < s_z < 0.12$).

* The drilled part information has not been fully received. But it is unalloyed steel. Following this, unalloyed St37 steel was calculated as k_s = 1550 N/mm^2 by reference from the relevant book (Akkurt, 1985).

3. Findings and Discussion

The damaged part was first examined by visual inspection (Figure 3). As a result of this process, it was observed that the fracture surface of the damaged part was broken directly without damage, with minimal plastic deformation, that is, without changing shape. The fracture occurred quickly and suddenly. On visual inspection, there was no sliding or friction effect; hollow structure and herringbone marks, often seen in ductile fracture, are not seen. A sign of static breakage was observed under sudden exertion. Due to the appearance of smooth-shiny separation surfaces, it was presumed to break as a brittle fracture.

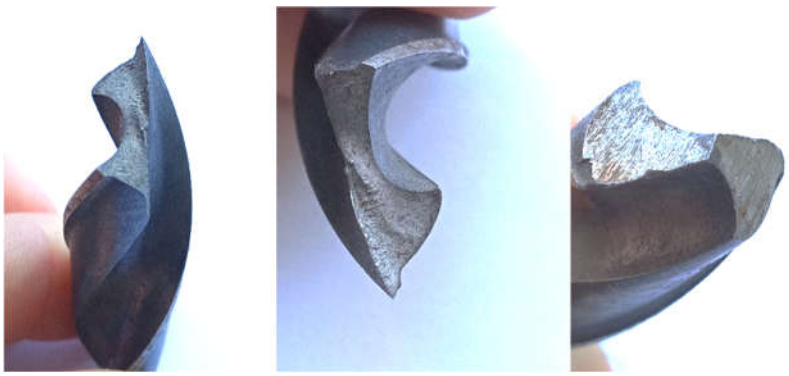

Figure 3. Visual inspection of the fracture surface

During operation, heat is released due to friction between the end mill and the workpiece and the operating temperature. For this reason, the use of coolant should be ensured not to damage the workpiece to be processed and the end mill. The coolant used during processing this damaged part is boron oil and water. Information has been received that the cylindrical end mill has often been sharpened. It has been found that the armor layer is damaged by abrasion during sharpening. It is assumed that damage does not occur due to corrosion in part. However, after the damage, it was observed that corrosion layers were formed on the surface in places due to the corrosive environment. Wear damage begins at the points where the cutting edge meets the protective armor. Particle rupture is also a common form of wear when drilling parts. When the end angle is smaller in the hole opened earlier, the stability is insufficient and may cause damage to the corners. In the damaged part, parts that break off from the surface are visible.

Figure 4 shows the images taken from the fracture surface with an optical microscope. Different cutting conditions occur on the cylindrical end mill because the chip angle varies throughout the mouth. The cutting speed varies throughout the mouth depending on the diameter of the mouth. The cutting speed is maximum around the end mill, zero in the center. Since the chip angle decreases towards the end of the mill, the flat part moves according to the lifting principle, not by cutting the material but by crushing it. This, in turn, led to an increase in the axial force and, with it, to a complication of the cutting conditions. However, this damage has almost no crushing because the end part of the cylindrical mill is mainly used to expand the hole. At the same time, since one side of the sharpened flat part is higher than the other side, it tends to shift to the right-left when the end mill comes into contact with the workpiece. As the clearance angle decreases, friction and wear between the clearance surface and the treated surface also increase. The most affected region by the cutting parameters is the core and the surrounding area. Improper grinding parameters may have caused microcracks on the cutting edges[10].

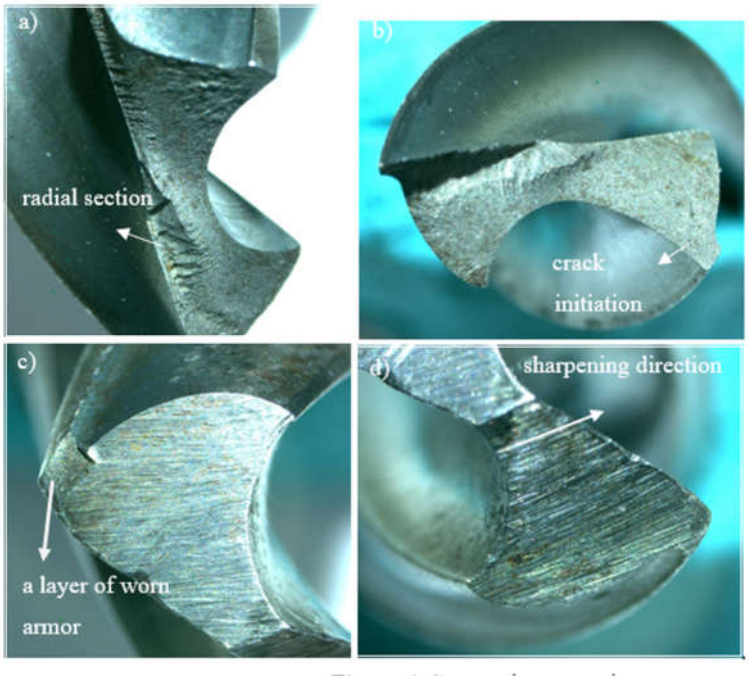

Figure 4. Stereomicroscope images

The following data were obtained using the formulas given in Section 2 (Table 1).

Table 1. Results of calculation

Rotation speed (RPM)	: 400
d (mm)	: 13
z (the number of groove)	: 2
Cutting speed (m/min)	: 8,16
Rate of feed (mm/min)	: 80
Total chip cross section (mm^2)	: 0,65
The total shear force (N)	: 2015

In addition to all these data, damage may have also been caused by the fact that the workpiece's appropriate number of revolutions, progress, and cutting speed was not processed. The drilling process may have been used for machining parts with an inappropriate hardness value. In addition, it can damage the armor layer by sharpening the end mill or making the drill not work well, causing it to break. (End mills can be sharpened at an angle of 118 if necessary to be economical, but this is not recommended because it damages the armor plating). A direct plunge may have been made for drilling a 13 mm hole. For drilling large holes of such diameters, it is recommended to drill holes in stages. The core region may have coincided with a more complex point in the processed material.

4. Conclusion and Recommendations

In this study, the fracture surface of a helical end mill was examined, and the rotation speed, cutting speed, feed, and shear force under operating conditions were calculated. The following results were obtained as a result of the operations performed:

The fracture surface is smooth and brittle with a crystalline appearance. Because it does not contain large plastic deformations, it is realized with low energy absorption.

The end mill has been sanded, blunted, and worn out. The armor layer around it was damaged, and the drill was made unusable. This has been one of the critical factors causing the fracture. It has been subjected to excessive mechanical stress by torsional load under static sudden forcing load conditions. The unreasonable load was applied to the part at a high cutting speed. In addition, there is a possibility that a harder point may have been contacted in the workpiece during the process.

It can occur fast at very high cutting speeds with free surface wear, plastic deformation, poor hole quality, and tolerance. At very low cutting speeds may be events, such as chip accumulation and longer expected cutting time. The cutting value recommendations can be checked to eliminate the problem of poor cutting tool life, such as increased coolant flow, filter cleaning, coolant holes, shortening the drill overflow distance, and workpiece stability control. If possible, a more wear-resistant quality can be selected. This can also happen when the tolerances on the end angles are not suitable for each other. This situation can be avoided with special production end mills[11]. This is an application chosen to prevent the case of chip jamming, mainly in materials that form a long chip structure, as well as when drilling deep holes. There should be a cooling fluid stream on the horizontal end mill that does not fall after exiting the milling machine with a length of at least 30 cm[12]. For this reason, internal coolant can be used in the design. In addition, this design can be produced more economically than conventional production methods with additive manufacturing.

5. References

[1] Özbek, İ. (1-92). Takım Çelikleri Sunumu. Metalürji ve Malzeme Mühendisliği. Sakarya Üniversitesi
[2]Korkmaz Çelik, "Yüksek Hız Takım Çelikleri (HSS)", Erişim: 10.05.2022. https://www.korkmazcelik.com/yuksek-hiz-takim-celikleri.
[3] Tjahjana, et al., (2019), "Failure Analysis of Super Hard End Mill HSS-Co", Open Engineering, 9(1):202-210.
[4] Yohanes W., et al., (2019), “Root Cause of End Mill Cutting Tool Failure,” AIP Conference Proceedings, 2097 030105, 1-7.
[5] Vipindas K., Jose, M., (2019), “Wear behavior of TiAlN coated WC tool during micro end milling of Ti-6Al4V and analysis of surface roughness”, Elsevier, Volumes 424–425,165-182, 15 April 2019.
[6] M., Sokovic, et al., (2004), “Wear of PVD-coated solid carbide end mills in high-speed dry cutting,” Journal of Materials Processing Technology, Elsevier, 157(1–12):422-426
[7] Song, Q., et al., (2021), “Fracture cause analysis of W6Mo5Cr4V2Al high-speed steel twist drill”, 46 (7), pp. 229-232.
[8] Viana, R., et al., (2009), “Influence of adhesion between coating and substrate on the performance of coated HSS twist drills,” 31 (4), pp. 327-332.
[9] Makine Takım, Erişim: 11.05.2022,
[10] Akkurt., M., (1985), İTÜ Makine Fakültesi, “Takım Tezgahları Talaş Kaldırma Yöntemleri ve Teknolojisi” Kitabı, Birsen Yayınevi.
[11] Sandvik Coromant, “Delik delme işleminde aşınma ve sorun giderme”, Erişim: 11.05.2022, https://www.sandvik.coromant.com/tr-tr/knowledge/drilling/pages/drilling-wear-and-troubleshooting.aspx .
[12]Sandvik Coromant, “Delik delme için ipuçları”, Erişim: 11.05.2022, https://www.sandvik.coromant.com/tr-tr/knowledge/drilling/pages/drilling-tips.aspx .

POST-PRODUCTION COPPER COATING APPLICATIONS WITH ADDITIVE MANUFACTURING

S. Melike Bulut*[0000-0002-8024-3541], **Tugce Tezel**[0000-0003-0139-442X], and **Volkan Kovan**[0000-0002-0599-525X]

[1] Akdeniz University, Engineering Faculty, Department of Mechanical Engineering, Antalya 07058, TURKEY

ABSTRACT

Copper has a high thermal and electrical conductivity. Since it is a soft and ductile metal, it is used in its pure form in many applications, including electrical installations, roofing, and industrial machines. Besides, it can be alloyed with other metals where strength, hardness, corrosion, deformation, and good resistance to creep are desired. Copper is widely used in the laser powder bed fusion (L-PBF) technique, one of the most common techniques in additive manufacturing technology. It is known that at the wavelengths used, they have specific difficulties since only a limited part of the energy is absorbed by the component, resulting in low-density printed parts. However, surface coating technologies are being developed, and copper alloy coatings are widely used to improve the surface performance defects of parts after production, provide oxidation-corrosion resistance and prevent wear in additive manufacturing technology. In this study, post-production copper applications with additive manufacturing were inspected.

Keywords: copper, nickel, coating, additive manufacturing

1. INTRODUCTION

Due to the complexity of conventional metalworking industries and processing methods and the high use of waste materials in production, additive manufacturing technologies have come to the forefront for creating complex structural parts. The applications of alloy-based surface coatings have been extensively developed and widely used to improve surface defects in near-surface areas of parts. In recent years, investigators have used copper alloy coatings to enhance surface quality, such as Laser Metal Deposition (LMD), Thermal Spraying techniques, Cold Spraying (CS), and Physical Vapor Deposition (PVD). Process optimization has been inspected in the research on additive manufacturing technology using copper alloys and is mainly focused on laser additive manufacturing technology. Process and performance analysis has provided a great theoretical basis for future research. However, it has been said that there is less interest in alternative manufacturing methods such as Electron Beam Melting (EBM) and electric arc/thermal plasma. The process parameters were identified by comparing the techniques of different additive manufacturing technologies. The impacts on the microstructure and mechanical quality of the three-dimensional components produced have been analyzed. The advantages and disadvantages of the three-printed parts created with each technology have been transferred. In the scope of additive manufacturing, the forthcoming focus of the production of copper-based alloys, which are the basis for the preparation of parts, was mentioned[1].

Laser Cladding (LC) is a kind of Direct Energy Deposition (DED) technique in which metallic powder or wire feedstock is collected on the part using a high-power laser to fix ripped parts or enhance surface qualities. The Laser Metal Deposition (LMD) method is also used to coat the surface by forming a molten layer on the part's surface by a similar principle. This method is used in many applications, especially in the aviation industry. Thermal spraying techniques are a coating process by spraying molten or heated coating materials onto the surface. Spraying (depending on the energy source) is carried out by methods such as flame-spraying, gas-detonation, and arc plasma spraying. Coatings deposited on the surface with thermal spraying techniques have a high adhesion due to their relatively dense and low porosity. Cold spraying involves deposition with desired powders coated on the part surface in a supersonic gas jet. Physical Vapor Deposition (PVD) is a process that occurs by vaporizing the material to be covered in a vacuum environment

and deposition it as a thin film on the surface of the part. The laser heat treatment process has become a preferred technology for observing parts' hardness and fatigue properties by offering the feasibility of localized heating area, superior processing speed, and processing of substantial, complicated parts. It is critical to complete the laser heat proceedings operation parameters to procure the intended material performance. Still, the high speed of the technique makes it tough to report the material's thermal past with basic measurement methods. In addition, it is costly to perform experiments to research the impact of process parameters. It is planned to construct a laser heat proceedings to be enforced by the as-deposited copper cold spray plating technique to provide a hardness decline of 30% throughout the thickness. An artificial neural net sample was advanced and used to reveal the laser heat approach situations that permit the intended hardness decline to be met. Thermal case histories were acquired by the thermal design of the laser heating period, and the eventuating hardness decline was found experimentally. Therefore, it has been said that this method can assist in selecting and optimizing process parameters at the end of the process[2].

The production of high-entropy alloys by additive manufacturing has been recently one of the most critical areas of considerable interest due to its distinguished mechanical characteristics and corrosion reluctance. Al0.25CoCrFeNiCu and Al0.45CoCrFeNiSi0.45 high entropy compounds were coated on stainless steel by applying the laser cladding method. Pre-alloyed high-entropy compounds produced by arc melting pursued by crunching have been used as a forerunner for laser cladding. Thus, the ideal laser power is significantly reduced from 1400W to 1600W, while the thermal reaction on the substrate is minimized. The laser cladding process has highly refined the dendritic microstructure while maintaining the dendritic area of arc melted compounds. And a certain degree of substrate dilution reaction has also been detected in the coating layers[3].

Therefore, in this study, the articles in the literature related to post-production copper coating applications with additive manufacturing were examined, and this review study was presented.

2. POST-PRODUCTION COPPER COATING APPLICATIONS WITH ADDITIVE MANUFACTURING

Fused Deposition Modeling (FDM), Selective Laser Melting (SLM), and Laser Metal Deposition (LMD) has been used as production methods in articles related to coating applications, cold spraying, electrodeposition, and Physical Vapor Deposition (PVD) have been widely used as a coating method. These studies investigated the effect of various parameters on coatings, such as scanning speed and part orientation, especially laser power. After that, the coating morphology, composition, and performance were analyzed.

In some studies in the literature, Ni-Co-Cu triple compound plating was processed by *Fran et al. (2022)* using ECAM (Electrochemical Additive Manufacturing). The morphology, corrosion resistance, chemical composition, and coating performance have been analyzed. The boost in the current density was caused by the capability growth of the coating speed. Therefore the coating thickness also increased (90 – 100 μm). For the chemical configuration, the boost in the ability provided more alive sites on the base material's exterior, and the plating's chemical property constantly approached the electrolyte. By observing the cross-section area of the plating, it turned out that it has a clear multilayer construction. In the tests, it was said that this triple coating has a perfect anti-corrosion property. The conclusion showed that the current density, plating structure, and chemical configuration vary depending on the possible parameters[4]. *Seneviratne et al. (2021)* evaluated the mechanical properties of Ultem™ 9085 Fused Deposition Modeling (FDM) printed samples by tensile and bending tests. They compared it with pieces of metallic plating thicknesses of about 75, 150, and 300 μm. Before mechanical tests, they performed nondestructive tests using x-ray computed tomography to evaluate the electroplated plating thickness alteration and comprehensive quality. In this way, most of the coating applications with the widely known electrolysis method involve improving the appearance of the parts. Still, they said this method could also increase the strength, hardness, and endurance of the plastic parts in the samples coated with electrolysis. Based on the use situation, the thickness of the composition of copper and nickel is adjusted to accomplish the essential combined qualities[5].

Tam et al. (2020) examined the copper platings in the closure welding section of a prototype steel container. Copper plating was made by two plating processes, namely by pyrophosphate electroplating bath in a conventional manufacturing situation and cold spraying. It was locally tempered using heating tape to

recover the ductility of its layers after cold spray coating. It was said that after 1 hour of heat approach at 350 °C under the inactive circumstance, heterogeneity was considerably decreased, and the microstructural properties suitable for the ongoing utilization were obtained[6]. *Rautio et al. (2022)* studied increasing the electrical conductivity and corrosion resistance of AlSi10Mg alloy produced by the Selective Laser Melting (SLM) technique by gold-nickel plating.

Gold-nickel coatings (Au-Ni) have been handled with electrodeposition (ED) and electroless deposition (ELD) techniques on the AlSi10Mg compound to enhance electrical conductivity and electrochemical action. To examine the coating strength, the surface dent hardness of the plated alloy was assessed. The conclusion disclosed that Au-Ni platings with a thickness of 2 and 10 μm could accomplish critical surface deficiencies such as pore formation[7]. *Korsholm et al. (2021)* evaluated the properties and preliminary performance of the components by using FDM modeling and coating a 1 μm copper layer with the physical vapor deposition (PVD) method and introducing a new way for the efficient production of prototypes of microwave components[8]. *Yang et al. (2018)* designed a technique for thick copper plating applications, a hand-made Cold Spraying (CS) system was used using a tip with an enlargement rate of 6.72 and a section length of 130 mm, which was cut with a wire electrode and removed after spraying. The development of interfacial microstructure and its mechanical behavior have been studied for sputtering and annealing conditions. The results showed that recrystallization occurs in two stages during spraying and tempering processes, and heat treatment on mechanical qualities ties was emphasized[9].

Laser Metal Deposition (LMD) is an additive manufacturing method developed recently. It has become the preferred technology for adapting materials' hardness and fatigue properties by offering a confined heating section, immense processing speed, and feasibility for processing complicated large materials. It is important to establish the laser heat approach process parameters to access the desired material action. Still, the great speed of the technique makes it tough to report the thermal past of the material with common measurement methods. In addition, it is costly to conduct experiments to investigate the reaction of progress parameters. *Razavipour et al. (2022)* aimed to design a laser heat treatment process on the deposited copper cold spray plating to supply a hardness decrease of 30% throughout the thickness. An artificial neural system exemplary has been improved to find the laser heat treatment conditions that allow the desired hardness decrease to be met. Thermal histories and thermal designing of the laser heating action were carried out; the resulting hardness contractions were acquired experimentally. Since the model can predict the regional hardness drop of the material according to the regional thermal past caused by multiple laser heat treatment conditions, it has been said that it can be used for objective in the elimination and optimization of various process parameters[10]. *Tillmann et al. (2022)* presented a new and innovative approach in which thermal spraying produces super-abrasive grinding wheels. For this aim, flat specimens and grinding stone hulls are plated with a commercial Fe-Al2O3 low-pressure (LP) cold gas spraying powder and nickel-coated diamond mixture with low-pressure LP cold gas spraying. Coatings have been studied metallographically for their combination. A well-embedded super abrasive content of 12% was obtained[11]. By *Li et al. (2019)*, Ti-B/TiC ceramic reinforced microlaminants were coated with a Laser Cladding (LC) technique on a TC17 titanium alloy substrate produced by Laser-deposition (LAM) additive manufacturing technology. Identifying AlCu2Mn microlaminants in laser-treated composites has contributed to the theoretical and experimental foundations for improving the quality of laser three-dimensional printing materials. It has been said to consolidate the laser-induced technological and related theoretical basis for producing micro-laminates modified with ultrafine nanocrystals on metal[12]. *Wang et al. (2021)* used a supersonic laser deposition (SLD) method combining laser cladding and cold spraying (CS) methods. They have used copper composite coating with different graphite content to facilitate instant heating of sprayed particles and deposition of low plasticity materials. By testing the wear and friction resistance of composite coatings with different graphite content, he explained the impact of graphite content on the wear resistance of combined plating[13]. *Olsen et al. (2021)* introduced a new system for generating conductive copper traces on 3D surfaces from different additive manufacturing technologies using 3D printing techniques. They performed dip-coating with copper nanoparticle ink, drying using a heat gun, and thermal curing by laser sintering. In the tests, the optimum laser top density was determined to obtain conductors with the lowest possible electrical resistance; it was said that the necessary prerequisites for enforcing this technology were presented[14]. *Garmendia et al. (2020)* coated AlSi10Mg powder with 1% copper by weight using a copper format solution curtailed to metallic copper after vacuum heat, proceeding to evaluate the impact of surface

modification of powdered raw materials used in additive manufacturing methods. The specimens were produced using Laser-Powder Bed Fusion (L-PBF). The samples from the plated powder exhibited an increased ultimate tensile strength and elongation at break compared to the AlSi10Mg materials. As a result, it was said that coating additions could be used to improve the usefulness of changing the combination of materials treated with L-PBF through the coating of powder feedstocks, as well as the mechanical qualities of materials after heat treatment[15]. *Obiegbu et al. (2019)* researched the wear resistance performance of Ti-6Al-4V coated with Al-Si-Sn-Cu reinforcement produced by Direct Laser Metal Deposition (DLMD). It has been said that the microstructural and tribological properties of coated samples produced with DLMD have improved and that their wear properties have shown an improved coefficient of friction (COF)[16]. *Stoll et al. (2019)* presented a new process for copper-ceramic composites produced by applying the Selective Laser Melting (SLM) method. It has produced 3D metallizations on Al2O3 by the DBC process, which is realized as melting copper or copper-based powder on ceramic substrates. It has formed spinel-like compounds by thermal finishing with Direct Copper Bonded (DBC) technology. It has also been said that high adhesion strengths of up to 44 N/mm2, decided by the shear test, can be achieved[17]. *Kang et al. (2018)* studied the impacts of particle size change on the homogeneity of Al-Fe alloys. Dry coating of Al particles with silica nanoparticles has significantly reduced interparticle Decoupling. The homogeneity of the powder mixture was studied optically in vibrated stack powder and thin extended layers, and solid samples were produced from various powder mixtures using LBM (Laser Beam Melting in metal powder bed) technology[18]. In addition, *Gharehbaghi et al. (2018)* researched the effect of Al-Fe-hybrid coatings on fifth-grade titanium alloy (Ti 6Al 4V). The impact of Fe on laser metal deposition (LMD) performed with different scanning speeds was investigated. It is noted that the increased laser power significantly raises the sediment width-height, heat-affected area surface, dilution ratio, sight ratio, and dust efficiency of each specimen due to the laser-material mutual effect[19]. On the other hand, *Zhao et al. (2019)* conducted an important study with powder metallurgy based on sintering techniques such as additive manufacturing technologies. To improve the sintering treatment of copper and Al alloys, Fe combined Aluminum powder with Cu particles and glued Fe nanoparticles to the surface of Al powder particles with the help of a polydopamine (PDA) plating. They said this compound powder shows improved sintering behavior, which can be attributed to the Al-Cu alloy phase created at the grain Fringes. It has been said that Fe-NP deposition and PDA coating approach with improved electrical and mechanical properties of sintered material is a decent reference technique for producing Al powders with enhanced sinterability[20].

3. RESULTS

Copper alloys are one of the essential alloys used in post-production coating applications with additive manufacturing and have an extensive range of application areas. This study relates the mechanical properties of copper alloy coatings to coating and production methods and reviews from more than 40 publications to outline the integration of copper plating into additive manufacturing. We are applying different surface coating technologies to improve surface performance by using alloy coating on the surface of parts by methods such as laser cladding, laser metal deposition, cold spraying, thermal spraying, and physical vapor deposition.

The assets of the three-printed materials achieved by each technique have been studied, and the forthcoming point of copper alloy additive manufacturing, which is the basis of the coating of the parts, has been foreseen. It is concluded that more attention should be paid to the heat treatment process, coating morphology, method parameters, electrical-thermal conductivity, and additive manufacturing processes. Significant differences in the mechanical properties of the studies have been reported, and the need for more examinations has been reported.

4. REFERENCES

[1] Wang, R., et al., (2021), "Research Progress of Copper and Its Alloys Surface Coating Technology and Additive Manufacturing Technology" 35 (19), pp. 19142-19152.
[2] Razavipour, M., et al., (2022), "Artificial Neural Networks Approach for Hardness Prediction of Copper Cold Spray Laser Heat Treated Coatings," 31 (3), pp. 525-544.
[3] Samoilova, O., et al., (2022), "Microstructural evolution of Al0.25CoCrFeNiCu and Al0.45CoCrFeNiSi0.45 high-entropy alloys during laser cladding".
[4] Zhang, F., et al., (2022), "Preparation of Ni-Co–Cu Ternary Alloy Coatings by the Low-Cost Electrochemical Additive Manufacturing," 24 (3), art. no. 2100788.
[5] Seneviratne, W., et al., (2021), "Electroplating polymer-based additive manufactured parts for enhanced structural performance," 3, pp. 1859-1871.
[6] Tam, J. et al., (2020), "Complex microstructural heterogeneity in electrodeposited and cold sprayed copper coating junctions," 404, art. no. 126479.
[7] Rautio, T., et al., (2020), "Enhancement of electrical conductivity and corrosion resistance by silver shell-copper core coating of additively manufactured AlSi10Mg alloy", 403, art. no. 126426.
[8] Korsholm, S.B., et al., (2021), "Fast production of microwave component prototypes by additive manufacturing and copper coating," 92 (3), art. no. 033509.
[9] Yang, K., et al., (2018), "Characterizations and anisotropy of cold-spraying additive-manufactured copper bulk," 34 (9), pp. 1570-1579.
[10] Razavipour, M., et al., (2022), "Artificial Neural Networks Approach for Hardness Prediction of Copper Cold Spray Laser Heat Treated Coatings," 31 (3), pp. 525-544.
[11] Tillmann, W., et al., (2022), "Qualification of the Low-pressure Cold Gas Spraying for the Additive Manufacturing of Copper–Nickel–Diamond Grinding Wheels," 31 (1-2), pp. 206-216.
[12] Li, J. et al., (2019), "Laser deposition-additive manufacturing of Ti–B/TiC ceramics reinforced microlaminates," 16 (4), pp. 1314-1320.
[13] Wang, J. et al., (2021), "Microstructure and Wear Resistance of Graphite/Cu Composite Coating. Prepared by Supersonic Laser Deposition", 48 (18), art. no. 1802015.
[14] Olsen, E., Overmeyer, L., (2021), " Laser sintering of copper conductive traces on primer pre-treated additive manufactured 3D surfaces", 6 (1), art. no. 015006.
[15] Garmendia, X., et al., (2020), "Microstructure and mechanical properties of Cu-modified AlSi10Mg fabricated by Laser-Powder Bed Fusion", 9, art. no. 100590.
[16] Obiegbu, M.-J.C., et al., (2019), "The Effects of Silicon and Copper on the Microstructure and Wear Resistance Performance of Al-Si-Sn-Cu/Ti-6Al-4V Composite Coatings", art. no. 8712023, pp. 20-25.
[17] Stoll. et al., (2019), "A novel approach of copper-ceramic-joints manufactured by selective laser melting" 11101, art. no. 1110109.
[18] Karg, M.C.H., et al., (2018), "Laser alloying advantages by dry coating metallic powder mixtures with SiOx nanoparticles," 8 (10), art. no. 862.
[19] Gharehbaghi., et al., (2018), "Experimental investigation of laser metal deposited icosahedral Al-Cu-Fe coatings on grade five titanium alloy," January, pp. 31-36.
[20] Zhao, Y., et al., (2019), "Biopolymer-Assisted Manufacturing of Aluminum-Copper Nanoparticle Composites with Enhanced Sinterability," 2 (9), pp. 5688-5694.

NEWTONIAN OLMAYAN AKIŞKANIN ŞIRINGA İÇERİSİNDEKİ AKIŞ ANALİZİ

FLOW ANALYSIS OF NON-NEWTONIAN FLUID INTO THE SYRINGE

Eray ERBAK[1]

[1]Ege Üniversitesi, Fen Bilimleri Enstitüsü, Makine Mühendisliği Bölümü, İzmir, Türkiye.

[1]https://orcid.org/ 0000-0003-0047-0910

Gökhan GÜRLEK [2]

[2] Ege Üniversitesi, Mühendislik Fakültesi, Makine Mühendisliği Bölümü, İzmir, Türkiye.

[2]https://orcid.org/0000-0001-5324-1818

Barış Oğuz GÜRSES [3]

[3]Ege Üniversitesi, Mühendislik Fakültesi, Makine Mühendisliği Bölümü, İzmir, Türkiye.

[3]https://orcid.org/0000-0002-2755-3452

Mert ŞENER [4]

[4]Ege Üniversitesi, Fen Bilimleri Enstitüsü, Makine Mühendisliği Bölümü, İzmir, Türkiye.

[4]https://orcid.org/0000-0002-9343-948X

ÖZET

Termoelektrik modüllerin kullanım alanı gün geçtikçe yaygınlaşmaktadır. Teknolojik gelişmeler ile farklı üretim yöntemlerinin bulunması ve farklı akışkanların termoelektrik modüllerde kulanılmaya başanması, termoelektrik modüllerin verimlerini arttırmaktadır. Termoelektrik modül üretiminde kullanılan akışkanlar genellikle şıringalı 3 boyutlu yazıcılarda çalışılmaktadır. Üretim için şimdiye kadar genellikle newtonian akışkanlar tercih edilmektedir. Ancak günümüzde newtonian olmayan akışkanlarla çalışmalar artmaktadır. Bu çalışma ise newtonian olmayan akışkanların, enjeksiyonlu basımı için gerekli olan kuvvetin hesaplanmasını içermektedir. Hesaplama deneysel çalışmalar ile nümerik analizlerin karşılaştırılmasını içermektedir.

Deney düzeneğine sabitlenen şırınga üzerine bırakılan sabit kütle, yerçekimi etkisi ile şırınganın içerisindeki akışkanı şırınganın ucundan dışarı itmektedir. Uygulanan sabit kuvvetlerin etkisi ile akışkanın hızı bilinmektedir. Deneyler ilk olarak hava ve su ile yapılmıştır. Hız verileri deneysel olarak iki akışkan için de bulunmuştur. Ansys yazılımı kullanılarak hazırlanan nümerik analizde elde edilen hız değerleri kullanılmıştır. Nümerik analizlerin sonucunda elde edilen kuvvetin, deneysel çalışmada kullanılan kuvvete yakındır. Su ve hava ile yapılan doğrulamanın ardından deneylere kalınlaşan bir akışkan olan diş macunu ile devam edilmiştir. Diş macunu viskozitesi için gerekli olan akış tutarlılığı katsayısı (k) ve akış davranışı katsayısı (n) değerleri için literatürden yararlanılmıştır. Nümerik analizlerin sonucunda elde edilen kuvvetin, deneysel çalışmada kullanılan kuvvete yakın olduğu görülmüştür.

Bu çalışma başka bir çalışma için ön çalışma niteliğindedir. Malzeme özelliği bilinen başka bir akışkan için gerekli kuvvet, bu analiz yöntemi ile kolayca hesaplanacaktır.

Anahtar Kelimeler: Kalınlaşan Akışkan, Non-Newtonian Akışkan, Diş Macunu

ABSTRACT

The usage area of thermoelectric modules is getting widespread day by day. The availability of different production methods and the use of different fluids increase the efficiency of thermoelectric modules. Fluids used in the production of thermoelectric modules are generally used in 3D printers. Until now, Newtonian fluids are generally preferred for production. Nowadays, studies with non-Newtonian fluids are increasing. This study includes the calculation of the force required for injection production of non-Newtonian fluids. The calculation includes comparison of experimental and numerical analysis.

The fixed mass left on the syringe fixed to the experimental setup pushes the fluid inside the syringe out of the syringe with the effect of gravity. The velocity of the fluid is known by the effect of the applied constant forces. Experiments were first carried out with air and water. Velocity data were experimentally found for both fluids. The velocity values obtained in the numerical analysis prepared using Ansys software were used. The force obtained as a result of the numerical analysis is close to the force used in the experimental study. After verification with water and air, the experiments were continued with toothpaste, which is a shear thickening fluid. The literature was used for viscosity values required for toothpaste. The force obtained as a result of the numerical analysis was found to be close to the force used in the experimental study.

This study is a preliminary study for another study. The force required for another fluid will be easily calculated with this method.

Keywords: Shear Thickening Fluid, Non-Newtonian Fluid, Toothpaste

INTRODUCTION

In nature, substances exist in basically three different states. These; solid, liquid and gas. At very high temperatures, the substance can also exist in the form of plasma. Liquid and gaseous substances are called fluids. The difference between solid and liquid state of matter is its resistance to shear stress. Solid materials first deform and then resist the applied shear stress. Liquids, on the other hand, continue to deform continuously, no matter how small the applied stress. Materials that constantly change shape under shear stress are called fluids. The image in Figure 1 shows this situation.

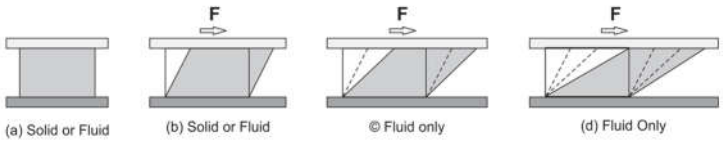

Figure 1: Solids and liquids under shear stress

In order to solve a fluid behavior, the part in which the fluid volume will be examined must be selected. We can assume that the fluid is formed in layers on top of each other. When a fluid comes into contact with a solid, its velocity is 0 m/s. In the fluid volume consisting of layers on top of each other, each layer slows down due to the effect of the previous layer. This deceleration volume is critical for predicting the behavior of the fluid. At the point where the ratio between the two velocity layers is 0.99, the effect becomes much less. This ratio is shown in Equation 1. If an analysis is made about fluids, it is necessary to examine below the point where the ratio of the two velocity layers is 0.99.

$$\frac{u}{u_\infty} = 0{,}99 \tag{1}$$

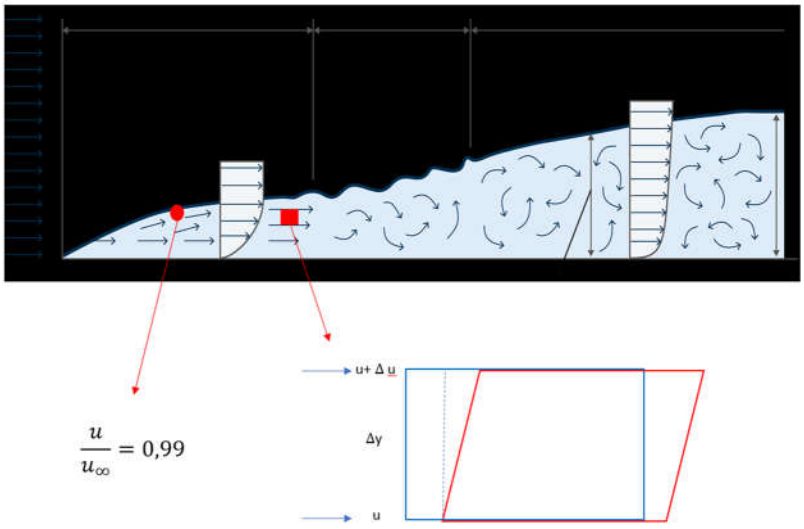

Figure 2: Boundary layer of fluid

$$\tan\Delta\beta = \frac{\Delta t \Delta u}{\Delta y} \tag{2}$$

$$\tan\Delta\beta = \frac{\Delta t \Delta u}{\Delta y} \tag{3}$$

$$\frac{\Delta\beta}{\Delta t} = \frac{\Delta u}{\Delta y} = \dot{\beta} \tag{4}$$

$$\tau \propto f(\dot{\beta}) \tag{5}$$

$$\tau = \mu \frac{du}{dy} = \mu \frac{d\beta}{dt} \tag{6}$$

The formula shown in Equation 6 is valid for fluids under the boundary layer. Using this formula, the "shear stress-rate of deformation" graph of the fluid can be drawn. This graph will be as in Figure 3 for water, oil and air.

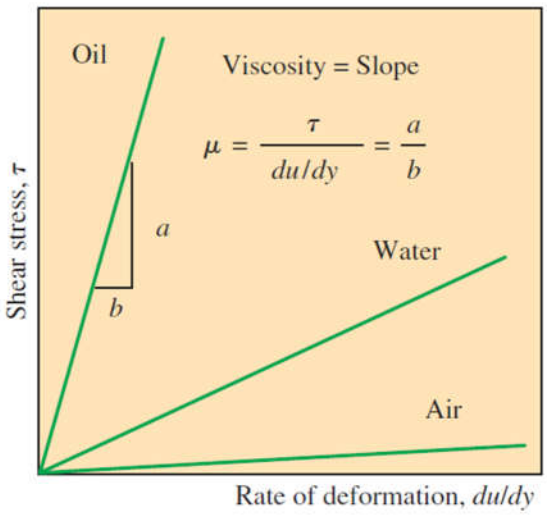

Figure 3: Shear stress-rate of deformation graph for water, oil and air

Fluids with the shape of y=mx, as in Figure 3, are called nowtonian fluids. But there are not only Newtonian fluids in our environment. There are also non-Newtonian fluids such as katcab, mayonnaise and toothpaste. The formulas in Table 1 are used to describe these types of fluids.

Table 1: Non-newtonian fluid models

$\eta = \eta_0$	Newtonian Model
$\eta = m\dot{\gamma}^{(n-1)}$ m = consistency index; n = power-law exponent	Power Law Model
$\eta = \eta_0(1+\lambda a)^{\frac{n-1}{a}}$ η_0 = zero shear viscosity; λ, a, and n are fitted parameters	Carreau-Yasuda Model
$\eta = \frac{\eta_0}{(1+(\lambda\dot{\gamma})^{1-n}}$ η_0 = zero shear viscosity; λ and n are fitted parameters	Cross Model

The graph of non-newtonian fluids is as in Figure 4.

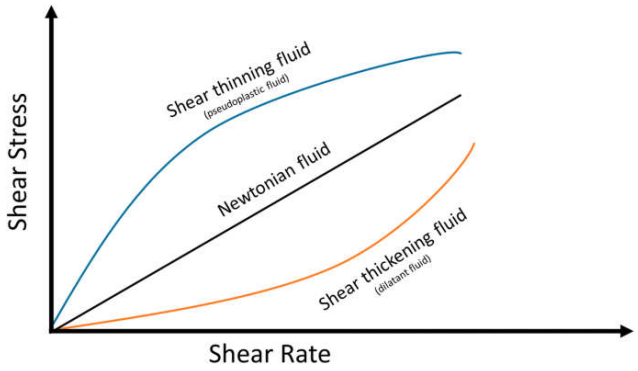

Figure 4: "Shear stress-shear rate" graph of newtonian and non-newtonian fluids

Toothpaste, which is the subject of this study, shows shear thinning property from non-newtonian fluids. The Power-Law model will be used during the study.

MATERIAL AND METHOD

Experimental Studies

Experiment 10 ml syringe and 0.3 mm diameter nozzle were used. During the experimental studies, the syringe was fixed to a platform. This process has been done to standardize the distance between the nozzle and the plate. Objects weighing 0.647 kg and 0.97 kg were left on the fixed syringe. A constant force is applied to the fluid in the syringe with the effect of gravity. As a result of the experiment, the flow time of

the fluid in the syringe was found. Experiments were repeated with 2 different masses. Two different fluids, water and toothpaste, were used. While water is a newtonian fluid, toothpaste is a shear thinning fluid. The equipment used during the experiment is shown in Figure 5.

Figure 5: Equipment used in the experimental study

Numerical Design of The System

As a result of experimental studies, the velocity of the fluid in the syringe and the force required to flow at this speed are known. Numerical analysis was also established in line with this information. Analysis was performed using the Fluid Flow module of Ansys software.

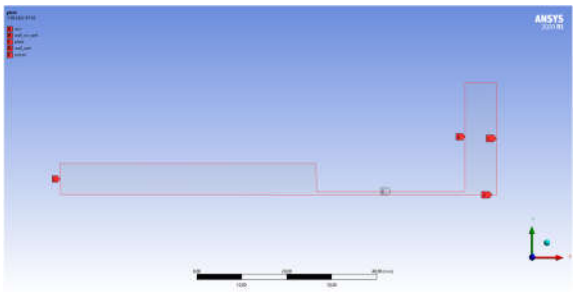

Figure 6: Numerical model

The flow was created as axisymmetric as seen in Figure 6.

The material properties required for analysis with water were used from the library of Ansys software. The properties required for the toothpaste were obtained using the literature. The "viscosity-shear rate" graph obtained with the data collected from the literature is in Figure 7. The graph created by taking the logarithm of this graph is in Figure 8.

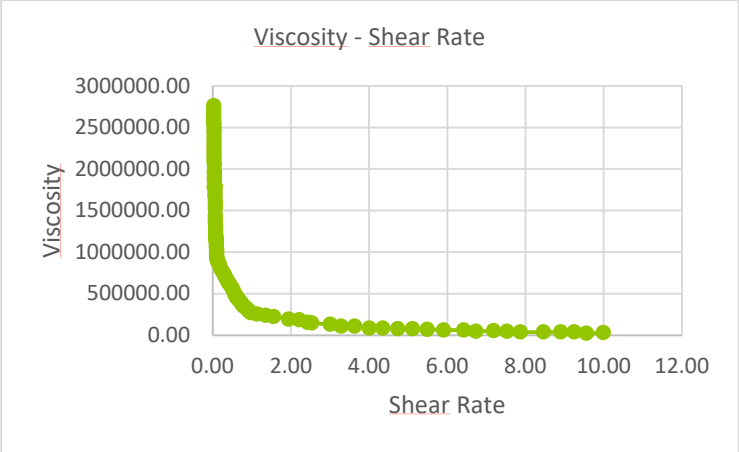

Figure 7: Viscosity-shear rate graph of toothpaste

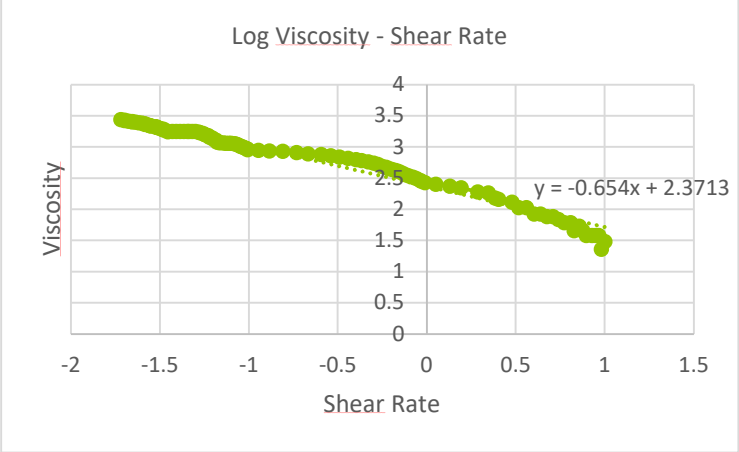

Figure 8: Log Viscosity-shear rate graph of toothpaste

Equation 7 is obtained from the "Log Viscosity-Shear Rate" graph in Figure 8.

$$y = -0{,}654x + 2{,}7313 \quad (7)$$

Consistency index (k) and Power Law Index (n) values obtained from Equation 7 are as follows.

Consistency index (k) = 2,3713

Power Law Index (n) = 1 - 0,654 = 0,346

These values are the viscosity values required for toothpaste. These data are used as in Figure 9.

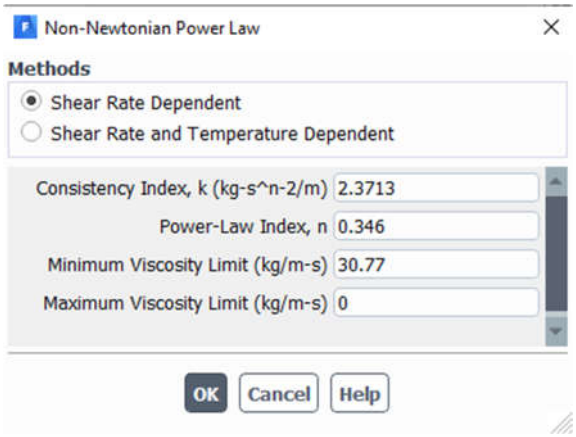

Figure 9: Power law model for toothpaste

During the numerical analysis, two different flow volumes were created. The first volume is the fluid itself. The second volume is air. The part indicated as A in Figure 6 moves in the +x direction according to the velocities obtained from the experimental studies. The part indicated as B in Figure 6 is the limits of the air volume. These parts are defined as Pressure outlet. The piston moving in the analysis discharges the fluid in the syringe into the air volume. This situation is illustrated in Figure 10.

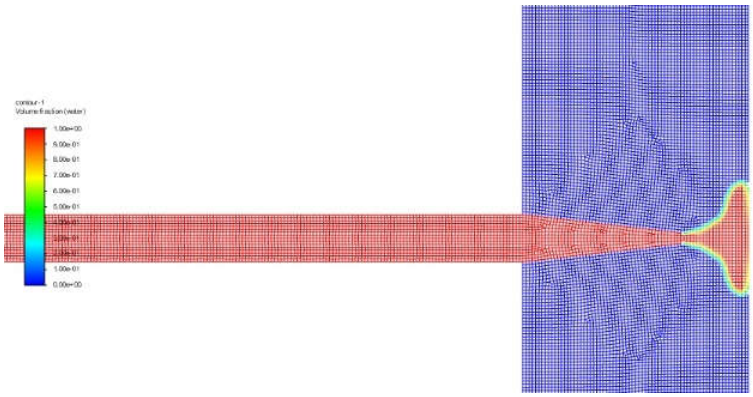

Figure 10: Flow profile in the numerical analysis result

RESULTS AND DISCUSSIONS

Flow visuals obtained as a result of numerical analysis are as in Figure 11.

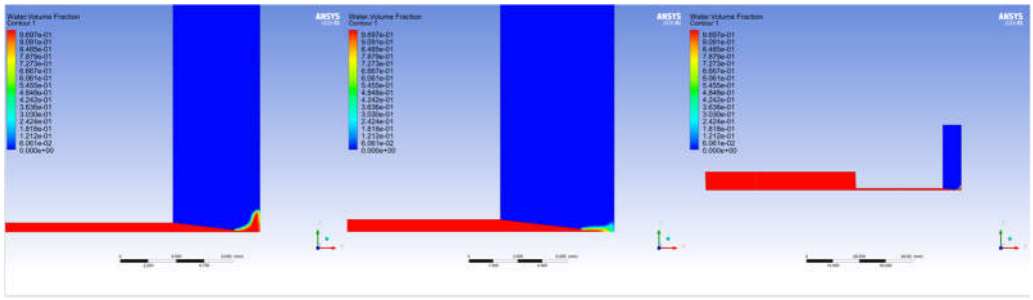

Figure 11: Flow profile in the numerical analysis result

The force values obtained as a result of experimental and numerical studies are as in Table 2.

Tablo 2: Results of numerical and experimental analysis

Fluid Material	Noozle Diameter (mm)	Weight (kg)	Time	Pressure In The Piston (Pa)	Mass calculated at the end of the analysis (kg)	% Error
Water	0,3	0,65	5,65	40208	0,63	2,48
	0,3	1	3,97	59542	0,93	6,47
Toothpaste	0,3	0,65	10	39807	0,62	3,45
	0,3	1	6,04	61964	0,97	2,67

CONCLUSION

As seen in Table 2, the mass calculated as a result of the numerical analysis is close to the mass used in the experimental study. The error rate is less than 10%. Experiments were first carried out with water, a Newtonian fluid. As a result of the analysis, it was seen that the values were found with an acceptable error. Calculation with non-newtonian fluid is also acceptable.

This study is a preliminary study of a start. For the production of PEDOT:PSS, which is one of the sub-work packages of a Tübitak project, the necessary force calculations must be made. The knowledge gained through this study will be used in the future for printing the ink prepared with PEDOT:PSS with a syringe.

ACKNOWLEDGMENTS

This work was supported by The Scientific And Technological Research Council of Turkey (Project Number 121M532)

REFERENCES

Çengel, Y. A., Turner, R. H., Cimbala, J. M., and Kanoglu, M. (2008). Fundamentals of thermal-fluid sciences (Vol. 703). New York: McGraw-Hill.

Munson, Bruce R., Young, Donald F., Okiishi, Theodore H. (2002). Fundamentals of Fluid Mechanics. United States.

Morris, Barry A. (2017) The Science and Technology of Flexible Packaging.

Drobny, Jiri George. (2014) Handbook of Thermoplastic Elastomers (Second Edition)

Bair, Scott. (2019) High Pressure Rheology for Quantitative Elastohydrodynamics (Second Edition). United States.

Bridges, Samuel., Robinson, Leon. (2020) A Practical Handbook for Drilling Fluids Processing. United States.

Bandyopadhyay, T. K., and S. K. Das. "Non-Newtonian and gas-non–Newtonian liquid flow through elbows–CFD analysis." *Journal of Applied Fluid Mechanics* 6.1 (2013): 131-141.

Morshed, Munzarin, et al. "Flow regime, slug frequency and wavelet analysis of air/Newtonian and air/non-Newtonian two-phase flow." *Applied Sciences* 10.9 (2020): 3272.

Scheven, Ulrich M., et al. "A cumulant analysis for non-Gaussian displacement distributions in Newtonian and non-Newtonian flows through porous media." *Magnetic resonance imaging* 25.4 (2007): 513-516.

Kumar, D., et al. "Non-Newtonian and Newtonian blood flow in human aorta: a transient analysis." *Biomedical Research (India)* 28.7 (2017): 3194-3203.

Aspinall, Sam R., Jane K. Parker, and Vitaliy V. Khutoryanskiy. "Role of mucoadhesive polymers in retention of toothpaste in the oral cavity." *Colloids and Surfaces B: Biointerfaces* 208 (2021): 112104.

COPPER CHLORIDE AND SILVER SELENITE ADDITIVE PEDOT:PSS BASED THERMOELECTRIC THIN FILM MANUFACTURING

BAKIR KLORÜR VE GÜMÜŞ SELENİT KATKILI PEDOT:PSS TABANLI TERMOELEKTRİK İNCE FİLM ÜRETİMİ

Şeyma ÖZKAN[1]

[1] Dokuz Eylül University, Graduate School of Natural and Applied Sciences, Department of Chemistry, İzmir, Turkey.

[1]ORCID ID: https://orcid.org/0000-0002-0255-3763

Gökhan GÜRLEK[2]

[2] Ege University,Faculty of Engineering, Mechanical Engineering Department, İzmir, Turkey.

[2]ORCID ID: https://orcid.org/0000-0001-5324-1818

Barış Oğuz GÜRSES[3]

[3] Ege University,Faculty of Engineering, Mechanical Engineering Department, İzmir, Turkey.

[3]ORCID ID: https://orcid.org/0000-0002-2755-3452

Yoldaş SEKİ[4]

[4] Dokuz Eylul University,Faculty Of Sciences, Department Of Chemistry, İzmir, Turkey.

ORCID ID: https://orcid.org/ 0000-0002-2225-1236

Mehmet SARIKANAT[5]

[5] Ege University,Faculty of Engineering, Mechanical Engineering Department, İzmir, Turkey.

[5]ORCID ID: https://orcid.org/0000-0001-7535-6819

Mert ŞENER[6]

[6]Ege University, Graduate School of Natural and Applied Sciences, Department of Mechanical Engineering, İzmir, Turkey.

[6]ORCID ID: https://orcid.org/0000-0002-9343-948X

Hicran BEŞİKCİ[7]

[7]Ege University, Graduate School of Natural and Applied Sciences, Department of Biomedical Technologies, İzmir, Turkey.

[7]ORCID ID: https://orcid.org/0000-0001-5360-7074

ABSTRACT

Conventional methods in electricity production first convert heat energy into kinetic energy and then this kinetic energy into electrical energy. With these methods, most of the heat energy remains as waste without being converted into electricity. This waste heat energy can be converted into electrical energy by the thermoelectric effect. When a thermoelectric system is formed between two metals with this effect, a potential difference is seen by creating a temperature gradient between the two ends. Electrical energy is obtained from the potential difference between these ends. The basis of this system is defined as the Seebeck effect. Thermoelectric materials are known as innovative products used in many fields. Because these materials, known as metals and semiconductors, are expensive and difficult of processing with, this field of

study has gravitated towards polymeric materials. Polymers with thermoelectric properties such as semiconductors are some of the reasons for preference due to their ease of processing, flexibility, and mechanical properties. PEDOT: PSS; since it is a flexible and biodegradable material with the highest success criteria among conductive polymers, it is widely used in solar cells, transparent electrode applications, and power devices that can be implanted oves the body. However, it has been observed that its thermoelectric properties are insufficient when used alone. In this study, Silver Selenite and Copper Chloride materials were added by using the doping method to increase the thermoelectric properties of the PEDOT: PSS polymer. PEDOT: PSS solution purchased as an aqueous solution was first purified and thin flexible films were prepared by adding Silver Selenite and Copper Chloride to the solutions prepared at different rates. It was created using different substrates with the Dr.Blade and drop-cast method. The electrical and thermal conductivity, density measurement, and surface morphology of the prepared thin films were investigated.

Keywords: PEDOT:PSS, Silver Selenite, Copper Chloride, Thermoelectric, Thin Films

HİPERELASTİK BİR MALZEMENİN MEKANİK ÖZELLİKLERİNİN BELİRLENMESİ

DETERMINING THE MECHANICAL PROPERTIES OF A HYPERELASTIC MATERIAL

Gökhan ÖZDEMİR[1]

[1]Ege Üniversitesi, Fen Bilimleri Enstitüsü, Makine Müh. Bölümü, İzmir, Türkiye.

[1]ORCID ID: 0000-0002-3004-2354

Mert ŞENER[1]

[1]Ege Üniversitesi, Fen Bilimleri Enstitüsü, Makine Müh. Bölümü, İzmir, Türkiye.

[1]ORCID ID: 0000-0002-9343-948X

B. Oğuz GÜRSES [2]

[2] Ege Üniversitesi, Mühedislik Fakültesi, Makine Müh. Bölümü, İzmir, Türkiye.

[2]ORCID ID: 0000-0002-2755-3452

ÖZET

Günümüz teknolojisinde tıbbi amaçlı kulanılan mikrorobotlar yaygınlaşmaktadır. Bu mikrorobotların kimi zaman uç işlevcileri için, kimi zaman ise tüm gövde için esnek hiperelastik malzemenin mekanik özelliklerinden yararlanılmaktadır. Hiperelastik malzemeler, ister zarar vermeyen dokusu olsun, isterse de yüksek deformasyon ve hareket kabiliyeti ile yarattığı mekanik avantajları olsun, süreklilik mekanizmaları ve mikrorobotlar için önemli bir yer tutmaktadır. Hiperelastik malzemeler sayesinde sistemler daha az mekanik parçadan oluşabilmektedir. Bu durum ise aşınma, gürültü, geri tepme vb. konularda avantajlar sağlamaktadır. Böylece daha uzun kullanım ömrü olan ve üretilmesi daha kolay mekanizmalar elde edilebilmektedir. Bu tip malzemeler, üretim kolaylığı ve kolay deformasyon özellikleri sayesinde mikro ölçekli robotik sistemler kurulmasında da oldukça kullanışlıdır. Bir mikrorobot ile bir prosedür gerçekleştirilmek istendiğinde oluşabilecek etkiler iyi tespit edilmelidir. Bu etkiler karşısında malzemenin vereceği tepkiler bilinmeli, ve kontrollü bir biçimde uygulanacak etkiler sonucundaki durum değişiklikleri önceden hesaplanabilmelidir. Tüm bunlar için malzemenin temel mekanik özelliklerinin belirlenmesi gerekmektedir. Malzemenin doğru tanımlanması, kurulacak sistemlerin modellenebilmesi ve malzemenin belirli etkiler altında davranışlarının doğru hesaplanabilmesi için en önemli etmendir. Hiperelastik malzemeler yapısı gereği nonlineer malzemelerdir. Dolayısıyla nonlineer bir malzeme modülüne sahiptir. Bu modülü doğru tanımlayabilmek için belirli malzeme modelleri geliştirilmiştir. Bu modeller için gerekli parametrelerin elde edilmesi amacı ile birçok çekme testi metodu bulunmaktadır. Çekme testleri sonucunda elde edilen verilere göre eğri uydurma yöntemi kullanılarak malzeme parametreleri, belirlenen malzeme modelleri için belirlenmektedir. İzotropik ve anizotropik olabilen hiperelastik malzemeler için genellikle sıkıştırılamaz malzeme tanımlaması yapılmaktadır. Bu çalışmada örnek bir kullanım alanı olarak, bağlı bir tıbbi mikrorobot sayılabilen esnek bronkoskopik kateterin eğilme kabiliyetini ölçebilmek için, bir hiperelastik malzemenin, malzeme modeli parametreleri tek eksenli çekme testi deneyleri ile belirlenmektedir. Ardından çekme testi, birim küp için Sonlu elemanlar metodu ile tekrarlanarak doğrulanmaktadır. Tüm bunların sonunda elde edilen malzeme modeli parametreleri kullanılarak, (hiperelastik bir malzemeden üretilen) manyetik esnek bronkoskopik kateterin, belirli yükler altındaki deplasmanı, deneyler ve sonlu elemanlar modeli ile belirlenmektedir. Oluşturulan hiperelastik malzeme modeli kullanılarak yapılan, sonlu elemanlar analizi sonuçları ile deneysel sonuçlar karşılaştırılmaktadır. Elde edilen verilere göre 100 mm uzunluğundaki esnek bir kirişin, hedef konumlara 0,5 mm ile 0,3 mm aralığında hata oranları ile eğildiği gözlemlenmektedir. Bu hatanın toplam

kateter boyuna göre ortalama hata oranı %0,4 olmakta ve geçerli bir malzeme modeli kurulduğunu göstermektedir.

Anahtar Kelimeler: Hiperelastik Model, Silikon, RTV, Malzeme Mekaniği

ABSTRACT

Microrobots used for medical purposes are becoming widespread in today's technology. The mechanical properties of the flexible hyperelastic material are sometimes used for the end-affectors of these microrobots, and sometimes for the whole body. Hyperelastic materials have an important place for continuum mechanisms and microrobots, whether they have non-destructive texture or mechanical advantages created by high deformation and mobility. Thanks to hyperelastic materials, systems can consist of fewer mechanical parts. This situation provides advantages in terms of wear, noise, recoil, etc.. Thus, mechanisms with a longer service life and easier to manufacture can be obtained. These types of materials are also very useful in the establishment of micro-scale robotic systems, thanks to their ease of production and easy deformation properties. When a procedure is desired to be performed with a microrobot, the effects that may occur should be well determined. The reactions of the material in the face of these effects should be known, and the changes in the situation as a result of the effects to be applied in a controlled way should be calculated in advance. For all these, it is necessary to determine the basic mechanical properties of the material. The correct definition of the material is the most important factor in modeling the systems to be installed and correctly calculating the behavior of the material under certain effects. Hyperelastic materials are nonlinear materials due to their structure. Therefore, it has a nonlinear material modulus. In order to define this module correctly, certain material models have been developed. There are many tensile test methods to obtain the necessary parameters for these models. According to the data obtained as a result of the tensile tests, the material parameters are determined for the material models by using the curve fitting method. For hyperelastic materials, which can be isotropic and anisotropic, generally incompressible materials are defined. In this study, the material model parameters of a hyperelastic material are determined by uniaxial tensile test experiments in order to measure the bending ability of a flexible bronchoscopic catheter, which can be counted as an tethered medical microrobot, as an example of use. Then the tensile test is verified by repeating the finite element method for the unit cube. Using the material model parameters obtained at the end of all these, the displacement of the magnetic flexible bronchoscopic catheter (made of a hyperelastic material) under certain loads is determined by experiments and a finite element model. The results of the finite element analysis using the created hyperelastic material model are compared with the experimental results. According to the data obtained, it is observed that a flexible beam of 100 mm length bends to the target positions with error rates in the range of 0.5 mm to 0.3 mm. The average error rate of this error over total catheter length is 0.4%, indicating that a valid material model has been established.

Keywords: Hyperelastic Model, Silicone, RTV, Material Mechanics

COMPARISON OF MACHINE LEARNING CLASSIFICATION TECHNIQUES IN R

Elif KOZAN[(a)], Filiz KARADAĞ[(b)], Agah KOZAN[(a)]

Dr., Ege University, Science Faculty, Department of Statistic, İzmir, Turkey (a)

Ege University, Science Faculty, Department of Statistic, İzmir, Turkey(b)

ORCID ID: 0000-0002-8267-074X

ORCID ID: 0000-0002-0116-7772

ORCID ID: 0000-0002-7387-9701

ABSTRACT

Machine learning is an important component of the growing field of data science. Machine learning provides the opportunity to make predictions through statistical methods and algorithms. Appropriate model selection while estimating affects the results considerably. Since the machine learning techniques used in each application problem perform differently, it is important to determine the appropriate technique by the researcher. In this study, comparative results of classification methods such as "Logistic Regression, K Nearest Neighbours (K-NN), Support Vector Machines (SVM), Kernel Support Vector Machines (Kernel SVM), Naive Bayes, Decision Trees and Random Forest" on real life data will be presented. This study is preliminary to the preparation of an R package that will automatically present the results of the classification techniques in the R program, which is planned to be carried out in the future. While presenting the comparative results of the techniques mentioned here, information about the R package, which is aimed to be brought to the literature, will be shared at the same time. The creation of the R package, which presents the results of practical comparison of classification techniques, will provide great convenience to researchers working in this field. Thus, it is aimed to provide a practical solution that will save time for those researchers in the selection of the appropriate model.

Keywords: Machine Learning, R programme, Classification algorithms, Random Forest, Decision Tree, SVM

ETHERNET INTERFACE DESIGN AND REALIZATION FOR SMART HOME COMPONENTS

Yuksel CELIK
Multitek Elektronik Research and Development Centre, Istanbul, TURKIYE
ORCID No:https://orcid.org/0000 0001 7799 4435
Dr. Murat TURE
Multitek Elektronik Research and Development Centre, Istanbul, TURKIYE
ORCID No:https://orcid.org/0000 0002 5744 4695

ABSTRACT

The smart home is defined that the connected house has wired and wireless infrastructure, providing easy communication for devices among themselves, the Internet, or the cloud. Therefore this is a system of high-tech devices in a modern residential building. Sometimes devices may not be the high-tech device or buildings may not be new and modern. The most difficult thing is ensuring that all of different devices are compatible with each other. While not will fully integrate with every device, they are overall great solutions that afford some control over things like smart lights, locks, speakers, cameras, and thermostats, all from one app instead of dozens. All devices can be reached Internet protocol. Some components do not have ethernet interfaces or the smart home can reach some system as a user, for example calling lifts. In this work, an ethernet interface has been designed and realized using only 8-bit microcontroller and SPI to LAN ethernet connector as cheap as possible. This interface has more option which are serial data, paralel data, general inputs-outputs pin, Analog Digital Converter, IIC (Inter-Integrated Circuit) etc... Also this can be used to control and monitoring more devices with using different protocol. TCP/IP connection has been used to communicate without loss data between device and monitor. A simple data format has been developed for this communication.

Keywords: Smart Home, Internet Protocol,

ÖZET

Akıllı ev , bir çok cihazın birbirleriyle kablolu ve/veya kablosuz kolayca haberleşebildiği ve bunlara Internet veya Bulut üzerinde erişimin sağlandığı konut sistemleri olarak tanımlanmaktadır. Bundan dolayı bir modern konut için yüksek teknoloji cihazlardan oluşturulmuş bir sistem olmaktadır. Bazen bu sistemler yüksek teknolojili cihazlardan oluşmayan, yeni ve modern olmayan binalar için kurulmak istenmektedir. En büyük zorluk, tüm bu farklı cihazların birbiriyle uyumlu olmasını sağlamaktır. Akıllı ışık, kilit, mikrofon, kamera ve termostat gibi bir çok cihazı tek bir uygulama ile izlemek ve kontrol etmek mümkün olmayabilir. Bütün bu aygıtlara İnternet Protokolu ile ulaşılabilmesi gerekmektedir. Örneğin, akıllı ev sisteminin bir parçası olarak düşünülen asansör çağırma için gerekli tuşuna erişim gibi bazı parçaların ethernet arayüzeyleri bulunmamaktadır. Bu çalışmada. 8-bitlik bir mikrodenetleyici ve SPI dan LAN'a bir ethernet kontrol tüm devresi ile minimum maliyetli bir Ethernet Arayüzey Devresi tasarlanmış ve gerçekleştirilmiştir. Bu arayüzey , seri veri, paralel veri, genel amaçlı giriş-çıkış uçları, Analog Dijital çevirici ve IIC(Inter-Integrated Circuit) erişim gibi bir çok özelliklere sahiptir. Bu arayüz devresi, farklı protokollar kullanan bir çok aletin izlenmesi ve kontrolu için kullanılabilir. Monitor ile cihazlar arasınaki iletişimde veri kaybını önlemek için TCP/IP bağlantı yöntemi kullanılmıştır. Bu haberleşme için basit bir veri biçimi geliştirilmiştir.

Anahtar Kelimeler: Akıllı Ev, Internet Protokolu**,** TCP/IP

Giriş

İnternet kullanımın artması beraberinde gerekli alt yapı yatırımlarının artmasını ve kapasitelerin artmasını sağlamıştır. Bu artışlar veri iletiminin hızınıda oldukça arttırmış ve maliyetini düşürmüştür. Hızlı ve ucuz iletişim sağlık sektöründen endüstriyel üretime günlük hayatını her noktasında etkisini göstermiştir. Böylece nesnelerin interneti (IoT) kavramı ortaya çıkmıştır. Nesnelerin miktar ve çeşitliliğinin artması bunların denetimi için gerekli sistemlerin ihtiyaçını arttırmıştır. Bu sistemlerin kurulum ve işletme maliyetleri kullanıcılar açısından mali ve teknik sorunlar ortaya çıkarmıştır. Bu gereksinim Bulut Sistemlerin geliştirilmesini desteklemiştir. Teknolojik gelişmeler günlük hayatımızın bir parçası olmuş ve konutların içine kadar girmiştir. Televizyon, müzik ve film oynatıcı cihazlarının uzaktan kontroluyla başlayan süreç ışıkların, perdelerin, ısıtıcıların, soğutucuların gibi bir çok sistemin uzaktan veya otomatik olarak devreye girmesi şeklinde devam ederek akıllı ev kavramının oluşmasını ve gelişmesini sağlamıştır. Yeni modern binalarda tüm sistemler ve iletişim hatları, global pazarda yer alan firmaların ortak geliştirdikleri ortak iletişim protokollarıyla uyumlu şekilde kurulabilmektedir. Yapım tarihi eski veya yeni olmasına rağmen bu sistemlerle uyumlu kurulmamış bazı binalarda da akıllı ev sistemi ve/veya akıllı ev sistemiyle izlenmeye uyumlu olmayan bazı cihazlar veya ihtiyaçlar bulunabilmektedir. Bu tip sistem ve aletler için sistemin var olan iletişim yöntemini yerel internet ağına bağlamak için bir arayüz devresine ihtiyaç vardır.

2. MATERYAL VE YÖNTEM

2.1. Akıllı Ev ve İletişim Yöntemleri

Akıllı ev sistemlerinde bulunan cihazlar bir denetleyici yardımıyla denetlenmesi ve istenilen biçimlendirmesi gerekmektedir. Bu işlev genellikle görüntülü haberleşme için kullanılan daire monitorü tarafından yapılmaktadır. Monitor olarak da sadece bir ekran yerine tablet bilgisayar kullanıldığında daire monitoru, ilave klavyeye gerek kalmadan istediğimiz değerleri girebilme ve işlemcisi yardımıyla denetleme organı ve hatta bir yerel sunucu işlevi görebilmektedir. Motorlu perde, sıcaklık kontrolu, güvenlik sistemleri gibi cihazları üreten bazı global üreticiler kendi aralarında özel iletişim yöntemleri (KNX, 2013) geliştirmişlerdir. Kablosuz iletişim olarak ta IEEE 802.15.4 standartlarına uygun olarak ZigBee (Tung, H.Y,, 2013), Bluetooth (Jim Kardach,1997) gibi bazı yöntemler geliştirilmiştir. Bunlara ilaveten IEEE Standartlarına uygun olmayan başka kablosuz yöntemlerde geliştirilmiştir. (Tiago D.P. Mendes, 2015). Bunlardan biride 433, 868 ve 915 MHz frekans bandlarında lisanssız ISM (Industry Scientific and Medical) frekans bandında çalışan RF alıcı-verici entegre devrelerdir (Çelik Y., Göktaş Ş., 2020). Bunlara ilaveten özellikle eski binalarda hala ethernet bağlantısı olmayan aletler olabilmektedir. Bazı kullanıcıların akıllı ev sistemlerinde gerçekleştirilmesi istediği özel çözümler olabilmektedir. Ethernet bağlantısı olamayan sistemleri akıllı ev ağına bağlamak için arayüz devresi gerekmektedir.

2.1.1 NXP S08PT32 ve WIZNET W5500 Tümdevresi ile Arayüz Tasarımı

8-bit Mikrodenetliyici olan S08PT32 ve Gömülü Ethernet tümdevresi (W5500) ile devre tasarlanmıştır.

NXP şirketine ait 8-bit mikrodenetleyici eşdeğer diğer mikrodenetleyicilerde olan ADC (Analog Digital Çevirici), Analog Karşılaştırıcı, Esnek Zaman Modulator birimi, IIC (Inter-Integrated Circuit), Gerçek Zaman Sayıcısı (RTC) , Seri Haberleşme Birimleri (SCI/UART), Seri Arayüz Birimi , sayısı 57 kadar artabilen Genel Amaçlı Giriş Çıkış ucuna sahiptir.

Gömülü ethernet devresi olarak kullanılan W5500 Tümdevresi TCP/IP yığını, 10/100 Ethernet Medya Erişim Kontrol (MAC) ve Fiziksel ehternet çıkışına sahiptir. SPI hattından biçimlendirildikten yine SPI dan kaydedicilerine yazılan veriyi fiziksel ethernet çıkışından İnternet Ağına veya İnternet ağından kendisine doğru gönderilen veriyi kaydedicilerine alarak SPI hattından okunmasını sağlayabilmektedir. Ayrıca TCP, UDP, ICMP, ARP, IGMP ve PPPoE protokollarını da desteklemektedir. Aynı anda bağımsız sekiz adet port açabilmektedir.

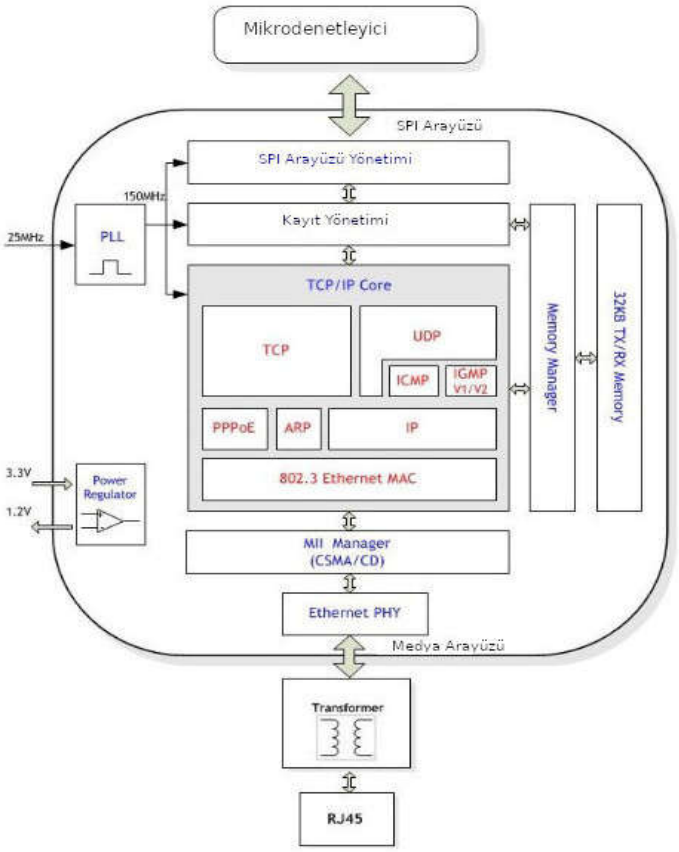

Şekil.1 Ethernet arayüzün katmanları ile görünümü

Belirtilen iki tümdevre kullanılarak çok amaçlı bir ethernet arayüz devresi şeklideki gibi gerçekleştirilmiştir. Ethernet üzerinden TCP/IP protokolu ile gönderilen veri biçimi Şekil.2 de verilmiştir.

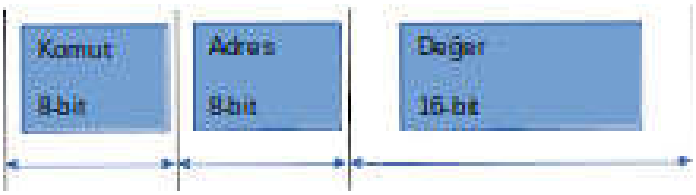

Şekil.2. TCP/IP de gönderilen veri biçimi

Mikrodenetleyici devre yönetici olarak, gömülü alt devre alt sistem olarak tasarlanmıştır. Mikrodenetleyicide geliştirilen yazılım öncelikle gömülü ethernet devresini biçimlendirme değerleri şekillendirip daha sonra belli aralıklarla ethernet hattı kontrol edilerek gelen veri kontrol edilmiştir. Gelen veri çözümlenerek istenilen komut gerekli modullere iletilmiştir. Moduller için giriş olarak tanımlananlardan gelen verilerde ethernet hattına aktarılmıştır.

Uygulama olarak Şekil.3 te görüldüğü gibi IP İnterkom tarafından asansör çağrılma fonksiyonu gerçekleştirilmiştir.

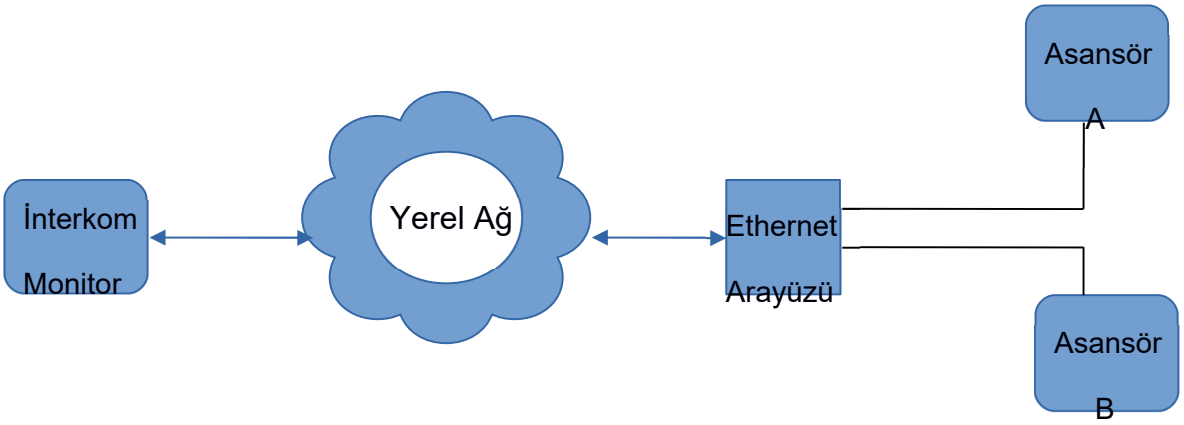

Şekil.3 İki asansörlü bir binada asansörlerin IP Interkom tarafında çağrılma devresi.

Uygulamanın yazılım akış diyagramı da Şekil.4 te verilmiştir.

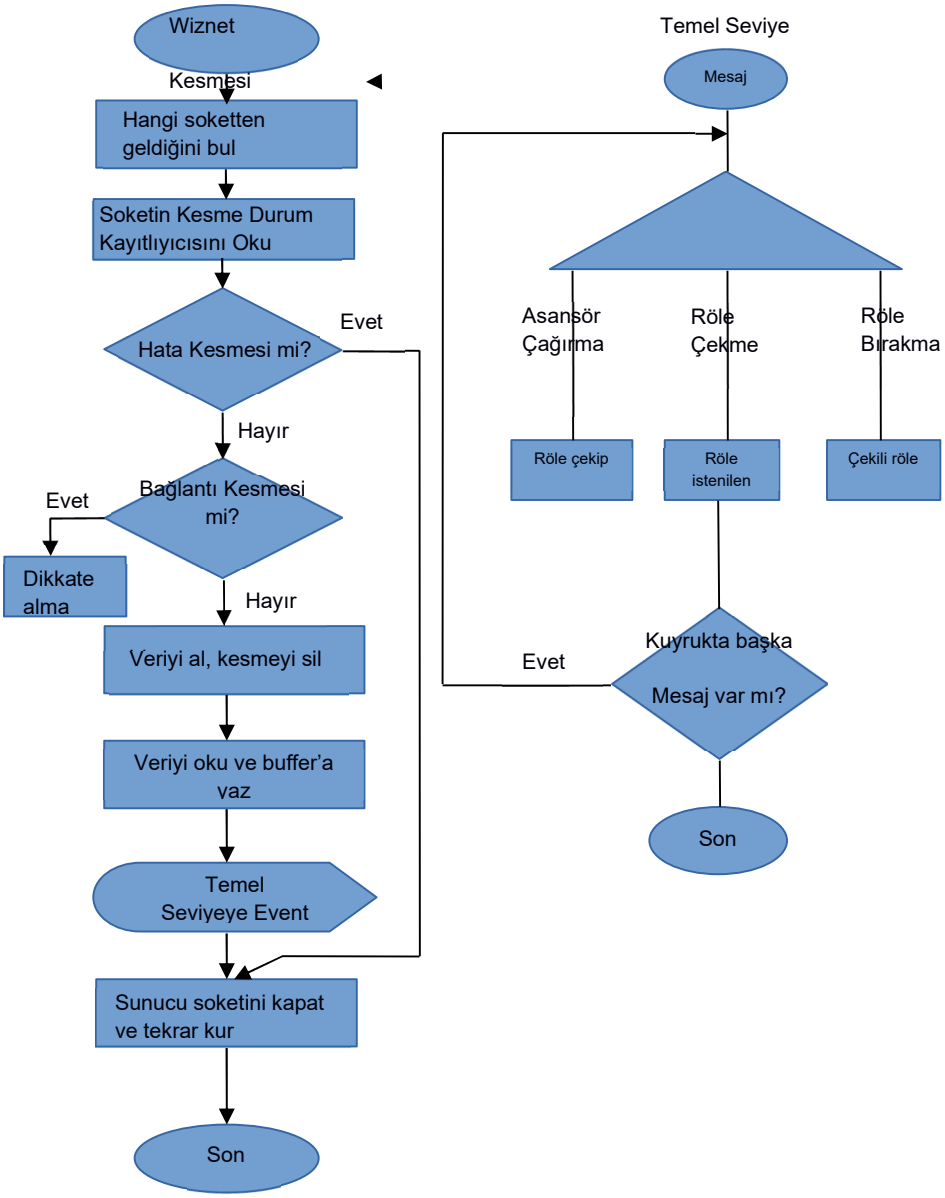

Şekil 4. Internet üzerinden asansör çağırma işlemi gerçekleştiren yazılımın akış diyagramı

3. SONUÇ VE ÖNERİLER

Geliştirilen çok amaçlı Ethernet Arayüz devresi ve Mikrodenetleyicinin Genel Amaçlı Uçları yardımıyla internet üzerinde iki asansör çağırma kontrolu gerçekleştirilmiştir. Mikrodenetliyiciye diğer modullerin yazılımları eklenerek tüm modulleri devreye almak mümkün olabilecektir.

KAYNAKLAR

1. Tung, H.Y.; Tsang, K.F.; Tung, H.C.; Chui, K.T.; Chi, H.R. The Design of Dual Radio ZigBee Homecare Gateway for Remote Patient Monitoring. IEEE Trans. Consum. Electron. 2013, 59, 756-764
2. *Kardach, Jim (5 March 2008). "Tech History: How Bluetooth got its name". eetimes. Retrieved 11 June 2013.*
3. Tiago D. P. Mendes, Radu Godina, Eduardo M. G. Rodrigues , João C. O. Matias and João P. S. Catalão, Smart Home Communication Technologies and Applications:Wireless Protocol Assessment for Home Area Network Resources. Energies 2015, 8, 7279-7311
4. Çelik Y., Göktaş Ş. RF Communication Desıgn And Implementation For Smart Home Applıcations, EJONX XI- International Conference on Mathematics-Engineering-Natural & Medical Science Proceeding Book,2021 Karak Jordan,
5. NXP Semiconductor, Technical Data, Document Number MC9S08PT60, Rev.6, 09/2019
6. W5500 Datasheet, Version 1.0.9, 22MAY2019

SIP CHAT CONTROLLED CLOUD INTERCOM

Ekrem YILMAZ
Multitek Elektronik Research and Development Centre, Istanbul, TURKIYE
ORCID No:https://orcid.org/0000 0002 2773 5555
Dr. Murat TURE
Multitek Elektronik Research and Development Centre, Istanbul, TURKIYE
ORCID No:https://orcid.org/0000 0002 5744 4695

ABSTRACT

The most important problem of the remote system is accessing to the device that are behind the NAT and/or the firewall. These IP addresses and these ports informations must be defined in all routing equipment. SIP (Session Interface Protocol) application can solve this difficulties without any definition. Security is also handled by TLS (Transport Layer Security) connection of SIP server. During the SIP registration, all appliance find their WAN (Wide Area Network) addresses and ports by the STUN (Session Traversal Utilities for NAT) server or the SIP registration authentication request messages. This ports can be open by the keep alive messages or some notices messages. SIP servers support chat messages and allow the third party application on the data of this messages. The cloud SIP server give the opportunities that the user can be found anywhere on the world. In this work, the gates of the cloud intercom are controlled by user's mobile phone. Also the specified gate's data can be observed by this application. The third party SIP clients' software are used both the door and GSM application. Free software of SIP server is used as the cloud SIP server and the control server. SIP chat messages are used to send the control data and the request information between the gates and the flat's owner.

Keywords: Cloud, Intercom, SIP, chat

ÖZET

Uzaktan denetlenebilen sistemlerin en önemli problemi, NAT (Network Address Translation – Ağ Adress Çevirimi) ve/veya güvenlik duvarının arkasında cihazlara erişimidir. Bunların IP (Internet Protocol) adresleri ve port bilgilerinin yönlendirici aygıtlarda tanımlanması gerekmektedir. SIP (Session Initiation Protocol – Çağrı Başlatma Protokolu) uygulamaları bu zorlukları herhangi bir tanımlama yapmadan çözebilmektedir. SIP sunucuya TLS (Transport Layer Security – Taşıma Katmanı Güvenliği) bağlantı ile güvenlik sorunuda çözülmüş olmaktadır. Tüm uygulamalar kendi dış dünyaya bağlandiği WAN (Wide Area Network – Geniş Alan Ağı) IP adres ve port değerlerini, SIP sunucuya kayıt olurken STUN (Session Traversal Utilities for NAT – Ağ) sunucu veya SIP Kayıt Şifre Onayı istenen mesajın içinde bulabilmektedir. Bu port bilgilerini yönlendirici tarafında sürekli açık bulundurulmasını da canlı tut (keep alive) mesajı veya bazı not bilgilerini belli sıklıkta göndermesiyle sağlayabilmektedirler. SIP sunucular sohbet (chat) mesajlarını destekleyip, bu mesaj bilgilerinin diğer uygulamalar tarafından işlenebilmesine izin vermektedirler. Bulut SIP sunucular, kullanıcıların dünyanın neresinde olursa olsun bu hizmeti kullanabilme fırsatını sunmaktadır. Bu çalışmada bulut interkom kapıları GSM mobil telefonları ile kontrol edilmiştir. Bu uygulama ile aynı zamanda belirlenen kapıların izlenmesi de sağlanmıştır. Kapılarda ve GSM uygulamalarında, SIP sunucudan bağımsız SIP müşteri uygulamaları kullanılmıştır. Bulut SIP sunucu ve kontrol sunucu olarak üçretsiz SIP sunucu yazılımları kullanılmıştır. Kapılar ve daire sahipleri arasında kontrol verileri ve izlenmek istenen gerekli bilgi verilerini iletimi için SIP sohbet mesajları kullanılmıştır.

Anahtar Kelimeler; Bulut, İnterkom, SIP, Sohbet Mesajı

Giriş

İnternet teknolojilerinin gelişimi akıllı ev kavramının içeriğini ve uygulamalarını daha da geliştirmiştir. Akıllı ev uygulamalarının uzaktan izlenmesi ve denetlenmesi çok daha kolay hale gelmiştir. Yatay ve dikey konutlara veya sitelerinine GSM Mobil Telefon uygulamaları ile erişim ve denetim çalışmaları hız kazanmıştır. Bulut Sunucuların kullanıma girmesiyle, her sitenin yönetimi için ayrı bir sunucu kullanmak yerine bir sunucu ile bağımsız bir çok sitenin akıllı ev sistemi kontrol edilebilir hale gelmiştir. Bulut sunucu ve öncesinde de en önemli soruni, kullanıcı olarakta tanımladığımız konuta uzaktan erişim olmaktadır. Kullanıcıların internet üzerinden dış dünyaya veri iletişimine, Şekil.1 de gösterildiği gibi en az bir yönlendiriciden geçmesi gerekmektedir. Kapılardan herhangi birinin GSM telefon uygulamalarından kontrol edilebilmesi için kontrol edilen kapının İnternet adresi ve port bilgisinin mobil uygulaması tarafında bilinmesi gerekmektedir. Bunun için İnternet adresinin ve portunun sabit olması, bu bilgilerin mobil uygulama tarafında tanımlanması, ilaveten Yönlendirici/Güvenlik Duvarında da gerekli tanımlamaların yapılması gerekmektedir. Yatay bir konut veya yatay konutlar sitesi için bu çalışmalar, ucuz olmasa da gerçekleştirilebilir. Ancak çok katlı dikey binalar ve/veya dikey binalar gurubu için bu çalışmalar hem pahalı, hem de çok sıkıntılı olmaktadır.

2. MATERYAL VE YÖNTEM

2.1. Yerel İnternet Ağı Üzerinden Görüntülü İnterkom Sistemleri

Yerel ağ üzerinden akıllı ev monitorü ile site üzerineki kapı ve güvenlik noktalarına ses ve görüntülü erişim için SIP yöntemi (RFC 3261)oldukça sık kullanılmaktadır. Aynı ağ üzerinde bulunan konut, güvenlik, ve kapı noktalarının fiziksel adresleri ile internet adresleri arasındaki bağlaşım geliştirilen bazı algoritmalar yardımıyla elde edilip sunucu olmadan da sabit adresli SIP yöntemiyle görüntülü iletişim sağlanabilmektedir. Internet adresi bilinen cihazların port bilgileri sahip tutularak kapı, güvenlik gibi noktaların denetimi de mümkün olmaktadır.

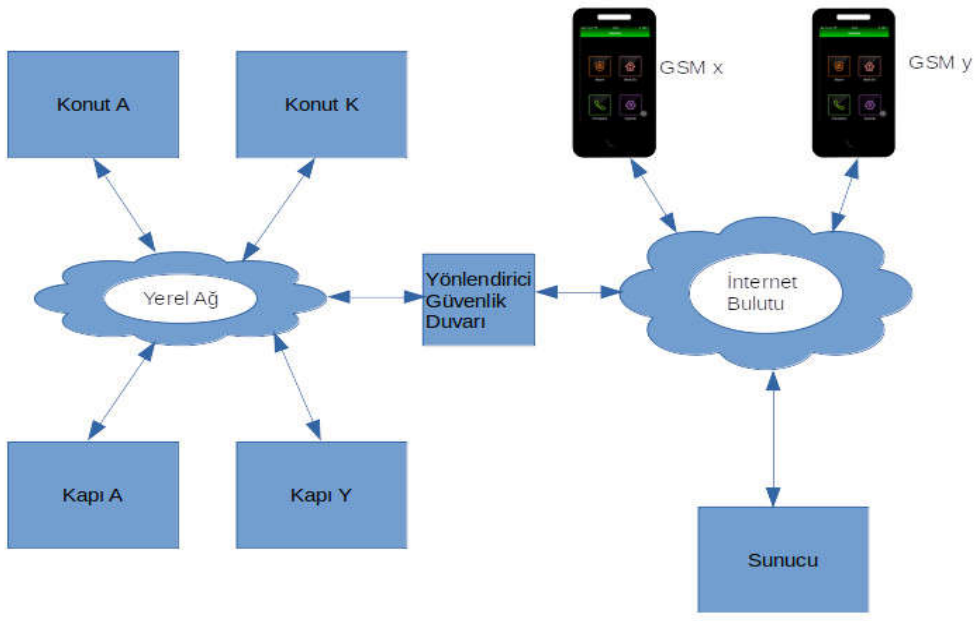

Şekil.1 Hem yerel hemde Bulut Kotrollu bir IP İnterkom sistemi

2.2. İnternet Bulutu Üzerinden Görüntülü İnterkom Sistemleri

Bulut üzerinden görüntülü interkom sistemi için mobil uygulamaların internet ve port bilgileri sürekli değişebileceği için bulutta bir sunucu olması gerekir. Sunucu, SIP sunucu olduğu gibi ilaveten proje gereği başka sunucularda olabilir. Interkom vasıtasıyla yapılan bazı kontrol ve izlemeler için ayrı portların tanımlanması gerekecekir. Bunun içinde Şekil.1 de görüldüğü gibi yönlendirici ve güvenlik duvarlarında ber bir uç noktası için tanımlamlar yapılmalıdır. Yeni yapıların yatay konutlar sitesi ve/veya dikey konutlar sitesi şeklinde yapıldığını gözönüne aldığımızda yüzlerce konut ve uç noktası olmaktadır. Burada interkom vasıtasıyla yapılan denetlemeler için yönledirici ve güvenlik duvarında yaptığımız tanımlamaların benzerlerinin mobil uygulamaya da taşınması gerekmektedir.

2.2.1 SIP Sohbet Ortamı

SIP sunucular kendi kullanıcılar arasında sohbet (chat) mesajlaşmalarına imkan tanımaktadır. Bu durumda konut sitesindeki herhangi bir noktaya SIP haberleşme portu kullanılarak sohbet mesajıyla ulaşabilmektedir. Mesajlaşmanın standartları RFC3428 ile tanımlanmaktadır. Bir çok firma açık kaynak kod uygulamasıyla SIP sunucu ve SIP kullanıcı (client) yazılımlarını ücretsiz kullanıma açmıştır. İlaveten SIP kullanıcı yazılımları SIP sohbet mesajlarının kullanımına da izin vermektedir.

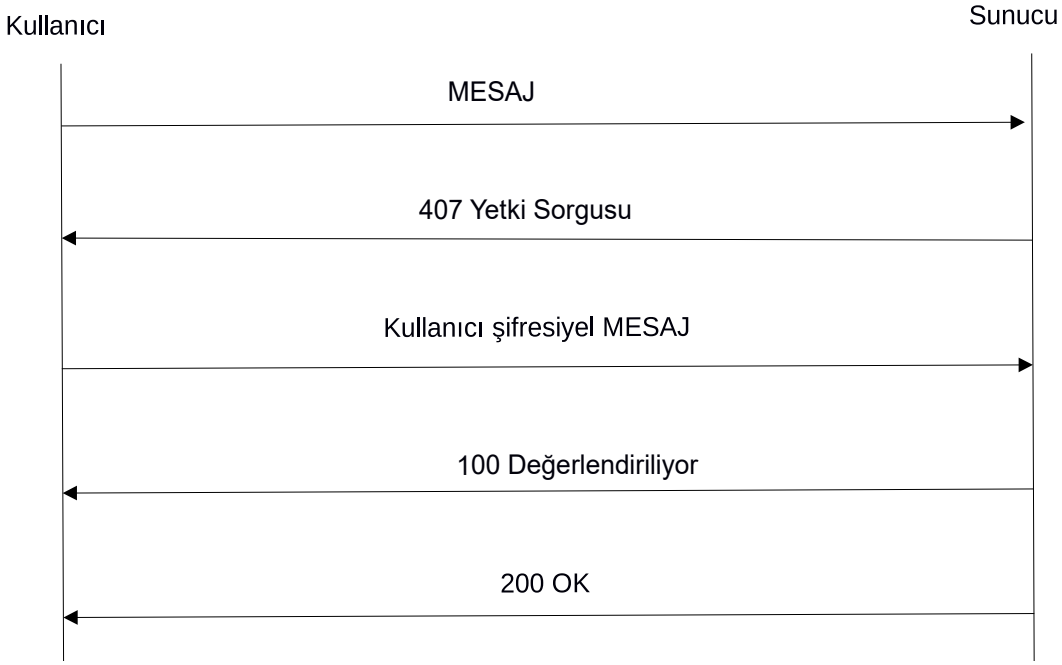

Şekil 2. SIP Mesaj akışı

Kullanılan SIP kullanıcı programının (Liblinphone 3.11.3) ChatRoom kütüphanesi buna izin vermektedir.

SIP sohbet iletisiyle gönderilen veriler komut olarak kabul edilerek Mobil Uygulamalardan uç noktaların denetim ve izlenmesi sağlanılmıştır. Kullanılan verilerin anlamları Tablo.1 de verilmiştir.

Mesaj Verisi	Mesaj Tipi

OPEN_DOOR	Emir
LED_ON	Emir
LED_OFF	Emir
LED_STATUS	İstek

Tablo.1 Kapı denetim ve izleme için kullanılan bazı Sohbet mesajları

Mobil uygulamadan gelen verilere göre uç nokta olarak belirlenen Kapı noktasının erişim blok diyagramı Şekil.3 de verilmiştir. Mobil uygulama yazılımı Linphone SIP Client kütüphanesi de kullanılarak Android ortamında geliştirilmiştir. Kapı uygulaması olarak Android ortamında da SIP haberleşmesi için yine Linphone SIP Client Kütüphanesi kullanılmış, ilave olarakta dış dünya ya erişim için IIC (Inter-Integrated Circuit) protokolu ile bir mikrodenetleyici (NXP S08PT32) kullanılmıştır.

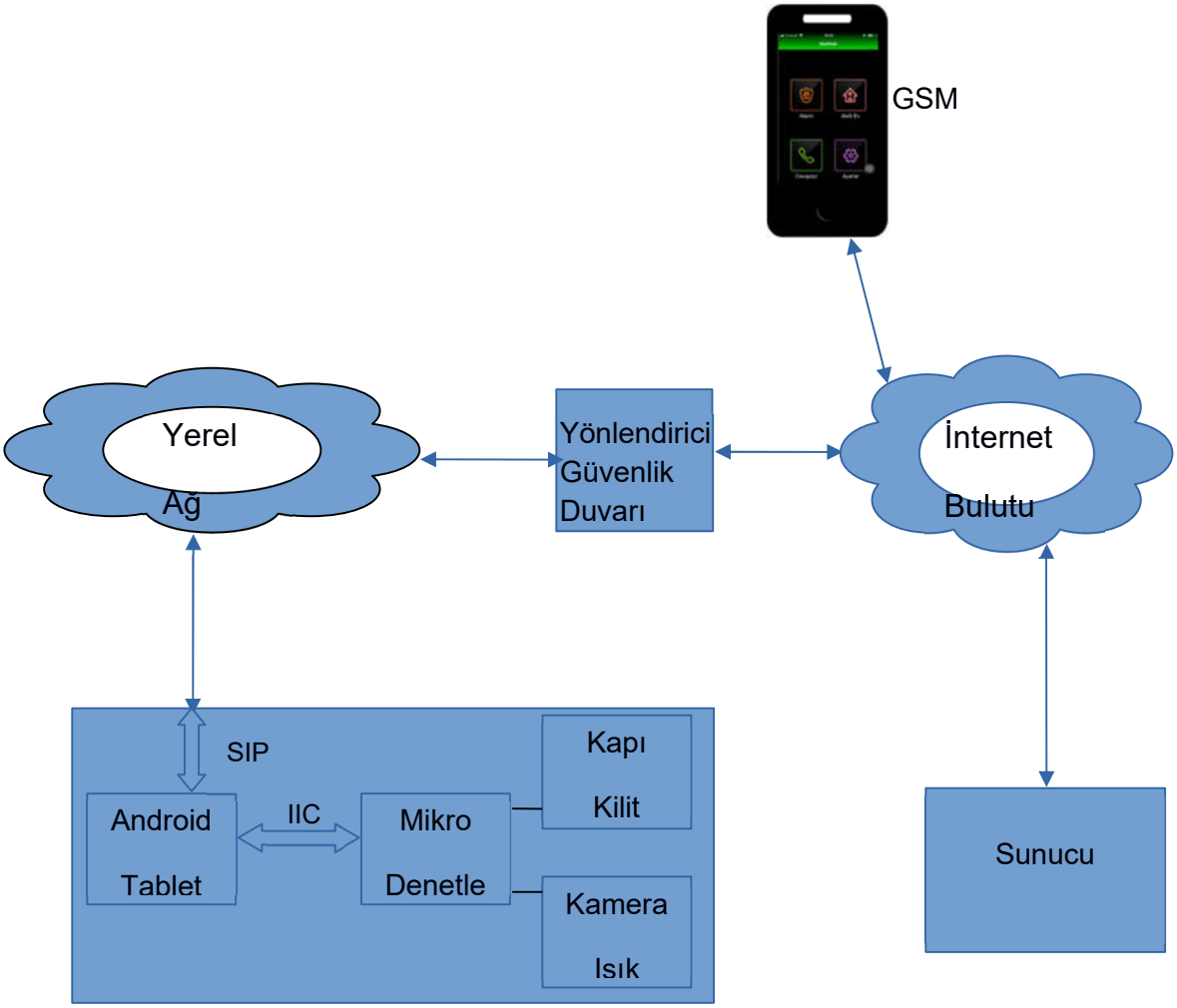

Şekil.3 GSM uygulamasından Kapı modülünün parçalarına erişim blok diyagramı

3. SONUÇ VE ÖNERİLER

Görüntülü Bulut Interkom sisteminde SIP Sohbet mesajları yardımıyla görüntünün daha kaliteli olabilmesi için kapının ışığı ayarlanmış ve kapının açılması kontrol edilmiştir. SIP yöntemiyle görüntülü haberleşme

yönteminde kullanılan portlar kullanılarak kontrol için Yönlendirici ve Güvenlik Duvarına ilave bir çalışma yapılmadan kontrol ve izleme erişimleri yapılmıştır. İlave Emir ve İstek mesajları tanımı ile bir çok denetim ve gözleme işlemi yapılabilecektir.

KAYNAKLAR

1- RFC 3261 Session Initiation Protocol, Rosenberg, J. Schulzrinne, H. Camarillo, G. Johnston A.ve diğerleri . Internet Engineering Task Force, June 2002
2- RFC 3428 Session Initiation Protocol (SIP) Extension for Instant Messaging, Rosenberg, J. Schulzrinne, H. ve diğerleri. Internet Engineering Task Force, December 2002
3- Liblinphone 3.11.1 https://download.linphone.org/releases/docs/liblinphone/3.11.1/c/group__chatroom.html
4 - NXP Semiconductor, Technical Data, Document Number MC9S08PT60, Rev.6, 09/2019https://download.linphone.org/releases/docs/liblinphone/3.11.1/c/group__chatroom.html

APPLICATION OF GREY-MARKOV GMM (1, 1) MODEL FOR FORECASTING NIGERIA ANNUAL SOYBEAN PRODUCTION

Isa Diadia Alhassan[1], Lawal Adamu[2]

[1,2]Department of Mathematics, Federal University of Technology, Minna, Nigeria

ABSTRACT

Providing reliable and dependable information, using a scientifically proven technique to the farmers, other Agricultural stakeholders and Government as a guide for better planning and sustainable Soybean production in Nigeria is the main focus of this paper. Many leguminous crops provide some protein, but Soybean is the only available crop that provides an inexpensive and high quality source of protein comparable to meat, poultry and eggs. A Grey-Markov model was developed to forecast the Nigeria annual Soybean production. The data used in this paper was collected from the United State Department of Agriculture (USDA) for a period of eleven years (2010- 2020). The result revealed a very high percentage forecasting accuracy of 97.7%, thus a high forecasting ability. This shows a reliable and dependable model. The results could assist the farmers, other agricultural stakeholders and government to plan and make better decisions aimed at reducing poverty and ensuring food security.

Keywords: Agriculture, Farmers, Government, Soybeans, Production, Nigeria, Forecasting, Grey-Markov.

EFFECT OF HEAT TREATMENTS ON PROXIMATE COMPOSITION OF SWEET POTATO TUBERS

Oyefeso, B. O.* and Udu, G. O.

Department of Agricultural and Environmental Engineering, Faculty of Technology, University of Ibadan, Ibadan, Nigeria.

ABSTRACT

Sweet potato is an important member of root and tuber crops which serve as a carbohydrate source for large populace in many developing countries. Its tuber is subjected to various heat treatment processes in its conversion from the raw form into final products which can be readily consumed. This study investigated the effects of heat treatment methods on the proximate composition of processed sweet potato tubers. White- and yellow fleshed sweet potato tubers used for this study were sourced locally from Bodija market in Ibadan metropolis, Oyo State, Nigeria. The tubers were subjected to three common heat treatment methods namely boiling, roasting and frying. Sweet potatoes from each of the heat treatments were subjected to proximate analysis. The results obtained shows that the heat treatment methods did not have any significant effect ($p \leq 0.05$) on the carbohydrate content of both varieties. Boiling, on the other hand, had significant effect ($p \leq 0.05$) on the ash, fibre and fat contents while it had no significant effect ($p \leq 0.05$) on the moisture and protein contents of both varieties. Roasting had no significant effect on the fat content although it had significant effect ($p \leq 0.05$) on the ash, fibre, protein and moisture contents of both varieties. All the investigated heat treatment methods had significant effects ($p \leq 0.05$) on the crude fibre and ash contents of both varieties. All the heat treatment methods effectively retained most of the nutrients in the sweet potato tubers within acceptable limits for human consumption. However, frying resulted in increased fat content which is often recommended to be avoided by the medical practitioners and dieticians to avoid the attendant health risks. Boiling is recommended when products of higher moisture and protein contents are desired.

Keywords: Sweet potato, frying, roasting, boiling, proximate composition

1. INTRODUCTION

Sweet potato (*Ipomoea batatas)* is a dicotyledonous plant of the *Convolvulaceae* family. It originated in Latin America from where it was brought to Europe, Africa, India, China and Japan (Woolfe, 1992). It is cultivated in over 100 developing countries and ranks among the seven most important food crops in over 50 of those countries (Bhattiprolu, 2000; Okorie and Onyeneke, 2012). They come in variety of colors and sizes and is rich in vitamins, minerals, antioxidants, fiber and beta carotene. It is appreciated for its very high nutritional value found in the tubers and the young aerial parts which serve as vegetables (Kure *et al.*, 2012).

The tubers are prepared for immediate consumption or processed into various products such as flour, chips, flakes etc. Its flour is very useful in baking and making various confectionary. The processing operations to which the tubers are subjected depend on the desired end products. The unit operations in the processing of sweet potato tubers include peeling, washing, cutting, heat treatments, milling, packaging etc. Heat treatments such as drying, frying, roasting and boiling are among the important processing operations in sweet potato tuber processing (Chukwu *et al*., 2012). Knowledge of the effects of various heat treatment methods on the quality attributes of the tubers is very important to the consumers and the food industry at large. This study was therefore, designed to investigate the effects of selected heat treatment methods on the proximate composition of sweet potato tubers.

2. MATERIALS AND METHODS

2.1 Materials Acquisition

Yellow- and white-fleshed varieties of sweet potato tubers used for the study were purchased at Bodija market in Ibadan, Oyo State. The tubers were packaged in a well ventilated sack and transported to Agricultural and Environmental Engineering Processing laboratory for samples preparation.

2.2 Sample preparation

One hundred and sixty grams of each cultivar was manually peeled and cut into smaller pieces using a sharp stainless-steel knife and washed properly with clean water. The samples were prepared by boiling 40 g of each cultivar with 500 mL of clean water in an aluminum pot for 20 minutes, roasting 40 g of each cultivar using coal, coal pot and wire mesh for 8 minutes and frying 40 g of each cultivar using 300 mL of vegetable oil for 5 minutes using a stainless-steel non-stick frying pan while 40 g fresh (untreated) samples of both cultivars were used as the control.

2.3 Proximate analysis

Proximate analysis of the heat-treated samples was carried out at the Department of Human Nutrition Laboratory, University of Ibadan, Nigeria, The percentage moisture content, carbohydrate, crude protein, fat, fibre and ash contents of the sweet potato tubers were determined according to Association of Official Analytical Chemists Official methods (AOAC, 2000).

2.4 Data analysis

Data obtained from the laboratory analysis were subjected to analysis of variance (ANOVA) and statistical analysis using Statistical Analysis System (SAS) version 9.4.

3. RESULTS AND DISCUSSION

The results of the proximate analysis carried out on the heat treated white-fleshed and yellow-fleshed sweet potato tubers are shown in Table 1. The moisture content ranged between 42.54 and 68.19% which are within the range of values obtained by Bahado-Singh et al. (2006) and Gouado *et al.* (2011). Roasted yellow-fleshed (RYF) sample had the lowest moisture content value of 42.54±0.04 while fried white-fleshed (FWF) sample had the highest value of 68.19±0.02. Fresh yellow-fleshed (CYF, as control) and boiled yellow-fleshed (BYF) samples were not significantly different ($p \leq 0.05$), having values of 59.67±0.02 and 59.64±0.08 respectively. The moisture contents of fresh white-fleshed (CWF, as control) and boiled white-fleshed (BWF) samples were not significantly different ($p \leq 0.05$), having values 61.65±0.05 and 61.61±0.08 respectively. Comparing the results obtained in this study with those by Adepoju and Adejumo (2015) on three sweet potato varieties, the moisture contents of the raw and boiled sweet potatoes were not significantly different, having values 69.80% and 66.20% respectively, which are higher than the values obtained in this study. This showed that the boiled sweet potato when compared to the raw (fresh) tubers contains almost the same amount of moisture.

Table 1: Proximate Composition of Sweet Potato

Samples	Moisture Content (%)	Crude Protein (%)	Crude Fat (%)	Crude Fibre (%)	Ash (%)	Carbohydrate (%)
CYF	59.67±0.02^{c}	1.66±0.06^{d,e}	0.09±0.01^{d}	1.74±0.03^{f}	1.06±0.01^{e}	37.52±0.08^{a}
BYF	59.64±0.08^{c}	1.71±0.05^{d,e}	0.04±0.00^{e}	1.41±0.01^{g}	1.51±0.02^{d}	37.13±0.13^{a}
FYF	43.57±0.03^{e}	1.90±0.13^{d,c}	2.41±0.01^{b}	2.37±0.06^{c}	3.53±0.05^{b}	48.59±0.12^{a}
RYF	42.54±0.04^{f}	3.57±0.13^{a}	0.10±0.00^{d}	3.20±0.0^{b}	3.01±0.04^{c}	50.78±0.13^{a}
CWF	61.65±0.05^{b}	1.46±0.06^{e}	0.15±0.01^{c}	4.90±0.07^{a}	0.77±0.02^{g}	35.97±0.05^{a}
BWF	61.61±0.08^{b}	1.61±0.05^{e}	0.11±0.01^{d}	1.82±0.01^{e}	0.85±0.02^{f}	35.83±0.12^{a}
FWF	68.19±0.02^{a}	2.01±0.08^{c}	2.98±0.03^{a}	1.45±0.05^{g}	4.34±0.04^{a}	22.50±0.05^{a}
RWF	44.69±0.16^{d}	2.70±0.25^{b}	0.10±0.00^{d}	2.03±0.06^{d}	1.53±0.05^{d}	51.00±0.12^{a}

Note: Values within each sample of sweet potato marked by the same letters within same column are not significantly different (p>0.05).

CYF: Control Yellow flesh; BYF: Boiled Yellow Flesh; FYF: Fried Yellow Flesh; RYF: Roasted Yellow Flesh; CWF: Control White Flesh; BWF: Boiled White Flesh; FWF: Fried White Flesh; RWF: Roasted White Flesh

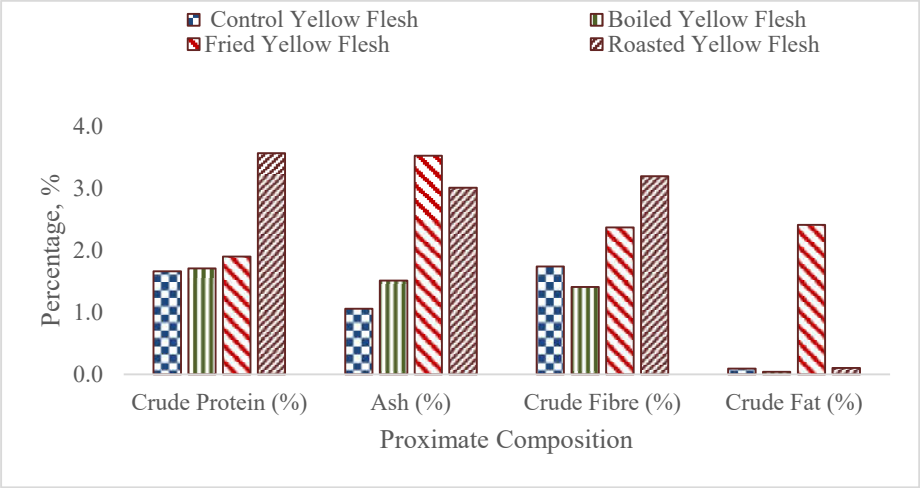

Figure 1-A: Proximate composition of Yellow-fleshed sweet potato

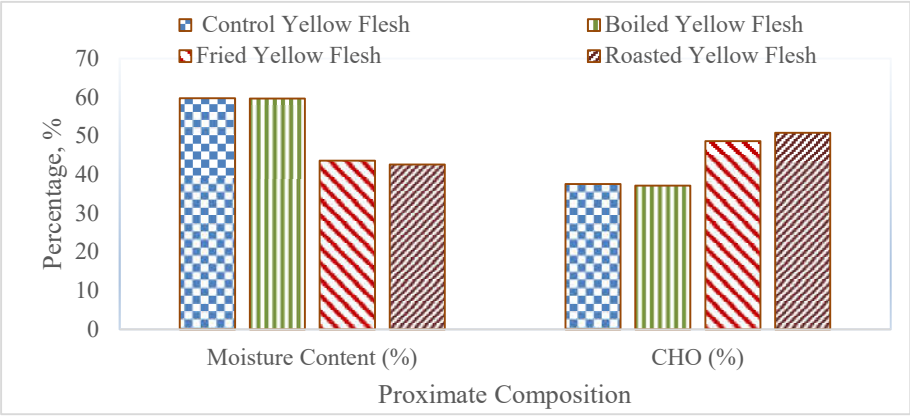

Figure 1-B: Proximate composition of Yellow-fleshed sweet potato

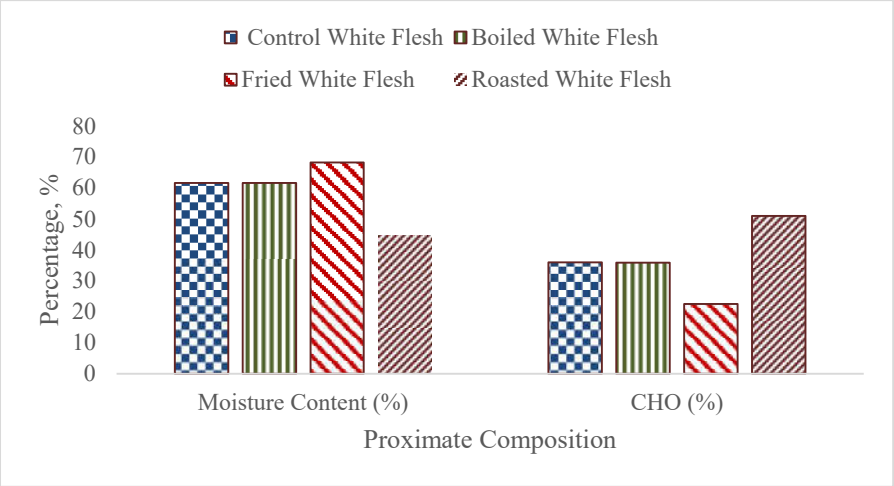

Figure 2-A: Proximate Composition of White-fleshed Sweet Potato

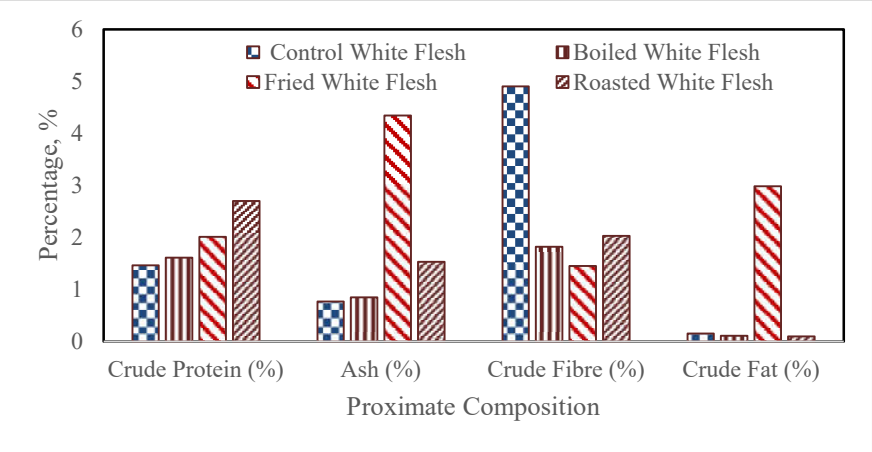

Figure 2-B: Proximate Composition of White-fleshed Sweet Potato

The crude protein obtained ranged between 1.46 and 3.57% with CWF having the lowest value of 1.46±0.06 and RYF having the highest value of 3.57±0.13. CYF and BYF were not significantly different ($p \leq 0.05$), with values 1.66±0.06 and 1.71±0.05 respectively. Also, CWF and BWF were not significantly different ($p \leq 0.05$) in moisture content, with values of 1.46±0.06 and 1.61±0.05 respectively. This showed that the boiled sweet potato tubers when compared to raw (fresh) samples contain almost the same amount of percentage protein. In a study conducted by Dincer *et al.* (2011), protein content of sweet potato ranged between 3.67 and 5.08% which is higher than the values obtained in this study.

The crude fat obtained ranged between 0.04 and 2.98% with BYF having the lowest value of 0.04±0.00 and FWF having the highest value of 2.98±0.03. CYF, RYF, BWF and RWF were not significantly different ($p \leq 0.05$) in fat content having values 0.09±0.01, 0.10±0.00, 0.11±0.01 and 0.10±0.00 respectively. Comparing these results to a study conducted by Akande *et al*. (2015), the fat content of heat-treated cocoyam flour ranged between 5.35 and 8.00% which is higher than the values obtained for sweet potato tubers in this study.

The crude fibre content ranged between 1.41 and 4.90% where BYF had the lowest value of 1.41±0.01 and CWF had the highest value of 4.90±0.07. BYF and FWF were not significantly different ($p \leq 0.05$), with values of 1.41±0.01 and1.45±0.05 respectively. When compared to the control sample, BYF and FWF reduced in fibre content. Also, when compared to a study conducted by Adepoju and Adejumo (2015), the fibre content of sweet potato ranged between 0.81 and 1.00% which is lower than the values obtained in this study.

The ash content ranged between 0.77 and 4.34% with CWF having the lowest value of 0.77±0.02 and FWF having the highest value of 4.34±0.04. BYF and RWF were not significantly different in ash content with values of 1.51±0.02 and 1.53±0.05. This compared to a study conducted by Ajala *et al.* (2014), the ash content of cocoyam flour ranged between 2.467 and 2.967% which is higher than the values obtained in this study.

The carbohydrate content varied between 22.50 and 51.00%. FWF had the lowest value of 22.50±0.05 and RWF had the highest value of 51.00±0.12. There were no significant differences ($p \leq 0.05$) in the total carbohydrate content of the samples when compared with the control samples. This is in agreement with the result obtained by Ikanone *et al.* (2014) where the carbohydrate content of sweet potato when boiled and fried were not significantly different ($p \leq 0.05$) from the control sample.

The carbohydrate contents of both varieties were not significantly affected by the heat treatment methods while other proximate compositions were significantly affected by, at least, one of the heat treatment methods.

4. CONCLUSION

The effect of selected heat treatment methods namely roasting, frying and boiling on the proximate composition of Nigeria-grown white- and yellow-fleshed sweet potato tubers was investigated in this study. All the investigated heat treatment methods had no significant effect on the carbohydrate content of both varieties. Boiling, on the other hand, had significant effect on the ash, fibre and fat contents while it had no significant difference on the moisture content and protein content of both varieties. Roasting had no significant effect on the fat content whereas it had significant effect on the ash content, fibre content, protein content and moisture content of both varieties. The heat treatments had significant effects on the crude fibre content and ash content of both varieties.

All the investigated heat treatment methods sufficiently retained most of the nutrients in the tubers after processing. However, frying resulted in increased fat content which is often recommended to be avoided by the medical practitioners and dieticians to avoid the attendant health risks. Boiling is recommended when products of higher moisture and protein contents are desired.

REFERENCES

Adepoju, A.L. and Adejumo, B.A. (2015). Some Proximate Properties of Sweet Potato (*Ipomoea batatas* L.) as Influenced by Cooking Methods. International Journal of Scientific and Technology Research, 4(3): 146-148.

Ajala, A.S. , Ogunsola, A.D. and Odudele, F.B. (2014). Evaluation of Drying temperature on proximate, thermal and physical properties of cocoyam flour. Global Journal of Engineering design and Technology, 3(4): 13-14.

AOAC (2000). Official Methods of Analysis. 17th Edition, The Association of Official Analytical Chemists, Gaithersburg, MD, USA. Methods 925.10, 65.17, 974.24, 992.16.

Bahado-Singh, P.S. ,Wheatly, A.O. , Ahmad, E.Y. and Asemota, H.N. (2006). Food processing methods influence the glycaemic indices of some commonly eaten West Indian carbohydrate-rich foods. British Journal of Nutrition, 96:476-481.

Bhattiprolu S. (2000). Color, Texture and Rehydration Characteristics of Ohmically Treated Sweet Potatoes. A Thesis Submitted to the Graduate Faculty of the Louisiana State University and Agricultural And Mechanical College, Louisiana.

Chukwu, O., Orhevba, B. A. and Mahmood, B. A. (2010). Influence of Hydrothermal Treatments on Proximate Compositions of Fermented Locust Bean (Dawadawa). Journal of Food Technology, 8 (3):99 – 101

Dincer, C., Karaoglan, M., Erden, F., Tetik, N., Topuz, A. and Ozdemir, F. (2011). Effects of baking and boiling on the Nutritional and Antioxidant properties of sweet potato cultivars. Plant Foods Human Nutrition, 66: 341-347.

Gouado, I., Demasse, M. A., Etame, L. G., Meyimgo, O. R., Solange, E. A. R. and Fokou, E. (2011). Impact of Three Cooking Methods (Steaming, Roasting on Charcoal and Frying) on the β-Carotene and Vitamin C Contents of Plantain and Sweet Potato. American Journal of Food Technology, 6: 994-1001.

Ikanone, C.E.O and Oyekan, P.O. (2014). Effect of Boiling and Frying on the Total Carbohydrate, Vitamin C and Mineral Contents of Irish (*Solanum tuberosum)* and Sweet Potato (*Ipomoea batatas*) Tubers. Official Journal of Nigerian Institute of Food science and Technology, 32(2): 33-39.

Kure, O.A., Nwankwo, L. and Wyasu, G. (2012). Production and quality evaluation of garri like product from sweet potatoes. Journal of Natural production and Plant Resources, 2(2): 318-321.

Okorie, S.U and Onyeneke, E.N. (2012). Production and Quality Evaluation of Baked Cake from Blend of Sweet Potatoes and Wheat Flour. Journal of Natural and Applied Science, Vol.3, No. 2.

Woolfe, J. A. (1992). Sweet potato; An untapped food resource. Cambridge University Press, Cambridge, UK, 29(1): 643-648.

SIZE AT REPRODUCTIVE MATURITY ONSET IN *GARCINIA KOLA* (HECKEL)

[1]Okonkwo, H.O, [2]Omokhua, G. E., and [2]Chima U. D.,

1. Swamp Forest Research station, Forestry Research Institute of Nigeria, Onne
2. Dept of Forestry and Wildlife Management, Faculty of Agriculture, University of Port Harcourt

ABSTRACT

Little is known of the life history of *Garcinia kola*; the present study is therefore designed to investigate the size of *G. kola* tree at reproductive maturity onset in the tropical rainforest-mangrove transition zone south of Nigeria. A total of twenty (20) trees were used in the study viz: ten (10) ten-year-olds at reproductive maturity onset, and ten (10) thirty-year-olds with several cycles of reproduction that make up two independent variables. Data collected were age of onset of flowering/fruiting and size at reproductive maturity onset. Relative size at reproductive maturity onset (RSOM) was estimated as size at reproductive maturity onset (SOM) divided by asymptotic maximal size (AMS). Data analysis was conducted using pairwise t-test and principal component analysis (PCA). Reproductive maturity onset (flower/fruit onset) was recorded in the ten-year-old stand ten (10) years after planting. Mean size at reproductive maturity onset (SOM) was height 5.32±1.7m, dbh 0.11±0.03m, total number of branches was 29.6±7.3m, crown depth 5.24±1.05m, crown diameter was 4.78±0.7m, and branch diameter 0.098±0.01m and asymptotic maximal size (AMS) was height 19.85±0.76m, dbh 0.95±0.09m, total number of branches 62±5m, crown depth 18.83±0.7m, crown diameter12.5±1.64m, and branch diameter 0.5±1.6m. Pairwise t-test analysis showed there was significant differences between SOM and AMS in all growth factors except leaf length, leaf breadth, and twig length. Highest relative size at reproductive maturity onset (RSOM) was recorded in leaf length 0.82, twig length 0.82, and leaf breadth 0.80, while, the lowest was branch diameter 0.11. Four components out of the total of eleven were extracted to explain the total variation in RSOM: Principal component one (PC1) explained 37.23%; PC2 26.4%, PC3 22.73%, and PC4 13.64%.

Keywords: Maturity, age, relative-size, reproductive, onset, asymptotic

IMPACT OF UREA-SULPHUR MIXTURE ADDITIVE IN SWEET POTATO PEEL UTILIZATION ON PERFORMANCE, HAEMATOLOGY AND BLOOD CHEMISTRY OF WEST AFRICAN DWARF SHEEP

***Micheal Taiwo AYANKOSO[1,2] and Azeez Olanrewaju YUSUF [2]**

[1]Department of Animal Science, Adekunle Ajasin University, Akungba-Akoko, Ondo State

[2]Department of Animal Production and Health, Federal University of Agriculture, Abeokuta, Ogun State

ABSTRACT

A 90- day study was conducted to investigate the impact of urea and sulphur mixture additive on the performance, haematology, blood serum chemistry and rumen ecology of West African Dwarf (WAD) sheep raised on intensive management system. Four diets (D1- D4) contained 30 % sweet potato peel were compounded with varying levels of sulphur and urea. D1 (control), D2 (control + 0.2 % Sulphur), D3 (control + 0.3% urea), D4 (control + 0.1% sulphur + 0.15% urea). Twenty WAD sheep weighed 12 kg and six (6) months age, approximately were used for study. The animals were grouped into four with five animals in each group which were randomly assigned into each of the four experimental diets. Data were obtained on the performance (feed intake and weight), haematology and blood chemistry, and rumen ecology of the animals which were subjected to one-way analysis of variance at 5 % level of probability. Performance in terms of weight gain was significantly ($P<0.05$) influenced by urea and sulphur additive with the highest in group of animals that received 0.2 % sulphur and control while the least was obtained in animals that received mixture of urea and sulphur. All parameters observed for haematology were significant expect for Basophils, monocytes and mean corpscular haemoglobin concentration which were not influenced ($P>0.05$). Individual supplementation of urea and suphur better influenced blood indices rather than when mixture was added. This study could be concluded that individual supplementation of sulphur on sweet potato peel diets improved the performance, blood and serum indices without any deletrious effect on the rumen ecology of WAD sheep

Keywords: Sweet potato peel, Urea, Sulphur, Additive, Performance

INTRODUCTION

Sheep and goats are reared for divers intentions which include but not limited to proceeds generation, spiritual purpose, family consumption, and food security especially when there is set back in crop production (Ozung *et al.,* 2011) but their production is confronted with different challenges in the tropics mostly during the dry season due to unavailability of forages in terms of quantity and quality, hence, militating against its performance and productivity which invariably affects human protein intake culminating into diseases such as Kwashorkor and general malformation of the general body systems (Osuji *et al.,* 1993, Aregheore, 2000 and Okai *et al.,* 2005). Use of non-convectional feedstuff is encouraged as an effort made to anticipate maximum productivity of livestock. Adequate inclusion of ingredients as additives or supplements with high protein can be used to optimize the utilization of roughages to increase the productivity of sheep for efficient consumption and maximum performance (Nsahlai, 1991). Unfortunately, these resources are costly and grossly insufficient leading to rivalry between man and animals (Pond *et al.,* 1995).

During the rainy season, forage crops are reasonably accessible and livestock tends to accumulate weight and retain their economic values (Babayemi *et al.,* 2003) but the major challenge confronting ruminant production is how to feed the animals throughout the year (Akinlade *et al.,* 2005). Dried or preserved forages can be leveraged on by ruminants during the scarce period when animals lose a considerable percentage of their body weight.

Malik *et al*. (2011) identified sweet potato peel as an important by-product which are readily available as kitchen waste produced all over the world, with highest being produced in Asia and Africa (FAO, 2020). Sweet potato possesses about 3.2 to 4.2 % N and can be used as supplement for energy in ruminat feeding. Sweet potato and its peels remain largely a food and feed product with minimum utilization procedures (Ma, 2019). Although, crude protein in sweet potato peel is far below the minimum requirement for maintenance production of ruminants. Like most other agricultural by-products, it is high in fibre and energy but deficient in crude protein. Research has shown that large quantities of crop by-products produced at homes, on private and government farms in Nigeria is unexploited year after year and majority are thrown away in waste bins, while others are left to decay in the field or burnt (Onyeonagu and Njoku, 2010). However, it has been reported that, West African Dwarf (WAD) sheep when fed these crop by-products are able to meet up with their maintenance requirement and optimal productivity levels when supplemented with other ingredients (Kalio, *et al.,* 2013; Kalio and Anyanwu, 2016). Therefore, urea and sulphur supplimentation as feed additives can further improve the nutritive value of sweet potato peels. Feed additives are products used in animal nutrition to improve the quality of feed for livestock and the quality of food for human from animal origin, or to improve the animals' performance and health (Akbar and Yaser, 2021).

Sulphur is an important component required for living, but mostly occurred in organic forms or metal sulphide. It is one of the fundamental natural elements required for protein synthesis and biochemical functioning of all living organisms. Sulphur supplementation has promoted the production and microbial protein in the rumen, as well as cellulose digestion (Qi *et al*., 1994).

Urea is commonly added to ruminant diet as a source of non-protein nitrogen that is rapidly hydrolyzed to ammonia in the rumen so as to improve the nutrition of low-quality agricultural by-products. Urea can be fed to ruminants as an economical replacement for protein in a ration. The amount of urea a ruminant animal can use depends on the digestible energy or total digestible nutrients content of the ration.

Haematological and biochemical indices of animals provide some alertness about the production performance abilities of West African Dwarf sheep (Orheruata and Akhuomobhogbe, 2006) and reveal the efficient approachability of the animal to its environments which include feeds and feeding (Esonu *et al.,* 2001) and is one of the quickest ways of adjudging medical and dietary health status of animal on feeding trier through blood analysis, this is because blood contains a numerous metabolites and other constituents which provide a valuable means for clinical investigation and nutritional status of man and animals (Okukpe *et al.,* 2011).

MATERIALS AND METHODS

Experimental site

This research work was carried out at the Teaching and Research Farms of the Department of Animal Production and Health, College of Animal Science and Livestock Production, Federal University of Agriculture, Abeokuta, located on Latitude 7° 15' N, Longitude 3° 26' E with an altitude of 76 m above sea level (Google earth map 2021). It is situated in the derived savannah zone of South-Western Nigeria with an average annual rainfall and temperature of 1,037 mm and 34.7ºC respectively (AccuWeather 2021) with a yearly average humidity of 83 % (Meteorological Station, FUNAAB).

Experimental materials

Fresh Sweet potato (*Ipomea batatas*) peels were purchased from chips processing industries in Abeokuta and its environment. The peels were sun-dried, ground and bagged in water-proof air tight containers for analysis and feeding trial. The urea was bought from the Ministry of Agriculture, Asero, Abeokuta, while sublime sulphur was obtained from local market in Abeokuta.

Experimental Animals and Management

Twenty (20) yearling West African Dwarf sheep weighing approximately 12kg were purchased from a reputable local market in Abeokuta, Ogun state, Nigeria. The animals on arrival were quarantined for 28 days in a pen that had been previously washed and disinfected using Iodophor® (Azintol) solution. The animals were treated against internal and external parasites using Ivomec at 1ml to 25kg body weight and Penstrep® (a broad spectrum antibiotics) at 2ml to 25kg body weight for three days. Each animal was also treated against ecto parasites using acaricide baths. They were also vaccinated with *peste des petits* ruminant (PPR) vaccine during the quarantined period. Thereafter, they were placed in individual pens having a raised slated floor and clean water was offered *ad-libitum* throughout the period of the experiment.

Experimental diet

The ground sweet potato peels were mixed with other ingredients - palm kernel cake (PKC), wheat offal, oyster shell, bone meal and table salt to compound concentrate diets (Table 1). The concentrate diets were formulated with varying levels of urea-sulphur mixture additives designed as treatment 1 (D1) which is the control diet (sweet potato peel based concentrate, SPPBC) with 0 % urea-sulphur additive, Treatment 2 (D2): SPPBC + 0.2 % Sulphur, Treatment 3 (D3): SPPBC + 0. 3% urea, Treatment 4 (D4): SPPBC + 0.1 % sulphur + 0.15 % urea.

Experimental Design

The twenty West African Dwarf sheep were divided into four groups of five animals per group where each animal was an experimental animal. The animals were randomly assigned into four experimental diets in a completely randomized design. The animals were fed at 4 % of their body weight which was adjusted weekly.

Data collection

Performance

Body weight: Weight of individual animal was measured at the commencement of the trial and subsequently on weekly basis throughout the experiment using Measuretech® digital hanging scale of 50 ±5 kg capacity.

Feed Intake: This was measured by recording the difference in the quantity of feed offered and quantity of feed refused.

Average daily gain (ADG): This was determined by dividing the total weight gained of each animal by the entire period of the experiment as shown in the formula below;

$$\text{ADG (g)} = \frac{\text{Final weight (g) - Initial weight (g)}}{\text{Number of days (days)}}$$

Average feed intake per day: It was determined by dividing the total feed intake by the number of days used for the experiment.

Feed conversion ratio: It was measured by estimating the ratio of feed intake to weight gain of each animal.

$$\text{Feed efficiency ratio} = \frac{\text{Daily feed intake (g/day)}}{\text{Daily weight gain (g/day)}}$$

Chemical Analysis: A fraction of the dried and milled experimental diets were ground and passed through a 2mm sieve before analysis. The crude protein of each of the samples was determined using the automated Kjeldahl method (AOAC, 2000). The dry matter was determined by drying at 65^{o}C for 48 hours in an oven while ash was measured by burning further at 600^{o}C for 24 hours in a muffle furnace. Ether extract was

determined according to the methods described by (AOAC, 2000). The neutral detergent fibre (NDF) and acid detergent fibre (ADF) composition were analysed using the method described by Van Soest *et al*. (1991).

Blood sample collection and analysis

About 10 ml of blood sample was collected via jugular venipunctures as descibed by (Frandson and Spurgeon, 1992) using hypodermic needles and syringe at the end of the experiment (12th week). About 5 ml of the blood sample was released into the sample bottle containing Ethylene Dimethyltetra Acetic Acid (EDTA) and Sodium fluoride (NaF) as anti-coagulant, and the bottles were gently mixed to ensure proper mixing of the blood with EDTA and NaF to prevent coagulation. The remaining 5ml of blood samples were dispensed into the plain blood sample without anti-coagulant to harvest serum. The blood smears were prepared immediately after the collection of samples. The red blood cell (RBC), packed cell volume (PCV) and haemoglobin (Hb) were determined by the capillary centrifuge while mean corpscular volume (MCV) and mean corpscular haemoglobin concentration (MCHC) were estimated from red blood cell, PCV and Hb in accordance to Schalm *et al*. (1986). White blood cell (WBC) was determined using Wintrobe method. Differential counts of white blood cell (neutrophils, eosinophils and lymphocytes) were determined using Giemsa's stain method by fixing thin blood smear in alcohol.

Statistical Analysis

The data collected were subjected to one-way Analysis of Variance (ANOVA) using the general linear model (GLM) procedure of SAS (2008). Significant differences among means were separated using the Duncan's Multiple Range Test.

RESULTS

Table 2 showed the result of proximate analysis (%) of sweet potato peel based diet with urea-sulphur mixture additives. Higher numerical values were obtained for crude protein ranging from 14.29 to17.96 which was inversely related to numerical values obtained for crude fibre ranging from 4.23 to 4.70 for treatments.

Table 3 showed influence of sweet potato peel based diet supplemented with urea-sulphur combination additives on performance of West African Dwarf (WAD) Sheep. Weight gain was observed to be significant ($P<0.05$) across the treatments with highest value (4688.57g) in animals fed 0.2 % sulphur, which was similar to those fed control (4600g), followed by those 0.15 % urea (4408.57g) and the least (4290g) was observed in those fed combinatnation of urea and sulphur. Also, higher numerical value (489.92g) was obtained for feed intake in animals fed comtrol diet while the least (469.44g) was obtained in those fed 0.2 % sulphur.

Haematological performance of WAD sheep fed sweet potato based diets supplemented with urea-sulphur mixture additives is presented in table 4. All the results obtained for haematology were significant ($P<0.05$) except for basophil and mean corpscular haemoglobin concentration (MCHC) which were similar ($P>0.05$). Higher similar trends were obtained for packed cell volume, haemoglobin and red blood cells in D3. D4 and D1 while the least were obtained in D2. White blood cell was higher in D1, D3,and D2 while the lower value was obtained in D4. Neutrophil was highest in D4, followed by D2 which is similar to the value obtained in D3. Lymphocyte had the highest value in animals in D3, D2, D1 while the least value was obtained in D4. Eosinophil was highest in D3 and D1, while the least was obtained in D2. Mean corpscular volume was higher in D3 and D1 while the least was obtained in D4 and D2.

Table 5 showed the effect of sweet potato peel supplemented with urea-sulphur combination additives on serum biochemical parameters. All the parameters observed were similar ($P>0.05$) except for cholesterol and aminotransferase. Cholesterol was observed to be significant ($P<0.05$) with the highest values in those animals that received D3 and D2, followed by D1 which was similar to D4. Aspartate aminotransferase was

also significant (P<0.05) with the highest values in animald that consumed D2, D4 and D1 while the least value was obtained in animals fed D3.

Table 7 and 8 showed the results of the effect of sweet potato peel supplemented with urea-sulphur mix additives on oxidative stability and rumen microbial population. All the parameters obtained were similar (P>0.05).

4.2 DISCUSSION

Diet utilization is an essential factor considered in animal production of which inclusion of sweet potato peels better influences the performance of experimental WAD sheep used in this study which gave higher numerical values in terms of feed intake and weight gain compare with the values reported Olorunnisomo (2010) for sheep fed maize and amaranth fodders which might be due to the inclusion of urea-sulphur mixture additives which might have probably influenced the palatability and utilization of the diets by the experimental animals. No deleterious depression in growth was observed in sheep fed diets containing 30 % inclusion of sweet potato peels. Higher weight gain was obtained for animals fed 0.2 % sulphur inclusion, which showed that the presence of sulphur has significant influence on the performance of the animals or might have better reacted with other ingredients to aid digestion and assimilation of the feed. However, non-significant effect of urea-sulphur additive was observed on feed conversion ratio (FCR) and weight gain which was similar to report of Thanh *et al.* (2012) who observed no effect of nitrates supplementation on weight gain in sheep but in contrast to that of Kalio *et al*. (2014) who fed WAD bucks with cassava peels treated with urea and broiler litter which might be due difference in types of animal and feed ingredient used which was also in consonance to the report of Trinh phuchao *et al.* (2009) who fed nitrate supplement to goat.

Observation of blood components remains one of the fastest and easiest means of predicting the health status of an animal. The packed cell volume values obtained in this study ranges between 25.00 - 34.33 L/L and it falls within the normal range (27 - 45 L/L) cited by Merck (2012) for healthy animal except for the group of animals fed 0.2 % sulphur inclusion, this implies that urea and combination of sulphur and urea can be supplemented into sweet potato peel diet for proper utilization of feed and improved performance. High PCV values obtained for WAD bucks fed sweet potato peels and other crop residues by Kalio *et al* (2013) corroborates PCV values obtained in this study . This is an indication that urea had influence the production of PCVwhich showed the soundness in the health status of animals, this is in consonnance with Njidda *et al.* (2014) who reported similar values for healthier sheep.

The value of haemoglobin obtained in this study was within the normal range (8 - 12 g/dl) normal range for sheep, this was also similar to the values obtained by Kalio *et al* (2013) for WAD bucks fed sweet potato peels, High parameters obtained for haemoglobin in this experiment showed that sweet potato peel supplemented with urea-sulphur mixture improves the iron content of the blood which is responsible for efficient respiratory activities in the body by transporting oxygen to tissues of the animal for oxidation of ingested food so as to release energy for other body functions as well as transport carbon dioxide out of the body of animals ((Maton *et al.,* 1993; Soetan *et al*., 2013). Generally, the values of WBC obtained in this study was higher than both the normal range reported for temperate sheep (4 x10^6/L-12 x 10^6 /L) (Schalm *et al*., 1986) and west African Dwarf sheep (15.24 x 10^6/L) of the tropics (Oduye, 1976). The increase in the WBC concentration obtained in this study is an indication of greater ability to resist disease infection which might have been aquired due to high plane of nutrition of the animals (Cheesbrough, 2004). This high concentration of WBC across the treatments might be due to presence of urea-sulphur additives in their diets. High WBC obtained is in contrast to the study of Kalio *et al.* (2013) who fed WAD bucks different crop residue and recording a low value of 8.30 x10^9/L for treatment with ordinary sweet potato, but in consonance to high values obtained by Saka *et al.* (2016) who fed different proportion of malted sorghum sprout to WAD goats. The higher leucocyte count in this study is an indicator of high level of immune response to infections or toxic substances which might be generated by the environment or additives in the feed (Bradbury *et al*., 1999).

Red blood cells (erythrocytes) serve as a carrier of haemoglobin which reacts with dissolved oxygen in the blood to form oxyhaemoglobin during respiration (Johnson and Morris, 1996) and subsequently aided transport of oxygen and removal of carbon dioxide in the body (Isaac *et al.* 2013; Soetan *et al*., 2013). The result of this study showed low value (2.6 – 3.3 x 10^{12}/L) of RBC which corroborates Anya *et al.* (2018) where pragmatic reduction in RBC counts of WAD goats were observed when fed increasing level of African yam bean seed meal. High value (11.45 - 15.22 x10^{12}/L) of RBC reported by Kalio *et al.,* (2013) who fed WAD bucks sweet potato peel with different crop residue which contradicts the result obtained for RBC in this current studywhich might be due to nutritional level of the ingredient used or season in which the experiment was carried out. The low value of RBC obtained in this study might also be attributed to immune response to infections or toxic substances in the feed while there was an an increase in WBC combacting the foreign objects in the body.

Higher values obtained in anmals fed urea-sulphur additives might be due to the presence of non-protein nitrogen which might have influenced the digestion of the feed coupled with the fact that sheep are known to be high cholesterol containing animals with capabitity to synthesize cholesterol from body fat. Values obtained in this study fall within the range (84-112.10 mg/dl) reported by (Hatta *et al*., 2019) who supplemented sheep's diets with shrimps waste without any deleterious effect. Aspartate aminotransferase (AST) decreased significantly in animals that received only urea additive. By implication, hazardous effect AST could be averted through the inclusion of urea to prevent conditions such as anorexia, coronary heart disease and muscular pathologies (Donald, 2016)

The micoflora (fungi, bacteria and fungi) level of the animals used in this study were not negatively influenced by the urea-sulphur additive and the pH were within the the normal range which permits efficiemt microbial activities in this animal. This is in line with the report of Qi *et al*. (1994) who said sulphur supplementation could be used to better influence the microbial rumen ecology of ruminants improved degradability of roughages.

Therefore, it could be concluded from this study that urea-sulphur additives is capable of inproving the utilization of sweet potato peels which invariably increase the feed intake and daily weight gain with better influence on the blood chemistry of the animals especially when added at 0.3 % level of urea.

REFERENCES

Accuweather. (2021). http://www.accuweather.com

Akbar, K. And Yaser K.D. (2021). Effect of different feed additives on growth performance and Production in livestock. Available at https://www.researchgate.net/publication/350655569. Accessed on 4th May, 2022.

Akinlade, A.J., Smith, J.W., Adekunle, I.O., Olanite, J.O. and Bamikole, M.A. (2005). Efeect of feed increasing levels of tropical kudzu (*Pueraria phaseoloides*) on feed intake, weight changes and manure production of weaned Ndama cattle fed a basal diet of poor quality guinea grass. *Bulletin of Animal Health Production in Africa*, 53(3):187-193.

Anya, M. I., Ozung, P.O., Okah, U., Ayuk, A. A. and Igwe, P.A. (2018). Blood Profile of West African Dwarf (WAD) Goats Fed Cassava Peel Meal Based- Diets Supplemented with African Yambean Concentrate. *Canadian Journal of Agriculture and Crops*, 3(2): 55-63

AOAC. (2000). Official methods of analysis. Association of Official Analytical Chemists. 17th ed. Arlington, VA, USA.

Aregheore, E. M. (2000). Chemical composition and nutritive value of some tropical by-product feedstuffs for small ruminants. In vivo and in vitro digestibility. *Animal Feed Science and Technology.* 85(1): 99-109.

Babayemi, O.J., Bamikole, M.A., Daniel, A.O., Ogungbesan, A. and Babatunde, A. (2003). Growth nutritive value and dry matter degradability of three *Tephrosia* species. *Nigerian Journal of Animal Production*, 30(1); 62-70.

Bradbury, M. G., Egan, S. V. and Bradbury, J. H. (1999). Determination of all forms of Cyanogen in cassava Roots and cassava Products Using Picrate paper kits. J.S. Clinical cases of Small ruminants in Zaria, Nigeria. *Bulletin of Animal Heath and Production in Africa*. 30:111-116

Cheesbrough, M. (2004). District Laboratory Practice in tropical Countries. Part 2, University Press Cambridge United Kingdom, 266-342.

Donald, W.S. (2016). Ecotoxicology Essentials: Environmental contaminants and their Biological Effects on Animals and Plants. Cooperative Wildlife Wesearch Laboratory and Department of Zoology, Southern Illinois University, Carbondale, IL, USA. p 475-490

Esonu, B.O., Oliver, O.E., Udedibie, A.B.I., Herbert, U., Epkpor, C.F., Okoli, I.C. and Iheukwumere, F.C. (2001). Performnce and blood chemistry of weaner pigs fed raw Mucuna (Velvet bean) meal. *Tropical Animal Production Investment*, 4: 49-54

FAO.(2020). Value Chain Analysis Highlights: Sweet potatoes in Lanao delSur Manila, Philippines, #2. Avalaible at fao.org/publications/car Accessed on 4th February, 2022.

Frandson, R.D. and Spurgeon, T.L. (1992). Anatomy and Physiology (4th Edition) Lea and Febiger, London.

Google Earth Map. (2021). http://www.earth.google.com

Hatta, M., Priyanto, R., Mas, M.S. and Prahesti K.I. (2019). Chemical characteristics and cholesterol level of local sheep with intensive fattening. IOP Conference Series: Earth and Environmental Science, 247: 012025.

Isaac, L.J., Abah, G., Akpan, B. and Ekaette, I.U. (2013). Haematological properties of different breeds and sexes of rabbits. Proceedings of the 18th Annual Conference of Animal Science Association of Nigeria. p. 24-27

Johnson, J.K. and Morris, D.D. (1996). Alterations in blood proteins. In B.P. Smith (Ed.), *International Animal Medicine* (2nd ed.). USA: Mosby Publishers.

Kalio, G. A., Ayuk, A. A. and Agwunobi, L. N. (2014). Performance of West African Dwarf (WAD) goats fed n-treated source and forage supplemented cassava peels in humid Cross River State, Nigeria. *American Journal of Experimental Agriculture.* 4(6): 629-638.

Kalio, G.A., Okafor, B.B. and Ingweye, J.N., (2013). Haematology and Biochemistry of West African Dwarf (WAD) Bucks fed crop by-products in Humid Tropical Nigeria. *The Experiment,* 18(2): 1227-1234.

Kalio, G,A and Anyanwu, N.J. (2016). Performance and haemato-Biochemical profiles of West African Dwarf (WAD) Does fed selected crop by-products in Nigeria. Agrosearch, 16(2): 41-50

Ma, D. (2019).Global market trends, challenges, and the future of the sweet potato processing industry. In: Mu, T. And Singh, J. Edition 2019. Sweet potato, Academic Press, 381-392. Available at feedipedia.org/node/26. Accessed on the 4th February, 2022.

Malik, A. A., Kudu, Y. S., Ibrahim, M. J., Agunbiade, A. A. and Oyedepo, M. T. (2011). Performance of growing rabbits fed graded levels of sweet potato (*Ipomea batatas*) peel meal diets supplemented with and without molasses. *Proceeding of the 35th Conference Nigeria Society for Animal Production, University of Abuja, Nigeria.* Pp. 280–283.

Maton, A., Hopkins, R. L. J., McLaughlin, C. W., Johnson, S., Warner, C. W., LaHart, D., and Wright, J. D. (1993). *Human Biology and Health*. Englewood Cliffs, New Jersey, USA: Prentice Hall

Merck Manual. (2012). Haematological reference ranges. Merck Veterinary Manual. Retrieved from http://www.merckmanuals.com/

Njidda, A.A., Shuai'Bu, A.A. and Isidahomen, C.E. (2014). Haematological and serum biochemical indices of sheep in semi-arid environment of Northern Nigeria. *J. Sci. Front. Res.*, *14*(2):49-56.

Nsahlai, I. V. (1991). The effect of quantity and quality of nitrogen upon straw utilization by steers. PhD Thesis. University of Reading, U.K. In: Ghana *Journal of Animal Science,* 5 (1): 16-22.

Oduye, O.O. (1976). Haematological values of Nigerian goats and sheep.*Tropical aninal Hith. Production*, 8: 131-136.

Okai, D. B., Abora, P. K. B., Davis, T. and Martin, A. (2005). Nutrient composition,availability, current and potential uses of "Dusa": A cereal by-product obtained from "koko"(porridge) production. *Journal of Science and Technology,* 25: 33-38.

Okukpe, K.M., Adeloye, A., Yousuf, M., Alli, O.I., Belewu, M. and Adebisi, A. (2011). Physiological response of West African Dwarf Goats to Oral Supplementation with Omega-3-fatty Acid. *Asian Journal of Animal Sciences*, 5(6): 365-372.

Olorunnisomo, O. A. (2010). Nutritive value of conserved maize, amaranth or maize-amaranth mixture as dry season fodder for growing West African Dwarf sheep. *Livestock Research for Rural Development.* 22: 191. http://www.lrrd.org/lrrd22/10/olor22191.htm

Onyeonagu, C. C. and Njoku, O. L. (2010). Crop Residues and Agro-Industrial by-products used in traditional sheep and goat production in Rural Communities of Markudi Local Government Area. *Journal of Tropical Agriculture, Food, Environment and Extension,* 9 (3): 161-169.

Orherunta, A.M. and Akhuomobhogbe, P.U. (2006). Haematological and blood biochemical indices in West African Dwarf goats vaccinated against *Pestes des peptit ruminants* (PPR). African *Journal of Biotechnology*, 5(9): 743-748.

Osuji, P. O., Nsahlai, I. V. and Khalil, H. (1993). Feed evaluation. ILCA Manual 5. ILCA (International Livestock Centre for Africa), Addis Ababa, Ethiopia. Pp. 40.

Ozung, P. O., Nsa, E. E., Ebegbulem, V. N. and Ubua, J. A. (2011). The potentials of small ruminant production in cross river rain forest zone of Nigeria: A review. *Continental Journal of Animal and Veterinary Research,* 3(1): 33-37.

Pond, W. G., Church, D. C. and Pond, K. R. (1995). Basic Animal Nutrition and Feeding, 4th Edition. John Wiley and Sons Inc., USA. Pp. 416-419.

Qi, K., Lu, C. D. and Owens, F. N. (1994). Effects of sulfate supplementation on performance, acid-base balance, and nutrient metabolism in Angora kids. *Small Ruminant Research,* 15: 19-29.

Saka, A. A., Sowande, O. S., Oni, O. A., Adewumi, O. O., Ogunleke, F.O. and Sodipe, O. G. (2016). Performance Evaluation and Haematological Parameters of West African Dwarf Goats Fed Diet Containing Graded Level of Raw and Fermented Malted Sorghum Sprout. *Nigerian Journal of Animal Science, 2*:444 – 457

SAS. (2008). Statistical Analysis System User's Guide. SAS Institute Inc; Cary, N.C. 27513. U.S.A.

Schalm, O.W., Jain, N.C., Carroll, E.J. (1986). Veterinary haematology 4th Edition Lea and FEBIGER, Philadephia.

Soetan K.O., Akinrinde A.S. and Ajibade T.O. (2013). Preliminary studies on the haematological parameters of cockerels fed raw and processed guinea corn *(Sorghum bicolor)*. Proceedings of 38th Annual conference of Nigerian Society for Animal Production. p.49-52.

Thanh, V. D., Thu, N. V. and Preston, T. R. (2012). Effect of potassium nitrate or urea as NPN sources associated with Mangosteen peel (*Garcinia mangostana*) on methane production, rumen parameters and growth performance of Phan Rang sheep in the Mekong Delta of Vietnam. *Livestock Research Rural Development.* 24:4. Retrieved from http://www.lrrd.org/lrrd24/4/thanh24073.htm

Trinh Phuchao, H. D., Preston, T. R. and Leng, R. A. (2009). Nitrate as fermentable nitrogen supplemented for goats fed forage based diets low in true protein. *Livestock Research Rural Development, 2*1: 1. Retrieved from http://www.lrrd.org/lrrd21/1/trin21010.htm

Van Soest, P.J., Robertson, J.B. and Lewis, B.A. (1991). Methods for dietary fibre, neutral detergent fibre, and non-starch carbohydrates in relation to animal nutrition. *Journal of Dairy Science*, 74: 3583–3597.

Wang, Z. and McAllister, T.A. (2002). Rumen Microbes, enzymes and feed digestion-A review. *Asian-Australas Journal of Animal Science,* 15(11): 1659-1676.

GUAVA PRUNING PRACTICES- AN OVERVIEW

Mujahid ALI

Water Management Research Farm, Renala Khurd, 56150 Okara, Pakistan

ORCID ID: 0000-0002-5200-1019

ABSTRACT

For sustainable guava production, pruning is indispensable in orchards. One of the prominent cultural and management practices in sustainable production from orchards is pruning. Orchard Pruning is one of the most important cultural practices in orchards. The life and bearing time of the orchard are prolonged by its proper implementation. Quality fruit production in developed countries has mainly because of proper and timely pruning. It ensures maintaining normal C:N ratio. The intensity of pruning is of utmost vital regarding next season's fruiting. Balance of vegetative and reproductive growth is key to providing desired results. Different cultivars have a specific level of pruning. Pruning starts as training from the first year of the plant. It could be manual or with a pruning machine. After pruning it could be sprayed with broad-spectrum fungicide. Pruning severity will increase with the increase in the planting density of the orchard. This review article focused on the significance, outcomes, and benefits of pruning with respective age and season/time of pruning in guava and its hazardous impacts of no pruning or improper methods of pruning.

Keywords; pruning; Psidium guajava, yield, growth, antioxidants

SOURCES OF AGRICULTURAL LABOUR PRODUCTIVITY GAP IN RURAL NIGERIA: A MICRO-LEVEL DECOMPOSITION

John Chiwuzulum Odozi

Department of Agricultural Economics and Extension, Faculty of Agriculture, Ajayi Crowther University, Oyo Town, P.M.B 1066, Oyo, Oyo State, Nigeria

ORCID NO: 0000-0001-9637-8195

ABSTRACT

Nigeria's agricultural productivity lags behind the rest of the economy despite the substantial number of people employed in the sector and its roles in poverty reduction and growth of the economy. Using the three waves of the Nigerian Living Standard Measurement Survey Data Set (2010/2011/ 2012/2013 and 2015/2016) and a microeconomic decomposition approach, the study estimated the extent of gap between agriculture and non-agriculture and the underlying sources. We use the Living Standards Measurement Survey – Integrated Surveys in Agriculture (LSMS-ISA) to measure labor productivity at the household level for Nigeria. The data set is multi-topic consists of Agriculture, Household and Community module files. The Household module consists of information on individual household member labour input in the last seven days and also information on labour payments to various livelihood activities carried out by households as well as capital payments and transfers. Only the household module was used to generate hours worked for all employed workers, whether they are self-employed, employed in wage work, or a mix of both. Our empirical strategy followed three steps. In the first step, household earnings were aggregated across labour employment activities. In the second step earnings generating function was estimated while in third step, labour productivity was decomposed using the Oaxaca-Blinder (OB) approach. A 34% labour productivity gap was accounted for on the basis of the elasticity estimates generated from the fixed effect labour productivity function and we find the gap to be driven by structural effects accounting 74% and endowment effecting accounting for 24%.

Keywords: labour productivity , Oaxaca decomposition, earning gap, structural transformation, agrarian change

EFFECT OF TREATING PEA SEEDS (*PISUM SATIVUM*) WITH FUNGICIDE ON THE ESTABLISHMENT OF SYMBIOSIS

LAABAS S., Boukirat D., Chaker H., Berber F.

University of Ahmed Ben Yahia el Wancharissi, Tissemsilt, Algeria

ABSTRACT

The massive use of phytosanitary products in agriculture has proven to be very effective and reliable in increasing crop productivity. Unfortunately, the application of these products, including various fungicides from different chemical families in agricultural practices, has a deleterious effect on beneficial microorganisms such as nitrogen-fixing bacteria and PGPRs, by limiting their physiological activities that contribute for soil fertility, and consequently on plant growth. A comparative trial was carried out in the greenhouse on two pea varieties (Onward and Gros Vert) with and without thiram treatment, in order to evaluate the effect of this fungicide on the establishment of symbiosis, and the microbial communities of rhizospheric soils. The results obtained show that the fungicide treatment and variety choice have no effect on the number of nodules and the fresh and dry weight of the aerial and root parts, and the low nodulation can be attributed to the low population of native rhizobia in the soil. In addition, a rhizospheric soil microflora count was carried out to determine and assess the bacterial concentration including PGPRs in each sample from two varieties tested with and without treatment. A low bacterial concentration was observed in the rhizospheric of the Gros Vert variety treated with the fungicide compared to the untreated control, and compared to the Onward variety; this result may be due to the seed treatment with thiram which affects the abundance of microflora in the soil; and the difference in response between cultivars of the same species.

Keywords: Pea (*Pisum sativum*), fungicides, nodulation, nitrogen fixation, rhizospheric microflora

THERMOELECTRIC MEASUREMENT OF 2D Bi_2Te_3-Ni and Bi_2Te_3-Cu THERMOELECTRIC JUNCTION DEVICES

Lasisi, A. R.[1, 2*], Rajeev Nepal[2], Prabesh Bajracharya[2] and Vinay Sharma[2]

1. Department of Physics, Federal College of Education, Kontagora, Nigeria.

2. Dixon Science Research Centre, Department of Physics, Morgan State University, Baltimore, MD, USA.

ABSTRACT

This paper reports the result of the thermoelectric voltage measurement of 2D (two-dimensional) magnetron sputtered/pulsed laser deposited Bi_2Te_3-Ni and Bi_2Te_3-Cu thermoelectric junction devices. The junctions were prepared from 99.9 % pure targets of Bi_2Te_3, Ni and Cu. The Bi_2Te_3 was deposited on the glass substrates using magnetron sputtering at room temperature, in a high vacuum chamber of base pressure of $1.04\ x10^{-8}$Torr. A power of 37 W was applied to the Bi_2Te_3 target and the thickness of the film was 25 nm. The Cu and Ni counter electrodes to make a thermoelectric junction were deposited by thermal evaporation and magnetron sputtering respectively through a shadow mask on the Bi_2Te_3 film. The devices were characterised using two points probe with a Keithley multimeter while the junction was heated with an infrared laser. The average power conversion efficiency of 0.38 % and 3.05 % were found for 2D Bi_2Te_3-Ni and Bi_2Te_3-Cu junction devices respectively. This study, therefore, concludes that, 2D Bi_2Te_3-Cu is a better device compared to 2D Bi_2Te_3-Ni junction device. Thus, it is recommended that, 2D Bi_2Te_3-Cu junction device should be employed in building an emergence power generator that powers small electronic devices, especially in remote areas.

FLOW AND HEAT TRANSFER PROPERTIES OF ELECTRICALLY CONDUCTING CARREAU HYBRID NANOFLUID OVER A 3-DIMENSIONAL ROTATING SHEET

Ephesus Olusoji Fatunmbi

Department of Mathematics and Statistics, Federal Polytechnic, Ilaro, Nigeria.

ABSTRACT

This study theoretically investigates flow and heat transfer properties of an electrically conducting Carreau Hybridized nanofluid along a 3-dimensional rotating stretching plate in saturated porous media. Copper (Cu) and Iron oxide (Fe_3O_4) nanoparticles are mixed together to form a hybrid nanofluid in ethylene-glycol base fluid under the influence of thermal radiation and non-uniform heat source. The mathematical equations which describes the physical problem are re-modeled from partial to ordinary deferential equations by means of similarity transformation variables while solution to the system of transformed equations is sought via Pseudo-Spectral Method (PSM). The outcomes of the numerical analysis are graphically displayed to discuss the impact of the various physical parameters that emerged from the main equations on the velocity and thermal fields as well as the dynamics of heat transfer mechanism and surface drag force. It is revealed that the hybridization of the nanoparticles induces a higher heat propagation than the unitary nanofluid for all the physical parameters considered whereas the strength of the surface drag force depreciates with higher magnitude of the fluid material term. Further, there exists a significant improvement in the heat transfer with higher magnitudes of thermal radiation term and stretching parameter but with the magnetic field there is a decrease in the heat transfer characteristics.

Keywords: Electrically conducting fluid; Heat transfer; Hybrid Nanofluid; Rotating Sheet; Nanoparticles.

THE USE OF MOBILE APPLICATIONS IN TERTIARY INSTITUTION CLASS: A COMPARATIVE PILOT STUDY OF THE STUDENTS' PERCEPTIONS AND REAL USAGE (CASE STUDY: FEDERAL COLLEGE OF EDUCATION, ZARIA)

Rafindadi Ibrahim Saad

Department of Computer Science, Federal College of Education, Zaria Kaduna State Nigeria

ABSTRACT

This paper was developed within the scope of a research paper that intends to characterize the use of mobile applications by the students of the Federal College of Education, Zaria during class time. The main purpose of this paper is to present the results of an initial pilot study that aimed to fine-tune data collection methods in order to gather data that reflected the practices of the use of mobile applications by students in a higher education institution during classes. In this paper we present the context of the pilot, its technological settings, the analysed cases and the discussion and conclusions carried out to gather mobile applications usage data logs from students of an NCE department of Computer Science, Our study gathered data from participants, taking theoretical classes in the Department of Computer Science FCE Zaria. The research was based on the Grounded Theory method approach aiming to analyze the logs from the access points of the Department. With the collected data, a profile of the use of mobile devices during classes was drawn. The preliminary findings suggest that the use of applications during the theoretical classes of the Department of Computer Science is quite high and that the most used applications are Social networks like Facebook and Instagram, Tick tok. During this pilot the accesses during theoretical classes corresponded to approximately accesses per student. We also concluded that the students agreed that accessing applications can distract them during these classes and that they have a misperception about their use of online applications during classes, as the usage time is, in fact, more intensive than what participants reported.

Keywords: Mobile application, Mobile usage, Higher education, Classes, Logs

STRENGTH IN MEDICAL CARE FRAMEWORKS: CYBER SECURITY AND COMPUTERIZED CHANGE IN PAKISTAN

MUHAMMAD FAISAL

TOP-TECH Artificial Intelligence Institute, Karachi, Pakistan.

ABSTRACT

The computerized change of the medical services area is a fundamental improvement as social orders move into post-modern, information based economy. there is reception of the most recent advancements and their applications in the well-being and care frameworks should be overseen successfully according to the viewpoint of their digital protection and flexibility. In any case, there is as yet a restricted comprehension of the key ideas that should characterize the essential vision of a versatile and feasible computerized change of the medical care area. Utilizing information gathered at the pinnacle of the COVID-19 pandemic from proprietors and C-level leaders from basic framework areas in the Pakistan, this examination broke down center develops that add to the expected trans-developmental, versatile and absorptive capacities with respect to well being frameworks advanced flexibility. The exploration found that a fair base of network protection information improvement, vulnerability the board, and thought for the area's elevated degrees of fundamental and hierarchical relationship are fundamental for its computerized strength and for the support ability of its computerized change endeavors. The paper depicts the ramifications of these discoveries for exploration and the executives practice.

Keywords: improvement, flexibility, Utilizing, expected, hierarchical, endeavors

NUMERICAL STUDY WITH EXPERIMENTAL COMPARISON OF THE THERMOPHYSICAL PROPERTIES OF POLYMER MATRIX POLYMER MATRIX COMPOSITES

***Abdessamad Belhaouzi1, Youssef Halimi1a, Souad Zyade1b and Mohamed Tahiri2**

1process and environmental engineering laboratory. Higher School of Technology of Casablanca. Hassan II Casablanca University

2Laboratory of Geosciences, Sciences Faculty of Hassan II University of Casablanca, Morocco

ABSTRACT

The aim of this work is to provide a numerical modeling of thermal conductivity of composite materials with organic matrices of saturated polyester resin (UPR) and various mineral charges (marble powder, expanded perlite, sand, etc.). For this purpose, a numerical study was conducted using the finite-element software COMSOL 3.5a to model the thermal transport of an elementary cell in order to calculate the effective thermal conductivity of composites. The influence of contact resistance, or the fraction of calcium carbonate, on effective thermal conductivity is given special consideration. The results show that the proposed digital model agrees well with experimental measurements and Hashin-Shtrikman analytical models.

Keywords: Finite elements, Composite materials, thermal conductivity, COMSOL

References

[1]. N. Benmansour., Doctoral Thesis., *University of Batna*: **2015**
[2]. A. Nait Alla., M. Feddaoui., H. Meftah., Comparison of two configurations to improve heat and mass transfer in evaporating two-component liquid film flow. *Int. J. Therm Sci*. 126. **2018** 194-204, DOI: 10.1016/j.ijthermalsci.2017.12.031
[3]. Wu, N.; Che, S.; Li, H.-W.; Wang, C.-N.; Tian, X.-J.; Li, Y.-F. A review of three-dimensional graphene networks for use in thermally conductive polymer composites: Construction and applications. *New Carbon Mater*. **2021**, 36, 911–926.
[4]. M. Karkri., B. Garnier., A.Boudenne., Numerical and experimental study of the thermophysical properties of spheres composite materials. *High Temperatures High Pressures*. **2011**; 40(1): 61-84.

ASSESSMENT OF MAGNETIC FIELD FROM POWER LINES FOR ITS ENVIROMENTAL IMPACTS

Engr. Ibrahim Aliyu Jumare,
Department of Physics With Electronics,
Federal University Birnin Kebbi, Kebbi State Nigeria
Engr. Aminu Bala Umar,
Department of Physics With Electronics,
Federal University Birnin Kebbi, Kebbi State Nigeria
Dr. Mohammed Sani Jaafaru (PhD),
Department of Biochemistry,
Kaduna State University, Kaduna State Nigeria

ABSTRACT

One of the primary causes of the magnetic field is power line wires. And, more recently, public outcry has erupted in response to claims of its magnetic fields' potentially harmful health consequences. The rapid increase in electric energy consumption as a result of technological advancements and global geographic expansion, makes it necessary for the existing transmission and distribution lines to be upgraded, and as a result, transmission cables pass across residential areas. Consequently, due to the exposure effect of extremely low frequency magnetic field on cancer, cardiac pacemaker, reproductive disorder, and other related cases, there is need to study and evaluate the magnetic field of ELF on existing 330kv lines in Nigeria, for both single and double circuit configurations. The parameters of transmission line towers and conductors, as well as electrical and geometrical data were provided by Transmission Company of Nigeria, allowing the magnetic fields under the conductors to be measured both within and outside the provided right-of-way (ROW). Furthermore, the results were compared with the international guide lines for maximum magnetic field exposure limit under 50Hz operational frequency. Conclusively, as a result of its environmental impact, new data concerning the phase arrangements was suggested to the Transmission Company of Nigeria (TCN), for deployment during any subsequent upgrade or expansion of 330kV lines in the future.

ARTIFICIAL INTELLIGENCE

Tannu Panchal
Bhagat Phool Singh Mahila Vishwavidhalya

ABSTRACT

What is artificial intelligence (AI)?

Artificial intelligence is the simulation of human intelligence processes by machines, especially computer systems. Specific applications of AI include expert systems, natural language processing, speech recognition and machine vision.

How does AI work?

As the hype around AI has accelerated, vendors have been scrambling to promote how their products and services use AI. Often what they refer to as AI is simply one component of AI, such as machine learning. AI requires a foundation of specialized hardware and software for writing and training machine learning algorithms. No one programming language is synonymous with AI, but a few, including Python, R and Java, are popular.

In general, AI systems work by ingesting large amounts of labeled training data, analyzing the data for correlations and patterns, and using these patterns to make predictions about future states. In this way, a chatbot that is fed examples of text chats can learn to produce lifelike exchanges with people, or an image recognition tool can learn to identify and describe objects in images by reviewing millions of examples.

AI programming focuses on three cognitive skills: learning, reasoning and self-correction.

Reasoning processes. This aspect of AI programming focuses on choosing the right algorithm to reach a desired outcome.

Self-correction processes. This aspect of AI programming is designed to continually fine-tune algorithms and ensure they provide the most accurate results possible.

Why is artificial intelligence important?

AI is important because it can give enterprises insights into their operations that they may not have been aware of previously and because, in some cases, AI can perform tasks better than humans. Particularly when it comes to repetitive, detail-oriented tasks like analyzing large numbers of legal documents to ensure relevant fields are filled in properly, AI tools often complete jobs quickly and with relatively few errors.

This has helped fuel an explosion in efficiency and opened the door to entirely new business opportunities for some larger enterprises. Prior to the current wave of AI, it would have been hard to imagine using computer software to connect riders to taxis, but today Uber has become one of the largest companies in the world by doing just that. It utilizes sophisticated machine learning algorithms to predict when people are likely to need rides in certain areas, which helps proactively get drivers on the road before they're needed. As another example, Google has become one of the largest players for a range of online services by using machine learning to understand how people use their services and then improving them.

DEVELOPMENT OF A SMART ARTIFICIAL INCUBATOR WITH A PETROLEUM LIQUID GAS ALTERNATIVE HEATING SOURCE CONTROL

Mu'azu Jibrin Musa, Kabir Ahmad Abubilal, Fatima Ashafa

Ahmadu Bello University, Nigeria, Dept. of Electronics & Telecommunications Engineering,

ORCID NO: 0000-0003-2006-6878

ORCID NO: 0000-0002-0593-1459

ORCID NO: 0000-0002-0079-3245

Yahaya Otuoze Salihu

Kaduna Polytechnic, Nigeria, Dept. of Computer Engineering,

ORCID NO: 0000-0002-8770-7572

Man-Yahaya Sani

Department of Electrical Engineering, Federal Polytechnic Bida, Niger, Nigeria,

ORCID NO: 0000-0002-3254-4518

ABSTRACT

Artificial egg incubation is significant aspect of modern agriculture in the area of animal production. This motivates many researchers to develop different types of egg incubator ranging from manually operated, Semi-automatic to fully automatic artificial incubators. From the available literature most of the electronically operated egg incubators suffer from one problem or another. Many of them suffer from very low efficiency of incubation due to poor control of the operating temperature and humidity at different stages of incubation. Others are associated with the problem of turning of the eggs' tray at wrong tilting angle and time. Lack of automated control of an alternative power supply and high energy consumption is a critical issue. This paper therefore, is to develop a smart artificial incubator that would address the problems of poor incubation performance by incorporating smart control mechanisms for both temperature and humidity. Also to address the challenges of high energy consumption by coming up with a fabrication and smart control for an alternative heating source using Petroleum Liquid Gas (PLG). Eggs tray tilting mechanism was developed using locally available materials, precise tilting at an angle of 45^0 was achieved through the deliberate manipulation of solid state relays and sealer switches. Delay was created using PIC16F877A to ignite the PLG. The main incubator control was by adopting the available XM-18 controller, which was improved by changing its initial configuration to operate on both AC and DC sources and to utilize the PLG heating alternative in the absent of AC heating source. In addition the incubation's real time dynamic parameters (temperature, humidity) were saved in the PIC 16F877A EPROM using the DS18B20 and DHT11 sensors for validation purposes. The complete incubator system was test-run for twenty one (21) days. The performance was evaluated using the incubation's dynamic parameters from the EPROM, energy consumption and percentage of hatchability as performance metrics as compared to the Mohammad *et al*., 2013. Average temperature and humidity, energy consumption and percentage of hatchability of 38.65 ^{0}C ≈ 38.9 ^{0}C, 63.7%, 300 W and 91% respectively were achieved.

Keywords: Egg incubator, Humidity, Petroleum Liquid Gas, Smart, Temperature

1. Introduction

There is increase in the global population growth which gave rise to increase in the demand of food. The amount of food need increase so also the amount of protein particularly animal derived protein (Henchion *et al*., 2017; Medical encyclopedia., 2021). Poultry is a good source of protein, but the production is limited through natural incubation. Incubation is of two types, the natural type and the artificial type. The natural incubation is done by the mother hen within average period of three weeks, while the artificial incubation is done by the use of a device called incubator (Wolfgang, 2018). An incubator can hatch large number of eggs at the same time depending on its capacity.

An incubator is a closed chamber system that controls parameters like temperature, relative humidity, ventilation and egg turning during incubation period. The performance of artificial incubation depends on how well the incubator controls these parameters like temperature, relative humidity and ventilation. Incubation temperature is the most critical of these parameters (Wolfgang, 2018 and Arnarson, 2017).

The incubator system hardware design can be broken down into subunits like: power supply unit, egg turner unit, microcontroller unit, temperature and humidity control units, timing unit, display unit and Keypad-input unit.

The power supply unit powers the entire system. The egg turner section consists of a bidirectional AC motor used for turning of the egg tray regularly. The microcontroller unit serves as the brainbox of the systems that monitors and control the motor for egg turning, temperature and humidity as well as display of operating parameters of the incubator.

So far, it is evident that a lot of research work has been done in developing incubators with different important features (Oriolowo *et al*., 2007). What is evident here is that none of the existing works is smart enough to accurately respond to environmental changes in order to efficiently operate the incubator for higher incubation efficiency, better performance in terms of energy consumption and to also provide an alternative automatic Petroleum Liquid Gas (PLG) heating source.

The rest of this paper is structured as follows. In section 2, the methodology and main components are discussed. In section 3 the challenges and design formulation are presented. The preliminary result is presented in Section 4 while Section 5 concludes the paper.

2. Development of an alternative PLG heating source

Develop of a smart alternative heating source using PLG and electrical control mechanism to compensate unforeseen power failure. Metal fabrication will be in-cooperated to provide the gas cylinder switching arm, which will be controlled through the decision taking in the PIC16F877A. Two MQ2 gas sensors would be used, the first MQ2 is for internal gas detection to ensure proffer switching ON of the gas and trigger ignition. The second MQ2 is for external gas detection of leakage if any and quickly switch off the gas. 12 V DC fans would be put in place to enable channel the warm air to the incubator chamber and evacuate excess warm air where necessary from the chamber. All decisions are taking in the PIC16F877A.

2.1 Design and implementation of the PLG into the existing XM-18 controller

The design, implementation and integration of the Petroleum Liquid Gas (PLG) control into the existing XM-18 incubator controller will enhance the hatchability of the eggs. XM-18 controller is an automatic egg incubator controller, which has a reputable history of high % of hatchability and very low chick's mortality if operated on an uninterrupted AC power supply (Musa *et al*., 2022). In some developing countries power is unstable for incubator to operate optimally, this leads to the poor performance of the XM-18. There for the need to improve the XM-8 to run on DC and utilize the PLG in absent of Power from the grid. Figure 1 and Figure 2 shows the components for the PLG and the integration of the XM-18 with the PLG respectively.

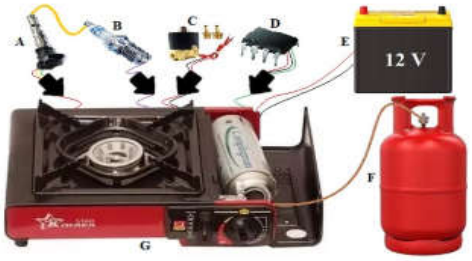

Figure 1. PLG Controller set-up

Figure 2. XM-18 interface with PLG

Auto PLG unit comprises of the ignition coil, sparking plug, camp stove and the microcontroller PIC16F877A. The ignition coil is connected to the sparking plug to enable coming up with the require sparking of about 100 kV DC. A code was written in C to the PIC16F877A to enable come up with the required pulses of 0.004 s (250 Hz frequency). Solenoid control valve controlled the LPG flow which heats the needed temperature for the incubator.

A. PLG unit with XM-18

PIC16F877A finds its applications in a huge number of devices. It was used to control the flow of the PLG. Figure 3 shows the interface of the PLG and the XM-18.

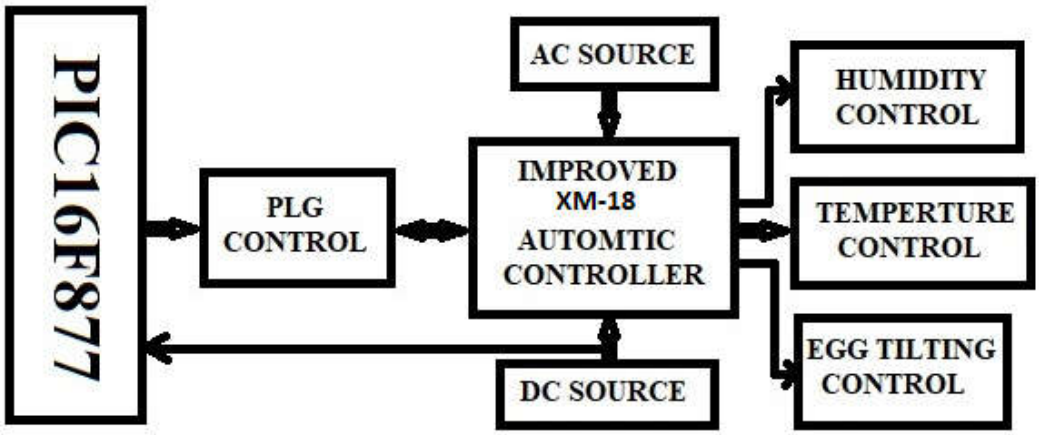

Figure 3. PIC16F877A connected to PLG with Energy sources and XM-18

The PLG controller will be monitoring the XM-18 to automatically switch the PLG in absent of AC power and to also switch off the PLG in the present of AC power. Figure 4 shows a typical control block diagram of XM-18.

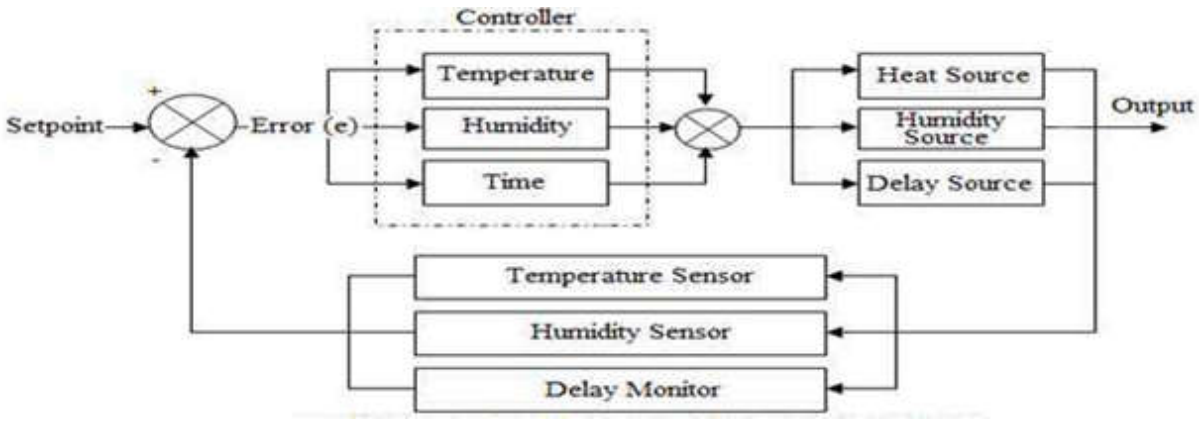

Figure 4. Typical XM-18 Control block diagram

The temperature and humidity of the incubator is controlled by the XM-18. The system will compare the desired value with that of the XM-18. The microcontroller uses the feedback from the sensor and gives the suitable output voltage based on the error. The error is the difference between the user-defined set point (the desired value) and the measured process variable (the actual value).

3. Challenges of existing incubator

The artificial (manual, semi-automatic and automatic) incubators suffer from high mortality due to frequent power failure more especially in some developing countries. Many incubator users depend on the heating source from the grid supply, the power inverter and kerosene. All this has an inherent problem.

3.1 Humidity Control when Incubating Chicken Eggs

Under artificial incubation, the requirement for humidity is not as strict as that for temperature. The chicken embryos are more adaptive to humidity range, based on the fact that the water contained in chicken eggs is also enough for its embryonic development. For high hatchability, humidity must be properly controlled and it should be kept within 60%. To achieve this, DHT11 is used to sense the humidity.

3.2 Require temperature range for embryonic development

Chicken eggs have adaptive capacity awards ambient temperature, and some eggs can still hatch under temperature range of 36-40.5 ℃ (96.5-105 ℉). When an incubation machine is utilized, the temperature mentioned above is not the most favourable temperature. Instead, the most appropriate temperature for incubation is 38.9 ℃ (100 ℉) and the most appropriate temperature during hatching process is 37.0 ℃-37.5 ℃ which XM-18 can accurately provide. DS18B20 is used to sense the temperature.

A. Influence of high temperature to embryonic development

Under high temperature, the chicken embryo develops very fast, which may lead to a shortening of incubation period, which can leads to increase of embryo death rate or decreases the quality of chicks. When the temperature is over 47 ℃, the embryo dies within 2 hours. When chicken eggs incubated for 16 days under 40.6 ℃ for 24 hours, the hatchability will fall down to some degree, under 43.3 ℃ for 9 hours, hatchability declining to a great extent, under 48.9 ℃ (120 ℉) for one hour, 100% of the embryos in the incubator die (Mesquita, 2021).

B. Influence of low temperature to embryonic development

When the temperature is under appropriate temperature, the incubation period will be longer and the death rate will increase and when incubated under 35.6 ℃ (96 ℉), most of the embryos die in the egg shells

C. Egg tilting control

In natural Incubation, mother hen frequently turns eggs with its feet and beak. This kind of intuitive work by hen is to warm every part of the embryo, avoid adhesion of embryo with egg shell, so as to increase hatchability (Niranjan, 2021).

3.3 Power Measurement Set-up

The overall energy consumption of the incubator was measured using the set-up as shown in Figure 5.

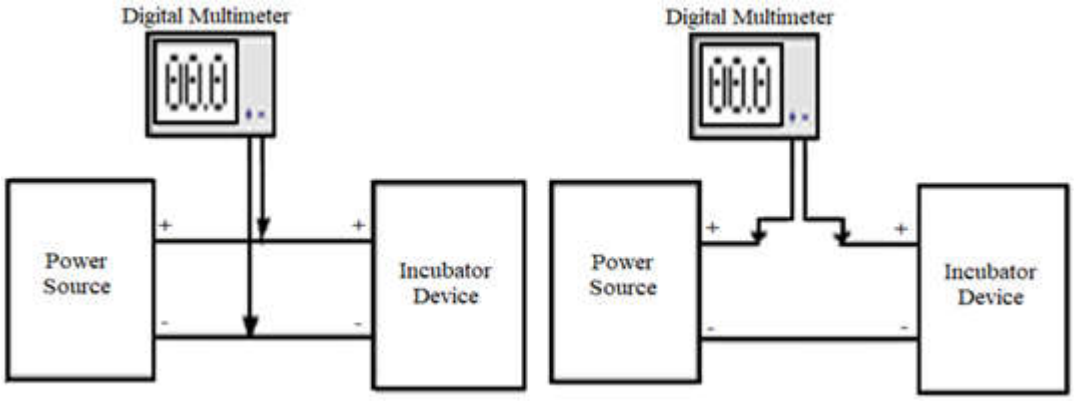

(a) Voltage Measurement (b) Current Measurement

Figure 5. Power measurement set-up

Energy consumption expression is as shown in the following equation (1) to (3)

Energy consumption expression is as shown in equation (1) (Akinpelu *et al.,* 2020):

$$E = Pt \quad (1)$$

where E is energy consumption in J, P is the power of the device in W, t is time which the energy was consumed.

Power P expression is as shown in equation (2) (Charles and Matthew, (2013):

$$P = IV \quad (2)$$

where I is the current in A, V is the current in V.

Hence the expression for the system's energy consumption can be express as equation (3) using equation (1) and (2):

$$E = (IV)t \quad (3)$$

The energy consumption as measured using power meter was found to be 300 W.

The average temperature and relative humidity, obtained are 38.9 ℃ and 63.7% respectively and the energy consumption as measured using power meter was at 300 W.

The percentage of hatchability is obtained using equation (4).

$$\%\ of\ hatchability = \frac{No.of\ eggs\ that\ hatched}{Total\ number\ of\ fertile\ eggs} \quad (4)$$

The percentage of hatchability of the proposed PLG with XM-18 was found to have an improvement of 2.79% over the work of Mohammed *et al*., (2013) (HEFINC840).

4. Result and Discussion

The overall reading of eighteen days of incubation gives the readings of the temperature and humidity as in Table1 to Table 2.

Table 1. Parameter readings from the incubator day 1-9

Days	1	2	3	4	5	6	7	8	9
Temp. ℃	38.7	38.9	38.9	38.8	38.9	38.9	38.8	38.9	38.7
Hum. (%)	64	66	60	65	63	63	67	64	64

Table 2. Parameter readings from the incubator day 10-18

Days	10	11	12	13	14	15	16	17	18
Temp. ℃	38.8	38.8	38.9	38.9	38.9	38.8	38.9	38.9	38.9
Hum. (%)	66	63	66	67	62	60	60	64	63

Figure 6 show that, the temperature of the incubator is within the expected limits since all the readings are in between the Upper Control Limit (UCL) and the Lower Control Limit (LCL). An average temperature of 38.9 ℃ was achieved throughout the incubation period.

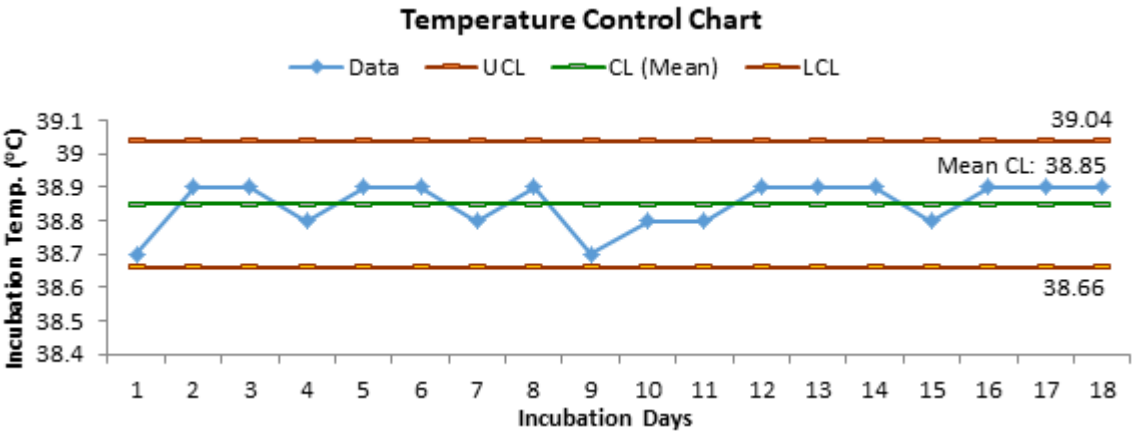

Figure 6. Temperature readings from the Incubator

Figure 7 show the humidity of the incubator within the eighteen days of incubation.

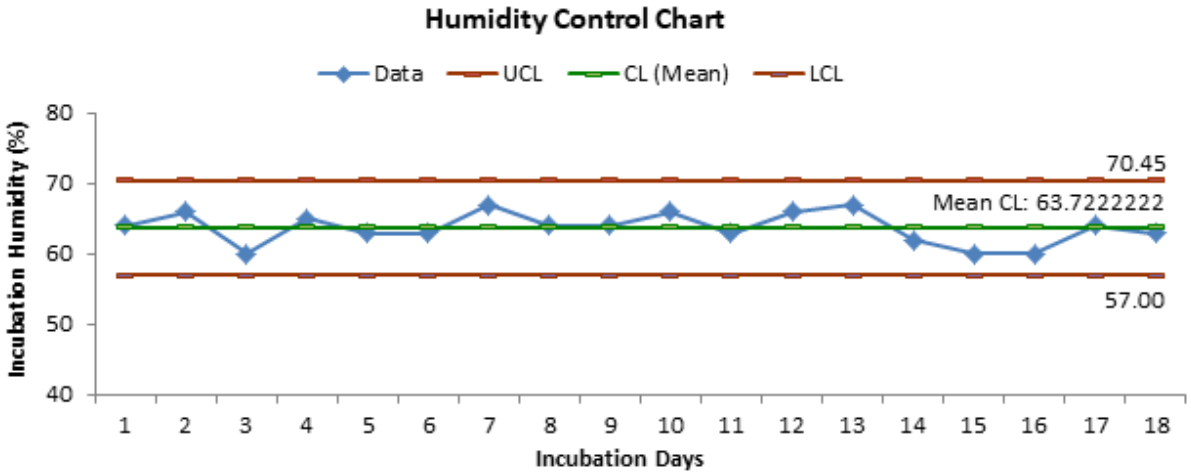

Figure 7. Relative Humidity Readings from the Incubator

Similarly, the humidity readings recorded are all within the optimal acceptable limit of incubation humidity. An average humidity of 63.7% was recorded. Hence, no single humidity value was out of the accepted incubation humidity range as compare to the humidity obtained in Mohammad *et al*., 2013 which has an error of 5.6%.

5. Conclusion

It can be concluded that a development of a smart artificial incubator with a PLG alternative heating source control using XM-18 can provide an improvement over HEFINC840 and other prominent incubator controllers. The percentage of hatchability was improved by 2.79% as compared by Mohammad *et al*., 2013. Acceptable average temperature and humidity of 38.9 ℃ and 63.7% was achieved respectively. An improvement of 5.6% in humidity was also recorded as against the Mohammad *et al*., 2013.

5.1 Recommendation for further work

Less expensive source of heating should be explored to enable low production cost of chicks.

References

Henchion M. Moloney A. P. Hyland J. Zimmermann J. McCarthy S. (2021). “Review: Trends for meat, milk and egg consumption for the next decades and the role played by livestock systems in the globe production of proteins,” Animal The international journal of animal biosciences, Science Direct, 15, pp. 1–14.

Medical encyclopedia. (2021). “Protein in diet,” Retrieved July 14, 2021, from Medlineplus: https://medineplus.gov

Wolfgang, N. D. (2018). “Design of a Semi - Automatic Artificial Incubator,” European Journal of Applied Engineering and Scientific Research, pp. 4–14.

Arnarson A. (2017). “8 Signs and Symptoms of Protein Deficiency,” Retrieved July 22, 2021, from healthline media: https://www.healthline.com/nutrition/protein-deficiency-symptoms#TOC_TITLE_HDR_8

Oriolowo Z. N. Maude F. A. Raji A. and Musa M. J. (2007). "Design and construction of an automatic electric incubator for hatching chicken eggs," 8th international conference, gold in Nigeria Agricultural Engineering and the millennium development. Yola, Adamawa State, Nigeria, pp. 215–220.

Musa M. J. Salihu Y. O. Yusuf M. Usman Z. G. (2022). "Improved XM-18 Controller using Petroleum Liquid Gas Based Automatic Heating Alternative for Egg Incubation in Developing Countries," in IEEE 5th Information Technology for Education and Development (ITED). Nile University of Nigeria, Abuja, Nigeria, pp. 1–4.

Mesquita M. A., Araujo I. C., and Cafe M. B. (2021). "Results of hatching and rearing broiler chickens in different incubation systems," Poutry Science, Science Direct, 100(1), pp. 94–102

Akinpelu A., Usikalu M. R., Onumejor C. A. (2020). "Construction of High Precision AC-DC Power Supply," International Journal of Recent Technology and Engineering (IJRTE), 8(6), pp. 2049–2051.

Niranjan, L., Venkatesan, C., Suhas, A. R., Satheeskumaran, S., and Nawas, S. A. (2021). "Design and implementation of chicken egg incubator for hatching using IoT," International Journal Computational Science and Engineering, 24(4), pp. 363–372.

Charles K. A., Matthew N. O. S., (2013) "Fundamentals of electric circuits," 5th Edition, McGraw-Hill, a business unit of The McGraw-Hill Companies, Inc., 1221 Avenue of the Americas, New York, NY 10020.

Mohammad A., Musa M. J., Ahmad K., Garba S., and Almustapha M. D. (2013) "Design and Performance of HEFINC840 Micro-controller Based Incubator," NIAE International Conference, Uyo, pp. 21–24.

BUILDING BLOCK FOR A SPOT WELDER

Felix A. HIMMELSTOSS, Ferhat YAMAN, Karl H. EDELMOSER

University of Applied Sciences, Faculty of Electronic Engineering and Entrepreneurship, Power Electronics Section, Vienna, Austria.

ABSTRACT

To make the spot-welder more flexible and to optimize the welding process concerning energy and weld strength, the following concept can be used. With the help of a PFC-link a bulk-capacitor is charged. The spot-welder consists of several building blocks which are connected to this DC-link. Each building block has a large capacitor which is charged with its own DC/DC converter and has control wires which connect the building block to the superimposed control system (it is also possible to make the control wireless using radio or infrared transmission). The DC/DC converter works as a current source and charges the capacitor up to a predetermined value (given from the control circuit in accordance to the welding technology). With the help of decoupling diodes, which are in series with the discharging switch, the building blocks feed the cable to the first welding electrode. The second welding electrode is connected via a cable with the other side of the capacitors. To avoid overvoltage due to the parasitic inductances, free-wheeling diodes have to be used. With the active switches the current of the building blocks can be interrupted arbitrarily. By this flexible system and in interaction with the superimposed control, different amplitudes and a very flexible timing of the pulses are possible. So it is feasible to generate a defined current profile to optimize the welding process. The complete concept, the design of the building blocks and the superimposed control are described.

Keywords: spot welding, capacitor charging, pulse power, retrofit

Introduction building block for a spot welder

Spot-welding (sketch in Figure 1.a) is done by pressing the two pieces which shall be connected together and by sending a large current through the contact point. A traditional spot welder uses capacitors which can be interconnected to provide the necessary pulse energy. These capacitors are charged and discharged over the welding spot. Because of the necessary high currents, thyristors are used to trigger the discharging. According to the welding technology several pulses can be sent to the welding spot. The voltage of the capacitors can be changed with a transformer with several taps and a connected rectifier and the strength of the pulse by connecting capacitors together. For each welding task the machine has to be connected by hand: mounting the cables, changing the tap of the transformer, and connecting several capacitors in parallel.

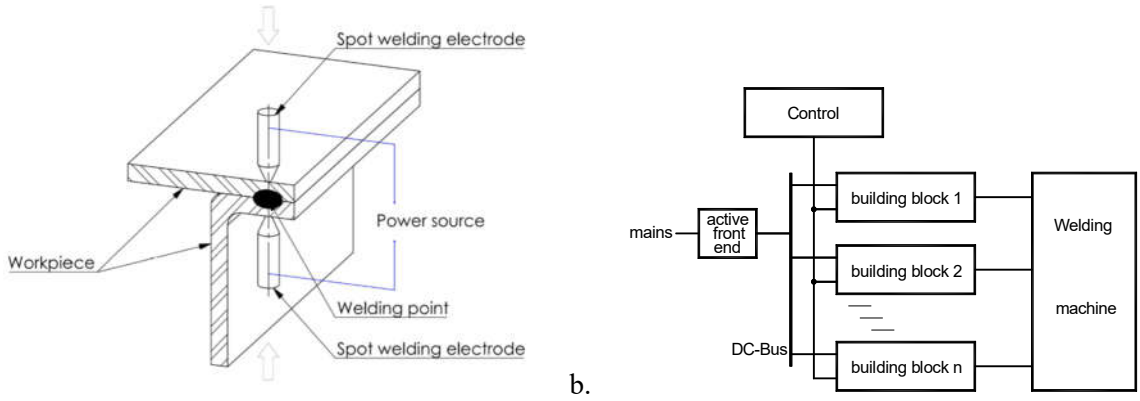

a. b.

Figure 1. (a) principle of spot welding, (b) concept.

To make the spot-welder more flexible and to optimize the welding process concerning energy and weld strength, the following concept can be used (Figure 1.b). This concept can also be used to retrofit an already existing apparatus. With the help of a power factor corrector (PFC) a link bus is supplied (consisting of a large bulk-capacitor). The bulk capacitor can also be replaced by a powerful battery behind a charger.

The proposed spot-welder consists of several building blocks which are connected to the DC-link. Each building block has a large capacitor for storing the energy of the welding current pulse, which is charged by its own DC/DC converter from the bulk capacitor and has control wires, which connect the building block to the superimposed control system (it is also possible to use a field bus or to make the control wire-less using radio or infrared transmission). The DC/DC converter works as a current source and charges the capacitor C up to a predetermined value (given from the control circuit in accordance to the welding technology). With the help of decoupling diodes which are in series with the discharging switch the building blocks feed the cable to the first welding electrode. The second welding electrode is connected via a cable with the other side of the capacitors. To avoid overvoltage due to the parasitic inductances, when the active switch is turned off, free-wheeling diodes have to be used.

Comprehensive descriptions of Power Electronics can be found in the text books (Zach 1, Mohan 2, Rozanov 3). Some hints to the actual literature about spot welding are now given. In (Lei 4) an analysis of welding defects is shown. The calibration of high current pulses is treated in (Hlavacek 5). The effects of welding time and welding current to weld nuggets is described in (Baskoro 6, Chen 9). A full bridge converter with high frequency transformer and rectification on the secondary side is explained in (Xiao-Jie 7). Small spot welding systems are also used in the textile industry (Suchy 8). The identification of electrical parameters in a spot welding system can be found in (Wang 10). That phase-controlled thyristor welders are still useful is shown in (Shopov 11).

Concept of the building block

Figure 2.a shows the power concept of one building block to generate positive current pulses. V_{in} represents the DC link, which is supplied e.g. by a PFC from the mains. The next block represents the DC/DC converter K which charges the capacitor C. To avoid a negative voltage across the capacitor C, a diode D_1 is connected in parallel. The main switch which controls the current pulse is realized by a MOSFET S which is driven by the driving circuit DRV and is connected to the superimposed control system. Instead of the MOSFET also an IGBT (especially when higher voltages are used) could be implemented. Due to the relative low necessary voltage of the capacitor C, it is better to use low voltage MOSFETs with high current ability to reduce the losses and to avoid elaborate cooling. The diode D_2 is the decoupling diode to avoid a back current through the body diode of the MOSFET switch S. D_3 is the free-wheeling diode to avoid overvoltage at the switch caused by the inductance of the welding cables. The load, consisting of the resistance of the welding cables, the resistance of the point to weld, and the inductance of the whole circuit, is connected between the connectors A_1 and A_2.

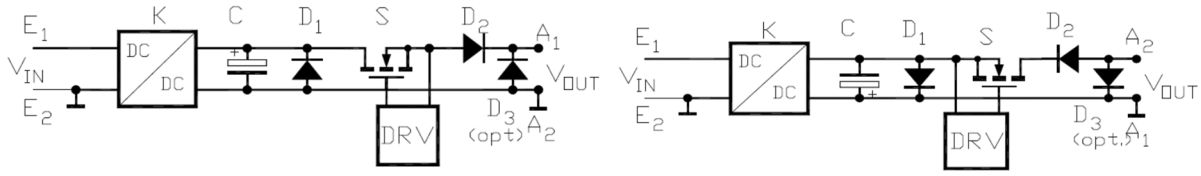

Figure 2. Basic circuit diagram of the building block: (a) for positive currents, (b) for negative currents (Himmelstoss 12).

If negative current pulses have to be produced, the circuit according Figure 2.b can be used. The function is equal to the positive current block. The DC/DC converter used in this case is a standard inverting Buck-Boost converter. For the positive building block, a normal Buck converter can be used.

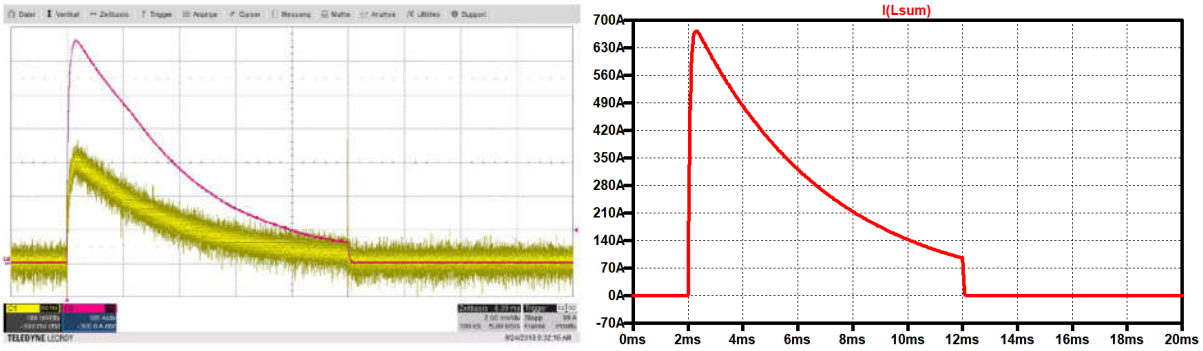

Figure 3. Positive current pulse: (a) measurement with a current probe (100 A/div, dark red), with a shunt (100 mV/div, green); (b) simulation (red).

Figure 3 shows the result for an experiment. The measured results show a good accordance with the simulation (the parameters for the simulation are shown in the circuit of the negative pulse system in Figure 4). In the simulation all inductors of the welding circuit are summed up in the value LL. The noise of the digital oscilloscope and the noise of the shunt have to be reduced by sampling the shunt signal with a fast sampler and by taking always e.g. ten successive samples and calculating the mean value; (the used oscilloscope can make this filtering only for repetitive signals).

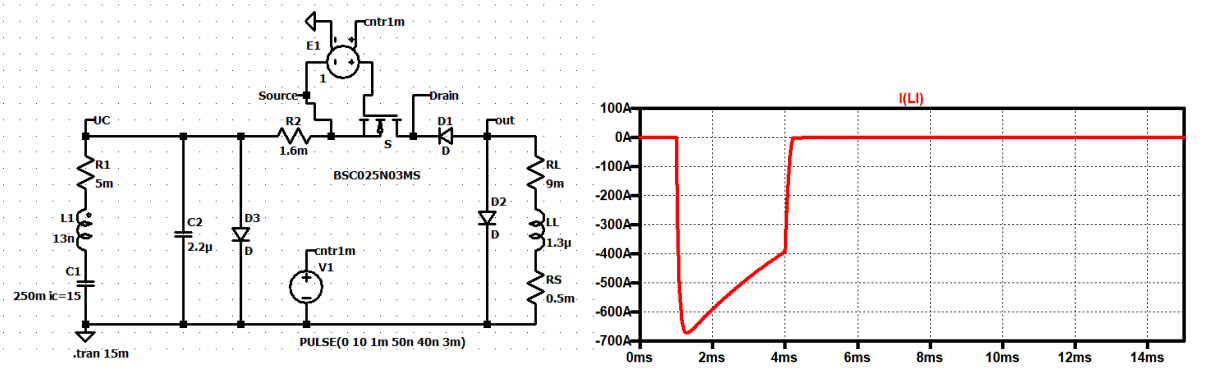

Figure 4. Generation of a negative pulse: (a) simulation circuit, (b) negative current pulse (red).

Figure 4 shows the simulation circuit and the negative current pulse through the welding spot. Again all the parasitic inductors are included in LL. The parasitic inductor and the equivalent series resistor of the capacitor are included in the model and the values are taken from the data sheet of the capacitor. The small capacitor in parallel to the big electrolyte one helps during turn-off of the switching transistor. It should be mounted as near as possible to the drain and to the anode of the free-wheeling diode to reduce the effective parasitic inductance and to avoid large over-voltage (in the simulation it is used as a path for the parasitic inductor of the capacitor, and in reality we use a bigger one). When the overvoltage is too high, one has to use a snubber for the active switch. This has to be dimensioned for the maximum current.

If positive and negative current pulses are necessary, the diode D2 has to be replaced by an anti-serial transistor and the freewheeling diode has to be connected in series to an anti-serial transistor. The influence of the parasitic inductance could also be reduced by a bidirectional avalanche diode (or two unidirectional ones which are connected anti-serial). This is only possible, however, for low repetition rates.

Charging of the bulk capacitor

A simple charging circuit is a Buck converter which is controlled by a simple hysteresis controller is treated.

Realization of the two-point controller with a comparator

Figure 5.a shows the charging concept for the positive pulse. With the help of a Buck converter consisting of the electronic switch M, the diode D, the inductor L, the capacitor C is charged. The converter is operated as a current source. The comparator U_2 works as a two-point controller with hysteresis for the current. A second comparator U_1 stops the charging process when the capacitor voltage reaches the reference value U_{Ref}. This is the voltage controller. The driver of the MOSFET is symbolized by the block DRV. Figure 5.b shows the same concept for negative charging. The same control concept is used here for the inverting Buck-Boost converter.

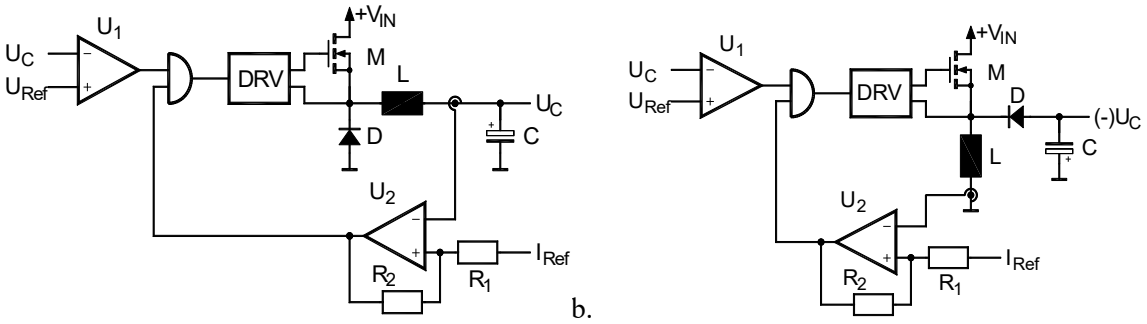

Figure 5. (a) positive charging, (b) negative charging.

Figure 6 shows the simulation circuit of the charging stage for the positive stage. The power electronics consists of a transistor M1, an inductor L1, and a diode D3. The input voltage is modelled by a voltage source V2. The capacitor to be charged is C1. The hysteresis of the current controller is adjusted by the resistors R1 and R2. The reference value of the charging current (mean value for a symmetric hysteresis) is increased after 10 ms (one can see a small break in the voltage curve). The voltage increases linearly. After it reaches the desired voltage, the other comparator (U1) stops the charging process.

The hysteresis must be chosen smaller compared to the one realized with an operational amplifier, because the OPA is slower and goes into saturation. An amplifier is made to amplify and not to be used as a comparator!

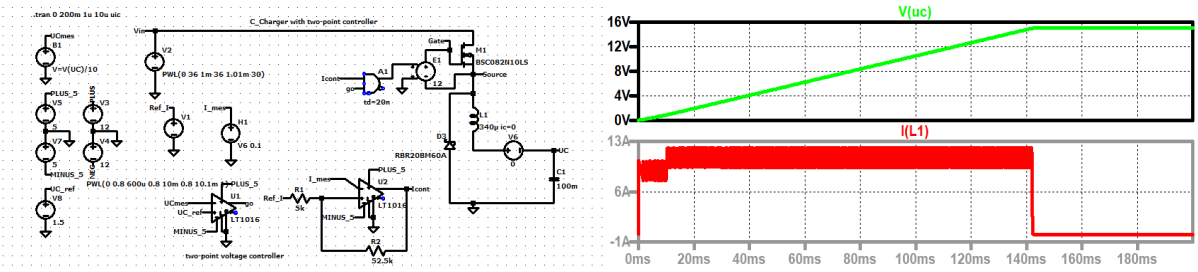

Figure 6. Charging of the capacitor: (a) principal circuit, (b) capacitor voltage (green), current through the inductor or charging current (red).

How long does it last to charge a capacitor with a constant current to a certain voltage level U_C? The repetition rate of the stages is limited by the charging current.

From the basic equation of the capacitor for the change of the voltage

$$\Delta u_C = \frac{1}{C}\int_0^t i_C dt \qquad (1)$$

one gets for the constant current I_0

$$T_{charge} = \frac{U_{end} \cdot C}{I_0}. \qquad (2)$$

The stored energy in the capacitor depends on the value of the capacitor and the square of the voltage according to

$$W_{end} = \frac{C \cdot U_{end}^2}{2} . \quad (3)$$

Using a two-point controller with the hysteresis I_H the frequency of the controller changes with the voltage across the capacitor. The voltage across the capacitor is practically constant during one switching period (remember we need large capacitors to store enough energy for the welding process). Therefore, we write a capital letter for $U_C(t)$ to mark that the voltage is constant when the frequency is calculated. The current should increase by I_H during the on-time of the active switch, and the voltage across the inductor is the difference between the input and the output voltages. The necessary on-time is therefore

$$T_{on} = L \frac{I_H}{U_1 - U_C(t)} . \quad (4)$$

During the off-time of the active switch the current decreases by I_H and the voltage across the inductor is now the negative output voltage. Therefore, one gets

$$T_{off} = L \frac{I_H}{U_C(t)} . \quad (5)$$

Adding these two time values gives the switching period of the controller

$$T = \frac{L \cdot I_H \cdot U_1}{[U_1 - U_C(t)] \cdot U_C(t)} . \quad (6)$$

The switching frequency can now be written according to

$$f = \frac{U_C(t) \cdot [U_1 - U_C(t)]}{U_1 \cdot L \cdot I_H} . \quad (7)$$

To obtain the maximum switching frequency in dependence on the capacitor voltage, one has to derivate the frequency in accordance to the capacitor voltage and set the result zero

$$\frac{df}{dU_C(t)} = \frac{U_1 - 2U_C(t)}{U_1 \cdot L \cdot I_H} = 0 . \quad (8)$$

The maximum switching frequency occurs, when the output voltage is equal to the half of the input voltage. At the beginning of the charging process, the on-time is short and the off-time is long and the nearer the output voltage gets to the input voltage, the longer are the on-times and the shorter are the off-times of the controller (and therefore the on- and off- times of the electronic switch of the charging converter).

Negative charging with the help of a Buck-Boost converter

To generate a negative voltage out of a positive one, a Buck-Boost converter is used. The circuit and the control equipment with two two-point controllers is shown in Figure 5.b. The function is analogue to the system shown in Figure 6. The simulation is shown in Figure 7. One has to mention that the absolute value of the capacitor voltage can be increased to a higher voltage than that of the input.

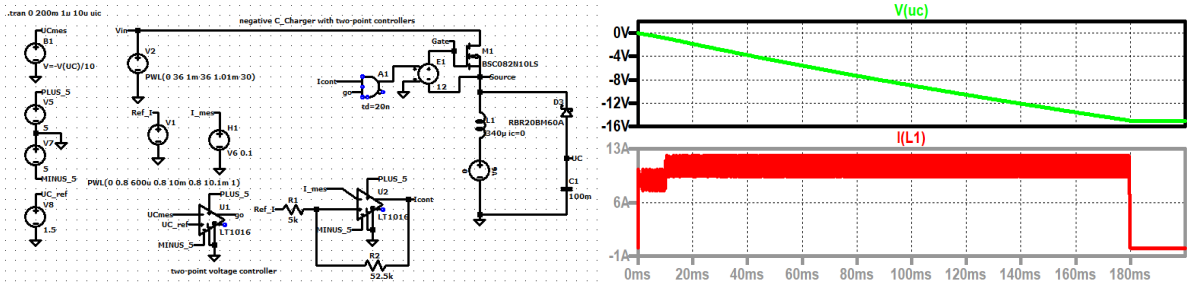

Figure 7. Negative charging of the capacitor: (a) principal circuit, (b) capacitor voltage (green), current through the inductor or charging current (red).

Combination of building blocks

In this section the combination of building blocks is shown.

Double pulse

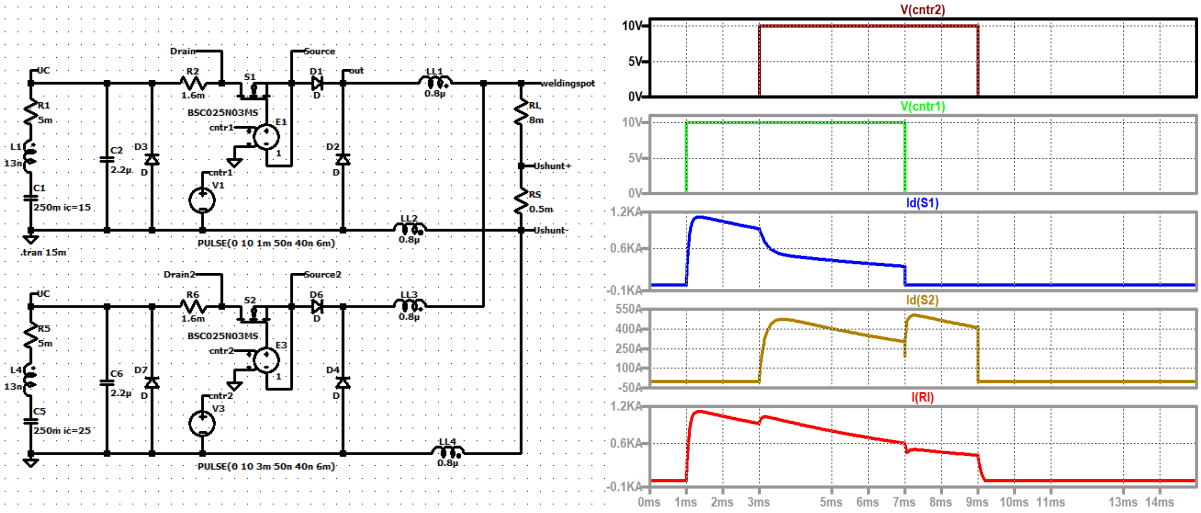

Figure 8. Double positive current pulse: (a) circuit, (b) control signal of the second stage (black), control signal of the first stage (green), current through first stage (blue), current through second stage (brown), output (welding) current (red).

Figure 8 shows the combination of two positive stages. In the simulation to each cable an inductor is attached (including a small resistor of 1 mΩ). The second stage is turned on 2 ms later than the first one.

One can see a feedback on the first stage caused by the load. The shunt for measuring the welding current is in series to the welding spot and measures the whole current. The current is high a longer time. The two systems superpose each other, due to the reverse voltage caused by the welding spot and the inductance of the cables.

Combination of a positive and a negative current pulse

When a positive and a negative pulse have to be applied to the load, the free-wheeling paths of the stages have to be altered. To avoid a short for the other pulse, an anti-serial transistor has to be connected to the free-wheeling diodes. In Figure 9 the circuit and simulation results are shown. The free-wheeling path is turned on e.g. when the main switch is turned on and is turned off after the current is zero or latest before the other stage is turned on. When the current is turned off, the current commutates into the free-wheeling diode.

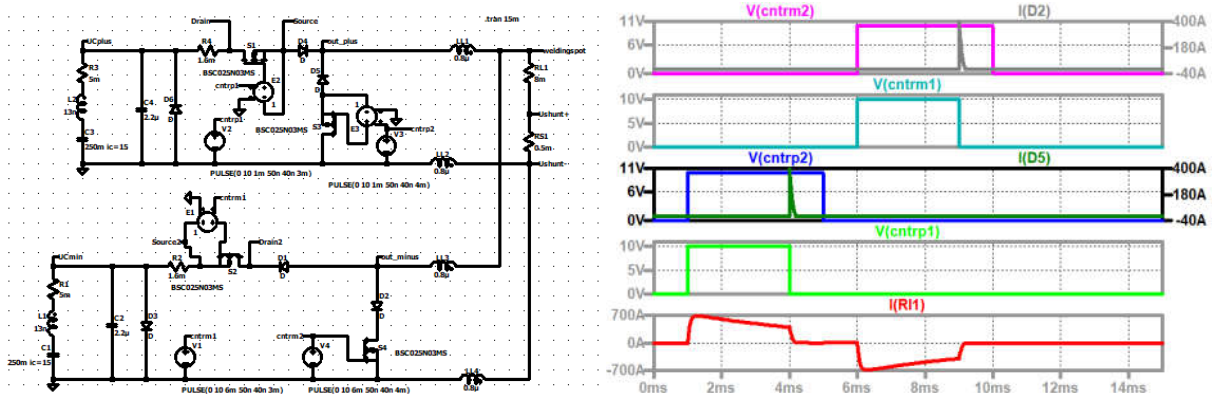

Figure 9. Positive-negative current puls: (a) circuit, (b) control signal of the free-wheeling path of the negative pulse (violet) and through the associated diode (grey); control signal for the negative stage (turquoise); control signal of the free-wheeling path of the positive pulse (blue) and through the associated diode (brown); control signal of the positive stage (green); output (welding) current (red).

Generation of the control pulses of the system

In the hand-operation the delay time for the main transistor and the turn-on time for each stage is loaded by increasing or decreasing the values with the help of the blue buttons minus and plus (Figure 10.a).

Figure 10.b shows the summery of the input data for three stages. One can see graphically the pulses and the values of the turn-on times and the delay times.

Figure 11 shows the display and the resulting control signals for an example.

a. 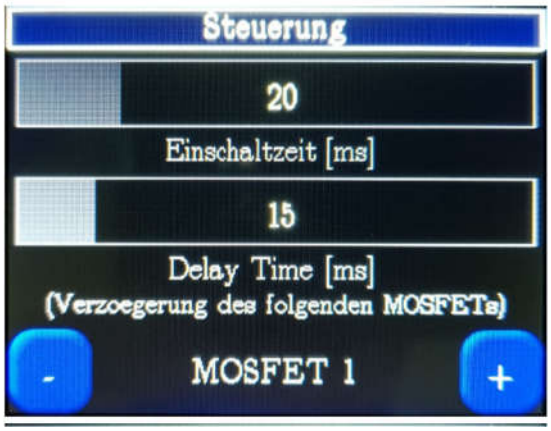

b. 

Figure 10. (a) display for one stage during input: upper value on-time, lower value delay time; (b) summery on the display: up to down the pulses for the stages.

Figure 10.b shows the summery of the input data for three stages. One can see graphically the pulses and the values of the turn-on times and the delay times.

Figure 11 shows the display and the resulting control signals for an example.

a. 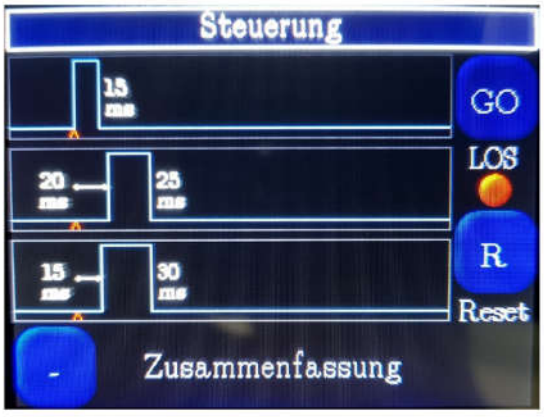

b. 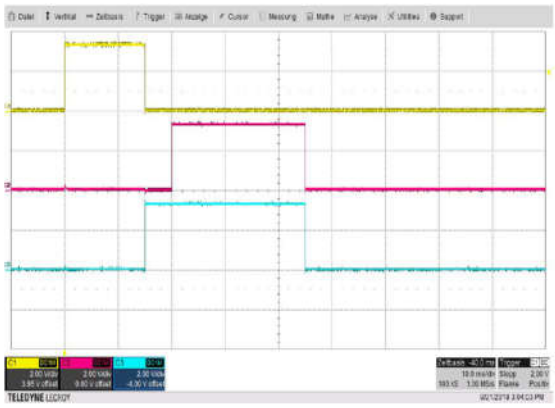

Figure 11. Example for the pulse generation: (a) picture of the display, measured control pulses.

Calculation of the current pulse

Summing all resistors to R, and all inductors to L, writing for the knee-voltage V_D one can write for the current

$$\frac{1}{C}\int_0^t idt + u_C(0) = Ri + V_D + L\frac{di}{dt}. \quad (9)$$

Transforming into the Laplace domain leads to the current in the frequency domain according to

$$I(s) = \frac{u_C(0)-V_D}{L}\frac{1}{s^2+s\frac{R}{L}+\frac{1}{CL}}. \quad (10)$$

The poles are at

$$s_{1,2} = -\frac{R}{2L} \pm \sqrt{\left(\frac{R}{2L}\right)^2 - \frac{1}{CL}}. \quad (11)$$

The poles of this equation are important for using the easiest correspondence equation. Both poles are real, one is near the origin and one if far to the left. With s_1 and s_2 for the poles and $s_2<s_1$ one gets the current according to

$$i = \frac{u_C(0)-V_D}{L}\frac{exp(-s_1t)-exp(-s_2t)}{s_2-s_1}. \quad (12)$$

Design of the building block

The currents are very high, therefore all semiconductors are stressed by a large forward current. This is the reason why thyristors are normally used in welding applications. Thyristors are very robust concerning high current. The main disadvantage of them is the fact that conducting ends only when the current reaches zero (in reality after the reverse recovery peak). In fact, there exist circuits to extinguish the thyristor, but they are relatively slow, compared to an active switch like a MOSFET or an IGBT.

In this design a MOSFET was used with an on-resistor of 1.6 mΩ and a maximum current of 1600 A (for pulses and a mean value of 500 A appropriately cooled). The maximum drain-source voltage is 75 V. A gate drive with an optocoupler is used, supplied by a small DC/DC converter. The blocking diode was combined with the free-wheeling diode in a power module consisting of two Schottky diodes with common cathode. The main advantage is that the wiring inductance is small. The diodes have an average current of 400 A and can withstand much higher pulse currents.

The capacitor has 220 mF and will be short circuited. This is an extreme stress for the device. In parallel to the electrolyte capacitor a ceramic capacitor is connected. Future studies have to be done to get deeper insight into the lifetime of capacitors which are short circuited regularly.

For security reason a bidirectional avalanche diode is placed in parallel to the free-wheeling diode (not shown in the figures), if the circuit opens unrequested. This element can dissipate the energy of the stray inductance.

Current measurement looks simple, but in reality it is quite challenging. Using shunts leads to three problems. First: there is a parasitic inductance in series to the resistive part of the shunt, which produces an additional voltage drop depending on the change of the current (derivative of the current). This means the shunt voltage is larger when the current increases and is lower when the current decreases. Second: the measurement resistor must be small to avoid losses and interaction with the system, therefore, the measurement signal is small and can easily be disturbed and is very noisy. Third: due to the skin effect the resistive part is not constant. To keep the parasitic inductor low, a coaxial design is advisable. Figure 12 shows such a design. A detailed description of this coaxial shunt is given in (Himmelstoss 13).

a. 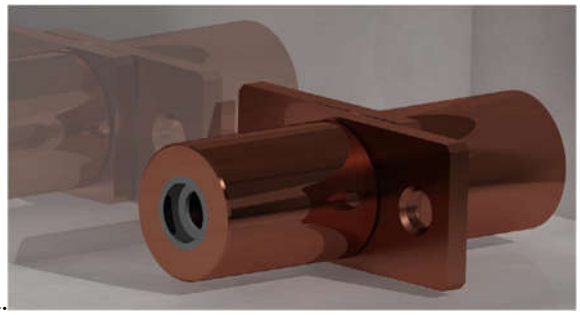 b. 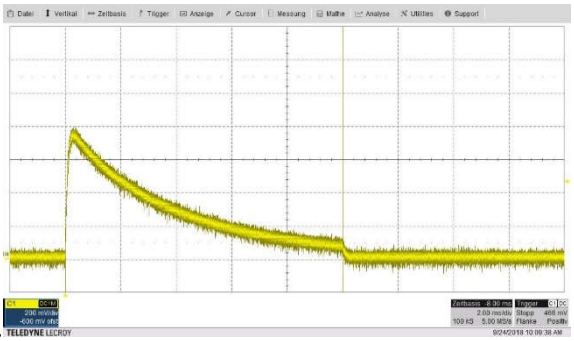

Figure 12. Current measurement device (a) coaxial shunt, peak current 1.6 kA.

Conclusion

The concept of realizing the spot-welder out of such building blocks has the following advantages:

- No retroaction to the mains during charging the capacitors
- No manual wiring of the capacitors to groups when changing the welding process is necessary
- The voltage across the capacitors and therefore their energy content can be different
- Grouping the capacitors is flexible and controlled by the discharging switches
- It is possible to interrupt the current flow by turning off the active switch
- energy content can be regulated precisely
- Flexible energy profiles can be realized
- By clocking the discharge switch and in interaction with the load and wiring inductance together with the free-wheeling diode predefined current forms are possible

By this flexible system in interaction with the superimposed control, different amplitudes and a very flexible timing of the pulses are possible. So it is feasible to generate a defined current profile to optimize the welding process. The here shown concept is well suited to modernize older step welding machines.

It should be mentioned that there are more possible applications than spot welding. Large current pulses with adjustable strength and duration are necessary for diverse technological processes e.g. hardening of materials, or for test equipment.

References

1. Zach, Franz. (2022). Power Electronics, in German: Leistungselektronik, Frankfurt: Springer, 6th edition.
2. Mohan, Ned & Undeland, Torre & Robbins William. (2003). Power Electronics, Converters, Applications and Design. New York: W. P. John Wiley & Sons.
3. Rozanov, Yuriy & S. Ryvkin, Sergey & Chaplygin, Evgeny & Voronin, Pavel. (2015) *Power Electronics Basics*, CRC Press.
4. Lei, X.-C. & Zhou, P. & Li, R.-X. (2009). "Analysis of Welding Defects in Spot Welding Process U-I Curves," 2009 Third International Conference on Genetic and Evolutionary Computing, pp. 201-204, doi: 10.1109/WGEC.2009.110.
5. Hlavacek, J. & Knenicky, M. & Draxler, K. (2020). "Calibration of Unipolar High Current Impulses for Resistance Spot Welding," 21st International Scientific Conference on Electric Power Engineering (EPE), pp. 1-4, doi: 10.1109/EPE51172.2020.9269221.
6. Baskoro, A. S. et al. (2014). "Effects of welding time and welding current to weld nugget and shear load on electrical resistance spot welding of cold rolled sheet for body construction," 2014 International Conference on Electrical Engineering and Computer Science (ICEECS), pp. 289-293, doi: 10.1109/ICEECS.2014.7045264.

7. Xiao-Jie, Y. et al. (2021), "Research on adaptive control of medium frequency DC resistance spot welding," 2021 International Conference on Artificial Intelligence and Electromechanical Automation (AIEA), pp. 30-34, doi: 10.1109/AIEA53260.2021.00014.
8. Suchý, S. & Rostás, K. & Soukup, R. (2022). "Encapsulation Methods for Resistance-Welded Contacts in Smart Textiles," 45th International Spring Seminar on Electronics Technology (ISSE), pp. 1-5, doi: 10.1109/ISSE54558.2022.9812820.
9. Chen, X. et al. (2022) "Effect of welding current and welding time on nugget size in RSW," ICETIS 2022; 7th International Conference on Electronic Technology and Information Science, pp. 1-4.
10. Wang, X. & Zhou, K.. (2021). "Electrical Parameter Identification of Medium-Frequency DC Resistance Spot Welding System Using Intelligent Algorithm," in IEEE/ASME Transactions on Mechatronics, vol. 26, no. 4, pp. 1791-1802, Aug. 2021, doi: 10.1109/TMECH.2021.3075479.
11. Shopov, Y. & S. Filipova-Petrakieva. (2021). "Phase Control Scheme with High Accuracy and Symmetry of the Control Pulses," 13th Electrical Engineering Faculty Conference (BulEF), pp. 1-3, doi: 10.1109/BulEF53491.2021.9690797.
12. Himmelstoss, F. & Edelmoser, K. (2018). “Vorrichtung zur Erzeugung hoher Stromimpulse mit kontrollierter Energieabgabe“, Austrian patent application AT 519343 A1 filed 10.11.2016.
13. Himmelstoss, F. A. & Edelmoser, K. H. (2017). “Current Measurement Device for High and Fast Changing Currents,” Power Conversion and Intelligent Motion PCIM 2017, Nuremberg, May 16-18, pp. 1311-1314, ISBN 978-3-8007-4424-4.

DETERMINATION OF HYDROCARBON PIPELINE TIME OF LEAK USING DISTRIBUTED ACOUSTIC SENSING MODEL

Amadi Oko Amadi

Department of Electrical Engineering and Computer Science, Texas A and M University, Kingsville USA

Lawrence Oborkahle.

Department of Electrical/Electronic Engineering, Michael Okpara University of Agriculture Umudike

Yabesh Toppo

Department of Chemical Engineering, Texas A and M University, Kingsville USA

Ekikere Umoren Udo.

Department of Electrical/Electronic Engineering, Michael Okpara University of Agriculture Umudike

Lokesh Ganta

Department of Mechanical Engineering, Texas A and M University, Kingsville USA

ABSTRACT

Leak is a catastrophic incident in pipeline operations, techniques to obtain zero-delay leak occurrence is of global interest. This paper use continuity equation of fluid dynamics model and obtain actual time leak occurs in hydrocarbon pipeline. In practices, time leak occurred is not time leak observed by team of pipeline operators monitoring workstations employed to detect the leak and the swift response of the acoustic alarm in mass balance approach. The model simulated in MATLAB display high accuracy by reducing the field leak time-period drastically from 863.937 to 16.43 seconds. The model is recommended for pipeline actual time leak detection estimate.

Keywords: Leak time, leak detection, Error, Discrepancy, Continuity equation and model.

1.0 Introduction

Pipeline is the fastest save means of transporting gases, liquid, and solid product. During pipeline operation, leak detection and the time the leak occurs are of primary concern to the pipeline operators. An efficient or pipeline of high integrity is the one with a very infinitesimal leak that was timely managed, quantified and controlled to obtain a negligible volume loss to the surroundings, some scholarly work has been made. Wang *et al* (2017) developed pipeline leak detection by using time-domain statistical feature of acoustic sensor characterized and identified by its waveforms, absolute amplitudes, and the frequency-domain energy distribution. Conversely the characteristics fades because of wave distortion under the condition of varying pipeline transportation. The experimental results from the field tests demonstrate the effectiveness of the actual leak time with the characterized feature extraction. Jin (2019) worked on leak detection using negative pressure wave (NPW) technique. He discovered that the Leak detection time is around the time required by the pressure wave to travel from the leak location to the pressure transmitter. In addition, which can provide an accurate leak location. Obibuike et al (2019) developed a mathematical model for time of leak estimation in a natural gas pipeline using pressure wave method to estimate the actual time the leak occurs in the pipeline as compare with the mass balance method, the proposed model was fast in comparison. Quy and Kim (2021) develop a work on real-time leak detection for a gas pipeline using a k-nearest neighbor classifier and hybrid acoustic emission features for detecting leak at a real time. To achieve the result, they

develop trained k-NN classifier algorithms that are embedded on the microcontroller unit to detect leak at a real-time. The system offers a reasonable alarm triggering without a false alarm despite adding white noise input signal but yield high average classification accuracy. Javad *et al* (2022) review comparative study on computational method for pipeline leakage detection and localization at a real-time using Mass/volume balance, negative pressure wave, pressure point analysis, statistical methods, and real-time transient modeling. Their study the strength, weakness and limitation recorded a commendable result on leak location speed across a line under study. North American Energy Pipelines magazine (2022) develop the evolution of pipeline leak detection at extended real-time transient model (E-RTTM) using pattern recognitions algorithm, they made assertion that Pipeline monitoring for its integrity originated from a simple mass balance approaches, for innovation of the entire systems the signature analysis technique habits leak pattern recognition to endlessly study this data and determine the pipeline's leak pattern. Conversely E-RTTM uses relative values, which continues to work effectively under turbulent pipeline conditions, without any significant effect on its sensitivity

2.0 Method

This work is analytical model, housed by the derivative of continuity equation as a tool in fluid dynamics, it postulates that the flow area of the pipeline is directly proportional to the flow velocity. This can be mathematically representing as,

$$A \propto u \quad (1)$$

$$R = Au = constant \quad (2)$$

Where, R, is the volume flow rate, A, is the flow area and u, is the flow velocity.

In this paper we obtain accurate time at which the leak occurs mathematically.

To achieve the models' following assumptions are made:

1. The hydrocarbon pipeline is having a single inlet and single outlet.
2. The fluid flowing in the hydrocarbon pipeline is non-viscous
3. The flow is incompressible, and the fluid flow is steady.

Understanding the Bernoulli's principle, we consider figure 3 diagram:

Figure 1: Simple hydrocarbon pipeline flow rate diagram

In this model, we consider the hydrocarbon flow for a short interval of time in the pipeline. So, assume that short interval of time as dt , at this time, the fluid will cover a distance of dx_1 with a velocity u_1 at the sending end (inlet) of the hydrocarbon pipeline.

At this time, the distance covered by the hydrocarbon will be:

$$dx_1 = u_1 dt \quad (3)$$

Now, at the sending end of the pipe, the volume of the fluid that will flow into the pipe will be: $V = A_1 dx_1 = A_1 u_1 dt$ (4)

It is known that mass (m) = Density (ρ) × Volume (V). So, the mass of the fluid in dx_1 region will be:

$dm_1 = Density \times Volume$ (5)

$\rho_1 A_1 u_1 dt = dm_1$ (6)

Hence the mass change at the sending end (inlet) will be

$\frac{dm_1}{dt} = \rho_1 A_1 u$ (7)

Similarly, the mass change at the receiving end (outlet) will be:

$\frac{dm_2}{dt} = \rho_2 A_2 u_2$ (8)

Therefore equating 7 and 8,

$\rho_1 A_1 u_1 = \rho_2 A_2 u_2$ (9)

This can be written in a more general form as:

$\rho\, A\, u$ = constant (10)

Hence, equation (10) concurs with the law of conservation of mass in fluid dynamics. Since the fluid is incompressible as it travels, the density remains constant for steady flow, therefore,

$\rho_1 = \rho_2$ (11)

Hence, equation (9) becomes:

$A_1 u_1 = A_2 u_2$ (12)

This equation can be written in general form as:

$R = A_1 u_1 = A_2 u_2$ = constant (13)

Because the pipeline is laid horizontally; geometry involves radial motion, we adopt cylindrical coordinate configuration.

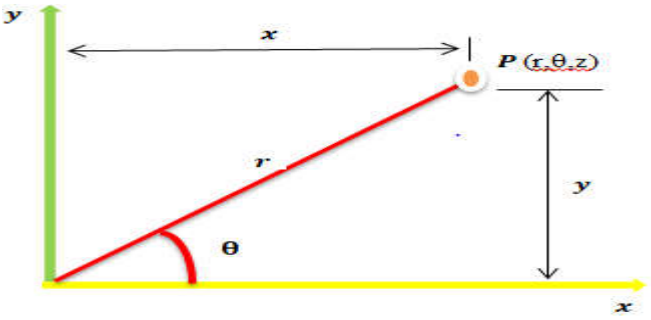

Figure 2: The model of cylindrical coordinate system as fluid phase changes during flow

The velocity components in these directions are in polar form as u_r , u_θ, u_z

Equation for such model coordinates for a point P (r, θ, z)

Consequently, if the gradient operator is written as,

$\nabla P = \frac{1}{r}\frac{d}{dr}(rP) + \frac{1}{r}\frac{d}{d\theta}(P) + \frac{1}{r}\frac{d}{dz}(P)$ (14)

Hence the radial motion continuity equation becomes,

$\frac{d\rho}{dt} + \frac{1}{r}\frac{d}{dr}(r\rho u_r) + \frac{1}{r}\frac{d}{d\theta}(\rho u_\theta) + \frac{d}{dz}(\rho u_z) = 0$ (15)

The equations govern the control volume analysis of an incompressible flow weather flow is steady (steady state) or unsteady (transient state).

At a steady state, the equation in three-dimensional stead flows becomes,

$$\frac{1}{r}\frac{d}{dr}(r\rho u_r) + \frac{1}{r}\frac{d}{d\theta}(\rho u_\theta) + \frac{d}{dz}(\rho u_z) = 0 \quad (16)$$

Where,

ρ is the gas density

u_r , u_θ. u_z Are the volumes of the velocity in three dimensions, but at a steady state of u_r

$\frac{1}{r}\frac{d}{dr}(ru_r) = 0$ (17)

Hence flow in u_r – direction becomes,

$$\frac{d}{dr}(\rho u_r) = 0 \quad (18)$$

Equation (18) becomes possible when there is no mass accumulation

Hence integrating with respect to r

$$\rho u_r = constant \quad (19)$$

Using equation (2).

$$\rho A u = \rho A u_r = constant \quad (20)$$

Consequently

$\rho_1 A_1 u_1 = \rho_2 A_2 u_2 = \frac{dm_1}{dt} = \frac{dm_2}{dt} = 0$ (21)

It is mass rate in the inlet pipeline minus the mass rate out pipeline

$$M_{inlet} - M_{outlet} = 0 \quad (22)$$

$$M_{inlet} = M_{outlet} \quad (23)$$

$\rho_1 A_1 u_1 - \rho_2 A_2 u_2 = 0$ (24)

Therefore, when there is leak the equation becomes,

$$M_{inlet} - M_{outlet} = M_{LEAK} \quad (25)$$

2.1: The time of leak model architecture.

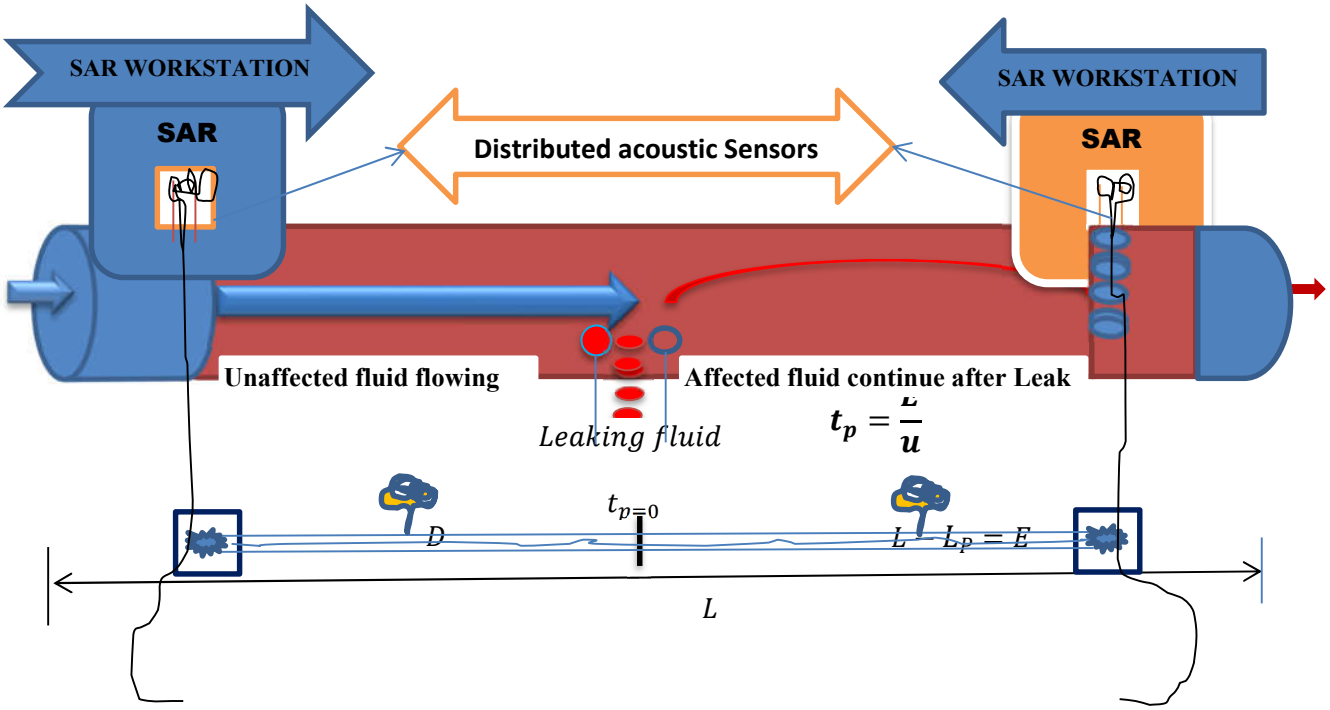

Figure 3: Pipeline bench setup for Determination of Leak Period

The figure shows the unaffected fluid flow distance (L_P) and affected fluid part (E) with the total distance of the pipeline length (L) used for the bench setup to capture Nigeria 614km Ajokuta Kaduna and Kano hydrocarbon pipeline. Thus, in this model, we considered it as a horizontal pipeline of equal cross-sectional area transporting hydrocarbon at steady rate isothermal condition and understand that leak detection time is not the same time the leak occurs in the pipeline, thus,

T_L, is the time the first mass of fluid exits the leak opening (time of leak). T_O, is the time the leak was observed by the pipeline monitoring team

t_p , is the time-period between when the leak occurred and when it was detected

Mathematically the above assumption is express as; $\{T_L\} < \{T_O\}$

If M is a fluid mass without leak through the pipeline, then when leak occurs the mass of fluid loss M_L at a time interval between when the leak occurred and when it was detected is.

$$t_P = (T_O - T_L) \qquad (26)$$

The T_O is a human time given by the monitoring team at the workstation, hence if we have t_p as the time interval period between when the leak occurred and when it was detected, then we calculate the time of leak T_L as,

$$t_P = (T_O - T_L) \qquad (27)$$

Recall that the distance travelled by the fluid from the sending end to the receiving end is given as Velocity x Time = Distance

To satisfy the interest of the work (Time of leak determination using DAS) we have,

$$L - L_P = E \qquad (28)$$

As the distance travelled by the fluid, from the sending end to the receiving end is identified as the affected part as shown in figure 4.

Thus.

$$u = \frac{E}{t_P} \tag{29}$$

Equation (29) is a general equation for time of leak used in this paper

Consequently, using equation (2) and (10), the flow rate of the affected hydrocarbon R_D documented at the exit point is given by the equation as,

$$R_D = UA \tag{30}$$

V is the velocity of the hydrocarbon travelling downstream to the output of the pipeline, m/s

A , is the cross-sectional area of the pipeline.

Combining equation (29) with equation (30), it can be rewritten as.

$$R_D = \left(\frac{E}{t_p}\right)\frac{\pi d^2}{4} \tag{31}$$

However, cross-multiplying and making t_p a subject of the formula, it becomes,

$$t_p = 0{,}785d^2\left(\frac{E}{R_D}\right) \tag{32}$$

Hence, the actual time the leak happened is T_L , and is equal to the time leak was observed and documented is T_O , minus the time-period t_p it happened as deduced in equation (26) and was rewritten as,

$$T_L = T_O - t_p \tag{33}$$

2.2: leak period determination using DAS model

Due to high rate of false alarm involves on the use of mass balance method in resolve of leak period, we proposed distributed acoustic sensing that uses the principle of sound wave during leak, when leaks occur, sound wave is emitted, such wave is detected by optic fiber sensors, comes as alarm system and travels along the pipeline parts. Hence equation 29 is the velocity of the acoustic wave V_{AW}traveling along the pipeline body. Thus, the equation becomes

$$t_p = \frac{L-L_P}{U_{AW}} \tag{34}$$

Given that velocity of the sound wave along the medium of a steel pipe wall is 5100 m/s, 5940m/s and 5960 m/s range helps to implement equation 34 and in turn calculate the time of leak (T_L) since the monitoring team can provide the time the leak is observed (T_O) from equation 33

2.3: Time of leak model simulation

The result in time of leak simulation were obtained in two techniques, the mass balance as used by many authors shown in equation (26) and the proposed model using sound wave of distributed acoustic sensing as shown equation (33) in determination of time of leak.

3.0: Result and discussion

3.1 Result of time of leak using mass balance techniques

Table 1: The Leak time profile of mass balance field data

Line ID	Leak period (t_p)mins	Time leak was Recorded (t_O)	Actual time of leak occurred (T_L)
L25	15.0101	01:30am	01.15am
L8	05.0012	05:40am	05.35am
L31	12.2540	12:09am	11.57am
L32	08.3004	03:16pm	03.08pm
L33	11.4021	08:52pm	08.41pm
L34	08.1202	12:50am	12.42am
L30	06.2013	07:53am	07.47am
L28	19.2001	03:05pm	02.46pm
L10	44.1012	08:09am	07:25am

This table shows a leak time profile of the mass balance with acoustic alarm systems used by the monitoring team, at different line ID that represent different length of pipeline incident under operation. Though it is a field data but equation (29) and (33) satisfy the leak period recorded by the team of operator with errors of human factor and instrument (false alarm) that will be addressed by the proposed model.

3.2: Results for Time of Leak Using distributed acoustic sensing (DAS) Method

Table 2: Time of leak simulation result using the proposed model

Line ID	Pipeline length [km]	Distance of Leak location (L_P) [km]	Leak period (t_P) mins
L25	50	11.09	0.1088
L8	44	15.71	0.0791
L31	90	17.60	0.2025
L32	99	21.22	0.2175
L33	91	12.85	0.2185
L34	105	11.62	0.2611
L30	196	1.38	0.5442
L28	196	6.18	0.5308
L10	128	19.95	0.3022

The table used equation (34) as it affects the study to simulate leak period (t_P) of different pipeline length and distance of leak location(L_P) using 357.6km/minutes as a speed of sound in a solid (steel pipeline). The result recoded leak period means of 0.2738 minutes or 16.43 seconds.

Table 3: Leak period ((t_P) comparison of acoustic wave sensing and mass balance approach

Line ID	Pipeline length [km]	Distance of Leak location (L_P) [km]	Mass balance approach Leak period (t_p)mins	Distributed Acoustic wave sensing approach Leak period ((t_P) min
L25	50	11.09	15.0101	0.1088
L8	44	15.71	05.0012	0.0791
L31	90	17.60	12.2540	0.2025
L32	99	21.22	08.3004	0.2175
L33	91	12.85	11.4021	0.2185
L34	105	11.62	08.1202	0.2611
L30	196	1.38	06.2013	0.5442
L28	196	6.18	19.2001	0.5308
L10	128	19.95	44.1012	0.3022
Total			127.5906	2.4647
Mean value			14.3990 mins or 863.937 sec	0.2738 mins or 6.43 sec

The leak period simulation result using acoustic wave signal during leak shows a mean value of 0.2738 minutes or 16.43 seconds against 14.3990 minutes or 863.937 seconds of mass balance approach. The

inference drawn, that shows high mean value reduction of leak period detected with the proposed model when compare with mass balance techniques, satisfies that sound wave travel faster than the fluid in the pipeline and consolidate the use of the model to verify the actual leak period in pipeline operation without in shut of the system under operation.

4.0 Conclusion

The mathematical equations were developed analytically to obtain the time of leak in hydrocarbon pipeline of different line ID of Nigerian gas company (NGC) under monitor, the model results indicate the flux between the time the alarm trigger for the leak occurrence and the actual time the leak occurs are not the same. The mean value leak period difference between mass balance approach and acoustic wave sensing shows the model (acoustic) effective nature on triggering the alarm for time of leak accuracy and sensitivity. The longer time of the alarm files for false alarm error and inefficient nature from the fluid exit time to the time the monitoring team detected the exit. For absolute pipeline high integrity monitoring of hydrocarbons, the model fine its use in several places such as SAR, SCADA, and SRS workstations. More so, where human habitations leave at the pipeline right of way, loss of live and properties on much delay in time of leak detection will be high, catastrophic when not addressed and the volume loss will retard the economic growth contributed by such product pipeline.

Reference

1. Obibuike Ubanozie Julian, Ekwueme Stanley Toochukwu, Ohia Nnaemeka Princewill, Igbojionu Anthony Chemazu, Igwilo Kevin Chinwuba, Kerunwa Anthony. Mathematical Model for Time of Leak Estimation in Natural Gas Pipeline. Petroleum Science and Engineering. Vol. 3, No. 2, 2019, pp. 68-73. doi: 10.11648/j.pse.20190302.15
2. Schlumberger. (2014). OLGA Dynamic Multiphase Flow Simulator. http://www.software.slb.com/products/foundation/Pages/olga. Aspx
3. Quy TB and Kim JM (2021) Real-Time Leak Detection for a Gas Pipeline Using a *k*-NN Classifier and Hybrid AE Features. MDPI Sensors (Basel) doi: 10.3390/s21020367
4. Javad Sekhavati, Seyed Hassan Hashemabadi, and Masoud Soroush, (2022) Computational methods for pipeline leakage detection and localization: A review and comparative study, Journal of Loss Prevention in the Process Industries, Volume 77, ISSN 0950 4230, https://doi.org/10.1016/j.jlp.2022.104771.
5. *North American Energy Pipelines* magazine is a free trade publication for industry professionals, 2022, August 3-4
6. F. Wang, W. Lin, Z. Liu, S. Wu, and X. Qiu, "Pipeline Leak Detection by Using Time-Domain Statistical Features," in IEEE Sensors Journal, vol. 17, no. 19, pp. 6431-6442, 1 Oct.1, 2017, doi: 10.1109/JSEN.2017.2740220
7. Jin Mingang (2019). Investigation on Parameters Affecting the Performance of Negative Pressure Wave Leak Detection Systems.Paper prepared for presentation at the PSIG Annual Meeting held in London, England.

HOW CAN ARTIFICIAL INTELLIGENCE INCREASE THE ACCURACY OF PRODUCTION FORECASTING?

Mohammad Bakhtiary

School of Chemical and Petroleum Engineering Shiraz, University, Shiraz, Iran

Masoud Shafiei

Enhanced Oil Recovery Research Center School of Chemical and Petroleum Engineering Shiraz, University, Shiraz, Iran

Masoud Riazi

Enhanced Oil Recovery Research Center School of Chemical and Petroleum Engineering Shiraz, University, Shiraz, Iran

Yousef Kazemzadeh

3-Department of Petroleum Engineering, Faculty of Petroleum, Gas, and Petrochemical Engineering, Persian Gulf University, Bushehr, Iran

ABSTRACT

Production prediction has always been one of the most challenging parameters in the advancement of economic programs and optimization in oil and gas fields the conventional methods available for production forecasting that have been used in the oil and gas industry require a lot of accurate petrophysical, geological, rock, and fluid data, etc. to forecast production. In addition, complex and time-consuming methods related to history matching will cause slowness and inaccuracy in numerical calculations. In the last two decades, with the advancement of computing technology and the familiarity of oil companies with data analysis, data-based modeling methods have been used as a successful solution for predicting oil and gas production. Data-based methods do not have problems related to other conventional methods. In this work, DNN, SVR, GRU, CNN-GRU models have been developed to predict the oil production of a well in one of Iran's oil fields. Overall, among the developed models, the CNN-GRU model achieved the best results for both the training data with a R^2 value of 99% and the test data with a R^2 value of 97%. Also, in terms of performance metrics, the CNN-GRU model showed excellent performance compared to other methods In addition, the combination of CNN-GRU model with GRU achieved much better results in the training and testing phase compared to the conventional GRU, so that the value of R^2 in the CNN-GRU model compared to the GRU method for training and The test data has been improved by 2% and 5% respectively. Also, when considering all data points, the performance metrics calculated using the results estimated by CNN-GRU were the best.

Keywords: Production prediction, Data-based methods, DNN, SVR, GRU, CNN-GRU, conventional methods

DYSFUNCTIONAL ANALYSIS OF A PRODUCTION SYSTEM BASED ON MOUNTED CARLO SIMULATION

APPLICATION: METAL SHEET PRODUCTION LINE

UNIT: COLD ROLLING MILL, COMPANY: SIDER –ANNABA-ALGERIA

Dalila Khalfa, Hichem Bouras, Oussama Meghlaoui, Mounira Djemai

Annaba University Algeria

ABSTRACT

The objective of this study is to find an adequate analytical approach to the functioning of the production system, to highlight the obstacles that can reduce the performance of the manufacturing process in the company.

Through this work, we tried to implement a production system analysis method for the "cold rolling mill" unit based on performance indicators named: Monte Carlo simulation. The application of this approach requires knowledge of the data is essential such as:

- The global architect and the systematic sequence of the system.

- The principles arisen difficulties that periodically repeat themselves.

we presented the internal structure of the process and their manufacturing specifics implemented at the level of the "cold rolling mill unit", thus we gave an exploitation of knowledge obtained through this study to make a statistical analysis and obtain a global view which reflects the real operation of a production system.

Applying the Monte Carlo simulation approach has the crater of translating functional data into practical information that can be easily interpreted (numerical and graphical results).

Based on these results, decisions will be made leading to the continuous improvement of the "cold rolling mill" production system.

Keywords: Monte Carlo simulation, modeling of the industrial process, production, industrial company

UX STUDY ON HANDHELD AUGMENTED REALITY GAMES BY APPLYING SPRADLEY'S NINE DIMENSIONS DESIGN PRINCIPLE

Pushkar Pandey[1]

[1]Indian Institute of Technology, Department of Design, Kanpur 208016, India.

[1]ORCID ID: https://orcid.org/0000-0002-5894-1036

Renu Kundu[2]

[2]Indian Institute of Technology, Department of Design, Kanpur 208016, India.

[2]ORCID ID: https://orcid.org/0000-0002-5894-1036

ABSTRACT

The first step in researching augmented reality was making a head-mounted three-dimensional display at the beginning of 1968. The idea behind a three-dimensional display is to show the user a perspective image from a different point of view that changes as the user moves. Since that time, the majority of growth in augmented reality has been driven by technology. The researcher's emphasis on AR's technological aspects, such as its hardware and software, has resulted in very few initiatives directed toward user experience and exploration studies. To address the transition of the notion of augmented reality from research/laboratories to the general user, it is necessary to approach the technology in a more user-friendly, user-centric manner. In this study, we focus on handheld augmented reality (HAR) gaming applications and propose to employ Spradley's nine dimensions to investigate components of handheld augmented reality experience so that designers may comprehend the human-centric design approach. we posed a questionnaire to a diverse sample of 215 individuals. After the questionnaire we select 35 individuals and provide them our iPhone11 to play AR Gamest for direct observation.

In the result we found out 61.9% user know about HAR games, 8.1% of users played the AR game without understanding that it is known handled augmented reality implies that even after utilising augmented reality, many are unaware of it. 28.2% (strongly agree) and 32.5% (agree) on the issue that it is easier to get skilled at AR games. We conclude our research by finding out there are 4 insights related to the HAR games. The detail about these insights are discussed in context with the human-centric design in HAR games.

Keywords: handheld augmented reality (HAR), user-centric, Spradley's nine dimensions, human-centric design

SENTIMENT ANALYSIS FOR PRODUCT RECOMMENDATION ON AMAZON'S MOBILE PHONE REVIEWS USING MACHINE LEARNING TECHNIQUES

Menaouer BRAHAMI

Dr., National Polytechnic School of Oran - MA, Systems Engineering Department, Algeria

ORCID ID: 0000-0003-0045-9797

Mohammed SABRI

Dr., National Polytechnic School of Oran - MA, Systems Engineering Department, Algeria

Chaya KEDİDİR

Phd., National Polytechnic School of Oran - MA, Systems Engineering Department, Algeria

Fatma DEHBI

Phd., National Polytechnic School of Oran - MA, Systems Engineering Department, Algeria

ABSTRACT

The product reviews serve as feedback for businesses in terms of performance, product quality, and the decision-making process of customers. As well, exploiting and analyzing customer product reviews in sentiments become an advantage for businesses and researchers on most e-commerce platforms. Moreover, it is becoming necessary for companies to examine customer reviews on online platforms such as Amazon to understand better how customers rate their products and services. Furthermore, recommender systems are information filtering systems from the massive amounts of product reviews that are generated dynamically based on customers' preferences, interests, and behaviours. Amazon is an example of the world's largest online retailer that allows its customers to write reviews and rate its products freely. In this paper, we present a new sentiment analysis for product recommendations approach on Amazon electronics product reviews based on the one hand, on detecting the sentiment (positive or negative) associated with mobile phone reviews using Natural Language Processing (NLP) and Machine Learning techniques and, on the other hand, by using the combination features (hybrid filtering) and KNN supervised learning to build our recommendation system for recommending electronic products that have received positive reviews. The research presented in this paper used a well-known strategy in sentiment analysis for feature extraction with text information namely the Bag of Words (BoW), TF-IDF, and Word Embedding. We evaluate their performance on one real-world dataset from Amazon and compare them with one state-of-the-art method. The experimental results of evaluating the recommender system, performed on 400,000 customer reviews, an ensemble of online datasets, yielded an accuracy of 95.94%, Recall of 95%, F1 score of 94%, and RMSE of 4.5%. The proposed approach helps SMEs companies use sentiment analysis to understand customer experiences using Amazon reviews.

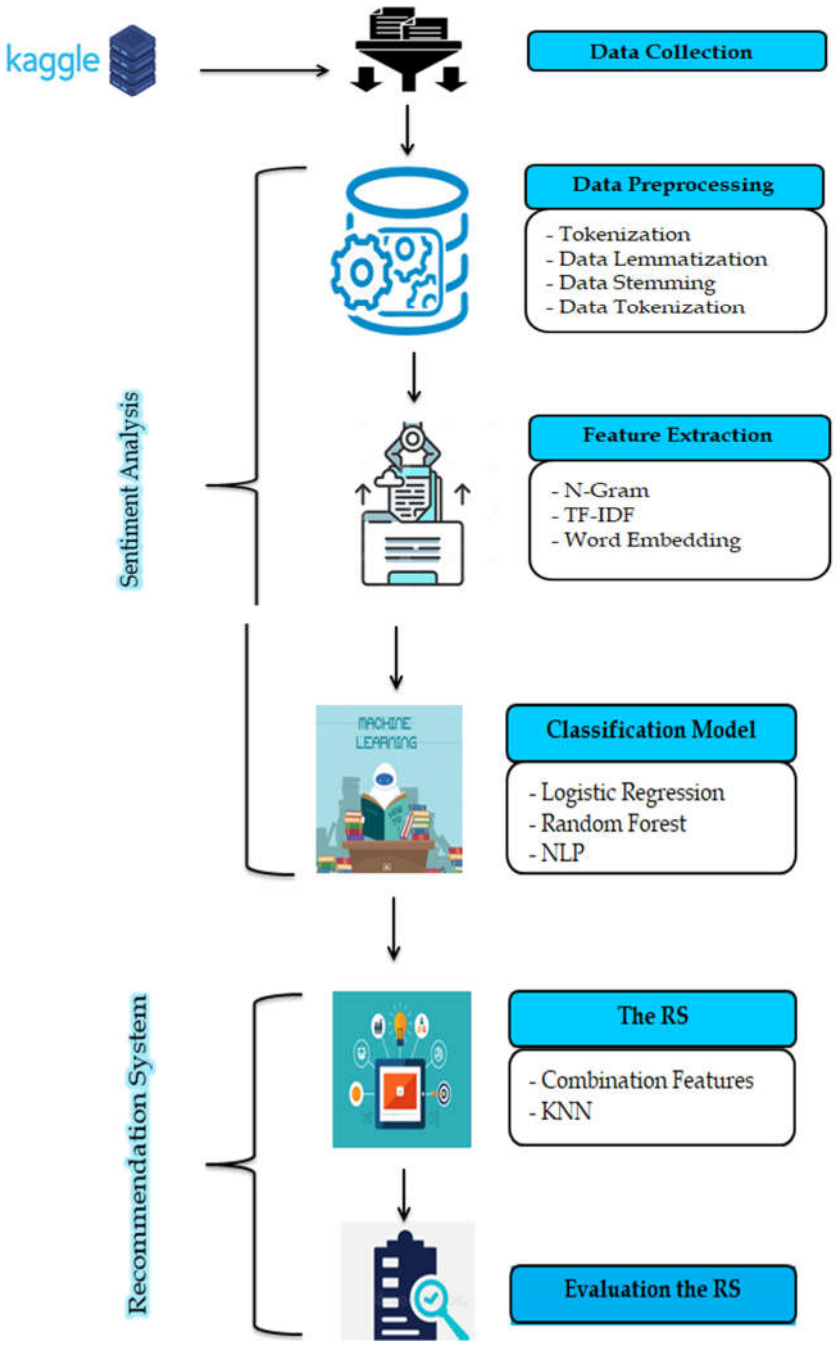

Figure. 1. *Main Steps of the proposed sentiment analysis for product recommendations Approach*

Keywords: Knowledge Management, Sentiment Analysis, Recommender Systems, Machine Learning, Product Reviews, Bag of Words, TF-IDF, Word Embedding, Decision Support System.

FEATURE ANALYSIS OF IOT BOTNET ATTACKS USING DEEP LEARNING

Menaouer BRAHAMI
Dr., National Polytechnic School of Oran - MA, Systems Engineering Department, Algeria
ORCID ID: 0000-0003-0045-9797
Mohammed SABRI
Dr., National Polytechnic School of Oran - MA, Systems Engineering Department, Algeria
Oussama CHETA
Phd., National Polytechnic School of Oran - MA, Systems Engineering Department, Algeria
Ahlem KHIAR
Phd., National Polytechnic School of Oran - MA, Systems Engineering Department, Algeria

ABSTRACT

With the advancements in world technologies like processing power, high speed internet (4G, 5G) and the increasing availability of cheap electronics, the Internet of Things phenomenon (IoT) emerged. This enabled electronic objects to connect to the internet, interact with each other, and interact with the physical world through the internet. Consequently, this increase in the number of connected devices, coupled with limited security measures and an absence of consensus regarding IoT device norms and standards, has made them an easy target for Botnet attacks, where these devices are hijacked and used to steal data and launch other types of massive attacks. Besides, security issues have also arisen with the network growth and as a result of the health situation of Covid-19. However, intrusion detection or detecting Botnet attacks in such big data is challenging.

In this paper, Advanced deep learning techniques have been proposed for automatic detection of the malicious behavior of Botnet attacks and extraction of useful knowledge related to this behavior. This research aims to provide an inclusive analysis of malicious behavior detection of Botnet attacks based on deep learning techniques followed by extracting useful information related to this behavior detection system using a Deep Learning explanation technique called SHAP (see Figure 1). Moreover, network traffic datasets coming from IoT devices are fully explored and analyzed. Deep learning techniques for malicious behavior detection of Botnet attacks have been critically evaluated based on different performance metrics (accuracy, precision, recall, f-1 score, and detection rate). Furthermore, existing challenges and possible solutions for network security and privacy have been discussed.

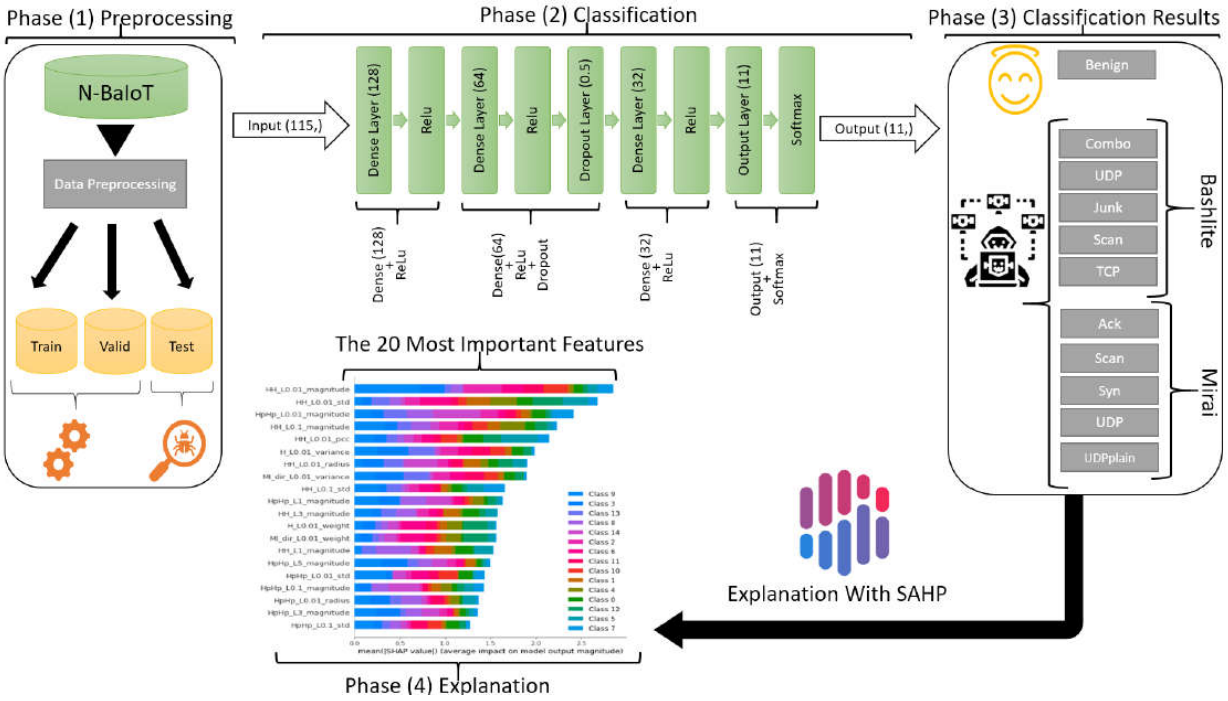

Figure. 1. *Main Steps of the proposed IoT Botnet Attacks Classification and Feature Analysis Using MLP and SHAP*

In this work, our prime objectives are to:

1. Produce two working deep learning models for classifying Botnet attacks;

2. Show some of the capabilities of the SHAP method for explaining black-box deep learning models' behavior;

3. Present our findings and discuss the obtained results with by performing feature analysis.

Keywords: Deep Learning, Intrusion Detection, Feature Analysis, Dimensionality Reduction, IoT, Botnet, SHAP.

EFFECT OF PIGMENT COATING ON SOME PERFORMANCE PROPERTIES OF DENIM FABRICS

Gamze OKYAY[1]

[1] Malatya Turgut Ozal University, Yeşilyurt Vocational School, Department of Design, Malatya, Turkey

[1]ORCID ID: https://orcid.org/0000-0003-1312-3897

Münevver ERTEK AVCI [2]

[2] Malatya Turgut Ozal University, Yeşilyurt Vocational School, Department of Textile, Clothing, Footwear, and Leather, Malatya, Turkey

[2]ORCID ID: https://orcid.org/0000-0002-7360-7407

Hilal BİLGİÇ[3]

[3] Malatya Turgut Ozal University, Yeşilyurt Vocational School, Department of Textile, Clothing, Footwear, and Leather, Malatya, Turkey

[3]ORCID ID: https://orcid.org/0000-0002-5195-9890

ABSTRACT

In this study, the effect of pigment coating on some performance properties of denim fabrics was investigated. For this purpose, three different raw denim fabric structures were first pre-treated and then coated with a pigment coating substance. Tensile and tear strength, seam slippage, rubbing, and washing fastness properties of reference fabrics as well as pre-treated and pigment coated fabric samples were evaluated using statistical analysis methods. Pigment coating generally slightly reduced the mechanical properties of the fabric. In overall, it had no effect on rubbing and washing fastness.

Keywords: Pigment, Coating, and Denim Fabric.

1. Introduction

Denim is typically a twill fabric with indigo-dyed warp yarns and undyed weft yarns, resulting in a blue top and ecru back appearance. Originally created for workers' clothing, this fabric has now gained immense popularity and is embraced by all, irrespective of gender, age group, and profession, due to its great durability, longer washing cycle, and ability to adapt to changing fashion trends [1]. Accordingly, denim manufacturers face significant challenges in developing innovative products in terms of both appearance and use due to the expansion of the denim industry and the demand for denim for fashion in recent years [2]. Denim fabric finishing is one of the most extensively used finishing treatments that have enormous practice, because of its effects on appearance and comfort [3]. There are almost countless variations of dry and wet processing techniques used by designers and textile chemists to achieve fashionable looks that are distinctive and desirable [4-6]. One of these techniques is coating technology. When applied on a fabric surface, it not only adds a functional edge to the fabric but also gives it a brilliant shine. Pigment coating is one of the most popular coating techniques commonly used in denim. With the pigment coating, the fabrics can gain a new look after each wash. However, the biggest limitation of this technique is that the fabric performance properties can be adversely affected [7]. Therefore, in this study, tensile and tear strength, seam slippage, rubbing, and washing fastness properties of reference fabrics as well as pre-treated and pigment-coated fabric samples were evaluated using statistical analysis methods.

2. Experimental

2.1. Materials

In this study, three different types of raw denim fabric structures (Çalık Denim) were used and the structural properties of the fabrics used are given in Table 1. Pigment substance (PC, Bercolin, Bersa Tekstil ve Kimya San. Ltd. Şti) was employed as a coating agent.

Table 1. The structural properties of the three different types of raw denim fabrics

(DE1: First, DE2: Second, and DE3: Third type raw denim fabrics

Notation	Warp yarn (Ne)	Weft yarn (Ne)	Pattern	Warp density (Threads/cm)	Weft density (Threads/cm	Dry weight (onz)	Washed weight (onz)
DE1	18/1 dual core-spun (46% Tencel, 30.67 % cotton, 16.76% T400, and 6.57% Lycra)	14.1/1 ring-spun (100% cotton)	3/1 Z twill	28.0	21.0	9.5	10.5
DE2	18/1 dual core-spun (76.31% cotton, 16.76% T400, 6.93% Lycra	14.1/1 ring-spun (100% cotton)	3/1 Z twill	28.0	20.5	7.5	9.0
DE3	10/1 dual core-spun (87.04% cotton, 9.31% T400, 3.65% Lycra	8.6/1 ring-spun (100% cotton)	3/1 Z twill	22.4	16.0	11.0	12.0

2.2. Methods

2.2.1. Pre-treatment

The pre-treatment processes applied to raw denim fabric structures are displayed in Table 2.

Table 2. Pre-treatment process applied to the three different types of raw denim fabrics

(DE1: First, DE2: Second, and DE3: Third type denim fabrics, and PT: Pre-treatment

Notation	Pre-treatment process
DEPT1	Backside tangent burning, burning, effective washing, dry fixation, standard finish, and sanforizing
DEPT2	Backside tangent burning, frontside burning + mercerizing, calendaring, dry fixation, and sanforizing
DEPT3	Backside tangent burning, burning, mercerizing, calendaring, dry fixation, and sanforizing

2.2.2. Coating

The pre-treated denim fabric structures were coated according to the rotation printing method. Table 3 summarizes the recipe for coating.

Table 3. The coating recipe applied to the

three different types of pre-treated denim fabrics

(DE1: First, DE2: Second, and DE3: Third type denim fabrics, and PC: Pigment coating

Notation	Coating recipe
DEPC1	46.1 g/kg Pigment, 150 g/kg binder, 12 g/kg thickener, 5 g/kg anti-foam, and 2 g/kg ammonia
DEPC2	15 g/kg Pigment, 500 g/kg coating paste, 12 g/kg thickener, and 8 g/kg coating catalyst
DEPC3	15 g/kg Pigment, 150 g/kg binder, 12 g/kg thickener, 5 g/kg anti-foam, and 2 g/kg ammonia

2.2.3. Analysis

All denim fabric specimens were initially conditioned in the laboratory under standard atmospheric conditions (20 ± 1ºC and 65 ± 2% R.H.) for 24h according to TS EN ISO 139. The tensile and tear strength, seam slippage, rubbing, and washing fastness analyses of the denim fabric samples were carried out based on the ASTM 5034, ASTM D1424, ASTM D434, AATCC 8, and ISO 105-C06 standards, respectively. Tensile strength and seam slippage analyses were performed on the SDL ATLAS tensile strength instrument. SDL ATLAS Elmendorf tear strength instrument was used for tear strength analysis. The rubbing and washing fastnesses were determined by using SDL ATLAS Electronic crock meter and Rotawash testing aparatus, respectively. Since the mechanical properties of the woven fabrics in the warp and weft directions may be different, they were carried out in both directions. Tensile and tear strength and seam slippage analyzes were performed with 5 replicates and the average of these repetitions was determined as the final value. Error bars were calculated from the coefficient of variation (CV%) of the mean of the test results. Analyses of rubbing and washing were conducted in one repetition and this value was recorded as the final value. The experimental study data were entered into the IBM® SPSS 26 statistical package software by using a one-way analysis of variance (ANOVA). The significance of the coating type was analyzed at a 95% confidence interval (CI).

3. Result and Discussion

In this part, the tensile and tear strength, seam slippage, rubbing, and washing fastness properties of the denim fabrics produced were evaluated comparatively with statistical analysis methods.

Tensile strength

The maximum amount of tensile stress that a material can bear before failure is known as its tensile strength. The tensile strength findings in the warp and weft directions of the denim fabric samples are displayed in Figure 1. The ANAVO results show that for the first and third type fabrics, the influence of coating type on tensile strength was statistically significant (p=0.000) in both the warp and weft directions at a 95% confidence interval. For the DE2 samples, it was significant (p=0.000) in the warp direction but not significant (p=0.488) in the weft direction. In all samples, pre-treatment and pigment coating slightly decreased the fabric tensile strength in the warp direction. In the weft direction, the pretreatment almost did not change the results, while the pigment coating increased slightly.

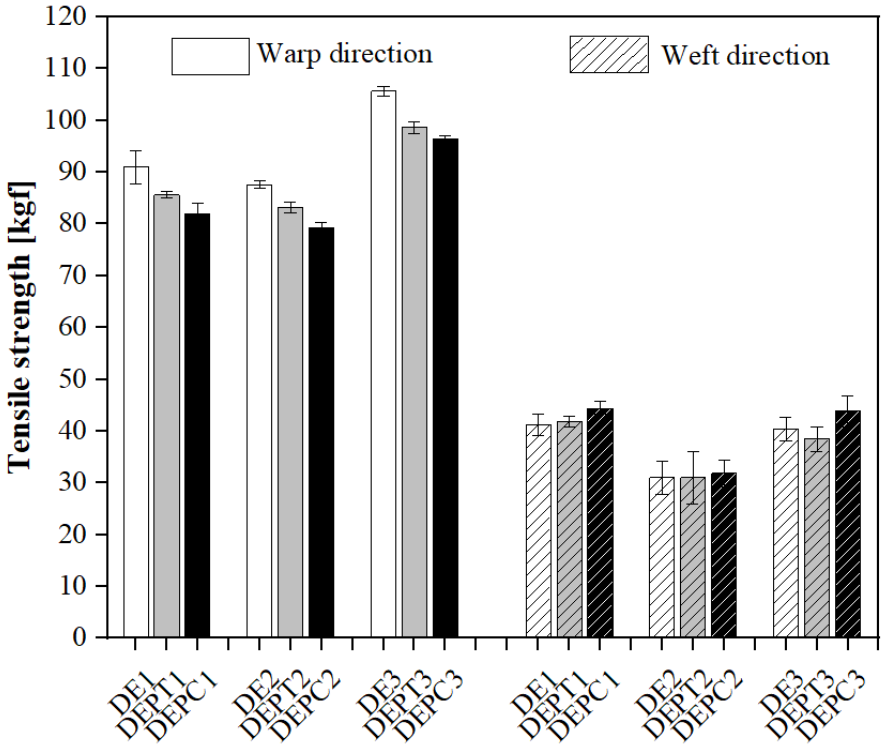

Figure 1. The tensile strength results of the denim fabric specimens.

(DE1: First, DE2: Second, and DE3: Third type raw denim fabrics,

PT: Pre-treatment and PC: Pigment coating).

Tear strength

Under specific conditions, the force necessary to begin or continue to tear a fabric in either the weft or warp direction is defined as tearing strength. Figure 2 shows the denim fabric samples' tear strength results for the warp and weft directions. When the tear strength values of the different denim fabrics structure were evaluated statistically, the ANOVA findings reveal that coating type was significant (p=0.000) for all fabric types in both weft and warp directions. Similar to the findings for tensile strength, pre-treatment and pigment coating on denim fabric structure led to a decrease in the tear strength values in the warp direction (Figure 2). While pretreatment in the weft direction did not change the results, the pigment coating decreased considerably. It is thought that the decrease in tear strength values in the warp and weft direction was due to the fact that the coating material penetrates into the fabrics and limited the movement of the warp and weft threads.

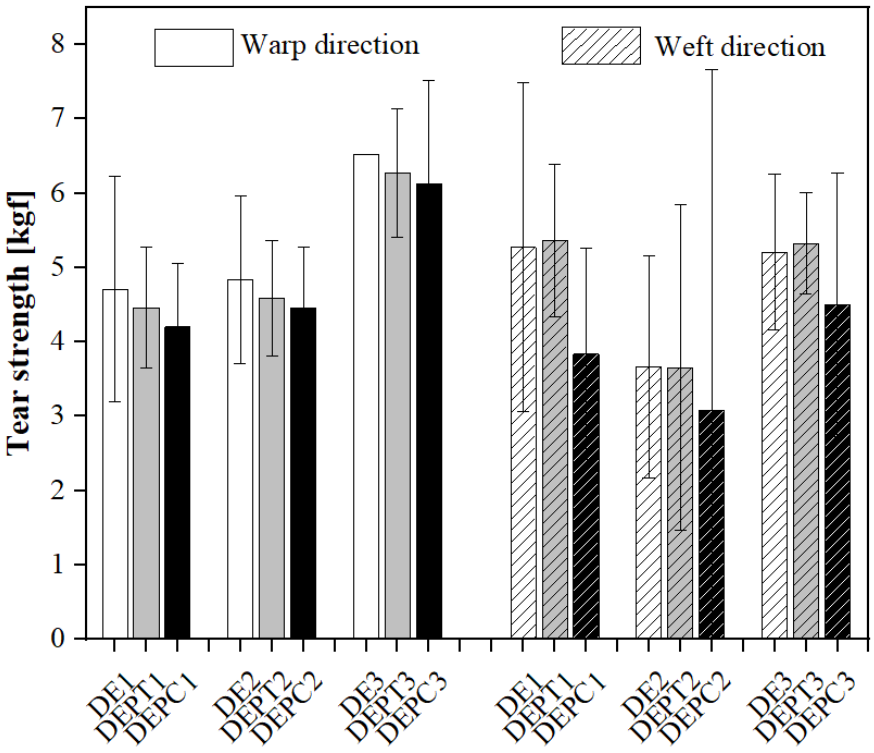

Figure 2. The tear strength results of the denim fabric specimens (DE1: First, DE2: Second, and DE3: Third type raw denim fabrics, PT: Pre-treatment and PC: Pigment coating).

Seam slippage

Seam slippage is a fabric's essential characteristic and a key component of the specification for fabrics. Seam slippage occurs when a fabric seam opens under a defined force. The results of seam slippage in both the warp and weft directions of the denim fabric structures are given in Figure 3. The ANOVA results indicate that the effect of coating type on the seam slippage was insignificant ($p>0.05$) for all fabric types in both weft and warp directions. Regardless of fabric direction, pretreatment either slightly increased or decreased the seam slippage values. Except for the DEPC3 sample, pigment coating raised the seam slippage values in the warp direction, but lowered them for all samples in the weft direction. The improvement in seam slippage in the weft direction might be due to the pigment coating material increasing slippage by reducing friction.

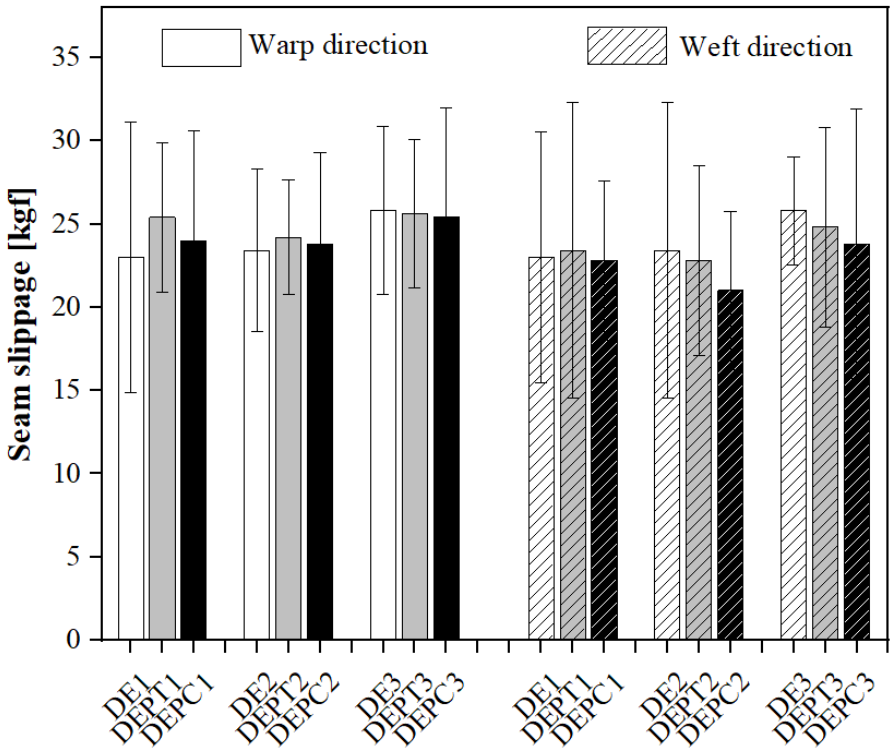

Figure 3. The seam slippage results of the denim fabric specimens (DE1: First, DE2: Second, and DE3: Third type raw denim fabrics, PT: Pre-treatment and PC: Pigment coating).

Rubbing and washing fastness

The rubbing and washing fastness findings of the denim fabric samples are illustrated in Table 4. A p-value could not be obtained for rubbing and washing fastness. Pre-treatment and pigment coating did not change dry and wet rubbing fastness for all denim fabric types. While pre-treatment improved color change in the first and second type fabrics, pigment coating did not cause any change. Both pre-treatment and pigment coating had no effect on the color change for the third type of fabric. While both pretreatment and pigment coating generally improved staining in the first type of fabrics, it did not cause any change in the second and third fabric types.

Table 4. The rubbing and washing fastness results of the denim fabric specimens (DE1: First, DE2: Second, and DE3: Third type raw denim fabrics, PT: Pre-treatment and PC: Pigment coating).

Notation	Rubbing fastness			Washing fastness					
	Dry crocking	Wet crocking	Color change	Staining					
				Acetate	Cotton	Nylon	Polyester	Acrylic	Wool
DE1	3~4	1~2	3~4	3~4	3~4	3~4	4	4	4
DEPT1	3~4	1~2	4	4	4	4	4	4~5	4~5
DEPC1	3~4	1~2	4	4~5	4~5	4~5	4~5	4~5	4~5
DE2	3~4	1~2	3~4	4~5	4~5	4~5	4~5	4~5	4~5
DEPT2	3~4	1~2	4	4~5	4~5	4~5	4~5	4~5	4~5
DEPC2	3~4	1~2	4	4~5	4~5	4~5	4~5	4~5	4~5
DE3	4~5	1~2	4	4~5	4~5	4~5	4~5	4~5	4~5
DEPT3	4~5	1~2	4	4~5	4~5	4~5	4~5	4~5	4~5
DEPC3	4~5	1~2	4	4~5	4~5	4~5	4~5	4~5	4~5

4. Conclusion

In this study, three different raw denim fabric structures were first pre-treated and then coated with a pigment substance to test the effect of pigment coating on some fabric performance properties. The tensile and tear strength, seam slippage, rubbing, and washing fastnesses of these fabrics were compared with statistical analysis methods. When the results were evaluated in general, while the pigment coating slightly reduced the mechanical properties of the fabrics, it did not cause any change in rubbing fastness and color change.

Acknowledgments

The authors appreciate the contributions of Çalık Denim, Malatya, Turkey, who carried out fabric manufacturing, coating, and analyses.

References

[1]. Memon, N.A. (2018). Cotton denim fabrics market: challenges and opportunities. *Pakistan Textile Journal*, *67*(6), 50-50.

[2]. Khalil, E. (2015). Sustainable and ecological finishing technology for denim jeans. *AASCIT Communication*, *2*(5), 159-163.

[3]. Mondal, M.I.H., & Khan, M.M.R. (2014). Characterization and process optimization of indigo dyed cotton denim garments by enzymatic wash. *Fashion and Textiles*, *1*(1), 1-12.

[4]. Khalil, E., & Islam, M.M. (2015). Wrinkle finish on denim by resin treatment: a review. *AASCIT Communication*, *2*(3), 82-87.

[5]. Sarkar, J., & Khalil, E. (2014). Effect of industrial bleach wash and softening on the physical, mechanical and color properties of denim garments. *IOSR Journal of Polymer and Textile Engineering*, *1*(3), 46-49.

[6]. Sarkar, J., Khalil, E., & Solaiman M. (2014). Effect of enzyme washing combined with a pumice stone on the physical, mechanical and color properties of denim garments.

[7]. Apparel resources. (2014). Coating finishes. https://apparelresources.com/fashion-news/trends/coating-finishes/, [Accessed 19 August 2022].

COMPARATIVE STUDY OF SLAKED LIME AND TSP ON HEAVY METAL IMMOBILIZATION FROM WASTEWATER

Mahamane Chapiou SOULEY GARBA[1], Erol KAYA[2]

[1] Dr., Dokuz Eylul University, The Graduate school of Natural and Applied Sciences, Mineral Processing Program

[2]Prof. Dr., Dokuz Eylul University, Faculty of Engineering, Mining Engineering Department, Mineral Processing Division

[1]ORCID ID: 0000-0002-3182-3769; [2]ORCID ID: 0000-0001-7874-7321

ABSTRACT

Slaked lime ($Ca(OH)_2$) and triple superphosphate (TSP) are the precipitating agents that stabilize heavy metal ions from wastewater through the formation of metal hydroxide and metal phosphate. This process known as chemical precipitation technology is influenced by many factors such as pH, metal concentrations and dosage of precipitating agent. This study aims to evaluate the effectiveness of $Ca(OH)_2$ and TSP for heavy metal immobilization from wastewater containing divalent ions of Cu, Fe, Mn, Sr and Zn through the precipitation test under different conditions and analyze the precipitates (residue) obtained after precipitation with $Ca(OH)_2$ and TSP separately.

The obtained experimental results demonstrated that the addition of high dosage of $Ca(OH)_2$ and TSP separately, immobilize effectively Cu, Fe, Mn, Sr and Zn metal ions with immobilization efficiency ranging from 90 to % 99.9% at pH values of 11.58 and 3.43 respectively. In addition, the effectiveness of $Ca(OH)_2$ decreases strongly as the pH drop to 2, 3, and 5 while the immobilization rates in all-metal ions using TSP are greater than 90%. The X-ray analyses reveal the presence of copper iron sulfide ($CuFeS_2$) and calcium zinc hydroxide hydrate in the treated residue with lime, whereas, it was found the formation of copper phosphate, iron phosphate, manganese phosphate and zinc phosphate in the treated residue with TSP.

Keywords: Slaked lime, triple superphosphate, immobilization, precipitation process, wastewater.

OHMİK ISITMA İŞLEMİNİN PROTEİN İLAVELİ SÜTLERDE *Listeria Monocytogenes* İNAKTİVASYONU ÜZERİNE ETKİSİ*

EFFECT OF OHMIC HEATING ON THE INACTIVATION OF *Listeria Monocytogenes* IN PROTEIN-ADDED MILK

Ramazan Yasin AYYILDIZ[1], Hatice Ahu KAHRAMAN[2]

[1]Burdur Mehmet Akif Ersoy Üniversitesi, Sağlık Bilimleri Enstitüsü, Gıda Hijyeni ve Teknolojisi Anabilim Dalı

[1]Burdur Mehmet Akif Ersoy University, Institute of Health Sciences, Department of Food Hygiene and Technology

[2]Burdur Mehmet Akif Ersoy Üniversitesi, Veteriner Fakültesi, Gıda Hijyeni ve Teknolojisi Anabilim Dalı

[2]Burdur Mehmet Akif Ersoy University, Faculty of Veterinary Medicine, Department of Food Hygiene and Technology

ÖZET

Listeria monocytogenes gıda kaynaklı hastalıklara sebep olan en önemli gıda patojenlerinden biridir. Süte uygulanan pastörizasyon işlemi, sütteki patojen mikroorganizmaları ve enzimleri etkisiz hale getirirken, ürünün aroma ve besinsel özelliklerinde birtakım olumsuzluklara neden olabilmektedir. Son yıllarda yapılan araştırmalar gıdaların yapısal özelliklerine zarar vermeden patojen inaktivasyonunu sağlayan yenilikçi teknolojiler üzerinde yoğunlaşmaktadır. Bu yenilikçi teknolojilerden biri olan ohmik ısıtma, kitlesel ve hızlı bir ısıtma sağlayarak etkin bir mikrobiyal inaktivasyon sağlamaktadır. Bu çalışmanın amacı, farklı elektrik alan şiddetindeki ohmik ısıtma (OI) işleminin protein tozu ilaveli sütlerde *L. monocytogenes* inaktivasyonu üzerine etkilerini belirlemektir. Bu kapsamda; 200 ml cam kavanozlara aktarılan % 1.5 yağ oranına sahip süt örnekleri içerisine %2,5, %5 ve % 7,5 oranında protein tozu ilave edildi, ardından 80 °C 15 dk otoklavlanarak pastörize hale getirildi. Örnekler içerisine % 0.5 oranında 10^7düzeyinde *L. monocytogenes* 4b (ATCC 13932) suşu inokule edildi. OI işlemi, paslanmaz çelik elektrotlar, K-tipi termocupl, datalogger ve 0-250 V, 10 amper, AC akım sağlayan güç kaynağı kullanılarak oluşturulan laboratuvar tipi pilot ünitede gerçekleştirildi. Patojen ilave edilmiş süt örnekleri OI işlemiyle 62 °C'ye kadar ısıtıldı, ardından steril enjektör yardımıyla örnekler alınıp yayma plak yöntemiyle ekimler yapıldı. Elde edilen sonuçlar varyans analizi ile değerlendirildi. Sonuç olarak *L. monocytogenes*' in inaktivasyon oranının ohmik ısıtma işleminin süresine, protein konsantrasyonuna ve uygulanan voltaj gradientine bağlı olduğu görüldü.

Anahtar Kelimeler: İnaktivasyon, *Listeria monocytogenes*, Ohmik Isıtma, Protein tozu, Süt,

ABSTRACT

Listeria monocytogenes is one of the most important food pathogens causing foodborne diseases. Pasteurization process may cause some negativities in the aroma and nutritional properties of the milk product while the inactivation of pathogenic microorganisms and enzymes. Research in recent years has focused on innovative technologies that provide pathogen inactivation without damaging the structural properties of foods. Ohmic heating, one of these innovative technologies, provides massive and rapid heating, providing an effective microbial inactivation. The aim of this study was to determine the effects of ohmic heating (OI) treatment at different electric field strengths on *L. monocytogenes* inactivation in protein added milk. For this purpose; 2.5%, 5% and 7.5% protein powder were added to the 200 ml 1.5% fat-milk into glass jars, then pasteurized by autoclaving at 80 °C for 15 minutes. *L. monocytogenes* 4b (ATCC 13932) strain was inoculated (0.5%) into the samples. OI process was carried out in a laboratory pilot unit using

stainless steel electrodes, K-type thermocouple, datalogger and power supply providing 0-250 V, 10 A, AC current. Pathogen-added milk samples were heated up to 62 °C, then samples were taken with the sterile injectors and spreaded on the Oxford agar plates. Obtained results were evaluated by analysis of variance. As a result, it was seen that the inactivation rate of *L. monocytogenes* depended on the ohmic heating time, protein concentration and applied voltage gradient.

Keywords: İnactivation, *Listeria monocytogenes*, Ohmic Heating, Milk, Protein Powder

*Bu çalışma Burdur Mehmet Akif Ersoy Üniversitesi Bilimsel Araştırma Projeleri Komisyonunca desteklenmiştir. Proje Numarası: 0812-YL-22/2017K12-41003

EFFECT OF DIFFERENT DISTANCE METRICS ON CLUSTERING OF GEOGRAPHIC POINTS

Merhad Ay[1]

[1]Erciyes University, Faculty of Engineering, Industrial Engineering Department, Kayseri, Turkiye

[1]ORCID ID: https://orcid.org/0000-0002-6892-7924

Lale Ozbakir[2]

[2]Erciyes University, Faculty of Engineering, Industrial Engineering Department, Kayseri, Turkiye

[2]ORCID ID: https://orcid.org/0000-0002-8103-7715

ABSTRACT

Clustering algorithms usually make distance measurements on the attributes of the points and label the closest (similar) points with the same cluster tag. The most widely used clustering algorithm is the K-means algorithm. In the literature, Euclidean distance is frequently used as the distance metric in the K-means algorithm. In addition, there are distance metrics such as Manhattan, Minkowski, Haversine which are rarely used in clustering studies. In this study, the effects of the Earth's geoid structure on the clustering quality are investigated while clustering geographic points. In the study, the Vincenty distance metric which gives the closest value to the distance between two points considering the shape of the Earth, and the Euclidean distance metric which calculates the distance on a plane, are used as the distance metrics in the K-means algorithm. Using these distance metrics, 69765 demand points in a city are clustered according to various cluster numbers (k=3, 4, 5, 6, 7, 8, 9, 10, 15, 20 and 50) with the K-means algorithm. There are various performance measures in the literature to measure clustering performance. These performance criteria are calculated by considering the distances between the elements and the clusters generated. Davies-Bouldin and Silhouette performance criteria are used to measure clustering quality in the study. The Davies-Bouldin criterion considers the distances of the elements within the cluster from the cluster center and the distances between the clusters. The Silhouette performance criterion determines the suitability of all cluster elements by focusing on their distances from the elements in the same cluster. Performance results showed that there is no significant performance difference between clustering studies using Euclidean or Vincenty distance metrics in small areas such as cities. When the quality of the clusters formed by both distance metrics are examined, it is determined that they are of similar quality.

Keywords: K-means, Vincenty, Euclidean, Clustering.

INTEGRATION OF BIG & STREAMING DATA TECHNOLOGIES AND AN APPLICATION

Merhad Ay

Erciyes University, Faculty of Engineering, Industrial Engineering Department, Kayseri, Turkiye

ORCID ID: https://orcid.org/0000-0002-6892-7924

ABSTRACT

Data volume and sizes have increased with the developments in technology and the big data notion has become important nowadays. In addition, the dynamic processing, storage, analysis, and interpretation of hundreds of streaming data from different sources are important for the competition and fast decisions. In this sense, technology companies such as Apache, Facebook and Google have shifted their investments to big and streaming data technologies. In this study, technologies related to reliable storage of streaming data, processing and analysis of big data are investigated and an application is employed with temporal-spatial data on their integration with each other. Apache Kafka, Zookeepers and Spark Streaming modules are used together in the applied study. Kafka is an open-source technology offered by Apache company in the sense that data from multiple sources can be stored reliably and accessed at any time without any data confusion. To use Kafka system, a resource management system is needed, and Apache company Zookeeper resource management system is used in this regard. Metadata of Kafka servers, data headers and snippets are kept under record by the Zookeeper. On the other hand, Spark Streaming technology is used to process and analyze the streaming data. As a result, it is concluded that such open-source technologies can be used by integrating into real life applications and are effective in making fast and accurate decisions for companies.

Keywords: Big data, streaming data, data mining, integrated systems.

INDUCTION OF ENZYMATIC BROWNING IN BANANA PEELS BY PULSED ELECTRIC FIELD

Manazza Ayub[1]

[1]Erciyes University, Engineering, Department of Food Engineering, Kayseri, Turkey.

[1]ORCID ID: https://orcid.org/ 0000-0002-4994-8367

Dr. Mustafa Fincan[2]

[2] Erciyes University, Engineering, Department of Food Engineering, Kayseri, Turkey.

[2]ORCID ID: https://orcid.org/ 0000-0002-9394-6449

ABSTRACT

The induction of enzymatic browning in banana peel tissue by the pulsed electric field (PEF) was studied using a computer vision system (CVS) and an electrical conductivity-based disintegration index. Banana peel slices were subjected to the 15µs-pulses at the electric field strength of 3.3 kV/cm by varying pulse numbers and pulse repetition rates (PRR); a series of RGB images were captured over 180 minutes and converted to L*a*b* images. The degree of browning was evaluated visually and quantitatively by driving browning index (BI) from L* images and associated with disintegration index (DI).

PEF induced a rapid brown discoloration, almost completed within 60 min after the treatment. The level and uniformity of browning across tissue were influenced by the change in PRR and pulse number and showed a relationship with DI. Among the variables, decrease in PRR produced most notable changes in terms of browning and energy utilization. The decrease in PRR from 1Hz to 0.1Hz in the 5 trains of pulses provided the highest increase in BI (from 44.3 ±12.78 to 71.68±5.5) with a small DI increase (from 42.88±0.43 to 46.34±2.29). Moreover, energy consumption required to achieve near-total browning could be achieved by reducing the frequency from 1 Hz to 0.1 Hz in the 15 trains of pulses. With the decrease in PRR, the tissue tended to become more uniformly brown suggesting an increase in electrophoretic effect at low PRRs. The results have further implied that PEF could be utilized as an energy-efficient alternative for inducing desirable enzymatic browning in various other plant tissue processing, such as in manufacturing black tea, black olive, and brown sun-dried apricot, locally known as Gün Kurusu.

Keywords: Pulsed electric field, Enzymatic browning, Banana peel, Computer Vision

EL BOMBA TAPALARI İÇİN BARİYER MEKANİZMASI GELİŞTİRİLMESİ

DEVELOPING A BARRIER MECHANISM FOR HAND GRENADE FUZES

Serhad YILDIZ [1]

[1]Kırıkkale Üniversitesi, Fen Bilimleri Enstitüsü, Savunma Teknolojileri Anabilim Dalı, Kırıkkale, Türkiye.

[1]ORCID ID: https://orcid.org/0000-0002-8697-4329

Zühtü Onur PEHLİVANLI[2]

[2]Kırıkkale Üniversitesi, Mühendislik Fakültesi, Metalurji ve Malzeme Mühendisliği Bölümü, Kırıkkale, Türkiye.

[2]ORCID ID: https://orcid.org/0000-0002-3094-5174

ÖZET

El bombaları, kurşun bazlı birincil piroteknik bileşenlerden (kurşun azid, kurşun stifnat) oluşmaktadır. Herhangi bir nedenle piroteknik bileşenlerden birisi istemeden etkinleştirilirse, el bombası kaçınılmaz olarak patlayabilmektedir. İstenmeyen bir patlama ölümcül yaralanmalara neden olabilmektedir. Tek veya kapalı bir depolama alanında çok sayıda el bombası depolanırsa ve el bombası istemeden patlarsa, tüm depolama alanı patlayabilir ve büyük hasara neden olabilmektedir. Yapılan çalışma, el bombası tapalarının şok dalgaları, ısı vb. etkilerle istemdışı patlamalarını önlemek için patlayıcı zincirde bir bariyer mekanizmasının geliştirilmesi ile ilgilidir. Birincil patlayıcı aktif olsa bile patlayıcı zincirinin kesilmesi büyük önem taşımaktadır. Bu tasarımla, birincil patlayıcının kasıtsız olarak başlatılmasıyla patlayıcı zinciri başlatma potansiyeli ortadan kaldırılmıştır. El bombası tapalarında istenmeyen patlamaları önlemek için iki farklı bariyer mekanizmaları geliştirilmiştir. Yapılan çalışmada bu mekanizmaların güvenilirliği ve işlevselliği incelenmiştir. Yeni geliştirilen bariyer mekanizmalarının emniyetli durumda primer patlayıcıdan gelen enerjiyi gecikmeli eczaya ulaştırmaması, emniyetsiz durumda ise enerjiyi gecikmeli eczaya aktarması gerekmektedir. Elde edilen deneysel sonuçlar karşılaştırılarak iki sistemin farklılıkları ve istem dışı patlamaları önleme potansiyelleri belirlenmiştir. Bariyer mekanizması-1 ve bariyer mekanizması-2'den oluşan el bombası tapalarına fonksiyon yapma (4.0-5.1 saniye) ve fonksiyon yapmama testleri uygulanmıştır. Bariyer mekanizması-1 ile yapılan testlerde başarılı sonuçlar elde edilmiştir. Ayrıca maliyet, işçilik, üretim, test edilebilirlik, montaj kolaylığı, operasyon sırasında hızlı ve kolay kullanım, depolama ve lojistik ortamlarına uyumluluk açısından bariyer mekanizması-1 modeli uygun olarak değerlendirilmiştir.

Anahtar Kelimeler: Tapa, El bombası, Emniyet, Bariyer mekanizması, Mühimmat.

ABSTRACT

Hand grenades consist of lead-based primary pyrotechnic components (lead azide, lead styfnate). If for some reason one of the pyrotechnic components is unintentionally activated, the hand grenade can inevitably explode. An unintentional explosion can cause fatal injuries. If a large number of grenades are stored in a single or enclosed storage area and the grenade detonates unintentionally, the entire storage area can explode and cause extensive damage. The work done showed that the grenade fuzes were exposed to shock waves, heat, etc. It concerns the development of a barrier mechanism in the explosive chain to prevent involuntary detonations with impacts. Even if the primary detonator is active, it is of great importance to cut the detonator chain. With this design, the potential to start the detonator chain by inadvertent initiation of the primary detonator is eliminated. Two different barrier mechanisms have been developed to prevent unwanted explosions in hand grenade fuzes. In this study, the reliability and functionality of these mechanisms were examined. The newly developed barrier mechanisms should not transmit the energy from the primary

explosive to the delayed detonator in a safe state, and transfer the energy to the delayed detonator in an unsafe state. By comparing the experimental results obtained, the differences of the two systems and their potential to prevent unintentional explosions were determined. Functioning (4.0-5.1 seconds) and non-functioning tests were applied to the grenade fuzes consisting of barrier mechanism-1 and barrier mechanism-2. Successful results were obtained in the tests performed with the barrier mechanism-1. In addition, the barrier mechanism-1 model was evaluated in terms of cost, workmanship, production, testability, ease of assembly, fast and easy use during operation, and compatibility with storage and logistics environments.

Keywords: Fuze, hand grenade, safety, barrier mechanism, ammunition.

Giriş

El bombası, bir insan tarafından yaklaşık 40 metreye kadar fırlatılabilen, içi infilak maddesi veya kimyasal maddelerle dolu olan ve bu maddeleri harekete geçiren, ateşleme tertibatını ihtiva eden küçük bir bomba türüdür. Genellikle savunma, taarruz, sis, göz yaşartıcı ve eğitim maksadıyla kullanılmaktadır.

Tüm mühimmatlarda olduğu gibi el bombalarında da; ateşleme zincirini başlatan ve aynı zamanda patlamanın istenilen zamandan ve konumdan önce gerçeklememesi için gerekli güvenlik özelliklerini barındıran mekanizma tapalardır. El bombalarındaki tapa düzeneği; tapa gövdesi, tapa gövdesine yerleştirilmiş bir patlayıcı zinciri ve tapa gövdesine kurma yayı ile dönebilir şekilde tutturulmuş bir ateşleme çekici, kabze ve çekme pimi içerir. Tapa tasarımları, el bombasının patlama tehlikesi alanının dışına atılmasını sağlamak için patlamanın başlamasından itibaren bir gecikme süresini sağlamalıdır. Bu süre geleneksel el bomba tapalarında piroteknik veya mekanik bir geciktirme elemanı tarafından sağlanmaktadır. Üretim aşamasından kullanım noktasına kadar, el bombası tapası çeşitli dinamik ve ataletsel girdiler yaşayacaktır. Ataletsel girdiler, örneğin, fabrikada üretime yüklenen yükler, muayene, paketleme, yük yüklemesi, nakliye, depolama ve lojistik dağıtımından kaynaklanan darbeler ve bir dizi titreşim girdisini içerir. Tapa tüm bu girdileri ve bunların kombinasyonlarını reddetmek üzere tasarlanmıştır. Tapa tasarımları, el bombasının patlama tehlikesi alanının dışına atılmasını sağlamak için patlamanın başlamasından itibaren bir gecikme süresini sağlamalıdır El bombaları tipik olarak patlayıcı veya kimyasal bir dolgu maddesi içeren plastik, kompozit, metal v.b. içerir.

El bombaları tapalarında genel olarak; gövde, patlayıcı (gecikmeli ve hassas), iğne mekanizması, kabze, kabzeyi gövdeye sabitleyen çekme halkası ve çekme pimi bulunur. Çekme halkası tapa gövdesinden ayrıldığında, el bombasının ateşlenmesini önlemenin tek yolu, kullanıcının kabzeyi tutmasıdır. Çünkü çekme pimi çıkarıldıktan sonra kabzenin küçük bir miktar bile farkında olmadan (Bu, kullanıcının bilgisi olmadan meydana gelebileceğinden, el bombası hala kullanıcının elindeyken veya bir kıyafet ürününe bağlıyken çalışabilir) serbest bırakılması, yay yüklü iğne mekanizmasının patlayıcı zincirini başlatmasına neden olur. Kabze bırakıldığında, el bombası ateşlenme süreci başlar ve el bombası kısa süre sonra patlar. Böyle bir olasılık, kullanıcı ve kullanıcının yakın çevresinde yer alan tüm unsurlar için telafisi mümkün olmayacak düzeyde ağır sonuçlar doğurur. Ayrıca çekme halkasının yanlışlıkla bir nesneye takılması ve el bombasından ayrılması da mümkündür. Bu nedenle el bombalarındaki güvenliği sağlamak için tapa mekanizmalarını gerekli güvenlik mekanizmalarını sağlaması gerekmektedir.

Farklı el bombası sistemleri ve güvenlik mekanizmalarına ilişkin bazı çalışmaların yapılarak özellikle patent çalışmaları ile sunulduğu ve tescillendiği görülmektedir [1-13]. Campagnuolo ve ark. [1] tarafından yeni bir el bombası tasarlanmıştır ve bu el bombası çift güvenlik özelliğine sahiptir. Sibum [2] konvansiyonel bomba tapalarına göre istemdışı aktivasyona karşı daha iyi güvenlik sağlayan uygun maliyetli bir el bombası tapası geliştirirek çalışmasını patent ile tescillemiştir. Knight ve ark. [3] tarafından ise el bombalarının güvenliği için elektromekanik tapa geliştirilerek tescillenmiştir. Yeni geliştirilen elektromekanik tapa güvenilirlik ve güvenlik için birbiriyle ilişkili mekanik ve elektronik güvenlik mantığını içermektedir. Bu tapa bir manyeto vurucu jeneratörü, kabze, çekme halkası, elektronik ünite ve mikro elektromekanik sistemli güvenlik ve kurma mekanizması MEMS (S&A) den oluşacak şekilde tasarlanmıştır. Dirubbio ve ark. [4] tarafından Amerikan menşeli M213 Bomba tapasının güvenlik sorunlarını önlemek amacıyla çalışmalar yapılmıştır. Campagnuolo ve ark. [5] tarafından yapılan çalışmalarda birincil patlayıcının kasıtsız olarak başlatılmasıyla patlayıcı zinciri başlatma potansiyeli ortadan kaldırılmıştır. Anjangwon [6] tarafından K413 el bomba tapa

üzerinde bazı tasarımlar yapılmıştır. Yeni tasarlanan el bomba tapa gövdesine, içindeki basıncı ölçebilen bir basınç göstergesi eklenmiştir. Bu sayede el bomba kullanıcının elindeyken primerin aktif olup olmadığı görülebilmektedir. Lauch [7] tarafından yapılan çalışmanın amacı, kullanıcı tarafından el bombasının ilk durumunu gösteren bir araç sağlamaktır. Bu sayede kullanıcı, el bombası primerinin devreye girip girmediğini ve dolayısıyla tapanın çalışıp çalışmadığını kolaylıkla gözlemleyebilmektedir. Veksler [8] tarafından yapılan çalışma, el bombası tapalarının şok dalgaları, ısı parçaları vb. nedenlerle istemdışı olarak patlamasını önlemek için patlayıcı zincirinde bir bariyer mekanizmasının geliştirilmesi ile ilgilidir. Hakala ve ark. [9] tarafından yapılan çalışma, çift güvenlik anahtarlı el bombası klapesi hakkındadır. Geleneksel el bombaları tek güvenliğe sahiptir. Bu güvenlik çekme pimi ile sağlanmaktadır. Bu pim bir kez dışarı çekildikten sonra tekrar takılamaz. Çünkü çekme piminin yapısı bozulmaktadır. Ancak yeni geliştirilen çift emniyet sistemli emniyet şalterleri tekrar tekrar çevrilerek emniyetsiz hale getirilebilmektedir. Dubno ve ark. [10] tarafından gelişmiş bir el bombası güvenlik mekanizması tasarlanmıştır. Amaç, ateşleme mekanizmasının kazara serbest kalmasını önlemek için el bombası için bir güvenlik mekanizması sağlamaktır. Padula [11] tarafından kamalı pimi sabitleyen özellik, mevcut el bombası tasarımına dahil edilmiştir. Yeni tasarımı ile kopilyanın kazara geri çekilmesi riskinin pratik olarak ortadan kaldırıldığı bir yapı sunulmuştur. Halsnes ve ark. [12] tarafından el bombaları için, emniyetin devre dışı bırakılmasının kolayca tersine çevrilebileceği basit bir emniyet mekanizması tasarlanmıştır. Kaiponen ve ark. [13] tarafından taşıma süresi boyunca çekme halkasını el bombası üzerine sabitlemek için bir mekanizma tasarlanmıştır. Campagnuolo ve ark. [14] tarafından M67 ve ASM Bombalarında kullanılan M228 ve M213 tapalarında M55 detonatörü yerine ikincil patlayıcı PBXN-5 kullanılmıştır. Böylece Kurşun azid ve kurşun stefenat miktarı azaltılmıştır. Ayrıca bu el bombalarında ana patlayıcı COMP-B yerine PBXN-109 duyarsız patlayıcılar kullanılmıştır. Bu değişikliklerle birlikte tapaların güvenliği artırılmıştır. Fowler [15] tarafından yapılan çalışmada tapalar patlayıcı içerdiğinden, mühimmatın atış anına kadar depolama ve nakliye durumlarında güvenli olması gerektiği, herhangi bir yanlış kullanım durumunda personele ve çevresine zarar vermemesi ve tapa tasarımı yapılırken bunların dikkate alınması gerektiği ortaya konulmuştur. El bombası tapaları ile ilgili birçok yaralanmalı ve ölümlü kaza yaşanmıştır [16-25]. Son yıllarda Türkiye'de el bombası tapaları ile ilgili kazalar rapor edilmiştir.

Literatürde yapılan çalışmalar ışığında, el bombası tapalarında kullanılan piroteknik unsurlar silahlı kuvvetlerde büyük endişelere yol açmaktadır. Bu nedenle bu tapalar patlamaya karşı çok hassastır. El bomba tapaları için farklı şekillerde ek güvenlik sistemlerinin geliştirilmesi gerekliliği ortaya çıkmaktadır. Bu kapsamda yeni tasarlanan tapaya bariyer mekanizmaları eklenmiştir. Bu mekanizmalar kullanıcı tarafından etkinleştirildikten sonra el bombası çalışmaya hazır hale gelmektedir.

Materyal ve Metot

El bombası tapasında patlayıcı zinciri; birincil kapsülü patlatmak için ateşleme çekici, geciktirici eczayı yakmak için detonatör ve son olarak da güçlendiricinin patlaması şeklindedir. Birincil detonatör istemdışı patlarsa, mevcut sistemde (Şekil 1) patlayıcı zincirini kesecek bir yapı olmadığı için patlama meydana gelecektir. Bu nedenle, Şekil 2 ve Şekil 3'teki bariyer mekanizması-1 (BM1) ve bariyer mekanizması-2 (BM2), el bombasının tapasını daha güvenli hale getirmek ve istemdışı patlamaları (patlayıcı zinciri kesmek) önlemek için tasarlanmıştır. Bu tasarımlar ile birincil patlayıcının istemdışı olarak devreye girmesiyle patlayıcı zincirini başlatma potansiyeli ortadan kaldırılmıştır.

Şekil 1. Mevcut el bomba tapası ve bileşenleri

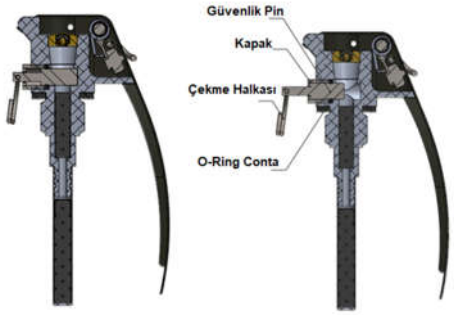

Şekil 2. BM1el bombası tapasının emniyetli (sol) ve emniyetsiz (sağ) kesit görünümü

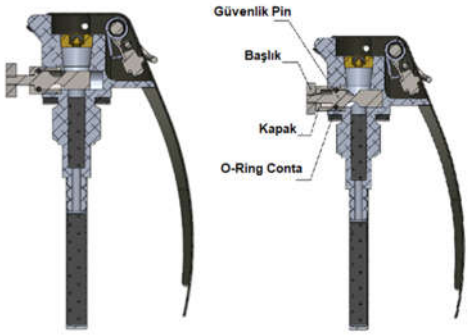

Şekil 3. BM2 el bombası tapasının emniyetli (sol) ve emniyetsiz (sağ) kesit görünümü

Yapılan Testler

Yeni geliştirilen bariyer mekanizmaları, birincil patlayıcıdan gelen enerjiyi güvenli bir durumda geciktirmeli elemana iletmemeli ve enerjiyi emniyetsiz durumda geciktirmeli elemana aktaracak şekilde tasarlanmıştır. Tasarım doğruluğunu belirlemek ve ürünün kullanılabilirliğini test etmek amacıyla geliştirilen her iki mekanizma da ölçüsel ve görsel testler, fonksiyon yapma ve fonksiyon yapmama testlerine tabi tutulmuşlardır. Her bir test için beş farklı numune test edilerek ortalama sonuçları alınmış ve değerlendirilmiştir.

Ölçüsel ve Görsel Kontrol

BM1 ve BM2'den oluşan el bombası tapasının tüm parçaları ölçü aleti ve mastar ile ölçülerek boyutsal olarak kontrol edilmiştir. Boyut kontrolünde kullanılan tüm mastar ve ölçü aletlerinin kalibrayonu yapılmıştır.

Fonksiyon Yapma Testi

Fonksiyon yapma testleri için bariyer mekanizması kullanıcı tarafından güvenli konumdan güvenli olmayan konuma getirilir. Emniyet mandalı çıkarılır ve tapa sütre arkasından fırlatılır. Detonatörün gecikmeli elemanı yaktığı görülecektir. Tapalar için standart fonksiyon yapma süresi 4.0-5.1 saniyedir. Bu süre aralığında aktive olan mekanizmalara fonksiyon yapmış olarak kabul edilmektedir. Geçikme süresi ölçümleri Şekil 4'de görülen dijital ölçüm cihazında yapılmıştır.

Fonksiyon Yapmama Testi

Fonksiyon yapmama testinde bariyer mekanizması güvenli bir konumdadır. Emniyet mandalı çıkarılır ve tapa sütre arkasından fırlatılır. Detonatörün gecikmeli elemanı yakmadığı görülmelidir.

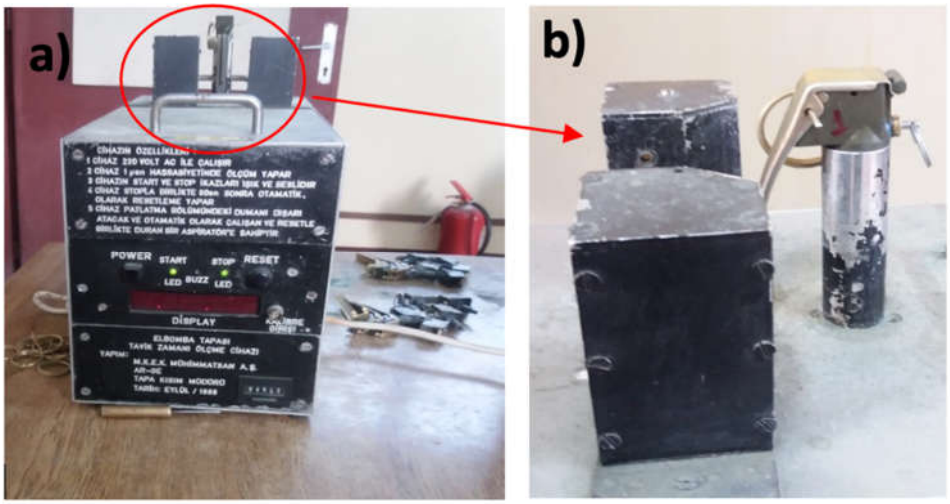

Şekil 4. a) El bombası tapa gecikme süresi ölçüm cihazı, b) El bombası tapasının ölçü cihazına bağlanması

Tartışma ve Sonuç

BM1 ve BM2'den oluşan el bomba tapalarına fonksiyon yapma (4.0-5.1 saniye) ve fonksiyon yapmama testleri uygulanmıştır. Fonksiyon yapma test sonuçları Şekil 5'de fonksiyon yapmama test sonuçları ise Tablo 2'de verilmiştir.

Fonksiyon yapması için mekanizmaların 4.0 ile 5.1 saniye aralığında aktif olması gerekmektedir ve Şekil 5'de verilen test sonuçlarına göre BM1 mekanizmasına ait tüm numunelerin bu zaman aralığında fonksiyon yaptıkları görülmektedir. BM2 mekanizmasına ait numunelerin sadece bir tanesinin istenilen zaman aralığında fonksiyon gerçekleştirdiği ancak diğer tüm numunelerin fonksiyon sürelerinin arttığı görülmektedir (Şekil 5).

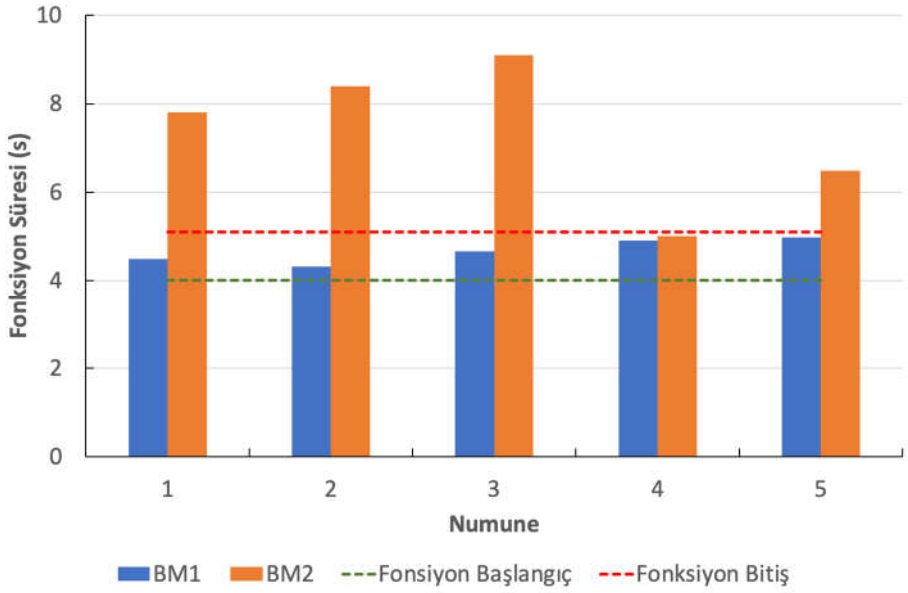

Şekil 5. BM1 ve BM2 mekanizmalarının fonksiyon süreleri grafiği

BM1 ve BM2 mekanizmalarına fonksiyon yapma testlerinden sonra fonksiyon yapmama testleri uygulanmış ve elde edilen sonuçlar Tablo 2'de verilmiştir. BM1 mekanizmasındaki numunlerin tamamının fonsyion yapmadığı görüldü (Tablıo 2). Ancak BM2 mekanizmasına ait numunelerin bir numune hariç fonksiyon

yaptıkları görüldü. BM1 ve BM2 mekanizmaları fonksiyon yapma açısında karşılaştırılarak BM2 mekanizmasının uygun olduğu belirlendir.

Tablo 2. BM1 ve BM2 mekanizmalarının fonksiyon yapmama testi sonuçları

Numune	Fonksiyon Durumu	Numune	Fonksiyon Durumu
BM1-1	-	BM2-1	√
BM1-2	-	BM2-2	√
BM1-3	-	BM2-3	-
BM1-4	-	BM2-4	√
BM1-5	-	BM2-5	√

√ : Fonksiyon yaptı, - : Fonksiyon yapmadı

Tartışma

Askeri açıdan son derece kritik olan mühimmat tapalarında emniyet ve güvenlik büyük önem taşımaktadır. Bu çalışmada, geleneksel el bombası tapalarına göre, istemdışı patlamaya karşı daha iyi güvenlik sağlayan, uygun maliyetli bir el bombası tapasının geliştirilmesi amaçlanmıştır.

- BM1 ve BM2'den oluşan el bombası tapalarına fonksiyon yapma (4.0-5.1 saniye) ve fonksiyon yapmama testleri uygulanmıştır.
- BM2 fonksiyon yapma testinde 4 adet numune 4.0-5.1 saniye aralığının dışında fonksiyon yapmıştır. Ayrıca fonksiyon yapmama testinde 4 adet numune fonksiyon yapmıştır. Bu sebeplerden BM2'den uygun sonuçlar alınamamıştır.
- Maliyet, işçilik, üretim, test edilebilirlik, montaj kolaylığı, operasyon sırasında hızlı ve kolay kullanım, depolama ve lojistik ortamlarına uyumluluk ve test sonuçlarına göre BM1 başarılı olarak değerlendirilmiştir.

Kaynaklar

[1] Campagnuolo C.J., Andrews W. J. (2017). Dual Safety Fuze For Grenade, Patent No: US 9,638,503 B1.
[2] Sibum K. (2013). Hand Grenade Fuse, Patent No: US 8.408,134 B2.
[3] Knight R., Wood R., Hoang T., Barham O. (2014). Electro-Mechanical Fuze For Hand Grenade, Patent No: US 8,887.640 B1
[4] Dirubbio V., Galinski E. (1990). Safety Fuze For A Hand Grenade, Patent No: US 4,926,752.
[5] Campagnuolo C.J., Gonsalves V., Andrews W. J., Kotevski N. (2014). Flying Primer For Hand Grenade Fuze, Patent No: US 8,857,341 B1.
[6] Anjang W. (2018). Safety device of a hand grenade fuse, Patent No: KR20180031093A.
[7] Lauch R. (2018). Hand grenade with an explosive train initiation indicator, Patent No: US 10,024,641 B1.
[8] Veksler Isar. (2012). Grenade mechanism, Patent No: WO 2012/080998 Al.
[9] Hakala A., Harju O. (2018). Hand grenade tube for hand grenade, Patent No: FI127331B.
[10] Dubno R. C., Dubno A. M. (1975). Hand Grenade Wıth Safety Mechanısm, Patent No: 3,865,027.
[11] Padula W. V. (1972). Hand Grenade Safety Lock Pull Rıng Assembly, Patent No: 3,765,337.
[12] Halsnes O., Wulvik E. (1999). Safety pin for hand grenades, Patent No: EP 1 094 293 A1.
[13] Kaiponen R. T., Liimatainen H. (1987). A hand-grenade pin, Patent No: EP0215160B1.
[14] Campagnuolo C.J., Gonsalves V., Andrews W. J. (2009). Insensitive Munition Solutions for Anti-Structure Munition Grenade. 53rd Annual Fuze Conference May 19-21, 2009.
[15] Fowler S. E. Safety and Arming Device Design Principles, Naval Air Warfare Center Weapons Division, China Lake, CA, 1999
[16] https://www.haberler.com/elazig-da-el-bombasi-kazasi-4-sehit-haberi/.Erişim tarihi: 27.08.2021

[17] https://www.milliyet.com.tr/gundem/tunceli-de-operasyonda-el-bombasi-kazasi-2-uzman-cavus-yarali-1148434. Erişim tarihi: 28.08.2021
[18] https://www.haberler.com/el-bombasi-patladi-1-sehit-haberi/. Erişim tarihi: 21.08.2021
[19] https://www.hurriyet.com.tr/gundem/cephanelikte-patlama-25-sehit-21390973. Erişim tarihi: 17.07.2021
[20] https://www.hurriyet.com.tr/gundem/hakkaride-askeri-birlikte-el-bombasi-patladi-5-yarali-40004152. Erişim tarihi: 31.08.2021
[21] https://www.aa.com.tr/tr/turkiye/hakkaride-mevzide-el-bombasi-patladi-1-asker-sehit/661128#!. Erişim tarihi: 03.09.2021
[22] https://www.elazigsonhaber.com/gundem/el-bombasi-kazaen-patladi-h11114.html.Erişim tarihi: 12.09.2021
[23] https://www.haberler.com/el-bombasi-kazaen-patladi-1-sehit-2-yarali-10383678-haberi/ Erişim tarihi: 26.08.2021
[24] https://www.aa.com.tr/tr/turkiye/agrida-kazara-el-bombasi-patladi-1-sehit-2-yarali/1197579. Erişim tarihi: 27.08.2021
[25] http://beyazgazete.com/haber/2020/1/16/hakkari-de-egitim-kazasinda-sehit-olan-askerler-icin-toren-duzenlendi-5409728.html. Erişim tarihi: 27.08.2021

HAVAN TAPALARI İLE İLGİLİ OLASI KAZALARI ÖNLEMEK İÇİN YENİ GÜVENLİK SİSTEMLERİNİN GELİŞTİRİLMESİ

POSSIBLE ACCIDENTS RELATED TO MORTAR FUZES DEVELOPMENT OF NEW SAFETY SYSTEMS FOR PREVENTION

Serhad YILDIZ [1]

[1]Kırıkkale Üniversitesi, Fen Bilimleri Enstitüsü, Savunma Teknolojileri Anabilim Dalı, Kırıkkale, Türkiye.

[1]ORCID ID: https://orcid.org/0000-0002-8697-4329

Zühtü Onur PEHLİVANLI[2]

[2]Kırıkkale Üniversitesi, Mühendislik Fakültesi, Metalurji ve Malzeme Mühendisliği Bölümü, Kırıkkale, Türkiye.

[2]ORCID ID: https://orcid.org/0000-0002-3094-5174

ÖZET

Havan mühimmatları zorlu muharebe alanlarında en çok tüketilen mühimmatlardan birisidir. Bu mühimmatların yoğun kullanımı kazara patlama risklerini de beraberinde getirmektedir. Bu çalışmada; havan mühimmat tapalarındaki güvenlik eksikliklerini gidererek kullanımdan önce düşme, nakliye veya üretim sırasındaki hatalar nedeniyle oluşabilecek patlamaların ve kayıpların önlenmesi amacıyla yeni bir üst gövde ataşleme pim sistemi tasarlanmıştır. Yeni tasarlanan üst gövde ateşleme pim sistemi için test numuneleri hazırlanarak, tapanın emniyetli olup olmadığını ve genel olarak ivmelenme sırasında ortaya çıkabilecek kararlı haldeki eylemsizlik yüklerine karşı malzeme güvenilirliğinin, bütünlüğünün ve performansının nasıl etkilendiğini belirlemek amacıyla, kurulma süresi, G kuvveti ve düşürme testlerine tabi tutulmuştur. Yapılan testler sonucunda yeni tasarlanan havan üst gövde ateşleme pim sistemi, en az 1000 G eksenel ivme kuvveti ile namluda devreye alınmış ve ateşleme pim sistemi, mühimmat namluyu terk ettikten sonra serbest bırakılmıştır ve bu sayede namluda patlama olasılığı ortadan kaldırılmıştır. Kurulma süresi testlerinde ise numunelerdeki eksenden kaçık durumda bulunan rotorun kurulma süresi testinde en az 0,8 saniye sonra patlayıcı zinciri eksenine geldiği görülmüştür. Yapılan düşürme testlerinde de mevcut sistemin 4 metre yükseklikte güvensiz konuma geçerek patlarken yeni tasarlanan sistemin 9 metre yükseklikten düşmesi durumunda dahi aktif olmadığı ve patlamanın gerçekleşmediği tespit edilmiştir. Yapılan testler ve elde edilen bulgular sonucunda yeni geliştirlen güvenlik sistemini mevcut havan tapalarına ve yeni tapa tasarımlarına entegre edilerek, havan tapa sistemlerinin daha güvenilir hale getirilebileceği görülmüştür.

Anahtar Kelimeler: Mümimmat, Tapa, Güvenlik Kurma Mekanizması, Ateşleme Pim Sistemi

ABSTRACT

Mortar ammunition is one of the most consumed ammunition in difficult combat areas. Intensive use of these ammunition brings with it the risk of accidental explosion. In this study; A new upper body attachment firing pin system has been designed in order to eliminate the safety deficiencies in mortar ammunition fuzes and to prevent explosions and losses that may occur due to falling before use, errors during transportation or production. Test samples were prepared for the newly designed upper body firing pin system and subjected to arming time, G-force and drop tests to determine whether the fuze is safe and how the material reliability, integrity and performance are generally affected against steady-state inertial loads that may occur during acceleration. As a result of the tests, the newly designed mortar upper body firing pin system was activated in the barrel with an axial acceleration force of at least 1000 G, and the firing pin system was released after the ammunition left the barrel, thus eliminating the possibility of explosion in the barrel. In the arming time

tests, it was observed that the rotor, which was out of axis in the samples, came to the axis of the explosive chain after at least 0.8 seconds in the arming time test. In the drop tests, it was determined that while the existing system went into an unsafe state at a height of 4 meters and exploded, the newly designed system was not active even if it fell from a height of 9 meters and the explosion did not occur. As a result of the tests and findings, it has been seen that the newly developed security system can be made more reliable by integrating the existing mortar fuzes and new fuze designs.

Keywords: Ammunition, Fuze, Safety Arming Mechanism, Firing Pin System

Giriş

Havan mühimmatı, genellikle, fırlatıldıktan sonra aktif olan ve hedef etkiye tepki olarak ateş eden bir tapa tertibatı ile donatılmıştır. Ateşlemeden önce veya hemen sonra kazaları önlemek ve güvenliği artırmak için, birçok havan topu tapası, fırlatma sırasında ve önceden tanımlanmış bir gecikmeden sonra uygulanan gerileme kuvvetlerine tepki veren bir safety and arming (S&A) mekanizması içerir. Bu S&A mekanizması gerekli güvenliği sağlamaktadır. Ancak tapanın burnunda bulunan ateşleme iğnesi, ateşleme sırasında gerileme kuvvetinin etkisiyle ters yönde hareket etmektedir. Bu sırada S&A mekanizması kurulu olursa veya istenen gecikme süresinden çok daha kısa sürede kurulum olursa patlama meydana gelmektedir. Bu nedenle, güvenlik önlemlerinin dezavantajlarının üstesinden gelen başka bir güvenlik mekanizmasının sağlanması avantajlı olacaktır. Havan mühimmat tapalarına ikincil güvenlik eklemek hem istemsiz patlamayı hem de arızayı önemli ölçüde azaltan gelişmiş bir güvenlik cihazı sağlamaktadır.

Alon [1] tarafından yeni tasarlanan güvenlik tertibatı, S&A mekanizmasını kilitleyerek kurulmasını engellemektedir. Ayrıca daha güvenilir bir montaj sağlamaktadır. S&A mekanizmasının çalışabilmesi için öncelikle mevcut atalet pimlerinin geri çekilmesi, ikinci olarak ise ateşleme iğnesinin hareketini engelleyen bilyanın (gövde ile ateşleme iğnesi arasındaki kilitleme cihazı) serbest bırakılması gerekmektedir. Perrin [2] tarafından DM111S ve DM183 havan tapalarına ikinci bir güvenlik eklemek için bir çalışma yapılmıştır. Tapanın burnuna türbin yapısı eklenmiştir. Bu sayede kuyruk dengeli (havada dönmeyen) mühimmatın burun kısmı uçuş sırasında oluşturulan hava akımı ile döndürülerek bir santrifüj etkisi yaratılmıştır. Rotor üzerindeki emniyeti ortadan kaldırmak için atalet kuvvetine ek olarak merkezkaç kuvvetine de ihtiyaç duyulmaktadır ve gerekli olan santrifüj yaklaşık 7000 RPM'dir. Ziemba [3] tarafından 20 mm M56 Yüksek Patlayıcı Ateşli mühimmatta kullanılan M505A3 tapası için geliştirilen klips mekanizmaları, tapanın kurulumunu geciktirerek, mühimmatın personel ve teçhizat güvenliği için silah sisteminden çıktıktan sonra belirli bir mesafeye kadar patlamasını engellemiştir [3]. Will ve ark. [4] tarafından mekanik uçak bomba tapalarındaki pervanenin yüksek basınca dayanamadığı kanıtlanmıştır, bu nedenle bomba yüksek hızlı bir uçaktan fırlatıldığında istenilen etkiyi bırakamamaktadır. Bu dezavantajın üstesinden gelmek için yeni geliştirilmiş bir elektrik kontrol sistemli tapa tasarlanmıştır. Campagnuolo ve ark. [5] tarafından yapılan çalışmalarda M67 ve ASM el bombalarında kullanılan M228 ve M213 tapaları çok miktarda kurşun bazlı birincil patlayıcı içerdiğinden, bu tapaların oldukça hassas olduğu belirtilmiştir. Bu tapalarda M55 detonatörler kullanılmaktadır. Bu detonatörde kullanılan birincil patlayıcı yerine ikincil patlayıcı PBXN-5 kullanılmıştır. Böylece kurşun azid ve kurşun stefenat miktarı azaltılmıştır. Ayrıca ana patlayıcı COMP-B yerine PBXN-109 duyarsız patlayıcı kullanılmıştır. Bu değişikliklerle birlikte tapaların güvenliği artırılmıştır. Geaney ve ark. [6,7] 30 mm M789 Yüksek Patlayıcılı Çift Amaçlı (HEDP) mühimmatta kullanılan M759 tapasının yumuşak hedeflerde (kum, toprak v.b.) daha etkili fonksiyon yapmasını geliştirmek için tapa üzerinde bazı değişiklikler yapmışlardır. Gregorio ve ark. [8] tarafından M751 tapasında güvenilirlik ve tek emniyet gibi olumsuzlukların giderilmesi ve MIL-STD-1316'daki güvenlik gereksinimlerinin karşılanması için çalışmalar yapılmıştır.

Kroon ve ark. [9] tarafından yayınlanan raporda 2016 yılında Kidal/Mali'de Hollanda'ya ait Airmobile Brigade havan birliğinde 60 mm havan eğitim atışı yapılırken havan mühimmatı namlu içinde patlamıştır. Bu kazada 2 asker ölmüş ve 1 asker ağır yaralanmıştır. Bu kaza en ince detaylarına kadar incelenerek rapor (TNO 2016 R11512) olarak yayınlanmıştır ve raporda erken patlamanın, tapa için uygun olmayan sıcaklık-nem koşulları ve tapa "güvenli" pozisyondayken detonatör-yemleme şarjı arasındaki bariyer diskinin işlevini yerine getiremediği için meydana geldiği ortaya konulmuştur. Bahsedilen bu kazanın yanı sıra, son yıllarda dünyanın çeşitli yerlerinde havan tapası kaynaklı birçok kaza [10-16] yaşanmıştır. Lee ve ark. [17] tarafından yapılan çalışmalarda havan mühimmatlarının hedefe burun üzeri temas etmemesi (örneğin, ağaç dallarının

veya benzerlerinin yavaşlaması nedeniyle mühimmatın dengesini kaybetmesi, bataklık gibi yumuşak bir yüzey nedeniyle tapa burun kısmının çökmemesi veya mühimmatın kuyruk stabil kanadının anormalliği nedeniyle yan üzeri düşmesi durumunda) tapanın çalışmaması veya burun kısmının arızalanmasına neden olduğu belirtilmektedir. Bu sebepten yeni bir tapa geliştirilmiştir. Yeni sistem mevcut çarpmalı yapıya göre daha kesin bir şekilde patlamayı mümkün kılmaktadır. Garber [18] tarafından 40 mm'lik bombaatar mühimmat tapasına mekanik otomatik intihar mekanizması dahil edilerek patlamamış mühimmat sayısı azaltılmış ve böylece çevre güvenliği artırılmıştır.

Jeonga ve ark. [19] tarafından topçu mühimmat tapalarında kullanılmak üzere gecikmeli kurmalı minyatür bir mekanik SAD (Güvenlik ve Kurma Cihazı) geliştirilmiştir. Zhijian ve ark. [20] tarafından MEMS düzlemsel zikzak yuvası, orta ve büyük kalibreli mühimmat tapaları için tasarlanmıştır. Bu tasarım, düşme etkisi ivmesi ile yumuşak atış ivmesi arasında ayrım yapabilmektedir. Tapanın fırlatma ortamında güvenilir bir şekilde etkinleştirilebilmesi ve nakliye sırasında güvenli bir şekilde korunması sağlanmıştır.

İncelenen çalışmalarında tapaların istenilen zaman ve mekân dışında patlamalarını önlemek, taşıma ve depolama durumlarındaki güvenliklerini de arttırmak amacıyla çok farklı çalışmaların yapıldığı görülmektedir. Ancak mevcut yapılan çalışma ve geliştirmelere rağmen hala bazı tapa sistemlerinin hala yeterli güvenlik sistemlerine sahip olmadığı bilinmektedir. Bunlarda birtanesi de havan mühimmatlarında kullanılan tapa sistemleridir. Havan tapa sistemlerinin taşıma esnasında ve mühimmatın havan içersinde patlamalarını önlemek güvenlik mekanizmalarını arttırmak amacıyla bu çalışma başlatılmış ve kuyruk dengeli havan mühimmatında kullanılan havan tapasının burun kısmı güçlendirilerek yeniden tasarlanmıştır. Tasarlanan yeni sistem ile tapalı mühimmatların taşıma sırasında ve havan sistemi içeridinde kaza sonucu patlamalarını önleyecek ilave bir güvenlik sistemine sahip yeni mühimmat tapası geliştirilmiştir.

Materyal ve Metot

Çalışmada incelenen mevcut ve yeni tasarlanan havan tapası Şekil 1.a-b'de gösterilmiştir. Mevcut havan tapasının iğne sisteminin hareketini kısıtlayacak herhangi bir emniyet yer almamaktadır. Ancak yeni tasarlanan üst gövde iğne sistemi emniyetli hale getirilmiştir. Bu emniyet namlu çıkışında eksenel ivme kuvvetinin sonlanmasıyla aktif olmaktadır. Mevcut havan tapasında bulunan iğne sistemi, atış esnasında merminin aldığı ivmenin etkisiyle atış yönünün ters istikametine doğru geri çekilmektedir. Bu sırada eğer tapanın güvenlik kurma mekanizması kurulu ise iğne detonatöre çarpmakta ve infilak gerçekleşmektedir (Şekil 2.b). Yeni tasarlanan üst gövde de ise bu ihtimal bertaraf edilmiştir (Şekil 3).

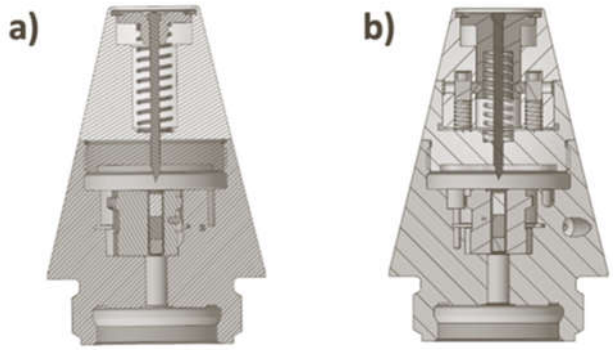

Şekil 1. a) Mevcut iğne sistemli havan tapası, b) Yeni ateşleme sistemli havan tapası

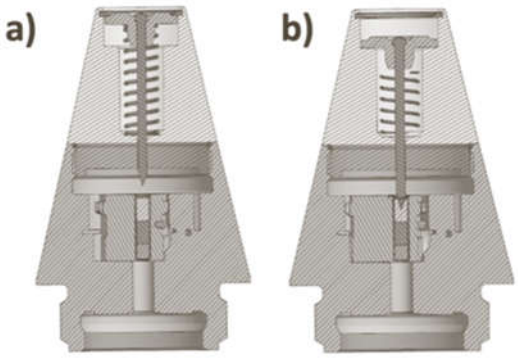

Şekil 2. Mevcut üst gövdenin a) Atış öncesi ve b) Atış anı kesit görüntüleri

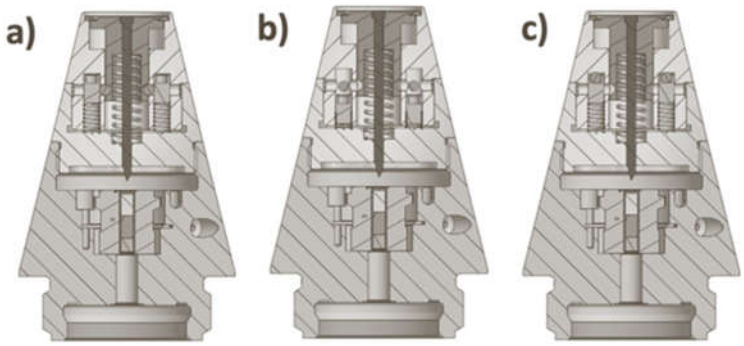

Şekil 3. Yeni havan tapasının a) Atış öncesi, b) Atış anı >1000 G ve c) Namlu çıkışı kesit görüntüleri

Tapa ateşlemesi sırasında mühimmatın ters yönü arka atalet kuvvetine maruz kalmaktadır. Bu atalet kuvveti, yeni tasarlanan üst gövdenin güvensiz hale gelmesi için gereklidir. Atalet kuvveti (G kuvveti) değeri, 60, 81 ve 120 mm havan mühimmatının yaklaşık sıfır barutla çalışabileceği bir değerin (en az 1200G) altında olmalıdır. Bu nedenle yeni tasarlanan üst gövde max.1000G'de kurulacak şekilde tasarlanmıştır. Bu atalet kuvveti değerini doğrulamak için bazı testler yapılmıştır. Öncelikle yeni tasarlanan üst gövdenin parçaları mastar ve ölçüm cihazı ile %100 olarak kontrol edilmiştir. Daha sonra test numuneleri hazırlanarak alt gövde testleri, üst gövde testleri ve tapa komplesi testleri olmak üzere üç ana başlıkta testlere tabi tutulmuştur. Bu testlerin uygulama metodolojileri farklı olmakla beraber, her üçü de tapanın emniyetli olup olmadığını ve genel olarak ivmelenme sırasında ortaya çıkabilecek kararlı haldeki eylemsizlik yüklerine karşı malzeme güvenilirliğinin, bütünlüğünün ve performansının nasıl etkilendiğini belirlemek amacıyla yapılmıştır.

Kurulma Süresi Testi

Hazırlanan alt gövde kompleleri öncelikle ölçüsel ve görsel olarak (mühimmat arayüz vidasının mastar kontrolü, yükseklik kontrolü, kötü işçilik belirtileri vb.), ardından kurulma süresi test cihazıyı yardımıylada kurulma süresi belirlenmiştir (Şekil 4).

Şekil 4. Kurulma süresi test cihazı

G Kuvveti Testi

Tapa içerisindeki iğne sisteminin atış sırasında namlu içinde maruz kaldığı eksenel ivmelenme hareketini görebilmek amacıyla G kuvveti testine tabi tutulmuşlardır. G testi yapılırken iki adet üst gövde karşılıklı olarak Şekil 5'de gösterilen G tezgâhına, yataklama aparatı kullanılarak yatay şekilde, üst gövde burun kısmı iç tarafa bakacak şekilde yerleştirilmiştir. Daha sonra cihaz çalıştırılarak numunelerin G kuvvetleri belirlenmiştir.

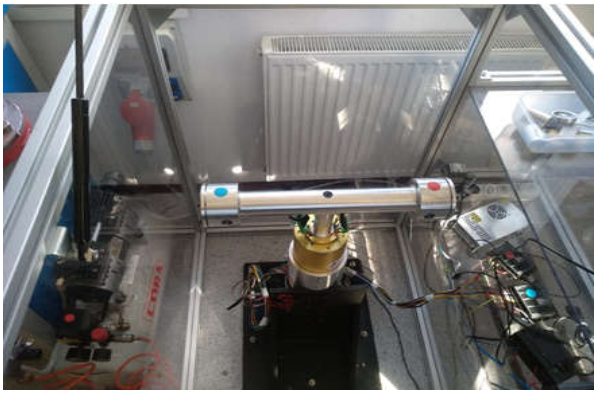

Şekil 5. G kuvveti testlerinin yapıldığı G test cihazı

Düşürme Testi

Alt gövde ve üst gövde testlerine tabi tutulan numuneler daha sonra düşürme testlerine tabi tutulmuştur. Düşürme testinde tapalar 6 kg'lık mermi ağırlığını temsil eden bir aparat üzerine ve tapa dibi üzerine düşecek şekilde monte edilerek 40 mm kalınlıktaki çelik levha üzerine düşürülmüştür. Düşürme işleminde tapa numuneleri standarta uygun olarak 3-9 metre arasındaki bir yükseklilerden düşürme testine maruz bırakılmıştır. Düşürme testi sonrasında tapa kontrol edilerek sistemin aktive olup olmadığı gözle muayene ile belirlenmiştir.

Sonuç ve Tartışma

Kurulma Zamanı Test Sonuçları

Alt gövdenin testlerinde tüm numunelerin ölçüsel ve görsel olarak uygun olduğu ve tüm numunelerdeki eksenden kaçık durumda bulunan rotorun kurulma süresi testinden en az 0,8 saniye sonra patlayıcı zinciri eksenine geldiği görülmüştür (Şekil 6).

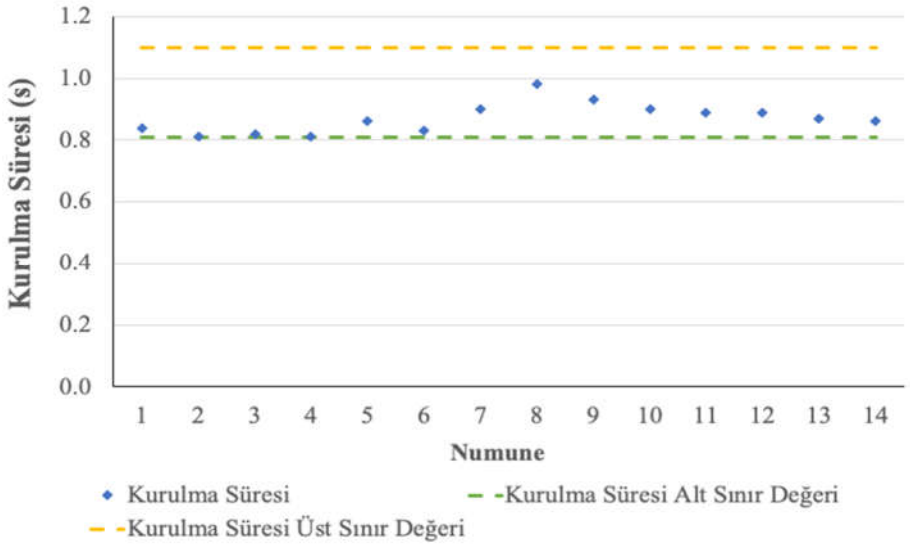

Şekil 6. Yeni tararlanan sisteme ait numunelerin kurulma süresi test sonuçları

Yeni tasarlanan güvenlik mekanizmalı tüm numuneler kurulma süresinin alt sınırı olan 0,8 saniye ile üst sınır olan 1,1 saniye zaman aralığı içerisinde aktive oldukları Şekil 6 da görülmektedir. Elde edilen test sonuçları yeni tasarlanan güvenlik mekanizmasının kurulma süresi açısında uygun olduğu ve kullanılabilirliği göstermiştir.

G Kuvveti Test Sonuçları

Üst gövde testlerinde tüm numunelerin ölçüsel ve görsel olarak uygun olduğu ve yeni ateşleme sistemli üst gövdenin emniyetsiz pozisyona geçtiği G değeri yay tansiyon cihazından faydalanılarak ve G testi yapılarak yaklaşık 1000 G olarak bulunmuştur. Ayrıca mevcut havan tapa üst gövdesi de G testine maruz bırakılmıştır. Mevcut iğnenin 1000 G ivme ile geri çekildiği Şekil 7'de detonatör ile aynı mesafeye yerleştirilen mukavvanın delinmesinden görülmektedir. Mukavva GKM içerisinde yer alan detonatörü temsil etmektedir. Tapa komplesi testlerinde tüm numunelerin ölçüsel ve görsel olarak uygun olduğu, düşürme testi uygulandıktan sonra; mevcut üst gövdeli tapalarda, iğnenin detonatörleri patlattığı ancak tasarlanan üst gövdeli tapalarda iğnenin detonatörle hiçbir şekilde temas etmediği, tapanın emniyetli olduğu gözlemlenmiştir.

Test sonuçlarında da anlaşıldığı gibi yeni tasarım ateşleme sistemli üst gövdenin en az 1000 G eksenel ivme kuvvetiyle kurulumunun başladığı ve eksenel ivme bittikten sonra (namlu çıkış) kurulumunu tamamladığı için, hiçbir durumda namlu içinde aktive olmadığı görülmüştür. Ancak mevcut havan tapasının üst gövdesinin atış anında 1000 G eksenel ivme kuvvetiyle namlu içinde aktif bir şekilde geri çekildiği görülmüştür. Bu sebepten namlu içinde ateşleme iğnesinin patlayıcı zincirinin ilk halkası olan detonatörün patlamasını önlemek, güvenlik açısından hayati öneme sahip olacaktır. Çünkü kuyruk dengeli havan tapasında bulunan ateşleme iğnesi, atış esnasında merminin aldığı ivmenin etkisiyle atış yönünün ters istikametine doğru geri çekilmektedir. Tapanın alt gövde içerisinde yer alan güvenlik ve kurma mekanizması eğer kurulu ise (yani rotorda bulunan detonatör patlayıcı zinciri ile aynı eksene gelmişse) iğne detonatöre çarpar ve infilak gerçekleşir. Yapılan bu çalışmalar neticesinde, sisteme eklenen ilave emniyet mekanizmasının bu durumu ortadan kaldırdığı yapılan testlerle kanıtlanmıştır.

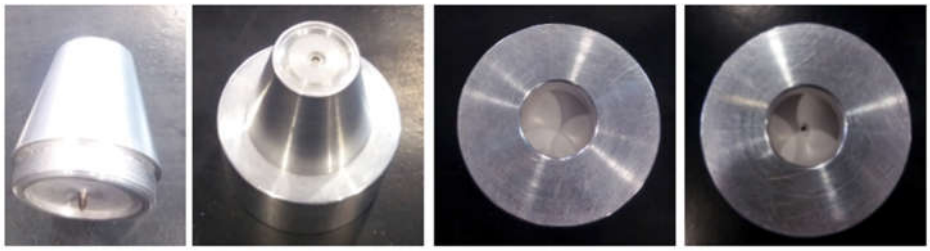

Şekil 7. Mevcut üst gövde mekanizmasının G testi sonuç görüntüleri

Düşürme Test Sonuçları

Düşürme testi uygulanan mevcut ve yeni sisteme ait numunelerin test sonuçları Tablo 1'de gösterilmiştir. 3 - 9 m yüksekliklerden düşürme testleri uygulandıktan sonra; mevcut üst gövdeli tapalarda, iğnenin detonatörleri patlattığı ancak yeni tasarlanan üst gövdeli tapalarda iğnenin detonatörle hiçbir şekilde temas etmediği, tapanın emniyetli olduğu gözlemlenmiştir. Mevcut sistem sadece 3m yükseklikte için patlatma yapmamıştır.

Tablo 1. Düşürme testi sonuçları

Düşürme Yüksekliği (m)	Yeni Sisteme Numuneleri	Mevcut Sistem Numuneleri
3	√	√
4	√	x
5	√	x
6	√	x
7	√	x
8	√	x
9	√	x

√ : Patlamadı, x : Patladı

Tartışma

Askerî açıdan son derece kritik olan mühimmat tapalarında güvenlik ve emniyet büyük önem arz etmektedir. Bu sebepten havan tapalarının istemsiz olarak fonksiyon yapmasından kaynaklanabilecek can kayıpları ve maddi hasarları engellemek amacıyla tapa sistemlerine ilave güvenlik mekanizması tasarlanmıştır. Mühimmat tapalarında, her türlü olumsuz senaryoda silah sisteminin ve personelin emniyette kalmasını sağlayan güvenlik kurma mekanizması bulunmaktadır. Özellikle bu mekanizmanın, havan tapasında kazara devreye girmesi halinde, mühimmatın namlu içinde patlamasına neden olacağı değerlendirilmiştir. Bu nedenle yeni tasarlanan üst gövde ateşleme pimi sistemi, atış sırasında namluda en az 1000 G eksenel ivme kuvveti ile kuruluma başlaması ve namludan çıktıktan sonra kurulumu tamamlaması nedeniyle namlu içinde mühimmatın patlaması önlenmiştir. Bu durum yapılan G ve düşürme testleriyle kanıtlanmıştır. Düşürme testlerinde güvenlik kurma mekanizması kurulu yeni ateşleme sistemli tapa ile mevcut ateşleme sistemli tapa kıyaslanmıştır. Mevcut tapanın 4-9 metre aralığında patladığı ancak yeni tapanın 4-9 metre aralığında patlamadığı görülmüştür. Bu çalışma neticesinde mevcut havan tapalarına ve yeni tapa tasarımlarına bu güvenlik sisteminin entegre edilmesi tapaya ikincil emniyet kazandıracaktır. Ayrıca bu emniyet sayesinde tapanın dünyada ve ülkemizdeki günümüz teknolojisi olan otomatik yüklemeli silah sistemleriyle entegre kullanımı sağlanmıştır.

Kaynaklar

Alon H. (2015). Safety Assembly For An Ammunition Fuze, Patent No: EP 2 943 740 B1.

Perrin M. (2017). Junghans Defence New Generation Fuzes to İmprove Munition Efficiency, Parari 2017, Canberra.

Ziemba R. T. (1993). Arming Delay, Dual Environment Safe, Füze, Patent No: US 5,243,912.

Will A.S., Renato B., Bufler N.C. (1961). Bomb Füze, Patent No: US 2,981,190.

Campagnuolo C.J., Gonsalves V., Andrews W. J. (2009). Insensitive Munition Solutions for Anti-Structure Munition Grenade. 53rd Annual Fuze Conference May 19-21, 2009.

Geaney J., Schwartz B., Recchia S. (2009). Fuze Technology Integration (FTI) Improved 30 mm. NDIA Fuze Conference Orlando, Florida May 19-21, 2009

Geaney J. (2010). Fuze Technology Integration (FTI) Improved 30 mm - The Fuzing Evolution-Smaller, Smarter, and Safer. 54rd Annual Fuze Conference, Kansas City, Missouri USA 11-12 May 2010.

Gregorio M., Mogendovich E. (2007). Universal Dual Safe Training Fuze For Mortars. 51st NDIA Fuze Conference, Nashville, USA May 22-24, 2007

Kroon E. J., Bouma R.H.B., Hooijmeijer P.A. (2016). Mortar exercise accident Mali: General technical research questions regarding the debris, Dutch Safety Board, Report TNO R11512, 2016.

Karppinen T., Valonen K. (2005). Mortar Accident at the Rovajärvi Shooting Zone, Report B3/2005Y, 2005.

Https://www.staradvertiser.com/2010/12/01/hawaii-news/misfired-mortar-not-defective-juryfinds/

Https://www.dailymail.co.uk/news/article-2296569/Pictured-Seven-US-Marines-killed-tragiclive-training-exercise-Nevada.html

14-Https://www.theguardian.com/us-news/2017/may/03/us-army-photographer-hilda-claytonphoto-death. Erişim tarihi: 13.06.2021

Http://en.protothema.gr/three-soldiers-killed-at-volos-greece-by-mortar-shell-blast/ Erişim tarihi: 14.05.2021

Https://www.unian.info/society/10178507-mortar-blast-at-training-ground-ukroboronprom-saysno-alternative-in-ukraine-to-molot-model.html. Erişim tarihi: 12.06.2021

Https://www.haberturk.com/sirnak-haberleri/16920461-sirnakta-havan-topu-atisi-sirasinda Patlama. Erişim tarihi: 12.06.2021

Lee K., Kim B.S., Choi Y. (2016). Shell Fuse Has A Firing Pin Which İs Operated By The Change Of İnertia On İmpact, Patent No: KR101666216B1.

Garber K. (2014). Self-destruction mechanism for a fuze, Patent No:WO2014106565A1

Jeonga J., Eoma J., Leea S., Limb D. W., Jang Y., Seo K. W., Choi S., Leec C. J., Ohd J. S., Miniature Mechanical Safety And Arming Device With Runaway Escapement Arming Delay Mechanism For Artillery Fuze, Sensors and Actuators 279 (2018), pp. 518-524

Zhijian Z., Weirong N., Xiaofeng W., Zhanwen X. Study on Parameters of MEMS Planar Zigzag Slot for Fuze. Key Engineering Materials Vols. 609-610 (2014) pp 813-818.

FARKLI ÜRETİM PARAMETRELERİNDEKİ 308L KAPLAMALARIN KAVİTASYON EROZYONU DİRENÇLERİNİN İNCELENMESİ

INVESTIGATION OF CAVITATION EROSION RESISTANCE OF 308L COATINGS IN DIFFERENT PRODUCTION PARAMETERS

Fatih Nedim YORULMAZ

Manisa Celal Bayar Üniversitesi, Mühendislik Fakültesi, Metalurji ve Malzeme Mühendisliği Bölümü, Manisa, Türkiye.

ORCID ID: 0000-0003-1726-9965

Hülya DURMUŞ

Manisa Celal Bayar Üniversitesi, Mühendislik Fakültesi, Metalurji ve Malzeme Mühendisliği Bölümü, Manisa, Türkiye.

ORCID ID: 0000-0002-7270-562X

ÖZET

Östenitik paslanmaz çelikler pek çok sektörde uygulama alanı bulan çelik grubudur. Östenitik paslanmaz çelikleri, yapısında bulunan krom ve nikel elementleri sayesinde korozyona ve kavitasyon erozyonuna karşı dayanıklıdır. Yüzeylerinde bulunan çok ince krom oksit (Cr_2O_3) tabakası pasifleşerek oksidasyon, korozyon ve kavitasyon erozyonunun oluşumunu engellemektedir. Nikel miktarı %8' den fazla olduğunda östenit oda sıcaklığında kararlı duruma gelir ve bu yapı sayesinde östenitik paslanmaz çelik adını almaktadır. Östenitik paslanmaz çeliklerin süneklik özellikleri yüksektir ve haddelemeyle sertleştirilebilirler. Ayrıca kaynak işlemlerinde kullanılabilme özelliğine sahiptirler. Petrokimya, deniz yapılarında, nükleer ve arıtma tesisleri ve medikal ürünlerde östenitik paslanmaz çelikler kullanılmaktadır. Östenitik paslanmaz çelik grubunda yer alan 308L, yapısındaki östenit ve δ-ferrit taneler sayesinde yüksek korozyon direncine sahiptir. Korozyon direncinin yanı sıra kavitasyon erozyonuna karşı da direnç göstermektedir. Östenitik paslanmaz çelikler ilave tel olarak kullanılıp, TIG kaynağı ile kolayca kaplanmaktadır. TIG kaynağı, düşük ısı girdisi, düzgün kaynak dikişi ve yüksek kaliteli kaynak yapabilme özellikleri sayesinde östenitik paslanmaz çeliklerin kaplama olarak kullanılmasını sağlamaktadır. Östenitik paslanmaz çelik kaynak metallerinin mikro yapıları esas metalin mikroyapısından daha farklı bir mikroyapıya sahiptir. Kaynak tellerinin kullanımı kaynak metalinin iç yapısını değiştirebilir. Östenitik paslanmaz çeliklerin kaplama yapıldıktan sonra katılaşma başlayınca östenit ve δ-ferrit taneleri oluşmaktadır. Kaplamadan sonra oluşacak mikroyapı önceden tahmin etmek için Schaeffler diyagramı kullanılmaktadır. Bu diyagram sayesinde seyrelme, yapı içerisindeki δ-ferrit ve östenitik oranı tahmin edilmektedir. Östenitik paslanmaz parçalarının sıvı ortamında yaygın hasar kaynaklarından biri olan kavitasyon erozyonu (CE), yalnızca parçanın kullanım ömrünü azaltmakla kalmaz, aynı zamanda yeni sorunları beraberinde getirir. Kavitasyon erozyonu (CE), yüksek hızlı akışkana maruz kalan bileşenlerin yüzeyinde sıklıkla meydana gelen bir aşınma türüdür. Sıvı ortamında, negatif basınç bölgesinin varlığı, kavitasyon kabarcıklarının oluşumunu teşvik etmekte ve daha sonra, bu kabarcıklar yüksek basınç bölgesine ulaştıklarında patlamaktadır. Kavitasyon kabarcıklarının sürekli patlamasının, mikro jet ve şok dalgası ile döngüsel stres etkisi üretebileceği ve bu durum da kavitasyon erozyonuna sebep olmaktadır. Oluşan stres malzemelerin akma mukavemetini aştığında önemli plastik deformasyona neden olmaktadır. Ayrıca, gerilme malzemelerin çekme mukavemetinin sınırlarını aştığında, yüksek kavitasyon erozyonu hasarına dönüşebilecek olan tane sınırları veya kayma bantları etrafında bazı mikro çatlaklar oluşturmaktadır. Bu çalışmada, S235JR çelik altlık plakalar üzerine 308L östenitik paslanmaz çelik tel, TIG kaynağı ile 140 A ve 180 A akım kullanılarak üç paso şeklinde kaplama yapılmıştır. Kaplama işleminden sonra numuneler ASTM G-32 standartlarına uygun titreşimli ultrasonik kavitasyon erozyonu testi uygulanmıştır. Testten önce ve sonra numunelerin ağırlıkları hassas terazi ile ölçülmüştür.

Numunelerdeki kütle kaybı hesaplanmıştır. 1, 3, 5 saatteki kayıpları hesaplamak için oluşturulan altlık malzemede ve 308L kaplanmış numunelerde kavitasyon erozyonu karşılaştırılmıştır. Kavitasyon erozyonu testinin süresi arttıkça kavitasyon erozyonunun arttığı test öncesi ve sonrası yapılan stereo ve optik mikroskop incelemelerinde de gözlemlenmiştir.

Anahtar Kelimeler: Östenitik paslanmaz çelik, 308L, Kavitasyon erozyonu, Mikroyapı.

ABSTRACT

Austenitic stainless steels are a steel group that finds application in many sectors. Thanks to the chromium and nickel elements in the structure of austenitic stainless steels, it is resistant to corrosion and cavitation erosion. The very thin chromium oxide (Cr_2O_3) layer on their surface becomes passivated and prevents the formation of oxidation, corrosion and cavitation erosion. When the nickel content is more than 8%, austenite becomes stable at room temperature and thanks to this structure, it is called austenitic stainless steel. Austenitic stainless steels have high ductility and can be hardened by rolling. They also have the feature of being used in welding processes. Austenitic stainless steels are used in petrochemicals, marine structures, nuclear and refining plants, and medical products. 308L, which is in the austenitic stainless steel group, has high corrosion resistance thanks to the austenite and δ-ferrite grains in its structure. In addition to its corrosion resistance, it also resists cavitation erosion. Austenitic stainless steels are used as additional wires and are easily coated with TIG welding. TIG welding enables the use of austenitic stainless steels as coatings, thanks to its low heat input, smooth weld seam and high quality weldability. The microstructure of austenitic stainless steel weld metals has a different microstructure from the microstructure of the base metal. The use of welding wires can change the internal structure of the weld metal. Austenite and δ-ferrite grains are formed when solidification begins after coating of austenitic stainless steels. The Schaeffler diagram is used to predict the microstructure that will form after coating. With this diagram, the dilution, the ratio of δ-ferrite and austenitic in the structure are estimated. Cavitation erosion (CE), one of the common sources of damage in the liquid environment of austenitic stainless parts, not only reduces the service life of the part, but also introduces new problems. Cavitation erosion (CE) is a type of wear that often occurs on the surface of components exposed to high velocity fluid. In the liquid medium, the presence of the negative pressure zone promotes the formation of cavitation bubbles, which then burst when they reach the high pressure zone. Continuous bursting of cavitation bubbles can produce cyclic stress effect with micro jet and shock wave, which causes cavitation erosion. When the resulting stress exceeds the yield strength of the materials, it causes significant plastic deformation. Also, when the stress exceeds the limits of the tensile strength of the materials, it creates some microcracks around the grain boundaries or slip bands that can turn into high cavitation erosion damage. In this study, three-pass coating was applied on S235JR steel backing plates using 308L austenitic stainless steel wire, TIG welding with 140 A and 180 A current. After the coating process, vibratory ultrasonic cavitation erosion test was applied to the samples in accordance with ASTM G-32 standards. Before and after the test, the weights of the samples were measured with a precision balance. The mass loss in the samples was calculated. To calculate the losses in 1, 3, 5 hours, the cavitation erosion of the formed substrate and 308L coated samples were compared. As the duration of the cavitation test increased, it was also observed in the stereo and optical microscope examinations performed before and after the test that the cavitation erosion increased.

Keywords: Austenitic stainless steel, 308L, Cavitation erosion, Microstructure.

GİRİŞ

Östenitik paslanmaz çelikler, paslanmaz çeliklerin en yaygın kullanılan türüdür ve genel olarak 300 serisini kapsamaktadır. Yapılarının büyük bir kısmı krom ve nikel alaşım elementinden oluşması ile birlikte az miktarlarda molibden ve/veya mangan da içermektedir. Yapıdaki krom elementi sayesinde Cr_2O_3 (krom oksit) tabakası diğer adı ile pasivasyon tabakası oluşmaktadır. Bu tabaka korozyon ve kavitasyon erozyonuna karşı direnç sağlamaktadır (Türkan 2013; Yüksel 2001; Murat 2018; Gökmen 2009). Ayrıca az miktarda bulunan mangan kaynaklanma sırasında sıcak çatlak oluşumuna karşı direnç sağlamaktadır (Şahin 1990). Östenitik paslanmaz çelikler petrokimya, deniz yapılarında, nükleer ve arıtma tesisleri ve medikal ürünlerde kullanılmaktadır (Köse ve Kaçar 2014).

Östenitik paslanmaz çeliklerin 300 serisi içinde yer alan 308L östenitik paslanmaz çeliği, yapısında krom, nikel ve kısmen mangandan dolayı korozyon ve kavitasyon erozyonu direncine sahiptir. 308L yüksek kaynak kabiliyeti sayesinde kaynak ve kaplama işlemlerinde sıkça tercih edilmektedir. Kaynak yöntemi olarak birçok yönteme uygundur, fakat TIG iyi kaynak dikişi, kolay yapılabilirliği, her pozisyonda ve yüksek kaliteli kaynak yapabilme özellikleri sayesinde 308L için uygun kaynak dikişini kolayca sağlamaktadır (Murat 2018; Nevcanoğlu 2019).

TIG kaynağında gereken ısı, tükenmeyen tungsten bir elektrot ve iş parçası arasında oluşan ark tarafından sağlanmaktadır (Şekil 1). Nozülden gönderilen asal gaz (He ve/veya Ar) kaynak dikişinin etrafını tamamen korumaktadır. Bu yöntem endüstride sıkça tercih edilen bir kaynak yöntemdir (Durgutlu vd., 2005; Althouse vd., 1999). 308L kaynak teli ile yapılan kaplama işlemi sonucunda kaplama kısmında oluşan östenit içerisinde delta ferrit taneleri korozyon ve kavitasyon erozyonu direncinde düşme oluşturmamaktadır.

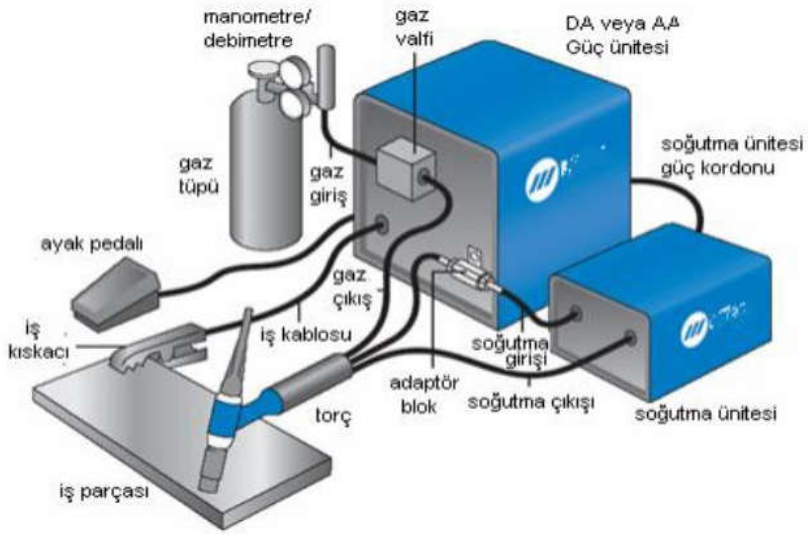

Şekil 1. TIG kaynağı cihazı (Metal Uzmanı 2022)

Kavitasyon (cavity) kelimesi, latince çukur, oyuk gibi anlamlara gelen "cavus" kelimesinden türemiştir (Basumatary 2017; Whitesides 2012). Kavitasyon erozyonu, içinden yüksek hızlı sıvının geçtiği pompa çarkları, hidrolik türbinler ve gemi pervaneleri gibi mühendislik bileşenlerinde sıklıkla meydana gelen tipik bir hasar şeklidir (Şekil 2). Östenitik paslanmaz çelik sıvı ortamda çalışan parçalarının en yaygın hasar biçimlerinden biri olan kavitasyon erozyonu (CE), yalnızca parçanın güvenilirliğini azaltmakla kalmaz, parçayı deformasyona uğrayarak kullanım ömrünü kısıtlamaktadır (Tian vd. 2022; Li vd. 2022).

Şekil 2. Gemi pervanesinin yüzeyinde oluşan kavitasyon erozyonu (Sampson 2008)

Sıvı ortamda, negatif basınç bölgesinin varlığı, kavitasyon kabarcıklarının oluşumunu sağlayacak ve daha sonra, bu kabarcıklar yüksek basınç bölgesine ulaştıklarında patlayacaklardır. Parçanın yüzeyinin yakınında meydana gelen kavitasyon kabarcıklarının lokalize döngüsel çökmeleri, malzeme kaybına neden olup bileşenlerin kapasitelerini düşürmektedir. Kraterler (oyuklar veya çukurlar) ve çatlaklar genellikle aşınmış yüzeyde bulunur, hasarlar büyük stres konsantrasyonlarına neden olmaktadır. Yüzeydeki stres konsantrasyonu, yorulma çatlağının kolayca çekirdeklenmesine ve yorulma ömrünün azalmasına neden olur. (Karimi ve Martin 1986; Stephens 2000; Schijve 2004; Gao ve Zhang 2022),

Kavitasyon erozyonuna olası etkilerini tespit edebilmek için kullanılan birçok test yöntemi vardır. Bu yöntemlerden yaygın olarak kullanılan ultrasonik titreşimli kavitasyon erozyonu testidir. Bu test ASTM G-32 standartlarında hazırlanmaktadır (Şekil 3). Bir sıvı içerisinde titreşimli bir uç yardımı ile test parçasına sürekli olarak kavitasyon baloncukları fırlatılır ve parçanın kavitasyona uğratılır (Şekil 4).

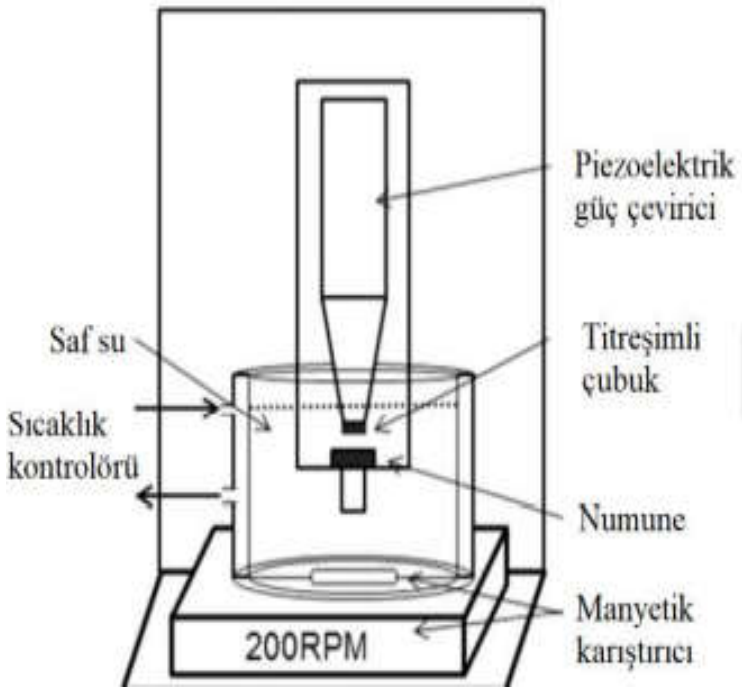

Şekil 3. ASTM G-32 standartlarında hazırlanan test düzeneği (Taillon vd. 2016)

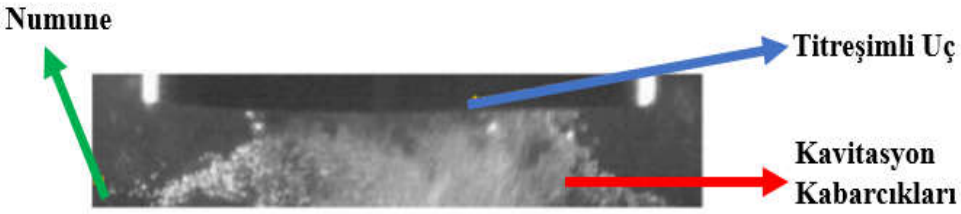

Şekil 4. Test sırasında oluşan kavitasyon kabarcıkları (Li vd. 2022)

Bu çalışmada, çelik altlıklar üzerine 308L östenitik paslanmaz çeliğinden kaplamaların kavitasyon erozyonu karşısındaki davranışları incelenmiştir. S235JR (St37) çelik üzerine 308L östenitik paslanmaz çelik TIG kaynağı ile üç farklı akımda ve üç paso şeklinde kaplanmıştır. Kaplama işleminden sonra ASTM G-32 standartlarında hazırlanan test düzeneğinde kavitasyon erozyonu testleri ve karakterizasyonları gerçekleştirilmiştir.

YÖNTEM

Altlık malzemesi olarak S235JR (St37) çeliği kullanılmıştır. Altlık üzerine farklı akımlar (140 A ve 180 A) ve 17 V voltaj kullanılarak TIG Kaynağı ile üç paso şeklinde 2 mm çapında 308L östenitik paslanmaz çelik teller ile kaplama yapılmıştır. Tablo 1 ve 2' de altlık ile kaplamanın kimyasal içeriği verilmiştir.

Tablo 1. 308L ve 316L paslanmaz çeliklerinin kimyasal içeriği (% ağ.)

	C	Cr	Ni	Mn	Mo	Si
308L	0,02	19	9	2,1	0,02	0,4

Tablo 2. Altlık malzemesinin kimyasal içeriği (ağ.)

	C	Mn	Cu	Al	Mo	Si	P	S
S235JR	0,16	0,4	0,03	0,04	0,03	0,016	0,05	0,017

Kaplama işleminden sonra oluşan parçaların şematik görüntüsü Şekil 5'de yer almaktadır; açık gri renk altlık malzemesi: S235JR çeliği, mavi renk 308L östenitik paslanmaz çelik kaplamaları göstermektedir. Oluşan numunelerin kodları Tablo 3'te verilmiştir.

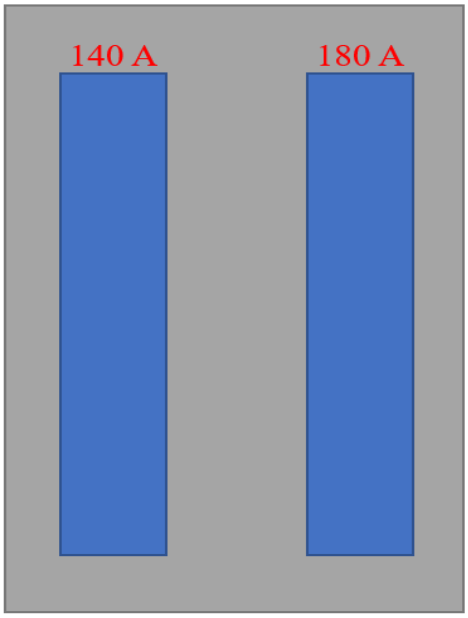

Şekil 5. 308L tel ile kaplama işlemi yapılan numunelerin şematik görünümü

Tablo 3. Numunelerin kodlanması

Numune kodu	Kaynak teli	Akım (A)	Gerilim (V)
84	308L	140	17
88	308L	180	17

Kaplama uygulanan parçalar ASTM G-32 standartlarına göre hazırlanmış olan titreşimli ultrasonik kavitasyon erozyonu cihazına uygun ölçülerde kesilmiştir (Şekil 6). Kesilen numunelere zımparalama ve parlatma işlemi uygulanmış ve teste hazır hale getirilmiştir. Test için uçtan uca genlik 50 ± 2 µm titreşim frekansı ise 20 kHz olarak ayarlanmıştır. Cihaza sabitlenen numuneler 2000 ml saf su ile dolu bir beher içerisine yerleştirilmiştir. Titreşimli uç ile numune arasından 0,5 mm mesafe ayarlanmıştır. Saf suyun sıcaklığı 25 ± 3 °C de tutulması için beher dışarısında soğutma işlemi yapılmıştır. Farklı test numuneleri kullanılarak testin süresi 1, 3 ve 5 saat olarak test uygulanmıştır.

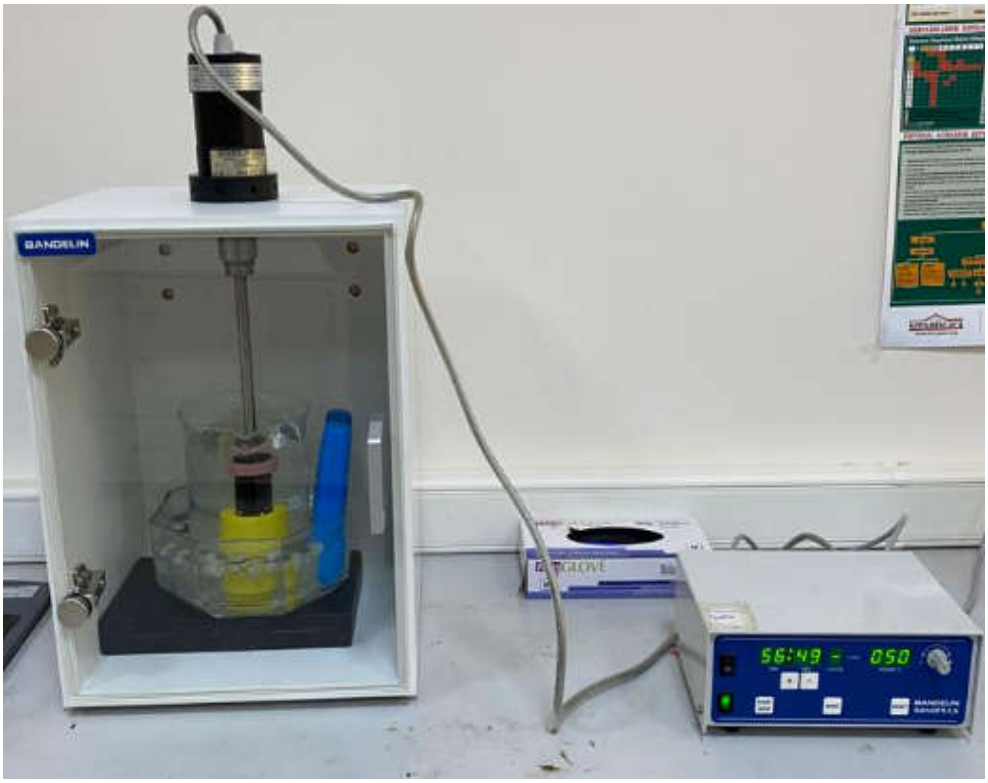

Şekil 6. Kavitasyon erozyonu test cihazı (ASTM G-32)

Numuneler test sonrasında kurutma için 60 °C de 24 saat etüvde bekletilmiştir. Testten önce ve sonra makro ve mikro görüntüleri sırasıyla stereo ve optik mikroskopla alınmıştır. Nikon marka Clemex yazılımlı 6,7 – 40x büyütmeli Stereo ve 50 - 1.000x Büyütmeli Optik Mikroskoplar kullanılarak incelenmiştir. Kümülatif kütle kaybının bulunması için numuneler testten önce ve sonra hassas terazi kullanılarak ağırlıkları ölçülmüştür.

BULGULAR ve TARTIŞMA

TIG kaynağı ile kaplama yapılan 308L kaynak telinin kaplamadan sonra soğuması sırasında yapıda östenit ve ferrit fazları oluşmuştur. Bu fazların yapı içerisinde oranına tahmin etmek için birçok yöntem bulunmaktadır. Bu yöntemlerden biri de Schaeffler Diyagramı yöntemidir. Bu diyagramda östenit fazı içerisinde ferrit miktarı tahmin edilmektedir. Ayrıca katılaşma modunu da tahmin edilmesine yardımcı olmaktadır.

Östenitik paslanmaz çeliklerin katılaşma modu dörde ayrılmaktadır; östenitik (A veya Ö), östenitik-ferritik veya birincil östenit (AF veya ÖF), ferritik-östenitik veya birincil ferritik (FA veya FÖ) ve ferritik (F) moddur. Bu çeliklerin katılaşma modlarında oluşan ferrit ve östenit dönüşümleri; Ö modda tam östenit, ÖF modunda östenit + östenitik ve ferrit, FÖ modda östenit + çıtasal (skeletal) ferrit ve östenit + levhalı ferrit ve son olarak F modunda östenit + iğnemsi ferrit ve ferrit + Widmanstatten östenit'ten oluşmaktadır (Tümer 2012; Rajani, vd. 2012; Lippold ve Kotecki 2005).

Schaeffler Diyagramı kullanılması için $Cr_{eş}$ ve $Ni_{eş}$ değerleri hesaplanmalıdır. Bu hesaplamalar Denklem (1) ve (2) ile yapılmaktadır (Türkan 2013).

$$Cr_{eş} = \%Cr + \%Mo + 1{,}5\%Si + 0{,}5\%Nb \quad (1)$$

$$Ni_{eş} = \%Ni + 30\%C + 0.5\%Mn \quad (2)$$

Bu denklemler kullanılarak hesaplanan $Cr_{eş}$ ve $Ni_{eş}$ değerleri hesaplanmıştır. Buna göre 308L için $Cr_{eş}$ değeri 19,62 ve $Ni_{eş}$ değeri ise 10,65' tir.

Hesaplanan bu değerler Schaeffler Diyagramında (Şekil 7) katılaşma modunu ve yüzde ferrit oranını göstermektedir. Katılaşma modu ferritik-östenitik veya birincil ferritik modudur. Bu modda östenit + çıtasal (skeletal) ferrit ve östenit + levhalı ferritler oluşmaktadır. Yüzde ferrit değeri ise diyagrama göre %9 olarak belirlenmiştir.

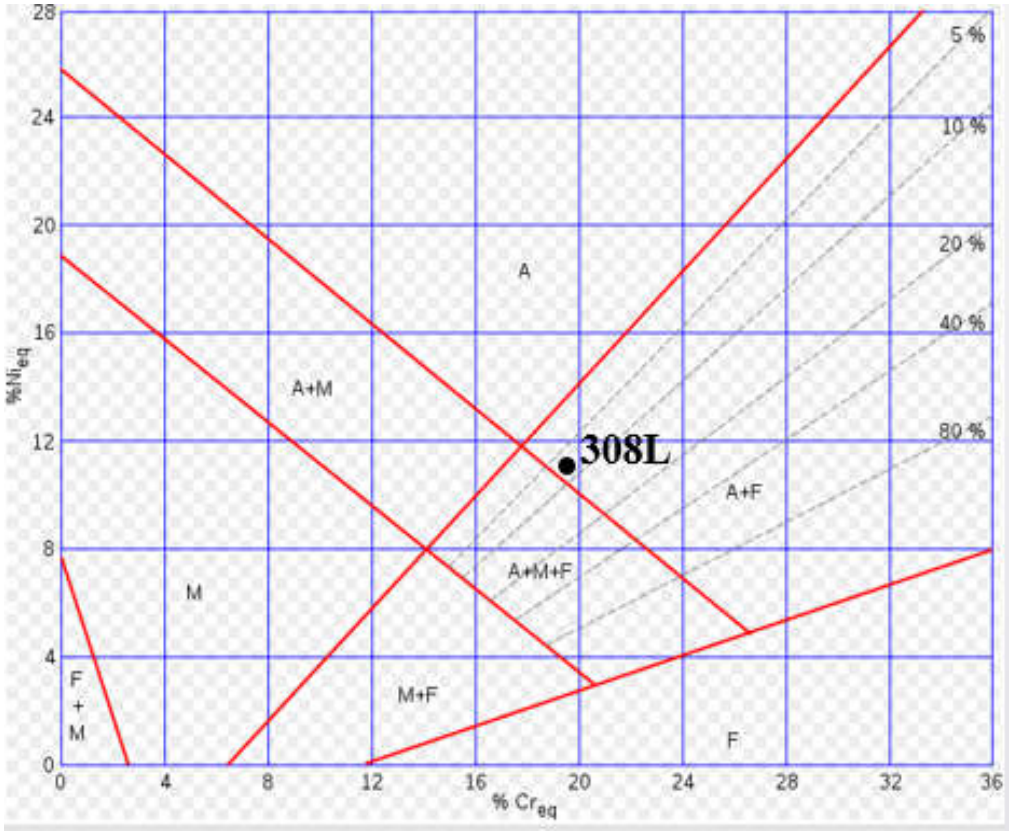

Şekil 7. Schaeffler Diyagramı (Wikimedia 2022)

Ultrasonik kavitasyon erozyonu testi uygulanan numunelere testin uygulanması için zımparalama işleminden sonra parlatma işlemi uygulanmıştır. Kavitasyon erozyonu testi uygulandıktan sonra numunelerin mikroyapı görüntüleri optik mikroskop yardımı ile alınmıştır (Şekil 8 ve 9).

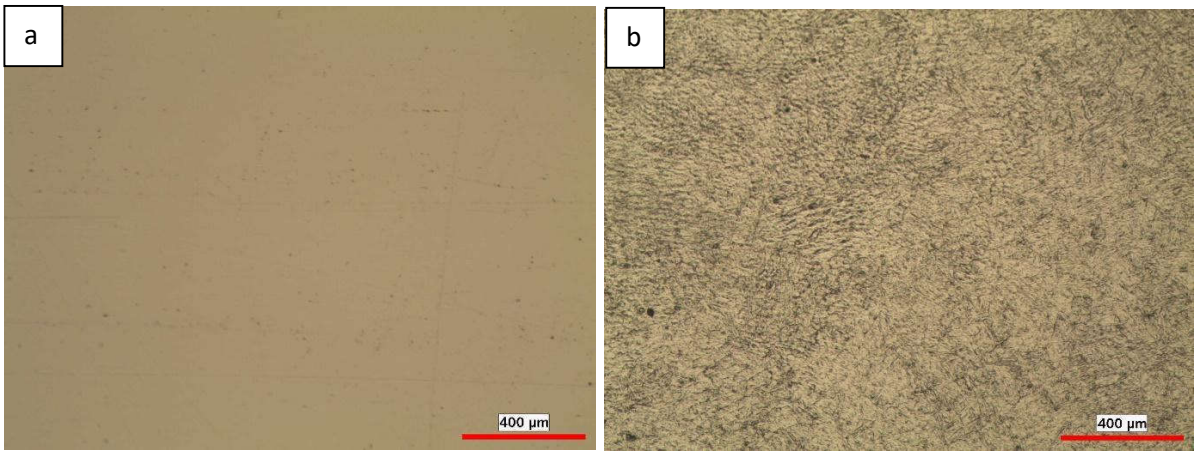

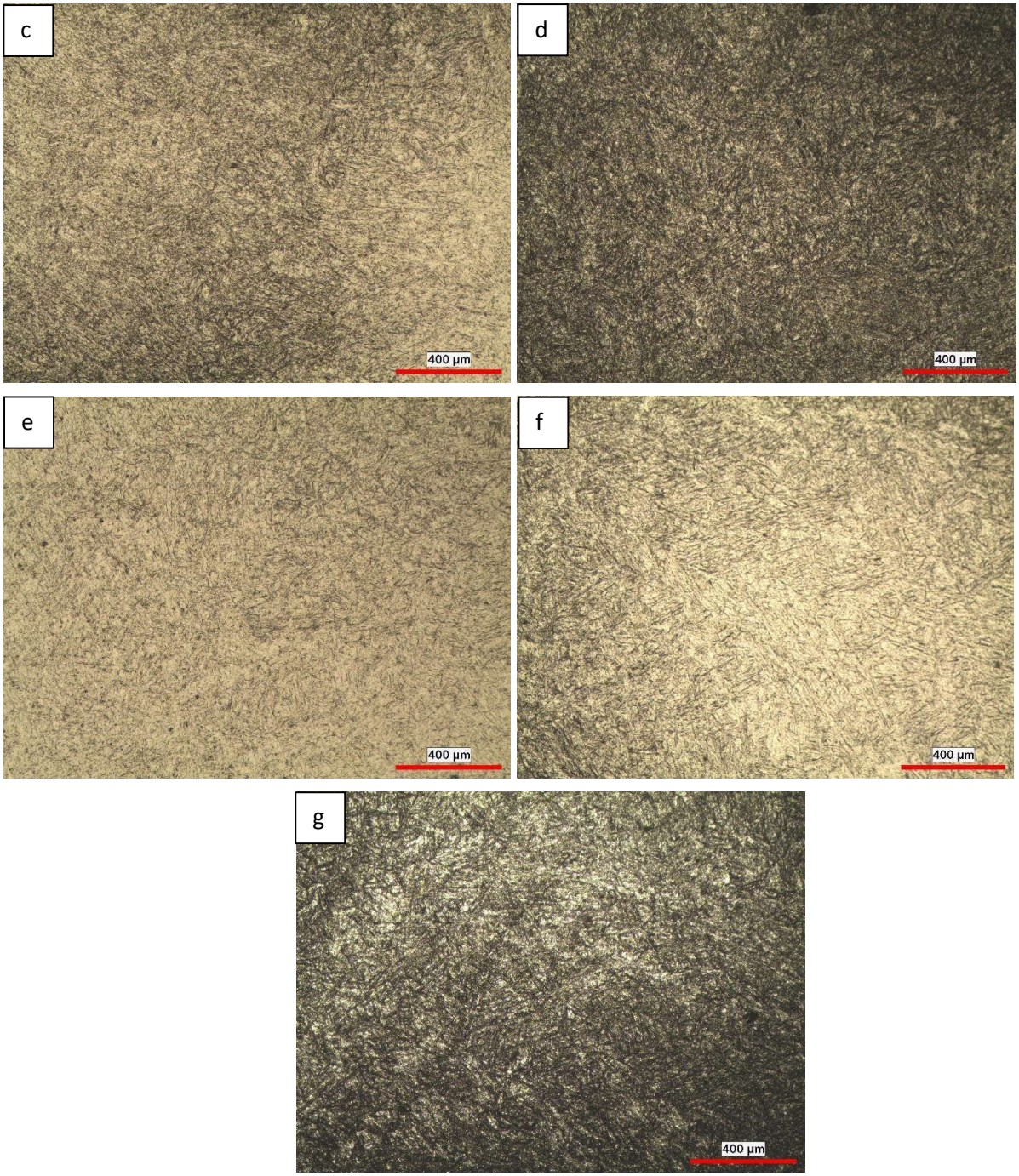

Şekil 8. 84 ve 88 kodlu numunelerin kavitasyon erozyonu testinden önce ve farklı süreler sonrası optik mikroskop görüntüleri; (a) test öncesi, (b) 84 - 1 saat, (c) 84 - 3 saat , (d) 84 - 5 saat , (e) 88 - 1 saat, (f) 88- 3 saat ve (g) 88- 5 saat

Şekil 8' de test sonrasında herhangi bir dağlama işlemi olmamasına rağmen numunelerin optik mikroskop görüntüleri dağlanmış gibi görülmektedir. Dağlama işleminin yapılmadığı Şekil 8a' da görülmektedir. Bu durum kavitasyon erozyonunun ilk olarak tane sınırlarında başladığı göstermektedir. Tane sınırlarındaki stres artmaktadır ve daha sonra tane sınırlarından başlayan kopmalar meydana gelmektedir. Bu da deformasyonu oluşturmaktadır (Tian vd. 2022). Şekil 8 incelendiğinde östenit ve ferrit fazları görülmektedir. Farklı akımlarda kaplama yapılan 308L kaynak telinin akımın farklı olması kavitasyon erozyonu testi sonunda mikroyapıda herhangi bir farklılığa yol açmamıştır. Kavitasyon erozyonu testi süresinin artması mikroyapı

görüntüsündeki tane sınırlarının daha belirgin hale gelmesine sebep olmuştur. Alınan mikroyapı görüntüleri kavitasyon erozyonunun daha az yoğun olduğu bölgelerden alınmıştır.

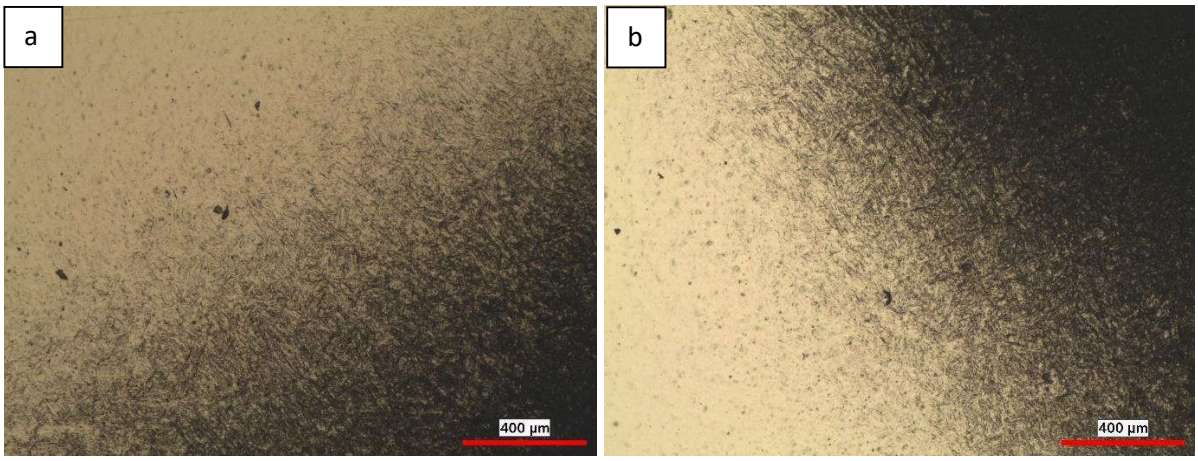

Şekil 9. 84 ve 88 kodlu numunelerin 5 saatlik kavitasyon erozyonu testi sonucunda oluşan görüntüler

Şekil 9 incelendiğinde 5 saatlik kavitasyon erozyonu testi sonrasında kavitasyon erozyonun yoğunlaştığı bölgede optik mikroskobun görüntü elde edemediği görülmektedir. Kavitasyon erozyonunun oluşan bölgenin görüntüleri stereo mikroskop ile makro ölçüde alınmıştır (Şekil 10).

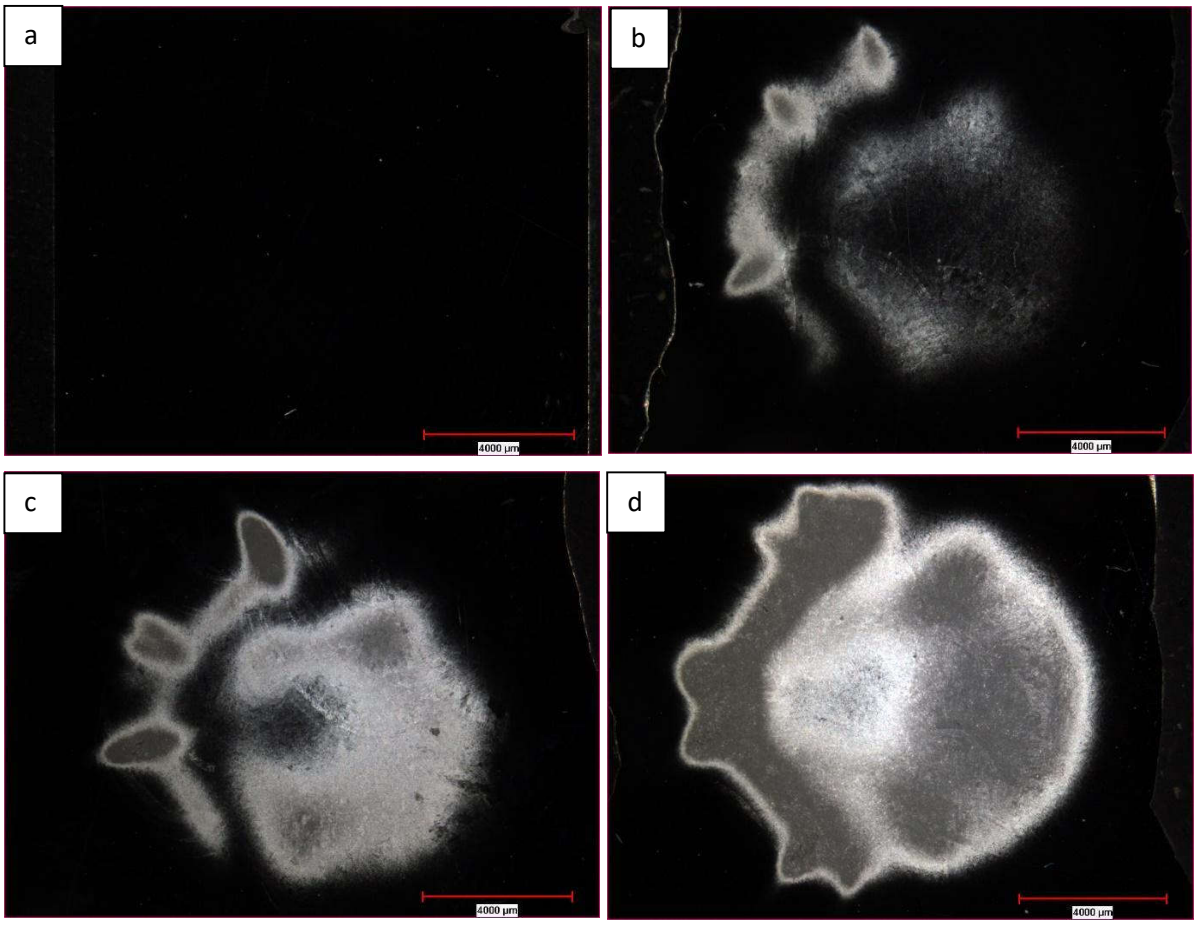

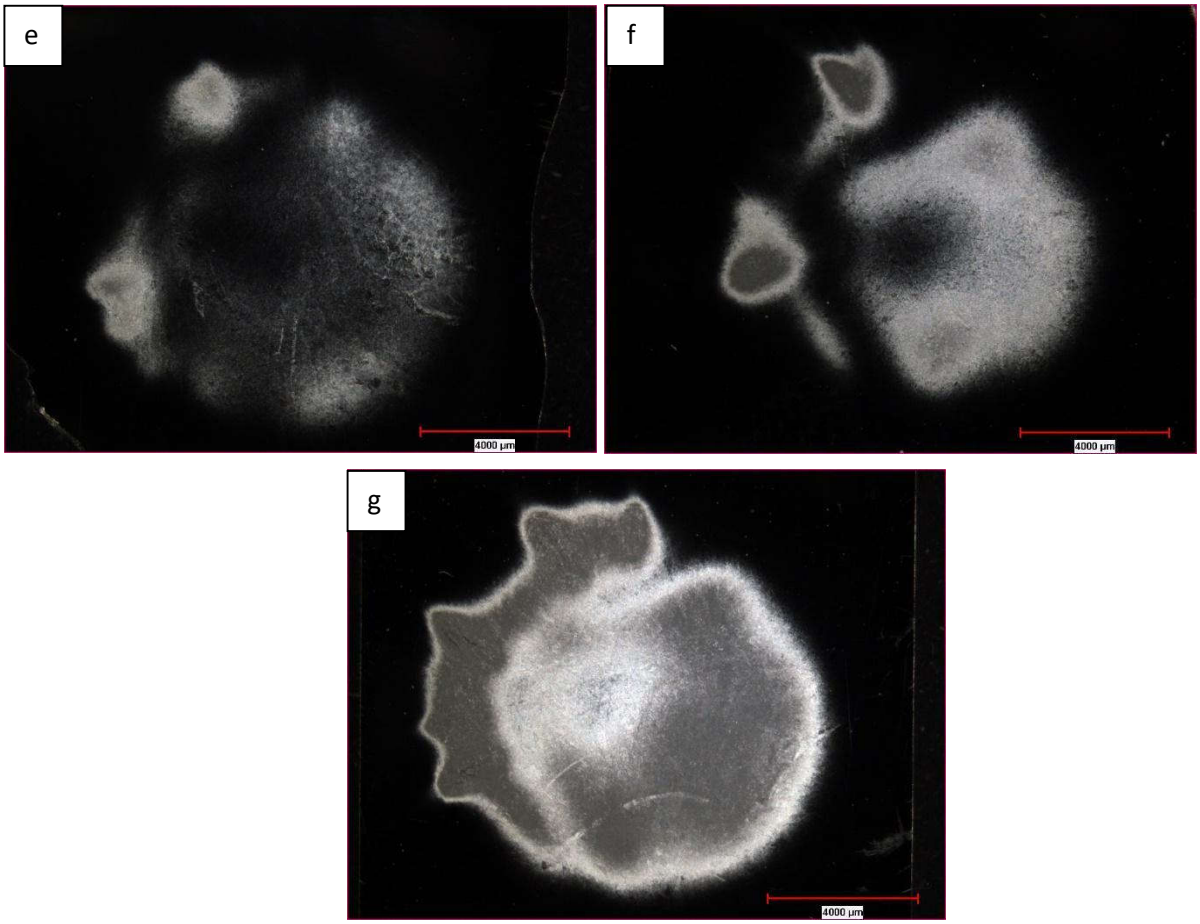

Şekil 10. 84 ve 88 kodlu numunelerin kavitasyon erozyonu testinden önce ve farklı süreler sonrası oluşan stereo mikroskop görüntüler; (a) test öncesi, (b) 84 - 1 saat, (c) 84 - 3 saat , (d) 84 - 5 saat , (e) 88 - 1 saat, (f) 88- 3 saat ve (g) 88- 5 saat

Şekil 10 incelendiğinde kavitasyon erozyonu test süresinin artması, kavitasyon erozyonundan dolayı kayıpları ve kavitasyon erozyonuna uğrayan alanın büyümesine neden olmuştur. Bu büyüme kavitasyon erozyonu gerçekleştiren ultrasonik titreşimli uçun (13 mm) dışına çıkmamıştır. Şekil 10a' da test öncesinde numunenin yüzeyinde herhangi bir çizik veya kaplama için kullanılan kaynak yönteminden oluşan bir hata bulunmamaktadır. Kavitasyon erozyonunun oluşumu numunenin yüzeyinde homojen olarak gerçekleşmemiştir. Gao ve ark.'nın yaptığı çalışmalarda bu durum ele alınmıştır ve şema ile gösterilmiştir (Gao ve Zhang 2022). Bu çalışmada da kavitasyon erozyonu homojen olarak dağılmamaktadır. Kavitasyon erozyonu süresi arttıkça deformasyon miktarı da artmıştır. Bu da numunenin yüzeyinde çatlaklara ve çukurlara sebep olmuştur (Şekil 10 c, d, f ve g). Bu durum literatürdeki uzun süreli kavitasyon erozyonu testi uygulanan çalışmalarda da görülmektedir (Li vd. 2022; Tian vd. 2022; Gao ve Zhang 2022; Gao ve Zhang 2019).

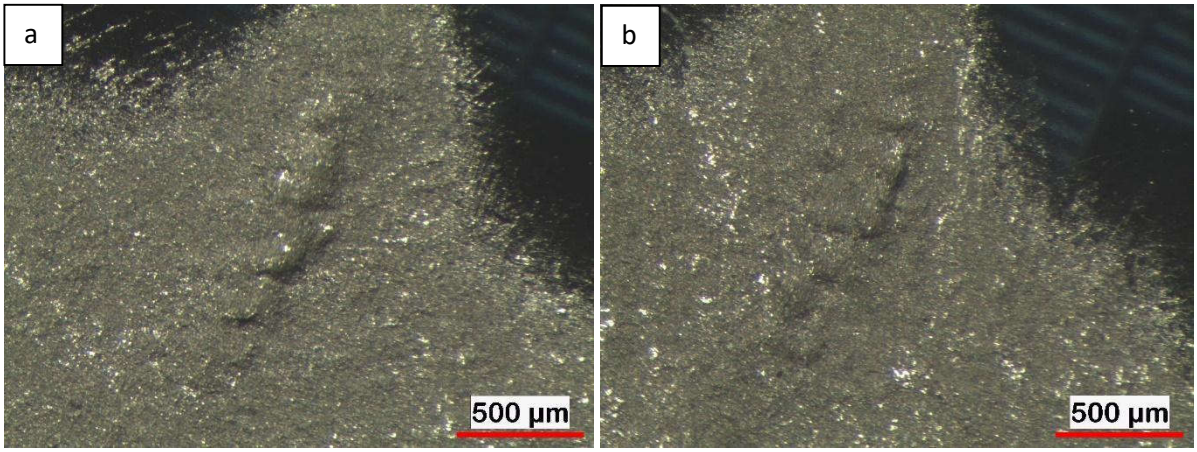

Şekil 11.84 ve 88 kodlu numunelerin sonra 5 saatlik kavitasyon erozyonu testi sonucunda oluşan çatlakların stereo mikroskop görüntüleri

Taneler arasındaki tutarsız hareket, tanede ve/veya tane sınırında strese neden olmakta ve biriken stres, tanenin ve/veya tane sınırının deformasyonuna neden olur. Birikmiş gerilme dayanım sınırına ulaştığında, tane sınırında ve/veya tanede çatlak oluşur (Hattori ve Mikami 2009; Gao ve Zhang 2019). Kavitasyon erozyon koşullarına daha fazla maruz kaldığında, daha fazla deformasyonla birlikte çatlak büyümeye devam eder. Plastik deformasyon sınırına ulaşıldığında, taneler ayrılır ve ilk kavitasyon kraterini oluşturarak ayrılır. (Tian vd. 2022). Deformasyon ve stresin sürekli olması ile parça deformasyona uğramaktadır (Şekil 11).

Kavitasyon erozyonu testinden önce ve sonra numunelerin kütle kaybının hesaplanması için numuneler hassas terazide tartılmıştır. Çıkan sonuçlar yardımı ile ağırlık kaybı oranı, MDRP (ortalama derinlik penetrasyon oranı) ve Re (kavitasyon erozyon direnci) değerleri hesaplanmıştır. Malzemelerin erozyon hasarı, MDPR ve R_e cinsinden ifade edilir. MDPR ve R_e, Denklem (3) ve (4) kullanılarak hesaplanmıştır:

$$MDRP\ (\mu m h^{-1}) = \frac{\Delta W}{10 \rho A \Delta t} \quad (3)$$

$$R_e\ (h\mu m^{-1}) = \frac{1}{MDRP} \quad (4)$$

Burada ΔW, mg cinsinden ağırlık kaybı, Δt ise saat cinsinden zaman aralığı, A ise cm^2 cinsinden numunenin yüzey alanı ve ρ ise g/cm^{-3} cinsinden numune yoğunluğudur (Bregliozzi vd. 2005). Bu denklemler kullanılarak oluşturulan grafikler Şekil 12' de verilmiştir.

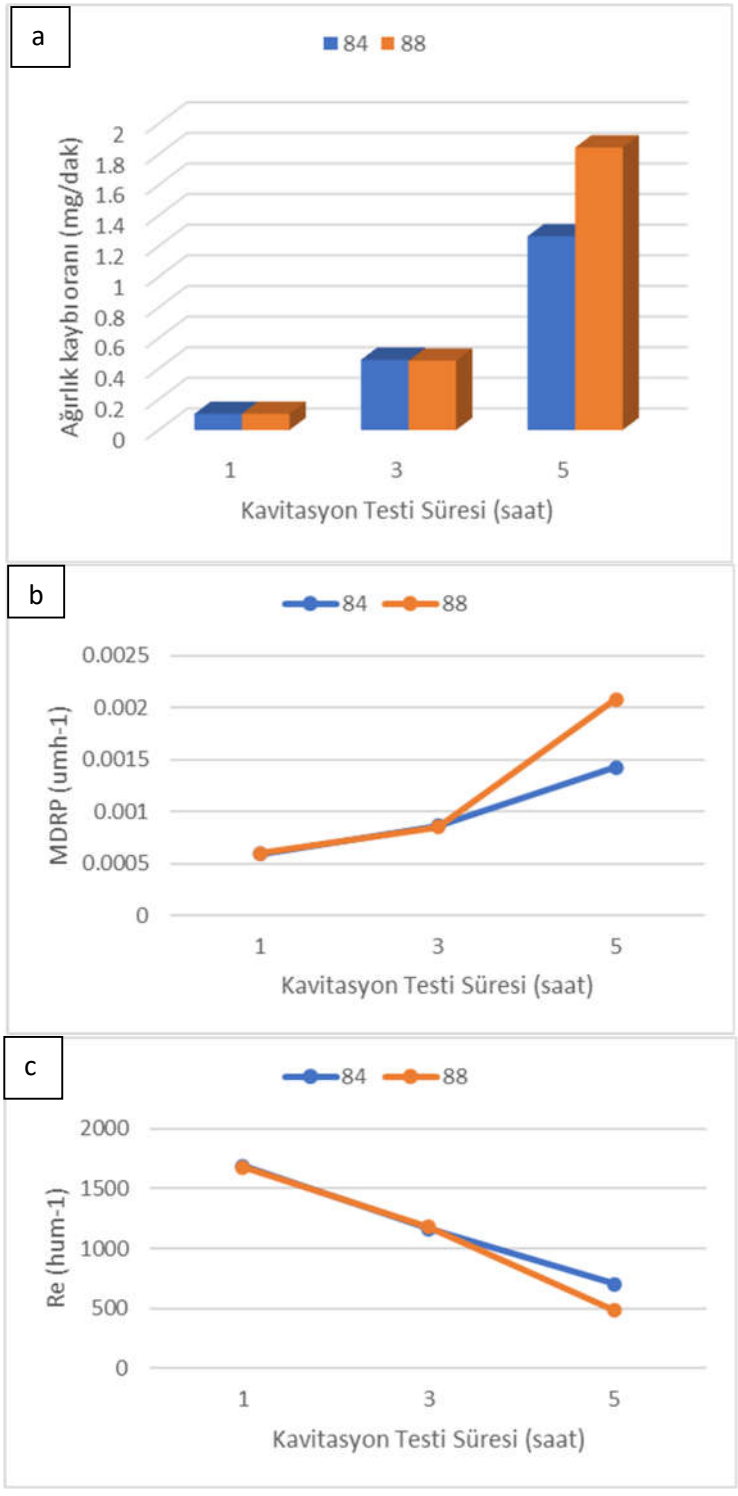

Şekil 12. (a) Ağırlık kaybı oranı, (b) MDRP değerleri ve (c) R_e değerleri

Şekil 12 incelendiğinde kavitasyon erozyonun geçen süre ile birlikte doğru orantılı olarak arttığı görülmektedir. Şekil 12a' da dakika başına malzeme kaybının mg cinsinden verildiği grafik görülmektedir. Bu grafiğe göre 84 ve 88 numuneler arasında 1. ve 3. saatler arasında çok az bir fark bulunuyorken, 3. saatten sonra farkın arttığı görülmektedir. 5. saatin sonunda ise 84 numaralı numune ile 88 numaralı numune arasında yaklaşık olarak % 40 oranında ağırlık kaybı farkı bulunmaktadır. Bu durumun oluşması Şekil 12b' de ortalama derinlik penetrasyon oranı (MDPR) değeri ile daha net bir şekilde anlatılmaktadır.

Şekil 12b' de 84 ve 88 kodlu numunelerin MDRP değerleri yer almaktadır. 88 kodlu numunenin 3. saatten sonra daha fazla ağırlık kaybetmesine neden olmakla birlikte daha derin kavitasyon erozyonuna maruz kaldığı görülmektedir. Bu durum R_e değerlerine de yansımaktadır.

Şekil 12c' de ise, 88 numaralı numunenin kavitasyon erozyonu direnci 84 nolu numuneye göre daha düşüktür. 84 ile 88 numaralı numuneler arasında 220 $h.\mu m^{-1}$'lik kavitasyon erozyonu direnci farkı bulunmaktadır.

SONUÇ

308L östenitik paslanmaz çelik teller ile farklı akımlarda TIG kaynağı kullanılarak kaplama yapılmış numunelerin faz yapıları diyagramlar sayesinde hesaplanmış, mikroyapı ve makroyapı incelemeleri yapılmış, kavitasyon erozyonu testleri gerçekleştirilmiş ve bu incelemeler sonucunda aşağıdaki sonuçlara varılmıştır.

1. Kaplama işleminden sonra her iki akım değerinde de oluşan yapı Schaeffler Diyagramına göre mikroyapıda östenit fazı ile birlikte %9 delta ferrit fazı bulunmaktadır.
2. Kavitasyon erozyonu ilk olarak tane sınırlarında başlamıştır. Ayrıca kavitasyon erozyonu testi sonucunda, mikroyapıdaki ferrit ve östenit tanelerinde bir değişim olmadığı gözlenmiştir.
3. Kavitasyon erozyonun oluşumu numunenin her yerinde homojen olarak bir dağılım sağlamamıştır. Pürüzlülük test sonuçlarına göre numune yüzeyindeki bazı noktalarda kavitasyon derinken, bazı noktalarda daha az kavitasyon erozyonu oluşmuştur.
4. Kavitasyon erozyonu test süresine bağlı olarak numunelerin ağırlık kaybı oranları süreye bağlı olarak artmıştır. 1 ve 3. saatlerde ağırlık kaybı oranları 140 A ve 180 A ile kaplama yapılmış numunelerde yakın sonuçlar elde edilmişken 5. saatte 140 A ile kaplama yapılmış numunede ağırlık kaybı oranı 180 A ile üretilen numuneye göre daha az elde edilmiştir. 180 A ile ısı girdisinin fazla olması ve tane boyutlarının büyük olmasından dolayı daha fazla malzemenin kavitasyon erozyonuna maruz kaldığı düşünülmektedir.
5. Kavitasyon erozyonu test süresine bağlı olarak MDRP sonuçlarında ise 140 A ile üretilen kaplanmış numunenin, 5 saat kavitasyon erozyonuna maruz kalmış durumdaki MDRP değeri 180 A ile üretilmiş kaplama numunesine göre daha düşük olduğu görülmüştür.
6. Kavitasyon erozyonu süresi ilerledikçe kaplama üretiminde kullanılan akım değerinin önemli olduğu görülmüştür. 1 ve 3. saatlerde kavitasyon erozyonu test sonuçları birbirine çok yakın elde edilirken 5. saatte kavitasyon erozyonu direncinin 140 A ile üretilen kaplamanın 180 A ile üretilen kaplamaya göre daha yüksek olduğu tespit edilmiştir. Stereo mikroskop görüntüleri ve pürüzlülük test sonuçları bunu desteklemektedir.

TEŞEKKÜR

Bu çalışma Manisa Celal Bayar Üniversitesi Bilimsel Araştırma Projeleri Koordinasyon Birimi tarafından desteklenmiştir. Proje Numarası: 2021-112

KAYNAKLAR

Althouse, A.D., Turnquist, C.H., Bowditch, W.A., Bowditch, K.E., (1999), ''Gas Tungsten Arc Welding'', Modern Welding, Goodheart-Willcox Pub., p327- 328.

Basumatary, J. (2017). Cavitation erosion-corrosion in marine propeller materials, Faculty of Engineering and the Environment, University of Southampton, Ph.D. Thesis.

Bregliozzi, G., Di Schino, A., Ahmed, S.U., Kenny, J.M., & Haefke, H. (2005). Cavitation wear behaviour of austenitic stainless steels with different grain sizes. Wear, 258(1-4), 503-510.

Durgutlu, A., Kahraman, N., Gülenç, B., (2005), ''Bakır ve Çelik Levhaların Örtülü Elektrod ve TIG Kaynak Yöntemleri ile Birleştirilmesi ve Arayüzey Özelliklerinin İncelenmesi'', Gazi Üniversitesi. Müh. Mim. Fak. Der., V. 20 (2): s 183-190

Gao, G., & Zhang, Z., (2019), ''Cavitation erosion behavior of 316L stainless steel'', Tribol. Lett. 67, 112.

Gao, G., & Zhang, Z. (2022). Cavitation erosion mechanism of 2Cr13 stainless steel. Wear, 488, 204137.

Gökmen, M., (2009), ‘’Paslanmaz Çeliklerin Gazaltı Kaynak Yöntemleri ile Kaynağında Koruyucu Gaz ve İlave Metalin Mekanik Özelliklere Etkisi,’’ Sakarya Üniversitesi, Fen Bilimleri Enstitüsü, Metal Eğitimi Anabilim Dalı, Sakarya.

Hattori, S., Mikami, N., (2009), ‘’Cavitation erosion resistance of stellite alloy weld overlays’’, Wear 267 (11), 1954–1960.

Karimi, A., Martin, J.L., (1986), ‘’Cavitation erosion of materials’’, Metall. Rev. 31, 1–26,

Stephens, R.I., (2000), ‘’Metal Fatigue in Engineering’’, Second ed., Wiley-lnterscience, New York.

Köse, C., and Kaçar R., (2014), "The effect of preheat & post weld heat treatment on the laser weldability of AISI 420 martensitic stainless steel." Materials & Design 64: 221-226.

Li, Z.X., Zhang, L.M., Udoh, I.I., Ma, A.L., & Zheng, Y.G. (2022). Deformation-induced martensite in 304 stainless steel during cavitation erosion: Effect on passive film stability and the interaction between cavitation erosion and corrosion. Tribology International, 167, 107422.

Lippold J.C, Kotecki D.J., (2005), ‘’Welding metallurgy and weldability of stainless steels’’. John Wiley&Sons, Amerika, 8-16.

Metal Uzmanı, (2022), TIG Kaynağı Şematik gösterimi, https://www.metaluzmani.com/tig-kaynagi-sematik-gosterim-ve-ozet-bilgi/

Murat, M.G., (2018), ‘’Savunma Sanayinde Kullanılan 420 ve 304L Paslanmaz Çeliklerin TIG Kaynağı Sonrası Korozyon ve Mekanik Özelliklerinin İncelenmesi,’’ Kırıkkale Üniversitesi, Fen Bilimleri Enstitüsü, Savunma Teknolojileri Anabilim Dalı, Kırıkkale.

Nevcanoğlu, A., (2019), ‘’TIG Kaynağı Yöntemi ile Birleştirilmiş Inconel 718 Süper Alaşım Malzemenin Kaynak Sonrası Özelliklerinin İncelenmesi,’’ Marmara Üniversitesi, Fen Bilimleri Enstitüsü, Metalurji ve Malzeme Mühendisliği Anabilim Dalı, İstanbul.

Rajani, H.Z., Torkamani, H., Sharbati, M., & Raygan, S. (2012), ‘’Corrosion resistance improvement in Gas Tungsten Arc Welded 316L stainless steel joints through controlled preheat treatment’’. Materials & Design, 34, 51-57.

Sampson, R. (2008). 'Cavitation', School of Marine Science and Technology, Newcastle University, 1, pp. 1–68.

Schijve, J., (2004), ‘’Fatigue of Structures and Materials’’, Second ed., Aviation Industry, Beijing.

Şahin, Ş., (1990), “Paslanmaz Çeliklerin Kaynak Kabiliyeti”, Y.Lisans Tezi, Selçuk Üniversitesi, Makine Anabilim Dalı, s:6-7, Konya.

Taillon, G., Pougoum, F., Lavigne, S., Ton-That, L., Schulz, R., Bousser, E., Savoie, S., Martinu, L. & Sapieha, J. E. K. (2016). Cavitation erosion mechanisms in stainless steels and incomposite metal–ceramic HVOF coatings, Wear, Vol. 364-365, pp. 201–210.

Tian, Y., Zhao, H., Yang, R., Liu, X., Chen, X., Qin, J., McDonald, A., & Li, H. (2022). In-situ SEM investigation on stress-induced microstructure evolution of austenitic stainless steels subjected to cavitation erosion and cavitation erosion-corrosion. Materials & Design, 213, 110314.

Tümer, M., (2012), ‘’Koruyucu Gaz Kompozisyonunun Özlü Tel Ark Kaynak Yöntemi ile Birleştirilen Paslanmaz Çeliklerin Mekanik Ve Mikroyapı Özelliklerine Etkisi,’’ Sakarya Üniversitesi, Fen Bilimleri Enstitüsü, Metal Eğitimi Anabilim Dalı, Sakarya.

Türkan, M., (2013), ‘’Kaynaklı ve Kaynaksız Östenitik Paslanmaz Çeliklerin Korozif Ortamlardaki Çekme Davranışları,’’ Pamukkale Üniversitesi, Fen Bilimleri Enstitüsü, Makina Mühendisliği Anabilim Dalı, Denizli.

Whitesides, R.W., (2012). Interesting Facts (and Myths) about Cavitation, Vol. 225. PDHonline, Fairfax.

Wikimedia, (2022), Schaeffler Diyagramı, https://commons.wikimedia.org/wiki/File:Diagramme_schaeffler.svg

Yüksel, M., (2001), ‘’Malzeme Bilgisi’’, Cilt 1, TMMOB Makina Mühendisleri Odası, Ankara.

COMPRESSIVE STRENGTH OF CLAYEY SOILS REINFORCED WITH BAYBURT STONE (BAYBURT TUFFITE)

Necmi YARBAŞI[1]

[1]Atatürk University, Faculty of Engineering, Civil Engineering Department, Erzurum, Turkey.

[1]ORCID ID: https://orcid.org/0000-0003-4259-1278

Rıdvan KUL[2]

[2]Atatürk University, Graduate School of Sciences, Graduate student, Erzurum, Turkey.

[2]ORCID ID: https://orcid.org/0000-0003-1336-4471

ABSTRACT

In today's world where climate changes are common, negative changes are observed in geotechnical properties in parallel with this change in soils that form the basis of engineering structures. This negative situation reveals the necessity of strengthening the soils with weak geotechnical properties. For this purpose, natural, synthetic, or various chemicals are used as additional additives. In this study, Bayburt stone (Bayburt tuffite), a natural rock, was pulverized and added to clayey soil with high plasticity and the changes in uniaxial unconfined compressive strength were investigated. Clay soil (CS) mixtures reinforced with Bayburt stone powder (BTP) in three different ratios (5%, 10%, and 15% dry weight) were cured in a laboratory environment (+20ºC) for 7, 14, and 28 days. At the end of these three different curing times, the unconfined compressive strength (UCS) values of the samples were obtained with a uniaxial unconfined pressure device. When the strength values obtained were examined, it was observed that the highest strength was 34.38% with the mixture of CS + 5% BTP at the end of 28 days of curing. After this mixture, at the end of the 28-day cure, the other highest strengths; It was determined as 18.75% in the CS+10 BTP mixture and 10.94% in the CS+15 BTP mixture.

Keywords: Clay soil, Bayburt Tuffite, strength

1. Introduction

Soil improvement/reinforcement is defined as improving the physical and mechanical properties of the soil (strength, bearing capacity, settlement, swelling, deformations, etc.) by mixing various additives. The use of natural, synthetic or various chemicals as additives in soil stabilization/reinforcement has increased significantly in the last decade. Strengthening works by mixing clayey soils, various waste/residue materials and especially natural rock fibers, which are called common and problematic soils, are continuing at an increasing pace (Prabakar and Sridhar, 2002; Akbulut et al., 2007; Yarbaşı et al., 2007; Hejazi et al., 2012; Maliakal and Thiyyakkandi, 2012; Yarbasi, 2019; Kalkan et al., 2020; Yarbasi, 2020; Yarbasi and Kalkan, 2020).The use of natural rocks or minerals as an alternative material in soil improvement has become increasingly important in recent years. When geotechnical engineers are confronted with such high-low plasticity clayey soils in large areas, they have now turned to improvement-reinforcing studies with natural rocks or minerals in order to optimize the engineering properties of these soils. Today, improvement studies are carried out in various application areas with Bayburt tuffite (Bayburt stone) in soils with weak geotechnical properties. From these studies; Yılmaz, F. et al., (2015). In their study titled "Soil Stabilization with Using Waste Materials against Freezing Thawing Effect", it was observed that samples stabilized with green Bayburt Stone mixtures had higher freeze-thaw durability compared to unstabilized samples. These mixtures can be successfully used as additives to increase the freeze-thaw effects of cohesion. Aykut, C. (2017). In the thesis study on "Investigating the usability of Bayburt stone wastes in geopolymer brick

production, it was concluded that geopolymer bricks produced from Bayburt stone and travertine wastes have zero CO_2 emission, higher strength and more economical. Tas et al., (2018). In their study titled "Soil Stabilization with Fly Ash and Bayburt Stone", industrial wastes of fly ash and Bayburt stone were used for soil stabilization. Low plasticity clayey soil was used within the scope of the study, and they determined that the mixture containing 10% of Bayburt stone and 25% fly ash gave the highest strength value according to uniaxial unconfined compressive strength values. In this study, it was aimed to improve/reinforce the clayey soils defined as problematic soils by using Bayburt tuffite (Bayburt stone) dust, which is a natural rock type, and to determine the strength of the new mixture material formed.

2. Materials

2.1. Clay soil (CS)

The CS samples used in this study were obtained from the deposits of the Oltu Oligocene sedimentary basin, Erzurum, Northeast Turkey. This soil with green color and high plasticity ise over-consolidated and it has clayey-rock characteristics in natural conditions (Kalkan and Bayraktutan, 2008). The CS sample and its granulometry curve are shown in Figure 1, and the physical and mechanical properties in Table 1.

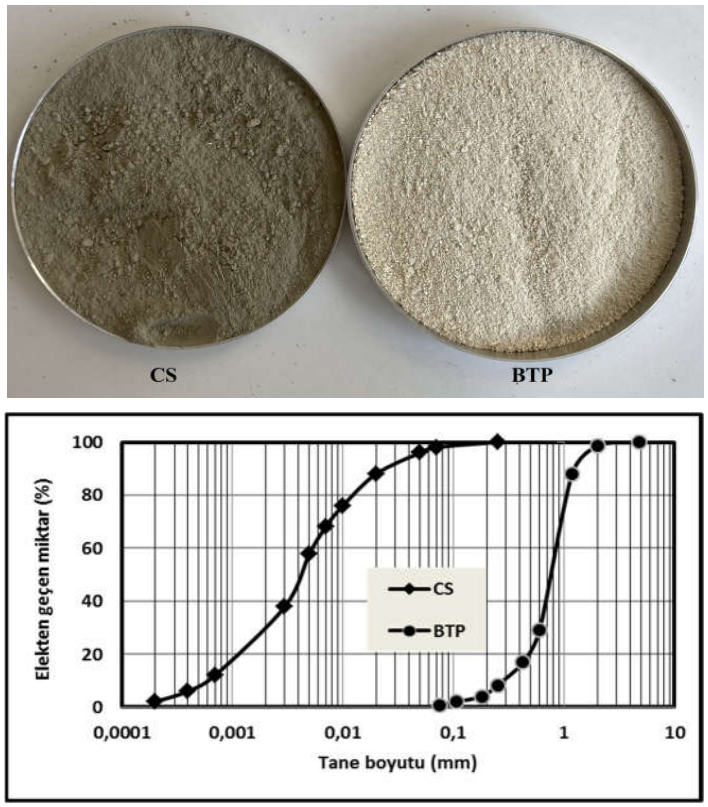

Figure 1. CS and BTP samples and granulometry curves

2.2 Bayburt tuffite (Bayburt stone) powder (BTP)

Bayburt tuffite (Bayburt stone), constituting the second important element of this study, are rocks deposited in Eocene aged lacustrine basins outcropping in large areas in and around Bayburt province. It is seen in yellow-white color, sometimes with green spots on a white background, and sometimes in yellow and green wavy colors (Yılmaz et al., 2005). The BTP sample and its granulometry curve are shown in Figure 1, and the physical and mechanical properties in Table 2.

Table 1. Physical and mechanical properties of CS (Kalkan and Bayraktutan, 2008)

Characteristics	Values
Specific weight, Gs	2.64
Sand (%)	10.0
Silty (%)	58.0
Clay (%)	32.0
LL, %	68
PL, %	28
PI, %	40
[1]Optimum water amount, %	25.8
[1]Max. dry weight, (kN/m^3)	14.1
[2]Soil category	CH

[1]Obtained from Standard Proctor Test.

[2]Soil class according to Unified Soil Classification System (USCS).

Table 2. Chemical and physical properties of BTP (Yılmaz, 2015)

Chemical properties	**Values**
Total SiO_2 (%)	69.96
Al_2O_3 (%)	12.25
Fe_2O_3 (%)	0.33
CaO (%)	2.52
MgO (%)	1.20
SO_3 (%)	0.05
K_2O (%)	2.43
Na_2O (%)	0.57
Cl (%)	0.0280
Glow loss	10.08
Physical properties	**Values**
Specific gravity (g/cm^3)	2.31
Specific surface area (cm^2/g)	7193
Pozzolan activation	8.8

3. Experimental Procedure

Mixture samples of CS and BTP were obtained by adding 5%, 10%, and 15% of the dry weight of the CS sample to BTP under dry conditions. Mixing ratios are 100% CS (MIX0), 95% CS+5% BTP (MIX1), 90% CS+10% BTP (MIX2) and 85% CS+15% BTP (MIX3). Each mixture was compressed under standard proctor energy at the optimum water content determined by the compression test (ASTM D. 698-78). The mixtures were mixed manually for at least 3 minutes at the required sensitivity. 5%, 10% and 15% BTP added to CS were subjected to a uniaxial free pressure device (ASTM D. 2166) after curing in the laboratory for 7, 14, and 28 days and 3 (three) samples were prepared for the consistency of the results. The arithmetic average of each mixture and the results were taken. Unlimited compressive strength values (UCS) values were determined at a constant loading rate of 0.5 mm/min.

4. Experimental results

Three different ratios (5%, 10%, and 15%) mixtures of BTP reinforced CS floor were cured in a laboratory environment at +20 ºC for 7, 14, and 28 days, and UCS values were obtained with a free pressure device. When the strength values obtained were examined and compared with the main material (witness) MIX0 (CS), it was observed that the highest strength was increased by 34.38% with the MIX1 (CS+5% BTP) mixture at the end of 28 days of curing. Following this mixture, at the end of the 28-day cure in the other highest strengths; It was 18.75% in the MIX2 (CS+10% BTP) mixture and 10.94% in the MIX3 (CS+15% BTP) mixture. The UCS graph of BTP reinforced CS soil mixes is shown in Figure 2. Examples and fracture patterns of the examined specimens are shown in Figure 3.

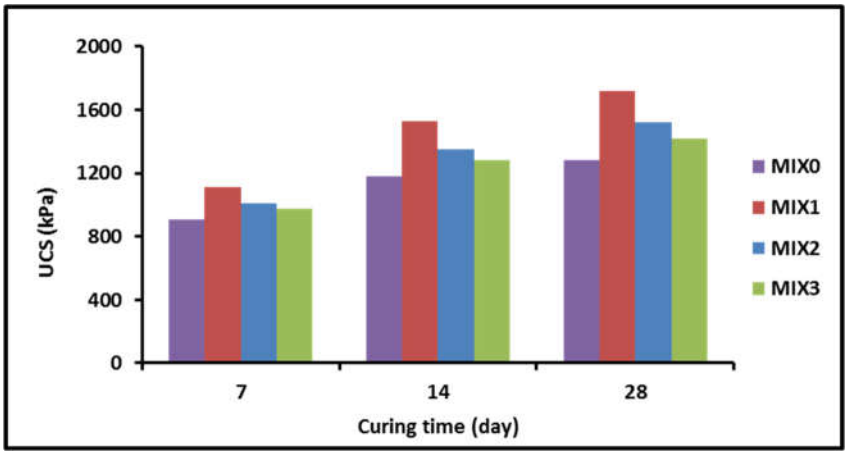

Figure 2. UCS distribution of mixture samples

Figure 3. Breakage patterns of the mixture samples after 28 days of curing

4. Conclusions

The strength values of CS reinforced with BTP at three different mixing ratios were determined with a uniaxial free pressure device. Among the BTP reinforced CS mixtures, the highest strength value was obtained in the MIX1 mixture after 28 days of curing. When the strength values of the three different mixtures were compared with the strength values of the base material (witness) MIX0, it was observed that there was a 34.38% strength increase in the MIX1 mixture. The other highest strength values following this mixture are respectively at the end of 28 days of curing; It was 18.75% in the MIX2 mixture and 10.94% in the MIX3 mixture. Therefore, it is concluded that BTP can be used as a sustainable and environmentally friendly material that reduces improvement/reinforcement costs.

Acknowledgements

This experimental research was supported by the Scientific Research Project of Atatürk University with the ID number of 10401 code of FYL-2022-10401. So, the authors thank the authorities of the Ataturk University for the support.

Declaration of Conflict of Interests

There are no known competing financial interests or personal relationships that could have appeared to influence the work reported in this paper.

Referances

Akbulut S, Arasan S, Kalkan E. (2007). "Modification of clayey soils using scrap tire rubber and synthetic fibers". Applied Clay Science 38 (1-2), 23-32.

ASTM D. 2166, 2006. "Standard Test Method for Unconfined Compressive Strength of Cohesive Soil". American Society for Testing and Materials. West Conshohocken, Pennsylvania, USA.

ASTM D. 698-78, 2012. "Fundamental Principles of Soil Compaction". American Society for Testing and Materials. West Conshohocken, Pennsylvania, USA.

Aykut, C. 2017."Investigation of the usability of Bayburt stone waste in the production of geopolymer bricks". Master's thesis, Bayburt University (Turkey), Institute of Science and Technology.

Hejazi, S.M., Sheikhzadeh, M., Abtahi, S.M., Zadhoush, A. 2012. "A Simple Review of Soil Reinforcement by Using Natural and Synthetic Fibers". Construction Building Material 30, 100-116.

Kalkan, E., Bayraktutan, M. 2008. "Geotechnical evaluation of Turkish clay deposits": a case study in Northern Turkey. Environmental Geology 55 (5), 937-950.

Kalkan, E., Yarbasi, N., Bilici, O. 2020. "The Effects of Quartzite on the Swelling Behaviors of Compacted Clayey Soils". International Journal of Earth Sciences Knowledge and Applications 2 (2) 92-101.

Maliakal, T., Thiyyakkandi, S. 2012. "Influence of randomly distributed coir fibers on the shear strength of clay". Geotechnical Geology Engineering 31, 425-433.

Prabakar, J., Sridhar, R.S. 2002. "Effect of random inclusion of sisal fiber on strength behavior of soil". Construction and Building Materials 16, 123-231.

Tas et al., 2018. "Soil Stabilization with Fly Ash and Bayburt Stone" Bayburt University (Turkey) Journal of Science Vol 1, Issue 1.

Yarbasi, N. 2019. "Performance of granular soils reinforced with obsidian (volcanic glass) additives in different proportions subjected to freeze-thaw". Pamukkale University Journal of Engineering Sciences 25 (6), 764-767.

Yarbaşi, N., 2020. "Effect of Freezing-Thawing on Clayey Soils Reinforced with Human Hair Fibers". Journal of Natural Fibers 17 (6), 921-931.

Yarbasi, N., Kalkan, E. 2020. "The Mechanical Performance of Clayey Soils Reinforced with Waste PET Fibers". International Journal of Earth Sciences Knowledge and Applications 2 (1) 19-26.

Yarbaşı, N., Kalkan, E., Akbulut, S. 2007. "Modification of the geotechnical properties, as influenced by freeze-thaw, of granular soils with waste additives". Cold Regions Science and Technology 48 (1), 44-54.

Yılmaz, A.O. Alp., İ., Demir, C., Arslan, M., Kolaylı, H., 2005. "Physical, Mechanical, Petrographic Properties of Bayburt Tuff (Bayburt Stone)", TMMOB, Chamber of Mining Engineers. https://www.maden.org.tr/resimler/ekler/ef6f97160533672_ek.pdf)

Yılmaz, F. 2015. "Investigation of Usability of Tuffite Stones with Lime in Soil Stabilization with Standard Experiments and Computed Tomography Technique" (Doctoral Thesis). Obtained from the National Thesis Center of the Council of Higher Education. (Thesis No. 397321).(Turkey).

BURDUR İLİ ÇAVDIR İLÇESİ MERMER OCAK ALANININ JEOLOJİK VE HİDROJEOLOJİK ÖZELLİKLERİNİN İNCELENMESİ

INVESTIGATION OF GEOLOGICAL AND HYDROGEOLOGICAL CHARACTERISTICS OF THE MARBLE QUARRY FIELD OF THE CAVDIR DISTRICT OF BURDUR PROVINCE

İbrahim İskender SOYASLAN[1]

[1]: Doç. Dr., Burdur Mehmet Akif Ersoy Üniversitesi, Mühendislik Mimarlık Fakültesi, İnşaat Mühendisliği Bölümü

ORCID NO: 0000-0001-5282-8094

ÖZET

Toridler olarak adlandırılan ve bugünkü jeolojik yapısını Alpin orojenezi sonrası kazanmış olan çalışma alanı yüksek bir mermer potansiyeline sahiptir. Aynı zamanda Isparta Büklümü olarak tanımlanmış tektonik bir kuşağın sol kanadında yer almaktadır. Çalışma alanının tektonik yapısına rağmen ticari olarak Burdur Beji olarak isimlendirilen ve Mesozoyik Kireçtaşlarından oluşan mermer türü bölgede geniş bir yayılıma sahiptir. Son yıllarda Burdur Beji açık krem ve kahve renge sahip olması, çok kolay cila alması, honlama ve eskitme yapılabilmesinden ötürü giderek talep görmeye başlamıştır. Bu artan talebe bağlı olarak ekonomik değerindeki artış bölgedeki mermer ocaklarının sayısının hızlı bir şekilde artmasına sebep olmuştur. Son yıllardaki küresel ısınma, hızlı nüfus artışı ve endüstrileşme tattlı su kaynaklarının da öneminin artmasına sebep olmuştur. Göller Bölgesinde yer alan çalışma alanı yakın çevresinde Gölhisar ve Yazır Gölü, Yapraklı, Kozağaç ve Çavdır baraj gölleri bulunmaktadır. Başta tarımsal sulama olmak üzere farklı amaçlar için kullanılan su kaynaklarının su kalitesinin ve miktarının korunması bölge için büyük önem taşımaktadır. Bu bakımdan çalışma alanı ve yakın çevresinde yapılacak her türlü madencilik faaliyetinin su kaynaklarına olası olumsuz etkilerinin belirlenmesi ve gerekli tedbirlerin alınması gerekmektedir.

Bu bildirinin amacı Burdur ili çavdır ilçesi sınırları içerisinde açılması öngörülen mermer ocağı ve çevresinin jeolojik ve hidrojeolojik özelliklerinin ortaya koyarak, madencilik faaliyetinin su kaynaklarına olası olumsuz etkilerinin tespit edilmesidir. Bu amaçla çalışma alanının yapısal jeolojisi, stratigrafisi, hidrolojisi ve hidrojeolojisi detaylı arazi çalışmaları içe belirlenmiştir. Çalışma alanının jeoloji ve hidrojeoloji haritaları hazırlanarak, litolojik birimlerin hidrojeolojik özellikleri ve yeraltı suyu dinamiği ortaya konmuştur. Sonuçta mermer ocak işletmesinin jeolojik ve hidrojeolojik özellikleri dikkate alındığında madencilik faaliyetinin yüzey ve yeraltı suları açısından olumsuz bir etkisinin olmayacağı sonucuna varılmıştır.

Anahtar Kelimeler: Hidrojeoloji, jeoloji, madencilik, mermer,

ABSTRACT

The study area, which is called the Taurides and gained its current geological structure after the Alpine orogeny, has a high marble potential. It is also located on the left flank of a tectonic belt defined as the Isparta Bend. Despite the tectonic structure of the study area, the marble type commercially called Burdur Beige and consisting of Mesozoic Limestones has a wide distribution in the region. In recent years, Burdur Beige has started to be in demand due to its light cream and brown color, easy polishing, honing and aging. Due to this increasing demand, the increase in its economic value has led to a rapid increase in the number of marble quarries in the region. Global warming, rapid population growth and industrialization in recent years have led to an increase in the importance of freshwater resources. Gölhisar and Yazır Lake, Yapraklı, Kozağaç and Çavdır dam lakes are located in the immediate vicinity of the study area located in the Lakes Region. It is of great importance for the region to protect the water quality and quantity of water resources used for different purposes, especially agricultural irrigation. In this respect, it is necessary to determine the

possible negative effects of all kinds of mining activities to be carried out in the study area and its vicinity on water resources and to take necessary precautions.

The aim of this paper is to determine the possible negative effects of mining activity on water resources by revealing the geological and hydrogeological characteristics of the marble quarry and its surroundings, which is envisaged to be opened within the borders of Çavdır district of Burdur province. For this purpose, the structural geology, stratigraphy, hydrology and hydrogeology of the study area were determined in detailed field studies. By preparing the geological and hydrogeological maps of the study area, the hydrogeological characteristics of the lithological units and the groundwater dynamics were revealed. As a result, considering the geological and hydrogeological characteristics of the marble quarry operation, it was concluded that the mining activity would not have a negative impact on surface and groundwater.

Keywords: Hydrogeology, geology, mining, marble

GİRİŞ

Doğal taşlar, madencilik faaliyeti sonucunda çıkarıldıktan sonra kullanım amacına uygun olarak işlenebilen doğal bir malzemedir. İnsanlık tarihi sürecince yapı malzemesi olarak kullanılan doğal taşlar, en eski inşaat malzemelerinden biridir. Günümüzde de hem yapı malzemesi hem de endüstriyel hammadde olarak çok farklı alanlarda kullanılmaktadır. Ülkemizde doğal taş sektörünün son yıllardaki giderek artan gelişimine bağlı olarak mermer ocak sayısında da ciddi artışlar görülmektedir. Alp Himalaya dağ kuşağı üzerinde bulunan ülkemkiz yaklaşık 5,1-13,9 milyar ton muhtemel mermer potansiyeli sahip olduğu resmi raporlarda yer almaktadır. Yine bu raporlarda ülke mermer miktarının bölgelere göre dağılımı; %32 Ege Bölgesi, %26 Marmara Bölgesi, %11 İç Anadolu Bölgesi ve geriye kalan %31'lik oranın diğer bölgelere bulunmaktadır. Ülkemizin, 2020 yılı toplam doğal taş ihracatının yaklaşık %95'ini mermer ihracat oluşturmaktadır. Mermer ihracat gelirinin yaklaşık %60 işlenmiş mermer ve geriye kalan %40'ı ise blok mermer ihracatından elde edilmektedir (Ekonomi Bakanlığı, 2021).

Son yıllarda Burdur il sınırları içerisinde çıkarılan ve ticari olarak Burdur Beji olarak isimlendirilen mermer türünün iç ve dış piyasalarda rağbet göremesi sonucunda, Burdur ile sınırları içerisinde çok sayıda mermer ocağı açılmıştır. Burdur ilinin göller bölgesinde bulunması ve açılan mermer ocaklarının işletme aşamasındaki madencilik faaliyetlerinin yüzey ve yeraltı sularına olası olumsuz etkileri halk ve sivil toplum kuruluşları tarafında zaman zaman endişe ile karşılanmaktadır. Oysa madencilik faaliyetleri arasında patlayıcı madde ve ağır metal gibi çevreye zararlı etkisi olacak maddeleri doğal taş madenciliğinde kullanılmamaktadır. Bunun yanında doğal taş madenciliğinin çevrebilim açısında en önemli risk faktörleri; ses kirliliği, toz kirlilliği, yüzey ve yeraltı sularında askıda katı madde miktarı ve görsel kirlilik olarak sayılabilir.

Bölgedeki mermer ocaklarında kullanılan madencilik yöntemi açık ocak işletmeciliği şeklinde olup, patlatma yapılmamaktadır. Açık işletme yönteminde üretim, ocağın basamaklar oluşturularak ilerletilmesi şeklinde gerçekleştirilir. Ocak alanında iş makineleri ile yerinden alınan mermer bloklarının direk olarak kamyonlara yüklenmesi ile mermer işleme fabrikalarına nakledilir. Mermer madenciliğinde amaç kırık ve çatlaksız blok üretimi olduğundan dolayı hiçbir şekilde patlatmalı bir üretim yöntemi kullanılmamaktadır. Mermer üretiminde, mermer içerisine açılan sondaj deliklerinden kesici elmas tellerin geçirilmesi suretiyle uygulanan kesme yöntemi kullanılır. Elmas tel ile mermer üretimi sırasında herhangi bir kimyasal kullanımı ve patlatma işlemi yapılmamaktadır.

Bu çalışmanın amacı, mermer madenciliğinin yapılması sırasında çevrede bulana akiferlere, beslenme alanlarına, kuyu ve kaynaklara herhangi bir etkisinin olup olmadığı, çevrede bulunan yerleşim yerlerinin içme ve kullanma sularına bir zararı olup olmayacağının hidrojeolojik olarak ortaya konulmasıdır. Bu amaçla proje sahası ve yakın civarının yeraltı suyu kaynakları ve yüzey suları, bölgenin jeolojisi, geçmiş yıllarda yapılan etüt çalışmalarına ait verilere ve arazi gözlemlerine dayanılarak kuyu, kaynak, çeşme, gölet, akarsu ve diğer kaynaklar ayrıntılı olarak araştırılmıştır.

Çalışma Alanı

Çalışma alanı Burdur İli, Çavdır İlçesi sınırları içerisinde olup 1/25.000 ölçekli topoğrafik haritada N23-d3 ve N23-d4 nolu paftalar içerisinde bulunmaktadır (Şekil 1). Faaliyet alanı Burdur İlinin kuş uçumu yaklaşık 90 km güney batısında, Gölhisar ilçesinin 14 km. güney doğusuna, Çavdır İlçesinin 10 km. güney batısında ve Kozağacı köyünün 4 km. kuzeybatısında yer almaktadır. Mermer Ocak sahasının en yakın noktasından itibaren en yakın yerleşim yeri; kuzeydoğu yönünde 1200 m mesafede Uylupınar Köyü'ne ait Bağarası Mahallesine ait evler bulunmaktadır. Ayrıca ocak sahasının en yakın noktasından itibaren güneydoğu yönünde 2500 m mesafede Kozağacı Köyü ve kuzeybatı yönünde 4300 m mesafede Kargalı Köyü'ne ait yerleşimler yeralır.

Çalışma alanının coğrafi özellikleri; İlin doğal yapısı oldukça engebeli olup, Burdur ili morfolojisinin %61'i dağlık, %3'ü yayla, %19'u ova ve %17si engebeli özelliğe sahiptir. Çalışma alanının Kuzeydoğusunda Yuvadağı (1330 m), doğusunda Dikmen Tepe (1222 m), Havutbaşı Tepe (1196 m), güneydoğusunda Büyükkılıç Tepe (1650 m) ve Karasivri Tepe (1495 m), güneyinde Armutlu Tepe (1713 m), Tokattaş Tepe (1645 m) ve Cebel Tepe (1602 m), güneybatısında Koçaş Dağı (2095 m), Yedikardeş Tepe (1930 m) ve Çal Dağı (1943 m), batısında Gözlem Kayası (1618 m), ve Ortataş Tepe (1605 m), kuzeyinde Eğriçalı Tepe (1279 m), Koca Tepe (1364 m), Sarımeşe Tepe (1371 m) ile çevrilidir.

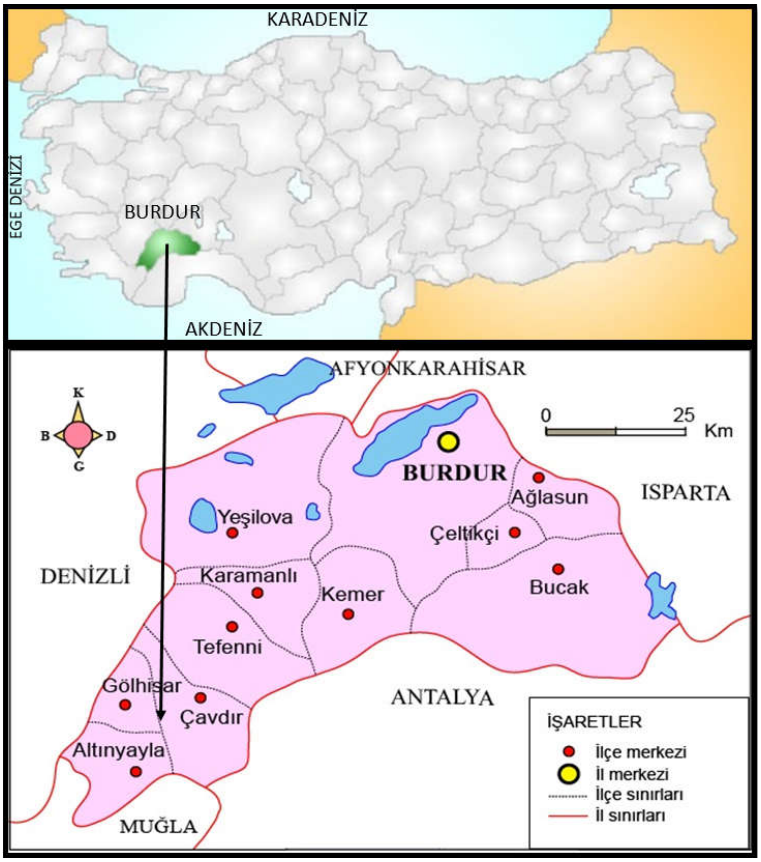

Şekil 1. Çalışma alanına ait yer bulduru haritası

Mermer Ruhsat alanı engebeli dağlık alan içerisindeki iki derin vadinin birleşim yerinde bulunan iki tepe ve bu iki tepeyi birbirine bağlayan sırttan oluşmaktadır. Çalışma alanının etrafı engebeli dağlık bir jeomorfolojik topoğrafya sunmaktadır. Bu yüksek topoğrafya arasındaki derin vadilerin içerisinde oluşmuş taban düzlüklerinde tarımsal faaaliyet yapılabilecek alan bulunmamasından dolayı her hangi bir tarımsal

faaliyet yapılmamaktadır. Dar düzlük ve hafif eğimli tepe ve dağ eteklerinde dağınık olarak küçük baş besi alanları bulunmaktadır.

Çalışma alanı ve yakın çevresinde engebeli bir yapının hakim olduğu, dağ ve tepelerin uzanımının genellikle kuzey-güney yönünde uzanım gösterdiği ve bu uzanıma paralel olarak gelişim gösteren vadiler boyunca eğimin azaldığı yöne doğru kuru dere yataklarının geliştiği görülmektedir (Şekil 2).

Çalışma alanı yaklaşık olarak 1000-1350 m. kotları arasında değişen yükseltilere sahiptir. Tepe ve sırt morfolojisinin egemen oldugu çalışma alanının güneyinde yüzeysel akışlar topografik eğim yününde tepe yamaçlarında görülmektedir. Çalışma alanı ve bu alanının doğu ve batı kesimlerinde jeomorfolojik yapıyı oluşturan hakim unsurlar, tepeler ve bu tepelerden başlamak üzere kuzeybatı-güneydoğu doğrultusunda uzanan sırtlardır. Mermer ocak alanına ulaşım, çalışma alanının güneyinde bulunan Kozağacı Köyü'nden gelen stabilize yol sağlanmaktadır.

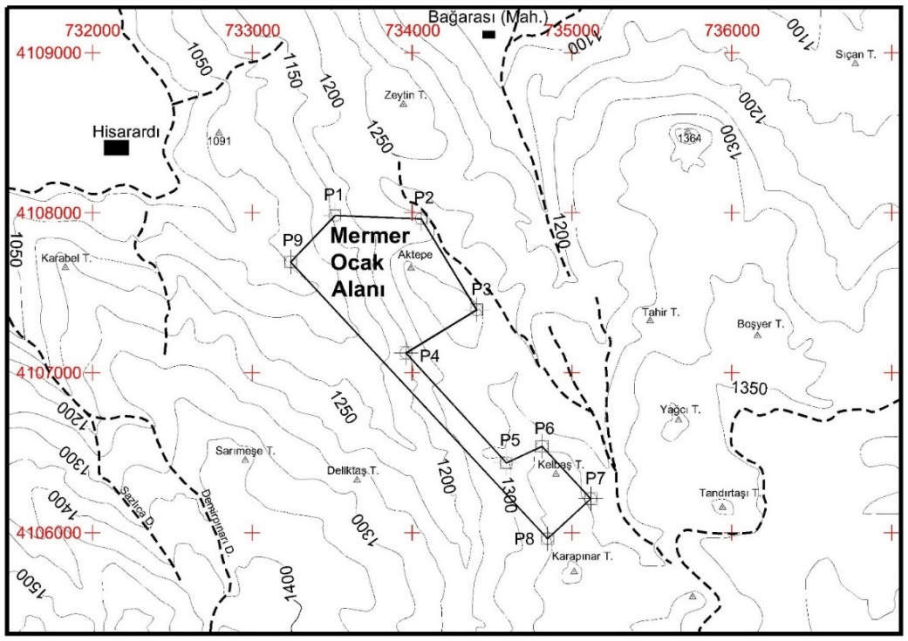

Şekil 2. Çalışma alanının topoğrafik haritası

İklim; Göller Bölgesi olarak da bilinen ve Akdeniz bölgesinin batısında yer alan Burdur İli, içerisinde birçok göl, gölet ve barajın bulundurmaktadır. Dolayısıyla yüzey ve yeraltı suları açısından önemli bir potansiyele sahiptir. İlin doğal yapısı engebeli olmakla beraber 950 m üzerindedir ve ortalama yukseltisi 1000 m'dir. İlin iklim özellikleri sahip olduğu ortalama rakımdan dolayı Akdeniz ikliminden farklılık göstererek, karasal iklime geçiş özellikleri taşımaktadır. Fakat özellikle güney kesimlerinde Akdeniz iklimi daha belirgin iken kuzey kesimlerinde karasal iklim daha baskındır. Dolayısıyla Burdur İli'nin iklim özelliği kurak ve yarı kurak olarak sınıflandırılabilir. Burdur İli'nin en yağışlı ayı Aralık, en kurak ayı ise Ağustos ayı olup, ortalama yağış miktarı yılllık ortalama 426,9 mm'dir. Burdur İline ait (1932-2022) ölçülen meteorolojik istatistikler Tablo 1'de verilmiştir.

Tablo 1. Burdur İli'ne ait 1932-2021 yılları arası meteorolojik istatistikler (MGM, 2022)

BURDUR	Ocak	Şubat	Mart	Nisan	Mayıs	Haziran	Temmuz	Ağustos	Eylül	Ekim	Kasım	Aralık	Yıllık
Ortalama Sıcaklık (°C)	2,5	3,8	3,9	11,6	16,5	21	24,6	24,6	20,2	14,5	8,8	4,3	13,0
Ortalama En Yüksek Sıcaklık (°C)	6,7	8,8	12,6	17,8	23,1	28	31,9	32,2	27,9	21,5	14,4	8,4	19,4
Ortalama En Düşük Sıcaklık (°C)	-0,9	-0,3	1,9	6	10,2	13,9	17	16,9	12,9	8,4	4,1	0,9	7,6
Ortalama Güneşlenme Süresi (saat)	3,8	5	5,9	7,1	9	10,8	11,8	11	9,2	7,2	5,5	3,3	7,5
Ortalama Yağışlı Gün Sayısı	10,29	8,82	10,24	8,94	10,65	9,71	3,35	4	4,24	7,35	5,82	9,29	7,7
Aylık Toplam Yağış Ort. (mm)	56,7	41,0	44,9	42,4	45,1	29,2	13,1	9,5	15,7	32,2	36,4	60,7	426,9
En Yüksek Sıcaklık (°C)	16,8	23,4	27,8	30,7	35,4	38,7	41,0	41,0	39,0	32,7	26,5	20,5	41,0
En Düşük Sıcaklık (°C)	-16,7	-15	-11,6	-7	-0,4	3,8	9	8,8	3,4	-2,4	-12	-15,3	-16,7

Yağış; Yıllık ortalama 426,9 mm yağış alan Burdur İli'ne, en çok yağış düşen aylar Aralık ve Ocaktır. Yani en fazla yağışı aylık ortalama 60,7 mm olmak üzere Kış aylarında alır. Buna karşın en az yağışı ise aylık ortalama 9,5 mm ile Ağustos ayında görülmektedir. İl genelinde yağış rekoru Burdur Merkez'de 2009 yılında 800 mm olarak ölçülmüştür.

Sıcaklık; Burdur İli'nin yıllık sıcaklık ortalaması güney ilçelerinde daha fazla ve kuzey ilçelerinde daha az olmak üzere 13,0 ^{0}C dir. En soğuk ay ortalaması 2,5 ^{0}C ile Ocak ayı, en düşük sıcaklık ortalaması -0,9 ^{0}C ile yine Ocak ayında gerçekleşmiştir. En sıcak ay ortalaması 24, ^{0}C ile Temmuz ve Ağustos, en yüksek sıcaklık ortalaması ise 32,2 ^{0}C ile Ağustos ayında ölçülmüştür. Tarihinde en düçük sıcaklık Ocak ayında -16,7 ^{0}C ve en yüksek sıcaklık ise Temmuz ayında 41 ^{0}C olarak ölçülmüştür.

JEOLOJİ

Çalışma kapsamında oluşturulan mermer ocak alanı ve yakın çevresinin 1/25.000 ölçekli genel jeoloji haritası ve bölgesel jeolojiyi aydınlatmak amacıyla Isparta Büklümü'nü içine alan genelleştirilmiş jeoloji haritası ilgili bölümlerde verilmiştir. Yeşilbarak napı, aşağıdan yukarıya doğru Gömbe ve Yavuz birimleri olarak farklı yapısal istiflerden oluşmaktadır. Elmalı formasyonu Gömbe birimini ile temsil etmektedir. Elmalı formasyonu Beydağları otoktonu ve Likya naplarının arasında süreklilik göstermektedir. Tektonik olarak Yeşilbarak napını üzerlemiş olan Likya napı, bölgede farklı naplar ile (Bodrum, Marmaris ofiyolit, Domuzdağı, Gülbahar ve Tavas napı) temsil edilir.

Marmaris ofiyolit napı, Kızılcadağ ofiyolitik melanjı ve olistostromları ile Marmaris peridoti ile tanımlanır. Jura Kretase yaşlı Orhaniye formasyonu; çört, radyolarit, kalsitürbidit ve çörtlü kireçtaşlarından meydana gelir. Orhaniye formasyonu, Gülbahar napını ile temsil edilir. Çalışma alanındaki allokton konumlu bir başka birim olan Orta Triyas yaşlı Yuvadağı formasyonunu ise Domuzdağ napını temsil eder. Bölgedeki Kuvaterner yaşlı alüvyon ise neootokton örtü kayalarını temsil etmektedir.

Çalışma alanı ve çevresi için birimlerin litolojik özellikleri dikkate alınarak 5 temel birim ayırt edilecek genel jeoloji haritası hazırlanmıştır (Şekil 3). Genel jeoloji haritasında ayırt edilen birimler, otokton birim olarak Kuvaterner yaşlı güncel sedimanlardan oluşan Alüvyon, allokton birimler ise Marmaris peridotiti, Kızılcadağ melanj ve ofiyoliti ile bu birimin için olistostrom konumlu olarak yer alan Yuvadağ ve Orhaniye formasyonlarıdır. Alüvyon ile Marmaris peridotiti arasında uyumsuz bir dokanak bulunmakla birlikte, Marmaris peridotiti ve Kızılcadağ ofiyolitik melanjı arasında ise bindirmeli bir dokanak bulunmaktadır.

Alüvyon (Qal); Çalışma alalnı ve yakın çevresindeki Alüvyon yelpazesi, birikinti konisi, yelpaze deltası, göl ve akarsu sekileri Kuvaterner yaşlı güncel çökelimler birer jeomorfolojik birim oluşturduklarından dolayı, "jeomorfolojik birimler" olarak ayırt edilerek ayrıca ele değerlendirilebilir. Çalışmanın amacı gözönüne alındağında Kuvaterner yaşlı birimlerin çalışma alanının kuzeybatı bölümünde dar bir alanda yüzeylenmelerinden dolayı Alüvyon olarak ayırtedilmiş ve haritalanmıştır.

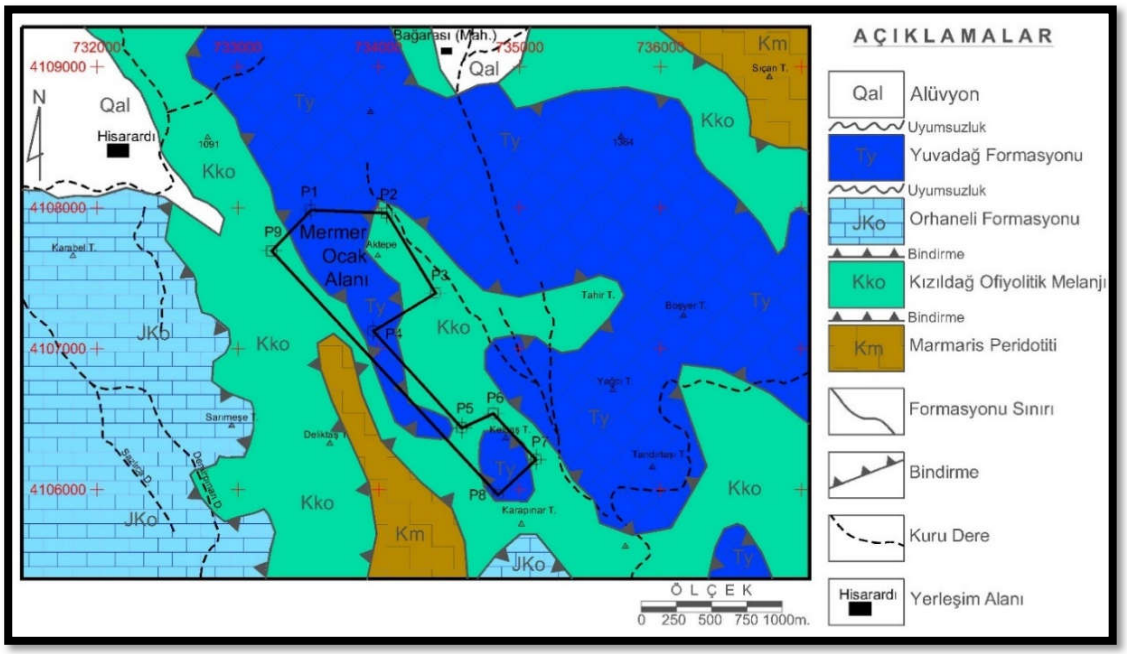

Şekil 3. Çalışma alanının genel jeoloji haritası

Kızıldağ Ofiyolitik Melanji (Kko); Kızıldağ Ofiyolitik Melanjı, Koçyigit (1981) tarafından "İç Toros Napı" olarak ta adlandırılan Allokton kökenli birimdir.

Bu karmaşık harzburjit, gabro, spilit ve serpantinden meydana gelen bazik ve ultrabaziklerle beraber kireçtaşı bloklarının yığışımından meydana gelir. Birimin Burdigaliyen sonrasında nap olarak bölgeye tektonik olarak yeleşmiştir. Birim özellikle bölgede Burdur Gölünün kuzeybatısında çakıltaşı, Miyosen birimler üzerinde ve havzada Pliyosen çökellerin altında bulunduğu tespit edilmiştir (Bilgin vd., 1990). Ofiyolit ve içerisindeki olistostromal konumlu kireçtaşı bloklarından oluşan melanj özellikli birimi Poisson (1977) isimlendirmiştir. Birim, nispeten peneplen morfoloji gösteren bölümlerde volkanik kökenli birimler ve serpantinitten meydana gelir (Döğen, 1992). Birim, bölgede ve özellikle çalışma alanının tam ortasında kuzeybatı-güneydoğu yönünde bir uzanım sunmaktadır.

Orhaneli Formasyonu (JKo); Gülbahar napı ile temsil edilen formasyon çörtlü mikrit ve radyolarit seviyelerini içerir. Birim, çalışma alanının batısında yer alır ve Hisarardı Köyünün güneyinden itibaren güneye doğru yayılım göstermektedir.

Birimin alttan üste doğru istifi, koyu renkli, oolitik kireçtaşından başlayıp, çört, radyolarit, pelajik kökenli kireçtaşı ve türbiditik kökenli kireçtaşı şeklinde devam eder. Birim gri, krem, kirli sarı renkli, kıvrımlı, bazen volkanit ve çört-radyolarit düzeyli mikritlerden meydana gelir. Açık renkli ve orta kalın tabakalı dolomitik kireçtaşları çok yaygın olmasa da Orhaniye formasyonu içerisine zaman zaman tespit edilmiştir (Şenel vd., 1989).

Yuvadağ Formasyonu (Ty); Şenel vd. (1989) tarafından adlandırılmış olan birim neritik kireçtaşı ve dolomitik kireçtaşlarından meydana gelir. Formasyon, çalışma alanı ve yakın çevresinde özellikle Gölhisar güneydoğusunda geniş alanlarda mostra vererek yayılım gösterir. Çalışma alanının ortasında yer alan Kızıldağ ofiyolitik melanjı içerisinde tektonik bir dokanak ile yer almaktadır. Birim orta kalınıktaki tabakalı yapısı yanı sıra kalın ve masif görünümde sumaktadır. Birimin hâkim litolojisi açık renklerdeki kireçtaşı, rekristalize kireçtaşı ve dolomitik karakterdeki kireçtaşlarından oluşmaktadır. Birimi karakterize eden en önemli özelliği, çok fazla sayıda algli içeren ve seyrek olarak gastrapod ile megaladon izlerine sahip çatlaklı yapısıdır.

HİDROLOJİ

Faaliyet alanının kuzeybatı yönünde 3200 m mesafede Gölhisar Gölü bulunmaktadır. Faaliyet alanının kuzeydoğu yönünde kuş uçumu 7200 m Bayındır Dere'si ve batı yönünde 8400 m mesafede Dalamana Çayı bulunmaktadır. Bölgede vadi tabanlarında ve düzlük alanlarda genelde mevsimsel olarak akış özelligi gösterebilen dere yataklarının mevcutiyeti topoğrafik harita üzerinden görülebilmektedir. Arazi çalışmalarının yapıldığı Kasım ayında bu derelerin bir çogunda su varlığına rastlanılmamıştır. Yıl içerisinde çoğunlukla kuru olan bu derelerden işletme aşamasında su kullanımı söz konusu değildir. Çalışma alanı büyük ölçüde drenaj yapılmasına uygun eğime sahiptir. Çalışma alanı ve civarındaki yer alan dereler ve kuru dereler çalışma alanının topoğrafik haritası (Şekil 2) ve hidrojeoloji haritasında (Şekil 4) belirtilmiştir.

Gölhisar Ovası içerisinde devamlı akışa sahip en önemli yüzeysel akış unsurları Aksu deresi, Bayındır çayı, Değirmen deresi ve Kocapınar deresidir. Bu derelerin düzenli akım rasat ölçümleri maalesef bulunmamaktadır. Ayrıca mevsimsel olarak düşen yağış miktarına bağlı olarak akışa çok sayıda dere bulunmaktadır. Ovada bulunan bu yüzeysel akış elemanları havza içerisinden akışa geçip yine havza içerisine boşalmaktadır (Yılmaz, 2015).

Yılmaz (2015) tarafından Gölhisar ovası için hidrolojik bütçe elemanları tek tek analiz edilerek emniyetli kullanılabilir yeraltı suyu potansiyeli hesaplanmıştır. Gölhisar Ovası'nın en önemli beslenim elemanı yağış olup, ova için eş yağış eğrileri yöntemi kullanılarak ortalama yağış miktarı 577.10 mm ve bu ortalama yağıştan beslenim miktarı 868.35 x 106 m^3/yıl olarak belirlenmiştir (Yılmaz, 2015).

HİDROJEOLOJİ

Çalışma alanı ve yakın çevresinde yer alan su noktaları; mevsimsel akışa geçen kaynaklar, sondaj ve keson kuyular, göletler, mevsimlik ve sürekli yüzeysel akışlardan oluşmaktadır. Çalışma alanı yakın çevresinde sürekli yüzeysel akışları; Aksu deresi, Bayındır çayı, Değirmen deresi ve Kocapınar deresi oluşturmaktadır. Bu akarsular havzanın en önemli yüzeysel akış olan Dalaman Çayı'na boşalmaktadır.

Dalaman Çayı; Boncuk Dağlarının kuzey yamaçlarındaki kaynaklardan doğan Dalaman Çayı, kuzeydoğu yönünde Gölhisar çukurluğuna doğru akışa geçer. Doğu ve batı yönlerinden akışa geçen yüzeysel akışlarla beslenen Dalaman Çayı Muğla il sınırlarındaki Dalaman Ovasına doğru akışına devam ettirir. Dalaman Çayının denize yaklaştıkça hakim olan peneplen morfoloji akışı giderek yavaşlamaktadır. Sonunda Dalaman Çayı, Sarısu civarında sığ bir bataklıkla formundaki alandan denize dökülür. (İÇDR, 2012).

Gölhisar Gölü; Yaklaşık olarak 7 km^2'lik yüz ölçümüne sahip olan Gölhisar Gölü, tektonik kökenli oluşuma sahip çukurluğun Dalaman Çayı alüvyonları tarafından önünün kapatılması ve sonrasında bu çukur alanın suyla dolması sonucunda meydana gelmiştir. Sığ bir göl olan Gölhisar Gölü'nün beslenme alanı daha çok diptendir. Gölün en derin noktası ise yaklaşık 6 m ile güneydeki Karaburun civarındadır. Deniz seviyesinden yüksekliği 931 m olan gölün kuzeydoğu kısmındaki yer alan bir kanal vasıtası ile fazla suları Dalaman çayına bırakılmaktadır.

Yapraklı Barajı; Dalaman Çayı üzerine 1991 yılında yapımı tamamlanmış olan baraj Gölhisar-İbecik su yolu üzerinde Kısık mevkiinde civarında yer alır. Baraj gölünün beslenimi, civardaki yüksek dağlardan gelen yağış sularıyla gerçekleşmektedir. Geniş bir su toplama havzasını alanına sahip olan Yapraklı Barajını besleyen çok sayıda yüzeysel akış bulunmaktadır. Bu yüzeysel akışlar; Altınyayla, Arıkaya, Ayvacık, Çameli, Darpak, Gürsu, İbecik, İmamlar, Kalaklar, Pırnaz, Yeşildere'deki tüm dere ve çaylardır. Sulama amaçlı olarak inşa edilenb Yapraklı Baraj ile Gölhisar ve Acıpayam ovasında yaklaşık olarak 2000 ha alanda sulu tarım yapılmaktadır. Gölhisar ovası ve yakın çevresinde özellikle alüvyon ortamda tarımsal sulama amaçlı açılmış sondaj kuyuları bulunmaktadır. Ovada özel kişilere ait sondaj ve sığ kuyu olmak üzere toplam 653 fazla kuyu bulunmaktadır (Yılmaz, 2015).

Litolojik Birimlerin Hidrojeolojik Özellikleri; Çalışma alanı ve yakın çevresinde bulunan jeolojik birimler fiziksel özellikleri ve akifer olabilme potansiyelleri dikkate alınarak hidrojeoloji haritası hazırlanmıştır (Şekil 4).

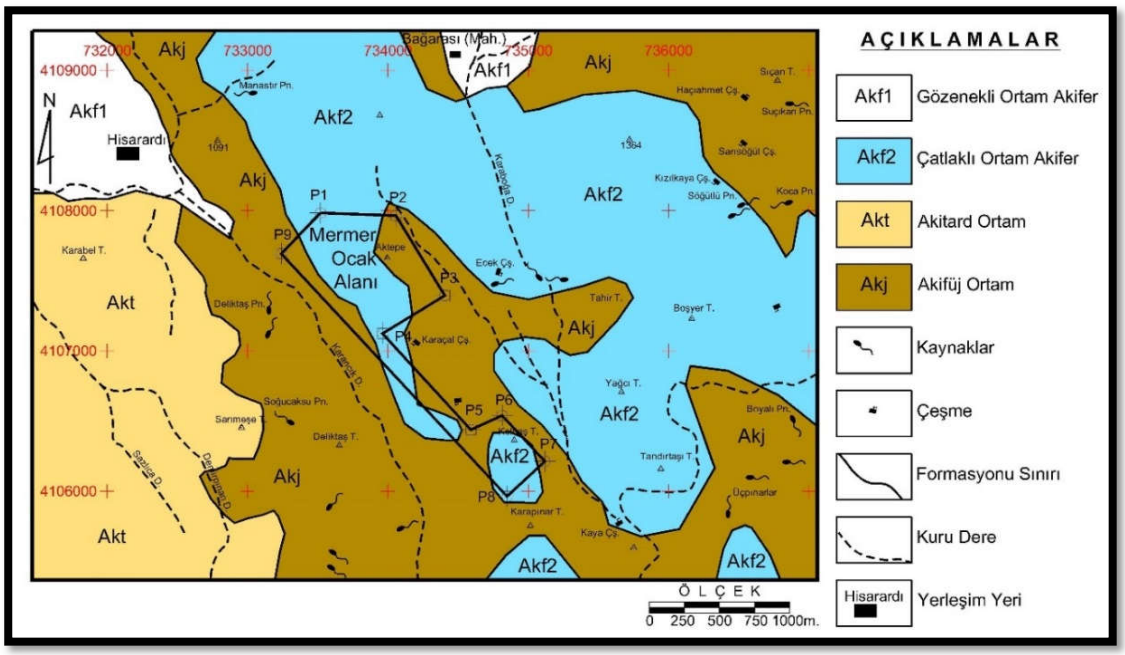

Şekil 4. Çalışma alanının hidrojeoloji haritası

Buna göre hidrojeolojik ortamlar; gözenekli ortam akiferi (Akf-1), çatlaklı kaya ortam akiferi (Akf-2), akitard ortam ve akifüj ortam (Akj) olarak sınıflandırılmıştır. Çalışma alanı kuzeyinde yüzeyleyen alüvyon ***Gözenekli Ortam Akiferi*** (Akf-1), Yuvadağ ormasyonu ***Çatlaklı Kaya Ortam Akiferi*** (Akf-2), Orhaniye formasyonu ***Akitard Ortam*** (Akt), Kızılcadağ ofiyolitik melanjı ile Marmaris peridotiti v ***Akifüj Ortam*** (Akj) olarak ayırtlanmıştır.

Gözenekli Ortam Akifer (Akf1); Gölhisar Ovasında daha geniş bir yayılıma sahip olan Alüvyon inceleme alanında kuzeyinde yüzeylenen ve verimi fazla olan taneli ortam akiferini temsil etmektedir. Çimentolanmamış ve gevşek tutturulmuş farklı boyutlardaki sediman yığışımından oluşan litolojiye sahip birim özellikle çakıl ve kum içeriklerinin arttığı seviyelerinde yeraltı suyu taşıdıklarından çalışma alanının en önemli akiferini oluşturmaktadır.

Çatlaklı Kaya Ortam Akiferi (Akf2); Çalışma alanında yer alan Yuvadağ formasyonu ***Çatlaklı Kaya Ortam Akiferi*** olarak tanımlanmıştır. Birimi oluşturan kireçtaşlarının, süreksizlik düzlemlerindeki boşluklarında yeraltı suyu taşıyabilen bir yapıa sahiptir. Kireçtaşlarının kalınlıkları ve süreksizliklerinin yoğunluğu, dolgu durumu ve kesişme durumları gibi özelliklerine bağlı olarak değişmekle birlikte önemli miktarlarda yeraltı suyu üretimi yapılabilmektedir. Çatlaklı Kaya Ortam Akikeri, çalışma alanı içerisinde ise kuzeybatı-güneydoğu boyunca çalışma alanın tam ortasından geçecek şekilde bir yayılım sunmaktadır.

Akitard Ortam (Akt); Çalışma alanında yayılımı kısıtlı olan ve su bulundurma açısından çok yavaş su geçirme özelliğine sahip yarı geçirimli özellik sunan Orhaniye formasyonları Akitard Ortam olarak ayırtlanmışlardır. Birim içerisindeki dolomitik kireçtaşlarında az miktarda su taşıma özelliğine sahipken; çört, şeyl, radyolarit ve volkanitlerin su taşıma özelliği bulunmamaktadır (Yılmaz, 2015).

Akifüj Ortam (Akj); Kızılcadağ ofiyolitik melanjı ve Marmaris Peridotiti birimi geçirimsiz özelliğe sahip ***Akifüj Ortam*** olarak ayırtlanmıştır. Kızılcadağ ofiyolitik melanjı geçirimsiz birimlerden oluşmakta, içerisindeki olistostrom konumlu konglomera, kiltaşı, silttaşı ve kumtaşı bulundurmaktadır. Birim içinde bulunan kireçtaşları kısıtlı su taşıma kapasitesine sahip olmasına rağmen bulundukları konumdan dolayı yeraltı suyunu iletebilecek özellik taşımamaktadır.

Yüzey ve Yeraltı Sularının Etkileşimi; Proje sahasında yapılan arazi etüdü sırasında ve yapılan araştırmalarda ruhsat sahasının özellikle kuzeyinde ve güneydoğusunda küçük debili mevsimsel kaynak noktaları tespit edilmiştir. Yağışlı aylar dışında bu kaynakların çoğundan boşalım olmamaktadır. Bölgede yol

kenarlarında, yerleşim merkezleri içinde ve bazı vadilerin tabanlarında çeşmeler mevcuttur. Bu çeşmeler çoğunlukla hayvanların su ihtiyacı için kullanılmaktadır.

Yılmaz (2015) tarafından yapılan araştırmada, Gölhisar Ovası'nda alüvyon, kireçtaşı ve konglomera litolojilerinden yeraltı suyu üretimi yapıldığı ve çalışma alanında yeraltı suyu akım yönünün ovanın güneyine doğru olduğu tespit edilmiştir. Ayrıca ovada yeraltı suyu seviyesi 960-1644 m arasında; yeraltı suyunun yüzeyden derinliği ise 4–57 m arasında tespit edilmiştir.

Ocak sahasında yapılacak madencilik faaliyetleri sırasında patlayıcı kullanımı söz konusu değildir. Bu nedenle ocak işletme sahasına yakın sondaj kuyularının ocak sahasındaki maden üretim çalışmalarından fiziksel olarak titreşim ve sarsıntı gibi nedenlerden olumsuz etkilenmeyeceklerdir. Doğal malzeme sınıfında yer alan mermer malzemesinin kazılması ve nakliyesi sırasında herhangi bir kimyasal işlem uygulanmayacak olması bölgede yer alan yeraltı ve yüzey su kaynaklarının kirlenme riskini ortadan kaldırmaktadır.

Ruhsat sahasının akifüj (geçirimsiz) ortam içerisindeki olistostrom konumlu çatlaklı kaya akiferi seviyelerden oluşması, alınacak olan sızdırmazlık ve drenaj tedbirleri ve işletme kotunun yeraltı suyu seviyesinin çok üzerinde olması ve mermer çıkarılması sırasında patlayıcı madde kullanılmaması nedenlerinden dolayı, inceleme alanında kuyuların ve kaynakların olumsuz etkilenmesi ihtimali büyük ölçüde ortadan kalkmaktadır. Dolayısıyla çatlaklı kaya akifer özelliğindeki ocak sahasının etrafı tamamen geçirimsiz karakterdeki akifüj ortam tarafından sarılması, bir başka ifade ile akifüj ortam içindeki yerel olistostrom konumlu mermer ocağından kaynaklanacak her hangi bir kirletici sızıntısının yeraltı suyuna karışma ihtimali hidrojeolojik olarak bulunmamaktadır.

İçme Suyu Kaynak ve Kuyuları İle Etkileşim; Mermer ocağı işletme aşamasında, ocak sahasında herhangi bir kimyasal işlem yapılmayacak olması ve mermerin doğal hammadde sınıfında bulunması nedeniyle kimyasal-tehlikeli risk oluşturmayacak olması, su kaynaklarının kirlenmesi riskini alınacak olan tedbirlerle de büyük ölçüde azaltmaktadır.

Ocak işletmeciliği sırasında içme suyu hatlarına ve depolarına herhangi bir müdahale olmamalı, ocak sahası içerisinde veya yakın civarında büyük su birikintilerinin oluşması engellenmelidir. Madencilik faaliyetleri sırasında oluşabilecek su birikintileri ve yağışlar sonrasında ocak sahasından yapılacak su tahliyesi topoğrafik eğim ve su noktaları dikkate alınarak, yüzey ve yeraltı su noktalarının olumsuz etkilenmeyeceği şekilde kaynaklara ters yönde yapılmalıdır.

İşletme sahasının su noktalarına olan mesafesi ve işletme taban kotunun yeraltı ve yüzey sularının kotlarının üzerinde bırakılması, ruhsat sahasını oluşturan birimlerin yarı geçirimli yapıda olmaları ve işletmecilik sırasında kirlilik ve atık ölçümü konusunda alınacak tedbirlerle de içme suyu kaynaklarının ocak sahası ve eleme tesisi işletmeciliğinden olumsuz etkilenmemesi sağlanmalıdır.

SONUÇ

Çalışma alanı ve çevresi için birimlerin litolojik özellikleri dikkate alınarak 5 temel birim ayırt edilecek genel jeoloji haritası hazırlanmıştır. Otokton birim olarak Kuvaterner yaşlı güncel sedimanlardan oluşan Alüvyon, allokton birimler ise Marmaris peridotiti, Kızılcadağ melanj ve ofiyoliti ile bu birimin için olistostrom konumlu olarak yer alan Yuvadağ ve Orhaniye formasyonları ayırt edilerek genel jeoloji haritası hazırlanmıştır. Alüvyon ile Marmaris peridotiti arasında uyumsuz bir dokanak bulunmakla birlikte, Marmaris peridotiti ve Kızılcadağ ofiyolitik melanjı arasında ise bindirmeli bir dokanak bulunmaktadır.

Hidrojeoloji bölümünde; su noktaları, litolojik birimlerin hidrojeolojik özellikleri, akifer ortamlarının hidrojeolojik özellikleri, yeraltı suyu dinamiği, su kimyası ve su kaynaklarının hidrojeolojik etkileşimleri açıklanmıştır. Su kaynaklarının hidrojeolojik etkileşimi başlığı, yüzey ve yeraltı sularının etkileşimi ve içme suyu kaynak ve kuyularının ile etkileşim olmak üzere iki alt konu başlığında açıklanmıştır.

Çalışma alanı kuzeyinde yüzeyleyen alüvyon ***Gözenekli Ortam Akiferi*** (Akf-1), Yuvadağ formasyonu ***Çatlaklı Kaya Ortam Akiferi*** (Akf-2), Orhaniye formasyonu ***Akitard Ortam*** (Akt), Kızılcadağ ofiyolitik melanjı ile Marmaris peridotiti v ***Akifüj Ortam*** (Akj) olarak ayırt edilerek hidrojeoloji haritası hazırlanmıştır.

Gölhisar Ovası'nda alüvyon, kireçtaşı ve konglomera birimlerinden yeraltı suyu alındığı, çalışma alanında yeraltı suyu akım yönünün güneye doğru olduğu tespit edilmiştir. Ovada yeraltı suyu tablasının rakımı 960-1644 m arasında; yeraltı suyunun yüzeyden derinliği ise 4–57 m arasında değişmektedir.

Ruhsat sahasının akifüj (geçirimsiz) ortam içerisindeki olistostrom konumlu çatlaklı kaya akiferi seviyelerden oluşması, alınacak olan sızdırmazlık ve drenaj tedbirleri ve işletme kotunun yeraltı suyu seviyesinin çok üzerinde olması ve mermer çıkarılması sırasında patlayıcı madde kullanılmaması nedenlerinden dolayı, inceleme alanında kuyuların ve kaynakların olumsuz etkilenmesi ihtimali büyük ölçüde ortadan kalkmaktadır. Dolayısıyla çatlaklı kaya akifer özelliğindeki ocak sahasının etrafı tamamen geçirimsiz karakterdeki akifüj ortam tarafından sarılması, bir başka ifade ile akifüj ortam içindeki yerel olistostrom konumlu mermer ocağından kaynaklanacak her hangi bir kirletici sızıntısının yeraltı suyuna karışma ihtimali hidrojeolojik olarak bulunmamaktadır.

Sonuç olarak; (i) mermer ocak işletmesinin yapılacağı litolojik birimin (olistostrom) geçirimsiz Kızılcadağ ofiyolitik melanjı içerisinde bulunması, (ii) işletme kotunun yeraltı suyu seviye kotunun çok üzerinde oluşu, (iii) işletme sahası ve yakın çevresinde işletmeden olumsuz etkilenebilecek kaynak ve içme suyu sondaj kuyusunun bulmaması, (iv) çalışma alanının jeomorfolojik yapısının yüzey ve yeraltı suları kirliliği açısından kapalı bir küçük havza özelliğinde olmasından göz önüne alındığında mermer ocak işletmesinin hidrojeolojik olarak olumsuz bir etkisinin olmayacağı sonucunda varılmıştır.

KAYNAKLAR

Alçiçek, M. C. (2001). Çameli Havzasının Sedimantolojik İncelemesi (Geç Miyosen-Geç Pliyosen, Denizli, GB Anadolu). Ankara: Ankara Üniversitesi, Fen Bilimleri Enstitüsü, Doktora Tezi.

Alçiçek, M. C., Veen, J. H., & Özkul, M. (2006). Neotectonic development of the Çameli Basin, southwestern Anatolia, Turkey. A. H. Robertson, & D. Mountrakis içinde, Tectonic Development of the Eastern Mediterranean Region (s. 591-611). London: Special Publications.

Barka, A., Reilinger, R., Saroğlu, F., & Sengor, A. M. (1997). The Isparta Angle: its importance in the neotectonics of the eastern Mediterranean region. International Earth Sciences Colloquium on the Aegean Region (IESCA- 1995) (s. 3-17). İzmir: Proceedings 1.

Bilgin, Z. R., Karaman, T., Öztürk, Z., Şen, M. A., & Şenel, M. (1990). Yeşilova-Acıgöl Civarının Jeoloji Raporu. Ankara: Maden Tetkik Arama Enstitüsü, MTA Rapor No:9071.

Çapan, U. (1980). Toros Kuşağı Ofiyolit Masifinin (Marmaris, Mersin, Pozantı, Pınarbaşı ve Divriği) İç Yapıları, Petrografisi ve Petrokimyalarına Yaklaşımlar. Ankara: Hacettepe Üniversitesi, Fen Bilimleri Enstitüsü, Doktora Tezi.

Döğen, A. (1992). Tefenni (Burdur) Civarının Jeolojisi ve Kromit Yatakları. Konya: Selçuk Üniverisitesi, Fen Bilimleri Enstitüsü, Yüksek Lisans Tezi.

Dumont, J. F., Uysal, Ş., Şimşek, Ş., Karamanderesi, I. H., & Leouzey, J. (1979). Güneybatı Anadolu'daki Grabenlerin Oluşumu. Maden Tetkik Arama Enstitüsü Dergisi,(97), 7-17.

Ekonomi Bakanlığı. (2021). Doğal Taş Sektörü (Sektör Raporları). Ankara: Ekonomi Bakanlığı, İhracat Genel Müdürlüğü Maden, Metal ve Orman Ürünleri Daire Başkanlığı. https://ticaret.gov.tr/data/5b87000813b8761450e18d7b/Do%C4%9Fal%20Ta%C5%9Flar%20Sekt%C3%B6r%20Raporu%202021.pdf adresinden alındı

Elitez, İ. (2010). Çameli ve Gölhisar Havzalarının Miyosen-Kuvaterner Jeodinamiği, Burdur-Fethiye Fay Zonu, GB Türkiye. İstanbul: İstanbul Teknik Üniversitesi, Yüksek Lisans Tezi.

Elitez, İ., Yaltırak, C., & Akkök, R. (2009). Morphotectonic Evolution of the Middle of Burdur-Fethiye Fault Zone: Acıpayam, Gölhisar and Çameli Area, SW Turkey. International Symposium on Historical Earthquakes and Conservation of Monuments and Sites in the Eastern Mediterranean Region 500th Anniver (s. 296-297). 10-12 September 2009, İstanbul: Proceedings.

İ.Ç.D.R. (2012). İl Çevre Durum Raporu-Muğla. Muğla: Muğla Valiliği, Çevre ve Şehircilik İl Müdürlüğü.

Koçyiğit, A. (1981). Isparta Büklümünde (Batı Toroslar) Toros Karbonat Platformunun evrimi. Türkiye Jeoloji Kurumu Bülteni, 24, 15-23.

MGM. (2022, 08 01). Meteoroloji Genel Müdürlüğü. Resmi İstatistikler (Burdur): https://www.mgm.gov.tr/veridegerlendirme/il-ve-ilceler-istatistik.aspx?m=BURDUR adresinden alındı

Poisson, A. (1977). Recherches geologique dans les Taurides occidentales these doct. d'etat orsay. N.1902.

Price, S. P., & Scott, B. (1994). Fault-block rotations at the edge of a zone of contiental extension, SW Turkey. J. Struct. Geol.(16), 381-392.

Sarıkaya, A. R., & Seyrek, T. (1976). Yeşilova-Tefenni Peridotit Masifindeki Krom ve Nikel zenginleşmeleri projeksiyon raporu. Ankara: Maden Tetkik Arama Enstitüsü, MTA Rapor No:5764.

Şenel, M., Selçuk, H., Bilgin , Z. R., Şen, A. M., Karaman, T., Dinçer, M. A., . . . Bilgi, C. (1989). Çameli (Denizli)- Yeşilova (Burdur)- Elmalı (Antalya) ve kuzeyinin jeolojisi. Ankara: Maden Tetkik Arama Enstitüsü Rapor No:9429 (yayımlanmamış).

Thuizat, R., Whitechurch, H., Montigny, R., & Juteau, T. (1981). K-Ar Dating of Some İnfra-Ophiolitic Metamorphic Soles from the Eastern Mediterranean. New İvidence for Oceanic Thrusting Before Obduction Earth Planet. Sci. Lett.(52), 302-310.

Yalçınkaya, S., Ergin, A., Taner, K., Afşar, P. Ö., Dalkılıç, H., & Özgönül, E. (1986). Batı Toroslar'ın jeoloji raporu. Ankara: Maden Tetkik Arama Enstitüsü Rapor No:7898 (Yayımlanmamış).

Yılmaz, E. İ. (2015). Gölhisar (Burdur) Ovasının Hidrojeoloji İncelemesi. Isparta: Süleyman Demirel Üniversitesi, Fen Bilimleri Enstitüsü, Yüksek Lisans Tezi.

YERALTI BARAJLARINDA İŞLETME, İZLEME VE KORUMA NASIL OLMALI: TEKNİK, KURUMSAL VE YASAL YÖNLERİYLE BİR DEĞERLENDİRME

HOW TO OPERATE, MONITOR AND PROTECT UNDERGROUND DAMS: AN EVALUATION OF TECHNICAL, INSTITUTIONAL AND LEGAL ASPECTS

Ahmet APAYDIN

Giresun Üniversitesi, Mühendislik Fakültesi, İnşaat Mühendisliği Bölümü, Giresun-Türkiye.

ORCID NO: 0000-0002-6437-7208

ÖZET

Yeraltı barajlarının yerüstü barajlarına göre buharlaşma kaybının ve arazi işgalinin olmaması, kirlenmeye ve başka dış etkilere karşı daha güvenli olması gibi önemli avantajları bulunmaktadır. Ayrıca yeraltısularının kuraklıklara karşı yerüstü sularına göre daha geç tepki vermesi ve böylece kurak dönemlerde yerüstü kaynaklarının azalmasıyla meydana gelen su açığını kapatması yeraltı barajlarının diğer olumlu bir özelliğidir. Bu nedenle ülkemizin özellikle yarı kurak bölgelerinde su ve gıda ihtiyacının sürdürülebilir bir şekilde karşılanabilmesi için yeraltı barajı ve yeraltısuyu yapay besleme yöntemlerinin uygulanmasına ihtiyaç bulunmaktadır. Ancak bu tür projelerden başarılı sonuçlar elde edilebilmesi için sadece yer seçiminin uygun, planlama ve projenin optimum, inşaatın projeye uygun bir şekilde arzu edilen standart ve kalitede yapılması yetmemekte, işletme süresince izleme, bakım-onarım, yönetim ve koruma çalışmalarının eksiksiz yapılması gerekmektedir. Ülkemizde 2000'li yılların başlarında Ankara, Kırıkkale, Çorum, Eskişehir, Elazığ gibi yarı kurak bölgelerde az sayıda da olsa yeraltı barajları inşa edilmiştir. Devlet Su İşleri Genel Müdürlüğü tarafından 2019-2023 dönemini kapsayacak şekilde uygulamaya konulan Yeraltı Barajları Eylem Planı'yla ülkemizde çok sayıda yeraltı barajı ve yeraltısuyu yapay besleme yapısının inşa edilmesi nedeniyle konu daha da önem kazanmıştır. Sel nedeniyle gövde ve diğer yapıların hasar görmemesi için akarsu yatak düzenlemesi ve gerekiyorsa baraj havzasında sediment depolama yapıları inşa edilmesi gibi çeşitli önlemlerin alınması, su alma yapısı, kuyular ve yapay besleme yapılarının siltasyonla tıkanmasına karşı önlemler alınarak durumu işletme süresince izlenmesi, baraj rezervuarında su seviye değişimi, debiler ve kirleticilerin etkisinin işletme boyunca izlenmesi gerekir. Ayrıca hem barajın, hem de yeraltısuyu kaynağı dikkate alınarak koruma sınırlarının belirlenmesi ve Resmi Gazete'de ilan edilmesi ve koruma hükümlerinin uygulanması son derece önemlidir.

Anahtar Kelimeler: Yeraltı barajı, Yapay besleme, İşletme, İzleme, Koruma.

ABSTRACT

Underground dams have important advantages over surface reservoirs such as no evaporation losses and no land occupations, being safer against pollution and other external effects. In addition, another positive feature of underground dams is that groundwater responds to droughts later than surface waters and thus eliminates the water deficit that occurs in surface resources during dry periods. For this reason, there is a need to implement underground dam and groundwater artificial recharge methods in order to ensure sustainable water and food security, especially in semi-arid regions of our country. However, in order to achieve successful results, it is not enough to choose the appropriate site, plan and project optimally, and the construction to be done in the desired standard and quality in accordance with the project, but it is necessary to carry out the monitoring, maintenance-repair, management and protection works in the next operation phase. In our country, in the early 2000s, some underground dams were built in semi-arid regions such as Ankara, Kırıkkale, Çorum, Eskişehir and Elazığ, albeit in small numbers. This issue has become more importance due to the construction of many underground dams and groundwater artificial recharge structures

in our country within the scope of the Underground Dams Action Plan to be implemented in the 2019-2023 period, which was implemented by the General Directorate of State Hydraulic Works. In order to prevent the structures from being damaged due to flooding, stream bed arrangement and, if necessary, construction of sediment storage structures is essential. On the other hand, water intake structures, wells and artificial recharge structures should be monitored by taking precautions against clogging with siltation, water level change in the dam reservoir, flow rates and the effects of pollutants should be monitored throughout the operation. In addition, it is extremely important to determine the protection limits by considering both the dam and the groundwater source, to be announced in the Official Gazette and to apply the protection provisions.

Keywords: Underground dam, Artificial recharge, Operation, Monitoring, Protection.

1. GİRİŞ

Yeraltı barajları ve yeraltısuyu suni besleme yapıları birkaç yıldır Türkiye'nin gündemindedir. Tarım ve Orman Bakanlığı'na bağlı Devlet Su İşleri (DSİ) tarafından "Cumhuriyetin Yüzüncü Yılında Yüz Yeraltı Barajı" sloganıyla 2019 yılında uygulamaya konulan "Yeraltı Barajları Eylem Planı" kapsamında yeraltı barajları kuraklığa karşı bir çözüm olarak sunulmaktadır. Projede yeraltı barajları ile birlikte yeraltısuyu yapay besleme projeleri de yer almaktadır. Başlangıçta yüz adet olarak planlanan sayı 2022 yılı Ocak ayı itibariyle 150'ye ulaşmış ve yetkililerce 60 adedinin tamamlandığı bildirilmiştir.

Türkiye'de geçtiğimiz yüzyılın ikinci yarısında içme ve sulama amacıyla bazı küçük yeraltı barajları (Apaydın vd., 2005), 2000'li yıllarda ise daha büyük ve daha işlevsel yeraltı barajları inşa edilmiştir (Apaydın 2009; Apaydın 2014; Apaydın vd. 2015). Yahşihan ve Bahşılı (Kırıkkale), Malıboğazı (Ankara), İskilip (Çorum), Baskil (Elazığ) ve Sancar (Eskişehir) yeraltı barajları bunlardan en çok bilinen örneklerdir (Apaydın, 2014). 2013 yılında hizmete giren Elmadağ-Kargalı (Ankara) barajı hem yerüstü, hem de yer altı depolaması olmasıyla (Apaydın ve Zengin, 2016) ülkemizde bilinen ilk denemedir.

Türkiye'de Yeraltı Barajları Eylem Planı'ndan önce az sayıda da olsa yeraltısuyu yapay besleme tesisleri de inşa edilmiştir. Ceylanpınar Ovaları Sulama Projesi (Güneydoğu Anadolu Bölgesi) bünyesinde yer alan 13 yeraltısuyu yapay besleme barajının planlama ve kesin proje çalışmaları 2013 yılında yapılmıştır. İki barajın (Cudi ve Büyük Cırcıp) yapımına 2013 yılında başlanmış ve 2015 yılında tamamlanmıştır (Ali ve Doğan, 2017). Diğer barajlar yeraltı suyu besleme ve taşkın kontrolü amaçlıdır (Apaydın, 2022).

Ülkemizin özellikle yarı kurak bölgelerinde su ve gıda ihtiyacının sürdürülebilir bir şekilde karşılanabilmesi için büyük ve klasik su depolama yapılarıyla birlikte yeraltı barajı ve yeraltısuyu yapay besleme tesisleri gibi alternatif projelere ihtiyaç bulunmaktadır. Yeraltısularının uzun süren kuraklıklardan yerüstü rezervuarlarına göre daha geç ve genellikle daha az etkilenmesi ve böylece kurak periyotlarda yerüstü kaynaklarında meydana gelen su açığını kapatması önemli bir hususdur. Buharlaşma kayıpları ve kirlenme yönüyle de yerüstü rezervuarlarına göre daha güvenli olması önemli avantajıdır.

Yeraltı barajlarının yer seçimi, elde edilecek su miktarının hesaplanması, potansiyelin meteorolojik koşullara göre değişiminin analizi, en uygun su alma yönteminin seçimi, barajın projelendirilmesi ve inşaatı uzmanlık gerektiren özel bir alandır. Yeraltı barajları ve yeraltısuyu yapay besleme projeleri konusunda yukarıda belirtilen hususlara ek olarak, inşaat tamamlandıktan sonra, başka bir ifadeyle işletme evresinde yapılacak işler ve alınması gereken önlemler başlı başına bir konudur. İzleme, koruma ve yönetim konularında yerüstü barajlarından farklı, kendine özgü çalışmalara ihtiyaç bulunmaktadır. İnşa etmekle iş bitmemekte, tesisten yüksek verimle uzun süreli hizmet alınabilmesi için ilave çalışmalar yapmak gerekir. Bilindiği kadarıyla Yeraltı Barajı Eylem Planı kapsamında tesislerin işletme evresiyle ilgili henüz bir hüküm bulunmamaktadır.

Bu bildiri, yeraltı barajlarında inşaat sonrasında yapılabilecek izleme, ölçüm, koruma ve yönetim konularını kapsamaktadır. Konu, dünyada ve ülkemizde inşa edilen örneklerden faydalanılarak ele alınmakta, özellikle Yeraltı Barajları Eylem Planı kapsamında 2023 yılında tamamlanması planlanan projeler için faydalı olacağı öngörülmektedir.

YERALTI BARAJLARINDA İŞLETME SÜRESİNCE KARŞILAŞILABİLECEK SORUNLAR

Sellerde Hasar Görme

Özellikle vadi alüvyonlarında inşa edilen yeraltı barajlarının yer üstünde bulunan yapıları (Şekil 1) veya gömülü yapıların yüzeye yakın olan kısımları sellerde zarar görebilmektedir. Su alma yapısı ve gövdenin yüzeyde devamı olan yapılar yüksek debili ve basınçlı suyun etkisiyle yıkılabilmektedir. Drenaj boruları sellerde taban aşınması nedeniyle hasar görebilmektedir. Hatta bu durum, plastik beton gövdeli yeraltı barajlarında, gövde üzerindeki başlık betonunun hasar görmesi ve bu nedenle taban aşınmasının derine doğru devam etmesi halinde plastik beton gövde için de söz konusu olabilir. Toprak gövdeli Ankara-Kalecik-Malıboğazı yeraltı barajında baraj inşaatından bir yıl sonra (2005) meydana gelen selde gözlem kuyuları, eksen yerinde karayolu altından yüzeysel akışı sağlayan büzler hasar görmüştür (Apaydın, 2022). Kret seviyesi doğal talveg kotundan iki metre derinde olduğundan taban oyulması oraya kadar inmemiş ve bu sayede gövde zarar görmemiştir. Ancak, hasar gören yapıların yeniden inşası ve yatak düzenlemesinin yeniden yapılması gerekmiştir.

Yeraltı barajlarında taban oyulmasının tersine, sellenmelerle gelen sediment malzemenin gövde arkasında birikmesi ve yer üstündeki yapıların sediment malzeme altında kalması da söz konudur. Yeraltı barajları Eylem Planı kapsamında inşa edilen ilk örneklerden olan Bartın-Bahçecik ve İzmir-Kiraz yeraltı barajlarında gövde üzerinde boylu boyunca başlık betonu ve onun üzerinde beton set inşa edilmiştir. Akarsuya gövde üzerinden geçiş için uygun kesit bırakılmışsa da şiddetli yağışlarla debisi ve seviyesi yükselen akarsuyun taşıdığı sediment malzeme gövde arkasında depolanarak talveg seviyesi yükseltmektedir. Yeraltı barajlarında gövde arkasında kaba taneli sediment malzeme kalınlığının sellenmelerle artması ilave depolama hacmi elde edilmesi yönüyle olumlu olmakla birlikte, su alma yapısı, gözlem kuyuları, işletme kuyularına ait baraka veya pompa istasyonlarının sediment malzeme altında kalma ihtimali vardır.

Şekil 1. Malıboğazı (a), İskilip (b), Kiraz (c) ve Bahçecik (d) yeraltı barajlarında yerüstündeki yapıların inşaat tamamlandıktan hemen sonraki görüntüleri. Oklar akış yönünü göstermektedir (foto a ve b, A.Apaydın, c ve d, www.dsi.gov.tr, erişim tarihi, 19 Mayıs 2022)

Çevre Arazileri Su Basması

Vadi alüvyonlarında inşa edilen yeraltı barajlarında ve yeraltısuyu yapay besleme yapılarında gövde üzerinde akışı sağlayacak yapı inşa edilmesine ve uygun kesit bırakılmasına rağmen şiddetli yağışlarda debinin yükselmesiyle çevredeki arazilere taşabilmektedir. Bunun haricinde, bir çevirme yapısıyla yatağından alınıp yeraltısuyu yapay besleme alanlarına kontrolsüzce verilen yüksek debili su, besleme alanından taşarak çevre arazileri su altında bırakabilmektedir. İzmir'in Tire ilçesinde Eğridere'nin sularının çevrilmesiyle

uygulamaya konan yeraltısuyu yapay besleme alanına 2022 yılı Şubat ayı başında gerçekleşen şiddetli yağışlarla aşırı su gelmiş ve besleme alanı dolarak, fazla su çevre arazileri su altında bırakmıştır (Şekil 2).

Şekil 2. İzmir-Tire-Eğridere yeraltısuyu yapay besleme alanında taşkın sonrası görüntüler (www.egepostasi.com, www.sabah.com, erişim tarihi 21.05.2022)

Siltasyon Nedeniyle Tıkanma

Yeraltı barajlarında sel sularının yıkıcı ve aşındırıcı etkileri olmakla birlikte, ağzından sediment malzemenin girmesi halinde su alma yapısının dolması ve boru giriş ağzının tıkanması da söz konusudur. Tıkanma, bu şekilde olduğu gibi, drenaj boruları ve su alma yapısı etrafında içten dışa doğru tane boyu küçülecek şekilde filtreleme yapılmaması veya iletim borusu girişine filtre konmaması halinde de meydana gelebilmektedir. Bu gibi olumsuzluklar proje ve inşaat evresinde göz önünde tutulmalı ve gerekli önlemler alınmalıdır. Ayrıca su alma yapısının giriş ağzı suların yükselebileceği seviyeden daha yüksek olmalıdır.

Tabanda Geçirimsiz Çamur Tabakası Oluşması

Gövde arkasında kalıcı veya geçici göl oluşan yeraltı barajları ile yeraltısuyu yapay besleme barajlarının ve besleme hendeklerinin tabanında bir süre sonra kil-silt malzemeden oluşan kaymak tabakası oluşmaktadır (Şekil 3). Bu malzeme geniş bir alan kaplaması ve yeterince kalın olması halinde rezervuardan akifere yüzey akışından beslenmeyi engellemektedir. Yeraltı barajlarında böyle bir durumun çoğunlukla dar bir alanda meydana gelmesi ve barajın geniş bir akifer alanından beslenmesi nedeniyle önemli bir sorun olmamakla birlikte, yapay besleme tesislerinin sürekli gözlem altında tutulması, temizlik ve bakım-onarımının yapılması projenin başarısı için önemlidir.

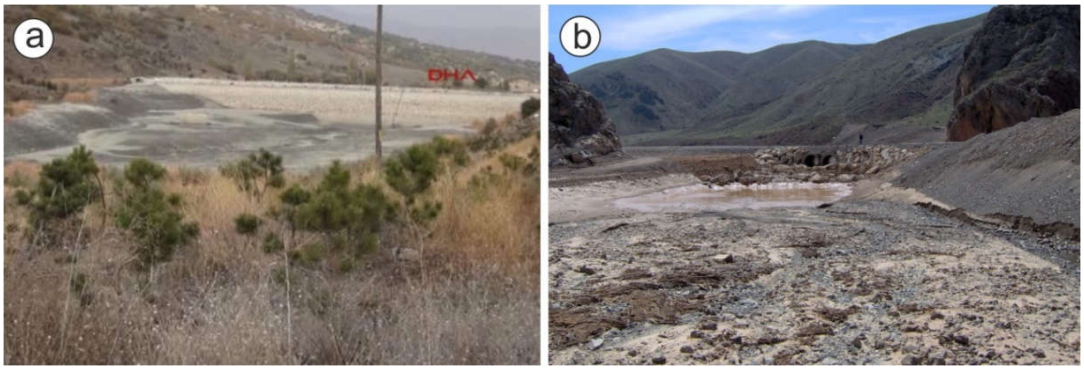

Şekil 3. Yeraltı barajlarında gövde arkasında ince malzemenin çökelmeyesiyle çamur tabakasının oluşmaya başlaması (a: Yeraltı ve yerüstü depolamalı Elmadağ-Kargalı barajında 2016 yılında kuraklık nedeniyle suların çekildiği andaki, b: Malıboğazı yeraltı barajında inşaat tamamlandıktan yaklaşık 1 yıl sonraki görüntü)

Kimyasal Etki ve Kalite Değişimi

Yeraltı barajlarında doğal ve insan kaynaklı olmak üzere iki farklı kalite sorunu olabilmektedir. Bütün hidrolik projelerde olduğu gibi, yeraltı barajlarında da suyun kimyasal özelliklerinin ve kalitesinin kullanma amacına uygun olması esastır. Bunun için yer seçiminde suyun kalitesi ve projenin potansiyel potansiyel kirleticilere karşı duyarlılığı araştırılarak ortaya konmalıdır. Gövde arkasında su seviyesi yüzeye yakın olan sistemler yüzeysel kirleticilere karşı daha kırılgandır. Ayrıca, gövde arkasında yeraltısuyu seviyesinin geniş bir alanda yükselmesiyle yeni durumda su-kayaç etkileşimi farklı olabilir ve bu durum yeraltısuyu kimyasında farklılaşmaya neden olabilir. Baraj öncesinde su kalitesinde sorun olmasa bile zamanla olabilecek değişimler de dikkate alınarak baraj havzasında kirlilik yönüyle önlemler alınmalıdır. Bu önlemler yönetsel ve yasal hükümlerle güvence altına alınmalıdır.

Yeraltı barajlarında yeraltısuyu kimyasında zamanla meydana gelen değişime örnek olabilecek bir çalışma Japonya'da Sunagawa yeraltı barajında yapılmıştır. Miyako adasındaki baraj bölgesinde 1975 yılında 5 mg/l olan nitrat konsantrasyonu (Kondo vd. 1977) tarımsal gübreleme sonucunda artmaya başlamış, yeraltı barajı inşa edilmeden önce 1988 yılında nitrat konsantrasyonu 10 mg/l tespit edilmiştir. Baraj inşa edildikten sonra yeraltısuyu akımı ve seviyesinin değişmesiyle nitrat konsantrasyonun nasıl değişeceğini tahmin etmek zor olmuştu; çünkü yeraltısuyu sistemi daha önce görülmemiş şekilde çok değişmiştir (Imaizumi vd. 2002). Bu amaçla barajın planlama, inşaat ve işletme süresince gözlem kuyularında nitrat konsantrasyonu izlemeye alınmıştır. Baraj inşa edildikten yedi yıl sonra 2000 yılında nitrat konsantrasyonu 2,69-9,75 mg/l arasında değişmekte, ortalaması 6,38 mg/l idi. Baraj öncesinde en yüksek konsantrasyon baraja yakın alt bölgeler olup, baraj inşasından sonra da durum değişmeyerek en yüksek konsantrasyon yine baraj gövdesi arkasında tespit edilmiştir. Yeraltısuyundan kuyularla sulama başlamasından iki yıl sonra nitrat konsantrasyonu 2,14 mg/l ile 8,34 mg/l arasında tespit edilmiştir (ortalama 5,77 mg/l). Üç yıl önce baraj gövdesi arkasında var olan yüksek konsantrasyon zonu o yıl kaybolmuştur. Burada dikkat çeken başka bir bulgu daha elde edilmiştir. Su seviyesi baraj inşasından sonra yükseldiğinde, kireçtaşlarından oluşan vadoz zonun bulunduğu bölgede nitrat konsantrasyonu azalmış, killerden oluşan vadoz zonun bulunduğu diğer bölgelerde ise yükselme eğilimine girmiştir (Ishida vd. 2006). Japonya'daki bu örnekten de anlaşılacağı üzere, baraj inşaatı sonrasında gözenekli jeolojik ortamdan ibaret olan rezervuarda kimyasal değişim su seviyesinin yükselmesine, yükselme ile temas edilen jeolojik ortamın kimyasına, akım sistemindeki değişime ve başka doğal ve insan kaynaklı faktörlere (tarımsal faaliyet vb.) bağlıdır.

YERALTI BARAJLARINDA İZLEME, BAKIM-ONARIM VE YÖNETİM

Barajların yapısal ve işlevsel güvenliğinden emin olmak, can ve mal güvenliğinden emin olmak ve gelecekte yapılacak benzer projeler için veri toplamak (Aşık, 2000) ve barajın işletme ömrünü (faydalı ömür) mümkün olduğunca arttırarak en verimli bir şekilde faydalanmak amacıyla denetim altında tutulması gerekir. Bunun için işletme boyunca izleme konusu son derece önemlidir. Yeraltı barajlarında izleme konusu çok yönlüdür.

Tesisin herhangi bir hasar veya zarar görmesine karşı izlenmesi gerektiği gibi, aynı zamanda tesisi besleyen yeraltısuyu sisteminin ve aynı zamanda onunla etkileşim halinde olan hidrolojik havzanın da izlenmesi gerekir. Bunun için rezervuarda gözlem kuyuları açılarak yeraltısuyu seviyesinin periyodik olarak izlenmesi gerekir. Ayrıca, cazibeli yeraltı barajlarında kullanım süresince (içme suyu barajlarında sürekli, sulama barajlarında sulama mevsimi boyunca) debinin de ölçülerek debi değişiminin yeraltısuyu seviyesi ile ilişkisi ortaya çıkarılmalıdır. Yeteri derecede uzun süreli ve kesiksiz veri elde edildiğinde, rezervuardaki su seviyesi ile debi arasındaki ilişki grafiklenerek bir anahtar eğri oluşturulması da mümkündür. Böylece, yeraltı barajının mevsimsel yağışa bağlı beslenme salınımlarına ve vananın açılarak sistemin boşaltılmasına karşı tepkisinin analiz edilmesi mümkün olabilecektir. Bütün bu veriler tesisin en verimli bir şekilde işletilmesine hizmet etmiş olacak, örneğin sulama amaçlı cazibeli yeraltı barajlarında su seviyesinin ve buna bağlı olarak debinin yüksek olduğu yağışlı yıllarda daha fazla arazinin sulanabileceği, tersi durumda ise temkinli olunması gerektiği konusunda çiftçiler bilgilendirilebilecektir. Benzer şekilde, kuyulardan pompajla su elde edilen yeraltı barajlarında da yeraltusuyu seviyesinin yüksek olduğu yağışlı dönemlerde kuyu verimlerinin ne kadar yüksek olacağı, tersi durumda ise ne kadar düşük olacağı hususunda su kullanıcıları bilgilendirilebilecektir. Yeraltıuyu seviye değişimlerinin izlenmesi sadece doğal meteorolojik faktörlere karşı değil, aynı zamanda sisteme insan kaynaklı etkilerin de analizi için önemlidir. Örneğin, vadi alüvyonlarında inşa edilen yeraltı barajlarını besleyen akifer vadi boyunca kilometrelerce uzanabilmektedir. Dolayısıyla, çok uzak mesafelerde dahi aşırı çekim, akiferi besleyen akarsuyun başka yere çevrilmesi gibi müdahaleler barajın verimini etkileyebilmektedir. Dolayısıyla, işletme boyunca yeraltı barajlarında izlemenin doğal ve yapay etkenlere karşı çok yönlü bir şekilde yapılması ve elde edilecek verilerin buna göre yorumlanması önem taşımaktadır. Yeraltı barajlarında sistem dinamiği ve sisteme yapılacak dış etkilere sistemin verdiği fiziksel tepki yönüyle izlemenin yanında diğer önemli bir husus da Bölüm 2'de ifade edildiği gibi barajı besleyen yeraltısuyu sisteminin kimyasal, biyolojik ve fiziksel yönden kirlenme ihtimaline karşı da izlenmesidir.

Yeraltı barajlarında kuyulardan pompaj ile su çekilen sistemlerde enerji maliyeti yüksek olduğundan su kayıplarını en aza indiren modern sulama yöntemlerinin seçilmesi ve sulama süresince kayıpları en aza indirecek uygulamaların yapılması önemlidir. Cazibeli sistemlerde ise, mutlaka vana sistemi kurulmalı, örneğin sulama barajlarında sulama mevsimi haricinde vana kapatılarak suyun boşa akması önlenmeli, suyun akiferde depolanmasına izin verilmelidir. Bu konuda en iyi örneklerden biri Ankara'nın Kalecik ilçesinde inşa edilen Malıboğazı yeraltı barajıdır. Barajın 500 m mansabında ve ayrıca suyun Gökçeören Sulama Kanalına döküldüğü yerde (2 km mansabında) olmak üzere iki kontrol vanası bulunmaktadır (Şekil 4). Sulama mevsimi dışında (genellikle Eylül sonu-Mayıs başı arası) bu vanalar kapalı tutularak yeraltısuyu seviyesi akifer içinde yükselmekte, sulama mevsimi başlangıcında ise vanalar açılarak yeraltısuyu deposu yavaş yavaş boşalmaktadır. İçme suyu amaçlı yeraltı barajlarında ise, iletim hattında herhangi bir arıza durumunda onarım süresince suyu boşa akıtmamak için baraj çıkışında bir vana sistemi kurulması gerekir. Gerekiyorsa bir vana da dağıtım deposu girişinden önce de monte edilebilir. İskilip yeraltı barajında, gövde altından HDPE boruya alınan su, barajın 500 m mansabında depoya aktarılmakta, buradan eski iletim hattı ile şehre verilmektedir. Depo girişinde bir vana sistemi bulunmaktadır.

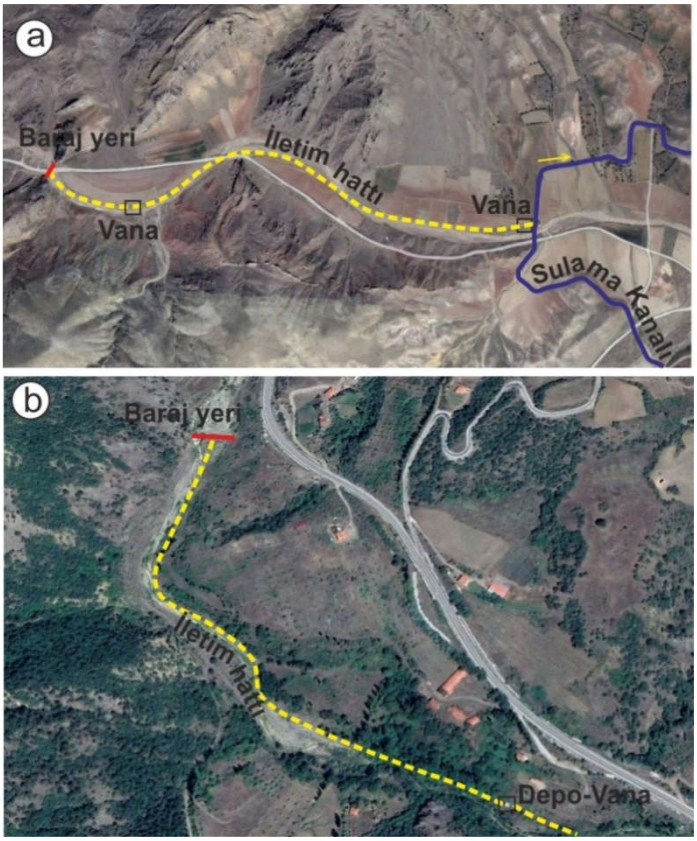

Şekil 4. Malıboğazı (a) ve İskilip (b) yeraltı barajında gövde altından su alan iletim hattının ve vana yerlerinin konumu

YERALTI BARAJLARINDA KORUMA ÖNLEMLERİ

Yeraltı barajlarında tesisin korunması ve su kaynağının korunması olmak üzere iki koruma husus söz konusudur. Tesisin korunması (2.1) Bölümünde söz edildiği gibi, öncelikle taşkınlara karşı koruma ve tesisin zarar görmemesi için güvenlik önlemlerinin alınması şeklindedir. Özellikle su alma yapısına dışarıdan olabilecek müdahaleyi engellemeye yönelik yükseltme veya tel örgü içine alma, uyarı tabelası asma gibi pratik önlemlerin alınması gerekir. Su kaynağının korunması ise hem miktar, hem de kalite yönüyle olmalıdır. Koruma sınırlarının ve koruma hükümlerinin belirlenmesi ayrıntılı çalışmaları gerektirir. Yeraltı barajı havzasında baraj su bütçesini olumsuz etkileyebilecek mesafe içinde kuyu, drenaj vb. yapılarla her türlü yeraltısuyu çekimi kontrol altına alınmalı, yeraltısuyu beslenmesini olumsuz yönde etkileyecek faaliyetler de sınırlandırılmalıdır. Ayrıca, yeraltı barajı havzasında baraj suyunun kalitesini olumsuz yönde etkileyebilecek faaliyetler gerekiyorsa tamamen yasaklanmalıdır. Bu kapsamda, içme amaçlı yeraltı barajlarında insan kaynaklı kirleticilere karşı koruma alanları belirlenmelidir. Sonuç olarak, yeraltı barajı havzalarında belirlenecek koruma alanlarında baraj su bütçesini olumsuz etkileyebilecek faaliyetler ile kirletici faaliyetler konusunda yasaklayıcı ve sınırlayıcı hükümler belirlenerek Resmi Gazete'de ilan edilerek uygulanmalıdır. İlan edilen hususların uygulanıp uygulanmadığı yetkili kurumlarca (DSİ ve Çevre Bakanlığı ile Valiliklere bağlı kurumlar) denetlenmelidir.

Türkiye'de içme suyu temin edilen yerüstü rezervuarları ile ilgili koruma hükümleri Su Kirliliği Kontrolu Yönetmeliği'nde, yeraltısuları ile ilgili hükümler ise Yeraltısuları Kanunu ve Yeraltısularının Bozulmaya ve Kirlenmeye Karşı Korunması Yönetmeliği'ne dayanarak uygulamaya konan İçme Suyu Temin Edilen Akifer ve Kaynakların Koruma Alanlarının Belirlenmesi Tebliği'nde yer almıştır. 10 Ekim 2012 tarih, 28437 sayılı Resmi Gazete'de yayımlanan söz konusu tebliğin 4. maddesinde kuyu, kaynak, kaptaj, tünel, galeri ve benzeri su noktası ve su yapısı için koruma alanlarının DSİ tarafından belirleneceği, koruma şartları ve sınırları ile birlikte Resmî Gazete'de ilan edileceği belirtilmiştir. Tebliğde, yıllık ortalama debisi 50 l/s ve üzerinde olan kaynaklar için mutlak, birinci ve ikinci derece koruma alanları, yıllık ortalama debisi 50 l/s'nin

altında olan kaynaklar için mutlak koruma alanı, içme suyu temin edilen kuyular için mutlak koruma alanı ilan edileceği, mutlak koruma alanı dışındaki faaliyetler için ilave tedbirler gerekli görülürse DSİ tarafından belirleneceği hükme bağlanmıştır. 6,7,8,9 ve 10. maddelerde koruma alanlarının nasıl belirleneceği ve sınırlarının ne olacağı açıklanmaktadır.

Noktasal olan veya çok dar bir alan kaplayan içme suyu tesisi ile ona su sağlayan akifer alanın korunmasına ait hükümler içeren söz konusu tebliğde tesis olarak kuyu, kaynak, kaptaj, tünel, galeri ve benzeri su noktası ve su yapısı kastedilmektedir. Yeraltı barajı yer almamaktadır. Tebliğde yer alan su noktası ve su yapılarına göre yeraltı barajları gövdesi, gövde arkasındaki su alma yapısı, varsa drenaj boruları ve yapay besleme tesisleri ile daha karmaşık olup, daha geniş alana yayılmaktadır. Buna göre Tebliğ'de 50 l/s'nin üzerindeki kaynaklar için geçerli olan mutlak, birinci ve ikinci derece koruma alanları içme suyu temin edilen yeraltı barajları için de uygulanmalıdır. Buna uygun olarak 6,7,8,9 ve 10. maddelerde belirtilen hükümlere göre koruma alanları belirlenmelidir. Konu ile ilgili olarak Tebliğ'de ilave düzenlemeler yapılmalıdır.

SONUÇ VE ÖNERİLER

Yerüstü depolamalarına göre birçok avantajı bulunan yeraltı barajları ülkemizde küçük ve orta ölçekli su ihtiyaçlarının karşılanması veya yerüstü rezervuarlarının kuraklıklardan olumsuz etkilendiği zamanlarda takviye görevi yapmasıyla önemi son yıllarda anlaşılmaya başlamıştır. Yeraltı barajlarının yer seçimi, planlama-projelendirme ve inşaatı kadar işletilmesi, izlenmesi ve korunması da kendine özgü hususlar içermektedir. 2019-2023 dönemini kapsayan Yeraltı Barajları Eylem planı ile birlikte ülkemizde yeraltı barajları ve yeraltısuyu yapay besleme yapılarının sayısı artmış, bundan sonra da daha da artacağı tahmin edilmektedir. Mevcut ve gelecekte inşa edilecek projeler için aşağıdaki hususların yerine getirilmesi önerilmektedir.

1- Vadi alüvyonlarında inşa edilen yeraltı barajlarında sel tehlikesine veya gövde arkasında göllenmeye karşı baraj arkasındaki su alma yapısı, pompa istasyonu, kuyu barakası, kaptaj veya depo gibi yapıların yüksekliği suyun yükselebileceği seviye dikkate alınarak belirlenmelidir. Sediment malzeme altında kalma riskini ortadan kaldırmak veya hafifletmek için akış yukarısında sediment tutucu yapılar (tersip bentleri) inşa edilmesi ve böylece baraj yerine gelebilecek malzeme miktarının minimize edilmesi en etkin çözümdür. Bununla da yetinmeyip, işletme süresince bütün yapılar sürekli olarak gözlem altında tutulmalı, gerektikçe malzeme temizliği, yatak düzenlemesi, bakım-onarım gibi işlemler yapılmalıdır.

2- Yeraltı barajlarında veya yeraltısuyu yapay besleme yapılarında kret seviyesinin talvegden yüksek olması halinde sellerde gövde arkasında yükselen suyun taşarak çevre arazilere zarar vermesini önlemek amacıyla yatak düzenlemesi yapılmalı ve işletme süresince gözlem altında tutulmalı, gerektikçe malzeme temizliği, yatak düzenlemesi, bakım-onarım gibi işlemler yapılmalıdır. Ayrıca, akarsudan çevirmeli olan yeraltısuyu yapay besleme tesislerinde çevirme yapısı suyu kontrollü bir şekilde verecek şekilde inşa edilmeli, sellerde akarsu debisi fazla yükselse bile yapay besleme alanına verilen su, zeminin infiltrasyon kapasitesini aşmamalıdır.

3- Su alma yapısı, drenaj boruları veya yapay besleme kuyularında siltasyon sonucu tıkanmaları önlemek için bu yapıların çevresinde uygun granülometriye sahip malzeme ile filtre zonu inşa edilmelidir. Besleme kuyularının zarar görmesine engel olmak için kuyuya doğrudan su vermek yerine, kuyu etrafında inşa edilecek filtre malzemesi içinden geçirildikten sonra besleme yapılması tercih edilmeli, mümkün olduğunca askıda katı maddeden arındırılmış su ile besleme yapılmalıdır.

4- Yeraltı barajı veya yeraltısuyu yapay besleme projelerinde planlama aşamasında başlayan izleme çalışmalarına inşaat ve işletme boyunca devam edilmelidir. Özellikle yeraltısuyu seviyesi değişimi, cazibeli projelerde debi değişimi, debi değişimi ile seviye değişimi ilişkisi, kuyulardan pompajlı projelerde kuyu verimlerindeki değişim, bu değişimin yeraltısuyu seviyesi ile ilişkisi, seviye değişimlerinin kimyasal bileşime etkisi gibi hususların izlenmesi gerekir. Su kaynağı, su yapısı ve işletmenin buna göre yönetilmesi, elde edilecek bilgilerin ve deneyimlerin başka projelerde faydaya dönüştürülmesi çok önemlidir.

5- Yeraltı barajlarını besleyen havzada çevresel etkilerin zamanla değişmesine ek olarak rezervuarda depolanan yeraltısuyu, su seviyesinin yükselmesiyle farklı mineralojik-kimyasal özelliklere sahip jeolojik ortamlarla temas ederek kimyasal yönden farklılaşabilmekte, değişen koşullara göre yeraltısuyu dinamiğinde

de değişme olduğundan bunların su kalitesine belirgin etkileri olabilmektedir. Bu gibi hususların inşaat öncesi çalışmalarla ortaya konması ve beklenen kimyasal etkiler yönüyle işletme boyunca düzenli izleme yapılması gerekmektedir. İzlemeden elde edilecek bulgulara göre teknik, idari ve yasal hükümler uygulanmalıdır.

6- Türkiye'de içme suyu temin edilen yerüstü barajları için Su Kirliliği Kontrolu Yönetmeliği'nde koruma hükümleri bulunmakta ve uygulama buna göre yapılmaktadır. Yealtı barajları için herhangi bir hüküm bulunmamaktadır. İçme Suyu Temin Edilen Akifer ve Kaynakların Koruma Alanlarının Belirlenmesi Tebliği'nde ise içme suyu temin edilen kaynaklar ve kuyular ile bunlar üzerinde kurulan tesislerin korunmasına yönelik hükümler yer almaktadır. Bu tebliğde yeraltı barajlarının da yer alması, yeraltı barajları için de mutlak, birinci ve ikinci derece koruma alanları belirlenmesi ve Resmi Gazete'de ilan edilmesi, böylece yeraltı barajları da kirlenmeye karşı koruma yönüyle yasal güvence altına alınmış olması gerekir.

KAYNAKLAR

Ali, E., Doğan, A. (2017). Modeling of Büyük Cırcıp Groundwater Recharge Dam using HYDRUS-1D, *Avrupa Bilim ve Teknoloji Dergisi (European Journal of Science and Technology)*, Cilt 7, No. 11, S.7-17.

Apaydin, A. (2022). Multi-parameter analysis for impermeability performance of slurry wall under dams: Two case studies in central Turkey, *Arabian Journal of Geosciences* (2022) 15:11.

Apaydın, A., Zengin E. (2016). A combined surface and groundwater storage project: the Elmadag dam, Turkey, *Quarterly Journal of Eng. Geology and Hydrogeology*, (Technical Note) doi:10.1144/qjegh2015-096, Vol. 49, pp. 237–243.

Apaydın, A., Demirci Aktaş, S., Kaya S. (2015). Ankara-Çankırı-Çorum Bölgesinde Yeraltı Barajları Konusunda Güncel Gelişmeler, MÜHJEO'2015 Ulusal Mühendislik Jeolojisi Sempozyumu, Mühendislik Jeolojisi Derneği ve KTÜ Jeoloji Müh. Bölümü Ortak Etkinliği, 3-5 Eylül 2015 Trabzon s. 397-404.

Apaydın, A. (2014). Yer seçiminden işletmeye yeraltı barajları, DSİ Genel Müdürlüğü Destek Hiz. Daire Başkanlığı Basım ve Foto-Film İşletme Müdürlüğü ISBN:978-605-64763-0-3, web:http://www.dsi.gov.tr/docs/yayinlarimiz.

Apaydin, A. (2009). Malibogazi Groundwater Dam: An Alternative Model for Semi-Arid Regions of Turkey, *Environmental Earth Sciences*, (2), 339-345.

Apaydın, A., Demirci Aktaş, S., Ekinci, O. (2005). Su Kaynaklarının Değerlendirilmesinde Farklı Bir Yaklaşım: Yeraltı Barajları, II. Ulusal Su Mühendisliği Sempozyumu Bildiriler Kitabı, 153-165, 21-24 Eylül 2005 Gümüldür-İzmir.

Aşık, Y. (2000). Baraj Kreti Üzerindeki Noktaların Yatay Harekelerinin Ölçülmesi İçin Bir Elektronik Ölçü Aleti Tasarımı ve İmalatı, Doktora Tezi, KTÜ-FBE, Trabzon.

Imaizumi M, Okushima S, Shiono T, Takeuchi M, Komae T. (2002). Soil water intrusion into a Ryukyu rimestone aquifer in Komesu underground dam basin southern part of Okinawa Island (in Japanese). *Trans* JSIDRE 221:11–23.

Ishida, S., Tsuchihara, T., Imaizumi, M. (2006). Fluctuation of NO3-N in groundwater of the reservoir of the Sunagawa Subsurface Dam, Miyako Island, Japan, Technical Report, Paddy Water Environ (2006), DOI 10.1007/s10333-006-0037-7.

Kondo H, Tase N, Hirata T. (1997). Nitrogen isotope ratio of nitrate of groundwater in Miyako Island Okinawa Prefecture (in Japanese). *J JAGH* 39(1):1–15.

YERALTI BARAJLARININ GÖVDE VE KAPASİTE YÖNÜNDEN YERÜSTÜ BARAJLARI İLE KARŞILAŞTIRMASI

COMPARISON OF UNDERGROUND DAMS WITH SURFACE DAMS IN TERMS OF DAM BODY AND CAPACITY

Ahmet APAYDIN

Giresun Üniversitesi, Mühendislik Fakültesi, İnşaat Mühendisliği Bölümü, Giresun-Türkiye.

ORCID NO: 0000-0002-6437-7208

ÖZET

Barajların gövde yüksekliği ve depolama hacmi en önemli kimlik bilgilerindendir. Dünyada ve Türkiye'de gövde yüksekliği en fazla olan barajlar çoğunlukla enerji amaçlıdır. Bunların çoğunlukla depolama kapasiteleri de yüksektir. 2022 yılı itibariyle Türkiye'de gövde yüksekliği en yüksek olan ilk beş baraj enerji amaçlı olup, gövde yükseklikleri 200-270 m arasındadır. Bunlar sırasıyla, Yusufeli, Deriner, Ermenek, Keban ve Berke barajıdır. İçme, sulama, sanayi vb. ihtiyaçları karşılamak amacıyla inşa edilen yerüstü depolama yapılarında gövde yüksekliği 8-10 m ile 200 m arasında değişmektedir. Dünyada ve Türkiye'de yeraltı barajları ile ilgili olarak gövde yüksekliği kriterine göre bir sınıflama bulunmamaktadır. Dünyanın bazı bölgelerinde kaya ortamlarında enjeksiyon veya kesişen kazık yöntemiyle inşa edilen yeraltı barajlarında yükseklik 50 m'nin üzerine çıkmıştır, ancak vadi alüvyonlarında inşa edilenlerde genellikle 30 m'den daha düşüktür.

Ülkemizde bu güne kadar inşa edilen yerüstü barajlarından sulama ve içme amaçlı olanların depolama hacimleri milyondan milyar metreküpe kadar geniş bir aralıktadır. Gövde yükseklikleri ise 15-200 m arasında olup, çoğunlukla 100 m'nin altındadır. Türkiye'de Tarım ve Orman Bakanlığı tarafından 2019-2023 yıllarını kapsayacak şekilde uygulamaya konan Yeraltı Barajları Eylem Planı'ndan (YEP) önce inşa edilen yeraltı barajlarında en yüksek gövdeli olanı 31,5 m ile Elazığ Baskil yeraltı barajıdır. Gövde yüksekliği Ankara-Kalecik-Malıboğazı yeraltı barajında 20,6 m, Yahşihan yeraltı barajında 14 m, İskilip yeraltı barajında ise 13 m'dir. Yıllık kapasite ise Baskil'de ortalama 6, Malıboğazı'nda 0,8-2, İskilp'te 0,7-1,6 hm^3'dür. YEP kapsamında 2021 yılı sonuna kadar inşa edilen yeraltı barajlarında depolama hacimleri 1 hm^3'ün altındadır. Bakanlığın açıklamasına göre 100 adet tesisten 50 hm^3 su elde edileceği açıklanmıştır. Buna göre tesis başına ortalama depolama kapasitesi 0,5 hm^3 olmaktadır. Bu miktar, eylem planından önce inşa edilenlere göre daha düşüktür, ancak inşa edilecek daha büyük barajlarda kapasitenin 1 hm^3'ün üzerine çıkması muhtemeldir. Dünyada ise bugüne kadar bilinen en büyük yeraltı barajı Japonya'da olup, gövde yüksekliği 69,5 m, maksimum kapasite 10 hm^3 civarındadır. Sonuç olarak, yerüstü barajlarına göre birçok avantajı bulunmakla birlikte, yeraltı barajlarının depolama kapasiteleri daha küçük olup, daha küçük ölçekli su ihtiyaçlarını karşılayabilecek özelliktedirler.

Anahtar Kelimeler: Yerüstü barajı, yeraltı barajı, gövde yüksekliği, depolama hacmi

ABSTRACT

The wall height and storage volume of the dams are among the most important identification information. The highest dams in the world and in Turkey are mostly for energy purposes. They often also have high storage capacities. As of 2022, the first five dams, which are the highest in Turkey, are for energy purposes and their heights are between 200-270 m. These are Yusufeli, Deriner, Ermenek, Keban and Berke dams, respectively. The height of the surface storage structures built to meet drinking, irrigation, industry and similar needs varies between 8-10 m and 200 m. There is no classification for underground dams in the

world and in Turkey according to the body height criterion. In some parts of the world, underground dams built by grouting or piling in rock environments have a height of over 50 m, but those built in valley alluviums are usually less than 30 m.

The storage volumes of the surface dams built in our country for irrigation and drinking purposes range from one million to one billion cubic meters. Their height is between 15-200 m, mostly below 100 m. Elazig Baskil underground dam, with 31.5 m, has the highest body among the underground dams built before the Underground Dams Action Plan (YEP) implemented by the Ministry of Agriculture and Forestry in Turkey to cover the years 2019-2023. The height is 20.6 m in the Ankara-Kalecik-Malıboğazı underground dam, 14 m in the Yahşihan underground dam, and 13 m in the İskilip underground dam. The annual capacity is 6 hm^3 in Baskil, 0.8-2 in Malıboğazı, and 0.7-1.6 hm^3 in İskilip. In the underground dams built by the end of 2021 within the scope of the YEP, the storage volumes are below 1 hm^3. According to the statement of the Ministry, it has been announced that 50 hm^3 of water will be obtained from 100 facilities. Accordingly, the average storage capacity per facility is 0.5 hm^3. Although this amount is lower than those built before the action plan, the capacity is likely to exceed 1 hm^3 for larger dams to be built. The largest underground dam known to date in the world is in Japan, with a height of 69.5 m and a maximum capacity of around 10 hm^3. Consequently, although they have many advantages over surface dams, underground dams have smaller storage capacities and are capable of meeting smaller water needs.

Keywords: Surface dam, underground dam, dam wall height, storage volume

GİRİŞ

Dünyada su depolama yapılarının inşaatı özellikle Mezopotamya bölgesinde sulama ve içme amacıyla başlamış, zamanla boyutları büyümüş ve kullanma amaçları çeşitlenmiştir. 20. Yüzyılın ikinci yarısından itibaren gövde tipleri çeşitlenerek yüksekliği 300 m'ye ulaşan barajlar inşa edilmeye başlanmıştır. 21. Yüzyılın ilk çeyreğinde ise yükseklik rekoru 300 m'yi aşmıştır.

Baraj mühendisliğinde gövde yüksekliği ve depolama hacmi en önemli iki unsurdur. Yükseklik ile depolama hacmi arasında her zaman doğrusal bir ilişki olmayabilmekle birlikte, gövdesi yüksek barajların depolama kapasiteleri de genellikle yüksektir. Diğer parametrelerin etkisi saklı tutulmak kaydıyla, enerji barajlarında yükseklik, su elde etme amaçlı barajlarda ise depolama hacmi en önemli unsurdur.

Su elde etmek amacıyla inşa edilen yerüstü barajları yağışlı zamanlarda akışa geçen veya debisi yükselen akarsuyun baraj rezervuarında depolanarak yıl boyunca veya ihtiyaç oldukça kullanılması esasına dayanır. Akarsu debilerinin özellikle kurak-yarıkurak bölgelerde mevsimsel değişiminin fazla olması, zamanla artan su ve gıda ihtiyacının karşılanmasında depolama yöntemini zorunlu hale getirmiştir. Bu nedenle Türkiye'de ve dünyanın birçok bölgesinde baraj yapımı son yıllarda hız kazanmıştır. İnşa edilen barajların yükseklikleri ve depolama kapasiteleri çok değişkendir. Örneğin, Türkiye'de hayvan sulama amaçlı olan çok küçük yapılar hariç içme, sulama, sanayi, turizm vb. çeşitli ihtiyaçlar için inşa edilmiş olan yerüstü barajlarının yükseklikleri 8-10 m'den 150-200 m'ye, depolama kapasiteleri ise 100 bin m^3'ten birkaç milyar m^3'e kadar değişmektedir (Öziş, 1983; Erkek ve Ağıralioğlu, 2002; Berkün 2002, 2005; Aşık 2016; Altınbilek 1977).

Uluslararası Büyük Barajlar Komisyonu'nun (ICOLD) tanımına göre; su depolama yapılarında yüksekliği akarsu seviyesinden 15 m üzerinde olanlar baraj (dam), 15 m'nin altında olanlar gölet (small dam) olarak adlandırılır. Türkiye'de bu tanım geçerli olsa da yüksekliği 40-50 m'nin de üzerine çıkan göletler de bulunmaktadır. Başka bir ifadeyle, uygulamada baraj-gölet sınırı net olmayıp ICOLD'un kabul ettiği sınırın epeyce üzerindendir.

Yerüstü barajlarında rezervuar hacmi tamamen su ile dolduğundan, depolama hacmi yerüstü barajları için çok önemli olmakla birlikte, yeraltı barajlarının kapasitesini ifade etmede tek başına yeterli değildir. Çünkü yeraltı barajlarının rezervuarında su taneler arasındaki boşluklarda veya kayaların kırık, çatlak veya erime boşluklarında depolanabilmektedir. Başka bir ifadeyle, yerüstü rezervuarlarının tamamı su ile dolmasına karşın, yeraltı rezervuarının ancak bir kısmı sudan ibaret olup, hacmin büyük bir kısmı jeolojik malzemeden ibarettir. Yeraltı barajlarının yerüstü barajlarına göre birçok avantajı olmakla birlikte, bu özelliği en önemli dezavantajıdır. Hacmin tamamını kullanamama dezavantajına ilave olarak, rezervuarın depolama kapasitesinin hesaplanmasının zorluğu veya bunu belirlemek için bir dizi arazi ve laboratuvar

araştırmalarının yapılması zorunluluğu ise ayrı bir problemdir. Üstelik, bu gerçekleştirilse bile rezervuarın sınır ve beslenme koşullarının ortaya konması da başlı başına bir iştir (Apaydın 2014, 2022).

Bu bildiride, dünyada ve ülkemizde bugüne kadar inşa edilenler göz önüne alınarak yerüstü barajları ile yeraltı barajlarının gövde boyutları ve depolama kapasitesi yönüyle karşılaştırması yapılmaktadır. Elbette ki, zamanla bu tür değerlendirmeler yeni boyut ve kapasiteler söz konusu oldukça revizyona ihtiyaç duyacaktır.

DÜNYADA VE TÜRKİYE'DE YERÜSTÜ BARAJLARININ YÜKSEKLİK VE KAPASİTE ARALIĞI

Bir barajın depolayacağı veya hizmete sunacağı su ve enerji miktarı o barajın en önemli performans özelliklerindendir. Mühendislik yönünden bakıldığında ise gövde yüksekliği bir barajın en önemli kimlik bilgilerindendir. Çoğu zaman, baraj denince diğer özelliklerinden önce akla gövde yüksekliği gelmektedir. Yüksek baraj inşa etme sadece mühendislik yönüyle değil, aynı zamanda ekonomik ve siyasal yönden de bir güç gösterisi olarak algılanmaktadır.

Kısa adı ICOLD olan Uluslararası Büyük Barajlar Komisyonu'na göre dünyada 900,000 baraj yapılmıştır. Bunlardan 45000 adedi Büyük Baraj sınıfındadır. Bunların yüksekliği 15 m'den fazla veya yüksekliği 5-15 m arasında olup depolama hacmi 3 milyon m^3'ten fazladır (Hull, 2009). Son 10-15 yılda Türkiye'de Bin Günde 1000 Gölet eylem planı kapsamında ve bunun haricinde inşa edilenlerle, İran, Çin, Hindistan gibi ülkelerdeki yoğun baraj inşaatları göz önüne alındığında toplam sayının 1 milyona doğru yaklaştığı da bir gerçektir. Gövde yüksekliği 150'm den fazla, gövde hacmi 15 milyon m^3 'den ve rezervuar kapasitesi 25 milyar m^3'den fazla olan **depolamalar Çok Büyük Baraj kategorisindedir ve bu boyuttaki barajların sayısı 20. Yüzyılın sonlarında 300'ü aşmıştır (Dorcey, 1997).**

Su yapıları ile ilgili çeşitli kaynaklarda (www.enerjiatlasi.com;) dünyada en yüksek olarak Çin'de 2014 yılında inşa edilen 305,5 m yüksekliğindeki Jinping-I Barajı yazılmaktadır. Onu 1988 yılında Tacikistan'da inşa edilen 300 m yükseklikteki Nurek Barajı takip etmektedir. Yine Tacikistan'da inşaatı devam eden (Nurek Barajı'nın menbasında) ve yazılı kaynaklarda sıralamada gösterilmeyen ancak proje yüksekliği 335 m olan Rogun Barajı birinci sıraya yerleşecektir. Bazı kaynaklarda barajın gövde yüksekliğinin 335 olacağı veya ikinci seçenek olarak 305 m'ye düşeceği ifade edilmektedir. Ancak bu konuda güvenilir bir veriye henüz erişilememiştir. Ayrıca yapımına devam edilen İran'daki Bakhtiari Barajı (Bahtiyari Barajı) 325 metre yüksekliğe, Çin'deki Shuangjiangkou Barajı da 312 metre yüksekliğe sahip olacaktır.

Dünyada ve Türkiye'de gövde yüksekliği en fazla olan barajlar çoğunlukla enerji amaçlıdır. Bunların çoğunlukla depolama kapasiteleri de yüksektir. 2022 yılı itibariyle Türkiye'de gövde yüksekliği en yüksek olan ilk beş baraj enerji amaçlı olup, gövde yükseklikleri 201-270 m arasındadır (Tablo 1). İçme, sulama, sanayi vb. ihtiyaçları karşılamak amacıyla inşa edilen yerüstü depolama yapılarından gövde yüksekliği 8-10 m ile 200 m arasında değişmektedir. Türkiye'de gövde yüksekliği 100 m'nin üzerinde olan bazı barajlar Tablo 2'de listelenmiştir.

Tablo 1. Türkiye'de en yüksek gövdeli enerji barajları

Sıra	Baraj Adı	Nehir	Gövde Yüksekliği (m)	Kapasite (hm^3)	Yılı
1	Yusufeli (Artvin)	Çoruh	270	2130	2022
2	Deriner (Artvin)	Çoruh	249	1969	2013
3	Ermenek (Karaman)	Göksu	230	4582	2009
4	Keban (Elazığ)	Fırat	210	31000	1974
5	Berke (Osmaniye)	Ceyhan	201	427	1999

Tablo 2. Türkiye'de enerji üretilmeyen (sulama, içme vb. amaçlı) bazı yüksek barajlar

Sıra	Baraj Adı	Nehir	Gövde Yüksekliği (m)	Kapasite (hm^3)	Yılı
1	Burgaz (İzmir)	Küçükmenderes	115	33	2014
2	Kirazlıdere (Kocaeli)	Kirazlıdere Ç.	109	60	1999
3	Çamlıdere (Ankara)	Bayındır Ç.	106	1220	1985
4	Aktaş (İzmir)	Aktaş Ç.	105	44	2018
5	İkizdere (Aydın)	İkizdere Ç.	101	213	2011
6	Eğrekkaya (Ankara)	Hamam Ç.	100	112	1992

YERALTI BARAJLARININ BOYUTLARI VE KAPASİTELERİ

Boyut ve Kapasiteyi Belirleyen Unsurlar

Yeraltı barajlarının yerüstü barajlarına göre birçok avantajı bulunmakla birlikte en önemli dezavantajı, depolama kapasitesinin çoğunlukla daha düşük olmasıdır. Bunun ana nedeni, yerüstü barajlarında rezervuarın tamamen su ile dolu iken, yeraltı barajı rezervuarında suyun ancak taneler arasında, kırık-çatlaklar veya karstik boşluklar içinde depolanmasıdır. Başka bir ifadeyle, yerüstü barajı tamamen dolu iken (su seviyesi dolusavak eşik kotunda iken) depolanan su hacmi toplam rezervuar hacmine eşittir. Yeraltı barajlarında ise rezervuar suya doygun olsa bile depolanan su miktarı en fazla toplam gözenek hacmi kadardır. Üstelik, yerüstü barajında su alma kotu üzerindeki suyun (aktif hacim) cazibe ile, bu seviye altındaki suyun (ölü hacim) pompajla alınması mümkündür. Yeraltı barajlarında ise akifer içindeki suyun cazibeyle veya kuyulardan pompajla tamamen çekilebilmesi mümkün değildir. Başka bir ifadeyle, yeraltı barajlarında yeterli beslenme ile rezervuar suya doygun olsa bile elde edilebilecek su miktarı gözeneklilik durumu, özgül tutma ve buna bağlı olarak depolama kapasitesine bağlıdır. Bununla birlikte, yeraltı barajlarında kapasite sadece rezervuar hacmi ve depolama kapasitesi ile sınırlı değildir. Baraj rezervuarına akiferin menba tarafından akım veya yerüstü su kaynaklarında her mevsim beslenmenin olması bu olumsuzluğu büyük ölçüde ortadan kaldırmaktadır.

Türkiye'deki Yeraltı Barajlarının Boyut ve Kapasiteleri

Türkiye'de, Tarım ve Orman Bakanlığına bağlı Devlet Su İşleri Genel Müdürlüğü (DSİ) tarafından 2019-2023 yıllarını kapsayacak şekilde uygulamaya başlanan Yeraltı Barajları Eylem Planı (YEP)'ndan önce inşa edilen yeraltı barajlarında gövde yüksekliği 31,5 m ile Elazığ Baskil'de inşa edilen yeraltı barajıdır. Ankara-Kalecik-Malıboğazı yeraltı barajında gövde yüksekliği 20,6 m'dir. Bu iki baraj da sulama amaçlı ve toprak dolgu olup, geçirimsizlik gövde ortasındaki sıkıştırılmış killi malzemeyle sağlanmaktadır. Yahşihan yeraltı barajı 14 m, İskilip yeraltı barajı ise 13 m gövde yüksekliğine sahiptir. Kret uzunlukları sırasıyla, 92, 50, 20, 55 m'dir. Yıllık kapasite ise Baskil'de ortalama 6, Malıboğazı'nda 0,8-2, İskilip'te 0,7-1,6 hm^3'dür (Tablo 3). Yeraltı Barajları Eylem Planı kapsamında inşa edilen barajlarda basına yansıyan verilere göre depolama hacimleri veya elde edilebilecek su miktarı 1 hm^3'ün altındadır. Bakanlığın eylem planı açılış töreninde yaptığı açıklamaya göre 100 adet tesisten 50 hm^3 su elde edileceği açıklanmıştır. Buna göre tesis başına ortalama depolama kapasitesi 0,5 hm^3 olmaktadır. Bu miktar, Eylem Planı'ndan önce inşa edilen örneklere göre daha düşük olmakla birlikte, eylem planı kapsamında büyük barajlarda kapasitenin 1 hm^3'ün üzerine çıkması muhtemeldir.

Tablo 3. Türkiye'de YEP'den önce inşa edilen önemli yeraltı barajlarında gövde ve kapasite verileri

Baraj Adı	Yahşihan	Malıboğazı	İskilip	Elmadağ	Baskil
Yer	Kırıkkale	Ankara-Kalecik	Çorum	Ankara	Elazığ
İnşa Yılı	2003	2005	2010	2012	2011
Amacı	İçme	Sulama	Sulama	Sulama	Sulama
Akifer	Kum-çakıl	Kum-çakıl	Kum-çakıl	Kum-çakıl	Kum-çakıl
Gövde Tipi	Beton+Kil	Toprak (kil)	Toprak	Kil Çekirdekli Kaya	Toprak (Kil)
Yükseklik (m)	14	20,6	13	26	31.5
Kret Uzunluğu (m)	20	50	55	213	92
Kapasite (hm^3/yıl)	0,7	1,0	1,0	2,5	200
Su Alma Yöntemi	Cazibeli	Cazibeli	Cazibeli	Pompajlı	Cazibeli

Yurt Dışındaki Yeraltı Barajlarının Boyut ve Kapasiteleri

Geçmişi çok daha eskilere dayanmakla birlikte, 19. Yüzyılın son çeyreğinde dünyanın pek çok bölgesinde, özellikle Güney ve Doğu Afrika ve Hindistan'da çeşitli büyüklükte yeraltı barajları yapılmaya başlanmıştır (Hanson ve Nilsson 1986; Nissen-Petersen 1982; Nilsson 1988; Foster vd. 2002; Zarkesh vd. 2012). Eski yeraltı barajlarının kapasiteleri yakın zamandaki barajlardan daha küçüktür ve kırsal küçük yerleşimlerde evsel ihtiyaçları karşılamak amacıyla kullanılmıştır. Yeraltı barajları, 1990'lardan itibaren daha büyük yerleşim yerlerinin içme suyu ihtiyacının karşılanması ve geniş tarım alanlarının sulanması için inşa edilmiştir. Ancak literatürde bu barajlara ait veriler sınırlıdır veya çok azına ait yeterli veri vardır. Geçen yüzyılın ikinci yarısında İran'da (Hartung vd. 1987) ve 2000-2001'de Hindistan'da (Raju vd. 2006) birkaç adet, Kore'de son yüzyılda 6 yeraltı barajı inşa edilmiştir. 1990'lardan sonra Çin ve Japonya'da bazı büyük yeraltı barajları inşa edilmiştir (Nagata vd. 1993; Ishida vd. 2003; Apaydın, 2014), 1990'larda Brezilya'da kuraklığa karşı kırsal bölgelerde yaklaşık beş yüz küçük ölçekli yeraltısuyu depolama yapısı (Foster vd. 2002; Foster ve Tuinhof, 2004) ve Kenya'da bazı sediment depolama barajları inşa edilmiştir (Hut vd. 2007; Ertsen ve Hut, 2009). Dünyada son zamanlarda çeşitli amaç ve ölçekte su temini (Ishida vd., 2011; Zarkesh vd., 2012; Raju vd., 2013; Jamali vd., 2013; Cantalice vd, 2016; Luiz vd, 2018) ve tuzlu su girişimini önlemek amacıyla (Kaleris ve Ziogas 2013; Botero-Acosta ve Donado 2015; Abdoulhalik ve Ahmed 2017; Chang vd, 2019) yeraltı barajları konusunda çalışmalar yapıldığı görülmektedir.

Yukarıda sözü edilenlerden literatürde erişilebilen ve yeterli verisi olan projeler incelendiğinde, büyük yeraltı barajlarının Japonya'da inşa edildiği görülmektedir (Tablo 4). Bu barajlarda gövde yüksekliği en fazla 69,5 m olup, maksimum kapasite 10 hm^3 civarındadır. Bu ölçüler küçük ölçekli bir yerüstü barajına karşılık gelmektedir.

Tablo 4. Dünyada literatüre giren bazı önemli yeraltı barajlarında gövde ve kapasite verileri

Baraj Adı	500 Adet	Nare	Sunagawa	Fukuzato	Komesu	Nakahara
Yer	Brezilya	Burkina Faso	Japonya	Japonya	Japonya	Japonya
İnşa Yılı	2000	2004	1993	1988	2003	2009-?
Amacı	İçme-sulama	Sulama	Sulama	Sulama	Sulama	Sulama
Akifer	Kum-çakıl	Kum-çakıl	Kireçtaşı	Kireçtaşı	Kireçtaşı	?
Gövde Tipi	Toprak, Beton, Jeomembran	Kil çekirdekli kum-çakıl	Jet Kolon	Jet Kolon	Jet Kolon	Jet Kolon
Yükseklik (m)	Ort. 4 m	11	49	27	69,5	55
Kret Uzunluğu (m)	Ortalama 50	207	1677	1790	2320	2350
Kapasite (hm^3/yıl)	Ort. 10.000	0,8	9,5	10,5	3,5	1,5
Su Alma Yöntemi	Cazibeli-pompajlı	Pompajlı (3 kuyu)	Pompajlı	Pompajlı	Pompajlı	Pompajlı

SONUÇ VE ÖNERİLER

Yerüstü barajlarında uygulanan gövde tiplerinden birçoğu yeraltı barajlarına da uygulanabilmektedir. Dünyada ve Türkiye'de bugüne kadar inşa edilen su depolama yapıları göz önüne alındığında, yeraltı barajları gövde boyutları (özellikle yükseklik ve kret uzunluğu) ve depolama hacmi yönünden yerüstü barajlarına göre daha küçüktür. Yeraltı barajında depolanan su miktarı aynı depolama hacmine sahip yerüstü barajlarına göre genellikle daha azdır, ancak kurak bölgelerde kurak aylarda (örneğin, Türkiye'de yaz ve sonbahar başlangıcında) yerüstü barajlarına çoğunlukla hiç su gelmemekte, bu süre boyunca rezervuardaki su

harcanmaktadır. Yeraltı barajlarında ise kurak aylarda rezervuara yeraltısuyu akışı yavaş da olsa devam etmektedir. Bu nedenle kurak bölgelerde yeraltı barajları yerüstü barajlarına göre daha güvenli ve sürdürülebilirdir. Ancak, akiferde yeraltısuyu hareketi yavaş ve karmaşık olduğundan, sadece gövde yüksekliğine bağlı olan rezervuarın değil, akiferin tamamında yeraltısuyu dinamiğinin barajın planlama çalışmalarında arazi ve laboratuvar testleriyle ortaya konması gerekir. Böylece, işletme süresince cazibe ile veya kuyulardan çekimle boşalan suya karşılık, rezervuara giren suyun pozitif etkisinin de dikkate alınmasıyla optimum işletme modelinin kurulması ve uygulanması projenin başarısı için son derece önemlidir.

KAYNAKLAR

Abdoulhalik, A., Ahmed, A.A. (2017). The effectiveness of cutoff walls to control saltwater J. Environ. Manage. 199, 62–73.

Altınbilek, D. (1977). Water Resources System Engineering, Middle East Technical University, Civil Eng. Depth, Water Resources Laboratory, Technial Publication, No: 12, Ankara.

Apaydın, A. (2014). Yer Seçiminden İşletmeye Yeraltı Barajları, DSİ Genel Müdürlüğü Destek Hiz. Daire Başkanlığı Basım ve Foto-Film İşletme Müdürlüğü ISBN:978-605-64763-0-3, web:http://www.dsi.gov.tr/docs/yayinlarimiz.

Apaydın, A. (2022). Türkiye'de Yeraltı Barajlarının Uygulanabilirliği ve "Yeraltı Barajları Eylem Planı"nın Değerlendirilmesi, Konya Mühendislik Bilimleri Dergisi, c.10, s. 1, 130-146.

Aşık, Y. (2016). Barajların Kontrolü ve Denetiminin Önemi, GÜFBED/GUSTIJ (2016) 6 (1): 33-40

Berkün, M. (2005). Su Kaynakları Mühendisliği, Birsen Yayınevi, 439 s.

Berkün, M. (2002). Su Kaynakları, Su Yapıları ve ÇED, TMH-Türkiye Mühendislik Haberleri Dergisi, Sayı 419, 43-47.

Botero-Acosta, A., Donado, L.D. (2015). Laboratory scale simulation of hydraulic barriers to seawater intrusion in confined coastal aquifers considering the effects of stratification. Procedia Environ. Sci. 25, 36–43.

Cantalice, J.R.B., Piscoya, V.C., Singh, V.P., et al. (2016). Hydrology and water quality of a underground dam in a semiarid watershed. Afr. J. Agric. Res. 11 (28), 2508–2518.

Chang, Q, Zheng T, Zheng X, Zhang B, Sun Q, Walther M (2019). Effect of subsurface dams on saltwater intrusion and fresh groundwater discharge, Journal of Hydrology 576, 508–519.

Dorcey, T. (1997). Large Dams, Workshop Proceedings, Gland, Switzerland.

Erkek, C., Ağıralioğlu, N. (2022). Su Kaynakları Mühendisliği, BETA Basım Aş. 240 s.

Ertsen, M., Hut, R. (2009). Two waterfall do not hear each other. Sand-storage dams, sciences and sustainable development in Kenya. Physics and Chemistry of the Earth, 34, 14-22.

Foster, F., Tuinhof , A. (2004). Brazil, Kenya: Subsurface dams to augment groundwater storage in basement terrain for human subsistence, World Bank Sustainable Groundwater Management Lessons from Practice, pp. 1–8.

Foster, S., Azevedo, G., Baltar, A. (2002). Subsurface dams to augment groundwater storage in Basement Terrain for Human Subsistence-Brazilian Experience" World bank, GWMATE Case Profile Collection, Vol. 5, P. 5.

Hanson, G., Nilsson, A. (1986). Groundwater dams for rural-water supplies in developing countries. Ground Water, vol 24, no:4, 497-506.

Hull, H. (2009). Large Dams, Human and Environmental Benefits and Costs, University of Wisconsin-Nres: 523 International Resource Management.

Hut, R., Ertsen, M., Joeman, N., Vergeer, N., Winsemius, H., Giessen, N. (2007). Effects of sand storage dams on groundwater levels with examples from Kenya. Physics and Chemistry of the Earth 33 (2008) 56–66.

Luiz, D.S.G.J., Vieira, F.P., Mannathal, H.V. (2018). Use of electrical resistivity tomography in selection of sites for underground dams in a semiarid region in southeastern Brazil. Groundwater Sustain. Dev S2352801X17301868.

Nagata, S., Enami, N., Nagata, J., Katho, T. (1993). Design and construction ofcutoff walls for subsurface dams on Amami and Ryukyu islands in the most southwestern part of Japan. IAH Selected Papers on Environmental Hydrogeology, 4, 229–245.

Ishida, S., Kotoku, M., Abe, E., Fazal, M.A., Tsuchihara, T., Imaizumi, M. (2003). Construction of subsurface dams and their impact on the environment. RMZ – Materials and Geoenvironment, 50, 149–152.

Ishida, S., Tsuchihara, T., Yoshimoto, S., Imaizumi, M. (2011). Sustainable use of groundwater with underground dams. Japan Agricultural Research Quartely, 45(1): 51-61.

Jamali, I.A., Olofsson, B., Mörtberg, U. (2013). Locating suitable sites for the construction of subsurface dams using GIS. Environ. Earth Sci. 70 (6), 1–15.

Kaleris, V.K., Ziogas, A.I. (2013). The effect of cutoff walls on saltwater intrusion and groundwater extraction in coastal aquifers. J. Hydrol. 476, 370–383.

Nilsson, A. (1988). Groundwater dams for small-scale water supply, Intermediate Technology Publications Ltd. London, pp. 69.

Nissen-Petersen, E. (1982). Rain Cathchment and water supply in rural Africa: A manual. Holder&Stoughton, Great Britain. 83 p.

Öziş, Ü. (1983). Su Yapıları, Ege Üniversitesi Matbaası, İzmir.

Öziş, Ü. (2002). Dörtbin Yıl Boyunca Türkiye'de Su Yapıları, İMO Türkiye Mühendislik Haberleri Dergisi, 17-28.

Raju, N.J., Reddy, T.V.K., Munirathban, P. (2006). Subsurface dams to harvest rainwater—a case study of the Swarnamukhi River basin, Southern India Hydrogeology Journal 14: 526–531.

Zarkesh, MMK., Ata, D.,Jamshidi, A. (2012). Performance of underground dams as a solution for sustainable management of Drought, Journal of Biourbanism, 1-45.

https://www.enerjiatlasi.com/en-yuksek-barajlar/ (erişim tarihi: 1 Eylül 2022).

DEĞİŞEN İKLİM SENARYOLARI DOĞRULTUSUNDA ADAPTİF MİMARLIK VE GELECEK POTANSİYELLERİ

ADAPTIVE ARCHITECTURE AND FUTURE POTENTIALS IN ACCORDANCE WITH CHANGING CLIMATE SCENARIOS

Burcu Buram ÇOLAK [1]

[1]Gazi Üniversitesi, Mimarlık Fakültesi, Mimarlık Bölümü, Ankara, Türkiye.

[1]ORCID ID: https://orcid.org/0000-0001-7932-6422

İdil AYÇAM [2]

[2]Gazi Üniversitesi, Mimarlık Fakültesi, Mimarlık Bölümü, Ankara, Türkiye.

[2]ORCID ID: https://orcid.org/0000-0001-7170-5436

ÖZET

Sanayileşmenin yüksek olduğu sera salımının fazla olduğu yerlerde enerji ve fosil yakıt kullanım oranları da fazladır. Bunun en önemli sebeplerinden biri insan faktörüdür. Zamanla bu durum nedeniyle küresel düzeyde oluşan çevreyle ilgili etki tüm dünyayı etkileyecek ölçüde büyük çaplı sonuçlar doğurmuştur. Gelecekte yaşanacak iklim değişikliklerden kaynaklı doğabilecek sonuçlardan etkilenecek bölgelerde hızlı önlemler alınması ve uyum stratejilerinin geliştirilebilmesi gerekmektedir. Değişen iklim senaryolarının getirdiği süreç ile küresel ölçekten bina ölçeğine kadar insanları etkilemektedir. Değişen iklim senaryolarından kaynaklı riskleri azaltmak ve yaşam kalitesini sürdürülebilir kılmak günümüzün en önemli konusu haline gelmiş bulunmaktadır. Tam da bu noktada bina ölçeğinden insan ölçeğine kadar etkilenen değişimleri göz önünde bulundurduğumuzda teknolojinin en çok etkilendiği alanlardan biri olan yapı alanında değişime gidilmesi zorunlu kılınmıştır. Alışılmış geleneksel mimari tasarım anlayışı ve yapım sistemlerinin dışına çıkıp daha yenilikçi teknolojilerin kullanıldığı koşullara uyum sağlayabilen yapılar tasarlamak, değişen iklim senaryolarının risklerini en aza indirgemek için önem arz etmektedir. Adaptif binaların genellikle cephe ve kabuklarında dinamik oluşuyla karşımıza çıkan koşullara uyarlanabilirlik tüm iç sistemleri de harekete geçirebilen kompleks bir sistemdir. Multidisipliner olup, mühendislerin ve mimarların ortak iş birliği ile tasarlanan adaptif yapılar değişen performans ihtiyaçlarına uyum sağlayarak binaların bütüncül performansını ve kullanıcı konforunu arttırmaktadır. Tüm bu sebeplerden dolayı çalışma kapsamında koşullara duyarlı ve uyarlanabilen adaptif mimarlık ve gelecek potansiyelleri incelenmektedir. Konu ile alakalı ilgili literatür araştırmaları yapıldıktan sonra adaptif mimari örnekleri üzerinden inceleme ve değerlendirme yapılmaktadır. Bu çalışma değişen iklim senaryoları doğrultusunda değişmesi ön görülen mimari tasarımlara yeni bir bakış açısı ile adaptif mimarlığı ele alarak yapılacak olan araştırma ve bina tasarımlarına ön bilgilendirme niteliğinde ışık tutmayı hedeflemektedir.

Anahtar Kelimeler: Adaptif Mimarlık, İklim Senaryoları, Teknoloji ve Mimarlık, Adaptif Cephe, Adaptif Bina Kabuğu.

ABSTRACT

Energy and fossil fuel usage rates are also high in places where industrialization is high and greenhouse emissions are high. One of the most important reasons for this is the human factor. It is necessary to take rapid measures and develop adaptation strategies in regions that will be affected by the consequences that may arise from future climate changes. It affects people from global scale to building scale with the process brought by changing climate scenarios. Just at this point, when we consider the changes that are affected from building scale to human scale, it is obligatory to make a change in the field of construction, which is

one of the areas where technology is most affected. It is important to design structures that can go beyond the traditional understanding of architectural design and construction systems and adapt to the conditions where more innovative technologies are used, to minimize the risks of changing climate scenarios. Adaptability to the conditions we encounter with the dynamic nature of the facades and shells of adaptive buildings is a complex system that can activate all internal systems. Multidisciplinary, adaptive structures designed with the joint cooperation of engineers and architects increase the holistic performance of the buildings and user comfort by adapting to the changing performance needs. For all these reasons, adaptive architecture that is sensitive and adaptable to conditions and its future potentials are examined within the scope of the study. After the relevant literature research on the subject is done, the analysis and evaluation are made on the examples of adaptive architecture. This study aims to shed light on the research and building designs that will be carried out by considering adaptive architecture with a new perspective on architectural designs that are predicted to change in line with changing climate scenarios.

Keywords: Adaptive Architecture, Climate Scenarios, Technology and Architecture, Adaptive Facade, Adaptive Building Shell.

1. GİRİŞ

İklim değişiklikleri hakkında yayınlanan senaryolar incelendiğinde küresel olarak ortalama sıcaklıkların 2100 yılına kadar 1-3.5 C° arasında artacağı ve buna bağlı olarak deniz seviyesinin de 15-95 cm arasında yükseleceği verilerine ulaşılmıştır. Gelecekte yaşanılacak sıcaklık ve sonucundaki diğer değişikliklere bağlı olarak yaşanılacak olan felaketler, seller, yangınlar, kuraklıklar, nem değişimleri vb. şeklinde sıralanabilmektedir. Bu felaketler sonunca tüm ekosistemden insan ölçeğine kadar tüm canlıların etkilenmesi kaçınılmazdır (Türkeş ve ark., 2000).

Değişen iklim senaryoları doğrultusunda yeni oluşabilecek koşullara çözüm getirebilecek teknolojilerin en çok kullanıldığı alanlardan biri olan yapı sektörüdür. Değişen iklim senaryoları ve bunun getirdiği sonuçlara karşı çözümler bulabilmeyi amaçlayan mimari tasarımlar sayesinde yapı maliyetleri düşürülürken enerji ve kullanılan kaynak verimliliğinin üst seviyeye çıkarılması da hedeflenmektedir. Mimari tasarımda değişen iklim koşullarına çözümler üretebilmek için tasarım aşamasında simülasyon programları aracılığıyla analizler yapılıp koşulların doğurabileceği sonuçların test edilmesi ve buna uygun sistemlerin geliştirilmesi önem arz etmektedir. Tüm koşulların mimari tasarım sonuçlanmadan; çevrenin etkisinin, iklim durumunun, rüzgâr etkisi, gün ışı ve gölgelenme durumu, aydınlatma ve havalandırma gibi konuların analiz edilmesi gerekmektedir (Kabadayı, 2019).

İklim değişikliğine uyarlanabilir adaptif mimari tasarımlar yapılabilmesi için teknolojinin getirilerinden faydalanması gerekmektedir. Teknoloji yardımıyla geliştirilmiş bilgisayar destekli tasarım programları ve analiz programları yardımıyla esnek tasarımlar yapılabilmesi kolaylaşmıştır. Esnek tasarım yaklaşımı zaman içerisinde meydana gelen değişimlere uyum sağlayabilen esnek mimari yapıların üretilmesini konu alan bir yaklaşımdır (İslamoğlu, 2018).

Forty (2000)' e göre esnek tasarım yaklaşımı; binaların gelecekte olabilecek muhtemel senaryolara göre adapte olabilen ve çeşitli alternatif çözümler sunarak tasarımı varsıllaştıran bir kavram olarak açıklanmıştır.

Habraken (2008)'e göre esneklik kavramı; hürriyet, yararlanma çeşitliliği, adaptasyon ve modifikasyon şeklinde ifade edilmiştir.

Schneider ve Till (2005, 2007)'e göre esneklik kavramı, yapı içerisindeki kullanıcıların binayı mevcut kullanımları ve ileride doğabilecek ihtiyaçlarını karşılayabilecek bir kavram olmakla birlikte, yapı kullanıcılarının gelecekteki ihtiyaçları karşılayabilmesi için bina sistemlerinin her koşula uyarlanabilir olmasını gerekliliğinin vurgulamaktadır.

Bu çalışma konu hakkında yapılan literatür araştırması yardımıyla adaptif cephe ve bina kabuklarını örnekler üzerinden incelemektedir. Çalışma kapsamında koşullara duyarlı ve uyarlanabilen adaptif mimarlık ve gelecek potansiyelleri konusuna vurgu yapılmaktadır. Konu ile alakalı ilgili literatür araştırmaları yapıldıktan sonra adaptif mimari örnekleri üzerinden inceleme ve değerlendirme yapılmaktadır. Bu çalışma değişen iklim senaryoları doğrultusunda değişmesi ön görülen mimari tasarımlara yeni bir bakış açısı ile adaptif

mimarlığı ele alarak yapılacak olan araştırma ve bina tasarımlarına ön bilgilendirme niteliğinde ışık tutmayı hedeflemektedir.

2. ADAPTİF MİMARLIK

1980'lerin başlarında kullanılmaya başlanan adaptif mimarlık kavramı çevrenin etkisinin önemini gözetirken çevre korunmasının önemine vurgu yapan aynı zamanda sürdürülebilirlik kavramına dikkat çeken çevresel etkilerin mimari tasarımı şekillendirmesi ve bu durumun sürdürülebilirliğinin sağlanması gerekliliğini benimseyen bir tasarım yaklaşımdır. Bu tasarım yaklaşımında bina içerisinde bulunan kullanıcıların konforlu ve çevre koşullarına uyumlu koşullarda yaşamlarını sürdürmesine olanak sağlamayı hedeflemektedir (Karakoç, 2015).

Adaptif yapılar iç ve dış ortam koşullarını analiz edip buna göre tepki verebilen, koşullara uygun değişebilen, yeni koşula uyarlayabilen ve binadaki diğer sistemleri aktifleştirebilen sistemler olarak tanımlanmaktadır. Adaptif cepheler ve bina kabukları çevresel koşullara göre hareket edip değişebilen mekanik sistemleri içeren farklı kurgularla bina cephe ve kabuğunda değişiklik yaratabilen ve bu sayede tasarımda da esnek olabilen olarak adlandırılmaktadır. Çevresel koşullardaki değişimler bina cephelerinin ve kabuklarının da değişime uyarlanabilir olmasını zorunlu hale getirmektedir.

Koşullara adapte olabilirlik özelliğini en çok yönlendiren kavram iklimde meydana gelen değişikliklerdir. İklimde meydana gelen değişikliklerin ve bunların çevreye etkisi nedeniyle bina kullanıcıları olumsuz koşullara maruz kalabilmektedirler. Bu olumsuz koşullardan etkilenmemesi için bina kullanıcıların konforunu sağlayan adaptif tasarımların yapılması önem arz etmektedir (Ghamari, Asefi, 2010).

Literatür araştırmaları, 20. yüzyıldan önce inşa edilen bina kabuklarının yeterince dinamik olmayışı ve çevresel etkilere uyum sağlayamayışı bu binalardaki yaşam konforunu düşürmekte ve aynı zamanda binaların ömrünü azaltıp bina işletim maliyetlerini arttırmakta olduğunu belirtmektedir. Günümüzde teknolojinin de gelişmesi sayesinde hareketli cepheler ve bina kabuklarının tasarlanması, binanın hareket kabileyetinin olmayışından dolayı meydana gelen sorunların giderilmesinde önem arz eden bir rol oynamaktadır (Karakoç, 2015).

3. ADAPTİF MİMARLIĞIN ÖRNEKLER ÜZERİNDEN DEĞERLENDİRİLMESİ

3.1. Design Hub, 2012

Avustralya, Melbourne'de 2012 yılında inşa edilmiş olan yapı sergi kompleksi olarak kullanılmaktadır. Bina kabuğu geometrik formların sistematik olarak kurgu oluşturulması ile tasarlanmıştır (Şekil 1).

Şekil 1. Design Hub, 2012 , Avustralya, Melbourne, Bina Görünüşleri (Gardiner, 2013)

Cephede bulunan geometrik modüller aktif olarak güneş hareketine duyarlı hareket etmektedir. Bina kabuğunda yer alan modüller adaptif olma kabiliyeti sayesinde güneş hareketlerine göre uyarlanabilir hareket etmektedir. Aynı zamanda kabuk gün ışığına duyarlı, iç mekânda gölge ve aydınlatma kontrolü yapabilmektedir. Tüm bu özellikleri ile birlikte depoladığı güneş enerjisini modülde yer alan PV paneller sayesinde enerjiye dönüştürmektedir. İç mekânda optimum termal konforu sağlarken görsel konfor adaptasyonu da sağlamaktadır (Şekil 2).

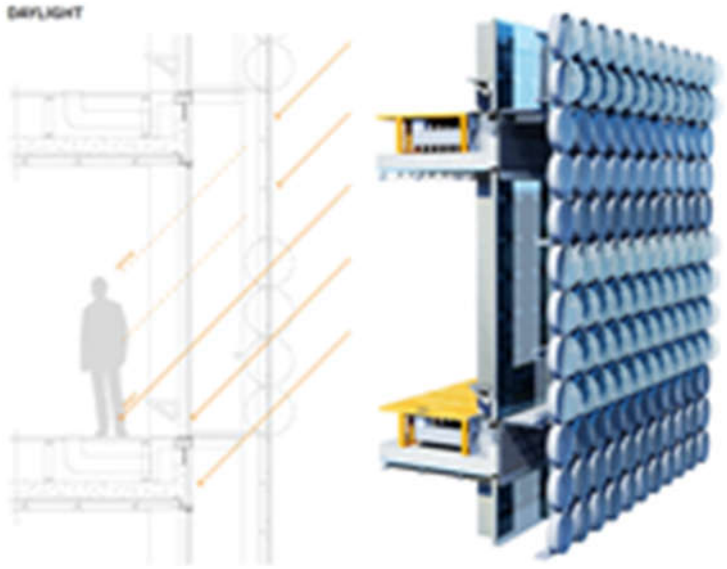

Şekil 2. Design Hub, 2012 , Avustralya, Melbourne, Bina Sistem Detayı (Kurtperenchio, 2022)

3.2. The Esplanade, Singapore, 2002

Singapore'da tiyatro binası ve konser salonu olarak kullanılan, 2002 yılında inşa edilen yapı biyomimikri bir mimari yaklaşım ile kirpi hayvan figüründen esinlenerek tasarlanmıştır (Şekil 3). Yapıda adaptif olma özelliği açılır kapanır kinetik sistem olarak yapıya hizmet veren yapı kabuğunda yer almaktadır.

Şekil 3. The Esplanade, Singapore, 2002, Bina Görünüşleri (Structurae, 2022)

The Esplanade bina kabuğu adaptif olma kabiliyeti sayesinde güneş hareketlerine göre uyarlanabilir hareket etmektedir. Aynı zamanda kabuk gün ışığına duyarlı, iç mekânda gölge ve aydınlatma kontrolü yapabilmektedir. İç mekânda optimum termal konforu sağlarken görsel konfor adaptasyonu da sağlamaktadır (Şekil 4).

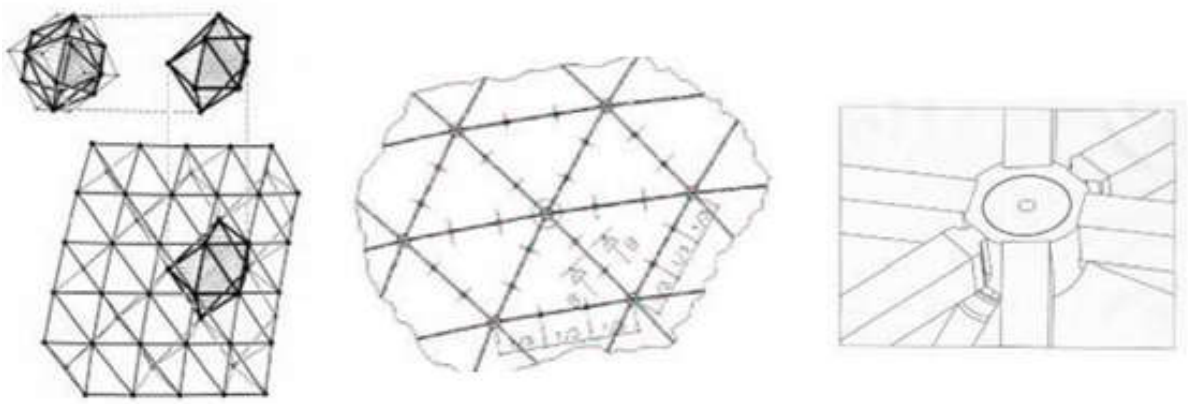

Şekil 4. The Esplanade, Singapore,2002, Modül Çizimleri (Sanchez-Alvarez, 2002: 3-6)

3.3. The Water Cube, Chaoyang, China, 2008

2008 yılında Çin'nin Chaoyang bölgesinde inşa edilen Pekin Ulusal Su Sporları Merkezi binası 'The Water Cube' adı ile tanınmaktadır. Yapı biyomimikri bir mimari yaklaşım ile adını aldığı su köpüklerinden esinlenilerek tasarlanmıştır (Şekil 5).

Şekil 5. The Water Cube, Chaoyang, China, 2008, Bina Görünüşleri (Mirkazemi and Mousavi, 2020)

The Water Cube bina kabuğu ve cephesinin adaptif olma kabiliyeti sayesinde yapı içerisinde doğal havalandırma ve termal izolasyon sağlamaktadır. Aynı zamanda yapı cephe ve kabuğunda bulunan su köpüğü modülleri yardımıyla dijital medya teknolojisi yardımıyla görsel bir şölen sunmaktadır. Işıklandırma için güneş enerjisinden yararlanmaktadır. İklime göre uyarlanabilir olması özelliği yardımı ile iç mekânda optimum termal konforu sağlarken görsel konfor adaptasyonu da sağlamaktadır (Şekil 6).

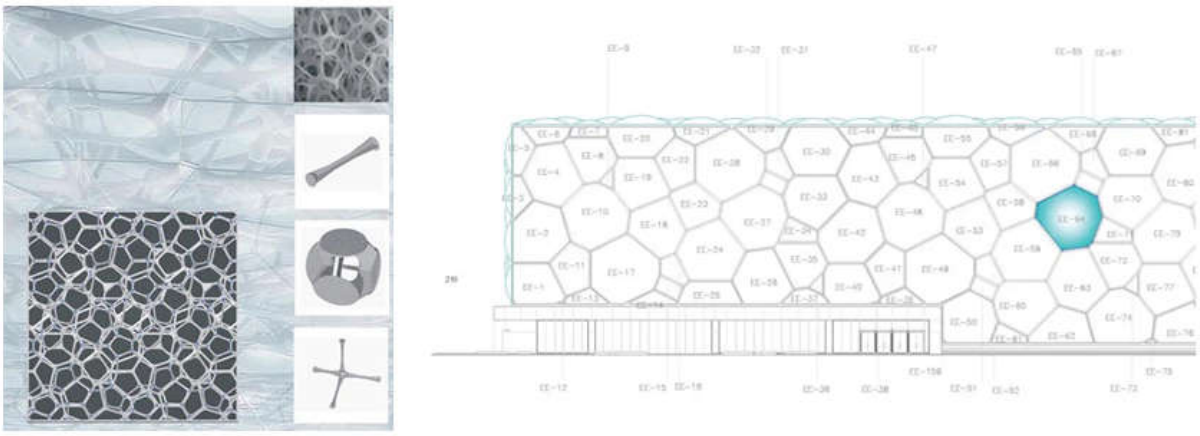

Şekil 6. The Water Cube Yapı Çizimleri (Arquidocs, 2008)

4. ADAPTİF MİMARLIĞIN GELECEK POTANSİYELLERİ

1. Adaptif mimari tasarımlarda önem arz eden en önemli kriter olan sürdürülebilirlik yapını çevre ile uyumlu olabilmesi ve çevreye uygun olarak pasif sistemler kullanmasının bir sonucudur. Bina cephe ve bina kabukların çevreye iklime uygun olarak tasarlanması çok önemlidir. Bu sayede hava kirliliğinin önüne geçilerek, CO2 emisyonu azaltılarak, çevrenin daha yaşanılabilir bir yer olabilmesi sağlanmaktadır (Boyle, 2004).
2. Adaptif tasarım yaklaşımı ile tasarlanmış binalarda aktif sistemlerden ziyade pasif sistemleri kullanmak ve bu şekilde enerji maliyetleri konusunda ciddi tasavvuf sağlanmaktadır (Ghamari ve Asefi, 2010).
3. Adaptif tasarım yaklaşımı ile tasarlanmış binalarda yapı toplam enerji maliyetleri giderleri konusunda ciddi azalmalar olduğu yapılan araştırmalar sonucunda görülmektedir. Bunun nedeni olarak bina için gerekli olan enerjinin fazlasını çevre yardımı ile üretebildiği ve hatta bazı durumlarda bu ürettiği enerjinin fazlasını depolayıp çevreye de yardımcı olabildiği görülmektedir.
4. Adaptif cephelerin kullanımıyla günümüzde dışarıdan enerji alınmamasının yanı sıra bazı durumlarda ve bölgelerde binayı işletenler tarafından dışarıya elektrik enerjisi bile satılabilmektedir (Karakoç, 2015).
5. Adaptif tasarım yaklaşımı ile tasarlanmış binaların dikkat çeken özelliği olarak adaptif olabilme özelliğinin getirdiği esneklikten dolayı yapının görünüşünün oluşturduğu estetik kurgudur (Drozdowski, 2011).

5. SONUÇ

Çalışma genel olarak değerlendirildiğinde değişen ilkim senaryolarına bağlı olarak doğacak sonuçlarına yapıların çözüm üretebilmesi için performansa dayalı adaptif tasarımlar yapılması ve bunların yapılabilmesi içinde konunun derinlemesine iyi anlaşılması önem arz etmektedir.

Koşullara adapte olabilen yapılar sadece değişen iklim ve çevresel koşullara çözüm üretmekle kalmayıp aynı zamanda kullanıcı konforunu sağlarken bina ömrünü uzatıp, enerji kaynaklarını tasavvufla kullanıp bina işletim maliyetlerini azaltabilmektedir.

Çevresel etkenler doğrultusunda performansa dayalı olarak oluşan tepkiler, bina kabuklarının ve cephelerin değişmesini ve farklı morfolojiler oluşturmasına imkân vermektedir. Bu çalışma, ileride yapılacak olan çalışmalar için, yol gösterici bir ön çalışma niteliğinde olup gerekli ön literatür çalışma ve örnekleri sunması açısından önemlidir.

Çalışma günümüzde yapılmış olan yapılara entegre edilecek olan ve gelecekte yapılacak olan adaptif bina ve kabuk tasarımlarında projenin içeriğine uygun ve bina ihtiyacına göre çevreye en uyumlu aynı zamanda

çevre koşullarından yararlanabilen konseptler oluşturulabilesi için bir rehber görevi görmeyi hedeflemektedir.

6. KAYNAKÇA

Arquidocs, 2008. https://arquidocs.wordpress.com/2008/08/25/water-cube-en-beijing/ (E.T. 25.07.2022).

Azahner, 2022. https://www.azahner.com/works/stony-brook/ (E.T. 15.08.2022).

Boyle, G. 2004. Renewable Energy. New York: Oxford University Press in association with the Open University.

Decanteddesign, 2015. https://decanteddesign.com/2015/03/31/adaptive-building-wall-roof-shading-systems-from-adi-adaptive-building-initiative-are-not-new-but-this-is-a-little-compilation-see-blogroll-for-a-link-to-the-adi-site/ (E.T. 15.08.2022).

Drozdowski, Z. 2011. The Adaptive Building Initiative: The Functional Aesthetic of Adaptivity. Architectural Design, (pp.118-123).

Forty, A. 2000. Words and Buildings, Thames & Hudson, London.

Gardiner, 2013. https://divisare.com/projects/227798-sean-godsell-architects-rory-gardiner-earl-carter-rmit-design-hub (E.T. 10.09.2022).

Ghamari H. & Asefi H. (2010). Toward Sustainability by the Application of Intelligence Building Systems. The Second International Conference on Sustainable Architecture and Urban Development, Amman, Jordan.

Habraken, N. J. 2008. Design For Flexibility. Building Research & Information, 36 (3), 290-296.

İslamoğlu, Ö. & Usta, G., (2018). Mimari Tasarımda Esneklik Yaklaşımlarına Kuramsal Bir Bakış. The Turkish Online Journal of Design, Art and Communication- TOJDAC ISSN: 2146-5193, October 2018, 8 (4), 673-683.

Kabadayı, H. İ. 2019. İklim Değişikliğine Odaklanan Mimari. https://www.inanckabadayi.com.tr/Blog/iklim-degisikligine-odaklanan-mimari. (E.T. 18 Ocak 2021).

Karakoç, E. 2015. Performansa Dayalı Adaptif Bina Kabuğu Tasarımı. İstanbul Teknik Üniversitesi, Fen Bilimleri Enstitüsü, Bilişim Anabilim Dalı Mimari Tasarımda Bilişim Programı Yüksek Lisans Tezi.

Kurtperenchio, 2022. https://www.kurtperenchio.com/case-study-rmit-design-hub (E.T. 10.09.2022).

Mathworld, 2022. https://mathworld.wolfram.com/DualTessellation.html (E.T. 30.07.2022).

Mirkazemi, S. M. & Mousavi, S. Y. (2020). Designing Adaptive Shells with the Approach of Geometrical Patterns in Nature. 7th International Conference on Innovation in Science and Technology, Amsterdam, Netherlands, (pp. 172-179).

Sanchez-Alvarez, J. 2002. The geometrical processing of the free-formed envelopes for the Esplanade Theatres in Singapore. Proc. IASS, (pp. 3-8). Corpus ID: 218484014.

Schneider, T. & Till, J., (2005). Flexible Housing: Oppourtunities and Limits,(pp.157-166).

Schneider, T. & Till, J., (2007). Flexible Housing, Architectural Press Elsevier Linancre, Jordan Hill, Oxford.

Structurae, 2022. https://structurae.net/en/structures/esplanade-theatres-on-the-bay (E.T. 30.07.2022).

Türkeş, M. & Sümer, U. M. ve Çetiner, G. (2000). Küresel iklim değişikliği ve olası etkileri. Çevre Bakanlığı, Birleşmiş Milletler İklim Değişikliği Çerçeve Sözleşmesi Seminer Notları (13 Nisan 2000, İstanbul Sanayi Odası), 7-24, ÇKÖK Gn. Md., Ankara.

SOLAR DECATHLON YARIŞMALARININ SÜRDÜRÜLEBİLİRLİK İLKELERİ KAPSAMINDA GELİŞİMİ

DEVELOPMENT OF SOLAR DECATHLON COMPETITIONS WITHIN THE SCOPE OF SUSTAINABILITY PRINCIPLES

Fulya GÖKŞEN[1]

[1]Gazi Üniversitesi, Mimarlık Fakültesi, Mimarlık Bölümü, Ankara, Türkiye.

[1]ORCID ID: https://orcid.org/0000-0002-9754-0956

İdil AYÇAM [2]

[2]Gazi Üniversitesi, Mimarlık Fakültesi, Mimarlık Bölümü, Ankara, Türkiye.

[2]ORCID ID: https://orcid.org/0000-0001-7170-5436

ÖZET

Binaların inşa edilmesi ve mevcut binaların yenilenmesindeki zorluğun üstesinden gelebilmek amacıyla işgücünün doğru yönlendirilmesi ve gerekli becerilerle donatılması gerekmektedir. Bu nedenle, mimarlık, mühendislik ve ilgili diğer disiplinlerdeki öğrencilerin yapı biliminin temelleri konusunda eğitilmesi ve bu ilkelerin bina tasarımına nasıl yansıtılacağını öğrenmesi temel gereksinimlerden biridir. Bu yaklaşımı referans alarak hareket eden ABD Enerji Bakanlığı (DOE), "Solar Decathlon" adı altında üniversiteler arası bir yarışma düzenleyerek öğrencileri; sürdürülebilir, ekolojik ve enerji etkin bina tasarımı, yenilenebilir enerjiyle çalışan yüksek performanslı ve düşük karbonlu binalar, en son teknolojiler ve malzemeler hakkında eğitmeyi ve farkındalık yaratmayı amaçlamaktadır. "Solar Decathlon" yarışması aracılığıyla öğrenciler yeni fikirler deneyerek mimari tasarım, teknoloji ve uygulama becerilerini geliştirmekle birlikte geleceğimizi etkileyecek olan iklim sorununu çözmek için ihtiyaç duyulan donanımları kazanmış olmaktadır. Ve dahası toplumu da eğitmeyi hedefleyerek sonuç ürünlerini sergilenmekte, enerji tüketimi ve sürdürülebilirlik konularında sosyal bilinç oluşturmaya çalışmakta ve yol gösterici bir rol üstlenmektedir.

Çalışma kapsamında ise, "Solar Decathlon" yarışmasının başlangıç tarihi olan 2002 yılından günümüze kadarki süreçte geçirdiği dönüşüm nitel araştırma yöntemlerinden veri toplama ve iz sürme metotları kullanılarak incelenmiştir. Her yılın kazanan projeleri, sürdürülebilirlik ilkeleri üzerinden karşılaştırılarak bir analiz gerçekleştirilmiş, geçmişten geleceğe bir değerlendirme yapılmak istenmiştir. Elde edilen verilere göre yarışma, Uluslararası Solar Decathlon etkinlikleri ile dünyanın dört bir yanındaki on binlerce öğrenci için sıfır enerjili tasarım eğitimi ve deneyimini arttırmaktadır. Solar Decathlon yarışması, sürdürülebilirlik ilkelerini bina tasarımı ve uygulamalarına entegre etmeyi, yeni malzeme ve tekniklerin kullanımını, ve yenilenebilir enerji üretimi gibi alanları en iyi şekilde harmanlamayı öğretmektedir. Öğrencilerin yanı sıra, mimar, mühendis ve ilgili diğer paydaşlarında tasarım ve inşa aşamaların da bu uygulamaları daha yaygın kullanımını sağlamak, kullanıcıları bilinçlendirmek gibi faydaları olacaktır. Sahip olduğu tüm bu özellikleri ile yarışmanın gelecekte yüksek bir potansiyele sahip olduğu öngörülmektedir.

Anahtar Kelimeler: Solar Decathlon, Yarışma, Eğitim, Enerji Etkin Tasarım, Sürdürülebilirlik.

ABSTRACT

To overcome the challenge of constructing new buildings and renovating existing buildings, the workforce needs to be properly guided and equipped with the necessary skills. Therefore, it is one of the basic requirements for students in architecture, engineering, and other related disciplines to be educated in the fundamentals of building science and learn how to reflect these principles in building design. Taking this

approach as a reference, the US Department of Energy (DOE) organizes an inter-university competition under the name of “Solar Decathlon” that aims to educate and raise awareness about sustainable, ecological, and energy-efficient building design; high performance, and low-carbon buildings powered by renewable energy; the latest Technologies, and materials. Through the “Solar Decathlon” competition, students develop their architectural design, technology and application skills by trying new ideas and gaining the necessary equipment to solve the climate problem that will affect our future. Moreover, it aims to educate the society, exhibits the result products, tries to create social awareness on energy consumption and sustainability, and plays a guiding role.

Within the scope of the study, the transformation of the "Solar Decathlon" competition from the start date of 2002 to the present day was examined by using data collection and tracing methods from qualitative research methods. An analysis was carried out by comparing the winning projects of each year to the theme that dominated that year, and an evaluation was made from the past to the future. According to the data obtained, the competition increases the zero-energy design education and experience for tens of thousands of students around the world through the International Solar Decathlon events. The Solar Decathlon competition teaches how to integrate sustainability principles into building design and practices, use new materials and techniques, and best blend areas such as renewable energy generation. In addition to students, architects, engineers, and other relevant stakeholders will also have benefits, such as making these applications more common in the design and construction stages and raising awareness of users. With all these features, it is predicted that the competition has high potential in the future.

Keywords: Solar Decathlon, Competition, Education, Energy Efficient Design, Sustainability.

1. GİRİŞ

Yapılı çevrenin küresel ve yerel çevre sorunları üzerindeki olumsuz etkisinin ortaya çıkması, 1970’lerden itibaren artan enerji krizi ve yakıt fiyatlarındaki artış üzerine ülkeler enerji tüketimini azaltmak amacıyla yeni yöntemler geliştirmek için çözüm arayışına girmişlerdir. Bu amaç doğrultusunda başlatılan uygulamalardan biri de ABD Enerji Bakanlığı (DOE) tarafından düzenlenen “Solar Decathlon” yarışması olup ilk olarak 2002 yılında Washington, D.C.'deki National Mall'da halka açık bir etkinlikle başlamıştır [1; 12].

Yarışma iki aşamadan oluşmaktadır. “Yapım/İnşa yarışması (Build challenge)”, iki yıllık bir tasarım ve uygulama sürecini içermektedir. İlk Solar Decathlon Yapım Yarışması 2002'de yapılmıştır. Daha sonra 2005, 2007, 2009, 2011, 2013, 2015, 2017 ve 2020'de iki yılda bir gerçekleştirilmiştir [12]. “Tasarım yarışması (Design challenge)”, bir veya iki dönem olabilmektedir. İlk olarak 2014 yılında DOE (ABD Enerji Bakanlığı) öğrenci tasarım yarışması olarak başlamış, 2018 yılına gelindiğinde “Tasarım Yarışması/Desing Challange” olarak adlandırılmış olup günümüze kadar her yıl düzenlenmiştir. Her iki yarışmada da katılımcılar mimari, mühendislik, enerji üretimi, enerji verimliliği ve daha birçok özelliği içeren ve her yıl güncellenen 10 kategoride yarışmaktadır [22].

Ek olarak yapının tasarım ve uygulama aşamalarının proje bazlı öğrenimini tamamlamak için Bina Bilimi Eğitimi kursu organize edilmiştir. Solar Decathlon’a katılan öğrencilerin, üniversite tarafından hazırlanan kursları veya yarışmanın organizatörleri tarafından sunulan eğitim kaynakları aracılığıyla temel yapı bilimi ilkelerini öğrenmeleri gerektiği düşünülmektedir. Dolayısıyla bu eğitimin amacı, tüm katılımcıların binaların enerjiyi nasıl ve neden kullandığının arkasındaki bilimsel ilkelere ilişkin güçlü bir temel bilgi ile yarışmaya başlamasını sağlamaktır. Ayrıca yarışma ekibinin multidisipliner takımlardan oluşması desteklenmekte olup ekip çalışması ödüllendirilmektedir [23].

“Solar Decathlon” yarışması ile öğrencileri; sürdürülebilir, ekolojik ve enerji etkin bina tasarımı, yenilenebilir enerjiyle çalışan yüksek performanslı ve düşük karbonlu binalar, en son teknolojiler ve malzemeler hakkında eğitmek ve onlarda farkındalık yaratmak hedeflemektedir. Öğrencilerin gelişimine katkı sağlamakla birlikte hem uzmanlardan hem de kendileri gibi diğer katılımcılardan yeni bilgiler öğrenmek ve liderlerin tecrübelerinden faydalanmak için eşsiz bir deneyim sunulmaktadır. Katılımcılar yarışmada özellikle yenilenebilir enerji ile çalışan yüksek enerji verimli binalar tasarlamak ve hatta inşa etmek durumundadır. Kazananlar, sadece mimari değil mühendislik, enerji tasarrufu, verimli, yenilikçi, pazar potansiyeli yüksek, yaratıcı, esnek ve akıllı tasarım gibi tüm bu parametreleri en iyi harmanlayan ekiplerdir [12; 23; 24].

"Solar Decathlon" yarışması zamanla uluslararası olarak genişlenmiş olup kendi etkinliklerine ev sahipliği yapan; Avrupa, Çin, Latin Amerika, Afrika, Hindistan ve Orta Doğu gibi diğer ülkelere de yayılarak 15 uluslararası etkinlikle yüzlerce ekip ve 20.000'den fazla katılımcıyı orfanizasyonlarına dahil etmiştir [12; 25; 26].

Çalışma kapsamında amaçlanan, "Solar Decathlon" yarışmasının başlangıç tarihi olan 2002 yılından günümüze kadarki süreçte geçirdiği dönüşümü nitel araştırma yöntemlerinden veri toplama ve iz sürme metotlarını kullanarak incelemektir. Her yılın kazanan projeleri, sürdürülebilirlik ilkeleri üzerinden karşılaştırılarak bir analiz gerçekleştirilmiş, geçmişten geleceğe bir değerlendirme yapılmak istenmiştir.

2. SOLAR DECATHLON YARIŞMA KATEGORİLERİ

2. 1. Solar Decathlon Build Challenge/İnşa Yarışması Kategorileri

Solar Decathlon Yapım Yarışmasında yarışan takımlar tamamen işlevsel evler tasarlar ve inşa eder. Ekipler yönergelere uygun evler inşa eder, sergiler ve işletir. Her evin uygulanmış proje üzerinden performansı kapsamlı bir şekilde ölçülür ve öğrenciler birden fazla jüriye sunar. İnşa mücadelesinde, 10 Kategoriden her biri bağımsız olarak puanlanır ve yarışmanın sonunda en fazla puana sahip olan takım kazanır [12].

Solar Decathlon 2002

2002 yılı sonbaharında, Amerika Birleşik Devletleri'ndeki kolej ve üniversite öğrencilerinden oluşan 14 takım tarihteki ilk Solar Decathlon'da yarışmıştır. Amaç, enerji verimliliği yüksek, tamamen güneş enerjisiyle çalışan evler tasarlama ve inşa etmektir. Ekipler bu amaçla Washington DC, National Mall'daki bir "Güneş Köyü"nde biraraya getirilmiş olup mimari, mühendislik, enerji üretimi, enerji verimliliği ve daha birçok özelliği içeren 10 kategoride yarışmıştır. Kategoriler Tablo 1'de yer almaktadır. Her takım toplamda 1.100 puana kadar kazanabilir. Puanlar hem öznel olarak jüri tarafından değerlendirilmekte hem de objektif bir şekilde ölçüme dayanarak verilmektedir. En çok puan alan takım, Colorado Üniversitesi, 875.302 puan kazanarak genel kazanan olmuştur [24; 27].

Tablo 3. 2002 Solar Decathlon Build Challenge/İnşa Yarışmasında yer alan 10 kategori [27]

2002 Yılı Yarışma Kategorileri	Alt Kategorileri
Tasarım ve Yaşanabilirlik	• Yapısal Bütünlük • İşlev ve Konfor • Estetik
Sunum ve Simülasyon	• Bir evin tasarımını geliştirmek için kullanılan bilgisayar simülasyonlarının kalitesi, yeniliği ve eksiksizliği • Mimari tasarımların netliği • Mühendislik tasarımının anlaşılırlığı ve mimari tasarımla entegrasyonu
Grafik ve İletişim	• İş planı • Kitleye uygun içerik geliştirme • Tutarlı bir format ve tasarım geliştirmek • Yaratıcı olmak ve ilgi yaratmak
Konfor Bölgesi	• Bir ev içinde belirli sıcaklık aralıklarını korumak • Yolcunun konfor ihtiyaçlarını karşılamak
Soğutma	• Taze gıda soğutucu bölmesinde 32°-40°F sıcaklık aralığının korunması • Dondurucu bölmesinde 40°-0°F sıcaklık aralığının korunması • Düşük elektrik enerjisi tüketimini korumak
Sıcak su	• Günlük duş testleri • İki çamaşır testi • Günlük bulaşık yıkama testleri
Enerji dengesi	• Günlük işler için enerji kullanımı: • Enerji talebi gereksinimlerini karşılamak veya aşmak • Yarışma başladığında evin pil sisteminde depolanan enerjiye eşit veya daha fazla miktarda enerji depolamak
Aydınlatma	• Hem gündüz hem de gece kabul edilebilir aydınlatma seviyelerini korumak
Ev Ofisi	• Ev ofis kullanımı için uygun şekilde aydınlatılmış ve şartlandırılmış bir alan tasarlama
Ulaşım	• Organizatörler tarafından sağlanan “Ford Th!ink Neighbor” elektrikli araçları için yeterli elektrik enerjisinin sağlanması • Evlerden önceden belirlenmiş gezileri tamamlaması • En fazla kilometre kredisi biriktirme

Solar Decathlon 2005

2005 sonbaharında, Amerika Birleşik Devletleri, Porto Riko, Kanada ve İspanya'daki kolej ve üniversite öğrencilerinden oluşan takımlar ikinci Solar Decathlon'da yarışmıştır. Ekipler, Washington DC, National Mall'daki bir "güneş köyünde" enerji verimliliği yüksek ve tamamen güneş enerjisiyle çalışan evler tasarlamak ve inşa etmek için 10 kategoride yarışmıştır. Bu kategoriler Tablo 2’de yer almaktadır.

Güneş evinin mimarisi, yaşanabilirliği, konforu ve cihazları için sürekli bir elektrik kaynağı sağlama, aydınlatma ve bir adet elektrikli araba şarj etme gibi özelliklerine göre değerlendirilir. Ayrıca evler, günlük kullanım için sıcak su sağlayabilmelidir. Yarışmanın tasarım ve enerji ile ilgili gereksinimlerine ek olarak, evlerinin tasarımının gelişimi hakkında belgeler sağlamalı ve kullanıcılarla iletişim kurmalıdır [2; 28].

Tablo 4. 2005 Solar Decathlon Build Challenge/İnşa Yarışmasında yer alan 10 kategori [28].

2005 Yılı Yarışma Kategorileri	Alt Kategorileri	Puanlama
Mimari	• Ekipler, güneş ve enerji verimliliği teknolojilerini sorunsuz bir şekilde evlerin tasarımlarına entegre eden çekici, yüksek performanslı evler tasarlamalı ve inşa etmelidir.	200
Konut	• Evler yaklaşık 70 m2'olmalıdır. Ancak yine de yaşanabilir olmalı ve günümüz ailelerinin ihtiyaçlarını karşılamalıdır.	100
Belgeleme	• Ekipler, Solar Decathlon projesinin şematik tasarımı, tasarım geliştirme, inşaat vb. gibi tüm aşamaları belgelemelidir.	100
İletişim	• Kalıcılığın sağlanması için çalışmaların başkaları ile paylaşılması gerekmektedir. Ekipler, web siteleri ve halka açık turlar aracılığıyla evlerinin teknik yönleri ve deneyimlerini geniş bir kitleye iletmelidir..	100
Konfor Bölgesi	• Sıcaklık ve nem kontrolü sağlanmalıdır.	100
Aletler	• En verimli cihazlar seçilmelidir.	100
Sıcak Su Kullanımını	• Günlük duş testleri • İki çamaşır testi • Günlük bulaşık yıkama testleri	100
Aydınlatma	• Hem gündüz hem de gece kabul edilebilir aydınlatma seviyelerini korumak	100
Enerji Dengesi	• Evlerin elektrik ihtiyacını karşılamak için güneş enerjisi sisteminden akülere giren enerji miktarı ve akülerden çekilen elektrik enerjisi miktarı ölçülerek puanlanmaktadır.	100
Ulaşım	• Bir önceki yarışma ile aynı içerik.	100

Solar Decathlon 2007

2007 Ekim ayında, Amerika Birleşik Devletleri, Porto Riko, Kanada, İspanya ve Almanya'daki kolej ve üniversite öğrencilerinden oluşan yirmi takım üçüncü Solar Decathlon'da yarışmıştır [3; 4; 5].

Tablo 5. 2007 Solar Decathlon Build Challenge/İnşa Yarışmasında yer alan 10 kategori [5]

2007 Yılı Yarışma Kategorileri	Alt Kategorileri	Puanlama
Mimari	• Sağlamlık • Ticaret • Yenilikçi Tasarım	200
Mühendislik	• Mühendislik Tasarımı ve Uygulaması • Enerji Analizi	150
Pazar Potansiyeli	• Pazara uygun maliyet	150
İletişim	• Bir önceki yarışma ile aynı içerik.	100
Konfor Bölgesi	• Sıcaklık ve nem kontrolü sağlanmalıdır.	100
Aletler	• Bir önceki yarışma ile aynı içerik.	100
Sıcak Su	• Bir önceki yarışma ile aynı içerik.	100
Aydınlatma	• Bir önceki yarışma ile aynı içerik.	100
Enerji Dengesi	• Bir önceki yarışma ile aynı içerik.	100
Ulaşım	• Bir önceki yarışma ile aynı içerik.	100

Solar Decathlon 2009

2009 Ekim ayında Amerika Birleşik Devletleri, Kanada, Almanya ve İspanya'daki kolej ve üniversite öğrencilerinden oluşan yirmi takım, enerji verimli ve tamamen güneş enerjisinine bağlı olan evi tasarlamak, inşa etmek ve işletmek için dördüncü ABD Enerji Bakanlığı Solar Decathlon'da yarışmıştır. Evler için aranan temel gerekilikler [6; 7]:

- Cazip ve yaşaması kolay olması,
- Rahat ve sağlıklı iç ortam koşulları sunması,
- Yeterli aydınlatma sağlaması,
- Ev aletlerine enerji sağlaması,
- Sıcak su sağlaması,

• Enerji üretimi ve tüketimini dengelemesi beklenmektedir.

Tablo 6. 2009 Solar Decathlon Build Challenge/İnşa Yarışmasında yer alan 10 kategori [6]

2009 Yılı Yarışma Kategorileri	Alt Kategorileri	Puanlama
Mimari	• Mimari Unsurlar • Bütüncül Tasarım • Yenilikçi Tasarım	100
Pazar Potansiyeli	• Yaşanabilirlik • İnşa edilebilirlik • Pazarlanabilirlik	100
Mühendislik	• İşlevsellik • Verimlilik • Yenilik • Güvenilirlik	100
Aydınlatma Tasarımı	• Elektirikli Aydınlatma Kalitesi • Günışığı kalitesi • Kullanım kolaylığı • Esneklik • Enerji verimliliği • Bina Entegrasyonu	75
İletişim	• Bir önceki yarışma ile aynı içerik.	75
Konfor Bölgesi	• Sıcaklık ve nem kontrolü sağlanmalıdır. • Temperature in the range of 72°F (22.2°C) to 76°F (24.4°C) • Relative humidity between 40% and 55%	100
Sıcak Su	• Sıcak su yarışması ile su ısıtma sisteminin evlerin günlük olarak yıkama ve banyo yapmak için kullandığı tüm sıcak suyu sağlayabildiğini göstermektedir (15 galon, 110°F/43.3°C).	100
Ev Aletleri	• En verimli cihazlar seçilmelidir. • Buzdolabı sıcaklık aralıklarını 34°F/1.11°C ila 40°F/4.44°C arasında tutun. • Dondurucu sıcaklık aralıklarını -20°F/-28.9°C ila 5°F/-1.5°C arasında koruyun. • Yarışma haftası boyunca 10 çamaşır yıkayın ve kurutun. • Yarışma haftası boyunca bulaşık makinesini beş kez çalıştırın.	100
Ev Eğlencesi	• Ev Eğlencesi yarışması, bir evin ev olmak için gereken özelliklere sahip olup olmadığını ölçer.	100
Net Ölçüm	• Enerji dengesi • Enerji fazlası	150

Solar Decathlon 2011 ve 2013

2011 Eylül ayında, Kanada, Yeni Zelanda, Belçika ve Çin'deki kolej ve üniversite öğrencilerinden oluşan ondokuz takım Solar Decathlon'da yarışmıştır. Maryland Üniversitesi birinciliği kazanmıştır [10; 8; 9].

2013 Ekim ayında ise Amerika Birleşik Devletleri, Avusturya, Kanada ve Çek Cumhuriyeti'ndeki kolej ve üniversite öğrencilerinden oluşan ondokuz takım yarışmıştır. Avusturya Takımı: Viyana Teknoloji Üniversitesi kazanan ilan edilmiştir [11].

Ekipler, evlerin performansını, ne kadar yaşanabilir ve uygun fiyatlı olduklarını ölçmek için tasarlanmıştır. Her kategori maksimum 100 puan değerindedir ve yarışma toplam 1.000 puandır. 2011 ve 2013 yıllarında yer alan kategoriler aynı olduğu için birleştirilerek Tablo 5'te verilmiştir. Ek olarak yarışmanın değerlendirilmesi aşağıda yer alan üç aşamada gerçekleştirilmiştir [11; 9]:

• Görev tamamlama

Ekipler yemek pişirme, bulaşık yıkama ve çamaşır yıkama gibi ev işlerini inşa ettikleri binada gerçekleştirmektedir.

• Performans İzleme

Ekipler evlerin konforlu iç ortam sıcaklık aralığını (71°-76°F/21.7°-24.4°C) korumak gibi belirli kriterlere göre performansını ortaya koymaktadır.

• Jüri değerlendirmesi

Alanında uzman jüri üyeleri (mimarlık, mühendislik ve iletişim vb.), ölçülemeyen özellikler (estetik ve tasarım ilhamı gibi) için puan vermektedir.

Tablo 7. 2011 ve 2013 Solar Decathlon Build Challenge/İnşa Yarışmasında yer alan 10 kategori [11; 9]

2011 ve 2013 Yılı Yarışma Kategorileri	Değerlendirme	Alt Kategorileri	Puanlama
Mimarlık Yarışması	Jürili	• Mimari Unsurlar • Bütüncül Tasarım • Aydınlatma • Yenilikçi Tasarım • Belgeleme	100
Pazar Temyiz Yarışması	Jürili	• Bir önceki yarışma ile aynı içerik.	100
Mühendislik Yarışması	Jürili	• İşlevsellik • Verimlilik • Yenilik • Güvenilirlik • Belgeleme	100
İletişim Yarışması	Jürili	• Bir önceki yarışma ile aynı içerik.	100
Uygun Maliyet Yarışması	Jürili	• Bir önceki yarışma ile aynı içerik.	100
Konfor Bölgesi Yarışması	Ölçülen	• Bir önceki yarışma ile aynı içerik.	100
Sıcak Su Yarışması	Ölçülen	• Bir önceki yarışma ile aynı içerik.	100
Ev aletleri Yarışması	Ölçülen	• Bir önceki yarışma ile aynı içerik.	100
Ev Eğlencesi Yarışması	Ölçülen	• Bir önceki yarışma ile aynı içerik.	100
Enerji Dengesi Yarışması	Ölçülen	• Bir önceki yarışma ile aynı içerik.	100

Solar Decathlon 2015

Solar Decathlon 2015, ABD Enerji Bakanlığı tarafından, 8-18 Ekim tarihlerinde Irvine, California'daki Orange County Great Park'ta gerçekleştirilmiştir. Ondört ekip, en uygun maliyetli, enerji açısından verimli ve güneş enerjili evi tasarlamak, inşa etmek ve işletmek için yarışmıştır. Finalde, Stevens Teknoloji Enstitüsü kazanarak birinci olmuştur [13].

Final yarışmasında, genel kazananı belirlemek için takımlar ve evleri 10 kategoride (Tablo 6) yarışmışlardır. Hedef [13]:

- Uygun maliyetli, çekici ve yaşaması kolay olması,
- Konforlu ve sağlıklı iç ortam koşulları sunması,
- Yemek pişirmek, temizlik yapmak, eğlenmek ve işe gidip gelmek için enerji sağlanması,
- Yeterli sıcak su sağlanması,
- Tükettiğinden çok enerji üretmesi beklenmektedir.

Tablo 8. 2015 Solar Decathlon Build Challenge/İnşa Yarışmasında yer alan 10 kategori [13]

2015 Yılı Yarışma Kategorileri	Değerlendirme	Alt Kategorileri	Puanlama
Mimarlık	Jürili	• Mimari konsept ve tasarım yaklaşımı • Mimari uygulama ve yenilik • Belgeleme	100
Pazar Potansiyeli	Jürili	• Bir önceki yarışma ile aynı içerik.	100
Mühendislik	Jürili	• Bir önceki yarışma ile aynı içerik.	100
İletişim	Jürili	• İletişim stratejisi • Elektronik iletişim • Halka açık sergi malzemeleri • Halka açık sergi sunumu • Görsel ve işitsel sunum	100
Uygun Maliyet	Jürili	• Bir önceki yıl ile aynı içerik.	100
Konfor Bölgesi	Ölçülen	• Bir önceki yıl ile aynı içerik.	100
Ev aletleri/Beyaz Eşya	Ölçülen	• Buzdolabı sıcaklığının 34°F (1,11°C) ile 40°F (4,44°C) arasında tutulması • Dondurucu sıcaklığının -20°F (-28.9°C) ile 5°F (-1.5°C) arasında	100

		tutulması • Belirli bir süre içinde çamaşır yıkamak • Aktif veya pasif kurutma yöntemleri kullanarak bir çamaşır yükünü yıkamadan önce toplam ağırlığına eşit veya daha az toplam ağırlığa döndürmek • Bulaşık makinesine yerleştirilen bir sıcaklık sensörünün 120°F'ye (48.9°C) ulaşması gereken bir noktada, bulaşık makinesini eksiksiz, kesintisiz bir döngü boyunca çalıştırmak • Belirli bir süre içinde 5 pound (80 oz veya 2.268 kg) suyu buharlaştırmak için bir mutfak aleti kullanarak pişirme simülasyonu.	
Ev Hayatı	Ölçülen	• Belirtilen zaman dilimlerinde tüm ışıkların açılması • Yarışma boyunca birkaç kez duştan 10 dakika veya daha kısa sürede 15 galon (56.8 l) sıcak su (110°F/43.3°C) üretmek • Belirli zaman dilimlerinde televizyon ve bilgisayar çalıştırma • Komşular için iki akşam yemeği partisine ev sahipliği yapmak • Komşular için bir film gecesi düzenlemek.	100
Ulaşım	Ölçülen	• Yarışma haftasında sekiz kez iki saat veya daha kısa sürede 25 mil veya daha fazla sürüş için tam puan verilmiştir.	100
Enerji Dengesi	Ölçülen	• Enerji üretimi • Enerji tüketimi	100

Solar Decathlon 2017

Solar Decathlon 2017, ABD Enerji Bakanlığı tarafından 5-9 ve 12-15 Ekim tarihlerinde, Colorado Üniversitesi'ndeki 61. and Peña İstasyonunda, Denver Uluslararası Havalimanını "Union Station" şehir merkezine bağlayan A hattı banliyö treninde gerçekleştirilmiştir. Onbir ekip, en uygun maliyetli, enerji açısından verimli ve cazip güneş enerjili evi tasarlamak, inşa etmek ve işletmek için yarışmış olup İsviçre Takımı, NeighborHub ile genel rekabeti kazanmıştır [14].

2017 yılında gerçekleştirilen yarışma, aşağıda verilen parametreleri vurgulamak için zorlu yeni kategorilerle zenginleştirilmiştir:

- İnovasyon/yenilik,
- Su kullanımı ve yeniden kullanım stratejileri,
- Akıllı enerji kullanımı,
- Pazar potansiyeli.

Ayrıca Solar Decathlon 2017 yarışması şunları vurgulamaktadır:

- Uygun maliyetli mimari ve mühendislik tasarımı,
- Enerji tasarruflu ısıtma ve soğutma sistemleri, cihazlar ve elektronikler,
- Kullanıcı sağlığı ve konforu,
- İletişim.

Solat Decathlon etkinlik tarihinde ilk kez 2017 yılında takımlar para ödülü almaya hak kazanmıştır. Yarışma alanında başarılı bir şekilde güneş evi inşa eden her takım, en az 100.000 $ almaya hak kazanmıştır. Dereceye girenler ise:

- 1. 300.000 $
- 2. 225.000 $
- 3. 150.000 $
- 4. 125.000$
- 5. ve üzeri, 100.000 $ kazanmaktadır.

Tablo 9. 2017 Solar Decathlon Build Challenge/İnşa Yarışmasında yer alan 10 kategori [14]

2017 Yılı İnşa Yarışma Kategorileri	Değerlendirme	Alt Kategorileri	Puanlama
Mimarlık	Jürili	• Mimari konsept ve tasarım yaklaşımı • Mimari uygulama ve yenilik • Belgeleme	100
Pazar Potansiyeli	Jürili	• Pazar potansiyeli • Yaşanabilirlik • Maliyet etkinliği • İnşa edilebilirlik	100
Mühendislik	Jürili	• Yaklaşım • Tasarım • Verimlilik • Performans • Belgeleme	100
İletişim	Jürili	• İletişim stratejisi • Uygulama • Yerinde iletişim	100
İnovasyon Yarışması	Jürili	• Araştırma • Sürdürülebilirlik • İnovasyon/Yenilik • Dayanıklılık ve Güvenilirlik	100
Su Yarışması	Jürili	• Koruma/tasarruf • Islah ve yeniden kullanım • Peyzaj	100
Sağlık ve Rahatlık		• 68°F (20°C) ve 74°F (23,3°C) arasındaki sıcaklıklar • %35 ile %60 arasında bağıl nem • Milyonda 1.000 parçadan daha az iç mekan CO2 seviyeleri • Dışarıdan evin içine ve içeriden dışarıya hava akışını en aza indiren, böylece o havayı ısıtmak veya soğutmak için gereken enerji miktarını azaltan sıkı bir bina kabuğu.	
Ev aletleri/Beyaz Eşya	Ölçülen	• Buzdolabı sıcaklığının 34°F (1,1°C) ile 40°F (4,4°C) arasında tutulması • Dondurucu sıcaklığının -20°F (-28.9°C) ile 5°F (-1.5°C) arasında tutulması • Birkaç yük çamaşır yıkamak • Aktif veya pasif kurutma yöntemleriyle birden fazla çamaşır kurutma • Yarışma sırasında 5 pound (80 oz veya 2,3 kg) suyu birkaç kez buharlaştırmak için bir mutfak aleti kullanarak pişirme simülasyonu • En az 110°F (43.3°C) ortalama sıcaklıkta 10 dakika veya daha kısa sürede 15 galon (56.8 L) su çekerek birkaç duşu simüle etmek.	100
Ev Hayatı	Ölçülen	• Yarışmanın her günü birkaç saat boyunca evin her yerinde konforlu ışık seviyelerini korumak • Her gün birkaç saat televizyon ve bilgisayar kullanmak • Komşular için iki akşam yemeği partisine ev sahipliği yapmak • Komşular için oyun gecesi düzenlemek • 75 dakika içinde en az 25 mil (40,2 km) elektrikli araç kullanmak.	100
Enerji Yarışması	Ölçülen	• Bir önceki yarışma ile aynı içerik.	100

Solar Decathlon 2020

Solar Decathlon 2020 etkinliği, Nisan 2021'de Golden, Colorado'daki Ulusal Yenilenebilir Enerji Laboratuvarı'nda gerçekleştirilmiştir. Katılımcılar, yapı endüstrisindeki gerçek dünya sorunlarına yaratıcı çözümler üretmek için yerel kullanıcıları için eksiksiz, işlevsel evler tasarlamakta ve inşa etmektedir. En iyi performans gösteren takımlar, 2021'de Ulusal Ev Müteahhitleri Birliği (NAHB) Uluslararası Müteahhitler etkinliğinde sergilenmek üzere davet edilmiştir [15].

Tablo 10. 2017 Solar Decathlon Build Challenge/İnşa Yarışmasında yer alan 10 kategori [15].

2020 Yılı İnşa Yarışma Kategorileri	Alt Kategorileri	Puanlama
Enerji Performansı	• Enerji Verimliliği • Enerji Üretimi • Net-Sıfır - Artı Enerji • Talep Karşılama • Şebekeden Bağımsız İşlevsellik	100
Mühendislik	• Farklı teknoloji ve entegrasyon • Enerji ve çevresel performans • Ön ve uzun vadeli maliyet analizi • Güvenilirlik	100
Finansal Fizibilite ve Uygun Maliyet	• Pazar potansiyeli • Maliyet etkinliği • İnşa edilebilirlik	100
Dayanıklılık	• Konumu için geçerli afet risklerine dayanma ve kurtarma • Felaketler sonrası yaygın olarak meydana gelen şebeke kesintileri sırasında kritik işlevleri sürdürmek • Yerel iklim koşullarına uyum sağlamak	100
Mimarlık	• Mimari konsept ve tasarım yaklaşımı • Mimari uygulama ve yenilik • Belgeleme	100
İşlevler	• Amaçlanan işlev ne kadar etkin bir şekilde yerine getirilmektedir	100
Pazar Potansiyeli	• Hedef kullanıcıya hitap etmesi • Yaklaşımı • Pazar potansiyeli	100
Konfor ve Çevre Kalitesi	• Binanın belirli sıcaklık, nem ve gürültü seviyelerinde çalışma yeteneği değerlendirilir • Verimli havalandırma, filtreleme, seyreltme ve malzeme seçimi stratejileri incelenir	100
İnovasyon / Yenilik	• Araştırma • Sürdürülebilirlik • İnovasyon/Yenilik • Dayanıklılık ve Güvenilirlik	100
Sunum	• Tasarım ve enerji performansı stratejisini ilgili kitlelere doğru ve etkili bir şekilde iletme yeteneğini değerlendirilir.	100

2.2. Solar Decathlon Design Challenge/Tasarım Yarışması Kategorileri

Güneş Dekatlonu tasarım yarışması ilk olarak 2014 yılında DOE (ABD Enerji Bakanlığı) öğrenci tasarım yarışması olarak başlamıştır. 2018 yılına gelindiğinde "Tasarım Yarışması/Desing Challange" olarak adlandırılmış olup günümüze kadar her yıl düzenlenmiştir [22].

Güneş Dekatlonu Tasarım Yarışmasında yarışan takımlar bir veya iki akademik dönem boyunca konut veya ticari bina tasarımları oluştururlar. Katılımcılar, inşaat endüstrisindeki gerçek dünya sorunları için yaratıcı çözümler üretmekte ve sıfır enerjili binalar için hızla artan talebini ne kadar iyi karşıladıkları konusunda değerlendirilmektedir [16].

Şekil 1 Güneş dekatlonunun tasarım ve inşa yarışmalarının yapısını göstermektedir. Tasarım Yarışmasına katılan ekipler; yeni konut, güçlendirme, bitişik nizam konut, çok aileli bina, ofis binası ve eğitim binası olmak üzere 6 klasmandan birinde yarışmayı tercih etmektedir. Takımlar galip gelmek için 10 kategorinin tamamında iyi performans göstermelidir. Bu kategoriler tasarım yarışmasında sabit olup "mimarlık, mühendislik, pazar potansiyeli, dayanıklılık ve farklı koşullara karşı direnç (resilience), çevresel etki, bütünleşik performans, kullanıcı deneyimi, konfor ve çevresel kalite, enerji performansı, sunum" olarak belirlenmiştir [17].

Şekil 12. Güneş Dekatlonunun Yapısı [17]

Tasarım Yarışması ile "Solar Decathlon" yarışmasının etkisi artmakta, ticari binalara ve daha çeşitli konut bina türlerini içermesi ile birlikte, katılımcı sayısında önemli bir artış olduğu görülmekte ve ülke genelinde üniversite kurumu müfredatına önemli ölçüde entegre edildiği belirtilmektedir [23].

2. 3. Bölüm Değerlendirmesi

Solar Decathlon inşa yarışması kapsamında projelerin değrelendirilmesi için belirlenen temel kategorilerin yıllar içindeki değişimi hazırlanan tablolar üzerinden incelendiğinde:

2002 yılında istenen özelliklere bakıldığında temelde, tasarım ve yaşanabilirlik, sunum ve simülasyon, grafik ve iletişim, konfor bölgesi, soğutma, sıcak su, enerji dengesi, aydınlatma, ev ofisi, ulaşım olmak üzere 10 başlıktan oluşmaktadır. Amaç, enerji verimliliği yüksek, tamamen güneş enerjisiyle çalışan evler tasarlama ve inşa etmektir.

2005 yılında ekiplerden özellikle güneş ve enerji verimliliği teknolojilerini sorunsuz bir şekilde konutların tasarımlarına entegre eden cazip, yüksek performanslı evler tasarlamları ve inşa etmeleri istenmiştir. Bir önceki yıl var olan özelliklere ek olarak; aletler başlığı eklenmiş olup en verimli cihazların kullanılması teşvik edilmiştir. Belgeleme ile ekiplerden projelerinin şematik tasarımı, gelişimi, inşaat vb. gibi tüm aşamaların belgelenmesi istenmiştir. Bir önceki dönemde soğutma ayrı bir kategori iken konfor bölgesi yarışma kategorisi içerisine dahil edilmiştir.

2007 yılında, mimaride sağlamlık, pazar potansiyeli ve yenilikçi tasarım vurgulanmıştır. Bir önceki yıl var olan özelliklere ek olarak; mühendislik kategorisi eklenmiş tasarım ve inşa aşamalarının birbirine entegre edilmesi istenmiştir. Ayrı bir başlık olarak ele alınan simülasyon, enerji analizi olarak mühendislik yarışması altında değerlendirilmeye başlanmıştır. Pazara uygun maliyeti teşvik etmek için pazar potansiyeli kategorisi ilk defa bu yıl dahil edilmiştir.

2009 yılında istenen özelliklere bakıldığında mimaride, bütüncül ve yenilikçi tasarım ön plana çıkmaktadır. Pazar potansiyeli kategorisine uygun maliyet dışında yaşanabilirlik, inşa edilebilirlik ve pazarlanabilirlik eklenmiştir. Mühendislik yarışmasında, verimlilik ve yeniliğe ek olarak işlevsellik ve güvenilirlik eklenmiştir. Enerji dengesi, net ölçüm kategorisi altına alınarak, enerji fazlasına çözüm üretilmesi seçeneği eklenmiştir. Son olarak bu yıl ilk defa ev eğlencesi kategorisi getirilerek, bir evin ev olmak için gereken özelliklere sahip olup olmadığı ölçülmektedir.

2011 ve 2013 yıllarında istenen özellikler aynı olup tek başlık altında değerlendirilmiştir. 2011 ve sonrasında yarışmanın değerlendirilmesi üç aşamada gerçekleştirilmiştir.

- Görev tamamlama: Ekipler yemek pişirme, bulaşık yıkama ve çamaşır yıkama gibi ev işlerini inşa ettikleri binada gerçekleştirmektedir.

- Performans izleme: Ekipler evlerin konforlu iç ortam sıcaklık aralığını (71°-76°f/21.7°-24.4°C) korumak gibi belirli kriterlere göre performansını ortaya koymaktadır.
- Jüri değerlendirmesi: Alanında uzman jüri üyeleri (mimarlık, mühendislik ve iletişim vb.), ölçülemeyen özellikler (estetik ve tasarım ilhamı gibi) için puan vermektedir.

Mimaride, bütüncül, yenilikçi tasarım ve ek olarak önceki dönemlerde ayrı bir kategoride yer alan aydınlatma tasarımı ve belgeleme bu kategori altında değerlendirmeye alınmıştır. Uygun maliyet pazar potansiyeli kategorisi altından çıkarılarak ayrı bir başlık olarak ölçülmüştür. Diğer kategoriler ise aynı kalmıştır.

2015 yılında katılımcılardan beklenen özellikler temelde, uygun maliyetli, çekici ve yaşaması kolay olması, konforlu ve sağlıklı iç ortam koşulları sunması, yemek pişirmek, temizlik yapmak, eğlenmek ve işe gidip gelmek için güç sağlanması, yeterli sıcak su sağlanması, tükettiğinden çok enerji üretmesidir. 2011-2013 yılları ile aynı özellikler beklenmekte olup tek fark ulaşım kategoridir. Belirlenen mil sayısını tamamlayan projelere puan verilecektir.

İlk kez 2017 yılında takımlar para ödülü almaya hak kazanmıştır. 2017 yılında katılımcılardan beklenen özelliklere bakıldığında diğer yıllardan farklı olarak, su yarışma kategorisi getirilerek; koruma/tasarruf, ıslah ve yeniden kullanım, peyzaj içerikleri eklenmiştir. İnovasyon, mimari ve mühendislik kategorilerinin alt başlığı olmaktan çıkarak ayrı bir kategori olarak değerlendirilmiştir. Uygun maliyet kategorisi ise tekrardan pazar potansiyeli başlığına dahil edilmiştir.

2020 yılında katılımcılardan beklenen özellikler incelendiğinde, enerji performansı başlığı altında, enerji üretimi ve verimliliğine ek olarak net-sıfır, artı enerji ve şebekeden bağımsız işlevsellik özellikleri beklenmektedir. Dayanıklılık (resilience) başlığı ilk defa ayrı bir kategori olarak eklenmiş olup afet risklerine karşı dayanıklılık ve kurtarma, felaketler sonrası yaygın olarak meydana gelen şebeke kesintileri sırasında kritik işlevleri sürdürmek gibi küresel sorunlar ön plana çıkarılarak çözüm bulunması istenmiştir. Yeni eklenen diğer bir kategori ise işlev yarışmasıdır. Projenin amaçlanan işlevi ne kadar etkin bir şekilde karşılayacağı ölçülmek istenmektedir. İletişim kategorisi yerine ise sunum kategorisi getirilmiş olup içerik olarak aynı özelliktedir. Bu başlık ile tasarım ve enerji performansı stratejisini ilgili kitlelere doğru ve etkili bir şekilde iletme yeteneği değerlendirilir.

Güneş Dekatlonu tasarım yarışmasında kategoriler sabit olup "mimarlık, mühendislik, pazar potansiyeli, dayanıklılık ve farklı koşullara karşı direnç (resilience), çevresel etki, bütünleşik performans, kullanıcı deneyimi, konfor ve çevresel kalite, enerji performansı, sunum" olarak belirlenmiştir.

3. SÜRDÜRÜLEBİLİRLİK İLKELERİ KAPSAMINDA YARIŞMANIN GELİŞİMİNİN İNCELENMESİ

Sürdürülebilir ve ekolojik yapı tasarımında, binanın bulunduğu yerle kurduğu anlamsal bağ sayesinde mimarisini özgün hale getiren bir takım farklılıklar ortaya çıkarmaktadır. Bu kapsamda yer alan projeler incelendiğinde her bir yapının farklı birçok tasarım parametresi baz alınarak kurgulandığı görülmektedir. Yerel ve bölgesel öncelikler, mimari tasarım zenginliğini ve çeşitliliğini artırmaktadır. Gökşen, F., [18]'nin tez çalışması kapsamında incelenen örnek yapılar ve literatür taramalarının analizi sonucunda sürdürülebilir ve ekolojik yapı tasarımında aşağıda verilen 8 ana başlığın ön plana çıktığı görülmektedir. Solar decathlon yarışmasının kazanan projeleri bu başlıkların referans alındığı bir tablo üzerinden bir araya getirilerek incelenecektir.

1. Sürdürülebilir düşünce ve tasarım ilkeleri
2. Ekolojik mimari ve yapay çevre tasarımı
3. Bina kabuğu
4. Bina geometrisi
5. Mekân organizasyonu
6. Yapı malzemesi seçimi

7. İklimlendirme sistemleri

8. Atık yönetimi

Sürdürülebilir düşünce ve tasarım ilkeleri başlığı altında beklenen özellikler: Tasarımın temel hedefleri, küresel ve yerel çevre sorunlarına sunduğu çözümler, enerji duyarlı yapı tasarımının ön planda tutulması, yerel kültür ve mimariyi yansıtan ürünler ortaya konması, fosil yakıtlar yerine yenilenebilir enerji kullanımın teşvik edilmesi, disiplinler arası bir çalışma sonucu tüm paydaşların katkıları ile geliştirilen ortak bir ürün olması vurgulanmaktadır.

Ekolojik mimari yapay çevre tasarımı başlığı altında beklenen özellikler: Doğal çevrenin korunması, bölgesel iklim özellikleri, yerel doku ve topoğrafya ile uyumlu mimari tasarım gerçekleştirilmesi örnek verilebilir.

Yapı kabuğu iç ve dış ortamı birbirinden ayıran, yatay, düşey ve eğimli yapı bileşenlerinden oluşan bir yapı öğesidir [19]. Kabuğun tasarımındaki temel hedef minimum ısıtma ve soğutma enerjisine dayalı konforlu bir iç mekan yaratmaktır [20; 21]. Dolayısıyla bina kabuğu başlığı altında beklenen özellikler: Düşey yapı elemanları ve çatıda kullanılan yapı malzemelerinin katman özellikleri ve kalınlıklarının yüksek oranda hava ve nem sızdırmazlığına sahip olacak şekilde seçilmesi, geri dönüştürülebilir malzemeler tercih edilmesidir.

Bina geometrisi başlığı altında beklenen özellikler: Yerleşim bölgesine ve iklim özelliklerine uygun, güneş ve hakim rüzgar yönünün dikkate alan, binanın formunu bu özelliklere göre şekillendiren bir tasarıma sahip olmasıdır.

Mekan organizasyonu başlığı altında beklenen özellikler: yerel kültüre ile uyumlu, kullanıcı konfor ve sağlığını düşünen, mevsime göre esnek kullanım sunabilen, tampon bölgeler barındıran açık ve yarı açık mekanlar ile desteklenebilen, farklı fonksiyonlara evrilebilecek alanlar tasarlanmasıdır.

Yapı malzemesi seçimi başlığı altında, bölgeyle ve iklimle uyumlu yerel malzeme kullanımı veya doğal ve geri dönüştürülebilen malzeme tercih edilmesi ön plana çıkmaktadır.

İklimlendirme sistemleri başlığı altında, Doğal aydınlatma ve havalandırmanın önemi, gerekliyse gölgeleme elemanlarının kullanılması, enerji verimliliği sağlanması için pasif sistemlere başvurulması, fosil yakıtlar yerine yenilenebilir kaynakları kullanarak aktif sistem tasarımlarını binaya entegre etmek gibi özellikler beklenmektedir.

Son olarak atık yönetimi ilkesi ile ise geri dönüşümlü malzeme tercih edilmesi, yağmur suyunun toplanması, gri su arıtma sistemi, siyah su kullanımı, katı atık veya biyolojik atık dönüşümü gibi parametrelerin projelere dahil edilmesi beklenmektedir.

Tablo 9. Yapım/İnşa Yarışmasının Kazan Projeleri

		2002 **Colorado Üniversitesi, Boulder** **BASE+**	**2005** **Colorado Üniversitesi, Denver ve Boulder**	**2007** **Technische Üniversitesi Darmstadt**
Sürdürülebilir Tasarım Kriterleri				
1	Sürdürülebilir düşünce ve tasarım ilkeleri	Yerel mimariyi dikkate alan yenilenebilir enerji kullanımı.	Doğal malzemelerin kullanılması, inovasyon, enerji verimliliği, modülerlik ve erişilebilirlik.	Doğal malzemeler, inovasyon, enerji verimliliği
2	Ekolojik mimari yapay çevre tasarımı	Değişen bütçelere, iklimlere ve şantiyelere uyum sağlar.	Her yere uyumlanabilir, Erişilebilir.	Verimliliği büyük ölçüde kurulduğu yerel iklime bağlıdır.
3	Bina kabuğu	Yalıtımlı panel	Duvarlarda biyo-tabanlı yapısal yalıtımlı paneller. Hareketli Çatı.	Meşe panjurlar. Parafin içeren özel bir duvar kaplaması denenmiştir (Faz değiştiren duvar sistemi).
4	Bina geometrisi	–	–	–
5	Mekân organizasyonu	Amerikan evi, Bölgeye uyarlanabilen modüler tasarım.	–	–
6	Yapı malzemesi seçimi	–	Kullanılan inşaat ve mobilya malzemeleri organik, Tamamen geri dönüştürülmüş ve doğal malzemelerden yapılmıştır.	Alman Meşesi, Doğal ahşap ve cam, Yerel malzeme kullanımı.
7	İklimlendirme sistemleri	Aktif sistem, Güneş enerjisi kullanımı, PV panel, Isı pompası.	Yüksek performanslı cam Güneş enerjisi kullanımı, PV panel.	Sıcak su ve iklim kontrolü sağlayacak sistemler, Pasif ve aktif güneş enerjisini birleştiren fotovoltaik paneller.
8	Atık yönetimi	–	Geri dönüştürülebilen malzeme kullanımı.	–

Tablo 9 (devamı). Yapım/İnşa Yarışmasının Kazan Projeleri

	Sürdürülebilir Tasarım Kriterleri	**2009 Darmstadt Üniversitesi**	**2011 Maryland Üniversitesi**	**2013 Avusturya Takımı: Viyana Teknoloji Üniversitesi**
				
1	Sürdürülebilir düşünce ve tasarım ilkeleri	Enerji verimliliği, Yeni teknoloji, yenilenebilir enerji kullanımı.	Enerji ve su tasarrufu, geri dönüşüm ve yağmur suyu yönetimi. Bütünsel tasarım.	Sağlıklı, sürdürülebilir bir gelecek ve birçok yaşam tarzına ve iklime uyum sağlayabilecek bir konsept.
2	Ekolojik mimari yapay çevre tasarımı	Çevre üzerinde minimum etki ve maksimum işlev.	Çevre üzerinde minimum etki ve maksimum işlev.	Çeşitli iklim bölgelerine uyum sağlar ve çeşitli yaşam tarzlarını karşılayabilir.
3	Bina kabuğu	Tek kristalli silikon panel ve alüminyum şeritler üzerine yerleştirilmiş ince film güneş pillerinden yapılmış dış cephe kaplaması, Vakum yalıtım panelleri ve alçıpandaki özel malzemeler.	Yalıtım, yüksek sızdırmazlık, enerji ve su sızmasına karşı koruyan entegre katman, havalandırmalı bir rainscreen, güneş duvarı.	–
4	Bina geometrisi	Kompakt tasarım, Küp.	Yağmur suyunu toplamayı sağlayan kelebek çatı hattı.	Kompakt tasarım.
5	Mekân organizasyonu	–	Kullanıcı konforu, Nem kontrolü, Esnek alan planlaması.	Esnak tasarım, değiştirilebilir mimari elemanlar. İç ve dış ile kamusal ve yarı kamusal alanlar.
6	Yapı malzemesi seçimi	Evin konforlu sıcaklıkları korumasına yardımcı olmak için vakum yalıtım panelleri ve alçıpanda özel malzemeler yer almaktadır.	Ahşap kaplama.	Ahşaptan yapılmış yenilenebilir ve çevre dostu yapı ve yalıtım malzemeleri.
7	İklimlendirme sistemleri	PV panel, Güneş pili, Pencerelerde, otomatik panjurlar eve giren güneş ısısı miktarını kontrol etmeye yardımcı olmaktadır.	Doğal aydınlatma, Sıcaklık, nem, aydınlatma ve diğer parametreleri izleyen ve ayarlayan bir ev otomasyon sistemi, PV panel, güneş duvar.	Otomatik bir perde ve tente sistemi ile birleştirilen pasif güneş tasarımı, çatı katında fotovoltaik panel, güneş duvarı. Merkezi bir hizmet odası, bir fotovoltaik monitör, havalandırma, sıhhi tesisat ve sıcak su temini dahil olmak üzere evin ihtiyaç duyduğu tüm otomatik mekanik sistemleri içerir. Isı pompası. Enerji geri kazanımlı havalandırma ünitesi.
8	Atık yönetimi	–	Yağmur suyu kullanımı, Gri su kullanımı.	Yağmur suyu toplama, Elektrikli bisikletlere veya araçlara güç sağlamak.

Tablo 9 (devamı). Yapım/İnşa Yarışmasının Kazan Projeleri

	Sürdürülebilir Tasarım Kriterleri	2015 Stevens: Stevens Teknoloji Enstitüsü, Sure House	2017 İsviçre Takımı NeighborHub	2020 Yapım Colorado Boulder Üniversitesi (CU Boulder) SPARC Evi
				
1	Sürdürülebilir düşünce ve tasarım ilkeleri	Savunmasız kıyı yerleşimleri için enerji verimli, güneş enerjili, fırtınaya dayanıklı bir ev.	Eenilenebilir enerji, su yönetimi, atık yönetimi, mobilite, gıda, malzeme seçimleri ve biyolojik çeşitlilik. Akuaponik sistemli iki dikey sera vardır.	Tasarım ilkeleri: Sürdürülebilirlik, Performans, Erişilebilirlik, Esneklik ve Kullanıcılardır.
2	Ekolojik mimari yapay çevre tasarımı	Yerel topografya ile çalışan afet durumunda yükseltilebilir tasarım.	İklim değişikliği ve kaynak tükenmesi gibi kritik zorluklara çözüm aramak.	Çevre koruma, ekonomik refah ve sosyal eşitlik sürd. ilkelerine dayanmaktadır.
3	Bina kabuğu	Yoğun yalıtım, hava sızdırmazlığı, akıllı inşaat teknikleri ve yüksek performanslı pencereler.	PV panellerinden enerji üreten ve pasif güneş stratejileri kullanarak su ve alan ısıtması için güneşten gelen ısıyı toplayan duvarları içerir. Çatı aynı zamanda su toplamak ve yiyecek yetiştirmek için kullanılan verimli bir yüzeydir. Yeşil çatı.	Yüksek düzeyde yalıtılmış, hava sızdırmazlığı dahil olmak üzere performansı artıran çoklu tasarım stratejileri içerir.
4	Bina geometrisi	Kompat tasarım.	Kompat tasarım.	Kompakt tasarım.
5	Mekân organizasyonu	Esnek alan kullanımı.	Kullanıcıların ihtiyaçlarını karşılamak için değişebilen çok işlevli alanlar ile tasarlanmıştır. Esnek Tasarım.	Esnek bina sistemleri.
6	Yapı malzemesi seçimi	–	Ev ve ev içindeki mobilyalar için lamine kaplama kereste kullanılmaktadır.	Ahşap yapı, ahşap kaplama ve koyun yünü yalıtımı gibi düşük karbonlu malzemeler içerir.
7	İklimlendirme sistemleri	Doğal gün ışığı, Güney cephede mimari olarak entegre edilmiş, fiber kompozit panjurlar, pasif güneş kontrolü sağlar, Entegre PV paneller, Hibrit ısı pompası.	Entegre PV paneller, Fotovoltaik (güneş enerjisi) sistemine ek olarak, elektrik üretmek için boyaya duyarlı "Gratzel" güneş pilleri ve sıcak su, alan ısıtması kendi ürettikleri güneş enerjisi panelleri kullanıyor.	Doğal havalandırma ve gün ışığını en üst düzeydedir. Isı pompaları, enerji geri kazanımlı vantilatör, ısı pompası su ısıtıcısı, güneş panellerinde maksimum güç noktası izleme ve merkezi kontrol sistemi vardır. Entegre PV paneller.
8	Atık yönetimi	–	Sıfır su "kuru" bir tuvalet, atıkları işlemek ve geri dönüştürmek için solucanlar kullanır.	–

Tablo 10. Tasarım Yarışmasının Kazanan Projeleri

Sürdürülebilir Tasarım Kriterleri		2019 Virginia Politeknik Enstitüsü ve Eyalet Üniversitesi TreeHAUS	2020 Miami Üniversitesi (Oxford, Ohio) The Peace Village
			
1	Sürdürülebilir düşünce ve tasarım ilkeleri	Ağaçların kaynakları toplama ve dağıtma biçiminden ilham alınmıştır. Net-pozitif, rejeneratif bağlantılı bir konut projesidir.	Net sıfır enerjili, uygun fiyatlı bir konut geliştirme projesidir.
2	Ekolojik mimari yapay çevre tasarımı	Ev, bağlamsal ekolojinin işbirlikçisi olarak görülür. Çevre ekosistemini desteklemektedir. Karbon ayak izini azalma.	Gelecek için adaptasyon ve yeniden büyüme fırsatları sağlamak. Permakültür bahçe tasarımı.
3	Bina kabuğu	Yüksek yalıtım ve hava sızdırmazlığı.	Hava geçirmezlik, süper yalıtımlı duvarlar, kapılar ve pencereler ve yerinde yenilenebilir enerji üretimi.
4	Bina geometrisi	Prefabrik modül.	Bina yönlenmesine dikkat edilmiştir. Prefabrik tasarım.
5	Mekân organizasyonu	Modüler tasarım.	Modüler tasarım.
6	Yapı malzemesi seçimi	Ahşap yapı malzemesi.	–
7	İklimlendirme sistemleri	Doğal havalandırma, Entegre PV paneller, Anerobik aerobik çürütme, PV ve biyogazla beslenen yedek birleşik ısı ve güç (chp) kaynağı.	Doğal havalandırma. Çatıda entegre PV paneller, passive house ve net zero tasarım özelliklerini barındırmaktadır.
8	Atık yönetimi	Yağmur Suyu Toplama, Gıda Atıkları, Geridönüştürülebilir yapı malzemesi.	Yağmur Suyu Toplama.

Tablo 10(devamı). Tasarım Yarışmasının Kazanan Projeleri

Sürdürülebilir Tasarım Kriterleri		2021 Northwestern Üniversitesi (Evanston, Illinois) NU Home	2022 Georgia Teknoloji Enstitüsü, Englısh Avenue Yellow Jackets
			
1	Sürdürülebilir düşünce ve tasarım ilkeleri	Kentsel alanda yer alan bireysel aile evlerinin, enerji tasarruflu evlerin çok yönlü, pazarlanabilir, konforlu ve ekonomik olabileceğini göstermektedir.	Boş ve terk edilmiş evleri uygun fiyatlı, sağlıklı ve enerji tasarruflu evlere dönüştürmek için tekrarlanabilir bir model oluşturmaktır.
2	Ekolojik mimari yapay çevre tasarımı	Yerel mimari ile uyumlu konut. Kaynak bilinçli bir yaşam tarzının erişilebilir olmasını sağlamak.	Mahalleye katkıda bulunmayı öngörmektedir. mevcut konutların performansını dönüştürmeyi, tarihi korumayı, iklime özgü müdahaleyi, termal konforu, maliyet etkinliğini, su koruma tekniklerini ve net sıfır enerjiyi desteklemektedir. Geleneksel üçgen çatı formu, English Avenue mahallesinin kimliğine verdiği önemden dolayı korunmuştur.
3	Bina kabuğu	Isıl performansı ve sızdırmazlığı yüksek yapı kabuğu, Pasif Ev standartlarını karşılamaktadır.	Isıl performansı ve sızdırmazlığı yüksek yapı kabuğu, Pasif Ev standartlarını karşılamaktadır.
4	Bina geometrisi	Kompakt tasarım.	–
5	Mekân organizasyonu	Çok işlevli olması ve değişimlere açık olması esneklik kazandırmaktadır.	–
6	Yapı malzemesi seçimi	Selüloz yalıtımı geri dönüştürülmüş malzemelerden yapılır ve yüksek termal dirence sahiptir, iç mekan hava kalitesini artırır, akustik yalıtım sağlar ve biyofilik tasarımı bütünleştirir. Dış paneller ve mobilyalar için geri kazanılmış ahşap kullanılır.	Isıl bariyer için mineral yün ve üflemeli selüloz ürünleri seçilmiştir. Ek olarak, Çevresel Yaşam Döngüsü Değerlendirmesi aracılığıyla test edilen ahşap ve biyo-bazlı malzemeler.
7	İklimlendirme sistemleri	Doğal havalandırma ve aydınlatma, Gün ışığı sensörleri, Entegre PV paneller, elektirikli araç şarjı, hava kaynaklı ısı pompası, Isı pompalı su ısıtıcısı ve düşük akışlı armatürler hem su hem de enerji tasarrufu sağlar.	Enerji geri kazanımlı havalandırma, Doğal gün ışığı, entegre PV paneller, akıllı termostatlar ve kontrol sistemleri.
8	Atık yönetimi	Gri suyun yeniden kullanımı.	Yağmur Suyu Toplama, Gri suyun yeniden kullanımı.

3. 1. Bölüm Değerlendirmesi

"Solar Decathlon" yarışmasının kazanan projeleri sürdürülebilirlik ilkeleri kapsamında değerlendirildiğinde.

2002 yılının kazanan projesi, yerel mimariyi dikkate alan yenilenebilir enerji kullanan, değişen bütçelere, iklimlere ve şantiyelere uyum sağlayabilen, yerel mimariyi yansıtan amerikan evi tasarımına sahip olan, aktif sistem, güneş enerjisi kullanımı, pv panel ve ısı pompası gibi sistemleri barındıran bir projedir.

2005 yılının kazanan projesi incelendiğinde, bir önceki yıla göre malzeme seçimine daha çok dikkat edildiği, doğal ve geri dönüştürülebilen malzemelerin tercih edildiği ve erişilebilirliğin ön plana çıkarıldığı görülmektedir. Diğer bir farklı özelliği ise tasarımda özellikle her yere uyumlanabilir olması için çalışılmıştır.

2007 yılının kazanan projesi sürdürülebilirlik ilkeleri kapsamında incelendiğinde: yenilikçi tasarım ve teknoloji kullanımının ön planda tutulduğu kazanan projede, faz değiştiren malzeme, parafin içeren özel bir duvar kaplaması denenmiştir. Böylece pasif olarak ısı depolaması sağlanabilmiştir. Farklı bir diğer özelliği binanın verimliliğinin büyük ölçüde yerel iklime bağlı olmasıdır. Bu özellikler dışında yerel ve doğal malzeme, yenilenebilir enerji kullanımı vb. gibi genel olarak bir önceki yıl ile aynı özellikleri barındırmaktadır.

2009 yılının kazanan projesi incelendiğinde: ekolojik mimari yapay çevre tasarımı kapsamında, çevre üzerinde minimum etki maksimum işlev amacıyla tasarlandığı vurgulanmıştır. Yenilenebilir enerji kullanımı dışında, teknoloji ve yenilikçi tasarım dikkate alınarak, duvar panellerinde vakumlu yalıtım, pencerelerde otomatik panjur sistemi kullanılmıştır.

2011 yılının kazanan projesi, enerji ve su tasarrufu, geri dönüşüm ve yağmur suyu yönetimi, bütünsel tasarım temel alınarak gerçekleştirilmiştir. Proje, çalışma kapsamında ele alınan tüm sürdürülebilirlik ilkelerini karşılamaktadır. Çevre üzerinde minimum etki, doğal ve geri dönüştürülebilir malzeme kullanımı, yüksek yalıtım, enerji verimliliği ve yenilebilir enerji kullanımı gibi ortak özelliklerin yanı sıra, yağmur suyunu toplamaya destek olan çatı tasarımı, gri su kullanımı, ev otomasyon sistemleri, güneş duvarı, nem kontrolü ve cephede havalandırmalı bir rainscreen kaplama sistemi gibi pasif sistemleri de barındırması ile diğer projelerden ayrılmaktadır.

2013 yılının kazanan projesi de bir önceki yıl gibi sürdürülebilirlik ilkelerinin tamamını karşılamaktadır. Sağlıklı, sürdürülebilir bir gelecek ve birçok yaşam tarzına ve iklime uyum sağlayabilecek bir konsept üzerinde durulmuştur. Merkezi bir hizmet odası, bir fotovoltaik monitör, havalandırma, sıhhi tesisat ve sıcak su temini dahil olmak üzere evin ihtiyaç duyduğu tüm otomatik mekanik sistemleri içerir. Otomasyon sistemleri bu projede ön plana çıkmaktadır. Ek olarak öne çıkan ve farklılık gösterendiğer bir özelliği ise elektrikli bisikletlere veya araçlara güç sağlamaktır.

2015 yılının kazanan projesi, sürdürülebilir düşünce ve tasarım ilkeleri kapsamında savunmasız kıyı yerleşimleri için enerji verimli, güneş enerjili, fırtınaya dayanıklı bir ev konsepti üzerinde durulmuştur. Yerel topograf ile çalışarak afet durumunda yükselebilen bir tasarıma sahip olması iklim değişikliği ile ortaya çıkan afetlere karşı bir çözüm önerisi olarak karşımıza çıkmaktadır. Bu özelliği ile önceki yıllardan önemli ölçüde ayrılmaktadır.

2017 yılının kazanan projesi çalışma kapsamında belirlenen tüm sürdürülebilirlik ilkelerini karşılamktadır. Sürdürülebilir düşünce ve tasarım ilkeleri kapsamında; yenilenebilir enerji, su yönetimi, atık yönetimi, mobilite, gıda, malzeme seçimleri ve biyolojik çeşitlilik gibi tasarım özellikleri üzerinde yoğunlaşmış olup iklim değişikliğine ek olarak kaynak tükenmesi gibi kritik zorluklara çözüm aramaktadır. Projede akuaponik sistemli (sucul yetiştiricilik ve topraksız tarımın entegre edildiği sistem) iki dikey sera vardır. Yeşil çatı aynı zamanda su toplamak ve yiyecek yetiştirmek için kullanılan verimli bir yüzeydir. Sıfır su "kuru" bir tuvalet, atıkları işlemek ve geri dönüştürmek için solucanlar kullanır. Tüm bu özellikleri ile önceki yılların kazanan projelerinden ayrılmaktadır.

2020 yılının kazanan projesi, sürdürülebilirlik, performans, erişilebilirlik, esneklik ve kullanıcı konforunu düşünen tasarım ileklerini barındırmaktadır. Ek olarak, çevre koruma, ekonomik refah ve sosyal eşitlik sürdürülebilir kalkınma ilkelerine dayanmaktadır.

Tasarım yarışmasının kazanan projeleri sürdürülebilirlik ilkeleri kapsamında değerlendirildiğinde ise:

2019 yılının kazanan projesi Treehause, ağaçların kaynakları toplama ve dağıtma biçiminden ilham alınarak tasarlanmıştır. Özellikle net-pozitif kavramı ön plana çıkarılmış, rejeneratif bağlantılı bir konut projesidir. Ev, bağlamsal ekolojinin işbirlikçisi olarak görülür. Çevre ekosistemini desteklemekte ve karbon ayak izini azaltmaya yönelik çözüm üretmektedir. Yağmur suyu toplama, gıda atıklarını dönüştürme, geridönüştürülebilir yapı malzemesi kullanımı gibi özellikleri barındırmaktadır.

2020 yılının kazanan projesi, net-sıfır enerjili, uygun fiyatlı bir konut geliştirme projesidir. Gelecek için adaptasyon ve yeniden büyüme fırsatları sağlamak, permakültür bahçe tasarımı, yağmur suyu toplama, passive house ve net-zero tasarım özelliklerine sahiptir.

2021 yılının kazanan projesi, kentsel alanda yer alan bireysel aile evlerinin, enerji tasarruflu evlerin çok yönlü, pazarlanabilir, konforlu ve ekonomik olabileceğini göstermektedir. Yerel mimari ile uyumlu konut, kaynak bilinçli bir yaşam tarzının erişilebilir olmasını istemektedir. Pasif ev standartları karşılanmakta ve gri su yeniden kullanılmaktadır.

2022 yılının kazanan projesi, boş ve terk edilmiş mevcut evleri uygun fiyatlı, sağlıklı ve enerji tasarruflu evlere dönüştürmek için tekrarlanabilir bir model oluşturmakta olup mahalleye katkıda bulunmayı öngörmektedir. Mevcut konutları dönüştürmeyi, tarihi korumayı, iklime özgü müdahaleyi, termal konforu, maliyet etkinliğini, su koruma tekniklerinsahiptir-sıfır enerjiyi desteklemektedir. Geleneksel üçgen çatı formu, English Avenue mahallesinin kimliğine verilen önemden dolayı korunmuştur. Çevresel Yaşam Döngüsü Değerlendirmesi aracılığıyla test edilen ahşap ve biyo-bazlı malzemeler kullanılmış, yağmur suyu toplama ve gri suyun yeniden kullanımı gibi özelliklere sahiptir.

4. SONUÇ

2002 yılında başlayan yarışma Amerikada güneş enerjisinin evlerde tasarlanması, inşa edilmesi ve yönetilmesi üzerine idi. Zamanla pazar potansiyeli yüksek ve yenilikçi tasarımlar beklenmiştir. 2010 yılında yarışma Avrupaya'da yayılarak yerel koşullara uyum sağlamaya başlamıştır. Her geçen yıl mekan organizasyonunda esnek ve değiştirilebilen çok işlevli alanların tasarlanması daha çok vurgulanmakta ve öne çıkmaktadır. Mimaride ise bütüncül tasarım istenmektedir. 2015 yılında artık sadece solar enerji değil dünya çapında farklı ülkelerde yerel bağlama uygun enerji etkin ve yenilenebilir enerji kaynaklarına yönelik olmaya başlamıştır. 2017 yılında su yarışması önemli bir kategori olarak yarışmaya dahil edilmiş, koruma/tasarruf, ıslah ve yeniden kullanım gündeme getirilmiştir. 2020 yılına gelindiğinde, net-sıfır, artı enerji ve şebekeden bağımsız işlevsellik ön plana çıkmış, farklı koşullara karşı direnç (resilience) başlığı ilk defa ayrı bir kategori olarak eklenmiştir. Böylece afet risklerine ve sonrasında oluşacak olan sorunlara karşı önlem ve dayanıklılık gibi küresel sorunlar ön plana çıkarılarak çözüm bulunması istenmiştir. 2019 ve sonrasında tasarım yarışması da dahil olmak üzere katılımcılardan beklenen güneş enerjisi kullanımından ziyade daha çok küresel sorunlara çözüm yönünde olmuştur. Bu nedenle karbon ayak izini azaltma, afetler, kaynakların tükenmesine karşı çözüm getirilmesi beklenmiştir.

Projelerde ise bu bilincin 2015 yılından itibaren başladığı çevresel ve küresel sorunları dikkate alan tasarımlar sundukları görülmektedir. Sonraki yıllarda da bu yönde şekillenmeye devam etmiş olup kazanan projelerin bu kapsamda birçok önlem aldığı gözlemlenmiştir. Topraksız tarım, iklime uyumlu bir ekosistem yaratma teknikleri, kaynak bilinçli bir yaşam tarzına yönlendirme, esnek tasarım, yağmur suyu ve gri su kullanımı, geridönüştürülebilirlik, yenilenebilir enerji kullanımı, biyo-yakıt kullanımı, sıfır-enerji, artı-enerji gibi çözümler örneklerden bir kaçı olarak verilebilir. Etkinlik her geçen yıl teknoloji ve işgücü avantajlarını arttırmıştır.

Tasarım Yarışması ile "Solar Decathlon" yarışmasının etkisi artmış sadece konut değil ticari yapılarda yarışmaya dahil edilmiştir. Kazanan projeler incelendiğinde tekil bina değil daha çok yerleşim ölçeğinde peyzaj da dahil olmak üzere planlama yapılmaya başlanmış, 2022 yılının kazanan projesinde de görüleceği gibi mevcut binaların yenilenmesi de yarışma kapsamına dahil edilerek var olan konut stoğunu iyileştirme yönünde adımlar atıldığı söylenebilir. Tasarım yarışması ile kentsel dokudaki konutların yeniden kullanımı, yenilenmesi, yeniden inşası ve yeni fonksiyon verilmesi, yeniden tanımlaması mimari sorun olarak karşımıza çıkmaktadır. Ek olarak kaynakların yeterli ve verimli kullanılması, iklimsel koruma ve sürekli yaşam döngüsü kentsel beğlamda değerlendirilmektedir.

Özetle, Uluslararası Solar Decathlon etkinlikleri, dünyanın dört bir yanındaki on binlerce öğrenci için sıfır enerjili tasarım eğitimi ve deneyimini arttırmaktadır. Solar Decathlon yarışması, sürdürülebilirlik ilkelerini bina tasarımı ve uygulamalarına entegre etmeyi, yeni malzeme ve tekniklerin kullanımını, ve yenilenebilir enerji üretimi gibi alanları en iyi şekilde harmanlamayı öğretmektedir. Öğrencilerin yanı sıra, mimar, mühendis ve ilgili diğer paydaşlarında tasarım ve inşa aşamaların da bu uygulamaları daha yaygın kullanımını sağlamak, kullanıcıları bilinçlendirmek gibi faydaları olacaktır. Sahip olduğu tüm bu özellikleri ile yarışmanın gelecekte yüksek bir potansiyele sahip olduğu öngörülmektedir. Ek olarak, enerji verimliliği ve iklim değişikliği bilincinin Türkiye'de eğitim gören öğrencilere de aşılanabilmesi için yarışmaya katılımın desteklenmesi ve teşvik edilmesi gerekmektedir.

KAYNAKLAR

[1]. Voss, K., Hendel, S. ve Stark, M. (2021). Solar Decathlon Europe – A review on the energy engineering of experimental solar powered houses. *Energy and Buildings*, *251*, 111336. doi:10.1016/J.ENBUILD.2021.111336

[2]. Moon, S., Nahan, R., Warner, C. ve Wassmer, M. (2005). Solar Decathlon 2005 : The Event in Review, 62.

[3]. Zamrodah, Y. (2016). Powered by The Sun 2007 Solar Decathlon, *15*(2), 1–23.

[4]. Yeang, K. (2007). The US solar decathlon 2007. *Architectural Design*, *77*(4), 120–121. doi:10.1002/ad.498

[5]. DOE Solar Decathlon: 2007'den Öne Çıkanlar. (2007).*U.S. Department of Energy*. 7 Eylül 2022 tarihinde https://www.solardecathlon.gov/past/2007/index.html adresinden erişildi.

[6]. DOE Solar Decathlon: 2009'dan Öne Çıkanlar. (2009).*U.S. Department of Energy*. 7 Eylül 2022 tarihinde https://www.solardecathlon.gov/past/2009/index.html adresinden erişildi.

[7]. Tech, V. (2009). U.S. Department of Energy: Solar Decathlon 2009.

[8]. Hutzel, B., Kilmer, O., Qian, Z. C., Kilmer, R. L., Cory, C. A., Horton, W. T., … Day, J. (2011). Preparing for the 2011 Solar Decathlon. *ASEE Annual Conference and Exposition, Conference Proceedings*, (May 2014). doi:10.18260/1-2--18621

[9]. DOE Solar Decathlon: Solar Decathlon 2011'den Öne Çıkanlar. (2011).*U.S. Department of Energy*. 7 Eylül 2022 tarihinde https://www.solardecathlon.gov/past/2011/index.html adresinden erişildi.

[10]. Yount, R. (2012). U.S. Department of Energy Solar Decathlon 2011. *European University Institute*, (2), 2–5. https://eur-lex.europa.eu/legal-content/PT/TXT/PDF/?uri=CELEX:32016R0679&from=PT%0Ahttp://eur-lex.europa.eu/LexUriServ/LexUriServ.do?uri=CELEX:52012PC0011:pt:NOT adresinden erişildi.

[11]. DOE Solar Decathlon: Solar Decathlon 2013'ten Öne Çıkanlar. (2013).*U.S. Department of Energy*. 7 Eylül 2022 tarihinde https://www.solardecathlon.gov/past/2013/index.html adresinden erişildi.

[12]. Solar Decathlon: Solar Decathlon Hakkında. (2002).*U.S. Department of Energy*. 7 Eylül 2022 tarihinde https://www.solardecathlon.gov/about.html adresinden erişildi.

[13]. Solar Decathlon: Solar Decathlon 2015'ten Öne Çıkanlar. (2015).*U.S. Department of Energy*. 7 Eylül 2022 tarihinde https://www.solardecathlon.gov/2015/index.html adresinden erişildi.

[14]. Solar Decathlon: Solar Decathlon 2017'den Öne Çıkanlar. (2017).*U.S. Department of Energy*. 7 Eylül 2022 tarihinde https://www.solardecathlon.gov/2017/index.html adresinden erişildi.

[15]. Solar Decathlon: İnşa Mücadelesi 2020 Hakkında. (2020).*U.S. Department of Energy*. 7 Eylül 2022 tarihinde https://www.solardecathlon.gov/2020/build/challenge.html adresinden erişildi.

[16]. Tokuç, A. ve Köktürk, G. (2020). Geleceğin Akıllı Evleri: Avrupa Güneş Dekatlonu 2014Örneği.

[17]. Romero, R., Simon, J., Ryan, T., Peterson, Z. ve Torcellini, P. (2021). US Department of Energy Solar Decathlon Competition Guide: 2021 Design Challenge and 2023 Build Challenge. https://www.osti.gov/biblio/1769818 adresinden erişildi.

[18]. Gökşen, F. (2017). *Sürdürülebilir Konut Tasarımında Enerji Etkin Yapı Kriterlerinin Belirlenmesi Ve Doğu Akdeniz Bölgesi İçin Bir Tasarım Modeli Önerisi*. https://tez.yok.gov.tr/UlusalTezMerkezi/tezSorguSonucYeni.jsp adresinden erişildi.

[19]. Rich, P. ve Dean, Y. (2012). *Principles of Element Design*. *Principles of Element Design*. doi:10.4324/9780080938585

[20]. Goldsmith, N. (2006). Building skin. *Fabric Architecture*, *18*(3), 14–15. doi:10.1007/978-3-7643-7729-

8_1
[21]. Knaack U., and Koenders, E. (2018). *Building Physics of the Envelope*. (U. Knaack ve E. Koenders, Ed.)*Building Physics of the Envelope*. doi:10.1515/9783035609493
[22]. Solar Decathlon: Tasarım Yarışması Hakkında. (2019).*U.S. Department of Energy*. 7 Eylül 2022 tarihinde https://www.solardecathlon.gov/2019/design/challenge.html adresinden erişildi.
[23]. Young, M., Romero, R., Stershic, J., Ryan, T., Carr, H. J., Young, M., … Carr, H. J. (2022). The Future of Building Science Education with the U.S. Department of Energy Solar Decathlon, (June). https://www.osti.gov/biblio/1874938 adresinden erişildi.
[24]. Eastman, M., Hayter, S., Nahan, R., Stafford, B., Warner, C., Hancock, E. ve Howard, R. (2004). Solar Decathlon 2002: The Event in Review, 141.
[25]. Kos, J. R. ve Souza, B. M. De. (2014). Educating home users through a solar house: The Ekó House experience. *Energy and Buildings*, *83*, 181–185. doi:10.1016/J.ENBUILD.2014.03.080
[26]. Sánchez, S. V. (2012). *Solar Decathlon Europe 2012: Improving Energy Efficient Buildings*.
[27]. DOE Solar Decathlon: Solar Decathlon 2002'den Öne Çıkanlar. (2002).*U.S. Department of Energy*. 7 Eylül 2022 tarihinde https://www.solardecathlon.gov/past/2002/ adresinden erişildi.
[28]. DOE Solar Decathlon: 2005'ten Öne Çıkanlar. (2005).*U.S. Department of Energy*. 7 Eylül 2022 tarihinde https://www.solardecathlon.gov/past/2005/ adresinden erişildi.

2D FINITE ELEMENT SIMULATION OF ELLIPTIC HOLE AUXETICS

Süleyman Nazif ORHAN[1]

[1]Erzurum Technical University, Engineering and Architecture Faculty, Civil Engineering Department, Erzurum, Turkey.

[1]ORCID ID: 0000-0002-1357-6039

Kemal SOLAK[2]

[2]Erzurum Technical University, Engineering and Architecture Faculty, Civil Engineering Department, Erzurum, Turkey.

[2]ORCID ID: 0000-0001-6957-2689

ABSTRACT

Auxetic structures, which have a negative Poisson's ratio, are worth investigating with their exceptional features. Since high auxetic behavior induces low stiffness and restricts the use of the auxetic structure, there is an upward tendency in the literature for improving the stiffness value of the structures. Different geometric shapes and designs of auxetic structures have been offered in the literature to enhance their mechanical performance. In this study, conventional peanut-shaped unit cell which is a type of elliptic hole auxetics was modified to enhance stiffness while retaining the auxetic behavior of structure. A novel unit cell was created by adding stiffener to the conventional peanut-shaped unit cell and these two types of unit cells were rotated 6 and 12 degrees. Thus, a total of 6 different 4x8 planar sheets were obtained from these unit cells. Numerical analyses were performed using the Static Structural module of Ansys software and all models were subjected to a 2 mm displacement as uniaxial tension. The numerical model was validated with a test data in the literature and the boundary conditions and material properties were kept unchanged for all models. Structures were meshed with 10-node tetrahedron elements and the Poisson's ratio and stiffness values were calculated from the same nodes of the structures. As a result of the analyses, it was discovered that the increase of the rotation angle increased the stiffness value while decreasing the auxetic behavior. It was also revealed that the stiffener-added models exhibited higher auxeticity and stiffness than their counterparts. The maximum von Mises values in all models were found in the curvilinear areas of the elliptic perforation. These findings may facilitate the design process of the 2D auxetics and provide new insights for their fabrication and implementation.

Keywords: 2D auxetic, finite element simulation, elliptic hole auxetic, stiffness

THESIS TOPIC: ASSESSMENT OF THE SAFETY AND SECURITY OF COMMERCIAL MOTORCYCLE OPERATION IN AKURE, ONDO STATE, NIGERIA

Triumph Temitope AROWOSAFE

Federal University Of Technology, Akure, Ondo State, Nigeria

ABSTRACT

Commercial motorcycles are seen to constitute a serious threat to the security, lives and properties of citizens. Their operators are said to engage in many criminal acts, causing accidents on roads, death of many innocent citizens, thus neglecting its purpose of conveying people and goods which is its transport functions in society. This study therefore examines the level of safety and security associated with operation of commercial motorcycles in Akure with a view to engendering policy response that could enhance the safety of the operators of commercial motorcycles and residents. Questionnaire and field observation were used to collect required data. Two set of questionnaires were administered; one on the residents and the other on the operators of commercial motorcycles in the study area. A total of 130 Motorcycle operators and 70 passengers were sampled. Descriptive statistics were employed in the data analysis. The study revealed that all commercial motorcyclists were males, while there was even distribution of gender among the residents with 55.7% and 44.3% female and males respectively. Majority of the motorcyclists (53.8%) are with secondary school education, most of whom were in the age group of 25 to 34 years, while majority of the residents are within the age of 21 to 40 years bracket of which (80.5%) were literates. Findings also revealed that unemployment situation in the state has led many (85.1%) people, particularly the youth; into the commercial motorcycle operation in the city. As a result of that, many of them (46.2%) did not engage in formal training and has results in high rate of commercial motorcycle crashes in the city, which have claimed many lives and rendered some impotent. Other problems associated with motorcycle include over speeding, a leading problem in the area coupled with the fact that, some operators now use motorcycles to perpetuate grievous crimes. In order to have safe, efficient public transportation, government should create more job opportunities for people, upgrading the existing three-wheel cycles and improve on the operational efficiencies of city taxies, imposing sanctions to enforce strict compliance among okada riders which will go a long way in reducing road accidents, crimes and thus reducing the influx of commercial motorcycles.

Keyword: Commercial motorcycle, okada riders(motorcycle riders), safety, security and Residents

HEAT TRANSFER PERFORMANCE OF INTERRUPTED MICROCHANNEL HEAT SINK USING AL_2O_3-WATER NANOFLUID AND EULERIAN MULTIPHASE TECHNIQUE

Opeoluwa Joseph Balogun[1*] , Ayodeji Samuel Binuyo[1]

[1]Department of Mechanical Engineering, Obafemi Awolowo University, P.M.B 13, Ile-Ife, Nigeria.

Orchid id: 0000-0002-9424-019X

ABSTRACT

The heat generated in electronic devices or electronic systems is conducted through the base material and then conveyed by combining thermal conduction, convection, and radiation to the surroundings through numerous components such as heat sinks. The thermal and hydraulic performance of an interrupted microchannel heat sink was investigated numerically in this research. A multiphase mixture of Al_2O_3 and water nanofluid was used as the working fluid. The effects of Reynolds number, nanofluid volume concentration, and rib edge configuration on the Microchannel Heat Sink's thermo-hydraulic performance were investigated using Fluent software. The results showed that the heat sink's performance was significantly improved by using Al_2O_3-water nanofluid and rib edge modification. The maximum temperature of the heat exchanger's bottom surface and the thermal resistance were reduced when the Reynolds number or nanoparticle concentration were increased.

This improved the uniformity of the temperature of the heat sink as regions with the likelihood of hot spots were drastically reduced. The convective heat transfer coefficient increased with an increase in the nanofluid concentration and Reynolds number. For instance, at Re = 100, increasing the concentration from 0.5 to 4 percent gave a 63.15 percent enhancement in the convective heat transfer coefficient for the Interrupted microchannel Heat sink-Base (IMCH-B). Under similar conditions, a 69.35 percent enhancement occurred for Interrupted microchannel Heat sink-Fillet (IMCH-F). Similarly, at 0.5 percent concentration for IMCH-F, an increase in Reynolds number from 100 to 700 gave a 76.79 percent. The thermal enhancement criteria (TEC) showed the IMCH-F has the best thermal performance across the various volume concentrations and Reynolds numbers.

Keywords: microchannel heat sink, nanofluids, Eulerian-Eulerian, thermohydraulic, TEC

SAFETY ASSESSMENT OF MILKING PRACTICES AMONG SMALLHOLDER DAIRY CATTLE FARMERS IN OYO STATE, NIGERIA

Popoola Moshood ABIOLA

Federal College of Animal Health and Production Technology, PMB Moor Plantation, Ibadan, Oyo state, Nigeria

ABSTRACT

A cross-sectional study was conducted in Oyo state to assess milking practices among smallholder dairy cattle farmers. Data were collected from 123 randomly selected dairy farmers using structured interview schedule. The data were collected on their socio-economic characteristics, dairy cattle production characteristics and their milking practices. Result showed that most of the respondents were female, married, had no formal education and had 9-12 years of milking experience. Results of the study also showed that all respondents practiced hand milking, with once (97.6%) and twice (2.4%) milking frequency per day. None of the respondents clean their barn before milking and 55.3% used stream water for farm activities. Plastic containers were commonly used for storage and transportation of milk by all respondents. None of the respondents clean udder and teat of the cow before milking and did not practice post-milking dipping of teats. There were significant association between years of experience of milk processing of the respondents and their milking practices such as modes of milking, milking area, cleaning of milking area, milking frequency, mode of cleaning milk container, milk containers used by the respondents, removing foremilk, filtering milk, milk storage and period of milk to reach collectors after milking. In conclusion, hygienic milking practices by dairy farmers are generally poor and this has direct impact on milk handling which could justify poor quality of raw milk obtained from cattle. Thus, it is imperative to create awareness on milking hygiene practices and milk post-harvest handling for smallholders in dairy industry to minimize milk-borne diseases. Farmers should also be trained on improved technologies on milking, processing and post-harvest handling of milk and milk products.

Keywords: Dairy, handling, hygiene, milk, practices

INTRODUCTION

Dairying and Livestock form the backbone of agriculture and deserve adequate focus in order to enhance the economic condition of farmers. Among livestock enterprises dairying has a prominent role in upliftment of socio-economic status of farmers. It assures a balanced development of the rural economy (Benin *et al.,* 2003), it also ensures the food security to the millions of people living in rural, urban and peri-urban areas (Jha, 2003). Diary production sector is one of the major economies of the world which satisfies nutritional requirements of the world through high quality milk and meat. It does not only give milk and meat but also manure, skin, horn, bone.

Local production and processing of milk in Nigeria has typically revolved around women who manage the process and the proceeds from the sale of the milk. Yields are very low due to poor genetic composition of local cattle breed, poor feeding practices and archaic production practices. A portion of the produced milk and related domestically processed milk-products are sold in the informal markets and to formal dairy processors and some kept for home consumption.

Despite the nutritional benefits of milk and its major contribution to livelihoods of pastoral communities, production and marketing systems along milk value chain the enterprise face numerous challenges. According to Kebede and Megerrsa (2018), beyond the stage of milk production by cattle, microorganisms may contaminate milk at various stages of milking, processing and distribution. The ill health of the cow and

its environment, improperly cleaned and sanitized milk handling equipment, and unhygienic workers who milk the cow, and come in contact with milk due to a number of reasons could serve as sources of contamination for the milk. Lack of refrigeration facilities at farm and household level in developing countries of tropical regions, with high ambient temperature implies that raw milk will easily be spoiled during storage and transportation (Godefay and Molla, 2000). Microorganisms can multiply and cause changes to milk quality once they gain entrance into the milk and their presence particularly the pathogenic microorganisms can cause harm to consumers by causing human illnesses and diseases (Barros et al., 2011). Therefore, milk and milk product handling need special care to reduce spoilage and food borne illness (Ashenafi and Beyene, 1994; Degraaf et al., 1997).

The main contributory factor to poor quality and safety is poor hygiene during milk harvesting and handling. Most of the challenges are related directly to the quality and safety of the milk and consequently lead to enormous losses of the milk along the chain. Poor hygiene is as a result of interaction of several risk factors along the milk value chain. Thus, the need for this study to sought to assess milking hygiene practices among smallholder dairy cattle farmers in Oyo state, Nigeria.

METHODOLOGY

Location of the study

The study was conducted in Oyo state. The state is located in south geo political zone of Nigeria; Oyo state was one of the three state carved out of the formal western region of Nigeria in 1976. It consists of 33 Local Government Areas (LGA) and 29 Local Council development areas. The state covered a land area of 28,454square/kilometers and it is bounded in the south by Ogun state, in the by Kwara state, in the west it is partially bounded by Ogun state and partially the Republic of Benin, while in the east by Osun state. The landscape consists of Old hard rocks and dome shaped hills. Which rise gently from about 500 meters in the southern part and reaching a height of about 1,219meters above sea level in northern part.

The state has a population of 5.6million people, (NPC, 2006) with climatic conditions that favour agriculture. The people of the area are predominantly farmers who cultivate cash and arable crops. Some of the farmers are also involved in livestock production. Within Oyo state, the zebu cattle (White Fulani and other Zebu breeds) are herded in the low land and land progressively used by the Yoruba for crop production. The major crops grown in the state include cassava, maize, yam, sorghum, cocoa, cocoa yam, melon, peppers soya bean and okra, the major livestock reared in the state include cattle, sheep, goat, fish production and poultry production.

Population of the study

The target population of this study consist of women dairy milk processors who are predominantly Fulani.

Sampling procedure and sampling size

Two-stage sampling procedure was adopted for this study. The first stage involved purposive selection of 9 LGAs where dairy farmers are predominant in Oyo state such as; Ido, Iseyin, Lagelu, Ogbomosho North, Saki East, Saki West, Ibarapa East, Oyo West and Itesiwaju and list of these women farmers were generated in each of the LGA from their Associations. The second stage involved random selection 123 respondents from the list generated in each of the LGA

Data Collection

Data were collected on socio-economic characteristics of the respondents, using an interview guide to obtain information from the respondents, dairy cattle production enterprises and their milking practices. These data were collected using a well structured interview schedule.

Data analyses

Data were subjected to descriptive statistics and Chi-square analysis using SPSS (V.23).

Results and Discussion

The socio-economic characteristics of the respondents is presented in Table 1. Result revealed that most (62.6%) of the respondents were above 25 years old, while few (4.9%) were within the age range of 11-15 and 5-10 years old respectively. The mean age of the respondents was 27.4 years. This is an indication that most of the respondents were youth who are capable of carrying out the rigorous activities associated with dairy milk production. It has been previously reported by some studies that age is positively and significantly related to production efficiency (Girei, *et al.,* 2013). The result also revealed that most (69.1%) of the respondents were married, 17.9% were single while few (13.0%) were widow. This is expected base on the result obtained for age of the respondents in which they were expected to have been married. One of the most important factors affecting the level of productivity on peasant farms is the composition and size of farming family (Opara, 2010). Married respondents are likely to be under pressure to produce more, not only for family consumption but also for sale (Opara, 2010). All the respondents were Muslims. The result shows that 45.5% of the respondents had no formal education, 33.3% had primary education, 19.5% had secondary education while 1.6% had tertiary education. This implies that most of the respondents were not mostly literates in terms of Western education. **Most (**45.5%) of the respondents had household size of 11-20 members, while few of them had between 41-50 (8%) and 31-40 (3.3%) members respectively. According to Omoregbe *et al.* (2013) large family sizes may be used as a source of family labour. The mean household size of the respondents was 18 members. This result disagrees with report of earlier studies that reported 2-6 members as the modal family size among household (Odebode and Popoola, 2016; Popoola *et al.,* 2017)**. The r**esult also shows that majority (49.6%) of the respondents earned between ₦18,000-₦22,000, 14.6% earned between ₦23,000- ₦ 27,000, 21.1% earned < ₦18,000, 8.9% earned > ₦32,000 while 2.4% earned between ₦28,000-₦32,000.

Table 1: Socio economic characteristics of the respondents

Variables	Frequency	Percentage	Mean
Age (years)			
5-10	6	4.9	
11-15	8	6.5	
16-20	16	13.0	
21-25	16	13.0	
>25	77	62.6	27.4
Marital status			
Single	22	17.9	
Married	85	69.1	
Widowed	16	13.0	
Religion			
Islam	123	100.0	
Educational status			
Primary	41	33.3	
Secondary	24	19.5	
Tertiary	2	1.6	
No formal Education	56	45.5	
Household size			
5-10	12	9.8	
11-20	56	45.5	
21-30	41	33.3	18
31-40	10	8.1	
41-50	4	3.3	
Income (₦)			
<18,000	26	21.1	
18,000-22,000	61	49.6	
23,000-27,000	18	14.6	29,173.41
28,000-32,000	3	2.4	
>32,000	11	8.9	

Cattle production enterprise for dairy production/processing by the respondents

Table shows the cattle production enterprise for dairy processing by the respondents. The result revealed that most of (30.9%) of the respondents had 9-12years of dairy processing experience. This implies that respondents had enough experience in dairy processing as this may help them to cope with constraints

associated with diary processing. Oluwatayo *et al.* (2008) reported that farmers with more years of experience would be more efficient, accept innovations easily, and have better understanding of the environment and market situations. The mean years of experience of the respondents in dairy processing was 26.7 years. Majority (30.9%) of the respondents had between 31- 40 herds of cattle; more than half of the respondents got their cattle through inheritance (82.9%), few respondents also got their cattle through purchase and inheritance (4.9%), 4.1% got their cattle through gift, inheritance and contract respectively (Fig. 1). As revealed in this result most of the respondents obtained their cattle by inheritance; this is an indication that cattle production is a means of lineage and succession business as part of culture of the dairy farmers (Fulani). Result also showed that majority (77.2%) of the respondents possessed White Fulani cattle, 12.2% of the respondents reared Sokoto Gudali, 5.7% of the respondents owned N'dama, 2.4% owned Red Bororo, 1.7% owned Muturu and 0.8% owned Keteku This is due to the fact White Fulani cattle give reasonable quantity of milk as it is regarded as the indigenous breed of cattle raised for dual purposes (beef and milk) in Nigeria.

Table 2: Cattle production enterprise for daily respondents

Variable	Frequency	Percentage	Mean
Years of experience			
5-8	13	10.6	
9-12	38	30.9	
13-16	31	25.2	
17-20	31	25.2	26.7
>20	10	8.1	
Herd size			
<10	6	4.9	
10-22	13	10.6	
21-30	34	27.6	
31-40	38	30.9	50
41-50	13	10.6	
>50	19	15.4	
Breed of cattle			
Red Bororo	3	2.4	
White Fulani	95	77.2	
Muturu	2	1.6	
Sokoto Gudali	15	12.2	
N'dama	7	5.7	
Keteku	1	0.8	

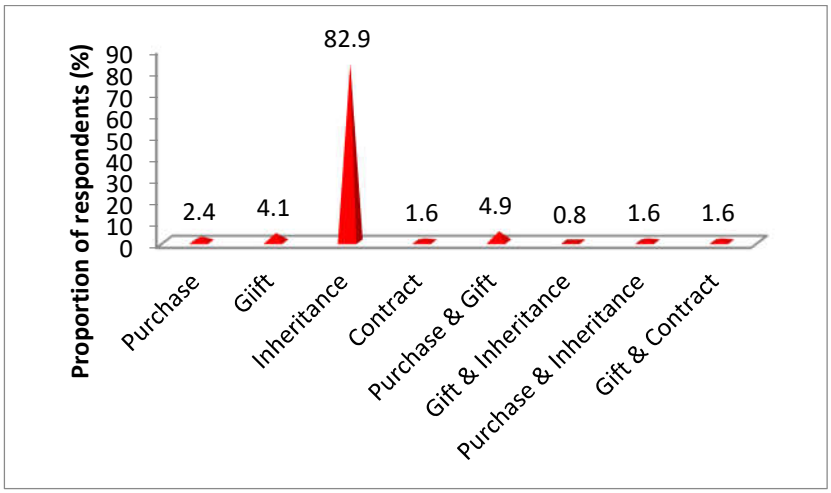

Figure 1: Sources of respondents' cattle

Milking methods and milk handling practices of respondents is shown in Table 3. The result showed that all the respondents practiced hand milking; do not clean the milking area, do not wash udder and teats of their cattle, remove foremilk and do not store in refrigerator. Result further revealed that most of the respondents milk their animals once a day (89.4%), use stream water in their operation (55.3%), do not wash their hands before milking (80.5%), use plastic containers to collect milk (98.4%), clean their milking utensils with water only (69.1%), take the milk to collectors immediately after milking (87.8%) and the milk were collected mostly at the farm gate (83.7%). Result of this study agreed with reports of Milligo et al. (2008) who reported that all smallholder farmers in peri urban areas in Burkina Faso practiced hand milking. Also, Kebede and Megerrsa (2018) reported that in Ethiopia, most of the respondents cleaned their barn before milking and 98% used treated pipe water supply for farm activities. While plastic containers were also commonly used for storage and transportation of milk.

Table 3: Milking methods and milk handling practices of respondents

Variables	Frequency	percentage
Method of milking		
Hand milking	123	100
Machine milking	-	-
Cleaning of milking area		
Yes	-	-
No	123	100
Milking frequency		
Once a day	110	89.4
Twice a day	13	10.6
Water source		
Well water	10	8.1
Pipe water	45	36.6
Stream water	68	55.3
Hand washing before milking		
Washing with water only	24	19.5
Washing with soap and water	-	-
Do not wash at all	99	80.5
Washing udder and teats		
Washing with water	-	-
Do not wash at all	123	100
Milk containers used		
Plastic	121	98.4
Stainless steel	2	1.6
Cleaning of milk utensils		
Cleaning with soap and water	38	30.9
Cleaning with water only	85	69.1
Removing foremilk		
Yes	123	100
No	-	-
Milk storage		
In refrigerator	-	-
Do not store at all	123	100
Time to reach collectors		
Immediately after milking	108	87.8
Within one hour	15	12.2
Points of milk collection		
Farm gate	103	83.7
In the barn	20	16.3

Table 4 shows the association between dairy cattle production enterprise of respondents and their hygienic milking practices. Result revealed that there were significant relationship ($p<0.05$) years of experience of farmers; herd size and hygienic milking practices of the respondents. However, there was no significant relationship between breeds of cattle; sources of cattle and hygienic milking practices of the farmers.

Table 4. Association between dairy cattle production enterprise of respondents and their hygienic milking practices

Variables	df	χ^2	p-value
Years of experience	4	8.334	0.001
Herd size	5	2.575	0.001
Breeds of cattle	5	9.365	0.345
Sources of cattle	7	7.308	0.276

df – Degree of freedom; χ^2- Chi square; p –value ($p<0.005$)

Conclusion

Hygienic milking practices by respondents (dairy farmers) are generally poor, this has direct impact on milk handling which is responsible for poor quality of raw milk obtained and processed. Thus, it is imperative to create awareness on hygiene milking practices and milk post-harvest handling for smallholders in dairy industry to minimize milk-borne diseases. Farmers should also be trained on improved technologies on milking, processing and post-harvest handling of milk and milk products.

References

Ashenafi M and Beyene F (1994). Microbial load, mycoflora, and keeping quality of raw and pasteurized milk from a dairy Farm. *Bull. Anim. Health Prod. Afr. 42:55-59.*

Barros L.S.S, Sóglia S.L.O, Ferreira M.J, Rodrigues M.J and Branco M.P.C. (2011). Aerobic and anaerobic bacteria and Candida species in crude milk. *J. Microbiol. Antimicrob. 3:206-212.*

Benin S, Pender J and Ehui S (Editors) 2003 Policies for sustainable land management in the East African highlands. Summary of Papers and Proceedings of a Conference held at the United Nations Economic Commission for Africa (UNECA), Addis Ababa, Ethiopia, 24-26 April 2002. Socio-economics and Policy Research Working Paper 50. International Livestock Research Institute (ILRI), Nairobi, Kenya. Pp 90-95. http://www.ifpri.org/divs/eptd/ws/papers/eptws13.pdf

DeGraaf T, Romero Zuniga, Cabalellero M, and Dwinger R.H (1997). Microbiological quality aspects of cow's milk at a smallholder cooperative in Turrialba, Costa Rica. Revue d'Élevage et de Médecine Vétérinaire des Pays *Tropicaux 50(1):57-64.*

Girei, A.A., Dire, B. and Iliya, M.M. and Salihu, M. (2013).Stochastic Frontier Production Function on the Resource Use Efficiency of Fadama II Crop Farmers in Adamawa State, Nigeria. *European Journal of Agricultural and Forestry Research, 1(2): 1-15267*

Godefay B and Molla B (2000). Bacteriological quality of raw milk from four dairy farms and milk collection center in and around Addis Ababa*. Berliner und Munchener Tierarztliche Wochenschrift, 113(7-8):276-278.*

Jha. B.J.K. (2003). Indian dairy in the emerging trade order, and unpublished report submitted to the *Institute of Economic Growth,* Delhi, p. 1–7.

Kebede L.G and Megerrsa S.A. (2018). Assessment of dairy farmers' hygienic milking practices and awareness on cattle milk-borne zoonoses in Bishoftu, *Ethiopia. Vol. 10(2), pp. 45-54. DOI: 10.5897/JVMAH2017.0602*

Milligo V, Ouedraogo GA, Agenas S, Svennersten-Sijaunja K (2008). Survey on dairy cattle milk production and milk quality problems in peri-urban areas in Burkina Faso. Afr. J. Agric. Res. 3:215-224.

Odebode S.O. and Popoola M.A. (2016). Comparative analysis of income generation from sheabutter production by rural women in Saki West and ATISBO Local Government Areas, Oyo state, *Nigeria. Science and Engineering Perspectives 11: 71-83*

Oluwatayo, A. E. (208). Efforts to Increase Improved Dairy Cattle in Tanzania. In: Proceedings of stakeholders workshop (Ministry of Livestock and Fisheries Development); 23 November, 2010, *Dar es Salaam, Tanzania. 102-114pp.*

Omoregbe J.O, Khan H., Bashaasha B. and Mutetikka (2013). Analysis of Householdsize Disparity In Agricultural Extension Service Delivery: The Case of Gedeb Woreda, West Arsi Zone, Oremia Regional State*. MSc Thesis, Alemaya University, Ethiopia.*

Opara, U.N. (2010). Personal and Socio-Economic Determinants of Agricultural Information Use by Farmers in the Agricultural Development Programme (ADP) Zones of Imo State, Nigeria: *Library Philosophy and Practice. P. 32*

Popoola M.A., Adebisi G.L., Osijinrin O.E., Babarinde G.T., Lawal A.M. and Kunuji O.M (2017). Determinants of backyard poultry production as strategy for food security among households in Ibadan Metropolis. Nigeria. *Proceedings of 6th ASAN-NIAS Joint Annual Meeting. September 10-14, 2017. Abuja*

AFFINITY POLYMER MEMBRANE CONTAINING TOA AND TOPO AS CARRIERS FOR THE RECOVERY OF Ni (II) AND Co(II) FROM WASTE LI-ION BATTERIES

Zakaria HABIBI[1], S. OUKKASS[1], S. MAJID[1], Y. CHAOUQI[1,2], M. HLAIBI[1] ,K.TOUAJ[1]

[1]Laboratoire Génie des Matériaux pour Environnement et Valorisation (**GeMEV**), Faculté des Sciences Aïn Chock, Université Hassan II, Casablanca, Maroc.

[2]Laboratoire de Recherche sur les Matériaux Textiles (**REMTEX**),ESITH Casablanca, Maroc.

ABSTRACT

The growth of the lithium-ion battery industry requires a secure supply of raw materials and proper management of end-of-life batteries.

Functional recycling of lithium-ion batteries would meet both economic and environmental needs. It would ensure the continued availability of cobalt and nickel for industrial applications and allow waste reduction.

The majority of heavy elements are toxic and harmful to living organisms, even at low concentrations.

For this work, we prepared two Polymer Inclusion Membranes (**PIMs**), based on the polymer support Polyvinylidene difluoride (**PVDF**) and two extractive agents: Trioctylphosphine oxide(**TOPO**) andTrioctyl amin(**TOA**).These membranes were characterized and have adopted to achieve the oriented processes for the facilitated extraction and recovery of **Co (II)**and **Ni(II)** ions. The obtained results were used to determine the values of different parameters: macroscopic permeability **(*P*),** initial flux **(J_0)** and microscopic apparent diffusion coefficient **(*D**)** and association constant **(K_{ass})** relating to the substrate movement through the membrane. The influence of several factors, initial substrate concentration, acidity and temperature (**C_0**, **pH**, **T**) was studied. The results indicate that the various parameters **(*P*, *J*, *D**** and **K_{ass}**) vary greatly with the temperature of the medium and the performance of the used membrane increases with temperature factor. Similarly, these studies made it possible to determine the values of activation parameters, (***E_a*, *$\Delta H^{\neq}$*** *and* ***$\Delta S^{\neq}$***), and to elucidate a mechanism by ***successive jumps of Co (II) and Ni(II) ions on fixed sites*** of the immobilized extractive agent molecules in the membrane phase.

Finally, we treated the filtrate of a type of Li-ion battery because we relied on the same membrane which showed good results in the first experiments.

Keywords: Li-ion battery, cobalt, nickel, polymer membrane with inclusion

PREPARATION AND CHARACTERIZATION OF A BIO-ADSORBENT FROM *MORINGA OLEIFERA* POD WASTE

Yosra Raji[1,2], Meriem Saadouni[1], Issam Mechnou[2], Abdelfattah elmahbouby[2], Omar Cherkaoui[1], Souad Zyade[2,3].

[1]Laboratory for Research on Textile Materials (REMTEX), Higher School of Textile and Clothing Industries(ESITH),Casablanca,Morocco.
[2]Genie Laboratory of Materials for Environment and Valorization (GeMEV), Aïn Chock Faculty of Sciences, Hassan II University, Casablanca, Morocco.

ABSTRACT

Pollution of water by non-biodegradable organic pollutants, such as dyes, requires the use of highly efficient processes. Studies have shown that the use of synthetic materials for wastewater purification can be seriously hazardous to health and the environment . Among the proposed solutions, adsorption techniques on adsorbent materials are less expensive processes concretely from plant waste. In this context we are interested in the adsorbent capacity of plant waste from the pods of the *Moringa Oleifèra* plant. The method of elaboration of activated carbon studied is thermal flach carbonization at 900°C followed by chemical activation by sulphuric acid. The prepared adsorbent was characterized using elemental analysis, FT-IR, SEM, TGA and EDX respectively. The effects of operational parameters, such as pH, moisture content, ash content, porosity and iodine value on the adsorbent were also studied and compared with those of commercial activated carbon. The characterization analysis done on the adsorbent showed that it has a low ash content (2.15%), low moisture content (2.65%) and acceptable diode number (586 mg/g). The performance of the synthesized adsorbent is evaluated for the removal of dye (methylene blue). In this work, we found that the adsorption isotherms of the studied adsorbent/adsorbate systems are satisfactorily described by the Langmuir mathematical model where the maximum adsorption capacity of activated carbon is 595 mg/g. The adsorption tests showed that equilibrium is established after 30 min and the kinetics are well described by the second order model. The thermodynamic study revealed a spontaneous and endothermic process and the adsorption is of physical type.

Keywords: Moringa Oleifèra, adsorption, activated carbon

STUDY OF DESIGN AND PERFORMANCE OF A HYBRID SOLAR-POWERED SYSTEM IN SUMMER CLIMATE

Mokhtar Noori Saddam [1, a),]

[1]Mech. Eng. Dept. College of Engineering, University of Thi-Qar, AL-Nasiriyah, Iraq

ABSTRACT

The paper presents the recent studies that specialize in optimizing the efficiency of air-conditioning (AC) systems using alternative energy. For this purpose, several advanced AC plants (absorption, adsorption, and desiccant) are designed. Their technology and components are described during this chapter. It also discusses the energy intake of the alternative energy use in air-conditioning, especially in rural regions where the electricity shortage is frequent, yet because the reduction of the energy costs and also the pollution rate. A comparison between solar AC systems and traditional AC systems at the extent of the designs, costs, and effectiveness is created at the tip of the chapter. Solar AC systems have many environmental benefits compared with those who are driven by conventional vapor compression cycles. In fact, traditional AC systems operate with chlorofluorocarbons and hydrofluorocarbon refrigerants that impact on ozone depletion. The solar AC systems reported during this paper present a noteworthy worldwide solution to scale back the harmful effects (high-energy consumption and pollution) of traditional AC systems. In fact, research studies revealed that absorption, adsorption, and desiccant systems allowed saving energy up to 80, 50, and 52%, respectively, due to the optimization of their designs at the amount of using environmentally unfriendly refrigerants, investing within the free and clean alternative energy to power them, moreover as at the extent of the selection of the components that comprise them. Therefore, these systems also reduced the pollution rate up to 95% (about 3000 kg of CO2), especially the absorption systems. additionally, their use is remarkably suitable in rural regions where the electricity isn't available or its shortage is frequent. Some solar AC systems are equipped with chilled or quandary tanks, which might be utilized in various activities (household, agricultural, and so on). However, their coefficient of performance is below 1 in most cases compared with the normal AC systems that their coefficient can reach the worth 3. Moreover, the installation and maintenance costs of the solar AC systems are relatively high. Hence, we will reach a long-term sustainability. Nonetheless, the look of those systems, especially adsorption and desiccant AC systems is complex.

Keywords: AC systems, solar energy, coefficient of performance

COMPARISON OF EVACUATED TUBE AND FLAT PLATE SOLAR COLLECTOR – A REVIEW

Rawan Adnan[1] , Mokhtar Noori Saddam[2]

[1]Mech. Eng. Dept. College of Engineering, University of Thi-Qar, AL-Nasiriyah, Iraq

[2]Mech. Eng. Dept. College of Engineering, University of Thi-Qar, AL-Nasiriyah, Iraq

ABSTRACT

Solar energy is an enormous and mostly untapped resource. Solar energy remains used mainly in small direct-use application such as water heating. Solar energy is used as direct light and heat from sun that is yoked with a scale of ever-needful innovative technology such as solar water heating,Solar Air heating, Photosynthesis, etc. It is a universal energy used by most of peoples. It is renewable and ecofriendly energy. Solar collector traps solar energy. A collector of solar collects heat by gripping process. Solar collector is describing as a device deliberate to attract incident solar radiation, transference the energy to fluid transient in contact with it usually liquid or air. Heat pipes are primary heat receiving device in solar collector. Heat pipe heat exchanger is a device which is used to transmit the heat from one side to another place using an evaporation-condensation cycle. In solar collector, three types of solar collectors are being used. The names of heat pipes are evacuated tube, flat plate solar collector and focused solar collector. The performance of heat pipes is determined by working fluid. Now day's Nano fluids are used in heat pipe. In otherwise Nano fluid describes the fluid requiring Nano particles is called Nano fluid. Nano fluid plays an important task in water heater, power generation. This paper presents an over views of comparative performance study of flat-plate and evacuated solar collector. Studies of Nano fluids reveals that high thermal conductivities and heat transfer coefficient compared to those of conventional fluids and When compared those kind of solar collectors, high performance has been given by evacuated tube solar collectors. If modification of flat plate integrated with heat pipe, it can give better performance than the plain flat plate solar collector. Evacuated tubes are having snow-shed problems due to creating vacuum inside the tube. Flat plate can shed snow very easily in little sun shed. If uses of Nano fluid in solar collectors, it reduces the dry out problems and also high thermal capacities through literatures.

DEVELOPMENT OF AN IMPROVED SMS OPERATING EGG TRAY TURNING SYSTEM

Mu'azu Jibrin Musa
Ahmadu Bello University, Dept. of Electronics & Telecommunications Engineering, Nigeria.
ORCID NO: 0000-0003-2006-6878
Yahaya Otuoze Salihu
Kaduna Polytechnic, Dept. of Computer Engineering, Nigeria.
ORCID NO: 0000-0002-8770-7572
Abdullahi Ismail Beli
Kaduna Polytechnic, Dept. of Electrical and Electronics Engineering, Nigeria.
ORCID NO: 0000-0002-9217-1709
Abubakar Abisetu Oremeyi
Kogi State Polytechnic Lokoja, Nigeria.
ORCID NO: 0000-0001-6668-9275

ABSTRACT

The natural way of egg incubation produces chicks in small numbers than the number required worldwide. This shortage in chick production by natural incubation led to the conception and development of artificial incubators, which range from manual, semi-automatic, and fully automated incubators. The high mortality rate in the chick's egg incubation is a result of the poor turning of eggs at the right angle of 45^0 and 135^0 on both sides to horizontal respectably, and also inappropriate delay in turning, high or low temperature less than or higher than 38.9 ^{0}C and low or high humidity, which is out of the range 60% to 75% in chicks' incubation. This paper aims to present a design to tackle the inherent issues associated with egg tray turning to minimize the high rate of pre-hatching mortality of embryos. The Egg tray was constructed using woods of different dimensions, the turning was achieved using a bidirectional D.C. motor, and the delay was created using microcontroller PIC16F877A. A program is written to the PIC16F877A to create the given delay using the flow code for the decision. Global Systems for Mobile communication (GSM) was incorporated to permit a remote command and checking of the egg trays run the device from all over the world using the ATtention command (AT). A low-cost SIMCOM SIM900 GSM modem was used to provide the communication link between the GSM and the turning system. The turning mechanism was compared with the manual egg turning, which is insufficient, gives room for errors, is labor intensive, porous in transmitting bacteria to the eggs, and causes extreme mortality to the chicks'. The design was also compared to a semi-automatic turning system, which is labor intensive and needs a physical operator to operate. Further comparison was conducted with the fully automated turning system, which was made up of a complex structure that did not provide an exact turning angle, the operator cannot know the status of the turning system at a distance, and also the operator cannot command the turning system via a Short Message Services (SMS) to operate at a distance. Hatchability of 84.0% was recorded on tilting the egg trays 45^o in both directions and 71.1% when the tilted angle was 20^o. The proposed turning system was found to be robust, eliminate human intervention, prevent the spray of bacteria to the eggs, cut-off high labor, and permit remote operation of the turning system.

Keywords: Automated mechanism, Egg tray, GSM, SMS, Turning system,

1. Introduction

Incubation is the process of keeping the fertile eggs warm to allow proper development of the embryo into a chick (Lumchanow and Udomsiri, 2017, Tona *et al*., 2022). Natural incubation is the process where the birds sit on the egg to provide the required condition until they hatch (Thomas *et al*., 2022). Due the shortage in chick production led to the development of artificial incubators. Artificial incubation is the process of keeping the fertile eggs in an enclosure where some key environmental conditions are controlled for hatching (Dutta and Anjum, 2021). In artificial incubation a relatively large number of eggs are hatched throughout the year, hence it addresses the demands of chick production. The artificial incubator is faced with the challenges of high mortality if one of the three conditions (temperature, humidity, and egg tilting) of incubation are not mated. Making an efficient incubator at low cost is another challenge because egg embryos are frangible, even a slight increase or decrease in temperature, humidity, turning of eggs, and ventilation can affect the development of the chick and time for hatching (Patricia *et al*., 2020). The temperature should be kept between 38.9 ºC (± 0.5 ºC), while the humidity should be kept at a range of 60% to 70% for optimum results during incubation (Musa *et al*., 2022). Egg tilting is compulsory during the first 18 days of incubation, without which almost all the embryos will stick to the egg's shell and die.

The rest of this paper is structured as follows. In section 2, the methodology and design formulation are presented. In section 3 the challenges of the existing incubators. The preliminary result and discussion are presented in Section 4 while Section 5 concludes the paper.

2. Methodology

The method used in coming up with the concept of the mechanism includes the following major sub-modules PIC16F877A, GSM module, limit switch, and bidirectional DC motor.

A. PIC MCU 16F877A

The PIC (Peripheral Interface Controller) 16F877A is one of the most renowned microcontrollers in the industry. It has four ports A to D, which are used for input and output control of other electronic devices. It has an internal EPROM, which permits data storage for future analysis. Figure 1 shows the typical configuration of PIC16F877A (Mousam, 2016).

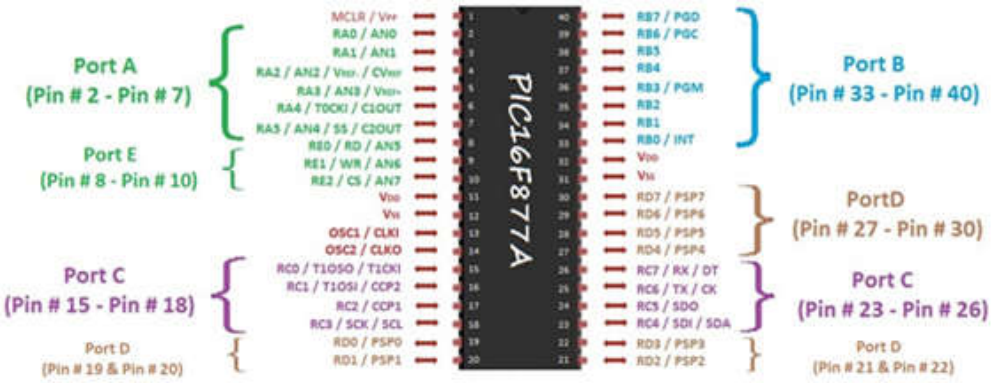

Figure 1. Typical Pin-out of PIC16F877A (Mousam, 2016).

A microcontroller is a single chip computer consisting of a central processing unit; Memory; Input ports and Output ports. At the heart of the microcontroller, there is a Central Processing Unit **(**CPU**)**. PIC microcontroller has some very special features that make it very attractive in different applications. These features are as follows (Mousam, 2016):

Power-on Reset (POR); Power-up Timer (PWRT); Oscillator Start-up Timer (OST); Watchdog Timer (WDT) with its on-chip RC oscillator for reliable operation; Code-protection; Power saving SLEEP mode; Selectable oscillator options Serial In-System Programming - via two pins (ROM devices support only Data

EEPROM programming). In this research work, the PIC16F877A is sufficient enough to handle all the controls of the proposed incubator and data storage. Delay was created using Timer1 of the PIC16F877A for egg turning. Nested loops were also created to produce the desired software delay.

B. GSM module

The GSM interface was designed and implemented for remote monitoring, and control, and to also provide a real-time EPROM saving of the dynamic parameters and a timer to keep track of the incubation days. The interface was developed through the D9 male and female ports of the GSM modem (SIMCOM SIM900) and the serial port of the GSM respectively. AT commands were used in C++ language to enable two ways of communication with the incubator via the Short Message Service (SMS). Unique codes were dedicated to each task for easy messaging. Incubator's parameters were saved in the EPROM throughout the incubation period with the help of a CR2032 CMOS battery for validation purposes. Figure 2 shows the GSM module used.

Figure 2. SIMCON SIM900 GSM Module

The GSM module was selected due to its ability to send and receive SMS, operate on the Quad Band 850, 900, 1800, and 1900 MHz, and can also be controlled via AT commands (Adi *et al.,* 2019).

C. Limit switch

Two limit switches are positioned at some point to enable cutting the supply voltage to the motor when the required angle reaches. Figure 3 shows a typical limit switch.

Figure 3. Limit switch

The limit switch was so designed with a normal close (NC) and normally open (NO) terminal. In the incubator turning mechanism, the NC terminal was used to cut off the voltage supply when engaged.

D. Bidirectional DC motor

A bidirectional DC motor with an internal gear arrangement was used due to its high torque and slow rotation. Figure 4 shows the bidirectional DC motor used.

Figure 4. DC bidirectional gear motor

The motor's synchronous speed, slip, torque, and starting current can be expressed as (Dejan and Bodan, 2016):

$$\eta_{sync} = \frac{120\,f}{p} \quad (1)$$

where $\eta_{sync}$is synchronous speed, f is the frequency, p is the poles

The slip can be expressed as:

$$s = \frac{\eta_{sync} - \eta_m}{\eta_{sync}} \times 100\% \quad (2)$$

where s is the slip, η_m is the mechanical shaft speed

The torque τ_{ind} can be expressed as:

$$\tau_{ind} = \frac{P}{\omega_m} \quad (3)$$

where, ω_m is the rotation per min, P is power in kW

The motor's starting current I_L can be expressed as:

$$I_L = \frac{S_{start}}{\sqrt{3}\,V_T} \quad (4)$$

where, S_{start} is the product of the rated hp and code factor, V_T is the rated voltage

Figure 5 shows the connection of the DC motor to the tray control mechanism.

Figure 5. Motor connection to tray turning

The final arrangement of the egg tray turning mechanism is shown in Figure 5.

E. Motor driver

The DC motor driver circuit was designed using IRF540 N-channel MOSFET to provide the driving voltage of 12 V to the bidirectional DC motor. Figure 6 shows the 12 V motor driving circuit. Figure 6 shows the motor driver circuit used.

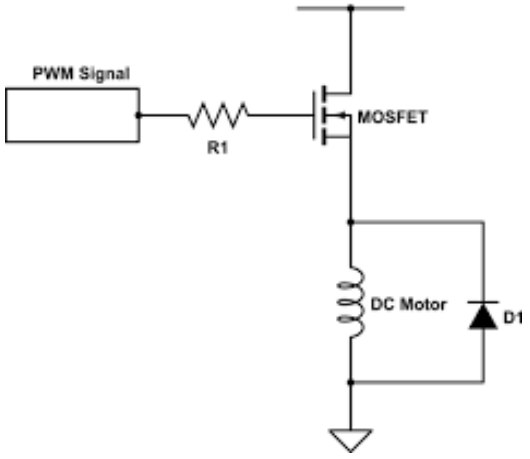

Figure 6. DC motor driver circuit

The driving circuit is made up of MOSFET, resistor, and diode (Ariful *et al*., 2017).

F. Tilting mechanism

This is the mechanism used for the tuning of the eggs' tray at an interval through an angle of 45^0. It contains control circuitry, a relay board, an electric motor (bidirectional), gear, and mechanical links.

Figure 7 shows general egg tray tilting parameters (French, 1997).

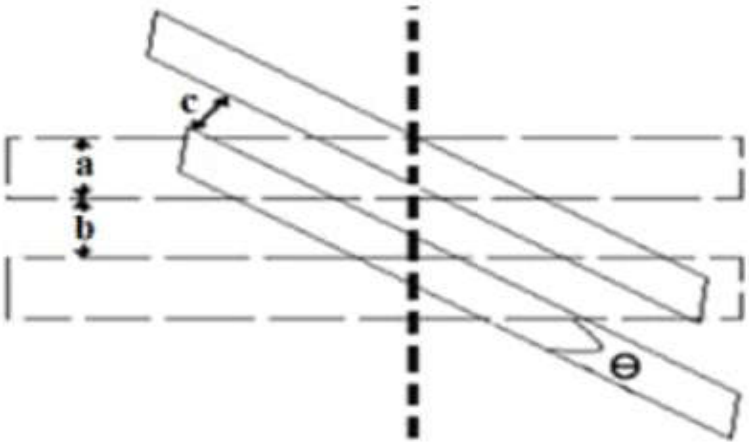

Figure 7. Tilting parameters (French, 1997)

The effect of tilting the trays with respect to the spacing between them can be expressed as in equation (5):

$$C = [cos\theta(a + b)] - a \qquad (5)$$

Where θ is the angle of tilt, C is the space between trays at $\theta = 45^o$, a is the wideness of each egg tray and b is the spacing between two trays at $\theta = 0^o$. Figure 8 shows the bidirectional tilting angles of the egg trays.

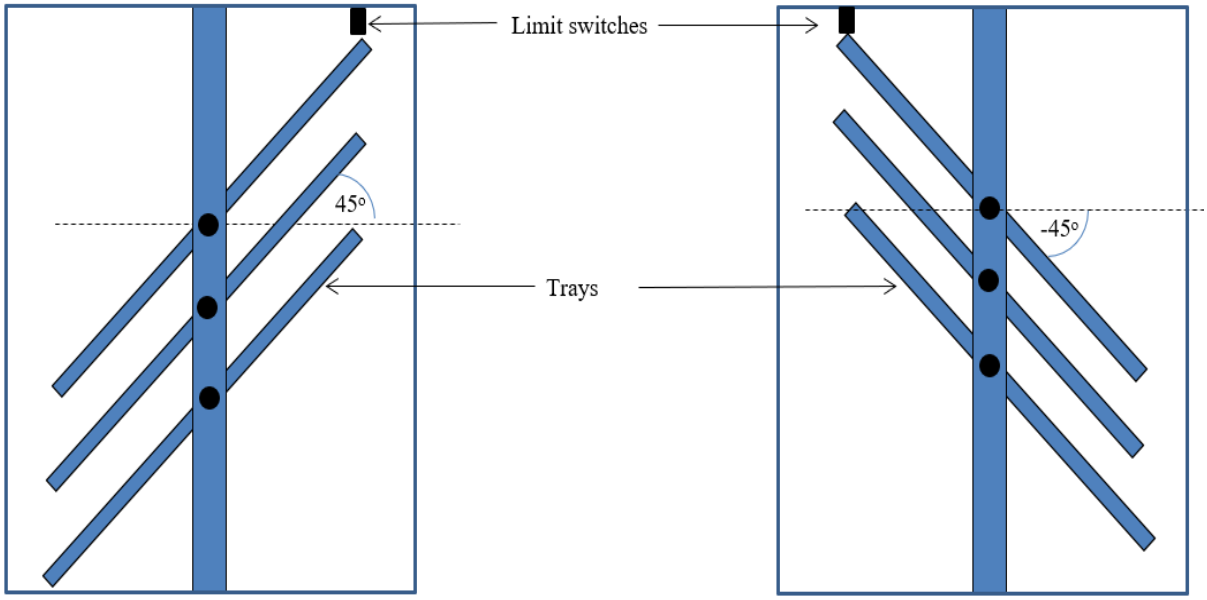

Figure 8. Tilting of egg trays to angles of 45° and -45°

The egg trays tilt anticlockwise at an angle of $\theta = 45^o$ to the horizontal and clockwise at an angle of $\theta = -45^o$ respectively. By so doing 247 eggs were recorded hatched out of 294 fertile eggs. The limit switch was also positioned to keep the tray at $\theta = 20^o$ angle and $\theta = -20^o$ to the horizontal respectively to study the effect of tilting on egg hatchability. This allows comparing the effect of the tilting between the angle of 20° and 45° on the hatchability. All other conditions such as temperature and humidity were kept constants

3. Challenges of the existing incubators

Conventional incubators are faced with several inherent problems which include the absence or inappropriate turning of the egg trays during the incubation period. Lack of proper titling angle of the egg tray leads to a high mortality rate of the embryos, which resulted in the tendency of an embryo to stick to the egg shells (Elibol and Brake, 2006). To prevent this, the eggs must be tilted every 4 hours at an angle of 45° to the horizontal in both directions.

4. Results and discussion

The proposed smart incubator is compared to the Manual, Semi-automatic, and fully automatic incubators. Table 1 shows the improvement of the proposed smart incubator against the conventional incubators.

Table 1. Comparison of the proposed smart incubator against the conventional incubators

SN	Manual	Semi-Automated	Fully automated	Proposed Smart
1.	Eggs are rotated manually	Trays are rotated manually to the desired angles	Trays are rotated automatically to the desired angles	Trays are rotated automatically to the desired angles
2.	Equilibrium gets disturbed whenever the door is opened	Equilibrium gets disturbed whenever the door is opened	Equilibrium has no disturbance due to the opening of doors	Equilibrium has no disturbance due to the opening of doors
3.	Consumes more power	Consumes power	power is conserved	power is conserved
4.	System status can not be queried	System status can not be queried	System status can not be queried	The status of the system can be queried remotely
5.	Can not be remotely operated	Can not be remotely operated	Can not be remotely operated	Remote operation is possible
6.	It can not send SMS in case of an alarm	It can not send SMS in case of an alarm	It can not send SMS in case of an alarm	It can send SMS in case of an alarm

From Table 1 is clear that the proposed smart incubator has many advantages over conventional incubators. Table 2 shows the effect of tilting angle on egg hatchability.

Table 2: Effect of tilt angle on hatchability

Angle of tilt	No. of Eggs	Chicks Hatched	% Hatched (%)
20º	294	209	71.1
45º	294	247	84.0

Hatchability of 84.0% was recorded when the eggs are tilted through an angle of 45º from a total of 294 fertile eggs and 71.1% when the tilted angle was altered to 20º using the same number of fertile eggs and the same incubation parameters.

5. Conclusion

The experiment data shows that tilting the eggs tray at 45° increased the percentage of the hatching by 12.9% as compared to 20°. This shows how critical the angle of tilt is to the hatchability of the eggs. Turning the eggs at greater angles reduced the dead embryos during the later stages of incubation and consequently, the eggs left on the hatching trays were reduced.

References

Lumchanow, W., and Udomsiri, S. (2017). "Chicken embryo development detection using self-organizing maps and K-mean clustering," 2017 International Electrical Engineering Congress (iEECON), pp. 1-4.

Tona, K., Voemesse, K., N'nanlé, O., Oke, O. E., Kouame, Y. A. E., Bilalissi, A., Meteyake, H., and Oso, O. M. (2022). "Chicken Incubation Conditions: Role in Embryo Development, Physiology and Adaptation to the Post-Hatch Environment," Front. Physiol. 13:895854, pp. 1-15.

Thomas, D. A., Reji, C., Joys J., and Jose, S. (2020). "Automated Poultry Farm with Microcontroller based Parameter Monitoring System and Conveyor Mechanism," 4th International Conference on Intelligent Computing and Control Systems (ICICCS), pp. 639-643.

Dutta, P., and Anjum, N. (2021). "Optimization of Temperature and Relative Humidity in an Automatic Egg Incubator Using Mamdani Fuzzy Inference System," 2nd International Conference on Robotics, Electrical and Signal Processing Techniques (ICREST), 2021, pp. 12-16.

Givisiez, P. E. N., Moreira, F. A. L. B., Santos, M. R. B., Oliveira, H. B., Ferket, P. R., Oliveira, C. J. B., Malheiros, R. D. (2020). "Chicken embryo development: metabolic and morphological basis for in ovo feeding technology," Poult Sci., 99(12), pp. 6774–6782.

Musa, M. J., Salihu, Y. O., Yusuf, M., Usman, Z. G. (2022). "Improved XM-18 Controller using Petroleum Liquid Gas Based Automatic Heating Alternative for Egg Incubation in Developing Countries," in IEEE 5th Information Technology for Education and Development (ITED). Nile University of Nigeria, Abuja, Nigeria, pp. 1–4.

Mousam, G., Suman, G., Pradip, K. S., and Goutam, K. P. (2016). "Design and Implementation of PIC16F877A Microcontroller Based Data Acquisition System with Visual Basic Based GUI," 7th International Conference on Intelligent Systems, Modelling and Simulation (ISMS), pp. 419–423.

Adi, P. D. P., Prasetya, D., Setiawan, A. B., Arifuddin, R. (2019). "Design of tsunami detector based sort message service using arduino and SIM900A to GSM/GPRS module," Proceedings of the 2nd International Conference on Advance and Scientific Innovation, ICASI, Banda Aceh, Indonesia, pp. 1-13.

Dejan, P., and Bodan, V. (2016). "Calculation of Induction Motor Starting Parameters Using MATLAB," Infotech-Jahorina 15, pp. 879–884.

Arifu, I., Shamim, A. K. M., Ullah, H., and Bhuiyan, M. A. S. (2017). "Design and Implementation of a Low-cost MOSFET Based Chopper Drive DC Motor Speed Control," Journal of Science and Technology, 9(20), pp. 1-4.

French, N. (1997) "Modeling incubation temperature: the effects of incubator design, embryonic development, and egg size," Poultry Science 76, pp. 124–133.

Elibol, O., and Brake, J. (2006). "Effect of Egg Turning Angle and Frequency During Incubation on Hatchability and Incidence of Unhatched Broiler Embryos with Head in the Small End of the Egg." Poultry Science Association Inc., 85(8), pp. 1433-1437.

COMPARISON OF STATISTICAL NEURAL NETWORK AND LOGISTIC REGRESSION IN CLASSIFICATION OF CHILD HIV STATUS

Tolulope. O. James

Department of Mathematics, Kebbi State University of Science and Techonogy, Aliero, Nigeria

ABSTRACT

There are several methods and choice of model to classify and diagnosis medical data according to diverse diseases and outcomes. In this paper, the performance of statistical neural network(SNN) that is multilayered perceptron and logistic regression (LR) were compared in classification of Child HIV status. The classifiers performance was estimated by the confusion matrix, the Area under the ROC curve (AROC). The result shows that the mean square error(MSE) values obtained from SNN were lesser than those obtained from LR. Also in LR and SNN the area under ROC curve was 0.98 and 1.0 respectively, it shows that logistic regression and neural networks were similar in classification subjects but the neural network perform better than the conventional logistic regression.

Keywords: Statistical neural network, logistic regression, Classification, child, HIV status.

ON PARAMETRIC REACCELERATED OVERRELAXATION (PROR) METHOD FOR LINEAR SYSTEMS

[1]I. O. Isah, [2]A. Ndanusa, [3]M. D. Shehu and [4]A. Yusuf

[1]Department of Mathematical Sciences, Prince Abubakar Audu University, Anyigba, Nigeria

[2,3,4]Department of Mathematics, Federal University of Technology, Minna, Nigeria

Abstract: In this paper, the application of Parametric Reaccelerated Overrelaxation (PROR) method is extended to more classes of coefficient matrices of linear systems. The PROR method is a three-parameter method derived and analysed for consistently ordered matrices. Convergence properties of the PROR method for cases when the coefficient matrix of the linear system is an $L-$ matrix or irreducible matrix with weak diagonal dominance are investigated, analysed and established. Numerical examples are solved to authenticate the effectiveness of the PROR method for these classes of matrices.

Keywords: AOR, ROR, PROR, spectral radius, L-Matrix, irreducible matrix.

2010 Mathematics Subject Classification: 65 XX, 65MXX, 65NXX, 65F10, 65F15, 65M06.

Introduction

Partial differential equations (PDEs) play a major role in many problems in Mathematics, Physics, Engineering, Economics and other science and non-science related fields. The Poisson equation, for example, is ubiquitous in electromagnetism, fluid dynamics among others. The discretization of PDEs by finite differences usually results in very large and sparse linear systems for which iterative methods have been deployed to solve. Numerous such iterative methods have been developed and are continuously being sought. Methods such as Gauss-Seidel [1] and Jacobi [2] have been introduced. Young [3] introduced the SOR method which is an extrapolated Gauss-Seidel method that gives faster convergence than the Jacobi and Gauss-Seidel methods. Hadjidimos [4] introduced the AOR, a two-parameter generalization of the SOR method which also gives better convergence results than the SOR. Thereafter, several modifications of the SOR and AOR methods have been made in an attempt to speed up the rate of convergence of the methods. These include Avdelas and Hadjidimos [5] who optimized the AOR method for the special case when the coefficient matrix of the linear system is consistently ordered. Youssef [6] developed a different version of the SOR for solving linear algebraic systems using the hidden explicit characterization of linear functions which was named the KSOR method. Youssef and Taha [7] introduced some new forms of the modified successive overrelaxation (MSOR) named MKSOR, MKSOR1 and MKSOR2 methods. Wu and Liu [8] proposed a new version of the AOR named the quasi accelerated overrelaxation method (QAOR). Youssef and Farid [9] derived another variant of the AOR called the KAOR. Vatti *et al.* [10, 11] proposed two different versions of the AOR called parametric accelerated overrelaxation (PAOR) method and the reaccelerated overrelaxation (ROR) method for consistently ordered matrices. Isah *et al.* [12] derived the PROR method, a three-parameter generalization of the ROR and PAOR methods aimed at further improving the convergence of the AOR method. This present work seeks to extend the applicability of the PROR method to more classes of matrices.

***Definition 1*:** A square matrix $A = (a_{ij})$ is called reducible if there exists a set K as the union of two disjoint nonempty subsets S and T that satisfies $a_{ij} = 0$ for $i \in S$ and $j \in T$. A square matrix that is not reducible is said to be irreducible. A matrix $A = (a_{ij})$ is irreducible if and only if its directed graph $G(A)$, is strongly connected.

***Definition 2*:** A square irreducible matrix $A = (a_{ij}) \in R^{n\times n}$ is said to be weakly diagonally dominant if $|a_{ii}| \geq \sum_{j=1, j\neq i}^{n} |a_{ij}|, \quad i = 1, 2, \ldots, n.$

***Definition 3*:** A square matrix $A = (a_{ij}) \in R^{n\times n}$ is an $L-$ matrix if $a_{ij} \leq 0$ $(i \neq j)$ and $a_{ii} > 0,$ for all $i, j = 1(1)n$

Materials and Methods

PROR Method

Consider the linear system arising from the discretization of a PDE given by:

$$Bx = c \tag{1}$$

The usual splitting of B in (1) gives

$$(D - L_B - U_B)x = c \tag{2}$$

where $D, -L_B, -U_B$ are the diagonal, strictly lower and strictly upper parts of B respectively.

Equation (2) results in

$$(I - L - U)x = b \tag{3}$$

or equivalently

$$Ax = b \tag{4}$$

where $A = I - L - U, \ b = D^{-1}c, \ L = D^{-1}L_B, \ U = D^{-1}U_B$

The Parametric Reaccelerated over-relaxation (PROR) method for solving (4) is denoted by $M_{\alpha,r,\omega}$ and given by

$$x^{(n+1)} = [(1+\alpha)I - \omega L)]^{-1}\{[(1+\alpha-r+r\omega)I + (r-\omega-r\omega)L + (r-r\omega)U]x^{(n)} + (r-r\omega)b\} \tag{5}$$

where the iteration matrix, $L_{\alpha,r,\omega}$ is represented as

$$L_{\alpha,r,\omega} = [(1+\alpha)I - \omega L)]^{-1}\{[(1+\alpha-r+r\omega)I + (r-\omega-r\omega)L + (r-r\omega)U] \tag{6}$$

The PROR method, $M_{\alpha,r,\omega}$ in (5) reduces to some known methods for specific choices of the parameters (α, r, ω) as follows:

$M_{0,r,\omega}$ gives the Reaccelerated over-relaxation (ROR) method, i. e. for $(\alpha, r, \omega) = (0, r, \omega)$)

$M_{0,1,0}$ gives the Jacobi method i. e. for $(\alpha, r, \omega) = (0,1,0)$

Convergence Analysis of PROR Method

Irreducible Matrices with Weak Diagonal Dominance

Lemma 1 (Varga (1981))

Let $A \geq O$ be an irreducible $n \times n$ matrix. Then,

i. A has a positive real eigenvalue equal to its spectral radius, $\rho(A)$.

ii. To $\rho(A)$, there corresponds an eigenvector $x > 0$.

iii. $\rho(A)$ increases when any entry of A increases.

iv. $\rho(A)$ is a simple eigenvalue of A.

Theorem 1: If A is an irreducible matrix with weak diagonal dominance. Then, for any $\alpha > -1$, $M_{\alpha,r,\omega}$ converges for all $0 \leq r \leq 1$ and $0 \leq \omega \leq 1$

Proof

Let λ be the eigenvalue of the iteration matrix, $L_{\alpha,r,\omega}$ of the PROR method.

Suppose for some λ, $|\lambda| \geq 1$, then the spectral radius of $L_{\alpha,r,\omega}$, $\rho(L_{\alpha,r,\omega}) \geq 1$.

Since λ is an eigenvalue, the relationship for the characteristic equation holds. That is

$$|L_{\alpha,r,\omega} - \lambda I| = 0 \tag{7}$$

which implies that

$$|[(1+\alpha)I - \omega L)]^{-1}[(1+\alpha-r+r\omega)I + (r-\omega-r\omega)L + (r-r\omega)U] - \lambda I| = 0 \tag{8}$$

$$|[(1+\alpha)I - \omega L)]^{-1}\{[(1+\alpha-r+r\omega)I + (r-\omega-r\omega)L + (r-r\omega)U] - \lambda I[(1+\alpha)I - \omega L)]\}| = 0 \tag{9}$$

That is

$$|(1+\alpha-r+r\omega)I + (r-\omega-r\omega)L + (r-r\omega)U - \lambda I[(1+\alpha)I - \omega L)]| = 0 \tag{10}$$

$$\left|I - \frac{r-\omega-r\omega+\lambda\omega}{\lambda(1+\alpha)-(1+\alpha-r+r\omega)}L - \frac{r-r\omega}{\lambda(1+\alpha)-(1+\alpha-r+r\omega)}U\right| = 0 \tag{11}$$

$$|Q| = 0 \tag{12}$$

where $Q = I - \frac{r-\omega-r\omega+\lambda\omega}{\lambda(1+\alpha)-(1+\alpha-r+r\omega)}L - \frac{r-r\omega}{\lambda(1+\alpha)-(1+\alpha-r+r\omega)}U$ (13)

We state that the coefficients of L and U in (13) are less than one in modulus. To prove this, it is necessary and sufficient to prove the inequalities:

$$|\lambda(1+\alpha) - (1+\alpha-r+r\omega)| \geq |\lambda\omega - \omega + r - r\omega| \tag{14}$$

and

$$|\lambda(1+\alpha) - (1+\alpha-r+r\omega)| \geq |r - r\omega| \tag{15}$$

Now, let $\lambda^{-1} = qe^{i\theta}$ where $0 \leq q \leq 1$, q and θ are real numbers. Then from (14), we obtain

$$\left|\frac{1}{q}(cos\theta - isin\theta)(1+\alpha) + r(1-\omega) - (1+\alpha)\right| \geq \left|\omega\left[\frac{1}{q}(cos\theta - isin\theta) - 1\right] + r(1-\omega)\right| \tag{16}$$

Further manipulation of (16) gives

$$[(1+\alpha)^2 - \omega^2] + [(1+\alpha)^2 - \omega^2]q^2 - [(1+\alpha)^2 - \omega^2]2qcos\theta + 2qrcos\theta(1-\omega)[(1+\alpha) - \omega] - 2q^2r(1-\omega)[(1+\alpha) - \omega] \geq 0 \tag{17}$$

It is observed that (17) holds for $\alpha = 0$ and $\omega = 1$.

For $\alpha \neq 0$ and $\omega \neq 1$, (17) becomes

$$[(1+\alpha) + \omega] + [(1+\alpha) + \omega]q^2 - [(1+\alpha) + \omega]2qcos\theta + 2qrcos\theta(1-\omega) - 2q^2r(1-\omega) \geq 0 \tag{18}$$

For $\alpha > -1$, the expressions in brackets in (18) are all nonnegative for all $0 \leq r \leq 1$ and $0 \leq \omega \leq 1$. Thus, (18) holds for all real values of θ if and only if it holds for $cos\theta = 1$. Therefore, (18) can be written as

$$[(1+\alpha) + \omega] + [(1+\alpha) + \omega]q^2 - [(1+\alpha) + \omega]2q + r(1-\omega)2q - 2q^2r(1-\omega) \geq 0 \tag{19}$$

$$(1-q)\{[(1+\alpha) + \omega](1-q) + 2qr(1-\omega)\} \geq 0 \tag{20}$$

and since $0 < q \leq 1$, (20) is also true.

Similarly, after series of simple transformations involving (15), we obtain

$$(1+\alpha)^2 + 2q(1+\alpha)cos\theta[r(1-\omega)-(1+\alpha)]+q^2[r(1-\omega)-(1+\alpha)]^2 - q^2r^2(1-\omega)^2 \geq 0 \quad (21)$$

Simplifying (21) gives

$$(1+\alpha)^2 + (1+\alpha)^2q^2 - 2q(1+\alpha)^2cos\theta + 2qr(1-\omega)(1+\alpha)cos\theta - 2q^2r(1-\omega)(1+\alpha) \geq 0 \quad (22)$$

which for same reason as in (18), must be satisfied for $cos\theta = 1$ leading to

$$(1+\alpha)(1-q)[(1+\alpha)(1-q) + 2qr(1-\omega)] \geq 0 \quad (23)$$

which is again true for $0 < q \leq 1$.

Now, since A has weak diagonal dominance and is irreducible, then $D^{-1}A = I - L - U$ also shares the same properties as A. The same is true of matrix Q in (13) since the moduli of the coefficients of L and U are less than one and not equal to zero. This implies that Q is a nonsingular matrix. i.e. $|Q| \neq 0$, which contradicts (12) and consequently (7) indicating that $|\lambda| \ngeq 1$ and thus $\rho(L_{\alpha,r,\omega}) < 1$. Hence, the $M_{\alpha,r,\omega}$ converges.

L − Matrices

Theorem 2: If A is an $L-$matrix, then for any $\alpha > 0$ and for all r and ω such that $0 < \omega < r < 1$, the PROR method, $M_{\alpha,r,\omega}$ converges if and only if the Jacobi method, $M_{0,1,0}$ converges.

Proof

It is trivial that if $M_{\alpha,r,\omega}$ converges, so does $M_{0,1,0}$ since $M_{\alpha,r,\omega}$ reduces to $M_{0,1,0}$ for some specific choices of parameter values. Hence, we only need to show that if $M_{0,1,0}$ converges, then $M_{\alpha,r,\omega}$ also converges.

Let $\tilde{\lambda} = \rho(L_{\alpha,r,\omega})$ be the spectral radius of $L_{\alpha,r,\omega}$. Suppose $\rho(L_{\alpha,r,\omega}) \geq 1$, based on this assumption, we can easily see that

$$[(1+\alpha)I - \omega L)]^{-1} = \frac{1}{1+\alpha}\left[I - \frac{\omega}{1+\alpha}L\right]^{-1} = \frac{1}{1+\alpha}\left[I + \frac{\omega}{1+\alpha}L + \left(\frac{\omega}{1+\alpha}\right)^2 L^2 + \left(\frac{\omega}{1+\alpha}\right)^3 L^3 + \cdots + \left(\frac{\omega}{1+\alpha}\right)^N L^N\right] \geq 0 \quad (24)$$

But

$$L_{\alpha,r,\omega} = [(1+\alpha)I - \omega L)]^{-1}[(1+\alpha-r+r\omega)I + (r-\omega-r\omega)L + (r-r\omega)U]$$
$$= \frac{1}{1+\alpha}\left[I + \frac{\omega}{1+\alpha}L + \left(\frac{\omega}{1+\alpha}\right)^2 L^2 + \left(\frac{\omega}{1+\alpha}\right)^3 L^3 + \cdots + \left(\frac{\omega}{1+\alpha}\right)^N L^N\right][(1+\alpha-r+r\omega)I + (r-\omega-r\omega)L + (r-r\omega)U] \geq 0 \quad (25)$$

which shows that $L_{\alpha,r,\omega}$ is nonnegative.

Also, $\tilde{\lambda}$ is an eigenvalue of $L_{\alpha,r,\omega}$. Let the corresponding eigenvector of $\tilde{\lambda}$ be v. This implies that

$$L_{\alpha,r,\omega}v = \tilde{\lambda}v \quad (26)$$

$$[(1+\alpha)I - \omega L)]^{-1}[(1+\alpha-r+r\omega)I + (r-\omega-r\omega)L + (r-r\omega)U]v = \tilde{\lambda}v \quad (27)$$

After some simple manipulations, (27) yields

$$\left[\frac{r-\omega-r\omega+\omega\tilde{\lambda}}{r-r\omega}L + U\right]v = \left[\frac{(1+\alpha)\tilde{\lambda} - (1+\alpha) + r - r\omega}{r-r\omega}\right]v \quad (28)$$

It is observed from (28) that $\frac{(1+\alpha)\tilde{\lambda}-(1+\alpha)+r-r\omega}{r-r\omega}$ is an eigenvalue of $\frac{r-\omega-r\omega+\omega\tilde{\lambda}}{r-r\omega}L + U$ corresponding to the eigenvector v. Thus,

$$\frac{(1+\alpha)(\tilde{\lambda}-1) + r(1-\omega)}{r-r\omega} \leq \rho\left(\frac{r(1-\omega)+\omega(\tilde{\lambda}-1)}{r(1-\omega)}L + U\right) \quad (29)$$

It is clear from (29) that

$$\frac{r(1-\omega)+\omega(\tilde{\lambda}-1)}{r(1-\omega)} \geq 1 \tag{30}$$

Therefore,

$$0 \leq \frac{r(1-\omega)+\omega(\tilde{\lambda}-1)}{r(1-\omega)} L+U \leq \left(\frac{r(1-\omega)+\omega(\tilde{\lambda}-1)}{r(1-\omega)}\right)(L+U)$$
$$= \frac{r(1-\omega)+\omega(\tilde{\lambda}-1)}{r(1-\omega)}\left(L_{0,1,0}\right) \tag{31}$$

where $L_{0,1,0}$ is the Jacobi iteration matrix.

Combining (29) and (31) gives:

$$\frac{(1+\alpha)(\tilde{\lambda}-1)+r(1-\omega)}{r-r\omega} \leq \rho\left[\left(\frac{r(1-\omega)+\omega(\tilde{\lambda}-1)}{r(1-\omega)}\right)(L+U)\right]$$
$$= \frac{r(1-\omega)+\omega(\tilde{\lambda}-1)}{r(1-\omega)}\rho\left(L_{0,1,0}\right) \tag{32}$$

which yields

$$\frac{(1+\alpha)(\tilde{\lambda}-1)+r(1-\omega)}{r(1-\omega)+\omega(\tilde{\lambda}-1)} \leq \rho\left(L_{0,1,0}\right) \tag{33}$$

That is

$$\rho\left(L_{0,1,0}\right) \geq \frac{(1+\alpha)(\tilde{\lambda}-1)+r(1-\omega)}{\omega(\tilde{\lambda}-1)+r(1-\omega)} \geq 1 \tag{34}$$

which proves that for $\tilde{\lambda} \geq 1$, so is the spectral radius of Jacobi iteration matrix, i. e. $\rho\left(L_{0,1,0}\right) \geq 1$

Now on the other hand, we can easily show that for $\tilde{\lambda} < 1$

$$\rho\left(L_{0,1,0}\right) < 1 \tag{35}$$

which implies that for $\tilde{\lambda} < 1$, $\rho\left(L_{0,1,0}\right) < 1$ and so we conclude that if $M_{0,1,0}$ converges, so does $M_{\alpha,r,\omega}$.

Choice of Optimum Values of Parameters, α, r and ω

The formulae derived by Isah *et al.* [12] for optimum values of the parameters α, r and ω of the PROR method suffices for $L-$matrices and irreducible matrices with weak diagonal dominance. These formulae are presented in what follows:

Let λ and μ be the eigenvalues of the iteration matrices of the PROR and Jacobi methods respectively, $\underline{\mu}$ and $\bar{\mu}$ are respectively the minimum and maximum of μ and k is any real constant, $k \neq 0$. The formulae for optimum values are categorized into three cases as follows:

Case I: When $\underline{\mu} = \bar{\mu}$ and $k = 1$

then $\omega = \frac{2(1+\alpha)}{1+\sqrt{1-\bar{\mu}^2}}$, $r = \left(\frac{1+\alpha}{\sqrt{1-\bar{\mu}^2}}\right)\left(\frac{1}{1-\omega}\right)$

Case II: When $\underline{\mu} \neq \bar{\mu}$ and $k > 1$

then $\omega = \frac{2(1+\alpha)}{1+\sqrt{1-\bar{\mu}^2}}$, $r = \left(1+\alpha+\omega+\frac{\bar{\mu}^2-\underline{\mu}^2}{2}\right)\left(\frac{1}{1-\omega}\right)$

Case III: When $\underline{\mu} \neq \bar{\mu}$ and $k < 1$

then $\omega = \frac{2(1+\alpha)}{1+\sqrt{1-\bar{\mu}^2}}$, $r = \left(1+\alpha+\omega+\frac{\bar{\mu}^2-\underline{\mu}^2}{2}\right)\frac{\left(\frac{1}{1-\omega}\right)}{2}$

Results and Discussion

The spectral radii of the PROR method are computed and compared with those of AOR and some recent methods for two test problems using MATLAB software.

Problem 1: The Poisson equation described by:

$$\nabla^2 u = -1 \tag{36}$$

discretized on a unit square region with homogenous boundary conditions and $h = \frac{1}{4}$ whose coefficient matrix is an irreducible matrix with weak diagonal dominance given by

$$\begin{pmatrix} 4 & -1 & 0 & -1 & 0 & 0 & 0 & 0 & 0 \\ -1 & 4 & -1 & 0 & -1 & 0 & 0 & 0 & 0 \\ 0 & -1 & 4 & 0 & 0 & -1 & 0 & 0 & 0 \\ -1 & 0 & 0 & 4 & -1 & 0 & -1 & 0 & 0 \\ 0 & -1 & 0 & -1 & 4 & -1 & 0 & -1 & 0 \\ 0 & 0 & -1 & 0 & -1 & 4 & 0 & 0 & -1 \\ 0 & 0 & 0 & -1 & 0 & 0 & 4 & -1 & 0 \\ 0 & 0 & 0 & 0 & -1 & 0 & -1 & 4 & -1 \\ 0 & 0 & 0 & 0 & 0 & -1 & 0 & -1 & 4 \end{pmatrix} \begin{pmatrix} u_{11} \\ u_{21} \\ u_{31} \\ u_{12} \\ u_{22} \\ u_{32} \\ u_{13} \\ u_{23} \\ u_{33} \end{pmatrix} = \begin{pmatrix} \frac{1}{16} \\ \frac{1}{16} \\ \frac{1}{16} \\ \frac{1}{16} \\ \frac{1}{16} \\ \frac{1}{16} \\ \frac{1}{16} \\ \frac{1}{16} \\ \frac{1}{16} \end{pmatrix} \tag{37}$$

where ∇^2 is the second order Laplacian operator given by $\nabla^2 = \frac{\partial^2}{\partial x^2} + \frac{\partial^2}{\partial y^2}$ Source: Ndanusa [13]

Problem 2: Consider the linear system $Ax = b$ whose coefficient matrix, A is an $L-$ matrix and known vector, b are given respectively by:

$$A = \begin{bmatrix} \frac{43}{9} & \frac{-4}{3} & \frac{-10}{9} & 0 \\ \frac{-5}{3} & \frac{49}{9} & 0 & \frac{-10}{9} \\ \frac{-13}{9} & 0 & \frac{49}{9} & 0 \\ 0 & \frac{-13}{9} & \frac{-5}{3} & \frac{55}{9} \end{bmatrix} \text{ and } b = \begin{bmatrix} \frac{5}{9} \\ \frac{8}{27} \\ \frac{22}{9} \\ \frac{62}{27} \end{bmatrix}$$

Source: Ndanusa [13].

The results are presented in the succeeding tables. The following notations are adopted:

L_{AOR} = Iteration matrix of AOR iterative method.

L_{ROR} = Iteration matrix of ROR iterative method.

L_{PAOR} = Iteration matrix of PAOR iterative method.

L_{PROR} = Iteration matrix of PROR iterative method.

$\rho(L_{AOR})$ = Spectral radius of L_{AOR}.

$\rho(L_{ROR})$ = Spectral radius of L_{ROR}.

$\rho(L_{PAOR})$ = Spectral radius of L_{PAOR}.

$\rho(L_{PROR})$ = Spectral radius of L_{PROR}.

Table 1: Result of Spectral Radii of L_{AOR} and L_{PROR} for Problem 1

r	ω	$\rho(L_{AOR})$	α	$\rho(L_{PROR})$
0.1	0.05	0.9701815784	− 0.72	0.8938259051
0.2	0.10	0.9392572158	− 0.70	0.8000000000
0.3	0.15	0.9071493683	− 0.68	0.7176916485
0.4	0.20	0.8737715508	− 0.66	0.6461529340
0.5	0.25	0.8390268063	− 0.64	0.5846884864
0.6	0.30	0.8028058133	− 0.62	0.5326153234
0.7	0.35	0.7649845198	− 0.60	0.4891965894
0.8	0.40	0.7254211490	− 0.58	0.4535068106
0.9	0.45	0.6839523539	− 0.56	0.4240915512

Table 1 reveals the result of the spectral radius of L_{PROR} computed alongside the spectral radius of L_{AOR} for problem 1. Obviously, the PROR scheme gives faster convergence than the AOR since $\rho(L_{PROR},) < \rho(L_{AOR},) < 1)$, for all values of the parameters α, r and ω.

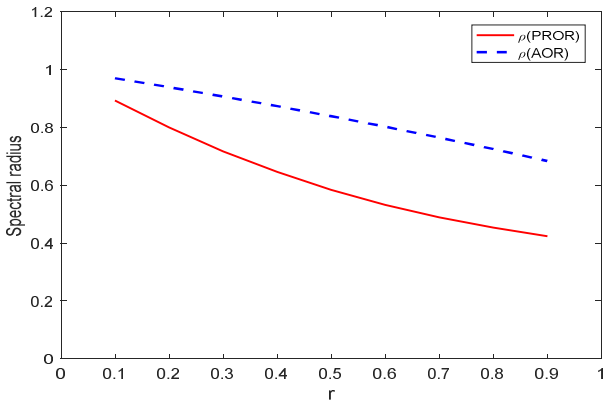

Figure 1: Spectral radii of L_{PROR} and L_{AOR} iteration matrices

Figure 1 represents the graphical illustration of the PROR iteration matrix, L_{PROR} compared with that of AOR iteration matrix, L_{AOR}. It is observed that L_{PROR} clearly converges faster than the AOR iterative method.

Table 2: Result Spectral Radii of $L_{ROR}, L_{PAOR},$ and L_{PROR} with Optimum Parameters for Problem 1

Method	α	r	ω	Spectral Radius(ρ)
ROR	-	−7.056	1.1716	0.2108096000
PAOR	− 0.5	0.6680	0.5858	0.3360000000
PROR	− 0.5	1.6124	0.5858	0.3357121600
ROR	-	−7.0560	1.1716	0.2108096000
PAOR	− 0.4	0.7765	0.7029	0.2941666667
PROR	− 0.4	2.6139	0.7029	0.2943161500
ROR	-	−7.0560	1.1716	0.2108096000
PAOR	− 0.3	0.8850	0.8201	0.2642857143
PROR	− 0.3	4.9197	0.8201	0.2643629000
ROR	-	−7.0560	1.1716	0.2108096000
PAOR	− 0.2	0.9935	0.9373	0.2418750000
PROR	− 0.2	15.8370	0.9373	0.2412248750
ROR	-	−7.0560	1.1716	0.2108096000
PAOR	− 0.1	1.1020	1.0544	0.2244444444
PROR	− 0.1	−20.256	1.0544	0.2243626667
ROR	-	−7.0560	1.1716	0.2108096000
PAOR	0.1	1.3200	1.2887	0.2000000000
PROR	0.1	−4.56960	1.2887	0.1993122909
ROR	-	−7.0560	1.1716	0.2108096000
PAOR	0.2	1.4280	1.4059	0.1900000000
PROR	0.2	−3.5181	1.4059	0.1899973250

In Table 2, we display the spectral radii of L_{ROR}, L_{PAOR}, and L_{PROR} for different combinations of optimum values of α, r and ω for problem 1. The table reveals that the spectral radius of the PROR iteration matrix decreases with each increased value of α such that $\rho(L_{PROR}) < \rho(L_{PAOR}) < \rho(L_{ROR}) < 1$ for $\alpha > 0$, indicating faster convergence of the PROR method for $\alpha > 0$.

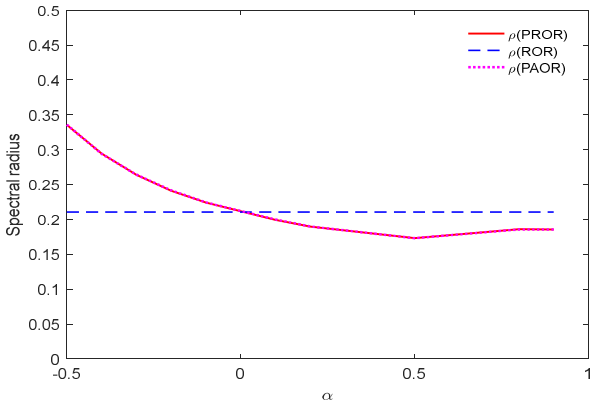

Figure 2: Spectral radii of L_{PAOR}, L_{ROR} and L_{PROR} iteration matrices for different α

Figure 2 illustrates the convergence performance of L_{PROR} in comparison with L_{PAOR} and L_{ROR} and different values of α, r and ω for problem 1. It is observed that the PROR and PAOR methods coincide but converge faster than ROR method for $\alpha > 0$.

Table 3: Result of Spectral Radii of L_{AOR} and L_{PROR} for Problem 2

r	ω	$\rho(L_{AOR})$	α	$\rho(L_{PROR})$
0.1	0.05	0.9503990534	− 0.72	0.8257401890
0.2	0.10	0.8994734663	− 0.70	0.6774234232
0.3	0.15	0.8471403706	− 0.68	0.5521621613
0.4	0.20	0.7933071755	− 0.66	0.4474730513
0.5	0.25	0.7378697740	− 0.64	0.3611387985
0.6	0.30	0.6807102814	− 0.62	0.2910417590
0.7	0.35	0.6216941438	− 0.60	0.2506311101
0.8	0.40	0.5606663840	− 0.58	0.1916145370
0.9	0.45	0.4974466381	− 0.56	0.1471552806

Table 3 shows the result of the spectral radius of L_{PROR} when compared with that of L_{AOR} for problem 2. It is evident from the table that the PROR scheme also converges faster than the AOR as $\rho(L_{PROR},) < \rho(L_{AOR},) < 1)$ for all values of the parameters α, r and ω.

Table 4: Result Spectral Radii of $L_{ROR}, L_{PAOR},$ and L_{PROR} with Optimum Parameters for Problem 2

Method	α	r	ω	Spectral Radius(ρ)
ROR	-	-14.6410	1.0753	0.1020897389
PAOR	− 0.5	0.5835	0.5376	0.1664908276
PROR	− 0.5	1.2621	0.5376	0.1664908277
ROR	-	-14.6410	1.0753	0.1020897389
PAOR	− 0.4	0.6873	0.6452	0.1450010033
PROR	− 0.4	1.9370	0.6452	0.1450010034
ROR	-	-14.6410	1.0753	0.1020897389
PAOR	− 0.3	0.7910	0.7527	0.1296626301
PROR	− 0.3	3.1988	0.7527	0.1296626301
ROR	-	-14.6410	1.0753	0.1020897389
PAOR	− 0.2	0.8948	0.8602	0.1181677120
PROR	− 0.2	6.6402	0.8602	0.1181677121
ROR	-	-14.6410	1.0753	0.1020897389
PAOR	− 0.1	0.99857	0.9678	0.1092341909
PROR	− 0.1	30.9750	0.9678	0.1092341910
ROR	-	-14.6410	1.0753	0.1020897389
PAOR	0.1	1.2061	1.1828	0.0962546465
PROR	0.1	-6.5972	1.1828	0.0962546463
ROR	-	-14.6410	1.0753	0.1020897389
PAOR	0.2	1.3099	1.2903	0.0913931118
PROR	0.2	-4.5114	1.2903	0.0913931117
ROR	-	-14.6410	1.0753	0.1020897389
PAOR	0.5	1.6212	1.6129	0.0807127950
PROR	0.5	-2.6449	1.6129	0.0807127946

Table 4 gives the spectral radius of L_{PAOR} presented alongside the spectral radii of $L_{ROR},$ and L_{PAOR} for different optimum values of r and ω obtained using derived formulae in terms of the chosen values of α applied on problem 2. The table shows that $\alpha > 0$ gave $\rho(L_{PROR}) = \rho(L_{PAOR}) < \rho(L_{ROR}) < 1$ indicating that the PROR method converges faster than the ROR method with same convergence result as PAOR method for these values of α.

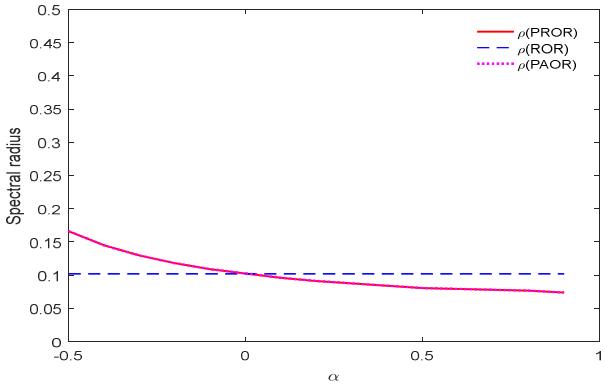

Figure 3: Spectral radii of L_{PAOR}, L_{ROR} and L_{PROR} iteration matrices for different α

Figure 3 shows the convergence behaviour of L_{PROR}, L_{PAOR} and L_{ROR} iterative matrices for different values of α, r and ω for problem 2. The table shows that the PROR and PAOR method virtually coincide but also converge faster than the ROR method for this problem when $\alpha > 0$.

Discussion

Tables 1 and 3 represent the spectral radii of the iteration matrices of the PROR method compared with those of AOR for problems 1 and 2 respectively. The results as revealed in the table confirm theoretical convergence results. Also, in Tables 2 and 4, we presented the convergence results for the case of optimum values of the parameters computed using the functional relations for each of the methods for problems 1 and 2 respectively. In Table 2, it is observed that the spectral radius of the PROR coincides with that of PAOR while it is better than that of ROR method, indicating faster convergence than the ROR methods. The results in Table 4 also revealed that the PROR method agrees with other methods for this problem. Figures 1, 2 and 3 are further proofs of the suitability of the PROR method for the classes of matrices under review.

Conclusion

This research has extended the analysis of a recent and fast converging iterative solver named the PROR method to more classes of matrices that may arise from the discretization of elliptic PDEs. The numerical examples solved revealed that the method is suitable for $L-$ matrices and irreducible matrices with weak diagonal dominance.

References

[1] Seidel, L., Abh bayer akad wiss. Naturwiss. Kl. 11(3), 81–108, 1874.
[2] Jacobi, C. G. J., Gessamelte werke. Berlin: G. Reimer. pp 467, 1884.
[3] Young, D. M., "Iterative methods for solving partial difference equations of elliptic type". Doctoral Thesis, Harvard University, Cambridge, MA. pp 74. 1950.
[4] Hadjidimos, A., "Accelerated overrelaxation method", *Mathematics of Computation*, (32) 141:149-157, 1978
[5] Avdelas G. & Hadjidimos, A., "Optimum accelerated overrelaxation method in a special case". *Mathematics of computation,* 36(153),183-187, 1981.
[6] Youssef, I. K., "On the successive overrelaxation method", *Journal of Mathematics and Statistics*, 8(2), 176-184, 2012.
[7] Youssef, I. K. & Taha, A. A., "On the modified successive overrelaxation method"., *Applied Mathematics & Computation.*, 219(9), 4601- 4613, 2013.
[8] Wu, S., & Liu, Y., "A new version of accelerated overrelaxation iterative method", *Journal of Applied Mathematics, (725360)*, 1-6, 2014
[9] Youssef, I. K. & Farid, M. M., "On the accelerated overrelaxation method". *Pure and Applied Mathematics Journal*, 4(1), 26 – 31, 2015.
[10] Vatti, V. B. K., Rao, G. C. & Pai S. S., "Parametric overrelaxation (PAOR) method", *Numerical optimization in Engineering and Sciences, Advances in Intelligent Systems and Computing,* 979, 283-288, 2020.
[11] Vatti, V. B. K., Rao, G. C. & Pai, S. S., "Reaccelerated overrelaxation (ROR) method", *Bulettin of the International Mathematical Virtual Institute*, 10(2), 315-324, 2020.
[12] Isah, I. O., Ndanusa, A., Shehu, M. D. & A. Yusuf, "Parametric reaccelerated overrelaxation (PROR) method for numerical solution of linear systems", *Science World Journal,* 17(1), 60-64, 2022.
[13] Abdulrahman Ndanusa, "Preconditioned successive overrelaxation iterative method for solving partial differential equations of elliptic type", Doctoral Thesis, Federal University of Technology, Minna, Nigeria, 2012.

MARKOV CHAIN ANALYSIS OF THE ACADEMIC CAREER PROGRESSION

Babayemi, A.W., *James, Tolulope O and Isah, Z.F

Department of Mathematics, Kebbi State University of Science and Technology, Aliero, Nigeria

ABSTRACT

There are many reasons for academics being under pressure in the Nigerian universities, but striving for academic promotion is regarded as one of the most influential factors. In this study, the career progression rates in academic staff, the rate of absorption and the duration of time taken before attaining the highest academic rank, was determined. Data were gotten from the establishment department in Kebbi State University of Science and Technology Aliero. The rank considered were: Graduate assistant, Lecturer (Assistant lecturer, Lecturer 11, Lecturer 1), Reader and Full Professor. The only absorbing state in the chain, is the state of retirement of staff and we assumed there are no death and expulsion occur during the period investigated. The result showed that, the average time taken before attaining the highest rank in the university stand at average of 10.27 years, and that the probability of absorption is certain, i.e. every staff that join the university system has a perfect probability of being a professor if there are no death or expulsion, he will definitely have retired successfully.

Keyword: Academic c`areer progression, markov chain, probability, academic rank

ANALYSIS AND NUMERICAL SOLUTION OF FRACTIONAL ORDER microRNA IN LUNG CANCER

Mohammed Baba Abdullahi[1*]& Amiru Sule[2]

[1]School of Mathematics and Computing, Department of Mathematics/Statistics

Kampala International University, Kampala Uganda.

[2]Faculty of Science, Department of Mathematical Science

Federal University Gusau

Abstract: Lung cancer arises after cells in the lungs split overwhelmingly, triggering tumors to develop. The tumor can decrease an individual capability to breathe, and the disease can extent to other parts of the body. It is one of the most common source of cancer and cancer-related deaths worldwide. In this paper, mathematical model of fractional order microRNA in lung cancer is analyzed. The model analysis is carried out to establish the stability of the equilibrium points and basic reproduction number. To obtain the model's scheme of fractional differential equations, the Caputo fractional derivative operator of order is used. To find an approximate solution to a system of nonlinear fractional differential equations, the Laplace–Adomian Decomposition Method is used. It was possible to acquire the solution of fractional differential equations in the form of an infinite series. Numerical simulations are presented to show the methods reliability and simplicity.

Keywords: Fractional Order, microRNA, Numerical Solution, Analysis & Lung Cancer

EFFECT OF DOUBLE-DIFFUSIVE STAGNATION POINT FLOW OF EYRING - POWELL NANOFLUID ON A SLENDER STRETCHING SHEET WITH NON-UNIFORM HEAT SOURCE SINK AND INCLINED MAGNETIC FIELD

Asha S. K.[*] **and Gayitri Mali**[1]

[*,1] Department of Mathematics, Karnatak University, Dharwad – 580003, Karnataka, India.

Abstract: In the present paper, influence of double diffusive convective stagnation point flow in a slender stretching sheet under the influence of inclined magnetic field and non-uniform heat source sink is studied. The suitable similarity transformations are utilized for the conversion of nonlinear differential equations. These converted equations are solved by means of Differential Transformation method (DTM) with the support of symbolic software Mathematica. Further, the effects of appropriate parameter on velocity profile, solute, nanoparticle concentration and temperature profiles are shown graphically with some suitable discussion. It is found that velocity decreases with a rise of magnetic parameter and also non-uniform heat source sink enhances the thermal profile of the system. But, opposite behaviour can be seen in solute concentration and nanoparticle concentration profiles. Such results can be useful in design and structure of materials, where implementation of variable thickness decreases the weight of stretched element and boosts the usage of materials.

Keywords: Slender Stretching Sheet, Stagnation point flow, Non-uniform Heat Source Sink, Eyring-Powell Nanofluid.

TWO-WEIGHTED INEQUALITIES FOR GENERALIZED FRACTIONAL INTEGRAL OPERATOR IN GENERALIZED WEIGHTED MORREY SPACES

Zaman V. Safarov
Azerbaijan State Oil and Industry University, Baku, Azerbaijan
Institute of Mathematics and Mechanics of NAS of Azerbaijan, Baku, Azerbaijan

ABSTRACT

$$\|f\|_{M^{p,\phi}_{\omega}} = \sup_{x\in R^n, r>0} \phi(x,r)^{-1}\|\omega\|^{-1}_{L_p(B(x,r))}\|f\|_{L_{p,\omega}(B(x,r))},$$

where $1 \le p < \infty$, ϕ is a positive measurable function on $R^n \times (0,\infty)$, ω is a non-negative measurable function on R^n, $B(x,r)$ is an open ball in R^n and $f \in L^{loc}_{p,\omega}(R^n)$. Here, $L_{p,\omega}(B(x,r))$ denotes the weighted L_p -space of measurable functions f for which

$$\|f\|_{L_{p,\omega}(B(x,r))} \equiv \left\|f_{\chi_{B(x,r)}}\right\|_{L_{p,\omega}(R^n)} = \left(\int_{B(x,r)} |f(y)|^p \omega(y)dy\right)^{\frac{1}{p}}.$$

For a measurable function ρ: $(0,\infty) \to (0,\infty)$ the generalized fractional integral operator I_ρ are defined by

$$I_\rho f(x) = \int_{R^n} \frac{\rho(|x-y|)}{|x-y|^n} f(y)dy$$

for any suitable function f on R^n.

Definition. *The weight function* (ω_1, ω_2) *belongs to the class* $A_{p,q}(R^n)$ *for* $1 \le p,q < \infty$, *if the following statement*

$$\sup_{x\in R^n, r>0} |B(x,r)|^{\frac{1}{p}-\frac{1}{q}-1}\left(\int_{B(x,r)} \omega_2^q(y)dy\right)^{\frac{1}{q}}\left(\int_{B(x,r)} \omega_1^{-p'}(y)dy\right)^{\frac{1}{p'}}$$

is finite.

We assume that $\int_0^{\frac{1}{\infty}} \frac{\rho(t)}{t^n}\frac{dt}{t} < \infty$, so that the generalized fractional integral operator I_ρ is well defined, at least for characteristic functions $1/|x|^{2n}$ of complementary balls: $f(x) = \frac{\chi_{R^n\setminus B(0,1)}(x)}{|x|^{2n}}$. Furthermore, we also assume that ρ satisfies the growth condition: there exist constants $C > 0$ and $0 < 2k_1 < k_2 < \infty$ such that

$$\sup_{r/2<t\le 3r/2} \frac{\rho(t)}{t^n} \le C_1 \int_{k_2 r}^{k_1 r} \frac{\rho(t)}{t^n}\frac{dt}{t}, r > 0.$$

This condition is weaker than the usual doubling condition for the function $\frac{\rho(t)}{t^n}$: there exists a constant $C > 0$ such that $\frac{1}{C_1}\frac{\rho(t)}{t^n} \le \frac{\rho(r)}{r^n} \le C_1\frac{\rho(t)}{t^n}, r > 0$, whenever r and t satisfy $r, t > 0$ and $\frac{1}{2}t \le r \le 2t$.

Theorem. *Let* $1 < p < q < \infty$, $\rho(r) \leq Cr^{\frac{n}{p}-\frac{n}{q}}$ *and* $(\omega_1, \omega_2) \in A_{p,q}(R^n)$. *Let the functions* $\phi_1(x,r)$ *and* $\phi_2(x,r)$ *fulfill the condition*

Then the operator I_ρ *is bounded from* $M_{\omega_1}^{p,\phi_1}(R^n)$ *to* $M_{\omega_2}^{q,\phi_2}(R^n)$.

Keywords: integral operator, Morrey space, function

FRANK OPERATOR WITH COMPLEX HESITANT FUZZY SETTINGS FOR DEALING WITH MULTIPLE-ATTRIBUTE DECISION-MAKING PROBLEMS

Shamim Akhter[1], Muhammad Sajjad Ali Khan[2] and Wali Khan Mashwani[1]

[1]Institute of Numerical Sciences, Kohat University of Science & Technology, Pakistan

[2]Department of Mathematics, Khushal Khan Khattak University, Karak, Pakistan

Abstract: In this paper, the Frank operator is used in complex hesitant fuzzy settings to analyses multiple-attribute decision-making (MADM) problems. In contemporary information fusion theory, the Frank operator is a conventional mean type aggregation operator with strong modelling capabilities, with special advantages for aggregating multi-dimension arguments. The Frank operator excels at capturing the interaction between several input arguments. We develop the complex hesitant fuzzy Frank (CHFF) operator for aggregating complex hesitant fuzzy data, inspired by the Frank operator notion. Investigated certain desired qualities including monotonicity, boundedness, and idempotency along with some instances. In addition, we went into great detail about a few unique cases involving different CHFF operator parameter values. We further develop the complex hesitant fuzzy Frank weighted arithmetic (CHFFWA) operator and complex hesitant fuzzy Frank weighted geometric (CHFFWG) operator to aggregating CHF information in situations where the input arguments are of varying importance. On this foundation, a method for dealing with MADM problems involving complex hesitant

fuzzy information is developed.

Keywords: Decision Making Models, Fuzzy Sets, Hesitant Fuzzy Set , Complex Fuzzy Sets and Complex Hesitant Fuzzy Sets

PHYLLOPLANE MYCOFLORA OF *NERIUM OLEIFERA* IN A NATIONAL HIGHWAY IN TAMIL NADU, INDIA

Dr. S. Bhuvaneswari[1]

[3]Department of Botany, Bharathi Women's College (A), Broadway, Chennai, India

Ms. D. Divyasri[2]

Ms. Mayuri[2]

[2]Research and Development, MARINA LABS, Nerkundram, Chennai, India

Dr. N.K. Udaya Prakash[3]

[3]Department of Biotechnology,

Vels Institute of Science, Technology and Advanced Studies (VISTAS),

Pallavaram, Chennai, India

https://orcid.org/0000-0003-2489-7118

ABSTRACT

Phylloplane fungi are the ones which grow on the surfaces of leaves. The fungi which are growing on phylloplane are continuously challenged by wind, temperature and moisture thus facing a unique microclimatic environment. The fungi growing on the plants in Highways are further challenged with the deposition of dust and vehicular emissions. This made the authors to develop interest to find out the diversity of mycoflora on the leaf surfaces of one such plant *Nerium oleifera.* Leaf samples of *Nerium oleifera* were collected from Vandalur to Dindivanam covering a stretch of 90 kms in a National Highway (NH-45) in the State of Tamil Nadu, India. The samples were collected at a distance of approximately 1 kilometer interval each. Altogether a total of 75 samples were collected and brought to the laboratory using a sterile ziplock bags. The samples were analysed for the presence of phylloplane mycoflora using leaf washing technique. Potato Dextrose Agar was used to isolate the fungi. A total of 34 species classified under 21 genera were isolated. Among the species isolated 4 species belongs to Zygomycota, 1 to Ascomycota and the remaining to Mitosporic fungi. Among the species, *Aureobasidium pullulans* was found to be dominant contributing around 90% of Colony forming units recorded. *Alternaria alternata, Aspergillus terreus, Curvularia lunata, Bipolaris australiensis* and *Nigrospora sphaerica* are the other significant contributors. It is clearly evident that the dominant species are of Dematiaceous in nature which is pigmented thus having resistance to UV and heat radiation. Their xerophilic nature makes them to adapt to the deposition of dust on the leaf surface. The study aptly demonstrates the adaptability of these microfungi to their microclimatic i.e. phylloplane environment.

Keywords: Phylloplane mycoflora, *Nerium oleifera*, NH-45 Chennai, Leaf washing technique, *Aureobasidium pullulans*

POTENTIAL ANTIBACTERIAL ACTIVITY OF QUERCETIN AGAINST MULTIDRUG-RESISTANT STRAIN *AEROMONAS HYDROPHILA*

Mahendra Kumar Savita[1],

[1] Amity University, Amity Institute of Biotechnology,

Lucknow, Uttar Pradesh, India -227105

[1]ORCID ID: https://orcid.org/0000-0002-5175-254X

Vinay Dwivedi[2]

[2] Dr. APJ Abdul Kalam University, Naraina Vidyapeeth Engineering, and Management Institute,

Department of Biotechnology, Kanpur-, Uttar Pradesh, India -208020

[1]ORCID ID: https://orcid.org/0000-0001-8294-0298

Prachi Srivastava[1]

[1] Amity University, Amity Institute of Biotechnology,

Lucknow, Uttar Pradesh, India -227105

[1]ORCID ID: https://orcid.org/0000-0003-4138-5464

ABSTRACT

Overuse of antibiotics in past three decades creates multiple drug resistance (MDR) in microbes poses a serious threat to human as well as aquatic health and complicates treatment. Therefore, it is essential to employ a technique that efficiently treats MDR bacteria and averts environmental weakening. Flavonoids have the capability to damaged bacterial cell membranes. A common flavonoid called quercetin is known to have antibacterial properties. This study's goal was to look into how quercetin affected common Gram-negative fish pathogen *Aeromonas hydrophila,* the key causative of bacterial hemorrhagic septicemia disease. Bacterial strains (MTCC ID-1739) were purchased from MTCC Chandigarh and used to measure minimum inhibitory concentrations by broth micro-dilution method using LB broth. By employing an incremental increase method, precise MICs were found. The inhibitory value increased with increasing test flavonoid concentrations. With mean minimum inhibitory values ranging from 0.35 to 1.0 mg/mL, the results showed that quercetin had an antibacterial effect against the bacteria chosen to infect fish. Quercetin was initiated to inhibit *Aeromonas hydrophila* at a concentration of 350 mcg/mL and complete inhibition was introduced at a concentration of 450mcg/ml. No significant inhibition was assessed before 350 mcg/ml. This suggests that quercetin may offer interesting sources for anti-bacterial drugs and may serve as "a model" for pharmaceutical development. Finding the antibacterial mechanism of action may be crucial for furthering the development of these substances. Additionally, the potential of quercetin as a novel antibacterial agent is examined, as well as the rising role of new technologies in this regard.

Keywords: Fish pathogens, *Aeromonas hydrophila*, Quercetin, minimum inhibitory concentrations.

NON-ISOTHERMAL MODELING OF 1D SMA SPRING INVOLVING ENTROPY CHANGE OF THE SYSTEM

Rabiu Ahmad Abubakar

The State Key Laboratory of Fluid Power Transmission and Control, Zhejiang University,

310027, Hangzhou, China

Abstract: In the current paper, suitable thermomechanical coupling models for the SMA wire are formulated based on energy and momentum conservation law. And a modified Landau phenomenological model is proposed for the dynamics of phase transformation of SMA. Entropy change in SMA wire undergoing phase transition is modeled and incorporated into the developed model. The proposed phenomenological SMA wire models are further extended to the SMA spring.

Landau free energy density $F_l(T,\lambda)$ related to the stretch ratio in the model is formulated and plotted at different temperatures. Numerical algorithm simulations are performed via Legendre wavelets-spectral approach for a non-isothermal dynamic system.

Keywords: *Entropy change; Shape memory alloys; Martensite transformation; pseudoelasticity; differential model.*

1 Introduction

Shape memory alloy (SMA) material can be trained to memorize different shapes when the temperature changes [1,2]. Therefore it converts thermal energy to mechanical [3–5]. This unique plastic-like deformation and recovery behavior is referred to as shape memory effects (SME)[6–8]. The history of this material started in the year 1800. It is discovered by William Buchler and his corworkers[9]. After this discovery, NINOL was given to the material with NI standing for nickel and NOL standing for Naval Ordinance Laboratory, where this incident occurred [10]. The material generates a loud strange sound in a cold state, and in a hot state, the sound is different [7]. After some time, researchers all over were attracted to this material behavior for various engineering applications [11,12]. After some serious investigation, it is discovered that the material has a unique property that is different from other metal alloys [13]. This material has the ability to recover energy up to 10^6 J/m^3, and the critical temperature depends on nitinol percentage content with a maximum limit of 363 K [14].

SMAs find application in many engineering applications like actuation impact absorption, sensor, and vibration isolation [15], to mention a few, due to reversible hysteresis properties under cyclic mechanical loading, despite the fact that they have low-frequency responses [16]. Apart from the medical field, they are not up to the level of commercialization due to the absence of detailed models describing their complex behavior. There are many mathematical models in existence [17,18]. But still not sufficient for exact simulation of their complex behaviors.

The most popular alloys are NiTi-based (Nitinol), Fe-based, and Cu-based [19]. Nitinol is bio-compatible and has a single crystal structure. Cu-based alloys, which are brittle SMAs, have gotten highest inelastic recovery strain of about 10% because of the thermo-elastic phased change and are more delicate in application [20], and have less temperature dependence, loading rate, grain size, and lower pseudoelastic behavior [21]. Fe-based SMAs exhibit high ductility, large hysteresis, and lower shape recovery (4 %). In addition to the shape memory effect and pseudoelasticity effect, SMAs exhibit other properties like rubber-like effects resulting from aging and allowing reversible and de-twinning of martensite variants [22].

Recently researchers developed an interest in a breakthrough in material design by introducing a new concept of entropy change during the martensitic phase transformation of SMAs [23]. This concept concerns creating multielement metallic material close to equimolar composition with the entropy of mixing higher than in the existing material, thus giving high phase stability [24]. The solid solution has high entropy and bulk intermetallic compounds, and some of them have a B2 structural body [25], and NiTi SMA austenite belongs to this. Therefore, modeling such a structure is now necessary to capture its behavior involving entropy change.

2 Modeling of SMA wire

For the coupled thermo-mechanical field derivation, the dynamics of the thermomechanical field is formulated using the law of conservation energy [5]. This law states that when a system undergoes a process, the total energy remains constant but only changes from one form to another or a combination of a different form of energy, and this is the basis of the first law of thermodynamics.

$$\Delta Q = \Delta e + W - H_L. \quad 1$$

where ΔQ is the energy input to the system, Δe is the change in internal interfaces during transformation, W is the mechanical energy associated with strain energy of transformation, and H_L is the waste heat. It involves frictional loss F_L and energy loss due to entropy is E_L.

And,

$$.H_L = -(F_L + E_L)$$

The frictional part is already expressed in ref. [5] . Therefore, the entropy is expressed as:

$$E_L = -T_1 \Delta s, \quad 2$$

where T_1 is the critical temperature Δs is the entropy change $\Delta s = S_M - S_A$. When the quantity of the material is considered, Eq. 2 becomes:

$$E_L = -\rho T_1 \Delta s \quad 3$$

For phase transformation to a current SMA temperature T, the entropy change is derived as:

$$\Delta s = \int_{T_1}^{T} \frac{dQ}{T}.$$

And,

$$dQ = C_V dT.$$

Hence,

$$\Delta s = \int_{T_1}^{T} \frac{C_V dT}{T}$$

$$\Delta s = C_v In \frac{T}{T_1} \quad 4$$

Therefore, substituting Eq. 4 in Eq 2.

$$E_L = -\rho C_v T_1 In \frac{T}{T_1}$$

Let,

$$k_5 = \rho C_v T_1,$$

Therefore,

$$E_L = -k_5 In \frac{T}{T_1}, \quad 5$$

where k_5 is the material constant for phase change specific entropy. The negative sign relates to the latent heat of transformation. Using the law of logarithm,

$$E_L = -(k_5 InT - k_5 InT_1) \quad 6$$

Hence, these forms of energy involved are expressed as follows:

$$\Delta e = \rho e_t - \sigma^T : (\nabla_v) + \nabla \cdot q = Z, \quad 7$$

where ρ is the density, σ is the stress tensor, e is the internal energy, q is the heat flux vector, and Z is the thermal loading.

By employing the thermodynamic equilibrium conditions, the thermo-mechanical free energy function (Q) is related to stress σ and internal energy e.

$$\sigma = \rho \frac{\partial Q}{\partial \eta} \quad ; \quad e = Q - T\frac{\partial Q}{\partial \eta}, \quad 8$$

where T is the temperature, and η stands for Cauchy-Lagrangian strain tensor.

$$\varepsilon(x,t) = u_x, \quad 9$$

where x is the axis of the material, and u is the displacement. The free energy function Q can be represented in terms of the Landau free energy function as:

$$Q(T,\varepsilon) = -c_v InT + E_L + Q(T)Q(\varepsilon) + \sigma$$

$$Q(T,\varepsilon) = -c_v InT + k_5 InT_1 - k_5 InT + Q(T)Q(\varepsilon) + \sigma,$$

$$Q(T,\varepsilon) = -(c_v + k_5)InT + Q(T)Q(\varepsilon) + (\sigma + k_5 InT_1) \quad 10$$

where c_v is the specific heat constant, the term $Q(T)Q(\varepsilon)$stands for the thermo-mechanical coupling contribution. By substituting the free energy function defined in Eq. 6-10 in Eq. 1 and using Landau-Ginzburg-Devonshire theory, the following coupled governing equations are obtained:

$$(c_v + k_5)\frac{\partial T}{\partial t} = k_4 \frac{\partial^2 T}{\partial x^2} + k_1 T\varepsilon \frac{\partial \varepsilon}{\partial t} + Z,$$

$$\rho \frac{\partial^2 u}{\partial t^2} = \frac{\partial \sigma}{\partial x} + \Upsilon \frac{\partial}{\partial t}\frac{\partial^2 u}{\partial x^2} - k_g \frac{\partial^4 u}{\partial x^4} - k_5 T_1 + F. \quad 11$$

And,

$$\sigma = k_1(T - T_1)\varepsilon + k_2\varepsilon^3 + k_3\varepsilon^5,$$

where k_1, k_2, k_3, and k_g are the re-normalized material constant, ρ is the material density, T is the current SMA temperature, ε is the strain, and is calculated as $\varepsilon = \frac{\partial u}{\partial x}$, c_v is the specific heat capacitance, k_4 is the normalized material constant, Υis the internal friction coefficient, F and Z are the mechanical and the thermal loading. The term $k_5 InT_1$ is reduced to $k_5 T_1$ for simplicity.

Because of the complication, strong nonlinearity, and coupling between the thermal and elastic fields in Eq. 11, it is further simplified by introducing other equations:

$$v = \frac{\partial u}{\partial t};\ \varepsilon = \frac{\partial u}{\partial x}; g = \frac{\partial^2 \varepsilon}{\partial x^2} \quad 12$$

And also, the average temperature change $\frac{T-T_1}{T_1}$ is used to reduce the nonlinearity.

Substituting Eq. 12 in. Eq. 11, the new governing equation is:

$$\left.\begin{aligned} &(c_v + k_5)\frac{\partial T}{\partial t} = k_4 \frac{\partial^2 T}{\partial x^2} + k_1 T\varepsilon \frac{\partial \varepsilon}{\partial t} + Z, \\ &\rho \frac{\partial v}{\partial t} = \frac{\partial \sigma}{\partial x} + \Upsilon \frac{\partial}{\partial x}\frac{\partial v}{\partial x} - k_g \frac{\partial^2 g}{\partial x^2} - k_5 T_1 + F, \\ &\sigma = k_1\left(\frac{T-T_1}{T_1}\right)\varepsilon + k_2\varepsilon^3 + k_3\varepsilon^5. \end{aligned}\right\} \quad 13$$

And the elastic equation takes the following:

$$\rho\frac{\partial v}{\partial t}=\frac{\partial}{\partial x}\left(\sigma+\Upsilon\frac{\partial v}{\partial x}-k_g\frac{\partial g}{\partial x}\right)-k_5T_1+F$$

Now the new equations are:

$$\left.\begin{aligned}
&v=\frac{\partial u}{\partial t};\ \varepsilon=\frac{\partial u}{\partial x};g=\frac{\partial^2\varepsilon}{\partial x^2},\\
&(c_v+k_5)\frac{\partial T}{\partial t}=k_4\frac{\partial^2T}{\partial x^2}+k_1T\varepsilon\frac{\partial\varepsilon}{\partial t}+Z,\\
&\rho\frac{\partial v}{\partial t}=\frac{\partial}{\partial x}\left(\sigma+\Upsilon\frac{\partial v}{\partial x}-k_g\frac{\partial g}{\partial x}\right)-k_5T_1+F,\\
&\sigma=k_1\left(\frac{T-T_1}{T_1}\right)\varepsilon+k_2\varepsilon^3+k_3\varepsilon^5.
\end{aligned}\right\}\quad 14$$

Equation 14 can capture the phase transformation of SMAs because the thermal and mechanical energy fields are coupled together. Therefore, 1-D SMA wire dynamics can be modeled using these equations by setting appropriate initial and boundary conditions.

3 SMA spring modeling

The modeling of the SMA spring is already given in ref. [26]. The stretch ratio is defined as the final length of the SMA spring per the original length.

$$\lambda=\frac{final\ length}{original\ length}=\frac{L_f}{L_o}=\frac{p_1}{p_o},\quad 15$$

where λ is the stretch ratio, L_f is the final length, L_o is the original length, p_1 is the current pitch, p_o is the reference pitch. Fig. 1 shows the SMA spring in shrank and stretched forms.

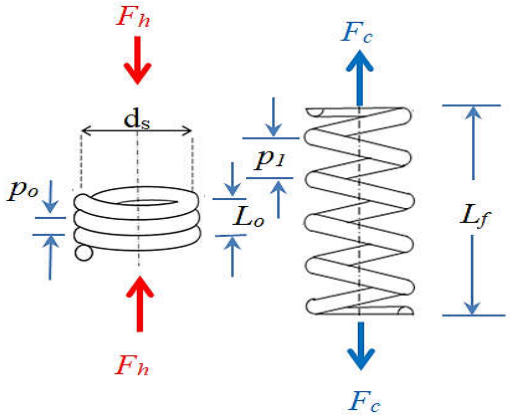

Figure 1 SMA spring

For the thermo-mechanical coupling dynamics of the SMA spring, the equation can also be obtained by slightly modifying those for the SMA wire by replacing the strain of the SMA wire with the stretch ratio of the SMA spring and the axial stress σ with shear stress τ. Therefore, Eq. 14 is modified as:

$$\left.\begin{aligned}
&v=\frac{\partial u}{\partial t};\ \lambda=\frac{\partial u}{\partial x};g=\frac{\partial^2\lambda}{\partial x^2},\\
&(c_v+k_5)\frac{\partial T}{\partial t}=k_4\frac{\partial^2T}{\partial x^2}+A_1T\lambda\frac{\partial\lambda}{\partial t}+Z,\\
&\rho\frac{\partial v}{\partial t}=\frac{\partial\tau}{\partial x}+\Upsilon\frac{\partial}{\partial x}\frac{\partial v}{\partial x}-k_g\frac{\partial^2g}{\partial x^2}-k_5T_1+Fr,\\
&\tau=A_1\left(\frac{T-T_1}{T_1}\right)\lambda+A_2\lambda^3+A_3\lambda^5.
\end{aligned}\right\}\quad 16$$

where r is the SMA wire radius. A_1, A_2, and A_3 are the SMA spring material constants.

3 Numerical algorithm via Legendre wavelets-spectral approach

In this method, wavelet functions are constructed by the mother wavelet function's expansion and translation. Legendre polynomials are used to drive it. The family of Legendre wavelet is represented as:

$$\psi_{w,p}(x) = \begin{cases} \sqrt{p+\frac{1}{2}}\,2^{\frac{k}{2}}P_p\left(2^k x - 2w + 1\right), & for \quad \frac{w-1}{2^{k-1}} \le x \le \frac{w}{2^{k-1}} \\ 0, & otherwise \end{cases}, \qquad 17$$

where $p = 0,1,w,M-1, w = 1,2,3,w, 2^{(k-1)}$ $\sqrt{p+\frac{1}{2}}$ is the coefficient for orthogonality. $P_p(x)$ are the Legendre polynomials with order p.

A function $f(x)$ defined in the interval [0, 1] is expanded as:

$$f(x) = \sum_{w=1}^{\infty}\sum_{(p=0)}^{\infty} H_{w,p}\,\psi_{w,p}(x) = H^T\psi(x) \qquad 18$$

When $f(x)$is truncated, Eq. 3.10 can be rewritten as:

$$f(x) = \sum_{w=1}^{k-1}\sum_{p=0}^{M-1} H_{w,p}\,\psi_{w,p}(x) = H^T\psi(x), \qquad 19$$

where H is the spectral space coefficient

$$H = [h_{10}, h_{11}, \ldots, h_{M-1}, h_{20}, .., h_{2M-1} \ldots, h_{2^{(k-1)}0} \ldots, h_{2^{(k-1)}M-1}]^T,$$

and $\Psi(x) = \left[\psi_{10}(x), \ldots, \psi_{M-1}(x), \psi_{20}(x), \ldots, \psi_{2M-1}(x), \ldots, \psi_{2^{k-1}0}(x), \ldots, \psi_{2^{k-1}M-1}(x)\right]^T$

4 Operational matrix of derivative

The calculation of derivative in spectral space is performed as an operational matrix form:

$$\frac{\mathrm{d}\Psi(x)}{\mathrm{dx}} = D\Psi(x) \qquad 20$$

where D is an $2^k M \times 2^k M$ operational matrix defined as:

$$D = \begin{pmatrix} B & 0 & \cdots & 0 \\ 0 & B & & 0 \\ \vdots & & \ddots & \vdots \\ 0 & 0 & \cdots & B \end{pmatrix}, \qquad 21$$

where B is a $M \times M$ matrix that is defined as:

$$W_{z,s} = \begin{cases} 2^{k+1}\sqrt{(2z-1)(2s-1)}, & z = 2, \ldots, M,\ S = 1, \ldots, z-1,\ and\ (z+s)\ odd, \\ 0, & otherwise. \end{cases} \qquad 22$$

The vector H in Eq. 18 is the spectral space coefficient applied to calculate the derivative by multiplying the matrix D.

Upon applying the Legendre wavelets method, the partial differential equation in Eq. 16 is written as follows:

$$L_o U + N_{non}(x, y, U^{)} = 0, \qquad 23$$

where L_o is the matrix of the linear operator, N_{non} is the matrix of the nonlinear operator and

$$U = [u_x, u_y]^T$$

The system is solved by using the T weight formula.

$$TL_o U^{(w+1)} + (1-T)L_o U^w + N_{non}(t, x, U^w) = 0, \qquad 24$$

Where w is the current time layer

5 Numerical experiment

Some experiments are performed to see the nonlinear behavior of SMA spring involving phase transformation. The experiments are performed using the SMA spring estimated parameters obtained [26]:

A_1=0.65 kg/(s^{2}m^{o}C), A_2=-56.5 kg/(ms^{2}m^{o}C), A_3=31.7 kg/(ms^{2}m^{o}C),

T_1= -49.4^{o}C, ρ=1.11 x10^4 kg/m^3, C_v = 1.1454x10^3 kg/s^2m^{o}C,

k_4 = 0.6960 mkg/s^3 ^{o}C, k_g = 1.5x10^6 kg/s^2, r =1.6/2 x 10^{-3} m.

The first experiment is performed under mechanical and thermal loading, changing with time, and the simulation time is 1s.

$$F = 4 \times 10^3 \, sin^3(4\pi t) \text{ N}$$

$$Z = 4 \times 10^3 \, sin^3(4\pi t) \text{kg}/(s^3 m)$$

The boundary conditions for this case are:

$$T_x(0,t) = 0, \quad T_x(L,t) = 0,$$

$$g(0,t) = 0, \quad g(L) = 0$$

$$u_x(0,t) = 0, \quad u_x(L,t) = 0.$$

And the initial condition is taken as follows:

$$T = 0, \; v = 0, \; \lambda = 0, \frac{dT}{dt} = 0, \quad \frac{dv}{dt} = 0, \quad \frac{d\lambda}{dt} = 0$$

Fig. 3(a) shows a graph of the temperature distribution curve with a sinusoidal pattern, and the thermomechanical coupling effect occurs. Martensite-austenite phase transformation. Stretch ratio distribution is shown in Fig. 3(b), with a strong nonlinear thermomechanical coupling effect. Switch between positive and negative values as t = 0-1s occurs. And also, in the middle (x=0.5), the value of the stretch ratio is zero throughout the time. Fig. 3(c) indicates the displacement distribution evolution due to the thermomechanical coupling effect. The graph produces an alternating between concave and convex curves switching between positive and negative values for t = 0 to t = 1s. It indicates austenite- twin martensite phase transformation when the loading value exceeds a certain value. The phase transformation here is due to mechanical loading.

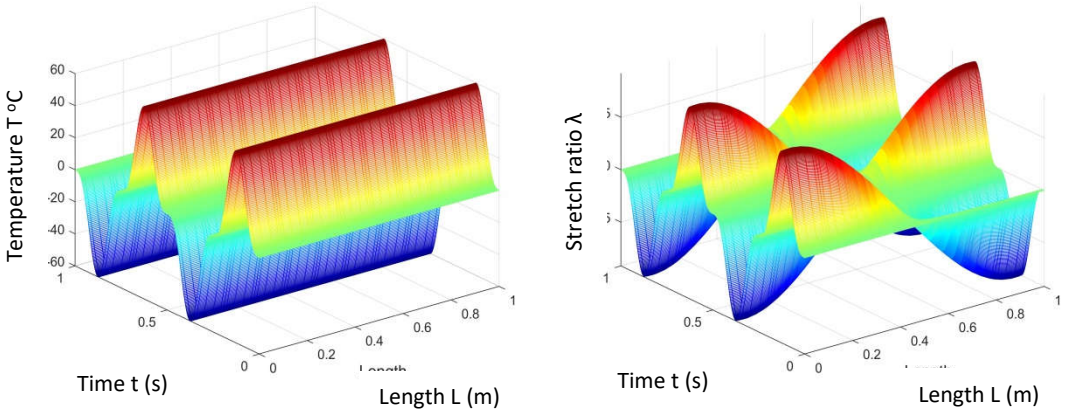

(a) (b)

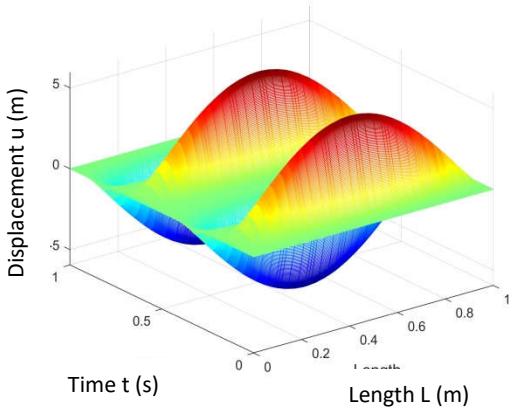

(c)

Figure 3 Simulation results of SMA spring under thermal and mechanical loading,

The second experiment is performed under constant mechanical and thermal loading, changing with time, and the simulation time is 1s.

$F = 4 \times 10^3$N and $Z = 4 \times 10^3\, sin^3(4\pi t)\text{kg}/(s^3 m)$.

Fig. 4(a) shows a graph of the temperature distribution curve and is similar to Fig. 4(a). Fig 4(b) shows the stretch ratio distribution. A strong nonlinear thermomechanical coupling effect switches from positive to negative values at x = 0.5. From 0 to 1s, the curve keeps in an alternating form. Fig. 4(c) presents the displacement distribution evolution with the thermomechanical coupling effect. The graph produces a convex curve with positive values only. The phase transformation here is due to mechanical loading.

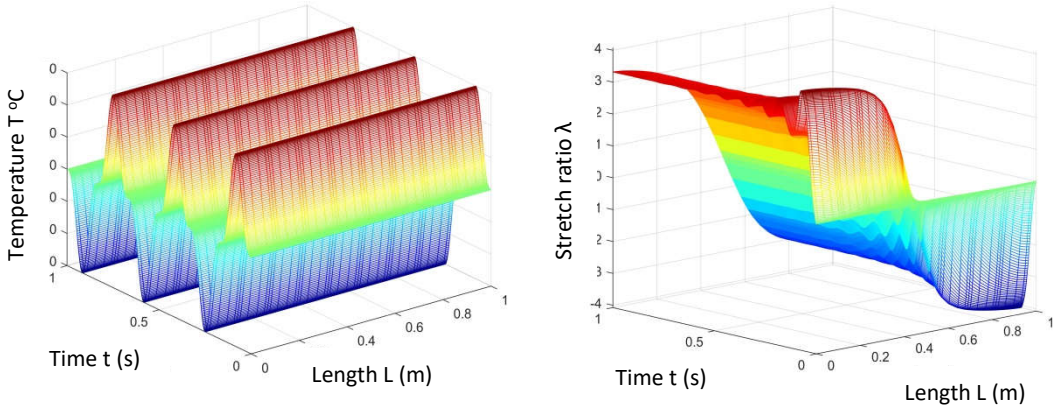

(a) (b)

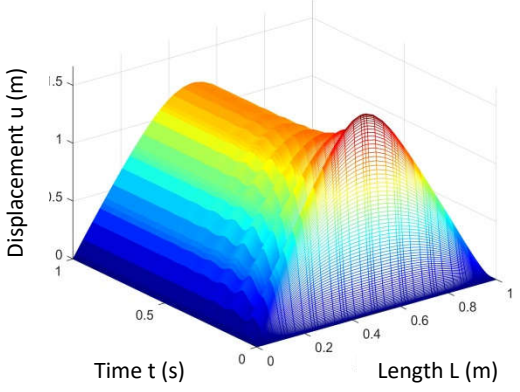

(c)

Figure 4 Simulation results of SMA spring under thermal and constant mechanical loading

The Landau free energy density $F_l(T,\lambda)$ related to the stretch ratio in Eq. 16 is formulated as:

$$F_l(T,\lambda) = \frac{A_1}{2}\left(\frac{T-T_1}{T_1}\right)\lambda^2 - \frac{A_2}{4}\lambda^4 + \frac{A_3}{6}\lambda^6. \qquad 17$$

Using the estimated SMA spring parameters, the $F_l(T,\lambda)$ is plotted as a function of stretch ratio in Fig. 2:

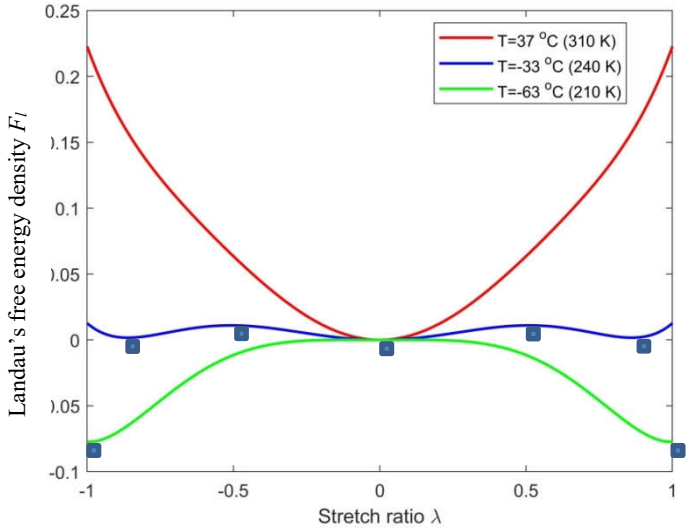

Figure 2 Landau free energy density at different temperatures

6 Conclusion

Modeling of 1D SMA wire and spring, involving entropy change of the system, is performed using suitable thermomechanical coupling models based on energy and momentum conservation law. And a modified Landau phenomenological model is proposed for the dynamics of phase transformation of SMA. Landau free energy density $F_l(T,\lambda)$ related to the stretch ratio in the models is formulated and plotted at different temperatures, followed by some simulations under non-constant temperature conditions. Therefore, the entropy change due to phase transformation is successfully captured and incorporated into the 1D SMA structure.

Reference

[1] HALAHLA A M, ABU Y B, ALMASRI A H. et al. The effect of shape memory alloys on the ductility of exterior reinforced concrete beam-column joints using the damage plasticity model[J]. Engineering Structures, Elsevier, 2019, 200(September): 109676.

[2] SHIVA S, YADAIAH N, PALANI I A. et al. Thermomechanical analyses and characterizations of TiNiCu shape memory alloy structures developed by laser additive manufacturing[J]. Journal of Manufacturing Processes, Elsevier, 2019, 48(February 2018): 98–109.

[3] ZHU J J, LIANG N G, HUANG W M. et al. Energy Conversion in Shape Memory Alloy Heat Engine Part I: Simulation. Journal of Intelligent Material Systems and Structures[J]. Journal of Intelligent Material Systems and Structures, 2001, 12(2): 133–140.

[4] MELNIK RODERICK V N, WANG L, MATUS P. et al. Computational Aspects of Conservative Difference Schemes for Shape Memory Alloys[C]//GERHARD GOOS, JURIS HARTMANIS C L. International Conference on Computational Science and Its Applications. Berlin, Heidelberg: Springer, 2003: 791–800.

[5] WANG L, MELNIK R V N. Thermo-mechanical wave propagations in shape memory alloy rod with phase transformations[J]. Mechanics of Advanced Materials and Structures, 2007, 14(8): 665–676.

[6] CHURCHILL C B, SHAW J. THERMO-MECHANICAL MODELING OF A SHAPE MEMORY ALLOY HEAT ENGINE[C]//Proceedings of the ASME 2011 Conference on Smart Materials, Adaptive

Structures and Intelligent Systems. Scottsdale, Arizona, USA: ASME, 2011: 641–650.
[7] LECCE L, ANTONIO C. Shape Memory Alloy Engineering[M]. LECCE L N C. Amsterdam: Elsevier, 2015.
[8] ALEXANDRAKIS V, MANUEL J, PÉREZ-CHECA A. Combinatorial synthesis of Ni–Mn–Ga-(Fe, Co, Cu) high-temperature ferromagnetic shape memory alloys thin films[J]. Scripta Materialia, Elsevier Ltd, 2020, 178(March): 104–107.
[9] FRITSCH E, IZADI M, GHAFOORI E. Development of nail-anchor strengthening system with iron-based shape memory alloy (Fe-SMA) strips[J]. Construction and Building Materials, Elsevier Ltd, 2019, 229: 117042.
[10] HUANG H, YAO P, SU Y. Stress relaxation behavior of columnar-grained Cu–Al–Mn shape memory alloys[J]. Materials Science & Engineering A, Elsevier B.V., 2019, 768(September): 138432.
[11] FEI X, HAIFENG Y, KUN L. et al. Forming and two-way shape memory effect of NiTi alloy induced by laser shock imprinting[J]. Optics and Laser Technology, 2019, 120(April): 105762.
[12] HONARMANDI P, JOHNSON L, ARROYAVE R. Bayesian probabilistic prediction of precipitation behavior in Ni-Ti shape memory alloys[J]. Computational Materials Science, Elsevier, 2020, 172(September 2019).
[13] ADARSH S H, SAMPATH V. Hot deformation behavior of Fe-28Ni-17Co-11.5Al-2.5Ta-0.05B (at.%) shape memory alloy by isothermal compression[J]. Intermetallics, Elsevier Ltd, 2019, 115(December): 106632.
[14] CHO H, TAKEDA Y, SAKUMA T. Fabrication and Output Power Characteristics of Heat-Engines Using Tape-Shaped SMA Element[J]. Advanced Structured Materials, 2017, 73: 1–15.
[15] PIRBHULAL S, ZHANG H, ALAHI E E. et al. A Novel Secure IoT-Based Smart Home Automation System Using a Wireless Sensor Network[J]. Sensors, 2016, 17(69): 1–19.
[16] ASHWIN R, A. R. S, J. N. R. Design of Shape Memory Alloy (SMA) Actuators[M]. HOLM ALTENBACH, MAGDEBURG, GERMANYLUCAS F.M. DA SILVA, PORTO P. TX USA: Springer, 2015.
[17] FINNEY K A. Ocean Thermal Energy Conversion[J]. Internation Journal of trend in scientific research and development, 2008, 1(1): 17–23.
[18] MA Z, WANG Y, WANG S. et al. Ocean thermal energy harvesting with phase change material for underwater glider[J]. Applied Energy, Elsevier Ltd, 2016, 178: 557–566.
[19] OTSUKA K, WAYMAN C M. Shape Memory Materials[M]. OTSUKA K, C. M. WAYMAN. Cambridge University Press., 1999.
[20] BANSIDDHI A, SARGEANT T D, STUPP S I. et al. Porous NiTi for bone implants : A review[J]. Acta Biomateria, 2008, 4(4): 773–782.
[21] ARAKI Y, ENDO T, OMORI T. Potential of superelastic CueAleMn alloy bars for seismic applications[J]. Earthq. Eng. Struct. Dyn., 2011, 40(1): 107-115.
[22] CISSE C, ZAKI W, BEN T. A review of constitutive models and modeling techniques for shape memory alloys[J]. International Journal of Plasticity, Elsevier Ltd, 2016, 76(January): 244–284.
[23] FIRSTOV G S, KOSORUKOVA T A, KOVAL Y N. et al. High Entropy Shape Memory Alloys[J]. Materials Today: Proceedings, Elsevier Ltd., 2015, 2(November): S499–S503.
[24] FIRSTOV G S, KOSORUKOVA T A, KOVAL Y N. et al. Directions for High-Temperature Shape Memory Alloys' Improvement: Straight Way to High-Entropy Materials?[J]. Shape Memory and Superelasticity, Springer International Publishing, 2015, 1(4): 400–407.
[25] GUO S, LIU C T. Phase stability in high entropy alloys: Formation of solid-solution phase or amorphous phase[J]. Progress in Natural Science: Materials International, Chinese Materials Research Society, 2011, 21(6): 433–446.
[26] ABUBAKAR R A, YUTIAN H, WANG F. et al. Modeling and Experimental Validation of the Hysteretic Dynamics of Shape Memory Alloy Springs[J]. INTERNATIONAL JOURNAL ON SMART SENSING AND INTELLIGENT SYSTEMS, 2020, 30(1): 1–9.

MODELING OF 1D SMA SPRING UNDER CONSTANT TEMPERATURE INVOLVING ENTROPY CHANGE OF THE SYSTEM

Rabiu Ahmad Abubakar

The State Key Laboratory of Fluid Power Transmission and Control, Zhejiang University,

310027, Hangzhou, China

Abstract: Based on conservation law of energy and momentum, suitable thermomechanical coupling models for the SMA wire are formulated. A modified Landau phenomenological model is proposed for SMA's dynamics of phase transformation. Entropy change in SMA wire undergoing phase transition is modeled and incorporated into the developed model. The proposed phenomenological SMA wire models are further extended to the SMA spring. Numerical algorithm simulations are performed under constant temperatures via Legendre wavelets-spectral approach for a non-constant temperature dynamic system.

Keywords: *Shape memory alloys; Martensite transformation; Entropy change; pseudoelasticity; differential model.*

1 Introduction

Interest in smart materials, like shape memory alloy (SMA), is rapidly developing due to their unique properties. Smart materials have attracted increasing attention from mathematicians, physicists, control theorists, and engineers. SMA is a kind of material that can be trained to memorize different shapes [2–4]. Moreover, when deformed, it can regain its original shape [5,6] as the temperature increases, thus converting thermal energy to mechanical type [7–9]. This unique property of the plastic-like deformation and subsequent full recovery is called shape memory effects (SMEs) [10–12]. The history of this noble alloy material started in the 1800s when William Buehler and his coworkers discovered its behaviors of shape recovery capability [13]. Following this, the NINOL was given to the material in which N.I. stands for nickel and NOL, attributing it to the Naval Ordinance Laboratory, where the behavior was first discovered [14]. The material produced a strange loud sound on a cold stage, different from that at the hot stage [11]. Over a decade, the material has drawn the researcher's attention for various engineering applications [15,16]. After rigorous investigation, it was concluded that the material had a unique property [17] that made it different from other alloy materials and then named it NITINOL associating it to the laboratory. This alloy can recover energy up to 10^6 J/m^3, and the transformation temperature depends on Ni-content with an upper limit of 363 K [18].

SMAs have reversible hysteresis properties under cyclic mechanical loading [19]**.** This makes them essential materials in many engineering applications such as actuation impact absorption, sensor, and vibration isolation [20], to mention a few. Except for the medical fields, such as wearable devices and telehealth care, SMAs have not been commercialized due to the lack of a detailed model describing their behaviors. Many mathematical models have been constructed for SMA from different perspectives [21,22]. However, due to the complex behavior of SMA, an exact and simple model has not yet been developed.

2 SMA wire and SMA spring modeling overview

Because of the complex behavior of SMA, for the past two decades, many mathematical models of shape memory alloys (SMAs) have been constructed from a different perspective [23,24]. This will help better understand the physical mechanism behind the martensitic transformation, which will help the design and fabrication of SMA devices. The research on SMA models can be mainly divided into micro-mechanical and phenomenological ones [25]. The characteristics of SMA originate from the microscopic changes in the crystal

lattice and are related to factors such as stress, temperature, and loading history[26]. Recently SMA spring has aroused researchers' attention due to its outstanding features in actuators. Compared to an SMA wire as an actuator, when the SMA wire is formed as an SMA spring, it creates a larger displacement. However, the pursuit of modeling its dynamic process is still under the spotlight. Here the review on the modeling of the SMA wire pseudoelasticity is presented and then extended to the SMA spring.

SMAs micro-structural features like phase nucleation, martensite twin growth, interface motion, etc., are modeled at grain crystal based on Ginzburg landau theory [27]. Traditional phenomenological models, such as the Preisach model, have the advantage of being simple in physics and mathematics [28]. Polynomial energy expression is used to constitute these model equations and is written in terms of variables like strain and temperature. Falk's polynomial model is one of the earliest constitutive models developed for SMAs [29]. Landau-Devonshire-like free energy is used in this work based on the similarity of the ferromagnetic materials' electromagnetic curves under the uniaxial stress-strain action of SMAs. The phase transition is assumed to happen at the strain-stress curve's negative slope. Later the martensite transformation is remodeled using Ginzburg-Landau's theory based on continuum thermodynamics [30]. For austenite and martensite, the domain walls are obtained from equilibrium conditions. However, the model cannot be applied to 3D due to the unphysical minima's appearance. Therefore in the attempt to solve this, the order parameter is used by Levitas et al. to average out the variables that describe the atomic lattice vibrations [31]. But the equations are somehow complex and need to be further simplified. Mahapatra and Melnik introduced a 3D simulation using the finite element method. Ginzburg-Landau's theory is used to develop a mesoscale phase-field model for SMAs nanowires martensitic transformation. The model showed the SMAs martensitic transformations based on the momentum and energy equations with bi-directional coupling via temperature, strain, and strain rate. Although there are some achievements in the microstructure's evolution and its effect on SMA response, there are drawbacks in the domain due to rescaling [32].

Ginzburg-Landau kinetic time-dependent equations were also used to develop a phase-field model for SMAs martensitic transformation, focusing on generating invariant habit planes and nuclei growth [33]. But the approach used here is not simpler. Claire Morin *et al*. introduced a Zaki–Moumni (ZM) model [34]. Here stain rate induced by the mechanical pseudoelasticity is considered, but the achievement is only at a high strain rate, probably due to the localization effect. Wang Jun et al. developed a constitute model for simulation of SMA nitinol at different loading rates [35]. The cyclic pseudoelasticity of polycrystalline SMAs describes the model. But the constitute model equations are not easy to execute. Other methods have been employed to verify the model cyclic capability in a multi-axial problem.

SMA springs are an important kind of actuator employed in different applications and have attracted the attention of several researchers. The helical SMA spring has good behavior because it gives more design possibilities than the SMA wire or bar. The design criteria include actuation force, stiffness, length, and direction (tension/compression), which determine the spring specifications like wire diameter, pitch angle, spring diameter, and the number of coils [36]. Recently, the SMA spring has attracted researchers' attention due to its outstanding actuators and vibration control features. SMA spring results in a much larger displacement than an SMA wire as an actuator. When SMA wire is formed as a spring, it is used in the vibration isolation solution for its internal damping capability and pseudoelasticity. Because of the complex thermo-mechanical behaviour of SMA springs, the pursuit of its modeling and dynamic process is still under the spotlight. There is much difficulty in making their modeling, which also affects their applications.

Recently researchers developed an interest in a breakthrough in material design by proposing a new concept of entropy change during the martensitic phase transformation of SMAs [37]. This concept concerns creating multielement metallic material close to equimolar composition with the entropy of mixing higher than in the existing material, thus giving high phase stability [38]. High entropy alloys are solid solutions, bulk metallic glasses, and intermetallic compounds. Some of them have a B2 type of structure [39] to which NiTi SMA austenite belongs. Therefore, modeling such a structure is now necessary to capture its behavior involving entropy change.

3 Modeling of SMA wire

For the coupled thermo-mechanical field derivation, the dynamics of the thermal field is formulated using the law of conservation energy [9]. This law states that when a system undergoes a process, the total energy remains constant but only changes from one form to another or a combination of a different form of energy, and this is the basis of the first law of thermodynamics.

$$\Delta Q = \Delta e + W - H_L. \quad (1)$$

where ΔQ is the energy input to the system, Δe is the change in internal interfaces during transformation, W is the mechanical energy associated with strain energy of transformation, and H_L is the waste heat. It involves frictional loss F_L and energy loss due to entropy is E_L.

And,

$$.H_L = -(F_L + E_L)$$

The frictional part is already expressed in ref. [9] . Therefore, the entropy is expressed as:

$$E_L = -T_1 \Delta s, \quad (2)$$

where T_1 is a reference transformation temperature and $\Delta s$is the entropy change from austenite to martensite $\Delta s = S_M - S_A$. When the quantity of the material is considered, Eq. 2 becomes:

$$E_L = -\rho T_1 \Delta s \quad (3)$$

For phase transformation to a current SMA temperature T, the entropy change is derived as:

$$\Delta s = \int_{T_1}^{T} \frac{dQ}{T}.$$

And,

$$dQ = C_V dT.$$

Hence,

$$\Delta s = \int_{T_1}^{T} \frac{C_V dT}{T}$$

$$\Delta s = C_v In \frac{T}{T_1} \quad (4)$$

Therefore, substituting Eq. 4 in Eq 2.

$$E_L = -\rho C_v T_1 In \frac{T}{T_1}$$

Let,

$$k_5 = \rho C_v T_1,$$

Therefore,

$$E_L = -k_5 In \frac{T}{T_1}, \quad (5)$$

where k_5 is the material constant representing the phase-independent specific entropy. The negative sign relates to the latent heat of transformation. Using the law of logarithm,

$$E_L = -(k_5 InT - k_5 InT_1) \quad (6)$$

Hence, these forms of energy involved are expressed as follows:

$$\Delta e = \rho e_t - \sigma^T : (\nabla_v) + \nabla \cdot q = Z, \quad (7)$$

where ρ is the density, σ is the stress tensor, e is the internal energy, q is the heat flux vector, and Z is the thermal loading.

By employing the thermodynamic equilibrium conditions, the thermo-mechanical free energy function (Q) is related to stress σ and internal energy e.

$$\sigma = \rho \frac{\partial Q}{\partial \eta} \quad ; \quad e = Q - T\frac{\partial Q}{\partial \eta}, \tag{8}$$

where T is the temperature, and η is the Cauchy–Lagrangian strain tensor.

$$\varepsilon(x,t) = u_x, \tag{9}$$

where x is the axis of the material, and u is the displacement. The free energy function Q can be represented in terms of the Landau free energy function as:

$$Q(T,\varepsilon) = -c_v InT + E_L + Q(T)Q(\varepsilon) + \sigma$$
$$Q(T,\varepsilon) = -c_v InT + k_5 InT_1 - k_5 InT + Q(T)Q(\varepsilon) + \sigma,$$
$$Q(T,\varepsilon) = -(c_v + k_5)InT + Q(T)Q(\varepsilon) + (\sigma + k_5 InT_1) \tag{10}$$

where c_v is the specific heat constant, the term $Q(T)Q(\varepsilon)$stands for the thermo-mechanical coupling contribution. By substituting the free energy function defined in Eq. 6-10 in Eq. 1 and using Landau-Ginzburg-Devonshire theory, the following coupled governing equations are obtained:

$$(c_v + k_5)\frac{\partial T}{\partial t} = k_4\frac{\partial^2 T}{\partial x^2} + k_1 T\varepsilon\frac{\partial \varepsilon}{\partial t} + Z,$$
$$\rho\frac{\partial^2 u}{\partial t^2} = \frac{\partial \sigma}{\partial x} + \Upsilon\frac{\partial}{\partial t}\frac{\partial^2 u}{\partial x^2} - k_g\frac{\partial^4 u}{\partial x^4} - k_5 T_1 + F. \tag{11}$$

And,

$$\sigma = k_1(T - T_1)\varepsilon + k_2\varepsilon^3 + k_3\varepsilon^5,$$

where k_1, k_2, k_3, and k_g are the re-normalized material constant, ρ is the material density, T is the current SMA temperature, ε is the strain, and is calculated as $\varepsilon = \frac{\partial u}{\partial x}$, c_v is the specific heat capacitance, k_4 is the normalized material constant, $\Upsilon$is the internal friction coefficient, F and Z are the mechanical and the thermal loading. The term $k_5 InT_1$ is reduced to $k_5 T_1$ for simplicity.

Because of the complication, strong nonlinearity, and coupling between the thermal and elastic fields in Eq. 11, it is further simplified by introducing other equations:

$$v = \frac{\partial u}{\partial t};\ \varepsilon = \frac{\partial u}{\partial x}; g = \frac{\partial^2 \varepsilon}{\partial x^2} \tag{12}$$

And also, the average temperature change $\frac{T-T_1}{T_1}$ is used to reduce the nonlinearity.

Substituting Eq. in. Eq. 12, the new governing equation is:

$$\left.\begin{aligned}
&(c_v + k_5)\frac{\partial T}{\partial t} = k_4\frac{\partial^2 T}{\partial x^2} + k_1 T\varepsilon\frac{\partial \varepsilon}{\partial t} + Z,\\
&\rho\frac{\partial v}{\partial t} = \frac{\partial \sigma}{\partial x} + \Upsilon\frac{\partial}{\partial x}\frac{\partial v}{\partial x} - k_g\frac{\partial^2 g}{\partial x^2} - k_5 T_1 + F,\\
&\sigma = k_1\left(\frac{T-T_1}{T_1}\right)\varepsilon + k_2\varepsilon^3 + k_3\varepsilon^5.
\end{aligned}\right\} \tag{13}$$

And the elastic equation takes the following:

$$\rho\frac{\partial v}{\partial t} = \frac{\partial}{\partial x}\left(\sigma + \Upsilon\frac{\partial v}{\partial x} - k_g\frac{\partial g}{\partial x}\right) - k_5 T_1 + F$$

Now the new equations are:

$$\left.\begin{aligned}
&v = \frac{\partial u}{\partial t};\ \varepsilon = \frac{\partial u}{\partial x}; g = \frac{\partial^2 \varepsilon}{\partial x^2},\\
&(c_v + k_5)\frac{\partial T}{\partial t} = k_4\frac{\partial^2 T}{\partial x^2} + k_1 T\varepsilon\frac{\partial \varepsilon}{\partial t} + Z,
\end{aligned}\right\} \tag{14}$$

$$\rho\frac{\partial v}{\partial t}=\frac{\partial}{\partial x}\left(\sigma+\Upsilon\frac{\partial v}{\partial x}-k_g\frac{\partial g}{\partial x}\right)-k_5T_1+F,$$
$$\sigma=k_1\left(\frac{T-T_1}{T_1}\right)\varepsilon+k_2\varepsilon^3+k_3\varepsilon^5.$$

Equation 14 can capture the phase transformation of SMAs because the thermal and mechanical energy fields are coupled. Therefore, 1-D SMA wire dynamics can be modeled using these equations by setting appropriate initial and boundary conditions.

In this section 1D SMA spring model is simulated under constant temperature, Eq. 14 reduced to:

$$\left.\begin{aligned} v=\frac{\partial u}{\partial t};\ \lambda=\frac{\partial u}{\partial x};g=\frac{\partial^2\lambda}{\partial x^2}\\ \rho\frac{\partial v}{\partial t}=\frac{\partial}{\partial x}\left(\sigma+\Upsilon\frac{\partial v}{\partial x}-k_g\frac{\partial g}{\partial x}\right)-k_5T_1+F\\ \sigma=k_1\left(\frac{T-T_1}{T_1}\right)\varepsilon+k_2\varepsilon^3+k_3\varepsilon^5\end{aligned}\right\} \quad 15$$

Only the elastic strain equation is considered for the dynamic case under constant temperature. But because phase transformation occurs, the entropy effect is still involved. Therefore

For the thermo-mechanical coupling dynamics of the SMA spring, Eq. 15 is slightly modified by replacing the strain of the SMA wire with the stretch ratio λ of the SMA spring and the axial stress σ with shear stress τ.

$$\left.\begin{aligned} v=\frac{\partial u}{\partial t};\ \lambda=\frac{\partial u}{\partial x};g=\frac{\partial^2\lambda}{\partial x^2},\\ \rho\frac{\partial v}{\partial t}=\frac{\partial \tau}{\partial x}+\Upsilon\frac{\partial}{\partial x}\frac{\partial v}{\partial x}-k_g\frac{\partial^2 g}{\partial x^2}-k_5T_1+Fr,\\ \tau=A_1\left(\frac{T-T_1}{T_1}\right)\lambda+A_2\lambda^3+A_3\lambda^5,\end{aligned}\right\} \quad 16$$

where r is the SMA wire radius. A_1, A_2, and A_3 are the SMA spring material constants.

3 Numerical algorithm via Legendre wavelets-spectral approach

The numerical simulation is done using the Legendre wavelets spectral approach for static and dynamic cases at a constant temperature. Phase transformation analysis is presented finally. In this method, wavelet functions are constructed by the mother wavelet function's expansion and translation. Legendre polynomials are used to drive it. The family of Legendre wavelet is represented as:

$$\psi_{w,p}(x)=\begin{cases}\sqrt{p+\frac{1}{2}}\,2^{\frac{k}{2}}P_p\left(2^kx-2w+1\right), & for\quad \frac{w-1}{2^{k-1}}\le x\le\frac{w}{2^{k-1}}\\ 0, & otherwise\end{cases}, \quad 17$$

where $p=0,1,w,M-1,w=1,2,3,w,2^{(k-1)}$ $\sqrt{p+\frac{1}{2}}$ is the coefficient for orthogonality. $P_p(x)$ are the Legendre polynomials with order p.

A function $f(x)$ defined in the interval [0, 1] is expanded as:

$$f(x)=\sum_{w=1}^{\infty}\sum_{(p=0)}^{\infty}H_{w,p}\,\psi_{w,p}(x)=H^T\psi(x) \quad 18$$

When $f(x)$is truncated, Eq. 3.10 can be rewritten as:

$$f(x)=\sum_{w=1}^{k-1}\sum_{p=0}^{M-1}H_{w,p}\,\psi_{w,p}(x)=H^T\psi(x), \quad 19$$

where H is the spectral space coefficient

$$H=[h_{10},h_{11},\dots,h_{M-1},h_{20},..,h_{2M-1}\dots,h_{2^{(k-1)}0}\dots,h_{2^{(k-1)}M-1}]^T,$$

and $\Psi(x)=\left[\psi_{10}(x),\dots,\psi_{M-1}(x),\psi_{20}(x),\dots,\psi_{2M-1}(x),\dots,\psi_{2^{k-1}0}(x),\dots,\psi_{2^{k-1}M-1}(x)\right]^T$

4 Operational matrix of derivative

The calculation of derivative in spectral space is performed as an operational matrix form:

$$\frac{\mathrm{d}\Psi(x)}{\mathrm{dx}} = D\Psi(x) \quad 20$$

where D is an $2^k M \times 2^k M$ operational matrix defined as:

$$D = \begin{pmatrix} B & 0 & \cdots & 0 \\ 0 & B & & 0 \\ \vdots & & \ddots & \vdots \\ 0 & 0 & \cdots & B \end{pmatrix}, \quad 21$$

where B is a $M \times M$ matrix that is defined as:

$$W_{z,s} = \begin{cases} 2^{k+1}\sqrt{(2z-1)(2s-1)}\,, & z = 2, \ldots, M,\ S = 1, \ldots, z-1,\ and\ (z+s)\ odd, \\ 0, & otherwise. \end{cases}$$

22

The vector H in Eq. 19 is the spectral space coefficient applied to calculate the derivative by multiplying the matrix D.

Upon applying the Legendre wavelets method, the partial differential equation in Eq. 16 is written as follows:

$$L_o U + N_{non}(x, y, U^{)} = 0, \quad 23$$

where L_o is the matrix of the linear operator, N_{non} is the matrix of the nonlinear operator and

$$U = [u_x, u_y]^T$$

The system is solved by using the T weight formula.

$$TL_o U^{(w+1)} + (1-T)L_o U^w + N_{non}(t, x, U^w) = 0,$$

24

Where w is the current time layer

5 Numerical experiment

A series of experiments are carried out to investigate the nonlinear behavior of SMA spring involving phase transformation. The experiments are performed using the SMA spring estimated parameters obtained [40]:

A_1=0.65 kg/(s^{2}m^{o}C), A_2=-56.5 kg/(ms^{2}m^{o}C), A_3=31.7 kg/(ms^{2}m^{o}C),

T_l= -49.4^{o}C, ρ=1.11 x10^4 kg/m^3, C_v= 1.1454x10^3 kg/s^2m^{o}C,

k_4 = 0.6960 mkg/s^3 ^{o}C, k_g = 1.5x10^6 kg/s^2, r =1.6/2 x 10^{-3} m.

The simulation is performed under dynamics conditions with coefficients k = 3 and M = 6 in Eq. 16. The simulation time used is 1s, and the time step-size $\Delta t = 0.0001$is used. The mechanical loading, which changes with time, is:

$$F = 4 \times 10^{-1}\, sin^3(6\pi t)\ \text{N}.$$

The free energy function employed here is:

$$F_l(T, \lambda) = \frac{k_1}{2}\left(\frac{T-T_1}{T_1}\right)\lambda^2 - \frac{k_2}{4}\lambda^4 + \frac{k_3}{6}\lambda^6.$$

For the first simulation, the temperature is set at 37 ^{o}C (310 K). Under this mechanical loading, the SMA spring switches between martensite to austenite phases. Fig. 1(a) shows the 3D displacement

simulation result. It is shown that the austenite phase is transformed into a twins martensite phase when loading attains a certain value. Thus, the phase transformations are caused by the applied mechanical loading. Fig. 1(b) shows the 3D graph of the stretch ratio. Fig. 1(c) shows the 2D relationship between stress and strain and comparison with experimental data. It can be seen that there is good agreement between them. Fig. 1(d) shows the 2D Landau's free energy density function, and it has one local minimum corresponding to austenite.

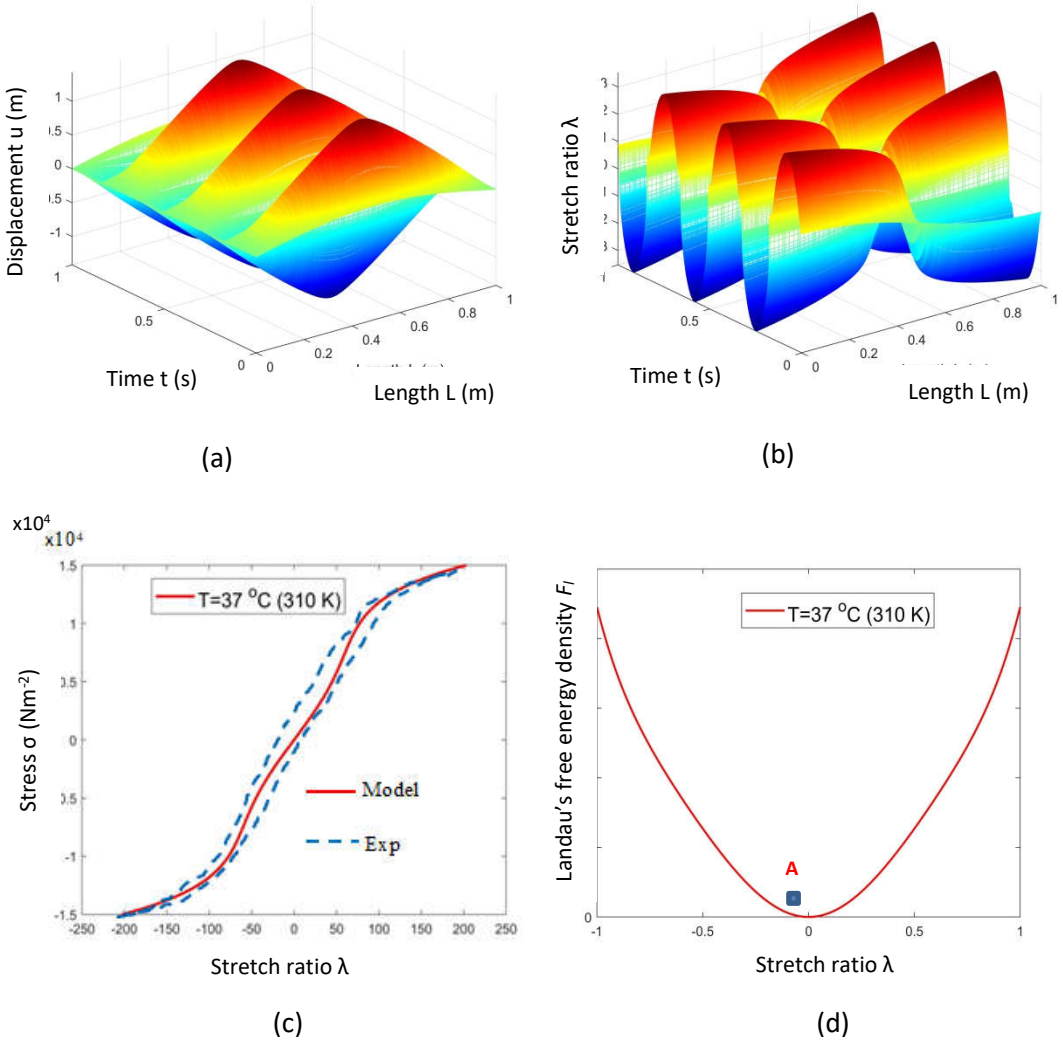

Figure 1 Simulation results of SMA spring under dynamic conditions at 37 ºC (310 K)

For the second simulation, the temperature is set at 0 ºC (273 K). Under the same mechanical loading, the SMA spring switches between martensite to austenite phases. Fig. 2(a) shows the 3D displacement simulation result. It is shown that the austenite phase is transformed into a twins martensite phase when loading attains a certain value. Thus, the phase transformations are caused by the applied mechanical loading. Fig. 2(b) shows the 3D graph of the stretch ratio. Fig. 2(c) shows the 2D relationship between stress and strain and comparison with experimental data. It can be seen that there is good agreement between them. Fig. 2(d) shows the 2D Landau's free energy density function. It has one local minimum corresponding to martensite and two local maxima corresponding to two austenites.

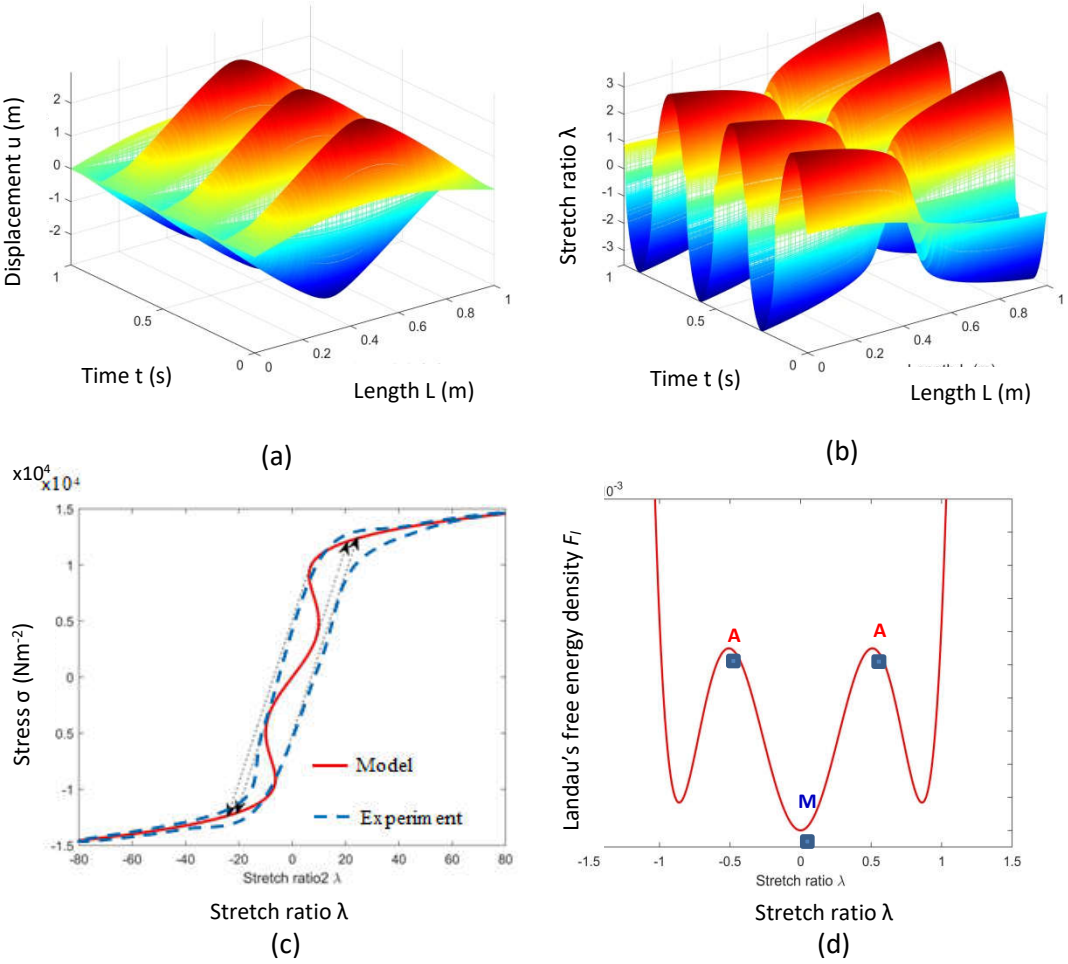

Figure 2 Simulation results of SMA spring under dynamic conditions at -33 °C (240 K)

For the third test, only simulation is conducted for feasibility analysis, with no comparison with experimental data because the temperature set in this case is very low (-63 °C/210 K) and is not achievable in the laboratory. Under the same mechanical loading, only martensite exists at this temperature. Fig. 3(a) shows the 3D displacement simulation result. Fig. 3(b) shows the 3D graph of the stretch ratio. Fig. 3(c) shows the 2D relationship between stress and strain, and Fig. 3(d) shows

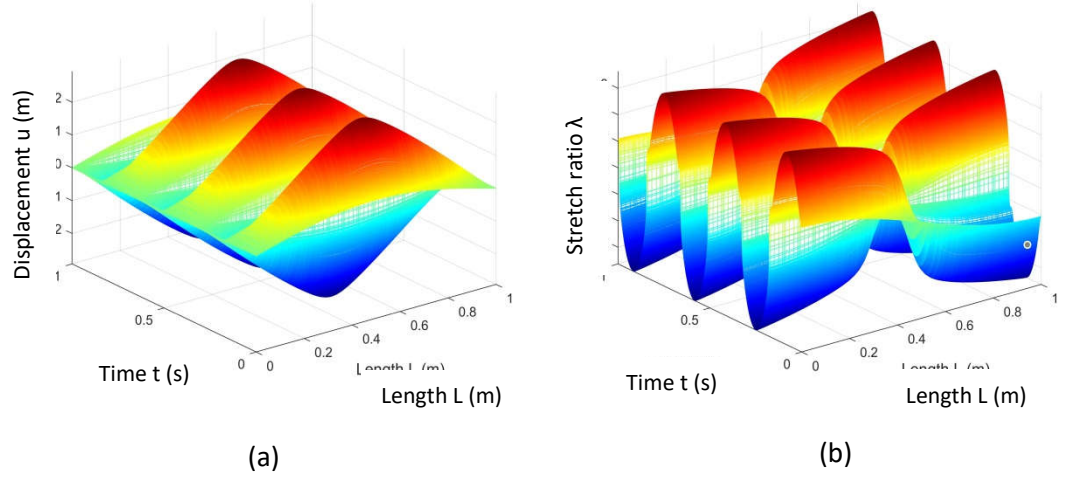

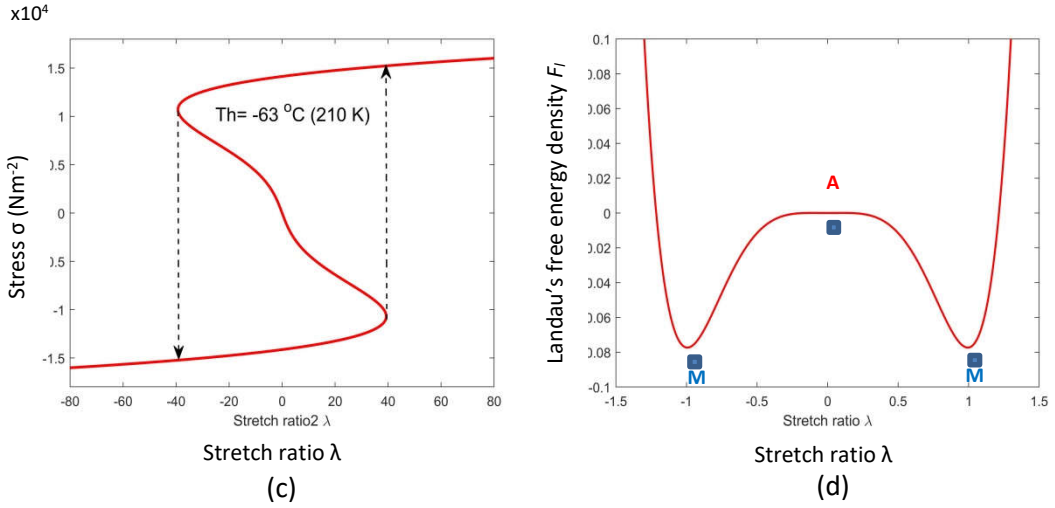

Figure 3 Simulation results of SMA spring under dynamic conditions at -63 °C (210 K)

For the static case under constant temperature, the term involving time in Eq. 16 turns to zero, and the equation reduces to:

$$\left.\begin{aligned} &v = \frac{\partial u}{\partial t};\ \lambda = \frac{\partial u}{\partial x};\ g = \frac{\partial^2 \lambda}{\partial x^2}, \\ &Fr = k_g \frac{\partial^2 g}{\partial x^2} - \frac{\partial \tau}{\partial x} + k_5 T_1, \\ &\tau = A_1 \left(\frac{T - T_1}{T_1}\right) \lambda + A_2 \lambda^3 + A_3 \lambda^5. \end{aligned}\right\} \qquad 25$$

The boundary conditions for this case are:

$$u(0,t) = 0, \quad u(L,t) = 0$$

$$g(0,t) = 0, \quad g(L) = 0.$$

In this test, the temperature is set at 37 °C (310 K). Thus, the initial condition should begin from the austenitic phase:

$$u_0(x) = 0.$$

Fig. 4 shows the of the static system for displacement and stretch ratio. There is also phase transition.

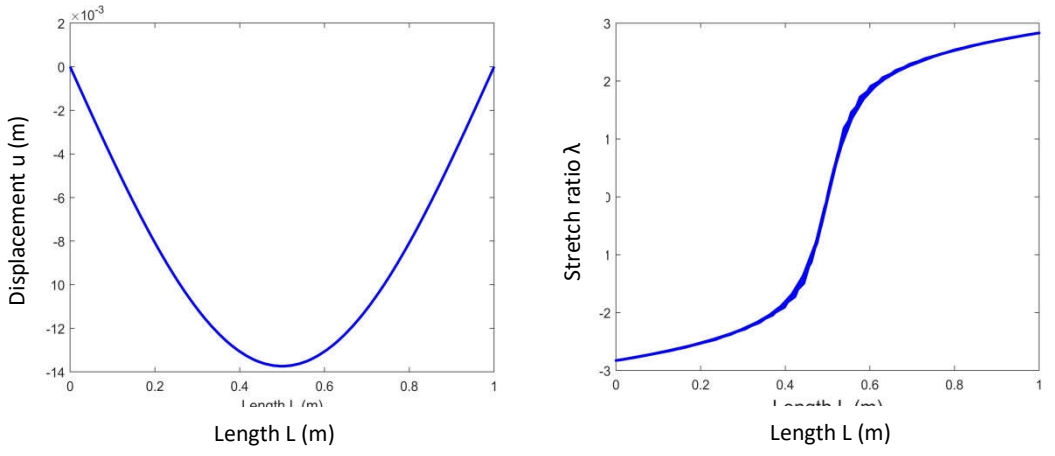

Figure 4 Simulation results of SMA spring under static condition

6 Conclusion

Modeling of 1D SMA wire and spring, involving entropy change of the system, is performed using suitable thermomechanical coupling models based on energy and momentum conservation law. And a modified Landau phenomenological model is proposed for the dynamics of phase transformation of SMA. Landau free energy density $F_l(T, \lambda)$ related to the stretch ratio in the models is formulated and plotted at different constant temperatures, followed by some simulations. Therefore, the entropy change due to phase transformation is successfully captured and incorporated into the 1D SMA structure.

Reference

[1] WANG L, MELNIK RODERICK V N. Thermomechanical Waves in SMA Patches under Small Mechanical Loadings[C]. DONGARRA M B D van A M A S, //International Conference on Computational Science. Amsterdam: Springer, 2004: 645–652.
[2] SITTNER P. Deformation twinning in martensite affecting functional behavior of NiTi shape memory alloys[J]. Materialia, 2019, 9(March): 100506.
[3] MACHADO L G, SAVI M A, JANEIRO R De. et al. Medical applications of shape memory alloys[J]. Brazilian Journal of Medical and Biological Research, 2003, 36(6): 683–691.
[4] NAGENDRA M R, TAMILSELVAN M, SADHASIVAM C. Computation and investigation of an SMA engine using low heat recovery[J]. International Journal of Pure and Applied Mathematics, 2018, 118(20): 57–62.
[5] HALAHLA A M, ABU Y B, ALMASRI A H. et al. The effect of shape memory alloys on the ductility of exterior reinforced concrete beam-column joints using the damage plasticity model[J]. Engineering Structures, 2019, 200(September): 109676.
[6] SHIVA S, YADAIAH N, PALANI I A. et al. Thermomechanical analyses and characterizations of TiNiCu shape memory alloy structures developed by laser additive manufacturing[J]. Journal of Manufacturing Processes, 2019, 48(February 2018): 98–109.
[7] ZHU J J, LIANG N G, HUANG W M. et al. Energy Conversion in Shape Memory Alloy Heat Engine Part I: Simulation. Journal of Intelligent Material Systems and Structures[J]. Journal of Intelligent Material Systems and Structures, 2001, 12(2): 133–140.
[8] MELNIK RODERICK V N, WANG L, MATUS P. et al. Computational Aspects of Conservative Difference Schemes for Shape Memory Alloys[C]. GERHARD GOOS, JURIS HARTMANIS C L,//International Conference on Computational Science and Its Applications. Berlin, Heidelberg: Springer, 2003: 791–800.
[9] WANG L, MELNIK R V N. Thermo-mechanical wave propagations in shape memory alloy rod with phase transformations[J]. Mechanics of Advanced Materials and Structures, 2007, 14(8): 665–676.
[10] CHURCHILL C B, SHAW J. THERMO-MECHANICAL MODELING OF A SHAPE MEMORY ALLOY HEAT ENGINE[C]//Proceedings of the ASME 2011 Conference on Smart Materials, Adaptive Structures and Intelligent Systems. Scottsdale, Arizona, USA: ASME, 2011: 641–650.
[11] LECCE L, ANTONIO C. Shape Memory Alloy Engineering[M]. LECCE L N C,. Amsterdam: Elsevier, 2015.
[12] ALEXANDRAKIS V, MANUEL J, PÉREZ-CHECA A. Combinatorial synthesis of Ni–Mn–Ga-(Fe, Co, Cu) high temperature ferromagnetic shape memory alloys thin films[J]. Scripta Materialia, 2020, 178(March): 104–107.
[13] FRITSCH E, IZADI M, GHAFOORI E. Development of nail-anchor strengthening system with iron-based shape memory alloy (Fe-SMA) strips[J]. Construction and Building Materials, 2019, 229: 117042.
[14] HUANG H, YAO P, SU Y. Stress relaxation behavior of columnar-grained Cu–Al–Mn shape memory alloys[J]. Materials Science & Engineering A, 2019, 768(September): 138432.
[15] FEI X, HAIFENG Y, KUN L. et al. Forming and two-way shape memory effect of NiTi alloy induced by laser shock imprinting[J]. Optics and Laser Technology, 2019, 120(April): 105762.
[16] HONARMANDI P, JOHNSON L, ARROYAVE R. Bayesian probabilistic prediction of precipitation behavior in Ni-Ti shape memory alloys[J]. Computational Materials Science, 2020, 172(September 2019).

[17] ADARSH S H, SAMPATH V. Hot deformation behavior of Fe-28Ni-17Co-11.5Al-2.5Ta-0.05B (at.%) shape memory alloy by isothermal compression[J]. Intermetallics, 2019, 115(December): 106632.
[18] CHO H, TAKEDA Y, SAKUMA T. Fabrication and Output Power Characteristics of Heat-Engines Using Tape-Shaped SMA Element[J]. Advanced Structured Materials, 2017, 73: 1–15.
[19] ASHWIN R, A. R. S, J. N. R. Design of Shape Memory Alloy (SMA) Actuators[M]. HOLM ALTENBACH, MAGDEBURG, GERMANYLUCAS F.M. DA SILVA, PORTO P, 编. TX USA: Springer, 2015.
[20] PIRBHULAL S, ZHANG H, ALAHI E E. et al. A Novel Secure IoT-Based Smart Home Automation System Using a Wireless Sensor Network[J]. Sensors, 2016, 17(69): 1–19.
[21] FINNEY K A. Ocean Thermal Energy Conversion[J]. Internation Journal of trend in scientific research and development, 2008, 1(1): 17–23.
[22] MA Z, WANG Y, WANG S. et al. Ocean thermal energy harvesting with phase change material for underwater glider[J]. Applied Energy, 2016, 178: 557–566.
[23] SHAW C, JOHN B C. Thermo-mechanical modeling of a shape memory alloy heat engine.[C]//Conference on Smart Materials, Adaptive Structures and Intelligent Systems,. Scottsdale, Arizona, USA: ASME, 2011: 641–650.
[24] BROWNE A L, ALEXANDER P W, MANKAME N. et al. Sma Heat Engines : Advancing From a Scientific Curiosity to a Practical Reality[C]//SMART MATERIALS, STRUCTURES & NDT in AEROSPACE Conference. .
[25] HE X, TONG Z, DU H. et al. Modeling microstructure evolution in shape memory alloy rods via Legendre wavelets collocation method[J]. Journal of Materials Science, 2019, 54(23): 14400–14413.
[26] WANG F, DU H, WANG L. Mechanics of Materials A modified Landau phenomenological constitutive model for the tension – compression asymmetry in one-dimensional Shape Memory Alloys[J/OL]. Mechanics of Materials, 2021, 156(October 2020): 103795. https://doi.org/10.1016/j.mechmat.2021.103795. DOI:10.1016/j.mechmat.2021.103795.
[27] CISSE C, ZAKI W, BEN T. A review of constitutive models and modeling techniques for shape memory alloys[J]. International Journal of Plasticity, 2016, 76(January): 244–284.
[28] HE X, DU H, TONG Z. et al. A dynamic hysteresis model based on Landau phenomenological theory of fatigue phenomenon in ferroelectrics[J/OL]. Materials Today Communications, 2020, 25(July): 101479. https://doi.org/10.1016/j.mtcomm.2020.101479. DOI:10.1016/j.mtcomm.2020.101479.
[29] FALK F. Ginzburg-Landau theory of static domain walls in shape-memory alloys[J]. Z. Phys. B Condensed Matter, 1983, 51(2): 177–185.
[30] XU G L, CUI Y W. Ginzburg-Landau Modeling for Martensitic Transformation Coupled with Composition Redistribution[J]. Diffusion Foundations, 2018, 15: 154–180. DOI:10.4028/www.scientific.net/df.15.154.
[31] LEVITAS V I, PRESTON D L. Three-dimensional Landau theory for multivariant stress-induced martensitic phase transformations. I. Austenitemartensite[J]. Physical review. B, Condensed matter, 2002, 13(66): 134206.
[32] DHOTE R P, MELNIK RODERICK V N, ZU J. Three-Dimensional Phase Field Model Of Proper Martensitic Transformation[J]. Meccanica, 2014, 49(7): 1561–1575.
[33] ARTEMEV A, JIN Y, KHACHATURYAN A G. THREE-DIMENSIONAL PHASE FIELD MODEL OF PROPER MARTENSITIC TRANSFORMATION[J]. Acta materillia, 2001, 49: 1165–1177.
[34] MORIN C, MOUMNI Z, ZAKI W. A constitutive model for shape memory alloys accounting for thermomechanical coupling[J]. International Journal of Plasticity, 2011, 27(5): 748–767.
[35] WANG J, MOUMNI Z, ZHANG W. A thermomechanically coupled finite-strain constitutive model for cyclic pseudoelasticity of polycrystalline shape memory alloys[J]. International Journal of Plasticity, 2017, 97(October): 194–221.
[36] ENEMARK S, SANTOS I F, SAVI M A. Modeling, characterization and uncertainties of stabilized pseudoelastic shape memory alloy helical springs[J]. Journal of Intelligent Material Systems and Structures, 2016, 27(20): 2721–2743.
[37] FIRSTOV G S, KOSORUKOVA T A, KOVAL Y N. et al. High Entropy Shape Memory Alloys[J/OL]. Materials Today: Proceedings, 2015, 2(November): S499–S503. http://dx.doi.org/10.1016/j.matpr.2015.07.335. DOI:10.1016/j.matpr.2015.07.335.
[38] FIRSTOV G S, KOSORUKOVA T A, KOVAL Y N. et al. Directions for High-Temperature Shape

Memory Alloys' Improvement: Straight Way to High-Entropy Materials?[J]. Shape Memory and Superelasticity, 2015, 1(4): 400–407. DOI:10.1007/s40830-015-0039-7.

[39] GUO S, LIU C T. Phase stability in high entropy alloys: Formation of solid-solution phase or amorphous phase[J/OL]. Progress in Natural Science: Materials International, 2011, 21(6): 433–446. http://dx.doi.org/10.1016/S1002-0071(12)60080-X. DOI:10.1016/S1002-0071(12)60080-X.

[40] ABUBAKAR R A, YUTIAN H, WANG F. et al. Modeling and Experimental Validation of the Hysteretic Dynamics of Shape Memory Alloy Springs[J]. INTERNATIONAL JOURNAL ON SMART SENSING AND INTELLIGENT SYSTEMS, 2020, 30(1): 1–9.

NON-ISOTHERMAL MODELING OF 1D SMA SPRING USING CHEBYSHEV COLLOCATION METHOD

Rabiu Ahmad Abubakar

The State Key Laboratory of Fluid Power Transmission and Control, Zhejiang University,

310027, Hangzhou, China

Abstract: Thermo-mechanical coupling models for the SMA spring are formulated based on energy and momentum conservation law. A modified Landau phenomenological model is proposed for the dynamics phase transformation of SMA. The proposed phenomenological SMA spring models are applied on SMA spring with two fixed ends. Landau free energy density related to the stretch ratio in the model is formulated. 3D Numerical algorithm simulations are performed via Chebyshev Collocation Method.

Keywords: *Shape memory alloys; Martensite transformation; pseudoelasticity; differential model.*

1 Introduction

The potential applications of shape memory alloys (SMA) increase interest in the material's analysis and modeling through theoretical approaches. SMA is a kind of material that can be trained to memorize different shapes [1–3]. Moreover, when deformed, it can regain its original shape [4,5] as the temperature increases, thus converting thermal energy to mechanical type [6–8]. This unique property of the plastic-like deformation and subsequent full recovery is called shape memory effects (SMEs) [9–11]. The history of this noble alloy material started in the 1800s when William Buehler and his coworkers discovered its behaviors of shape recovery capability [12]. Following this, the NINOL was given to the material in which N.I. stands for nickel and NOL, attributing it to the Naval Ordinance Laboratory, where the behavior was first discovered [13]. The material produced a strange loud sound on a cold stage, different from that at the hot stage [10]. Over a decade, the material has drawn the researcher's attention for various engineering applications [14,15]. After rigorous investigation, it was concluded that the material had a unique property [16] that made it different from other alloy materials and then named it NITINOL associating it to the laboratory. This alloy can recover energy up to 10^6 J/m^3, and the transformation temperature depends on Ni-content with an upper limit of 363 K [17].

Although SMAs show a low-frequency response, they have reversible hysteresis properties under cyclic mechanical loading [18]**.** This makes them essential materials in many engineering applications such as actuation impact absorption, sensor, and vibration isolation [19], to mention a few. Except for the medical fields, such as wearable devices and telehealth care, SMAs have not been commercialized due to the lack of a detailed model describing their behaviors. Many mathematical models have been constructed for SMA from different perspectives [20,21]. However, due to the complex behavior of SMA, an exact and simple model has not yet been developed.

NiTi-based (Nitinol), Fe-based, and Cu-based alloys are the most popular [22]. Nitinol is bio-compatible and single-crystal. Cu-based alloys, which are brittle SMAs, have the highest inelastic strain recovery (up to 10 %) because of the thermo-elastic phased change and are more delicate in application [23]. Compared to Nitinol, Cu-based alloys exhibit less temperature dependence, loading rate, grain size, and lower pseudoelastic behavior [24]. Fe-based SMAs exhibit high ductility, large hysteresis, and lower shape recovery (4 %). In addition to the shape memory effect and pseudoelasticity effect, SMAs exhibit other properties like rubber-like effects resulting from aging and allowing reversible and de-twinning of martensite variants [25].

3 Modeling of SMA spring

SMA spring thermo-mechanical coupling dynamic models are built based on the law of conservation energy [8], with the stretch ratio of the SMA spring as an order parameter and shear stress τ.

$$\left.\begin{aligned} v &= \frac{\partial u}{\partial t};\ \lambda = \frac{\partial u}{\partial x};\ g = \frac{\partial^2 \lambda}{\partial x^2}, \\ c_v \frac{\partial T}{\partial t} &= k_4 \frac{\partial^2 T}{\partial x^2} + A_1 T \lambda \frac{\partial \lambda}{\partial t} + Z, \\ \rho \frac{\partial v}{\partial t} &= \frac{\partial}{\partial x}\left(\tau + \Upsilon \frac{\partial v}{\partial x} - k_g \frac{\partial g}{\partial x}\right) + Fr, \end{aligned}\right\} \quad 1$$

And,

$$\tau = A_1 \left(\frac{T - T_1}{T_1}\right)\lambda + A_2 \lambda^3 + A_3 \lambda^5.$$

These equations are for the 1D modeling of nonlinear dynamics of SMA spring. The model is for a single crystalline structure and can be modified for modeling polycrystalline structures.

The Landau free energy density $F_l(T, \lambda)$ related to the stretch ratio in Eq. 1 is formulated as:

$$F_l(T, \lambda) = \frac{A_1}{2}\left(\frac{T - T_1}{T_1}\right)\lambda^2 - \frac{A_2}{4}\lambda^4 + \frac{A_3}{6}\lambda^6. \quad 2$$

2 Thermal dependency

For analysis of elastic waves in SMA spring, the modified elastic equation Eq. 1 linearizes at the point (τ_L, λ_L) at which $\tau_L = 0$:

$$\rho \ddot{u} = \frac{\partial}{\partial x} k_L \lambda + \Upsilon \frac{\partial}{\partial t}\frac{\partial \lambda}{\partial x} - k_g \frac{\partial^4 u}{\partial x^4}, \quad 3$$

where, the mechanical loading is dropped out. k_L is the stiffness constant for linearization and is dependent on temperature.

From Fig. 1, when the SMA spring is at high temperature, only austenite is stable, and there is no phase transformation. Here $\lambda_L = 0$ so k_L is formulated as:

$$k_L = A_1\left(\frac{T - T1}{T1}\right) \quad 4$$

At lower temperatures, the linearization is carried out by three points. Here the stable points are calculated using the following formula:

$$A_1 \left(\frac{T - T_1}{T_1}\right) + A_2 \lambda^2 + A_3 \lambda^4 = 0, \quad 5$$

And,

$$\lambda_L = \sqrt{\frac{-A_3 \pm \sqrt{A_2^2 - 4A_1 A_3\left(\frac{T - T_1}{T_1}\right)}}{2A_3}}, \quad 6$$

$$\lambda_L = \pm 1.34$$

These two values are associated with the stretch ratio for martensite plus ($\lambda_L = +1.34$) and minus ($\lambda_L = -1.34$). The coefficient k_L is calculated as:

$$k_L = A_1 \left(\frac{T - T_1}{T_1}\right) + A_2 \lambda^2 + A_3 \lambda^4 \quad 7$$

k_L has the same value for the two stable points at martensite plus and minus.

For the intermediate temperature cases, the dependence of k_L on temperature is complicated since both austenite and martensite may occur, and there may be four values $\lambda_L$to satisfy $\tau_L = 0$. Though the symmetry property still exists for martensitic variants, wave motions are different between austenite and martensite states.

For the wave motion in Eq. 33, the solution is given as:

$$u(z) = u(x - Vt) = u(z), \quad z = x - Vt, \qquad 8$$

here *V* is the wave velocity. Upon substitution, the following equation is obtained:

$$k_g \frac{\partial^2 \lambda}{\partial x^2} = \pm(k_L - \rho V^2)\lambda - \Upsilon V \frac{\partial \lambda}{\partial x} \qquad 9$$

The problem is now computed as an ordinary differential equation, and its general solution is:

$$\lambda(z) = (C_1 + C_2 z)e^{z\sqrt{(k_L - \rho V^2)/k_g}} \qquad 10$$

Where C_1 *and* C_2 are the coefficient to be determined by boundary conditions. The viscous term is temporarily neglected.

When the *V* is less than the velocity of sound, $V_s = \sqrt{k_L/\rho}$then $k_L - \rho V^2 > 0$ and there is a limited solution because the exponential function has a positive index and will become infinity. This indicates that no waves can propagate in the material when *V* is smaller than the velocity of sound. The velocity of sound of the material depends on the temperature; therefore, the allowed speed for wave propagation in the SMA spring varies along with the temperature.

When the viscous term is considered, the wave propagation will always be accompanied by dissipation effects. And will characterize the following equation:

$$|\lambda(z)| = e^{-\xi\omega z}, \quad \xi = \frac{\Upsilon V}{2\sqrt{(\rho V^2 - k_L)k_g}} \qquad 11$$

$$\omega = \sqrt{\frac{(\rho V^2 - k_L)}{k_g}}, \qquad 12$$

Where the initial amplitude is 1, the exponential coefficient estimates the dissipation effect$\xi\omega = \frac{\Upsilon V}{2k_g}$. When *V* is large enough, the dissipation effect will be induced, and it is temperature-dependent.

4 Numerical Methodology

In Numerical simulation, modeling success depends on how well the original differential model is treated. A good method that converts a partial differential model (PDE) to a nonlinear PDE is always a welcome idea.

The difficulties associated with the coupled systems above equations stress-strain dependency is a non-monotonic function. Therefore, reducing the system to a system of differential-algebraic equations (DAE) will be good.

5 Chebyshev Collocation Method

In this method, a set of Chebyshev points $\{x_i\}$ are chosen along the length for good pseudo spectral approximation as:

$$x_i = \frac{L\left(1 - \cos\left(\frac{\pi i}{V}\right)\right)}{2}, \qquad i = 1,2 \ldots\ldots\ldots\ldots V \qquad . \qquad 15$$

Using the above nodes, *v, T,* and M_{ex} distributions in the spring can be expressed in linear approximation as:

$$f(x) = \sum_{i=1}^{V} \quad M_{ex_i}\Phi_i(x), \qquad 16$$

where *f(x)* represents any of *u, v, T, σ* and $M_{ex_i}$is the function value at x_i, $\Phi_i(x)$ is the i^{th} interpolating polynomial is :

$$\Phi_i(x_j) = \begin{cases} 1, & i = j, \\ 0, & i \neq j. \end{cases} \quad 17$$

Here it is seen that the Lagrange interpolants satisfy the interpolating needs. By obtaining *f(x)* approximately, the *∂f(x)/∂x* can be easily gotten the derivative function $\Phi_i(x)$ with respect to *x*:

$$\frac{\partial f}{\partial x} = \sum_{i=1}^{V} f_i \frac{\partial \Phi_i(x)}{\partial x}, \quad 18$$

And in the same way for higher-order derivatives, all these approximations are formulated in matrix form for easy programming.

6 Multi-Domain Decomposition

The spectral method has good accuracy for discretization and is applied here. The domain is *Dm = [0, L]* is decomposed evenly into sub-domains *O* intervals with an overlapping region between pair intervals, as shown in Fig. 2.

And,

$$Dm = \bigcup_{c=1}^{c=C} Dm_c, \quad 19$$

where *C* is the number of sub-domain chosen, the Chebyshev collocation method is applied to approximate the solution and its derivatives in each interval. For each pair of consecutive intervals, the coupling is set as:

$$y_c^n = y_{c+1}^2, \qquad y_c^{n-1} = y_{c+1}^1, \quad 20$$

where the *c* subscript is the interval node while the *n* subscript is the node number in each interval. y_c^n is the variable function at each value point x_c^n. This can be any of the dependent variables. $x_c^n$is the same node as $x_{(c+1)}^2$, and x_c^{n-1} is the same node as x_{c+1}^1. The value of the derivatives function is estimated by averaging their values in two intervals involved.

$$\left.\frac{\partial y}{\partial x}\right|_{x_c^{n-1}} = \frac{1}{2}\left(\sum_{i=0}^{V} y_c^i \left.\frac{\partial \Phi_i(x)}{\partial x}\right|_{x_c^{n-1}} + \sum_{i=0}^{V} y_{c+1}^i \left.\frac{\partial \Phi_i(x)}{\partial x}\right|_{x_{c+1}^1} \right),$$

$$\left.\frac{\partial y}{\partial x}\right|_{x_c^{n}} = \frac{1}{2}\left(\sum_{i=0}^{V} y_c^i \left.\frac{\partial \Phi_i(x)}{\partial x}\right|_{x_c^{n}} + \sum_{i=0}^{V} y_{c+1}^i \left.\frac{\partial \Phi_i(x)}{\partial x}\right|_{x_{c+1}^2} \right). \quad 21$$

For the second-order, the approximation can be obtained by taking an average of the node in the overlapped region.

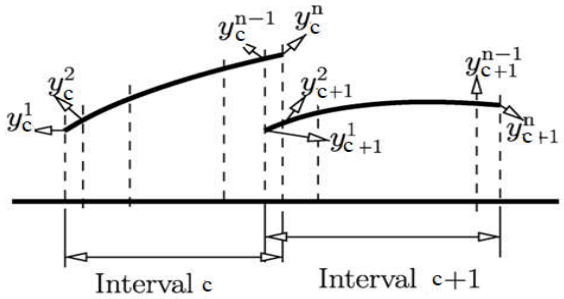

Figure 2 Domain decomposition and discretization

7 The method of backward differentiation formula

The partial differential equations in Eq. 2.32 are converted to ordinary differential equations by combining the multi-domain decomposition methods with Chebyshev collocation methods. The last row in Eq. 2.23 is discretized using the Chebyshev collocation methods. Therefore the whole system can be written by combining the ordinary differential equations and algebraic equations as:

$$Y\frac{dX}{dt} + V[t, X, Z(t)] = 0, \qquad 22$$

where X is the vector that collects all the variables solved, Y is a singular matrix, and V is a vector that collects a nonlinear function generated by spatial discretization. Second-order backward differentiation is used for implicit algorithms. Hence the DAE system is converted into a set of algebraic systems at each time level by discretizing the time derivative as:

$$j\left(\frac{3}{2}X^n - 2X^{n-1} + \frac{1}{2}X^{n-2}\right) + \Delta tN\left(t_n, X^n, Z(t_n)\right) = 0, \qquad 23$$

where n stands for the current computational time layer, iteration has to be carried out in this computational time layer using Newton's method by X^n use of X^{n-1} and X^{n-2}. By employing this algorithm, the unknown vector X is resolved at all specific instances. The iteration is stopped when the residual is smaller than $1\text{x}10^{-6}$.

8 Modeling 1-D SMA spring under thermal

Consider an SMA spring in Fig. 3 with a fixed boundary subjected to thermal loading only.

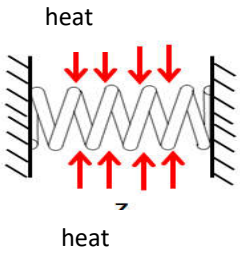

Figure 3 SMA spring under thermal loading

For this case, Eq. 1 is reduced to:

$$v = \frac{\partial u}{\partial t};\ \lambda = \frac{\partial u}{\partial x};\ g = \frac{\partial^2 \lambda}{\partial x^2},$$

$$c_v\frac{\partial T}{\partial t} = k_4\frac{\partial^2 T}{\partial x^2} + k_1 T\lambda\frac{\partial \lambda}{\partial t} + Z,$$

$$\rho\frac{\partial v}{\partial t} = \frac{\partial}{\partial x}\left(\tau + \Upsilon\frac{\partial v}{\partial x} - k_g\frac{\partial g}{\partial x}\right), \qquad 24$$

$$\tau = A_1\left(\frac{T-T_1}{T_1}\right)\lambda + A_2\lambda^3 + A_3\lambda^5.$$

The initial condition is $T=T_a$; the boundary conditions for this case are:

$$u(0,t) = 0, \quad u(L) = 0; g(0,t) = 0, \quad g(L,t) = 0; \text{ and } T_x(0,t) = 0, \quad T_x(L,t) = 0,$$

9 Numerical experiment

In this section, numerical experiments are performed. Using the estimated parameters obtained in experiment 1 above for SMA spring. A_1=0.65 kg/(s^{2}m^{o}C), A_2=-56.5 kg/(ms^{2}m^{o}C), A_3=31.7 kg/(ms^{2}m^{o}C), T_1= -49.42^{o}C, ρ=11100 kg/m^3, C_v = 1.1454x10^3 kg/s^2m^{o}C, k = 0.6960mkg/s^3 ^{o}C, k_g = 1.5x10^6 kg/s^2, r =1.6/2 x 10^{-3} m. T_a =15 ^{o}C.

For this case, the thermal loading applied is: $Z = 600\sin(3\pi t)\text{kg}/(s^3 m)$. Fig. 4a shows the displacement of the SMA spring with two fixed ends. The graph produced a hyperbolic form, and there is no displacement at

the two boundaries. Fig. 4(b) represents the temperature graph, producing a sinusoidal curve with a strong nonlinear thermo- mechanical coupling behavior. Fig. 4(c) presents a stretch ratio graph. It shows a strong nonlinear thermo-mechanical couple behavior like the temperature graph. The stretch ratio starts with a larger value and with a small value. There is a clear indication of the pseudoelastic effect.

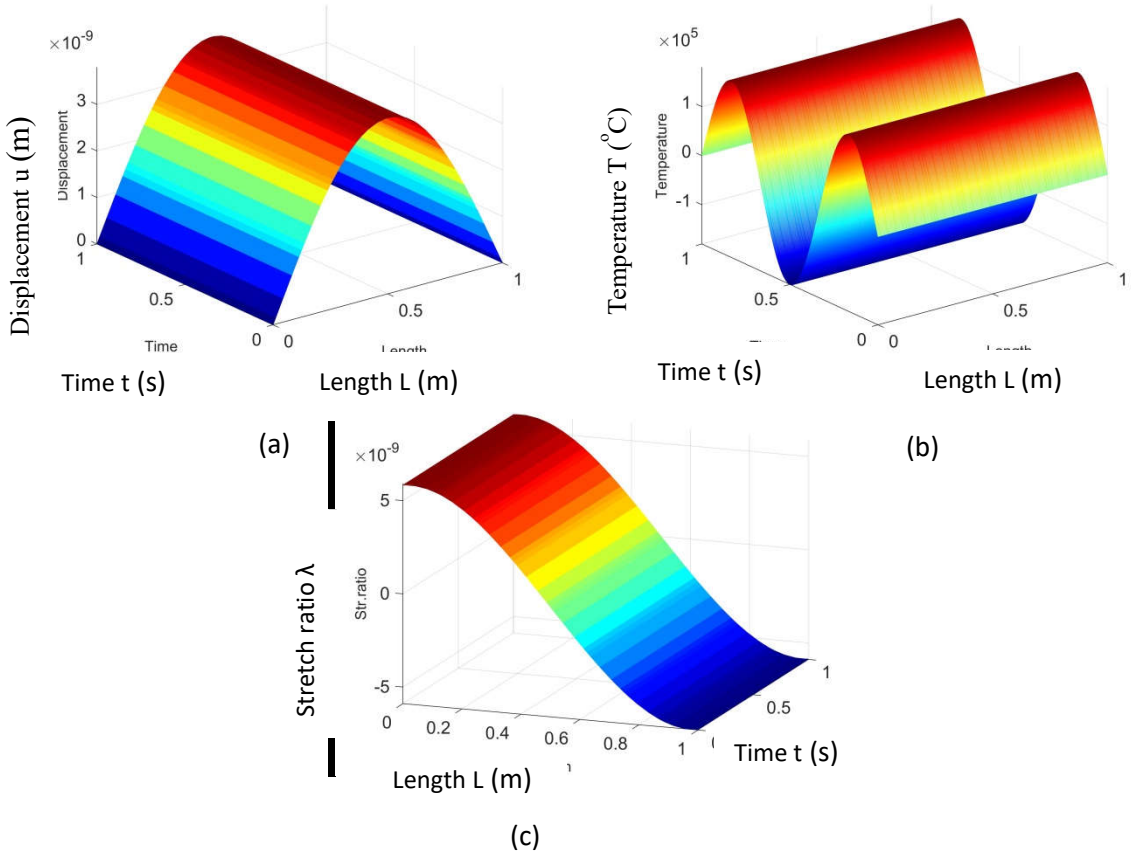

Figure 4 Simulation results of SMA spring under thermal loading only

9 Conclusion

Modeling of SMA spring thermomechanical coupled equations are performed, and the simulation results are presented under the thermal loading for an SMA spring with two fixed ends. Therefore, the coupled modeling equations for SMA spring are established.

References

[1] SITTNER P. Deformation twinning in martensite affecting functional behavior of NiTi shape memory alloys[J]. Materialia, 2019, 9(March): 100506.
[2] MACHADO L G, SAVI M A, JANEIRO R De. et al. Medical applications of shape memory alloys[J]. Brazilian Journal of Medical and Biological Research, 2003, 36(6): 683–691.
[3] NAGENDRA M R, TAMILSELVAN M, SADHASIVAM C. Computation and investigation of an SMA engine using low heat recovery[J]. International Journal of Pure and Applied Mathematics, 2018, 118(20): 57–62.
[4] HALAHLA A M, ABU Y B, ALMASRI A H. et al. The effect of shape memory alloys on the ductility of exterior reinforced concrete beam-column joints using the damage plasticity model[J]. Engineering Structures, 2019, 200(September): 109676.
[5] SHIVA S, YADAIAH N, PALANI I A. et al. Thermomechanical analyses and characterizations of TiNiCu shape memory alloy structures developed by laser additive manufacturing[J]. Journal of

Manufacturing Processes, 2019, 48(February 2018): 98–109.
[6] ZHU J J, LIANG N G, HUANG W M. et al. Energy Conversion in Shape Memory Alloy Heat Engine Part I: Simulation. Journal of Intelligent Material Systems and Structures[J]. Journal of Intelligent Material Systems and Structures, 2001, 12(2): 133–140.
[7] MELNIK RODERICK V N, WANG L, MATUS P. et al. Computational Aspects of Conservative Difference Schemes for Shape Memory Alloys[C]. GERHARD GOOS, JURIS HARTMANIS C L,//International Conference on Computational Science and Its Applications. Berlin, Heidelberg: Springer, 2003: 791–800.
[8] WANG L, MELNIK R V N. Thermo-mechanical wave propagations in shape memory alloy rod with phase transformations[J]. Mechanics of Advanced Materials and Structures, 2007, 14(8): 665–676.
[9] CHURCHILL C B, SHAW J. THERMO-MECHANICAL MODELING OF A SHAPE MEMORY ALLOY HEAT ENGINE[C]//Proceedings of the ASME 2011 Conference on Smart Materials, Adaptive Structures and Intelligent Systems. Scottsdale, Arizona, USA: ASME, 2011: 641–650.
[10] LECCE L, ANTONIO C. Shape Memory Alloy Engineering[M]. LECCE L N C,. Amsterdam: Elsevier, 2015.
[11] ALEXANDRAKIS V, MANUEL J, PÉREZ-CHECA A. Combinatorial synthesis of Ni–Mn–Ga-(Fe, Co, Cu) high temperature ferromagnetic shape memory alloys thin films[J]. Scripta Materialia, 2020, 178(March): 104–107.
[12] FRITSCH E, IZADI M, GHAFOORI E. Development of nail-anchor strengthening system with iron-based shape memory alloy (Fe-SMA) strips[J]. Construction and Building Materials, 2019, 229: 117042.
[13] HUANG H, YAO P, SU Y. Stress relaxation behavior of columnar-grained Cu–Al–Mn shape memory alloys[J]. Materials Science & Engineering A, 2019, 768(September): 138432.
[14] FEI X, HAIFENG Y, KUN L. et al. Forming and two-way shape memory effect of NiTi alloy induced by laser shock imprinting[J]. Optics and Laser Technology, 2019, 120(April): 105762.
[15] HONARMANDI P, JOHNSON L, ARROYAVE R. Bayesian probabilistic prediction of precipitation behavior in Ni-Ti shape memory alloys[J]. Computational Materials Science, 2020, 172(September 2019).
[16] ADARSH S H, SAMPATH V. Hot deformation behavior of Fe-28Ni-17Co-11.5Al-2.5Ta-0.05B (at.%) shape memory alloy by isothermal compression[J]. Intermetallics, 2019, 115(December): 106632.
[17] CHO H, TAKEDA Y, SAKUMA T. Fabrication and Output Power Characteristics of Heat-Engines Using Tape-Shaped SMA Element[J]. Advanced Structured Materials, 2017, 73: 1–15.
[18] ASHWIN R, A. R. S, J. N. R. Design of Shape Memory Alloy (SMA) Actuators[M]. HOLM ALTENBACH, MAGDEBURG, GERMANYLUCAS F.M. DA SILVA, PORTO P, 编. TX USA: Springer, 2015.
[19] PIRBHULAL S, ZHANG H, ALAHI E E. et al. A Novel Secure IoT-Based Smart Home Automation System Using a Wireless Sensor Network[J]. Sensors, 2016, 17(69): 1–19.
[20] FINNEY K A. Ocean Thermal Energy Conversion[J]. Internation Journal of trend in scientific research and development, 2008, 1(1): 17–23.
[21] MA Z, WANG Y, WANG S. et al. Ocean thermal energy harvesting with phase change material for underwater glider[J]. Applied Energy, 2016, 178: 557–566.
[22] OTSUKA K, WAYMAN C M. Shape Memory Materials[M]. OTSUKA K, C. M. WAYMAN. Cambridge University Press., 1999.
[23] BANSIDDHI A, SARGEANT T D, STUPP S I. et al. Porous NiTi for bone implants : A review[J]. Acta Biomateria, 2008, 4(4): 773–782.
[24] ARAKI Y, ENDO T, OMORI T. Potential of superelastic CueAleMn alloy bars for seismic applications[J]. Earthq. Eng. Struct. Dyn., 2011, 40(1): 107-115.
[25] CISSE C, ZAKI W, BEN T. A review of constitutive models and modeling techniques for shape memory alloys[J]. International Journal of Plasticity, 2016, 76(January): 244–284.

COMPARATIVE BIOGAS PRODUCTION MEASUREMENT FOR LABORATORY SCALE EXPERIMENT

M. Ahmad, A. A. Zuru, C. Muhammad and M. Musa

ABSTRACT

This research presents the study carried out on the use of an alternate gas collection medium that measures the mass rather than the volume of the biogas produced for laboratory scale experiment using Urine Drainage Bag (UDB). Four methods were designed for calibration of the UDB: (a) Measurement of Mass of Water in Urine Bag and its Corresponding Volume in Measuring Cylinder (Random) (b) Measurement of Incremental Mass of Water in Urine Bag and its Corresponding Volume in Measuring Cylinder resulted in linear wit (c) Measurement of Volume of Air in Urine Drainage Bag as Function of Mass of the Air and (d) Measurement of Volume of Air in Urine Bag based on Volume of Water Displaced in Measuring Cylinder. The four methods gave good calibration result but led to exaggerated results. The comparative analysis of the monitoring of biogas yield using mass measurement in lieu of volume measure was carried using 10 Digesters split into two sets of 5 digestated labeled A1, A2, A3, A4, A5 and B1, B2, B3, B4 and B5. Set A Digesters were monitored using downward displacement of water in measuring cylinder and while Set B Digesters were monitored by weighing the mass of biogas at same interval of time. Results show that biogas yield could monitored by measuring mass at suitable intervals but conversion of the yield in mass to yield in volume could not done successfully using the calibration equation. Only conversion on assumption of ideal gas behaviour as proposed by Rajesh B. & Rajneesh K. (2019) gave excellent fit.

1.0 Introduction and Literature Review

For centuries, energy in its entire ramification has always been an essential input to all aspects of human development, especially for the modern age. It is indeed the livewire for industries producing the fuel for the manufacturing and transportation goods and for other conventional power generations and utilizations. Consequently, global energy consumption has about doubled in the last three decades of the past century (Divya *et al*., 2014). In 2012, about 87% of the primary energy consumption was from fossil fuels (33% oil, 24% natural gas, 30% coal), 4% from nuclear fuels, 9% from renewable resources, of which the main one is hydroelectric, 7%, whereas the remaining 2% consists of non-commercial biomasses, such as wood, and other types of fodder, that in rural-economies still constitute the main resources (Arent, *et al.,* 2014).

This trend will only increase giving the increasing rise of educated people with their attendant change in lifestyle which depends largely on energy for transportation, recreation, and production. Unfortunately, fossil fuels have been identified as having a major negative impact on our environment as the primary agents of global warming because of their utilization in transportation producing gases such as Carbon (II) oxide and other Green House Gases (GHG). For instance, In 2013, the Intergovernmental Panel on Climate Change (IPCC) Fifth Assessment Report concluded that "It is *extremely likely* that human influence has been the dominant cause of the observed warming since the mid-20th century (IPPC, 2013). For these reasons, there is increasing interest in replacing fossil fuels with Renewable Energy sources (also called Bioenergy) as mitigation options. Renewable energy resources are available in both developed and developing countries in significant quantities (Stocker *et.al*, 2013).

In this research work, the renewable energy source of interest is biogas from biomass. Biomass which is a material that comes from renewable biological materials such as plants, animals, and microbes. It is made into fuels using different methods such as chemical processes that convert the carbohydrates into sugars, and sugars into alcohol – a liquid bioenergy fuel (*Syed*, 2006). Moreover, Biomass resources such as cattle dung,

agricultural wastes, and other organic wastes have been one of the main energy sources for mankind since the dawn of civilization**.** Experts have proposed biogas as one of these new sources of renewable energy. In 2000, the global energy generation from biogas was about 280,000 TJ and reached almost 1.3 million TJ by 2014, with a typical annual increase of 13.2% in biogas production (IEA, 2016; Vasco-Correa *et al.*, 2018). In 2017, biogas generation was projected at about 61.7 billion m^3, with almost half of it ~~was~~ being produced in the European Union (World Bioenergy Association 2019; Vasco-Correa *et al.*, 2018).

The most common method to obtain biogas is anaerobic digestion, which is frequently used in the processing of municipal wastewater for sludge degradation and stabilization, and the decomposition of food waste and other compounds in weirs (Demirbas, 2010). Anaerobic digestion is generally classified as (a) Psychrophilic (less than 15 °C), (b) Mesophilic (15 to 45 °C) and (c) Thermophilic (45 to 65 °C). The mesophilic and thermophilic digestions are more important because in the psychrophilic range the production of biogas is very low (Nijaguna, 2002). It is well known in kinetics that temperature is a very important factor as it affects the rate of reaction and influences the effects on solubility of metals and gases such as **CO_2** and consequently could impact on the buffering and composition of the biogas. It is also well established that the solubility of gases increases with increase in pressure and decreases with an increase in temperature and also varies with the molecular nature of the gas. Thus, Methane (CH_4) can be considered a less soluble hydrocarbon in water because of its smaller size and because it has the potential of causing minimum disruption to water's hydrogen bonds. This effect is so low that its solubility in water can be considered virtually zero. On the other hand, CO_2 is very polar and its solubility is high in water. Solubility of CO_2 and CH_4 at 1.0 atmosphere (101.325 kPa) and temperature (Petersson and Wellinger, 2009).

The partial pressure of gas in the headspace of the digester can be held within a constant range. But CO_2 can hydrate and dissociate in the aqueous phase and vary the function of pH and other factors. The reaction scheme can be expressed by equation 1 (Dixon and Kell, 1989):

$$CO_2 + H_2O \leftrightarrow H_2CO_3 \leftrightarrow HCO_3^- + H^+ \leftrightarrow CO_3^{2-} + 2H^+ \text{ ----------1}$$

When pH value is < 8, the concentration of carbonate ions may be neglected and the hydration reaction can be expressed as:

$$CO_2 + H_2O \leftrightarrow H_2CO_3 \leftrightarrow HCO_3^- + H^+ \text{----------2}$$

When alkalinity is less than 1000 mg/L, pH starts to change rapidly. A total alkalinity of 1.5 g $CaCO_3$/L is recommended for an adequate performance of the anaerobic systems (Hawkes et. al.,1997)

In view of the issues raised above, several studies have been conducted to investigate the accuracy of biogas measurements in laboratory scale experiments as described below. Particularly relevant to this paper, are laboratory scale experiments (Bagudo et.-al., 2008; Bagudo et.-al. 2011; Tambuwal et.-al, 1997; Yusuf et-al., 2011; Zuru et.-al., 2000, and Zuru et.-al., 2004, that measure the quantity and composition of biogas by using downward displacement of water in a measuring cylinder inverted into a water trough as shown in Figure 1:

Figure1: Laboratory Set-up for Measurement of Biogas Yield using Downward Displacement of Water

The biogas generated in the plastic digester is channeled through the PVC-tube into a Measuring Cylinder ($500cm^3$, $1000cm^3$ or $2000cm^3$) filled with water and inverted into a plastic trough containing water. As the biogas is generated it bubbles into the measuring cylinder and displace the water downward into the plastic trough. The volume of water displaced downward in the cylinder is read off as the volume of biogas generated: In most experiments mentioned above, readings were taken at 24 hour intervals. The sources of error in such set-ups are:

(i) High initial pressure is required to displace a column of $2000cm^3$ of water in the cylinder, hence there will be error in the initial volume of biogas;

(ii) Reading of the volume of biogas when the water meniscus is between two consecutive minimum calibration of the cylinder:

(iii) Error due to solubility of CO_2 at the interface between the head-pressure of biogas and water in the cylinder;

(iv) The evapouration of barrier solutions after a long time; and

(v) Error due to high production beyond capacity of cylinder within reading interval, e.g production of more than $2000cm^3$ biogas in 10hours while using $1000cm^3$ cylinder. This results in sustained biogas loss through the trough until the Cylinder is refilled regularly.

As pointed out above, the major drawback of the liquid displacement gas collecting and measuring system is inaccuracy due to biogas solubility/diffusion through the barrier solution. Liquids such as simple tap water, oil, acidified water and carbonated water are widely used as barrier solutions. The solubility and diffusion varies with type of liquid, atmospheric pressure, temperature, density of liquid, gas composition. Therefore, the same correction factor cannot be applied for every time of gas measurement. A study reported that underestimations of CO_2 in the biogas could be as high as 30% with the use of Warburg liquid displacement gas measurement system. Gas solubility errors can be eliminated by collecting gas in gas bags and measuring the gas volume with liquid column meters (Guwy, 2004).

2.0 Statement of the Research Problem

This paper addresses a challenge believed to have significant impact on the quantity of biogas produced in laboratory-based experiments: that is, the most common and widely accepted method of biogas collection based on liquid displacement. This type of gas collection is used for broad laboratory-based volume measurement because of it's simplicity, low-cost, easy to set up and use, and capable of working for a long

period without support. The use of the liquid displacement method requires that measurements taken directly from the gas column (e.g. liquid levels) are used to calculate gas volumes. The major drawback of the liquid displacement gas collecting and measuring system in the case of biogas, is the inaccuracy due to solubility of sum component of biogas such as carbon (IV) oxide (CO_2) in the barrier solutions, loss of gas due to diffusion or low-pressure production which cannot bubble out to displace the liquid in the cylinder. Moreover, this measurement technique could result in the suppression of anaerobic digestion because the high amounts of dissolved CO_2 can affect the pH of the medium and, consequently, can alter the microbial activity (Mould *et al.*, 2015). A study by Guwy, (2010) shows that underestimations of CO_2 in the biogas could be as high as 30% with the use of a liquid displacement gas measurement system. The vaporization of barrier solutions after a long period can also result in inaccuracies. Therefore, to address these challenges, it is theorized that gas solubility errors and associated setbacks can be eliminated by collecting gas in a gas bag (urine bag) and measuring the "gas mass" in lieu of "gas volume".

3.0 Aim and Objective

This main aim of the study is to examine the feasibility of monitoring biogas yield by weighing the mass of biogas in urine bag at given intervals over a given retention period and compare same with existing method of measuring the yield by downward displacement of water in measuring cylinder;

The specific objectives are:

(i) Calibrate the urine bag for measurement of mass and volume of gas and liquid;

(ii) Design experiment to collect and measure biogas yield using urine bag at given interval of time (hours) and retention period (days);

(iii) Set up parallel experiment as in (ii) above but measuring the biogas yield using downward displacement of water in measuring cylinder; and

(iv) Compare the daily, weekly and total biogas yield from cow dung using both Mass Measurement in Urine Bag and Volume Measurement by Downward Displacement of water in measuring Cylinder.

4.0 Theoretical Framework for Calibration of Urine Bag

The theoretical framework of the method for calibration of the Urine bag is based on the relationship between mass, volume and density through the equation:

$$Density\ (\rho) = \frac{Mass\ (m)}{Volume\ (V)} \text{ ----------(3)}$$

Based on equation (3), it is theorized that the volume of a fluid will be directly proportional to the mass of the fluid which will be described by the following equation (4):

$$V = \frac{m}{\rho} + k \text{ ----------(4)}$$

Where k is the intercept of a linear plot between Volume (V) of the fluid and its Mass (m). Thus, if a series of volume of a fluid are plotted against the corresponding masses, an acceptable linear plot will give the density of the fluid from its slope. If the density of the fluid is reproduced within acceptable error margin, then measurement of mass of the fluid is a good indirect method of measuring volume of the fluid. Consequently, the yield of biogas can be ascertained by measuring its mass in lieu of its volume.

The second basic assumption is that the mass (M_{bio}) of the Total Biogas produced in 56 days will be equivalent to the volume (V_{bio}) of the Total Biogas produced in 56 days. Thus, the Volume (V_{bio}) will be related to the Mass(M_{bio}) by transformation of equation (3) to express the density of biogas (ρ_{bio}) by the equation (5):

$$\rho_{bio} = \frac{M_{bio}}{V_{bio}} \text{----------(5)}$$

Where ρ_{bio} is the density of the biogas at the experimental temperature and pressure. Thus, the Density (ρ_{bio}) of Biogas will be calculated using Equation (5) and compared with literature values.

The third assumption considered the biogas to approximate ideal gas as proposed by Rajesh B. & Rajneesh K. (2019). Thus, the volume of biogas produced over a Hydraulic Retention Time (HRT) and temperature (T) could be calculated with the formula:

$$V_{bio} = \frac{M_{bio}\ x\ R_{bio}\ x\ T}{M_r x\ P_{atm}} \text{----------(6)}$$

Where:

V_{bio} = Volume of biogas;

M_{bio} = Mass of biogas;

M_r = Molar Mass of Biogas = 28.94 Kg/Mol (Rajesh B. & Rajneesh K., 2019)

R_{bio} = Molar gas constant for biogas = 287.32 J/Kg.K (Rajesh B. & Rajneesh K., 2019)

P_{atm} = Atmospheric Pressure = 101.235kPa

T = Temperature in Kelvin = T ^{O}C + 273.16

5.0 MATERIALS AND METHOD

5.1 Materials

The materials used are basically cow dung as the substrate, a 2-litre flexible PVC Urine Drainage Bag product of YILI Medicals and 2000cm^3 Measuring Cylinder product of VITLAB.

5.2 Methods

5.2.1 Calibration of Urine Bag for Measurement of Mass of Biogas

In order to employ equation (4) in calibrating the Urine Bag for measurement of mass of biogas, three (3) experiments were designed as follows:

(a) Method 1: Measurement of Mass of Water in Urine Bag and its Corresponding Volume in Measuring Cylinder (Random).

Five (5) empty Urine Drainage Bags (UDR) were randomly picked from pack of 10 UDRs and labelled A, B, C, D, and E. Each was filled with tap water and weighed to get 1,801; 1,895; 1,855; 1,869 and 1,874g respectively. The water in each Urine Drainage Bag was carefully transferred into a 2000cm^3 measuring cylinder to get the following corresponding volume of water: 1,820; 1,930; 1,890; 1,910 and 1920 cm^3, for bags A, B, C, D and E, respectively. The volumes (V) were plotted against mass (M) to get the linear plot shown in Figure 2.0.

(b) Method 2: Measurement of Incremental Mass of Water in Urine Bag and its Corresponding Volume in Measuring Cylinder

The Urine bag with highest mass (1,895g) of water in 3.2.1(a) above with corresponding volume (1,930cm^3) was identified as the reference bag and the mass was divided by 5 to give 379g. Thereafter, this figure (379g) was multiplied by 1, 2, 3, 4 and 5 to get five masses 379, 758, 1,137; 1,516 and 2,274g. These quantities of water were injected into separate Urine Drainage Bags and transferred separately into 2,000cm^3 measuring cylinder to obtain the corresponding volumes as 806, 1,156; 1,540 and 1,916 cm^3 respectively. The volumes were plotted against mass to get the linear plot shown in Figure 3.0.

(c) Measurements of Mass and Volume of Air in Urine Bag

Two (2) sets of experiments were conducted in this section:

(i) Method 3: Measurement of Volume of Air in Urine Drainage Bag as Function of Mass of the Air

This experiment is designed to examine the relationship between the mass and volume of air in Urine Drainage Bag which simulates how biogas fills the Urine Drainage Bag.

First, six (6) Urine Drainage Bags were randomly picked from a pack of 10 UDRs and labelled A, B, C, D, E, and F. A hand pump was used to pump 1, 2, 3, 4, 5, 6, 7, 8, 9, 10, 11,12,13, 14 and 15 pump strokes of air were pumped into each Urine Drainage Bag and weighed. The volume of the cylinder of the hand pump was calculated to be 173.20 cm^3 implying that 1 pump stroke is equivalent to 173.20cm^3 of Air. Therefore, the volume of air corresponding to the above strokes are: 173, 346, 520, 693, 866, 1,039; 1,212; 1,386; 1,559; 1,732; 1,905; 2,078; 2,252; 2,425; and 2,598, respectively. The corresponding mass (g) of air are: 4, 5, 7, 9, 10, 11, 11, 12, 12, 12, 13, 13, 14, 14 and 14g, respectively. A plot of volume of Air in Urine Drainage Bag against Mass (g) is given Figure 4.

(ii) Method 4: Measurement of Volume of Air in Urine Bag based on Volume of Water Displaced in Measuring Cylinder

This experiment is designed to simulate the current method of measuring volume of biogas by displacement of water in measuring cylinder.

In view of the finding in c(i) above, 15 strokes of Air were pumped into each of six (6) Urine Drainage Bags labelled A, B, C, D, E and F and weighed to get 12, 13, 12, 11, 12 and 12g, respectively. The discharge pipe of each urine bag was directed into an inverted water-filled 2,000cm^3 measuring cylinder in a bowl half-filled with water and the volume of water displaced by the Air in the six UDBs was found to be 1,500; 1,600; 1,510; 1,460; 1,500 and 1,520 cm^3, respectively. Therefore, the average mass of the air that could fill a Urine Drainage Bag is 12g and the corresponding average volume of water displaced in the cylinder is 1,515cm^3. In other words, 1g of Air displaces 126.25cm^3.

5.2.2 Comparative Measurement of Biogas Yield using Downward Displacement of Water in Measuring Cylinder and Mass of Biogas in Urine Drainage Bag

This experiment is designed to monitor and compare daily biogas yield based on measuring (i) volume of water displaced in measuring cylinder and (ii) mass of biogas in urine drainage Bag. Hence, all experiments were conducted simultaneously under same environment and readings taken at the same time.

Ten (10) plastic Jerry cans (5 litres each) were used as digesters for the generation of biogas with cow dung as the substrate. Five (5) measuring cylinders (2,000cm^3 Capacity each) and Five (5) Urine Drainage Bag (2-Litres capacity each) were used as gas measuring devices.

(a) Method 5: Measurement of Biogas Yield by Downward Displacement of Water in Measuring Water

A set of five digesters (5 litre Capacity each) tagged SET A was prepared by mixing 1.0kg of cow dung with 2000cm^3 of water to obtain a slurry of 1:2 ratio of substrate to water as recommended by Bagudo *et.al.,* (2011). The temperature and pH of the slurries were recorded and the digesters sealed, with their cover lid fitted with 1.0-meter PVC plastic hose-pipe as a conduit for the biogas into the inverted measuring cylinder in bowl of water. The digesters were labelled A_1, A_2, A_3, A_4 and A_5 and the volume of biogas generated was measured by displacement of water in the measuring cylinder at interval of 12hours per day for a retention period of 56 days, as recommended by Bagudo et al (2011) and Zuru et al., (2004). The results obtained are summarised in Table 1 and presented in Figure 8

(b) Method 6: Measurement of Biogas Yield by Weighing Mass (g) of Biogas in Urine Drainage Bag

Another set of five digesters (5-litre Capacity each) tagged SET B were prepared exactly as described in 3.2.2(a) above and labelled B_1, B_2, B_3, B_4 and B_5. However, in this case the 1.0-meter PVC plastic hose-pipe conduit outlet for biogas was connected to a weighed 2-Litre Urine Drainage bag for measuring the mass of biogas generated as recommended by Surve *et al.,* (2015). Thus, the mass of biogas generated was monitored by weighing the urine bag and its content (Figure 9) at intervals of twelve (12) hours over a retention period of 56 days.

It is pertinent to note that the two sets of digester, A & B, were set-up simultaneously and the volume of water displaced in the cylinder and mass of Urine bag were noted at the same time at intervals of 12 hours over a retention period of 56 days.

Figure 2: Measurement of Biogas mass in the Urine Drainage Bag

6.0 RESULTS AND DISCUSSION

6.1 Result of the Calibration of the Urine Drainage Bag using Mass and Volume of Water in Filled Urine Bag

The result of the measurements of mass of water in filled randomly picked Urine Drainage Bag as a function of the corresponding volume of water displaced in a measuring cylinder (Method 1) is shown in Figure 2 below.

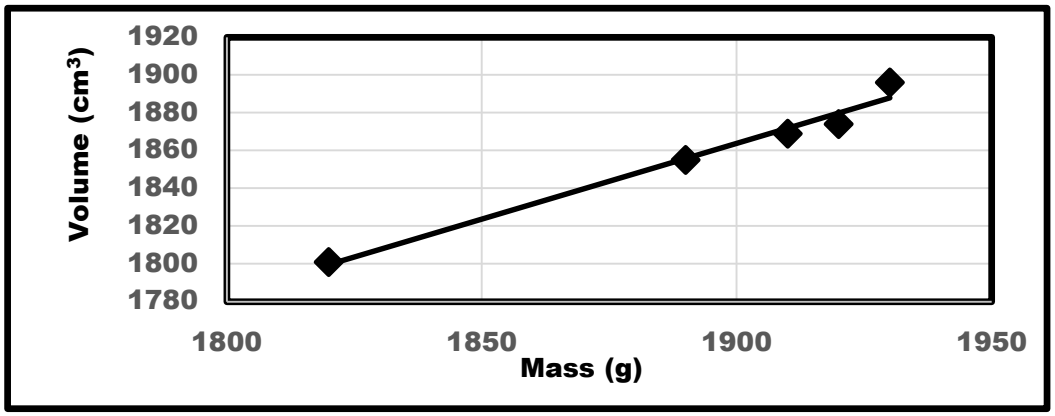

Figure 3: Linear Plot for Calibration of Urine Bag with Water Displacement (Random)

The figure revealed that the relationship between the volume of water in Urine Drainage Bag and its corresponding mass is linear and defined by equation (7) with correlation coefficient of 0.9782:

$V = 0.8018m + 340.37$ ----------(7)

Therefore, using equation (7) the density of water is computed from the slope as 1.2472g/cm^3 at 28.5^{o}C and 101.325kPa. Comparing this to 0.9967g.cm^3 at 26.7^{o}C and 101.325kPa as reported by Water Science School, (2018), this gives 18.39% relative error in determining density of water. This implies a 18.39% likely error should the urine drainage bag be adopted for measuring the density of water by measuring the mass and volume of water in filled Urine Drainage Bag.

6.2 Result of the Calibration of the Urine Drainage Bag using Volume of Water as Function of its Regular Incremental Mass

The result of the measurements of regular incremental mass of water in Urine Drainage Bag as a function of the corresponding volume of the displaced water in measuring cylinder (Method 2) is shown in Figure 4 below

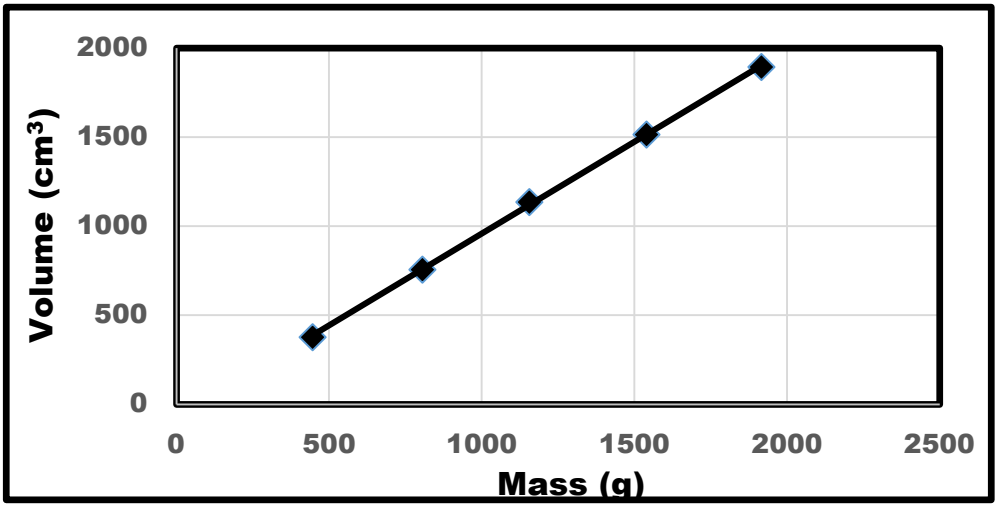

Figure 4: Linear Plot for Calibration of UDB with Water Displacement (Incremental Mass)

The figure shows a linear relationship between the volume and mass defined by equation (8) with correlation coefficient of 0.9997:

$V = 1.0313m - 72.455$----------(8)

Similarly, using equation (8) the density of water is computed from the slope as 0.9696g/cm^3 at 28.5^{o}C and 101.325kPa. When compared to 0.9967g/cm^3 at 26.7^{o}C and 101.325kPa (Water Science School, 2018). This gives a relative error of 9.43% in determining density of water. This implies a 9.43% likely error should the UDB be adopted for measuring the density of water by measuring the incremental mass and volume of water in UDB ba.

It is obvious that the incremental method is twice more accurate than the random filled Urine Drainage Bag method. However, in design of biogas experiment this will require preparation of digester slurries with fixed water quantity but regular incremental mass of substrate which will affect the water to substrate ratio and indeed the yield. Therefore, filled UDB method is preferable.

6.3 Result of the Calibration of the UDB Using Air

The result of the measurements of mass of air in Urine Drainage Bag as a function of its volume (Method 3) is shown in Figure 5 below.

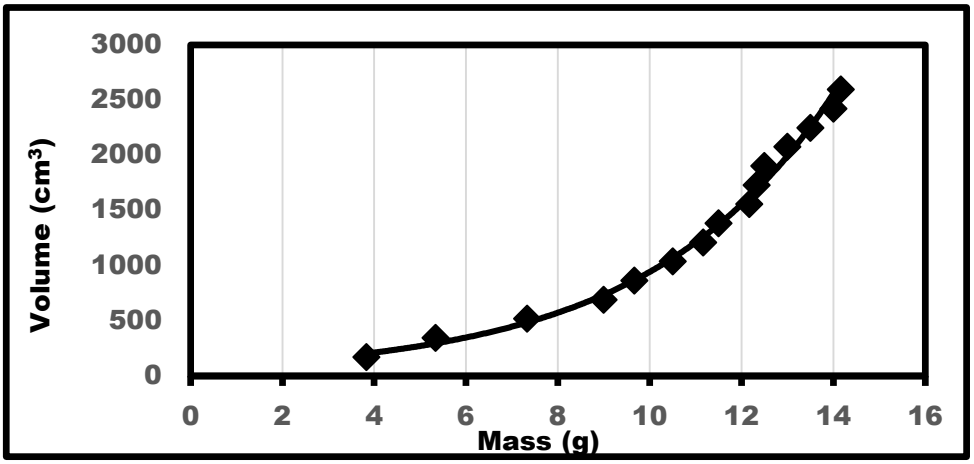

Figure 5: Variation of Volume of Air in UDB as function of its Mass

The figure shows an exponential relationship between the volume and mass of air defined by equation (9) below with correlation Coefficient = 0.9912:

$V = 77.649e^{0.2496m}$----------(9)

Equation (9) shows that the volume of air in the UDB varies exponentially with the corresponding mass. This is in tune with the reality since as more gas enters the bag, internal pressure of the existing air in the urine drainage bag will rise and counter the incoming air. Therefore, the increase in volume to be accommodated in the bag will reduce in an asymptotic manner.

Since the average mass of air that fills a UDB is 12.0g, then using Equation 9, volume of 12.0g of Air is computed as 632.2cm^3 which means that 1.0g of Air is equivalent to 52.68cm^3 or density of Air is 0.0190g/cm^3 at 28.5^{o}C and 101.325kPa. However, the density of air is given as 1.2250 kg/m^3 (0.00123g/cm^3) at 15^{o}C and 101.325kPa (Richard Shelquist (2019)). Thus, when Equation 9 is applied to the monitoring of biogas yield using mass of biogas in UDB (Method 6) to compute the corresponding volume of biogas a relative error of 1444.7% will be made. This underscores the weakness of the assumption.

6.4 Result of the Calibration of the UDB Mass of Air as Function of Displaced Water in Cylinder

The experiment revealed that the average mass of 15 pump strokes of air that could fill a UDB is 12.0g and the corresponding average volume of water displaced in the cylinder is 1,515cm^3. This implies that 1.0g of Air displaces 126.25cm^3 of water in a measuring cylinder or the density of the air is 0.0079g/cm^3 at 28.5^{o}C and 101.325kPa. When compared to the density of air, 1.2250 kg/m^3 (0.00123g/cm^3) at 15^{o}C and 101.325kPa, as reported by Richard Shelquist (2019), this gives a relative error of 542.28% in determining the density of air which underlines the weakness of the method.

However, since 1 Pump Stroke of Air is computed to be 173.2cm^3 based on the configuration of the cylinder of the pump, then the volume of 15 pump strokes of air which is 12.0g will be equivalent to 2,078cm^3. This implies that there is a relative error of 27.09% in estimating the volume of air by displacement of water in measuring cylinder.

Thus, the Volume of biogas is calculated from the mass using equation:

$Volume = 126.25\ x\ Mass\ of\ Biogas$.....(10)

6.5 Results of Comparative Study of Biogas Yield by Measuring Mass of Biogas in UDB and Water Displacement in Measuring Cylinder

The total biogas yield over the Hydraulic Retention Time of 56 days from the two sets of 5-biogas digesters labelled SET A and SET B are presented in Figures 6 and 7 respectively and summarized in Tables 4.1 and 4.2 respectively.

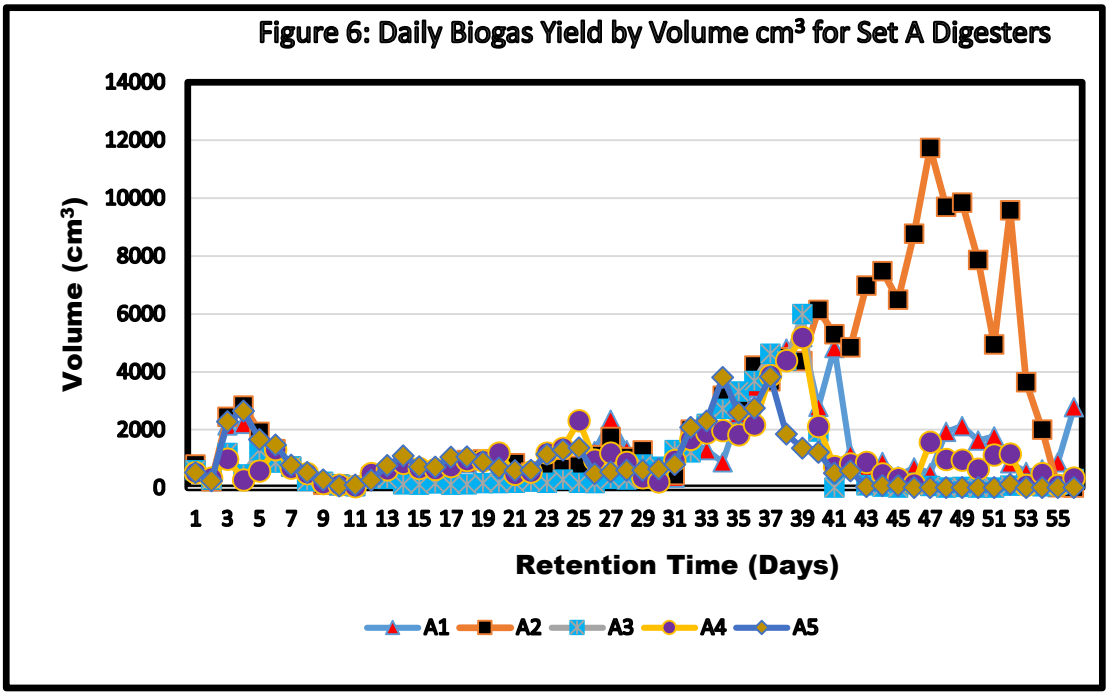

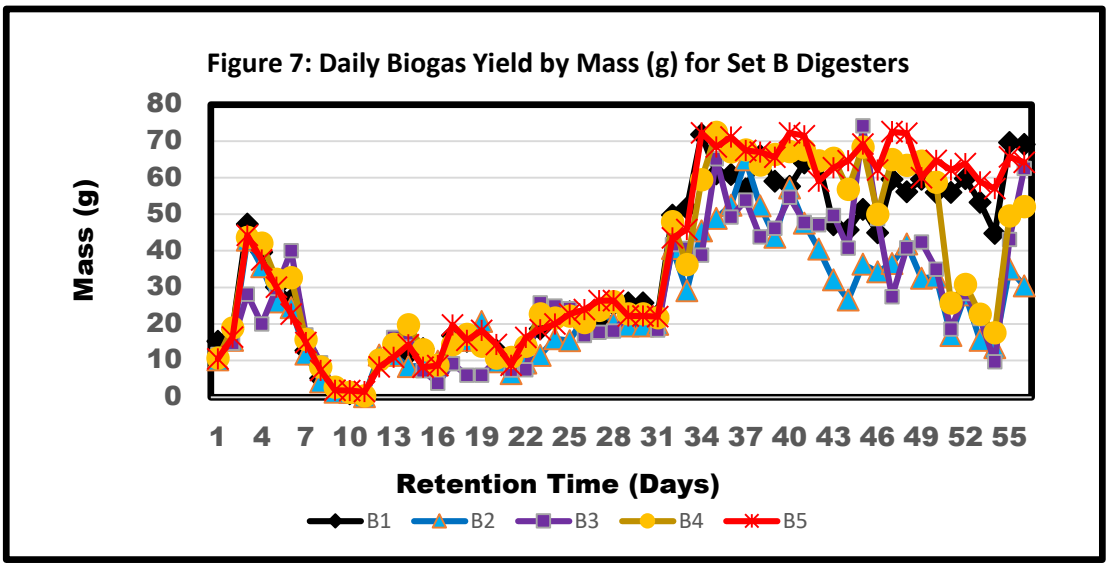

Table 4.1 Biogas Yield (Volume) over Retention Period of 56 Days for SET A Digesters

Digester	A1	A2	A3	A4	A5
Volume cm^3	73,880.00	158,690.00	43,999.00	58,920.00	49,701.00
Vol dm^3	0.07	0.16	0.04	0.06	0.05

Table 4.2 Biogas Yield (mass) over Retention Period of 56 Days for SET B Digesters

Digester	B1	B2	B3	B4	B5
Mass (g)	1,972	1,403	1,536	1,931	2,139
Mass (Kg)	1.97	1.40	1.54	1.93	2.14

The 10 Digesters were assumed to have same slurry concentration and composition but the biogas yield for SET A was monitored by displacement of water in measuring cylinder and the biogas yield for SET B was monitored by weighing the mass of biogas in UDB. Careful examination of Figure 6 shows that the yield of Digester A_2 was significantly higher than those of Digesters A_1, A_3, A_4 and A_5 in the 8^{th} week. Therefore, the Fisher's Fisher Pairwise Comparisons test was conducted to ascertain if the difference is significant. The test shows (Appendix I) that the means of biogas yield of Digesters A_1, A_3, A_4 and A_5 are not significantly different, while that of Digester A_2 is significantly different from those of Digesters A_3, A_4 and A_5 but not significantly different from that of Digester A_1. This suggests that the composition of the slurry in Digester A_2 is different. This is clearer is clearer in Table 4.1 with the volume (158,690cm^3) of Digester A_2, being twice more than that of each of the other four digesters A1, A3, A4 and A5.

On the other hand, Figure 7 shows the plot of daily biogas yield for the SET B Digesters which reveals a clustering of the five digesters which suggests that the composition of the slurries in the five digesters are similar. This is corroborated by the Fisher's Pairwise Comparisons test which shows (Appendix II) that the means of biogas yield of Digesters B_1, B_2, B_3, B_4 and B_5 are not significantly different. These imply that the composition of the slurry in Digester A2 has different composition from the those of the other nine digesters. Therefore, the biogas yield for Digester A2 and the Corresponding Digester B2 will not be used for further analysis. Only four digesters each for Sets A and B will be used for the analysis as given in Table 4.3 below:

Table 4.3 Comparative Analysis of Total Biogas Yield Measured by Mass and Volume

SET A Digester	**Volume (cm^3) in 56 days**	**SET B Digester**	**MASS (g) in 56 Days**	**Volume (cm^3) based on Ideal Gas Model Equation (6)**	**Volume (cm^3) Based on Mass of Air in Urine Bag. Equation (9)**	**Volume (cm^3) based on Displaced Water in Measuring Cylinder Equation (10)**
A1	73,880	**B1**	1,972.08	58,298.63	103,889.17	248,975.10
A3	43,999	**B3**	1,536.03	45,408.12	80,918.06	193,923.79
A4	58,920	**B4**	1,930.93	57,082.15	101,721.39	243,779.91
A5	49,701	**B5**	2,139.11	63,236.37	112,688.31	270,062.64
Average	56,625		1,894.53	56,006.32	99,804.23	239,185.36
Relative Diff (%)				-1.10	76.43	323.12
Density g/cm^3	0.0335			0.0338	0.0190	0.0079
Relative to Lit 0.00125g/cm3	2,580			2,604	1,420	532

The comparative analysis of the total biogas yield of the two sets of digesters assumes that the composition of the slurries of Digesters SET A and SET B have the same homogenous composition. Moreover, since all the digesters were digested under the same environmental conditions, the total yield of all the digesters will be the same within experimental error irrespective to the parameters used in measuring the yield. Consequently, to compare the biogas yield of the two sets, two approaches are used:

(a) the total of biogas yield of SET B, which were measured by mass (g), are converted to volume (cm^3) and compared directly (Table 4.3);

(b) The density (g/cm^3) of biogas is calculated using equation (3) and compared to literature value of 1.15–1.25 kg/m^3 or 1.15–1.25 x 10^{-3} g/cm^3**;** and

(c) assume the biogas to approximate ideal gas as proposed by Rajesh B. & Rajneesh K. (2019) and calculate the volume from mass using equation (6).

The results in Table 4.3 from three equations described earlier. Equation (6) assumes that biogas behaves, ideally. It is therefore not surprising that it practically reproduced the Total Biogas yield within 99.9%. The means that if the biogas production is monitored by measuring the mass of biogas produced, the yield in terms of volume could be calculated using equation 6. On the other hand, the assumption that Equation (9) simulates the reality of biogas filling of UDB, does not lead to acceptable result because the relative difference between the total volume of biogas generated in 56 days as measured using mass measurement, is 76.43% larger than the volume obtained by downward displacement of water in a cylinder. Similarly, the biogas yield calculated on calibration of UDB using the water displacement method does not lead to acceptable result because the relative difference between the volume calculated from mass measurement is 323.12 % higher than that obtained by the existing water displacement method. Moreover, calculation of the density of biogas using the total biogas yields determined using Mass Measurement and the corresponding Volume measurement, resulted in a density of 0.0335g/cm^3 compared to literature 0.00125g/cm^3 which is about 2,580% higher.

6.6 Summary of Findings

From analysis of Figures 6 and 7, and the results in Table 4.3, the following findings are made:

(i) The Biogas yield at laboratory scale experiments could be monitored by measuring the mass of biogas produced in lieu of volume measurement at given interval of time;

(ii) A method of Calibration of the Urine Drainage Bag that could give reproduceable results is necessary;

(iii) Total biogas yield in volume (cm^3) calculated using mass measurement based on the assumption that biogas approximate ideal gas behaviour give high correlation between mass and volume measurements;

(iv) Biogas yield measured by monitoring biogas mass with the assumption that filling of UDB by biogas is governed by exponentials expression give larger quantity of biogas compared to yield measured using water displacement method;

(v) Biogas yield measured by monitoring biogas mass with UDB calibrated by water displacement method give larger quantity of biogas compared to yield measured using water displacement method;

(vi) Calculation of the density of biogas based on Total Biogas yield measured by monitoring volume and mass simultaneously give highly on realistic result; and

(vii) Though mass measurement could eliminate errors due to solubility of CO_2 and partial pressure on headspace, it introduces other challenges moisture trapped in gas bobbles transferring into the UDB thereby increasing the mass.

7.0 Conclusion

Biogas yield could be successfully monitored in laboratory scale experiments and the volume computed using the equation proposed by Rajesh B. & Rajneesh K. (2019) based on biogas approximating real gas behaviour.

References

Abdulhamid M. S., Muazu B., and Kamaluddeen K., (2019). Comparative Biogas production by Anaerobic Digestion Using Sugarcane Bagasse, Cow Dung and Chicken Droppings Obtained from Katsina Metropolis as Substrates. UMYU Journal of Microbiology Research. 4(2): 70-74.

Adegunloye D. V. and Abe A. S., (2020). Co-Digestion of Cow Dung With Some Cereal Wastes for Biogas Production. Nigerian Research Journal of Chemical Sciences. 8(1): 37-51.

Adeniran K.A., Adepoju P.O., and Adepoju T.F., (2019). Comparative Study of Biogas Production from Plantain Peels Mixed with Poultry Droppings and Poultry Droppings Only. Journal of Environmental Science and Technology. *13 (2): 94- 105.*

Association of Official Analytical Chemist (AOAC), (2016) Official methods of Analysis. Association of Analytical Chemist's 14th edition. Alinton. Virginia, 2(2): 20-9.

Arent, D.J., Wise, A., Gelman, R., (2014). The status and prospects of renewable energy for combating global warming. *Energy Economics* 33, 584–593.
Bagudo, B.U., Garba, B., Dangoggo, S. M. and Hassan, L.G. (2011). The Qualitative Evaluation of Biogas Samples Generated from Selected Organic Wastes. *Scholars Research Library*, 3 (5):549-555.

Bagudo, B. U., Garba, B., Dangoggo, S. M. and Hassan, L.G. (2008). Comparative Study of Biogas Production from Locally Sourced Substrate Materials. *Nigeria Journal of Basic and Applied Sciences*, 16(2): 262-266.

Baki, A. S. (2004). Isolation and Identification of Microbes Associated with BIOGAS Production at Different Retention Time Using Cow Dung. M.Sc. dissertation, Usmanu Danfodiyo University Sokoto, Nigeria, (2004). 18–21 October.

Buck, A. L. (1981), "New equations for computing vapor pressure and enhancement factor", J. Appl. Meteorol., 20: 1527–1532 ·

Buck A. L. (1996), *Buck Research CR-1A User's Manual, Appendix 1.*

Cheng, S., Li, Z., Mang, H.P., Huba, E.M., Gao, R., and Wang, X., (2014). Development and Application of Prefabricated Biogas Digesters in Developing Countries. *Renewable Sustainable Energy Revision* 34, 387-400.

Chomini M. S., Kambai, C., John W. C., Chomini, A. E. and Fatoke V., (2021). Comparative Anaerobic Co-Digestion Effects of Some Agricultural Biomass on Their Digestates Biochemical Properties. Nig. J. Pure & Appl. Sci. 34 (1), 3929-3940.

Clinton S.W., Peter A. K. and Daudi M. N., (2020). Co-digestion of Pretreated Chicken Goat and Untreated Cow Manure at Different Substrate to Inoculums Ratios and Total Solids for Biogas Production. Bioresource technology, 99(17), 8288-8293.

Demirbas, A. and Demirbas, M.F. (2010) Green Energy and Technology, Algae Energy, Algae as a New Source of Biodiesel. Springer, London, 139-157.

Dixon N. M. and Kell D. B. (1989) , "The control and measurement of 'CO2' during fermentations," Journal of Microbiological Methods, Vol 10, p.p 155 -176, 1989.

Egbekun, M.K. and Ehieze, M.U., (1997). Proximate Composition and Functional Properties of Full Fat and Defatted Beniseed (Sesamum indicum L.) Flour. *Plant Foods for Human Nutrition*, 51, 35-41.

Ezekoye, V. A. (2019). Biogas Generation From Plant and Animal Wastes, Its Purification, Compression and Storage/Usage. International Journal of Scientific Research. 2(7), 31-34.

Fatima M. , Aliyu A., Ummasalma A. S. and Hadiza G., (2018). Biogas Production From Cow Dung for Sustainable Energy Generation. *UMYU Journal of Microbiology Research.* 3(1): 81-86.

Gomez, K.A. and Gomez A.A., (1984). Statistical Procedures for Agricultural Research (2 ed.). John wiley and sons, NewYork, 680p.

Guwy A. J. (2004), "Equipment used for testing anaerobic biodegradability and activity," Reviews in Environmental Science and Bio/Technology, Vol. 3, p.p 131–139, 2004.

Guwy A. J., (2010). Equipment used for Testing Anaerobic Biodegradability and Activity. *Environmental Science and Bio/Technology,* 3(6), 131–139.

Hawkes F. R., Guwy A. J., Rozzi A. G. and Hawkes D. L. (1997);, "A new instrument for on-line measurement of bicarbonate alkalinity," Water Research, Volume 27, 1993, p.p 167-170, 1997

Hendriks, A. T. and Zeeman, G., (2009). Pretreatments to Enhance the Digestibility of Lignocellulosic Biomass. *Bioresource Technology*, 100(1), 10–18.

Ibarra-Gonzalez, P., and Rong, B.G. (2019). A Review of the Current State of Biofuels Production from Lignocellulosic biomass using thermochemical conversion routes. *Chin. J. Chem. Eng*., 27: 1523–1535

International Energy Agency (IEA). (2016). IEA Bioenergy Task 37 Country Reports Summary 2015. http://www.ieabioenergy.com/wpcontent/uploads/2015/01/ IEA-Bioenergy-Task-37-CountryReport-Summary 2014_Final.pdf.

International Society of Automation (2016). 67 T.W. Alexander Drive, Research Triangle Park NC 27709.

IPCC, (2013): Summary for Policymakers. In: Climate Change 2013: The Physical Science Basis. Contribution of Working Group I to the Fifth Assessment Report of the Intergovernmental Panel on Climate Change [Stocker, T.F., D. Qin, G.-K. Plattner, M. Tignor, S.K. Allen, J. Boschung, A. Nauels, Y. Xia, V. Bex and P.M. Midgley (eds.)]. Cambridge University Press, Cambridge, United Kingdom and New York, NY, USA.

Khalid A., Arshad M., Anjum M., Mahmood T., and Dawson L., (2011). The anaerobic digestion of solid organic waste. Waste Manag. 1(8):1737-44. doi: 10.1016/j.wasman.2011.03.021. Epub 2011 May 6. PMID: 21530224.

Massé D.I., Talbot G. and Gibert Y., (2011). In Farm Biogas Production: A Method to Reduce GHG Emissions and Develop More Sustainable Livestock Operations, *Animal Feed Sci. and Techn*., 16(6); 436-445.

Mohammad A., Prakash P., Tareq A., and Gordon M., (2020). Potential of Biocrude Production from Camel Manure via Hydrothermal Liquefaction: A Qatar Case Study. *12th International Exergy, Energy and Environment Symposium (IEEES-12), Dec 20-24, 2020, Doha, Qatar.*

Moses A. O., O. O. & Noor A. A., (2018). Quality of Optimized Biogas Yields From Co-Digestion of Cattle Dung with Fresh Mass of Sunflower Leaves, Pawpaw and PotatoPeels. *Cogent Engineering*. 5:1, 1538491.

Morris, J. A., & Feldman, D. C. (1996). The Dimensions, Antecedents and Consequences of Emotional Labor. Academy of Management Review, 21, 986-1010.

Mould, R., Morgan, K. E., and Kliem, E. K., (2015). A Review and Simplification of the in-Vitro Incubation Medium. *Animal Feed Science and Technology*, 172 (155): 155-172.

Muhammad C., Muhammad M., Muhammad S. J. , Musa U. D., Aliyu S. B., (2019). Assessment of Low Temperature Refining Process of Castor Seed Oil for Biodiesel Production. *American Journal of Chemical and Biochemical Engineering,*3(1): 1-6.

Musa I. T, Tinia I. M., Razif M. H., and Azni I., (2014). Effect of Carbon to Nitrogen Ratio of Food Waste on Biogas Methane Production in a Batch Mesophilic Anaerobic Digester, International Journal of Innovation, Management and Technology, 5(2); 116-119.

Néel B., and Deike L., (2021). Collective Bursting of Free-Surface Bubbles, and the Role of Surface Contamination. *Journal of Fluid Mechanics, 917*(46): 265- 272.

Nijaguna B. T. 2002; "Biogas Technology," New Age International, pp.46-48, 2002

Ukpai, P. A. and Nnabuchi, M. N., (2012). Comparative Study of Biogas Production from Cow Dung, Cow Pea and Cassava Peeling using 45 Litres Biogas Digester. *Advances in Applied Science Research,* 3 (3):1864-1869.

OECD. (2020). Renewable energy (indicator), https://doi.org/10.1787/aac7c3f1-en (accessed on 07 April 2020).

Okeh, C.O., Onwosi, C.O. and Odibo, F.J.C., (2014). Biogas Production from Rice Husks Generated from various Rice Mills in Ebony State, Nigeria. *Renewable Energy,* 62, 204- 208.

Orhorhoro, E. K., Ebunilo, P. O. and Sadjere, G. E. (2017). Experimental Determination of Effect of Total Solid (TS) and Volatile Solid (VS) on Biogas Yield. *American Journal of Modern Energy*, 3(6), 131-135

Ozor, O. C., Agah, M. V., Ogbu, K. I., Nnachi, A. U., Udu-ibiam, O. E. and Agwu, M. M. (2014). Biogas Production using Cow Dung from Abakaliki Abattoir in South-Eastern Nigeria. International Journal of Scientific & Technology Research, 3(10), 2277-8616.

Petersson A. and Wellinger A. (2009), "Biogas upgrading technologies – developments and innovations," IEA Bioenergy, 2009. Available online: www.iea-biogas.net

Pham C. H., Triolo J. M., Cu T.T.T, Pedersen L, and Sommer S. G., 2013; Validation and Recommendation of Methods to Measure Biogas Production Potential of Animal Manure, Asian-Australasian Journal of Animal Sciences (AJAS) ,Vol. 26, No. 6 : 864-873 June 2013 https://doi.org/10.5713/ajas.2012.12623

Pipatmanomai S., Kaewluan S., and Vitidsant T., (2014). Economic Assessment of Biogas-to-Electricity Generation System with H_2S Removal by Activated Carbon in Small Pig Farm. *Applied Energy*, 86, 669-674.

Prakash P., (2011). Master Thesis: Biogas Measurement Techniques and the Associated Errors. *Environmental Science and Technology,* 3(1),22-67.

Rajesh B. and Rajneesh K. (2019) Experimental and numerical study of biogas, methane and carbon dioxide produced by pre-treated wheat straw and pre-digested cow dung, International Journal of Sustainable Engineering, 12:4, 240- 247, DOI: 10.1080/19397038.2019.1605548

Richard Shelquist (2019). An Introduction to Air Density and Density Altitude Calculations, https://wahiduddin.net/calc/density_altitude.htm accessed 28-03-2022.

Sajeena B. B., Jose P.P. and Madhu G., (2013). Effect of Total Solid Concentration on Anaerobic Digestion of the Organic Fraction of Municipal Solid Waste. *International Journal of Scientific and Research Publications,* 3(8), 1–5.

Sindibu T., Solomon S.S., and Ermias D., (2018). Biogas and Bio-fertilizer Production Potential of Abattoir Waste as Means of Sustainable Waste Management Option in Hawassa City, Southern Ethiopia. *Journal of Applied Science and Environmental Management*. 22 (4) 553 – 559.

Surve P., Konde H., Yadav S., Makhare P. and 'Shaikh Ummid I. (2015). An Investigation of Compression and Purification of Biogas and It's use for Domestic Instant Water Heating Application. International Journal of Engineering Sciences & Research Technology (I2OR), Publication Impact Factor: 3.785 (ISRA), Journal Impact Factor: 2.114 ISSN: 2277-9655.

Sumarli S., Citrakara U. S., Retno W., and Sukarni S., (2019). Physicochemical Characteristics of Corn Silk as Biomass Fuel Feedstock. Conference Series: Materials Science and Engineering. 515 012103.

Stocker, T.F., D. Qin, G.-K. Plattner, L.V. Alexander, S.K. Allen, N.L. Bindoff, F.-M. Bréon, J.A. Church, U. Cubasch, S. Emori, P. Forster, P. Friedlingstein, N. Gillett, J.M. Gregory, D.L. Hartmann, E. Jansen, B. Kirtman, R. Knutti, K. Krishna Kumar, P. Lemke, J. Marotzke, V. Masson-Delmotte, G.A. Meehl, I.I. Mokhov, S. Piao, V. Ramaswamy, D.Randall, M. Rhein, M. Rojas, C. Sabine, D. Shindell, L.D. Talley, D.G. Vaughan and S.-P. Xie, (2013): Technical Summary. In: Climate Change 2013: The Physical Science Basis. Contribution of Working Group I to the Fifth Assessment Report of the Intergovernmental Panel on Climate Change. Cambridge University Press, Cambridge, United Kingdom and New York, NY, USA.

Syed, Z. I., (2006). A Case Study to Bottle the Biogas in Cylinders as Source of Power for Rural Industries Development in Pakistan. World Applied Sciences Journal 1 (2): 127-130, ISSN 1818-4952.

Soroush D., Prashant K., Christian E., and Wolfgang R., (2021). On the Effect of Biogas Bubbles in Anaerobic Digester Mixing. *Biochemical Engineering Journal, 173, 108088.*

Tambuwal, A.D., Dangoggo, S.M. and Zuru A.A. (1997). Physico-Chemical Studies on Biogas. *Nigerian Journal of Renewable Energy*, 5 (1 & 2): 98-100.

Tambuwal, B.M., Baki, A.S., Bello, A., Musa, A.R. and Bello, M.R. (2019). Biogas Generation Using Cattle Rumen Contents. *Acta Scientific Medical Sciences* 3(4): 22-30.

Tambuwal A.D and Ogbiko C., (2018). Proximate and Chemical Analyses of Selected Agricultural Wastes Used for Biogas Production. *Science Research Annals.* 9(1): 56-60.

Vasco-Correa, J., Khanal, S., Manandhar, A., and Shah, A. (2018). Anaerobic digestion for bioenergy production: global status, environmental and techno-economic implications, and government policies. *Biores Technol,* 247:1015–1026.

Water Science School (2018); Water Density, US Geological Survey.https://www.usgs.gov/special-topics/water-science- school/science/water-density#overview, accessed 8-03- 2022.

Wijngaarden L. V., (2010). Mechanics and physics of bubbles in liquids. Martinus Nijhoff Publishers, p.p 38-40.

World Energy Council (2017), World Energy Resources report. Published by World

Yavini T. D., Azuaga I. C., and Agabison J., (2014). Evaluation of the Effect of Total Solids Concentration on Biogas Yields of Agricultural Wastes. *International Research Journal of Environment Science*. 3(2), 70-75.

Yusuf M.O.L., Debora A. and Ogheneruona D.E., (2011). Ambient Temperature Kinetic Assessment of Biogas Production Co-digestion of Horse and Cow Dung, *Res. Agr. Eng.,* 57(3), 97–104.

Zuru, A.A., Dangoggo, S.M., Birnin-Yauri, U.A. and Tambuwal A.D., (2004). Adoption of thermogravimetric Kinetic Models for Kinetic Analysis of Biogas Production Article in Renewable Energy DOI: 10.1016/S0960-1481(03)00074-0.

Zuru, A.A., Saidu, H., Odum, E.A. and Onuorah, O.A., (2000). A Comparative Study of Biogas Production from Horse, Goat and Sheeps Dungs. Nigerian Journal of Renewable Energy Vol., 6, Nos 1 & 2. pp. 43-47.

APPENDIX 1 Calibration of Urine Bag using Random Mass Bag and Volume of Water in Cylinder

Urine bags	Mass of Empty bag	Mass of Water in urine bag (g)	Volume of water in cylinder (ml)
A	8g	1801	1820
B	8g	1895	1930
C	8g	1855	1890
D	8g	1853	1870
E	8g	1869	1910
F	8g	1874	1920

APPENDIX 2: Calibration of Urine Bag Using Volume of Water as Function of Mass of Water

S/N	Mass (g)	Volume (ml)
1.	379	446
2.	758	806
3.	1137	1156
4.	1516	1540
5.	1896	1916

Table 4.3: Calibration of Urine Bag Using Mass of Air and Volume of Water Displaced in a Cylinder

Urine bag	No of Strokes	Mass of (Bag + Air)(g)	Volume (ml)
A	15	12	1,500
B	15	13	1,600
C	15	12	1,510
D	15	11	1,460
E	15	12	1,500
F	15	12	1,520
Average	**15**	**12**	**1,515**

HEAVY METAL IONS DETECTION BY ELECTROCHEMICAL SENSING METHOD WITH LOW TEMPERATURE SYNTHESIZED OF NANOSTRUCTURED MgNiO2 BASED ELECTRODE

Mohammad Imran[a,d] , Eun-Bi Kim[b], Mohammad Shaheer Akhtar[c], Dong-Heui Kwak[d], Sadia Ameen[a]

[a]Advanced Materials and Devices Laboratory, Department of Bio-Convergence Science, Jeonbuk National University, Jeongeup Campus, 56212, Republic of Korea

[b]Energy Materials & Surface Science Laboratory, Solar Energy Research Center, School of Chemical Engineering, Jeonbuk National University, Jeonju 54896, Republic of Korea

[c]New & Renewable Energy Material Development Center (NewREC), Jeonbuk National University, Jeonbuk, Republic of Korea

[d]Environmental Engineering Laboratory, Department of Bioactive Material Sciences,

Jeonbuk National University, Jeonju 54896, Republic of Korea,

ABSTRACT

The industrial wastes from textiles and dyes factories cause the severe threat to environment. In particular, the heavy metal ions are the main source for the toxicity of aquatic ecosystem. Thus, a rapid and sensitive detection method is required for toxicological assessment, ecological protection and human health. In this work, $MgNiO_2$ nanostructures were synthesized by a simple and cost-effective hydrothermal method for the electrochemical sensing application for the detection of heavy metal ions. The synthesized $MgNiO_2$ nanostructures were thoroughly characterized in terms of morphology, crystal quality, structural and electrochemical properties by various analysis tools. The morphological analysis revealed that synthesized $MgNiO_2$ exhibited a rose like structure having the average size of 20~25nm. The XRD patterns of synthesized $MgNiO_2$ were well matched with JCPDS card 24-0712, corresponding to crystallographic planes of spinal structure. To check the sensing behavior, the synthesized $MgNiO_2$ nanostructures were used as electro-active electrode to fabricate the electrochemical sensor towards heavy metal ions. The reasonable and rapid sensing behavior to heavy metal ions was recorded by the fabricated electrochemical sensor based on synthesized $MgNiO_2$ electrode.

Keywords- MgNiO2, Heavy metals, cyclovoltammetry, electrochemical sensor

BIO-ELECTRO FENTON PROCESS FOR TREATMENT OF ANTIDEPRESSANT POLLUTANT: PERFORMANCE ENHANCEMENT

Loubna Rachidi

PhD student., Faculty of Sciences of Rabat, University Mohammed V, Laboratory of Materials, Nanotechnology and Environment

Ghizlan Kaichouh

Pr., Faculty of Sciences of Rabat, University Mohammed V, Laboratory of Materials, Nanotechnology and Environment

Aicha Guessous

Pr., Faculty of Sciences of Rabat, University Mohammed V, Laboratory of Materials, Nanotechnology and Environment

ABSTRACT

The Electro-Fenton process design as being one of the most powerful and environmentally friendly emerging technologies for the remediation of wastewater containing organic compounds such as aromatics, which is also widely applied for the degradation of pharmaceutical products (Nidheesh and Gandhimathi, 2012; Barhoumi et al., 2016).

Nevertheless, Electro- Fenton processes used for complete mineralization can be expensive, and hence its combination with a biological treatment can significantly reduce operating costs.

in this study, the objective is to apply two processes electro-Fenton and biologic by coupling each other. In this sense, a follow-up of the mineralization of the pollutant antidepesseur, the biodegradability of the by-products of electrolysis during the electro-Fenton process and the biological treatment were examined.

To confirm the improved coupling between the electro-Fenton process and biological treatment, an activated sludge culture of the by-product solutions was performed after 2h or 3 h of electrolysis. To this end, the results obtained showed that the mineralization rates of the biodegradable part of the by-products of the pollutant antidepressant by activated sludge is almost fast and reaches 72%, 80% after 2 days of culture for a pretreatment time of 2h and 3h respectively.

Keywords: Electro-Fenton, Biodegradability.

ZAMAN SKALASINDA DÖRDÜNCÜ MERTEBEDEN SINIR DEĞER PROBLEMİNİN SİMETRİK ÇÖZÜMLERİNİN VARLIĞI

EXISTENCE OF SYMMETRIC SOLUTIONS FOR FOURTH ORDER BOUNDARY VALUE PROBLEMS ON TIME-SCALES

Sümeyra İBİŞ[1]

[1]Ege Üniversitesi, Fen Bilimleri Enstitüsü, Matematik Bölümü, İzmir, Türkiye

[1]ORCID ID: https://orcid.org/0000-0002-9207-1564

Erbil ÇETİN[2]

[2]Ege Üniversitesi, Fen Fakültesi, Matematik Bölümü, İzmir, Türkiye

[2]ORCID ID: https://orcid.org/0000-0002-3785-7011

ÖZET

Bu çalışmada $a, b \in \mathbb{T}$, $\alpha, \beta \geq b - a$ ve $\mathbb{T}$ herhangi bir simetrik zaman skalası (yani $t_1 \leq t_2$ için $t_1 = b - t_2 + a$) olmak üzere

$$-\left(-\zeta^{\Delta\nabla}\right)^{\Delta\nabla} = f(t,\xi), \qquad t \in \mathbb{T}_{\kappa^2}^{\kappa^2}$$
$$-\left(-\xi^{\Delta\nabla}\right)^{\Delta\nabla} = g(t,\zeta), \qquad t \in \mathbb{T}_{\kappa^2}^{\kappa^2}$$

dinamik denklem sistemi

$$\zeta(t) = \zeta(b - t + a), \qquad \alpha\left[(\zeta^{\Delta\nabla})^{\Delta}(\sigma(a)) - (\zeta^{\Delta\nabla})^{\Delta}\rho^2(b)\right] = \zeta^{\Delta\nabla}(t_1) + \zeta^{\Delta\nabla}(t_2)$$
$$\xi(t) = \xi(b - t + a), \qquad \beta\left[(\xi^{\Delta\nabla})^{\Delta}(\sigma(a)) - (\xi^{\Delta\nabla})^{\Delta}\rho^2(b)\right] = \xi^{\Delta\nabla}(t_1) + \xi^{\Delta\nabla}(t_2)$$

dört noktalı sınır değer koşullarıyla birlikte ele alınmıştır. Ayrıca, bu çalışma boyunca $f(t,0) \equiv g(t,0) \equiv 0$ olmak üzere $f: \mathbb{T} \times [0,\infty) \to [0,\infty)$ ve $g: \mathbb{T} \times [0,\infty) \to [0,\infty)$ ile tanımlanan fonksiyonların ld-sürekli ve simetrik olduğu kabul edilmiştir. Bu çalışmada temel amacımız, ele aldığımız dördüncü mertebeden dört noktalı sınır değer problem sisteminin en az bir veya en az iki simetrik pozitif çözümünün varlığını göstermektir. Bunun için öncelikle problemin Green fonksiyonu elde edilmiştir. Ayrıca bu fonksiyon yardımı ile dördüncü mertebeden dinamik denklem sistemi integral denklem şeklinde ifade edilmiştir. Daha sonra Banach uzayında tanımlanan operatörün tamamen sürekli olduğu gösterilmiştir. Krasnosel'skii sabit nokta teoremi yardımı ile uygun koni belirlenerek bu operatörün sabit noktalarının varlığı gösterilmiştir. Sonuç olarak, problemimizin yeterli ve uygun koşullar altında en az bir veya en az iki simetrik pozitif çözümünün var olduğu ispatlanmıştır. Daha sonra ana sonucu destekleyen örneklere yer verilmiştir.

Anahtar Kelimeler: Zaman Skalası, Sınır Değer Problemler Sistemi, Krasnosel'skii Sabit Nokta Teoremi, Pozitif Çözüm, Simetrik Çözüm

ABSTRACT

In this study, we consider the dynamic equation system

$$-\left(-\zeta^{\Delta\nabla}\right)^{\Delta\nabla} = f(t,\xi), \qquad t \in \mathbb{T}_{\kappa^2}^{\kappa^2}$$
$$-\left(-\xi^{\Delta\nabla}\right)^{\Delta\nabla} = g(t,\zeta), \qquad t \in \mathbb{T}_{\kappa^2}^{\kappa^2}$$

with four-point boundary conditions

$$\zeta(t) = \zeta(b - t + a), \qquad \alpha\left[(\zeta^{\Delta\nabla})^{\Delta}(\sigma(a)) - (\zeta^{\Delta\nabla})^{\Delta}\rho^2(b)\right] = \zeta^{\Delta\nabla}(t_1) + \zeta^{\Delta\nabla}(t_2)$$
$$\xi(t) = \xi(b - t + a), \qquad \beta\left[(\xi^{\Delta\nabla})^{\Delta}(\sigma(a)) - (\xi^{\Delta\nabla})^{\Delta}\rho^2(b)\right] = \xi^{\Delta\nabla}(t_1) + \xi^{\Delta\nabla}(t_2)$$

where $\mathbb{T}$ is bounded symetric time scale (with $a = min\mathbb{T}$, $b = max\mathbb{T}$) and $\alpha, \beta \geq b - a$. Also throughout this study, $f, g: \mathbb{T} \times \mathbb{R}^+ \to \mathbb{R}^+$functions are assumed ld-continuous and symmetric such that $f(t, 0) \equiv g(t, 0) \equiv 0$. Our main purpose in this study is to show the existence of at least one or at least two symmetric positive solutions of the fourth order four-point boundary value problem system. Firstly, the Green's function of the problem is obtained. In addition, with the help of this function, the fourth order dynamic equation system is expressed as an integral equation. Then, it is shown that the operator defined in Banach space is completely continuous. The existence of fixed points of this operator is shown by determining the appropriate cone with Krasnosel'skii fixed point theorem. As a result, the existence of at least one or at least two symmetric positive solutions of the problem under suitable and sufficent conditions has been proven. In finally, examples are given that support the main result.

Keywords: Time Scale, Boundary Value Problems System, Krasnosel'skii Fixed Point Theorem, Positive Solution, Symmetric Solution

PHOTOCATALYTIC DEGRADATION OF SULFAMETHAZINE IN THE PRESENCE OF COPPER/PERYLENE DIIMIDE SUPRAMOLECULAR CATALYSTS

Ozan Can Yıldız [1]

[1] Ege University, Faculty of Engineering, Chemical Engineering Department, İzmir, Turkey

[1]ORCID ID: https://orcid.org/0000-0002-7603-0455

Burcu Palas [2]

[2] Ege University, Faculty of Engineering, Chemical Engineering Department, İzmir, Turkey

[2]ORCID ID: https://orcid.org/0000-0002-2815-0057

Gülin Ersöz [3]

[3] Ege University, Faculty of Engineering, Chemical Engineering Department, İzmir, Turkey

[3]ORCID ID: https://orcid.org/0000-0002-5875-5946

ABSTRACT

Wastewaters contaminated with veterinary antibiotics poses a serious problem for surface and drinking water. Among various antibiotic groups, sulfamethazine receives great attention since it is used in large quantities in the treatment of human and animal infections and kidney disorders. Presence of sulfamethazine in water bodies threaten to environmental and human health due to its recalcitrant and persistent nature. Therefore, it is of significance to develop efficient and environmentally friendly treatment systesm for the removal of veterinary antibiotics. In this frame, the main target of this study is the removal of veterinary antibiotic, sulfamethazine from aqueous solutions by photo Fenton-like oxidation using supramolecular catalysts. Copper impregnated perylene diimidide (Cu/PDI) supramolecular catalyst was synthesized and its photocatalytic performance was investigated under visible light irradiation. A parametric study was carried out by the application of response surface methods to investigate the interactive effects of reaction parameters. Box-Behken Design was used to examine the influences of catalyts loading, pH and oxidant dosage on sulfamethazine degradation. The optimum reaction conditions were determined in the parametric studies and kinetic studies were carried out under these optimum conditions. In the presence of Cu/PDI catalyst, 80.5% sulfamethazine removal was obtained under the optimum conditions, which were determined as 1 g/L catalyst loading, pH 7, and 7.88 mM initial hydrogen peroxide concentration. The degradation of sulfamethazine fit to second order reaction rate model and the activation energy was calculated as 27.3 kJ/mol in the presence of Cu/PDI catalyst.

Keywords: Photocatalytic Degradation, Veterinary Antibiotic, Supramolecular Catalyst, Response Surface Methods, Kinetic Study

METAL OXIDE BASED SOLAR CELLS: IMPROVEMENT IN CELL PERFORMANCE

Saadet YILDIRIMCAN[1,2]

[1]Mersin University, Vocational School of Technical Sciences, Department of Medical Services and Techniques, Program of Opticianry, Mersin, Turkey

[2]Mersin University, Department of Nanotechnology and Advanced Materials, Institute of Science, Mersin, Turkey

ORCID ID: https://orcid.org/0000-0002-9044-6908

ABSTRACT

Researchers have recently focused on solar cell studies due to the increasing need for eco-friendly, renewable and sustainable energy sources. Metal oxide materials are widely used in many applications such as optoelectronic devices, lasers, biosensors, photocatalysis and solar cells. These materials are of great interest in such studies because of their functional properties such as optical, magnetic and electronic. Especially, metal oxide thin film studies play an important role in solar cell applications. The morphological and crystallographic structure, surface roughness, film thickness and porous structure of the obtained metal oxide thin films are crucial parameters affecting the solar cell efficiency. Besides, different production techniques such as chemical vapor deposition, spin coating, dip coating, DC sputtering, molecular beam epitaxy, thermal evaporation and pulsed laser deposition are used in the production of metal oxide materials. These materials can be coated layer by layer on substrates such as indium doped tin oxide (ITO) and fluorine doped tin oxide (FTO) glass. In addition, there are many studies on different types of solar cells in the literature. Some of them are dye-sensitized, multi-junction, perovskite, organic, hybrid and silicon solar cells. The solar cell efficiency and other photovoltaic properties can be analyzed using the solar simulator device. The photovoltaic parameters (fill factor, efficiency, open-circuit voltage and short-circuit current) of solar cell varies according to the production method and the type of used metal oxide. In the present study, the production methods of metal oxide semiconductor materials and their effects on solar cell efficiency will be discussed.

Keywords: Metal Oxide, Production Method, Solar Cell, Efficiency

PRELIMINARY RESULTS ON THE ELECTROMAGNETIC ACTUATOR INTEGRATED MAGNETIC PARTICLE IMAGING SYSTEM

ELEKTROMANYETİK AKTÜATÖR ENTEGRE MANYETİK PARÇACIK GÖRÜNTÜLEME SİSTEMİ ÜZERİNE ÖN SONUÇLAR

Mert ŞENER[1]

[1] Ege University, Graduate School of Natural and Applied Sciences, Department of Mechanical Engineering, İzmir, Turkey.

[1]ORCID ID: https://orcid.org/0000-0002-9343-948X

Hicran BEŞİKCİ[2]

[2]Ege University, Graduate School of Natural and Applied Sciences, Department of Biomedical Technologies, İzmir, Turkey.

[2]ORCID ID: https://orcid.org/0000-0001-5360-7074

Şeyma ÖZKAN[3]

[3] Dokuz Eylül University, Graduate School of Natural and Applied Sciences, Department of Chemistry, İzmir, Turkey.

[3]ORCID ID: https://orcid.org/0000-0002-0255-3763

Barış Oğuz GÜRSES[4]

[4] Ege University, Engineering Faculty, Department of Mechanical Engineering, İzmir, Turkey.

[4]ORCID ID: https://orcid.org/0000-0002-2755-3452

Mutlu BOZTEPE[5]

[5] Ege University, Engineering Faculty, Department of Electrical & Electronics Engineering, İzmir, Turkey

[5] https://orcid.org/0000-0002-2750-5784

Aysun BALTACI[6]

[6] Ege University, Engineering Faculty, Department of Mechanical Engineering, İzmir, Turkey.

[6]ORCID ID: https://orcid.org/0000-0003-1818-6651

ABSTRACT

The sending of a structure to the human body in order to eliminate health problems has occupied science fiction cinema and literature for many years. This dream has gained a reality today with the help of micromanufacturing methods and developments in robotics and has taken the name of microrobotics. Micro/nano robots, as their names suggest, are micrometer or nanometer sized robotic systems that can perform desired functions. Microrobots, which are at the intersection of MEMs and robotics, are robots with a characteristic size of less than 1 mm. Microrobots, which are a new research topic, are predicted to have medical applications such as drug delivery, micromanipulation and biopsy in the future. Studies on magnetic manipulator systems have reached a certain maturity in applying force and torque. For example, the OCTOMAG system has reached the initiation phase of clinical trials and will likely find clinical application in the coming years. The most important feature of OCTOMAG that makes it unique is that the microrobot can be observed optically through the pupil throughout the operation. This feature is unique to intraocular operations and is not present in other intracorporeal operations. This shortcoming is one of the biggest

obstacles to the introduction of microrobotic technology into clinical trials. Magnetic particle imaging (MPI) method is a new imaging method that determines the positions of structures in space based on the non-linear magnetic responses of magnetic particles and has minimal harm to human health. The applications of the MPI method on the orientation of microparticle and catheter systems are a current issue, and especially its application in targeted drug delivery is being studied. In this study, a magnetic particle imaging system is designed and integrated to an eight coils electromagnetic actuator system. Gradient and excitation coils are designed with electromagnetic finite element method. Position of the Fe3O4 based microrobot is monitored by the proposed MPI system.

Keywords: Magnetic particle imaging, electromagnetic actuator, microrobot

ASPERGİLLUS TÜRLERİ: FARKLI ORGANİZMALAR ÜZERİNDEKİ PATOJENİTESİ, BİYOTEKNOLOJİK KULLANIMI VE BİYOBOZUNMA KAPASİTESİ

ASPERGILLUS SPECIES: PATHOGENICITY ON DIFFERENT ORGANISMS, BIOTECHNOLOGICAL USE AND BIODEGRADATION CAPACITY

Saniye Elvan ÖZTÜRK[1]

[1]Aksaray Üniversitesi, Fen Edebiyat Fakültesi, Moleküler Biyoloji ve Genetik Bölümü, Aksaray, Türkiye.

[1]ORCID ID: https://orcid.org/0000-0003-4399-8299

ÖZET

Aspergillus cinsi üyelerinin yaklaşı olarak 400 türü bulunmaktadır. Bunlardan bazıları toksik özellik gösterirken bazıları göstermemektedir. Aspergillus cinsi ile yapılan çalışmalar son yıllarda giderek önem kazanmıştır.

Aspergillus üyelerinin faydaları listelendiğinde organik (selüloz gibi) ve sentetik (polietilenglikol gibi) materyalleri degrede etme ve ayrıca enzim üretebiliyor olmaları vardır. Bu yüksek çeşitlilikte iş yapabilme kapasitesi ise bazı Aspergillus türlerinin (Örneğin *Aspergillus flavus*) doğada diğerlerinden daha sık karşılaşılmasına neden olmaktadır.

Aspergillus türlerinin patojenik etkilerini ise hem bitkilerde, hem insanlarda hem de hayvanlarda görmek mümkündür. Toksik etkiler gösteren suşların da çeşitli biyokontrol yöntemleriyle ortamdan uzaklaştırılması sağlanmaya çalışılmaktadır. Bu amaçla bazı bitki sekonder moleküllerinin önemi de giderek artan ilgiye sahiptir.

İklim koşullarındaki değişiklikler ve çevre kirliliğinin artışı gibi etmenler canlılar üzerinde geri dönüşü imkânsız sonuçlar ortaya çıkarmaktadır. Bu sebeplerle çevreye zarar vermeyen ya da nispeten daha az zararlı yöntemlerin araştırılması giderek önem kazanmaktadır. Tarımsal uygulamalarda bu metotların yaygınlaşması sayesinde de insan ve hayvan sağlığına verilen zararın yok edilmesi ya da aza indirgenmesi planlanmaktadır. Ayrıca sentetik maddelerin (örneğin polietilenglikol) bozundurulması ve bunlardan doğal ikincil bileşikler sentezlenmesine ve hatta toksik olan mikotoksinlerin azaltımına kadar pek çok alanda çevre duyarlı metotlar kullanılabilecektir.

Yaygın olarak Aspergillus türlerini ortadan kaldırma yöntemi olarak kimyasal ve fiziksel uygulamalar kullanılmaktadır. Ancak bu yöntemlerin yukarıda bahsi geçen sebeplerle kullanımlarının kısıtlanması gerekmektedir. Bu nedenle toksik Aspergillus türlerinin kontrol altına alınması için kullanılan biyolojik yöntemlerden biri de uçucu yağların kullanımıdır. Uçucu yağların bu türlerin toksisitesini ve aflatoksin üretiminini kısıtladığı bulunmuştur. Diğer taraftan uçucu yağ kullanımının çeşitli sınırlamaları mevcuttur. Bu nedenle alternatif yöntemlere gidilmiştir. Nanoenkapsülasyon yöntemleri bu nedenle geliştirilen yöntemlerden biridir. Biyolojik yöntemlerde bitki ekstraktlarının kullanımına ek olarak bazı mantar ve bakterilerin izolatlarının da benzer aktiviteye sahip oldukları bulunmuştur.

Aspergillus türlerinin yayılımı ekonomik hasara ve sağlık sorunlarına yol açmakta, ancak değişen çevresel koşullar da bu türlerin yayılmaya devam etmesine neden olmaktadır. Ancak çevre dostu yöntemlerin geliştirilmesi ve yayılım yapan türlerin toksik olmayan türler lehine değiştirilmesi sayesinde verilen zararın azaltılması/yararlı ürünlere dönüştürmede kullanılmaları planlanmaktadır.

Anahtar Kelimeler: Aspergillus, Patojenite, Biyobozunma, Aflatoksin, Biyokontrol, Uçucu yağlar.

ABSTRACT

There are approximately 400 species of members of the genus Aspergillus. Some of these show toxic properties, while others do not. Studies with the genus Aspergillus have become increasingly important in recent years.

Listing the benefits of Aspergillus members is their ability to degrade organic (such as cellulose) and synthetic (such as polyethyleneglycol) materials and also to produce enzymes. This high diversity of work capacity causes some Aspergillus species (eg *Aspergillus flavus*) to be encountered more frequently in nature than others.

It is possible to see the pathogenic effects of Aspergillus species in plants, humans and animals. It is tried to ensure that the strains that show toxic effects are removed from the environment by various biocontrol methods. For this purpose, the importance of some plant secondary molecules is of increasing interest.

Factors such as changes in climatic conditions and increase in environmental pollution cause irreversible consequences on living things. For these reasons, it is becoming increasingly important to research methods that do not harm the environment or are relatively less harmful. Thanks to the widespread use of these methods in agricultural practices, it is planned to eliminate or minimize the damage to human and animal health. In addition, environmentally sensitive methods can be used in many areas, from the degradation of synthetic materials (for example, polyethyleneglycol) and the synthesis of natural secondary compounds from them, and even the reduction of toxic mycotoxins.

Chemical and physical applications are commonly used as a method of eliminating Aspergillus species. However, the use of these methods should be restricted for the reasons mentioned above. Therefore, one of the biological methods used to control toxic Aspergillus species is the use of essential oils. Essential oils have been found to limit the toxicity and aflatoxin production of these species. On the other hand, there are various limitations to the use of essential oil. Therefore, alternative methods have been used. Nanoencapsulation methods are one of the methods developed for this reason. In addition to the use of plant extracts in biological methods, isolates of some fungi and bacteria have also been found to have similar activity.

The spread of Aspergillus species causes economic damage and health problems, but changing environmental conditions cause these species to continue to spread. However, it is planned to use them in reducing the damage/conversion into useful products by developing environmentally friendly methods and changing the spreading species in favor of non-toxic species.

Keywords: Aspergillus, Pathogenicity, Biodegradation, Aflatoxin, Biocontrol, Essential oils.

CHANGES IN POSTURAL CONTROL AND KINEMATIC VARIABLES IN RESPONSE TO ANKLE JOINT TAPING IN PROFESSIONAL BASKETBALL PLAYERS

Hande ARGUNSAH[1]

[1]Acıbadem Mehmet Ali Aydınlar University, Faculty of Engineering and Natural Sciences, Biomedical Engineering Department, Istanbul, Turkey.

[1]ORCID ID: https://orcid.org/ 0000-0002-5776-1797

ABSTRACT

Ankle sprain is the most common cause of injury in team sports, from 38 to 50% of total sports injuries, and the risk of recurrence is high as twice. The major reason for recurrent ankle sprains is the chronic instability of the ankle joint, which could be related either to peroneal muscle weakness, proprioceptive deficits, or mechanical instability. Ankle taping has been one of the most common ankle support systems that restricts ankle inversion and plantar-flexion motion. The reduction is generally greater for athletes with a history of ankle sprain, although positive effects have also been shown for those with no prior injury. However, it is not exactly clear if the ability for ankle taping to reduce the prevalence of the ankle sprains is due to the mechanical restriction provided by the tape and/or due to the proprioceptive value of the adhesive tape. The purpose of this study is to investigate the effects of ankle taping on professional basketball players' postural control during the landing phase of high jump and to compare the lower extremity spatiotemporal parameters for taped and non-taped conditions. Xsens MVN wearable motion capture system is used for data collection and 12 elite male basketball players participated in the study. The results show that, kinesio taping has the potential to increase strength and better performance and balance immediately after the application. In the frontal plane, taped participants were less ankle joint inversion (mean difference= 4.1 degrees SD= 0.658).

Keywords: kinesio-tape, Xsens MVN, ankle sprain, injury prevention

INTRODUCTION

Ankle sprain is the most common cause of disability in team sports, from 38 to 50% of total sports injuries, and the risk of recurrence is high as twice (Garrick, 1977). The major reason for recurrent ankle sprains is the chronic instability of the ankle joint, which could be related either to peroneal muscle weakness, proprioceptive deficits, or mechanical instability. Furthermore, it is a common injury for athletes who perform cutting maneuvers, landings, or frequent jumps or make contact with other players. In basketball, handball, soccer, and volleyball, ankle sprains represent from 60 to %90 of the injuries, and the 75% of the athletes affected have relapses that can force them to give up their competitive practice. For these reasons, several external ankle support systems, such as athletic tape, orthoses, and high-top shoes, have been designed. These systems attempt to support the ankle joint during rehabilitation and to prevent injury or its recurrence.

It is not exactly clear if the ability for ankle taping to reduce the prevalence of the ankle sprains is due to the mechanical restriction provided by the tape and/or due to the proprioceptive value of the adhesive tape. While some researchers have considered performance-related consequences, the majority of ankle taping research has considered the effects on ankle joint range of motion (ROM). It is the assumption of these investigations that restriction of joint ROM represents the quantity of stability provided by each appliance. Common to ankle taping is the concept of restricting excessive ankle inversion while allowing normal ankle dorsiflexion and plantar flexion.

In this study, a wearable IMU-based body motion analysis system, Xsens MVN, will be used. The reasons why we use this system are 1) it allows us to collect data from athletes not in the laboratory environment, but

during training or during exhibition 2) contrary to camera-based systems, it is much cheaper and does not require any laboratory 3) it is much more faster than other systems (calibration, data collection, etc.).

The purpose of this study is to investigate the effects of ankle taping on lower extremity kinematics and postural control in professional basketball players during the landing phase of high jump. The importance of this study is to clarify the lack of understanding of the effects of ankle taping on the ankle sprain injury. At the end of this study, the expectation is to determine a significant difference between taped and non-taped subjects with the comparison of the kinematic data of ankle, knee, hip and the mass center of gravity. The effects of ankle taping on the postural control and lower extremity kinematics in elite basketball players during the landing phase of high jump by using a wearable motion capture system will be investigated for the first time in literature. The training and exercise routines of the players will be unconstrained, and the data will be collected in basketball court. The obtained results will reveal the effects of ankle taping in reducing the ankle injury rate quantitatively.

METHODS AND MATERIALS

Xsens MVN is a motion capture solution that enables the capture of 3D kinematics data in different environments. MVN ensures real-time and accurate human motion analysis. Xsens' motion trackers capture the smallest twitches to high dynamic movements on-body ensuring full 3D motion analysis. MVN uses 17 wireless sensors which are fitted on the body with adjustable straps and uses a software-based on built-in time codes and remote-control plugins.[1]

Despite that growing application areas, the errors caused during segment positioning & sensor-the-segment calibrations has prevented inertial motion capture systems to become a commodity. Xsens has developed a new motion capture engine that aims at overcoming the major error sources of current solutions, in order to provide an accurate and consistent solution.

This new technology combines the data of all motion trackers with advanced biomechanical models resulting in immunity to the effects of magnetic distortions. Also, the sensor- to-segment calibration procedure doesn't rely on the data from the magnetometers, allowing the calibration to be performed anywhere.

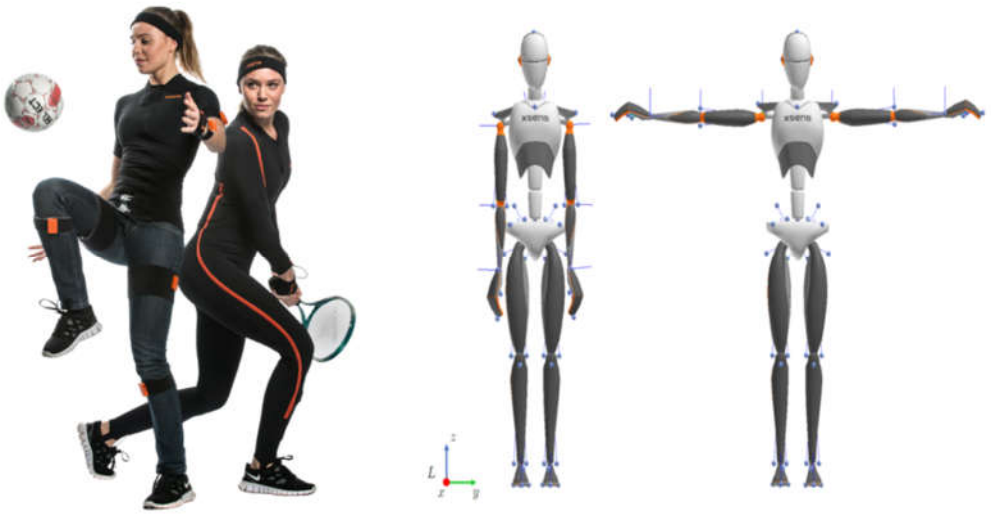

Figure 1: (Taken from XSens website) (Left): Xsens MVN consists of 17 inertial and magnetic motion trackers. Data from wireless (MVN Awinda) or wired (MVN Link) trackers is transmitted by a wireless connection to a PC where the data is further processed and visualized.(Right): Xsens MVN avatar in N-pose (left) and T-pose (right). In the T-pose, all segment coordinate frames are aligned with the common coordinate frame L shown at the bottom left.

The hardware system of Xsens MVN (Fig. 1) streams data wirelessly to a PC/laptop. To capture the motion of the human body, 17 motion tracker sensors are attached to the feet, lower legs, upper legs, pelvis, shoulders, sternum, head, upper arms, forearms, and hands. The sensor modules are inertial and magnetic measurement units that contain 3D gyroscopes, 3D accelerometers and 3D magnetometers. Each module runs an advanced signal processing pipeline that includes patented StrapDown Integration (SDI) [8]–[15] algorithms to send the data at a relatively low rate (e.g. 60Hz) while preserving the accuracy of sampling at a much higher rate (e.g. >1kHz).

Figure 2: (a) Ankle taping (b) Jumping from 30cm bench

XSens MVN Software system processes the data frame by frame real-time and does automatic reprocessing. Data is processed frame by frame, progressing forward in time. The engine combines the data of all motion trackers with advanced biomechanical models to obtain the position and orientation of all human body segments. The reprocess HD mode adds the feature of processing data over a larger time window to get an optimal (and more consistent) estimate of the position and orientation of each body segment. To provide full six-degree-of-freedom tracking of body segments with connected inertial sensor modules, each body segment's orientation and position can be estimated by, respectively, integrating the gyroscope data and double integrating the accelerometer data in time.

Twelve elite male basketball players participated in this study. Healthy shoulder ROM data were obtained from thirty healthy participants. With a 0.05 significance level, this sample size is deemed fit for the comparison-based experiment. The groups consist of participants aged between 18-25 years with no neuromuscular, motor-impaired disease, no previous surgery or injury that previously caused permanent functional impairment of the upper extremity of their body, with a normal body mass index. (BMI 18.5-24.9). Each participant read and signed an informed consent that was approved by the Institutional Review Board of Acibadem Mehmet Ali Aydınlar University.

RESULTS

Participants were given a standard experimental protocol, which last for maximum 30 minutes. In the meantime, Xsens MVN sensors were placed on the participants. Participants' body measurements (height, foot length, arm span, wrist/knee/hip height), weight and age information were noted and the system was calibrated separately for each participant.

Ankle, knee, hip kinematic data of the participants' dominant lower extremity were collected:

a) with ankle wrap present

b) without ankle wrap

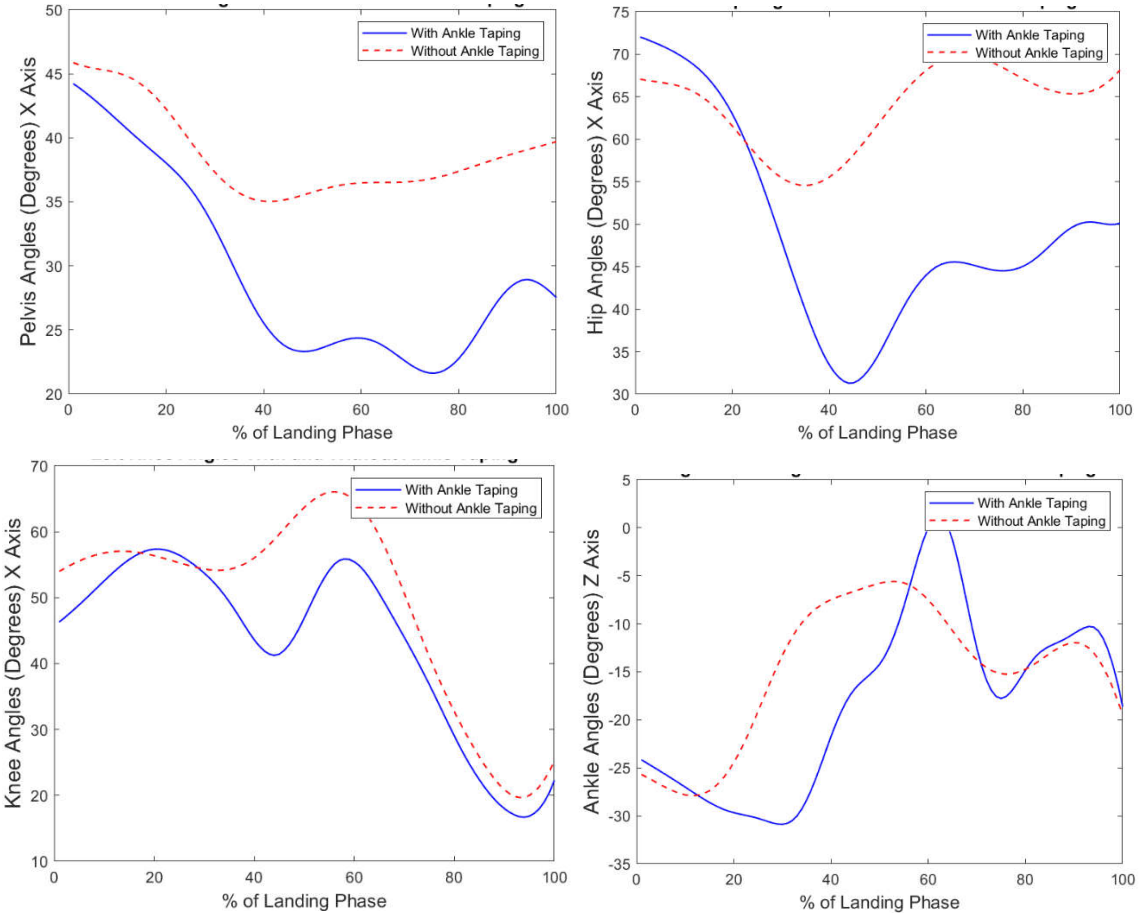

Figure 3: Dominant lower extremity joints' range of motion and movement trajectories dıring the landing phase of high jump from a standard 30 cm bench

According to the initial results (Figure 3), kinesio taping has the potential to increase strength and better performance and balance immediately after the application. In the frontal plane, taped participants were less ankle joint inversion (mean difference= 4.1 degrees SD= 0.658).

DISCUSSION

Sport injuries result in pain, loss of playing or working time, as well as medical expenditure. Among these sport injuries, ankle sprain is the most common sports-related musculoskeletal injury among all athletes, regardless of age or level of participation (MacKean, 1995). (Garrick, 1977) demonstrated that ankle injuries continue to constitute a significant threat to atheletes in sports and most other activities. The ankle is almost unique in that the vast majority (85%) of injuries are of a single type, sprains, and an equally high proportion of the sprains involve the same (lateral) structures. Thus, in athletes, the lateral ligament complex of the ankle is the most frequently injured single structured in the body. (McKay, 2001) indicates that in basketball, ankle injuries are among the most common injuries sustained and they are also amongst the most severe. In an attempt to ascertain the type and frequency of ankle injuries in athletes of similar ages in a wide variety of sports, the results of a 2 year study, (Garrick, 1977), of four high schools were examined. During the investigation where certified athletic trainers examined all injuries, 2,840 participants in 14 sports sustained 1,176 injuries. 14% of which involved the ankle. The over-all injury rate for all sports was 0,415 (or 41 injuries per 100 participants per season). The rate of occurence of ankle injuries was 6 (5.7%) per 100 participants per season, 1 ankle injury for every 17 participants. Of these ankle injuries, the vast majority (85%) were sprains. Ankle sprains were most common in basketball where they constituted 38 and 45% of all injuries in men's and women's basketball. Furthermore, incurring ankle sprains while playing basketball may be considered de rigueur for elite players, with more than 90% of elite players reporting a history of at

least 1 ankle sprain (J. Leanderson, 1993). The incidence of reccurrent ankle sprains has been reported to exceed 75% among basketball players at various levels of competition. In games and practices, ankle ligament sprains with 26.2% and 26.8% are one of the most common reported injuries (Dick Randall, 2003).

The high incidence of ankle sprains, the cost of it and the potential negative chronic results required preventive measures. Prophlactic taping, ankle taping, braces, specially designed shoes and neuromuscular training (eg, balance board training) have been developed as preventive techniques for ankle sprains (Verhagen & Bay, 2010). Widespread belief in the effectiveness of ankle taping and the extremely high incidence of lateral ankle sprains among athletes resulted in frequently use of the procedure. (Moiler vd., 2006) demonstrated that ankle taping and bracing are considered effective and reducing both incidence and severity preventive measures for ankle injuries. Furthermore, both techniques are more effective in participants that have a history of any ankle injuries. (Verhagen & Bay, 2010) indicates that taping is a particularly effective for previously injured athletes. There is another preventive measure combination which is including ankle taping and wearing of high-top shoes was more effective in preventing reinjuries than either ankle taping alone or merely wearing high-top shoes (Rovere vd., 1988). Another study with using a electrogoniometer shows that taping is the most effective at extremes of motion (Laughman, 1980). In addition to reduce the injury risk, ankle taping may also effect the activity of the muscles that around ankle joint, including the tibialis anterior (TA), peroneus longus (PL), peroneus brevis (PB), and soleus (SOL) (Gribble, 2006; Hertel, 2002; Ross, 2004; Wilkerson, 2002). In addition to this, taping limits excessive range of motion (ROM) at the tibiotalar and subtalar joints and may also increase local prioprioceptive output (Beynnon, 1991; Refshauge, 2000; Robbin, 1995). (Osbahr, 2013) indicates that proper ankle taping decreases inversion and plantar flexion which is important because inversion and plantar flexion is the most common injury mechanisms of the ankle. However there are still some contradictions about the effects of the ankle taping tecqhnique on ankle sprains. (Chinn vd., 2014) concluded that, ankle tape altered frontal-plane and sagittal-plane kinematics at the ankle while walking and jogging in shoes on a treadmill. In each case, the ankle was positioned more neutrally with tape. The changes seen in the taped condition may contribute to a reduced risk of ankle sprains due to better positioning of the ankle throughout the gait cycle. Futhermore, the study indicates that the tape may protect the ankle via its mechanical properties as well as its neuromuscular effect on ankle position just before critical aspects of gait, such as toe-off and foot-floor clearance. The findings of another study (Wilkerson, 1991) suggest that incorparation of the subtalar sling significantly enhances protection against an inversion sprain, but at the expense of a slightly greater restriction of plantar flexion. When ankle taping is being used as a prophylactic measure to prevent ligament injury in normal uninjured ankles, performance considerations may justify the use of the less restrictive standard method. However it also mentions that when ankle taping is being used to protect recently injured ligaments, or stabilize an ankle with chronic instability, the benefit of having nearly twice as much residual restriction of inversion seems to outweigh any performance decrement that may be caused by subtular sling. Based on another study, just ankle taping is not enought, but the combination of an external tape with neuromuscular training may achieve the the best preventive outcomes with minimal burden for the athlete (Verhagen & Bay, 2010). To the contrary, (Jeffriess, 2015) demonstrated that ankle taping will not affect planned or reactive agility as measured by the Y-shaped agility test in healthy male basketball players. Moreover, taping method also caused a decrease in muscle activity for the inside leg of the planned and reactive cuts and finally there was generally minimal effect to the activity of the muscles about the ankle when the joint was taped. Similar to this study, (Abián-Vicén, 2008) indicates that the use of prophylactic ankle taping had almost no influence on the balance or jump performance or healthy young subjects. In contrast, it says ankle taping could increase the risk of injury during landings because the peak forces were increased in the taped condition. Finally, it says that use a proper of ankle taping, only when it is required, like in those instances where alternative methods have failed. The most probable explanation for these kind of inconsistencies can be the variations in tape application procedures.

CONCLUSION

Ankle taping has been one of the most common ankle support systems because it has been effective in restricting joint motion. The main purpose of ankle taping is to restrict ankle inversion and plantar-flexion motion. Non-elastic adhesive taping is used to prevent recurrence after an ankle sprain. Such tapings restrict

ankle inversion, as a prophylactic effect, reduce inversion movement speed and reduce the incidence of sprains. The reduction is generally greater for athletes with a history of an ankle sprain, although positive effects have also been shown for those with no prior injury.

REFERENCES

1. Abián-Vicén, Javier, Luis M Alegre, J Manuel Fernández-Rodríguez, Amador J Lara, ve Xavier Aguado. "Ankle Taping Does Not Impair Performance in Jump or Balance Tests", t.y., 7.
2. Alfuth, Martin, Dieter Klein, Raphael Koch, ve Dieter Rosenbaum. "Biomechanical Comparison of 3 Ankle Braces with and Without Free Rotation in the Sagittal Plane". Journal of Athletic Training 49, sy 5 (Ekim 2014): 608-16. https://doi.org/10.4085/1062-6050-49.3.20.
3. Alt, Wilfried, Heinz Lohrer, ve Albert Gollhofer. "Functional Properties of Adhesive Ankle Taping: Neuromuscular and Mechanical Effects Before and After Exercise". Foot & Ankle International 20, sy 4 (Nisan 1999): 238-45. https://doi.org/10.1177/107110079902000406.
4. Beynnon, Bruce D, Darlene F Murphy, ve Denise M Alosa. "Predictive Factors for Lateral Ankle Sprains: A Literature Review", t.y., 5.
5. Bicici, Seda, Nihan Karatas, ve Gul Baltaci. "® EFFECT OF ATHLETIC TAPING AND KINESIOTAPING ON MEASUREMENTS OF FUNCTIONAL PERFORMANCE IN BASKETBALL PLAYERS WITH CHRONIC INVERSION ANKLE SPRAINS", t.y., 13.
6. Callaghan, M J. "Role of Ankle Taping and Bracing in the Athlete." British Journal of Sports Medicine 31, sy 2 (01 Haziran 1997): 102-8. https://doi.org/10.1136/bjsm.31.2.102.
7. Chinn, Lisa, Jay Dicharry, Joseph M. Hart, Susan Saliba, Robert Wilder, ve Jay Hertel. "Gait Kinematics After Taping in Participants with Chronic Ankle Instability". Journal of Athletic Training 49, sy 3 (02 Haziran 2014): 322-30. https://doi.org/10.4085/1062-6050-49.3.08.
8. Dick, Randall, Jay Hertel, Julie Agel, Jayd Grossman, ve Stephen W Marshall. "Descriptive Epidemiology of Collegiate Men's Basketball Injuries: National Collegiate Athletic Association Injury Surveillance System, 1988–1989 Through 2003–2004", t.y., 8.
9. Fong, Daniel Tik-Pui, Youlian Hong, Lap-Ki Chan, Patrick Shu-Hang Yung, ve Kai-Ming Chan. "A Systematic Review on Ankle Injury and Ankle Sprain in Sports": Sports Medicine 37, sy 1 (2007): 73-94. https://doi.org/10.2165/00007256-200737010-00006
10. Fong, Daniel TP, Yue-Yan Chan, Kam-Ming Mok, Patrick SH Yung, ve Kai-Ming Chan. "Understanding Acute Ankle Ligamentous Sprain Injury in Sports". BMC Sports Science, Medicine and Rehabilitation 1, sy 1 (Aralık 2009): 14. https://doi.org/10.1186/1758-2555-1-14.
11. Fraser, John J., Rachel M. Koldenhoven, Susan A. Saliba, ve Jay Hertel. "RELIABILITY OF ANKLE-FOOT MORPHOLOGY, MOBILITY, STRENGTH, AND MOTOR PERFORMANCE MEASURES". International Journal of Sports Physical Therapy 12, sy 7 (Aralık 2017): 1134-49. https://doi.org/10.26603/ijspt20171134.
12. Garrick, James G. "The Frequency of Injury, Mechanism of Injury, and Epidemiology of Ankle Sprains*". The American Journal of Sports Medicine 5, sy 6 (Kasım 1977): 241-42. https://doi.org/10.1177/036354657700500606.
13. Gerber, J. Parry, Glenn N. Williams, Charles R. Scoville, Robert A. Arciero, ve Dean C. Taylor. "Persistent Disability Associated with Ankle Sprains: A Prospective Examination of an Athletic Population". Foot & Ankle International 19, sy 10 (Ekim 1998): 653-60. https://doi.org/10.1177/107110079801901002.
14. Ho, Yi-Hung, Cheng-Feng Lin, Chih-Han Chang, ve Hong-Wen Wu. "Effect of Ankle Kinesio Taping on Vertical Jump with Run-up and Countermovement Jump in Athletes with Ankle Functional Instability". Journal of Physical Therapy Science 27, sy 7 (2015): 2087-90. https://doi.org/10.1589/jpts.27.2087.
15. Hubbard, Tricia J., ve Mitchell Cordova. "Effect of Ankle Taping on Mechanical Laxity in Chronic Ankle Instability". Foot & Ankle International 31, sy 6 (Haziran 2010): 499-504. https://doi.org/10.3113/FAI.2010.0499.
16. Hume, Patria A., ve David F. Gerrard. "Effectiveness of External Ankle Support: Bracing and Taping in Rugby Union". Sports Medicine 25, sy 5 (1998): 285-312. https://doi.org/10.2165/00007256-199825050-00001.

17. Jeffriess, Matthew D, Adrian B Schultz, Tye S McGann, ve Samuel J Callaghan. "Effects of Preventative Ankle Taping on Planned Change-of-Direction and Reac- Tive Agility Performance and Ankle Muscle Activity in Basketballers", t.y., 13.
18. Kaminski, Thomas W., Jay Hertel, Ned Amendola, Carrie L. Docherty, Michael G. Dolan, J. Ty Hopkins, Eric Nussbaum, Wendy Poppy, ve Doug Richie. "National Athletic Trainers' Association Position Statement: Conservative Management and Prevention of Ankle Sprains in Athletes". Journal of Athletic Training 48, sy 4 (Temmuz 2013): 528-45. https://doi.org/10.4085/1062-6050-48.4.02.
19. Kaumeyer, Greg, ve Terry Malone. "Ankle Injuries: Anatomical and Biomechanical Considerations Necessary for the Development of an Injury Prevention Program". Journal of Orthopaedic & Sports Physical Therapy 1, sy 3 (Ocak 1980): 171-77. https://doi.org/10.2519/jospt.1980.1.3.171.
20. Kofotolis, Nikolaos, ve Eleftherios Kellis. "Ankle Sprain Injuries: A 2-Year Prospective Cohort Study in Female Greek Professional Basketball Players", t.y., 7.
21. Leanderson, J., G. Nemeth, ve E. Eriksson. "Ankle Injuries in Basketball Players". Knee Surgery, Sports Traumatology, Arthroscopy 1, sy 3-4 (Eylül 1993): 200-202. https://doi.org/10.1007/BF01560206.
22. MacKean, Lynne C., Gordon Bell, ve Robert S. Burnham. "Prophylactic Ankle Bracing Vs. Taping: Effects on Functional Performance in Female Basketball Players". Journal of Orthopaedic & Sports Physical Therapy 22, sy 2 (Ağustos 1995): 77-81. https://doi.org/10.2519/jospt.1995.22.2.77.
23. McKay, G D. "Ankle Injuries in Basketball: Injury Rate and Risk Factors". British Journal of Sports Medicine 35, sy 2 (01 Nisan 2001): 103-8. https://doi.org/10.1136/bjsm.35.2.103.
24. Meana, M., L. Alegre, J. Elvira, ve X. Aguado. "Kinematics of Ankle Taping after a Training Session". International Journal of Sports Medicine 29, sy 1 (Ocak 2008): 70-76. https://doi.org/10.1055/s-2007-965126.
25. Osborne, Michael D, ve Thomas D Rizzo. "Prevention and Treatment of Ankle Sprain in Athletes": Sports Medicine 33, sy 15 (2003): 1145-50. https://doi.org/10.2165/00007256-200333150-00005.
26. Refshauge, Kathryn M., Jacqueline Raymond, Sharon L. Kilbreath, Liset Pengel, ve Inger Heijnen. "The Effect of Ankle Taping on Detection of Inversion-Eversion Movements in Participants with Recurrent Ankle Sprain". The American Journal of Sports Medicine 37, sy 2 (Şubat 2009): 371-75. https://doi.org/10.1177/0363546508324309.
27. Riemann, Bryan L., Randy J. Schmitz, Michael Gale, ve Steven T. McCaw. "Effect of Ankle Taping and Bracing on Vertical Ground Reaction Forces During Drop Landings Before and After Treadmill Jogging". Journal of Orthopaedic & Sports Physical Therapy 32, sy 12 (Aralık 2002): 628-35. https://doi.org/10.2519/jospt.2002.32.12.628.
28. Smith, Ronald W., ve Stephen F. Reischl. "Treatment of Ankle Sprains in Young Athletes". The American Journal of Sports Medicine 14, sy 6 (Kasım 1986): 465-71. https://doi.org/10.1177/036354658601400606.
29. Stoffel, Karl K., Rochelle L. Nicholls, Andrianto R. Winata, Alasdair R. Dempsey, Jeffrey J. W. Boyle, ve David G. Lloyd. "Effect of Ankle Taping on Knee and Ankle Joint Biomechanics in Sporting Tasks": Medicine & Science in Sports & Exercise 42, sy 11 (Kasım 2010): 2089-97. https://doi.org/10.1249/MSS.0b013e3181de2e4f.
30. Teramoto, Atsushi, Hideji Kura, Eiichi Uchiyama, Daisuke Suzuki, ve Toshihiko Yamashita. "Three-Dimensional Analysis of Ankle Instability after Tibiofibular Syndesmosis Injuries: A Biomechanical Experimental Study". The American Journal of Sports Medicine 36, sy 2 (Şubat 2008): 348-52. https://doi.org/10.1177/0363546507308235.
31. Thacker, Stephen B., Donna F. Stroup, Christine M. Branche, Julie Gilchrist, Richard A. Goodman, ve Elyse A. Weitman. "The Prevention of Ankle Sprains in Sports". The American Journal of Sports Medicine 27, sy 6 (Kasım 1999): 753-60. https://doi.org/10.1177/03635465990270061201.
32. Thonnard, J.L., D. Bragard, P.A. Willems, ve L. Plaghki. "Stability of the Braced Ankle: A Biomechanical Investigation". The American Journal of Sports Medicine 24, sy 3 (Mayıs 1996): 356-61. https://doi.org/10.1177/036354659602400318.
33. Waterman, Captain Brian R, Major Brett D Owens, Captain Shaunette Davey, Captain Michael A Zacchilli, ve Lieutenant Colonel Philip J Belmont. "The Epidemiology of Ankle Sprains in the United States": The Journal of Bone and Joint Surgery-American Volume 92, sy 13 (Ekim 2010): 2279-84. https://doi.org/10.2106/JBJS.I.01537.
34. Wilkerson, Gary B. "Biomechanical and Neuromuscular Effects of Ankle Taping and Bracing", t.y., 10.

35. Wilkerson, Gary B. "Comparative Biomechanical Effects of the Standard Method of Ankle Taping and a Taping Method Designed to Enhance Subtalar Stability". The American Journal of Sports Medicine 19, sy 6 (Kasım 1991): 588-95. https://doi.org/10.1177/036354659101900606.
36. Willems, T., E. Witvrouw, K. Delbaere, A. De Cock, ve D. De Clercq. "Relationship between Gait Biomechanics and Inversion Sprains: A Prospective Study of Risk Factors". Gait & Posture 21, sy 4 (Haziran 2005): 379-87. https://doi.org/10.1016/j.gaitpost.2004.04.002.
37. Yeung, M S, K M Chan, C H So, ve W Y Yuan. "An Epidemiological Survey on Ankle Sprain." British Journal of Sports Medicine 28, sy 2 (01 Haziran 1994): 112-16. https://doi.org/10.1136/bjsm.28.2.112.
38. Refshauge K, Kilbreath SL, Raymond J. The effect of recurrentankle inversion sprain and taping on proprioception at the ankle. Med Sci Sports Exerc. 2000;32(1):10–5.
39. Robbin S, Waked E, Rappel R. Ankle taping improves proprioception before and after exercise in young men. Br J Sports Med. 1995;29(4):242–7.
40. Beynnon BD, Renstrom PA. The effect of bracing and taping in sports. Ann Chir Gynaecol. 1991;80(2):230–8.

LANDSAT 8 UYDUSU KULLANILARAK 2018-2021 YILLARI ARASINDA İSTANBUL'DAKİ KENTSEL ISI ADASININ İNCELENMESİ

INVESTIGATION OF URBAN HEAT ISLAND IN ISTANBUL USING LANDSAT 8 SATELLITE BETWEEN 2018–2021

Duygu ARIKAN[1]

[1]Konya Teknik Üniversitesi, Mühendislik ve Doğa Bilimleri Fakültesi, Harita Mühendisliği Bölümü, Konya, Türkiye.

[1]ORCID ID: https://orcid.org/0000-0001-9976-7479

Ferruh YILDIZ[2]

[2]Konya Teknik Üniversitesi, Mühendislik ve Doğa Bilimleri Fakültesi, Harita Mühendisliği Bölümü, Konya, Türkiye.

[2]ORCID ID: https://orcid.org/0000-0003-1248-8923

ÖZET

Zaman içerisinde nüfusun artması, hızlı kentleşmeye ve kentlerin genişlemesine neden olmaktadır. Bunun bir sonucu olarak doğal arazi örtüsü azalmakta ve geçirimsiz yüzeyler artmaktadır. Tüm bu etkenler kentlerdeki ısı durumunu da değiştirmekte ve iklim değişikliklerine neden olmaktadır. Kentleşme süreci ve iklim değişikliği arasındaki etkileşim çok yönlüdür. Ulaşım, su kaynakları, enerji, endüstriyel faaliyetler, nüfus, sosyo-ekonomik faaliyetler, sera gazı emisyonları, hava kirliliği gibi etkenler birbirine bağlıdır. Ayrıca, kentsel ısı adalarındaki artış ve sıcak hava dalgası sadece çevreyi ve ekonomiyi etkilemez. Aynı zamanda bireylerde sağlık problemlerine de neden olur ve yaşam kalitelerini olumsuz etkiler. Bu nedenle, büyüyen ve gelişen şehirlerde iklim değişikliği problemlerine karşılık kentsel planlamanın yapılması, gelişim açısından önem arz etmektedir. Teknolojinin gelişmesiyle uydularda bulunan termal veriler sayesinde kentsel ve kırsal alanlardaki ısı miktarı hesaplanabilmektedir.

Bu çalışmada 2018-2021 yılları arasında İstanbul'daki kentsel ısı adasının yıllara göre değişimi incelenmiştir. Çalışma alanının İstanbul seçilmesinin nedeni, nüfus yönünden ve kentsel gelişme yönünden hızlı büyüyen metropol bir şehir olmasındandır. Kentsel ısı adası çalışmalarında daha çok arazi kullanımı ve arazi örtüsü değişimi izlenilmekte ve NDVI (Normalleştirilmiş Fark Bitki Örtüsü İndeksi) kullanılmaktadır. Uydu görüntülerindeki bant kombinasyonlarından yararlanılarak NDBI (Normalleştirilmiş Fark Bina İndeksi) da hesaplanmıştır. Bu amaçla, Landsat 8 Collection 1 Tier 1 TOA Yansıtım verisi kullanılmıştır. Bu uydu misyonu, 2013 yılından itibaren, 12 adet spektral bandı ile hizmet vermektedir. Çalışmada TIR, RGB, Yakın Kızılötesi (NIR), kızılötesinin kısa dalga boyu (SWIR) bantları kullanılmıştır. Uydu görüntülerinin indirilmesi, ücretsiz erişim imkânı sağlayan Google Earth Engine platformu vasıtasıyla olmuştur. Haritaları oluşturmak için ArcGIS yazılımından yararlanılmıştır. Sonuç olarak zaman içerisinde bitki örtüsünün azaldığı ve yapıların artmış olduğu kanısına varılmıştır. Arazi yüzeyindeki bu değişimler kentsel ısı adasının yoğunluğunu arttırmıştır.

Anahtar Kelimeler: Kentsel ısı adası, NDVI, NDBI, Google Earth Engine.

ABSTRACT

Over time, the increase in population causes rapid urbanization and expansion of cities. As a result, natural land cover is decreasing and impermeable surfaces are increasing. All these factors also change the temperature situation in cities and cause climate changes. The interaction between the urbanization process

and climate change is multifaceted. Factors such as transportation, water resources, energy, industrial activities, population, socio-economic activities, greenhouse gas emissions, air pollution are interconnected. In addition, the increase in urban heat islands and the heat wave do not only affect the environment and the economy. It also causes health problems in individuals and affects their quality of life negatively. For this reason, urban planning in growing and developing cities against climate change problems is important in terms of development.

With the development of technology, the amount of heat in urban and rural areas can be calculated thanks to the thermal data found in satellites. In this study, the change of the urban heat island in Istanbul between the years 2018-2021 was examined. The reason for choosing Istanbul as the study area is that it is a fast growing metropolitan city in terms of population and urban development. In urban heat island studies, mostly land use and land cover change are monitored and NDVI (Normalized Difference Vegetation Index) is used. NDBI (Normalized Difference Building Index) was also calculated by using band combinations in satellite images. For this purpose, Landsat 8 Collection 1 Tier 1 TOA Reflectance data was used. This satellite mission has been in service with 12 spectral bands since 2013. In the study, TIR, RGB, Near Infrared (NIR), short wavelength (SWIR) bands of infrared were used. Satellite images were downloaded via the Google Earth Engine platform, which provides free access. The ArcGIS software was used to create the maps. As a result, it was concluded that the vegetation cover decreased and the structures increased over time. These changes in the land surface have increased the density of the urban heat island.

Keywords: Urban Heat Island, NDVI, NDBI, Google Earth Engine.

GİRİŞ

Kentsel ısı adası (KIA) kavramı, kentsel bir bölgenin ya da çevresinin ısınma derecesini ölçmektir (Z.-H. Wang, 2022). Bu kavram ilk olarak 1820 yılında Luke Howard tarafından yapılan çalışmayla literatüre girmiştir (Streutker, 2003). Dünya çapında kırsal bölgedeki (kentsel olmayan alan) ısı miktarının kentsel bölgelere göre daha az olduğu görülmektedir (Oke, 1982). Kentlerdeki yoğunlaşmış ısı üreten kaynak miktarının fazla olması, yaz veya kış mevsiminde kullanılan iklimlendirme cihazları, insan aktiviteleri sonucunda kentler üzerinde toz bulutu meydana getirmektedir (Tozam & Karaca, 2018). Bu durum da atmosferde olması gereken doğal sıcaklık miktarını etkilemekte ve daha da arttırmaktadır. Bölgesel olarak görülen sıcaklık farklılıkları, zaman içerisinde küresel bir probleme dönüşmeye başlamıştır. Çünkü, kent bölgelerindeki ısınmanın fazla olması su kalitesi, hava kalitesi, iklim ve çevre faktörünü de etkilemektedir. Bu durumda doğrudan insan sağlığını etkileyen bir durum olarak karşımıza çıkmaktadır (Arnfield, 2003; Grimm et al., 2008; Shepherd, 2005).

Bu problemlerin önüne geçilmesi veya en aza indirgenmesi amacıyla kentsel ısı miktarının belirlenmesi gerekmektedir. Kentsel ısı adasının ölçümü sabit meteoroloji istasyonları, kuleler, araçlara monte edilen sensörler aracılığıyla gerçekleştirilmektedir (Mirzaei & Haghighat, 2010; Schwarz, Schlink, Franck, & Großmann, 2012; Smoliak, Snyder, Twine, Mykleby, & Hertel, 2015). Bu ölçüm cihazlarının pahalı olması, kurulumu için gereken sürenin uzun olması gibi faktörlerden ötürü her şehirde bulunmamaktadır (Mirzaei & Haghighat, 2010). İzleme istasyonlarının sayısının az olması kentsel arazi kullanım alanlarının belirlenmesi ya da iklim değişikliğini izleme çalışmalarında yeterli veri sağlanamaması anlamına gelmektedir. (Jin & Dickinson, 2010; Weng, 2009; Zhou et al., 2018). Bu nedenle uydu görüntülerinden yararlanılmaktadır. Uydu görüntüsünü kullanılarak ilk kentsel ısı adası çalışması Rao tarafından gerçekleştirilmiştir (Krishna, 1972). Bu amaçla kullanılan çeşitli uydular bulunmakta ve teknolojinin gelişmesiyle sayıları da paralel şekilde artmaktadır. Bunlar; Landsat, Moderate Resolution Imaging Spectroradiometer (MODIS) ve Advanced Space-borne Thermal Emission and Reflection Radiometer (ASTER), Sentinel-3, Advanced Very High Resolution Radiometer (AVHRR), ve GOES'dir (Cui & De Foy, 2012; Gallo & Owen, 1998; Zhou et al., 2018).

Kentsel ısı adası, günümüzde pek çok araştırmacının konusu olmuştur. Çalışma bölgesi İstanbul seçildiği için, bu bölgede kentsel ısı adasını belirlemek için yapılan farklı çalışmaların birkaçı Tablo 1'de sunulmuştur.

Tablo1. İstanbul'da yapılan kentsel ısı adası çalışmaları

Çalışmanın Amacı	*Kullanılan Yöntem*	*Kaynak*
Kentsel ısı adası etkilerinin belirlenmesi	Linear regresyon yöntemi ve Mann-Kendall testinin kullanılması	Karaca, Anteplioğlu, and Karsan (1995)
Kentsel ısı adası etkisinden kaynaklanan yeraltı sularının araştırılması	Meteorolojik veriler, Yeraltı suyu sıcaklıkları, Yer kaynaklı ısı pompası değerleri arasında ilişki kurulması	Yalcin and Yetemen (2009)
Kentsel büyüme ve KIA arasındaki ilişki	Arazi Kullanımı/Örtü Sınıflandırması	Kaya, Basar, Karaca, and Seker (2012)
Yüzeysel KIA etkisinin kıyı bölgesi üzerinde değerlendirilmesi	Görüntülerin ön işlemesi ve Arazi Kullanımı/Örtü haritalanması	Dihkan, Karsli, Guneroglu, and Guneroglu (2015)
Mevsimsel kentsel ısı adası etkilerinin araştırılması	Arazi yüzey sıcaklığı ve istasyon verilerinin istatiksel değerlendirilmesi	Ünal et al. (2020)
Yüzey kentsel ısı adasında kent dokusunun üzerindeki rolünün değerlendirilmesi	The Ridge Regression Modeli, and Monte Carlo Simulasyonu	Okumus and Terzi (2021)

Küresel bir problem olan KIA, son yıllarda çok daha önemli bir konu olarak ileri sürülmüştür (Zhou et al., 2018). İstanbul ilinde hızlı ve yoğun bir yapılaşma olduğundan, yapmış olduğumuz bu çalışmada 2018-2021 yılı içerisinde kentsel ısı adasının durumu uydu görüntüsüyle incelenmiştir. Ayrıca NDVI bitki indeksi ve NDBI indeksi hesaplanmış olup, aralarında bir ilişki olup-olmadığı belirtilmiştir. Nüfus verileri sayesinde yıllık nüfus artışı olan bölgelerdeki KIA durumu incelenmiştir.

MATERYAL METOT

Çalışma Alanı

Türkiye'nin en uzun sahil şeridine sahip olan şehir, konum olarak ülkenin kuzey batı kısmında bulunmaktadır (Dihkan et al., 2015). İstanbul Asya ve Avrupa kıtaları üzerinde yer alan ve yüz ölçümü 5343 km^2'dir (Şekil 1). Nüfusu 16 milyona yaklaşan şehir Türkiye'nin en kalabalık şehridir(Ünal et al., 2020). Bu nüfusun %65.5 kadar kısmı Avrupa kesiminde, %35.5 kısmı ise Anadolu yakasında yaşamaktadır (TUİK, 2022). Nüfus yönünden Dünyadaki mega şehirler içerisinde 21. sıra da yer almaktadır. Şehirde kentleşme son 20 yılda hız kazanmıştır. Bu nüfus artışı bazı problemlere de sebep olmaktadır. Örneğin: yerleşim alanlarının kontrolsüz genişlemesi, enerji tüketim miktarının artması, arazi örtüsü ve arazi kullanımında değişiklikler meydana gelmektedir (Orhan, 2021). Tüm bu değişimler çevresel bozulmaları arttırmaktadır.

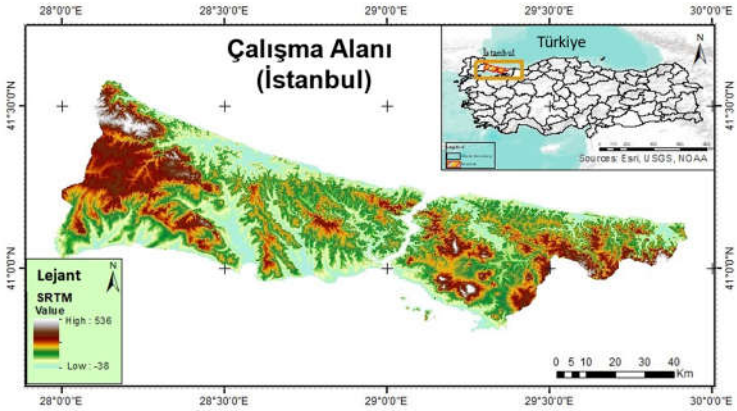

Şekil 1. Çalışma Alanı (İstanbul)

Çalışmada yapılan genel işlemler ve kullanılan veriler Şekil 2'de iş akış diyagramında sunulmuştur.

Şekil 2. İş-akış diyagramı

Çalışmada Kullanılan Veriler

Bu çalışmada, 2018-2021 yılları arasında İstanbul'daki kentsel ısı adası durumu incelenmiştir. Ayrıca, bölgedeki nüfus durumu, NDVI ve NDBI indeksleri ile ilişkileri ortaya konulmuştur. Verilerin indirilmesinde Google Earth Engine platformu kullanılmıştır. Çevrimiçi erişim imkanı sağlayan, büyük verilerin analiz edilmesinde ve hızlı bir şekilde görselleştirilmesinde, ücretsiz ve yardımcı bir yazılımdır (Ermida, Soares, Mantas, Göttsche, & Trigo, 2020).

KIA, NDVI ve NDBI verileri için Landsat 8 uydusuna ait görüntüler kullanılmıştır. Bu uydu 11 Şubat 2013 yılında fırlatılmıştır ve toplamda 12 adet spektral bandı bulunmaktadır. Çalışmada kullanılan bantlara ait genel özellikler Tablo 2'de sunulmuştur (Ermida et al., 2020). Bu uydu OLI ve TIR olmak üzere iki sensör içermektedir. Termal kızılötesi sensörü (TIR) sayesinde dünya yüzeyine ait termal veriler bant 10 ve bant11'e kaydedilmektedir (Khorrami & Gunduz, 2020).

Tablo2. Landsat 8 uydusunun çalışmada kullanılan bantlarına ait bilgiler

Uydu İsmi	***Kullanılan Bantlar***	***Dalgaboyu (µm)***	***GEE veriseti***	***Çözünürlük***	***Geçiş süresi***	***Görev Durumu***
Landsat 8 (OLI; TIRS)	Red : B4	0.64-0.67	C01/T1_SR	30 m	10:00 (16 gün)	11 Nisan 2013'ten günümüze kadar
	NIR : B5	0.85-0.88	C01/T1_SR	30 m		
	TIR : B10	10.6-11.19	C01/T1_TOA	100^2 m		

KIA etkisine neden olan faktörler arasında bitki yüzeyinin durumu da yer almaktadır. Çünkü, bitkilerin yansıtıcılık yapan yüzeylerde ısı dağılımını etkilemesi söz konudur (Yalcin & Yetemen, 2009). Bu amaçla yapmış olduğumuz çalışmada NDVI bitki endeksi hesaplanmıştır.

NDVI bitki endeksi, genellikle tarımsal amaçlı uygulamalarda tercih edilmektedir. Bitki türünün sağlıklı veya sağlıksız olmasının belirlenmesinde, bir bölgenin ormanlık ya da ağaçlık tespitinin yapımında, çayırlık arazilerinin durumu vb. çalışmalarda sıkça kullanılan bir yöntemdir (Becker-Reshef, Vermote, Lindeman, & Justice, 2010; İleri & Koç, 2022; J. Wang, Rich, Price, & Kettle, 2004). NDVI, -1 ve +1 arasında değer almaktadır. Eğer arazi örtüsü çalılık, mera, çimen, orman gibi alan ile kaplıysa NDVI pozitif değerleri

almaktadır. Eğer arazi örtüsü bitki değil de, kaya, beton, kum gibi yüzeyle kaplıysa NDVI negatif değer almaktadır.

Rouse Jr, Haas, Deering, Schell, and Harlan (1974), tarafından geliştirilen bu yöntemin temelinde kırmızı ve yakın kızılötesi bandın spektral yansıma değeri kullanılmaktadır. Landsat 8 uydusunun 4.bandı kırmızı bandı, 5.bandı ise yakın kızıl ötesi ifade eder ve yöntem;

$$NDVI = \frac{B5 - B4}{B5 + B4}$$

formülü ile elde edilir.

The Normalized Difference Built-up Index (NDBI), yerleşik alanları vurgulamak için kullanılmaktadır. NDBI indeksi de bitki indeksinde olduğu gibi -1 ve +1 arasında değer almaktadır (Zha, Gao, & Ni, 2003). Pozitif değer alması kentsel arazi alanlarının olduğunu, negatif değer alması durumu da kentsel olmayan araziyi temsil etmektedir (Zha et al., 2003).

Bu indeksin hesaplanabilmesi için, yakın kızıl ötesi bant ve kızılötesinin kısa dalga boyu yansıma değerleri kullanılmaktadır. Landsat 8 uydusunun 5.bandı yakın kızıl ötesini ve 6. Bandı ise kızılötesinin kısa dalga boyunu ifade eder ve yöntem;

$$NDBI = \frac{B6 - B5}{B6 + B5}$$

Eşitliğiyle hesaplanır.

SONUÇLAR VE TARTIŞMA

Kentsel ısı adasının etki durumu, kentin yapısına bağlı olarak değişmektedir. Bu nedenle, çalışmada İstanbul'un nüfus durumu, arazi kullanış biçimi tespit edilmiştir. Landsat uydu görüntüsünün 4,5 ve 10. bantlarından yararlanılarak NDVI ve NDBI indeksi hesaplanmış ve haritaları oluşturulmuştur.

Çalışmada, kentsel ısı adalarını belirlemek amacıyla 6^0C- 29^0C arasında 5 sınıfa ayrılmıştır. 2018 yılında sıcaklık 6^0C ile 18^0C arasında daha fazladır. Yıllar geçtikçe sıcaklık değerinde artışlar meydana geldiği görülmektedir (Şekil 3). 2019 yılında Arnavutköy, Esenyurt, Gaziosmanpaşa, Esenler, Sultangazi, Başakşehir, Beykoz gibi ilçelerde bir önceki yıla göre sıcaklık miktarında artışlar yaşanmıştır. 2021 yılında ise Esenyurt kısmında ciddi şekilde sıcaklık artışı görülmektedir. Yine bu yılda Fatih, Beyoğlu, Kadıköy gibi turistik mekanlarda ve Bahçelievler, Ataşehir, Maltepe, ilçelerin de sıcaklık ortalamaları 23^0C-27^0C olarak hesaplanmıştır. Pendik ise güney kısımlarında sıcaklık değerleri fazladır. 2021 yılında 2020 yılına kıyasla sıcaklık değerlerinde biraz azalma olmuştur. Çünkü bu zaman diliminde küresel bir hastalık olan COVID-19'dan dolayı bazı kısıtlamalar yapılmıştır. İnsan etkileşimin az olması, araç kullanımının azalması gibi etkenler olumlu sonuçlar üretmiştir. Ayrıca su yüzeylerin de kentsel ısı miktarı daha az olarak yansımaktadır.

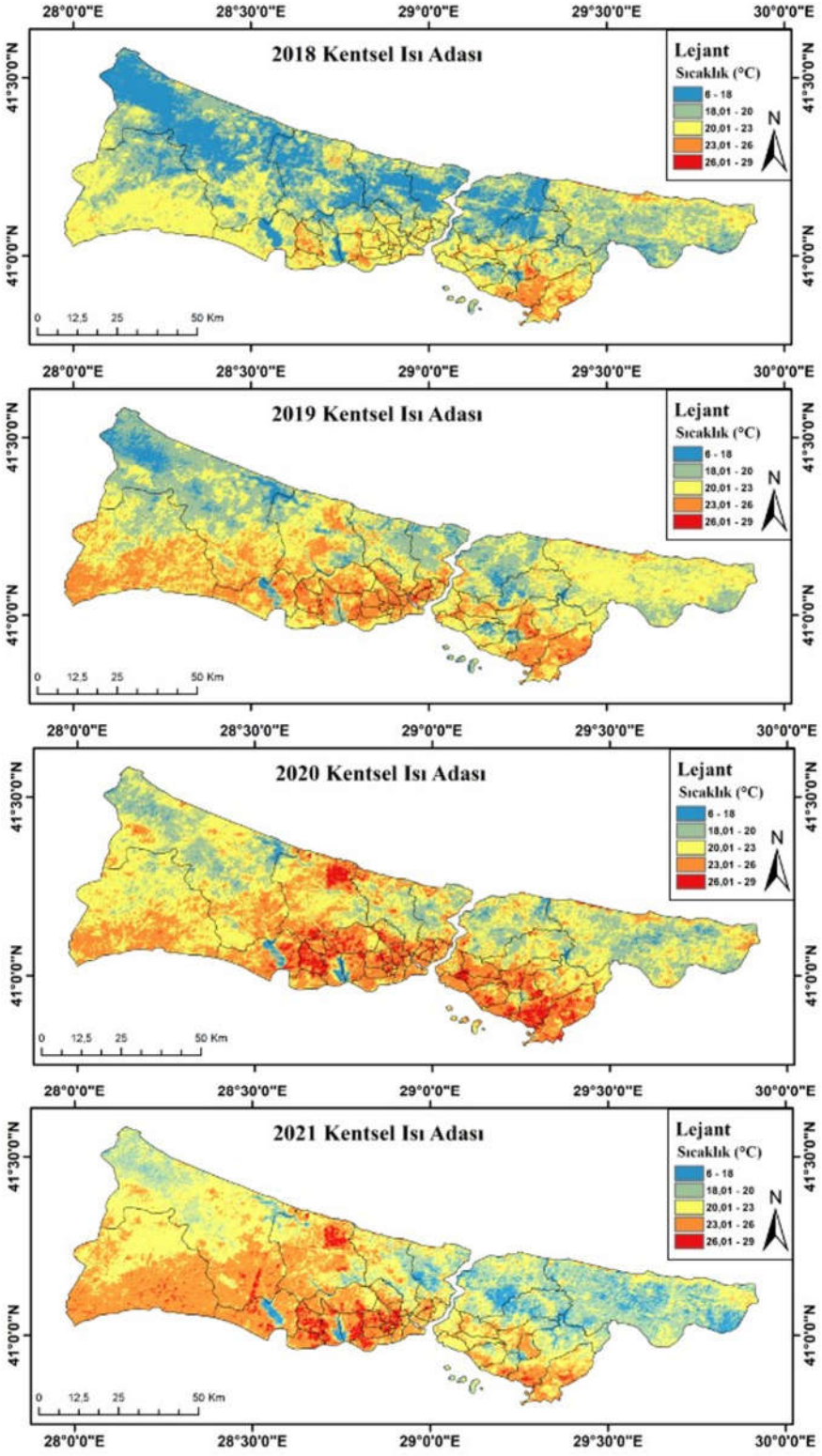

Şekil 3. 2018-2021 yılları arasındaki kentsel ısı adasına ait haritalar

2018 yılından 2021 yılına kadar toplamda 773.176 kişi artmıştır. İstanbul'un en kalabalık ilçesi Esenyurt, nüfusu en az olan ilçesi ise Adalar'dır. Şekil 4'de 2021 yılı İstanbul nüfus yoğunluğu haritası, Şekil 5' de ise 2018 yılından 2021 yılına kadar İstanbul'un ilçelerindeki nüfus miktarı ayrıntılı olarak verilmiştir. Nüfus ve kentsel ısı adası arasında pozitif bir ilişki olduğu görülmektedir. Nüfus miktarının fazla olduğu ilçelerde

(Esenyurt, Küçükçekmece, Bağcılar, Pendik, Bahçelievler) kentsel ısı miktarı fazla iken, nüfus miktarının az olduğu ilçelerde (Adalar, Şile, Çatalca'nın kuzey batı kısmı, Beşiktaş) KIA düşüktür.

Şekil 4. 2021 yılı İstanbul nüfus haritası

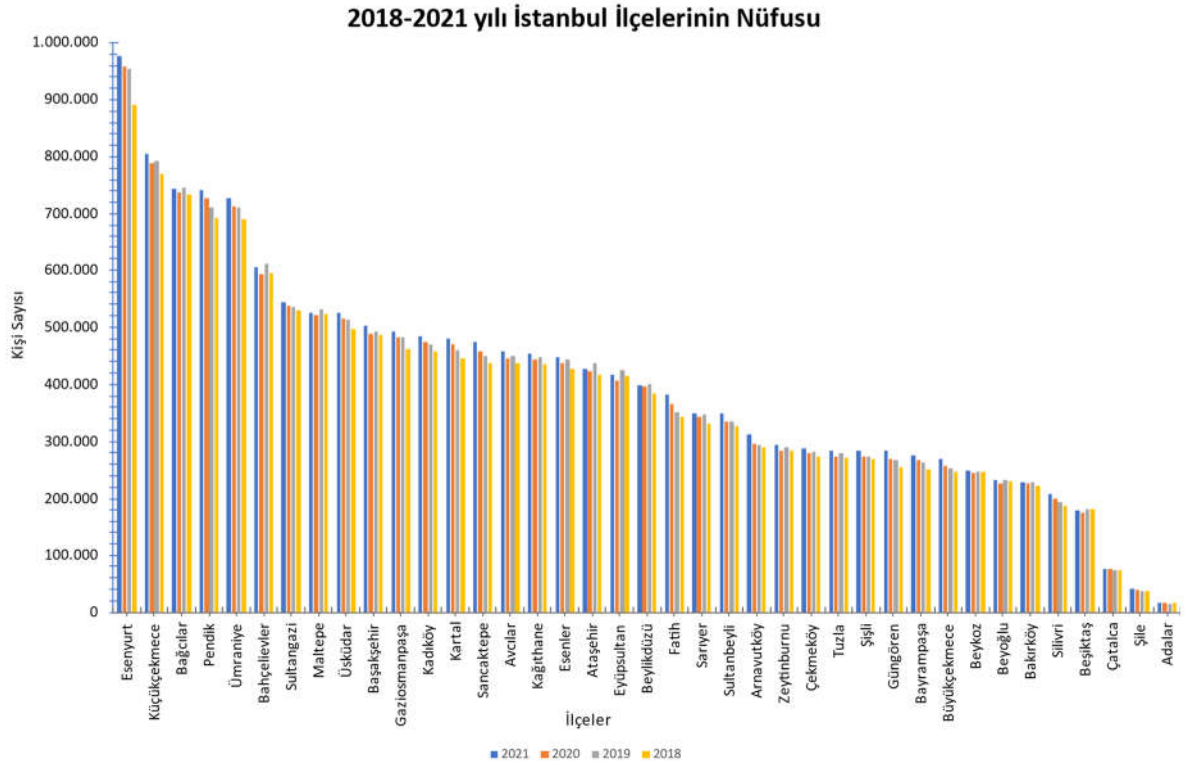

Şekil 5. 2018-2021 yılları arasında İstanbul ilçelerinin nüfus sayıları

Kentsel ısı adası, bitki örtüsü ve arazi yüzeyinde bulunan yapılarla doğrudan ilişkilidir (Yalcin & Yetemen, 2009). Şekil 6'da verilen haritalar irdelendiğinde kentsel ısı adası ile NDVI ve NDBI arasında bir ilişki kurulmuştur. Kentsel ısı adasının NDVI ile arasında negatif bir ilişki bulunurken, NDBI ile arasında pozitif

bir ilişki kurulabilmektedir. Kentlerdeki nüfusun miktarının artması yerleşim alanlarının büyümesinde etki etmektedir. Bu durum da doğrudan bitki örtüsünün ve doğal arazi örtüsünün zaman içerisinde azalmasına sebep olmaktadır. Bu etkenlerde şehrin yapısını ve geometrisi değiştirmektedir. Kentlerdeki yüksek katlı binalar ve farklı malzemeli (asfalt, beton, taş) yollar gün boyu güneş ışınlarını emmekte ve daha sonrasında ısıya dönüştürmektedir. Bu dönüşen ısı ise depolanmaktadır. Sonrasında tekrardan atmosfere salınarak kentteki hava sıcaklığını arttırmaktadır. Gece olduğunda ise, gün boyu absorbe edilen enerji atmosfere gönderilmektedir.

NDVI, bitki örtüsünün durumu hakkında ve bitkinin sağlıklı ve sağlıksız olması ile ilgili bilgiler vermektedir. Şekil 6'da NDVI haritası incelendiğinde 2018 yılından 2021 yılına kadar bitki örtüsünde zamanla bir azalma görülmektedir. Fakat 2021 yılında İstanbul'un Anadolu yakasının bir önceki yıla göre NDVI değerinde bir artış olduğu görülmektedir. Bunun sebebi olarak 2021 yılında ülkemizde COVID-19 pandemisi görüldüğü için virüsün bulaşma etkisini azaltmak amacıyla bazı kısıtlama ve tedbirler uygulanmıştır. Bu süre zarfında doğa kendini yenilemiş ve sağlıklı bitki örtüsünün yansıma değeri daha da artmıştır. Bitki örtüsünün sık olduğu Şile ve Çatalca bölgelerinde, kentsel ısı adasının miktarı düşüktür. Bitki örtüsünün varlığı, sıcaklık yoğunluğunu düzenlemektedir. Çünkü, bitki örtüsüyle kaplı alanlar üzerinde, yüzey ve yüzeye yakın yerlerde sıcaklık değerleri düşük olmaktadır. Tam tersi durumda bitki örtüsünün az olduğu yerlerde, sıcaklık değerlerinin yüksek olduğu tespit edilmiştir.

NDBI ise, kentsel arazi durumunu veya yerleşim alanlarını belirlemek amacıyla kullanılmaktadır. 2018 yılından 2021 yılına kadar kentsel alan artarken, bitki örtüsü de zamanla azalmaktadır. Nüfusun fazla olduğu bölgelerde NDBI yansıma değeri 1'e yakındır. Bu bölgelerde ise kentsel ısı adası değeri oldukça fazladır. Çünkü güneşten gelen enerji, kentsel bölgedeki yapılar tarafından emilmekte ve depolanmaktadır. Bu durum bölgeden bölgeye değişiklik gösterebilir. Gerek binaların geometrisi, yüksekliği, gerekse yapımında kullanılan malzemeler ısı miktarında değişikliğe yol açar. Ayrıca, yüksek katlı binaların bulunduğu yerlerde hava akımı az olduğundan ısı kaybı engellenmekte ve dağılmamaktadır. Bu nedenle kentsel ısı adası, yerleşim yelerlerinde daha fazla olmaktadır.

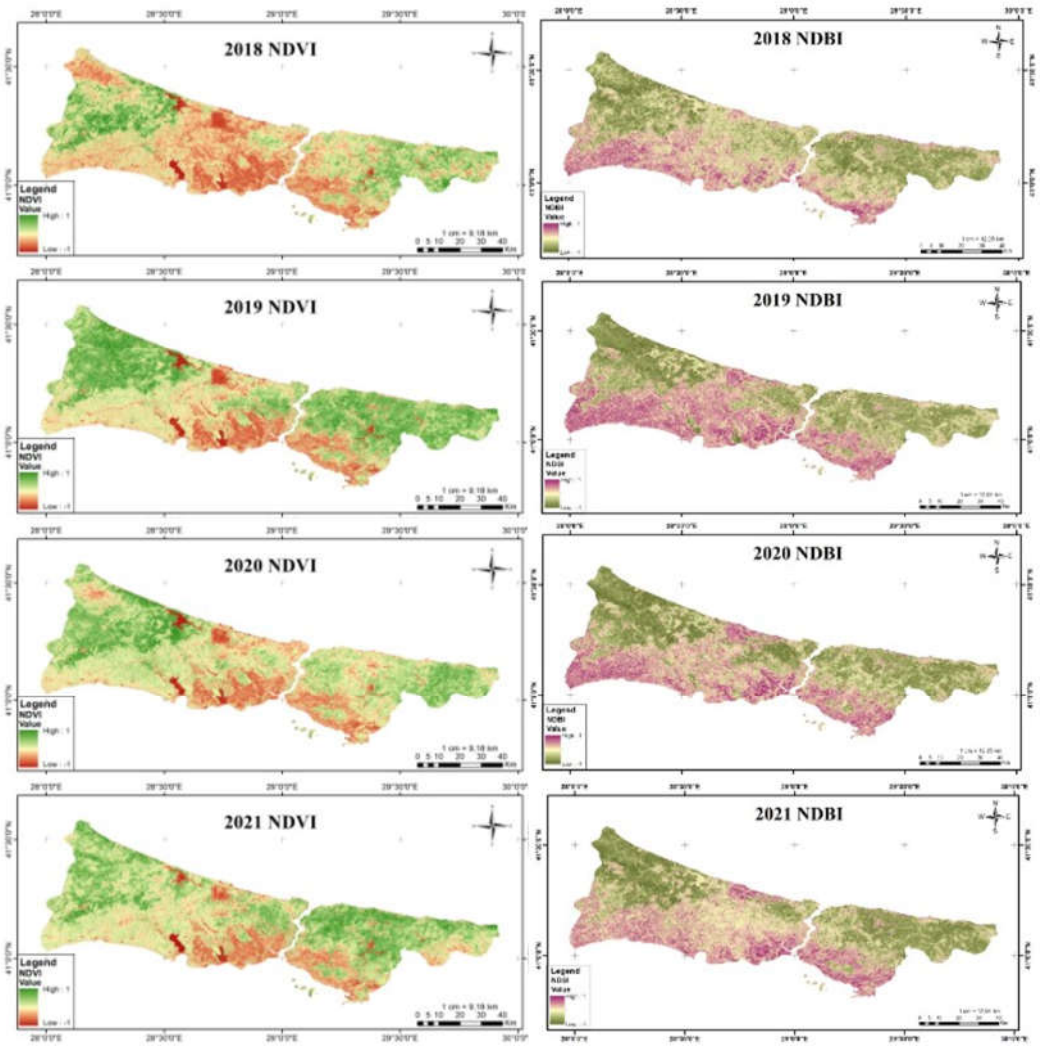

Şekil 6. 2018-2021 yıllarına ait NDVI ve NDBI haritaları

Kentlerin geometrik yapısı ve büyüklüğü, arazi durumunun çeşitli olmasından kaynaklı her kentin ısı adası farklı olmaktadır. Son yılların en önemli antropojenik sorunlarından biri olarak görülen bu problemin çözümü de bölgeden bölgeye farklılık göstermektedir. Bu nedenle kentleşme aktivitelerinin artarak devam ettiği ülkemizde hızlı çözümler üretebilmek için; kent ikliminin sürekli olarak izlenmesi gerekmektedir. Bunun için uzaktan algılama verileri sayesinde güncel durum izlenebilmektedir. Ayrıca araştırma bulgularında, nüfusun ve bina yapıların artması, yeşil alanların azalması sıcaklık parametresi üzerinde çok etkili olduğu görülmüştür. Bu nedenle, yapılarda ısının depolanmasını azaltacak malzemeler tercih edilmeli, çatı ve cephelerinde ayna gibi yansıtıcı özelliğine sahip malzemeler azaltılmalıdır. Kent merkezleri başta olmak üzere yeşil alanların yoğunluğu ve yapı alanlarındaki yeşil koridor alanlarının arttırılması sağlanmalıdır.

REFERENCES

Arnfield, A. J. (2003). Two decades of urban climate research: a review of turbulence, exchanges of energy and water, and the urban heat island. *International Journal of Climatology: a Journal of the Royal Meteorological Society, 23*(1), 1-26.

Becker-Reshef, I., Vermote, E., Lindeman, M., & Justice, C. (2010). A generalized regression-based model for forecasting winter wheat yields in Kansas and Ukraine using MODIS data. *Remote Sensing of Environment, 114*(6), 1312-1323.

Cui, Y. Y., & De Foy, B. (2012). Seasonal variations of the urban heat island at the surface and the near-surface and reductions due to urban vegetation in Mexico City. *Journal of Applied Meteorology and Climatology, 51*(5), 855-868.

Dihkan, M., Karsli, F., Guneroglu, A., & Guneroglu, N. (2015). Evaluation of surface urban heat island (SUHI) effect on coastal zone: The case of Istanbul Megacity. *Ocean & coastal management, 118*, 309-316.

Ermida, S. L., Soares, P., Mantas, V., Göttsche, F.-M., & Trigo, I. F. (2020). Google earth engine open-source code for land surface temperature estimation from the landsat series. *Remote Sensing, 12*(9), 1471.

Gallo, K. P., & Owen, T. W. (1998). Assessment of urban heat Islands: A multi-sensor perspective for the Dallas-Ft. worth, USA region. *Geocarto International, 13*(4), 35-41.

Grimm, N. B., Faeth, S. H., Golubiewski, N. E., Redman, C. L., Wu, J., Bai, X., & Briggs, J. M. (2008). Global change and the ecology of cities. *science, 319*(5864), 756-760.

İleri, O., & Koç, A. (2022). Monitoring the available forage using Sentinel 2-derived NDVI data for sustainable rangeland management. *Journal of Arid Environments, 200*, 104727.

Jin, M., & Dickinson, R. E. (2010). Land surface skin temperature climatology: Benefitting from the strengths of satellite observations. *Environmental research letters, 5*(4), 044004.

Karaca, M., Anteplioğlu, Ü., & Karsan, H. (1995). Detection of urban heat island in Istanbul, Turkey. *Il Nuovo Cimento C, 18*(1), 49-55.

Kaya, S., Basar, U. G., Karaca, M., & Seker, D. Z. (2012). Assessment of urban heat islands using remotely sensed data. *Ekoloji, 21*(84), 107-113.

Khorrami, B., & Gunduz, O. (2020). Spatio-temporal interactions of surface urban heat island and its spectral indicators: a case study from Istanbul metropolitan area, Turkey. *Environmental Monitoring and Assessment, 192*(6), 386. doi:10.1007/s10661-020-08322-1

Krishna, R. (1972). Remote sensing of urban heat islands from an environmental satellite.

Mirzaei, P. A., & Haghighat, F. (2010). Approaches to study urban heat island–abilities and limitations. *Building and environment, 45*(10), 2192-2201.

Oke, T. R. (1982). The energetic basis of the urban heat island. *Quarterly Journal of the Royal Meteorological Society, 108*(455), 1-24.

Okumus, D. E., & Terzi, F. (2021). Evaluating the role of urban fabric on surface urban heat island: The case of Istanbul. *Sustainable Cities and Society, 73*, 103128.

Orhan, O. (2021). Mersin ilindeki kentsel büyümenin yer yüzey sıcaklığı üzerine etkisinin araştırılması. *Geomatik, 6*(1), 69-76.

Rouse Jr, J., Haas, R. H., Deering, D., Schell, J., & Harlan, J. C. (1974). *Monitoring the vernal advancement and retrogradation (green wave effect) of natural vegetation*. Retrieved from

Schwarz, N., Schlink, U., Franck, U., & Großmann, K. (2012). Relationship of land surface and air temperatures and its implications for quantifying urban heat island indicators—An application for the city of Leipzig (Germany). *Ecological indicators, 18*, 693-704.

Shepherd, J. M. (2005). A review of current investigations of urban-induced rainfall and recommendations for the future. *Earth Interactions, 9*(12), 1-27.

Smoliak, B. V., Snyder, P. K., Twine, T. E., Mykleby, P. M., & Hertel, W. F. (2015). Dense network observations of the Twin Cities canopy-layer urban heat island. *Journal of Applied Meteorology and Climatology, 54*(9), 1899-1917.

Streutker, D. R. (2003). *A study of the urban heat island of Houston, Texas*: Rice University.

Tozam, İ., & Karaca, Ü. B. (2018). Kentsel Isı Adası Etkisi ve Serin Çatılar. *TC İstanbul Kültür Üniversitesi, İstanbul, 9*, 12-13.

Ünal, Y. S., Sonuç, C. Y., Incecik, S., Topcu, H. S., Diren-Üstün, D. H., & Temizöz, H. P. (2020). Investigating urban heat island intensity in Istanbul. *Theoretical and Applied Climatology, 139*(1), 175-190.

Wang, J., Rich, P., Price, K., & Kettle, W. (2004). Relations between NDVI and tree productivity in the central Great Plains. *International journal of remote sensing, 25*(16), 3127-3138.

Wang, Z.-H. (2022). Reconceptualizing urban heat island: Beyond the urban-rural dichotomy. *Sustainable Cities and Society, 77*, 103581.

Weng, Q. (2009). Thermal infrared remote sensing for urban climate and environmental studies: Methods, applications, and trends. *ISPRS Journal of photogrammetry and remote sensing, 64*(4), 335-344.

Yalcin, T., & Yetemen, O. (2009). Local warming of groundwaters caused by the urban heat island effect in Istanbul, Turkey. *Hydrogeology journal, 17*(5), 1247-1255.

Zha, Y., Gao, J., & Ni, S. (2003). Use of normalized difference built-up index in automatically mapping urban areas from TM imagery. *International journal of remote sensing, 24*(3), 583-594.

Zhou, D., Xiao, J., Bonafoni, S., Berger, C., Deilami, K., Zhou, Y., . . . Sobrino, J. A. (2018). Satellite remote sensing of surface urban heat islands: Progress, challenges, and perspectives. *Remote Sensing, 11*(1), 48.

TUİK, 2022. URL: https://www.tuik.gov.tr/

THE ADVANTAGES OF ORNAMENTAL PLANTS FOR ENVIRONMENTAL AND HUMAN HEALTH

Mert Çakır[1]

[1]Süleyman Demirel University, Faculty of Architecture, Department of Landscape Architecture, Isparta, Turkey.

[1]ORCID ID: https://orcid.org/0000-0003-0079-0375

Bahar Sancar[2]

[2]Kocaeli University, Faculty of Agriculture, Department of Agricultural Economics, Kocaeli, Turkey.

[2]ORCID ID: https://orcid.org/0000-0002-3687-1495

ABSTRACT

Plants are crucial to the sustainability of life on earth and play a significant role in maintaining the ecological balance. Plants that stand out or add to the visual appeal of space with their flowers, leaves, fruits, or other distinguishing characteristics are known as 'ornamental plants'. Ornamental plants have been used for functional and aesthetic purposes throughout history. There is an ongoing movement from rural to urban areas as a result of the growing global population, the advancement of technology, and the growth of the industry. People migrate away from rural areas as a result, and the hectic pace of metropolitan life has a negative impact on their physical and mental health. With fewer green spaces in cities, ornamental plants are now more important than ever for their aesthetic appeal as well as to reduce nature-related longings and to create more habitable settings. Ornamental plants have a wide range of uses in environmental management. Ornamental plants reduce heat accumulation, and air, and noise pollution and increase air and life quality. According to their intended usage, ornamental plants are categorized into four different classes. These include cut flowers, outdoor and indoor ornamental, and bulbous-tuberous plants. The many and varied uses of ornamental plants contribute positively to urban biodiversity. Ornamental plants are an important commercial industry and a sector that contributes to the economy of a nation. The results of investigations on the advantages of ornamental plants for human and environmental health were summarized in this paper.

Keywords: Plant Design, Biodiversity, Indoor Plants, Outdoor Plants

1. INTRODUCTION

There is a constant movement from rural to urban areas as a result of the growing global population, the advancement of technology, and the growth of the industry. People migrate away from rural areas as a result, and the hectic pace of metropolitan life has a negative impact on their physical and mental health. People can no longer interact with the natural environment due to the growing urbanization of the world. There is substantial proof that urbanization increases the prevalence of physical and psychological disorders globally (Skar and Krogh, 2009). The importance of the natural environment for people's physical and mental health has also been stressed by scientific investigations.

Plants are crucial to the sustainability of life on earth and play a significant role in maintaining the ecological balance. Humans and other living things cannot exist without plants. They are useful in foodstuffs, pharmaceuticals, and many other industries (Amlekar et al., 2014). Additionally, plants provide a natural environment in the space where a person works physically as well as psychological relaxation and revivification. The environment's physical and mental wellness is significantly improved by using plants in both indoor and outdoor design (Shibata, 2001; 2004; Yannick et al., 2009).

Ornamental plants are plants that increase visual quality with their flowers, leaves, fruits, and forms. Ornamental plants have been used for functional and aesthetic purposes throughout history (Baktır, 2013; Jaggi, 2013). Today, in addition to aesthetic appearance, the importance of using ornamental plants has increased in order to eliminate the longing for nature and create more livable environments with the decrease of green areas in cities (Korkut et al., 1995; Yazgan et al., 2005). Ornamental plant cultivation has a long history in human culture, although it only started growing in importance at the turn of the 20th century. According to their intended usage, ornamental plants are categorized into four different classes and are shown in Figure 1 (Anonymous, 2022a). These include cut flowers, seasonal flowers, interior ornamental plants, outdoor ornamental plants, and bulbous and tuberous plants (Uslu, 2002; Ay, 2009; Kazaz, 2012; Yazici and Gülgün, 2016; Gülgün and Yazici, 2016).

Figure 1. Classifying ornamental plants

Numerous research has been done on the interactions between people and ornamental plants, both indoor and outdoor (Lohr, 2000; Lohr and Pearson-Mims, 2000; Relf and Lohr, 2003). According to these research, plants promote productivity (Lohr et al., 1996), reduce mental weariness (Tennessen and Cimprich, 1995), speed up the healing of illnesses and maladies (Ulrich, 1984), and improve air quality (Wood et al., 2002). It has been stated that ornamental plants can elevate mood and inspire good feelings (Adachi et al., 2000; Shibata and Suzuki, 2002; 2004).

The many and varied uses of ornamental plants contribute positively to landscape and urban biodiversity (Figure 2) (Anonymous, 2022b). In regions that have been damaged or eroded, ornamental plants can be used as vegetation to filter out noise, dust, heat buildup, and air pollution while also giving the area a uniform appearance. They have a variety of usage areas that are used, including sports fields, playgrounds, recreation areas, parks, gardens, homes, and other public spaces (Ugberugbhe, 1997). At the same time, ornamental plants provide ecological and aesthetic functions to people such as complementary, attractive, emphasizing, and directing (Miller, 1992).

Figure 2. An example of the use of ornamental plants

In conclusion, ornamental plants not only enhance the aesthetics of the space in which they are employed but also directly promote human mental and physical health. At the same time, ornamental plants constitute an important commercial industry and a sector that supports the nation's economy. In this study, studies on the benefits of ornamental plants for human and environmental health and their results were reviewed. The benefits of ornamental plants were determined.

2. THE BENEFITS OF ORNAMENTAL PLANTS FOR HUMAN HEALTH

Scientific studies have shown the positive effects of plants on human health since the early 1970s. The design of indoor and outdoor areas with nature in mind can have significant positive effects on human quality of life, according to subsequent studies (Ulrich, 1984; Kellert, 2005).

Recently, it is thought that the negative conditions caused by rapid urbanization affect people negatively. People who move away from nature and have less interaction with the natural environment can have physical and psychological disorders. Urban green spaces increase the quality of life of people, contribute to the identity of the city and create recreational areas (Aydemir et al., 2004). In this context, urban green spaces relieve people psychologically and meet the need to get away from the city to a significant extent. The quiet and unique atmosphere of natural green spaces are environments that reduce the stress of daily life, meet the need for breathing fresh air, as well as provide both physical and mental relaxation (Chiesura, 2004). The World Health Organization (WHO) defines health as “a state of complete physical, mental and social well-being and not merely the absence of disease or infirmity” (Frumkin, 2001).

Today, people living in big cities spend at least 80% of their lives indoors. When people spend time in enclosed spaces, the air quality of the environment has a significant impact on their health. A major threat to human health results from the concentration of pollutants in the air reaching hazardous levels. Plants can clean the air and swiftly remove contaminants from the environment (Abbass et al., 2017; Brili et al., 2018). People's performance and health are directly impacted by the environment's declining air quality (Konijnendijk, 2003; Sevik et al., 2013; 2016). Ornamental plants have been found to have a relaxing and inspiring effect on people in the setting in which they live (Lohr et al., 1996). At the same time, ornamental plants are used in interactions between people and nature to reduce all types of air pollution, prevent distraction, improve working efficiency, manage mental fatigue, stress, and low blood pressure, and quickly heal diseases (Lewis, 1993; Lohr, 2000; Djukanovic, 2002; Tani and Hewitt, 2009; Cetin, 2016; Sevik et al., 2017).

Ornamental plants help to create healthy living environments in people's living environments. It needs areas to support its social demands and a natural setting for psychological leisure at the same time (Bozkurt and Ulus, 2014; Cengiz et al., 2017). It has been predicted that people having ornamental plants in their workplaces and rooms can improve the mood of employees and awaken positive thoughts (Figure 3) (Adachi et al., 2000; Shibata and Suziki, 2001; 2002; 2004; Anonymous, 2022c).

Figure 3. Use of ornamental plants to benefit human health

Humans have long had a close relationship with the environment, but in recent years it has been claimed that environmental harm and modernization brought on by increased urbanization exacerbate people's feelings of loneliness and despair (Mayer and Frantz, 2004; Speldewinde et al., 2009; 2011; Van Haaften and Van De. Vijver, 1996). Because of this, it is anticipated that the presence of ornamental plants in living spaces will have a substantial impact on welfare and psychology. Table 1 provides a summary of the advantages of ornamental plants for human health (Hall and Knuth, 2019).

According to Doxey et al. (2009), people's use of plants at work and at home may have an impact on their quality of life, mood, and mental health. The usage of indoor plants has been shown in other research to have favorable impacts on people's mood, stress levels, relief from mental weariness, and performance (Dijkstra et al., 2008).

Tablo 1. The benefits of ornamental plants for human health (Hall and Knuth, 2019)

Reduces anxiety and stress
Minimizes the lack of attention, helps to concentrate
Increases awareness and visual response
Reduces depression
Strengthens memory
Increases happiness and quality of life
Reduces post-traumatic stress disorder
Increases creativity
Increases productivity and attention
Reduces dementia
Improves self-esteem

Ornamental plants have been shown to reduce stress in most people. In a 1979 study by Ulrich, it was shown that stressed-out college students' viewpoints on plants increased, their pleasant feelings increased, and their levels of fear and fury reduced (Frank, 2003). Lohr et al. (2007) discovered that having plants around the office lowers stress levels. When utilized inside, plants have been shown to boost productivity and lower systolic blood pressure by one to four units (Lohr et al., 2007).

Ordinarily, people use ornamental plants to alter the mood in the office. Most individuals emotionally associate ornamental plants with enhancing the workplace (Larsen et al., 1998). The impact of indoor plants on productivity, attitudes, and perceptions in the workplace was studied by Larsen et al. (1998). As a consequence of the investigation, it was discovered that the plants utilized positively raised staff welfare levels and boosted production.

It has been discovered that using plants in hospital settings or being around plants outside helps patients recover more quickly and have less pain after surgery (Ulrich, 1989). Additionally, studies have demonstrated that the presence of ornamental plants at workplaces can lessen signs of emotional and physical discomfort, lower the need for sick days, and lessen weariness and headaches by 20–25% (Fjeld et al., 1998; Fjeld, 2002).

2. THE BENEFITS OF ORNAMENTAL PLANTS FOR ENVIRONMENTAL HEALTH

More than half of the world's population now resides in cities, according to recent statistics (Worldwatch Institute, 2007). People's connections to the natural world have diminished as urbanization has increased. Plants continue to improve the environment at every spatial scale, despite humans moving farther away from the natural world.

The greatest advantage of plants is that they create oxygen, which gives the atmosphere the substance that enables people to breathe and survive on this planet. Two mature trees can produce enough oxygen for a family of four, while one mature tree may produce an average of 260 pounds of oxygen per year (Environment Canada, 2005). Similar to this, a family of four can get enough oxygen from just 15 by 15 meters of natural grass (Virginia State University, 2004).

Strategic placement of ornamental plants can improve the environment in practical ways. It is crucial in decreasing noise in regions used for fences or borders, establishing resting spaces, lowering light and glare reflected on buildings, and giving shade (Robinette, 1972; GrowerTalks, 2006). Table 2 provides a summary of the functional characteristics of plants (Ertunç, 2011).

Table 2. Functional characteristics of ornamental plants (Ertunç, 2011).

Helping buildings to be connected and integrated with the environment
Having an important role in defining areas and determining their boundaries
Directing and separating vehicle and pedestrian traffic
Helping to determine scale in cities
Creating visual barriers and ensuring privacy
Improving to urban identity, indoor and outdoor spaces
Identifying and highlighting levels on sloping areas
Creating a landscape
Protecting from wind, dust and noise, providing shading
Providing climate control
Giving a homogeneous appearance
Protecting from natural disasters (such as preventing erosion, reducing wind speed)

The ability of ornamental plants to store carbon is crucial for reducing the rise in atmospheric carbon dioxide concentrations. Carbon dioxide is a greenhouse gas that contributes to global warming (Alley et al., 2007). Burning fossil fuels and altering land usage are the main causes of the atmosphere's elevated carbon dioxide

concentrations (Alley et al. 2007). Green areas should be established both indoors and outdoors to address this dangerous issue (McPherson, 2005). Establishing green areas with ornamental plants that sequester carbon also cuts down on carbon footprints (Carbon Footprint, 2007; Eilperin, 2007).

Due to their capacity to filter pollutants from the air, plants are frequently referred to as the "lungs of cities" (McPherson, 2005). Human mortality and disease rates are decreased by plants that serve as natural filters and minimize air pollution (Powe and Willis, 2004). The following are some ways that plants can reduce air pollution (Figure 4) (McPherson, 2005; Anonymous, 2022d).

- Gaseous pollutants (such as ozone, nitrogen oxides, and sulfur oxide) are absorbed through the leaves.
- The temperature is lowered by evapotranspiration and it also reduces ozone concentrations.
- They improve the quality of the air by increasing the amount of oxygen.
- They accumulate airborne particulate matter (dust, ash, pollen, etc.) on leaves and slow its rate in the air.

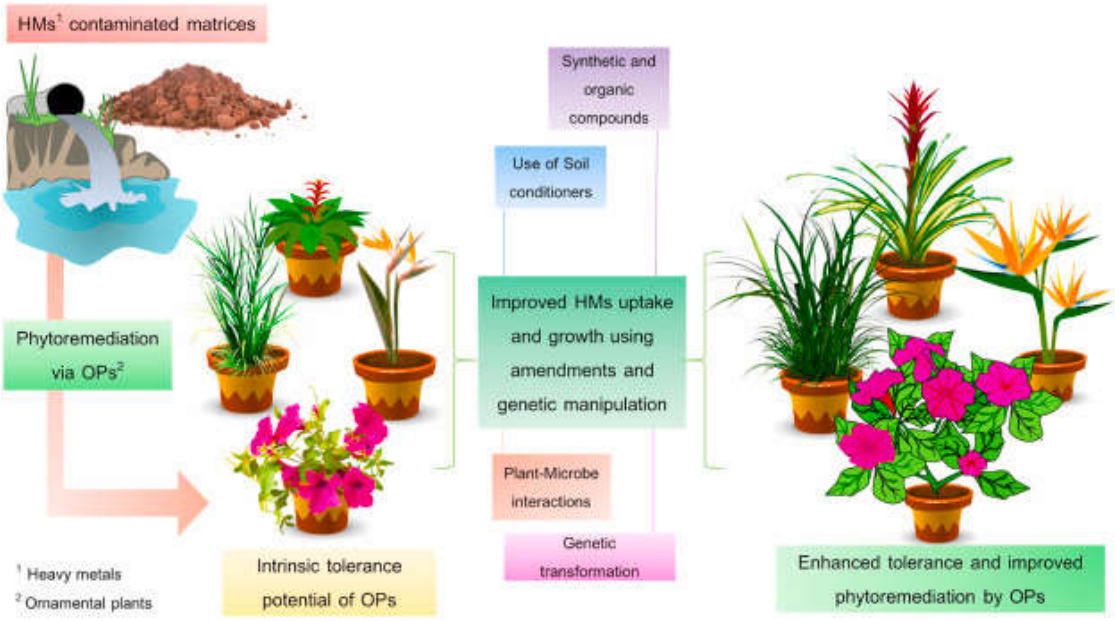

Figure 4. Ecological benefits of ornamental plants

Both urbanization and the proportion of people who spend their time indoors are growing (Orwell et al., 2004). Numerous studies have shown that indoor volatile compound concentrations (VOC) are higher than outside levels (Sakai et al., 2004). Studies have shown that plants serve as atmospheric filters both indoors and outdoors and that they improve the air quality in the space in which they are employed (Orwell et al., 2004; Liu et al., 2007).

Ornamental plants not only help to improve air quality but also have significant benefits in terms of water management. Through filtration and purification techniques, they are used to eliminate soil and air pollutants, prevent water contamination, and even stop floods by storing water. For instance, wetlands and green spaces filter and store water when sewage overflows into groundwater. In green areas such as home gardens, parks, sports fields, and medians, water retention is achieved by using turfgrasses (University of Minnesota, 2006). In urban areas, plants can be used by designing them according to rainwater collection areas in order to manage water flow (Inglis, 1999). Plants around ponds or streams improve soil structure, minimizing water erosion and reducing sedimentation in waterways (Brack, 2002).

In terms of both plant production and use in parks and gardens, ornamental plants support the preservation and expansion of biodiversity. It serves as a haven for a variety of birds and other animals while ornamental plants are being produced and ready for use (Canadian Christmas Tree Growers Association, 2004). The

development of landscape corridors improves plant biodiversity and inhibits the invasion of exotic species, according to studies done in South Carolina (Damschen et al., 2006). Additionally, it has been found that regions connected by landscape corridors have 20% more plant species than those without such corridors (Damschen et al., 2006).

RESULTS

Research has demonstrated the positive effects of ornamental plants on both the emotional and physical well-being of people and the environment. It has been proven from the studies that working in settings with ornamental plants benefits employees in terms of productivity, creativity, improved mental and physical health, upbeat mood, decreased stress levels, and decreased pain perception. A major factor in the rise in the use of ornamental plants to address environmental and health issues is the research on ornamental plants and their advantages. In order to effectively manage the environment, maintain a healthy ecosystem, safeguard the ecological balance, and improve human quality of life, ornamental plants must be used in a variety of ways. They offer numerous environmental advantages such as heat buildup, water management, and a decrease in noise and air pollution. Every day and in every aspect of life, plants are necessary. Ornamental plants should therefore be added to all areas where people live and spend time, and their use should be encouraged, in order to promote both human and environmental health.

REFERENCES

Abbass, O. A., Sailor, D. J., & Gall, E. T. (2017). Effectiveness of indoor plants for passive removal of indoor ozone. Building and Environment, 119, 62-70.

Adachi, M., Rode, C.L.E. and Kendle, A.D. (2000). "Effects of floral and foliage displays on human emotions," HortTechnology, vol. 10, no. 1, pp. 59–63.

Alley, R. et al. (2007). Climate Change 2007: The Physical Science Basis- Summary for Policymakers. Intergovernmental Panel on Climate Change. Retrieved Feb. 19, 2007 from: http://www.ipcc.ch/SPM2feb07.pdf.

Amlekar, M., Manza, R. R., Yannawar, P., & Gaikwad, A. T. (2014). Leaf features based plant classification using artificial neural network. IBMRD's Journal of Management and Research, 3(1): 224-232.

Anonymous, (2022a). https://slideplayer.com/slide/5879689/

Anonymous, (2022b). https://thefarmpeople.in/blogs/news/benefits-of-ornamental-gardening

Anonymous, (2022c). https://www.healthline.com/health/healthy-home-guide/benefits-of-indoor-plants

Anonymous, (2022d). https://www.sciencedirect.com/science/article/pii/S0013935121000748

Ay, S. (2009). Süs Bitkileri İhracatı, Sorunları ve Çözüm Önerileri: Yalova Ölçeğinde Bir Araştırma. Suleyman Demirel University Journal Of Faculty Of Economics & Administrative Sciences . 2009, Vol. 14 Issue 3, P423-443. 21p.

Aydemir, E.S., Öksüz, A.M., Aydemir, Ş., Beyazlı, D.Ş., Ökten, N., Sancar, C., Özyaba, M., Türk, Y.A. (2004). Kentsel Alanların Planlanması ve Tasarımı, 285-335 s, Trabzon.

Baktır, İ. (2013). Türkiye'de süs bitkilerinin dünü, bugünü ve yarını. V. Süs Bitkileri Kongresi Bildiriler Cilt-1, Yalova, 13-16.

Bozkurt. S, G. ve Ulus, A. (2014). Rekreasyonel Amaçlı Kullanılan Alışveriş Merkezlerinde iç Mekan Bitkilerinin Organizasyonu ve Kullanım Parametrelerinin İstanbul (Avrupa Yakası) Örneğinde incelenmesi. İstanbul Üniversitesi Orman Fakültesi Dergisi, 64(2), 24-40.

Brack, C. L. (2002). Pollution Mitigation and Carbon Sequestration by an Urban Forest. Environmental Pollution 116: 195-200.

Brilli, F., Fares, S., Ghirardo, A., de Visser, P., Calatayud, V., Muñoz, A., ... & Menghini, F. (2018). Plants for sustainable improvement of indoor air quality. Trends in plant science, 23(6), 507-512.

Canadian Christmas Tree Growers Association. (2004). Environmental Issues: Why Buy a Real Christmas Tree. http://www.christmastree.net/env_eng.htm.

Carbon Footprint. (2007). Carbon Footprint Homepage. Retrieved Mar. 8, 2007 from: http://www.carbonfootprint.com/.

Cengiz, B., Kaya, B. &Yakan O. E. (2017). Kampüs Binalarında İç Mekan Bitkisel Tasarım: Bartın Üniversitesi Örneği. I. Uluslararası Sosyal Bilimler ve Eğitim Araştırmaları Sempozyumu. 3-5 Kasım, Antalya-Türkiye.s:1-17

Cetin, M. (2016). A Change in the Amount of CO2 at the Center of the Examination Halls: Case Study of Turkey. Studies on Ethno-Medicine, 10(2), 146-155.

Chiesura, A. (2004). The Role Of Urban Parks For The Sustainable City. Landscape and Urban Planning, 68(1), 129-138.

Damschen, E. et al. (2006). Corridors Increase Plant Species Richness at Large Scales. Science 313 (5791): 1284-1286.

Dijkstra, K., Pieterse, M.E. and Pruyn, A. (2008). Stress-reducing effects of indoor plants in the built healthcare environment: The mediating role of perceived attractiveness. Preventive Medicine 47:279-283.

Dijkstra, K., Pieterse, M.E., Pruyn, A. (2008). Stress reducing effects of indoor plants in the Built healthcare environment. Preventive Medicine 47: 279-283.

Djukanovic, R., Wargocki, P., & Fanger, P. O. (2002). Cost-benefit analysis of improved air quality in an office building. In Proceedings of Indoor Air 2002 (Vol. 1, pp. 808-813).

Doxey, J.S., Waliczek, T.M., Zajicek, J.M. (2009). The Impact of Interior Plants in University Classrooms on Student Course Performance and on Student Perceptions. HortScience 44(2): 384-391.

Eilperin, J. (2007). Plant a Tree Then Book a Flight to NY. Toronto Star, Section Travel-K, pp. 10-11.

Environment Canada. (2005). You Asked Us. http://www.ec.gc.ca/envirozine/english/issues/58/any_questions_e.cfm.

Ertunç, Z. (2011). Antakya Kent Dokusunda Kullanılan Çok Yıllık Süs Bitkilerinin Peyzajda Kullanımları. Yüksek Lisans Tezi. Mustafa Kemal Üniversitesi Fen Bilimleri Enstitüsü, Peyzaj Mimarlığı Anabilim Dalı, Hatay, s. 127.

Fjeld, T. (2002). "The effects of plants and artificial daylight on the wellbeing and health of office workers, school children and health-care personnel," Proceedings of International Plants for People Symposium, Floriade, Amsterdam, NL.

Fjeld, T., Veiersted, B., Sandvik, L., Riise, G. and Levy, F. (1998). "The effect of indoor foliage plants on health and discomfort symptoms among office workers," Indoor Built Environ. Vol. 7, pp. 204-209.

Frank, M.S. (2003). The Benefits of Plants and Landscaping. Florida Gardening. Retrieved Feb. 23, 2007 from: www.floridagardening.org/download/BenefitofPlants.pdf

Frumkin, H. (2001). Beyond Toxicity: Human Health and the Natural Environment. American Journal of Preventive Medicine 20 (3): 234-240.

GrowerTalks. (2006). Sky-High and Green. Retrieved Feb. 5, 2007 from: http://www.growertalks.com/archive/articles/306.asp

Gülgün Aslan, B., Yazici, K. (2016). Üretimden Pazarlamaya Türkiye De Süs Bitkileri. TÜRKTOB (19), 64-69.

Hall, C. and Knuth M. (2019). An Update of the Literature Supporting the Well-Being Benefits of Plants: A Review of the Emotional and Mental Health Benefits of Plants. Journal of Environmental Horticulture 1 March 2019; 37 (1): 30–38.

Inglis, M. (1999). Stormwater Management Pond- Parkland Dedication. Landscape Trades September: 22-24.

Jaggi, D. (2013). A Micropropagation System For Carnation (Dianthus caryophyllus)-An Important Ornamental Plant. Master's Thesis. Thapar University, Departmant of Biotechnology and Environmental Sciences, Patiala, 8-9.

Kazaz, S. (2012). Odunsu Süs Bitkilerinin Çoğaltma ve Yetiştirme Teknikleri. Ders notları, Ankara Üniversitesi Ziraat Fakültesi Bahçe Bitkileri Ana Bilim Dalı.

Kellert, S. (2005). Designing and understanding the human-nature connection.Washington Island.

Konijnendijk, C. C. (2003). A decade of urban forestry in Europe. Forest policy and Economics, 5(2), 173-186.

Korkut, A., Yıldırım, T., Görür, G., Çakmak, S. (1995). Türkiye'de Süs Bitkileri Tüketim Projeksiyonları Ve Üretim Hedefleri", IV. Türkiye Ziraat Mühendisliği Teknik Kongresi, Tarım Haftası'95 Kongre Kitabı, 2. Cilt, T.C. Ziraat Bankası Kültür Yayınları No:26, 697-714, Ankara.

Larsen, L. et al. (1998). Plants in the Workplace: The Effects of Plant Density on Productivity, Attitudes, and Perceptions. Environment and Behaviour 30 (3): 261-281.
Lewis, C.A. (1993) Green nature, human nature (University of Illinois Press,Chicago).
Liu, Y. J. et al. (2007). Which Ornamental Plant Species Effectively Remove Benzene From Indoor Air? Atmospheric Environment 41 (3): 650-654.
Lohr, V. and C.H. Pearson-Mims. (2000). Physical discomfort may be reduced in the presence of interior plants. HortTechnology 10:53–58.
Lohr, V. I. (2009). What are the benefits of plants indoors and why do we respond positively to them?. In II International Conference on Landscape and Urban Horticulture 881 pp. 675-682
Lohr, V. I., Pearson-Mims, C. H. and Goodwin, G. K. (2007). Interior Plants May Improve Worker Productivity and Reduce Stress in a Windowless Environment. Plants in Buildings. Retrieved Feb. 23, 2007 from: http://www.plants-inbuildings.com/whyplantsstressreduction.php.
Lohr, V.I, Pearson-Mims, C.H. and Goodwin, G.K. (1996). Interior plants may improve worker productivity and reduce stress in a windowless environment. J. Environ. Hort. 14:97-100.
Lohr, V.I. (2000). Human-horticulture relationships in North and South America. Acta Hort, 523:109-114.
Mayer, F.S., Frantz, C.M.P. (2004). The connectedness to nature scale: ameasure ofindividuals'feelingin community with nature. J. Environ. Psychol. 24: 503–515.
McPherson, E. G. (2005). Trees With Benefits. American Nurseryman April 1: 34-40.
Miller, G.T. (1992). Environmental Science, fourth edition, 1992.
Miller, G.T. (1992). Environmental Science, fourth edition, 1992.
Orwell, R. L. et al. (2004). Removal of Benzene by the Indoor Plant/Substrate Microcosm and Implications for Air Quality. Water, Air and Soil Pollution 157: 193-207.
Powe, N. A. and K. G. Willis. (2004). Mortality and Morbidity Benefits of Air Pollution (SO2 and PM10) Absorption Attributable to Woodland in Britain. Journal of Environmental Management 70 (2): 119-128.
Relf, P.D. and V.I. Lohr. (2003). Human issues in horticulture. HortScience 38:984–993.
Robinette, G. O. (1972). Plants, People, and Environmental Quality. Washington DC: US Department of the Interior, National Parks Service.
Sakai, K. et al. (2004). A Comparison of Indoor Air Pollutants in Japan and Sweden: Formaldehyde, Nitrogen Dioxide, and Chlorinated Volatile Organic Compounds. Environmental Research 94: 75-85.
Sevik, H., Çetin, M., & Işınkaralar, K. (2016). Bazı İç Mekan Süs Bitkilerinin Kapalı Mekanlarda Karbondioksit Miktarına Etkisi. Düzce Üniversitesi Bilim ve Teknoloji Dergisi, 4(2).
Sevik, H., Cetin, M., Guney, K., & Belkayali, N. (2017). The Influence of House Plants on Indoor CO. changes, 2(2), 2.
Sevik, H., Karakas, H., & Karaca, U. (2013). Color-Chlorophyll relationship of some indoor ornamental plant. International Journal of Engineering Science & Research Technology, 2(7), 1706-1712.
Shibata, S. and Suzuki, N. (2001). "Effects of indoor foliage plants on subjects' recovery from mental fatigue," N. Amer. J. Psychol. vol. 3, pp. 385-396.
Shibata, S. and Suzuki, N. (2004). "Effects of an indoor plant on creative task performance and mood," Scandinavian Journal of Psychology, vol. 45, pp. 373-381.
Skar, M. and Krogh, E. (2009). "Changes in children's nature-based experiences near home: From spontaneous play to adult-controlled, planned and organized activities," Children's Geographies, vol. 7, no. 3, pp. 339-354.
Speldewinde, P.C., Cook, A., Davies, P., Weinstein, P. (2009). A relationship between environmental degradation and mental health in rural Western Australia. Health Place 15: 865–872.
Speldewinde, P.C., Cook, A., Davies, P., Weinstein, P. (2011). The hidden health burden of environmental degradation: disease comorbidities and dryland salinity. EcoHealth 8: 82–92.
Tani, A., Hewitt, C. N. (2009). Uptake of aldehydes and ketones at typical indoor concentrations by houseplants. Environmental Science & Technology, 43(21), 8338- 8343.
Tennessen, C.M. and Cimprich, B. (1995). Views to nature: Effects on attention. J. Environ. Psychol. 15:77-85.
Ugberugbhe, K. (1997). The Nigeria Environment. Federal Ministry of works housing and Environmental Protection, Vol. 1, No. 1 pp3.

Ulrich, R. (1989). The Role of Trees in Human Well-Being and Health. Proceedings from Fourth Urban Forestry Conference Conference. St. Louis, Missouri.

Ulrich, R.S. (1984). View through a window may influence recovery from surgery. Science 224:420–421.

University of Minnesota. (2006). Environmental Benefits of a Healthy, Sustainable Lawn. http://www.sustland.umn.edu/maint/benefits.htm.

Uslu, A. (2002). İthal Süs Bitkileri İle Ekonomik/Ekolojik Park Tasarımı Gerçekleşebilirmi? II. Ulusal Süs Bitkileri Kongresi, 22-24 Ekim 2002, Antalya.

Van Haaften, E.H., Van De Vijver, F.J.R. (1996). Psychological consequences of environmental degradation. J. Health Psychol. 1: 411–429.

Virginia State University. (2004). Nutrient Management for Lawn Service Companies. http://www.ext.vt.edu/pubs/turf/430-400/430-400.html#L2

Wood, R.A., Orwell, R.L., Tarran, J., Torpy, F. and Burchett, M. (2002). Pottedplant/growth media interactions and capacities for removal of volatiles from indoor air. J. Hort. Sci. Biotechnol. 77:120-129.

Worldwatch Institute. (2007). Cities Key to Tackling Poverty and Climate Change. http://worldwatch.org/node/4839.

Yannick, J., Brengman, M., Willems, K., Kathleen, W. (2009). The effects of urban retail greenery on consumer experience: Reviewing the evidence from a restorative perspective. Urban Forestry and Urban Greening 9:57–64.

Yazgan, M.E., Korkut, A.B., Barış, E., Erkal, S., Yılmaz, R., Erken, K., Gürsan, K., Özyavuz, M. (2005). Süs Bitkileri Üretiminde Gelişmeler. Ziraat Mühendisleri Odası Teknik Kongresi, 3-7 Ocak 2005.

Yazici, K., Gülgün, B. (2016). Tr83 Illerinde Süs Bitkileri Sektörünün Mevcut Durumu Ve Gelistirilmesi Üzerine Bir Arastırma. Selçuk Gıda Tarım Bilimleri Dergisi, 3(1), 18-24.

URBAN SCALE MICRO AGRICULTURE PRACTISES

Bahar Sancar[1]

[1]Kocaeli University, Faculty of Agriculture, Department of Agricultural Economics, Kocaeli, Turkey.

[1]ORCID ID: https://orcid.org/0000-0002-3687-1495

Mert Çakır[2]

[2]Süleyman Demirel University, Faculty of Architecture, Department of Landscape Architecture, Isparta, Turkey.

[2]ORCID ID: https://orcid.org/0000-0003-0079-0375

ABSTRACT

The demand for staple foods rises along with the global population. The world population, which was approximately 7.5 billion in 2016, is projected to increase to 8.5 billion in 2030 and to 9.7 billion by 2050. In order to meet the staple food needs, there should be a parallel growth in agricultural production of 70%. Chemical goods are now being utilized extensively in agricultural areas to meet this requirement, and as a result, their detrimental impacts on human health and the environment are starting to be clearly seen. Urban agriculture, permaculture, roof-terrace-balcony gardening, hobby gardening, and vertical gardening are examples of urban scale micro-agriculture techniques. It is well known that agricultural goods produced in small-scale areas in and around cities significantly contribute to world food production and that this sort of agriculture offers some ecosystem services, such as promoting healthy soils. Urban agriculture has a number of ecological advantages, including a decrease in waste production, an increase in biodiversity and air quality, and a reduction in the environmental effect of food storage and transportation. The purpose of this study was to establish the advantages of micro agriculture at an urban size and to examine micro-agriculture practices globally and in Turkey.

Keywords: Agricultural Methods, Alternative Agriculture, Food Supply, Micro-agriculture

1. INTRODUCTION

Agriculture encompasses the production of plant and animal goods (including forestry and fishery activities), as well as the harvesting, transportation, preservation, and sale of products. (Karluk, 1999). Agricultural practices meet the basic nutritional needs of people. Risk and unpredictability are considerable since agricultural production is reliant on climatic conditions. As a result, the requirements for supply and demand in agricultural production are adaptable and diverse (Türkoglu, 2015). The demand for staple foods rises along with the global population. While there were roughly 7.5 billion people on the planet in 2016, that number is projected to rise to 8.5 billion in 2030 and 9.7 billion in 2050. In order to meet the staple food needs, there should be a parallel growth in agricultural production of 70% (FAO, 2017). The cultivation of species with the greatest efficiency, the use of chemical pesticides and fertilizers, and the employment of technology have all contributed to a large increase in production since the green revolution of the 20th century. However, the excessive use of chemical products negatively affects both people and the environment (Bhandari, 2014; Walter et al., 2017). Due to the results of improper agricultural policies and excessive water use in the world, it has become necessary to make some agricultural lands unusable alongside these environmental issues, to get maximum efficiency in the smallest area, and to do this in a sustainable and environmentally friendly way (Shamshiri et al., 2018).

According to Vagsholm et al. (2020), it is deemed inevitable to design ways to minimize waste and losses in production systems that aim to reduce losses and waste while achieving the highest production. Traditional agricultural practices serve as the foundation for the change process in agriculture, and it is important to incorporate smarter techniques based on data gathered utilizing a variety of trend technologies (Lioutas et al., 2021).

In addition to meeting the nutritional needs of the world population, agriculture has an indispensable place in the economy due to its features such as meeting the raw material source in the economy, industry, and contributing directly or indirectly to exports. Environmental, social, and economic impacts on agriculture reduce considerably as the population grows, and food production rises (Pittelkow et al., 2015; Lidicker, 2020, Pineiro et al., 2020; Ofosu et al., 2020; Singh and Singh, 2020; Tamburino et al., 2020). Agriculture plays a key role in the economy for the growth and development of many countries (Abioye et al., 2020). Agriculture is a dominant sector in nine nations and contributes 6.4% of global economic productivity (Pathan et al., 2020).

In 2007, for the first time in the world, the urban population exceeded the rural population. According to estimates, 34% of the world's population will reside in rural areas in 2050, with the remainder residing in urban areas. People today are looking for diverse locations to breathe because they live uniform lives with urban growth. It has been disregarded that the natural life cycle is supported by atmospheric events including air, water, sun, rain, and wind, which are in risk of extinction given the technological growth they are undergoing (Unal and Akyuz, 2018). In order to address this urban risk, save urban wildlife, and develop new living spaces, micro-gardens are used as an alternative to traditional living arrangements. Micro agriculture refers to agricultural activities that are typically conducted on urban sites that are smaller than 5 decares. Urban agriculture, permaculture, roof-terrace-balcony gardening, hobby gardening and vertical gardening (green wall) can be listed among the micro-agricultural practices that can be applied on an urban scale.

The following explanation explains how micro-agricultural activities carried out on an urban scale contribute to production: A one square meter micro garden may produce 100 onions in 120 days, 30 kg of tomatoes annually, 36 lettuce every 60 days, and 10 cabbages every 90 days (FAO, 2010). Micro-agriculture techniques, which provide daily direct access to fresh, nutrient-rich vegetables, enable people to meet their vitamin, mineral, and plant protein demands in accordance with their unique capacities. Additionally, it offers an additional revenue stream from the selling of low-volume goods. The goal of this study is to determine the benefits of micro agriculture in urban settings and examine micro-agriculture practices in the world and in Turkey.

2. MICRO AGRICULTURAL PRACTICES

With the technological and sociological advancements that occurred immediately following the Industrial Revolution, humans are migrating away from nature by adopting new living forms, and new city types are emerging. Urban air temperatures have risen in all cities as a result of the rapid acceleration of urbanization, population growth, and migration, as well as the unchecked use of old energy sources, which are classified as non-renewable, which have led to major environmental issues worldwide. Due to the increased awareness of these negative effects on the environment and human health, the idea of sustainability was put on the map with the intention of resolving the issues by creating sustainable living environments. Sustainable space design is vital for the environment, economics, and energy efficiency.

Agricultural activities that focus on growing crops and increasing productivity in limited agricultural areas (usually less than 5 decares) in urban, semi-urban and rural areas are called micro agriculture. Micro-agriculture practices include urban agriculture, permaculture, roof, terrace and balcony gardening, hobby gardening and planting vegetables, fruit and ornamentals in vertical gardens, as well as growing plants in locally available recycled materials (e.g. plastic boxes, old rubbers and polyethylene bags) (Barclay, 2013).

The FAO attempted to popularize micro agriculture in 2010 with a project in Central and South America and African countries (Gabon, Namibia, Niger, Senegal and Rwanda) (WHO/FAO, 2003; FAO, 2010; UN, 2011; Metropolis, 2014; UMGI, 2014). With the help of this project, it has been determined that low-income families meet their nutritional needs and obtain an additional income source by selling their surplus products.

As a result of not only low-income families but also people who want to produce their own basic needs, those who produce as a hobby, people who are bored with the hectic pace and crowded nature of the city, as well as people who want to produce in the areas where they live (balcony, roof, etc.), these applications have gained popularity in recent years. It is anticipated that the growing popularity of micro agriculture will have benefits for society, the economy, and the environment in the face of issues like urbanization, population growth, and malnutrition (Climate Action, 2010).

Micro agriculture practices are suitable for all age groups and are an extremely productive method. Micro farming techniques have various benefits. These are suitable for cities because they are quick and affordable, take up little space, produce results quickly (in 45 to 90 days), don't require the use of chemical pesticides and fertilizers, purify the air, help with household waste management by recycling waste products, and harvest rainwater. Additional benefits of micro agriculture practices as an environmentally friendly approach can be listed as follows; integrated use of domestic waste as compost and fertilizer to increase productivity, zero tillage aimed at increasing biodiversity, mulching and protective agricultural practices such as insect culture (Ba and Ba, 2007; Climate Action, 2010; FAO, 2010; BBC, 2012; Barclay, 2013; Metropolis, 2014).

2.1. Urban Agriculture

These agricultural activities provide a significant portion of the daily food and fuel requirements of residents in and around the city. An alternate production model to industrial agriculture is urban agriculture. Urban waste and natural resources are used in cities for production in order to meet personal needs or to generate additional revenue from plant and animal goods (Mougeot 2000; Smit et al. 2001; FAO 2007).

Economic activity, location, land, scale, product and producer are common components of urban agricultural activities (Stewart et al. 2013). There are empty urban areas in all cities where agricultural activities can be carried out. These areas can be listed as areas that are not suitable for construction, free public or other property, temporarily unused areas, empty areas belonging to the public, and residential surfaces such as roofs and balconies (Smit and Nasr, 1992).

Urban agriculture has many benefits in terms of environmental sustainability. It contributes positively to environmental restoration and rehabilitation and urban landscape in order to recover the areas where wastes are accumulated within the urban landscape and unused areas. In addition, air pollution and fuel consumption are reduced due to the shortening of distances in the transportation of products. The increase in green areas provides many opportunities for the urban people in terms of physical, psychological and health (Beatley, 2000). The environmental benefits of urban agriculture are summarized in Table 1 (Smit et. al 2001; FAO 2007; Knizhnik, 2012).

Table 1. Environmental benefits of urban agriculture

Increases biodiversity
Creates habitat for wildlife
Creates a microclimate
Reduces the heat island effect
Improves air quality and humidity
Improves the urban landscape
Provides positive effects on human health
Creates physical recreation areas
Provides protection from sun and rain
Reduces noise and dust
Enables the evaluation of unused areas and roofs, terraces and balconies
Reduces ecological footprint
Offers recreational opportunities

Urban agriculture contributes to the solution of environmental problems by using urban wastes (compost production, irrigation with waste water) as a production source (Cofie et al. 2006). Urban forests and urban agricultural areas contribute to green areas on the condition of creating microclimate and increasing biodiversity and ensuring its sustainability (Konijnendijk, 2004). It minimizes energy consumption and lessens the ecological impact of cities by speeding up the processes of fresh, daily food production and transportation from producer to consumer. Urban agricultural areas provide services including landscape maintenance, quality time, and enjoyment while also increasing the amount of green space. The planning and management of recreational areas should be based on agro-ecological production methods related to eco-sanitation / sustainable waste management, and these functions should be integrated with urban agricultural areas (FAO, 2007).

In terms of environmental sustainability, urban agriculture has some negative environmental effects. Intensive use of chemical pesticides and fertilizers causes pollution of water resources, and the use of nitrate-rich fertilizers (such as chicken fertilizer) causes groundwater pollution. As a result of the misuse of marginal areas in the city, sensitive ecosystems are damaged (FAO, 2007).

Urban agriculture has certain detrimental consequences on the environment in terms of environmental sustainability. Water resources are contaminated by the frequent use of chemical fertilizers and pesticides, and groundwater is contaminated by the use of fertilizers high in nitrate. Sensitive ecosystems in the city are harmed as a result of the improper usage of marginal areas (FAO, 2007).

2.2. Permaculture

Permaculture, also known as sustainable agriculture, is an ecological design approach applied in accordance with agricultural practices and sustainability principles that aim to benefit the nature and the world of which they are a part, by taking the physical and mental needs of people and the functioning of the natural ecosystem as a reference. This approach first emerged in the 1970s in Australia with the study of Bill Mollison and David Holmgren. Permaculture is also an earth science that creates human settlements where comprehensive solutions to ecological issues are generated by fusing agricultural practices with scientific knowledge, technology, and skills (Althouse, 2006; Anonymous, 2022a).

Scientists have defined permaculture in different ways at different times. According to Holmgren (2001), permaculture is a landscape design in which sustainable settlements and food production systems are applied to meet local needs and to consume resources in a healthy way. According to Kendiway (2009), permaculture has been defined by taking in the issues of meeting the urban needs of society such as healthy food, clean water, renewable energy and creating natural habitats in sustainable and flexible ways. According to Mollison (2017), permaculture is a design method in which rich and sustainable human settlements are created by observing natural systems.

With these concepts, the individual is meant to move from a position of ecosystem consumer to producer. A self-sufficient cycle, sustaining the lives of living and non-living beings that do not produce waste, and fostering beneficial relationships for all parties are the objectives of permaculture design. These objectives are achieved by integrating healthy food and energy production without harming the environment. These approach objectives aim to support effective and eco-friendly solutions. Nature, people, and other living things on earth are all covered by the three fundamental ethical principles. These regulations both direct the designs to be developed and the standards by which the area will be assessed (Mollison, 1979;1981; Althouse, 2006). The most fundamental component of these laws is the human, and everything is based on enhancing human life. Humans are the ones with the most work and obligation in this improvement. The goal of permaculture ethics is to create harmonious relationships with nature and use the proper techniques to address human needs. Holmgren (1981) and Mollison (2001) determined permaculture ethics and principles as in the Table 2.

Table 2. Permaculture ethics and principles

Permaculture Principles	Permaculture Ethics
Observing and interacting	Take care of the earth
Using energy effectively	To take care of people
Energy storage	Setting consumption limits
Get yield	
Building self-managing systems based on feedback	
Evaluating renewable resources	
Using appropriate technology	
Not producing waste	
Designing for repetitive details	
Combining elements	
Using small and slow solutions	
Providing and increasing diversity	
Utilizing interfaces and obtaining marginal value	
Responding to change creatively	
Giving functionality to components	
Supporting important functions	

2.3. Roof-Terrace-Balcony Gardening

The roof was once a building part whose surface consumed energy, but thanks to recently developed technology and science of building materials, it is now a building component that benefits the ecology. With the sustainable use of green roofs, the roof—which is typically a heat-absorbing, inert, and underutilized building material—has begun to develop into a space that offers living spaces outside the building and may also be used for activities (Eyüce, 2009).

The roof garden is an area often used for recreation, entertainment and as an additional outdoor living space for building occupants. Roof gardens play an important role in sustainable design and are also defined as living roofs, green roofs and eco-roofs (Coffman, 2007). A roof garden is a green area created by adding layers of environment and plants on a traditional roof system and has positive functions compared to traditional roofs in many respects (Pomegranate Center, 2005; Ekşi, 2014). In other words, roof gardens are important systems that improve the energy performance, air quality and urban ecology of the building without additional equipment, produce innovative solutions to the problems created by rain water, and take place in sustainable buildings with these features (Tohum, 2011).

Some cultures have employed planting studies on structures throughout history for aesthetic and environmental reasons (Osmundson, 1999; Ekşi, 2014). The Hanging Gardens of Babylon, which were built 2500 years ago, are where roof gardens first appeared. There were substantial, tiered, and densely planted terraces built on top of the city walls, it was discovered when the archaeological findings were studied (Tunbis, 1987). In order to insulate their homes from the elements and to fix the soil, people who lived in Northern Europe in the 18th century covered their roofs with dirt and planted herbaceous plants (Getter and Rowe, 2006; Eksi, 2014).

In order to meet the settlement need due to population growth, the construction of high-rise buildings has been increasing recently as a result of rapid urbanization (Duzenli et al., 2016). The decrease in natural vegetation and green areas and the high heat absorbing, dark colored materials used in roof coverings have caused an increase in atmospheric temperature with global warming (Turkes et al., 2000; Bulut, 2005; Tohum, 2011). Roof gardens contribute to urban areas in many ways. In addition to their aesthetic appearance, roof gardens provide economic, ecological and social benefits as long as they are built with a safe insulation system and correct projecting. These benefits are presented in Table 3. (Patterson, 2001; Dough et al., 2005; Jenrick, 2005; Environmental Affairs Department, 2006; Erkul & Sonmez, 2014). One of the most common applications applied to increase the amount of green space in cities today is roof gardens.

Table 3. The benefits of roof gardens

Economic Benefits	Ecological Benefits	Social Benefits
Reduction in replacement cost	Creating a natural habitat for plants and animals	Obtaining new usage areas
Reduction in heating cost	Reduction in environmental noise	Creating natural environments
Increasing the thermal insulation of the roof	Reduction in dust and smoke levels	
Extending the life of waterproofing	Changing the climate characteristics of the environment	
Reduction in drainage cost		
Reduction in the amount of waste water		
Creating space utilization		

There are two basic types of roof gardens. These are intensive and extensive roofs (Getter and Rowe, 2006). Intensive roofs are areas that are planted with medium-sized trees, shrubs, ornamental plants and plants of at least 30 cm in size and are established for aesthetic purposes that require maintenance (Uzun, 2002; Dunnet and Kingsbury, 2008; Eksi and Uzun, 2016). Extensive roofs are areas that are planted with plants that have the ability to recovery against any biotic and abiotic stress, have a narrow growing environment, need low maintenance, and are established to provide ecological benefits to the building and the city on which they are located (Dunnett and Kingsbury, 2004; Liu, 2004; Lazzarin et al., 2005; Environmental Affairs Department, 2006; Obendorfer et al., 2007; Dunnet and Kingsbury, 2008; Fioretti et al., 2010; Eksi and Uzun, 2016). The differences between dense and extensive roof systems are outlined in Table 4.

Table 4. Differences between intensive and extensive roof systems (Kuçukerbas, 1991; Kuçukerbas, 1993a;1993b; Koç and Gunes, 1998; Uzun, 2002; Eksi, 2006; Gemi, 2010; Eksi, 2012a; Aycam and Kınalı, 2013; Anonymous, 2022b).

Features	Intensive (Dense)	Extensive (Rare)
Infrastructure	Sometimes complex, labor-intensive, additional structural layers	Simple, lightweight, easy-to-implement layering
Habitat	Deep, low evaporation value, high weight, suitable environment for plant growth	Shallow, light, high evaporation, difficult environment for plants
Maintenance Needs	Low maintenance, easy	High maintenance needs, fertilization, irrigation, pruning activities
Vegetable Tissue	Ground cover, shrub, tree, habitat requirements are high	Ground cover or herbaceous, short height, low habitat requirements, durable
Height	25-100 cm	<15 cm
Irrigation	Always necessary	Mostly absent
Weight	250-1000 kg/m^2	50-150 kg/m^2
Possibility to walk	Available	None or limited
Water buffer	18-39 mm	4-12 mm
Roof load capacity	Requires extra strong roof structure	Mostly enough
Roof slope	Straight or in the form of terraces	Up to 45 degrees

Terrace garden is defined as an open green space arrangement with many functions that requires more or less maintenance, carried out with the help of special materials and techniques, on a straight or slightly sloping area of any building located on the ground or mostly above ground level. Terrace gardens are examined in two main groups. These are intensive and extensive terrace gardens.

Intensive terrace gardens: a type of terrace garden arrangement that requires a deep soil level, which is arranged with trees, shrubs and turfgrasses in a large area.

Extensive terrace gardens: a type of terrace garden arrangement where less soil is required in terms of soil depth than intensive, more turfgrasses, groups of shrubs or one-perennial ground cover plants.

Balconies and terraces are indispensable living spaces as a defined space where plants, birds, insects and similar living creatures live together with people and share a common space. In this regard, balconies and terraces, which are considered rooms of the house within the definition of open space, are also designed in parallel with this shaping if the design of all rooms of a house is shaped in accordance with the user's preferences. In this respect, communities with different cultures in different countries display their lifestyle

and culture on balconies and terraces, and use suitable plant species, furniture and accessories. Terrace and balcony gardens create environments where people can touch both their own lives and urban life. Planting applications are carried out with plants such as vegetables, fruit trees and ornamental plants in materials such as small pots and plastic on balconies and terraces. With this application, people produce their own food and contribute to the amount of green space in cities by creating green space where they live. In recent years, balconies and terrace gardens have gained importance in apartment-style buildings in cities and neighborhoods.

2.4. Hobby Gardening

As a result of the increase in urban areas, unplanned urbanization and the decrease in green areas, people have moved away from nature and are stuck between concrete structures. Due to this circumstance, people have conducted various searches. Hobby gardening, also known as urban small gardens, is one of these pursuits. Hobby gardens are places where urban dwellers and farmers interact, where people can produce a variety of fruits, vegetables, and ornamental plants, and where they can unwind (Erduran and Sulusoğlu, 2006).

Hobby gardens often cover areas up to 300 m2 and begin at 20 m2. For a year, a person who rents a hobby garden can grow any type of fruit, vegetable, or ornamental plant without the use of pesticides or chemical fertilizers. Basic amenities such a security building, parking, administrative and personnel building, a restroom, a prayer room, a children's playground, parcels, sitting places, a warehouse, trash cans, and a water tank are all present in hobby gardens.

The establishment of hobby gardens in the world was related to the economic crisis. In the industrial revolution, the living conditions of the workers were adversely affected and encouraged the establishment of dedicated gardens due to economic difficulties. Afterwards, the establishment of hobby gardens in countries for different purposes started to increase and hobby gardening is now carried out in many European countries. Hobby gardens, which have a history dating back to the 18th century in the world, started to be implemented in Turkey at the end of the 20th century. The first example in the world was established in England, and the first example in Turkey was established in the city of Bursa. As of 2015, there are 28 hobby gardens in Turkey. 7 of them are in Eskisehir, there are 5 in Istanbul, Konya, Kayseri, 2 in Bursa and Mersin, and one in Balıkesir and Gaziantep (Kef, 2015).

Recently, hobby gardens in some cities are considered as a kind of relaxation garden. The hobby garden allows people to get away from the busy pace of the city, spend free time in nature and grow organic vegetables and fruits (Oguz, 2000). People living in cities get both economic and psychological gains in order to deal with the soil, to cultivate, to grow plants, to take care of various plants and to obtain products in these areas, which they rent for certain periods. Spending time in these areas enables people to perform recreational activities (Yılmaz et al., 2006; Kılıc, 1995). At the same time, hobby gardens improve the urban open green space system and contribute positively to the urban ecosystem and urban aesthetics (Erduran et al., 2008). Common characteristics of hobby gardens are given in the Table 5 (Yılmaz et al., 2006; Onder and Polat, 2008, Kef, 2015).

Table 5. Common characteristics of hobby gardens

They are usually established by local governments and municipalities. However, there are also those established by individuals, associations and universities both in Europe and Turkey.
They are rented to city dwellers under specific terms and for a specific sum of money at specific times.
The facilities are managed by a voluntary association and an elected manager.
They contain necessary structures such as walking paths and parking areas.
They are situated inside the city or close by.
Area sizes should be 20-200 square meters.
Crops such as vegetables, fruits and flowers are grown.
They are built on first class agricultural land. Slope values should be less than 2%.

2.5. Vertical Garden (Green Wall)

Vertical gardening was first applied in 1915 by Patrick Blanc, an American geologist. It is a type of production that aims to increase the number of plants per unit area on the vertical axis without the need for soil (Fabian and Malte, 2011; Anirudh and Rekha, 2014). It is also known by names such as green wall, turfgrass wall and wall covered with greenery (De Bon et al., 2017). The vertical garden creates a three-dimensional view on the vertical axis by highlighting the soil volume. It can be used in groups or soliter in different heights and shapes with flowerpots or similar containers. Vertical garden can be applied inside and outside the building. The materials used must be environmentally friendly and reusable (Nwosisi and Nandwani, 2018).

In addition to their appealing appearance, vertical gardens have advantages for humans, such as improving their mental and spiritual health (Timur and Karaca 2013). The main purpose in vertical gardens is to create ecological, educational and environmental awareness. It creates a recreation area for those who want to grow plants. Healthy and fresh plants can be produced and consumed thanks to this environmentally friendly application (Nwosisi and Nandwani, 2018). The environmental benefits of vertical gardens are given in Table 6 (Wolverton et al., 1989; Elinc and Elinc, 2010; Tufekcioglu, 2010; Tekin and Oguz, 2011; Helzel and Batıgun, 2012; Grant, 2015; Blanc, 2018; Star, 2018; Yıldız, 2018).

Table 6. The environmental benefits of vertical gardens

Reduces energy consumption and increases energy efficiency
Reduces water consumption
Provides acoustic comfort and reducing noise pollution
Increases indoor-outdoor air quality
Supports biodiversity
Increases aesthetic comfort

The development of diseases and pests can be slowed down, the ecological environment can be enhanced, product quality can rise, and water waste can be avoided in the controlled environment utilized for vertical gardens. Additionally, vertical farming enables simple and less expensive product distribution in cities (Schans et al., 2014). Depending on their types, vertical gardens are categorized into two categories. These include living walls and green facades (Kalay and Özen, 2021).

Green facades are a vertical garden system created from climber plant groups or various plants. This system be mounted independently on existing walls or buildings such as columns and fences. Green facades are created by wrapping the plants in a mesh panel or netting system with cable, wire, or rope. In addition, there are different production methods according to their ability to grow with or without contact with the wall and in pots and soil (Kiasif and Selcuk, 2018).

Living walls are called as biological walls. It is a type of vertical garden planted with vertical modules, planted panels or plantation in the living walls system. Living walls can be made of polyester, plastic, synthetic fabric, metal, clay and concrete, and various plant species can be used at the desired density. Automatic systems are preferred in the maintenance (Agriculture Vertical Gardens, 2016).

3. MICRO AGRICULTURE PRACTICES IN THE WORLD AND IN TURKEY

3.1. Urban Agriculture

Examples from Turkey

Kuzguncuk City Garden (İstanbul)

One of Istanbul's most significant green spaces, Kuzguncuk, has been retained in its original form for approximately 700 years and still produces goods. This garden is protected by the Kuzguncuklular Association and the residents of Kuzguncuk Neighborhood. Kuzguncuk City Garden, formerly known as İlya

Garden, is used for both agricultural production and social gatherings. Additionally, permaculture design was used to build facilities like playgrounds, rest areas, and walking paths (Sayan, 2014).

Yedikule Gardens (İstanbul)

Yedikule Gardens in Istanbul, which is one of the important representatives of urban agriculture, both protect the agricultural heritage and have an important place in terms of the continuity of safe, healthy and local food production. The gardens in Yedikule have survived from the Ottoman period, and nowadays, thanks to the Yedikule Conservation Initiative, they are tried to be preserved as both a productive and social space (Sayan, 2014).

Examples from the World

Wolcott Street Farm (Brooklyn, New York, USA)

This urban agriculture region, which was developed by changing the vacant areas between the city center and the sea, was founded by a volunteer society. The goal of this farn is to turn barren land into vibrant urban farms, provide access to wholesome, reasonably priced produce, and develop the next generation of environmental leaders by introducing young people to the industry (Red Hook Farms, 2021).

Perth Urban Farm (Perth, Australia)

The aim of this area, which was created by transforming the free and unused land in the city into an urban farm, is to provide a learning experience to people of all ages, to encourage social capital and community participation, and to educate these people on the importance and ease of sustainable living practices. The area was created by volunteer individuals and is used for multiple purposes. A variety of fruits and vegetables are produced, poultry is raised, waste management is provided, and there is also arts and community room in the area and workshops for children and adults (Evans, 2021).

3.2. Permaculture

Examples from Turkey

Marmariç (İzmir)

Marmariç Ecological Life Association was established in İzmir's Bayındırlık district in 2005 in order to be an exemplary sustainable settlement and to share the experiences gained while creating this settlement, and it started to be implemented in 2009. The objectives of the project are to reduce the pressure on natural water resources, to take measures against the unstable precipitation regime due to climate change, to increase product diversity by reducing agricultural inputs in fertilization, irrigation, hoeing, pest and weed control, to create a self-sustaining and self-sustaining life culture model, and to spreading and sharing the experience gained during this period in various ways (Bakır et al., 2011).

Belentepe Permaculture Practice and Wildlife Farm (Bursa)

Studies on sustainable living using permaculture principles are being conducted in the high-altitude Belentepe, southwest of Bursa Uludağ, on a 15 decares facing south region. The farm features raised bed vegetable gardens, a greenhouse, an artificial pond, water retention ditches, an entry-level food forest, and a pasture for the animals. It also produces natural honey. Buildings with green roofs have been constructed from natural materials, and solar panels installed on the rooftops of the structures generate electricity (Anonymous, 2022f).

Examples from the World

Australian Permaculture Research Institute and JOHUD Greening the Desert (Jordan)

It is a successful example of overcoming all problems by using permaculture design in a five-hectare agricultural area where severe drought, yield loss and salinization are experienced (Anonymous, 2022c; 2022d).

Urban Permaculture Path to Freedom (Pasadena, USA)

It is a family project that started in the mid-1980s. It aims to experience the simple life and to meet the food needs throughout the year from an organic permaculture garden. During the project, they first started to use alternative energy sources in their homes. They ran their cars on homemade biodiesel. In addition to new technologies, they are researching the life solutions of past generations. They raise farm animals from which they use their fertilizers and eggs (Anonymous, 2022e).

3.3. Roof-Terrace-Balcony Gardening

Examples from Turkey

Meydan Shopping Center (İstanbul)

Established on an area of 128 thousand square meters in Ümraniye (İstanbul), the shopping center has been designed in accordance with modern life and ecological environment. The roof area is about 55,000 square meters, of which 30,000 square meters is green space. There is an extensive roof system with different slopes ranging from 0 to 125%. The project has received many awards both in terms of architecture and the technologies it uses (Aksoy and İcmek 2010, Anonymous 2017a).

Forum İstanbul Shopping Center (İstanbul)

Intensive plantation was applied on the green roof of the Forum İstanbul project, which was established on an area of approximately 250.000 square meters in Bayrampaşa, İstanbul. There is a green roof application of 3,500 m² in the project. In this project, it was thought that the soil depth should be greater and the pot system should not be used as much as possible, but this could not be realized and polygonal pots of various sizes were designed and palm, acacia and oaks were used (Tohum, 2011).

Examples from the World

Nanyang Technical University (Singapore)

The curved and green roof of Nanyang Science, Technology and Research University, located in a forest area in Singapore, was designed in 2006 according to the extensive roof system in order to adapt to the natural structure of the environment. The building, built on an area of approximately 18,000 m^2, has a slope of 60% (Anonymous 2017b, Aycam and Kınalı 2013).

Nine Houses (Switzerland)

Nine houses, whose construction was completed in Switzerland in 1993, are designed as single-family residences according to the intensive roof system. The total green roof area of this building, which consists of 9 residences and was built with the idea of integrating a building into the environment as much as possible and ensuring growth based on surface area, is 3.9950 m^2 (Anonymous 2017b). With the directive that came into effect in Switzerland, many city administrations are converting straight roofs to green roofs. In 2017, 29.5% of the straight roofs in Zurich have been green roofs (Tohum, 2011).

3.4. Hobby Gardening

Examples from Turkey

İzmir City Gardens (İzmir)

The area covered by İzmir City Gardens is 13 950 m^2. It consists of 44 parcels, each of which is 140-160 m^2. There are no garden houses in the parcels. İzmir City Gardens are also leased to retirees on a contractual basis for one year (Kılıç, 1995).

Atatürk Forest Farm Hobby Gardens (Ankara)

In 2000, hobby gardens were established in the Atatürk Forest Farm area in Ankara and attracted great interest from the citizens. The hobby garden, consisting of 520 parcels of 200 m^2, located on a total area of 60,000 m^2, has been rented for four years. Material storage, pergola, drinking and utility water services were provided in each parcel. Parking area and public use areas, cafeteria, children's playground and sports fields were built in the area. General maintenance of the area was carried out by Atatürk Forest Farm personnel and security and information services were provided (Erduran and Sulusoglu, 2006).

Examples from the World

Various places are reserved for hobby gardens in and outside the city, in the Netherlands. Sports fields, hobby garden complexes and educational gardens for students are included in areas such as Zuiderpark, Cloverleaf and Laag-Zestienhoven Park, which constitute the urban green system (Oguz, 2000; Yılmaz et al., 2006). Hobby gardens in the Netherlands play an important role in protecting and improving the environment in cities and villages (Anonymous, 2014).

Hobby gardens in the UK have a long history. The term hobby garden is referred to as "Guinea Garden", "Allotment Garden" and "Hobby Garden". In the United Kingdom, hobby gardens were established to provide income to poor people, partially different from their current purpose, in the first days of their establishment and they still continue their existence (Önder and Polat, 2008). Growing organic crops in hobby gardens in the UK is in high demand (Anonymous, 2012).

3.5. Vertical Garden (Green Wall)

Examples from Turkey

Siemens Vertical Garden

Turkey's first vertical garden is the Siemens Vertical Garden project, which was established in the Tarlabaşı region of Istanbul. 4000 living plants, 8 different plant species, were used in the vertical garden created on a 90 m^2 surface on the facade of a historical building. Plants and seagull symbols, Siemens logo, and nature theme were embroidered, which brought the environmental identity of the company to the fore (Çelik et al., 2015).

Armaggan Shopping Center Vertical Garden

In the Armaggan Shopping Center in Nuruosmaniye, Istanbul, the wall surface of the five-storey building, which is closed on four sides, is planted and the natural environment effect is tried to be provided aesthetically (Floraplus 2013).

Examples from the World

Vancouver International Airport Vertical Garden (Canada)

The 15 m high 195 m^2 facade, located at the international passenger door of the Vancouver International Airport, has been planted with a panel system by creating different textures and patterns with the use of various plant species symbolizing the "Coastal Mountains" in the region. According to the characteristics of the northern climate, plant species resistant to cold and wind were used. Before the plants were brought to the construction site, they were allowed to grow on the panels for a few months, after which the assembly of the frames, panels and irrigation system was completed in approximately 20 days. Due to the fact that the project was carried out in a region with a very cold and freezing climate, special systems and assembly methods were applied to adapt to winter conditions (GSKY 2013).

Sportplaza Mercator Vertical Garden (The Netherlands)

In the mixed-function Sportplaza Mercator project, which will serve for the Rembrant Park in Amsterdam, the roof and facade of the building are covered to form a porous surface using approximately 5000 species of shrubs and groundcovers. The entire building is planted with a modular system created with three-layer elements. These layers are in the form of steel mesh elements fixed to the structure, protection plates fixed to the inner surfaces of the steel mesh and a thin outer plate on it. The outer layers consist of a metal frame and felt-covered plastic sheets on which pots are placed in regularly formed cavities. The nutrient-rich water that enables plants to grow is transferred to the plants with the automatic hydroponic irrigation method built into the system (Lambertini and Leenhardt 2007).

4. RESULTS

As a result of rising population, rapid urbanization, quick industrialization, etc., today's cities have evolved into places where energy consumption and resource use are at their highest levels. In addition, many countries have had trouble acquiring agricultural items as a result of the COVID-19 pandemic circumstances. These circumstances have shown the need for various ecological applications to be made in urban settings, and along with the "return to nature and nature" theme, which has gained popularity recently, efforts to live in this manner within the constraints at hand have elevated micro-agriculture techniques to the fore. Along with the economic advantages of micro-agricultural practices, which can be organized individually or as a community in the city, there are also other advantages in terms of human health, which are supported by granting access to safer food, as well as social and psychological advantages, which are supported in conjunction with the leisure activity that will be brought about by caring for the soil and the production. Due to their great productivity and efficiency, micro-agriculture techniques can significantly improve food security. Micro-agricultural techniques are expected to significantly help address the problem of food insecurity and the need for food in urban areas without fertile fields. Micro-agricultural methods that contribute to the integrity of green spaces by safeguarding the city's existing natural green spaces should be included.

REFERENCES

Abioye, E., Abidin, Z., Shukri M., Saiful, A., Salinda, B., Mohamad, I., Muhammad, R., Abdulrahaman, O., Patrick, O., Muhammad,.R. (2020). A review on monitoring and advanced control strategies for precision irrigation. Computers and Electronics in Agriculture. 173.

Abul-Soud, M.A., Emam, M.S.A. & Abd El-Rahman Noha, G. (2015). The potential use of vermi-compost in soilless culture for producing strawberry. International Journal of Plant and Soil Science, 8(5): 1-5.

Aksoy, Y., İçmek, S. (2010). Çatı Bahçelerinin Kent Yaşamındaki Yeri ve Önemi: İstanbul Kentinden Örnekler. 5. Ulusal Çatı & Cephe Sempozyumu, İzmir, 15 -16 Nisan 2010.

Althouse, K. (2016). An Instructional Module on Permaculture Design Theory for Landscape Architecture Students, Utah State University.

Anirudh, G. & Rekha, B. (2014). Recent trends in agriculture: vertical farming and organic farming. Advances in Plants and Agriculture Research, 1(4): 00023.

Anonymous, (2012). http://forum.skyscraperpage.com/showthread.php?t=202452, European Housing Question, 15 Aralık 2013.

Anonymous, (2014). http://www.jardins-familiaux.org, Office International du Coin de Terre et Des Jardins Familiaux a.s.b.l. 9 Nisan 2014.

Anonymous, (2017a). http://www.mimdap.org/?p=61650

Anonymous, (2017b). http://greenroofs.org

Anonymous, (2022a). http://www.geofflawtononline.com/about/.

Anonymous, (2022b). Yeşil çatı türleri. http://www.green-urbanscape.com/tr/content/ye%C5%9Fil%C3%A7at%C4%B1-t%C3%BCrleri.

Anonymous, (2022c). http://permaculture.org.au/2007/03/01/greening-the-desert-now-on-youtube/

Anonymous, (2022d). http://permaculture.org.au./2009/12/11/greening-the-desert-ii-final/

Anonymous, (2022e). http://urbanhomestead.org/

Anonymous, (2022f). http://belentepe.org

Ayçam, İ., Kınalı, M. (2013). Ofis Binalarında Yeşil Çatıların Isıtma ve Soğutma Yüklerine Olan Etkilerinin Analizi. Tesisat Mühendisliği Dergisi, Sayı 135, Mayıs-Haziran 2013, s. 26-34.

Ba, A. and Ba, N. (2007). Micro-gardens in Dakar. December 2007, 30-31. In: http://www.ruaf.org/sites/default/files/UAmagazine%2019%20H11.pdf (November 2014).

Bakır, M.F., Akhuy, S., Aydemir, G. (2011). Permakültür El Kitabı ve Marmariç Örneği, Marmariç Ekolojik Yaşam Derneği, Mengi Basım Ambalaj Yayıncılık San. Tic. ve Ltd Şti., Türkiye.

Barclay, E. (2013). Why Micro-Gardening Could Go Big. In: http://www.northcountrypublicradio.org/news/npr/197998315/why-micro-gardening-could-go-big (November 2014).

BBC, (2012). Africa: Feeding the rising urban population. In: http://www.bbc.com/news/ business-19541723 (November 2014).

Beatley, T. (2000). Green Urbanism: Learning from European Cities. Washington D.C.: Island Press.

Bhandari, G. (2014). An overview of agrochemicals and their effects on environment in Nepal. Applied Ecology and Environmental Sciences, 2(2), 66–73. doi: 10.12691/aees-2-2-5.

Blanc, P. (2018). "A Scientific and Artistic approach by Patric Blanc Vertical Garden".https://www.verticalgardenpatrickblanc.com/sites/default/files/styles/slideshow/public/16766-0.jpg?itok=v3omvLtY

Bulut, Ü. (2005). Teras çatılar üzerine mimari bir değerlendirme. http://catider.org.tr/pdf/sempozyum/bildiri_8.pdf.

Çelik, A., Ender, E. & Zencirkıran, M. (2015). Dikey Bahçe ve Türkiye'deki Uygulamaları. Tarım Bilimleri Araştırma Dergisi, 8 (1), 67-70. Retrieved from https://dergipark.org.tr/tr/pub/tabad/issue/34798/385377

Climate Action, (2010). UN promotes the benefits of micro-gardens in Africa. In: http://www.climateactionprogramme.org/news/un_promotes_the_benefits_of_microgardens_in_africa (November 2014).

Cofie, O., Adam-Bradford, A. and Drechsel, P. (2006). Recycling of urban organic waste for urban agriculture. In R. van Veenhuizen. Cities Farming for the Future: Urban Agriculture for Green and Productive Cities, RUAF Foundation/IDRC/IIRR, Leusden.

Cofman, R.R. (2007). Vegetated Roof Systems: Design, Productivity, Retention, Habitat, And Sustainability In Green Roof And Ecoroof Technology, PhD Thesis, The Ohio State University, Ohio, USA.

De Bon, H., Holmer, R. J. & Aubry, C. (2015). Urban horticulture. Cities and Agriculture: Developing Resilient Urban Food Systems, Earthscan Food and Agriculture. Routledge, London and New York, pp. 218-254.

Doug, B., Hitesh, D., James, L. ve Paul, M. (2005). Report on the environmental benefits and costs of green roof technology for the city of Toronto.

Dunnett, N. ve Kingsbury, N. (2008). Planting green roofs and living walls. Portland, OR: Timber press.

Dunnett, N., Kingsbury, N., (2004). Planting Green Roofs and Living Walls. Timber Press, Oregon.

Düzenli, T., Mumcu, S. ve Eren, E. (2016). Peyzaj mimarlığında çatı bahçelerinin kullanım amaçları: Trabzon kenti örneği. Uluslararası Hakemli Tasarım ve Mimarlık Dergisi, 1(9), 129-142.

Ekşi, M. (2014). Çatı bahçesi kavramı ve terim kullanımı üzerine bir değerlendirme. Avrasya Terim Dergisi, 2(2), 26-35.

Ekşi, M. ve Uzun, A. (2016). Yeşil çatı sistemlerinin su ve enerji dengesi açısından değerlendirilmesi. İstanbul Üniversitesi Orman Fakültesi Dergisi, 66(1), 119-138.

Ekşi, M. (2006). Çatı ve teras bahçelerinde kullanılan konstrüksiyon elemanları ve yeni yaklaşımlar. İstanbul Üniversitesi Fen Bilimleri Enstitüsü Peyzaj Mimarlığı Anabilim Dalı.

Ekşi, M. (2012a). İstanbul'daki başlıca çatı bahçelerinin yapım esasları açısından değerlendirilmesi. Journal Of The Faculty Of Forestry, Istanbul University 62 (1):149-157.

Elinç, H.ve Elinç, Z. K. (2010). "Dikey Bahçelerde Kullanılan Süs Bitkilerinin Estetik Özellikleri" IV. Süs Bitkileri Kongresi Bildirirler (535-540), Alata Bahçe Kültürleri Araştırma Enstitüsü, Mersin.

Environmental Affairs Department, (2006). Green Roofs-Cooling Los Angeles; A Resource Guide. Environmental Affairs Department City, Los Angeles, CA.

Erduran, F., Kabaş, S., Ayhan, Ç.K. & Kelkit, A. (2008). Çanakkale kentinde hobi bahçesi amaçlı kullanılan alanların peyzaj mimarisi açısından değerlendirilmesi. Çanakkale Kenti Çevre Sorunları Sempozyumu, (s. 148-157).

Erduran, F., Sülüşoğlu, M. (2006). Hobi Bahçelerinin Kent Ekolojisinde ve Gelişiminde önemi ve Kocaeli-İzmit Örneği. VI. Ulusal Ekoloji ve Çevre Kongresi. Diyarbakır.

Erkul, E. ve Sönmez, A. (2014). Yeşil çatı sistemleri ve çevresel etkileri. Mimarlık Dergisi, 375(1), 52-58.

Evans, P, N. (2021). History of perth city farm. https://perthcityfarm.org.au/gardening/history/.

Eyüce, A. (2009). Doğa ve Mimarlık İlişkileri. 21. Uluslararası Yapı ve Yaşam Kongresi, Doğa, Kent ve Sürdürülebilirlik, 20-21 Mart, sf.6-10, TMMOB Mimarlar Odası Bursa Şubesi, Bursa.

Fabian, K. & Malte, E.K. (2011). Vertical farming: can urban agriculture feed a hungry world? Spiegel online news International, p. 4.

FAO, (2007). Profitability and sustainability of urban and peri-urban agriculture. ftp://ftp.fao. org/docrep/fao/010/a1471e/a1471e00.pdf, Erişim tarihi 15.01.2015.

FAO, (2010). Urban and peri-urban horticulture: With micro-gardens, urban poor "grow their own". In: http://www.fao.org/ag/agp/greenercities/pdf/FS/UPH-FS-6.pdf (November 2014).

FAO, (2017). The future of food and agriculture-trends and challenges. Food and Agriculture Organization of the United Nations, Rome.

Fioretti, R., Palla, A., Lanza, L.G., Principi, P. (2010). Green roof energy and water related performance in the mediterranean climate. Building and Environment,45(8), ss. 1890-1904.

Floraplus, (2013). http://www.foraplus.net/content/yesilvadi-den-dikey-bahce-verticalgarden.

Gemi, A. M. (2010). Çevre dostu çatılara örnek uygulamalı bir yaklaşım. 5.Ulusal Çatı ve Cephe Sempozyumu, Dokuz Eylül Üniversitesi Mimarlık Fakültesi Tınaztepe Yerleşkesi – İzmir, 15-16 Nisan, (183-189).

Getter K. L. ve Rowe, D. B. (2006). The role of green roofs in sustainable development. HortScience 41: 1276– 1286.

Grant, G. (2015). "Yeşil Çatılar, Yaşayan Duvarlar" https://www.ekoyapidergisi.org/yesil-catilar-yasayan-duvarlar

GSKY, (2013). http://gsky.com/projects

Helzel, M., & Batıgün, C. (2012). Paslanmaz Çelikten Yapılmış Yeşil Duvarlar.Euro Inox Bina Serisi, Cilt 17, 2-19.

Hemenway, T. (2009). Gaia's Garden: A Guide to Home-scale Permaculture, 2nd Edition, Chapter Tree, Designing the Ecological Garden, Chelsea Green Publishing Company.

Holmgren, D. (2001). The Essence of Permaculture, Extracts of Book Permaculture: Principles and Pathways to Sustainability, Holmgren Design Services, The Source of Permaculture Vision and Innovation.

Jenrick, K. (2005). Green Roofs: A Horticultural Perspective. Dissertation, Royal Botanic Gardens, Kew.

Kalay, F. (2019), "Patrick Blanc'in Dikey Bahçe Tasarımlarının Tasarım İlkeleri Doğrultusunda İrdelenmesi", MSGSÜ Fen Bilimleri Enstitüsü İç Mimarlık Anabilim Dalı Yüksek Lisans Tezi, İstanbul.

Kalay, F., Özen, E.S. (2021). Dikey bahçe uygulamalarının yaşanabilir çevreye sunduğu katkılar. Turkish Journal of Landscape Research, 4 (2), 64-77.

Karluk, R. (1999). Avrupa Birliği ve Türkiye, Beta Yayınevi, İstanbul, s.157.

Kef, F. Ş. (2015). Hobi bahçelerinin planlanması ve tasarımı: Konya Karatay Karaaslan Hobi Bahçesi. (Yüksek Lisans Tezi, Bartın Üniversitesi, Fen Bilimleri Enstitüsü, Bartın).

Kiasif, Ç.G.ve Selçuk, E. (2018). "Yeşillendirilmiş Konut Cephelerin Kentlerin Çevresel Kalkınmasına Etkisi", YTÜ Mimarlık Fakültesi İstanbul I. Konut Kurultayı, 10-11 Mayıs 2018, İstanbul.

Kılıç, H. (1995). İzmir Kenti Örneğinde Kent Küçük Bahçeleri Planlama Olanakları Üzerine Araştırmalar. Yüksek Lisans Tezi (yayımlanmamış), Ege Üniversitesi/Fen Bilimleri Enstitüsü, Peyzaj Mimarlığı Anabilim Dalı, Bornova - İzmir, 105 s.

Knizhnik, L.H. (2012). The Environmental Benefits of Urban Agriculture on Unused, Impermeable and Semi-Permeable Spaces in Major Cities With a Focus on Philadelphia, PA. Master of Environmental Studies Capstone Projects, University of Pennsylvania.

Koç, N., Güneş, G. (1998). Çatı bahçeleri düzenlemesine ilişkin teknik özellikler ve donanımlar. Pamukkale Üniversitesi Mühendislik Fakültesi Mühendislik Bilimleri Dergisi, Cilt 4, Sayı 1-2, (501-512).

Konijnendijk, C., Gauthier, M. and Veenhuizen, R. van. (2004). Trees and cities, growing together. Urban Agriculture Magazine, no 13. Editorial. Leusden, RUAF.

Küçükerbaş, E. V. (1993b). Çatı Bahçeleri. Mimarlar Odası İzmir Şubesi Ege Mimarlık Dergisi, Sayı 3, Sayfa: 41_42, İzmir.

Küçükerbaş, E.V. (1991). Ege bölgesi koşullarında sığ topraklar üzerinde az bakımla (ekstansif) bitkilendirme olanakları üzerinde bir çatı bahçesi örneğinde araştırmalar. E.Ü. Fen Bilimleri Enstitüsü Peyzaj Mimarlığı Anabilim Dalı, Doktora Tezi, İzmir.

Küçükerbaş, E.V. (1993a). Kentlerimizde yeni yeşil alanlar: çatı bahçeleri. Mimarlar Odası İzmir Şubesi Ege mimarlık Dergisi, Sayı1-2, Sayfa: 71-72, İzmir.

Lambertini, A. & Leenhardt, J. (2007). "Vertical Gardens: Bringing The City Of Life", Hudson,U.K.

Lazzarin, R.M., Castellotti, F., Busato, F. (2005). Experimental measurements and numerical modelling of a green roof. Energy and Buildings, 37(12), ss. 1260-1267.

Lidicker, W. Z. (2020). A Scientist's Warning to humanity on human population growth. Global Ecology and Conservation, Volume 24.

Lioutas, E.D., Charatsari, C. & De Rosa, M. (2021). Digitalization of agriculture: A way to solve the food problem or a trolley dilemma? Technology in Society 67(2021): 101744.

LIU, K. (2004), Sustainable Building Envelope -Garden Roof Sistem Performance, NRC-CNRC, RCI Building Envelope Symposium, November 4-5, ss. 1-14, New Orleans.

Metropolis, (2014). Study: Micro-Gardens in Dakar, Senegal. In: http://policytransfer.metropolis.org/case-studies/micro-gardens-in-dakar.pdf (November 2014).

Mollison, B. (1979). Permaculture: A Designers' Manual, Publishers for The Permaculture İnstitute, Second Edition.

Mollison, B. (1981). Introduction to Permaculture, Pamphlet I in the Permaculture Design Course Series Published By Yankee Permaculture.

Mollison, B. (2017). Permakültüre Giriş, Çevirmen: Egemen Özkan, Sürdürülebilir Yaşam Kitapları, Sineksekiz Yayınevi, İstanbul.

Mougeot, L. J. A. (2000). Urban Agriculture: Definition, Presence, Potentials And Risks, Growing Cities, Growing Food: Urban Agriculture at the Policy Agenda: A Reader on Urban Agriculture, Havana, Cuba, 6-9 November.

Nwosisi, S. & Nandwani, D. (2018). Urban Horticulture: Overview of Recent Development (Sustainable Development and Biodiversity Book 18). In: Urban Horticulture Sustainability for the Future. Ed. Nadwani, D. First edition, Springer, Cham, Switzerland, pp. 3-30.

Oberndorfer, E., Lundholm, J., Bass, B., Connelly, M., Coffman, R., Doshi, H., Dunnett, N., Gaffin, S., Kohler, M., Lui, K., Rowe, D.B., (2007). Green roofs as urban ecosystems: ecological structures, functions, and services. BioScience, 57(10), ss. 823-833.

Ofosu, G., Dittmann, R., Sarpong, D. and Botchie, D. (2020). Socio-economic and environmental implications of artisanal and small-scale mining (ASM) on agriculture and livelihoods, Environmental Science and Policy 106, April, 210-220.

Oğuz, D. (2000). Hobi bahçeleri ve Avrupa ülkelerinden örnekler. Ekin Dergisi, (14): 93- 97.

Önder, S. & Polat, A.T. (2008). Peyzaj tasarım süreci kapsamında Konya kenti için yeni bir hobi bahçesi oluşturulması. Selçuk Üniversitesi Ziraat Fakültesi Dergisi, 22(46), 18-25.

Osmundson, T., (1999). Roof gardens: history, design and construction. Norton Company, New York, 0–393– 73012–3.

Özkan, B., Kaplan, A., Aslan, N. & Kılıç, H. (1996). Ülkemizde kent küçük bahçe parklarının gelişimi üzerinde bir araştırma. Ekoloji ve Çevre Dergisi, 18, 18-21.

Pathan, M., Patel, N., Yagnik, H., Shah, M. (2020). Artificial cognition for applications in smart agriculture: A comprehensive review. Artificial Intelligence in Agriculture.

Patterson, S., (2001). Roofing design and practice, Upper Saddle River, N.J.:Prentice Hall

Piñeiro, V., Arias, J., Dürr, J. et al. (2020). A scoping review on incentives for adoption of sustainable agricultural practices and their outcomes. Nat Sustain 3, 809–820.

Pittelkow, C. M., Liang, X., Linquist, B. A., van Groenigen, K. J., Lee, J., Lundy, M. E., van Gestel, N., Six, J., Venterea, T., van Kessel, C. (2015). Productivity limits and potentials of the principles of conservation agriculture. Nature, 517: 365-368.

Pomegranate Center, (2005). Green Roof Manual: How to Replace your Dead Roof with a Living Landscape.

Red Hook Farms. (2021). Wolcott street farm, red hook farms. http://www.added-value.org/aboutus.

Sayan, H. S. (2014). Kentin gizli bahçeleri: kent bostanları. https://www.tarim.com.tr/Kentin-Gizli-Bahceleri-Kent-Bostanlari,29044h.

Schans Van der, J.W., Renting, H. & Rene, V.V. (2014). Innovations in urban agriculture, vol 28. Urban Agriculture Magazine, p. 10.

Shamshiri, R. R., Weltzien, C., Hameed, I. A., Yule, I. J., Grift, T. E., Balasundram, S. K., Pitonakova, L., Ahmad, D., Chowdhary, G. (2018). Research and development in agricultural robotics: A perspective of digital farming. International Journal of Agricultural and Biological Engineering, 11(4), 1–14.

Singh, K.M. and Singh, D. (2020). "Challenges of ensuring food and nutritional security in Bihar". Available at: https://mpra.ub.uni-muenchen.de/96679/1/MPRA_paper_96679.pdf

Smit, J. and Nasr, J. (1992). Urban agriculture for sustainable cities: using wastes and idle land and water bodies as resources. Environment and Urbanization 1992 pp.141-152.

Smit, J., Nasr, J. and Ratta, A. (2001). Urban Agriculture: Food, Jobs and Sustainable Cities, UNDP, Habitat II Series.

Stewart, R., Korth, M., Langer, L., Rafferty, S., Da Silva, N.R. and Van Rooyen, C. (2013). What are the impacts of urban agriculture programs on food security in low and middle-income countries? Environmental Evidence 2013, 2:7.

Tamburino, L., Bravo, G., Clough, Y., Nicholas, K.A. (2020). From population to production: 50 years of scientific literature on how to feed the World. Global Food Security, 24.

Tarım Dikey Bahçeler, (2016). Tarım Dikey Bahçeler. T.C. Milli Eğitim Bakanlığı. http://www.megep.meb.gov.tr/mte_program_modul/moduller/Dikey%20Bahçeler.pdf

Tekin, Ç.ve Oğuz, C. Z. (2011). "Yapı ile Yükselen Yeşil Duvarlar", New World Sciences Academy 6, (4), 1241-1249 İstanbul Türkiye.

Timur Ö B, Karaca E (2013) Vertical gardens. In Advances in Landscape Architecture. IntechOpen.

Tohum, N., (2011). Sürdürülebilir Peyzaj Tasarım Aracı Olarak Yeşil Çatılar. İstanbul Teknik Üniversitesi, Fen Bilimleri Enstitüsü, Peyzaj Mimarlığı Anabilim Dalı Yüksek Lisans Tezi.

Tüfekçioğlu, İ. (2010). Yerçekimine Meydan Okuyan Bahçeler. GEO, 39-40. https://www.researchgate.net/publication/340233475_Yercekimine_meydan_okuyan_bahceler

Tunbiş, M. (1987). Çatı bahçeleri. Journal of the Faculty of Forestry, 37(4), 103-116.

Türkeş, M., Sümer, U. M. ve Çetiner, G. (2000). Küresel iklim değişikliği ve olası etkileri. https://s3.amazonaws.com/academia.edu.documents/34390964/iklimetkileri.pdf?AWSAccessKeyId=AKIAIWOWYYGZ2Y53UL3A&Expires=1542510498&Signature=lScpjihwj91pjpyeh%2FT7ynwVngQ%3D&response-contentdisposition=inline%3B%20filename%3DKURESEL_IKLIM_DEGISIKLIGI_VE_OLASI_ETKIL.pdf

Türkoğlu, E. (2015). Küreselleşme ve Tarım Sektörü: Türkiye Örneği, Marmara Üniversitesi Sosyal Bilimler Enstitüsü, İktisat Anabilim Dalı, Uluslararası İktisat Bilim Dalı, Yüksek Lisans Tezi.

UMGI-Uganda Micro Gardening Initiative, (2014). Research: Tomato-consumption on household level in Uganda.

UN – Department of Economic and Social Affairs, Population Division, (2011). Population Distribution, Urbanization, Internal Migration and Development: An International Perspective. In:http://www.un.org/esa/population/publications/PopDistribUrbanization/PopulationDistribut ionUrbanization.pdf (November 2014).

Ünal, U., Akyüz, D.E. (2018). Yeşil Altyapı Uygulamaları Kapsamında Yağmur Hendeklerinin Önemi ve Sürdürülebilir Kent Anlayışı ile Değerlendirilmesi, İklim Değişikliği ve Çevre, 3(2): 55–63.

UZUN, A., (2002). Çatı bahçesi ders notları. İstanbul Üniversitesi Orman Fakültesi, Peyzaj Mimarlığı Bölümü.

Vågsholm, I., Arzoomand, N.S., Boqvist, S. (2020). Food security, safety, and sustainability—getting the trade-offs right. Frontiers in Sustainable Food Systems, 4, p. 16.

Walter, A., Finger, R., Huber, R., Buchmann, N. (2017). Opinion: Smart farming is key to developing sustainable agriculture. PNAS, 114(24), 6148–6150.

WHO/FAO, (2003). Diet, nutrition and the prevention of chronic diseases. WHO Technical Report Series 916. In: http://whqlibdoc.who.int/ trs/who_trs_916.pdf (November 2014).

Wolverton, B., Johnson, A., ve Bounds, K. (1989). Interior Landscape Plants for Indoor Air Pollution Abatement. Nasa John C. Stennis Space Centre Science and Technology Laboratory, 1-2.

Yıldız, M. (2018). Dikey Bahçe; Beton Yapıların Yeni Yeşil Yüzü Ekoyapı Dergisi: https://www.ekoyapidergisi.org/dikey-bahce-beton-yapilarin-yeni-yesil-yuzu

Yılmaz, H., Turgut, H. ve Demircan, N. (2006). Erzurum kent halkının hobi bahçesi hakkındaki görüşlerinin belirlenmesi, Atatürk Üniversitesi, Ziraat Fakültesi, Peyzaj Mimarlığı Bölümü, Süleyman Demirel Üniversitesi Orman Fakültesi Dergisi, A (1): 96-110.

THYMBRA SPİCATA TÜRÜNÜN UÇUCU YAĞ BİLEŞENLERİ VE BİTKİ BESİN ELEMENTLERİNİN BELİRLENMESİ

DETERMINATION OF ESSENTIAL OIL COMPONENTS AND PLANT NUTRIENT ELEMENT OF *THYMBRA SPICATA* SPECIES

Osman GEDİK[1]

[1]Kahramanmaraş Sütçü İmam Üniversitesi, Ziraat Fakültesi, Tarla Bitkileri Bölümü, Kahramanmaraş, Türkiye.

[1]ORCID ID: https://orcid.org/0000-0002-4816-3154

Ömer Süha USLU [2]

[2]Kahramanmaraş Sütçü İmam Üniversitesi, Ziraat Fakültesi, Tarla Bitkileri Bölümü, Kahramanmaraş, Türkiye.

[2]ORCID ID: https://orcid.org/0000-0003-0858-0305

Orçun ÇINAR[3]

[3]Batı Akdeniz Tarımsal Araştırma Enstitüsü, Antalya, Türkiye.

[3]ORCID ID: https://orcid.org/0000-0002-8356-384X

ÖZET

Tüm dünyada aroma ve baharat elde etmede yaygın bir şekilde kullanılan kekik, 60 farklı tür bitkinin genel ismidir. Bunlar içinde, *Satureja, Thymus, Origanum, Coridothymus ve Thymbra* cinsleri hem yayılım olarak hemde ekonomik açıdan büyük önem arz etmektedir. Bu çalışmada, Kahramanmaraş florasında doğal olarak yayılış gösteren ve kekik türleri arasında önemli bir yere sahip olan *Thymbra spicata*'nın uçucu yağ bileşenleri ve makro mikro besin element değerleri belirlenmiştir. Çalışmada kullanılan bitki materyali Kahramanmaraş Menzelet baraj gölü çevresinde doğal yetişme alanlarından çiçeklenme döneminde toplanarak laboratuvar ortamında gölgede kurutulmuştur. Çalışma Kahramanmaraş Sütçü İmam Üniversitesi Ziraat Fakültesi Tarla Bitkileri Bölümü Tıbbi ve Aromatik bitkiler laboratuvarında yürütülmüştür. Çiçeklenme döneminde toplanarak gölgede kurutulan herbadan Neo-clevenger cihazında su destilasyonu ile uçucu yağ elde edilmiş ve öğütülen herbadan makro-mikro besin elementlerinin değerleri belirlenmiştir. Uçucu yağ bileşenleri Batı Akdeniz Tarımsal Araştırma Enstitüsü (BATEM)'nde, makro-mikro besin element değerleri ise Kahramanmaraş Sütçü İmam Üniversitesi "Üniversite-Sanayi-Kamu İşbirliği Geliştirme Uygulama ve Araştırma Merkezi'nde (ÜSKİM)" yapılmıştır. Çalışma sonuçlarına bakıldığında *Thymbra spicata*'nın toprak üstü herbasında uçucu yağ oranı % 2.90 olarak belirlenmiştir. Elde edilen uçucu yağda 11 farklı bileşen tespit edilmiştir. Kekik türlerinde karakteristik bileşen olan karvakrol bu türde de başlıca bileşen olarak belirlenmiştir. Uçucu yağ bileşenlerinde karvakrol %79.68 ile başlıca bileşen olurken bu bileşeni %9.93 ile gama-terpinen, %4.60 ile cymene, %2.35 ile beta-karyofilen'nin takip ettiği görülmüştür. *Thymbra spicata* türünün kurutulan toprak üstü herbasında 9 farklı bitki besin elementinin oranları belirlenmiştir. Buna göre Ca 29965 mg/kg, Mn 47.755 mg/kg, Zn 24.24 mg/kg, Fe 212.9 mg/kg, Na 140.8 mg/kg, P 1163.5, Mg 35.98 mg/kg, K 15610 mg/kg ve Cu 13.46 mg/kg olarak belirlenmiştir. Bazı modern kültürler, hala yabani bitkileri baharat ve önemli besinsel mineral kaynağı olarak tükettikleri bilinmektedir. Bu sebeple bu bitkilerin uçucu yağ bileşenlerinin ve bitki besin elementlerinin belirlenesi önem arz etmektedir.

Anahtar kelimeler: *Thymbra spicata,* uçucu yağ, bitki besin elementleri

ABSTRACT

Thyme, which is widely used to obtain aroma and spice all over the world, is the general name of 60 different types of plants. Among them, *Satureja*, *Thymus*, *Origanum*, *Coridothymus* and *Thymbra* genera are of great importance both in terms of distribution and economy. In this study, essential oil components and macro-micro nutrient values of *Thymbra spicata*, which is naturally distributed in Kahramanmaraş flora and has an important place among thyme species, were determined. The plant material used in the study was collected from the natural growing areas around Kahramanmaraş Menzelet dam lake during the flowering period and dried in the shade in the laboratory environment. The study was carried out in Kahramanmaraş Sütçü İmam University Faculty of Agriculture, Department of Field Crops, Medicinal and Aromatic plants laboratory. Essential oil was obtained from the herb collected and dried in the shade during the flowering period by water distillation in the Neo-clevenger device, and the values of macro-micro nutrients from the ground herb were determined. Essential oil components were made in the West Mediterranean Agricultural Research Institute (BATEM), and macro-micro nutrient element values were determined in Kahramanmaraş Sütçü İmam University "University-Industry-Public Cooperation Development Application and Research Center (ÜSKİM)". Considering the results of the study, the essential oil rate in the above-ground herb of *Thymbra spicata* was determined as 2.90%. Eleven different components were determined in the obtained essential oil. Carvacrol, which is the characteristic component in thyme species, was determined as the main component in this species. While carvacrol was the main component in essential oil components with 79.68%, it was observed that this component was followed by gamma-terpinene with 9.93%, cymene with 4.60%, and beta-caryophyllene with 2.35%. The ratios of 9 different plant nutrients were determined in the dried aerial herb of *Thymbra spicata* species. Accordingly, Ca 29965 mg/kg, Mn 47.755 mg/kg, Zn 24.24 mg/kg, Fe 212.9 mg/kg, Na 140.8 mg/kg, P 1163.5, Mg 35.98 mg/kg, K 15610 mg/kg and Cu 13.46 mg/kg It was determined as. Some modern cultures are still known to consume wild plants as a spice and source of important nutritional minerals. For this reason, it is important to determine the essential oil components and plant nutrients of these plants.

Keywords: *Thymbra spicata*, essential oil, plant nutrients

Giriş

Ülkemizde ticareti yapılan ve yaygın olarak kullanılan, tamımı Lamiaceae familyasına bağlı kekik türlerinin dahil olduğu cinsler olup bunlar: *Origanum*, *Thymbra*, *Coridothymus*, *Satureja* ve *Thymus*'tur. İhracatı en çok yapılan ve uçucu yağ üretiminde kullanılan türler, *Origanum onites* (Bilyalı kekik, İzmir kekiği), *Origanum vulgare* subsp. *hirtum* (İstanbul kekiği, Kara kekik), *Origanum minutiflorum* (Sütçüler kekiği, Yayla kekiği, Toka kekiği), *Origanum majorana* (Beyaz kekik, Alanya kekiği), *Origanum syriacum* var. *bevanii* (dağ kekiği, Suriye kekiği, İsrail kekiği)'dir. Bunlar dışında ticareti yapılan diğer türler *Coridothymus capitatus* (İspanyol kekiği), *Thymbra spicata* ve *Thymbra sintenisii* (Sivri kekik), *Satureja cuneifolia, Satureja hortensis, Satureja montana, Satureja spicigera* (Trabzon kekiği), *Thymus eigii'*dir. Tüm bu türlerin ortak özelliği yüksek miktarda uçucu yağ içermeleri ve uçucu yağın ana bileşiğinin karvakrol ve/veya timol olmasıdır. Karvakrol ve/veya timol kekiğe kendine özgü kokusunu veren maddelerdir. Aynı zamanda karvakrol ve timol içeriği kekikte fiyatı belirleyen parametrelerdir. Bu türler arasında özellikle *Thymus, Origanum, Satureja, Thymbra* ve *Coridothymus* cinsleri hem yayılış olarak hem de ekonomik olarak büyük önem taşımaktadır (Anonim, 2020). *T. spicata* (karakekik, karabaş kekik, zahter) çok yıllık otsu, 20-40 cm boylanabilen, tüylü, esmer yeşil renkli, ucu sivri yapraklı, başak şeklinde toplanmış pembeleylak renkli çiçeklere sahiptir. İki çeşit mevcut; var. *spicata* ve var. *intricata* P. H. Davis. Batı ve Güney bölgelerde yabani. %1-2 verimli uçucu yağda, çoğunlukla karvakrol fazladır; ancak tüm kekiklerde olduğu gibi timol kemotipleride bulunur (Akgül, 1993). *T. spicata*'nın taze yapraklarından bazı illerde salata yapılır. Aslında bu tür, bütün Ortadoğuda bol yetişen kekik olarakta en çok kullanılan ve hemen aynı adla ("zaatar" Arapça'dan) bilinen baharattır (Akgül 1993). *T. spicata*'nın, gıda olarak tüketimine bakıldığında; kurutulmuş yaprak ve çiçekleri kullanılır. İlkbahar mevsiminde taze sürgün olarak toplanıp bunlardan ürün alma şeklindedir. Su buharı distilasyonuyla, kurutulmuş toprak üstü bölümlerinden uçucu yağ 'kekik yağı' ve geri kalan yağ altındaki su 'kekik suyu' biçiminde değerlendirilir (Baytop, 1999; Şekeroğlu, 2008; Koçer, 2021). Jeldi et al. (2022) bildirdiği üzere günümüzde modern tıp, uçucu yağlar ve bileşenlerinin terapötik etkilerinden faydalanır. Aslında, birçok uçucu bileşik (timol ve karvakrol antiseptik özellikleri için öjenol

analjezik özellikleri için) günümüzde farmasötik preparatlarda yaygın olarak kullanılan bileşenlerdir (Pauli, 2001). Koçer (2021)'in bildirdiği üzere; bu bitkiden elde edilen kurutulmuş çiçek hali yahut yapraklarından yapılan karışımın (% 1-5) halk ilacı olarak kullanımı mevcuttur. Çiçekli bir dal veya birkaç yaprak sıcak su içine atılıp sarımsı bir renge bürününceye kadar bekletilir ve yapılan infüzyon suya atılan kısımlar çıkarılarak çay olarak tüketilir (Baytop, 1999). Tansı ve Özgüven (1991) *Thymbra spicata* türünün uçucu yağ oranını %2.2 olarak, karvakrol bileşenini ise üç farklı biçim zamanında %60.85-66.73 aralığında belirlemiştir. Uçucu yağ oranı ile karvakrol miktarı bakımından en uygun hasat zamanın çiçeklenme dönemi olduğunu bildirmiştir. Baytop (1999), ülkemizde tıbbi aromatik bitkiler olarak nitelendirilen bu bitkilerin, kültüre alınmasıyla yüksek kaliteli, taze ve istenilen miktarda ucuza drog elde edilebileceğini rapor etmiştir.

Materyal ve Metot

Bitki materyali

Çalışmada kullanılan *Thymbra spicata* türüne ait bitki materyali Kahramanmaraş ili Menzelet baraj gölü çevresinde doğal yetişme ortamından çiçeklenme döneminde (Şekil 1) toplanarak laboratuvar ortamında gölgede kurutulmuştur.

Uçucu yağ izolasyonu ve bileşenlerinin belirlenmesi

Thymbra spicata türünün kurutulmuş herba kısımları öğütülerek su distilasyonu yöntemi ile üç saat boyunca Neo-clevenger cihazında uçucu yağları çıkarılmıştır. Uçucu yağ için 30 gram öğütülmüş numune örneği kullanılmıştır. Distilasyon sonucu elde edilen uçucu yağlar Batı Akdeniz Tarımsal Araştırma Enstitüsü (BATEM) laboratuvarında GC/MS cihazında analiz edilmiştir. Elde edilen uçucu yağların bileşenlerini belirleyebilmek için uçucu yağlar 1:100 oranında hekzan ile seyreltilmiştir. Uçucu yağ bileşen analizi GC/GC-MS (Gaz kromatografisi (Agilent 7890A)-kütle detektör (Agilent 5975C)) cihazı ile kapiler kolon (HP InnowaxCapillary; 60.0 m x 0.25 mm x 0.25 µm) kullanılarak yapılmıştır. Analizde taşıyıcı gaz olarak 0.8 mL/dk akış hızına sahip helyum gazı kullanılmış, numuneler cihaza 1 µl enjeksiyon hacminde 40:1 split oranı kullanılarak enjekte edilmiştir. Enjektör sisteminin sıcaklığı 250°C'de sabit tutulmuş, kolon sıcaklık programı 60°C (10 dakika), 60°C'den 220°C'ye 4°C/dakika ve 220°C (10 dakika) olacak şekilde programlanmıştır. Bu sıcaklık programı kullanıldığında toplam analiz süresi 60 dakika olarak gerçekleşmiştir. Kütle dedeksiyonu için tarama aralığı (m/z) 35-450 atomik kütle ünitesi ve elektron bombardımanı iyonizasyonu 70 eV olarak uygulanmıştır. Uçucu yağ bileşenlerinin teşhisi yapılırken Wiley ve Oil Adams kütüphanelerinin sonuçları kullanılmıştır. Elde edilen bileşenlerin yüzde oranları FID dedektör kullanılarak, bileşenlerin teşhisi ise MS dedektör kullanılarak tespit edilmiştir (Uysal Bayar ve Çınar, 2020).

Besin elementleri tayini (mg kg^{-1})

Toprak üstü herbası öğütülerek hazırlanın örnekten 1 gram tartılarak üzerlerine 3 mL % 65'lik HNO3 ve 1 mL % 30'luk HCl eklenerek mikrodalga sisteminde parçalama işlemi yapılmıştır. İşlem sonunda çözeltiler ultra saf su ile 50 mL'lik hacime tamamlanarak ICP-OES (Optima 2100 DV: Perkin Elmer Inc.) cihazında ölçümleri yapılmıştır. Bitki besin element tayini Kahramanmaraş Sütçü İmam Üniversitesi ÜSKİM laboratuvarında yapılmıştır.

Şekil 1. *Thymbra spicata* türünün araziden çekilmiş görüntüsü

Bulgular ve Tartışma

Bu çalışmada önemli kekik türlerinden birisi olan *Thymbra spicata* türünün uçucu yağ oranı, bileşenleri ve bitki besin element değerleri belirlenmiştir.

Tablo 1. *Thymbra spicata* türünün uçucu yağ bileşenleri

Peak	R.T.	Uçucu yağ bileşenleri	Bileşen oranı (%)
1	10,649	α-thujene	0.36
2	16,017	β-myrcene	0.68
3	16,767	α-terpinene	0.96
4	19,586	ɣ-terpinene	9.93
5	20,657	cymene	4.60
6	27,409	1-octen-3-ol	0.26
7	28,15	trans-sabinene hydrate	0.24
8	32,664	β-caryophyllene	2.35
9	43,614	caryophyllene oxide	0.44
10	47,581	thymol	0.52
11	48,297	carvacrol	79.68
Tanımlanan (%)			100
Uçucu yağ oranı (%)			2.90

Tablo 1'e bakıldığında; *Thymbra spicata* türünün toprak üstü kısımlarının oluşturduğu herba da uçucu yağ oranı %2.90 olarak belirlenmiştir. Bu uçucu yağın 11 farklı uçucu yağ bileşeni içerdiği belirlenmiştir. Uçucu yağ bileşenlerine bakıldığında başlıca bileşenin %79.68 ile karvakrol olduğu görülmektedir. Karvakrol yada

timol kekik olarak adlandırılan bitkilerin başlıca bileşenleridir. *Thymbra spicata*'nın uçucu yağında karvakrolu takip eden bileşenlere bakıldığında, %9.93 ile ɣ-terpinene, %4.60 ile cymene, %2.35 ile β-caryophyllene'nin takip ettiği görülmektedir. Koçer (2021)'in yapmış olduğu çalışmada *Thymbra spicata* türünün uçucu yağ oranını %2.73 olarak bildirmiştir. Uçucu yağın başlıca bileşenlerini ise cymene (%7.17), ç-terpinene (%12.30), o-cymene (%10.05), ve carvacrol (%65.15) olarak bildirmiştir. Bu çalışmadaki karvakrol oranı (%79.68), Koçer (2021)'in karvakrol değerinden yüksektir. Kızıl et al. (2015)'in *Thymbra spicata* türünün 30 farklı popülasyonu üzerinde yapılan çalışmaya göre başlıca uçucu yağ bileşeni olan karvakrol %12.7-97.9 aralığında değiştiği bildirmişlerdir.

Tablo 2. *Thymbra spicata* türünün bitki besin element değerleri

Bitki Besin Elementleri	**Ortalama değerler (mg/kg)**
Makro besin elementleri	**(mg/kg)**
Ca	29965
K	15610
P	1163.50
Mg	3598
Mikro besin elementleri	**(mg/kg)**
Mn	47.75
Zn	24.24
Fe	212.90
Na	140.80
Cu	13.46

Thymbra spicata türünün toprak üstü herbasında 9 farklı bitki besin elementinin değerlerine bakılmıştır. Tablo 2'ye bakıldığında, Ca 29965 mg/kg olarak, Mn 47.75 mg/kg, Zn 24.24 mg/kg, Fe 212.90 mg/kg, Na 140.80 mg/kg, P 1163.50 mg/kg, Mg 3598 mg/kg, K 15610 mg/kg, Cu 13.46 mg/kg olarak belirlenmiştir. Bayram (2018) on farklı kekik üreticisinin arazisinden temin edilen materyal üzerinde yapmış olduğu çalışmada P %17-37, K %1.96-3.29, Ca %1.17-3.30, Mg %0.27-0.35, Fe 51-335 mg kg^{-1}, Zn 14-45 mg kg^{-1}, Mn 59-85 mg kg^{-1}, Cu 13-38 mg kg^{-1} aralığında değişim gösterdiğini bildirmiştir. Aynı zamanda kekik yapraklarının besin elementi içerikleri ile ilgili araştırmaların çok sınırlı olduğunu da belirtmiştir (Bayram, 2018). Özcan et al. (2008) *Thymbra spicata* türünün toprak üstü herbasında, Ca 1925.7 ppm, K miktarını 1200.9 ppm, Mg miktarını 503.8 ppm, Mn 5.72 ppm, P 1150.2 ppm, Na 119.04 ppm ve Zn ise 3.54 ppm olarak belirlemiştir. Akgül (1993)'e göre kekik gibi yaprak baharatlarda kalsiyum, demir, magnezyum ve potasyum miktarı yüksektir. Sodyum (Na) miktarı genellikle baharatların genelinde düşüktür. Bu durum sodyumun (tuzun) sınırlandırıldığı beslenmelerde önemlidir. Az sodyumlu baharatların tuzun yerine lezzet vermek amacıyla kullanılması tavsiye edilebileceğini bildirmiştir.

Sonuç

Bu çalışmada Kahramanmaraş florasında doğal olarak yayılış gösteren *Thymbra spicata* türünün uçucu yağ bileşenleri ve bitki besin element değerleri belirlenmiştir. *Thymbra spicata* türünün kuru herbasında %2.90 uçucu yağ olduğu belirlenmiştir. Bu uçucu yağda toplam 11 bileşen belirlenmiştir. Uçucu yağ bileşenlerinin başlıcası karvakrol olup miktarının oldukça yüksek olduğu görülmüştür. Bitki besin element değerlerine bakıldığında makro besin elementlerinde en yüksek değere Ca sahipken mikro besin elementlerinde en yüksek değere Fe sahip olmuştur. Bu türün yaygın kullanımı, uçucu yağ oranı ve bileşenlerine bakıldığında kültüre alınarak tarımının yapılması önem arz etmektedir.

Kaynaklar

Akgul, A. 1993. Spice Science and Technology. Food Technology Association Publication, Ankara.

Anonim, 2020. T.C. tarım ve orman bakanlığı fabrika genel müdürlüğü üretim, kekik fizibilite raporu ve yatırımcı rehberi. Tarım Bakanlığı ve Ormancılık. Eğitim ve Yayın Dairesi Başkanlığı, Ankara.

Bayram, E.S. 2018. The relationships between nutrition and some quality parameters of oregano (Origanum onites L.) grown organically in the conditions of Denizliprovince. Harran J. Agric. Food Sci. 22, 225–235.

Baytop, T. 1999. Treatment With Herbs in Turkey. Nobel Medicine Book Stores, Istanbul, p. 480.

Baytop, T. 1999. Treatment With Herbs in Turkey. Nobel Medicine Book Stores, Istanbul, p. 480.

Jeldi, L., Taarabt, K.O., Mazrid, M.A., Ouahmaneb, L., Alfeddya, M.N. 2022. Chemical composition, antifungal and antioxidant activities of wild and cultivated Origanum compactum essential oils from the municipality of Chaoun, Morocco. S. Afr. J. Bot. 147, 852–858.

Kızıl, S., Toncer, O., Dıraz, E., Karaman, S. 2015. Variation of Agronomical Characteristics and Essential Oil Components of Zahter (*Thymbra spicata* L. var. *spicata*) Populations In Semi-Arid Climatic Conditions. Turk J Field Crops, 20(2): 242-251.

Koçer, O. 2021. Hatay Yöresinde Yetişen *Thymbra spicata* L. (Zahter/Karabaş Kekiği) Bitkisinin Uçucu Yağ Oran ve Bileşenlerinin Belirlenmesi. *Avrupa Bilim ve Teknoloji Dergisi*, (27), 446-449.

Özcan, M.M., Ünver, A., Uçar, T., Arslan, D. 2008. Mineral content of some herbs and herbal teas by infusion and decoction. Food Chemistry, 106: 1120-1127.

Pauli, A. 2001. Antimicrobial properties of essential oil constituents. Int. J. Aromather. 11, 126–133.

Şekeroğlu, N. 2008. Kilis ve yöresinde halk ilacı ve baharat olarak kullanılan bitkiler. Zeytindalı, Kilis Kültür Derneği Kilis Şubesi Yayını, 51: 6-11.

Tansı, S., Özgüven, M. 1991. *Thymbra spicata* L.' da Farklı Biçim Zamanlarının Drog Verimi ve Kaliteye Etkisi. 9. Bitkisel ilaç hammaddeleri toplantısı Eskişehir,16-19 Mayıs.

Uysal Bayar, F., Cınar, O. 2020. Yield and quality parameters of some cultivated *Origanum* spp. species. Derim 37, 10–17.

KURAKLIK STRESİNİN ÇÖREK OTUNDA ÇİMLENME VE FİDE GELİŞİMİ ÜZERİNE ETKİSİNİN BELİRLENMESİ

DETERMINATION OF THE EFFECT OF DROUGHT STRESS ON GERMINATION AND SEEDLING DEVELOPMENT IN BLACK CUMIN

Osman GEDİK[1]

[1]Kahramanmaraş Sütçü İmam Üniversitesi, Ziraat Fakültesi, Tarla Bitkileri Bölümü, Kahramanmaraş, Türkiye.

[1]ORCID ID: https://orcid.org/0000-0002-4816-3154

Ömer Süha USLU [2]

[2]Kahramanmaraş Sütçü İmam Üniversitesi, Ziraat Fakültesi, Tarla Bitkileri Bölümü, Kahramanmaraş, Türkiye.

[2]ORCID ID: https://orcid.org/0000-0003-0858-0305

Elif BOZDAĞ[3]

[3] Kahramanmaraş Sütçü İmam Üniversitesi, Ziraat Fakültesi, Tarla Bitkileri Bölümü, Kahramanmaraş, Türkiye.

[3]ORCID ID: https://orcid.org/0000-0002-9249-5367

Ali ACAR[4]

[4] Kahramanmaraş Sütçü İmam Üniversitesi, Ziraat Fakültesi, Tarla Bitkileri Bölümü, Kahramanmaraş, Türkiye.

[4]ORCID ID: https://orcid.org/0000-0002-8616-5070

ÖZET

Türkiye iklim koşullarında rahatlıkla yetiştirilebilen çörek otu, halk hekimliğinde kullanılan, baharat, koku verici ve lezzet artırıcı olarak mutfaklarda yer alan, gıda sanayinde hammadde olarak kullanılan katma değeri yüksek tıbbi ve aromatik bitkilerinden biridir. Tohum toprağa düştüğü andan itibaren yetişme periyotlarının herhangi bir döneminde kuraklıktan etkilenebilirler. Ancak özellikle çimlenme ve fide gelişimi dönemleri daha hassas oldukları bir evredir. Bu çalışmada tarımı yapılan iki farklı çörek otu türünün (*N. sativa* ve *N. damascena*) farklı kuraklık seviyelerinde çimlenme ve fide gelişim üzerine etkisi araştırılmıştır. Çalışma Kahramanmaraş Sütçü İmam Üniversitesi Ziraat Fakültesi Tarla Bitkileri Bölümü Tıbbi ve Aromatik bitkiler laboratuvarında yürütülmüştür. Araştırmada farklı çörek otu türlerinin kuraklık sitresine tepkilerini belirlemek için, kontrol (saf su), PEG-6000 kullanılarak -1.6, -3.5, -5.4 bar ozmotik basınca sahip kuraklık ortamları hazırlanmıştır. Deneme tesadüf parselleri deneme desenine göre 4 tekerrürlü olarak kurulmuştur. Çalışmada petri kaplarının tabanı iki kat filtre kağıdı ile kaplanmış ve her petriye 100 adet çörek otu tohumu ekilmiştir. Deneme 12 saat karanlık ve 12 saat aydınlık koşulları sağlayan iklimlendirme dolabında 14 gün boyunca takip edilmiştir. Deneme süresi sonunda petrilerden elde edilen fidelerde aşağıda belirtilen ölçümler alınmıştır. Araştırma sonuçlarına bakıldığında; radikula kuru ağırlık, plumula kuru ağırlık, fide kuru ağırlık ve kuraklık tolerans indeksi dışındaki parametrelerde *N. sativa* türü *N. damascena* türünden daha yüksek bir değere sahip olmuştur. Kuraklık seviyeleri açısından bakıldığında en yüksek değerler kontrol uygulamasından, en düşük değerler ise en yüksek kuraklık seviyesinden olan -5.4 bardan elde edilmiştir. Her iki türün kuraklık tolerans indeksi birbirine yakın olmasına rağmen *N. damascena* türü *N. sativa* türünden daha yüksek bir değere sahip olmuştur. Artan kuraklık seviyeleri çörek otunda çimlenme ve fide gelişimini olumsuz etkilediği görülmüştür.

Anahtar kelimeler: Çörek otu, PEG-6000, Kuraklık stresi, *Nigella*

ABSTRACT

Black cumin, which can be easily grown in the climatic conditions of Turkey, is one of the high value-added medicinal and aromatic plants used in folk medicine, used in kitchens as a spice, odorant and flavor enhancer, and used as a raw material in the food industry. From the moment the seed falls to the ground, it can be affected by drought in any period of the growing period. However, especially during the germination and seedling development periods, they are more sensitive. In this study, the effects of two different types of black cumin (*N. sativa and N. damascena*) on germination and seedling growth at different drought levels were investigated. The study was carried out in Kahramanmaraş Sütçü İmam University Faculty of Agriculture, Department of Field Crops, Medicinal and Aromatic plants laboratory. In the study, to determine the responses of different black cumin species to drought stress, using control (pure water) and PEG-6000; drought environments with -1.6, -3.5, -5.4 bar osmotic pressure were prepared. The experiment was set up in a randomized plot design with 4 replications. In the study, the bottom of the petri dishes was covered with two layers of filter paper and 100 black cumin seeds were planted in each petri dish. The experiment was followed for 14 days in an air-conditioning cabinet providing 12 hours of darkness and 12 hours of light. At the end of the trial period, the following measurements were taken on the seedlings obtained from the petri dishes. Looking at the results of the research; *N. sativa* species had a higher value than *N. damascena* in the parameters except radicula dry weight, plumule dry weight, seedling dry weight and drought tolerance index. In terms of drought levels, the highest values were obtained from the control application, and the lowest values were obtained from the highest drought level, -5.4 bar. Although the drought tolerance index of both species was close to each other, *N. damascena* had a higher value than *N. sativa*. It has been observed that increasing drought levels negatively affect the germination and seedling development of black seed.

Keywords: Black cumin, PEG-6000, drought stress, *Nigella*

Giriş

Çörek otu (*Nigella*), Ranunculaceae familyasına ait tek yıllık otsu bir bitkidir (Tanker ve ark., 2013). Çörek otunun dünyada 20-24 kadar türü olup, bunlardan 12-15'i Türkiye florasında yayılış göstermektedir (Ayhan, 2012; Başer, 2010). *N. sativa* ve *N. damascena* kültürü yapılan en önemli iki çörek otu türüdür (Ayhan, 2012; Baydar, 2016; Ürüşan, 2016). Çörek otu bitkisinin tohumu özellikle güney Asya ve Orta doğunun farklı bölümlerinde sağlıklı kalmak ve pek çok hastalıklarla savaşmak için uzun zamandan beri kullanılmaktadır. Çörek otu önemli bir ilaç ve baharat bitkisi olduğunun yanı sıra, halk arasında tohumları çoğu yemeklerde, pastalarda, böreklerde ve hamurlu ürünlerde lezzet verici olarak da kullanılmaktadır. İklim bilimciler, ülkemizin de içinde bulunduğu geniş alanlarda kuraklık tehlikesine işaret etmektedirler. Ayrıca, dünyada ve ülkemizde zaman zaman kurak periyotlar yaşanmakta ve bu dönemlerde tarımsal üretimde önemli oranda verim kayıpları ortaya çıkmaktadır (Çarpıcı ve Erdel, 2015). Çarpıcı ve Erdel (2015)'in bildirdiği üzere kuraklık terimi, sıcaklığın optimum isteklerin üzerine çıkması sonucu bitkinin aşırı su kaybederek solması ve bu durumun tüm şiddetiyle sürmesine bağlı olarak bitkinin ölmesine kadar varan bir olay olarak tanımlanmaktadır (Eriş, 1998). Kuraklığın kelime olarak sözlükteki anlamı ise, toprak faydalı rutubetinin tükendiği ve bu halin bitki gelişimini geciktirdiği ya da durdurduğu kuru bir dönemdir (Madran, 1984). Aslan ve Atış (2018)'ın bildirdiği üzere, tarımsal üretime kuraklığın iki temel etkisi bulunmaktadır. Birincisi, istenilen bitki çıkışını sağlayamama, ikincisi ise toprakta istenilenden daha az su bulunması nedeniyle gelişme ve verimde azalmadır (Saxena ve ark., 1993). Polyethylene glycol (PEG) çevresel kuraklığın laboratuvar koşullarında taklit edilmesi amacıyla sıklıkla kullanılmaktadır (Kaufman ve Eckard, 1971). Polietilen glikol (PEG), yüksek molekül ağırlıklı bir madde olup su alımını düzenleyerek, ortamı istenilen su stresi koşullarında tutmaktadır. Ayrıca PEG-6000 bitki köklerince alınmamakta ve toksik etki yaratmamaktadır (Çalıkoğlu ve Tilki 2002). Bitkiler tohum toprağa düştüğü andan itibaren yetişme periyotlarının herhangi bir döneminde kuraklıktan etkilenebilirler. Ancak özellikle çimlenme ve fide gelişimi dönemleri daha hassas oldukları bir evredir (Uslu et al., 202). Hamidi ve Safarnejad (2010), yonca çeşitleri üzerine yapmış olduğu çalışmada farklı kuraklık seviyelerinin (0, -3, -6 ve -9 bar) çimlenme yüzdesini,

çimlenme oranını, sapçık ve kökçük uzunluğu ile vigor indeksi önemli ölçüde azalttığını ve çeşitlerin kuraga dayanım yönünden büyük farklılıklar gösterdiklerini bildirmişlerdir. Arslan ve Atış (2018) mürdümük çeşitleri üzerine yapmış oldukları çalışmada, incelenen tüm özelliklerin artan kuraklık düzeylerinden olumsuz etkilendiği ve bu etkinin istatistiksel olarak önemli olduğu belirlenmiştir. Uslu et al. (2021) yapmış oldukları çalışmada kuraklık seviyesi kontrol uygulamasından -5.3 bar'a çıktığında radikula, plumula ve fide uzunluklarında istikrarlı bir azalma meydana geldiğini bildirmişlerdir.

Materyal ve Metot

Bu çalışmada tarımı yapılan iki çörek otu türüne ait tohum örneklerinin farklı kuraklık seviyelerinde (0, -1.6, -3.5, -5.4 bar) çimlenme ve fide gelişimi üzerine etkisi belirlenmiştir. Çalışmada *N. sativa* ve *N. damascena* türlerine ait tohum örnekleri kullanılmıştır. Bu çalışma Kahramanmaraş Sütçü İmam Üniversitesi Ziraat Fakültesi Tarla Bitkileri Bölümü Tıbbi ve Aromatik bitkiler laboratuvarında iklimlendirme kabininde yürütülmüştür. Araştırma tesadüf parselleri deneme deseninde iki faktörlü ve dört tekerrürlü olarak yürütülmüştür. Çimlendirme öncesinde tohumların yüzey sterilizasyonu için %5'lik sodyum hipoklorit kullanılmıştır. Tohumlar 5 dakika sodyum hipoklorit ile çalkalanmış ve ardından saf su ile iyice yıkanmıştır (Babakhani et al., 2011). Sterile edilen tohumlar kurutma kağıtları üzerine alınarak kurutulmuştur. Her petri kabına 100 adet çörek otu tohumu ve 10 ml PEG-6000 solüsyonundan ilave edildilmiştir. Petri kapları parafilm ile kapatılmış ve 12 saat karanlıkta 12 saat aydınlık olacak şekilde 24 °C'de 14 gün takip edilerek çimlenme oranına ve fide özelliklerine bakılmıştır. Çimlenme oranı, radikula uzunluğu, plumula uzunluğu, radikula yaş ve kuru ağırlığı, plumula yaş ve kuru ağırlığı, fide yaş ve kuru ağırlığı alınmış ve vigor indeksi ile kuraklık tolerans indeksleri hesaplanmıştır. Ölçümlerle ilgili detaylar aşağıda verilmiştir.

ÇO (%): Çimlenme oranı, çimlenen tohumların toplam tohum sayısına bölünmesi ve ardından 100 ile çarpılmasıyla bulundu (Maquire 1962).

ÇO: (Çimlenen Tohum Sayısı / Toplam Tohum Sayısı) × 100

Radikula ve pulumula uzunluğu: Tesadüfi olarak seçilen 10 tane fidenin radikula ve pulumula uzunlukları bir kumpas yardımı ile tohumdaki çıkış noktasından en uç kısmına kadar ölçülmüştür (Uslu et al., 2021).

Radikula yaş, pulumula yaş ve fide yaş ağrılıkları: Petri kaplarından tesadüfen seçilen 10 fidenin, radikula ve pulumula kısımları ayrılmış ve tartılarak radikula yaş ve pulumula yaş ağırlıkları belirlenmiştir. Radikula yaş ağırlık ile pulumula yaş ağrlık toplanarak fide yaş ağırlık değeri elde edilmiştir.

Radikula kuru, pulumula kuru ve fide kuru ağrılıkları: Radikula yaş ve pulumula yaş ağırlık için kullanılan örnekler 70 ℃'de 48 saat sabit ağırlığa gelinceye kadar bekletilerek kurutulmuş ve 0.0001 g hassasiyete sahip terazi kullanılarak kuru ağırlık tartımları yapılmıştır. Radikula ve pulumula kuru ağırlıkları toplanarak fide kuru ağırlık belirlenmiştir.

Vigor indeks: Vigor indeks değeri, fide uzunluğunun çimlenme oranı ile çarpılmasıyla bulunmuştur (Abdul-Baki ve Anderson, 1973).

Kuraklık Tolerans İndeksi=(TxTYA/T0TYA)x100

Burada, TYA= toplam yaş ağırlığı, Tx=X dozundaki toplam yaş ağırlığı, T0= kontrol uygulamasındaki toplam yaş ağırlığını ifade etmektedir (Arslan ve Atış, 2018).

Bulgular ve Tartışma

Çimlenme oranı (%)

Artan kuraklık stresi düzeylerinin çörek otunda çimlenme oranı üzerine etkisine bakıldığında, genotipler, kuraklık düzeyleri ve genotip x kuraklık düzeyi interaksiyonu %1 düzeyinde önemli bulunmuştur. *N. sativa* (%72) *N. damascena*'dan (%60.50) daha yüksek bir çimlenme oranına sahiptir. Kuraklık düzeylerine bakıldığında dozların artışına bağlı olarak çimlenme oranında düşüş meydana geldiği görülmektedir. En yüksek çimlenme oranı kontrol (0 bar) dozunda en düşük çimlenme oranı ise en yüksek kuraklık stres

düzeyinde (-5.4 bar) elde edilmiştir. Genotip x kuraklık düzeyi interaksiyonuna bakıldığında en yüksek çimlenme oranı istatistiki olarak aynı grupta yer alan her iki genotipin kontrol uygulamasında, en düşük çimlenme oranı ise yine aynı grupta yer alan her iki genotipin -5.4 bar kuraklık düzeyinden elde edilmiştir (Çizelge 1). Benzer çalışmalara bakıldığında; yonca tohumlarının çimlenmesi üzerine yapılan bir çalışmada, çeşitlerin, çimlenme yüzdesi bakımından -4.91 bar seviyesine kadar dayanabildiği ve bu seviyeden sonra çimlenme yüzdesi önemli ölçüde azaldığını bildirmişlerdir (Çarpıcı ve Erdel, 2015). Arslan ve Atış (2018)'ın çeşit × kuraklık düzeyi açısından sonuçlarına bakıldığında, tüm çeşitler için çimlenme oranlarında -12 bar ozmotik basınç seviyesine kadar önemli bir azalma meydana gelmemiştir. Kuraklık düzeyi -12 bar seviyesine çıktığında ise tüm çeşitlerin çimlenme oranı önemli derecede azalmıştır. Çalışılan tohum materyaline göre kuraklıktan etkilenme seviyeleri değişiklik göstermektedir.

Radikula Uzunluğu (mm)

Kuraklık stresi seviyelerinin iki farklı çörek otu genotipinin radikula uzunluğu üzerine etkisine bakıldığında; genotip, kuraklık düzeyi ve genotip x kuraklık düzeyi interaksiyonu %1 düzeyinde önemli bulunmuştur. Genotipler bakımından *N.sativa* (29.30 mm), *N. damascena* (16.69 mm)'dan daha yüksek bir değere sahip olmuştur. Kuraklık düzeylerine bakıldığında en yüksek radikula uzunluğu kontrol uygulamasından (39.43 mm) elde edilirken, en düşük ise en yüksek kuraklık stres seviyesi olan -5.4 bar uygulamasından (1.40 mm) elde edilmiştir (Çizelge 1). Genotip x kuraklık düzeyi interaksiyonuna bakıldığında en yüksek radikula uzunluğu *N. sativa*'nın kontrol uygulamasından elde edilirken, en düşük radikula uzunluğu istatistiki olarak aynı grupta yer alan her iki genotipin -5.4 bar kuraklık stresi seviyesinde elde edilmiştir (Çizelge 1). Kuraklık stres seviyelerinin artışına paralel olarak radikula boyunda düşüş görülmüştür.

Pulumula Uzunluğu (mm)

Artan kuraklık stresi seviyelerinin çörek otu genotiplerinin pulumula uzunluğu üzerine etkisine bakıldığında; genotipler %5, kuraklık düzeyi ve genotip x kuraklık düzeyi interaksiyonunun ise % 1 düzeyinde önemli olduğu görülmüştür (Çizelge 1). Pulumula uzunluğu bakımından *N. sativa* (46.88 mm) genotipi *N.damascena* (32.94 mm) genotipinden daha yüksek bir değere sahiptir. Kuraklık düzeyi bakımından en yüksek pulumula değeri 0 bar (kontrol) kuraklık düzeyinden elde edilirken en düşük pulumula uzunluğu -5.4 bar kuraklık düzeyi uygulamasından elde edilmiştir. Genotip x kuraklık düzeyi interakiyonuna bakıldığında en yüksek pulumula değeri *N. damascena*'nın kontrol uygulamasından (0 bar) elde edilirken, en düşük pulumula uzunluğu *N. sativa*'nın -5.4 bar kuraklık düzeyinden elde edilmiştir (Çizelge 1).

Fide Uzunluğu (mm)

Çizelge 1'e göre uygulanan kuraklık düzeylerinin çörek otunda fide uzunluğu üzerine etkisine bakıldığında genotipler, kuraklık seviyeleri ve genotip x kuraklık seviyeri intereksiyonunun %1 düzeyinde önemli olduğu görülmüştür. Fide uzunluğu bakımından *N. sativa* (29.30 mm), *N. damascena*'dan (16.69 mm) daha yüksektir. Kuraklık düzeylerine bakıldığında artan kuraklık seviyelerinde fide uzunluğunda düşüş görülmüştür. Genotip x kuraklık düzeyleri interaksiyonuna bakıldığında en yüksek fide uzunluğu *N. sativa*'nın kontrol dozundan, en düşük değer ise istatistiki olarak aynı grupta yer alan her iki genotipinde -5.4 bar kuraklık düzeyinde elde edilmiştir. Dolgun ve Çifci (2018)'nin yapmış olduğu çalışmada, makarnalık buğday çeşitlerinde farklı kuraklık seviyelerinde kuraklık stres ortalaması incelendiğinde en uzun fide 10.0 cm ile kontrol uygulamasında en kısa fide ise 3.9 cm ile 5.0 bar kuraklık stresi seviyesinde görülmüştür.

Radikula ve pulumula yaş ağırlık (gr)

Artan kuraklık düzeylerinin çörek otunun radikula ve pulumula uzunluğu üzerine etkisine bakıldığında, her iki özellik içinde genotipler, kuraklık düzeyleri ve genotip x kuraklık düzeleri istatistiki olarak %1 düzeyinde önemli olduğu görülmektedir. Genotipler bakımından her iki özelliktede *N. sativa* daha yüksek değerlere sahip olmuştur. Kuraklık seviyesi bakımından en yüksek değerler kontrol (0 bar) uygulamasından elde edilirken, en düşük değer her iki özellikte de en yüksek doz olan -5.4 bar kuraklık düzeyinden elde

edilmiştir. Genotip x kuraklık düzeyi interaksiyonuna bakıldığında her iki özellikte de en yüksek değer *N. sativa*'nın kontrol uygulamasından elde edilirken, en düşük değer her iki genotipin -5.4 bar kuraklık düzeyi uygulamasından elde edildiği görülmüştür (Çizelge 1). Dolgun ve Çifci (2018)'nin makarnalık buğday çeşitleri üzerine yaptıkları çalışmada kuraklık stres ortalamasına göre farklı kuraklık stresi seviyesindeki en yüksek kök yaş ağırlığı 211.1 mg ile kontrol uygulamasından elde edilmiştir.

Çizelge 1. Farklı kuraklık seviyelerinde çimlendirilen iki farklı çörek otu türünün çimlenme oranı (ÇO), radikula uzunluğu (RU), pulumula uzunluğu (PU), fide uzunluğu (FU), radikula yaş ağırlığı (RYA) ve pulumula yaş ağırlığına (PYA) ait ortalama değerler

		ÇO (%)	RU (mm)	PU (mm)	FU (mm)	RYA (gr)	PYA (gr)
Genotip	*N.damascena*	60.50 b	16.69 b	32.94 b	16.69 b	0.080 b	0.080 b
	N. sativa	72.00 a	29.30 a	46.88 a	29.30 a	0.161 a	0.110 a
Kuraklık Düzeyi (Bar)	0 (D_1)	95.50 a	39.43 a	32.18 a	71.61 a	0.226 a	0.170 a
	-1.6 (D_2)	84.50 b	30.50 b	25.09 b	55.60 b	0.155 b	0.152 b
	-3.5 (D_3)	54.50 c	20.67 c	9.95 c	30.62 c	0.102 c	0.058 c
	-5.4 (D_4)	30.50 d	1.40 d	0.42 d	1.82 d	0.001 d	1.38e-17 d
Genotip x Kuraklık Düzeyi (GxD)	Nd x D_1	96.00 a	30.99 c	33.80 a	64.79 b	0.142 c	0.152 bc
	Nd x D_2	85.00 b	27.20 d	27.13 c	54.33 cd	0.145 c	0.160 b
	Nd x D_3	44.00 d	6.52 e	3.21 f	9.74 e	0.032 d	0.007 e
	Nd x D_4	17.00 e	2.07 f	0.85 fg	2.92 f	0.002 e	1.38e-17 e
	Ns x D_1	95.00 a	47.86 a	30.56 b	78.42 a	0.310 a	0.187 a
	Ns x D_2	84.00 b	33.80 b	23.06 d	56.86 c	0.165 b	0.145 c
	Ns x D_3	65.00 c	34.82 b	16.69 e	51.51 d	0.172 b	0.110 d
	Ns x D_4	44.00 d	0.73 f	8.88e-16 g	0.73 f	1.38e-17 e	1.38e-17 e
Mean		66.25	23.00	16.91	39.91	0.121	0.095
CV		6.63	6.43	10.74	6.15	7.71	7.79
Lsd (Genotip)		3.20**	1.08**	1.32*	1.79**	0.007**	0.005**
Lsd (Kuraklık Düzeyi)		4.53**	1.52**	1.87**	2.53**	0.009**	0.007**
Lsd (Genotip x Kuraklık Düzeyi)		6.44**	2.20**	2.65**	3.73**	0.01**	0.01**

Fide yaş ağırlık (gr)

Çizelge 2'ye göre artan kuraklık düzeylerinin fide yaş ağırlık üzerine etkisine bakıldığında; genotipler, kuraklık düzeyleri ve genotip x kuraklık düzeyleri %1 seviyesinde önemli bulunmuştur. Genotipler bakımından *N. sativa* (0.273 gr), *N. damascena* dan (0.160 gr) daha yüksek bir değere sahip olmuştur. Kuraklık düzeyleri bakımından en yüksek fide yaş ağırlığı kontrol uygulamasından elde edilirken en düşük fide yaş ağırlığı -5.4 bar kuraklık düzeyinden elde edilmiştir. Genotip x kuraklık düzeyi interaksiyonuna bakıldığında en yüksek değer *N. sativa*'nın kontrol dozunda görülürken en düşük değer istatistiki olarak aynı grupta yer alan her iki genotipin -5.4 bar kuraklık düzeylerinde görülmüştür. Dolgun ve Çifci (2018)'nin çalışmasında kuraklık stres ortalaması değerlerine bakıldığında en yüksek fide yaş ağırlığı 406.6 mg ile kontrol uygulamasında en az ise 87.7 mg ile 5.0 bar kuraklık stresi seviyesinde görülmüştür. Bu çalışmada da benzer şekilde en yüksek fide yaş ağırlığı kontrol uygulamasından elde edilmiştir.

Radikula kuru ağırlık (gr)

Artan kuraklık düzeylerinin çörek otu genotiplerinde radikula kuru ağırlığı üzerine etkisine bakıldığında; genotipler, kuraklık düzeyleri ve genotip x kuraklık düzeyleri %1 seviyesinde önemli bulunmuştur. Genotipler bakımından *N. damascena* (0.966 gr), *N. sativa*'dan (0.705 gr) daha yüksek bir değere sahip olmuştur. Kuraklık düzeyleri bakımından en yüksek fide yaş ağırlığı kontrol uygulamasından elde edilirken en düşük fide yaş ağırlığı -5.4 bar kuraklık düzeyinden elde edilmiştir. Genotip x kuraklık düzeyi interaksiyonuna bakıldığında en yüksek değer *N. damascena*'nın -1.6 bar kuraklık düzeyinde görülürken en düşük değer *N. sativa*'nın -5.4 bar kuraklık düzeyi uygulamasından elde edilmiştir. Benzer şekilde Dolgun ve

Çifci (2018)'nin makaranalık buğday çeşitleri üzerinde yapmış olduğu çalışmada kuraklık stres ortalaması incelendiğinde en uzun kök 10.8 cm ile kontrol uygulamasında en kısa kök ise 3.2 cm ile 7.5 bar kuraklık stresi seviyesinde görülmüştür.

Çizelge 2. Farklı kuraklık seviyelerinin yetiştirilen iki çörek otu türünün fide yaş ağırlığı (FYA), radikula kuru ağırlığı (RKA), pulumula kuru ağırlığı (PKA), fide kuru ağırlığı (FKA), vigor indeksi (Vİ) ve kuraklık tolerans indeksine (KTİ) ait ortalama değerler

		FYA (gr)	RKA (gr)	PKA (gr)	FKA (gr)	Vİ	KTİ
Genotip	*N. damascena*	0.160 b	0.966 a	0.657	1.623 a	707.17 b	54.87 a
	N. sativa	0.273 a	0.705 b	0.710	1.415 b	975.09 a	54.77 b
Kuraklık Düzeyi (Bar)	0 (D_1)	0.396 a	1.012 a	1.006 a	2.001 a	1708.4 a	100.0 a
	-1.6 (D_2)	0.308 b	0.997 b	0.987 a	2.000 a	1173.2 b	83.1 b
	-3.5 (D_3)	0.161 c	0.945 b	0.741 b	1.687 b	472.6 c	35.3 c
	-5.4 (D_4)	0.001 d	0.390 c	0.00 c	0.390 c	10.11 d	0.8 d
Genotip x Kuraklık Düzeyi (GxD)	Nd x D_1	0.295 c	1.027 ab	0.985 a	2.012 ab	1554.28 b	100.00 b
	Nd x D_2	0.305 bc	1.105 a	1.072 a	2.175 a	1153.68 c	103.39 a
	Nd x D_3	0.040 e	0.955 bcd	0.572 b	1.152 c	108.50 e	14.41 e
	Nd x D_4	0.002 f	0.780 e	0.00 c	0.780 d	12.19 f	1.69 f
	Ns x D_1	0.497 a	0.997 bc	0.990 a	1.987 ab	1862.68 a	100.00 b
	Ns x D_2	0.312 b	0.890 d	0.940 a	1.827 b	1192.81 c	62.81 c
	Ns x D_3	0.282 d	0.935 cd	0.910 a	1.847 b	836.85 d	56.28 d
	Ns x D_4	0.00 f	0.00 f	0.00 c	0.00 e	8.02 f	0.1e-14 g
Mean		0.21	0.83	0.68	1.51	841.13	54.82
CV		4.31	6.76	21.00	11.05	7.60	2.51e-7
Lsd (Genotip)		0.006**	0.041**	0.104	0.122**	46.70**	0.10e-7**
Lsd (Kuraklık Düzeyi)		0.009**	0.058**	0.007**	0.173**	66.05**	0.14e-7**
Lsd (Genotip x Kuraklık Düzeyi)		0.01**	0.08**	0.21*	0.25**	95.04**	0.2e-7**

Pulumula kuru ağırlık (gr)

Çizelge 2'ye bakıldığında çörek otunda kuraklık düzeylerinin pulumula kuru ağırlık üzerine etkisi bakımından, kuraklık düzeyleri %1, genotip x kuraklık düzeyleri %5 düzeyinde istatistiki olarak önemli bulunurken, genotipler arasında önemli bir fark görülmemiştir. Kuraklık düzeylerine bakıldığında en yüksek pulumula kuru ağırlığı istatistiki olarak aynı grupta yer alan kontrol ve -1.6 bar kuraklık seviyesinden elde edilirken, en düşük pulumula kuru ağırlığı -5.4 bar kuraklık düzeyinden elde edilmiştir. Genotip kuraklık düzeyi interaksiyonuna bakıldığında en yüksek pulumula kuru ağırlık değerinin *N. damascena*'da aynı grupta yer alan kontrol ve -1.6 bar kuraklık düzeylerinden ve *N. sativa*'da aynı grupta yer alan kontrol, -1.6 ve -3.5 bar kuraklık düzeylerinden elde edilmiştir. En düşük pulumula kuru ağırlığı ise her iki genotipte de en yüksek kuraklık seviyesi olan -5.4 bar da elde edilmiştir.

Fide kuru ağırlık (gr)

Uygulanan kuraklık düzeylerinin çörek otunda fide kuru ağırlık üzerine etkisine bakıldığında; genotipler, kuraklık düzeyleri ve genotip x kuraklık düzeyleri %1 seviyesinde önemli bulunmuştur. *N. damascena* genotipi (1.623 gr), *N. sativa*'dan (1.415 gr) daha yüksek bir değere sahip olmuştur. Kuraklık düzeyleri bakımından en yüksek fide kuru ağırlığı istatistiki olarak aynı grupta yer alan kontrol ve -1.6 bar kuraklık düzeyi uygulamalarından elde edilirken en düşük fide yaş ağırlığı -5.4 bar kuraklık düzeyinden elde edilmiştir. Genotip x kuraklık düzeyi interaksiyonuna bakıldığında en yüksek fide kuru ağırlığı -1.6 bar kuraklık düzeyinde elde edilirken, en düşük fide kuru ağırlığı *N. sativa*'nın -5.4 bar kuraklık düzeyinde elde edilmiştir.

Vigor indeksi

Çizelge 2'ye göre kuraklık düzeylerinin çörek otunda vigor indeksi üzerine etkisine bakıldığında; genotipler, kuraklık düzeyleri ve genotip x kuraklık düzeyleri %1 seviyesinde önemli bulunmuştur. *N. damascena* genotipi (707.17), *N. sativa*'dan (975.09) daha düşük bir değere sahip olmuştur. Kuraklık düzeyleri bakımından en yüksek vigor indeks değeri kontrol uygulamasında, en düşük ise -5.4 bar kuraklık düzeyinden elde edilmiştir. Genotip x kuraklık düzeyi interaksiyonuna bakıldığında; en yüksek vigor indeksin *N. sativa*'nın kontrol uygulamasında elde edilirken en düşük değerin her iki genotiptede aynı grupta yer alan -5.4 bar kuraklık düzeyinde elde edilmiştir. Benzer çalışmalara bakıldığında, Çarpıcı ve Erdel (2015) yapmış oldukları çalışmada çeşitlerin vigor indeks özelliğinin -2.91 bar seviyesinden sonra kontrole oranla önemli ölçüde azaldığını bildirmiştir.

Kuraklık tolerans indeksi

Artan kuraklık düzeylerinin çörek otunda kuraklık tolerans indeksi üzerine etkisine bakıldığında; genotipler, kuraklık düzeyleri ve genotip x kuraklık düzeyleri interaksiyonu %1 düzeyinde önemlidir. *N. damascena* genotipi (54.87), *N. sativa*'dan (54.77) daha yüksek bir değere sahip olmuştur. Kuraklık düzeyleri bakımından en yüksek kuraklık tolerans indeks değeri kontrol uygulamasında, en düşük ise -5.4 bar kuraklık düzeyinden elde edilmiştir. Genotip x kuraklık düzeyi interaksiyonuna bakıldığında; en yüksek kuraklık tolerans indeksi *N. damascena*'nın -1.6 bar uygulamasında elde edilirken en düşük değerin -5.4 bar kuraklık düzeyinde elde edilmiştir.

Sonuç

Kuraklık, bitkilerin karşılaştığı en önemli abiyotik stres faktörlerinden birisidir. Bu çalışmada çörek otunda artan kuraklık seviyelerinin çimlenme ve fide gelişimini önemli ölçüde olumsuz yönde etkilediği görülmüştür. *N. damascena* türü *N. sativa* türünden daha yüksek kuraklık tolerans indeksine sahip olmuştur. Kuraklık düzeyleri açısından bakıldığında kontrolün dışındaki bütün seviyeler belirli oranlarda çimlenme ve fide gelişimini etkilemiştir. Genotip x kuraklık düzeyi interaksiyonuna bakıldığında artan kuraklık seviyeleri *N. damascena* da çimlenme oranını *N. sativa*'ya göre daha çok düşürmüştür.

Kaynaklar

Abdul-Baki, A.A., Anderson, J.D. 1973. Vigor determination in soybean seed by multiple criteria. Crop Science, 13: 630-633.

Aslan, H., Atış, İ. 2018. Bazı Yaygın Mürdümük Çeşitlerinde Kuraklık Stresinin Çimlenme ve Fide Gelişimine Etkisi. Mustafa Kemal Üniversitesi Ziraat Fakültesi Dergisi, 23(2): 218-231.

Ayhan, B. 2012. *Nigella sativa* L. Bitkisi Üzerine Fitoterapötik Çalışmalar. Yüksek lisans Tezi, Gazi üniversitesi, Ankara.

Babakhani, B., Khavari-Nejad, R.A., Hassan Sajedi, R., Fahimi, H., Saadatmand, S. 2011. Biochemical responses of alfalfa (*Medicago sativa* L.) cultivars subjected to NaCl salinity stress. African Journal of Biotechnology, 10(55): 11433-11441.

Başer, K.H.C. 2010. Çörek Otu (*Nigella sativa*). Bağbahçe Dergisi, 32(3): 26-27.

Baydar, H. 2016. Tıbbi ve Aromatik Bitkiler Bilimi ve Teknolojisi. Süleyman Demirel Üniversitesi Yayın No:51. Isparta.

Çalıkoğlu, M., Tilki, F. 2002. Orman ağacı tohumlarında çimlenme-su stresi ilişkisi. İstanbul Üniversitesi Orman Fakültesi Dergisi, 52(1): 77-88.

Çarpıcı, E.B., Erdel, B. 2015. Bazı yonca çeşitlerinde (*Medicago sativa* L.) kuraklık stresinin çimlenme özellikleri üzerine etkisi. Derim, 32(2): 201-210.

Dolgun, C., Çifci, E.A. 2018. Farklı Kuraklık Stresi Seviyelerinin Makarnalık Buğday Çeşitlerinde Çimlenme ve Erken Fide Gelişimi Üzerine Etkisi. Bursa Uludag Üniv. Ziraat Fak. Derg., 32(2): 99-109.

Eriş, A. 1998. Bahçe Bitkileri Fizyolojisi. Uludağ Üniversitesi Ziraat Fakültesi Ders Notları. 4. Baskı, No:11, 152s.

Hamidi, H., Safarnejad, A. 2010. Effect of drought stress on alfalfa cultivars (*Medicago sativa* L.) in germination stage. American-Eurasian Journal of Agricultural & Environmental Sciences. 8(6): 705-709.

Kaufman, M.R., Eckard, A.N. 1971. Evolution of stress control by polyethylene. Glycols by analysis of gulation. Plant Physiology, 47: 453-456.

Madran, N. 1984. Büyük Tarım Sözlüğü. Cilt I, Ankara.

Maquire, J.D. 1962. Speed of germination aid in selection and evaluation for seedling emergence and vigor. Crop Science 2: 176-177.

Saxena, N.P., Johansen, C., Saxena, M.C., Silim, S.N. 1993. Selection for drought and salinity tolerance in cool-season food legumes (Ed. KB. Singh, MC. Saxena). Breeding for Stress Tolerance in Cool-Season Food Legumes. United Kingdom, pp. 245-270.

Tanker, N., Koyuncu, M., Coşkun, M. 2013. Farmasötik Botanik, Ankara Üniversitesi Eczacılık Fakültesi Yayınları. Ankara.

Uslu Ö. S., Gedik, O., Alhumedi, M., Almınfı, K. 2021. Kuraklık Stresinin Bazı Yem Bezelyesi (*Pisum sativum* L.) Çeşitlerinin Çimlenme ve Fide Gelişimi Üzerine Etkisi. UAZİMDER Uluslararası Anadolu Ziraat Mühendisliği Bilimleri Dergisi 3(2): 28-36.

Ürüşan, Z. 2016. Bazı Çörek Otu (*Nigella sativa*, *Nigella damascena*) Genotiplerinde Tarımsal ve Kalite Özelliklerinin Belirlenmesi. Yüksek Lisans Tezi, Atatürk Üniversitesi, Erzurum.

THE POTENTIAL OF RAW TURKISH PUMPKIN SEED SHELLS ON DYESTUFF REMOVAL

Damla Kübra GÜRLENKAYA[1]

[1]Pamukkale University, Institute of Science, Environmental Enginnering Department, Denizli, Türkiye.

[1]ORCID ID: https://orcid.org/0000-0003-1875-8621

Levent GÜREL[2,*]

[2]Pamukkale University, Engineering Faculty, Environmental Engineering Department, Denizli, Türkiye.

[2]ORCID ID: https://orcid.org/0000-0002-4801-2735

ABSTRACT

Pumpkin is a very healthy foodstuff and found in the diet of many countries. Seeds of the pumpkins are also important food resources in Turkey. They are consumed by many people as dried fruits. The amount of produced seed shells is very high due to this consumption. The shells of this foodstuff are waste materials, and they are sent to landfills after consumption. It is very important to assess this kind of waste materials in color removal from aqueous media contamined with dye containing wastewaters. The aim of this study is to determine the dye removal potential of those waste materials (shells). Cationic dye (Y.28) was chosen as a model dye to simulate the textile wastewater. Pumpkin seeds were purchased from a market located in Denizli, Türkiye. The shells were separated from the seeds and dried under the sun. After that, the shells were cleaned using tap, distilled and deionized water and dried at 60°C for two days, milled and sieved and dried again at the same temperature for fortyeight hours. The pumpkin seed shell adsorbent was obtained at the end of this procedure. In treatment studies, this adsorbent material was contacted with dye solution at different pH values and adsorbent amounts. The most convenient pH for adsorption of Y.28 dye was found to be 10. At lower pH values (4, 6 and 8) the adsorbent was found very effective above a removal efficiency of 79%, too. The capability to remove basic dye at different pH values is a very precious feature, because of the variable pH values in textile wastewaters. The highest adsorbent capacity (46 mg/g) was obtained with 0.5 g adsorbent dosage per liter of treated dye solution. The highest dye removal efficiency (95%) was also achieved with 10 g/L adsorbent dosage. According to the results obtained with this waste material, it was concluded that this adsorbent in its raw form was very effective on removal of basic textile dye from dye contaminated solutions.

Keywords: Pumpkin seed shells, cationic textile dye, high removal efficiency, waste material

Acknowledgement: This work was supported by Pamukkale University (Project Number: 2020FEBE027)

*Corresponding Author: Levent GÜREL, Environmental Engineering Department, Faculty of Engineering, Pamukkale University, Denizli, Türkiye

İKLİM DEĞİŞİKLİĞİNİN ZİRAİ MÜCADELE AÇISINDAN DEĞERLENDİRİLMESİ

THE EVALUATION OF THE CLIMATE CHANGE IN TERMS OF PLANT PROTECTION

Ömer Süha USLU[1*]

[1]Kahramanmaraş Üniversitesi Sütçü İmam Ziraat Fakültesi Tarla Bitkileri Bölümü, Kahramanmaraş, Türkiye.

[2]ORCID ID: https://orcid.org/0000-0003-0858-0305

Osman GEDİK[2]

[2]Kahramanmaraş Üniversitesi Sütçü İmam Ziraat Fakültesi Tarla Bitkileri Bölümü, Kahramanmaraş, Türkiye.

[2]ORCID ID: https://orcid.org/0000-0002-4816-3154

Haroon KHAN[3]

[3]The University of Agriculture, Faculty of Plant Protection, Department of Weed Sceince, Peshawar, Pakistan.

[2]ORCID ID: https://orcid.org/0000-0003-0858-0305

ÖZET

Günümüzde "Küresel Isınma" insanoğlunun karşılaştığı en önemli ekolojik sorunlardan biridir. Küresel ısınmanın temel nedeni atmosfere salınan sera gazlarının miktarındaki artıştır. Bu gazların en önemlisi küresel ısınma üzerinde %50 etkisi olan CO^2'dir. Küresel ısınmanın neden olduğu iklim değişikliği ve tarım üzerindeki etkileri ile mücadele için tüm tarım muhatapları bilgilendirilmeli ve desteklenmelidir. Bilim adamları, küresel ısınmanın yabani otların, hastalıkların ve zararlıların baskısını artıracağını düşünmektedir. Bu artış aynı zamanda verim kaybını da artıracaktır. Tarla bitkileri, yabani otlar da dahil olmak üzere diğer bitkilerle rekabet halinde yaşar. Bu bitkiler virüs, mantar, akar, örümcek ve kuşlar tarafından ya desteklenir ve/veya saldırıya uğrar. İklim değişikliğinin bitkiler başta olmak üzere yeryüzündeki tüm canlıları ve bunların hastalık ve zararlı kaynaklarını etkilemesi kaçınılmazdır. Artan zararlı ve hastalık riskleri nedeniyle ekosistemde meydana gelen bozulma ve kuraklık gıda güvenliğini ve geçim kaynaklarını olumsuz yönde etkileyebilir. Bu durum ekonomik krizlere, zorunlu göçlere ve çatışmalara neden olabilir. Nem, sıcaklık ve CO2 miktarındaki herhangi bir değişiklik, bitki hastalık etkenlerinin dağılımını, gelişmesini, yayılmasını ve üremesini de etkiler. İklim değişikliği, daha önce zararlıların ve hastalıkların yaşayamadığı bölgelerde uygun iklim koşullarının oluşmasını sağlar. İklim değişikliği ayrıca bitki koruma ve pestisit kullanımı üzerinde olası etkilerle yabani otların, zararlıların ve hastalıkların ekolojisini de etkiler. Atmosferdeki artan karbondioksit ve ozon seviyeleri ve yoğun yağışlar da bitki fizyolojisini ve yapısını etkileyerek bitkiyi zararlılara ve hastalıklara karşı daha savunmasız hale getirebilir. Şiddetli fırtınalar ve yağmurlar bitkilerin direncini azaltabilir ve mantar ve bakteri enfeksiyonlarını artırabilir. Kuraklık durumunda, stres altındaki bitkiler hastalık ve zararlılara karşı normal dirençlerini kaybetme riskiyle karşı karşıyadır. Hastalık ve zararlılardaki artıştan dolayı çok geniş alanlarda zararlı sentetik toksik pestisitlerin kullanılması bitki ve insan sağlığı ile çevre ve biyolojik çeşitlilik üzerinde olumsuz sonuçlar doğurabilmektedir. Biyoçeşitliliğin korunması için yapılacak çalışmalar ve iklim değişikliğinin bitki koruma üzerindeki olumsuz etkisini azaltmaya yönelik iyileştirme çalışmaları oldukça önemlidir.

Anahtar Kelimeler: İklim değişikliği, Küresel ısınma, Tarım, Zirai mücadele

ABSTRACT

Today, "Global Warming" is one of the most important ecological problems faced by human beings. The main reason for global warming is the increase in the amount of greenhouse gases released into the atmosphere. The most important of these gases is CO_2, which has a 50% effect on global warming. All agricultural interlocutors should be informed and supported in order to combat climate change and its effects on agriculture caused by global warming. Scientists think that global warming will increase the pressure of weeds, diseases and pests. This increase will also increase the loss in yield. Field crops live in competition with neighbouring plants, including weeds. These plants are supported and/or attacked by virus, fungus, breeding, mite, spider, bird, and mammal. It is inevitable that climate change will affect all living things on earth, especially plants, and their sources of disease and pests. Due to increased pest and disease risks, ecosystem degradation and drought can adversely affect food security and livelihoods. This can lead to economic crises, forced migrations and conflicts. Any change in humidity, temperature and CO_2 amount also affect the distribution, development, spread and reproduction of plant disease agents. Climate change ensures the formation of suitable climatic conditions in regions where pests and diseases could not live before. Climate change also affects the ecology of weeds, pests and diseases, with possible effects on crop protection and pesticide use. Increasing levels of carbon dioxide and ozone in the atmosphere and heavy rainfall can also affect plant physiology and structure, making the plant more vulnerable to pests and diseases. Heavy storms and rains can reduce the resistance of plants and increase fungal and bacterial infections. In the event of drought, plants under stress risk losing their normal resistance to diseases and pests. Due to the increase in diseases and pests, the use of harmful synthetic toxic pesticides in very large areas may have negative consequences on plant and human health, as well as on the environment and biological diversity. Studies to be carried out for the protection of biodiversity and improvement efforts to reduce the negative impact of climate change on plant protection are very important.

Keywords: Climate change, Global warming, Plant protection, Agriculture

GİRİŞ

Tarımsal üretim uygarlığın ve teknolojinin etkisi altında kalmış büyük değişiklikler ve tarım devrimleri geçirmiştir. Son 100 yıldaki istisnai nüfus artışının (çevre koşullarındaki değişikliklerle birlikte) gıda arzının güvenliğini etkileyen birçok istenmeyen sonucu olmuştur. Artan dünya nüfusuna bağlı olarak bitkisel üretimde de talep artışı yaşanmaktadır. 2050 yılına kadar, artan talepleri karşılamak için küresel tarımsal üretimin büyük olasılıkla iki katına çıkarılması gerekecektir (Tilman ve ark., 2011). Son zamanlarda, iklim değişikliği, artan küresel sıcaklık ve atmosferik karbondioksit konsantrasyonları, ısı dalgaları, sel, yoğun fırtınalar, kuraklıklar ve diğer aşırı hava olaylarına yönelik yoğun araştırmalar yapılmaktadır. Bu nedenle, bu ve benzeri sebeplerle meydana gelen tarımsal verim kayıplarını azaltmak için araştırıcılar tarafından yukarıda bahsi geçen abiyotik faktörlere daha fazla önem verilmektedir. Tarımsal üretim ile ilgili olarak, özellikle kurak mevsimlerin tarımsal üretim için sınırlayıcı bir faktör olduğu bölgelerde, yağış düzenlerindeki değişiklikler potansiyel olarak sıcaklık artışından daha yüksek bir öneme sahiptir (Parry, 1990). İklim değişikliği ve hava şartlarındaki dengesizliklerden en çok etkilenecek olan zararlılardır. Sıcaklık artışı, zararlıların üreme, hayatta kalma, yayılma ve popülasyon dinamikleri ile zararlılar, çevre ve doğal düşmanlar arasındaki ilişkileri doğrudan etkiler. Özellikle önemli bir sorun haline gelebilen zararlı böceklerin, özellikle istilacı haşere türlerinin biyolojisi ve ekolojisi üzerinde yapılacak çalışmalar çok önemlidir. Yağış, atmosferik karbondioksit konsantrasyonları ve sıcaklık değişimlerinin ve iklim değişikliklerinin etkisi üzerine yapılan araştırmalar artırılmalıdır. Küresel ısınmanın neden olduğu iklim değişikliği ve tarım üzerindeki etkileri ile mücadele için tüm tarım muhataplarının ve paydaşlarının bilgilendirilmesi ve desteklenmesi gerekmektedir. Neredeyse her gün çok farklı platformlarda iklim değişikliğinin fırtına, sel ve orman yangınları gibi doğal afetleri şiddetlendirdiği, turizmi etkilediği, birçok türün neslinin tükenme tehlikesiyle karşı karşıya kaldığı veya tarım arazilerinin çöle dönüşmesi veya deniz seviyesi yükseldikçe üzerinde yerleşim olan kıta ve adaların terk edilmesi riski nedeniyle mülteci krizleri gibi kültürel değişimlere sebep olduğuna dair değerlendirmeler yapılmaktadır. İklim değişikliği tartışması giderek daha fazla yaygınlaşırken daha karmaşık hale gelmekte, aynı zamanda birçok farklı terim ya da kavram iklim değişikliği ile birlikte zikredilmektedir. Bu terimleri tanımak ve iyi anlamak iklim değişikliği konusunu daha iyi kavramamıza yardımcı olacaktır.

İKLİM DEĞİŞİKLİĞİ İLE İLGİLİ BAZI TERİMLER

Hava durumu

Farklı iklim şartlarında hava durumu yıl boyunca devamlı olarak değişmektedir. Bu değişim ve dalgalanma sürecinde aşırı sıcak ve aşırı soğuk gibi anormallikler, beraberinde küresel ısınma ve iklim değişikliğini tetikleyen en önemli etkenler arasında yer almaktadır. Avrupa Birliği Copernicus İklim Değişikliği Servisi, 2021 yılının dünya çapında kaydedilen en sıcak yıllar arasında yer aldığını ifade etmektedir (Anonim, 2022a). Bu tespit bir alarm özelliği de taşımaktadır. Bilim adamları, dünyanın 1,5 °C'den fazla ısınması halinde, dünyadaki ekosistemlerin tamamen çökmeye başlayacağını ifade etmektedir (Johansen, 2002).

Su

En önemli su kaynakları arasında yer alan yağışların fazlalığı da eksikliği de ciddi sorunlara yol açmaktadır. Değişen iklim şartları altında seller giderek artan bir sorun haline gelmiştir. 20. yüzyılın başlarına kıyasla, dünyanın çoğu yerinde hem daha güçlü hem de daha sık ve anormal seviyede yoğun yağış olayları yaşanmaktadır. Bununla birlikte kuraklık ta günümüz dünyasında daha yaygın bir problem haline gelmeye başlamıştır. Kuraklıkla birlikte tarımsal üretim için daha fazla su tüketilmeye başlamıştır. Tıpkı yüksek sıcaklıkların insanı daha fazla terletmesi gibi, hava sıcaklıkları bitkilerin daha fazla su kaybetmesine veya terlemesine sebep olur, bu da çiftçilerin daha fazla sulama suyu kullanması sonucunu doğurur.

İklim

İklim, istatistiksel verilere dayalı olarak zaman içinde hava durumunda meydana gelen değişimleri ifade etmektedir. İklim verileri, tarımsal üretimin sağlıklı bir şekilde sürdürülebilmesi açısından vazgeçilmez temel dinamikler arasında yer almaktadır. Uzmanlar, 2030 yılına kadar iklim değişikliğinin her yıl sıtma, ishal hastalığı, ısı stresi ve yalnızca yetersiz beslenme nedeniyle ek 250.000 ölüme neden olacağını tahmin etmektedir. İklimde meydana gelecek değişiklikler sebebi ile en ağır yükün çocukların, kadınların ve yoksulların üzerine düşeceği ve sağlık alanında kabul edilemeyecek seviyede ciddi ve büyük sorunlar yaşanacağı öngörülmektedir (Anonim, 2015).

Buzullar

Buzul tabakaları, 50 bin km^2'ye yaklaşan kıtasal buz kitleleridir. Ağustos 2019'da 24 saatlik bir süre zarfında Grönland kıtasının eriyerek 11 milyar ton buz kaybettiği bildirilmektedir. Yapılan yeni bir analize göre buzul erimesindeki bir önceki rekor % 15 oranında aşılmıştır. Uzmanlar, 1948'ten bu yana kayda geçirilen erime verilerine bakıldığında son incelemelerin "eşi benzeri görülmemiş bir seviyeye" işaret ettiğini belirtmektedirler. Bu kayıpların başlıca nedeni olarak, Grönland üzerindeki yüksek hava basınç sistemlerinin bloke olması gösterilmektedir. Devam eden karbon salımının Grönland'da aşırı erimeye yol açtığı söylenmektedir (Anonim, 2020). Buzul tabakalarının yazın biraz buz kaybetmesi (ve kışın birazını geri kazanması) normal olmakla birlikte, 2019 yılında erime mevsimi neredeyse bir ay erken başlamış ve rekor seviyede yüksek sıcaklıklara bağlı olarak çok ciddi buzul kaybı yaşanmıştır.

Küresel ısınma

Günümüzde "Küresel Isınma" insanoğlunun karşılaştığı en önemli ekolojik sorunlardan başında yer almaktadır. Küresel ısınmanın temel nedeni atmosfere salınan sera gazlarının miktarındaki artıştır. Bu gazların en önemlisi küresel ısınma üzerinde % 50 oranında etkisi olan CO^2'dir.

Karbondioksit

Kimyasal bir bileşik olan karbondioksit, solunum sonrası ya da diğer organik bileşiklerin yanması sonucu üretilen bir gazdır. Bitkiler fotosentez sırasında karbondioksiti gazını kullanarak bu gazı dünyadaki tüm yaşamın temel bir bileşeni haline getirir. Atmosferdeki Karbondioksit, Dünya yüzeyinden yayılan ısıyı atmosferde hapsederek gezegeni bitki ve hayvanların yaşaması ve gelişmesi için yaşanabilir hale getirmektedir. Bununla birlikte artan ve aşırı seviyede olan karbondioksit miktarı, beraberinde iklim değişikliği ile sonuçlanan sera etkisine sebep olmaktadır.

Metan

Metan, bir karbon ve dört hidrojen atomundan oluşan doğal bir gazdır. Yakıldığında diğer fosil yakıtlardan daha az karbondioksit salıyor, ancak atmosferdeki ısıyı yakalamada CO^2'den yaklaşık 30 kat daha güçlü, bu

da onu daha büyük bir iklim değişikliği tehdidi haline getiriyor. Atmosfere salınan metan miktarı, orman yangınları, bir takım doğal gaz kaynaklarının kendi kendine parçalanması ve özellikle hayvansal protein elde etmek için kurulan hayvancılık işletmeleri sebebi ile son 250 yılda iki kattan fazla artmıştır. Bu oran küresel ısınmanın % 20'sine sebep olmaktadır.

Fosil yakıtlar

Fosil yakıtlar, milyonlarca yıl önce yaşamış organizmalardan meydana gelen kömür, petrol ve doğal gaz gibi herhangi bir doğal yakıt olarak ifade edilebilir. Sanayi devrimi sırasında insanoğlu fosil yakıtlara bağımlı hale geldi. Günümüzde fosil yakıtlar, plastikten üretiminden ısınmaya kadar gündelik eşyaların neredeyse % 90'ında yer alır hale gelmiştir. Fosil yakıtların elde edilmesi için yapılan madencilik ve sondaj çalışmaları da, atmosfere yüksek düzeyde karbondioksit göndererek küresel ısınmayı şiddetlendirmektedir.

Okyanus asitliliği

Okyanus suyunun atmosferden karbondioksiti emmesi sonucu okyanuslardaki pH seviyelerinin düşmesi olarak okyanus asitliliği olarak ifade edilebilir. Deniz suyu doğal olarak 7'nin üzerinde hafif asidik bir pH seviyesine sahiptir (nötr pH 7'dir). Asitlenme pH'ı 7'nin altına düşürür. Bilim adamları okyanus asitlenmesinin popüler deniz ürünlerini olumsuz etkileyerek dünyadaki ekosistemlere ve ekonomilere zarar vereceğini bildirmektedir. 2030 yılına kadar okyanusların yaklaşık % 55'inin artan sıcaklıklar, asitlenme, azalan oksijen ve iklim değişikliğinin diğer belirtileri nedeniyle zarar görebileceği kaydedilmektedir.

Sera gazları

İnsanoğlu atmosferdeki karbondioksit oranını artırarak, sera etkisini tetiklemiştir. Fosil yakıtların yakılması sonucu açığa çıkan karbon dahil sera gazları, ısıyı atmosferde hapseder. Atmosferdeki bu gazların kombinasyonu ve fazlalığı gezegeni daha sıcak hale getirmekte ve hızlı iklim değişikliğine yol açmaktadır. Önemli sera gazları arasında su buharı, karbondioksit, metan, azot oksit ve ozon yer almaktadır.

Küresel sıcaklık ortalaması

NASA'nın Goddard Uzay Araştırmaları Enstitüsü (GISS), dünyanın küresel sıcaklığının 1880 yılından günümüze kadar yaklaşık 1 °C'den biraz daha fazla arttığını ifade etmektedir. 2017 yılında küresel sıcaklık ortalaması, 1951'den 1980'e kadar ölçülen sıcaklık ortalamasının 0.9 °C üzerinde olduğu tespit edilmiştir (Anonim, 2022b).

Biyoyakıtlar

Biyoyakıt, petrol gibi fosil yakıtların oluşumunda yer alan yavaş jeolojik süreçlerden ziyade, bitkiler kullanılarak elde edilmektedir. Biyoyakıtlar, özellikle taşımacılık sektöründe yakıt ihtiyacının karşılanmasına destek olmaktadır. Gelecek nesilleri güvence altına almak için fosil yakıt yerine yenilenebilir enerji üretimini ve kullanımını artırmak zorundayız.

Ozon tabakası

Ozon, insanları özellikle cilt kanseri gibi önemli bir sağlık sorununa sebep olan radyasyondan korur. Aerosoller gibi ozon tabakasını olumsuz etkileyen ürünlerin kullanımını kademeli olarak durdurmaya yönelik küresel bir anlaşma olan Montreal Protokolü imzalanmıştır. Süreç kontrol altına alınmaya çalışılmaktadır.

Deniz seviyesinin yükselmesi

Gezegen ısındıkça buzullar erimekte ve deniz seviyesi yükselmektedir. 1900'lerin başından bu yana küresel deniz seviyesi yaklaşık olarak 21 cm yükselmiştir. İklim değişikliği denilince aklımıza gelen bu terimlere daha farklı terimler de eklenebilir.

İKLİM DEĞİŞİKLİĞİNİN TARIM VE BİTKİ KORUMA ÜZERİNDEKİ ETKİLERİNE İLİŞKİN BAZI DEĞERLENDİRMELER

FAO, bitki hastalıkları ve zararlılarının dünyadaki verimi her yıl yüzde 20 ila 40 oranında azalttığını belirtiyor. Bu, yıllık 220 milyar doların üzerinde tarımsal ticaret kaybına neden oluyor. Milyonlarca insanın

aç kalmasına neden olmakta ve yoksul kırsal toplulukların birincil gelir kaynağı olan tarıma ciddi zararlar vermektedir. Küresel ısınma yabancı otların, hastalıkların ve zararlıların baskısını artıracak. Bu artış aynı zamanda verim kaybını da artıracaktır. En şiddetli verim kayıplarının, ısınmanın hastalık ve zararlı popülasyonlarını artırdığı bölgelerde yaşanması beklenmektedir. İklim değişikliğinin bitkiler başta olmak üzere yeryüzündeki tüm canlıları ve bunların hastalık ve zararlı kaynaklarını etkilemesi kaçınılmazdır. Artan zararlı ve hastalık riskleri nedeniyle ekosistem bozulması ve kuraklık gıda güvenliğini ve geçim kaynaklarını olumsuz etkileyebilir. Bu durum ekonomik krizlere, zorunlu göçlere ve bir takım çatışmalara neden olabilir. Artan nem, sıcaklık ve CO2 miktarı bitki hastalık etkenlerinin dağılımını, gelişmesini, yayılmasını ve üremesini etkilemektedir. İklim değişikliği, daha önce zararlıların ve hastalıkların yaşayamadığı bölgelerde uygun iklim koşullarının oluşmasını sağlar. İklim değişikliği ayrıca bitki koruma ve pestisit kullanımı üzerinde olası etkilerle yabancı otların, zararlıların ve hastalıkların ekolojisini de etkilemektedir. İklim değişikliği sebebi ile bazı türler kuzey küreye ve daha yüksek enlemlere, bazıları ise tropik bölgelerde daha yüksek sıcaklıklara göç edebilir, dolayısı ile hastalık ve zararlıların yayılımı ve dağılımı değişebilir. Atmosferdeki artan karbondioksit ve ozon seviyeleri ve yoğun yağışlar da bitki fizyolojisini ve yapısını etkileyerek bitkiyi zararlılara ve hastalıklara karşı daha savunmasız hale getirebilir (Şekil 1). Şiddetli fırtınalar ve yağmurlar bitkilerin direncini azaltabilir ve mantar ve bakteri enfeksiyonlarını artırabilir. Kuraklık durumunda, stres altındaki bitkiler hastalık ve zararlılara karşı normal dirençlerini kaybetme riskiyle karşı karşıya kalırlar. Hastalık ve zararlılardaki artıştan dolayı çok geniş alanlarda zararlı sentetik toksik pestisitlerin kullanılması bitki ve insan sağlığı ile çevre ve biyolojik çeşitlilik üzerinde olumsuz sonuçlar doğurabilmektedir. Biyoçeşitliliğin korunmasına yönelik yapılacak çalışmalar ve iklim değişikliğinin bitki koruma üzerindeki olumsuz etkisini azaltmaya yönelik iyileştirme çalışmaları oldukça önemlidir. Çeşitlilik, özellikle yapılacak ıslah çalışmaları ile tarımsal ürün üretim sistemlerinin iklim değişikliğinin etkilerine uyum sağlamasına yardımcı olabilir. 2002 yılındaki Dünya Gıda Zirvesi'nde gıda güvenliği şu şekilde tanımlanmıştır. “Gıda Güvenliği, tüm insanların her zaman, aktif ve sağlıklı bir yaşam için beslenme ihtiyaçlarını ve gıda tercihlerini karşılamak için yeterli, güvenli ve besleyici gıdaya fiziksel, sosyal ve ekonomik erişime sahip olmaları durumunda ortaya çıkar” İklim değişikliği gıda güvenliğinin dört boyutunu da etkiler: gıda üretimi, gıda erişilebilirliği, gıda kullanımı ve gıda sistemlerinin istikrarıdır. Gıda güvenliğinden yoksun olan insanlar, artan ürün kayıplarından ve yeni zararlı ve hastalık çeşitlerinden ilk etkilenenler olacaktır. Küresel ısınma ve hava olaylarındaki aşırı değişiklikler, muhtemelen bitki zararlıları ve hastalıklarının yaşam döngüsünü, epidemiyolojik özelliklerini ve yayılmasını etkileyecektir. Örneğin artan sıcaklıklar zararlıların çoğalmasını teşvik ederek gıda güvenliğini tehdit edebilir.

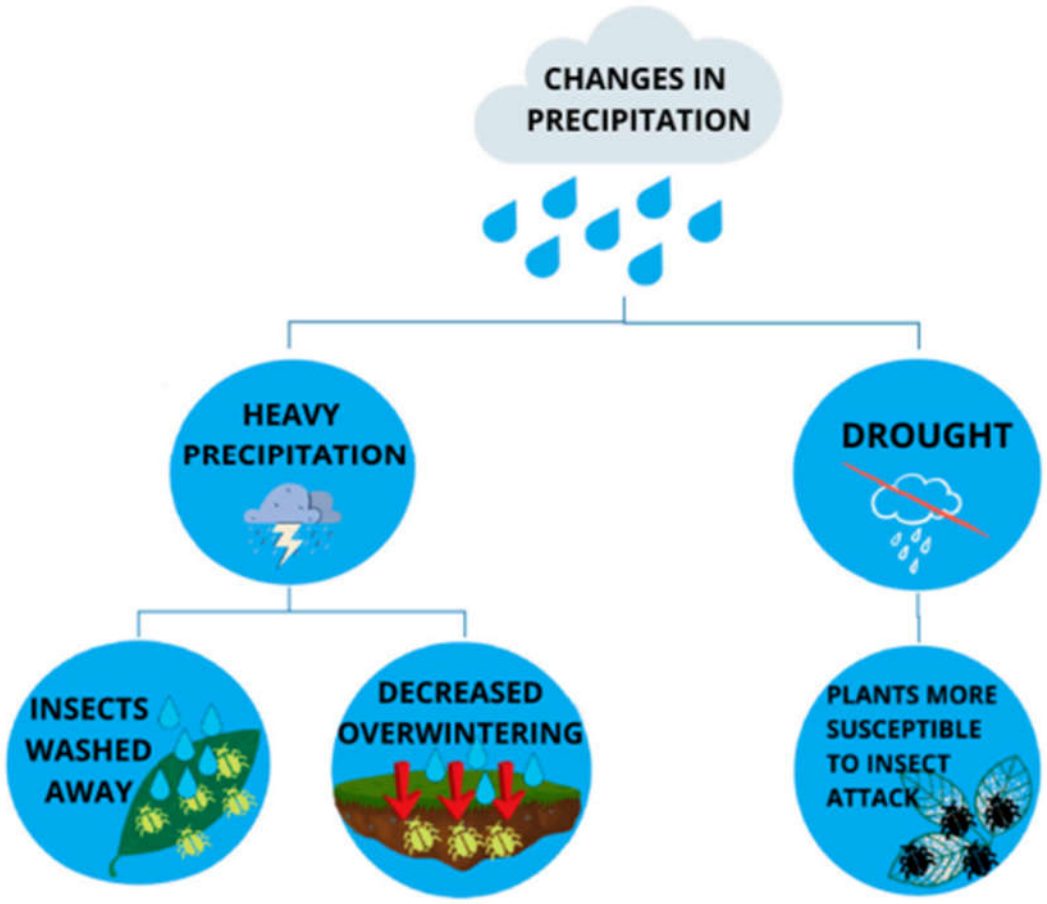

Şekil 1. Yağış miktarındaki değişikliklerin tarım zararlıları üzerine etkileri (Skendzic et al., 2021)

Küresel ısınma aynı zamanda zararlıların kış aylarında da hayatta kalmasını sağlar ve böylece zarar süresini uzatabilir. Ayrıca, örneğin, kasırgalar ve diğer şiddetli hava olayları zararlıları ve hastalıkları daha geniş bir alana yayabilir. İklim değişikliği aynı zamanda zararlıların ve hastalıkların daha önce yaşamaları mümkün olmayan alanlarda uygun iklim koşulları bulma ve dolayısıyla bu alanlara yayılma riskini de artırmaktadır. Yeni ıslah edilen çeşitler, bu tür alanlarda zararlı ve hastalık dağılımını daha da kolaylaştırabilir. Haşerelerin ve hastalıkların etkileri, yaygın konakçılarla etkileşimleri, daha da artabilir. Haşere risk analizi yapılırken iklim değişikliğinin etkisi üzerine daha fazla odaklanılmalıdır. Bu hassasiyet bitki sağlığını, biyolojik çeşitliliği ve gıda güvenliğini korumaya yardımcı olabilir. Bitki zararlılarının artan yayılmasına yanıt olarak, bazı potansiyel olarak zararlı sentetik toksik tarım kimyasallarının küresel kullanımı ve talebi, bitki sağlığı, insan sağlığı, biyolojik çeşitlilik ve çevre için olumsuz sonuçlarla çoğalabilir. Tarım ve ormancılık faaliyetleri, iklim değişikliğine uyum sağlamak için, özellikle zararlıların ve hastalıkların uluslararası yayılmasının önlenmesi ve zararlıları denetleme disiplinleri ile ilgili olarak yenilenmiş teknik bilgi gerektiren bitki ıslahında değişiklikler ve haşere kontrol uygulamalarında değişiklikler gerektirebilir. İklim değişikliği genetik erozyonu artırabilir ve bitkisel üretimde genetik çeşitliliğin olmaması bitki sağlığı için büyük bir risktir. Bitkilerdeki genetik çeşitlilik, tarımsal ürün üretim sistemlerinin iklim değişikliğine daha iyi uyum sağlamasına yardımcı olabilecek ve çevreye zarar verebilecek bazı tehlikeli pestisitler veya gübrelere olan ihtiyacı azaltabilecek önemli bir kalıtsal özellik kaynağıdır. İklim değişikliği, kültür bitkilerinin yanı sıra, birçok bitkinin yabani formlarının hayatta kalma yeteneğini de etkileyebilir. Bu nedenle, biyoçeşitliliğinin korunması çok önemlidir. Bitkilerin ve bitkisel ürünlerin, sınırları aşarken bitki sağlığı noktasında tedbirler alınması da her zaman önemlidir. Artan bitki hastalık ve zararlıları, önemli ekonomik kayıplara neden olabilir ve verimi ve hasat kalitesini düşürebilir, böylece potansiyel olarak önemli gıda kayıpları görülebilir. Ülkeler, bitkisel ürünlerin taşınmasında güvenli uluslararası ticaret ağları oluşturarak sağlıklı gıda kaynaklarının korunması için bitki sağlığı önlemlerinin uygulanmasını dikkate almalıdır.

SONUÇ

İklim değişikliği sürecinde, tarımsal üretim yapan işletmeler, hayvancılık işletmeleri, ormancılık ve su ürünleri çiftlikleri değişen koşullara uyum sağlamak zorundadır. Tarımın iklim değişikliğine uyum sağlaması ve önümüzdeki yıllarda gıda güvenliği ve beslenme hedeflerine ulaşılması gerekiyorsa, gıda üretim sistemleri ve bağımlı oldukları daha geniş ekosistemler giderek daha dayanıklı, çok işlevli ve çok amaçlı hale gelmek zorundadır. İklim değişikliğinin sonuçları ne olursa olsun, bir takım önlemler alınarak tarımsal ürünlerin koruma altına alınması imkan dahilindedir. Bu basit ve kolay önlemler neler olabilir. İklim değişikliğinin sonuçları ne olursa olsun, tarımın ve tarımsal üretimin muhafaza edilmesi noktasında alınabilecek bazı basit ve kolay önlemler nelerdir?

1) Tarımsal üretim yapılan alanları daha fazla gözlemlemeye, incelemeye ve araştırmaya ihtiyacımız var. Her canlı, her böcek bizim düşmanımız değildir. Hastalıklar ve zararlılar hakkında daha fazla bilgiye ihtiyacımız var. Mücadele yöntemleri hakkında daha fazla şey öğrenmemiz gerekiyor. Dolayısı ile onları daha yakından ve daha iyi tanımalıyız.

2) Hastalık ve zararlılarla mücadelede kültürel tedbirler artırılmalıdır. Bu nedenle biyoçeşitliliğin korunması ve arttırılması oldukça önemlidir. Doğal düşman kullanımı, karma ekim sistemleri, azaltılmış toprak işleme ve malçlama gibi uygulamalar çeşitlendirilebilir.

3) Çeşit ıslahına önem verilmelidir. Bu nedenle çok boyutlu ıslah çalışmaları yapılmalıdır. Özellikle hastalık ve zararlılarla mücadelede bitkilerin öne çıkan özellikleri belirlenmeli ve birbirleriyle buluşturulmalıdır. Üstün özelliklere sahip yeni çeşitler elde edilmelidir.

4) Münavebe yani aynı tarlada farklı bitkiler yetiştirmek, hastalık ve zararlıların gelişimini ve yayılmasını yavaşlatır. Tarladaki bitki artıkları, diğer mahsuller için zararlı olan patojenlerin konakçılarıdır. Rotasyon bu döngüyü bozar.

5) Topraklarımız, hastalık ve zararlılarla mücadelede sahip olduğumuz en önemli kaynaklardan birisidir. Fiziksel, kimyasal ve biyolojik yönden iyi bir tarla toprağı kültür bitkilerinin rekabet gücünü artırır.

Kaynaklar

Anonim, 2015. https://www.who.int/news/item/11-12-2015-new-climate-accord-could-save-lives-and-health-costs-from-both-climate-and-air-pollution. Erişim tarihi: 07/09/2022.

Anonim, 2020. https://www.bbc.com/turkce/haberler-dunya-53856423. Erişim tarihi: 07/09/2022.

Anonim, 2022a. https://www.copernicus.eu/en/copernicus-services/atmosphere. Erişim tarihi: 07/09/2022.

Anonim, 2022b. https://earthobservatory.nasa.gov/world-of-change/global-temperatures. Erişim tarihi: 07/09/2022.

Johansen, B.E., 2002. The Global Warming Desk Reference; Greenwood Publishing Group: Westport, CT, USA; ISBN 0-313-31679-1.

Parry, M., 1990. The potential impact on agriculture of the greenhouse effect. Land Use Policy, 7, 109–123.

Skendži´c, S.; Zovko, M.; Živkovi´c, I.P.; Leši´c, V.; Lemi´c, D. The Impact of Climate Change on Agricultural Insect Pests. Insects 2021, 12, 440. https://doi.org/10.3390/ insects12050440.

Tilman, D.; Balzer, C.; Hill, J.; Befort, B.L., 2011. Global food demand and the sustainable intensification of agriculture. Proc. Natl. Acad. Sci. USA, 108, 20260–20264.

THE ASSOCIATION BETWEEN RUMEN MICROBIOTA AND PRODUCTION PERFORMANCE IN DAIRY CATTLE

Dilan Deniz İlhan, MSc[1]

[1]Ege University, Faculty of Agriculture, Department of Animal Science, İzmir, Turkey.

[1]ORCID: https://orcid.org/ 0000-0002-3428-1854

Assistant Prof. Dr. Veysel Bay[2]

[2]Ege University, Faculty of Agriculture, Department of Animal Science, İzmir, Turkey.

[2]ORCID: https://orcid.org/0000-0002-9339-4840

ABSTRACT

The demand and need for animal protein increase every day due to the increase in the world population. Animal health has become an essential factor in ensuring maximum performance in livestock. Healthy microbiota significantly enhances production performance and animal welfare. Microbiota refers to a population that contains viruses, bacteria, archaea, and fungi in vital organs of living organisms. It is known that microbiota has 10 times more cells and 100 times more genes than the host. It is also known to affect host phenotypes immensely through gut microbiota, neural functions, and endocrine pathways. Furthermore, it plays a crucial role in digestion and absorption of feed, regulating intestinal mobility and homeostasis of the gut barrier.

Intestinal digestion and absorption are important factors for cattle's dynamic balance of the intestinal ecosystem. Although the number of bacterial species in the digestive system of cattle is estimated to be over 5,000, this number varies in line with ration, feeding strategy, and geographical location. Foregut and intestines in cattle contain a high number of viruses, fungi, bacteria, archaea, and protozoa which help ferment ingredients. Their bacterial concentration amounts to 10^{12}-10^{14} cells per milliliter (ml) of the ingredient. Healthy microbiota increases the fat content of milk and feed conversion ratio in cattle. Furthermore, microbiota in cattle is thought to improve animal welfare and reduce methane emissions positively.

This article reviews and examines literature data on the microbiota structure of cattle, its physiological and ecological interactions, and its impact on production performance and related parameters.

Keywords: Dairy cattle, rumen microbiota, productivity

THE GENETICS OF CASEOUS LYMPHADENITIS IN SMALL RUMINANTS

Assist. Prof. Dr. Veysel Bay[1]

[1]Ege University, Faculty of Agriculture, Department of Animal Science, İzmir, Turkey.

[1]ORCID: https://orcid.org/0000-0002-9339-4840

Dr. Çağrı Kandemir[2]

[2]Ege University, Faculty of Agriculture, Department of Animal Science, İzmir, Turkey.

[2]ORCID: https://orcid.org/0000-0001-7378-6962

Prof. Dr. Turgay Taşkın[3]

[3]Ege University, Faculty of Agriculture, Department of Animal Science, İzmir, Turkey.

[3]ORCID: https://orcid.org/0000-0001-8528-9760

ABSTRACT

Caseous Lymphadenitis (CLA) is a deadly bacterial disease caused by a bacterium called Corynebacterium pseudotuberculosis. It is common in sheep and goats and causes significant economic losses.

The swelling corresponding to the abscessed lymph node beneath the skin is the most important sign of bacterial disease (external form). Bacteria can sometimes enter the bloodstream and cause abscesses in internal organs like the liver, lungs, kidneys, or reproductive system.

Infected animals are thought to be a potential source of disease. Transmission occurs when organisms spread to the environment via abscess discharge or discharge from pulmonary lesions reaches the animals via coughing. Other animals in the herd are then put at risk due to contamination from contaminated equipment and the environment.

It results in economic losses due to the condemnation of animal skin and carcass. CLA is also thought to be linked to herd infertility and abortion. The external form of the disease is not fatal, but it can cause a decrease in the animal's live weight and milk yield, as well as deterioration of its skin and wool. It could also negatively affect animal welfare.

The true prevalence of caseous lymphadenitis in small ruminants is frequently underestimated because it is not a notifiable disease in many countries. However, in some countries, figures ranging from 8% to 90% have been reported.

C. pseudotuberculosis is susceptible to a variety of antibiotics in vitro, but clinical cases of CLA are frequently antibiotic-resistant. There is currently no effective CLA therapy available, and vaccine use is limited. To combat the disease effectively, a herd control program should be established to eliminate risk factors and protect small ruminants. In this case, selective breeding of CLA-resistant animals could be an option.

This review will go into detail about CLA, and genetic factors associated with CLA resistance.

Keywords: Caseous Lymphadenitis, small ruminants, genetics

ESKİŞEHİR ODUNPAZARI EVLERİNİN MEKAN SENTAKSI İLE İRDELENMESİ

EXAMINATION OF ESKISEHIR ODUNPAZARI HOUSES WITH SPACE SYNTAX

Esra ACAR

Fırat Üniversitesi, Mimarlık Fakültesi, Mimarlık Bölümü, Elazığ, Türkiye

ORCID ID: 0000-0002-7264-3705

Ayça GÜLTEN

Fırat Üniversitesi, Mimarlık Fakültesi, Mimarlık Bölümü, 23119, Elazığ, Türkiye

ORCID ID: 0000-0001-9837-8674

ÖZET

Toplumun sosyo kültürel yapısını en çok yansıtan fiziki çevrenin büyük bir bölümünü oluşturan konut yapıları temelde barınma ihtiyacını karşılayan bir mekansallık durumu olarak ele alınsa da, kent dokusunda bütüncül bir ifade ve kentlinin yaşamlarında fiziksel ve sosyal boyutlar olarak karşımıza çıkar. Bu yaklaşım ile beraber belirli bir bölgedeki aynı kültürde yerleşim gösteren bir topluluğun konut yapısının da benzer, hatta aynı özellikler taşıması da olağan hale gelmektedir. Jeopolitik konumundan dolayı Anadolu'da birçok uygarlığın yaşadığı dönemden bugüne kadar geçen süreç içerisinde geleneksel konutlar da kendine yer edinmiştir. Birçok uygarlığa ev sahipliği yapmış olan Eskişehir kentinde yer alan Odunpazarı evleri geleneksel Türk konut mimarisinin örneklerini barındıran ve geleneksel dokusunu geçmişten bugüne koruyarak süregelen bir yerleşim alanıdır. Çalışma kapsamında geleneksel Odunpazarı yerleşimini kitlelere tanıtmak, incelemek ve sentaktik olarak analizlerinin irdelenmesi hedeflenmiştir. Mekan sentaksı yöntemi, farklı bölgelerin, kentlerin, bina ölçeğindeki tasarım alternatiflerinin etkilerini araştırmak ve bunların sosyal yapı ile olan etkileşimlerini ve bununla birlikte anlamsal boyut ilişkilerini incelemek içinde kullanılan bir tekniktir. Bu doğrultuda Odunpazarı bölgesinde yaşayan toplumun yaşantısının konut üzerindeki etkileri üç geleneksel konut bağlamında incelenip analiz edilerek mekân kurgusundaki soyut ve somut veriler, mekân sentaksı yöntemiyle sayısal olarak elde edilmiştir. Elde edilen veriler sonucunda, yapıların zemin ve üst katlarında mekanlar arasındaki ilişkinin ve geçirgenliğin en fazla 1 nolu yapıda en az 2 nolu yapıda olduğu görülmüştür. Zemin ve üst katların entegrasyon değeri fazla ve dolayısıyla daha fazla sığ mekana sahip olan yapının 2 nolu yapı olduğu, en derin mekanlara sahip yapının 1 nolu yapı olduğu ortaya çıkmıştır. Ortalama derinlik değeri ise zemin kat ve üst katlarda farklılıklar göstermiştir. Sonuç olarak Odunpazarı evleri üzerinden morfolojik analizler gerçekleştirilerek, mekansal değerlendirmelerin geçmişin ve bugünün analiz edilerek geleceğe aktarılmasında önemli bir adım olduğu belirlenmiş ve geleneksel konutlar yeniden işlevlendirilirken doğru koruma yaklaşımları için karar alınması bağlamında altlık olacağı düşünülmüştür.

Anahtar Kelimeler: Geleneksel konut, Odunpazarı evleri, Mekan sentaksı

ABSTRACT

Although the housing structures, which constitute a large part of the physical environment that most reflects the socio-cultural structure of the society, are considered as a spatial situation that basically meets the need for shelter, they appear as a holistic expression in the urban fabric and as physical and social dimensions in the lives of the citizens. With this approach, it becomes commonplace for a community inhabiting the same culture in a particular region to have similar or even the same characteristics in the housing structure. Due to its geopolitical location, traditional houses have also taken their place in the process that has passed from the period when many civilizations lived in Anatolia to the present. Located in the city of Eskişehir, which has hosted many civilizations, Odunpazarı houses are an ongoing residential area that contains examples of

traditional Turkish residential architecture and preserves its traditional texture from the past to the present. Within the scope of the study, it is aimed to introduce and examine the traditional Odunpazarı settlement to the masses and to examine its analysis syntactically. The space syntax method is a technique used to investigate the effects of different regions, cities, and building-scale design alternatives, and to examine their interactions with the social structure, as well as their semantic dimension relations. In this direction, the effects of the life of the society living in the Odunpazarı region on the house were examined and analyzed in the context of three traditional houses, and the abstract and concrete data in the space setup were obtained numerically by the space syntax method. As a result of the data obtained, it was seen that the relationship between the spaces and the permeability in the ground and upper floors of the buildings were at most in the 1st structure and at least in the 2nd structure. It has been revealed that the structure with higher integration value of the ground and upper floors and therefore more shallow spaces is structure number 2, and the structure with the deepest spaces is structure number 1. The average depth value showed differences in the ground floor and upper floors. As a result, by performing morphological analyzes on Odunpazarı houses, it has been determined that spatial evaluations are an important step in analyzing the past and present and transferring them to the future, and it is thought that it will be a base for making decisions for the right conservation approaches while refunctioning traditional houses.

Keywords: Traditional house, Odunpazarı houses, Space syntax

ALTERNATIVE TECHNOLOGIES FOR THE USE OF WIND ENERGY ON SHIPS: FLETTNER ROTOR

Kenan Yiğit

Yildiz Technical University, Faculty of Naval Architecture and Maritime, Marine Engineering Department, Istanbul, Turkey.

ORCID ID: https://orcid.org/0000-0002-4165-4081

ABSTRACT

In this study, the Flettner rotor technology and the approaches to increasing the efficiency of this technology are examined. Wind energy has an important place in maritime history. Today, with the conversion of wind energy to alternative energy systems, both electrical energy and propulsion system needs can be met on ships. One of these alternative approaches is the Flettner rotor system. It provides an alternative propulsion system on board, using the Magnus effect. It is a cylindrical rotating device that is mounted vertically on the deck and powered by electricity. The electrical energy is used to drive the Flettner rotor by the electric motor. The Magnus effect is caused by the pressure difference on both sides of the rotating cylinder. Thus, a secondary energy source is obtained for ship propulsion by generating lift and drag forces. Although the origin of Flettner rotor technology dates back to the 1920s, it has recently come back into the limelight due to international regulations and restrictions in the maritime field. In the last decade, this technology has been applied to different types of ships, such as general cargo, ro-ro, passenger, tanker, bulk carrier, and ferry. Theoretical and practical studies show that Flettner rotor systems have the potential to reduce main engine fuel consumption by half depending on the referenced parameters. Although this rate is lower in practical applications, this technology offers a remarkable approach for zero-emission ship concepts. As a result, it can be said that Flettner rotor systems can be applied in practice and contribute significantly to energy efficiency. It is envisaged that the energy saving rate can be increased with initiatives such as developing the control system with various optimization techniques, using different material structures, testing new models in system design, and meeting the electrical energy needs with renewable energy sources.

Keywords: Ship, Flettner rotor, Renewable energy, Wind energy, Energy efficiency.

SOL-JEL YÖNTEMİ İLE SENTEZLENEN Eu^{3+}, Gd^{3+} VE Yb^{3+} KATKILI BİYOAKTİF CAM TOZLARININ IN VITRO BİYOAKTİVİTE, SİTOTOKSİSİTE VE 5-FLOROURASİL SALIM DAVRANIŞININ İNCELENMESİ

Begüm RAHMAN[1]

[1]Manisa Celal Bayar Üniversitesi, Mühendislik Fakültesi, Metalurji ve Malzeme Mühendisliği, Manisa, Türkiye.

[1]ORCID ID: https://orcid.org/0000-0003-3600-1155

Aylin M. DELİORMANLI [2]

[2]Manisa Celal Bayar Üniversitesi, Mühendislik Fakültesi, Metalurji ve Malzeme Mühendisliği, Manisa, Türkiye.

[2]ORCID ID: https://orcid.org/0000- 0001-7877-7635

Harika ATMACA[3]

[3]Manisa Celal Bayar Üniversitesi, Fen Edebiyat Fakültesi, Biyoloji Bölümü, Manisa, Türkiye.

[3]ORCID ID: https://orcid.org/0000-0002-8459-4373

ÖZET

Bu çalışmada sol-jel yöntemi ile sentezlenmiş farklı konsantrasyonlarda (%0.5, 1, 3, 5) evropiyum (Eu^{3+}), gadolinyum (Gd^{3+}), iterbiyum (Yb^{3+}) içeren biyoaktif cam tozlarının biyoaktiviteleri, in vitro sitotoksisiteleri ve antikanser ilaç salım davranışları incelenmiştir. Bu amaçla, nadir toprak elementi (RE^{3+}) katkılı silika bazlı 13-93 biyoaktif cam tozlarının yapay vücut sıvısı (SBF) içerisinde hidroksiapatit (HA) oluşturma davranışı farklı zaman aralıklarında FTIR spektrometre ve taramalı elektron mikroskobu kullanılarak incelenmiştir. Hazırlanan tozların in vitro sitotoksistesi pre-osteoblastik MC3T3-E1 ve osteosarkom SaOS-2 hücre hatları kullanılarak MTT yöntemi (3, 7 ve 14 gün) ile araştırılmıştır. Biyoaktif cam tozlarının bir antikanser ilacı olan 5-florourasil (5-FU) salım davranışı fosfat tamponlu salin içerisinde pH 7.4'de ve 37 °C'de test edilmiştir. Sonuçlar, nadir toprak elementi katkısının biyoaktif cam tozlarının in vitro biyoaktivitesi üzerinde olumsuz bir etkiye neden olmadığını göstermiştir. Diğer yandan 3 günlük hücre kültürü sonunda 5%Yb^{3+} içeren biyoaktif camlar dışındaki örneklerin tamamında SaOS-2 hücrelerine karşı herhangi bir sitotoksik etki gözlenmemiştir. 14 gün sonunda ise çalışma kapsamındaki tüm RE^{3+} katkılı biyoaktif cam örneklerin SaOS-2 hücreleri üzerinde toksik etkiye sahip olduğu anlaşılmıştır. Diğer yandan, MC3T3-E1 hücre hattı ile yapılan 3 günlük kültür çalışmaları sonucunda en yüksek RE^{3+} konsantrasyonuna sahip biyoaktif camların hücre canlılığında azalmaya neden olduğu anlaşılmıştır. İlaç salım çalışmalarının sonuçları 600 saat sonunda biyoaktif cam tozlarından fosfat tamponlu salin ortamına gerçekleşen kümülatif 5-FU salım miktarının RE^{3+} katkı çeşidi ve konsantrasyonuna bağlı olarak % 42-69 seviyesinde olduğunu göstermiştir. Çalışmada hazırlanan RE^{3+} içeren 13-93 biyoaktif cam tozlarının doku mühendisliği uygulamalarında kullanılma potansiyellerinin olduğu sonucuna varılmıştır.

Anahtar Kelimeler: Biyoaktif cam, Evropiyum, Gadolinyum, İterbiyum, MC3T3-E1, SaOS-2.

ABSTRACT

In this study, the bioactivity, in vitro cytotoxicity and anticancer drug release behavior of sol-gel derived bioactive glass powders containing Europium (Eu^{3+}), Gadolinium (Gd^{3+}), Ytterbium (Yb^{3+}) at different

concentrations (0.5, 1, 3, 5 wt.%) were investigated. For this purpose, the hydroxyapatite (HA) formation behavior of rare earth element (RE^{3+})-doped silicate-based 13-93 bioactive glass powders was investigated in artificial body fluid (SBF) at different time intervals using FTIR spectrometer and scanning electron microscope. In vitro cytotoxicity of the prepared powders was investigated by MTT method (3, 7 and 14 days) using pre-osteoblastic MC3T3-E1 and osteosarcoma SaOS-2 cell lines. The release behavior of 5-fluorouracil (5-FU), an anticancer drug, from bioactive glass powders was tested in phosphate buffered saline at pH 7.4 and 37 °C. The results of the study showed that the rare earth element addition did not cause any detrimental effect on the in vitro bioactivity of the studied bioactive glass powders. On the other hand, after 3 days of cell culture, no cytotoxic effect was observed against SaOS-2 cells in all of the samples, except for the bioactive glasses containing 5%Yb3+. At the end of 14 days, it was understood that all RE^{3+} -containing bioactive glass samples had a toxic effect on SaOS-2 cells. Additionally, as a result of 3-day culture studies with the MC3T3-E1 cell line, it was shown that there was a decrease in cell viability for bioactive glass powders at the highest RE^{3+} concentration. The results of the drug release studies showed that the cumulative 5-FU release rate from bioactive glass powders to phosphate buffered saline after 600 hours was 42-69% depending on the RE^{3+} additive type and concentration. It was concluded that the 13-93 bioactive glass powders containing RE^{3+} prepared in the study have the potential to be used in tissue engineering applications.

Keywords: Bioactive glass, europium, gadolinium, ytterbium, MC3T3-E1, SaOS-2.

1. GİRİŞ

Biyoaktif camlar sert ve yumuşak doku mühendisliği uygulamalarında ve bunun dışında diş hekimliği, kanser tedavisi, biyomedikal görüntüleme gibi farklı uygulamalarda kullanılan malzemelerdir [1-3]. Diğer yandan, lantanitler ya da nadir toprak elementlerine ait iyonların görünür ve yakın-infrared bölgelerinde fotolüminesans özellik gösterdiği bilinmektedir. Er^{3+}, Tm^{3+}, Gd^{3+}, Ho^{3+}, Nd^{3+}, Yb^{3+} gibi çeşitli nadir toprak elementleri iyonlarının katkılanmasıyla sentezlenen camların, kırmızı, yeşil ve mavi dalgaboylarında, görülebilir bölgede, üst dönüşüm vasıtası ile emisyona neden oldukları görülmüştür [4].

Nadir toprak elementleri arasında yer alan evropiyum (Eu^{3+}) katkılı biyoaktif cam tozlarının lüminesans ve ilaç (ibuprofen) salım özellikleri Fan ve arkadaşları [5] tarafından incelenmiş olup, sonuçlar sentezlenen lüminesant biyoaktif camların ilaç taşıyıcı sistemler olarak kullanılabileğini göstermiş ve vücuda salımı gerçekleşen ilaç miktarının tespit edilebilmesinin mümkün olacağı raporlanmıştır. Benzer şekilde, literatürde Eu^{+3} içeren ve mezogözenekli ilaç sistemlerinin bir anti-kanser ilaçı olan doksorubisin (DOX) salımının incelenmesi ve in vitro sitotoksisitesi üzerine yayınlanmış çalışmalar bulunmaktadır [6].

Biyomalzemelere lüminesans özellik kazandırmak için kullanılan bir diğer önemli nadir toprak elementi iterbiyum (Yb^{3+}) olup, diğer nadir toprak elementleri ile birlikte kullanıldığında sinerjistik etki görülmesine imkan tanımaktadır [6]. Ignjatović ve arkadaşları [7] tarafından gerçekleştirilen bir çalışmada Yb^{+3}/Gd^{+3} katkılı hidroksiapatit tozları sentezlenmiş, elde edilen malzemelerin lüminesans özelliklerinin belirlenmesi için FTIR, ışık eksitasyon-emisyon spektrumları incelenmiş ayrıca in vitro sitotoksisite testleri gerçekleştirilmiştir. Sonuçlar, sentezlenen malzemelerin çok yönlü biyomedikal görüntüleme uygulamalarında kullanılabileceğini göstermiştir [7].

Diğer yandan gadolinyum (Gd^{3+}) nadir toprak elementleri grubunda yer alan ve paramanyetik özellik gösteren bir metaldir [8]. Bu nedenle, manyetik rezonans görüntüleme (MRI) sinyallerini arttırmakta ve MRI kontrast maddesi olarak kullanılmaktadır. Yüksek termal, kimyasal ve fotokimyasal stabilitesinden ötürü fotoluminesans özelliklerin ön planda olduğu uygulamalarda da yer almaktadır [9]. Gadolinyumun kemik doku rejenerasyonu üzerinde olumlu etkiye neden olduğu raporlansa da etki mekanizmaları tam olarak bilinmemektedir. Borges ve arkadaşları [10] tarafından 2019 yılında yapılan bir çalışmada Gd^{3+} ve Yb^{3+} katkısı yapılmış biyoaktif camların yapısal özellikleri incelenmiştir. Ayrıca, 2.5-5 mol% miktarında Gd^{+3} katkısının biyoaktiviteyi arttırdığı raporlanmıştır. Benzer şekilde, Eu^{3+}, Gd^{3+} ve Yb^{3+} içeren 13-93 biyoaktif camların yapısal, morfolojik ve fotolüminesans özellikleri daha önce incelenmiştir [11]. Ancak belirtilen nadir toprak elementi iyonlarının 13-93 camlarının biyoaktivitesi, sitotoksisitesi ve ilaç salım davranışı henüz bilinmemektedir. Bu çalışmanın amacı belirtilen RE^{3+} iyonları içeren biyoaktif camların biyomedikal uygulamalarda kullanılabilirliğinin araştırılmasıdır.

2. DENEYSEL ÇALIŞMALAR

2.1. Sol-jel Yöntemi ile Biyoaktif Cam Sentezi

Katkısız, Eu^{3+}, Gd^{3+} ve Yb^{3+} katkılı (0.5, 1, 3, 5 ağırlıkça%) silika bazlı 13-93 biyoaktif cam ($6Na_2O$, $12K_2O$, $5MgO$, $20CaO$, $4P_2O_5$, $53SiO_2$; ağırlıkça %) tozları sol-jel metodu ile daha önce geliştirilmiş olan yönteme göre sentezlenmiştir [11]. Bu amaçla, 14.41 ml deiyonize suyun içine 0.0998 ml 65% nitrik asit eklenmiş sonrasında 9.92 ml TEOS eklenerek 1 saat karıştırmaya bırakılmıştır. Solusyon berrak hale geldiğinde sırası ile 0.475 ml trietil fosfat, 0.835 gr sodyum nitrat, 4.135 gr kalsiyum nitrat tetrahidrat, 1.579 gr magnezyum nitrat hegzahidrat ve 1.308 gr potasyum nitrat solusyona birer saat ara ile ilave edilmiştir. Nadir toprak elementi içeren camların sentezinde ek olarak evropiyum (III) nitrat pentahidrat, gadolinyum (III) nitrat pentahidrat, iterbiyum (III) nitrat pentahidrat kullanılmıştır. Toplam solusyon oda sıcalığında 24 saat karıştırılmış ardından yine oda sıcaklığında ağzı kapalı vaziyette cam şişenin içinde jelleşme için bekletilmiştir. Sonrasında jeller yaşlandırma işlemi için 48 saat 60°C sıcaklıkta etüvde tutulmuş ardından şişenin ağzı açılarak önce 24 saat 60 °C sıcaklıkta ve sonra 24 saat 120 °C de tutularak kurutma işlemi gerçekleştirilmiştir. Kuruyarak toz haline gelen biyoaktif cam tozları agat havanda dövülerek ufalanmış ardından 625 °C'de 4 saat kalsine edilmiştir. Tane boyut küçültme işlemi için yüksek hızlı planeter değirmen (Fritch, Pulverisette, Premium Line 7) kullanılmıştır.

2.2. Karakterizasyonlar

2.2.1. Biyoaktivite

In vitro biyoaktivite deneyleri yapay vücut sıvısı (SBF) içinde gerçekleştirilmiştir. Bu amaçla gerekli kimyasalların, Kokubo yöntemine göre [12] (NaCl, $NaHCO_3$, KCl, $K_2HPO_4{\bullet}3H_2O$, $MgCl_2{\bullet}6H_2O$, $CaCl_2$, Na_2SO_4 , $CH_2OH_3CNH_2$ (Sigma Aldrich)) ve 1 M HCl belirli bir sırada ultra- saf suya eklenip , 37 °C de magnetik karıştırıcı üzerinde devamlı karıştırılarak tam çözünmeleri sağlanmıştır. Sentezlenen biyoaktif cam tozları, pH'sı 7.4 olan yapay vücut sıvısı (SBF) içerisine konularak (1 gr örnek için 500 ml SBF) inkübatörde 37 °C'de 7 ve 28 gün bekletilmiştir. Daha sonra SBF'den çıkarılan örnekler önce etanol ile yıkanmış sonrasında 100 °C'de etüvde 24 saat kurutulmuştur. SBF'den çıkarılan yapıların yüzeyinde hidroksiapatit (HA) oluşumu taramalı elektron mikroskobu (SEM) ve FT-IR spektroskopisi kullanılarak incelenmiştir.

2.2.2. In Vitro Sitotoksisite

Çalışmalarda fare kalvariyal pre-osteoblatistik MC3T3-E1 (ATCC, USA) ile insan osteosarkoma hücre hatları (SaOS-2) (ATCC, USA) kullanılmıştır. Sentezlenen biyoaktif cam partikülleri kuru presleme yolu ile pelet haline getirilmiş 690 °C'de 1 saat sinterlenerek disk şeklinde skafoldlar hazırlanmıştır. Hazırlanan disk şeklindeki 3 boyutlu skafoldların çapları 7.5 mm olup yükseklikleri 1-2 mm seviyesindedir. Tüm örnekler %70'lik etanol ile yıkanmış ardından 350 °C de 15 saat tutularak sterilizasyon işlemi gerçekleştirilmiştir. Biyoaktif cam skafoldların sitotoksisitesinin belirlenmesi için, MC3T3-E1 preosteoblast hücre dizini, DMEM F–12, %10 FBS, %1 L-glutamine ve %1penisilin-streptomycine içeren kültür ortamında 37°C'de ve %95 hava- 5% CO_2 içeren inkübatörde bekletilmiştir. Hücreler, örneklerin üzerine 100 µl'de 5 x 10^4 hücre olacak şekilde aktarılmış 3, 7 ve 14 gün sonra hücre proliferasyonu ve sitotoksisitesi, kolorimetrik bir test yöntemi olan MTT ((3-(4, 5- dimethylthiazolyl-2)-2.5-diphenyltetrazolium bromide), ile değerlendirilmiştir.

Diğer yandan, SaOS-2 hücreleri önce %10 FBS ve %1 penisilin-streptomisin eklenen McCoy's 5A (L-Glutaminli) besiyerinde 75 cm^2 lik kültür kaplarında çoğaltılmıştır. MTT ile sitotoksisite analizi için biyoaktif cam örnekleri barındıran 24 gözlü kültür kaplarının her bir gözüne 2.5x10^5 hücre olacak şekilde hücre ekilmiş ve hücreler 14 güne dek inkübe edilmiştir.

MTT ile sitotoksisite analizi için kültürün belirli zamanlarında (3, 7, 14 gün) kültür kabının gözlerindeki kültür ortamı uzaklaştırılarak, her bir göze 600 µL serumsuz kültür ortamı ve 60 µL MTT (2.5 mg/mL, PBS içerisinde) eklenmiştir. Örnekler, 37°C'deki inkübatörde 4 saat bekletildikten sonra, gözlerdeki MTT içeren ortam uzaklaştırılarak ve her bir göze DMSO eklenmiş, sonrasında oluşan mor renkli formazan kristallerinin çözünmesi sağlanmıştır. Elde edilen çözeltinin absorbansı 570 nm'de ölçülmüştür.

2.2.3. İlaç Salım Davranışı

Çalışma kapsamında yapılan deneysel çalışmalarda ilaç modeli olarak bir antikanser ilacı olan 5-Fluorourasil (5-FU, Sigma Aldrich) kullanılmıştır. Belirli konsantrasyondaki ilaç solusyonu (0.15 g biyoaktif cam, 1 mg/ 100 ml solusyon) içinde 48 saat, karıştırılarak biyoaktif cam partiküllerin yüzeyine ilaç adsorpsiyonu gerçekleştirilmiştir. Sonrasında ilaç yüklü biyoaktif cam tozları santrifuj (10000 rpm) ile solusyondan ayrılmış ve sedimentler toplanmıştır. Kalibrasyon eğirisi eldesi için stok solusyonlar PBS içinde 0.50 - 25.00 µg/mL olarak hazırlanmış sonrasında absorbans değerleri UV-Vis spektrofotometresi (Thermo-Scientific Evolution 201) kullanılarak 266 nm'de elde edilmiştir. 5-FU yüklenmiş cam partiküller fosfat tampon çözeltisi ortamında bekletilerek ilaç salınım performansı belirlenmiştir. İlaç yükleme çalışmalarına benzer şekilde belirli zaman aralıklarında çözeltiden alınan örneklerin UV-Vis spektrofotometre ile absorbansı ölçülerek solüsyon içerisindeki ilaç konsantrasyonu belirlenmiştir.

3. BULGULAR VE TARTIŞMA

Sentezlenen biyoaktif cam tozlarının yüzeylerinde hidroksiapatit oluşturma davranışı yapay vücut sıvısı (SBF) içinde incelenmiştir. Bu amaçla nadir toprak element iyonları içeren biyoaktif cam tozları 7 ve 28 gün SBF içinde 37 °C'de statik koşullar altında bekletilmiştir. SBF içerisinde 7 gün bekletilen örneklerin FTIR analiz sonuçları ve SEM mikrografları sırası ile Şekil 1 ve Şekil 2'de verilmektedir. Aynı örneklerin SBF ile işlem görmemiş hali Şekil 1 (d)'de yer almaktadır. Örneklerin FTIR spektrumlarında 1100 cm^{-1}'de görülen pik, P=O gerilmesine aittir. 900 cm^{-1}'de oluşan düşük şiddetli yaygın pik CO_3^{2-} oluşumununa işaret etmektedir. Ayrıca, 560 ve 604 cm^{-1}'de görülen çift pik P-O vibrasyon modunda kristal fazda fosfat oluşumunu (ortofosfat) göstermektedir. Bir diğer deyişle spektrumda 560 ve 604 cm^{-1}'de piklerin varlığı biyoaktif camların yüzeyinde kristalin HA oluşumunu kanıtlamaktadır.

7 gün SBF içinde bekletilmiş RE^{3+} içeren biyoaktif cam tozlarına ait SEM mikrograflarında örneklerin tümünün yüzeyinde 2. bir faz maddenin oluşumu gözlenmektedir. Oluşan bu 2. faz madde, hidroksiapatite ait morfoloji ile örtüşmektedir (Şekil 2).

Şekil 3'de verilen FTIR spektrumlarına göre, 28 gün SBF içinde bekleyen örneklerde ise kristal fazda HA oluşumunu işaret eden piklerin şiddeti en yüksek halini almıştır. Bu durum, çalışma kapsamında sentezi yapılan biyoaktif cam tozlarının biyoaktif olduğunu, belirtilen konsantrasyonlarda yapılan Eu^{3+}, Gd^{3+} ve Yb^{3+} katkısının 13-93 biyoaktif cam tozlarının HA oluşturma davranışında olumsuz bir etkiye neden olmadığını göstermektedir.

SaoS-2 hücre hattı ile 3, 7 ve 14 gün yapılan hücre kültürü sonunda hücre canlılığının tespiti için yapılan MTT test sonuçları Şekil 4'de verilmektedir. Ayrıca belirtilen zaman dilimlerinde biyoaktif cam örnek içermeyen hücre kültürlerine (kontrol grubu) ait optik mikroskop görüntüleri de aynı şekilde yer almaktadır. Buna göre, 3 gün sonunda 5%Yb^{3+} içeren biyoaktif cam dışında örneklerin tamamında sitotoksik bir etki gözlenmemiştir. En yüksek konsantrasyonda Yb^{3+} içeren örnekte ise 3 günden itibaren hücre canlılığı %40 seviyelerine düşmüştür. Bu durum, Şekil 5'de verilen hücrelere ait optik mikroskop görüntülerinde de açık bir şekilde görülmektedir. 3 günlük hücre kültürü sonunda, katkısız ve 3% oranında RE^{3+} içeren örneklerin yüzeylerine ait SEM görüntüleri Şekil 6'da verilmektedir. Buna göre, örneklerin yüzeyinde SaOS-2 hücrelerinin varlığı açıkça görülmektedir. 3 günlük kültür sonunda hücrelerin skafoldlar üzerine tutunduğu ve yayılma davranışında olduğu anlaşılmaktadır. Diğer yandan, 7 gün sonunda sadece %1 ve %3 Gd^{3+} içeren örneklerin osteosarkom hücreleri üzerinde sitotoksik bir etkiye neden olmadığı anlaşılmaktadır. 14 gün sonunda ise hücre canlılığında dramatik düşüşler olduğu gözlenmiştir ve tüm örneklerde benzer sonuçlar alınmıştır. Artan Gd^{3+} konsantrasyonu ile de hücre canlılığında düşüş gözlenmiştir.

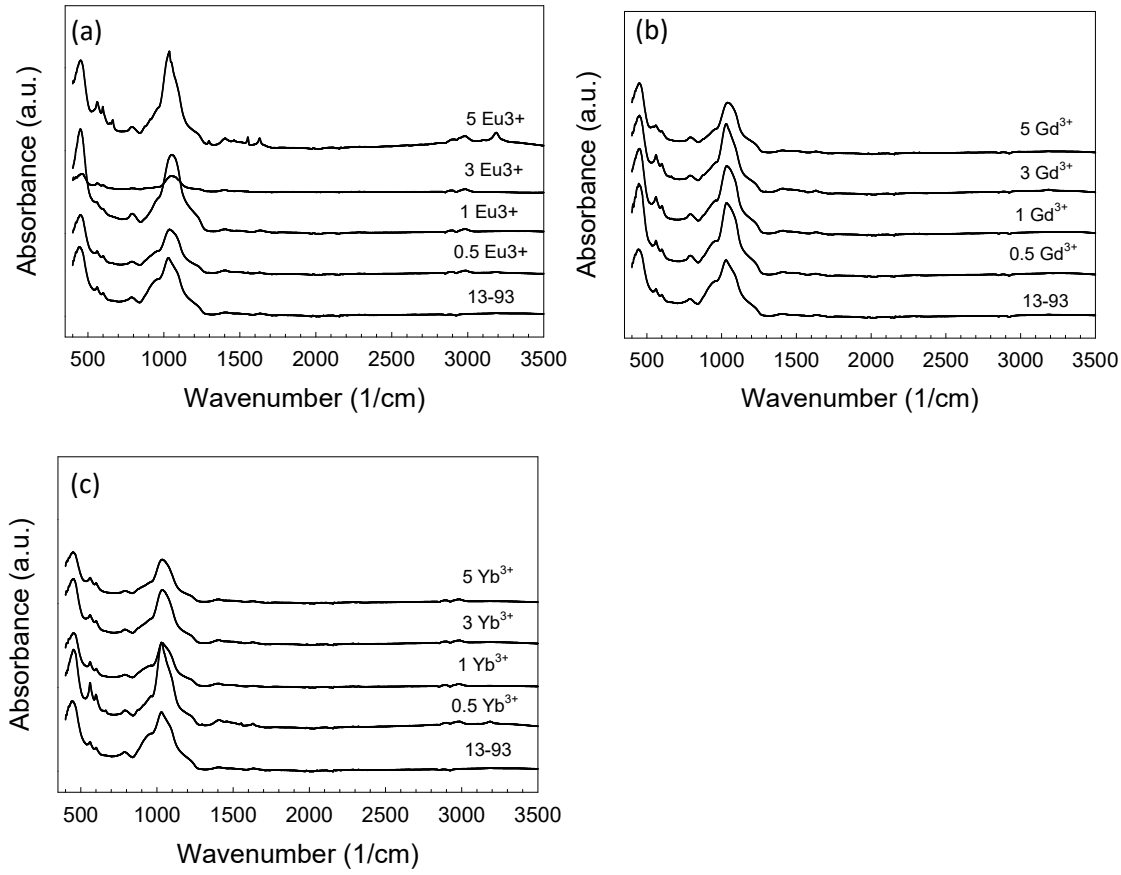

Şekil 1. (a) Eu^{3+}, (b) Gd^{3+}, ve (c) Yb^{3+} içeren biyoaktif cam tozlarının 7 gün SBF içinde bekletildikten sonraki FTIR spektrumları.

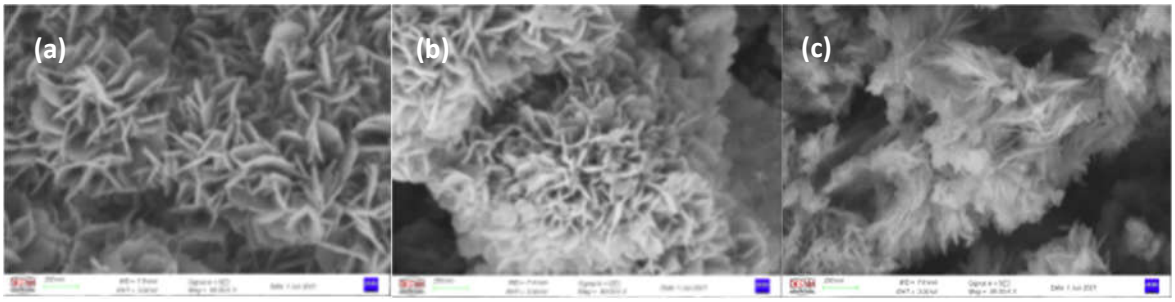

Şekil 2. SBF içinde 7 gün bekletilen (a) 5%Eu^{3+},(b) 5%Gd^{3+},(c) 5% Yb^{3+} içeren biyoaktif cam tozlarının SEM mikrografları.

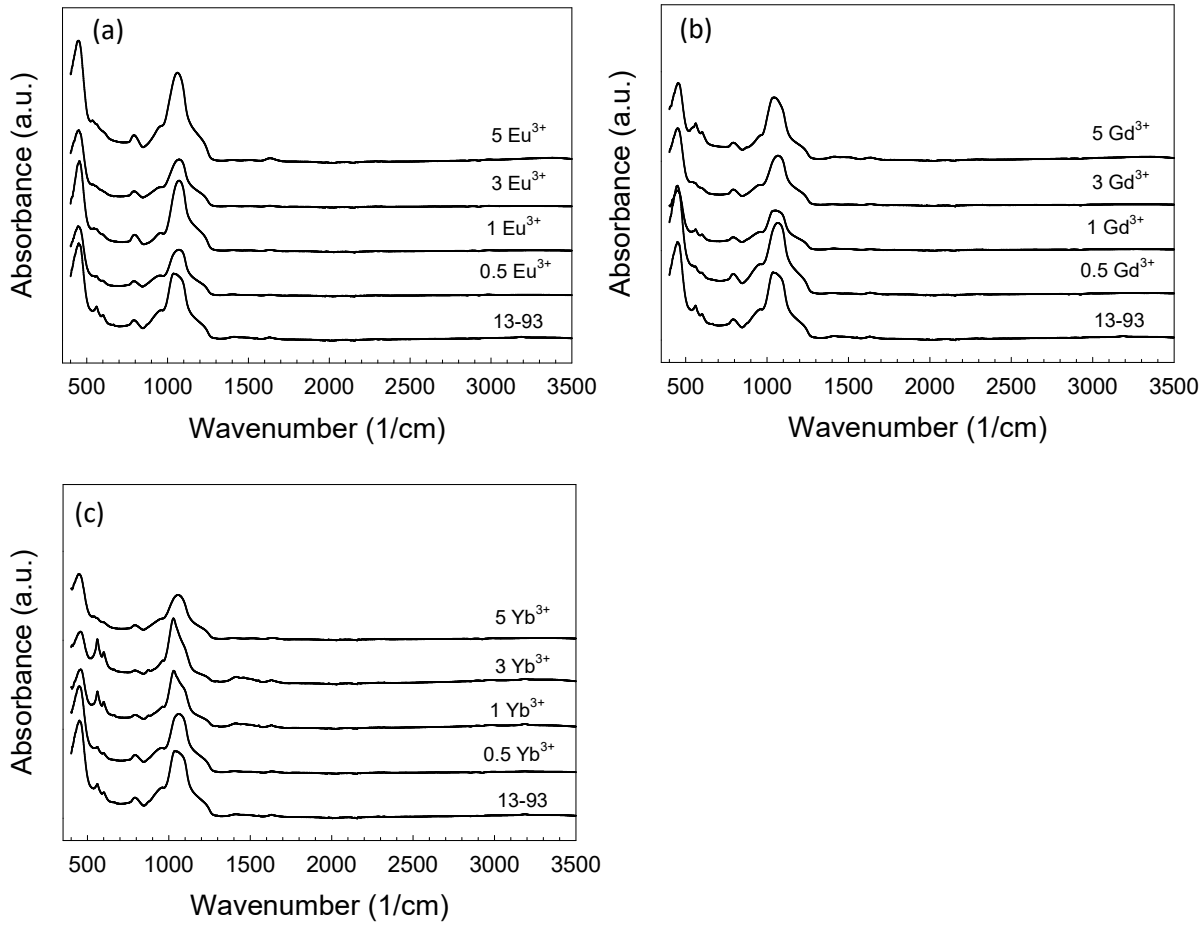

Şekil 3. (a) Eu^{3+}, (b) Gd^{3+}, ve (c) Yb^{3+} içeren biyoaktif cam tozlarının 28 gün SBF içinde bekletildikten sonraki FTIR spektrumları.

Benzer şekilde, osteoblastik MC3T3-E1 hücreleri ile yapılan 3, 7 ve 14 günlük hücre kültürüne ait MTT test sonuçları Şekil 7'de gösterilmektedir. Buna göre, 3 günlük kültür sonunda %3 konsantrasyona dek Yb^{3+} ilavesi veya %5'e dek Gd^{3+} ilavesi hücreler üzerinde herhangi bir sitotoksik etkiye neden olmamıştır. 7 günlük kültür süresi sonunda %5 Gd^{3+} içeren örneklerde hücre canlılığı oranının yaklaşık %80 seviyesinde olduğu görülmektedir. Ancak 14 gün sonunda tüm biyoaktif cam örneklerin hücre canlılığında önemli azalmalar olduğu görülmektedir. Bu durumun çalışılan biyoaktif cam örneklerin MC3T3-E1 hücrelerine karşı hızlı bir sitotoksik etki göstermesinden çok, 14 günlük kültür çalışmalarında hücre büyüme ortamının pH değişimine bağlı olarak ortaya çıkmış olabileceği düşünülmektedir.

Çalışma kapsamında ilaç salımı deneylerinde bir antikanser ilaci olan 5-FU kullanılmıştır. Şekil 8'de ilaç salım çalışmaları kapsamında hazırlanan 5-FU kalibrasyon eğrisi gösterilmektedir. İlaç solüsyonları PBS içerisinde ve karanlık ortamda hazırlanmıştır. R^2 değeri 0.99 olarak elde edildiğinden ilgili grafik, solüsyon içindeki ilaç konsantrasyonunun hesaplanmasında yüksek bir doğruluk oranı ile kullanılmıştır. 48 saat 5-FU solüsyonu içerisinde karıştırılarak bekletilen biyoaktif cam tozu örneklerine ait ilaç adsorpsiyon yüzdelerinin yaklaşık 28%-36% arasında olduğu anlaşılmıştır. Eu^{3+}, Gd^{3+} ve Yb^{3+} içeren biyoaktif cam tozlarına ait PBS içinde ilaç salım grafikleri Şekil 8'de verilmektedir. Buna göre, ilk 24 saat sonunda kümülatif ilaç salım yüzdesinin Eu^{3+}, Gd^{3+} ve Yb^{3+} katkılı örneklerde sırası ile ortalama %26, %25 ve %27 seviyesinde olduğu görülmüştür. 600 saat sonunda aynı grup örneklerden toplam ilaç salımının sırasıyla ortalama ~%55, %53, %65 mertebesinde olduğu anlaşılmıştır.

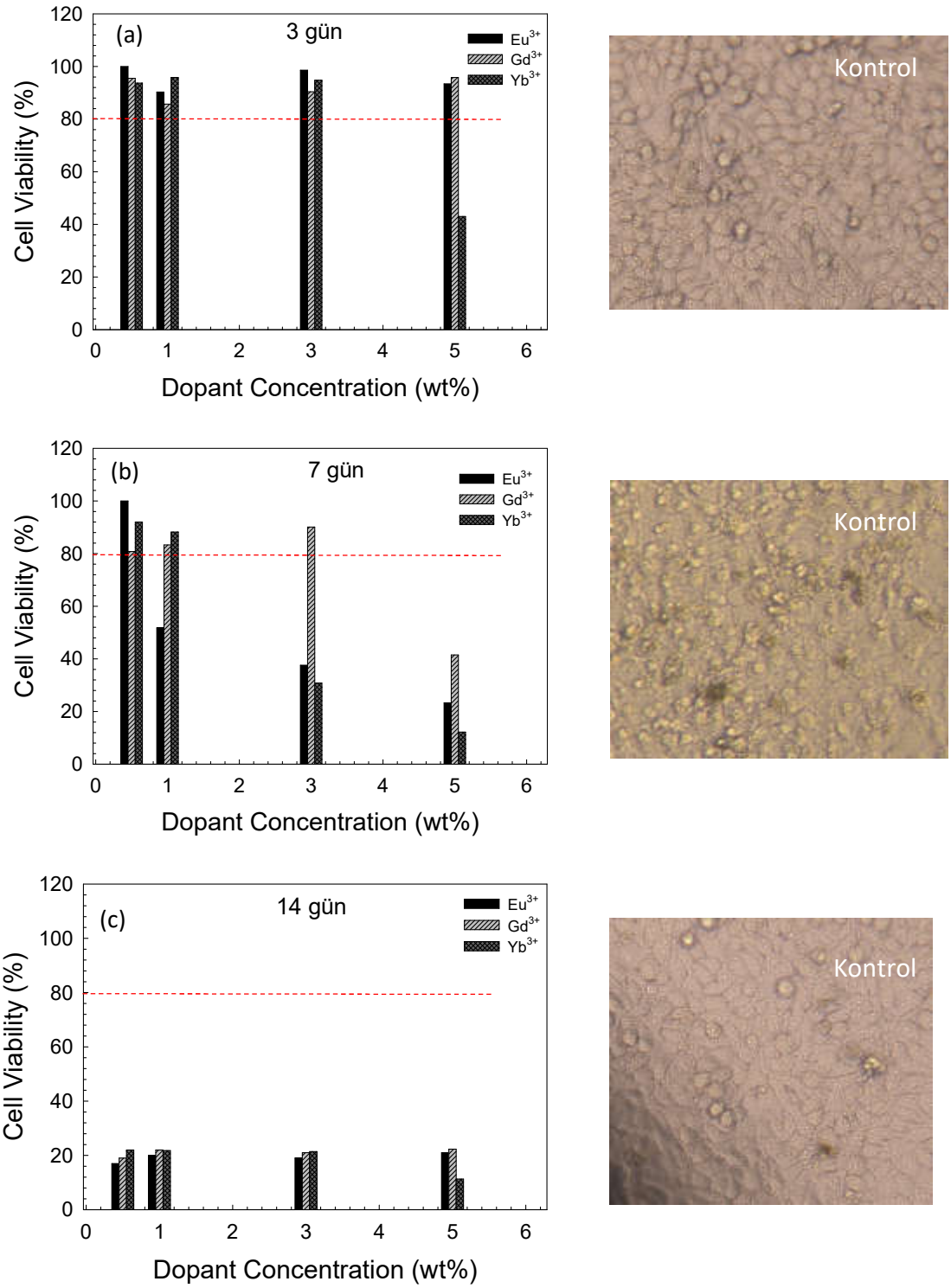

Şekil 4. Osteosarkom SaOS-2 hücre hattı kullanılarak (a) 3 gün, (b) 7 gün ve (c) 14 günlük hücre kültürü sonunda MTT test ile elde edilen hücre canlılığı grafikleri. Optik mikroskop görüntüleri, ilgili zaman dilimindeki kontrol grubu hücrelerin morfolojisini göstermektedir.

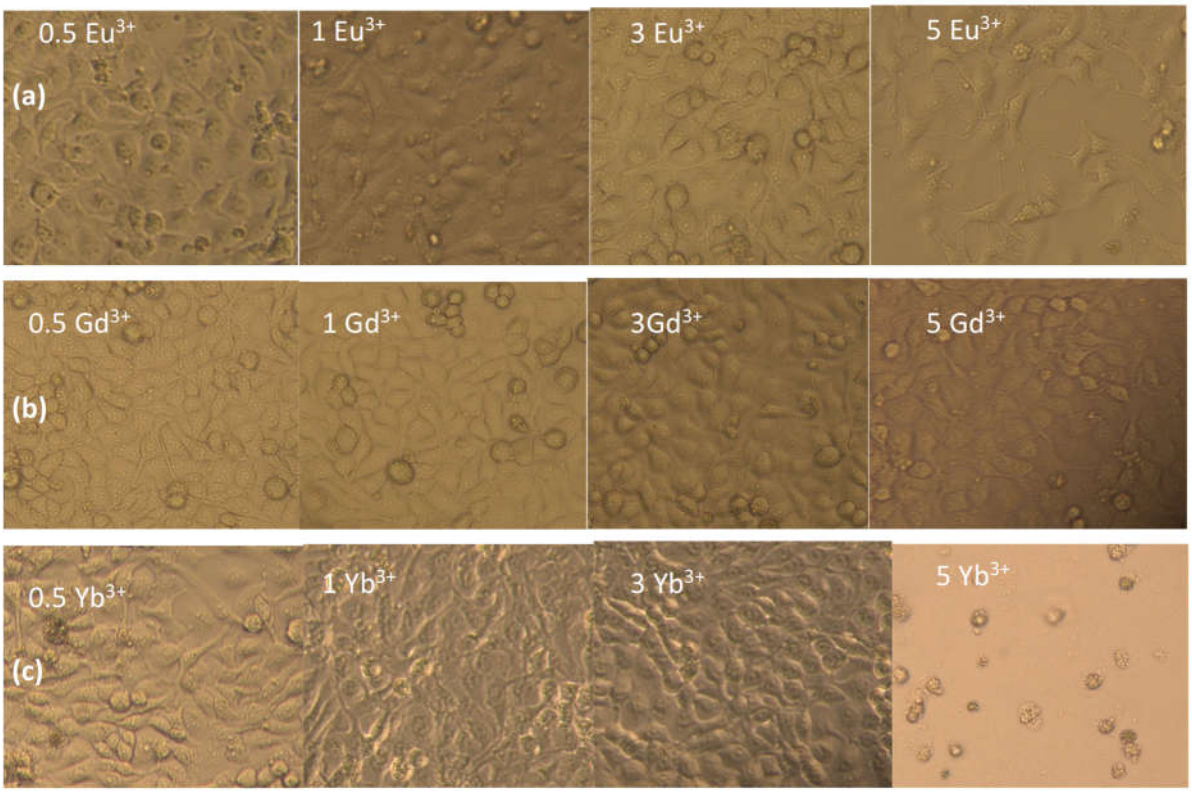

Şekil 5. Osteosarkom SaOS-2 hücre hattı (a) Eu^{3+}, (b) Gd^{3+} ve (c) Yb^{3+} içeren biyoaktif cam skafoldlar kullanılarak yapılan 3 günlük hücre kültürü (3D) sonunda hücre kültür kaplarında bulunan hücrelerin optik mikroskop görüntüleri (Büyütme 100x).

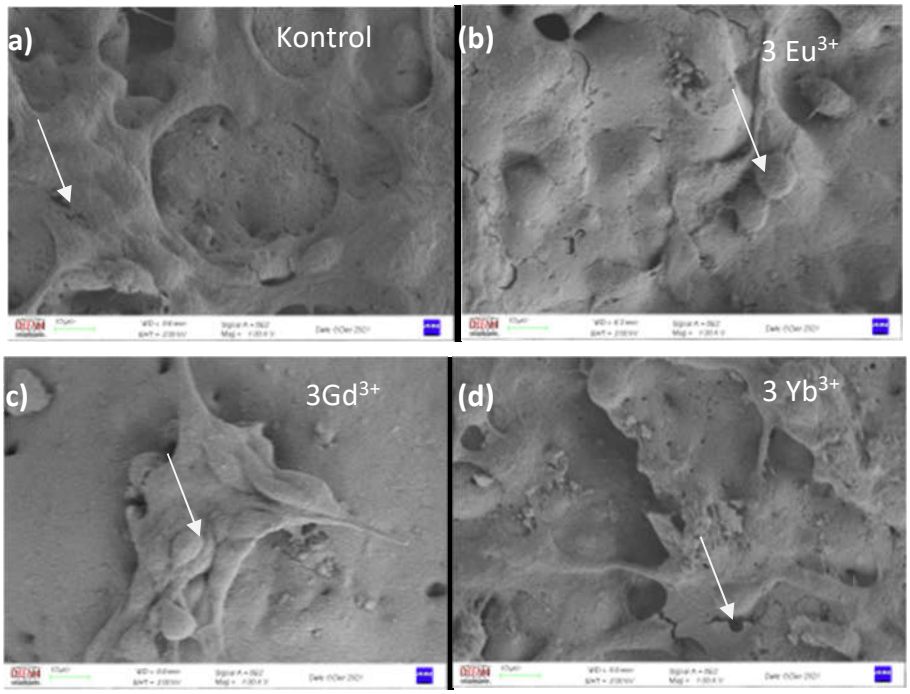

Şekil 6. Osteosarkom SaOS-2 hücre hattı kullanılarak yapılan 3 günlük hücre kültürü (3D) sonunda skafoldların yüzeyinde bulunan hücrelerin SEM görüntüleri (a) katkısız, (b) $3Eu^{3+}$, (c) $3Gd^{3+}$, (d) 3 Yb^{3+} içeren biyoaktif cam skafoldlar.

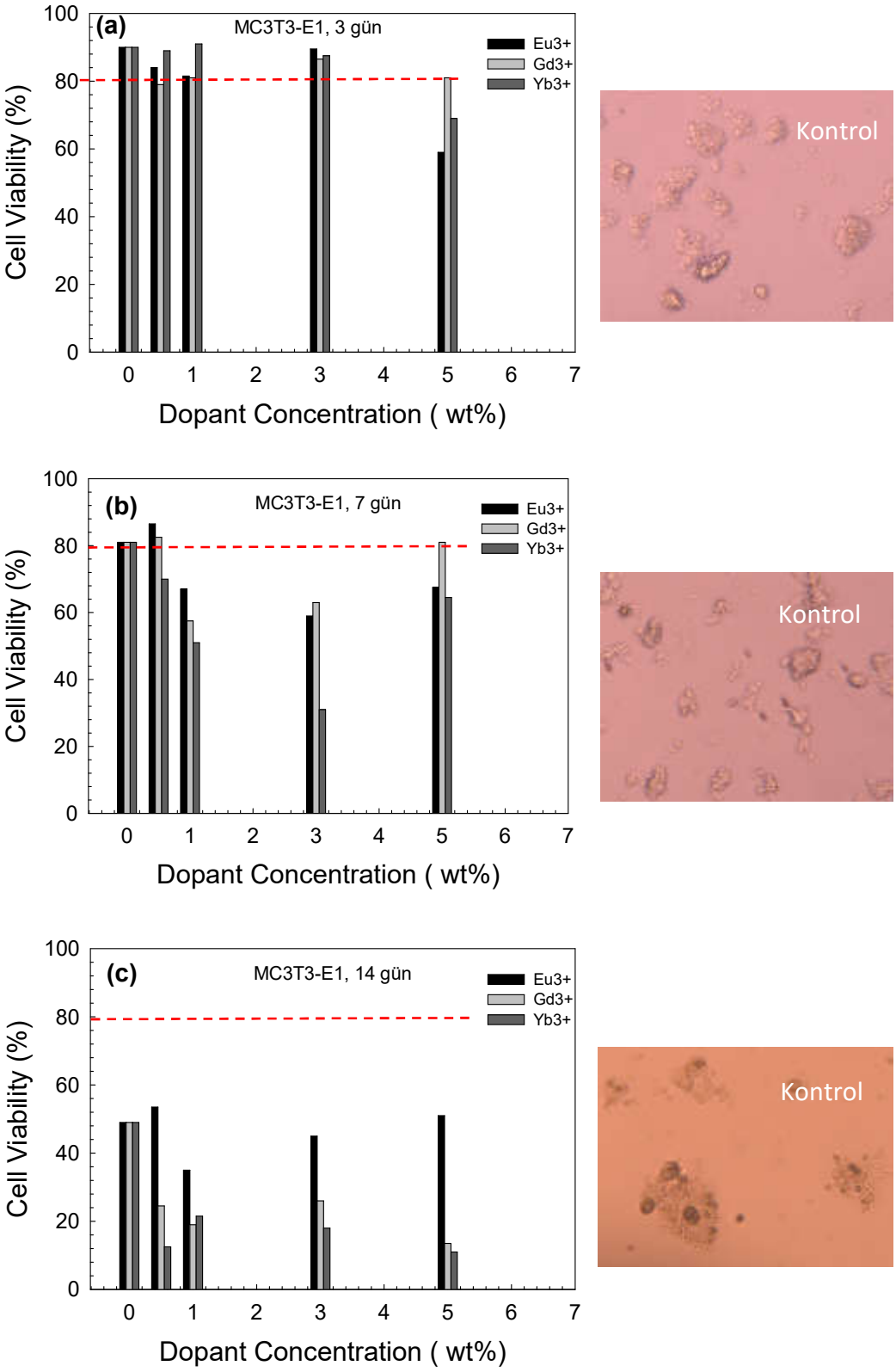

Şekil 7. Sol-jel ile hazırlanan biyoaktif cam skafoldlar ve osteoblastik MC3T3-E1 hücre hattı kullanılarak (a) 3, (b) 7 ve (c) 14 günlük hücre kültürü sonunda MTT test ile elde edilen hücre canlılığı grafikleri. Optik mikroskop görüntüleri, ilgili zaman dilimindeki kontrol grubu hücrelerin morfolojisini göstermektedir.

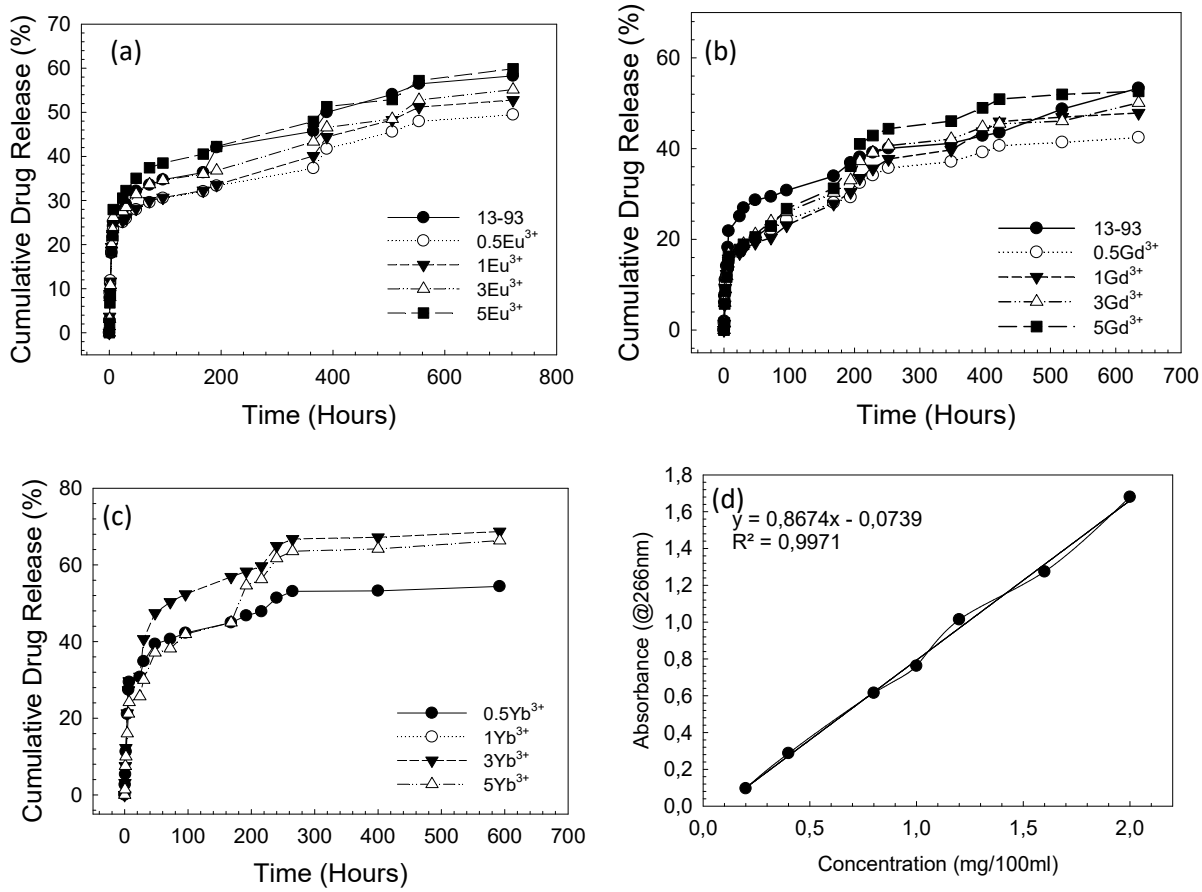

Şekil 8. Sol-jel yöntemi ile sentezlenmiş (a) Eu^{3+}, (b) Gd^{3+} ve (c) Yb^{3+} içeren biyoaktif cam tozlarının ilaç salım grafikleri (d) 5-FU kalibrasyon eğrisi.

4. SONUÇLAR

Bu çalışmada sol-jel yöntemi ile sentezlenmiş Eu^{3+}, Gd^{3+}, Yb^{3+} içeren biyoaktif cam tozlarının biyoaktiviteleri, in vitro sitotoksisiteleri ve antikanser ilaç salım davranışları incelenmiştir. Bu amaçla, nadir toprak elementi (RE^{3+}) katkılı silika bazlı 13-93 biyoaktif cam tozlarının SBF içerisinde HA oluşturma davranışı incelenmiş, in vitro sitotoksisiteleri pre-osteoblastik MC3T3-E1 ve osteosarkom SaOS-2 hücre hatları kullanılarak MTT yöntemi ile araştırılmıştır. Biyoaktif cam tozlarından PBS ortamına 5-FU salım davranışı pH 7.4'de test edilmiştir. Sonuçlar, RE^{3+} katkısının biyoaktif cam tozlarının in vitro biyoaktivitesi üzerinde olumsuz bir etkiye neden olmadığını göstermiştir. Diğer yandan 3 günlük hücre kültürü sonunda 5%Yb^{3+} içeren biyoaktif camlar dışındaki örneklerin tamamında SaOS-2 hücrelerine karşı herhangi bir sitotoksik etki gözlenmemiştir. 14 gün sonunda ise çalışma kapsamındaki tüm RE^{3+} katkılı biyoaktif cam örneklerin SaOS-2 hücreleri üzerinde toksik etkiye sahip olduğu anlaşılmıştır. Diğer yandan, MC3T3-E1 hücre hattı ile yapılan 3 günlük kültür çalışmaları sonucunda en yüksek RE^{3+} konsantrasyonuna sahip biyoaktif camların hücre canlılığında azalmaya neden olduğu anlaşılmıştır. İlaç salım çalışmalarının sonuçları 600 saat sonunda biyoaktif cam tozlarından gerçekleşen kümülatif 5-FU salım miktarının RE^{3+} katkı çeşidi ve konsantrasyonuna bağlı olarak %42-69 seviyesinde olduğunu göstermiştir.

TEŞEKKÜR

Bu çalışma 219M212 nolu TÜBİTAK projesi ve 2020-067 nolu BAP projesi kapsamında desteklenmiştir.

KAYNAKLAR

1. Hench, L.L. 1998. Bioceramics. Journal of the American Ceramic Society, 81, 1705-1728.
2. Brink, M., Turunen, T., Happonen, R., Yli-Urppo. 1997. A. Compositional Dependence of Bioactivity of Glasses in the System Na_2O-K_2O-MgO-CaO-B_2O_3-P_2O_5-SiO_2. Journal of Materials Science: Materials in Medicine, 37,114–21.
3. Rahaman M.N., Day D.E., Bal B.S., Fu Q., Jung S., B., Bonewald L.F. 2011. Biactive glass in tissue engineering. Acta Biomaterialia, 7(6), 2355-2373.
4. Kaya, A., 2016. Nadir Toprak İyonları ile Katkılandırılmış Çinko Oksit Tellürit (TeO2-ZnO) Camlarda Beyaz Işık Üretimi ve Karakterizasyonu, Yüksek Lisans Tezi, İstanbul Teknik Üniversitesi.
5. Fan, Y., Huang, S., Jiang, J., Li, G., Yang, P., Lian, H., Cheng, Z., Lin, J. 2011. Luminescent, mesoporous, and bioactive europium-doped calcium silicate (MCS: Eu3+) as a drug carrier. Journal of Colloid and Interface Science, 357, 280–285.
6. Zhang,Y., Hu, M., Wang,X., Zhou,Z., Liu,Y. 2018. Design and Evaluation of Europium Containing Mesoporous Bioactive Glass Nanospheres: Doxorubicin Release Kinetics and Inhibitory Effect on Osteosarcoma MG 63 Cells. Nanomaterials (Basel), 8(11): 961.
7. Li Q., Xing M., Chang L., Ma L., Chen Z.,Qiu J., Yu J., Chang J. 2019. Upconversion luminescence Ca–Mg–Si bioactive glasses synthesized using the containerless processing technique. Frontiers in Materials Science, 13, 399–409.
8. Ignjatović N.L., Mančić L., Vuković M., Stojanović Z., Nikolić M.G., Škapin S., Jovanović S., Veselinović L., Uskoković V., Lazić S., Marković S., Lazarević M.M., Uskoković D.P. 2019. Rare-earth (Gd^{3+},Yb^{3+}/Tm^{3+},Eu^{3+}) co-doped hydroxyapatite as magnetic, up-conversion and down-conversion materials for multimodal imaging. Nature Scientific Reports, 9, 16305.
9. Thompson, C.C. 2011. Gadolinium: compounds, production and applications. New York: Nova Science Pub Inc.,
10. Borges, R., Schneider, J.F., Marchi, J. 2019. Structural characterization of bioactive glasses containing rare earth elements (Gd and/or Yb). Journal of Materials Science, 54(17), 11390–11399.
11. Deliormanlı, A.M. Oğuzlar, S., Zeyrek Ongun, M. 2022. Effects of Eu^{3+}, Gd^{3+} and Yb^{3+} substitution on the structural, luminescence and decay properties of silicate-based bioactive glass powders. Journal of Materials Research, 37, 622–635.
12. Kokubo,T., Takadama, H. 2006. How useful is SBF in predicting in vivo bone bioactivity?. Biomaterials, 27,15,2907-2915, https://doi.org/10.1016/j.biomaterials.2006.01.017.

EISA YÖNTEMİ İLE GADOLİNYUM (III) VE İTERBİYUM (III) İÇEREN MEZOGÖZENEKLİ, 13-93 BİYOAKTİF CAM TOZLARININ HAZIRLANMASI, YAPISAL ÖZELLİKLERİNİN VE İN VİTRO BİYOAKTİVİTESİNİN İNCELENMESİ

Begüm RAHMAN[1]

[1]Manisa Celal Bayar Üniversitesi, Mühendislik Fakültesi, Metalurji ve Malzeme Mühendisliği, Manisa, Türkiye.

[1]ORCID ID: https://orcid.org/0000-0003-3600-1155

Aylin M. DELİORMANLI [2]

[2]Manisa Celal Bayar Üniversitesi, Mühendislik Fakültesi, Metalurji ve Malzeme Mühendisliği, Manisa, Türkiye.

[2]ORCID ID: https://orcid.org/0000- 0001-7877-7635

ÖZET

Evaporasyon ile indüklenmiş kendiliğinden birleşme (EISA), mezogözenekli, desenli ince filmlerin ve tozların sentezinde kullanılan etkili bir yöntemdir. EISA sentez yöntemi; sentez çözeltisinin hazırlanması, hidroliz, kurutma ve kalsinasyon olmak üzere dört basamaktan oluşur. Bu çalışmada, gadolinyum (Gd^{3+}) ve iterbiyum (Yb^{3+}) içeren 13-93 biyoaktif cam tozlarının, noniyonik surfaktan Pluronik F-127 varlığında EISA tekniği ile sentezi ve karakterizasyonu gerçekleştirilmiştir. Sentezlenen biyoaktif cam tozlarının yapısal ve morfolojik özellikleri FTIR spektrometre kullanılarak incelenmiş, ayrıca tozların tane boyutu, BET toplam yüzey alanı ve gözenek çapları ölçülmüştür. Biyoaktif cam tozlarının yüzeylerinde hidroksiapatit oluşturma yeteneği yapay vücut sıvısı içerisinde zamanın fonksiyonu olarak test edilmiştir. Sonuçlar, EISA ile sentez çalışmaları sırasında kullanılan triblok-kopolimer Pluronik F127 miktarının ve sonrasında polimerin yapıdan uzaklaştırma yönteminin hazırlanan biyoaktif cam tozlarının toplam yüzey alanı ve gözenekliliğini doğrudan etkilediğini göstermiştir. Buna göre, 1 g F-127 kullanılarak EISA yöntemi ile hazırlanan ve asit içerisinde bekletilerek işlem gören katkısız 13-93 biyoaktif cam tozlarının Single Point, BET ve Langmuir yüzey alanları sırasıyla 369, 372 ve 531.8 m^2/g olarak ölçülmüştür. Aynı şekilde hazırlanan 13-93 cam tozlarının ortalama gözenek çapı 24.03 Å olarak elde edilmiştir. Yapay vücut sıvısı içerisinde 7 ve 28 gün bekletilen katkısız ve Gd^{3+} ya da Yb^{3+} katkılı biyoaktif cam tozlarının in vitro biyoaktivitesinde bir azalma olmadığı ve yüzeylerinde HA oluşumu gerçekleştiği anlaşılmıştır. Çalışma kapsamında sentezi yapılan mezogözenekli biyoaktif cam tozlarının özellikle ilaç salım uygulamalarında kullanılabileceği sonucuna varılmıştır.

Anahtar Kelimeler: Biyoaktif cam, EISA, gadolinyum, iterbiyum.

ABSTRACT

Evaporation-induced self-assembly (EISA) is an effective technique used in the synthesis of mesoporous and patterned thin films and powders. EISA synthesis method consists of four main steps; the preparation of the synthesis solution: hydrolysis, drying and calcination. In this study, synthesis and characterization of 13-93 bioactive glass powders containing gadolinium (Gd^{3+}) and ytterbium (Yb^{3+}) were carried out by EISA technique in the presence of non-ionic surfactant Pluronic F-127. The structural and morphological properties of the synthesized bioactive glass powders were examined using FTIR spectrometry, and the particle size, BET total surface area and pore diameters of the powders were also measured. The ability to form hydroxyapatite on the surfaces of bioactive glass powders was tested as a function of time in simulated body fluid. The results showed that the amount of triblock-copolymer Pluronic F-127 used during the

synthesis with EISA and subsequently the method of removing the polymer from the structure directly affect the total surface area and porosity of the prepared bioactive glass powders. Accordingly, Single Point, BET and Langmuir surface areas of bare 13-93 bioactive glass powders prepared by EISA method using 1 g of F-127 and treated by soaking in acid were measured as 369, 372 and 531.8 m^2/g, respectively. The mean pore diameter of 13-93 glass powders prepared in this technique was recorded as 24.03 Å. Results also revealed that that there was no decrease in the in vitro bioactivity of bare and Gd^{3+} or Yb^{3+} doped bioactive glass powders, which were kept in simulated body fluid for 7 and 28 days, and HA deposition occurred on their surfaces. It was concluded that mesoporous bioactive glass powders synthesized within the scope of the study could be utilized specifily in drug delivery applications.

Keywords: Bioactive glass, EISA, gadolinium, ytterbium.

1. GİRİŞ

Biyoaktif camlar ilk olarak Hench ve arkadaşları tarafından [1,2] 1969 yılında 45S5 kodu ile ($45SiO_2$, $24.5CaO$, $24.5Na_2O$ ve $6P_2O_5$ ağırlık%) üretilmiştir. Sentetik hidroksiapatite göre hem osteokontüktif hem de osteoindüktif olmaları nedeni ile üstün özellikler gösteren malzemelerdir. Bu özelllikleri nedeniyle doku mühendisliği ve dental uygulamalarda ayrıca kanser tedavisinde (radyoaktif madde yüklü olarak) kullanılırlar. Ek olarak, biyomedikal görüntüleme uygulamalarında nadir toprak elementleri ile lüminesans özellik kazandırılmış biyoaktif camların kullanımına ilişkin çalışmalar mevcuttur [3,4].

13-93 kodlu biyoaktif camı da 45S5 gibi silika bazlı olup kalsiyum, fosfat, sodyum, magnezyum ve potasyum içeren ($6Na_2O$, $12K_2O$, $5MgO$, $20CaO$, $4P_2O_5$, $53SiO_2$; wt %) ve FDA tarafından onaylı bir cam kompozisyondur [5]. 13-93 biyoaktif cam tozlarının daha önce ergitme ve sol-jel yöntemi ile sentezi üzerine yayınlanmış çalışmalar mevcuttur [5-8].

Diğer yandan, EISA (Evaporation Induced Self Assembly, evaporasyonla indüklenmiş kendiğinden birleşme) mezogözenekli malzemelerin sentezinde kullanılan sol-jel prosesi ve surfaktanların birlikte kullanımını içeren bir yöntemdir [9]. Yöntem ilk kez mezo-yapılandırılmış silika ince filmlerin hazırlanması için tasarlanmıştır [9,10]. Son yıllarda, sol-jel kimyasının yüzey aktif maddelerle birleştirilmesiyle EISA yöntemi ile çok sayıda mezoyapılı malzeme hazırlanmıştır [10-12]. Mezogözenekli ince filmlerin oluşumunda, EISA yöntemi kapsamında yüzey aktif madde, çözünür metal alkoksit veya metal tuzu, alkol (tipik olarak etanol), su ve sıklıkla asitten (genellikle HCl) oluşan homojen bir çözelti karıştırılır. Bu solüsyondaki yüzey aktif maddenin başlangıç konsantrasyonu kritik misel konsantrasyonundan (CMC) çok daha düşüktür. Çözelti, bir substrat üzerine dökülür ve uçucu bileşenlerin (özellikle alkol, HCl ve su) buharlaşması hava ve film arasındaki arayüzeyde gerçekleşir. İlk aşamalarda (10-30 s), alkolün buharlaşması nedeniyle, metal oksit oligomerlerinin ve uçucu olmayan yüzey aktif maddenin konsantrasyonu artar. Yüzey aktif madde konsantrasyonundaki bu artış, organik-inorganik hibritin kendi kendine birleşmesini bir sıvı kristal fazı oluşmasını sağlar [13].

Literatürde EISA yöntemi ile 13-93 biyoaktif cam sentezi üzerine yayınlanmış bir çalışma bulunmamaktadır. Diğer yandan iterbiyum (Yb^{3+}) ya da gadolinyum (Gd^{3+}) katkısının 13-93 biyoaktif camlara görünür ışık bölgesinde lüminesans özellik kazandırdığı raporlanmıştır [14]. Belirtilen iyonları içeren hidroksiapatitlerde biyolojik özelliklerin ayrıca biyoaktivite ve yeni kemik oluşumunun gelişmiş olması gözönünde tutularak, belirtilen iyonların katkısının mezogözenekli biyoaktif camların SBF içindeki in vitro HA oluşturma yeteneğini arttıracağı düşünülmüştür. Bu şekilde özellik kazanan biyoaktif camların vücut içi resorpsiyon/degradasyonunun biyomedikal görüntüleme cihazları kullanılarak takip edilmesi ve ilaç yüklenen biyoaktif camlardan gerçekleşen vücut içi ilaç salım miktarının tespit edilmesi mümkün olacaktır. Bu amaçla, çalışma kapsamında iterbiyum (Yb^{3+}) ve gadolinyum (Gd^{3+}) katkılı mezogözenekli toz formunda 13-93 biyoaktif camlar EISA yöntemiyle sentezlenerek ilgili karakterizasyonlar yapılmıştır.

2. DENEYSEL ÇALIŞMALAR

2.1.Malzemeler

Katkısız, Yb^{3+} ve Gd^{3+} katkılı silika bazlı 13-93 biyoaktif cam ($6Na_2O$, $12K_2O$, $5MgO$, $20CaO$, $4P_2O_5$, $53SiO_2$; ağırlıkça %) toz sentezi için kullanılan kimyasallar: tetraetil ortosilikat (TEOS), kalsiyum nitrat tetrahidrat ($Ca(NO_3)_2.4\ H_2O$, magnezyum nitrat hegzahidrat ($Mg(NO_3)_2.6H_2O$), sodyum nitrat, $NaNO_3$, Potasyum nitrat, KNO_3, trietilfosfat (TEP), gadolinyum (III) nitrat pentahidrat, iterbiyum (III) nitrat pentahidrat ve nitrik asittir. EISA yöntemi ile sentez çalışmalarında kullanılan non-iyonik triblok kopolimer (PEO-PPO-PEO) Pluronik F-127 (Mw: 12600) Sigma Aldrich'den temin edilmiştir.

2.2. EISA Yöntemi ile Biyoaktif Cam Sentezi

Çalışmada EISA yöntemi ile mezogözenekli biyoaktif cam tozu sentezi için her birinde 14.30 ml deiyonize su ile 14.30 ml EtOH bulunan cam şişelerde farklı konsantrasyonlarda (0.125, 0.25, 0,5 ve 1 gr) Pluronic F-127 tri blok-kopolimer çözdürülerek 13-93 biyoaktif cam solüsyonları hazırlanmıştır. İşlemlere belirtilen solüsyonlara 0.1005 ml HNO_3 eklenerek devam edilmiş ardından 9.92 ml TEOS eklenerek ve oda sıcaklığında 1 saat karıştırmaya bırakılmıştır. Solusyon berrak hale geldiğinde sırası ile 0.475 ml TEP, 0.835 gr sodyum nitrat, 4.135 gr kalsiyum nitrat, 1.579 gr magnezyum nitrat ve 1.308 gr potasyum nitrat solusyona birer saat ara ile ilave edilmiştir. Deneysel çalışmalar sırasında başlangıç kimyasallarının, etanol ve su içerisindeki çözünme hızlarının farklı olduğu gözlemlenmiştir. Hazırlanan, içeriğinde 0.125, 0.25, 0,5 ve 1 gr F-127 kopolimeri olan, solüsyonlar yaklaşık 15 saat manyetik karıştırıcı yardımcı ile karıştırılarak homojen hale getirilmiştir. Homojenliğinden emin olunan karışım petri kabı içerisine boşaltılarak çeker ocak altında önce jelleşme ve yaşlandırma için ağzı kapalı olarak sonrasında evaporasyon için üzeri açık durumda 24 saat bekletilmiştir (Şekil 1).

Şekil 1. EISA yöntemi ile 13-93 bazlı biyoaktif cam sentezi sırasında çekilen fotoğraflar (a) başlangıç durumunda (b) etüvde 60 °C'de kurutma işlemi uygulandıktan sonra.

Diğer bir grup örnek, kurutma işlemi sonrasında yapıdaki F-127'yi hızlı bir şekilde uzaklaştırmak için 1 gr örnek/100 ml asit oranına göre derişik sülfürik asit solüsyonu içerisinde 1 saat bekletilmiş sonrasında deiyonize su ile defalarca (20-25 kez) yıkanarak pH değerinin yaklaşık 7 olması sağlanmıştır. Isıl işlemle polimerin sistemden düzgün bir şekilde uzaklaşması için örnekler önce 250 °C'de 4 saat bekletilmiş sonrasında 625 °C'de 4 saat tutulmuştur. Tane boyut küçültme işlemi için yüksek hızlı planeter değirmen (Fritch, Pulverisette, Premium Line 7) kullanılarak örnekler öğütülmüştür.

2.3. Karakterizasyonlar

Yapısal karakterizasyonlar, FTIR cihazı (Thermo-Scientific, Nicolet IS 20) ile ATR ataçmanı kullanılarak gerçekleştirilmiştir. Ayrıca sentezlenen tozların tane boyutları tane boyutu ölçüm cihazı (Malvern, Mastersizer 3000, UK) ile ölçülmüştür. Yüzey alanı ve gözenek boyutu ölçümleri, yüzey alanı (BET) ölçüm cihazı (Micromeritics marka Gemini VII 2390t model) kullanılarak yapılmıştır. Cihaz ile -196 °C'deki sıvı

azot ortamında azot gazı adsorpsiyonu tekniğine dayalı olarak katıların m^2/g olarak yüzey alanları, gözenek çapı ve dağılımını ölçülebilmektedir.

In vitro biyoaktivite deneyleri yapay vücut sıvısı (SBF) içinde gerçekleştirilmiştir. Sentezlenen malzemeler, pH'sı 7.4 olan SBF içirisine konularak (1 gr örnek için 500 ml SBF olacak şekilde) inkübatörde 37 °C' de 7 ve 28 gün bekletilmiştir. Daha sonra SBF'den çıkarılan örnekler önce etanol ile yıkanmış sonrasında 100 °C'de etüvde 24 saat kurutulmuştur. SBF'den çıkarılan yapıların yüzeyinde hidroksiapatit (HA) oluşumu FTIR spektroskopisi kullanılarak incelenmiştir.

3. BULGULAR VE TARTIŞMA

Farklı miktarlarda F-127 kullanılarak EISA yöntemi ile hazırlanan 13-93 biyoaktif cam tozlarının yapısal özelliklerinin incelenebilmesi için FTIR analizi yapılmıştır. EISA yöntemi ile sentezlenen biyoaktif cam tozlarının kalsinasyon sonrasındaki FTIR spektrumları Şekil 2 ve Şekil 3'de verilmektedir. 625 °C'de yapılan kalsinasyon işleminin yapıdaki F-127'nin uzaklaştırma için yeterli olduğu anlaşılmaktadır. Saf F-127, 2889 cm^{-1} (C–H gerilme titreşimi), 1342 cm^{-1} (O–H eğilme), ve 1111 cm^{-1} (C–O–C gerilme titreşimleri) bandlarını içermektedir [15]. 625 °C'deki ısıl işlem öncesinde örneklerin 250 °C'de 4 saat bekletilmesinin polimerin yapıdan uzaklaştırılmasında etkili olduğu görülmektedir.

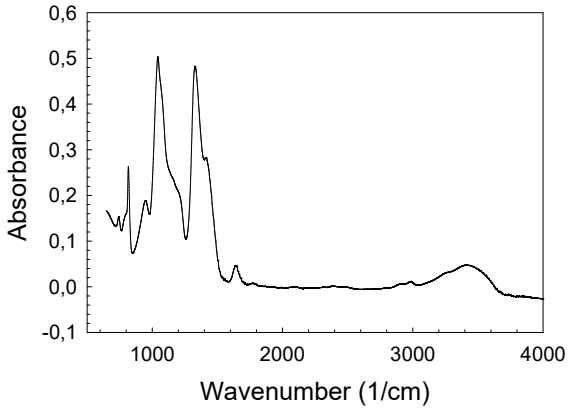

Şekil 2. EISA (0.250 g F127) ile hazırlanan 13-93 biyoaktif cam kserojellerin 120 °C'deki kurutma sonrası FTIR spektrumu.

Spektrumda 1380 cm^{-1} civarında görülen pik NO_3 simetrik gerilmesine aittir. Bu durum, başlangıç malzemelerinden gelen nitratların yapıdan tamamen uzaklaşmadığını göstermektedir. Benzer şekilde 1 g F-127 kullanılarak EISA yöntemi ile sentezlenmiş Gd^{3+} veya Yb^{3+} içeren biyoaktif cam tozlarının FTIR spektrumları Şekil 4'de ve asit içerisinde bekletilerek hazırlanan biyoaktif cam tozlarının kalsinasyon sonrasındaki FTIR spektrumları Şekil 5'de verilmektedir. Asit ile işlem görmemiş Gd^{3+} ve Yb^{3+} katkılı cam örneklerin IR spektrumunda bir farklılık gözlenmezken asit içerisinde bekletilen örneklerin spektrumunda ~580 cm^{-1}, 680 cm^{-1} ve 1090 cm^{-1}'de sülfürik asite ait kimyasal grupların (O=S=O, C-S-C) var olduğu anlaşılmaktadır.

EISA yöntemi kullanılarak hazırlanan biyoaktif cam tozlarının tane boyutu ölçüm sonuçlarına bakıldığında (Şekil 6), sentezlenen tozların medyan tane boyutunun ~3-10 μm aralığında olduğu ve tozların bi-modal tane boyutu dağılımına sahip olduğu görülmektedir. Nadir toprak iyonu ilavesinin EISA ile sentezlenen biyoaktif camların tane boyutu üzerinde bir değişikliğe neden olmadığı anlaşılmaktadır. Diğer yandan asit ile işlem görmüş biyoaktif cam tozlarının ortalama tane boyutunun daha küçük olduğu anlaşılmaktadır.

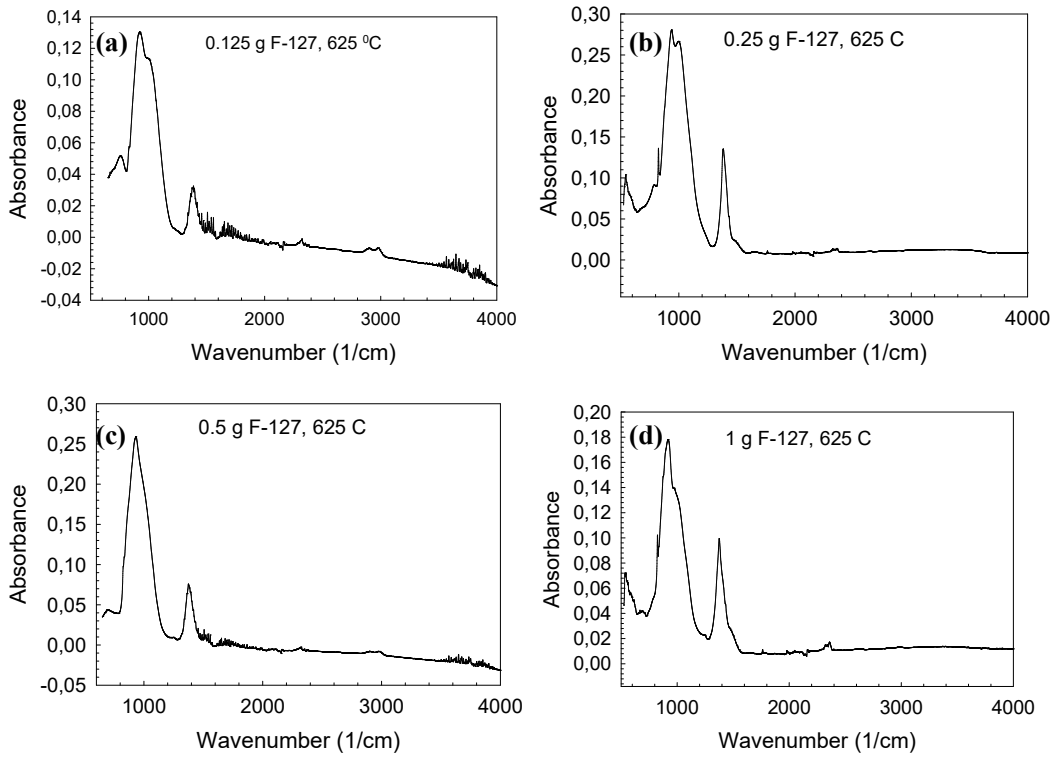

Şekil 3. Farklı miktarlarda F-127 blok-kopolimer kullanılarak EISA yöntemi ile sentezlenmiş (625 °C'de kalsine edilmiş) biyoaktif cam tozlarının FTIR spektrumları (a) 0.125 g, (b) 0.25 g, (c) 0.5 g, (d) 1 g F-127 ile hazırlanmış örnekler.

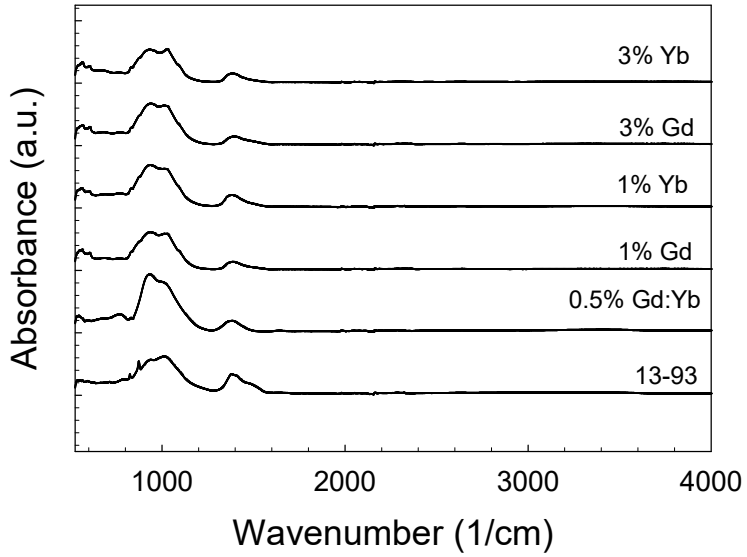

Şekil 4. EISA yöntemi ile 1 g F-127 kullanılarak sentezlenmiş Gd^{3+} ve Yb^{3}içeren biyoaktif cam tozlarının FTIR spektrumları.

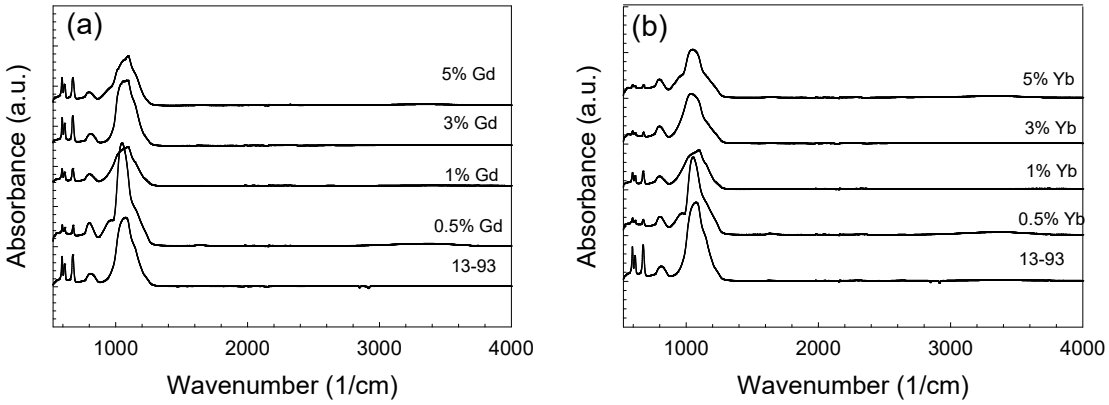

Şekil 5. EISA yöntemi (1 g F-127) ile sentezlenmiş ve asit ile işlem görmüş (a) Gd^{3+}, (b) Yb^{3+}içeren biyoaktif cam tozlarının FTIR spektrumları.

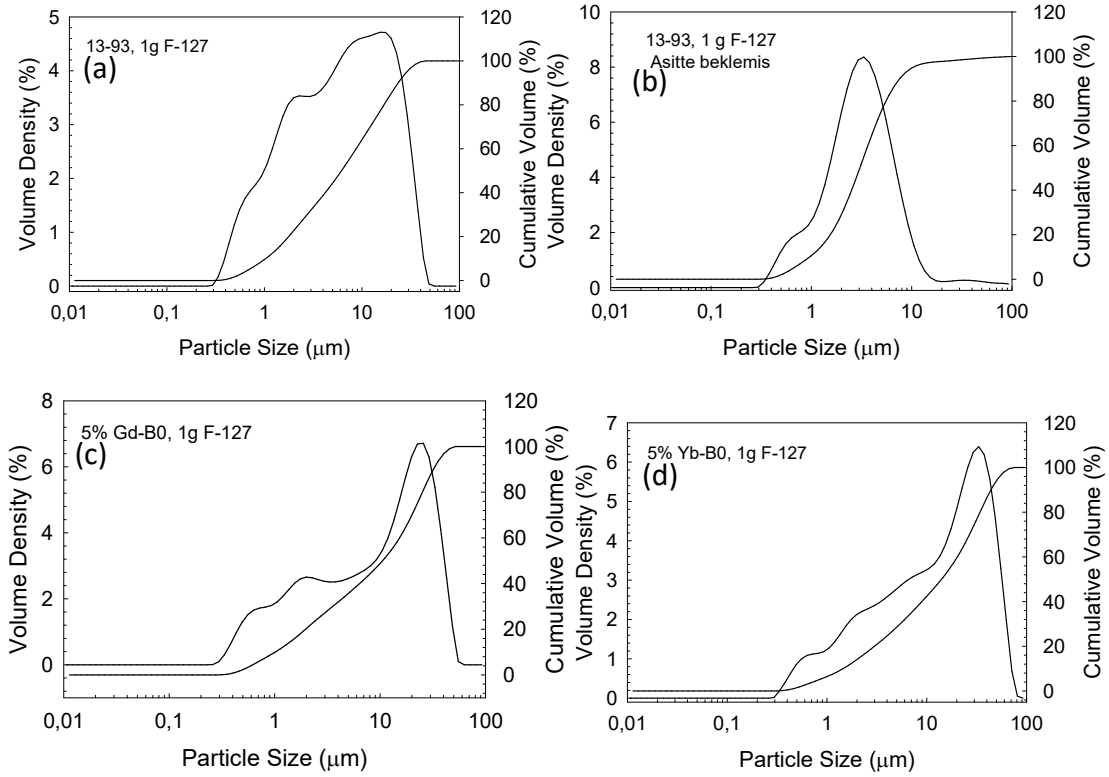

Şekil 6. EISA yöntemi ile (F127: 1 g) sentezlenen, 625 °C'de kalsine edilmiş biyoaktif cam tozlarının tane boyut dağılımını gösteren grafikler (a) 13-93, (b) 13-93, asit ile işlem görmüş, (c) 5%Gd^{3+}, (d) 5%Yb^{3+}.

Yapılan ölçüm sonuçlarına göre, 1 g F-127 ile hazırlanan ve sonrasında asit içerisinde bekletme yapılan katkısız 13-93 biyoaktif cam tozlarının medyan tane boyutu 3.05 μm iken, asit ile işlem görmemiş örnek için bu değer 6.18 μm olarak ölçülmüştür. Diğer yandan %5 Gd^{3+} ve %5 Yb^{3+} içeren biyoaktif cam tozu örnekleri için medyan tane boyutu 10.6 μm ve 9.69 μm olarak elde edilmiştir.

Farklı konsantrasyonlarda F-127 kullanılarak sentezlenen tozların BET yüzey alanı, Langmuir ve Single Point yüzey alanı değerleri Tablo 1'de verillmektedir. Buna göre EISA yöntemi ile sentezlenen cam tozlarının kullanılan F-127 miktarına bağlı olarak artan yüzey alanı değerlerine sahip olduğu görülmektedir. 1 gr F-127 içeren örneğin Langmuir yüzey alanı 8.19 m^2/g olarak ölçülmüştür. F127 konsantrasyonuna bağlı olarak artan yüzey alanının, örneklerin sahip olduğu mezogözenekliliğe bağlı olduğu düşünülmektedir.

Pluronik F-127 blok-kopolimer varlığında yüksek oranda mezogözenekler barındıran cam tozları sentezlenebilmektedir.

Asit içerisinde işlem görerek hazırlanan biyoaktif cam tozlarının toplam yüzey alanları ve gözenek çapı değerleri sırasıyla Tablo 2 ve Tablo 3'de verilmektedir. Buna göre, asit ile işlem görmüş örneklerin yüzey alanlarında yaklaşık 65 kat artış gerçekleşmiştir. Asit içerisinde bekletilerek EISA yöntemi ile hazırlanan (1 g F-127) katkısız 13-93 biyoaktif cam tozlarının Single Point, BET ve Langmuir yüzey alanları sırasıyla 369, 372 ve 531.8 m^2/g olarak ölçülmüştür. Sonuçlar ayrıca, 1 gr'dan daha yüksek miktarda F-127 içerecek şekilde hazırlanan örneklerin toplam yüzey alanın azaldığını göstermektedir. Buna göre F-127 miktarı 4 g olarak kullanıldığında toplam BET yüzey alanının 189 m^2/g olduğu anlaşılmaktadır. Sonuçlar asit ile işlem görerek hazırlanan örnekler için optimum F-127 mikarının 1 g olması gerektiğini göstermektedir.

Asit içerisinde bekletme işleminin sentezlenen tozların gözenek çaplarını da doğrudan etkilediği anlaşılmaktadır. EISA yöntemi ile 1 g F-127 kullanılarak hazırlanan 13-93 cam tozlarının gözenek çapı ~171 Å iken asit ile işlem görmüş örnekte bu değer 24.03 Å olarak elde edilmiştir. Gözenek boyutu 2 nm ile 50 nm arasında değişen malzemeler mezogözenekli malzemeler olarak sınıflandırılmaktadır [16]. Bu nedenle, proje kapsamında 1 g F-127 kullanılarak EISA yöntemi ile hazırlanan ve sonrasında asit ile işleme alınmış biyoaktif cam tozlarının mezogözenekli olduğu anlaşılmaktadır.

In vitro biyoaktivite çalışmalarının sonuçlarına göre, 1 g F-127 kullanılarak, asit ile işlem görümüş Gd^{3+} ve Yb^{3+} içeren biyoaktif cam tozlarının SBF içerisinde 7 gün ve 28 gün bekletildikten sonraki FTIR spektrumları sırasıyla Şekil 7'de gösterilmektedir. FTIR spektrumlarında 1100 cm^{-1}'de görülen pik, P=O gerilmesine aittir. 900 cm^{-1}'de oluşan düşük şiddetli yaygın pik CO_3^{2-} oluşumununa işaret etmektedir. Ayrıca, 560 ve 604 cm^{-1}'de görülen çift pik P-O vibrasyon modunda kristal fazda fosfat oluşumunu (ortofosfat, PO_4^{3-}) göstermektedir. SBF içerisinde bekletilen örneklerin tamamında 7 günden itibaren HA oluşumu gerçekleştiği anlaşılmaktadır.

Tablo 1. EISA yöntemi ile hazırlanmış 13-93 biyoaktif cam tozlarının yüzey alanı değerleri.

Yüzey Alanı-Modeli	**13-93 F127: 0.250 g**	**13-93 F127: 0.50 g**	**13-93 F127: 1.00 g**
Single Point (m^2/g)	2.9729	3.6937	5.8616
BET(m^2/g)	3.1035	3.8039	5.9672
Langmuir(m^2/g)	4.3238	5.2540	8.1943

Tablo 2. EISA yöntemleri ile hazırlanmış ve asit ile işlem görmüş katkısız, Gd^{3+} ve Yb^{3+} içeren biyoaktif cam tozlarının yüzey alanı değerleri.

Yüzey Alanı-Modeli	**13-93 F127: 1.00 g**	**13-93 F127: 2.00 g**	**13-93 F127: 4.00 g**	**5%Gd F127: 0.25 g**	**5%Yb F127: 0.25 g**
Single Point (m^2/g)	369.52	256.57	188.37	192.029	280.41
BET(m^2/g)	372.12	256.40	190.29	189.52	280.64
Langmuir(m^2/g)	531.88	363.34	272.73	265.44	398.53

Tablo 3. EISA yöntemleri ile hazırlanmış ve asit ile işlem görmüş katkısız, Gd^{3+} ve Yb^{3+} biyoaktif cam tozlarının ortalama gözenek genişliği (Å).

	13-93 F127: 1.00 g Asitsiz	**13-93 F127: 1.00 g**	**13-93 F127: 2.00 g**	**13-93 F127: 4.00 g**	**5%Gd F127: 0.25 g**	**5%Yb F127: 0.25 g**
Adsorpsiyon por genişliği (BET) (Å)	171.61	24.03	22.68	27.27	21.26	22.99
Desorpsiyon por genişliği (BET) (Å)	201.01	24.16	22.81	27.87	21.41	23.24
BJH Adsorpsiyon por genişliği (Å)	319.2	37.18	39.76	59.42	44.11	40.92
BJH Desorpsiyon por genişliği (Å)	379.5	35.44	37.10	55.50	41.60	39.04

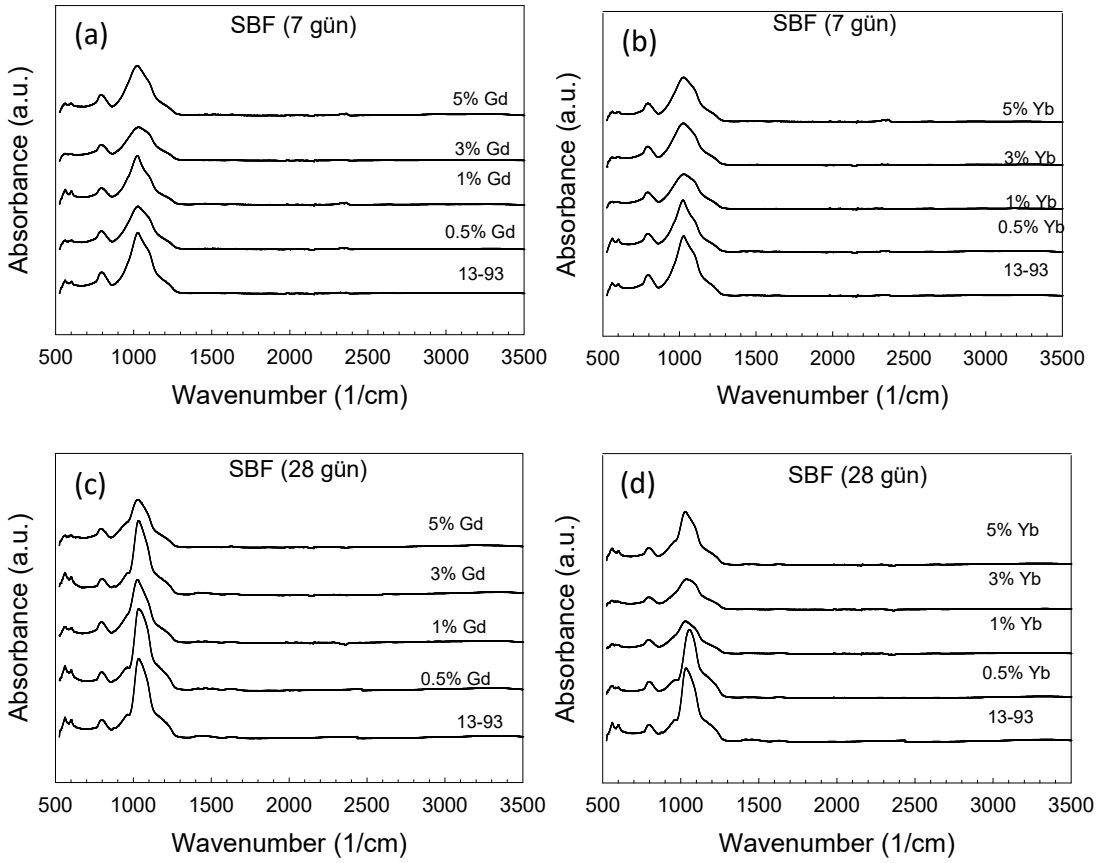

Şekil 7. Yapay vücut sıvısında 7 ve 28 gün bekletilmiş, asit ile işlem görerek EISA ile hazırlanmış (F127, 1 g) (a),(c) Gd^{3+}; (b),(d) Yb^{3+} içeren biyoaktif cam tozlarının FTIR spektrumları.

4. SONUÇLAR

Çalışmada Gd^{3+} ve Yb^{3+} içeren 13-93 biyoaktif cam tozlarının, Pluronik F-127 varlığında EISA yöntemi ile sentezi ve karakterizasyonu gerçekleştirilmiştir. Sentezlenen biyoaktif cam tozlarının yapısal ve morfolojik özellikleri FTIR spektrometre kullanılarak incelenmiş, ayrıca tozların tane boyutu, BET toplam yüzey alanı ve gözenek çapları ölçülmüştür. Biyoaktif cam tozlarının yüzeylerinde hidroksiapatit oluşturma yeteneği yapay vücut sıvısı içerisinde zamanın fonksiyonu olarak test edilmiştir. Sonuçlar, EISA ile sentez çalışmaları sırasında kullanılan F-127 miktarının ve sonrasında yapıdan uzaklaştırma yönteminin (asit içerisinde bekletme ve ısıl işlem ile) hazırlanan biyoaktif cam tozlarının toplam yüzey alanı ve gözenekliliğini doğrudan etkilediğini göstermiştir. Buna göre, 1 g F-127 kullanılarak hazırlanan ve asit ile işlem gören 13-93 biyoaktif cam tozlarının BET yüzey alanı 372 m^2/g olarak ölçülmüştür. Aynı şekilde hazırlanan 13-93 cam tozlarının ortalama gözenek çapı 24.03 Å olarak elde edilmiştir. Yapay vücut sıvısı içerisinde 7ve 28 gün bekletilen katkısız, Gd^{3+} ya da Yb^{3+} katkılı biyoaktif cam tozlarının in vitro biyoaktivitesinde bir azalma olmadığı ve yüzeylerinde HA oluşumu gerçekleştiği anlaşılmıştır.

TEŞEKKÜR

Bu çalışma 219M212 nolu TÜBİTAK projesi ve 2020-067 nolu BAP projesi kapsamında desteklenmiştir.

KAYNAKLAR

1. Hench, L. L., Splinter, R. J., Allen, W. C., Greenlee, Jr. T. K. (1971) "Bonding Mechanisms at the Interface of Ceramic Prosthetic Materials", Journal of Biomedical Materials Research, 2, 117–41.
2. Hench, L.L. (1998) Bioceramics , Journal of the American Ceramic Society 81, 1705-1728.
3. Kalaivani, S., Srividiya, S., Vijayalakshmi, U., Kannan, S. (2019) Bioactivity and up-conversion luminescence characteristics of Yb3+/Tb3+ co-doped bioglass system, Ceramics International, 45(15), 18640-18647.
4. Deliormanlı, A.M., Rahman, B., Oğuzlar, S., Ertekin, K. (2021) Structural and luminescent properties of Er3+ and Tb3+ doped sol-gel based bioactive glass powders and electrospun nanofibers, Journal of Materials Science, 56,2, 14487–14504.
5. Brink, M., Turunen, T., Happonen, R., Yli-Urppo, A. (1997) Compositional Dependence of Bioactivity of Glasses in the System Na_2O-K_2O-MgO-CaO-B_2O_3-P_2O_5-SiO_2, Journal of Materials Science: Materials in Medicine, 37,114–21.
6. Rahaman, M.N., Day, D.E., Bal, B.S., Fu, Q., Jung, S.,B., Bonewald L.F. (2011) Biactive glass in tissue engineering, Acta Biomaterialia, 7(6), 2355-2373.
7. Fu, Q, Rahaman, MN, Bal, BS, Brown, RF, Day, DE. (2008) Mechanical and in vitro performance of 13-93 bioactive glass scaffolds prepared by a polymer foam replication technique. Acta Biomater. 4(6):1854-64. doi: 10.1016/j.actbio.2008.04.019.
8. Deliormanlı, A.M., Yıldırım, M. (2016) Sol-gel Synthesis of 13-93 Bioactive Glass Powders containing Therapeutic Agents, J Austra. Ceram.Soc., 52 (2), 9-19.
9. Yang, H., Coombs, N., Sokolov, I., Ozin, G.A. (1996) Free-standing and oriented mesoporous silica films grown at the air-water interface. Nature. 381:589–592.
10. Brinker, C.J., Lu, Y., Sellinger, A., Fan, H. (1999) Evaporation-induced self-assembly: Nanostructures made easy. Adv. Mater. 11:579–585.
11. Grosso, D., Cagnol, F., Soler-Illia, G., Crepaldi, E., Amenitsch, H., Brunet-Bruneau, A., Bourgeois, A., Sanchez, C. (2004) Fundamentals of mesostructuring through evaporation-induced self-assembly. Adv. Funct. Mater. 14:309–322.
12. Smarsly, B., Antonietti, M. (2006) Block copolymer assemblies as templates for the generation of mesoporous inorganic materials and crystalline films. Eur. J. Inorg. Chem. 2006:1111–1119.
13. Mahoney, L, Koodali, RT. (2014) Versatility of Evaporation-Induced Self-Assembly (EISA) Method for Preparation of Mesoporous TiO_2 for Energy and Environmental Applications. Materials (Basel). 7(4):2697-2746. doi: 10.3390/ma7042697.
14. Deliormanlı,AM., Oğuzlar,S., Zeyrek Ongun M. (2022) Effects of Eu^{3+}, Gd^{3+} and Yb^{3+} substitution on the structural, luminescence and decay properties of silicate-based bioactive glass powders, Journal of Materials Research, 37, 622–635
15. Karolewicz, B., Górniak, A., Owczarek, A. et al. (2014) Thermal, spectroscopic, and dissolution studies of ketoconazole–Pluronic F127 system. J Therm Anal Calorim 115, 2487–2493. https://doi.org/10.1007/s10973-014-3661-2
16. Holban, A.M., Grumezescu,A.M., Andronescu, E. (2016) Chapter 10 - Inorganic nanoarchitectonics designed for drug delivery and anti-infective surfaces, Editor(s): Alexandru Mihai Grumezescu, Surface Chemistry of Nanobiomaterials, William Andrew Publishing, 301-327.

A MATHEMATICAL MODEL OF THE EFFECT OF DRAG FORCE CREATED BY BODY FLUIDS ON THE POSITION OF THE MAGNETIC MICROROBOT

Özge AKBÜLBÜL [1]

[1]Ege University, Graduate School of Natural and Applied Sciences, İzmir, Türkiye.

[1]ORCID ID: https://orcid.org/0000-0002-7892-6458

Aysun BALTACI [2]

[2]Ege University, Faculty of Engineering, Mechanical Engineering Department, İzmir, Türkiye.

[2]ORCID ID: https://orcid.org/0000-0002-9049-1610

Barış Oğuz GÜRSES [3]

[3]Ege Üniversitesi, Faculty of Engineering, Mechanical Engineering Department, İzmir, Türkiye.

[3]ORCID ID: https://orcid.org/ 0000-0002-2755-3452

ABSTRACT

Magnetic microrobots are small-scale devices that can be manipulated by external magnetic fields. It is foreseen that from past literature research it can be used in surgical procedures within the scope of clinical minimally invasive operations in the future. Microrobots can be used for procedures such as drug delivery, occlusion, and biopsy in areas of the body that are difficult to reach with standard operations. Considering its use in body fluids in in vivo environments in future applications, the resistance of the microrobot to the fluid in the body flow is an important factor in determining the position of the microrobot and providing its control, in brief, in order to receive feedback from the microrobot. In this study, it is mathematically modeled in MATLAB/Simulink for a cylindrical microrobot to be manipulated in 1 dimensional by an Electromagnetic Actuator (EMA) according to the drag force effect created in the aforementioned body fluids whose density is close to water. The effect of the drag force on the microrobot position was investigated.

Keywords: Microrobot, drag force, body fluids

INTRODUCTİON

Microrobots are small-scale manipulable devices at the micrometer scale that will find use in various fields, especially in biomedicine. Due to the small size of microrobots, it is predicted that they can be used especially in minimally invasive surgical procedures. Performing an invasive surgical procedure speeds up the patient's postoperative recovery. For this reason, operations performed through smaller incisions in invasive surgery with the contribution of microrobots will be a positive situation for both the patient and the surgeon in the future. It is thought that in the future in health applications, microrobots can be used with a user interface in surgical procedures to be performed with small incisions, and they can be used in procedures such as drug delivery, biopsy, unblocking in hard-to-reach areas. Microrobots can be manipulated electrically, chemically, optically, magnetically, through power sources such as batteries, and acoustically [1]. However, when most of these manipulation techniques are designed for a movement in the human body, they are not suitable because the power supply is not continuous. When magnetic manipulation, one of these manipulation techniques, is applied to a magnetic microrobot, motion can be achieved with the continuous external magnetic field effect of the power source. Microrobots with magnetic properties can be guided in the working area by magnetic field effect with devices called electromagnetic actuators. Electromagnetic actuators (EMAs) consist of coil systems induced by electric current, and they can make the object in the

working area make directional and rotational movements with the magnetic field effect they create [2]. It is predicted that the use of microrobots will become widespread with the production of these devices according to human size [3]. Considering that the microrobot will be used for sensitive in-vivo procedures, it is useful to focus on the precision of its control. The margins of error caused by external effects are of great importance in controlling the position of the microrobot [4]. By detecting these effects, the controller is adjusted more sensitively and the margin of error of the microrobot is reduced. One of the most important external effects is the microrobot's environment. Considering that researches have been started for the use of microrobot in in-vivo operations in the future, the effect of body fluids on the microrobot is the same as the imaging effect under the control of the microrobot [5]. In obtaining the position, speed and acceleration outputs of the microrobot, the external environment effects and imaging and the measurement of positional error margins are included in the feedback factors. These feedback factors, on the other hand, are important in determining the required force and torque in the direction of the microrobot, and in measuring the position, speed and acceleration outputs of the microrobot with the right precision.

In this study, the MATLAB/Simulink model of a cylindrical microrobot that will be guided in 1D by an electromagnetic actuator (EMA) according to the drag force effect created in body fluids with a density close to water, such as blood, cerebrospinal fluid (CSF), contrasted blood, plasma (serum), pancreatic fluid. It was modeled mathematically. The effect of drag force on the microrobot position was investigated.

Materials and Method

In our study, it was thought that the microrobot would be used in vivo. For this reason, first of all, a mathematical model has been studied that will perform the movement and observation of the microrobot in a fluid-filled tube in one direction.Since the fluid density will change the drag force effect; Microrobot position has been obtained for body fluids with a density close to water, such as blood, cerebrospinal fluid (CSF), contrast-enhanced blood, plasma (serum), pancreatic fluid.

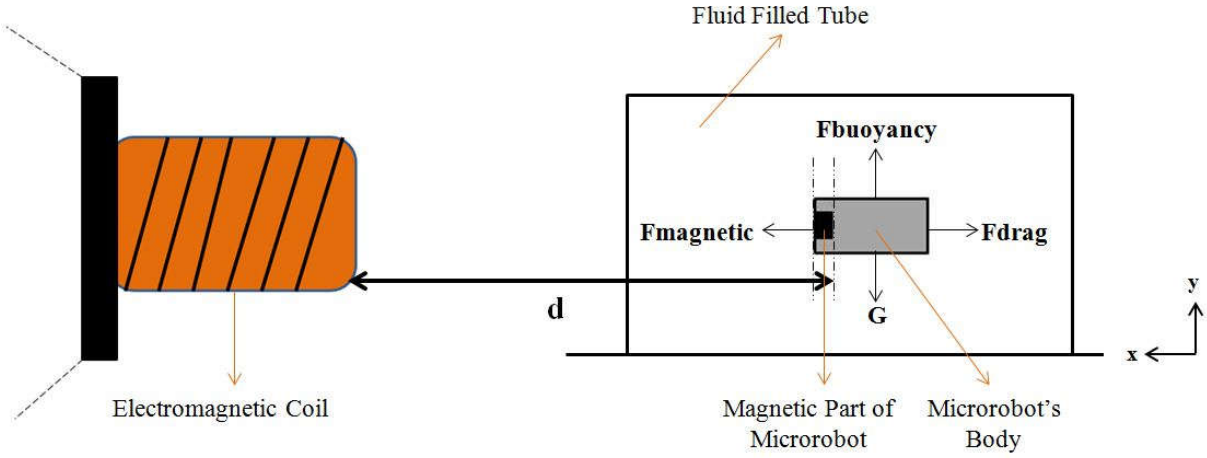

Figure 7. *Forces Acting on the Microrobot in the Fluid*

Consists of an electromagnetic coil that manipulates the microrobot to be directed in the x direction, that allow the position of the microrobot. Modeling is done by considering that there is a microrobot inside the fluid-filled tube. One of the important issues for microrobot control is that the microrobot, which is in body fluids with a density close to water, overcomes the drag force and is moved by the coil. The most important factor to consider when modeling a microrobot is the forces acting on the microrobot. Considering the microrobot in fluid, gravity is equal to the buoyancy force when the microrobot is suspended in the air. Force analysis is mainly in the horizontal direction [6]. When the microrobot is immersed in the fluid, the main actuation force working on the robot is the magnetic force, and the viscous force here is related to the speed of the microrobot (Equation 1):

$$F + F_d + m\frac{dv}{dt} = 0 \quad (1)$$

Here v is the speed of the microbot. In the horizontal direction, the drag force works against the motion of the microrobot. To manipulate the microrobot, the input magnetic force must overcome the drag force (F≥Fd). Here F is the magnetic force applied to the microrobot and Fd is the drag force of the fluid. The weight of the microrobot to be produced is determined by the connection between the buoyancy force (Eq. 2) and the weight.

$$F_b = V_r(\rho_r - \rho_f)g \quad (2)$$

$$(m_{microrobot}g) - \rho_{fluid}V_{microrobot}g = 0 \quad (3)$$

Equation 3 considers ρ, fluids of different densities (for water: 997 kg/m^3, for CSF 1000-1007 kg/m^3 [7], for Blood/Serum 1043-1060 kg/m^3 [8], for pancreatic fluid 1045-1128 kg/m^3 [9]). V is the volume of the microrobot and g is the gravitational acceleration. Here, the relationship that will enable the movement to be directed in the x direction is between the drag force and the magnetic force. This is given as a force input in the x direction to the microrobot block in the MATLAB/Simulink program. The velocity value is obtained by integrating these values once, and the position values are obtained by integrating the velocity value. In this way, the position in the x direction is obtained independently of each other. The magnetic force is given by [10]:

$$F = V(M.\nabla)B \quad (4)$$

Here V is the volume of the magnetic microrobot. M is the magnetization of the magnetic microrobot and B is the magnetic flux. ∇ is the gradient operator. In this case, there is only magnetic force acting in the x direction. In the COMSOL program, if a permanent magnet with a width of 250 mm and a height of 500 mm is defined at one end of the PDMS body microrobot (its mass is about 2.2 mg, its density is about 7800 kg/m^3), the magnetic field strength of the electromagnetic coil of the microrobot is calculated. Its magnetization is 5x10^5 A/m. The values seen in this interaction at the maximum and minimum d distance are in the range of 0.2-0.6 T. The magnetic force must be formed in such a way as to overcome the drag force on the microrobot that will move in the fluid.

The drag force (Eq. 5) on a cylindrical body in the fluid, for a laminar flow;

$$F_{d=}\frac{1}{2}c_D A\rho v^2_{terminal} \quad (5)$$

It is calculated by Stokes' Law (0.5>Re). Here, A is the surface area of the particle, ρ is the density of the fluid, $v_{terminal}$ is the final velocity of the microrobot, c_D is the drag coefficient.

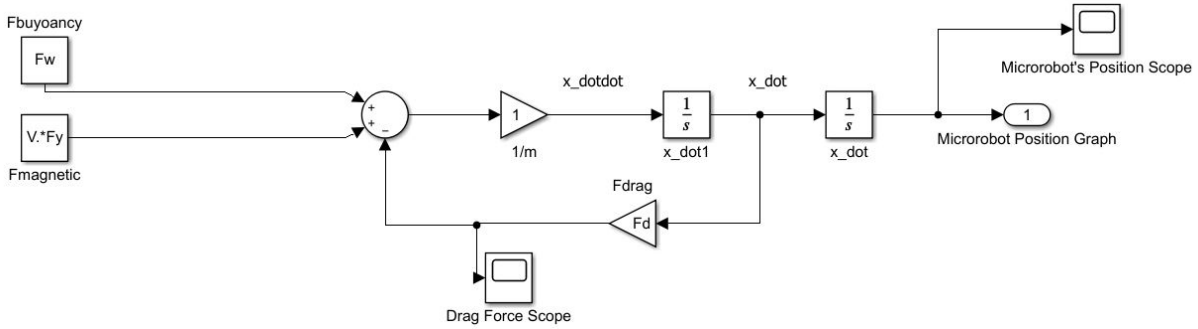

Figure 8. *The MATLAB/Simulink Model of Forces Acting on the Microrobot in the Fluid Indicated in Figure 1 (Microrobot's Dynamics).*

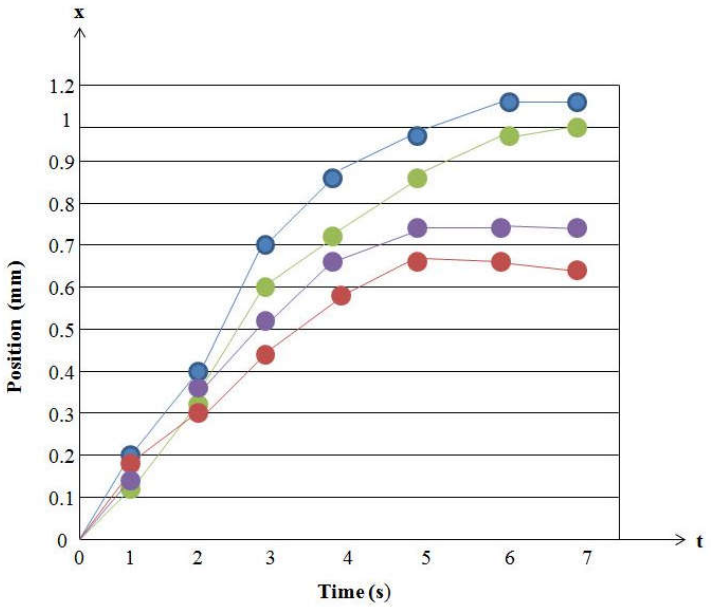

Figure 9. *Effects of Body Fluids of Different Densities on Microrobot Position via Drag Force (Blue Dot= Water, Green Dot=CSF, Red Dot= Blood/Serum, Purple Dot= Pancreatic Fluid)*

Results and Conclusions

In this study, the effect of the densities of different body fluids on the position of the microrobot through the drag force connection was investigated. A MATLAB/Simulink model (Figure 2) has been created to verify these calculations. It has been observed that the calculations made with equations on MATLAB MScript and the mathematical model created in MATLAB/Simulink give convergent results. It has also been shown on the Simulink model that more drag force occurs in blood/serum and pancreatic fluids, which are denser than water (Figure 3). Estimates of the area gradient required to resist fluid drag forces in different body fluids indicated that a minimum gradient of about 0.6 T/m would be required. This model essentially provides an approximation to the calculations of microrobot dynamics in itself. In order to examine the parameters affecting the dynamics of the whole system, mathematical models used in closed-loop controller systems [11] should be used. This model, which examines the microrobot dynamics, only includes the examination of a part of the system.

In addition, according to information from the literature, it is recommended to use the Burgers model consisting of a Maxwell and a Kelvin element to describe the properties of the vitreous, while mathematical modeling will be performed for image feedback such as the eye organ, but for more viscous body environments. These are two common models of viscoelastic behavior, elements consisting of a spring and a shock absorber in series and parallel, respectively. For those who will do research for viscous media, it is recommended to investigate these models [12]. In this study, the drag force effect of body fluids with a density close to water was investigated.

References

[1] H. Kim, J. Ali, U. K. Cheang, J. Jeong, J. S. Kim, and M. J. Kim, "Micro Manipulation Using Magnetic Microrobots," *J. Bionic Eng.*, vol. 13, no. 4, pp. 515–524, 2016.
[2] T. Xu, J. Yu, X. Yan, H. Choi, and L. Zhang, "Magnetic actuation based motion control for microrobots: An overview," *Micromachines*, vol. 6, no. 9, pp. 1346–1364, 2015.
[3] M. Sitti, "Miniature devices: Voyage of the microrobots," vol. 458, no. April, pp. 1121–1122, 2009.
[4] J. Jiang, Z. Yang, A. Ferreira, and L. Zhang, "Control and Autonomy of Microrobots: Recent Progress and Perspective," *Adv. Intell. Syst.*, vol. 4, no. 5, p. 2100279, 2022.
[5] F. Soto and R. Chrostowski, "Frontiers of medical micro/nanorobotics: In vivo applications and commercialization perspectives toward clinical uses," *Front. Bioeng. Biotechnol.*, vol. 6, no. NOV, pp. 1–12, 2018.
[6] A. Ghanbari, P. H. Chang, B. J. Nelson, and H. Choi, "Electromagnetic Steering of a Magnetic Cylindrical Microrobot Using Optical Feedback Closed-Loop Control," *Int. J. Optomechatronics*, vol. 8, no. 2, pp. 129–145, 2014.
[7] N. Masoumi *et al.*, "2D computational fluid dynamic modeling of human ventricle system based on fluid-solid interaction and pulsatile flow," *Basic Clin. Neurosci.*, vol. 4, no. 1, pp. 64–75, 2013.
[8] D. J. Vitello, R. M. Ripper, M. R. Fettiplace, G. L. Weinberg, and J. M. Vitello, "Blood Density Is Nearly Equal to Water Density: A Validation Study of the Gravimetric Method of Measuring Intraoperative Blood Loss," *J. Vet. Med.*, vol. 2015, pp. 1–4, 2015.
[9] N. Dhaka *et al.*, "Pancreatic fluid collections: What is the ideal imaging technique?," *World J. Gastroenterol.*, vol. 21, no. 48, pp. 13403–13410, 2015.
[10] S. Jeon *et al.*, "A Magnetically Controlled Soft Microrobot Steering a Guidewire in a Three-Dimensional Phantom Vascular Network," *Soft Robot.*, vol. 6, no. 1, pp. 54–68, 2019.
[11] Y. Shao, A. Fahmy, M. Li, C. Li, W. Zhao, and J. Sienz, "Study on Magnetic Control Systems of Micro-Robots," *Front. Neurosci.*, vol. 15, no. August, pp. 1–15, 2021.
[12] K. B. Yesin, K. Vollmers, and B. J. Nelson, "Modeling and control of untethered biomicrorobots in a fluidic environment using electromagnetic fields," *Int. J. Rob. Res.*, vol. 25, no. 5–6, pp. 527–536, 2006.

INVESTIGATING THE ENGINEERING CHARACTERISTICS OF ANTHILL SOIL AND LATERITE SOIL

Adegbesan Ololade O.; Ayegbusi Olufunke A.; Omisande Lawrence A.
Department of Civil Engineering
The Federal Polytechnic, Ilaro Ogun State Nigeria

ABSTRACT

Laterites are the products of intensive and long lasting tropical rock weathering which is intensified by high rainfall and elevated temperatures have found wide usage as materials for construction purposes and seen as sustainable construction materials in various aspects of civil and building construction projects because it is environmental friendly and having low energy consumption while anthills soils seen as nuisance to the environment have been a common natural resource seen in many communities because of their abilities to withstand long adverse weather. This research investigated the engineering characteristics of Anthill soil and Lateritic soil. Samples of lateritic soil and anthill soil were collected and subjected to various tests such as Sieve Analysis Tests, Atterberg Limit Tests, Compaction Test and California Bearing Ratio Test**.** Laterite has a maximum dry density and CBR value of 27.5kN/m^3 and 52.91% respectively. This is greater than 30% minimum suitable for sub-base of a road pavement while that of the anthills ranges fall within maximum dry density of 15.5kN/m^3 and CBR value of 41.80% respectively. The investigation revealed that the higher the clay content the lower the values of both the C.B.R and M.D.D thereby indicating that anthill soil compared favorably with laterite and is suitable for various embankment formation such as footpath, lawn tennis court, ramp, sub-base and base course in road construction work as a result of their C.B.R values. Also, anthill soil can be used to perform the function of water retaining reservoir as a result of its clay content

Keywords: Anthill, California Bearing Ratio, Compaction, Laterite, Maximum Dry Density

1.0 Introduction

Soil is the end product of the influence of the climate, relief (elevation, orientation, and slope of terrain), biotic activities (organisms), and parent materials (original minerals) acting over periods of time (Gilluly, Waters, Woodford,1975). Soil continually undergoes development by way of numerous physical, chemical and biological processes, which include weathering with associated erosion. Soil acts as an engineering medium, a habitat for soil organisms and a recycling system for nutrients and organic wastes. The weathering of parent material takes the form of physical weathering (disintegrating), chemical weathering (decomposition) and chemical transformation. Laterites are the products of intensive and long lasting tropical rock weathering which is intensified by high rainfall and elevated temperatures.

Laterite is a widely used materials for construction purposes and seen as sustainable construction materials in various aspects of civil and building construction projects because it is environmental friendly and having low energy consumption. Laterite has found applications in the construction of rural feeder roads, townships roads, intercity link roads, dams, airport runways, highways roads. Laterite is a material that is economically effective, easy to work, mostly abundant and inexpensive,

Since soil has a tremendous range of available niches and habitats, it contains most of the earth's genetic diversity. A handful of soil can contain billions of organisms, belonging to thousands of species. Anthills have been a common natural resource seen in many communities. However, some are dreaded because they are habitation for some dangerous creatures such as ants, snakes and other strange creatures. Anthills are made as a result of the by-product of worker ants digging concealed tunnels. These worker ants are also part of the genus Macrotermes called termites and are an important soil forming factor in many areas, helping in

soil turnover and creating small zones of better aired and more fertile soils by bringing soil material up from the subsurface to the surface (Olowofoyeku et al, 2016). The anthills so formed by these termites are hard and very resistant to weathering and erosions (Adeyemi & Salami, 2004). Anthill is made of different types of soil and engineers are interested in the engineering usefulness of the anthills as there is need to eliminate their habitats because of the nuisances they are causing to the environment (Adegbesan O.O, Ayegbusi O.A. and Omisande L.A 2020). Their ability to withstand long adverse weather has necessitated determining their characteristics and comparing same with laterite with the hope that they may be suitable to replace laterite for construction purposes and this will be justified through results that will be obtained from the various tests on the two samples: lateritic and anthill soils.

Adegbesan O.O, Ayegbusi O.A. and Omisande L.A. (2020) investigated the geotechnical properties of anthill soil through collection of anthill soils at three LGAs of Ogun State, The Atterberg limits results revealed that the anthills and their surrounding soil were predominantly soil with intermediate plasticity with their optimum moisture content (OMC) ranging from 7.14 – 18.60% while the maximum dry density (MDD) ranged from 1.054 – 2.40 Mg/m3. The Andre-Obayanju, O., & Imarhiagbe, O. J. (2019) carried out studies on the geotechnical evaluation of anthill soils Soils from anthills were collected from different parts of Edo State, and was subjected to some geotechnical tests – Atterberg, compaction, CBR and particle size tests – to ascertain the properties of the soils. The uniformity coefficient and coefficient curvature of the soils indicated that they are good subgrade materials for road construction. Variations in the properties of termitaria and their surrounding soil properties were investigated by Eneji, I. S., Sha'Ato, R., & Ejembi, S. E. in 2015 using routine soil analysis protocol. Their results showed that there was clear disparity in the texture (clay content), pH level, AP and TN within the mound and in the environs. Aluvihara, S., & Kalpage, C. S. (2020) did carried out particle size analysis of different clay types. They collected anthill clay, brick clay and roof tile clay samples from different regions in Sri Lanka. Each sample collected were oven dried for approximately 24 hours under the temperature of 1100C until the mass was becoming constant. The results for the moisture contents there were obtained 15.49% for anthill clay, 21.45% for brick clay and 25.97% for roof tile clay.

2.0 Methodology

2.1 Sample Collection

Samples of lateritic soil and anthill soil were collected and subjected to various tests. The sample of laterite was collected from the Ajegunle borrow pit along Papalanto- Ilaro Road. The samples of Anthill soil were collected from different locations which are all within Yewa South Local Government Area of Ogun State. They are as listed below:

i. Egbado college site 6.8972° N, 3.0219° E

ii. Ibeshe site I close to Dangote factory 7.0538°N, 2.9751°E

iii. Ajegunle 6.8828°N, 3.1223°E

iv. Federal polytechnic, Ilaro Campus. 6.8868° N, 3.0055° E

After the samples collected were brought to the laboratory and spread out in order to air dry them.

Experiments carried out on the soil sample included:

i. Sieve Analysis Tests

ii. Atterberg Limit Tests

iii. Compaction Test in accordance with BS 1377-2: 2022

iv. California Bearing Ratio Test in accordance with BS 1377-2: 2022

2.2 Sieve Analysis

The particles sieve analysis of a soil involves determining the percentage by weights of particle within the different size ranges. This is the determination of the percentage by weight of particles within the different size ranges as this will facilitate the description, classification and naming the soil appropriately based on standards such as unified, AASHTO and British soil classification systems.

2.3 Atterberg Limit Test

Plasticity of fine grained soil can be determined through the Atterberg limit test. The atterberg limit test consist of the following Liquid Limit (LL), Plastic Limit (PL), and shrinkage Limit respectively.

The Liquid limit and plastic limit are the upper and lower limit of the range of water content over which a soil exhibits plastic behavior.

Liquid limit (LL) A certain quantity of oven-dried soil sample was powdered and passed through 425μ (Micrometer) British Standard (B.S.) No. 40 sieve. The soil material was then mixed with distilled water until a thick homogeneous paste was formed and the paste was then placed in the cup of the liquid limit device. The soil was divided into two using standard grooving tool and the number of blows required to close groove were noted. Care was taken to ensure that the groove was closed by a flow of the soil and not by slippage between the soil and the cup. Plastic limit (PL) The PL defined the moisture content in percentage at which the soil crumbles when rolled into threads. The is performed by repetitively rolling an ellipsoidal soil mass by the finger on a glass plate. For this test carried out, some amount of the powdered soil sample already sieved through sieve B.S. No. 40 sieve was used. The test soil was carefully mixed with water and to such an extent of water content, which just allowed a thread of about 3 mm to be rolled. The rolled sample was achieved on a glass plate and the process was repeated until a thread of about 3 mm in diameter began to show signs of shears both longitudinally and transversely. Some of the crumbling materials were taken for water content determination, which when arranged, gives the plastic limit. Two of these determinations were obtained which were averaged to give the plastic limit. It is worth noting that P.L. > 35 (low plasticity) P.L between 35 and 50 (moderate plasticity) P.L. > 50 (high plasticity)

2.4 Shrinkage Limit Test

The test was carried out in accordance with British standard with the aim of knowing the moisture content expressed in percentage at which volume change ceases and to attain a quantitative indication of the amount of volume change which can occur.

2.5 Compaction Test

The process of densifying soil by packing the particles closer together with a reduction in volume of air is called compaction. The densities achieved by compaction are invariably expressed as dry densities, generally in mg/m^3 although, occasionally, the units' kg/m^3 is used. The moisture content at which maximum dry density is obtained for a given amount of compaction in known as the optimum moisture content. Compaction test was carried out to determine the optimum moisture content (O.M.C) and the maximum dry density (M.D.D) of the soil sample.

2.6 California Bearing Ratio (C.B.R) Test

California Bearing Ratio (C.B.R) The California Bearing Ratio (C.B.R) of a soil is gives the resistance of the soil to the penetration of a standard plunger. It helps in the determination of the suitability of a soil as sub-grade, sub-base and base materials.

3.0 Results and Discussion

3.1 Sieve Analysis

Table 1

SITE		SOIL SAMPLE	D10	D30	D60	CU	CC	CLAY CONTENT	CLASS
1	EGBADO	ANTHILL	0.18	0.28	0.47	2.61	0.93	26	SP/SC
	COLLEGE	LATERITE	0.16	0.28	0.38	2.38	1.29	23.5	WG
2	IBESHE	ANTHILL	0.15	0.24	0.44	2.93	0.87	47.5	SP/SC
		LATERITE	0.17	0.25	0.34	2.00	1.08	22.6	WG
3	FPI CAMPUS	ANTHILL	0.19	0.29	0.35	1.84	1.27	35.4	WG/SC
		LATERITE	O.21	0.29	0.49	2.33	0.82	25	SP
4	AJEGUNLE	ANTHILL	0.18	0.31	0.48	2.67	1.11	57.5	WG/SM
		LATERITE	0.19	0.29	0.54	2.84	0.82	30.9	SP
	CONTROL	LATERITE	1.00	0.62	0.50	4.50	1.53	16.4	WG

The Egbado college anthill soil contained 26% of clay based on the sieve analysis carried out, it has more than 50% of grain that is greater than 200mm US sieve sieze or 63 am BS or 0.075mm BS so it is classified as clayey SC sand based on the unified soil classification system, because C_u<6 and P.I>7 as shown in the graph while its laterite sample contained 23.5% of clay based on the sieve analysis carried out which has more than 50% of coarse fraction sand size. It is classified as silty sand based on the unified soil classification system because Cu<6 and P.I.< 7

Considering the anthill soil at Ibese, it contained 47.5% of clay based ob the sieve analysis carried out which has more than 50% of coarse fraction of sand sieve with C_u<6 and P.I>7, it is therefore classified as clayey sand (SC) based on the unified soil classification system while its laterite contained 22.6% of clay based on the sieve analysis carried out which has more than 50% of coarse fraction of sand size with Cu< 6 and P.I. < 4. It is classified as silty sand based on the unified soil classification.

The unified soil classification for the anthill and lateritic soil at Federal Polytechnic Ilaro is clayey sand because the anthill soil contained 35.4% of clay based on the sieve analysis carried out which has more than 50% of coarse fraction of sand size and its laterite contained 25.0% of clay based on the sieve analysis carried out which has more than 50% of coarse fraction of sand size. Both have C_u<6 and P.I>7

The anthill soil obtained at Ajegunle contained 57.5% of clay based on the sieve analysis carried out which has more than 50% of coarse fraction of sand sieve with C_u<6 and P.I>4, it is classified as silty (SM) sand based on the unified soil classification system while the lateritic soil contained 30.9% of clay based on the sieve analysis carried out which has more than 50% of coarse fraction of sand size with Cu< 6 and P.I. >7. It is classified as clayey sand based on the unified soil classification.

3.2 Atterberg Limits, Compaction and CBR Test

Table 2

	SOIL	SL %	LL	PL	PI	M.D.D kN/M^3 Mg/M^3	O.M.C (%)	CBR VALUE (%)	Remark
EGBADO COLLEGE	ANTHILL	7.36	29	20.81	8.19	18.8	14.40	40.77	GOOD FOR BASE/SUB-BASE
	LATERITE	8.62	20	14.49	5.51	19.60	11.87	36.51	
IBESHE	ANTHILL	12	39.5	30.16	9.34	19.8	14.7	24.18	GOOD FOR BASE/SUB-BASE
	LATERITE	9.26	19.0	15.40	3.96	17.20	9.81	33.33	
FPI CAMPUS	ANTHILL	7	27.1	18.87	18.4	24.4	7.00	34	GOOD FOR BASE/SUB-BASE
	LATERITE	4.76	34.2	31.35	2.85	19.9	10.40	41.80	
AJEGUNLE	ANTHILL	14	44.2	33.5	10.7	15.2	12.8	19.67	FAIR FOR SUB-BASE
	LATERITE	7.99	33	9.47	23.26	20.8	1.10	32.39	
CONTROL	LATERITE	6	20	10.51	9.49	27.5	10.4	52.91	EXCELLENT FOR BASE

Laterite has a maximum dry density and CBR value of 27.5kN/m^3 and 52.91% respectively. This is greater than 30% minimum suitable for sub-base of a road pavement. The Egbado college anthill has a maximum dry density of 18.8kN/m^3 and CBR value of 40.77% respectively. This is greater than minimum of 30% suitable for sub-base of a road pavement while its laterite sample has a maximum dry density of 19.60KN/m3 and CBR value of 36.51%

The Ibeshe anthill has a maximum dry density of 19.80kN/m^3 and CBR value of 24.18% respectively and its laterite sample has a maximum dry density of 17.20KN/m3 and CBR value of 33.33%. This is greater than the maximum of 30.5 required for a road sub-base

The anthill within the precinct of Federal Polytechnic Ilaro has a maximum dry density and CBR value of 24.0kN/m^3 and 34% respectively. This is greater than minimum required for road sub-base while the laterite collected within the vicinity too has a maximum dry density of 19.9KN/m3 and CBR value of 41.80%.

The anthill soil sample got at Ajegunle (Ilaro) has a maximum dry density of 15.5kN/m^3 and CBR value 19.67% respectively while laterite collected within the same axis too has a maximum dry density of 20.8KN/m3 and CBR value of 32.39%.

4.0 Conclusion

The investigation revealed that the higher the clay content the lower the values of both the C.B.R and M.D.D thereby indicating that anthill soil compared favorably with laterite and is suitable for various embankment formation such as footpath, lawn tennis court, ramp, sub-base and base course in road construction work as a result of their C.B.R values. Also, anthill soil can be used to perform the function of water retaining reservoir as a result of its clay content

5.0 Reference

Adegbesan, O. O., Ayegbusi, O. A., & Omisande, L. A. (2020). Assessment of The Geotechnical Properties of Anthills in Ogun State.

Adeyemi GO, Salami RO. (2004). Some Geotechnical Properties of Two Termite-reworked Lateritic Soils from Ago-Iwoye, South-Western Nigeria. Geotechnology. ISBN 133: 35-41.

Aluvihara, S., & Kalpage, C. S. (2020). Particle Size Analysis of Different Clay Types. In *International Conference of Advance Research and Innovation (ICARI-2020)*.

Andre-Obayanju, O., & Imarhiagbe, O. J. (2019). Geotechnical Evaluation of Anthill Soils from Parts Of Edo State, Southwestern Nigeria.

BS 1377 Methods of test for Soils for civil engineering purposes (England: British Standards Institution, 2022).

Eneji, I. S., Sha'Ato, R., & Ejembi, S. E. (2015). Comparative analysis of termiteria and surrounding soil properties in the University of Agriculture, Makurdi, Nigeria. *ChemSearch Journal*, *6*(1), 57-61.

Gilluly, Waters, Woodford (1975). *Principles of Geology* (4th ed.). USA: W.H. Freeman. ISBN 978-0716702696.

Olowofoyeku, A., Olatokunbo, O., Gideon, B., & Ayobami, B. (2006). Assessment of the Geotechnical Properties of Termite Reworked Soils.

MECHANICAL AND THERMAL MECHANICAL INTERACTIONS IN A FRACTIONAL ORDER MICROSTRETCH THERMOELASTIC HALF-SPACE

D.S.Pathania

Professor, GNDEC Ludhiana (Punjab) INDIA

Pradeep Kumar

C T University Ludhiana (Punjab) INDIA

ABSTRACT

The present investigation deals with the mechanical and thermal interactions in a fractional order microstretch thermoelastic half-space subjected to inclined mechanical forces acting at the boundary of the surface of the half-space. Integral transform technique (Laplace transform and Fourier transform) has been applied to solve the basic equations mathematically. The mathematical expressions of mechanical stresses coupled tangential stress, microstress and the temperature distribution has been obtained numerically. Some particular results and special cases also have been derived.

USE OF E-WASTE CABLES AS PART OF AGGREGATE OR FIBERS IN CONCRETE

Sandra JURADIN
University of Split Faculty of Civil Engineering, Architecture and Geodesy, Split, Croatia
ORCID ID: 0000-0001-5964-6226
Melina ČOTA
STAZUN d.o.o., SPLIT, Croatia
Jelena LOVRIĆ VRANKOVIĆ
University of Split Faculty of Civil Engineering, Architecture and Geodesy, Split, Croatia
Gabrijela GROZDANIĆ
University of Split Faculty of Civil Engineering, Architecture and Geodesy, Split, Croatia

ABSTRACT

Today, e-waste is considered the fastest growing waste on the planet as more than 48 million tons of it are produced every year. Only 15 to 20 % of the total e-waste is recycled and the rest usually goes directly into landfills. This paper presents the possibility of using e-waste cables as a possible replacement for fine and coarse stone aggregates or as reinforcement in the form of fibers. E-waste cables have not undergone any pre-treatment other than manual cutting to the appropriate length. Cables of different diameters were used so that the cut pieces corresponded to 0/4, 4/8 and 8/16 mm aggregate fractions. The amount of e-waste aggregate replacement was 1 and 5% of the total volume of aggregate in concrete. For one concrete mixture, e-waste cables, like 3 cm long fibers, were added to the amount of 1% of the total volume of concrete. A total of 8 concrete mixes were made and tested in the fresh and hardened stage. The workability was tested in a fresh state by the slump and ultrasonic pulse velocity, dynamic modulus of elasticity, compressive strength and flexural strength, σ-δ diagram, saturated water absorption and sorptivity were tested on 28-day-old concrete specimens. The addition of e-waste cables affected the mechanical and durability properties of the concrete due to poorer grain/fiber adhesion and cement matrix. For this reason, the use of this type of concrete is limited, and additional tests are recommended.

Keywords: e-waste cable, concrete, mechanical properties, durability, recycling.

INTRODUCTION

Plastic began to be mass-produced in the 1950s and its use has grown steadily since then. According to Guglielma (2017), 26 billion tons of plastic waste will be produced by 2050. Much of the plastic waste is disposed of in landfills and the environment, and the biggest problem is that plastic does not degrade easily. A large part of the waste consists of discarded electronic devices, including PVC cables and wires. One way to reuse electronic plastic waste is its incorporation into concrete as aggregate or fibers (Kaliyavaradhan and Ling, 2019).

Gregorova, Ledererova, and Stefunkova (2017) used ethylene vinyl acetate (EVA) waste, waste from electrical cable, and waste polystyrene as an aggregate in the lightweight concrete and concluded that the used aggregate had positive thermo-technical properties. Wang R., Tengfei, and Wang P. (2012) tested cement mortar with the addition of nonmetallic powder recycled from waste printed circuit boards. The powder to cement ratio by mass was 0, 5, 10, 15, 20, and 25%. The authors concluded that the powder decreased the bulk density of the hardened cement mortar and increased the air content in the fresh mortar.

More significant changes in the mechanical characteristics of the mortar begin when the powder to cement ratio by mass increases above 15%.

Gull and Balasubramanian (2014), Kurup and Kumar (2017a), and Kurup and Kumar (2017b) investigated the effect of PVC fibers on the properties of fresh and hardened concrete. Gull and Balasubramanian (2014) used plastic e-waste material (wire insulations) with different proportions (0%, 0.4%, 0.6%, 0.8 % and 1%) and different sizes (3 cm, 4 cm and 5 cm). The authors concluded that the best results were obtained if the length of fibers was 3 cm. Kurup and Kumar (2017a) added fibers in concrete in amounts of 0.6, 0.8, and 1% with respect to the weight of cement. The higher amount of PVC fibers influenced the workability of concrete, which resulted in lower slump values. PVC fibers had a positive impact on the compressive strength, flexural strength, split tensile strength, and modulus of elasticity of concrete. The recommended dose of PVC fiber, which improves the properties of concrete, was 0.8 % with respect to the weight of cement. Kurup and Kumar (2017b) tested the effect of recycled PVC fibers and silica on the shear strength of concrete and concluded that fibers improved the ductility behavior of tested concrete.

Rathore and Rawat (2019) studied the influence of e-waste as a partial replacement of coarse aggregate in the concrete mixture in quantities of 5%, 10%, 15%, 20%, 25%, and 30%. E-waste particle sizes were divided into three classes: less than 10 mm, between 10 and 15 mm, and up to 20 mm. The authors found that the mechanical properties of concrete were higher when coarse aggregate was replaced by 15% with two sizes of e-waste material.

In general, the incorporation of e-waste into concrete without reducing its properties can solve the problem of e-waste disposal and reduce environmental pollution. The aim of this paper is to examine the possible use of e-waste cables as a partial replacement of aggregates or as fiber reinforcement and to give a recommendation for the use of this type of concrete.

MATERIALS AND METHODES

In this study, a total of 8 mixtures were made: a control mixture, six mixtures in which a certain fraction of aggregate was replaced with e-waste aggregate in the amount of 1 and 5% of the total volume of aggregate and a mixture reinforced with e-waste fibers in the amount of 1% of the total volume. The cement used for all mixtures was ordinary Portland cement CEM II/B-M (S-LL) 42.5 N in the amount of 350 kg per m^3 and the water to cement ratio (w/c) was 0.50. The fractions of the crushed limestone aggregate used for concrete mixtures preparation were 0/4 mm, 4/8 mm and 8/16 mm.

For the needs of the research, PVC cables were collected from discarded electronic devices. All cables were divided into 3 series, according to diameter. The thinnest cables were used to make the 0/4 mm fraction; for 4/8 mm cables of medium thickness and 8/16 mm cables of maximum thickness. The PVC cables were then hand-cut to the required length. The aim was to keep the ratio of the length and diameter of the cut parts of the cable as close as possible to less than 3, in order to simulate the appearance of the aggregate grain. For fibers: thin cables were manually cut to a length of 3 cm, which is in line with the recommendation of Gull and Balasubramanian (2014). All three fractions of e-waste aggregates and e-waste fibers are shown in Figures 1 and 2. The volume fraction of aggregates in mixtures is shown in Figure 3 and the composition of mixtures is presented in Table 1.

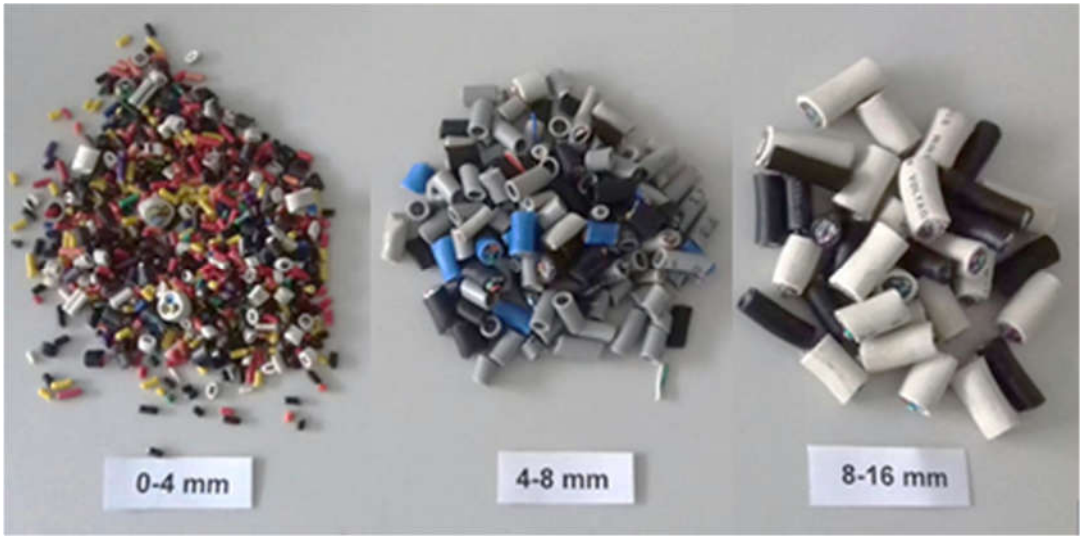

Figure 1. E-waste aggregate fractions

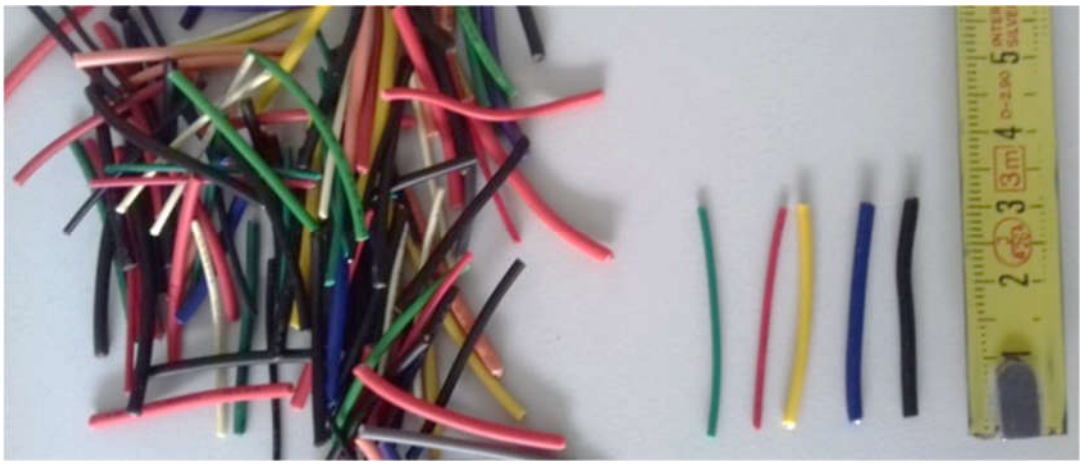

Figure 2. E-waste fibers

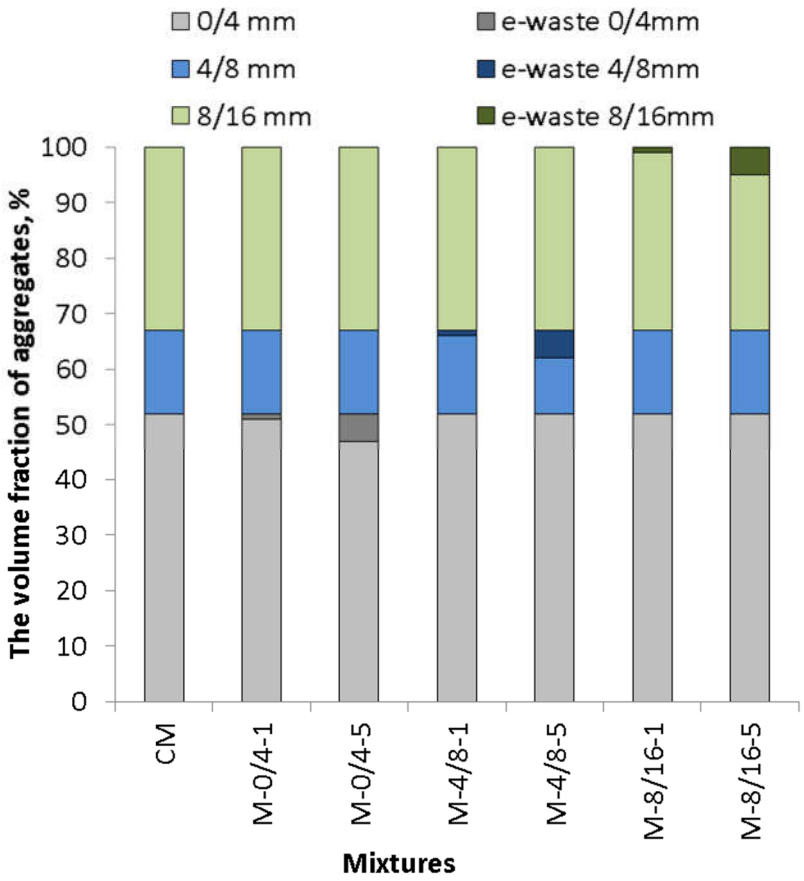

Figure 3. The volume fraction of aggregates in mixtures

CM represents the control mixture, M-F stands for the mixture with fibers from electric cables, and in mixtures from M-0/4-1 to M-8/16-5, the first number indicates the fraction of recycled e-waste aggregate and the second number indicates which percentage of the total aggregate was added to the mixture.

Table 1. Concrete mix constituents (kg per 1m^3)

	Mixtures	CM	M-0/4-1	M-0/4-5	M-4/8-1	M-4/8-5	M-8/16-1	M-8/16-5	M-F
	cement	350	350	350	350	350	350	350	350
	w/c	0.5	0.5	0.5	0.5	0.5	0.5	0.5	0.5
e-waste	0/4 mm	-	7.7	38.3	-	-	-	-	-
	4/8 mm	-	-	-	6.3	31.4	-	-	-
	8/16 mm	-	-	-	-	-	6.6	32.8	-
	fibers	-	-	-	-	-	-	-	11
aggregate	0/4 mm	971.5	950.9	868.7	971.5	971.5	971.5	971.5	957.5
	4/8 mm	280.2	280.2	280.2	261.6	186.8	280.2	280.2	276.2
	8/16 mm	616.5	616.5	616.5	616.5	616.5	597.8	523.1	607.7

The mixtures were made in a laboratory mixer and their workability was tested in a fresh state by the slump method in accordance with HRN EN 12350-2 Testing Fresh Concrete - Slump Test. To avoid the occurrence of segregation in concrete due to the addition of different types of aggregates, all mixtures had a slump class S1 (10-40 mm), Figure 4.

Figure 4. Testing workability by slump method: M-4/8-1

Specimens of concrete mixtures were prepared in moulds as cubes (150 mm), cylinders (100 mm x 200 mm), and prisms (100 x 100 x 500 mm). After 24 h, the specimens of the concrete mixtures were extracted from the moulds and cured in water at 20 ± 2 °C for the next 27 days. After that period, the dynamic modulus of elasticity, ultrasonic pulse velocity (UPV), compressive strength, flexural strength, σ-δ diagram, saturated water absorption, and sorptivity were determined.

Ultrasonic pulse velocity (v) was tested in accordance with HRN EN 12504-4:2021 Testing Concrete in Structures - Part 4: Determination of Ultrasonic Pulse Velocity. UPV was tested on cubes and calculated as:

$$v = L/T \quad (1)$$

where L was a distance between the centres of transducer faces and T the time taken by pulse to go through the specimen, Figure 5.

Figure 5. Testing ultrasonic pulse velocity

The dynamic modulus of elasticity E_{din} was calculated from UPV (v) assuming a Poisson's ratio of 0.2 and using the hardened concrete density (ρ) according to the formula:

$$Edin = 0.9 \cdot v^2 \cdot \rho \quad (2)$$

Compressive strength was tested on cube-shaped specimens according to EN 12390-3: Testing Hardened Concrete - Part 3: Compressive Strength of Test Specimens while flexural tensile strength was tested on prisms according to EN 12390-5: Testing Hardened Concrete - Part 5: Flexural Strength of Test Specimens.

The saturated water absorption (A) was calculated using (3):

$$A = \Delta M / M_d \cdot 100\% \quad (3)$$

where ΔM is the difference between the mass of a surface dry specimen in the air after immersion and the mass of an oven-dried sample in the air (M_d).

Sorptivity was calculated as an increase in mass due to the access of water on the underside of specimens divided with a cross-section of the specimen (cylinder with d = 100 mm) and the square root of time (1440 min).

$$S = \Delta m / (d^2 \cdot \pi / 4 \cdot t^{0.5}) \quad (4)$$

Specimens' weights were measured after 0, 2, 4, 8, 15, 30, 45, and 60 min, and 4 and 24 hours and shown in the water absorption (g) – time (min) diagram.

RESULTS AND DISCUSSION

Table 2 presents the results obtained from all the mixtures.

Table 2. Test results of hardened concrete

Mixtures	UPV m/s	E_{din} GPa	Compressive strength MPa	Flexural strength MPa	Saturated water absorption %	Sorptivity x 10^{-4} mm/min$^{0.5}$
CM	3771.6	30.3	45.8	7.0	6.7	1.92
M-0/4-1	3718.2	29.2	43.3	6.5	6.5	1.97
M-0/4-5	3667.1	28.4	38.8	6.2	7.4	1.83
M-4/8-1	3733.3	29.5	44.5	7.1	7.3	2.73
M-4/8-5	3613.9	27.3	29.6	5.4	8.0	1.94
M-8/16-1	3731.7	29.2	40.4	6.9	6.9	2.57
M-8/16-5	3704.6	28.8	32.8	5.6	7.5	2.31
M-F	3691.5	28.7	43.8	6.6	6.4	1.88

Figure 6 shows UPV and the dynamic modulus of elasticity relative to the control mixture CM. According to Table 2, for all concrete, quality was good because UPV had values above 3500 m/s. Figure 6 shows that the replacement of aggregates in the amount of 1% does not significantly affect the quality of concrete. Mixture M-4/8-5 achieved 96% of the value of the control mixture. The dynamic modulus of elasticity has a similar trend as UPV, Figure 6, and Table 2. The type of e-waste probably affected the obtained result.

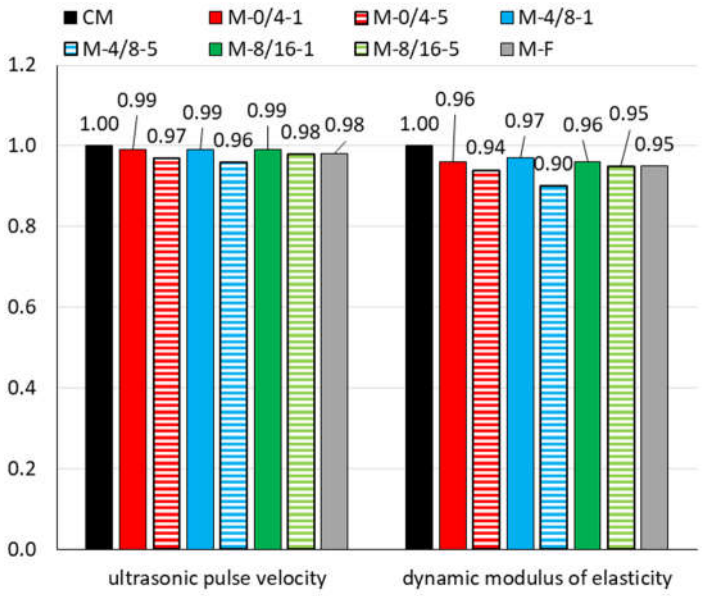

Figure 6. Dynamic modulus of elasticity and ultrasonic pulse velocity relative to mixture CM

E-cables, suitable for the 4/8 mm fraction after cutting to an appropriate length, have been split into two parts; a central part and a PVC sheath, Figure 7, even though they look compact in Figure 1. The concrete properties depend on the characteristics of the two matrices: cement and aggregate/fibers. If the PVC cylinder remains hollow or is filled with mortar during mixing and placing concrete, it will affect the test results.

Figure 7. E-cable after cutting

The impact of the addition of e-waste on compressive and flexural strength is shown in Figure 8 and Table 2. In the mixture M-4/8-5, the reduction in compressive strength is 35% compared to the control mixture. The compressive strength of both M-8/16-1 and M-8/16-5 mixtures in the range of 12 to 28% was also reduced by replacing the 8/16 mm aggregate with the e-waste aggregate.

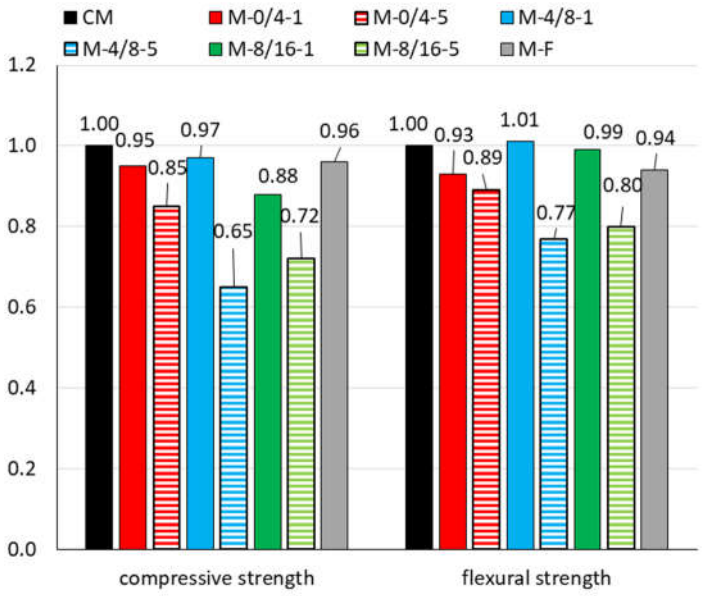

Figure 8. Compressive strength and flexural strength relative to mixture CM

Due to the smooth surface of the aggregate and fiber, the adherence between the grain or fiber and the matrix of concrete is weak, so slipping occurs, Figure 9. Due to the slippage, according to Figure 10, the fibers did not affect the change in the σ-δ diagram and did not impart good ductility. All specimens broke immediately after exceeding the tensile strength during testing. In order to improve this adhesion, the surface roughness of grain or fiber should be increased (Kaliyavaradhan and Ling, 2019). According to Figure 8 and Table 2, 1% of the aggregate replacement did not affect the flexural strength; however, 5% did. The greatest reduction of 23% is noticed in the mixture M-4/8-5.

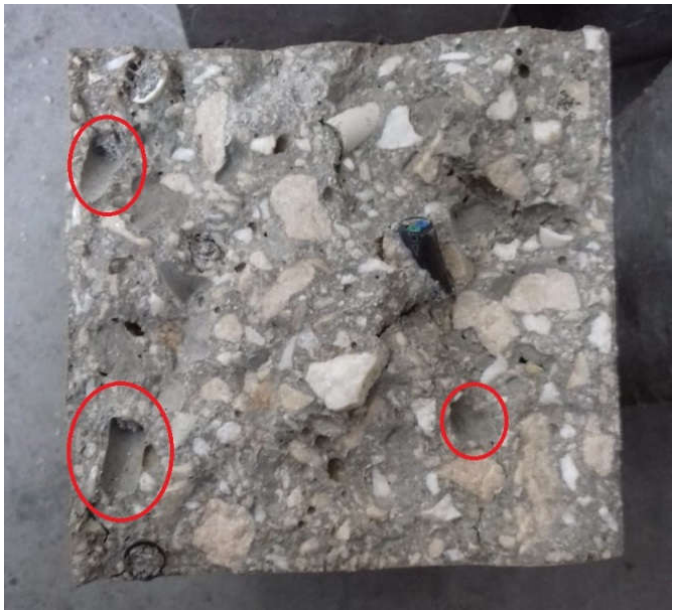

Figure 9. Cross-section of M-8/16-5 specimen

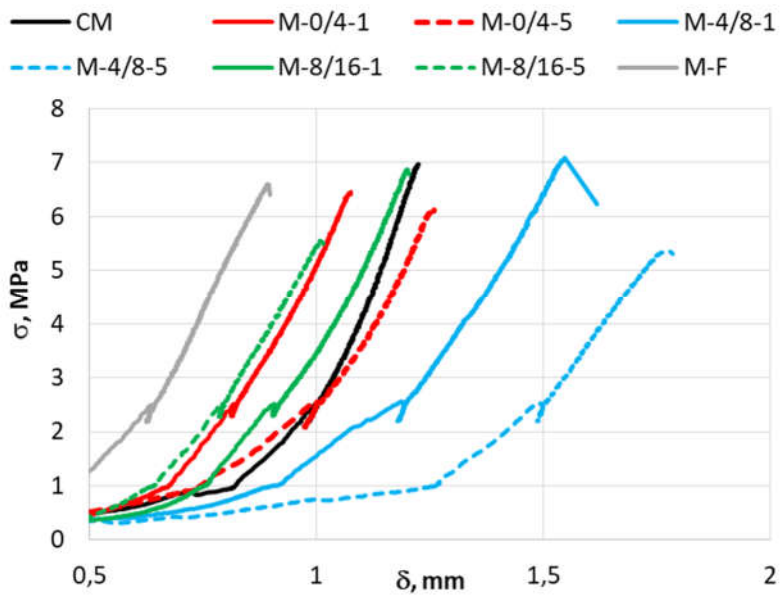

Figure 10. σ-δ diagram

Saturated water absorption is increased in specimens with a higher share of aggregate replacement, Figure 11.

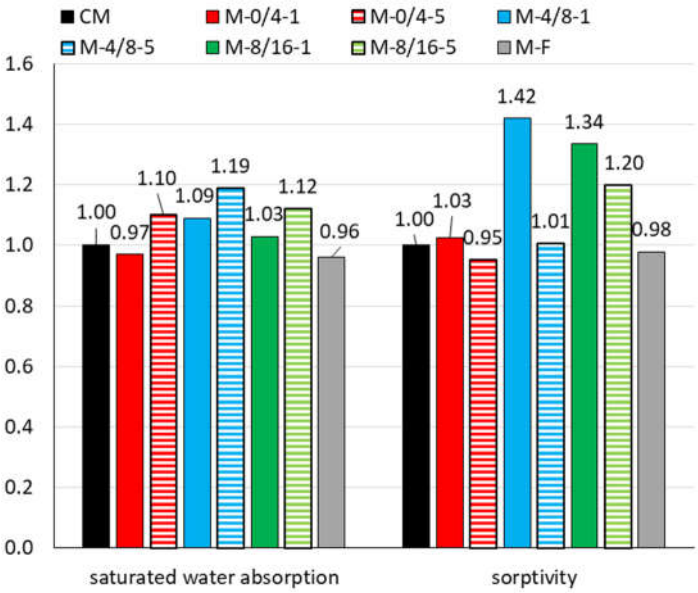

Figure 11. Saturated water absorption and sorptivity relative to mixture CM

In accordance with the Comité Euro-International du Béton (1989), the concrete quality will be poor if water absorption is higher than 5%. All mixtures have a value higher than 6%, even the control mixture, Table 2. The M-4/8-5 mixture has an absorption of 8%, probably due to the previously mentioned problem with the e-waste aggregate, Figure 7.

For the same reason, the M-4/8-1 mixture had the highest capillary absorption in 24 hours, Figure 12. In comparison with the control mixture, this mixture had 42% higher sorptivity, Figure 11. Mixtures M-0/4-5

and M-F had higher initial water absorption than the control mixture, but after 24 hours, the absorption was slightly lower, Figures 11 and 12.

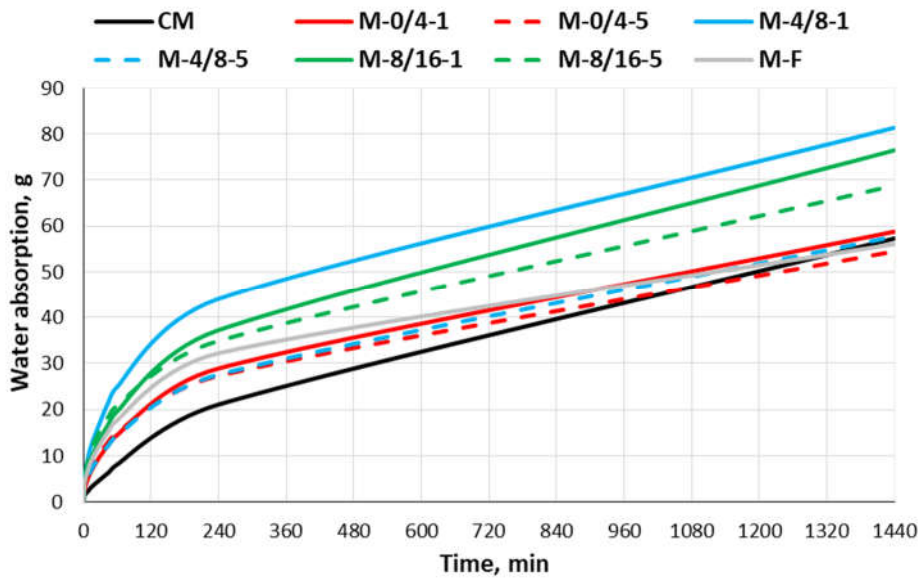

Figure 12. Water absorption – time diagram

Given that water absorption and sorptivity are indicators of concrete durability, it is clear that this type of concrete could only be installed in dry conditions, where is no risk of damage.

Kumar and Selvan (2017) have shown that splitting tensile and flexural strength of e-waste, as fine and coarse aggregate replacement concrete mixtures, were superior to that of referent concrete; therefore, proper selection of e-waste and other materials can enhance the strength, durability, and quality of concrete.

CONCLUSION AND RECOMMENDATION

Eight mixtures were tested in this paper: a control mixture, six mixtures in which 1 and 5% of aggregates were replaced with e-waste cables and a mixture in which 3 cm long e-waste cables were added as fiber reinforcement. Although the measured ultrasound pulse velocity showed that they are good concretes, replacing origin stone aggregate with e-waste aggregate, without compromising durability and strength criteria, requires extensive research. Due to the smooth surface of the waste cables, it was expected that the adhesion between the cement matrix and e-waste grain/fiber would not be satisfactory. It can be assumed that the poor Interfacial Transition Zone (ITZ) also led to lower mechanical and durable properties of the cement composite.

Future research should pay attention to:

- selecting the appropriate stable cable shape
- improving the unsuitable surface texture of replacement e-waste aggregates/fibers
- finding the optimal amount and shape of e-waste aggregate/fibers
- finding optimal mineral admixtures

for the purpose of improvement of the mechanical and durable properties of concrete. In this form, this type of concrete can only be placed in dry conditions where there is no risk of corrosion or chemical attack.

REFERENCES

Concrete (1989), F.I.B.I.F.S. Diagnosis and assessment of concrete structures state of art report; CEB Bulletin; Secretariat Permanent.

Gregorova V., Ledererova, M., & and Stefunkova, Z. (2017). Investigation of Influence of Recycled Plastics from Cable, Ethylene Vinyl Acetate and Polystyrene Waste on Lightweight Concrete Properties. Procedia Engineering, 195, 127 – 133.

Guglielmi, G. (2017). In the next 30 years, we'll make four times more plastic waste than we ever have. Science. https://www.science.org/content/article/next-30-years-we-ll-make-four-times-more-plastic-waste-we-ever-have (access on 07.05.2022)

Gull, I. & Balasubramanian, M. (2014). A new paradigm on experimental investigation of concrete for e-plastic waste management. International Journal of Engineering Trends and Technology, 10 (4), 180e186

Kaliyavaradhan, S. K., & Ling, T. C. (2019). Performance of concrete with PVC fibres. In Use of Recycled Plastics in Eco-efficient Concrete (pp. 369-385). Woodhead Publishing.

Kumar, A. A., & Selvan, R. S. (2017) Performance of Recycled E-waste as Aggregates in Green Concrete. Nature Environment and Pollution Technology, 16 (4), 1135 – 1140.

Kurup, A. R., & Kumar, K. S. (2017a). Novel fibrous concrete mixture made from recycled PVC fibres from electronic waste. Journal of Hazardous, Toxic, and Radioactive Waste, 21 (2), 04016020.

Kurup, A. R., & Kumar, K. S. (2017b).Effect of recycled PVC fibres from electronic waste and silica powder on shear strength of concrete. Journal of Hazardous, Toxic, and Radioactive Waste, 21 (3), 06017001e1-4.

Rathore, V. & Rawat, A. (2019). Effective utilization of electronic waste in concrete mixture as a partial replacement to coarse aggregates, AIP Conference Proceedings 2158, 020037; https://doi.org/10.1063/1.5127161

Wang, R., Zhang, T., & Wang, P. (2012). Waste printed circuit boards nonmetallic powder as admixture in cement mortar. Materials and Structures, 45(10), 1439–1445. doi:10.1617/s11527-012-9843-0

INDIA'S SMART CITIES MISSION AS A MEANS OF ACHIEVING UN NEW URBAN AGENDA 2016: INDIAN PERSPECTIVE POST COVID-19 ANALYSIS

Samuel Mores G. [1)*], **Kiran mai Yanamala**[2)]

[1)]Assistant Professor, Presidency University, Bangalore, India,

[2)]Research Scholar, Presidency University, Bangalore, India,

ABSTRACT

Worldwide Cities occupy approximately 2% of the total land. They contribute to 70% to GDP, over 60% to Global Energy Consumption, over 70% to Greenhouse Gas Emissions and 70% to global waste (The UN Habitat New Urban Agenda III, 2016). The statistics are very clear that Urbanization is present and inevitable. Urbanization has its own merits and demerits. Increasing Urbanization is posing various challenges and creating problems today. However, the same Urbanization can be a source of solutions that our world is facing today. With proper urban planning, a lot of problems are associated with urbanization can be avoided and mitigated. The discussions in The UN-Habitat New Urban Agenda III Conference, majority have agreed to the 'Smart City Model' as a solution to the problems faced by urbanization. India's Smart Cities Mission is efficient to promote sustainable and inclusive development. The study shall discuss how the Smart Cities Mission and UN New Urban Agenda contributes to urbanization and sustainability issues. The study also developed a model to ascertain significant parameters which shall provide a direction for future researches.

Keywords: UN-Habitat New Urban Agenda III, Smart Cities Mission, Sustainability, Sustainable Development Framework, Urbanization

BETONARME KÖPRÜLERİN DAİRESEL VE KARE DİREKLERİNDE TAKVİYE ANALİTİK VE SAYISAL ÇALIŞMASI

ANALYTICAL AND NUMERICAL STUDY OF REINFORCEMENT IN CIRCULAR AND SQUARE PILLARS OF REINFORCED CONCRETE BRIDGES

Domingos Brasil da Silva Junior

University Center of Piaui, İnşaat Mühendisliği Mezunu

Centro Universitário do Piaui, Graduando em Engenharia Civil

Sávio Torres Melo

University Center of Piaui (UNIFAPI), Mühendislik Sektörü Profesörü

Centro Universitário do Piaui, Professor do Setor de Engenharias

ORCID ID: 0000-0001-6725-1689

ÖZET

Betonarme yapılar, öngerilmeli beton ve metalik yapı gibi diğer yapısal yöntemlere göre daha sık meydana gelmektedir. Seçim üç faktörü ima eder: daha düşük teknik-ekonomik maliyet ve dayanıklılık, malzemelere erişim kolaylığı sunduğundan, çeliğin özelliklerini betonla birlikte sağlayarak, çekme ve basma gerilimlerine karşı direnç geliştirerek, malzemeyi daha yapışkan hale getirir. Bu koşullar göz önüne alındığında, bu araştırmanın amacı, Brezilya standartlarının hesaplama yöntemlerini değerlendirmek ve çalışmadan bu yana Eberick yazılımında kullanılanlarla karşılaştırmak için betonarme köprü sütunlarının güçlendirilmesine ilişkin analitik ve sayısal bir çalışma yapmaktır. Köprü direklerindeki güçlendirmenin önemi, mevcut gerçek durum karşısında daha iyi doğruluk sağlamak için sayısal yöntemin vurgulanmasının önemi ve konuyla ilgili az sayıda araştırma yapılması, bununla ilgili analizleri geliştirmek için bilgi eklemek amacıyla. bu sütunlar.

Anahtar Kelimeler: Betonarme. Köprü Sütunları. Zırh. Hesaplama Yöntemleri.

ABSTRACT

Reinforced concrete constructions occur more frequently compared to other structural methods, such as prestressed concrete and metallic structure. The choice implies three factors: lower technical-economic cost and durability, as it presents an ease of access to materials, it provides the characteristics of steel together with the concrete, developing resistance to traction and compression tensions, making the material more adherent. Given these circumstances, the objective of this research is to carry out an analytical and numerical study of the reinforcement of reinforced concrete bridge pillars in order to evaluate the calculation methods of Brazilian standards and compare with the one used in the Eberick software, since the study of the reinforcement in bridge pillars becomes important, the relevance of highlighting the numerical method to provide better accuracy in the face of the existing real situation and the small number of research related to the subject, with the purpose of adding information to improve the analysis regarding these pillars.

Keywords: Reinforced Concrete. Bridge Pillars. Armor. Calculation Methods.

MEVCUT ÇEVRE SENARYOSUNDA ELEKTRIKLI ARAÇLARIN KULLANIMI

THE USE OF ELECTRIC VEHICLES IN THE CURRENT ENVIRONMENTAL SCENARIO

João Leite Barbosa de Carvalho Filho

UniFacid Üniversitesi Merkezi, Elektrik Mühendisliği Mezunu

Centro Universitário UniFacid, Graduando em Engenharia Elétrica

Sávio Torres Melo

UniFacid Üniversite Merkezi, Mühendislik Sektörü Profesörü

Centro Universitário UniFacid, Professor do Setor de Engenharias

ORCID ID: 0000-0001-6725-1689

ÖZET

Pek çok kişi tarafından büyük bir teknolojik gelişme olarak görülen elektrikli araçlar pazar için yeni değil. Toyota Prius'un 1997'de piyasaya sürülmesinden bu yana, Kuzey Amerika pazarı çok sayıda elektrikli otomobil lansmanı gördü. Bu gerçek, büyük ölçüde ABD hükümetinin elektrikli araç üreticilerini ve tüketicilerini teşvik etmesine bağlanabilir. Şu anda dünya genelinde atmosfere karbondioksit salan milyarlarca araba var, bu nedenle elektrikli araçların yaratılması ve kullanılması, fosil yakıtlarla çalışan geleneksel araçlardan gaz salınımının yarattığı çevresel etkiyi azaltmaya geldi. Mevcut çalışma, doğamızı korumak ve çevre kirliliğini azaltmak için uzun yıllardır sürdürülebilir önerilerle gelişen mevcut dünyamızda, gezegenin ve üzerindeki herkesin refahı için bir elektrikli aracın verimliliğini ortaya koymayı amaçlamaktadır. BT. Bu nedenle, elektrikli araçların yerine yanmalı araçların ikamesi, gezegenimizi korumak ve böylece daha sürdürülebilir önlemlerin benimsenmesini teşvik etmek için dev bir adımdır.

Anahtar Kelimeler: Teknolojik Gelişme, Karbon Dioksit, Çevresel Etki.

ABSTRACT

Seen by many as a major technological advance, electric vehicles are not new to the market. Since the launch of the Toyota Prius in 1997, the North American market has seen a large number of electric car launches. This fact can be attributed in large part to the US government's encouragement of electric vehicle manufacturers and consumers. Currently there are billions of cars across the globe emitting carbon dioxide into the atmosphere, in view of this the creation and use of electric vehicles came to reduce the environmental impact generated by the release of gases from traditional vehicles that are powered by fossil fuels. The present work aims to present the efficiency of an electric vehicle in our current world, which for many years has been evolving with sustainable proposals, in order to preserve our nature and reduce environmental pollution, for the well-being of the planet and everyone on it. Therefore, the substitution of combustion vehicles for electric vehicles is a giant step to preserve our planet and thus encourage the adoption of more sustainable measures.

Keywords: Technological Advancement, Carbon Dioxide, Environmental Impact.

IMPACTS OF URBAN FORM AND SOCIOECONOMIC ELEMENTS ON DOMESTIC ELECTRICITY CONSUMPTION WITH RESPECT TO ITS IMPACTS ON LAND SURFACE TEMPERATURE (LST) AND CLIMATE CHANGE IN PAKISTAN

R. Sherwani[1], W. Abdul[2] , Aqsa Qalb[3] , Syed H. Arshad[4], Saima. Gulzar[5]

1 National University of Science and Technology, School of Civil Engineering and Environmental Sciences, Department of Urban and Regional planning, H-12, Islamabad, Pakistan, (PhD Scholar) and (Assistant Professor), School of Architecture and Planning, University of Management and Technology, C II, Johar Town, Lahore.

2 National Institute of Transportation, School of Civil Engineering and Environmental Sciences, Department of Urban and Regional planning, National University of Science and Technology, H-12, Islamabad, Pakistan (Assistant Professor).

3 National University of Science and Technology, School of Civil Engineering and Environmental Sciences, Institute of Geographical Information system, H-12, Islamabad, Pakistan, (PhD Scholar) and (Assistant Professor), School of Architecture and Planning, University of Management and Technology, C II, Johar Town, Lahore.

4 (Assistant Professor), School of Architecture and Planning, University of Management and Technology, C II, Johar Town, Lahore.

5 (Professor), School of Architecture and Planning, University of Management and Technology, C II, Johar Town, Lahore.

Abstract: Changing climatic rhythms have directly impact the built environment. The global energy scarcity and exceptional increase in energy consumption pushed energy optimization in the ambit of inevitable tasks. Energy crisis of the 1970s gave rise to the energy conservation principles but the idea of regulating domestic electricity demand through socio economic and urban form elements gained popularity in the early 2000s. Pakistan has 39% urban population while urbanization rate in Pakistan is 2.81%, devastatingly effected by the global climate change. This research investigates the effect of socio-economic features and urban form elements on domestic electricity demand and its impacts on Land Surface Temperature (LST) and pollutant emissions. Chemical effects of pollutants on the built environment, ultimately effects (LST) directing the earth towards radiating its skin being view of a remotely sensed sensor. The blistering earth surface behavior through rising (LST) by the built environment give flexibility to be used as an input for several models like thermal climate variability model in GIS. Land Surface Temperature is considered as an important indicator at all levels, local, regional, national and global. It serves as a vital element in determining urban climatology, urban heat island effects, calculation of greenhouse gases effects and their estimation, spatio-temporal rise in temperature by using various GIS models. Demographic change especially in south Asia, directly related to climate change and increasing thermal discomfort leads towards increase in energy consumption and ultimately increase in (LST), which is escalating the pollutant Like particulate matters (suspended particles, PM1, PM2.5, PM10) and enhance concentration of greenhouse gases like CH4, O3, Sox, NOx, CO and CO2. Efforts have been made viable to reduce the impacts of (LST) while using different algorithms in this research. Income level and household size is taken as socio economic characteristics. Street pattern, land cover, house size, no of storey, tree plantation, open to sky area are taken as elements of urban form. Electricity billing data is collected from the electric supply company, WAPDA and a questionnaire survey is conducted in five residential areas of Lahore as a case study. High resolution LANDSAT imagery is obtained and neighborhood plans are acquired. A total of 400 households are surveyed. The data is coded & analyzed in GIS and SPSS. Markove chain analysis for future trends in land-use and Single window algorithm, based on single thermal band ranging from 10.4-12.5 micrometer is used for (LST). Multivariate analysis techniques including correlation and regression analysis are employed.

Moreover, the paper intends to highlight major trends of electricity consumption, and pollutant emissions. The key findings show that two of the socio-economic features including income and household size significantly affect electricity consumption and pollutants emissions. This research concludes that significant reduction in electricity demand is possible through socio economic and urban form changes. Incorporation of PV installation, reduce the negative impacts of (LST) on climate change, leads for attaining sustainable development goals in Pakistan.

What will audience learn from your presentation?

- Interrelationship between Housing form, energy consumption, carbon emissions, its impacts on Land Surface Temperature (LST) and climate change impacts with reference to Pakistan
- The research will help to study the implementation of Markove chain analysis, single window algorithm for thermal band consideration in analysis for focusing on urbanization trends, its impacts on climate change, along with regression and correlation relationship in the developing countries like Pakistan
- It will get us together to think about the problems in running scenarios of Pakistan and to find sustainable solutions for the achieving sustainable development Goals in new energy paradigm in Pakistan

ŞUŞA ŞƏHƏRİNİN MÜASİR REKONSTRUKSİYASI VE İNNOVATİV TƏKLİFLƏR

MODERN RECONSTRUCTION OF THE CITY OF SHUSHA AND INNOVATIVE PROPOSALS

Vəfa Vəliyeva

Democratic Youth Public Union, Baku, Azerbaijan

ABSTRACT

Azərbaycanın mədəniyyət paytaxtı Şuşa şəhəri 28 illik əsarətdən sonra Azərbaycanın prezidenti ali baş komandan İham Əliyevin başçılığı altında 2020 - ci ildə 44 gün davam edən müharibənin uğurlu nəticəsi olaraq azad olundu.

1752-ci ildə Pənahəli xan tərəfindən inşa etdirilən Şuşa şəhəri konstruktiv olaraq 17 məhəllə prinsipinə uyğun təşkil olunmuşdur: (Seyidli, Culfalar, Quyuluq, Çuxur məhəllə, Dörd çinar, Dördlər qurdu, Hacı Yusifli, Çöl Qala, Qurdlar, Saatlı, Köçərli, Mamayı, Xoca Mərcanlı, Dəmirçilər, Hamamqabağı, Merdinli və Təzə məhəllə).

Şuşada yaşayan əhalinin sosial rifahini nəzərə alan Pənahəli xan hər məhəllədə ayrıca hamam, məscid və bulaq inşa etdirmişdi.

1992-ci il may ayının 8-də erməni birləşmələri tərəfindən işğal edilən Şuşa şəhəri Qarabağın bütün işğal olunmuş əraziləri kimi erməni vandalizminin qurbanı olmuşdur. Belə ki, Azərbaycanın bir çox maddi-mənəvi irsi dağıdılmışdır.

Hazırda Şuşada yenidənqurma işlərinə başlanılmışdır.

Şuşa şəhərinin rekonstruktiv bərpasının əsas prinsipləri olaraq aşağıdakı innovativ təklifləri irəli sürə bilərik:

-Dağıdılmış mədəni irsin yenidən bərpası;

-17 məhəllə prinsipinə dayanaraq şəhərin memarlıq ənənəsinin bərpası. Klassik ənənəyə yeni rəng qatılması üçün hər məhəllədə uşaq bağçası, məktəb və tibbi yardım məntəqəsinin tikilməsi;

-Şəhərin əsas memarlıq ənənələri nəzərə almaqla şəhər kənarında çağdaş şəhərsalma mədəniyyətinin tətbiqi;

-Şuşanın musiqi mədəniyyətinin beşiyi olduğunu diqqətə alaraq Şuşa şəhərinin mərkəzində yeni konservatoriya binasının inşası;

- Bakı şəhərində demoqrafik artımı nəzərə alaraq və gənc nəslin yenidən Şuşa şəhərinə yönləndirilməsi məqsədi ilə bəzi universitet binalarının tikintisi;

-Azərbaycanın Şərq-Qərb memarlıq ənənəsinə sahib olduğunu üçün Şuşa şəhərinin yenidən inkişaf etməsi məqsədi ilə yeni şəhərsalma prinsiplərini nəzərə alaraq Bakıda tətbiq edilən modern tikililərin Şuşa şəhərinə də tətbiqi;

-Etnoqrafiya, Xalçaçılıq və Mədəniyyət muzeylərinin klassik və çağdaş üslubların qarşılaşdırlması üslubunda tikilməsi;

-Şuşa şəhərinin təbii resurslarını nəzərə alaraq Cıdır düzündə yeni turbazaların yaradılması;

-Qarabağ atlarınının yenidən dünyaya tanıdılması üçün atçılığın inkişafı yönündə yeni atçılıq bazasının yaradılması;

-Azərbaycanın görkəmli mədəniyyət xadimlərinin xatirə gecələrinin keçirilməsi üçün yeni müasir üslubda bina tikilişi.

Açar sözlər: Innovasiya, susa, rekonstruksiya, sehersalma, milli, modern

ANALYSIS OF PATENT INFORMATION SEARCH BASED ON ROYAL JELLY

L.B. Umiraliyeva[1], M.S. Amangeldin[1], S.F. Kolosova[2], A.T. Ibraikhan[1]

[1]Kazakh Research Institute of Processing and Food Industry, Kazakhstan, Almaty city

[2]Sarsen Amanzholov East Kazakhstan University, Ust-Kamenogorsk city

ABSTRACT

In the global pharmaceutical industry, royal jelly enjoys close attention. Scientists from different countries study its beneficial properties and create medicinal preparations on its basis.

Royal jelly is a paste-like nutritious product that bees feed to the queen bee from the larval stage and throughout her life. The composition and quality of it depends on the size of the bee family and providing it with enough nectar and pollen. Royal jelly is formed in special glands of nurse bees and is secreted by them from 3 to 12 days of life.

Royal jelly is successfully used in the world as a dietary and therapeutic product. It seems relevant to obtain royal jelly on an industrial scale and manufacture various medicines and food additives based on it, which opens broad prospects for both beekeeping and consumers - represented by food, pharmaceutical and cosmetic industries, as well as the use of colostrum with a high nutritional value and biological value for functional products.

As a result of a patent search, technologies for obtaining royal jelly were studied, and a wide range of use of royal jelly in various industries was established.

Royal jelly is widely used in dermatology. It is recommended for the treatment of difficult to heal wounds, including bedsores and burns, with seborrhea and seborrheic eczema, impetigo of the hands and feet.

Royal jelly increases the body's resistance to infections. It has an immunoregulatory effect. It causes a significant increase in the body's resistance to infections by stimulating the production of macrophages and γ-globulin.

Royal jelly is used in the treatment of cardiovascular diseases such as angina pectoris, neurosis, post-infarction conditions, arterial hypertension, cerebral embolism, atherosclerosis.

Oral royal jelly has a beneficial effect in coronary heart disease, coronary atherosclerosis and in the rehabilitation period after myocardial infarction.

Royal jelly is also used for the prevention and treatment of diseases of the digestive tract and internal organs. Duodenal ulcers are particularly sensitive to the effects of this product.

In addition to the pharmaceutical industry, royal jelly is used in the food industry. So, it is used as a biologically active food supplement for the prevention of diseases and the improvement of the cardiovascular system. Royal jelly is used to produce products such as non-alcoholic rosehip drink, confectionery dragees, instant cereals, sports drink mix, mint-chocolate beef granules, fermented beef stew, honey milk, etc.

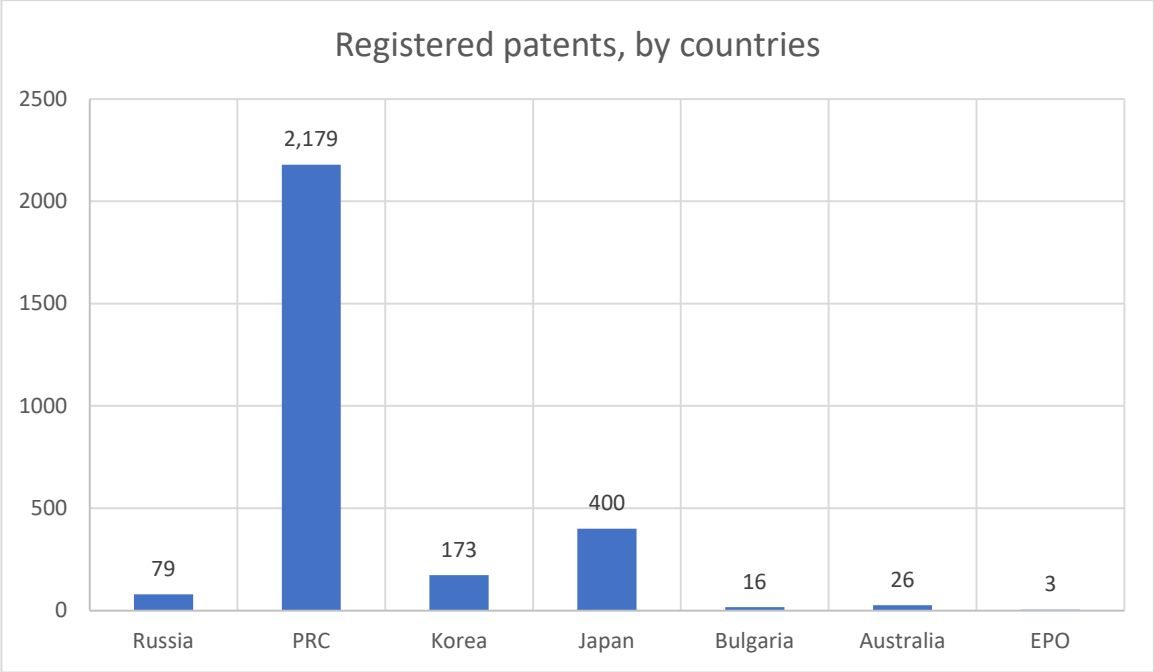

Chart 1. Number of registered patents between 2012-2022

The number of published preserved documents by years and countries for the study period was determined. Patents worked out: Russian Federation, China, Republic of Korea, Japan, Bulgaria, Australia, EPO.

As a result of the analysis of the patents of the above countries, it has been shown that the production of royal jelly and its processing are given considerable attention in China, Japan, and in the Republic of Korea.

According to the results of a patent search, it can be noted that one of the most important biological properties of royal jelly is the enhancement of metabolic processes and tissue renewal. This product enhances protein metabolism, increases the number of red blood cells and hemoglobin levels. It is assumed that the iron and zinc ions included in its composition contribute to this to a large extent.

Analysis and generalization of the selected scientific and technical information indicates the relevance of this active substance study. Therefore, our institute is currently working on the implementation of products based on royal jelly.

FOOD SECURITY AND BIODIVERSITY SUSTAINABILITY IN A CHANGING CLIMATIC SCENARIO IN PAKISTAN

Haroon KHAN[1]

[1]The University of Agriculture, Faculty of Crop Protection, Department of Weed Science & Botany, Peshawar, Pakistan.

[1]ORCID ID: https://orcid.org/0000-0001-6089-9407

Ömer Süha USLU[2]

[2]Kahramanmaraş Sütçü İmam University, Agriculture Faculty, Field Crops Department, Kahramanmaraş, Türkiye.

[2]ORCID ID: https://orcid.org/0000-0003-0858-0305

Osman GEDİK[3]

[3]Kahramanmaraş Sütçü İmam University, Agriculture Faculty, Field Crops Department, Kahramanmaraş, Türkiye.

[3]ORCID ID: https://orcid.org/0000-0002-4816-3154

ABSTRACT

Both natural and human processes contribute to climate change. It significantly affects agricultural productivity, food security, and biodiversity. The majority of endemic and specially adapted species are in danger of going extinct. In light of the fact that it sustains all life on Earth and serves as the major source of primary healthcare for more than 60-80% of humanity worldwide, worries about species extinction are valid. Although the effects of climate change on biodiversity and food security have been recognized, little research has been done in connection to the problem's global scope. The cornerstone of Pakistan's food security is agriculture. The agriculture industry has been falling in recent years while being crucial to our country's food security, economics, and prosperity. One of the main contributors to these hopeless agricultural conditions is climate change. Pakistan is one of the most climate-vulnerable nations in the world, coming in at number eight on the list of nations most at risk from climate change in 2021. The nation is highly prone to the multiple and interconnected hazards that a changing climate poses. A number of recent data, such as rising average temperatures and increased rainfall variability across the country, hint to a deteriorated climatic outlook. In addition, the frequency of climate-related calamities like floods, droughts, heat waves, etc. has grown recently. Over 80% of agricultural output comes from Pakistan's mostly irrigated agriculture system, which consumes 90% of the river water that is available. The base of food production, land, and water, are restricted and even declining resources because of factors like the changing climate. This review's objective is to draw attention to the effects of climate change on Pakistan's agricultural industry, biodiversity, and opportunities for mitigation in order to ensure resilient agricultural practices that ensure household food security. Strong policies, the introduction of high-yielding stress-resistant cultivars, the creation of climate-resilient irrigation systems, and agriculture are all necessary for attaining food security in this scenario.

Keywords: Climate Change, food security, biodiversity, Pakistan

INTRODUCTİON

Global Perspective

Agriculture is the foundation of Pakistan's food security. Agriculture has been diminishing in recent years while being vital to our country's food security, economics, and prosperity. Climate change is a key contributor to these deplorable agricultural conditions. Pakistan is one of the world's most climate-sensitive countries, placing eighth on the list of nations most vulnerable to climate change in 2021. The country is very exposed to the multiple and interconnected challenges presented by climate change. Recent data, such as rising average temperatures and increased rainfall variability across the country, indicate to a deteriorating climate picture.

Climate change has affected the environmental conditions for growing agricultural crops in many parts of the world; some benefit from it (polar regions gain more ice-free territory suitable for agricultural crops), while others suffer (rising surface temperature, unequal rainfall, and so on). Climate change reduces crop quantity and quality, as well as sugar content, color, and storage stability in fruits; increases in weeds, blight, and destructive insects in agricultural crops; decreases land fertility owing to rapid organic decomposition; and increases soil erosion due to higher rainfall.

Many African and Asian nations are suffering as a result of climate change. It is challenging to develop reaction capacities to reduce climate change causes and adapt to climate change impacts since there are many disadvantaged people on both continents. There are currently 7 billion people on our globe, and by 2050, that number is projected to increase to 9 billion. Currently, there are more than 800 million individuals that are food insecure. At a time when we are already battling to feed our expanding population, climate change will bring up additional difficulties. As a result of changing and unpredictable rainfall patterns, droughts, rising temperatures, an increase in the frequency and intensity of extreme weather, and pest and disease outbreaks, crop failures and animal losses will rise.

Given that global temperatures are currently rising at a rate of 0.2°C (0.1°C) every decade, the human-caused temperature increase passed 1°C over pre-industrial levels about 2017 and, if present trends continue, will reach 1.5°C around 2040. This temperature rise has been accompanied by an increase in ocean temperature, a 20-centimeter rise in sea level, a 40% decrease in Arctic sea ice, and an increase in the number of extreme weather events. As we produce more CO_2 into the atmosphere, climate change will endanger and complicate life on Earth (IPCC, 2018a). As a result, it is vital to establish adaptation strategies that optimize potential while conserving expenditures, resulting in long-term agricultural development.

National Perceptive

Agriculture is a critical economic sector in Pakistan, contributing 18.5% of GDP, employing 38.5% of the overall workforce, and accounting for around 60% of exports (PES, 2019). It serves as the raw material for a variety of value-added goods and supports the lives of 62% of the people (PES, 2017-18). It is considered that steady expansion in the agriculture sector is unavoidable for our economy's projected growth, yet owing to neglect in budgetary allocations and expenditure in this area, it has failed to meet projected growth objectives. Climate change has an influence on agriculture since it is an open business. Climate change impacts such as high temperatures, precipitation timing, intensity, and duration, aridity, desertification, reduced water availability, increased pests incidence in crops, and erosion have all had a significant impact on agricultural production worldwide, including in Pakistan. Pakistan is particularly exposed to climate change threats since it is located in an area where temperature rises are predicted to be greater than the world average.

Drought impacted not only Baluchistan, but the whole country in the previous several decades, lasting over 10 months, affecting around 2.2 million people, and resulting in 143 fatalities. In 2018, the government proclaimed a drought emergency, with extensive periods of drought hurting the lives and livelihoods of millions of people in Baluchistan and Sindh provinces. During this time, millions of animals died. Pakistan has experienced 78 floods affecting over 76 million people, 15 heat waves (e.g. in Karachi in 2015 and 2017), various cyclones (e.g. Yemy in 2007 affecting over 1.5 million people), and a series of calamitous droughts (10 were reported between 1998 and 2014). The unimpeded and vicious water flow from denuded

hillsides, caused by deforestation, exacerbates the intensity of avalanches in the lower Himalayas (ADB, 2017).

Pakistan is regarded as one of the world's most vulnerable countries to climate change (CC). Given its geographic, demographic, and climatic variety, Pakistan's high sensitivity to climate change is predictable. Due to the inherently arid environment and the significant reliance on water from glacier runoff, climate change threats to water, energy, and food security are especially serious. Its consequences may be observed in the increased intensity and frequency of catastrophic climatic disaster occurrences, as well as small but steady changes infiltrating many sectors of government function. Due to Pakistan's high sensitivity, expenses are predicted to be comparably high in compared to the rest of South Asia, where the ramifications on fragile industries are already expected to be massive. According to some estimates, climate change is already causing significant economic losses in Pakistan.

According to the evaluation of the Global Climate Risk Index 2020, Pakistan came in 5th with over 6 billion USD in damages from climate change. Pakistan has also been singled out by the World Bank as Asia's hotspot for being affected by global temperature and precipitation abnormalities that may heighten the severity, extent, and frequency of catastrophes. More and more people will need to relocate as a result of rising soil erosion, more and more frequent and severe floods along rivers, the salinization of farms, and melting glaciers in northern regions. On both the supply and demand sides, there are several mitigating options, with energy-saving strategies being the most effective. According to estimates, national adaptation needs range between 1.5 and 3.0% of GDP, and there is already a sizable worldwide shortage. The costs of Pakistan's yearly adaptation to climate change were anticipated to vary from 6 to 14 billion USD, or an average of 10.7 billion USD annually, through 2050, notwithstanding the difficulty of making such figures. A comparison of worldwide cost projections with existing levels of adaptation financing shows that predicted global adaptation needs are much higher than present investment levels, particularly in vulnerable developing nations like Pakistan (UNDP, 2017).

Climate Change and Agronomic Crops

Crops cultivated in both irrigated and spate farming systems are extremely vulnerable to water availability and temperature variations. Temperature increases (+0.500C-2.00C) are expected to reduce agricultural production by 8-10% by 2040. (Dehlavi et al., 2015). According to Iqbal et al., (2009), multiple modeling studies utilizing the crop-growth simulation model indicated a decline in the production of main crops, notably wheat and rice, as well as the duration of the growing season in four agro-climatic zones of Pakistan. The model anticipated that a 1.00C increase in temperature will result in a 14-day decrease in wheat growing season length in northern Pakistan compared to southern Pakistan.

In all agro-climatic zones, with the exception of the north, the same research found a 6% loss in wheat output and a 15–18% fall in fine-grain aromatic basmati rice yield by 2080. A combination of agronomic and social factors, including the availability of water, pesticides, labor, family characteristics, the number of women, past experiences, and exposure to extreme events and seasonal weather, are thought to have a significant impact on wheat crop production. High summer (kharif) rainfall is critical for winter (rabi) agricultural output (Iqbal et al., 2009).

Temperature increases influence most plants, resulting in decreased crop yields and complex growth responses. Under future warmer and drier weather, a 1°C rise in growth period temperature, for example, may reduce wheat productivity by 3-10%, winter wheat production by 5-35%, and maize yield by 2.4-45.6%. Even if precipitation remains constant, agricultural production might drop by 15% on average due to shorter crop growth periods and increased water stress induced by higher temperatures and evapotranspiration. Wheat output in Pakistan fell by 50%, as seen in (Table-1). Climate change may have a positive influence on agricultural crop output in other nations, for example, in desert places, rainfall rises during wet circumstances, and wheat yield in Mexico will increase by 25% in the future. Southern Pakistan's cereal crop yields have dropped by 15-20%.

Reddy KR *et al.,* 2002 found 8%, 3-17%, and 4-15% yield losses in cotton, coarse grains, and oilseeds crops, respectively, in Pakistan. Extreme temperatures and precipitation can prohibit crops from developing. Rising atmospheric CO_2 levels may have an indirect influence on crops through pest and disease impacts.

Table 1. Impact of climate change on cereal crop production

Crops	Country/Continent	Yield reduction (%)	Reference
Wheat	Australia	−32	Luo *et al.,* 2005
	Worldwide	−5.5	Lobell *et al.,* 2011
	China	−17.5	Yang *et al.,* 2017
	Asia	−7.7	Asseng *et al., 2017*
	Pakistan	**−50**	Hussain *et al.,* 2018
Rice	India	−8	Saseendran *et al.,* 2000
	Asia	−6.3	Masutomi *et al.,* 2009
	Italy	−12	Bregaglio *et al.,* 2017
Maize	Portugal	−17	Ahmed *et al.,* 2018
	Africa	−20	Yang *et al.,* 2017
	Pakistan	**−27**	Rurinda *et al.,* 2015
	USA	−27	Gunn *et al.,* 2018

Climate Change and Horticultural Crops

Global horticulture operations and output may be significantly impacted by climate change. Climate change will modify the growth patterns, flowering, and fruiting capacity of many perennial and annual horticultural plants. Changed seasonal conditions that affect hibernation, acclimatization, and subsequent flowering and fruiting are expected to provide considerable hurdles to some perennial fruit crops. Due to reduced cold damage and a longer growing season, other crops may benefit from the effects of climate change (Dixon, 2012).

There has been less focus on studying how climate change affects the growth cycle of vegetable crops. In commercial field vegetable crops, premature flowering might recur. Allium, brassica, beet, and carrot cultivation in the area will be negatively impacted by this. As the temperature at night rises, more people will breathe, shifting the assimilates' distribution into reproductive sinks. It will become more challenging to grow desirable high quality grades of vegetables like cucumbers and tomatoes as a result, as fruit size and quality would be lowered. The development of new cultivars that are better suited to the changing environment and market demands as well as a reevaluation of current cultivars may result from this.

Different crops respond differently to temperature triggers. Mango, for instance, has a bias toward temperature and tends to vegetate more in warmer climates. This reduces yield and quality by altering the size and number of leaves that emerge from the vegetative buds. Sharp temperature reductions result in mango being damaged by cold stress. Pathogen and pest damage are expected to increase as mango pathogens and other Lepidoptera species are fostered. Changes that increase rainfall during fruiting will be harmful. Mango crops' ascorbic acid and sugar content are reduced when light intensity is reduced during fruiting. Rising temperatures will have an impact on grape harvests, perhaps delaying fruit development and reducing quality.

Climate Change and Livestock

Livestock is a vital source of food in Pakistan. In Pakistan, the livestock industry generates 56.3% of agricultural production and 11.8% of national GDP, and it directly sustains over 8 million rural families (Pakistan Economic Survey 2014–15). Many people rely heavily on cattle to satisfy their food demands in hilly places where agriculture production is more challenging. Livestock management employs eight million people in the country and contributes for 35% of their income. Pakistan is the world's 4th largest milk

producer. Given the size of animal production, Pakistan generates considerable foreign money from exporting cattle and livestock byproducts (WFP, 2018). The emissions from this industry make up a sizable portion of all agricultural emissions in Pakistan. For instance, the only processes that produce close to 90% of the greenhouse gas emissions from agriculture are enteric fermentation and manure management, which together account for about 40% of Pakistan's overall GHG emissions (Ahmad *et al*., 2012).

Major obstacles to Pakistan's livestock production are posed by climate change. As temperatures increase, rainfall patterns change, and extreme weather events occur more frequently, it is expected that global cattle productivity would decline. It is generally known that increasing temperatures have a negative impact on feed intake, reproduction, and performance in a variety of livestock species. Indirect effects might include lower feed and fodder quality and availability, the rise of illnesses, and increased rivalry for resources with other industries (Sejian *et al*., 2018). Climate change's direct effects are anticipated to be more restricted in non-grazing systems, owing to the fact that putting animals in buildings allows for more control over production conditions.

Climate Change and Fisheries/ Aquaculture

Over 500 million people, either directly or indirectly, make their living via fisheries and aquaculture. Additionally, fish provides 400 million people in the highest poverty rates with essential minerals and at least 50% of their animal protein. Fish also provides essential nutrition to 3 billion people worldwide. Climate change endangers existing and future production levels, food security, and fishing industry jobs. Climate change is profoundly affecting ocean ecosystems, with consequences for marine animals, biodiversity, fisheries and aquaculture, coastal zones, and humanity.

The loss of marine biodiversity will be caused by physical and chemical changes in the ocean. Rising ocean temperatures, rising levels of carbon dioxide (CO_2), and hypoxia will have a direct influence on marine life (inadequate oxygen). As more carbon dioxide is absorbed by salt water, it becomes more acidic. Warmer saltwater has a lower concentration of oxygen (IPCC, 20018a). Production systems and livelihoods that are already in trouble due to overfishing, poor management, and the effects of other human causes are expected to deteriorate further as storm frequency and severity increase and extreme weather events become more common.

Climate Change and Forestry

Biological variety is a vital component of the ecological services that ecosystems provide to human society. Once degraded, biological variety is difficult to recover or replace since it contributes to the functioning of ecosystems. Particularly when it comes to rural subsistence, forests are a vital natural resource. It provides a number of essential ecosystem services, like as CO_2 reduction and environmental management, as well as timber, firewood, food, wildlife habitat, and other necessities. 4.19 million hectares of Pakistan's total land area are covered in forests or 5%.

Around 1.6 billion people (nearly 25% of the world's population) depend on forests for their livelihoods. Clean water and wholesome soils are only two of the $75–100 billion worth of goods and services that come from forests each year. 80% of the terrestrial biodiversity on the planet is found in forests. Approximately 5.01% of Pakistan's total geographical area is covered by forests. Numerous stakeholders are becoming more aware of the serious issue of deforestation. Climate change is projected to have a wide range of negative consequences for the ecosystem as a whole, notably for Pakistan's already fragile forestry sector. Climate change is most likely to result in lower production, changes in species composition, reduced forest area, biodiversity loss, and increased flood risks. Adaptation in the forestry industry comprises the need to repair and improve Pakistan's forests through sustainable forest management, with a special emphasis on how they are affected by climate change.

Climate Change and Water

The water business is one of the most vulnerable to climate change's consequences. Pakistan has the largest contiguous Indus Basin irrigation system in the world, which is heavily reliant on precipitation, glaciers, and snow melt, as well as ground water abstraction. Monsoon rains (50 million acre feet MAF) and river inflows are the IRS's primary sources of water (142 MAF). Ground water provides for approximately 48% of the surface water available at the canal head of the irrigation system. Water consumption is predicted to rise due to the world's fast growing population, rising social standards, expanded industry, and improved sanitation. Pakistan is one of the most water-stressed countries on the planet. Water shortage data suggest that the country is quickly nearing water scarcity. The circumstance necessitates wartime development and control of the country's water resources (Falkenmark *et al.,* 1989).

The current water deficit is around 20 MAF, with a predicted increase to 31 MAF by 2025. It is ascribed to policy errors, ill-conceived programs, wrongly constructed institutions, weak laws, and a lack of political will. In recent years, anxieties about the impact of climate change on Pakistan's already-depleted water supplies have intensified. A few of the ways that climate change is predicted to affect Pakistan's hydrologic resources include rising temperatures, increasing saltwater intrusion in coastal areas, an increased risk of glacial lake outburst floods, more intense rainfall, and altered monsoon and winter rainfall patterns.

Climate Change and Soil

Climate change might have a big impact on soils and the activities they do. Climate change will influence agricultural output because changes in soil temperature, air temperature, and rainfall affect crop maturity and potential yield. As the temperature rises, irrigation may be used to compensate for water shortages. Water scarcity, on the other hand, may make irrigation impossible. Increased land damage, or land degradation, will occur in the form of soil erosion, desertification, salinization, or loss of peat soils, diminishing the ability of soils to maintain agricultural needs.

The world's unique combination of soils and climate determines the kind and distribution of natural and semi-natural ecosystems, giving water, nutrients, and a growth medium. As the climate changes, so will the soil's ability to support current ecosystems, resulting in changes in vegetation growing in different parts of the world. Overall, climate change will have a significant influence on the jobs that soil performs, and this will have a huge impact on the future utilization of soils, usually needing extensive adaptations to meet the changing environment (Hillel and Rosenzweig, 1989).

CONCLUSİONS

Farmers in Pakistan continue to adopt traditional agricultural methods and use outdated technology in their agricultural areas, making them less sustainable. Pakistani agricultural communities are experiencing very serious issues in the 21st century, with agriculture directly or indirectly supporting 70% of the country's population. Agrarian economies, such as Pakistan's, are particularly sensitive to the effects of climate change. Evidently, these effects are causing a reduction in agricultural production in Pakistan, putting the country's economy and food security at risk. As a result, it is necessary to align the agricultural sector of the country with the framework of climate-compatible development. Existing archaic methods, such as inadequate on-farm water management, excessive tillage, pesticide usage, mono-cropping, intense cultivation, obsolete cropping patterns, climate fragile value chains, and so on, hinder agriculture growth potential in many regions of Pakistan. This may be due to a lack of knowledge about climate-smart agriculture. Climate change adaptation methods have the potential to significantly lessen the consequences of climate change in Pakistan.

REFERENCES

ADB, 2017, Climate Change Profile of Pakistan, Asian Development Bank Manila, Philippines.
Ahmed I, Rahman MH U, Ahmed S, Hussain J, Ullah A, Judge J. 2018. Assessing the impact of

climate variability on maize using simulation modeling under semi-arid environment of Punjab, Pakistan. Envir. Sci. & Pollution Res., 25(28): 28413- 28430

Asseng et al. 2017. Hot spots of wheat yield decline with rising temperatures. Global Change Biology. 23 (6): 2464-2472

Bregaglio *et al*. 2017. Identifying trends and associated uncertainties in potential rice production under climate change in Mediterranean areas. Agricultural and Forest Meteorology.237: 219-232

Cheke, R. A. & Tratalos, J. A. 2007 Migration, patchiness, and population processes illustrated by two migrant pests. Bioscience 57: 145 –154.

Climate Change 2013 (2018a): The Physical Science Basis. Contribution of Working Group I to the 5th Assessment Report of the Intergovernmental Panel on Climate Change [Stocker,T.F.,]

Dehlavi A, Groom B, Gorst A. 2015. Climate Change Adaptation in the Indus Ecoregion: A micro-econometric study of the determinants, impacts and cost effectiveness of adaptation strategies. Islamabad: World Wide Fund for Nature Pakistan.

Dixon GR. 2012. Climate change, plant pathogens and food production. Can. J. Plant Pathol. 34(3): 362–379

Falkenmark M, Lundqvist J, Widstrand C. 1989. Macro-scale water scarcity requires micro-scale approaches–aspects of vulnerability in semi-arid development. Nature Resources Forum.13(4): 258–267.

Hillel D, Rosenzweig, C. 1989. The green house effect and its implications regarding global agriculture, Research bulletin No.724. Massachusetts Agricultural Experiment Station, Amherst

Hussain J, Khaliq T, Ahmad A, Akhter J, Asseng S. 2018. Wheat responses to climate change and its adaptations: A focus on arid and semi-arid environment. International Journal of Environmental Research. 12: 1-10.

Iqbal, M.M, M. A. Goheer and A. M. Khan.2009. Climate Change Aspersions on Food Security of Pakistan. Science Vision. 15 (1). Islamabad.

Lobell DB, Schlenker W, Costa- Roberts J. 2011. Climate trends and global crop production since 1980. Science. 29: 616-620

Luo Q , Bellotti W, Williams M, Bryan B. 2005. Potential impact of climate change on wheat yield in South Australia. Agricultural and Forest Meteorology. 132(3- 4): 273-285

Masutomi Y, Takahashi K, Harasawa H, Matsuoka Y. 2009. Impact assessment of climate change on rice production in Asia in comprehensive consideration of process/parameter uncertainty in general circulation models. Agriculture, Ecosystems and Environment. 131(3-4): 281-291

Pakistan Economic Survey 2014-2015, Finance Division, Govt. of Pakistan.

Pakistan Economic Survey 2017-2018, Finance Division, Govt. of Pakistan.

Pakistan Economic Survey 2018-2019, Finance Division, Govt. of Pakistan.

Reddy KR et al. 2002. Simulating the impacts of climate change on cotton production in the Mississippi delta. Climate Research. 22(3): 271-281

Rurinda J, Van Wijk M. T, Mapfumo P, Descheemaeker K, Supit I, Giller K. E. 2015. Climate change and maize yield in southern Africa: What can farm management do? Global Change Biology. 21(12): 4588-4601

Saseendran S. A., Singh K. K., Rathore L. S., Singh S. V, Sinha S. K. 2000. Effects of climate change on rice production in the tropical humid climate of Kerala, India. Climatic Change. 44(4): 495-514

Sejian, V., Bhatta, R., Gaughan, J., Dunshea, F., & Lacetera, N. 2018. Review: Adaptation of animals to heat stress. Animal, 12(S2): 431-444.

UNDP, 2017, Pakistan – Climate Public Expenditure and Institutional Review, United Nations Development Program, Islamabad, Pakistan.

WFP, 2018. Climate Risks and Food Security Analysis: A Special Report for Pakistan. Islamabad, December 2018

Yang C, Fraga H, Van Ieperen W, Santos J. A. 2017. Assessment of irrigated Climate Change and Agriculture maize yield response to climate change scenarios in Portugal. Agricultural Water Management. 184:178-190

CLIMATE CHANGE AND RIVER WATER POLLUTION: AN APPLICATION TO THE GANGES IN KANPUR

Amitrajeet A. BATABYAL

Arthur J. Gosnell Professor of Economics, Rochester Institute of Technology, 92 Lomb Memorial Drive, Rochester, NY 14623-5604, USA

Karima KOURTIT

Open University, Heerlen, The Netherlands

Peter NIJKAMP

Open University, Heerlen, The Netherlands

ABSTRACT

We provide a theoretical framework to analyze how climate change influences the Ganges and how this influence affects pollution in the river caused by tanneries in Kanpur, India. We focus on two tanneries, A and B, that are situated on the same bank of the Ganges in Kanpur. Both produce leather and leather production requires the use of noxious chemicals. Tannery A is situated upstream from tannery B. Tannery $A's$ leather production depends only on labor use but tannery $B's$ leather production depends on labor use, the chemical waste generated by tannery A, and the natural pollution absorbing capacity of the Ganges. In this setting, we perform four tasks. First, we construct a metric that measures the climate change induced mean reduction in the natural capacity of the Ganges to absorb pollution in the time interval $[0, t]$. Second, we use this metric and determine the equilibrium production of leather by both tanneries in the benchmark case in which there is no pollution. Third, we ascertain how the benchmark equilibrium is altered when tannery B accounts for the negative externality foisted upon it by tannery A. Finally, we study the impact on leather production and on labor use when the two tanneries merge and then discuss the policy implications stemming from our research.

Keywords: Climate Change, Ganges River, Tannery, Unitization, Water Pollution

THE DAMAGE MECHANISMS OF ACRYLONITRILE BUTADIENE STYRENE

Hassan Bouhsiss,* , A. En-naji , A. Wahid , Abdekarim Kartouni , Mohamed El Ghorba

Laboratory of Physics of Matter Condensed, Faculte des Sciences Ben M'sik, Hassan II University of Casablanca, Avenue Driss El Harti, B.P 7955 Sidi Othman, Casablanca, Morocco

Laboratory of Control and Mechanical Characterization of Materials and Structures, National Higher School of Electricity and Mechanics, BP Oasis, Hassan II University, Casablanca, Morocco

Condensed Matter Physics Laboratory, Faculty of Sciences Ben M'Sik, University Hassan II of Casablanca, B.P. 7955, Casablanca, Morocco

ABSTRACT

Plastics play an important role in our daily lives due to their ease of installation and relatively low production costs. At present polymers are ubiquitous in all facets of our lives, hence the imminent need to detect the mechanical behavior of these said polymers. This research presents new developments in the field of fracture mechanics.

The present work will be devoted to the study of the mechanical behavior of a polymer of type Acrylonitrile Butadiene Styrene (ABS) under uniaxial tensile loading focusing on the influence of stress concentrations on the behavior of the studied ABS structures containing a combined defect.

The knowledge of the mechanical behavior of the components is essential to predict their service life in order to avoid any fatal failure in service. In this context, our study is based on the evolution of the stress concentration coefficient and the stress intensity factor of single and double notched specimens.

In order to achieve this objective we have damaged the studied material (ABS) by the realization of combined hole + single notch and hole + double notch defects.

Keywords: Mechanical behavior, Stress concentration coefficient, ABS, tensile, damage, service life, stress intensity factor, critical defect

CALCULATING THE AMOUNT OF WATER LEAKAGE INTO THE OPEN PIT MINE USING A DISCRETE FRACTURE NETWORK AND NUMERICAL SIMULATION AND WAYS TO CONTROL IT WITH A DRY PLAN FOR IT

Seyedeh Golaleh Hosseini,
PhD student in Amirkabir University, Faculty of Mining engineering
Kourosh Shahriar,
Professor in Amirkabir University, Faculty of Mining engineering
Mohammad Amin Karbala,
PhD in Amirkabir University, Faculty of Mining engineering

ABSTRACT

It is important to control and estimate the amount of water leakage into the open pit mine during the construction and exploration operation in the jointed rock mass. Not controlling this factor, more than any other factor is the main reason for additional costs and delays in the construction of mineral excavations. Therefore, the proper estimation of the water leakage amount in determining the optimal direction of mining excavation, cost estimation and determining the appropriate schedule can be a basic requirement. The input flow to mineral excavations is affected by various factors, one of the most important of which is the pattern of discontinuities in the rock mass, which accurate numerical simulation can help a lot in predicting the amount of flow to mineral excavations. The most effective pattern of discontinuity in the rock mass, which is also the main water flow transmission system, is a continuous network of separate fractures. Analytical and experimental studies have shown that three dimensional models of discrete fracture network (3D DFN), if randomly generated, provide better results to determine the amount of water leakage than other models. For this purpose, 3DEC software, which has the ability to randomly generate a network of separate fractures and solve the flow in the jointed system, has been used. This software has the ability to model joints in three dimensional based on statistical distribution functions and uses discrete element method to solve the flow. In a case study, its geological data is used to build a model. Using the network of different fractures, first the desired model was geometrically matched with the studied area and for the hydraulic calibration of the model, the data of lujan test conducted in the area was used. The results of this research show that the intensity of the flow is very sensitive to the aperture of the joints. Then the results of this step are compared with UDEC software in the next step and the amount of leakage is also confirmed with this software. In order to confirm the work with analytical formulas, the cubic law is the most compatible with the existing conditions of the area and the constructed model.

COMPARATIVE STUDY BETWEEN GNSS AND LASERGRAMMETRY

Mokrane Salwa[1*], El azzouzi Rachid[2]

[*1]Sultan moulay slimane university, Sciences and technologies faculty, Department of geomatics, geosciences and environment, Beni Mellal, Morocco. [2]Agronomic and Veterinary Institute Hassan II – IAV, Department of Geomatics and Topographic Engineering, Rabat, Morocco

ABSTRACT

Lately, data acquisition techniques have undergone changes which have made it possible to facilitate and automate the task in the field. Indeed, the advent of GNSS and the evolution of laser scanning techniques have resulted in precise three-dimensional surveys, extremely reliable and quick to perform.

This end-of-study project proposes, through an experimental study, a comparison between the lasergrammetry technique and GNSS. This comparison relates, on the one hand, to the quality of the results obtained from each of the two techniques, and on the other hand, to the cost, the production time and the criteria for choosing each of these techniques.

The realization of this comparison made it possible to deduce that the results obtained by the different techniques are not very different (an average of the differences of 4 cm for the distance, 3 gr for the deposit and 13 cm for the case of orthometric height) and are characterized by an overall satisfactory quality (the quality of the clouds of points are alike). In terms of execution time, lasergrammetry was the fastest during the completion of the field mission although its office phase remained relatively slow requiring a good understanding of the processing software. Regarding the selection criteria, lasergrammetry seems to us to be the most appropriate in the case of complex morphologies, thanks to the density of points surveyed, and to sites with difficult access since it is based on remote measurements. On the other hand, GNSS is more suited to less complex shapes, the survey of which generally requires a relatively smaller number of points.

Keywords: GNSS, lasergrammetry, laser scanning, Mobile Mapping System, three-dimensional surveys.

DESIGN AND ANALYSIS OF ADVANCED SPEED CONTROL METHODS FOR PLC AND HMI BASED INDUCTION MOTOR DRIVE

Dr. V. Thiyagarajan

Associate Professor, Sri Sivasubramaniya Nadar College of Engineering, Kalavakkam – 603 110, Chennai, Tamil Nadu, INDIA

ABSTRACT

The Programmable Logic Controller (PLC) based variable frequency speed control system has many advantages over variable frequency drive (VFD) and is one of the most ideal and promising speed control methods for three phase induction motors. Focus on the issue that the control system for variable frequency speed regulating of the motor base PLC makes it difficult to monitor the PLC and the VFD's operational status in real time. Variable Frequency Drives (VFDs) are used more frequently to provide a flexible method of speed control for industrial applications that require variable speed operation at almost all times because the speed and torque of AC motors depend on the voltage and frequency. Induction motors account for the vast majority of electrical machines used in industry because of their low cost and rugged construction. As a result, efficient control and stable operation are critical. Because of their ease of programmability, fast operation, and precise control, Programmable Logic Controllers (PLCs) are robust devices widely used in industries and process control applications. This paper describes a design and analysis of advance speed control system for variable-frequency induction motor drive based on PLC and HMI. An intelligent measurement and control system based on PLC and HMI for variable frequency speed regulating of the motor is presented in accordance with the design ideas and composition principle of a typical control system. In addition, the motor drive circuit and VFD control circuit are designed, and then the PLC control programme and HMI monitoring interface are created. The test results show that the system design is reasonable, the operation is stable, and the human-computer interaction interface is friendly, indicating that it can effectively solve the aforementioned problems.

Keywords: Induction motor, PLC, variable frequency drive (VFD), speed control and protection, MATLAB/Simulink